

**INFLUENCE OF DIAMETER, DISTINCTIVE MATERIAL  
AND GEOMETRY OF VERTICAL DRAIN WITH SOIL  
STRUCTURE EFFECTS ON CONSOLIDATION  
CHARACTERISTICS OF KAOLINITIC CLAY  
DUE TO RADIAL DRAINAGE**



**A Thesis Submitted to  
The Maharaja Sayajirao University of Baroda  
For the Degree of  
Doctor of Philosophy in Civil Engineering**

**By  
Manish V. Shah**

**Research Guides**

**Prof. (Dr). D.L. Shah**

**Prof. (Dr.) A.V. Shroff**

(Vide.MSU letter no. AC/III/136  
Dt. 17/5/2005)

**Geotechnical Engineering Division  
Applied Mechanics and Structural Engineering Department  
Faculty of Technology and Engineering  
The Maharaja Sayajirao University of Baroda  
Vadodara – 390 001  
July - 2012**

**Synopsis**

**“INFLUENCE OF DIAMETER, DISTINCTIVE MATERIAL AND GEOMETRY OF VERTICAL DRAIN WITH SOIL STRUCTURE EFFECTS ON CONSOLIDATION CHARACTERISTICS OF KAOLINITIC CLAY DUE TO RADIAL DRAINAGE”**

Amongst the various ground improvement techniques the vertical geodrain using radial drainage is preferable in soft cohesive soil. When a soil mass is subjected to compressible stresses, it causes a reduction in pore space and, if saturated the excess water is expelled with time till equilibrium condition is established for a given constant compressive stress. For cohesive soil, the time required to accomplish this, is more. Initially, before any reduction of pore space has occurred, the compressive stresses are carried by the water (called hydrostatic excess or excess pore water pressure). As the excess water drains, compressive stresses are transferred to the soil grains increasing the intergranular pressures. This complete process is known as ‘Consolidation’ of the soil and was first analyzed by Karl Terzaghi (1923) for a case of one-dimensional consolidation.

The model law of consolidation suggests that shorter the drainage path, faster the rate of the consolidation ( $t = T_v d^2 / C_v$  i.e.  $t \propto d^2$ ). In addition the rate of consolidation can be enhanced if higher horizontal permeability than vertical of soil is taken into advantage. These can be made possible by adopting central vertical geodrain (sand drain) where drainage path reduced by four fold Terzaghi (1936) where in excess water dissipates radially and vertically at faster rate.

Because of the certain limitations of conventional methods, the concepts of prefabricated vertical geodrains have entered into the practice particularly for ground improvement of soft marine clays. Some of the cost effective and eco-friendly prefabricated geodrains of natural materials seems to have not only expedite the rate of settlement but consequently accelerated the rate of gain in strength.



### **Historical Theoretical Developments**

Classical theoretical work of Terzaghi & Frohlich (1936,1943,1948), Rendulic (1935), Biot (1941), Carillo (1942), Silveira (1953) of three dimensional process of consolidation into plane radial flow have been resolved and gave solution by Barron (1948) considering 'equal strain' and 'free strain' conditions with and without peripheral smear and drain well resistance.

Kjellman (1948), Takagi (1957), Crezer (1957), Schiffman (1958), Hansbo (1960,1981), Mc Kinlay (1961), Aboshi (1961), Escario & Uriel (1961), Creyers (1961), Horne & Rowe (1964), DeLean (1965), Mikasa (1965), Christie (1966), Rowe & Barden (1966), Anandakrishnan et al. (1969), Sivareddy (1969), Berry Wilkinson (1969), Simon & Tan (1971), Taytovich et al. (1971), Sills (1975), Yamaguchi et al. (1976), Yoshikuni et al. (1974), Chaput & Thomann (1975), Brenner et al. (1983), Davis & Poulos (1968), Olson et al. (1977), Zeng & Xie (1989) extended the analysis of above classical works incorporating several additional factors viz. magnitude and rate of loading, permeability with respect to stratification, accounting linear and non-linear behavior with void ratio change and gave closed-form solution for pore pressure distribution in three dimensional process of consolidation considering with and without stratification.

Later on, Olson.R.E et al. (1974), Runesson et al. (1985), A.Altabbaa et al. (1987,1991), Goughnour. R. R et al. (1992,1994), H.D.lin et al. (1997), XioWuTang et al. (1998,2001), GuoFuZhu et al. (1998,2000), Xu-Sheng et al. (2004), Guo-XiongMei & JianHuaYin et al. (2003), Gorolmai et al. (2002), ToyoakiNogami et al. (2003), Tang et al. (2000,2001), Patrick Fox et al. (2003), Mesri et al. (1994), Leo.C.J (2004), Bergado et al. (1997,2002) have extended Barron's work numerically using Finite element method (FEM) and Finite difference method (FDM) concept for 'Free strain & Equal strain' conditions using appropriate softwares.

Some school of research workers worked numerically by assuming variable permeability of smear zone J.C.Chai et al. (1994,1997,2000,2001), probabilistic design approach by W.Zhov & H.P.Hong et al. (1999), plane strain modeling with smear effects

by B.Indraratna et al. (1997, 2000, 2005, 2008, 2010, 2011, 2012), soil compressibility and smear effects by Basu & Madhav et al. (1993, 2000, 2011), closed form solution for ramp loading by Chin Jian Leo (2004) adopting Finite Element approach for the extension of Hansbo's theoretical aspect for 'no smearing and well resistance' condition for band shaped drains.

### **Historical Experimental Developments**

Another school of research workers Barden et al.(1960), Aboshi-Monden(1961), Rowe-Shields (1965), Ramanjaneya(1969), Rowe et al.(1970), Escario Uriel (1971), Singh and Hattab (1980), I.Juran (1987), Holtz & Christopher (1987), J.Blewett et al. (2002), S.Hansbo (2004), Indraratna et al. (1998,2005), Shroff-Shah(2006) have developed experimental set-up for the measurement of consolidation of soft clay considering with and without horizontal top drainage layer, with and without pore pressure measurement either by using peripheral and central vertical drain in oedometer along with sophisticated instrumentation.Shroff A.V and Shah M.V (2006, 2007) modified hydraulically pressurized oedometer for the study of sequence of consolidation of soft clay through isochrones.

S.Hansbo (1983), R.Kremer (1983), Jamiolkowski et al. (1984), Bergado et al. (1991), Koerner et al. (1994), G.V.Rao (1994,1995,1997,2004), Chai.J.C. (1999), Sharma et al. (2000), Hird et al. (2000,2002), J.Chu et al. (2003), J.N.Mandal et al. (2003), Indraratna et al. (1998, 2005, 2010), Lee et al. (2007) have worked on different shapes of drains, type of drains, method of installation, spacing of drains using synthetic and non-synthetic natural fibers.

All the above research workers have concentrated on extension of Barron's theory considering its limitations to amalgamate smear effect, well resistance, variable permeability and non-linear behavior of void-ratio by adopting Finite element method, Finite difference method and probabilistic design approaches and have not arrived to one common consensus. Further they could not obtain theoretical formulation of radial pore pressure distribution during process of consolidation from first principle

## *APPENDIX-A*

considering non-homogeneity, time effects intrinsic to the soil skeleton and compressibility of the pore fluid and solids along with variation of compressibility and permeability.

Though some of the research workers have attempted in adopting experimental set-up for the measurement of consolidation but only few could measure pore pressure during the process.

They failed to accommodate these measurements at the various sequence of process of consolidation and its effect on effective stress with a use of Isochrones. No researcher could compare theoretical isochrones with experimental one.

Above researchers took pain in attempting in using various synthetics, non-synthetics and natural materials for vertical drain but missed the above measurements and analysis.

### **Aim and Objective:**

The aim of the present work is to study One-dimensional consolidation due to only radial flow of saturated soft clay with radial pore water pressure dissipation under constant magnitude of constant pressure using central vertical drain of different material, geometry (shapes) and 'n' value('n' is the ratio of drain radius to radius of zone of influence).

### **Theoretical Development of Present Work:**

The theoretical equations governing the one-dimensional consolidation of fully saturated clay with radial dissipation of pore pressure are derived on the basis of assumptions more general than those adopted:

## APPENDIX-A

$$\frac{\partial e}{\partial T_r} \equiv \left( \frac{r_e}{h} \right) \frac{\partial^2 e}{\partial R \partial Z} \mp \lambda \frac{\partial e}{\partial R} \quad \text{----- Shroff A.V & Shah M.V (2009)}$$

This is further simplified in the form as shown below.

$$\frac{\partial e}{\partial T_r} \equiv \left( \frac{r_e}{h} \right) \frac{\partial^2 e}{\partial R^2} \mp \lambda \frac{\partial e}{\partial R}$$

Taking,  $Z = \frac{z}{h}$ ,  $R = \frac{r}{r_e}$ ,  $T_r = \frac{C_r t}{r_e^2}$ ,  $\lambda = r_e \frac{C_e}{C_r}$

Where,

$e$  = void ratio

$T_r$  = Time factor

$r_e$  = radius of influence

$h$  = height of sample

$C_r$  = Coefficient of consolidation due to radial drainage

$z$  = vertical distance of the element from the bottom plane

$r$  = radial distance from drain to the points of measurement of pore pressure

$\lambda$  = lumped parameter

$$C_e = k_h k_o (1 + e_o) \left\{ \left( \frac{\rho_s}{\rho_f} + e \right) \frac{\partial \xi}{\partial \xi'} - \eta \right\} \quad (\text{Here, } k_h, k_o, e_o, \sigma', \rho^s, \rho^f \text{ have their}$$

*usual means*)

$$C_r = \left[ \frac{(1 + e_o)^2}{(1 + e)} * \frac{k_h k_o}{\rho_f} * \frac{d\sigma'}{de} \right] \frac{\partial \xi}{\partial \xi'}$$

This theoretical treatment incorporates non-homogeneity, time effects intrinsic to the soil skeleton along with physico-chemical changes, compressibility of pore fluid and solid, variation of compressibility and permeability during consolidation. The lump parameter ( $\lambda$ ) incorporates above all factors.

## APPENDIX-A

Further, although Darcy's law is assumed to be valid, recasted in a form in which it is the relative velocity of the soil skeleton and pore fluid flow reference to central drain characteristics that is related to the excess pore fluid pressure gradient.

Solution for the above theoretical equation is obtained using boundary condition of the problem for pore water pressure at any instant and initial pore water pressure by adopting Laplace Transform Technique. Curve expert software is used to compute theoretical relationships. From the data of consolidation ratio ( $U_r$ ) versus  $r/r_e$ , isochrone is drawn for particular value of  $T_r$  and further average degree of consolidation ( $U_{avg}$ ) for a given  $T_r$  is computed by ratio of area outside particular isochrone over total area. From the data of  $U_{avg}$  versus  $T_r$ , degree of consolidation versus  $T_r$  for a particular ( $\lambda$ ) parameter is presented. Similarly for various positive and negative values of ( $\lambda$ ) the trajectory of the curves can be obtained.

Solution of  $U_{R\ avg}$  of above

$$= \exp\left\{\left(\lambda/2\right)\right\} * \left[ \frac{\sinh\lambda/2 R}{\sinh\lambda/2} + 2\pi \sum_{n=1}^{\infty} \frac{(-1)^n . n \sin(n\pi R)}{\lambda^2/4 + n^2 \pi^2} \exp\left\{-\left(\lambda^2/4 + n^2 \pi^2\right)T\right\} \right] +$$

$$\exp\left\{-\left(\lambda/2\right)\right\} * \left[ \frac{\sinh\lambda/2 (1-R)}{\sinh\left(\lambda/2\right)} - 2\pi \sum_{n=1}^{\infty} \frac{n \sin(n\pi R)}{\lambda^2/4 + n^2 \pi^2} \exp\left\{-\left(\lambda^2/4 + n^2 \pi^2\right)T\right\} \right]$$

where, 'n' is integer

**Lumped Parameter ( $\lambda$ ):**

Change of tortuosity because of particle orientation under load variation reflecting soil structural changes (from edge to face and edge to edge or face to face) orientation is also accounted in lumped parameter ( $\lambda$ ).

Further ( $\lambda$ ) incorporates the changes in the ratio of coefficient of horizontal permeability( $k_h$ )/coefficient of vertical permeability( $k_v$ ) under load variation.

Also appropriate ( $\lambda$ ) parameter is assessed for variation in degree of saturation for a given drainage path (drain diameter), for various ratio of  $S_r/w$  for given pressures, where  $S_r$  is a degree of saturation and  $w$  is per cent water content at the end of constant loading.

The experimental investigations till today (literature) have revealed that type of the drain material in the prefabricated vertical geodrain has direct influence on the velocity with which it leaves the void space.

In the theoretical derivation for the present investigation also it reflects that the rate of outflow of fluid, that is rate of change of fluid in the element is dependant on excess fluid pressure gradient which will be function of the type of drain material used in fabricating vertical geodrain being ' $k$ ' will be function of both porosity and void ratio ' $e$ ' which ultimately reflects in coefficient of consolidation ( $C_r$ ) in the derivation.

Further lumped parameter ( $\lambda$ ) is the ratio of  $(C_e/ C_r) r_e$ , where ' $C_r$ ' is coefficient of consolidation due to radial drainage and ' $C_e$ ' is coefficient due to permeability and porosity which is to some extent due to small magnitude of radial strain which helps in redistributing loads to the surface at interface of drain giving same settlement supporting 'equal strain' condition. In turn ' $C_r$ ' will vary with the drain material reflecting in the values of ( $\lambda$ ). Maximum and minimum drainage path related to various shapes of the central drain orientation is coordinated to

## APPENDIX-A

related to rate of dissipation of the pore fluid, thereby degree of consolidation of clay with time. Longer the drainage path, lower the rate of consolidation and ( $\lambda$ ) will vary as per the above explanation

### **Experimental Developments of Present Work**

Experimental object of the present investigation is to modify existing hydraulically pressurized oedometer for the measurement of pore water pressure at various radial points to obtain experimental isochrones. It enables to measure sequence of consolidation at various  $r/r_e$  ratio for corresponding concentric planar location for given  $z/h$  at that time with reference to various factors influencing consolidation due to radial dissipation of pore water pressure. The system consisting of pore pressure and displacement transducers along with data acquisition system and printer interfaced with computer is used for settlement and pore water pressure measurements. Also simultaneously measurements of pore pressures are planned to carry out by conventional Bishop's pore pressure set-up and extensometer. The factors affecting measurements such as de-airing of the system, pressure loss through polypropylene pipe (system flexibility), preparation of deaired soft soil sample, smearless vertical drain installation, smooth polished frictionless base plate and middle ring of the oedometer, deairing of the porous stone, frictionless settlement rod are aimed to increase perfection and accuracy of the system.

A development of special radial and vertical permeability measurement set-up is planned to access the efficacy of the drain with equivalent pore space and clogging potential of the drain. The stiffness/flexibility of the drain is scheduled to be measure against the load variation in control triaxial compression set-up.

### **Experimental Programme**

The scheme to verify the proposed theory and the lumped parameter ( $\lambda$ ) is to conduct a series of consolidation tests with radial drainage through vertical geodrain at central location of a cylindrical saturated soil sample along with pore pressure measurements at three radial distances and displacement measurements so as to prove its efficacy

## APPENDIX-A

against various physical factors namely type of drain material, various shapes of the drain with different geometry of the drain. 'n' value (i.e. different diameters of drain related to influence zone). Various derived parameters are evaluated for the above and analysis was carried to access the structural variation with load, tortuosity changes with change of horizontal permeability and consolidation pressure ratio (CPR).

Prior to planning the actual experimental schedule preliminary experiments were carried out in order to design same initial thickness of sample, same physical properties of the drain, shapes of the drain and installation technique.

A series of consolidation tests considering all the above factors viz. drain material and shape of drain and various 'n' value, were conducted in 254mm & 152mm diameter oedometer having a pore pressure & displacement measurement system.

It is planned to use sand, polypropylene fabric, coir-jute fibers, and polypropylene fibers to fabricate vertical geodrains of different diameters in relation to diameter of oedometer to achieve various 'n' values. Fibers of jute and coir are treated chemically before fabricating geodrain to avoid algae formation during long term test.

To assess the influence of various shapes of the drain with different geometry of the drain on consolidation, plus shaped drain, tripod shaped drain, rectangular stripped drain (band) are adopted. The optimacy of 'n' value dictate the economy and the efficiency of the functioning of the drain. The experiments are designed and conducted for 'n' value equal to 11.04, 16.93 & 21.71 using various drains of above materials.

For the study of structural variation in soil, (i) the water content ratio (WCR) is evaluated considering the ratio of existing weight of water at particular load to weight of water at initial load (10KPa) for same weight of soil solid. (ii) consolidation pressure ratio (CPR) assessed considering load under testing to the load with which sample is preconsolidated initially before the commencement of test. For the analysis CPR as 2, 4, & 16 are accounted. (iii) permeability ratios with variation in horizontal permeability deduced from the above results are utilized to access the effect of tortuosity in the soil structure. Permeability ratio as 4.5, 9, 18 & 36 are accounted.

About 50 consolidation tests with radial drainage along with pore pressure and settlement measurements are planned and performed to examine the several factors



## APPENDIX-A

mentioned earlier. The schedule for the same is illustrated in the table mentioned earlier.

### Summary of Findings:

The experimental data from a variety of test performed during these investigations are examined critically and discussed from fundamental considerations.

From basic measurements of settlement for various interval of time the basic plot of dial gauge reading (dgr) vs.  $\log t$  for particular intensity of load are obtained for various factors influencing the consolidation due to only radial drainage. Similarly measurement of pore pressure at various radial points under particular intensity of pressure at different interval of time the basic plots of consolidation ratio versus log time and for different  $r/r_e$  are obtained.

From basic settlement plots the coefficient of consolidation due to radial drainage ( $C_r$ ) is deduced for various average degree of consolidation ( $U_{avg}$ ) under various different pressures for appropriate lumped parameter ' $\lambda$ ' fitting to the theoretical and experimental curve. Consequently pore pressure basic plots are utilized to access average degree of consolidation from experimental isochrones for various experimental time factors. Simultaneously coefficient of consolidation is computed from consolidation ratio vs.  $\log t$  for various pore pressure measurement points.

Void ratio computed at the end of every increment of pressure is plotted against effective log pressure from which compression index is calculated. Pattern of  $C_c$  values versus pressure is ascertained by  $C_c$  vs. pressure plot for various influencing factors.

While deciding various influencing factors some of the specific parameters are derived such as volumetric water ratio, drainage path ratio, permeability ratio, consolidation pressure ratio. The influence of these parameters on consolidation due to radial flow is analyzed critically. Also the experimental isochrone for above each parameter is compared with theoretical one along with comparison of theoretical ( $\lambda$ ) value with

## APPENDIX-A

average degree of consolidation vs. time factor. Further in analysis, the terms average degree of consolidation ( $U_{avg}$ ) and  $U_r$  has the same means unless specified.

### General Inferences:

- 1) There is a distinct behavior of soft soil during consolidation by vertical flow and only by radial flow.
- 2) Time – settlement curve (degree of consolidation) due to radial flow always lie below the vertical flow. This is because of shorter drainage path and horizontal permeability in radial flow compared to vertical flow.
- 3) Higher initial hydrodynamic lag is observed in dissipation of mid plane pore water pressure in vertical flow compared to radial flow. The tortousity of soil structure for a vertical flow causes delay in the dissipation in early stage of consolidation.
- 4) Under lighter load time taken for the consolidation due to radial flow is 16 times lesser than the vertical flow, while for 50% consolidation time taken for radial flow is 3 times; for 90% consolidation time taken is about 6 times lesser than the vertical one which also reflects in coefficient of consolidation due to radial drainage ( $C_r$ ) versus pressure relationship that is magnitude of  $C_r$  decreases at faster rate compare to vertical one.
- 5) The void ratio for a particular load decreases at faster rate in radial case compare to vertical one. Initial structural dynamic viscosity of the soil configuration resist the light consolidation load exhibiting initial hump more in vertical case.
- 6) The studies on consolidation of clayey soil due to vertical flow revealed that degree of saturation, drainage path; stress history, mineral type and soil structure play their important role on settlement characteristics of kaolinitic clays Shroff et al., (1972). The conclusions of present work are drawn considering the above factors and the influence of diameter ( $n'$ values), distinctive material and geometry of vertical drain with soil structure effects on consolidation characteristics of kaolinitic clay due to only radial drainage using hydraulically pressurized oedometer.

**Influence of Drain Diameter ('n' value)**

**I) Rate of Consolidation (Influence of 'n' value keeping same material of drain and same pressure)**

- It concludes that for 50% consolidation,  $n=11.04$  takes 48% and 71% less time compared to  $n=16.93$  and  $21.71$  for any drain material under light loading (upto 40kPa) and 53%, 63%, under constructional loading (160kPa and greater). Similarly for 80% consolidation,  $n=11.04$  takes 35% and 61% less time compared to  $n=16.93$  and  $21.71$  for any drain material under light loading and 37%, 54% under constructional loading.
- From pore pressure measurements, it infers that for 50% consolidation and mid plane radial point  $r_2$ ,  $n=11.04$  takes 59% and 76% less time compared to  $n=16.93$  and  $21.71$  for any drain material under light loading and 65%, 77%, under constructional loading. Similarly for 80% consolidation,  $n=11.04$  takes 42% and 61% less time compared to  $n=16.93$  and  $21.71$  for any drain material under light loading and 51%, 67% under constructional loading.
- In case of coir-jute drain(CJ) at 50% consolidation,  $n=11.04$  takes lowest time of 330min & 185min amongst other drains under light and construction loadings respectively. Also for 80% consolidation CJ and  $n=11.04$  remain effective exhibiting lowest time of 750min & 550min time under light and constructional loading respectively as discussed earlier.
- During settlement measurements it concludes that  $n=11.04$  for 50% consolidation shows 76% and 69% higher  $C_r$  value compare to  $n=16.93$  and  $21.71$  for any drain material under light loading and 81% and 75% under constructional loading. Similarly for 80% consolidation shows 67% and 60% higher  $C_r$  value compare to  $n=16.93$  and  $21.71$  for any drain material under light loading and 69% and 63% under constructional loading.
- During pore pressure measurements for middle radial point  $r_2$  it concludes that  $n=11.04$  for 50% consolidation shows 405% and 583% higher  $C_r$  value compare to  $n=16.93$  and  $21.71$  for any drain material under light loading and 483% and 580% under constructional loading. Similarly for 80% consolidation shows 227% and

## APPENDIX-A

239% higher  $C_r$  value compare to  $n=16.93$  and  $21.71$  for any drain material under light loading and 290% and 298% under constructional loading.

- $n=16.93$  is found to be more efficient then  $n=21.71$  under both light and constructional loadings.
- $n=16.93$  shows averagely 92% higher  $C_r$  value under light loading while 60% higher under constructional loading compare to  $n=21.71$  but 61% lower compare to  $n=11.04$  under light loading and 56% lower under constructional loading.

### *Coefficient of consolidation due to radial drainage ( $C_r$ ) vs. applied pressure*

- The general pattern of  $C_r$  vs. pressure for any 'n' value indicates that it increases with pressure, but at 50% consolidation variation in  $C_r$  value is higher compare to 80% consolidation. In pore pressure measurement under lighter loading there is variation in  $C_r$  value, but constancy is maintained after 50KPa for any 'n' value.
- For  $n=11.04$  the maximum value of  $C_r$  is  $8.09 \times 10^{-4} \text{ cm}^2/\text{sec}$  &  $7.02 \times 10^{-4} \text{ cm}^2/\text{sec}$  at 50% and 80% consolidation for CJ from settlement consideration.
- For  $n=16.93$  average  $C_r$  value ranges from  $1.46 \times 10^{-4} \text{ cm}^2/\text{sec}$  &  $3.49 \times 10^{-5} \text{ cm}^2/\text{sec}$  for 80% consolidation for constructional loading from settlement and pore pressure measurements respectively.

---

CJ = coir-jute drain, SW = sandwick drain, PF = polypropylene fiber drain  
SD = sand drain

### *Coefficient of consolidation due to radial drainage ( $C_r$ )-Degree of consolidation ( $U_r$ ) relationship*

- For  $n=21.71$  average  $C_r$  value ranges from  $1.78 \times 10^{-4} \text{ cm}^2/\text{sec}$  &  $4.7 \times 10^{-5} \text{ cm}^2/\text{sec}$  for 80% consolidation for constructional loading from settlement and pore pressure measurements respectively.

- Average  $C_r$  value for  $n=16.93$  remain in between  $n=11.04$  and  $n=21.71$ . The lowest average value of  $n=21.71$  signifies inefficiency of the drains of any material compare to drains of other 'n' value.

## II) Magnitude of Consolidation

### *Compression index ( $C_c$ ) vs. applied pressure*

- With the same drain  $C_c$  value shows increasing trend with higher 'n' value. It signifies that because of low rate of dissipation in higher 'n' values the magnitude of compressibility increases at particular period of interval. This behavior is similar for all drains.  $C_c$  value for coir-jute drain(CJ), Sandwich drain(SW), Polypropylene fiber drain(PF), Sand drain(SD) for  $n=11.04$  are 0.272, 0.279, 0.292, and 0.312 respectively.

### *Coefficient of horizontal permeability ( $k_h$ ) vs. applied pressure*

- The horizontal permeability ( $k_{h50}$ ) obtained by settlement decreases with increase in the pressure for almost all drains and for all 'n' values.
- From settlement analysis it concludes that  $n=11.04$  for 50% consolidation shows 278% and 289% higher  $k_h$  value compare to  $n=16.93$  and 21.71 for any drain material under light loading and 735% and 3025% under constructional loading. Similarly for 80% consolidation shows 190% and 200% higher  $k_h$  value compare to  $n=16.93$  and 21.71 for any drain material under light loading and 442% and 1862% under constructional loading.
- From pore analysis for middle radial point  $r_2$  it concludes that  $n=11.04$  for 50% consolidation shows 305% and 373% higher  $k_h$  value compare to  $n=16.93$  and 21.71 for any drain material under light loading and 732% and 2747% under constructional loading. Similarly for 80% consolidation shows 165% and 134% higher  $k_h$  value compare to  $n=16.93$  and 21.71 for any drain material under light loading and 454% and 1460% under constructional loading.
- $n=16.93$  shows more coefficient of transmissivity of pore water then  $n=21.71$  under both light and constructional loadings.

## APPENDIX-A

- From settlement analysis  $n=16.93$  shows averagely 47% and 512% higher  $k_h$  value under light loading and constructional loading compare to  $n=21.71$  but 37% and 77% lower compare to  $n=11.04$  under light loading and constructional loading for 50% consolidation under any drain material.
- From pore pressure analysis  $n=16.93$  shows averagely 63% and 411% higher  $k_h$  value under light loading and constructional loading compare to  $n=21.71$  but 45% and 73% lower compare to  $n=11.04$  under light loading and constructional loading for 50% consolidation under any drain material.
- From pore pressure analysis for 50% consolidation it concludes that  $K_h$  value of mid plane pore pressure for CJ works out to be 76% and 146% higher under light loading and constructional loading compare to PF for any 'n' value while for 80% consolidation CJ shows 33% and 77% higher value under light loading and constructional loading respectively.

### *Lumped parameter ( $\lambda$ ) vs. Degree of consolidation ( $U_r$ )*

- As 'n' value increases, drain diameter ('n' value) decreases. Experimental results almost match with theoretical results with  $\lambda=-0.2$  particularly for CJ for  $n=11.04$ ,  $\lambda = -0.19$  for  $n=16.93$  and  $\lambda = -0.18$  for  $n=21.71$  proves to be efficient amongst other drains. From theoretical considerations  $n=11.04$  proves to be efficient amongst other 'n' values.

### *Isochrones*

- From the consolidation ratio vs. radius of influence for various  $T_r$  values reveals that sequence of consolidation for CJ of  $n=11.04$  at any radius of influence seems to be efficient compare to all other drains. Comparing isochrones of all three 'n' values it is concluded that  $n=11.04$  is more effective compare to  $n=16.93$  and  $n=21.71$ , while  $n=16.93$  is more superior compare to  $n=21.71$  for all drain materials.
- Trajectory of isochrones for  $n=11.04$  lies above the  $n=16.93$  and  $n=21.71$  for both light and constructional loading. Also trajectory of isochrones for  $n=16.93$  lies above  $n=21.71$  for all drain materials and loadings.

### *Shear strength*

- Gain in shear strength was observed for all three 'n' values for any drain material after consolidation, but highest gain was observed in case of 'n' equal to 11.04 for any drain material. Average post shear strength increased to 150kPa from pre shear strength of 15kPa.

### **Influence of Distinctive Drain Materials:**

#### **I) Rate of Consolidation**

- From settlement and pore pressure measurement considerations it infers that for 50% consolidation, CJ under light loading takes 46% less time in compare to SW, 49% in compare to PF, 56% in compare to SD, while for 80% consolidation, CJ takes 31% less time in compare to SW, 35% in compare to PPD and 44% in compare to SD and under constructional loading CJ takes 45% less time in compare to SW, 58% less time in compare to PF, 58% in compare to SD, while for 80% consolidation CJ takes 29% less time in compare to SW, 41% in compare to PF and 47% in compare to SD for same 'n' value and permeability ratio.
- Rate of drainage of a radial points nearer to drainage being faster the time taken for particular % of consolidation is less in compare to radial points farther away, it also reflects this observation in settlement measurements to some extent showing more compressibility gradient towards central drain. It seems from the micrograph of several drains the pore space in terms of nanomeasurement is larger compare to other drains. This reflects the efficiency of CJ with respect to micro structure opening even under light and heavy constructional loading.

#### *Coefficient of consolidation due to radial drainage ( $C_r$ ) vs. Time*

- Looking to above inferences it is clear that CJ shows more rate of consolidation both at low and high pressures in compare to other drain materials from settlement and pore pressure measurement considerations because of higher horizontal permeability of drain of CJ.
- Effectiveness of PF seems too remote from reality compare to functioning of other drains. While effectiveness of SW is less than CJ but higher than SD.

## APPENDIX-A

### *Coefficient of consolidation due to radial drainage ( $C_r$ ) vs. applied pressure*

- Under any strain condition because of the flexibility CJ drain shows higher horizontal permeability compare to others.
- From the plots it is very clear that for all drain materials the initial nature of  $T_{r80}$  graph &  $T_{r50}$  graph decreases with initial applied pressure and at higher pressures it remains same that is nearly constant. It is because of the initial structural resistance existing in the clay water structure of the Kaolinite clay.
- Lesser variation in  $C_r$  value is observed for radial point's  $r_2$  and  $r_3$  for all drain materials and for all applied pressures. Though CJ shows more inter-rate of dissipation of excess hydrostatic pore water pressure even at successive pressures in compare to other drain materials.

## **II) Magnitude of consolidation**

### *Compression index ( $C_c$ ) vs. applied pressure*

- Amongst various drain material fibers of CJ orient in such a way that the rate of dissipation remain faster in spite of pressure increase though pressure effects their orientation but compare to other drains it maintains its efficaciousness. These reflect in the value of  $C_c$  of SW and CJ which results into effective compressibility of soil.

### *Coefficient of horizontal permeability ( $k_h$ ) vs. applied pressure*

- From the above discussion it indicates that  $K_h$  value of drain increases the efficacy of rate of drainage through soil thereby it reflects coefficient of transmissivity of water through soil. For any pressure the  $k_h$  value of CJ remains efficient compare to others.

### *Lumped parameter ( $\lambda$ ) vs. Degree of consolidation ( $U_r$ )*

- As ' $\lambda$ ' value decreases efficiency of drain material decreases. Experimental results almost match with theoretical results with  $\lambda=-0.2$  particularly for CJ proves to be efficient amongst other drains.



### *Isochrones*

- From the consolidation ratio vs. radius of influence for various  $T_r$  values reveals that sequence of consolidation for CJ at any radius of influence seems to be efficient compare to all other drains.

### *Shear strength*

- Considerable gain in shear strength of soft soil mass was observed at the end of consolidation for any drain material of same 'n' value. Maximum shear strength was in the range of 100 - 140 kPa compared to 6-18 kPa of initial shear strength. CJ has exhibited highest strength of 150kPa compared to other drains.

## **Influence of Geometry (shape) of Drain**

### **I) Rate of Consolidation**

- Considering settlement measurement it concludes that for 50% consolidation, CSSD of  $n=11.04$  takes 41% less time compared to any drain material under light loading and 48%, under constructional loading. Similarly for 80% consolidation, CSSD takes 39% less time compared to any drain material under light loading and 36% under constructional loading.

-----  
CSSD = Circular shape sand drain, BSSD = Band shape sand drain

PSSD = Plus shape sand drain, TSSD = Tripod or 'Y' shape sand drain

- From pore pressure measurements, it infers that for 50% consolidation and mid plane radial point  $r_2$ , CSSD of  $n=11.04$  takes 13% less time compared to other drain shapes under light loading and 20% under constructional loading. Similarly for 80% consolidation, CSSD takes 15% less time compared to other drain shapes under light loading and 18% under constructional loading.
- CSSD of  $n=11.04$  takes lowest time in compare to BSSD, PSSD, TSSD both under light and constructional loading. However BSSD for 50% consolidation takes 12% & 23% lower time in compare to PSSD & TSSD but 50% higher in compare to CSSD under light loading. Also PSSD takes 13% lower time

## APPENDIX-A

compare to TSSD but 70% higher in compare to CSSD. Similarly BSSD for 80% consolidation takes 12% & 12% lower time in compare to PSSD & TSSD but 53% higher in compare to CSSD under light loading. Also PSSD takes equal time compare to TSSD but 73% higher in compare to CSSD.

- Though from the point of rate of dissipation of pore pressure for a circular shape drain seems to be efficient, the band shape drain provide best construction facility during installation in terms of cost and speed of work.
- Based on the equivalent diameter concept the dimensions of various shapes of drain are worked out. Though surface area of plus shape and tripod shape drain work out to be higher then band shape and circular shape drain, the draining efficiency of circular and band shape is higher then other two shapes of drain. It may be due to right and acute angles of the drain which intercept the path of flow of water to some extent.
- Under compressional stresses the drain-clay interface are not remaining compatible with the deform shape of the drain, therefore the higher surface area of plus and tripod shape drain are not remaining advantageous for the easy flow of water from the central drain.

### *Coefficient of consolidation due to radial drainage ( $C_r$ )-Degree of consolidation ( $U_r$ ) relationship*

- From settlement analysis it concludes that CSSD of  $n=11.04$  for 50% consolidation shows 71% higher  $C_r$  value compare to other geometry of drains under light loading and 96% under constructional loading. Similarly for 80% consolidation shows 65% higher  $C_r$  value compare to other geometry of drains under light loading and 57% under constructional loading.
- From pore pressure analysis for middle radial point  $r_2$  it concludes that  $n=11.04$  for 50% consolidation shows 12% higher  $C_r$  value compare to other geometry of drains under light loading and 21% under constructional loading. Similarly for 80% consolidation shows 14% higher  $C_r$  value compare to other geometry of drains under light loading and 18% under constructional loading.

## APPENDIX-A

### *Coefficient of consolidation due to radial drainage ( $C_r$ ) vs. applied pressure*

- The general pattern of  $C_r$  vs. pressure for any shape of drain indicates that it increases with pressure, but at 50% consolidation variation in  $C_r$  value is higher compare to 80% consolidation. In pore pressure measurement under lighter loading there is variation in  $C_r$  value, but constancy is maintained after 50kPa for any shape of drain.
- Average  $C_r$  value for BSD remain in between CSD and PSD. The lowest average value of TSD signifies inefficiency of the drain geometry compare to geometry of other drains.

### *Compression index ( $C_c$ ) vs. applied pressure*

- It is observed that for CSD lower  $C_c$  value is obtained compared to other geometry of sand drains. It signifies that because of low rate of dissipation in other shapes of drains the magnitude of compressibility increases at particular period of interval. This behavior is similar for all drains.  $C_c$  value for CSD, BSD, PSD, and TSD for  $n=11.04$  are 0.161, 0.241, 0.271, and 0.282 respectively. Under no geodrain condition the value of  $C_c$  is 0.42.
- There is no much variation of Compression index with shape of drain, though the rate of drainage for a particular static loading seems to be faster in CSD compared to others.

-----  
CSSD = Circular shape sand drain, BSSD = Band shape sand drain

PSSD = Plus shape sand drain, TSSD = Tripod or 'Y' shape sand drain

### *Coefficient of horizontal permeability ( $k_h$ ) vs. applied pressure*

- From settlement analysis it concludes that  $n=11.04$  for 50% consolidation shows 274% higher  $k_h$  value compare to any shape of sand drain under light loading and 36% under constructional loading. Similarly for 80% consolidation shows 259% higher  $k_h$  value compare to any shape of sand drain under light loading and 9% under constructional loading.
- From pore pressure analysis for mid plane radial point  $r_2$  it concludes that CSD of  $n=11.04$  for 50% consolidation shows 143% higher  $k_h$  value compare

## APPENDIX-A

to any shape of sand drain under light loading and 15% lower under constructional loading. Similarly for 80% consolidation it shows 149% higher  $k_h$  value under light loading and 18% lower under constructional loading.

### *Lumped parameter ( $\lambda$ ) vs. Degree of consolidation ( $U_r$ )*

- Experimental results almost match with theoretical results with  $\lambda = -0.125$  particularly for CSSD,  $\lambda = -0.12$  for BSSD,  $\lambda = -0.11$  for PSSD and  $\lambda = -0.1$  for TSSD proves to be efficient amongst other drains. From the above analysis it can be said that Circular shape is more efficient in compare to other shapes in accelerating rate of consolidation.

### *Isochrones*

- From the consolidation ratio vs. radius of influence for various  $T_r$  values reveals that sequence of consolidation for CSSD of  $n=11.04$  at any radius of influence seems to be effective compare to other geometry of drains. Comparing isochrones of all four shapes it is concluded that CSSD is more effective compare to others, while BSSD is superior compare to PSSD & TSSD for same drain material. Trajectory of isochrones for CSSD lies above the BSSD, PSSD, TSSD for both light and constructional loading. Overall TSSD is in-effective in increasing rate of compressibility and dissipation of pore water pressure. Proposed theory fits very well with various shapes of sand drains of 'n' value 11.04 for all pressures.

### **Dynamic Analysis of Consolidated Clay Bed by Central Vertical Geodrain**

#### *Post vane shear strength of reinforced consolidated clay mass before application of seismic stresses*

- For sandwich of  $n= 16.93$  the results of vane shear strength indicates that strength increases from 14.6kpa to maximum of 113.7kpa i.e. 88% increment. It was also observed that strength is more towards the first radial point  $r_1$  while it is less at  $r_3$  i.e. 101.5kpa. But generally for analysis the mid radial point ( $r_2$ ) is consider in design. For  $n=21.71$  the strength increased from 12.1kpa to 99.1kpa i.e. 87% increment

## APPENDIX-A

without application of seismic stresses. In this case also the strength was maximum at  $r_1$  while it was minimum at  $r_3$  i.e. 97.4kpa. This results indicates that as the diameter of drain increases the soil shear strength also increases.

- In brief, before consolidation of the soil sample, the same strength (12.5kPa) for any radial distance is observed for all the 'n' value. The strength of consolidated soil mass at the end of 320kPa load intensity exhibit 9 times strength than 10kPa for  $n=16.93$ , while for  $n=21.71$  it is about 7.5 times. The strength at mid radial point is less than the strength nearer at drain and more than farthest radial point  $r_3$ .

### Post vane shear strength of reinforced consolidated clay mass after application of seismic stresses

- Under dynamic analysis, SW of  $n=16.93$ , the vane shear strength indicates that the % loss in strength is more during first or initial vibration, afterwards the loss in strength is more or less constant. The average strength for  $n=16.93$  decreased from 108.53kpa to 51.10kpa i.e. 53% decrement for vibration period of 5 seconds. While for  $n=21.71$  the average strength decreased from 99.0kpa to 46.3kpa i.e. 53% decrement, Initial earthquake shock (period of vibration equal to 5 sec) is sufficient to cause metastable condition in card house structure of soft clay for any 'n' value but smaller the 'n' value more resistance is offered against strength loss. In any  $n=16.93$  the % strength loss(46%) is less than  $n=21.71$ . Percentage loss in strength for any period of vibration is less in smaller 'n' value compare to higher 'n' value 11.04.
- For  $n=16.93$  under seismic stresses the results of vane shear strength for seismic period of 15 secs, 30 secs, 60 secs and 120 secs indicates that %loss in strength is 46% averagely remains constant though seismic periods was increased while if we consider the net effect in strength then it is only 6 to 8% which may be an indication of particle rearrangement or the card house structure of soft clay to have become horizontal whose metastability was not affected by adsorbed water at later stages to some extent. While or  $n=21.71$  the % loss in strength was averagely 68% which is much higher compare to  $n=16.93$  values. Also it was observed that there was no change in in-situ placed condition of sandwich or even no settlement of only

## APPENDIX-A

sandwich was observed nor any change in its diameter was observed indicating sandwich as a stable drain under seismic conditions which prevents the soft soil to get quick.

- Initial earthquake shock (period of vibration equal to 5 sec) is sufficient to cause metastable condition in card house structure of soft clay for any 'n' value but smaller the 'n' value more resistance is offered against strength loss. In any  $n=16.93$  the % strength loss(46%) is less than  $n=21.71$ . Percentage loss in strength for any period of vibration is less in smaller 'n' value compare to higher 'n' value 11.04.

### **Influence of Water Content Ratio (WCR)**

- As water content ratio increases the value of  $C_c$  increases for any drain material and for same 'n' value. For same water content ratio the variation in compression index ( $C_c$ ) value for different drain material indicate 0.556 for coir-jute drain (CJ), 0.546 for sandwich drain (SW), 0.538 for polypropylene fiber drain (PF) and 0.532 for sand drain (SD). From the pattern of variation it infers that for same  $C_c$  value the WCR remains in the ascending order of CJ, SD, PF and SW. For same WCR, the  $C_c$  values are descending order of CJ, SW, PF and SD.
- Coir-jute drain show lowest water content at the end of any load amongs various drains proving its ability to consolidate soil more compare to others.

### **Influence of Consolidation Pressure Ratio (CPR)**

- As CPR value increases the compression index ( $C_c$ ) value increases for any drain material. In the higher range of CPR value, the  $C_c$  value is in the order of CJ, SW, PF and SD while for lower range of same CPR value the sequence is in the order of CJ, SW, SD and PF.
- As CPR increases  $k_v$  and  $k_h$  increases for any drain material and therefore the ratio  $k_h/k_v$  increases as CPR increases for any drain material. Amongs various drains, CJ gives highest  $k_h/k_v$  of the order of 27 which indicates CJ drain s facilitates more gradient of water towards drain forming displacement

of particles in such a way that horizontal permeability of soil increases leading ratio more for end of any load.

### **Scanning Electron Microscopy**

Scanning electron microscopy (SEM) along with the quanti-image analyzer with system of MIC (micro-structure characterization) software has been employed to deduce the interpretation by this nano technology, which will give the relative compression of circular soil sample from extreme radial distance to interface of drain with soil.

#### *Influence of micro-porosity*

- From nano analysis of micrograph, it interprets that for same height level of sample the percentage micro pores are increasing from central drain radially to outer radial point. Between nearest radial point  $r_1$  and clay-drain interface the percentage decrease of micro pore is more compared to mid plane radial point  $r_2$  and outward radial point  $r_3$ . Because of faster rate of dissipation the achieved void ratio or porosity which is worked out is less in case of coir-jute drain compare to sand drain.
- Though, the micro pore distribution at interface(drain-soil) at any level (height) is less compare to  $r_1$ ,  $r_2$  and  $r_3$ , in general the distribution of the micro-porosity exhibit higher magnitude of consolidation with increase of depth at any radial point however, it has been confirmed this observation at mid plane radial point  $r_2$ . In general the degree of orientation(decrease of angle between particles) of particles in the soil structure undergoing consolidation indicate comparatively more face-to-face contact towards drain. Also this pattern is exhibited depth wise for any radial distance and drain material.

#### *Influence of angle of orientation*

- The software measurement for angle of angularity of one particle with other of various micrographs indicate that orientation of particle becomes more or less face to face to some extent as we approach towards drain from extreme radial point.

## APPENDIX-A

- In case of SD the degree of orientation during consolidation is more near the drain (radial point r1) compare to CJ, while more degree of orientation is observed in CJ at middle radial point r2 compare to SD, and almost same degree of orientation is observed in CJ & SD at farthest radial point r3.

### *Influence of Tortosity*

- Tortosity is a real measure of actual flow path towards radial direction towards central drain during consolidation process. Tortosity tends to unity in case of CJ drain compare to SD as mentioned earlier. Soil structure because of the gradient of flow in horizontal direction and vertical load help causes more quantum of face-to-face contact in the former case. For the same drain the depth wise tortosity also indicate the effect of over burden to some extent. In case of coir-jute drain the tortosity at interface and at mid radial point are almost same indicating uniform surface settlement unlike sand drain.

The theoretical relationship obtained between average degree of consolidation versus time factor for various values of  $\lambda$  both for positive and negative range fits well with the experimental results obtained from the laboratory studies. The above findings will definitely provide a ready solution to the design engineers and field persons in making the selection of effective drain material, optimum drain diameter(size) and easy workable drain geometry with respect to site conditions. The appropriate value of lumped parameter ( $\lambda$ ) will directly give the clue to design engineer regarding the selection of prefabricated vertical geodrain with respect to field conditions.

July, 2012

Manish V. Shah

**Ph.D Candidate**



## CERTIFICATE

This is to certify that Thesis entitled, **“INFLUENCE OF DIAMETER, DISTINCTIVE MATERIAL AND GEOMETRY OF VERTICAL DRAIN WITH SOIL STRUCTURE EFFECTS ON CONSOLIDATION CHARACTERISTICS OF KAOLINITIC CLAY DUE TO RADIAL DRAINAGE”** presented by **Mr. Manish Vrajlal Shah** for the award of the Degree of Doctor of Philosophy to The Maharaja Sayajirao University of Baroda, has been carried out by him in Geotechnical Engineering Laboratory of Applied Mechanics and Structural Engineering Department, Faculty of Technology and Engineering, Baroda. The matter in this Thesis has not been submitted for the award of any other degree or diploma.

Vadodara  
July, 2012

### Research Guides

**Dr. D. L. Shah**

Professor, Erstwhile Head  
Applied Mechanics Dept.

**Dr. A. V. Shroff**

(Vide.MSU letter no.  
(AC/III/136 Dt. 17/5/2005)  
Professor Emeritus  
Applied Mechanics Dept.

**Dr. I. I. Pandya**

Head  
Applied Mechanics Department

**Dr. A. N. Misra**

Professor & Dean  
Faculty of Technology and Engineering  
The Maharaja Sayajirao University of Baroda, Vadodara

## ACKNOWLEDGEMENT

The thesis is the result of continuous interaction between my guides **Prof. (Dr.) A.V. Shroff** and **Prof. (Dr.) D.L. Shah** and the author. Development of advanced theory and Procurement of newly developed drain materials used in the research is due to consistent support of my guides. Author owes a deep sense of gratitude to them for their invaluable direction, indefatigable zeal and the meticulous attention to all the facets of research work.

Author wishes to thank Prof. (Dr.) A.N. Misra, Dean, Faculty of Technology and Engineering, The M.S. University of Baroda for providing research facility and grant for the present research work.

Author wishes to thank Prof. (Dr.) I.I. Pandya, Head, Applied Mechanics Dept. and Prof. (Dr.) S.C. Patodi, Ex. head, Applied Mechanics Dept, Prof. (Dr.) K.R. Biyani, Ex. Head, Applied Mechanics Dept, Faculty of Technology and Engineering, The M.S. University of Baroda for providing all research facility during present research work.

Author wishes to thank Prof. M.N. Patel, Principal, L.D. College of Engineering and Prof. R.M. Manvar, Head, Applied Mechanics Dept., Prof. (Dr.) R.K. Gajjar, Ex. Head, Applied Mechanics Dept, L.D. College of Engineering, Ahmedabad and Ph.D & PG Dean (GTU) for providing all research facility and motivation during present research work.

Author is highly grateful to Department of Technical Education (DTE), Government of Gujarat for necessary permission and extending all research facility during present research work.

Author wishes to thank Prof. K.S. Agarwal, Ex. Principal, Polytechnic, The M.S. University of Baroda and Prof. P.J. Amin, Ex. Head, Applied Mechanics Dept., Prof. M.V. Marathe, Ex. Head, Applied Mechanics Dept., The M.S. University of Baroda for providing all research facility during present research work.

The author is indebted to Prof. (Dr.) A.P.Verma, of Mathematics Department, SVNIT, Surat for his precious guidance in theoretical work, especially in mathematical formulations and for providing valuable comments.

Author is benefited from supplement of research papers and the discussions of his research with Dr. N.H. Joshi, Associate Professor, Applied Mechanics Dept.

Author wishes to thank his respected teachers notably Prof. R.M. Bhagia, Dr. H.J. Shah, Dr. Bimal Shah, Dr. J.D. Rathod, Dr. N.K. Solanki, Shri G.S. Doiphode, Shri M.K. Maroliya, Shri V.R. Patel and Shri L.S. Thakur for their suggestions and help.

Author wishes to thank his respected teachers and colleagues notably Shri S.B. Bhagwat, Ms. D.S. Ghelani, Shri S.M. Patel, Shri M.M. Patel, Shri D.P. Shah, Shri M.J. Jethwa, Mrs. S.N. Pandya, Shri H.K. Patel, Mrs. Deepa Prabhu, Shri L.D. Dheman, Applied Mechanics Dept., Polytechnic, MSU for their suggestions and help.

Author wishes to express sincere thanks to his colleagues notably Prof. (Dr.) H.S. Patel, Prof. (Dr.) B.J. Shah, Prof. (Dr.) N.K. Arora, Prof. (Dr.) S.P. Dave, Prof. C.S. Sanghvi, Prof. B.A. Vyas, Prof. M.G. Vanza, Prof. P.G. Patel, Prof. A.J. Shah, Prof. M.D. Vakil, Prof. K.R. Parmar, Applied Mechanics Dept., L.D. College of Engineering, Ahmedabad

Author wishes to express sincere thanks to his colleagues and friends Prof. CD. Patel, Prof. C.N. Patel and Prof. Poonam Modi, Applied Mechanics Dept., L.D. College of Engineering, Ahmedabad.

Special thanks to my dear friends Vishal Arekar, Kannan Iyer, Kanan Salat and P.G. Students Tasneem Khan, Pritam Patil, Ekta Shah for their inspiration and help during the research.

Author wishes to express his appreciation to the laboratory staff namely Shri Ashok Parmar, Shri H.M. Patel, Shri Yogesh Pawar and Shri Milind Dave, Applied Mechanics Dept, MSU.

Author wishes to express his appreciation to the laboratory staff namely Shri Neelam Joshi, Sanjay Jadhav , Shri Chirag Pagedar and Shri Raju Patel, Applied Mechanics Dept, Polytechnic, MSU.

Author is thankful to Department of Metallurgy and Department of Textile Engineering, The M.S. University of Baroda for providing necessary testing facilities during the research.

Author is thankful to Department of Pharmacy and Department of Civil Engineering for providing distilled water for the testing.

Author is thankful to M/s TCR Advanced Engg Pvt. Ltd, GIDC, Vadodara for providing research help in Scanning Electron Microscopy and use of MIC software.

Author is grateful to Mr. Gajjarkaka of TAIRO, Faculty of Technology and Engineering, The M.S University of Baroda for their valuable help in preparing experimental set ups.

The accomplishment of the present research work is due to inexpressible and invaluable contribution of Madam Meenaben Shroff.

Special thanks to my dear brother and sisters for their rich motivation.

The present work is possible due to inexpressible and invaluable contribution of my wife, Krishna and son Rasesh and particularly my nephew Nishant.

The author extends his sincere gratitude to all who have directly or indirectly contributed during the research work.

**TO**

**MY PARENTS**

**AND**

**PARAMPUJYA GOSWAMI 108 SHREE INDIRABETIJI MAHODAYA**

## **CONTENTS**

| <b>Title</b>        |   | <b>Page No.</b> |
|---------------------|---|-----------------|
| SYNOPSIS            |   | I               |
| CERTIFICATE         |   | XXVII           |
| ACKNOWLEDGEMENT     |   | XXVIII          |
| LIST OF FIGURES     |   | XXXI            |
| LIST OF TABLES      |   | LVII            |
| LIST OF PHOTOGRAPHS |   | LIX             |
| LIST OF SYMBOLS     |   | LXIV            |
| LIST OF APPENDIX    |   | LXIX            |
|                     |   |                 |
| CHAPTER -1          | INTRODUCTION                              | 1               |
| CHAPTER -2          | CONSOLIDATION OF SOFT CLAY BY RADIAL FLOW | 4               |
| 2.1                 | Introduction                              | 4               |
| 2.2                 | Ground Improvement Methods                | 5               |
| 2.3                 | Type of Vertical Drains                   | 15              |
| 2.4                 | Sand Drains                               | 18              |
| 2.4.1               | Salient Features of Sand Drain            | 19              |
| 2.4.1.1             | Diameter of Drains                        | 19              |
| 2.4.1.2             | Spacing of Sand Drains                    | 19              |
| 2.4.1.3             | Depth of Sand Drains                      | 20              |
| 2.4.1.4             | Installation of Sand Drain                | 20              |
| 2.4.1.5             | Properties of Sand for Drains             | 20              |
| 2.4.2               | Blanket                                   | 21              |

|        |   |    |
|--------|---|----|
| 2.4.3  | Arrangement of Drains                                     | 21 |
| 2.4.4  | Rate of Loading   | 22 |
| 2.4.5  | Remarks on Vertical Sand Drains                           | 22 |
| 2.5    | Sandwicks   | 24 |
| 2.5.1  | Remarks on Vertical Sandwicks                             | 25 |
| 2.6    | Prefabricated Vertical Drains<br>(Band Drains)            | 25 |
| 2.6.1  | Wrapped Flexible Pipe Drains                              | 26 |
| 2.6.2  | Band Drains   | 26 |
| 2.6.3  | Polypropylene Wick Drains                                 | 28 |
| 2.6.4  | Wrapped and Unwrapped Drains                              | 29 |
| 2.6.5  | Polypropylene Fiber Drain                                 | 30 |
| 2.6.6  | Remarks on Prefabricated vertical drains<br>(Band drains) | 30 |
| 2.7    | Theoretical Review  | 31 |
| 2.7.1  | Terzaghi's Theory   | 32 |
| 2.7.2  | Rendulic's Solution                                       | 35 |
| 2.7.3  | Biot's Theory   | 36 |
| 2.7.4  | Carillo's Solution  | 36 |
| 2.7.5  | Barron's Theory   | 36 |
| 2.7.6  | Kjellman's Theory   | 43 |
| 2.7.7  | Silveira's Theory   | 44 |
| 2.7.8  | Richart's Theory  | 45 |
| 2.7.9  | Takagi's Theory   | 49 |
| 2.7.10 | Schiffman's Theory  | 49 |
| 2.7.11 | Hansbo Theory   | 51 |

|        |  |     |
|--------|--|-----|
| 2.7.12 | Escario-Uriel's Solution   | 53  |
| 2.7.13 | Horne's Solution   | 54  |
| 2.7.14 | Rowe's Theory  | 55  |
| 2.7.15 | Christie's Solution  | 57  |
| 2.7.16 | Anandkrishnan-Kappuswamy's Solution  | 58  |
| 2.7.17 | Siva Reddy – Murty's Solution  | 58  |
| 2.7.18 | Berry and Wilkinson's Theory   | 59  |
| 2.7.19 | Simons – Tan Solution  | 69  |
| 2.7.20 | Tsytovinch Martirosyan Kulkarni's Theory   | 70  |
| 2.7.21 | Creyer's Theory  | 71  |
| 2.7.22 | T.K.Tan's Theory   | 71  |
| 2.7.23 | Parikh, Verma and Shroff Theory  | 74  |
| 2.7.24 | Sill's Theory  | 74  |
| 2.7.25 | Yamaguchi Theory   | 74  |
| 2.7.26 | Yoshikuni and Nakanodo Theory  | 74  |
| 2.7.27 | Lee and Viliappan Theory   | 76  |
| 2.7.28 | Chaput and Thomann's Theory  | 76  |
| 2.7.29 | Brenner and Pbebaharan's Theory  | 77  |
| 2.7.30 | Vreeken and Duijn's Theory   | 78  |
| 2.7.31 | Table for Theoretical Developments   | 80  |
| 2.8    | Historical Experimental Developments   | 88  |
| 2.8.1  | Contribution by Some of the Research Workers in Experimental and Laboratory Investigations | 89  |
| 2.8.2  | Table for Laboratory Developments  | 113 |



|            |   |     |
|------------|---|-----|
| 2.9        | Critical Appraisal on Discrepancies and Limitations of Theoretical and Experimental Development till Date | 117 |
| CHAPTER -3 | SCOPE, PROGRAMME AND SCHEME OF INVESTIGATIONS   | 121 |
| 3.1        | Scope   | 121 |
| 3.1.1      | Theoretical Work  | 121 |
| 3.1.2      | Experimental Work   | 122 |
| 3.2        | Programme   | 125 |
| 3.2.1      | Objectives  | 125 |
| 3.2.2      | Experimental Schedule   | 125 |
| 3.3        | Scheme  | 126 |
| 3.3.1      | Parameters  | 126 |
| 3.3.2      | Plots   | 126 |
| 3.4        | Experimental Schedule   | 128 |
| 3.4.1      | Conventional Parameters   | 129 |
| 3.4.2      | Derived Parameters  | 132 |
| 3.4.3      | Scanning Electron Microscopy (SEM)  | 134 |
| 3.4.4      | Shear Strength Measurement of the Consolidated Clay Mass under Static and Dynamic Load                    | 136 |
| 3.5        | Properties of Various Materials Used In Laboratory Investigation  | 137 |
| CHAPTER -4 | THEORETICAL DEVELOPMENTS (ADVANCED THEORY OF CONSOLIDATION THROUGH RADIAL FLOW)                           | 145 |
| 4.1        | Physical Background   | 147 |
| 4.1.1      | Nature of change in Clay Colloid  | 147 |

|         |   |     |
|---------|---|-----|
| 4.1.2   | Nature of change in Fabric Structure  | 147 |
| 4.1.3   | Nature of Radial Flow of Pore Fluid   | 148 |
| 4.1.4   | Nature of Effective Stress Law  | 148 |
| 4.2     | Mathematical Formulation  | 149 |
| 4.2.1   | Governing Equations   | 149 |
| 4.2.1.1 | Co-ordinate Scheme  | 149 |
| 4.2.1.2 | Equilibrium Equation  | 150 |
| 4.2.1.3 | Equation of Continuity  | 151 |
| 4.2.1.4 | Flow Equation   | 151 |
| 4.2.1.5 | Effective Stress Law  | 153 |
| 4.2.1.6 | Permeability, Porosity and Fluid Density relationship   | 153 |
| 4.3     | Transformed Equations   | 154 |
| 4.4     | Analytical Solutions  | 164 |
| 4.4.1   | Boundary conditions   | 164 |
| 4.4.2   | Mathematical treatment  | 164 |
| 4.4.3   | Theoretical Relationships   | 169 |
| 4.4.4   | Plots showing the relationship between Average Degrees of Consolidation through radial drainage( $U_R, \%$ ) and Time factor ( $T_r$ ) for various values of lump parameter ( $\lambda$ )         | 172 |
| 4.4.5   | Table showing the relationship between Average Degrees of Consolidation through radial drainage( $U_R, \%$ ) and Time factor ( $T_r$ ) for various values of lump parameter ( $\lambda$ )         | 182 |
| 4.4.6   | Trajectory of Curves representing relation between Average Degree of Consolidation through radial flow ( $U_R, \%$ ) and Time factor ( $T_r$ ) for various values of lump parameter ( $\lambda$ ) | 186 |

|            |   |     |
|------------|---|-----|
| CHAPTER -5 | MEASUREMENT FACTORS AND EXPERIMENTAL SET-UP                           | 192 |
| 5.1        | Factors Affecting Measurement   | 192 |
| 5.1.1      | Drain Stiffness   | 193 |
| 5.1.2      | Selection of Gradation of Sand  | 196 |
| 5.1.3      | Smear and Well Resistance   | 196 |
| 5.1.5      | Side Friction   | 197 |
| 5.1.6      | System Inadequacies   | 198 |
| 5.1.7      | Shape of Porous Stone   | 199 |
| 5.1.8      | Radial co-ordinates and pore pressure                                 | 199 |
| 5.2        | Experimental Setups   | 200 |
| 5.2.1      | Review of experimental set-up   | 200 |
| 5.3        | Description of Present Setup  | 202 |
| 5.3.1      | Hydraulic Pressure System   | 202 |
| 5.3.2      | Modified Hydraulically Pressurised Oedometer                          | 205 |
| 5.3.3      | Settlement Measurement System   | 209 |
| 5.3.4      | Pore Pressure Measurement System                                      | 210 |
| 5.3.4.1    | Bishop's Pore pressure measuring system                               | 210 |
| 5.3.4.2    | Transducers and Data Acquisition System                               | 211 |
| 5.4        | Method of Soil Sample Preparation                                     | 213 |
| 5.5        | Vertical Drain Design, Selection, Fabrication, Testing & Installation | 215 |
| 5.5.1      | Vertical drains classification  | 215 |
| 5.5.2      | Drain design and guidelines   | 216 |
| 5.5.2.1    | Design of sand drain  | 216 |

|           |  |     |
|-----------|--|-----|
| 5.5.2.2   | Design of Geometrical Sand drains  | 216 |
| 5.5.2.3   | Design of Sandwicks (SW)   | 219 |
| 5.5.2.4   | Design of Coir-Jute drain (CJ)   | 221 |
| 5.5.2.5   | Design of Polypropylene fiber drain (PF)   | 227 |
| 5.6       | Testing Procedure  | 228 |
| 5.7       | Problems and their Remedial Measures   | 230 |
| 5.8       | De-Airing the Entire System  | 233 |
| 5.9       | Special Apparatus Developed To Measure Coefficient of Radial Permeability of Soil and Vertical Drain   | 233 |
| 5.10      | Scanning Electron Microscopy of Consolidated Samples   | 236 |
| Chapter-6 | RESULTS, ANALYSIS AND DISCUSSION   | 238 |
| 6.1       | Presentation of Results  | 238 |
| 6.2       | Method of Analysis/Determination of Parameters   | 239 |
| 6.2.1     | Determination of Coefficient of consolidation due to radial drainage ( $C_r$ ), Time factor for consolidation due to radial flow ( $T_r$ ), Degree of consolidation due to the radial drainage, for settlement reading, $U_r\%$ and for pore pressure readings ( $1-u_r/u_o\%$ ), Pore pressure ratio for radial flow ( $u_r/u_o\%$ ). | 239 |
| 6.3       | Analysis and Discussion: Consolidation due to radial drainage  | 266 |
| 6.3.1     | Type of Drain Material   | 267 |
| 6.3.2     | Diameter (size) of vertical drain – ‘n’ value  | 355 |
| 6.3.3     | Geometry (shape) of vertical drain   | 470 |
| 6.3.3.1   | Dynamic Analysis of Consolidated Clay Bed by Central Vertical Geodrain Sandwich of ‘n’16.93 and 21.71  | 521 |

|           |  |     |
|-----------|--|-----|
| 6.3.4     | Variation of Water content ratio (WCR)         | 525 |
| 6.3.5     | Variation of Consolidation Pressure Ratio(CPR) | 528 |
| Chapter-7 | SUMMARY OF FINDINGS                            | 530 |
|           | LIST OF RESEARCH PUBLICATIONS                  | 555 |
|           | REFERENCES                                     | 562 |
|           | APPENDIX                                       | 588 |
|           | VITAE  | 613 |

## LIST OF FIGURES

| Figure No. | Title   | Page No. |
|------------|---|----------|
| 2.1        | Classification of in-place treatment  | 16       |
| 2.2        | Cross-section of cardboard drain and insertion mandrel  | 16       |
| 2.3        | Cross-section of plastic geodrain drain and insertion mandrel   | 17       |
| 2.4        | Comparative efficiencies of geodrains and 0.18m diameter sand drains  | 17       |
| 2.5        | Cross-section of typical vertical drains (a) cardboard drain and mandrel (b) plastic drain and mandrel (c) drainage wick and casing pipe (d) rope drain and casing pipe   | 18       |
| 2.6        | Installation and Function of vertical sand drains   | 20       |
| 2.7        | Typical arrangements of sand drain  | 22       |
| 2.8(a)     | Typical PV drain products   | 27       |
| 2.8(b)     | Sketch of band drain installation rig and band drain delivery arrangement   | 28       |
| 2.9        | Typical section of zoned earth embankment, Lornex, USA  | 29       |
| 2.10       | Typical section of Geodrain   | 29       |
| 2.11       | Terzaghi's one dimensional consolidation  | 32       |
| 2.12       | Consolidation pressure distribution diagram   | 33       |
| 2.13       | Isochrones representing progress of consolidation of a layer of ideal clay for different types of drainage (after Terzaghi & Frohlich, 1936)  | 34       |
| 2.14       | Relation between Time factor and degree of consolidation in (a) Time factor plotted on arithmetic scale (b) on a logarithmic scale. The three curves $C_1$ , $C_2$ , $C_3$ correspond to three different cases of loading | 35       |
| 2.15(a)    | Plan of drain well pattern and fundamental concepts of flow within zone of influence of each well (Barron's theory)   | 37       |
| 2.15(b)    | Theoretical curve of average degree of consolidation vs Time factor for combined vertical and radial flow for range of 'n' values   | 38       |
| 2.16       | Theoretical curve of average degree of consolidation for radial flow for range of 'n' values  | 39       |
| 2.17       | Distribution of initial excess pore water pressure in soil cylinder with $n = 100$  | 40       |
| 2.18       | Average degree of consolidation for various values of 'n' under 'equal strain' condition at any given time  | 41       |

|      |   |    |
|------|---|----|
| 2.19 | Effect of smear and well resistance on 'equal strain' consolidation by radial flow to drain wells   | 42 |
| 2.20 | Schematic picture of soil cylinder dewatered by vertical drain (a) idealized case(left) (b) real case influence of smear and well resistance (right)  | 44 |
| 2.21 | Consolidation chart for cylindrical sample with external radial flow of water (after Silveria, 1953)  | 45 |
| 2.22 | Relationship between $K_h/K_v$ , $u$ and $r$ for $n=5$ and $n=15$ (after Richart, 1957)   | 46 |
| 2.23 | Relationship between $n$ and $f(n)$ or $v$ for $\frac{K_h}{K_s} = 20$ (After Richart 1954)  | 47 |
| 2.24 | Actual and equivalent well installations (after Richart, 1957)  | 47 |
| 2.25 | Distribution of initial excess pore water pressure in soil cylinder with $n = 100$  | 48 |
| 2.26 | Comparison of average consolidation rates in clay cylinders by radial drainage only for various values of 'n' (after Barron, 1948)  | 48 |
| 2.27 | Effect of size of drain well vs. time for consolidation(after Richart, 1957)  | 49 |
| 2.28 | Plot of isochrones (after Takagi, 1957)   | 50 |
| 2.29 | Exponents for equal strain sand drain problem with no smear, radial flow (after Schiffman, 1958)  | 51 |
| 2.30 | (a) Scheme of arrangement of the consolidation test in the triaxial apparatus with drainage towards the cylindrical surface (b) cylindrical element of the sample (after Escario et.al, 1961) | 53 |
| 2.31 | Approximate solution for effective coefficient of consolidation with horizontal drainage of soil consisting of horizontal permeability (after Horne, 1964)                                    | 54 |
| 2.32 | Theoretical relations between the geometry of the sample and the measured coefficient of consolidation (after Rowe, 1964)   | 55 |
| 2.33 | Influence of the ratio $b/a$ on the maximum value of $C_h$  | 56 |
| 2.34 | Plan showing location of discrete points in a cylinder of soil with a central vertical sand drain (after Christe, 1966)   | 57 |
| 2.35 | Consolidation of a cylinder of a soil with 30% secondary compression and radial drainage to a drain of diameter equal to one tenth of the diameter of cylinder (after Christe, 1966)          | 57 |
| 2.36 | Pore pressure distribution in a sand drain for case I   | 58 |
| 2.37 | Pore pressure distribution in a sand drain for case II  | 59 |

|         |   |    |
|---------|---|----|
|         | (after Sivareddy, 1969)   |    |
| 2.38    | Average degree of consolidation $\mu$ plotted against time factor $T$ for sand drain $n=20$ with smear $s_m = 1.1$ , free strain (after Berry et.al, 1969)                                    | 60 |
| 2.39    | Rate of dissipation of pore pressure plotted against time factor $T$ for sand drain $n=20$ with smear $s_m = 1.1$ , free strain (after Berry et.al, 1969)                                     | 60 |
| 2.40    | Rate of dissipation of pore pressure plotted against time factor $T$ for peripheral drain with smear for various values of $s_p$ , free strain (after Berry et.al, 1969)                      | 61 |
| 2.41    | Boundary conditions for central sand drain and peripheral drain (after Berry et.al, 1969)   | 61 |
| 2.42(a) | Average degree of consolidation $\mu$ plotted against time factor $T_1$ for a varying compressibility and permeability relationship, sand drain $n=20$ , free strain (after Berry et.al 1969) | 62 |
| 2.42(b) | Rate of dissipation of pore pressure plotted against time factor $T_1$ for a varying compressibility and permeability relationship, sand drain $n=20$ , free strain (after Berry et.al 1969)  | 63 |
| 2.43(a) | Average degree of consolidation $\mu$ plotted against time factor $T_1$ for a varying compressibility and permeability relationship, sand drain $n=10$ , free strain (after Berry et.al 1969) | 63 |
| 2.43(b) | Rate of dissipation of pore pressure plotted against time factor $T_1$ for a varying compressibility and permeability relationship, sand drain $n=10$ , free strain (after Berry et.al 1969)  | 64 |
| 2.44    | Comparison between Barron theory and the theory incorporating a varying compressibility and permeability for the case $C_c/C_k = 1.5$ , $p_i/p_o = 2$ , $n=10$                                | 64 |
| 2.45    | Average degree of consolidation $\mu$ plotted against time factor $T_1$ for varying compressibility and permeability relationship, peripheral drain, free strain                              | 65 |
| 2.46    | Rate of dissipation of pore pressure plotted against time factor $T_1$ for varying compressibility and permeability relationship, peripheral drain, free strain                               | 65 |
| 2.47    | Rheological Models (after Berry et.al, 1969)  | 67 |
| 2.48(a) | Rate of dissipation of pore pressure plotted against time factor $T$ for different values of $M$ , peripheral drain, free strain (Berry et.al, 1969)  | 67 |
| 2.48(b) | Average degree of consolidation $\mu$ plotted against time factor $T$ for different values of $M$ , peripheral drain, free  | 68 |



|         |  |    |
|---------|--|----|
|         | strain (Berry et.al, 1969)   |    |
| 2.49(a) | Rate of dissipation of pore pressure plotted against time factor T for different values of M, sand drain n=5, free strain (Berry et.al, 1969)  | 68 |
| 2.49(b) | Average degree of consolidation $\mu$ plotted against time factor T for different values of M, sand drain n=5, free strain (after Berry, et.al, 1969)  | 69 |
| 2.50    | Comparative plot of ratio $U/\sigma'_t - \sigma'$ against time factor T (after Simon-Tan, 1971)  | 69 |
| 2.51    | Plot of average degree of consolidation $\bar{U}$ against time factor T (after Simon-Tan, 1971)  | 70 |
| 2.52    | Plot of degree of consolidation against under root of time factor T for $\mu = 0.25, 0.50$ (after Creyer, 1961)  | 72 |
| 2.53    | Plot of $\Sigma (0, T)$ against $U_R (1, T)$ for $\mu = 0.25, 0.50$ (after Creyer, 1961)   | 73 |
| 2.54    | Settlement as function of $\sqrt{t}$ (curve I) and Ratio of lateral/vertical pressure $\delta e/q$ as function of $\sqrt{t}$ (curve II)  | 73 |
| 2.55    | Effect of drain resistance on consolidation rate (a) Notation (b) Values of $U_r$ (c) Values of $T_r(50)$ (d) Values of $T_r(80)$ (After Yoshikuni & Nakanodo, 1974)   | 75 |
| 2.56    | Effect of stratification on vertical drain performance (Lee & Valiappan, 1974)   | 76 |
| 2.57    | Nomograms for the function required for the design of vertical drains under progressive loading conditions (Chaput & Thomann, 1975)  | 77 |
| 2.58    | General view of 152mm dia. and 254mm dia. consolidation cell   | 90 |
| 2.59    | Laboratory models of sand drain formers (a) closed mandrel (circular shaped); (b) closed mandrel (hollow tube); (c) closed mandrel (cruciform shaped); (d) closed mandrel (star shaped); (e) open mandrel (auger shaped); (f) double wall jetting (g) jetted drains (Dutch method) | 91 |
| 2.60    | Laboratory model of sand drain formers   | 91 |
| 2.61    | Laboratory model of sand drain formers   | 92 |
| 2.62    | Inward radial flow consolidation tests: percentage consolidation against square root of time for various methods of consolidation  | 93 |
| 2.63    | Inward radial flow consolidation tests: rate of dissipation of pore pressure against time for various methods of consolidation   | 94 |
| 2.64    | Inward radial flow consolidation test: scale effects for   | 95 |

|      |   |     |
|------|---|-----|
|      | various methods of boring   |     |
| 2.65 | Inward radial flow consolidation tests: coefficient of consolidation versus loading for various methods of installation. A= auger, JM = jetted mandrel, CM= closed mandrel, OM = open mandrel | 96  |
| 2.66 | Inward radial flow consolidation tests: coefficient of consolidation versus loading for various methods of installation. A= auger, JM = jetted mandrel, CM= closed mandrel, OM = open mandrel | 96  |
| 2.67 | Inward radial flow condition tests: coefficient of consolidation against loading pressure for various methods of installation   | 97  |
| 2.68 | Inward radial flow consolidation tests: coefficient of permeability against pressure for various methods of installation  | 97  |
| 2.69 | Inward radial flow consolidation tests: coefficient of consolidation against loading pressure for various methods of installation   | 98  |
| 2.70 | Inward radial flow consolidation tests: coefficient of permeability against loading pressure for various methods of installation  | 98  |
| 2.71 | Influence of geometry of sample on equivalent Oedometer results (after Rowe, 1959)  | 99  |
| 2.72 | Summary of consolidation test results (after Rowe, 1959)  | 100 |
| 2.73 | Three dimensional consolidation curves and its analysis (after Aboshi, 1961)  | 101 |
| 2.74 | Values of the coefficient of consolidation of the blue clays from Huelva obtained by radial permeability test (after Escario et al, 1961)   | 102 |
| 2.75 | Theoretical consolidation curves for the axial and radial cases (after Mc Kinlay, 1965)   | 102 |
| 2.76 | Effect of drain diameter on measured coefficient of consolidation   | 103 |
| 2.77 | Comparison with previous experimental observations (after Rowe)   | 103 |
| 2.78 | Compression-Time curves obtained from R2 type tests   | 105 |
| 2.79 | Pore pressure dissipation curves from R2 type tests   | 105 |
| 2.80 | Compression-Time curves obtained from R4-2 type tests   | 106 |
| 2.81 | Pore pressure dissipation curves at various distances from centre of drain as measured from R4-2 type tests   | 106 |
| 2.82 | Comparison of measured and predicted pore pressures for various degrees of consolidation  | 107 |
| 2.83 | Variation of $C_{vr}$ with drain diameter ( $U_r = 90\%$ )  | 107 |

|      |  |     |
|------|--|-----|
| 2.84 | Model container  | 109 |
| 2.85 | Time-Settlement curves with vertical sand drain (radial and combined flow) and marine clay (vertical flow) using centrifuge modeling for loading (a) 0.1-0.2kPa (b) 0.2-0.5kPa (c) 0.5-1.0kPa (d) 1.0-2.0kPa           | 110 |
| 2.86 | Time-Degree of settlement curves with vertical sand drain (radial and combined flow) and marine clay (vertical flow) using centrifuge modeling for loading (a) 0.1-0.2kPa (b) 0.2-0.5kPa (c) 0.5-1.0kPa (d) 1.0-2.0kPa | 110 |
| 2.87 | Time-Degree of settlement curves of marine clay under vertical flow condition (theoretical and experimental) using centrifuge modeling for loading (a) 0.1-0.2kPa (b) 0.2-0.5kPa (c) 0.5-1.0kPa (d) 1.0-2.0kPa         | 111 |
| 2.88 | Time-Degree of settlement curves of marine clay under radial flow condition (theoretical and experimental) using centrifuge modeling for loading (a) 0.1-0.2kPa (b) 0.2-0.5kPa (c) 0.5-1.0kPa (d) 1.0-2.0kPa           | 112 |
| 2.89 | Time-Degree of settlement curves of marine clay under combined flow condition (theoretical and experimental) using centrifuge modeling for loading (a) 0.1-0.2kPa (b) 0.2-0.5kPa (c) 0.5-1.0kPa (d) 1.0-2.0kPa         | 112 |
| 4.1  | Configuration of clay element  | 150 |
| 4.2  | Simpsons rule to estimate degree of consolidation  | 169 |
| 4.3  | Consolidation ratio ( $U_r$ ) vs. Ratio of radial distance (R) for $\lambda = 0.7$   | 171 |
| 4.4  | Consolidation ratio ( $U_r$ ) against ratio of radial distance (R) for various time factor ( $T_r$ ) for $\lambda = 0.7$   | 172 |
| 4.5  | Consolidation ratio ( $U_r$ ) against ratio of radial distance (R) for various time factor ( $T_r$ ) for $\lambda = 0.6$   | 173 |
| 4.6  | Consolidation ratio ( $U_r$ ) against ratio of radial distance (R) for various time factor ( $T_r$ ) for $\lambda = 0.5$   | 173 |
| 4.7  | Consolidation ratio ( $U_r$ ) against ratio of radial distance (R) for various time factor ( $T_r$ ) for $\lambda = 0.4$   | 174 |
| 4.8  | Consolidation ratio ( $U_r$ ) against ratio of radial distance (R) for various time factor ( $T_r$ ) for $\lambda = 0.3$   | 174 |
| 4.9  | Consolidation ratio ( $U_r$ ) against ratio of radial distance (R) for various time factor ( $T_r$ ) for $\lambda = 0.2$   | 175 |
| 4.10 | Consolidation ratio ( $U_r$ ) against ratio of radial distance (R) for various time factor ( $T_r$ ) for $\lambda = 0.1$   | 175 |
| 4.11 | Consolidation ratio ( $U_r$ ) against ratio of radial distance (R) for various time factor ( $T_r$ ) for $\lambda = 0.05$  | 176 |
| 4.12 | Consolidation ratio ( $U_r$ ) against ratio of radial distance (R) for various time factor ( $T_r$ ) for $\lambda = 0.01$  | 176 |

|        |   |     |
|--------|---|-----|
| 4.13   | Consolidation ratio ( $U_r$ ) against ratio of radial distance (R) for various time factor ( $T_r$ ) for $\lambda = 0$                                | 177 |
| 4.14   | Consolidation ratio ( $U_r$ ) against ratio of radial distance (R) for various time factor ( $T_r$ ) for $\lambda = -0.01$                            | 177 |
| 4.15   | Consolidation ratio ( $U_r$ ) against ratio of radial distance (R) for various time factor ( $T_r$ ) for $\lambda = -0.05$                            | 178 |
| 4.16   | Consolidation ratio ( $U_r$ ) against ratio of radial distance (R) for various time factor ( $T_r$ ) for $\lambda = -0.01$                            | 178 |
| 4.17   | Consolidation ratio ( $U_r$ ) against ratio of radial distance (R) for various time factor ( $T_r$ ) for $\lambda = -0.2$                             | 179 |
| 4.18   | Consolidation ratio ( $U_r$ ) against ratio of radial distance (R) for various time factor ( $T_r$ ) for $\lambda = -0.3$                             | 179 |
| 4.19   | Consolidation ratio ( $U_r$ ) against ratio of radial distance (R) for various time factor ( $T_r$ ) for $\lambda = -0.4$                             | 180 |
| 4.20   | Consolidation ratio ( $U_r$ ) against ratio of radial distance (R) for various time factor ( $T_r$ ) for $\lambda = -0.5$                             | 180 |
| 4.21   | Consolidation ratio ( $U_r$ ) against ratio of radial distance (R) for various time factor ( $T_r$ ) for $\lambda = -0.6$                             | 181 |
| 4.22   | Consolidation ratio ( $U_r$ ) against ratio of radial distance (R) for various time factor ( $T_r$ ) for $\lambda = -0.7$                             | 181 |
| 4.23   | Average degree of consolidation( $U_r$ ) vs. Time factor ( $T_r$ ) for various values of ' $\lambda$ '  | 187 |
| 4.24   | Average degree of consolidation( $U_r$ ) vs. Time factor ( $T_r$ ) for various values of ' $\lambda$ ' on natural scale                               | 188 |
| 5.1(a) | Stiffness of sand drain installation  | 193 |
| 5.1(b) | Effect of sand drain on relative stiffness of a clay foundation   | 193 |
| 5.2    | Stress-Strain nature of various vertical geodrains  | 195 |
| 5.3    | Standard gradation curve of sand  | 195 |
| 5.4    | Types of mandrel for forming drainage well: (a) solid (b) hollow tube (c) cruciform (d) star (e) auger (f) double-wall jetting (g) dutch type jetting | 197 |
| 5.5    | Basic layout of pressure system   | 204 |
| 5.6    | General arrangement of ancillary equipment used with the Rowe cell  | 204 |
| 5.7    | Bottom plate with measurement points and loaction   | 207 |
| 5.8    | Sectional view of Oedometer with measurement points   | 207 |
| 5.9    | Typical stress – strain curve of coir fiber (Kulkarni, Satyanarayana et.al, 1981)   | 224 |
| 5.10   | Influence of diameter on mechanical properties on coir fibers (Tomczak, Satyanarayana et.al, 2007)  | 225 |
| 5.11   | Scanning electron micrographs of coir fiber at different  | 226 |

|      |   |     |
|------|---|-----|
|      | strain rates (a) and micrograph showing the end of fiber with pull out of microfibrils (b&c)                                      |     |
| 5.12 | Rowe cell connected to pore pressure panel for flushing and initial checks  | 233 |
| 6.1  | Stages of consolidation and analysis of log-time/settlement curve   | 241 |
| 6.2  | Plot of dial gauge reading vs. log't' and stages of consolidation   | 243 |
| 6.3  | Comparison of theoretical and experimental Degree of consolidation and fitting of experimental curve for $\lambda = -0.2$         | 248 |
| 6.4  | Dissipation of pore water pressure (degree of consolidation) vs. log't' for CJ drain of 'n'11.04 at three radial points at 160kPa | 251 |
| 6.5  | Experimental isochrones with respect to time for CJ of 'n'11.04   | 257 |
| 6.6  | Comparison of theoretical and experimental isochrones   | 260 |
| 6.7  | Comparison of degree of consolidation vs. experimental and theoretical time factor (Tr) for CJ of 'n'11.04                        | 265 |
| 6.8  | Comparison of degree of consolidation vs. experimental and theoretical time factor (Tr) for SD of 'n'11.04                        | 265 |
| 6.9  | Comparison of degree of consolidation vs. experimental and theoretical time factor (Tr) for SW of 'n'11.04                        | 265 |
| 6.10 | Degree of consolidation (Ur) vs. log't' in min for SD   | 268 |
| 6.11 | Degree of consolidation (Ur) vs. log't' in min for SW   | 268 |
| 6.12 | Degree of consolidation (Ur) vs. log't' in min for CJ   | 269 |
| 6.13 | Degree of consolidation (Ur) vs. log't' in min for PF   | 270 |
| 6.14 | Comparison of Degree of consolidation of various drain materials w.r.t 40kPa and 160kPa applied pressure                          | 271 |
| 6.15 | Degree of consolidation based on dissipation of excess hydrostatic pore water pressure vs. log't' in min                          | 273 |
| 6.16 | Degree of consolidation based on dissipation of excess hydrostatic pore water pressure vs. log't' in min                          | 273 |
| 6.17 | Degree of consolidation based on dissipation of excess hydrostatic pore water pressure vs. log't' in min                          | 274 |
| 6.18 | Degree of consolidation based on dissipation of excess hydrostatic pore water pressure vs. log't' in min                          | 274 |
| 6.19 | Comparison of drain material w.r.t radial point 'r1' at 40kPa pressure  | 276 |
| 6.20 | Comparison of drain material w.r.t radial point 'r2' at 40kPa pressure  | 276 |
| 6.21 | Comparison of drain material w.r.t radial point 'r3' at 40kPa pressure  | 277 |
| 6.22 | Comparison of drain material w.r.t radial point 'r1' at   | 277 |

|      |  |     |
|------|--|-----|
|      | 160kPa pressure  |     |
| 6.23 | Comparison of drain material w.r.t radial point 'r2' at 160kPa pressure  | 277 |
| 6.24 | Comparison of drain material w.r.t radial point 'r3' at 160kPa pressure  | 278 |
| 6.25 | Comparison of Degree of consolidation against drain material based on settlement and pore pressure measurements at 40kPa pressure  | 281 |
| 6.26 | Comparison of drain material based on settlement and pore pressure measurements at 160kPa pressure   | 281 |
| 6.27 | Coefficient of consolidation through radial drainage (Cr) vs. Degree of consolidation (Ur) for SD  | 286 |
| 6.28 | Coefficient of consolidation through radial drainage (Cr) vs. Degree of consolidation (Ur) for SW  | 286 |
| 6.29 | Coefficient of consolidation through radial drainage (Cr) vs. Degree of consolidation (Ur) for CJ  | 287 |
| 6.30 | Coefficient of consolidation through radial drainage (Cr) vs. Degree of consolidation (Ur) for PF  | 287 |
| 6.31 | Comparison of drain material for coefficient of consolidation through radial flow for various degree of consolidation at low and high pressure using settlement analysis | 288 |
| 6.32 | Coefficient of consolidation through radial drainage (Cr) vs. Degree of consolidation (Ur) at radial points r1, r2 and r3 for SD at all pressures                        | 290 |
| 6.33 | Cr vs. Ur for SD at radial points r1, r2, r3 at 40kPa pressure   | 291 |
| 6.34 | Cr vs. Ur for SD at radial points r1, r2, r3 at 160kPa pressure  | 291 |
| 6.35 | Coefficient of consolidation through radial drainage (Cr) vs. Degree of consolidation (Ur) at radial points r1, r2 and r3 for SW at all pressures                        | 291 |
| 6.36 | Cr vs. Ur for SW at radial points r1, r2, r3 at 40kPa pressure   | 292 |
| 6.37 | Cr vs. Ur for SW at radial points r1, r2, r3 at 160kPa pressure  | 292 |
| 6.38 | Coefficient of consolidation through radial drainage (Cr) vs. Degree of consolidation (Ur) at radial points r1, r2 and r3 for CJ at all pressures                        | 292 |
| 6.39 | Cr vs. Ur for CJ at radial points r1, r2, r3 at 40kPa pressure   | 293 |
| 6.40 | Cr vs. Ur for CJ at radial points r1, r2, r3 at 160kPa   | 293 |

|      |  |     |
|------|--|-----|
|      | pressure   |     |
| 6.41 | Coefficient of consolidation through radial drainage (Cr) vs. Degree of consolidation (Ur) at radial point's r1, r2 and r3 for PF at all pressures                   | 293 |
| 6.42 | Cr vs. Ur for PF at radial points r1, r2, r3 at 40kPa pressure   | 294 |
| 6.43 | Cr vs. Ur for PF at radial points r1, r2, r3 at 160kPa pressure  | 294 |
| 6.44 | Comparison of Coefficient of consolidation through radial flow against drain material basedon settlement and pore pressure measurements at 40kPa and 160kPa pressure | 294 |
| 6.45 | Coefficient of consolidation through radial drainage(Cr) vs. Applied pressure for SD at 50% and 80% degree of consolidation (Ur)                                     | 296 |
| 6.46 | Coefficient of consolidation through radial drainage(Cr) vs. Applied pressure for SW at 50% and 80% degree of consolidation (Ur)                                     | 297 |
| 6.47 | Coefficient of consolidation through radial drainage(Cr) vs. Applied pressure for CJ at 50% and 80% degree of consolidation (Ur)                                     | 297 |
| 6.48 | Coefficient of consolidation through radial drainage(Cr) vs. Applied pressure for PF at 50% and 80% degree of consolidation (Ur)                                     | 298 |
| 6.49 | Comparison of Drain material w.r.t coefficient of consolidation through radial drainage(Cr) against applied pressure at 50% degree of consolidation (Ur)             | 298 |
| 6.50 | Comparison of Drain material w.r.t coefficient of consolidation through radial drainage(Cr) against applied pressure at 80% degree of consolidation (Ur)             | 299 |
| 6.51 | Coefficient of consolidation through radial drainage(Cr) vs. Applied pressure for SD at 50% and 80% degree of consolidation (Ur) at radial points r1, r2, r3         | 302 |
| 6.52 | Coefficient of consolidation through radial drainage(Cr) vs. Applied pressure for SW at 50% and 80% degree of consolidation (Ur) at radial points r1, r2, r3         | 303 |
| 6.53 | Coefficient of consolidation through radial drainage(Cr) vs. Applied pressure for CJ at 50% and 80% degree of consolidation (Ur) at radial points r1, r2, r3         | 303 |
| 6.54 | Coefficient of consolidation through radial drainage(Cr) vs. Applied pressure for PF at 50% and 80% degree of  | 304 |

|      |   |     |
|------|---|-----|
|      | consolidation ( $U_r$ ) at radial points $r_1, r_2, r_3$  |     |
| 6.55 | Comparison of Drain material w.r.t coefficient of consolidation through radial drainage( $C_r$ ) against applied pressure at 50% $U_r$ at radial points $r_1, r_2, r_3$ | 304 |
| 6.56 | Comparison of Drain material w.r.t coefficient of consolidation through radial drainage( $C_r$ ) against applied pressure at 80% $U_r$ at radial points $r_1, r_2, r_3$ | 305 |
| 6.57 | Comparison of Drain material w.r.t $C_r$ against applied pressure for 50% & 80% $U_r$ based on settlement and pore pressure analysis                                    | 305 |
| 6.58 | Void ratio vs. Applied pressure for SD  | 307 |
| 6.59 | Void ratio vs. Applied pressure for SW  | 308 |
| 6.60 | Void ratio vs. Applied pressure for CJ  | 308 |
| 6.61 | Void ratio vs. Applied pressure for PF  | 308 |
| 6.62 | Comparison of Drain materials w.r.t void ratio( $e$ ) against applied pressure for $n=11.04$ (same ' $n$ ' value)   | 309 |
| 6.63 | Comparison of compression index ( $C_c$ ) with drain material for $n=11.04$   | 309 |
| 6.64 | Comparison of % microporosity of CJ and SD (' $n=11.04$ ') at various locations (Influence of drain material)   | 316 |
| 6.65 | Comparison of angle of orientation ( $\beta$ ) against ratio of radial distance ( $r/r_e$ ) of CJ and SD of ' $n=11.04$ ' (Influence of drain material)                 | 316 |
| 6.66 | Comparison of horizontal tortuosity ( $T_h$ ) and vertical tortuosity ( $T_v$ ) against depth of sample for CJ and SD of ' $n=11.04$ ' (Influence of drain material)    | 316 |
| 6.67 | Coefficient of consolidation through radial drainage( $C_r$ ) vs. Applied pressure for SD at 50% and 80% degree of consolidation ( $U_r$ )                              | 318 |
| 6.68 | Coefficient of consolidation through radial drainage( $C_r$ ) vs. Applied pressure for SD at 50% and 80% degree of consolidation ( $U_r$ )                              | 318 |
| 6.69 | Coefficient of consolidation through radial drainage( $C_r$ ) vs. Applied pressure for CJ at 50% and 80% degree of consolidation ( $U_r$ )                              | 319 |
| 6.70 | Coefficient of consolidation through radial drainage( $C_r$ ) vs. Applied pressure for PF at 50% and 80% degree of consolidation ( $U_r$ )                              | 319 |
| 6.71 | Comparison of Drain material w.r.t coefficient of horizontal permeability ( $k_h$ ) against applied pressure at 50% degree of consolidation ( $U_r$ )                   | 320 |
| 6.72 | Comparison of Drain material w.r.t coefficient of   | 320 |



|      |   |     |
|------|---|-----|
|      | horizontal permeability (kh) against applied pressure at 80% degree of consolidation ( $U_r$ )  |     |
| 6.73 | Coefficient of consolidation through radial drainage( $C_r$ ) vs. Applied pressure for SD at 50% and 80% degree of consolidation ( $U_r$ ) at radial points $r_1$ , $r_2$ , $r_3$ | 323 |
| 6.74 | Coefficient of consolidation through radial drainage( $C_r$ ) vs. Applied pressure for SW at 50% and 80% degree of consolidation ( $U_r$ ) at radial points $r_1$ , $r_2$ , $r_3$ | 323 |
| 6.75 | Coefficient of consolidation through radial drainage( $C_r$ ) vs. Applied pressure for CJ at 50% and 80% degree of consolidation ( $U_r$ ) at radial points $r_1$ , $r_2$ , $r_3$ | 324 |
| 6.76 | Coefficient of consolidation through radial drainage( $C_r$ ) vs. Applied pressure for PF at 50% and 80% degree of consolidation ( $U_r$ ) at radial points $r_1$ , $r_2$ , $r_3$ | 324 |
| 6.77 | Comparison of Drain material w.r.t coefficient of horizontal permeability (kh) against applied pressure at 50% $U_r$ at radial points $r_1$ , $r_2$ , $r_3$                       | 325 |
| 6.78 | Comparison of Drain material w.r.t coefficient of horizontal permeability (kh) against applied pressure at 80% $U_r$ at radial points $r_1$ , $r_2$ , $r_3$                       | 325 |
| 6.79 | Comparison of Drain material w.r.t kh against applied pressure for 50% & 80% $U_r$ based on settlement and pore pressure analysis   | 326 |
| 6.80 | Dissipation of hydrostatic excess pore water pressure ( $U_r/U_o$ ) vs. ratio of radial distance ( $r/r_e$ ) with respect to time for SD at 40kPa                                 | 328 |
| 6.81 | Dissipation of hydrostatic excess pore water pressure ( $U_r/U_o$ ) vs. ratio of radial distance ( $r/r_e$ ) with respect to time for SD at 160kPa                                | 328 |
| 6.82 | Dissipation of hydrostatic excess pore water pressure ( $U_r/U_o$ ) vs. ratio of radial distance ( $r/r_e$ ) with respect to time for SW at 40kPa                                 | 329 |
| 6.83 | Dissipation of hydrostatic excess pore water pressure ( $U_r/U_o$ ) vs. ratio of radial distance ( $r/r_e$ ) with respect to time for SW at 160kPa                                | 329 |
| 6.84 | Dissipation of hydrostatic excess pore water pressure ( $U_r/U_o$ ) vs. ratio of radial distance ( $r/r_e$ ) with respect to time for CJ at 40kPa                                 | 330 |
| 6.85 | Dissipation of hydrostatic excess pore water pressure ( $U_r/U_o$ ) vs. ratio of radial distance ( $r/r_e$ ) with respect to time for CJ at 160kPa                                | 330 |
| 6.86 | Dissipation of hydrostatic excess pore water pressure ( $U_r/U_o$ ) vs. ratio of radial distance ( $r/r_e$ ) with respect to  | 331 |

|       |  |     |
|-------|--|-----|
|       | time for PF at 40kPa   |     |
| 6.87  | Dissipation of hydrostatic excess pore water pressure ( $U_r/U_o$ ) vs. ratio of radial distance ( $r/r_e$ ) with respect to time for PF at 160kPa | 331 |
| 6.88  | Comparison of theoretical isochrones and experimental isochrones with respect to time factor ( $T_r$ ) for SD at 160kPa pressure                   | 332 |
| 6.89  | Comparison of theoretical isochrones and experimental isochrones with respect to time factor ( $T_r$ ) for SW at 160kPa pressure                   | 333 |
| 6.90  | Comparison of theoretical isochrones and experimental isochrones with respect to time factor ( $T_r$ ) for CJ at 160kPa pressure                   | 334 |
| 6.91  | Comparison of theoretical isochrones and experimental isochrones with respect to time factor ( $T_r$ ) for PF at 160kPa pressure                   | 335 |
| 6.92  | Comparison of Drain materials with respect to isochrones for time factors ( $T_r$ ) at 160kPa pressure   | 336 |
| 6.93  | Comparison of Drain materials with respect to isochrones for selected time factors ( $T_r$ ) at 160kPa pressure                                    | 337 |
| 6.94  | Comparison of Drain materials with respect to experimental isochrones for $T_r = 0.04$ time at 160kPa pressure                                     | 337 |
| 6.95  | Comparison of average degree of consolidation ( $U_r$ ) against theoretical and experimental Time factor ( $T_r$ ) for SD at 40kPa                 | 339 |
| 6.96  | Comparison of average degree of consolidation ( $U_r$ ) against theoretical and experimental Time factor ( $T_r$ ) for SD at 160kPa                | 339 |
| 6.97  | Comparison of average degree of consolidation ( $U_r$ ) against theoretical and experimental Time factor ( $T_r$ ) for SW at 40kPa                 | 340 |
| 6.98  | Comparison of average degree of consolidation ( $U_r$ ) against theoretical and experimental Time factor ( $T_r$ ) for SW at 160kPa                | 340 |
| 6.99  | Comparison of average degree of consolidation ( $U_r$ ) against theoretical and experimental Time factor ( $T_r$ ) for CJ at 40kPa                 | 341 |
| 6.100 | Comparison of average degree of consolidation ( $U_r$ ) against theoretical and experimental Time factor ( $T_r$ ) for CJ at 160kPa                | 341 |
| 6.101 | Comparison of average degree of consolidation ( $U_r$ )  | 342 |

|       |   |     |
|-------|---|-----|
|       | against theoretical and experimental Time factor (Tr) for PF at 40kPa   |     |
| 6.102 | Comparison of average degree of consolidation (Ur) against theoretical and experimental Time factor (Tr) for PF at 160kPa   | 342 |
| 6.103 | Comparison of average degree of consolidation (Ur) against experimental Time factor (Tr) for various Drain materials with lump parameter ' $\lambda$ '                  | 343 |
| 6.104 | Comparison of average degree of consolidation (Ur) against theoretical and experimental Time factors (Tr) for various Drain materials with lump parameter ' $\lambda$ ' | 343 |
| 6.105 | Comparison of average degree of consolidation (Ur) against theoretical and experimental Time factor (Tr) for SD at 40kPa  | 346 |
| 6.106 | Comparison of average degree of consolidation (Ur) against theoretical and experimental Time factor (Tr) for SD at 160kPa   | 347 |
| 6.107 | Comparison of average degree of consolidation (Ur) against theoretical and experimental Time factor (Tr) for SW at 40kPa  | 347 |
| 6.108 | Comparison of average degree of consolidation (Ur) against theoretical and experimental Time factor (Tr) for SW at 160kPa   | 348 |
| 6.109 | Comparison of average degree of consolidation (Ur) against theoretical and experimental Time factor (Tr) for CJ at 40kPa  | 348 |
| 6.110 | Comparison of average degree of consolidation (Ur) against theoretical and experimental Time factor (Tr) for CJ at 160kPa   | 349 |
| 6.111 | Comparison of average degree of consolidation (Ur) against theoretical and experimental Time factor (Tr) for PFat 40kPa   | 349 |
| 6.112 | Comparison of average degree of consolidation (Ur) against theoretical and experimental Time factor (Tr) for PF at 160kPa   | 350 |
| 6.113 | Comparison of average degree of consolidation (Ur) against experimental Time factor (Tr) for various Drain materials with lump parameter ' $\lambda$ '                  | 350 |
| 6.114 | Comparison of average degree of consolidation (Ur) against theoretical and experimental Time factors (Tr) for various Drain materials with lump parameter ' $\lambda$ ' | 351 |
| 6.115 | Comparison Ur vs. Tr for various Drain materials with lump parameter ' $\lambda$ ' on the basis of settlement and pore  | 351 |

|       |   |     |
|-------|---|-----|
|       | pressure analysis   |     |
| 6.116 | Comparison of vane shear strength of clay samples consolidated by various Drain materials   | 352 |
| 6.117 | Degree of consolidation ( $U_r$ ) vs. $\log t$ in min for SD  | 358 |
| 6.118 | Degree of consolidation ( $U_r$ ) vs. $\log t$ in min for SW  | 358 |
| 6.119 | Degree of consolidation ( $U_r$ ) vs. $\log t$ in min for CJ  | 359 |
| 6.120 | Degree of consolidation ( $U_r$ ) vs. $\log t$ in min for PF  | 359 |
| 6.121 | Comparison of degree of consolidation ( $U_r$ ) vs. $\log t$ in min for 'n' value with respect to drain material at 40kPa pressure  | 360 |
| 6.122 | Comparison of degree of consolidation ( $U_r$ ) vs. $\log t$ in min for 'n' 11.04 with respect to drain material at 160kPa pressure | 360 |
| 6.123 | Comparison of degree of consolidation ( $U_r$ ) vs. $\log t$ in min for 'n' 16.93 with respect to drain material at 40kPa pressure  | 361 |
| 6.124 | Comparison of degree of consolidation ( $U_r$ ) vs. $\log t$ in min for 'n' 16.93 with respect to drain material at 160kPa pressure | 361 |
| 6.125 | Comparison of degree of consolidation ( $U_r$ ) vs. $\log t$ in min for 'n' 21.71 with respect to drain material at 40kPa pressure  | 362 |
| 6.126 | Comparison of degree of consolidation ( $U_r$ ) vs. $\log t$ in min for 'n' 21.71 with respect to drain material at 160kPa pressure | 362 |
| 6.127 | Comparison of dissipation of pore water pressure against $\log t$ w.r.t 'n' value for SD at all pressures                           | 369 |
| 6.128 | Comparison of dissipation of pore water pressure against $\log t$ w.r.t 'n' value for SW at all pressures                           | 370 |
| 6.129 | Comparison of dissipation of pore water pressure against $\log t$ w.r.t 'n' value for CJ at all pressures                           | 371 |
| 6.130 | Comparison of dissipation of pore water pressure against $\log t$ w.r.t 'n' value for PF at all pressures                           | 372 |
| 6.131 | Comparison of dissipation of pore water pressure for 'n' values at nearest radial point 'r1' for various vertical drains            | 373 |
| 6.132 | Comparison of dissipation of pore water pressure for 'n' values at mid radial point 'r2' for various vertical drains                | 373 |
| 6.133 | Comparison of dissipation of pore water pressure for 'n' values at farthest radial point 'r3' for various vertical drains           | 374 |
| 6.134 | Comparison of dissipation of pore water pressure for 'n' values at nearest radial point 'r1' for various vertical                   | 374 |

|       |   |     |
|-------|---|-----|
|       | drains  |     |
| 6.135 | Comparison of dissipation of pore water pressure for 'n' values at mid radial point 'r2' for various vertical drains      | 375 |
| 6.136 | Comparison of dissipation of pore water pressure for 'n' values at mid radial point 'r3' for various vertical drains      | 375 |
| 6.137 | Comparison of degree of consolidation vs. time based on settlement analysis and pore pressure analysis at 160kPa pressure | 376 |
| 6.138 | Comparison of % porosity on 'n' value using MIC software  | 383 |
| 6.139 | Comparison of angle of orientation ( $\beta$ ) on 'n' value using MIC software  | 383 |
| 6.140 | Comparison of horizontal and vertical tortousity on 'n' value using MIC software  | 383 |
| 6.141 | Comparison of Cr against Ur for SD of 'n'11.04 at all applied pressures   | 385 |
| 6.142 | Comparison of Cr against Ur for SD of 'n'16.93 at all applied pressures   | 386 |
| 6.143 | Comparison of Cr against Ur for SD of 'n'21.71 at all applied pressures   | 386 |
| 6.144 | Influence of 'n' value on Cr vs. Ur for SD at 40kPa and 160kPa  | 387 |
| 6.145 | Comparison of Cr against Ur for CJ of 'n'11.04 at all applied pressures   | 387 |
| 6.146 | Comparison of Cr against Ur for CJ of 'n'16.93 at all applied pressures   | 388 |
| 6.147 | Comparison of Cr against Ur for CJ of 'n'21.71 at all applied pressures   | 388 |
| 6.148 | Influence of 'n' value on Cr vs. Ur for CJ at 40kPa and 160kPa  | 389 |
| 6.149 | Comparison of Cr against Ur for PF of 'n'11.04 at all applied pressures   | 389 |
| 6.150 | Comparison of Cr against Ur for PF of 'n'16.93 at all applied pressures   | 390 |
| 6.151 | Comparison of Cr against Ur for PF of 'n'21.71 at all applied pressures   | 390 |
| 6.152 | Influence of 'n' value on Cr vs. Ur for PF at 40kPa and 160kPa  | 391 |
| 6.153 | Comparison of Cr vs.'n' value at Ur50% and Ur80% at 40kPa   | 391 |
| 6.154 | Comparison of Cr vs.'n' value at Ur50% and Ur80% at 160kPa  | 392 |
| 6.155 | Coefficient of consolidation through radial drainage  | 397 |

|       |  |     |
|-------|--|-----|
|       | against Degree of consolidation for SD of 'n'11.04 at radial points for all pressures  |     |
| 6.156 | Coefficient of consolidation through radial drainage against Degree of consolidation for SD of 'n'16.93 at radial points for all pressures | 397 |
| 6.157 | Coefficient of consolidation through radial drainage against Degree of consolidation for SD of 'n'21.71 at radial points for all pressures | 398 |
| 6.158 | Comparison of Cr vs. Ur for various 'n' values of SD at radial points  | 398 |
| 6.159 | Comparison of Cr vs. Ur for various 'n' values of SD at radial points  | 399 |
| 6.160 | Coefficient of consolidation through radial drainage against Degree of consolidation for SW of 'n'11.04 at radial points for all pressures | 399 |
| 6.161 | Coefficient of consolidation through radial drainage against Degree of consolidation for SW of 'n'16.93 at radial points for all pressures | 400 |
| 6.162 | Coefficient of consolidation through radial drainage against Degree of consolidation for SW of 'n'21.71 at radial points for all pressures | 400 |
| 6.163 | Comparison of Cr vs. Ur for various 'n' values of SW at radial points  | 401 |
| 6.164 | Comparison of Cr vs. Ur for various 'n' values of SW at radial points  | 401 |
| 6.165 | Coefficient of consolidation through radial drainage against Degree of consolidation for CJ of 'n'11.04 at radial points for all pressures | 402 |
| 6.166 | Coefficient of consolidation through radial drainage against Degree of consolidation for CJ of 'n'16.93 at radial points for all pressures | 402 |
| 6.167 | Coefficient of consolidation through radial drainage against Degree of consolidation for CJ of 'n'21.71 at radial points for all pressures | 403 |
| 6.168 | Comparison of Cr vs. Ur for various 'n' values of CJ at radial points  | 403 |
| 6.169 | Comparison of Cr vs. Ur for various 'n' values of CJ at radial points  | 404 |
| 6.170 | Coefficient of consolidation through radial drainage against Degree of consolidation for PF of 'n'11.04 at radial points for all pressures | 404 |
| 6.171 | Coefficient of consolidation through radial drainage against Degree of consolidation for PF of 'n'16.93 at                                 | 405 |

|       |  |     |
|-------|--|-----|
|       | radial points for all pressures  |     |
| 6.172 | Coefficient of consolidation through radial drainage against Degree of consolidation for PF of 'n'21.71 at radial points for all pressures | 405 |
| 6.173 | Comparison of Cr vs. Ur for various 'n' values of PF at radial points  | 406 |
| 6.174 | Comparison of Cr vs. Ur for various 'n' values of PF at radial points  | 406 |
| 6.175 | Comparison of Cr value against 'n'values for various vertical drains at 40kPa applied pressure   | 407 |
| 6.176 | Comparison of Cr value against 'n'values for various vertical drains at 160kPa applied pressure  | 407 |
| 6.177 | Comparison of Cr against applied pressure for SD at 50% and 80% degree of consolidation  | 409 |
| 6.178 | Comparison of Cr against applied pressure for SW of various 'n' values at 50% and 80% degree of consolidation                              | 410 |
| 6.179 | Comparison of Cr against applied pressure for CJ of various 'n' values at 50% and 80% degree of consolidation                              | 410 |
| 6.180 | Comparison of Cr against applied pressure for PF of various 'n' values at 50% and 80% degree of consolidation                              | 411 |
| 6.181 | Comparison of Cr value on drain material for same 'n' 11.04 at Ur =50%   | 411 |
| 6.182 | Comparison of Cr value on drain material for same 'n' 11.04 at Ur =80%   | 412 |
| 6.183 | Comparison of Cr value on drain material for same 'n' 16.93 at Ur =50%   | 412 |
| 6.184 | Comparison of Cr value on drain material for same 'n' 16.93 at Ur =80%   | 413 |
| 6.185 | Comparison of Cr value on drain material for same 'n' 21.71at Ur =50%  | 413 |
| 6.186 | Comparison of Cr value on drain material for same 'n' 21.71 at Ur =50%   | 414 |
| 6.187 | Comparison of Cr against applied pressure for SD of various 'n' values at 50% and 80% degree of consolidation                              | 417 |
| 6.188 | Comparison of Cr against applied pressure for SW of various 'n' values at 50% and 80% degree of consolidation                              | 418 |

|       |  |     |
|-------|--|-----|
| 6.189 | Comparison of Cr against applied pressure for CJ of various 'n' values at 50% and 80% degree of consolidation                                | 418 |
| 6.190 | Comparison of Cr against applied pressure for PF of various 'n' values at 50% and 80% degree of consolidation                                | 419 |
| 6.191 | Comparison of Cr value on drain material for same 'n' 11.04 at Ur =50%   | 419 |
| 6.192 | Comparison of Cr value on drain material for same 'n' 11.04 at Ur = 80%  | 420 |
| 6.193 | Comparison of Cr value on drain material for same 'n' 16.93 at Ur =50%   | 420 |
| 6.194 | Comparison of Cr value on drain material for same 'n' 16.93 at Ur =80%   | 421 |
| 6.195 | Comparison of Cr value on drain material for same 'n' 21.71 at Ur =50%   | 421 |
| 6.196 | Comparison of Cr value on drain material for same 'n' 21.71 at Ur =80%   | 422 |
| 6.197 | Comparison of void ratio vs. applied pressure for SD   | 423 |
| 6.198 | Comparison of void ratio vs. applied pressure for SW   | 424 |
| 6.199 | Comparison of void ratio vs. applied pressure for CJ   | 424 |
| 6.200 | Comparison of void ratio vs. applied pressure for PF   | 424 |
| 6.201 | Comparison of compression index (Cc) against 'n' value for various vertical drains   | 425 |
| 6.202 | Comparison of coefficient of horizontal permeability (kh) against applied pressure for SD of various 'n' values                              | 427 |
| 6.203 | Comparison of coefficient of horizontal permeability (kh) against applied pressure for SW of various 'n' values                              | 427 |
| 6.204 | Comparison of coefficient of horizontal permeability (kh) against applied pressure for CJ of various 'n' values                              | 428 |
| 6.205 | Comparison of coefficient of horizontal permeability (kh) against applied pressure for PF of various 'n' values                              | 428 |
| 6.206 | Influence of 'n' value of various vertical drains on coefficient of horizontal permeability (kh) for Ur-50% & 80% at 40kPa pressure          | 429 |
| 6.207 | Influence of 'n' value of various vertical drains on coefficient of horizontal permeability (kh) for Ur-50% & 80% at 160kPa pressure         | 429 |
| 6.208 | Comparison of coefficient of horizontal permeability (kh) against applied pressure for SD of various 'n' values at radial point's r1, r2, r3 | 433 |
| 6.209 | Comparison of coefficient of horizontal permeability (kh)  | 434 |



|       |   |     |
|-------|---|-----|
|       | against applied pressure for SW of various 'n' values at radial point's r1, r2, r3  |     |
| 6.210 | Comparison of coefficient of horizontal permeability (kh) against applied pressure for CJ of various 'n' values at radial point's r1, r2, r3                  | 434 |
| 6.211 | Comparison of coefficient of horizontal permeability (kh) against applied pressure for PF of various 'n' values at radial point's r1, r2, r3                  | 435 |
| 6.212 | Influence of 'n' value of various vertical drains on coefficient of horizontal permeability (kh) for Ur-50% at 40kPa pressure at three radial points          | 435 |
| 6.213 | Influence of 'n' value of various vertical drains on coefficient of horizontal permeability (kh) for Ur-80% at 40kPa pressure at three radial points          | 436 |
| 6.214 | Influence of 'n' value of various vertical drains on coefficient of horizontal permeability (kh) for Ur-50% at 160kPa pressure at three radial points         | 436 |
| 6.215 | Influence of 'n' value of various vertical drains on coefficient of horizontal permeability (kh) for Ur-80% at 160kPa pressure at three radial points         | 437 |
| 6.216 | Comparison of isochrones of 'n' values (dissipation of excess hydrostatic pore water pressure) w.r.t time against ratio of radial distance at 160kPa pressure | 439 |
| 6.217 | Comparison of isochrones of 'n' values (dissipation of excess hydrostatic pore water pressure) w.r.t time against ratio of radial distance at 160kPa pressure | 440 |
| 6.218 | Comparison of isochrones of 'n' values (dissipation of excess hydrostatic pore water pressure) w.r.t time against ratio of radial distance at 160kPa pressure | 441 |
| 6.219 | Comparison of isochrones of 'n' values (dissipation of excess hydrostatic pore water pressure) w.r.t time against ratio of radial distance at 160kPa pressure | 442 |
| 6.220 | Comparison of isochrones of 'n'11.04 of SD w.r.t experimental and theoretical Time factors (Tr) at 160kPa pressure  | 443 |
| 6.221 | Comparison of isochrones of 'n'16.93 of SD w.r.t experimental and theoretical Time factors (Tr) at 160kPa pressure  | 443 |
| 6.222 | Comparison of isochrones of 'n'21.71 of SD w.r.t experimental and theoretical Time factors (Tr) at 160kPa pressure  | 444 |
| 6.223 | Comparison of isochrones of 'n'11.04 of SW w.r.t experimental and theoretical Time factors (Tr) at 160kPa   | 444 |

|       |  |     |
|-------|--|-----|
|       | pressure   |     |
| 6.224 | Comparison of isochrones of 'n'16.93 of SW w.r.t experimental and theoretical Time factors (Tr) at 160kPa pressure                 | 445 |
| 6.225 | Comparison of isochrones of 'n'21.71 of SW w.r.t experimental and theoretical Time factors (Tr) at 160kPa pressure                 | 445 |
| 6.226 | Comparison of isochrones of 'n'11.04 of CJ w.r.t experimental and theoretical Time factors (Tr) at 160kPa pressure                 | 446 |
| 6.227 | Comparison of isochrones of 'n'16.93 of CJ w.r.t experimental and theoretical Time factors (Tr) at 160kPa pressure                 | 446 |
| 6.228 | Comparison of isochrones of 'n'21.71 of CJ w.r.t experimental and theoretical Time factors (Tr) at 160kPa pressure                 | 447 |
| 6.229 | Comparison of isochrones of 'n'11.04 of PF w.r.t experimental and theoretical Time factors (Tr) at 160kPa pressure                 | 447 |
| 6.230 | Comparison of isochrones of 'n'16.93 of PF w.r.t experimental and theoretical Time factors (Tr) at 160kPa pressure                 | 448 |
| 6.231 | Comparison of isochrones of 'n'21.71 of PF w.r.t experimental and theoretical Time factors (Tr) at 160kPa pressure                 | 448 |
| 6.232 | Influence of isochrones on 'n' value w.r.t experimental and theoretical time factors (Tr) for CJ at 160kPa pressure                | 449 |
| 6.233 | Influence of 'n' value on experimental isochrones for various vertical drains of 'n'11.04 at 160kPa pressure                       | 450 |
| 6.234 | Influence of 'n' value on experimental isochrones for various vertical drains of 'n'16.93 at 160kPa pressure                       | 450 |
| 6.235 | Influence of 'n' value on experimental isochrones for various vertical drains of 'n'21.71 at 160kPa pressure                       | 451 |
| 6.236 | Comparison of theoretical and experimental average degree of consolidation (Ur) against Time factor (Tr) for SD at 40kPa pressure  | 452 |
| 6.237 | Comparison of theoretical and experimental average degree of consolidation (Ur) against Time factor (Tr) for SD at 160kPa pressure | 453 |
| 6.238 | Comparison of theoretical and experimental average degree of consolidation (Ur) against Time factor (Tr) for SW at 40kPa pressure  | 453 |

|          |  |     |
|----------|--|-----|
| 6.239    | Comparison of theoretical and experimental average degree of consolidation ( $U_r$ ) against Time factor ( $T_r$ ) for SW at 160kPa pressure | 454 |
| 6.240    | Comparison of theoretical and experimental average degree of consolidation ( $U_r$ ) against Time factor ( $T_r$ ) for CJ at 40kPa pressure  | 454 |
| 6.241    | Comparison of theoretical and experimental average degree of consolidation ( $U_r$ ) against Time factor ( $T_r$ ) for CJ at 160kPa pressure | 455 |
| 6.242    | Comparison of theoretical and experimental average degree of consolidation ( $U_r$ ) against Time factor ( $T_r$ ) for PF at 40kPa pressure  | 455 |
| 6.243    | Comparison of theoretical and experimental average degree of consolidation ( $U_r$ ) against Time factor ( $T_r$ ) for PF at 160kPa pressure | 456 |
| 6.244    | Comparison of lump parameter ( $\lambda$ ) vs. 'n' value based on settlement analysis  | 456 |
| 6.245(a) | Comparison of theoretical and experimental average degree of consolidation ( $U_r$ ) against Time factor ( $T_r$ ) for SD at 40kPa pressure  | 459 |
| 6.245(b) | Comparison of theoretical and experimental average degree of consolidation ( $U_r$ ) against Time factor ( $T_r$ ) for SD at 160kPa pressure | 459 |
| 6.246    | Comparison of theoretical and experimental average degree of consolidation ( $U_r$ ) against Time factor ( $T_r$ ) for SW at 40kPa pressure  | 460 |
| 6.247    | Comparison of theoretical and experimental average degree of consolidation ( $U_r$ ) against Time factor ( $T_r$ ) for SW at 160kPa pressure | 460 |
| 6.248    | Comparison of theoretical and experimental average degree of consolidation ( $U_r$ ) against Time factor ( $T_r$ ) for CJ at 40kPa pressure  | 461 |
| 6.249    | Comparison of theoretical and experimental average degree of consolidation ( $U_r$ ) against Time factor ( $T_r$ ) for CJ at 160kPa pressure | 461 |
| 6.250    | Comparison of theoretical and experimental average degree of consolidation ( $U_r$ ) against Time factor ( $T_r$ ) for PF at 40kPa pressure  | 462 |
| 6.251    | Comparison of theoretical and experimental average degree of consolidation ( $U_r$ ) against Time factor ( $T_r$ ) for PF at 160kPa pressure | 462 |
| 6.252    | Comparison of 'n' value w.r.t settlement and pore pressure analysis for vertical drains of 'n' 11.04   | 463 |

|       |   |     |
|-------|---|-----|
| 6.253 | Comparison of 'n' value w.r.t settlement and pore pressure analysis for vertical drains of 'n'16.93   | 463 |
| 6.254 | Comparison of 'n' value w.r.t settlement and pore pressure analysis for vertical drains of 'n'16.93   | 464 |
| 6.255 | Comparison of lump parameter ( $\lambda$ ) vs. 'n' value based on pore pressure analysis  | 464 |
| 6.256 | Comparison of vane shear strength against ratio of radial distance for CJ of all 'n' values   | 465 |
| 6.257 | Comparison of vane shear strength against ratio of radial distance for SW of all 'n' values   | 466 |
| 6.258 | Comparison of vane shear strength against ratio of radial distance for PF of all 'n' values   | 466 |
| 6.259 | Comparison of vane shear strength against ratio of radial distance for PF of all 'n' values   | 466 |
| 6.260 | Comparison of degree of consolidation vs. log't in min for CSSD   | 471 |
| 6.261 | Comparison of degree of consolidation vs. log't in min for PSSD   | 472 |
| 6.262 | Comparison of degree of consolidation vs. log't in min for BSSD   | 472 |
| 6.263 | Comparison of degree of consolidation vs. log't in min for TSSD   | 473 |
| 6.264 | Comparison of various geometry of sand drain at 40kPa and 160kPa pressure of 'n'11.04   | 473 |
| 6.265 | Comparison of degree of consolidation vs. log't' in min for CSSD at three radial points for all applied pressures                               | 478 |
| 6.266 | Comparison of degree of consolidation vs. log't' in min for PSSD at three radial points for all applied pressures                               | 478 |
| 6.267 | Comparison of degree of consolidation vs. log't' in min for BSSD at three radial points for all applied pressures                               | 479 |
| 6.268 | Comparison of degree of consolidation vs. log't' in min for BSSD at three radial points for all applied pressures                               | 479 |
| 6.269 | Comparison of degree of consolidation for various geometrical sand drains of mid radial point r2 at 40kPa and 160kPa pressure                   | 480 |
| 6.270 | Comparison of degree of consolidation for various geometrical sand drains based on settlement and pore pressure measurements at 40kPa pressure  | 480 |
| 6.271 | Comparison of degree of consolidation for various geometrical sand drains based on settlement and pore pressure measurements at 160kPa pressure | 481 |
| 6.272 | Comparison of Cr vs. Ur for CSSD at all pressures   | 482 |
| 6.273 | Comparison of Cr vs. Ur for PSSD at all pressures   | 483 |

|       |  |     |
|-------|--|-----|
| 6.274 | Comparison of $C_r$ vs. $U_r$ for BSSD at all pressures  | 483 |
| 6.275 | Comparison of $C_r$ vs. $U_r$ for TSSD at all pressures  | 484 |
| 6.276 | Influence of various geometrical shape of drain on $C_r$ vs. $U_r$ for all pressures   | 484 |
| 6.277 | Comparison of $C_r$ vs. $U_r$ for CSSD for all pressures at radial points $r_1$ , $r_2$ and $r_3$  | 488 |
| 6.278 | Comparison of $C_r$ vs. $U_r$ for PSSD for all pressures at radial points $r_1$ , $r_2$ and $r_3$  | 488 |
| 6.279 | Comparison of $C_r$ vs. $U_r$ for BSSD for all pressures at radial points $r_1$ , $r_2$ and $r_3$  | 489 |
| 6.280 | Comparison of $C_r$ vs. $U_r$ for TSSD for all pressures at radial points $r_1$ , $r_2$ and $r_3$  | 489 |
| 6.281 | Influence of Geometry of drain on $C_r$ (of mid radial point $r_2$ ) vs. $U_r$ at 40kPa and 160kPa pressure  | 490 |
| 6.282 | Influence of Geometry of drain on $C_r$ vs. $U_r$ at 160kPa pressure based on settlement and pore pressure analysis                                  | 490 |
| 6.283 | Comparison of $C_r$ vs. applied pressure for various geometrical drains at $U_r$ 50% and $U_r$ 80%   | 492 |
| 6.284 | Comparison of $C_r$ vs. applied pressure for geometrical drains at $U_r$ 50% at radial points $r_1$ , $r_2$ and $r_3$                                | 495 |
| 6.285 | Comparison of $C_r$ vs. applied pressure for geometrical drains at $U_r$ 80% at radial points $r_1$ , $r_2$ and $r_3$                                | 495 |
| 6.286 | Comparison of void ratio ( $e$ ) vs. applied pressure for various geometrical shape sand drains  | 497 |
| 6.287 | Comparison of Compression index ( $C_c$ ) vs. Geometrical shape sand drains of 'n' 11.04   | 497 |
| 6.288 | Comparison of coefficient of horizontal permeability( $k_h$ ) against applied pressure for geometrical drains at $U_r$ 50% and $U_r$ 80%             | 499 |
| 6.289 | Comparison of $k_h$ vs. applied pressure for geometrical sand drains for $U_r$ 50% at radial points $r_1$ , $r_2$ and $r_3$                          | 501 |
| 6.290 | Comparison of $k_h$ vs. applied pressure for geometrical sand drains for $U_r$ 80% at radial points $r_1$ , $r_2$ and $r_3$                          | 501 |
| 6.291 | Comparison of $k_h$ vs. applied pressure for geometrical sand drains for $U_r$ 50% based on settlement and pore pressure analysis                    | 502 |
| 6.292 | Comparison of $k_h$ vs. applied pressure for geometrical sand drains for $U_r$ 80% based on settlement and pore pressure analysis                    | 502 |
| 6.293 | Dissipation of hydrostatic excess pore water pressure ( $U_r/U_o$ ) vs. ratio of radial distance ( $r/r_e$ ) with respect to time for CSSD at 160kPa | 504 |

|       |   |     |
|-------|---|-----|
| 6.294 | Dissipation of hydrostatic excess pore water pressure ( $U_r/U_o$ ) vs. ratio of radial distance ( $r/re$ ) with respect to time for PSSD at 160kPa | 504 |
| 6.295 | Dissipation of hydrostatic excess pore water pressure ( $U_r/U_o$ ) vs. ratio of radial distance ( $r/re$ ) with respect to time for BSSD at 160kPa | 505 |
| 6.296 | Dissipation of hydrostatic excess pore water pressure ( $U_r/U_o$ ) vs. ratio of radial distance ( $r/re$ ) with respect to time for TSSD at 160kPa | 505 |
| 6.297 | Comparison of theoretical isochrones and experimental isochrones with respect to time factor ( $Tr$ ) for CSSD at 160kPa pressure                   | 506 |
| 6.298 | Comparison of theoretical isochrones and experimental isochrones with respect to time factor ( $Tr$ ) for PSSD at 160kPa pressure                   | 506 |
| 6.299 | Comparison of theoretical isochrones and experimental isochrones with respect to time factor ( $Tr$ ) for BSSD at 160kPa pressure                   | 507 |
| 6.300 | Comparison of experimental isochrones with respect to selected time factor ( $Tr$ ) for geometrical sand drains at 160kPa pressure                  | 507 |
| 6.301 | Comparison of theoretical and experimental average degree of consolidation ( $U_r$ ) against Time factor ( $Tr$ ) for CSSD at 40kPa pressure        | 509 |
| 6.302 | Comparison of theoretical and experimental average degree of consolidation ( $U_r$ ) against Time factor ( $Tr$ ) for CSSD at 160kPa pressure       | 509 |
| 6.303 | Comparison of theoretical and experimental average degree of consolidation ( $U_r$ ) against Time factor ( $Tr$ ) for BSSD at 40kPa pressure        | 510 |
| 6.304 | Comparison of theoretical and experimental average degree of consolidation ( $U_r$ ) against Time factor ( $Tr$ ) for BSSD at 160kPa pressure       | 510 |
| 6.305 | Comparison of theoretical and experimental average degree of consolidation ( $U_r$ ) against Time factor ( $Tr$ ) for PSSD at 40kPa pressure        | 511 |
| 6.306 | Comparison of theoretical and experimental average degree of consolidation ( $U_r$ ) against Time factor ( $Tr$ ) for PSSD at 160kPa pressure       | 511 |
| 6.307 | Comparison of theoretical and experimental average degree of consolidation ( $U_r$ ) against Time factor ( $Tr$ ) for TSSD at 40kPa pressure        | 512 |
| 6.308 | Comparison of theoretical and experimental average  | 512 |

|       |  |     |
|-------|--|-----|
|       | degree of consolidation ( $U_r$ ) against Time factor ( $T_r$ ) for TSSD at 160kPa pressure  |     |
| 6.309 | Comparison of theoretical and experimental average degree of consolidation ( $U_r$ ) against Time factor ( $T_r$ ) for CSSD at 40kPa pressure  | 514 |
| 6.310 | Comparison of theoretical and experimental average degree of consolidation ( $U_r$ ) against Time factor ( $T_r$ ) for CSSD at 160kPa pressure | 514 |
| 6.311 | Comparison of theoretical and experimental average degree of consolidation ( $U_r$ ) against Time factor ( $T_r$ ) for PSSD at 40kPa pressure  | 515 |
| 6.312 | Comparison of theoretical and experimental average degree of consolidation ( $U_r$ ) against Time factor ( $T_r$ ) for PSSD at 160kPa pressure | 515 |
| 6.313 | Comparison of theoretical and experimental average degree of consolidation ( $U_r$ ) against Time factor ( $T_r$ ) for BSSD at 40kPa pressure  | 516 |
| 6.314 | Comparison of theoretical and experimental average degree of consolidation ( $U_r$ ) against Time factor ( $T_r$ ) for BSSD at 160kPa pressure | 516 |
| 6.315 | Comparison of theoretical and experimental average degree of consolidation ( $U_r$ ) against Time factor ( $T_r$ ) for TSSD at 40kPa pressure  | 517 |
| 6.316 | Comparison of theoretical and experimental average degree of consolidation ( $U_r$ ) against Time factor ( $T_r$ ) for TSSD at 160kPa pressure | 517 |
| 6.317 | Influence of geometry of drain on experimental time factor (lump parameter) based on settlement and pore pressure analysis                     | 518 |
| 6.318 | Comparison of vane shear strength of consolidated clay mass by CSSD, PSSD, BSSD, TSSD  | 519 |
| 6.319 | %loss of shear strength vs. time interval in seconds   | 523 |
| 6.320 | Comparison of $C_c$ vs. WCR for various vertical drains  | 526 |
| 6.321 | Comparison of $C_c$ vs. Type of drain for same WCR   | 527 |
| 6.322 | Comparison of WCR vs. Type of drain for same $C_c$   | 527 |

## LIST OF TABLES

| Table No. | Title   | Page No. |
|-----------|---|----------|
| 2.1       | Comparison of various Ground Improvement Methods  | 5        |
| 2.2       | Grading Requirements for Sand Drain   | 21       |
| 2.3       | Grading of Blanket Material (Clean, coarse sand or Gravel)  | 21       |
| 2.4       | Summary of various researchers in theoretical development   | 80       |
| 2.5       | Experts based on Experimental set-up  | 113      |
| 2.6       | Experts based on Material properties  | 115      |
| 3.1       | Schedule of study parameters and related figure numbers   | 128      |
| 3.2       | Variation of Vertical Drain Materials   | 129      |
| 3.3       | Variation of 'n' values   | 130      |
| 3.4       | Various Geometry (shapes) of Vertical Drain   | 131      |
| 3.5       | Variation of Volumetric Water Ratio (VWR)*  | 132      |
| 3.6       | Variation of Consolidation Pressure Ratio (CPR)   | 133      |
| 3.7       | Schedule of SEM of consolidated clay samples with central vertical drain  | 134      |
| 3.8       | Schedule of measurement of vane shear strength  | 136      |
| 3.9       | Properties of Kaolinitic clay used for investigation  | 137      |
| 3.10      | Properties of sand used in Sand drain   | 137      |
| 3.11      | Properties of sand used in Sandwich drain   | 138      |
| 3.12(a)   | Physical Properties of polypropylene geotextile used for Sandwich drain   | 138      |
| 3.12(b):  | Mechanical and Hydraulic Properties of polypropylene geotextile used for Sandwich drain (photograph 3.1,3.2,3.3 and 3.4)                                  | 138      |
| 3.13      | Permittivity and transmittivity of vertical drain of geosynthetics in fabricating the drain (test on special radial permeability set-up, refer chapter 5) | 139      |
| 3.14      | Specific surface area of vertical geodrains used in present investigations  | 140      |
| 3.15      | Physical, Mechanical and Hydraulic Properties of Jute fibers (photograph 3.5)   | 141      |
| 3.16      | Physical and Mechanical Properties of Coir fibers   | 141      |



|      |   |     |
|------|---|-----|
| 3.17 | Properties of Polypropylene fibers used in Polypropylene fiber drain (PF) (photograph 3.6)  | 142 |
| 3.18 | Stress-Strain characteristics of various vertical geodrains used in laboratory investigations (photograph 3.7)                            | 142 |
| 5.1  | Typical chemical composition and physical properties of Coir fibers   | 222 |
| 5.2  | Tensile properties of coir fibers at different strain rate<br>(Mukherjee, Satyanarayana et.al, 1984)                                      | 225 |
| 5.3  | Schedule of Micrographs for MIC   | 237 |
| 6.1  | Comparison of time taken for 50% and 80% degree of consolidation of drain material based on settlement and pore pressure measurements     | 271 |
| 6.2  | Comparison of Cr values for various drain materials based on settlement and pore pressure analysis  | 288 |
| 6.3  | Comparison of time taken for 50% and 80% degree of consolidation for various 'n' value based on settlement and pore pressure measurements | 363 |
| 6.4  | Comparison of Cr values for various drain materials based on settlement and pore pressure analysis  | 392 |
| 6.5  | Percentage loss in strength at the end of each period due to seismic effect   | 522 |

## LIST OF PHOTOGRAPHS

| Photograph No. | Title  | Page No. |
|----------------|--|----------|
| 3.1            | Tensile test on geotextile used in fabricating Sandwich  | 139      |
| 3.2            | Air permeability test on geotextile used in Sandwich   | 140      |
| 3.3            | Bursting strength test on Geotextile used in Sandwich  | 142      |
| 3.4            | Sample of Sandwich drain ('n'11.04) along with polypropylene geotextile  | 143      |
| 3.5            | Sample of Coir-Jute fibers and Coir-Jute drain ('n'11.04) encapsulated by filter paper   | 143      |
| 3.6            | Sample of white Polypropylene fibers and Polypropylene fiber drain ('n' 11.04) encapsulated by filter paper                            | 144      |
| 3.7            | Stiffness test on vertical drains  | 144      |
| 5.1            | View of complete tri-axial set-up for stiffness test and sample of sandwich after failure  | 194      |
| 5.2            | Self compensating mercury pressure system  | 205      |
| 5.3            | Complete Oedometer assembly with its components  | 208      |
| 5.4            | Bottom plate with connections to pore pressure measuring points  | 208      |
| 5.5            | Complete hydraulically pressurized Oedometer set-up  | 209      |
| 5.6            | Complete view of laboratory of Consolidation of soft clays through radial flow   | 212      |
| 5.7            | Vane shear set-up with soil sample   | 214      |
| 5.8            | Mandrel of plus shape, circular shape, band shape & tripod shape   | 218      |
| 5.9            | Top platen installation, bore hole formation using circular mandrel and clay sample with central vertical sand drain ready for testing | 218      |
| 5.10           | Formation of plus shape , tripod shape and band shape bore hole using mandrel for geometrical shape sand drains                        | 218      |
| 5.11           | Sandwich ('n'11.04) ready for installation and clay sample with central sandwich   | 221      |
| 5.12           | Coir fibers, Bunch of coir and jute fibers of required length and coir-jute drain (CJ) of 'n'11.04                                     | 226      |
| 5.13           | Polypropylene fiber drain (PF) ready for   | 228      |

|        |   |     |
|--------|---|-----|
|        | installation and clay sample with central PF drain ready for testing  |     |
| 5.14   | (a) Sampler with radial drainage (b) Sampler with top cap (c) Set-up of sampler with top cap, centrally placed sample and bottom drainage valve (d) Complete radial permeability set-up | 235 |
| 6.1(a) | Micrographs of Sand drain (SD) of 'n'11.04 at locations $h_{tr2}$ , $h_{cr2}$ , $h_{br2}$   | 282 |
| 6.1(b) | Micrographs of Sand drain (SD) of 'n'11.04 at locations $h_{cr2}$ ,   | 282 |
| 6.1(c) | Micrographs of Sand drain (SD) of 'n'11.04 at locations $h_{br2}$   | 283 |
| 6.2(a) | Micrographs of Coir-Jute drain (CJ) of 'n'11.04 at locations $h_{tr2}$  | 283 |
| 6.2(b) | Micrographs of Coir-Jute drain (CJ) of 'n'11.04 at locations $h_{cr2}$  | 284 |
| 6.2(c) | Micrographs of Coir-Jute drain (CJ) of 'n'11.04 at locations $h_{br2}$  | 284 |
| 6.3    | Microscopic image of Sand drain (SD) at location $h_{tr2}$ and measurement of % porosity and angle of orientation ( $\beta$ ) using MIC software  | 310 |
| 6.4    | Microscopic image of Coir-Jute fiber drain (CJ) at location $h_{tr2}$ and measurement of % porosity and angle of orientation ( $\beta$ ) using MIC software                             | 311 |
| 6.5    | Microscopic image of Sand drain (SD) at location $h_{cr2}$ and measurement of % porosity and angle of orientation ( $\beta$ ) using MIC software  | 312 |
| 6.6    | Microscopic image of Coir-Jute drain (CJ) at location $h_{cr2}$ and measurement of % porosity and angle of orientation ( $\beta$ ) using MIC software                                   | 313 |
| 6.7    | Microscopic image of Sand drain   | 314 |

|      |   |     |
|------|---|-----|
|      | (SD) at location $h_{br2}$ and measurement of % porosity and angle of orientation ( $\beta$ ) using MIC software  |     |
| 6.8  | Microscopic image of Coir-Jute drain (CJ) at location $h_{br2}$ and measurement of % porosity and angle of orientation ( $\beta$ ) using MIC software       | 315 |
| 6.9  | Sectional view of consolidated clay sample (end of 320kPa pressure) with central vertical sand drain (SD) of $n = 11.04$                                    | 353 |
| 6.10 | Sectional view of consolidated clay sample (end of 320kPa pressure) with central vertical sandwich drain (SW) of $n = 11.04$                                | 353 |
| 6.11 | Sectional view of consolidated clay sample (end of 320kPa pressure) with central vertical coir-jute drain (CJ) of $n = 11.04$                               | 354 |
| 6.12 | Sectional view of consolidated clay sample (end of 320kPa pressure) with central vertical polypropylene fiber drain (PF) of $n = 11.04$                     | 354 |
| 6.13 | Microscopic image of Sand drain (SD,'n'11.04) at location $l_{brd}$ and measurement of % porosity and angle of orientation ( $\beta$ ) using MIC software   | 377 |
| 6.14 | Microscopic image of Sand drain (SD,'n'16.93) at location $l_{brd}$ and measurement of % porosity and angle of orientation ( $\beta$ ) using MIC software   | 378 |
| 6.15 | Microscopic image of Sand drain (SD,'n'21.71) at location $l_{brd}$ and measurement of % porosity and angle of orientation ( $\beta$ ) using MIC software   | 379 |
| 6.16 | Microscopic image of Coir-Jute fiber drain (CJ,'n'11.04) at location $l_{brd}$ and measurement of % porosity and angle of orientation ( $\beta$ ) using MIC | 380 |

|      |  |     |
|------|--|-----|
|      | software   |     |
| 6.17 | Microscopic image of Coir-Jute fiber drain (CJ,'n'16.93) at location $I_{brd}$ and measurement of % porosity and angle of orientation ( $\beta$ ) using MIC software | 381 |
| 6.18 | Microscopic image of Coir-Jute fiber drain (CJ,'n'21.71) at location $I_{brd}$ and measurement of % porosity and angle of orientation ( $\beta$ ) using MIC software | 382 |
| 6.19 | Sectional view of consolidated clay sample (end of 320kPa pressure) with central vertical sand drain (SD) of $n = 16.93$   | 467 |
| 6.20 | Sectional view of consolidated clay sample (end of 320kPa pressure) with central vertical sand drain (CJ) of $n = 16.93$   | 467 |
| 6.21 | Sectional view of consolidated clay sample (end of 320kPa pressure) with central vertical sand drain (PF) of $n = 16.93$   | 468 |
| 6.22 | Sectional view of consolidated clay sample (end of 320kPa pressure) with central vertical sand drain (SD) of $n = 21.71$   | 468 |
| 6.23 | Sectional view of consolidated clay sample (end of 320kPa pressure) with central vertical sand drain (SW) of $n = 21.71$   | 469 |
| 6.24 | Sectional view of consolidated clay sample (end of 320kPa pressure) with central vertical sand drain (CJ) of $n = 21.71$   | 469 |
| 6.25 | Sectional view of consolidated clay sample (end of 320kPa pressure) with central Plus shape sand drain (PSSD) of $n'11.04$   | 519 |
| 6.26 | Sectional view of consolidated clay sample (end of 320kPa pressure) with central Band shape sand drain (BSSD) of $n'11.04$   | 520 |

|      |  |     |
|------|--|-----|
| 6.27 | Sectional view of consolidated clay sample (end of 320kPa pressure) with central Tripod shape sand drain (TSSD) of n'11.04 | 520 |
| 6.28 | Shaking table with Oedometer, vane shear and vibration meter   | 521 |

## LIST OF SYMBOLS

| Symbol     | Description   |
|------------|---|
| CNS        | Cohesive non-swelling   |
| H          | Height / thickness of the sample  |
| R          | Radius of the soil sample or Oedometer  |
| K          | Permeability of the sand used for vertical drain                              |
| $C_r$      | Coefficient of consolidation through radial drainage                          |
| $C_v$      | Coefficient of consolidation through vertical drainage                        |
| PVD        | Prefabricated vertical drain  |
| t          | Time at any given instance  |
| $T_r$      | Time factor for consolidation through radial drainage                         |
| $T_{r,50}$ | Time factor for 50% consolidation through radial drainage                     |
| $T_{r,80}$ | Time factor for 80% consolidation through radial drainage                     |
| U          | Degree of consolidation due to combined linear and radial drainage            |
| $C_h$      | Coefficient of consolidation through horizontal drainage                      |
| R          | Ratio of $r/r_e$ with reference to isochrones                                 |
| r          | Any radial distance with reference to Oedometer                               |
| $r_e$      | Radius of influence   |
| $r_1$      | Radial point nearer to drain/first radial point with reference to Oedometer   |
| $r_2$      | Radial point at mid distance /second radial point with reference to Oedometer |
| $r_3$      | Radial point away from drain/third radial point with reference to Oedometer   |
| $U_R$      | Average degree of consolidation for radial flow                               |
| $U_r$      | Degree of radial consolidation  |
| $u_o$      | Initial pore water pressure   |
| $u_r$      | Pore water pressure at given radial point                                     |
| $T_r$      | Time factor for radial consolidation  |
| $r_w$      | Radius of filter well (drain) with reference to Barron's theory               |
| $k_v$      | Coefficient of vertical permeability  |
| $k_h$      | Coefficient of horizontal permeability  |
| U          | Degree of consolidation in general  |
| $U_z$      | Degree of vertical consolidation  |
| $T_h$      | Time factor for horizontal drainage   |
| e          | Void ratio  |

|            |   |
|------------|---|
| $n$        | Porosity  |
| $A.P$      | Applied pressure in kPa   |
| $n$        | Ratio of $r_e/r_w$  |
| $k_w$      | Permeability of well backfill   |
| $r_w$      | Radius of drain/well  |
| $de/dt$    | Rate of vertical strain   |
| $Q$        | Well discharge capacity   |
| $q'(z)$    | Rate of loading at time $t$   |
| $L$        | Characteristic length of the drain  |
| $k_c'$     | Coefficient of permeability in smeared zone   |
| $\Delta P$ | Pressure increment in kPa   |
| $q$        | Coefficient of volume compressibility of the pore fluid                                 |
| $r_w$      | Unit weight of pore fluid   |
| $v$        | Volume of pore fluid  |
| $lw$       | Degree of saturation  |
| $P_a$      | Atmospheric pressure  |
| $K_v$      | Coefficient of permeability in the vertical direction                                   |
| $K_r$      | Coefficient of permeability in the radial direction                                     |
| $S$        | Compression modulus   |
| $U(t)$     | Mean excess pore pressure   |
| $U_o$      | Initial excess pore pressure  |
| $V_j$      | Volume of soil below depth below $z = j(z)$   |
| $Q(t)$     | Total amount of ground water which has been transported through the drain upto time $t$ |
| $u_z$      | Vertical upward displacement  |
| $Be$       | Equivalent drainage diameter  |
| $C_{vr}$   | Coefficient of vertical consolidation for radial drainage                               |
| $U_R$      | Average degree of consolidation   |
| $T_r$      | Time factor for consolidation due to radial flow  |
| $\lambda$  | Lump parameter  |
| $C_r$      | Coefficient of consolidation due to radial drainage                                     |
| $C_e$      | Coefficient due to permeability and porosity  |
| WCR        | Water content ratio   |
| CPR        | Consolidation pressure ratio  |
| $k_h$      | Coefficient of permeability for horizontal flow   |



|           |   |
|-----------|---|
| $k_v$     | Coefficient of permeability for vertical flow                               |
| $C_r$     | Coefficients of consolidation due to radial flow                            |
| $T_r$     | Time factor for consolidation due to radial flow                            |
| $U_r$     | Degree of consolidation due to the radial drainage                          |
| $C_{cr}$  | Compression index for consolidation due to radial flow                      |
| $P_{cr}$  | Primary compression ratio for consolidation due to radial flow              |
| $u_r/u_o$ | Pore pressure ratio for radial flow   |
| $a_{vr}$  | Coefficient of compressibility due to radial flow                           |
| $m_{vr}$  | Coefficient of volume change due to radial flow                             |
| $P$       | Consolidation pressure  |
| SM        | Settlement analysis   |
| PM        | Pore pressure analysis  |
| $e$       | Void ratio  |
| $\zeta$   | Shear strength of soil  |
| $\beta$   | Angle of orientation  |
| SD        | Sand drain  |
| SW        | Sandwick  |
| CJ        | Coir-jute fiber drain   |
| PF        | Polypropylene fiber drain   |
| $n$       | ratio of radius of odometer to the radius of drain                          |
| Sa        | Surface area  |
| De        | Equivalent diameter of geodrain   |
| SEM       | Scanning electron microscopy  |
| $r$       | Radius of clay sample in general  |
| $r_d$     | Radius of drain   |
| $B_d$     | Breadth of drain  |
| $T_d$     | Thickness of drain  |
| $r_1$     | first radial point for measurement of pore pressure at a distance of $r/4$  |
| $r_2$     | second radial point for measurement of pore pressure at a distance of $r/2$ |
| $r_3$     | third radial point for measurement of pore pressure at a distance of $3r/4$ |
| $H$       | thickness of final consolidated clay sample                                 |
| $h_t$     | Top of final consolidated clay sample                                       |
| $h_c$     | Centre of final consolidated clay sample                                    |
| $h_b$     | Bottom of final consolidated clay sample                                    |

|            |  |
|------------|--|
| $h_{tr1}$  | Top of final consolidated clay sample at first radial point $r_1$                  |
| $h_{tr2}$  | Top of final consolidated clay sample at first radial point $r_2$                  |
| $h_{tr3}$  | Top of final consolidated clay sample at first radial point $r_3$                  |
| $h_{cr1}$  | Centre of final consolidated clay sample at first radial point $r_1$               |
| $h_{cr2}$  | Centre of final consolidated clay sample at first radial point $r_2$               |
| $h_{cr3}$  | Centre of final consolidated clay sample at first radial point $r_3$               |
| $h_{br1}$  | Bottom of final consolidated clay sample at first radial point $r_1$               |
| $h_{br2}$  | Bottom of final consolidated clay sample at first radial point $r_2$               |
| $h_{br3}$  | Bottom of final consolidated clay sample at first radial point $r_3$               |
| $l_{trd}$  | Clay-Drain interface at top of final consolidated clay sample at location $r_d$    |
| $l_{crd}$  | Clay-Drain interface at centre of final consolidated clay sample at location $r_d$ |
| $l_{brd}$  | Clay-Drain interface at bottom of final consolidated clay sample at location $r_d$ |
| $l_{tr1}$  | Clay-Drain interface at top of final consolidated clay sample at location $r_1$    |
| $l_{tr2}$  | Clay-Drain interface at top of final consolidated clay sample at location $r_2$    |
| $l_{tr3}$  | Clay-Drain interface at top of final consolidated clay sample at location $r_3$    |
| $l_{cr1}$  | Clay-Drain interface at centre of final consolidated clay sample at location $r_1$ |
| $l_{cr2}$  | Clay-Drain interface at centre of final consolidated clay sample at location $r_2$ |
| $l_{cr3}$  | Clay-Drain interface at centre of final consolidated clay sample at location $r_3$ |
| $l_{br1}$  | Clay-Drain interface at bottom of final consolidated clay sample at location $r_1$ |
| $l_{br2}$  | Clay-Drain interface at bottom of final consolidated clay sample at location $r_2$ |
| $\psi$     | Permittivity   |
| $\theta$   | Transmissivity   |
| $d_e$      | Oedometer diameter   |
| $d_w$      | Drain diameter   |
| $\Delta u$ | Initial pore water pressure  |
| $\Delta P$ | Applied incremental stress   |
| $C_e$      | Equivalent compressibility of pore water line and connection                       |
| $C_m$      | Compressibility of pore pressure measuring element                                 |
| $C_s$      | Compressibility of soil skeleton   |

|            |  |
|------------|--|
| $h_1, h_2$ | Initial levels of two mercury surfaces measured above some datum |
| $h_3$      | Level of sample measured above some datum                        |
| $\gamma_m$ | Unit weight of mercury   |
| $\gamma_w$ | Unit weight of water   |
| $A$        | Cross-sectional area of the cylinder                             |
| $\Delta L$ | Shortening of the spring   |
| $w$        | Weight of unit length of flexible tube filled with mercury       |
| $k$        | Spring stiffness   |
| LVDT       | linear variable differential transformer                         |
| DVM        | Digital volt meter   |
| PVD        | Prefabricated vertical drain                                     |
| CSSD       | Conventional circular shape sand drain                           |
| PSSD       | Plus shape sand drain  |
| TSSD       | Tripod shape sand drain  |
| BSSD       | Band shape sand drain  |
| MIC        | Micro structure characterization                                 |

## LIST OF APPENDIX

| <b>Sr.No.</b> | <b>List of Appendix</b>                        | <b>Appendix No.</b> | <b>Page No.</b> |
|---------------|--|---------------------|-----------------|
| 1.            | SYNOPSIS                                       | A                   | I               |
| 2.            | DATA ACQUISITION SYSTEM                        | B                   | 588             |
| 3.            | LABVIEW- 8.2 SOFTWARE                          | C                   | 591             |
| 4.            | CURVE EXPERT 3 SOFTWARE                        | D                   | 595             |
| 5.            | MICROSTRUCTURE<br>CHARACTERIZER SOFTWARE (MIC) | E                   | 601             |
| 6.            | VARIOUS TESTS ON CLAY                          | F                   | 607             |
| 7.            | VARIOUS TESTS ON SAND                          | G                   | 611             |

# CHAPTER-1

## INTRODUCTION

---

Amongst the various ground improvement techniques the vertical geodrain using radial drainage is preferable in soft cohesive soil. When a soil mass is subjected to compressible stresses, it causes a reduction in pore space and, if saturated the excess water is expelled with time till equilibrium condition is established for a given constant compressive stress. For cohesive soil, the time required to accomplish this, is more. Initially, before any reduction of pore space has occurred, the compressive stresses are carried by the water (called hydrostatic excess or excess pore water pressure). As the excess water drains, compressive stresses are transferred to the soil grains increasing the intergranular pressures. This complete process is known as 'Consolidation' of the soil and was first analyzed by Karl Terzaghi (1923) for a case of one-dimensional consolidation.

The model law of consolidation suggests that shorter the drainage path, faster the rate of the consolidation ( $t = T_v d^2 / C_v$  i.e.  $t \propto d^2$ ). In addition the rate of consolidation can be enhanced if higher horizontal permeability than vertical of soil is taken into advantage. These can be made possible by adopting central vertical geodrains or prefabricated vertical drains (PVDs) where drainage path reduced by four fold, Terzaghi (1936) where in excess water dissipates radially and vertically at faster rate. Because of the certain limitations of conventional methods such as sand drains, the concept of prefabricated vertical geodrains have entered into the practice particularly for ground improvement of soft marine clays. Some of the cost effective and eco-friendly prefabricated geodrains of natural materials seems to have not only expedite the rate of settlement but consequently accelerated the rate of gain in strength by increasing intergranular contacts.

Barron (1948) was the first to gave complete solutions of consolidation through inward radial flow using vertical drains considering 'equal strain' and 'free strain' conditions. He also considered well resistance and smear effects in his

solutions. The unique position of the classical theory is maintained even though experimental observations reveal worthwhile deviations from its mainly due to the imprecise picture of pore water pressure dissipation phenomena with time, physical nature of real soil and inefficient mathematical technique. To explain these discrepancies attention is generally focused on factors such as inefficient drain material, drain size, drain spacing, drain geometry, well resistance, smear effect, invalidity of Darcy's law, inadequacy of effective stress law and non-linearity of stress-strain law. Considerable amount of experimental and theoretical investigations of various research workers point out the chief factors and suggest the specifications for a realistic theory of consolidation by radial flow. It must incorporate for instance, the characteristics of drain material, drain diameter and drain geometry along with physico-chemical changes of clay, pore fluid and soil skeleton with due consideration to inelastic, time dependant, nonlinear and non quasistatic nature of stress-strain relationship of a real soil. A promising mathematical approach to the development of a realistic theory of consolidation of clays is seen in the works of Gibson et al. (1967) and Shroff et al. (1972).

Shroff and Shah (2008, 2010 and 2012) of the Applied Mechanics Department (Geotechnical Engineering Laboratory) of the M.S University of Baroda established a partial differential equation of consolidation through radial flow from fundamental considerations employing similar mathematical treatment. The equation has a form identical to the differential equation for the non-steady radial conduction of heat in a moving medium through vertical central heat dissipater as against the Terzaghi classical concept of heat flow through isotropic bodies. For solution of higher order partial differential equation derived from first principle of present theoretical investigation an EXCEL Macro program was developed.

The various experimental factors are treated by using hydraulically pressurized Oedometer for the measurement of pore water pressure at various radial points to obtain experimental isochrones that is sequence of consolidation and at various  $r/r_e$  ratio for corresponding concentric planar location for given  $z/h$  at that time with reference to various factors influencing consolidation due to radial dissipation of pore water pressure. Average degree of consolidation is computed

from trajectory of isochrones and influence of each parameter is obtained in form of value of lump parameter ( $\lambda$ ). The average degree of consolidation ( $U_R$ ) obtained experimentally for each influencing factor is then compared with theoretical one with respect to time factor ( $T_r$ ), and appropriate lump parameter ' $\lambda$ ' is determined. Under the above theoretical background the present work investigates experimentally the influence of factors like distinctive drain material, ' $n$ ' value (diameter of drain), geometry of drain along with soil structure effects on the consolidation characteristics of kaolinitic clay due to radial drainage.

## **CHAPTER-2**

### **CONSOLIDATION OF SOFT CLAY BY RADIAL FLOW**

---

#### **2.1 Introduction**

There are various methods of ground improvement for soft clays. One of the popular methods is using the vertical drains which have a distinct advantage of faster rate of consolidation and hence quicker gain in strength of soft clays. Vertical drains can either be sand drains, sand wicks, rope drain, or prefabricated band drains or composite geodrain. Sand drains are created in vertical holes made in soft clay, which is filled with sand. It is the earliest type of vertical drain while the geodrain is the recent development and most commonly used vertical drains which are prefabricated by fibers/fabrics of geosynthetic material.

In spite of several limitations, sand drain technique is the simplest technique, and is the most suitable method in countries having adequate availability of sand. This may prove to be cost effective solution for shallow depths in developing countries where labour costs are very low and where there are restrictions on imported equipments and materials. Beside vertical drains there are many other ground improvement techniques like addition of admixtures, vibroreplacement, stone columns, soil nailing, grouting, jet grouting, dynamic compaction, blasting, electro-osmosis and CNS layer. In the succeeding para, a description of various ground improvement techniques is given; and description of improvement by geodrain is then presented.

The development of soil improvement methods follows two different methodologies. In one methodology, emphasis has been on the improvement of material, as for example, with use of admixtures, thermal treatment, or by densification. In the other methodology, emphasis has been on the improvement of the system which contains the soil. Examples of this would be reinforcement using inclusions.



## 2.2 Ground Improvement Methods

**Table 2.1:** Comparison of various Ground Improvement Methods

| Methods                 | Sub-methods                   | Principle  | Most suitable soil condition                         | Maximum effective treatment depth | Special equipment required                                     | Special materials required   | Properties of treated material                            | Advantages & Limitations  | Relative cost |
|-------------------------|-------------------------------|--|--|-----------------------------------|--|--|---|---|---------------|
| 1.<br>Use Of Admixtures | <b>1.1 Remove and Replace</b> | Foundation soil excavated, improved by drying or admixture, and recompactd | Inorganic soils                                      | 7-10 m                            | Excavating, mixing and compaction equipment, dewatering system | Admixtures stabilizers.  | Increased strength and stiffness, reduced compressibility | Uniform, controlled foundation soil when replaced; may require large area dewatering. | High          |
|                         | <b>1.2 Structural Fills</b>   | Structural fill distributes loads to underlying soft soils                 | Use over soft clays or organic soils, marsh deposits | -----                             | Mixing and compaction equipment                                | Sand, gravel, flyash, bottom ash, slag, expanded aggregates , clam shell or oyster shell, incinerator ash. | Soft subgrade protected by structural load bearing fill   | High strength, good load distribution to underlying soft soils                        | low to high   |

|                       |  |  |  |                   |   |   |   |   |                  |
|-----------------------|--|--|--|-------------------|---|---|---|---|------------------|
|                       | <b>1.3<br/>Mix-In-<br/>Place Piles<br/>And Walls</b> | Lime,<br>Cement, or<br>Asphalt<br>introduced<br>through<br>rotating auger<br>or special in<br>place mixer  | All soft or<br>loose<br>inorganic soils  | >20 m             | Drill rig,<br>rotary<br>cutting and<br>mixing<br>head,<br>additive<br>proportionin<br>g<br>equipment. | Cement<br>,Lime,<br>Asphalt, or<br>chemical<br>stabilizer | Solidified<br>soil piles or<br>walls of<br>relatively<br>high<br>strength                   | Uses native<br>soil, reduced<br>lateral<br>support<br>requirements<br>during<br>excavation;<br>difficult<br>quality<br>control. | Moderate to high |
| <b>2.<br/>Thermal</b> | <b>2.1<br/>Heating</b>                               | Drying at low<br>temperatures;<br>alteration of<br>clays at<br>intermediate<br>temperatures<br>(400-600° C);<br>fusion at high<br>temperatures<br>(>1000°C). | Fine –grained<br>soils,<br>especially<br>partly<br>saturated<br>clays and<br>silts, loesses. | 15 m              | Fuel tanks,<br>burners,<br>blowers  | Fuel.   | Reduced<br>water<br>content,<br>plasticity,<br>water<br>sensivity<br>increased<br>strength. | Can obtain<br>irreversible<br>improvement<br>in properties,<br>can<br>introduce<br>stabilizers<br>with hot<br>gases.            | High             |
|                       | <b>2.2<br/>Freezing</b>                              | Freeze soft,<br>wet ground to<br>increase its<br>strength and<br>stiffness   | All soils  | Several<br>meters | Refrigeratio<br>n system  | Refrigerant   | Increased<br>strength and<br>stiffness,<br>reduced<br>permeability                          | No good in<br>flowing<br>ground<br>water,<br>temporary  | High             |

|                     |   |   |   |  |  |                                      |  |  |                  |
|---------------------|---|---|---|--|--|--------------------------------------|--|--|------------------|
| 3.<br>Reinforcement | <b>3.1<br/>Vibroreplacement,<br/>Stone And<br/>Sand<br/>Columns</b>   | Hole jetted into soft, fine-grained soil and back-filled with densely compacted gravel or sand.         | Soft clays and alluvial deposits        | 20 m   | Vibrofloat, crane or vibrocat                      | Gravel or crushed rock backfill      | Increased bearing capacity, reduced settlements                                    | Faster than precompression, avoids dewatering required for remove and replace; limited bearing capacity. | Moderate to high |
|                     | <b>3.2<br/>Root Piles,<br/>Soil Nailing</b>                           | Inclusions used to carry tension, shear, compression  | All soils                               | 7m   | Drilling and grouting equipment                    | Reinforcing bars, cement grout       | Reinforced zone behaves as a coherent mass   | In-situ reinforcement for soils that can't be grouted with admixtures.                                   | Moderate to high |
|                     | <b>3.3 Strips,<br/>Grids,<br/>Geotextiles<br/>&amp;<br/>Membranes</b> | Horizontal tensile strips, membranes buried in soil under embankments, gravel base courses and footings | Cohesionless soil, some C- $\phi$ soils | Can construct earth structures to heights of several tens of m | Excavating earth handling and compaction equipment | Metal or plastic strips, Geotextiles | Self-supporting earth structures, increased bearing capacity, reduced deformation. | Economical, earth structures coherent, can tolerate deformations, increased allowable bearing pressure.  | Low to moderate  |

|                            |   |   |                                   |                               |                                       |                         |  |   |  |
|----------------------------|---|---|-----------------------------------|-------------------------------|---------------------------------------|-------------------------|--|---|--|
| 4.<br>Injection & Grouting | <b>4.1<br/>Particulate<br/>Grouting</b>       | Penetration grouting fill soil pores with soil, cement , and/or clay                        | Medium to coarse sand and gravel. | For shallow to greater depths | Mixers, tanks, pumps, hoses           | Grout, water            | Impervious, high strength with cement grout, eliminate liquefaction danger.                        | Low cost grouts, high strength; limited to coarse-grained soils, hard to evaluate.    | Lowest of the grout system                                 |
|                            | <b>4.1<br/>Chemical<br/>Grouting</b>          | Solutions of two or more chemicals react in soil pores to form a gel or a solid precipitate | Medium silts and coarser          | Unlimited                     | Mixers, tanks, pumps, hoses           | Grout, water            | Impervious, low to high strength eliminate liquefaction danger                                     | Low viscosity, controlled gel time, good water shut-off; high cost, hard to evaluate. | High to very high  |
|                            | <b>4.2<br/>Pressure<br/>Injected<br/>Lime</b> | Lime slurry injected to shallow depths under high pressure                                  | Expansive clays.                  | Unlimited but 2-3 m usual     | Slurry tanks, agitators, pumps, hoses | Lime, water, surfactant | Lime encapsulate d zones formed by channels resulting from cracks, root holes, hydraulic fracture. | Only effective in narrow range of soil conditions                                     | Competitive with other solutions to expansive soil problem |

*Consolidation of soft clay by radial flow*

|  |   |  |   |                             |  |   |  |   |   |
|--|---|--|---|-----------------------------|--|---|--|---|---|
|  | <b>4.3<br/>Displacement Grout</b>       | High viscous grout acts as radial hydraulic jack when pumped in high pressure                                  | Soft, fine – grained soils, foundation soils with large voids or cavities | Unlimited but a few m usual | Batching equipment, high pressure pumps, hoses   | Soil, cement, water                         | Grout bulbs within compressed soil matrix.                                   | Good for correction of differential settlement, filling large void; careful control required.         | Low material cost, high injection cost. |
|  | <b>4.4<br/>Electrokinetic Injection</b> | Stabilizing chemicals moved into soil by electro-osmosis or colloids into pores by electrophoresis             | Saturated silts, silty clays (Clean sands in case of colloid injection).  | Unknown                     | Dc power supply, Anodes, Cathodes  | Chemical stabilizer, colloidal void fillers | Increased strength, reduced compressibility, reduced liquefaction potential. | Existing soil and structures not subjected to high pressures; no good in soil with high conductivity. | Expensive                               |
|  | <b>4.5<br/>Jet Grouting</b>             | High speed jets at depth excavate, inject, and mix stabilizer with soil to form columns or panels. Deep Mixing | Sand, Silts, Clays  |                             | Special jet nozzle, heavy air compressors, pumps pipes and hoses, high air pressure compressor | Water, stabilizing chemicals                | Solidified columns and walls   | Useful in soils that can't be permeation grouted, precision in locating treated zones.                |   |

|  |                                      |   |  |                                      |   |  |   |   |           |
|--|--------------------------------------|---|--|--------------------------------------|---|--|---|---|-----------|
| <b>5.1</b><br><b>In-Situ Deep Compaction of Cohesionless soils</b> | <b>5.1</b><br><b>Blasting</b>        | Shock waves and vibrations cause liquefaction and displacement, with settlement to higher density | Saturated, clean sands partly saturated sands and silts(collapsible loess) after flooding. | >30 m                                | Jetting or drilling machines                          | Explosives, backfill to plug drill holes, hole casings | Can obtain relative densities to 70-80 %; may get variable density, time-dependent strength gain. | Rapid, inexpensive, can treat any size areas; no improvement near surface, dangerous.   | Low       |
|  | <b>5.2</b><br><b>Vibratory Probe</b> | Densification by vibration, liquefaction induced settlement under overburden                      | saturated or dry clean sand  | 20 m (Ineffective above 3-4 m depth) | Vibratory pile driver and 750 mm dia. open steel pipe | None   | Can obtain relative densities of up to 80 %. Ineffective in some sands.                           | Rapid, simple, good underwater, soft under layers may damp vibrations, difficult to penetrate, stiff over layers, not good in partly saturated soils. | Moderate. |

*Consolidation of soft clay by radial flow*

|  |  |  |   |       |  |   |   |   |                  |
|--|--|--|---|-------|--|---|---|---|------------------|
|  | <b>5.3 Vibro Flotation</b>                       | Densification by vibration and compaction of backfill material               | Cohesionless soils with less than 20 % fines            | 30 m  | Vibroflot, crane, pumps                        | Granular backfill, water supply                         | Can obtain high relative densities, good uniformity   | Useful in saturated and partly saturated soils, uniformity  | Moderate         |
|  | <b>5.4 Compaction Piles</b>                      | Densification by displacement of pile volume and by vibration during driving | Loose sandy soils, partly saturated clayey soils, loess | >20 m | Pile driver, special sand pile equipment       | Pile material (often sand or soil plus cement mixtures) | Can obtain high densities, good uniformity            | Useful in soils with fines, uniform compaction, easy to check results: slow, limited improvement in upper 1-2 m.                        | Moderate to high |
|  | <b>5.5 Heavy Tamping (Dynamic-Consolidation)</b> | Repeated application of high intensity impacts at surface                    | Cohesionless soils, waste fills, partly saturated soils | 30 m  | Tampers of up to 200 tons, high capacity crane | None  | Can obtain good improvement and reasonable uniformity | Simple, rapid, suitable for some soils with fines, usable above and below water; requires control must be away from existing structures | Low              |

|                      |                        |  |  |  |  |   |  |  |   |
|----------------------|------------------------|--|--|--|--|---|--|--|---|
| 6.<br>Precompression | 6.1<br>Preloading      | Load is applied sufficiently in advance of construction so that compression of soft soils is completed prior to development of the site.   | Normally consolidated soft clays, silts, organic deposits, completed sanitary landfills. |  | Earth moving equipment, large water tanks or vacuum drainage systems sometimes used, settlement markers, piezometers | Earth fill or other material for loading the site; sand or gravel for drainage blanket. | Reduced water content and void ratio, increased strength                   | Easy, theory well developed, uniformity: requires long time (Vertical drains can be used to reduce consolidation time )                        | Low (Moderate if vertical drains are required ) |
|                      | 6.2<br>Surcharge Fills | Fill in excess of that required permanently is applied to achieve a given amount of settlement in a shorter time; excess fill then removed | Normally consolidated soft clays, silts, organic deposits, completed sanitary landfills. |  | Earth moving equipment settlement markers, piezometers   | Earth fill or other material for loading the site sand or gravel for drainage blanket.  | Reduced water content, void ratio and compressibility; increased strength. | Faster than preloading without surcharge, theory well developed; extra material handling can use vertical drains to reduce consolidation time. | Moderate  |



|  |                              |   |   |                |  |  |  |  |      |
|--|------------------------------|---|---|----------------|--|--|--|--|------|
|  | <b>6.3 Electro Osmosis</b>   | DC current causes water flow from anode towards cathode where it is removed   | Normally consolidated silts and silty clays |                | DC power supply, wiring, metering system | Anodes(usually rebars or aluminum) cathodes(well points or alloys) | Reduced water content and compressibility, increased strength, electrochemical hardening by sacrificial anode. | No fill loading required, can use in confined areas, relatively fast; non-uniform properties between electrodes, no good in highly conductive soils, only small area can be treated. | High |
|  | <b>6.4 Well Point System</b> | Well points are placed by jetting the annular space between the well point and the hole is filled with sand. This permits drainage of all the previous strata through the well point. Group of well | Large sandy areas                           | Shallow depths | Horizontal pipes, pumps                  | None   | -----  | In the fine silts and fine varved deposits, well points may not be able to function efficiently.   |      |

|  |  |   |  |                |       |       |       |   |          |
|--|--|---|--|----------------|-------|-------|-------|---|----------|
|  |  | points are connected together to horizontal pipes called headers and these in turn lead to pump.  |  |                |       |       |       |   |          |
|  | <b>6.5 Cohesive Non Swelling (CNS) Layer</b> | CNS layer thickness compatible to swelling pressure is interposed between the black cotton soil and the wing wall or the foundation of a structure or canal bank. | Stabilizing slopes, cuts in embankment | Shallow depths | ----- | ----- | ----- | To resist the swelling pressure being transmitted to the wing wall or any foundation. | Moderate |

Combinations of the two methods may be possible. One example would be the treatment of a cohesive soil backfill so it could be used in a permanent reinforced earth structure. Another might be the development of a technique that results in high strength so that ground may be utilized for the desired purpose.

Finally, three further aspects of soil improvement will gain consideration in the years ahead. Energy costs, both for producing the needed materials and for carrying out the work in the field, eco-friendly materials supporting green revolution and contributing in reducing global warming problems will be of increasing importance. Thirdly, increased attention should be given to the long term response of materials that are added to the ground.

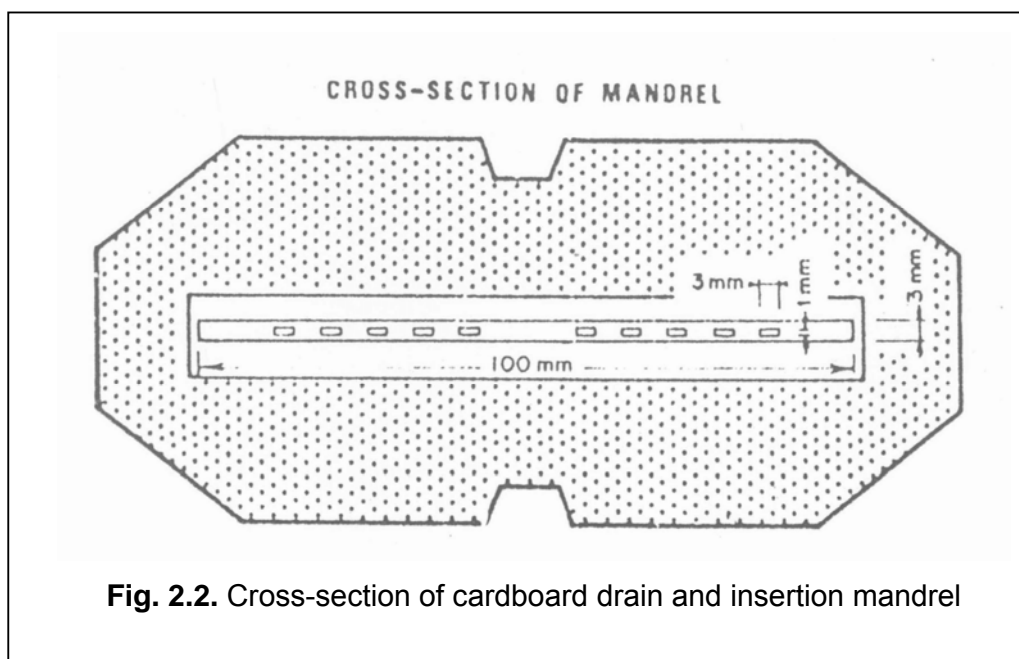
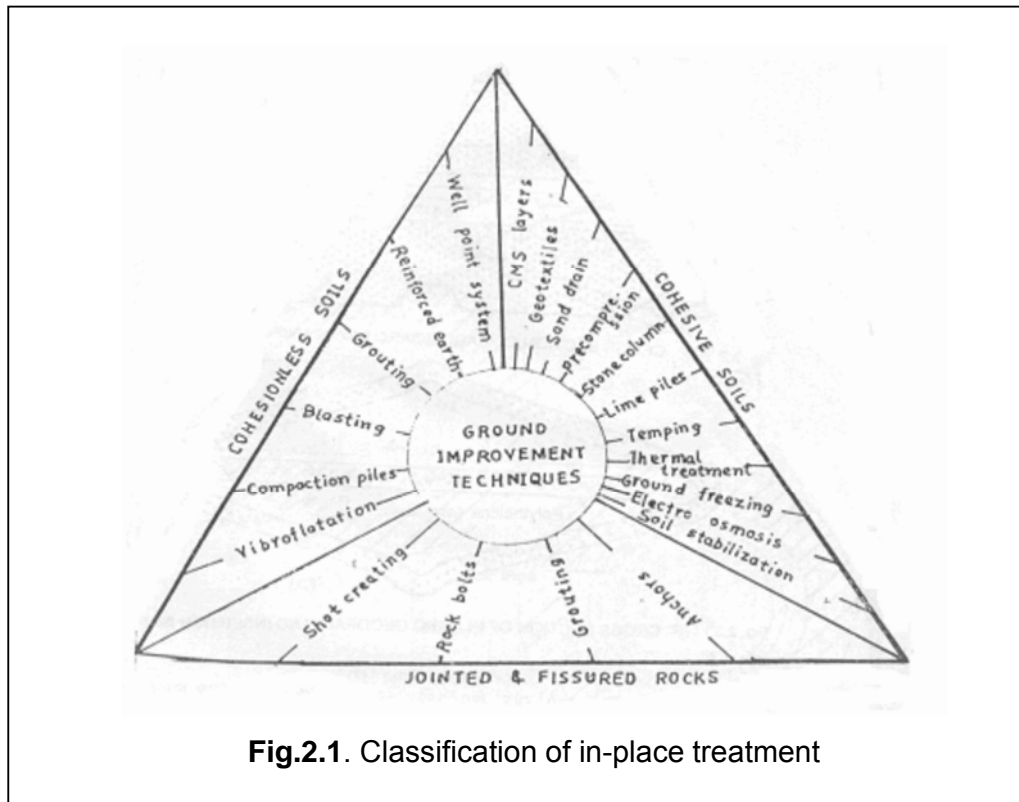
### **2.3 Type of Vertical Drains**

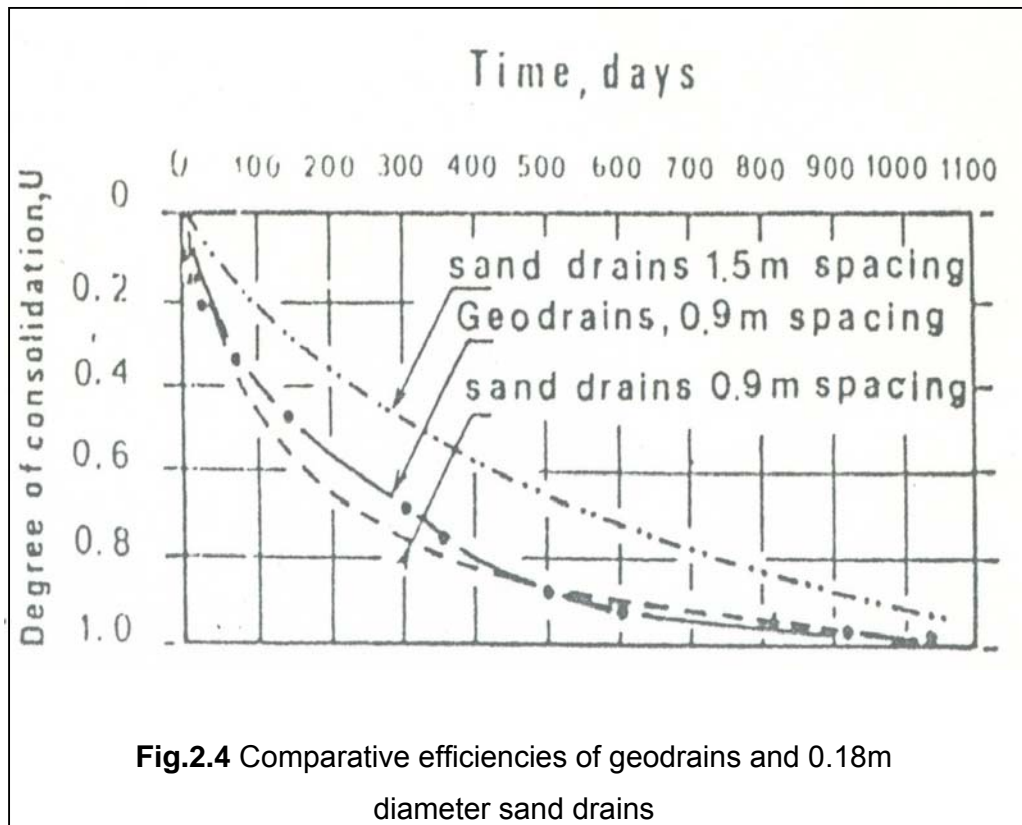
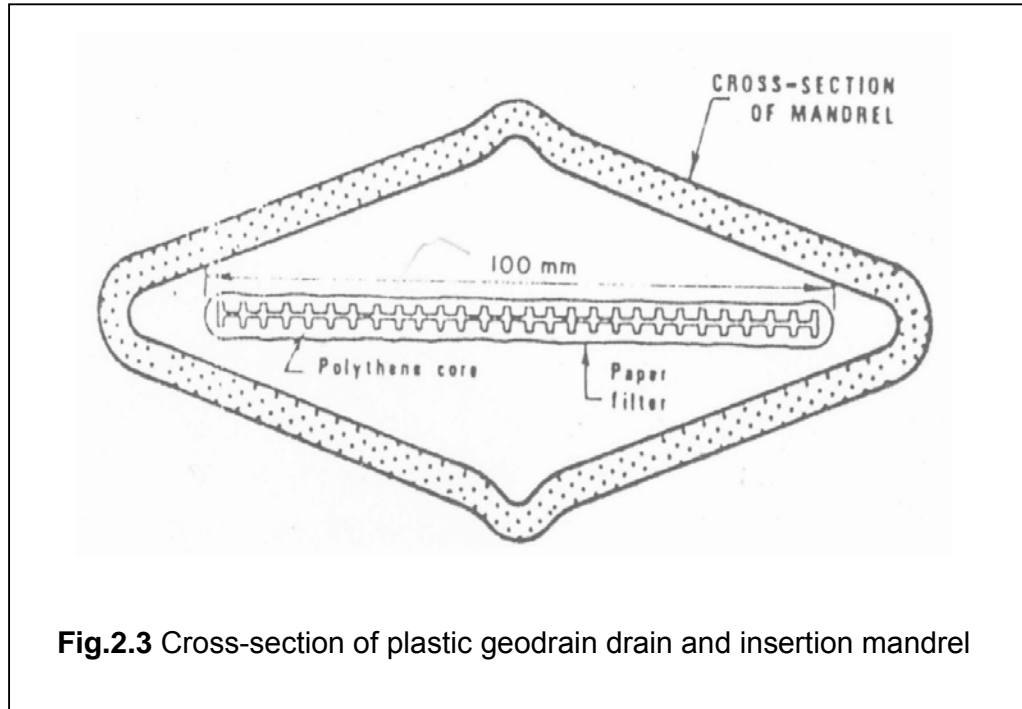
Acceleration of consolidation by different methods is widely used for improvement of soil. From 1930's sand drains have been used extensively for improving soft clays. This is done basically by employing concrete pile driving equipment which involves driving a casing with expandable shoe, followed by filling up with sand and subsequently extracting the casing 400 to 500 mm diameter drains are normally used for such work. In this context, Barron's study indicated the advantage of using smaller diameter drains, but it was found that arching of sand in the casing does not allow a very small diameter sand drain to be installed by the conventional technique.

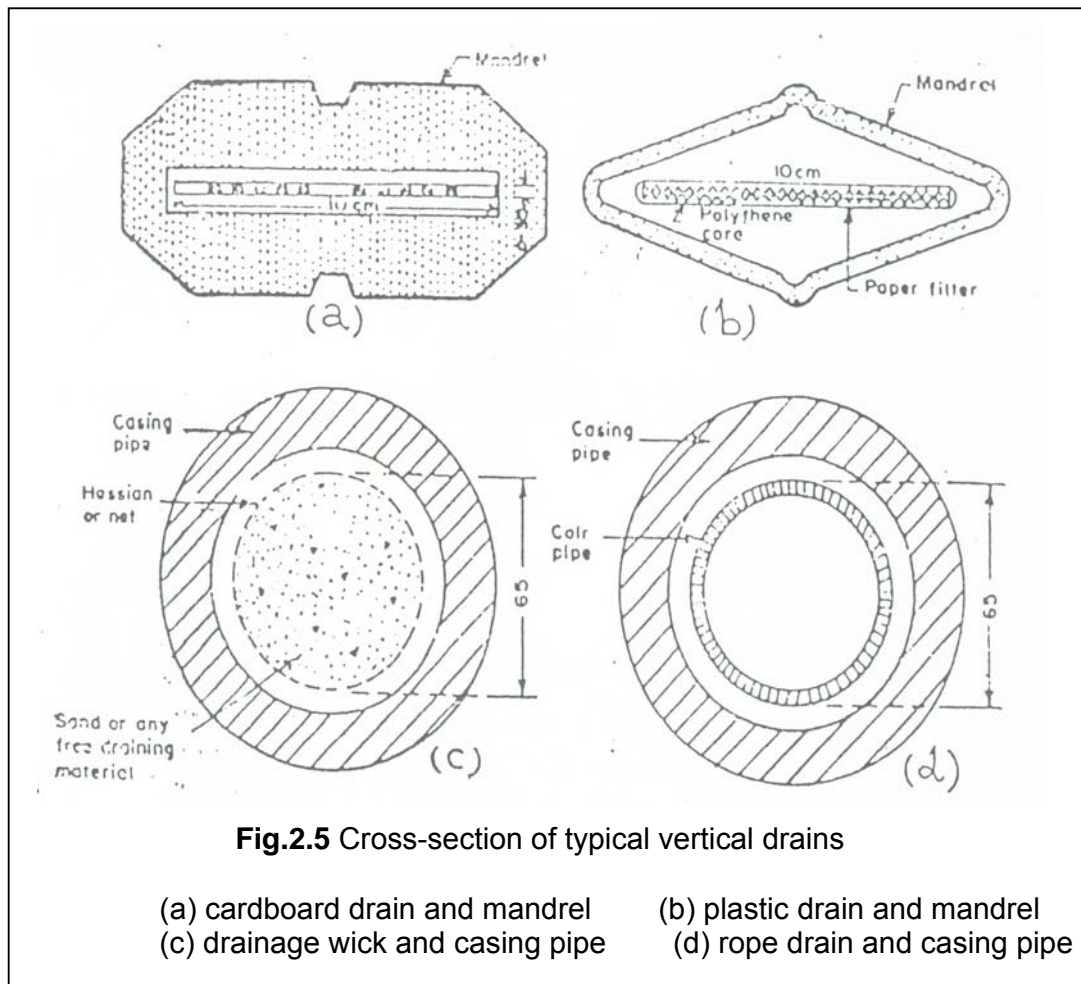
It was found that for drains longer than 20 m it is necessary to have more than 400 mm diameter drain. For smaller depths the diameter could be decreased, but even then for a 10 m long drain the diameter could not be reduced below 300 mm, Christie (1959). Many attempts were made in the 1960's to have smaller diameter sand drains, mainly using some form of jetting. By and large over the years sand drains, have been superseded by other forms of vertical drains. Only in recent years a novel technique of forming 200 mm diameter sand drain has been developed, Datye (1981).

The first break through in the construction of vertical drains took place in Sweden by Kjellamann (1948) with use of cardboard. These first card board drains were 100mm wide and 3 mm thick but other sizes have been used subsequently. Similar drains using different materials like plastic drains, fabric

drains and Geodrains are in use now days. These drains are termed as Geodrains. (Refer Fig. 2.1 to Fig. 2.5)







## 2.4 Sand Drains

Sometimes the natural rate of consolidation of a particular soil is too slow, particularly when the layer overlies an impermeable material and in order that the structure may carry out its intended purpose, the rate of consolidation must be increased. An example of where this type of problem can occur is an embankment designed to carry road traffic. It is essential that most of the settlement has taken place before the pavement is constructed if excessive cracking is to be avoided. This can be achieved by the installation of a system of sand drains, which is essentially a set of vertical boreholes put down through the soil layers, ideally to a firmer material and then backfilled with draining material, such as suitable graded sand. The preload is left in place prior to the construction of the intended structure long enough to induce settlement and then is removed. On thick deposits of soft clay, preloading alone may take a long time to bring about significant compression. In such circumstances, construction of sand drains alone or used in conjunction with preloading offer an effective

technique for ground improvement. Installation method of sand drain is subject to various disturbing effects, viz. smear, soil displacement and remoulding effects such as coating the sides of the drains with a thin film of mud and contamination of thin sand layers. Such disturbances have led to the trend of using drains of different materials, especially geodrains. Yet sand drains prove to be efficiently cost effective in developing countries in large projects, where improvement is required for quite a big area.

By the model law of consolidation, time required for consolidation varies as the square of the length of drainage path, which is the distance that a particle of pore water must travel upon expulsion. If for instance, the drainage path is reduced from  $H$  to  $H/2$ , the rate of consolidation increases four times. Thus, a vertical sand drain brings about a more than 2-fold decrease in the length of the drainage path because of the radial drainage of water towards the vertical drain. The horizontal distance for drainage, in case of sand drains is many times shorter than the distance for draining vertically, i.e.  $R < H$ , where  $R$  is radius of soil sample and  $H$  is height/thickness of soil sample.

Besides, the horizontal permeability of a cohesive soil is usually larger than its vertical permeability because of smaller size of the clay particles. Fig. 2.6 shows schematic view of installation and functioning of vertical sand drains.

Sand drains accelerate the expulsion and draining away of the pore water squeezed out of the voids of the soft soil by the earth fill, or by a structural load. Thus it speeds the rate of consolidation, relieves hydrostatic excess pressure and accelerates the increase in shear strength.

## **2.4.1 Salient Features of Sand Drain**

### **2.4.1.1 Diameter of Drains**

Varies in practice from 450mm in diameter to about 600mm in diameter.

### **2.4.1.2 Spacing of Sand Drains**

This depends on the type and permeability of the soil. Generally 2m to 5m center to center spacing is practicable. Sand drains are effective if the spacing is less than the thickness of the consolidating layer;  $2H$ .

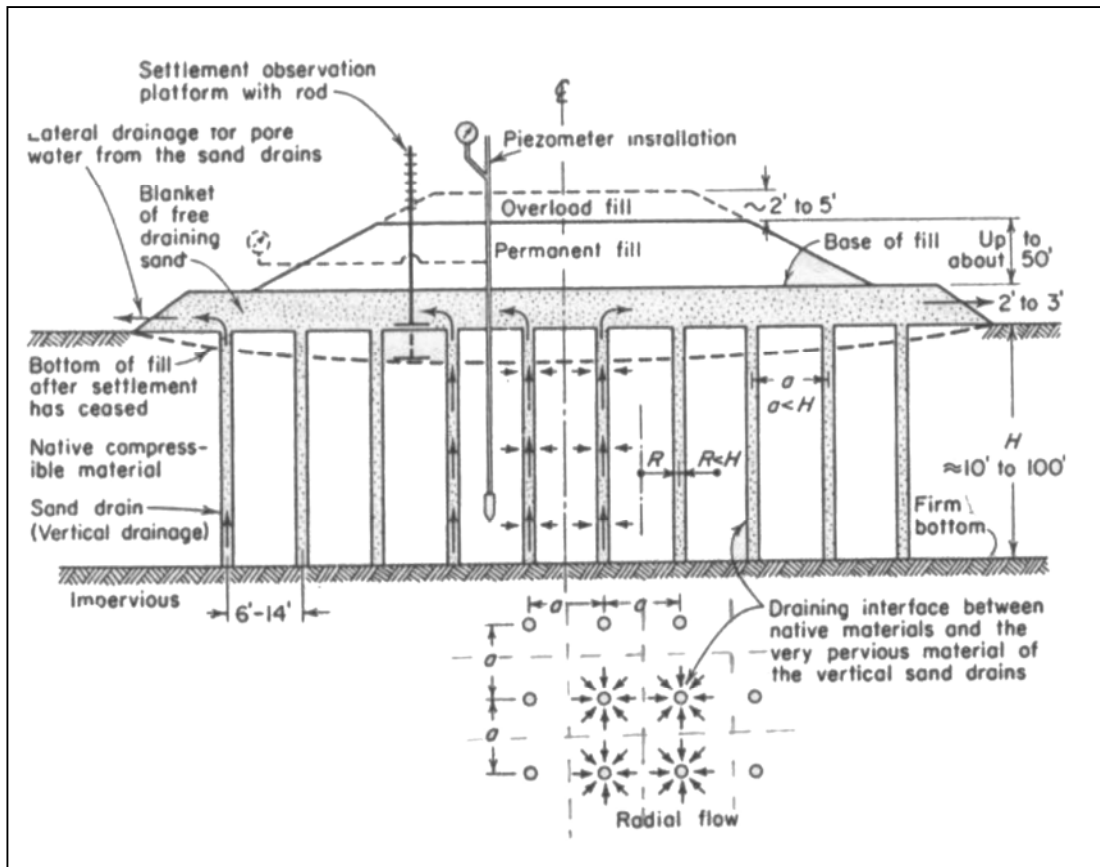


**Fig.2.6** Installation and Function of vertical sand drains

#### 2.4.1.3 Depth of Sand Drains

Sand drains have been placed to a depth from 4m to 25m and in some cases even upto 40m.

#### 2.4.1.4 Installation of Sand Drain

A sand drain is now usually installed by means of hollow steel pipe called mandrel which acts as a casing during the filling of the sand drain.

#### 2.4.1.5 Properties of Sand for Drains

The permeability of sand should be between  $k = 10^{-3}$  cm/sec and  $k = 10^{-4}$  cm/sec for application as sand drains. California Department of Highways has given following specifications.



**Table 2.2:** Grading Requirements for Sand Drain

| Sieve size | Percent Passing |
|------------|-----------------|
| 0.5"       | 90-100          |
| No. 8      | 25-100          |
| No. 30     | 5-50            |
| No. 50     | 0-20            |
| No. 100    | 0-3             |

According to other specification suggested by Kremer, Meyvogel, Weele and Jager, the percentage of particles, passing the 63 $\mu$ m sieve shall be less than 5 % of the fraction passing the 2 mm sieve. The proportion of sample that remains on the 250  $\mu$ m sieve shall not be less than 50 %. The loss due to heating to 960°C for the fraction smaller than 2 mm shall not be more than 3 %. The permeability of the sand should be  $k > 1.4 \times 10^{-4}$  m/s.

#### 2.4.2 Blanket

The blanket provides lateral drainage of pore water at the base of the fill from vertical sand drains. It is sometimes specified that the blanket material should contain not more than 5 % to 10 % of (-200) material (<0.074mm)

California Department of Highways has given following specifications:

**Table 2.3:** Grading of Blanket Material (Clean, coarse sand or Gravel)

| Sieve size | Percent Passing |
|------------|-----------------|
| 0.375"     | 80-100          |
| No. 8      | 5-50            |
| No. 30     | 0-20            |
| No. 50     | 0-5             |

#### 2.4.3 Arrangement of Drains

A typical arrangement of sand drains is shown in Fig.2.7. There are two situations when the sand drains are made to puncture through an impervious layer, when there is a pervious layer beneath it. This creates 2-way vertical

drainage as well as lateral and results in considerable speeding up of consolidation.

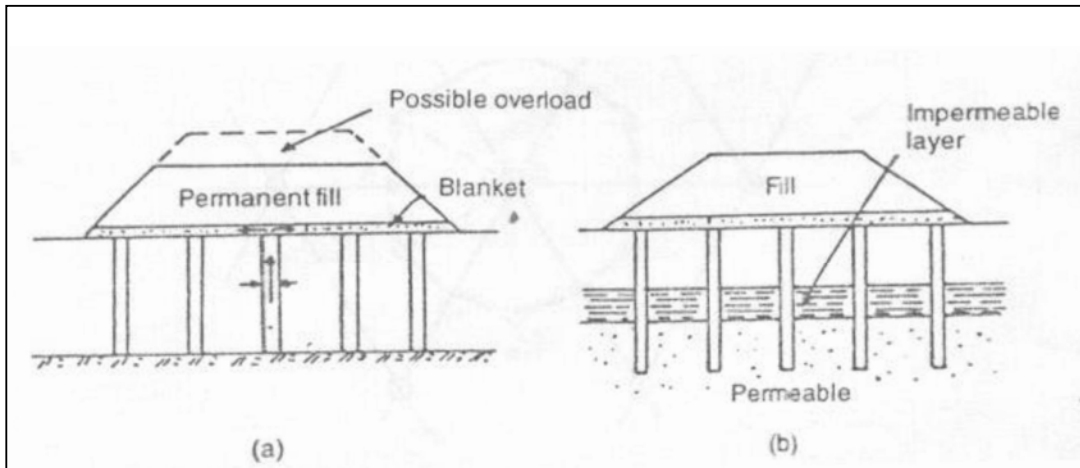


**Fig.2.7** Typical arrangements of sand drain

#### 2.4.4 Rate of Loading

The purpose of controlling the rate of construction of an earth embankment is to prevent the rupture of the native soil, and the shearing off of the sand drain which result in lateral displacement of the earth mass and/or formation of mud waves. The devices for controlling the rate of settlement of the fill and the development pore water pressures at various depths in soil underneath the fill are settlement observation platforms and the piezometers. The order of magnitude of induced pore water pressures while filling the embankment is up to  $80 \text{ kN/m}^2$  to  $105 \text{ kN/m}^2$ . By correlation of the rate of consolidation of the native soil with the pore water pressures at various depths in the native soil, it is possible to estimate the rate of loading viz, rate of application of the next safe lift of the fill material.

The amounts of settlement of soil from 1.2m to 6m have been attained in various instances without failure in shear.

#### 2.4.5 Remarks on Vertical Sand Drains

- Because of the low permeability of clay, little excess pore water can be drained out of the clay during the construction period of an earth embankment.
- Sand drain constitutes supplementary outlets for the excess pore water.

- Compressible soils with sand drains settle more rapidly than those without drains.
- Sand drains hasten primary consolidation.
- The higher horizontal permeability of the soil as compared to the vertical permeability allows quicker drainage of pore water and accounts for the effectiveness of sand drains in consolidating a soil.
- Consolidation by means of sand drain can be brought about easily in a relatively short time, 3 to 12 months, depending upon the thickness of the consolidating layer of soil, among other conditions and helps in attaining most of the settlement during the construction period of the fill.
- Sand drains are relatively weak in shear, particularly if shearing is effected by lateral displacement of the soil mass underneath the fill. Therefore the rate of loading the fill must be such as not to cause failure in shear of the soil mass.
- Vertical sand drains accelerate the increase in shearing resistance of the native material.
- Sand drains are successfully applicable where soil, drainage and geological conditions are proper and suitable for sand drains to apply.
- The theory of the functioning of the sand drains the pore water pressure relationships and the solution of spacing of vertical sand drains is based on advanced higher mathematics and requires the use of Bessel functions.
- To receive adequate drainage properties, sand has to be carefully chosen which might seldom be found close to the construction site, Yeung (1997).
- Drains might become discontinuous because of careless installation or horizontal soil displacement during the consolidation process.
- During filling bulking of the sand might appear which could lead to cavities and subsequently to collapse due to flooding.
- Construction problems and/or budgetary burdens might arise due to the large diameter of sand drains.
- The disturbance of the soil surrounding each drain caused by installation may reduce the permeability, the flow of water of water to the drain and thus the efficiency of the system.

- The reinforcing effect of sand drains may reduce the effectiveness of preloading the subsoil.

## **2.5 Sandwicks**

Now there are wide variety of vertical drains available, falling into two groups; the round and the band drains. Round drains include the traditional sand drain as well as the prefabricated sandwicks and wrapped pipe drains. Sandwicks are prepacked in a filter stocking and placed in a predrilled hole or into a mandrel, Hughes and Chalmers (1972). They were first produced with woven jute stockings but in recent years, polypropylene woven and melt-bounded fabrics are commonly used. Besides giving economy in the amount of sand, the stocking permits a large variety of drilling and driving methods to be used so that one can vary the installation equipment to suit the site and soil conditions and provide minimum disturbance and the economy.

The fabric stockings allow the sandwicks to be extremely flexible and tenacious. The ability to stretch and compress at various points in their length is an essential requirement for most prefabricated drains as it enables them to cope with vertical settlements and lateral deformations. The granular soil filling in sandwicks ensure that the drain remains open no matter what the outside soil pressure; provided the filter fabric is chosen carefully, neither it nor the sand should clog, so that the hydraulic discharge capacity of sandwicks is usually adequate. Wrapped flexible pipes drains consist of flexible usually corrugated plastic pipes surrounded by either a natural fiber layer or an engineering filter fabric similar to that used for sandwicks. They can be placed using almost all of the drilling and driving systems of installation. However, they are more usually placed inside a round mandrel. A non recoverable conical sealing and driving tip is used to anchor the pipe on withdrawal of the mandrel.

This drainage system has the advantage that checks can be made down the pipe to establish that there is continuity and clogging has not occurred. Dastidar (1969) described the use of prefabricated sandwich for the strength improvement of coastal marine clays at Kandla, India

### **2.5.1 Remarks on Vertical Sandwichs**

- As outer cover of drain is either made from geotextile or polypropylene the clogging potential of clay reduces greatly and due to this rate of consolidation increases more rapidly compare to sand drain which is in direct contact with soil.
- Due to continuity of outer cover made from various synthetic materials there installation becomes easy because nearly of circular shape filler material gets more densely packed and so bulging and shearing is greatly reduced compare to sand drains.
- As filler material sand does not get clogged easily various gradations of sand can be altered to get maximum advantage economize the overall cost of project.
- Sandwichs of smaller diameter is more efficient as compared to sand drain of higher diameters.
- During its installation smearing effect is sometimes more pronounced if proper boreholes are not made and if its vertical alignment is not checked at regular intervals.
- Dissipation of excess pore water pressure is rapid but lack of proper code provisions and guidelines have restricted the use of sandwichs in field.
- It was concluded that coefficient of consolidation through radial drainage  $C_r$  is significantly higher than due to vertical flow  $C_v$  for all load intensity.

### **2.6 Prefabricated Vertical Drains (Band Drains)**

The prefabricated vertical drains(band drains)/geodrains, commercially available in market, are superior to displacement sand drains with regards to disturbance and their continuity is not threaten by soil movements, irrespective of whether they take place in horizontal or vertical direction. Also time of installation is greatly reduced.

Kjellmann (1937) first reported the use of prefabricated geodrain. The band shaped prefabricated geodrain was made available in market by 1939. Wager reported about this geodrain, consisting of a grooved plastic core surrounded by wet resistance filter paper.

### **2.6.1 Wrapped Flexible Pipe Drains:**

It consists of flexible, usually corrugated plastic pipes, surrounded by either a natural fiber layer or an engineering filter fabric similar to that used for sandwicks. It can be placed using almost every drilling and driving systems available. However, generally they are placed inside a round mandrel. A non recoverable conical sealing and driving tip is used to anchor the pipe on withdrawal of the mandrel.

### **2.6.2 Band Drains:**

There are several types of band drains widely used. E.g. Alidrain, Castle drain boards, Colband drains, Mebra paper filter and polyester drains as shown in fig.2.8 (a). Band drain and round drains are the geodrains available today in the market. Band drains are placed by displacement methods. Band drains is introduced at the top of site to be installed by a system of rollers as described in fig.2.8 (b). As band drains are light, they need to be protected from wind and weather.

Runesson et al. (1977) using a band shaped vertical drain, the Kjellman's assumption that draining effect of a drain depends, to a great extent, upon the circumference of its cross sectional area. He used finite element method for analysis of the data.

Hansbo (1979) gave a simple solution for the consolidation of fine grained soils using a prefabricated band shaped drain, with regard to well resistance and smear and he has concluded that at higher discharges, well resistance is reduced and efficiency of drain improved. He recommended that filter around the vertical channels of core should be fine enough to prevent the entry of fines. This would reduce the long term discharge capacity of the drain.

Vreeken, Berg and Loxham (1983) investigated the effect of interface erosion of particles on the performance of band shaped vertical drain. It was noted that permeability of clay around filter of stand pipe changed remarkably during experiment due to erosion of particles. It was seen that permeability did not change significantly in stand pipe. It was also found that particle concentration in stand pipes were independent of time and ground water gradient.

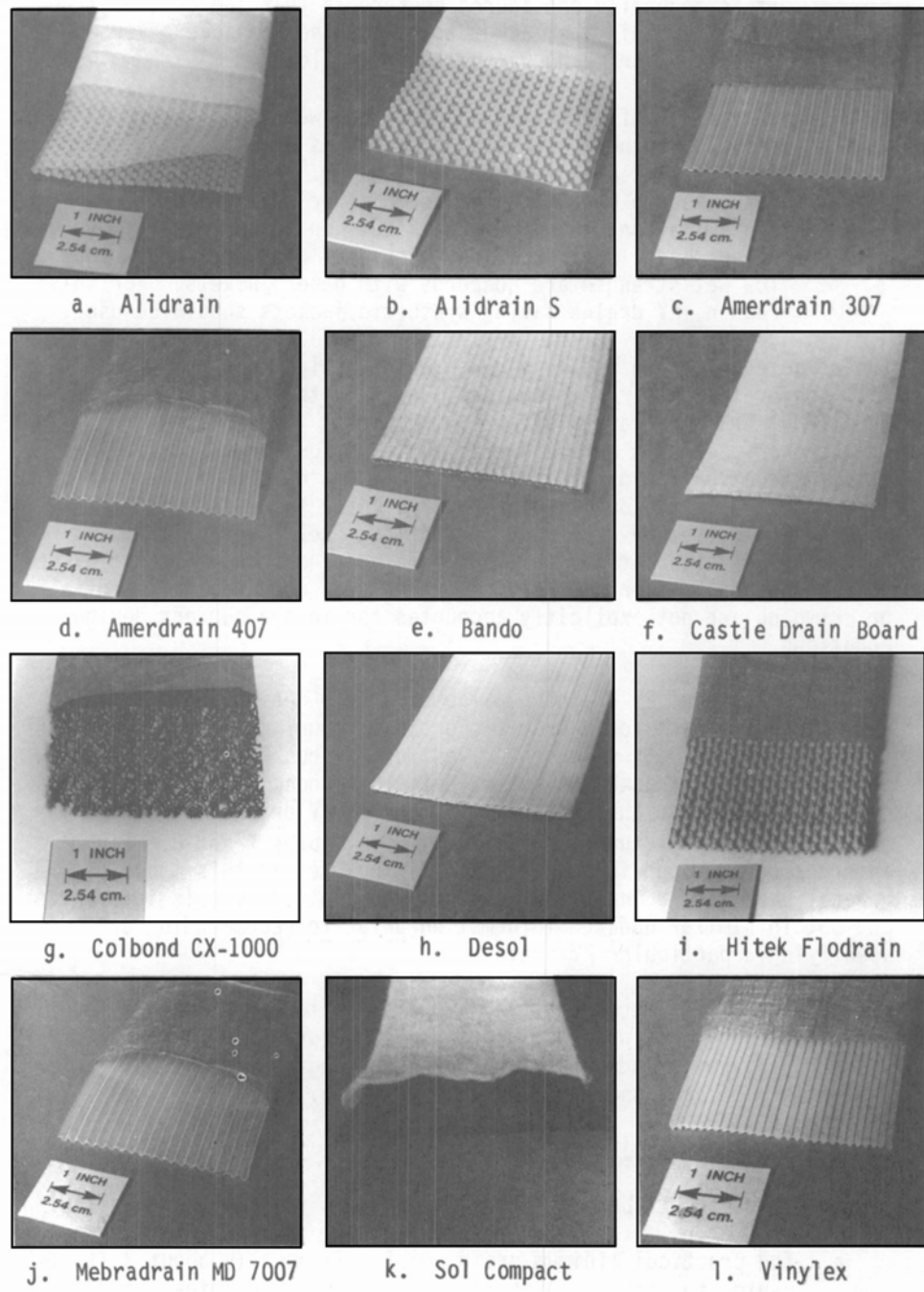


**Fig.2.8(a):** Typical PV drain products

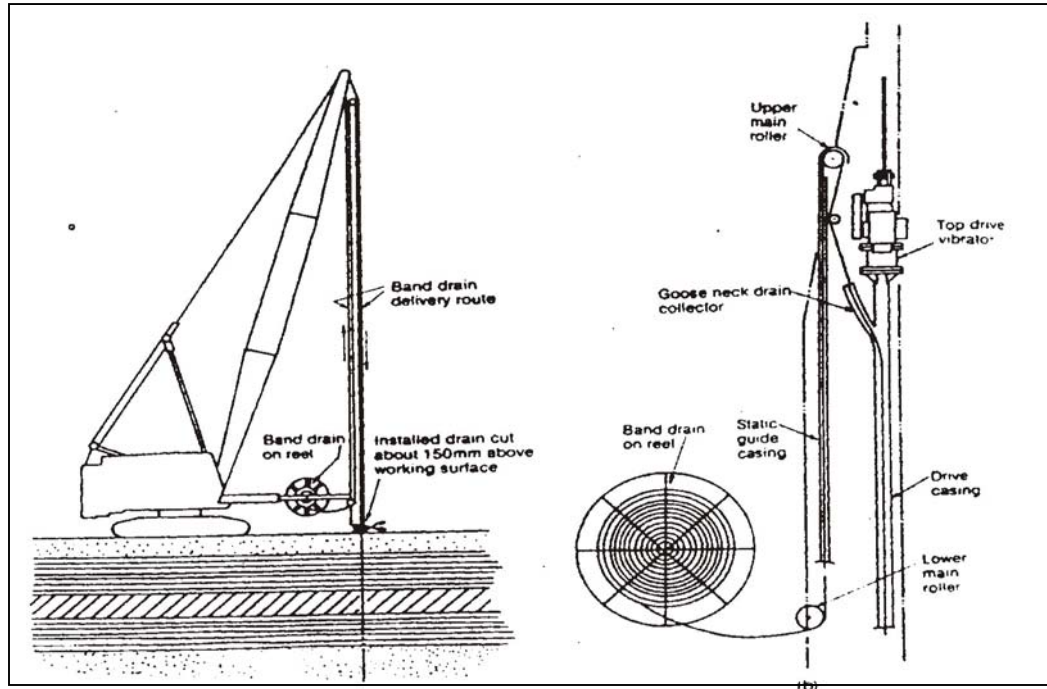


**Fig.2.8 (b)** Sketch of band drain installation rig and band drain delivery arrangement

### 2.6.3 Polypropylene Wick Drains:

Burke and Smucha (1981) described a polypropylene wick geodrain installed at Lornex dam in USA. The starter dam is a zoned earth embankment constructed of locally borrowed soils, as shown in Fig.2.9. It had crest width of 15m at elevation of 1146m length of approximately 830m, and volume of  $3.5 \times 10^6 \text{ m}^3$ . A zone of more permeable sand and gravel was used in the downstream shell to control seepage. Seepage through sandy layers in the soft deposits under the dam was controlled by the upstream blanket and the cutoff which extended down to the underlying glacial till. The geodrains shown in Fig. 2.10 which was used to drain the soft foundation, consisted of a multi-ribbed polyethylene plastic core 100mm wide by 4mm thick enclosed in a heavy filter paper cover. Use of this wick type of geodrain to enhance the strength of soft soil was found economical and cheaper as compared to other available method. Geodrain used was made of a multiribbed polyethylene plastic core, 100mm wide and 4mm thick, enclosed in a heavy filter paper cover. Geodrains were installed in dam. Geodrain enabled the early consolidation of soft soil foundation increasing the shear strength of soil at greater rate leading to completion of dam in two seasons and substantial saving in cost of project was made possible.



### 2.6.4 Wrapped and Unwrapped Drains:

Ali and Young (1988) used wrapped and unwrapped vertical drains to investigate the effect of lateral pressure on discharge capacity of drains at different hydraulic gradients. The two drains to be tested were cut to a length of 480mm and were inserted into rubber membranes before being pushed through the slot. Rubber membrane was used to prevent seepage from the drain the surrounding soil, which otherwise will not give actual discharge capacity of drain at the outlet tank. Ali and Yong recommended that vertical drains should be wrapped in geotextile to prevent the clogging of the drainage path. It was also confirmed that composite drains, wrapped with woven geotextile performs better than those wrapped with non-woven geotextile.

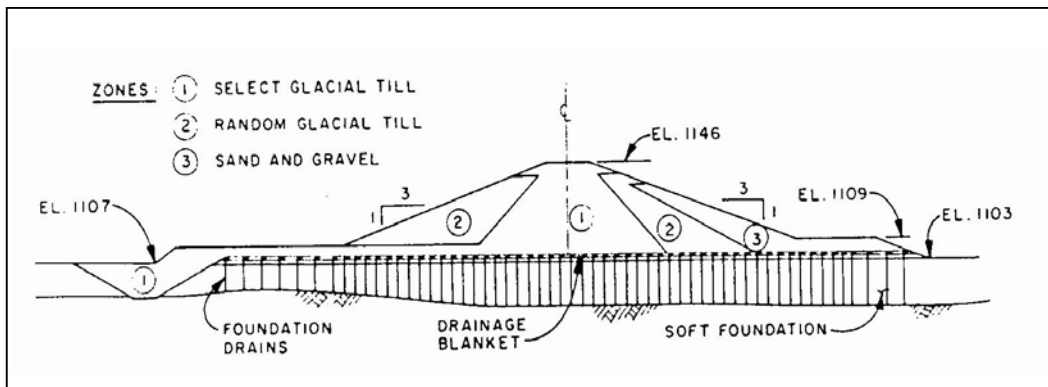


**Fig. 2.9** Typical section of zoned earth embankment, Lornex, USA

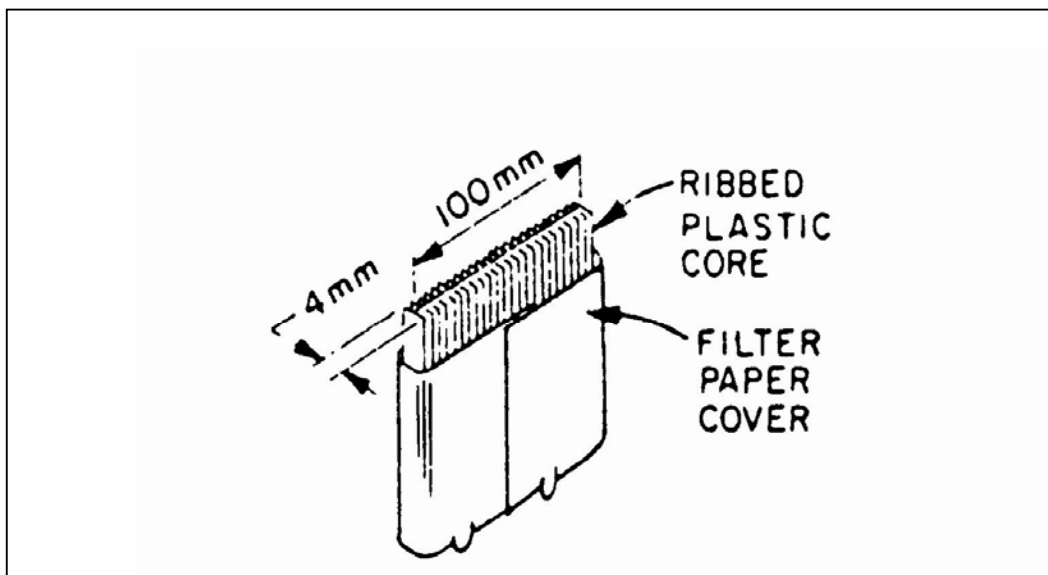


**Fig. 2.10** Typical section of Geodrain

### **2.6.5 Polypropylene Fiber Drain:**

Asundaria and Shroff (1989) examined the influence of prefabricated polypropylene fiber drain with consolidation analysis based on pore pressure dissipation data during consolidation. The drain was made of multifilament woven fabric as filter and polypropylene geotextile fiber as core. It was also concluded that the polypropylene fiber geodrain increased the rate of pore pressure dissipation effectively and allowed early consolidation for as particular construction loading. They recommended the geodrain to be used in field to improve the strength of soft foundation and to economize the ground improvement work.

### **2.6.6 Remarks on Prefabricated vertical drains (Band drains)**

- Band drain constitutes supplementary outlets for the excess pore water.
- Compressible soils with band drains settle more rapidly than those with sand drains.
- Band drains does not hasten primary consolidation.
- The higher horizontal permeability of the soil as compared to the vertical permeability, accounts for the effectiveness of band drains in consolidating a soil.
- Band drains are strong in shear, particularly if shearing is effected by lateral displacement of the soil mass underneath the fill.
- Number of theoretical solutions is available as per field conditions and so its applicability becomes more easy compare to traditional sand drains.
- Due to well established manufacturing process and due to ease in packing, transportation and installation band drains are preferred compared to other circular drains.
- Solutions with and without well resistance and smear effect are know well developed but still considering band drain as an equivalent circular drain in mathematical formulations as an assumption arises number of questions.
- Due to outside synthetic cover and inside corrugated plastic core flow paths or pore water dissipation becomes more fast but still there is no universal theory based on sequence of consolidation (isochrones) with respect to time.

## **2.7 Theoretical Review**

Classical theoretical work of Terzaghi & Frohlich (1936,1943,1948), Rendulic (1935), Biot (1941), Carillo (1942), Silveira (1953) of three dimensional process of consolidation into plane radial flow have been resolved and gave solution by Barron (1948) considering 'equal strain' and 'free strain' conditions with and without peripheral smear and drain well resistance.

Kjellman (1948), Takagi (1957), Crezer (1957) Schiffman (1958), Hansbo (1960,1981), Mc Kinlay (1961), Aboshi (1961), Escario & Uriel (1961), Creyers (1961), Horne & Rowe (1964), DeLean (1965), Mikasa (1965), Christie (1966), Rowe & Barden (1966), Anandkrishnan et al. (1969), Sivareddy (1969), Berry Wilkinson (1969), Simon & Tan (1971), Taytovich et al. (1971), Sills (1975), Yamaguchi et al. (1976), Yoshikuni et al. (1974), Chaput & Thomann (1975), Brenner et al. (1983), Davis & Poulos (1968), Olson et al. (1977), Zeng & Xie (1989) extended the analysis of above classical works incorporating several additional factors viz. magnitude and rate of loading, permeability with respect to stratification, accounting linear and non-linear behavior with void ratio change and gave closed-form solution for pore pressure distribution in three dimensional process of consolidation considering with and without stratification.

Later on, Olson.R.E. et al. (1974), Runesson et al (1985), A.Al Tabbaa et al. (1987,1991), Goughnour.R.R et al. (1992,1994), H.D.lin et al. (1997), XioWuTang et al. (1998,2001), GuoFuZhu et al. (1998,2000), Xu-Sheng et al. (2004), Guo-XiongMei & JianHuaYin et al. (2003), Gorolmai et al. (2002), ToyoakiNogami et al. (2003), Tang et al. (2000,2001), Patrick Fox et al. (2003), Mesri et al. (1994), Leo.C.J (2004), Bergado et al. (1997,2002) have extended Barron's work numerically using Finite element method (FEM) and Finite difference method (FDM) concept for 'Free strain & Equal strain' conditions using appropriate softwares.

Some school of research workers worked numerically by assuming variable permeability of smear zone J.C.Chai et al. (1994,1997,2000,2001), probabilistic design approach by W.Zhov & H.P.Hong et al. (1999), plane strain modeling with smear effects and vacuum consolidation by B. Indraratna et al.

(1997,2000,2005,2008,2010), soil compressibility and smear effects by Basu & Madhav (1993, 2000), closed form solution for ramp loading by Chin Jian Leo (2004) adopting Finite Element approach for the extension of Hansbo's theoretical aspect for 'no smearing and well resistance' condition for band shaped drains.

A review of many assumptions made in the many relevant theories is not possible with the confines of this chapter, but the assumptions made in the recent literatures are summarized below:

### 2.7.1 Terzaghi's Theory

In order to compute the amount of consolidation (or say settlement) after any given time 't', Terzaghi evolved this theory, which considers the very fact that the consolidation is directly based upon the expulsion of pore water. The equation is analogous to flow of heat in anisotropic media. Fig.2.11 shows a clay layer, of thickness H sandwiched between 2 layers of sand which serves as drainage faces.

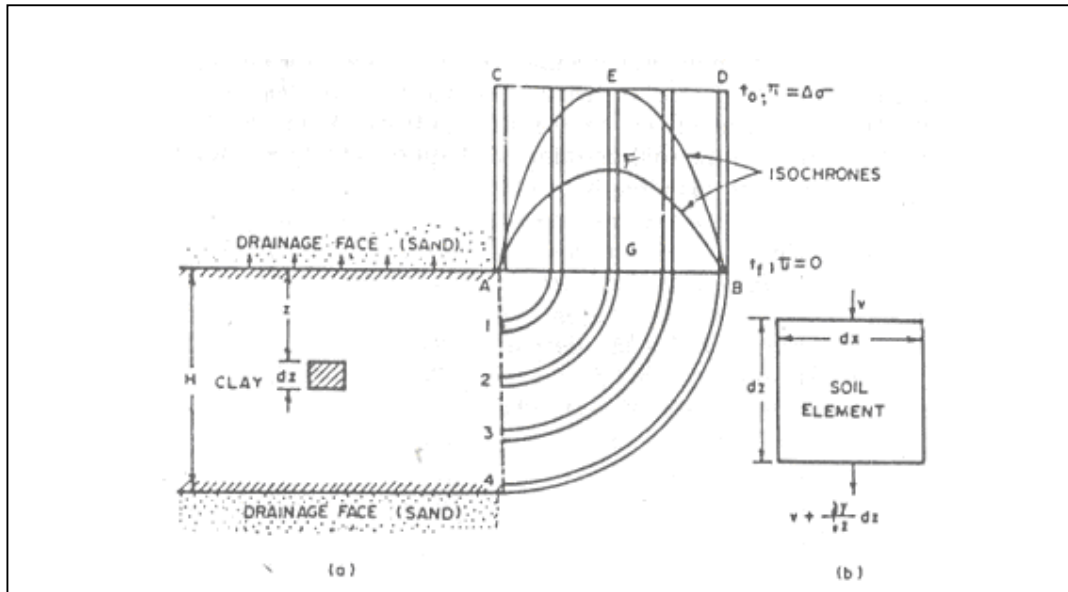


**Fig.2.11:** Terzaghi's one dimensional consolidation

The three dimensional consolidation equation is

$$\frac{\partial u}{\partial t} = C_{vx} \left( \frac{\partial^2 u}{\partial x^2} \right) + C_{vy} \left( \frac{\partial^2 u}{\partial y^2} \right) + C_{vz} \left( \frac{\partial^2 u}{\partial z^2} \right) \text{-----} 2.1$$

Solution of the consolidation equation 2.1 is done by means of Fourier series by using hydraulically boundary conditions.

In the case of sand drains, where the process of three dimensional consolidation is symmetrical about vertical axis, it is more convenient to express equation 2.1 into polar co-ordinates as

$$\frac{\partial u}{\partial t} = C_h \left[ \frac{\partial^2 u}{\partial r^2} + \frac{1}{r} \frac{\partial u}{\partial r} \right] + C_v \frac{\partial^2 u}{\partial z^2} \quad \text{-----} 2.2$$

If the radial flow takes place in planes at right angle to z axis, the term  $\frac{\partial^2 u}{\partial z^2}$  equals to zero and so from equation 2.2 reduces to (Refer Fig.2.12)

$$\frac{\partial u}{\partial t} = C_v \left[ \frac{\partial^2 u}{\partial r^2} + \frac{1}{r} \frac{\partial u}{\partial r} \right] \quad \text{-----} 2.3$$

Fig 2.13, gives the isochrones for different types of drainage and different distributions of consolidation pressures in vertical direction.

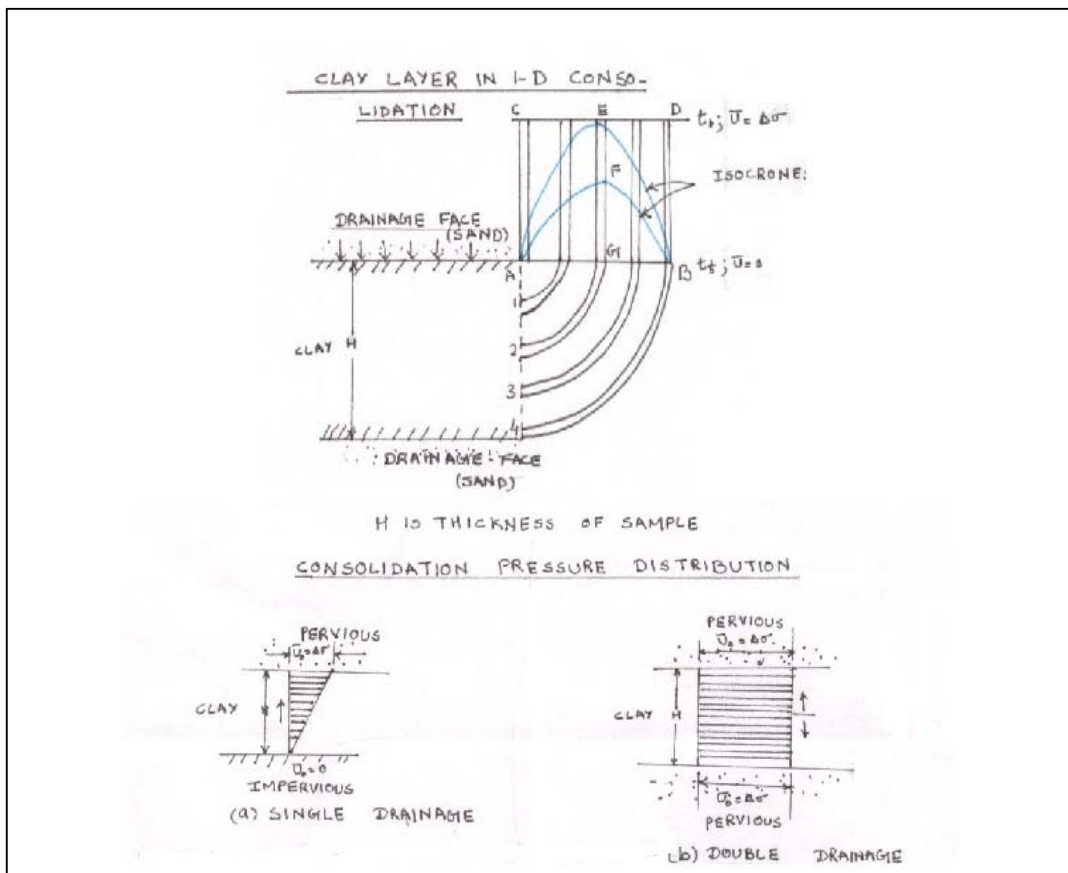
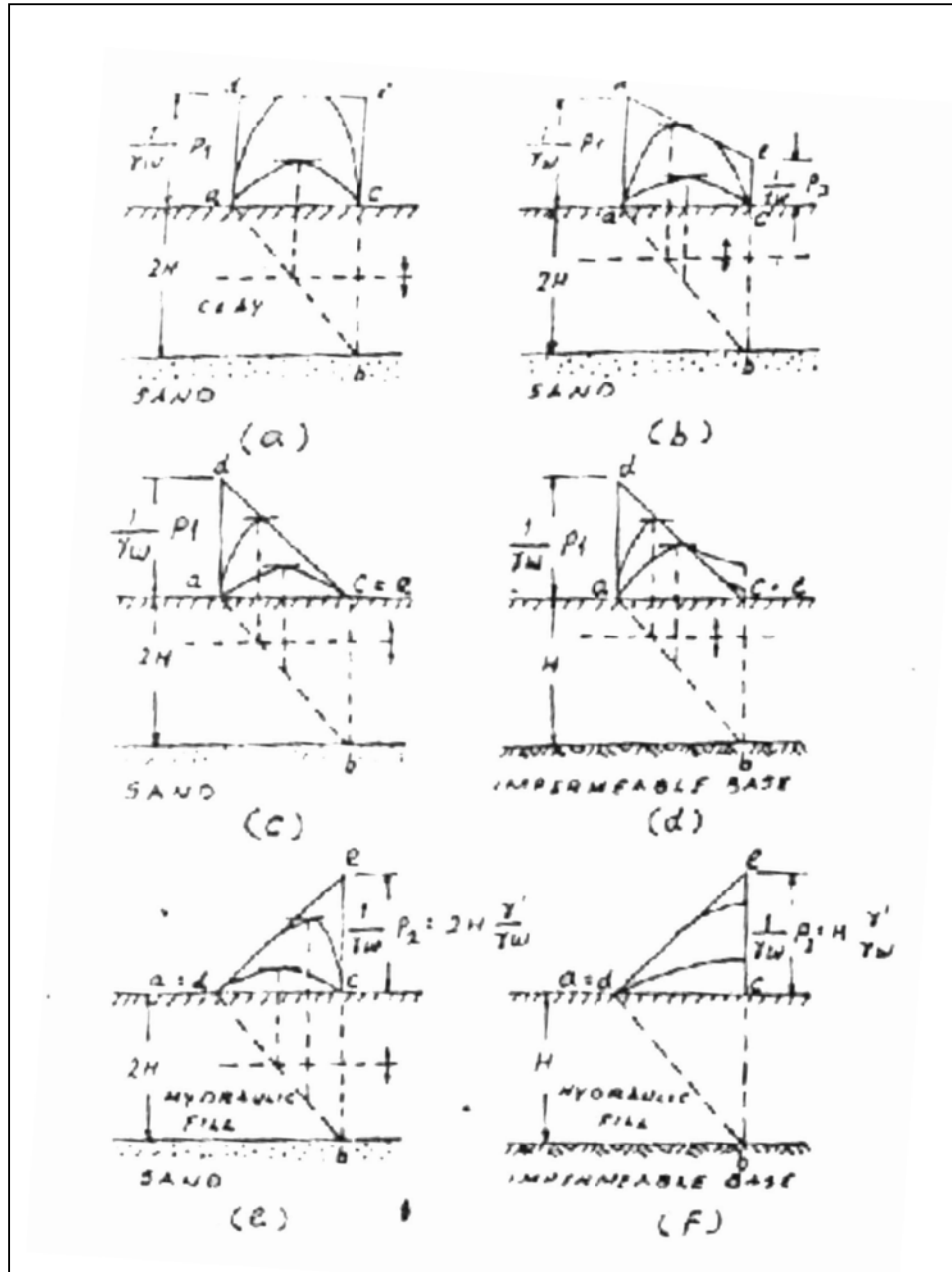
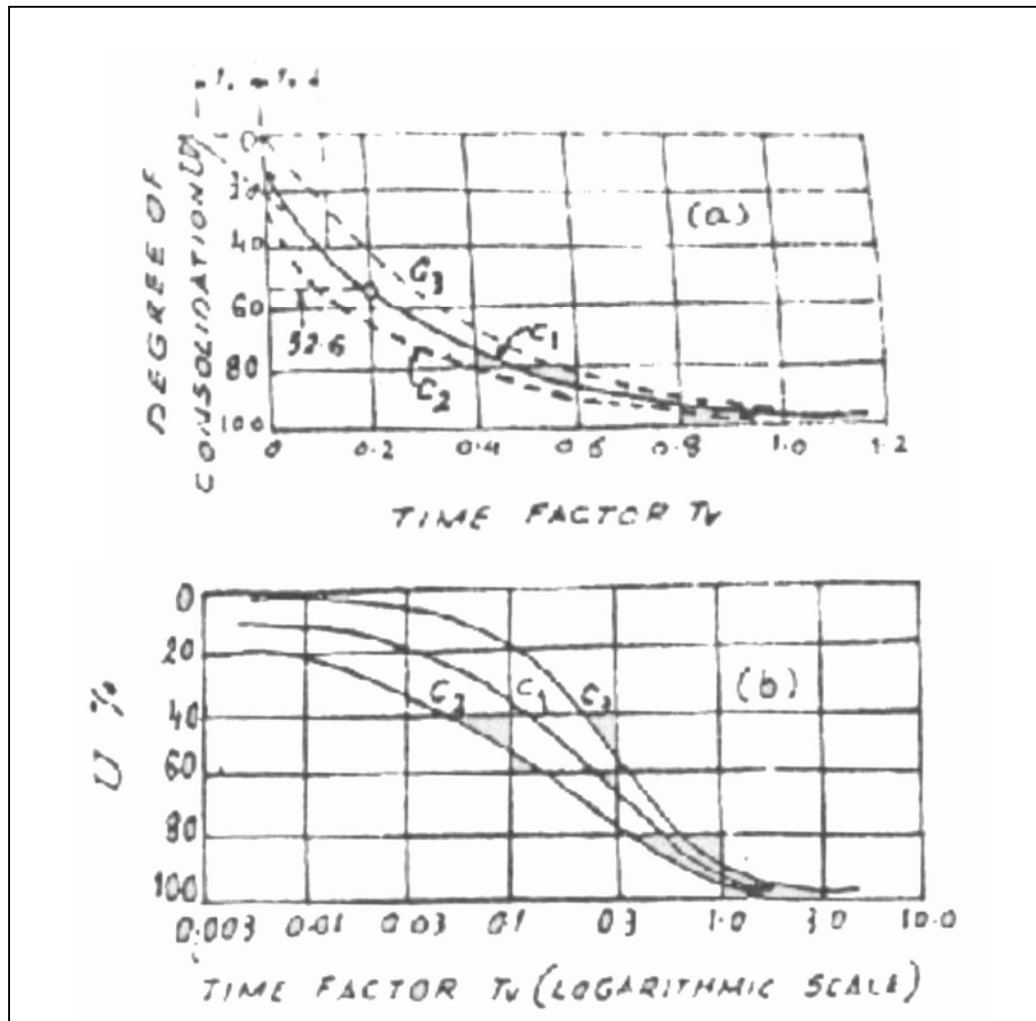


Fig. 2.12 Consolidation pressure distribution diagram



**Fig.2.13:** Isochrones representing progress of consolidation of a layer of ideal clay for different types of drainage (after Terzaghi & Frohlich, 1936)



**Fig.2.14:** Relation between Time factor and degree of consolidation in (a) Time factor plotted on arithmetic scale (b) on a logarithmic scale. The three curves  $C_1$ ,  $C_2$ ,  $C_3$  correspond to three different cases of loading

### 2.7.2 Rendulic's Solution

In case of radial drainage, only Rendulic (1935) showed the relation between the time,  $t$ , and the degree of consolidation,  $U_r$  %, giving the equation

$$U_r \% = 100 F(T_r) \quad \text{-----} \quad 2.4$$

Where  $T_r = (C_h/4R^2) \times t$  is the time factor for consolidation involving horizontal flow out of a cylindrical body with an outer body with an outer diameter  $2R$  towards a central filter well with diameter  $2r_w$ . The relation between the degree of consolidation,  $U_r$  %, and the time factor  $T$ , depends on the value of the ratio  $R/r$ . (Fig. 2.14)

In case of three dimensional flow, if the permeability of the soil in a vertical direction is different from that in a radial direction, the solutions for consolidation of the cylindrical block is given by Carrillo's solution (1942).

### 2.7.3 Biot's Theory (1941)

Biot (1941) presented with an extension of one dimensional case to three dimensional case. Established the validity of equation for any arbitrary load variables with time. Anisotropy of the mass and its influence upon stress distribution and settlement are not considered in his theory, in order to avoid heavy mathematics while presenting.

### 2.7.4 Carillo's Solution (1942)

Resolving the Terzaghi's consolidation equation into a plane radial flow and a linear vertical flow, Carillo (1942) presented a solution for the consolidation of soils. The main consideration of this solution was that at any point, with in the soil prism, which is consolidating under the specified pressure, the ratio between excess hydrostatic pressure at any given time 't' to the initial hydrostatic pressure is the product of the two ratio's obtained by considering the flow perpendicular to two faces first, and then flow perpendicular to the other face only.

In the case of anisotropic soil ( $K_v = K_h$  and  $C_v = C_h$ ), Terzaghi's consolidation equation modified to:

$$\partial u / \partial t = C_h [\partial^2 u / \partial r^2 + 1/r \partial u / \partial r] + C_v \partial^2 u / \partial z^2 \quad \text{2.5}$$

Degree of consolidation U% due to combined linear and radial drainage can be assessed by the equation

$$(100-U) = (1/100) (100-U_z) (100-U_r) \quad \text{2.6}$$

### 2.7.5 Barron's Theory (1948)

The first exhaustive treatment of the problem of the consolidation of a soil cylinder containing a central drain has been presented by Barron. (Fig.2.15) His theory was based on all of the simplifying assumptions of Terzaghi's uncoupled one dimensional consolidation theory.



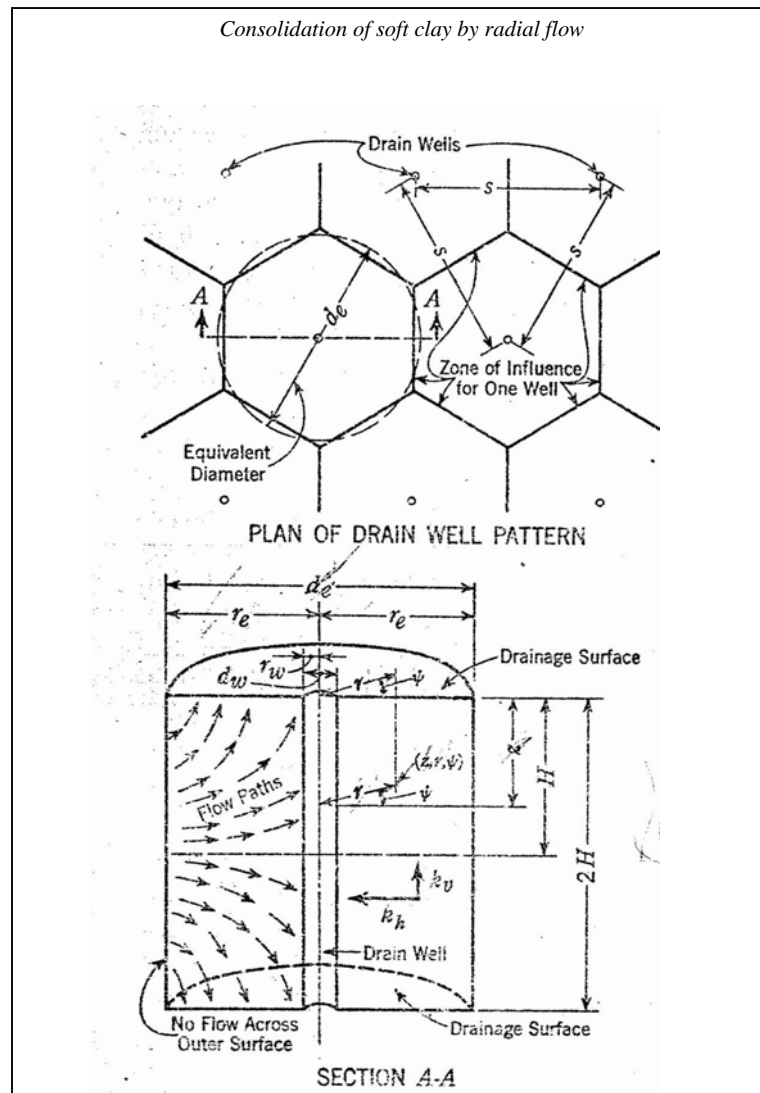


**Fig.2.15(a)** Plan of drain well pattern and fundamental concepts of flow within zone of influence of each well (Barron's theory)

Barron considered two types of vertical strains which might occur in a clay layer.

### 1. Free vertical strain :

The assumption is that the vertical surface stress remains constant during a consolidation process, and the resulting surface displacements are thus non uniform.

### 2. Equal vertical strain :

The assumption is that a vertical surface displacement is constant through out the drained area and the resulting vertical stress at the surface is thus non uniform. For both the strain conditions he included an analysis of the effect of

smear of the soil near the well boundary, and the effect of resistance of flow through the well itself.

CASE –I: Case of free strain consolidation with no smear and no well resistance

The equation for  $u_r$  and  $u_z$  were developed by R.E. Glover (1930) from the analogous heat flow problems which consists of Bessel's function, the time factor for consolidation by radial flow is,

$$T_h = [k_h(1+e)t] / (ar_w^2 de^2)$$

for  $U_r$ , where  $\ln$  in which  $k_h$  is the coefficient of permeability in horizontal direction equation for  $U_z$  and  $U_r$  were developed by Terzaghi (1925). Curves of  $U_r$  versus  $T_h$  for various of  $n$  are shown in figure 2.15(b) and 2.16.

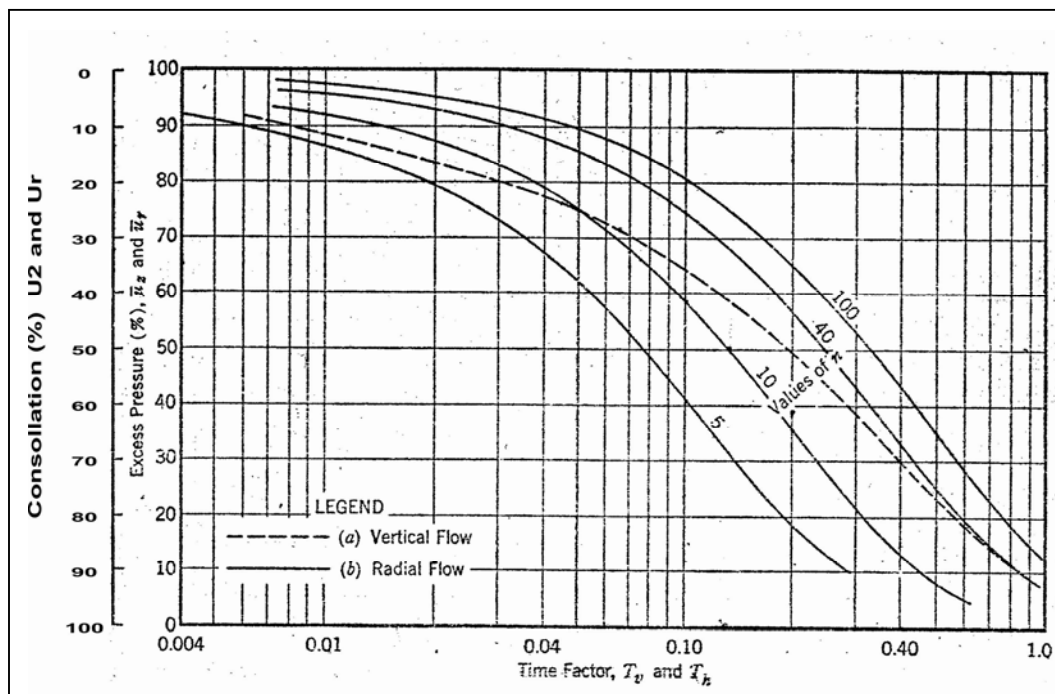


**Fig.2.15(b)** Theoretical curve of average degree of consolidation vs Time factor for combined vertical and radial flow for range of 'n' values

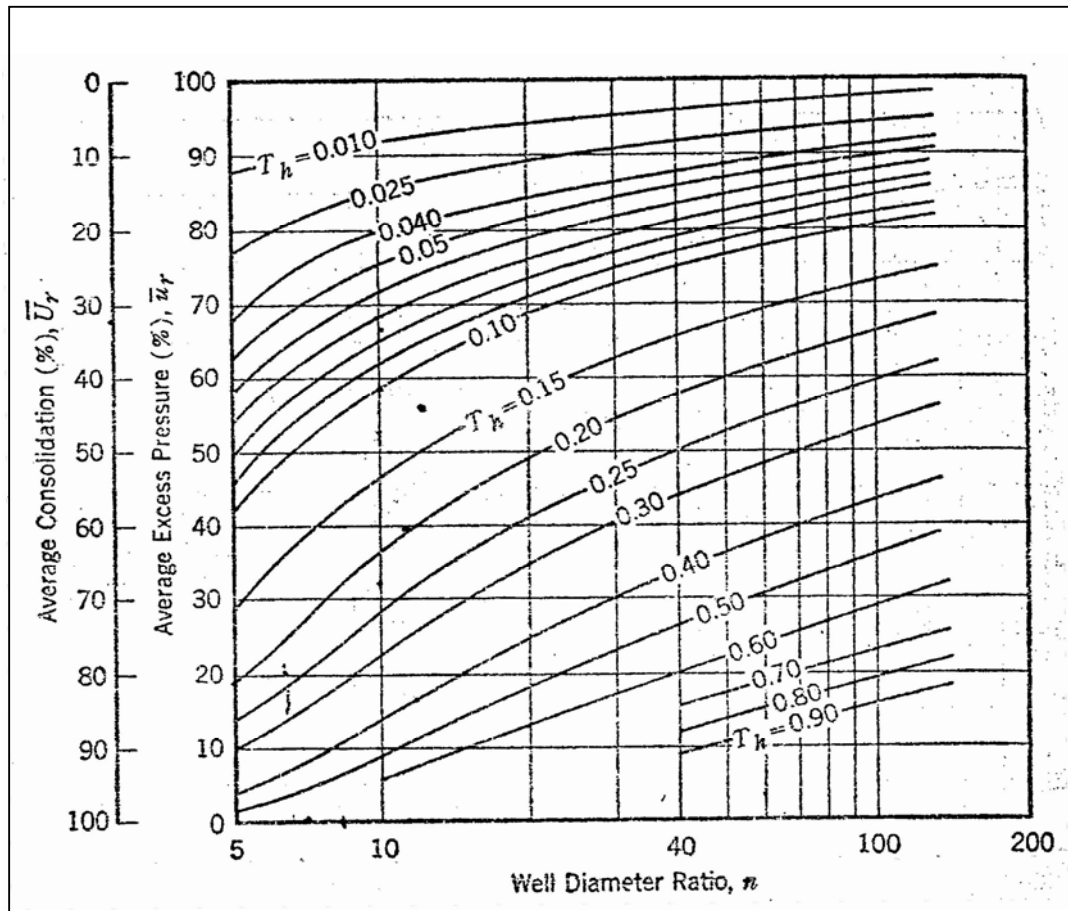


**Fig.2.16** Theoretical curve of average degree of consolidation for radial flow for range of 'n' values

CASE – II : Case of equal vertical strain with no smear and no well resistance  
When free strains are permitted, the soil adjacent to the well consolidates and compresses faster than the soil farther away from the drain this difference in rate of consolidation develops differential settlement of the upper surface of the soil mass and shears strains within the mass.

The differential equation for consolidation for these cases is given by

$$\frac{\partial u}{\partial t} = c_v \frac{\partial^2 u}{\partial z^2} + c_h \frac{\partial^2 u}{\partial r^2} + \frac{1}{r} \frac{\partial u}{\partial r} \quad \text{-----2.7}$$

in which  $c_h$  is the coefficient of consolidation for horizontal flow and equal to  $k(1+e)/a_v \cdot r_w$ . for radial flow only, this become,

$$\frac{\partial u}{\partial t} = c_h \frac{\partial^2 u}{\partial r^2} + \frac{1}{r} \frac{\partial u}{\partial r} \quad \text{-----2.8}$$

The solution for expression is

$$U_r = \frac{4u_0}{de^2 f(n)} re^2 \ln(r/r_w) - \frac{r^2 - r_w^2}{2} \quad \text{-----2.9}$$

In which

$$U = u_0 \cdot \epsilon \quad \text{-----2.10}$$

Is the base of natural logarithm,

$$= - 8 Tn/f(n) \quad \text{-----2.11}$$

$$\text{and } F(n) = (n^2/n^2 - 1) \ln(n) ( [3n^2 - 1]/4n^2 ) \quad \text{-----2.12}$$

The initial distribution of the hydrostatic excess pressure is not uniform as shown in Fig.2.17 but with passage of time the distribution approaches that for the free strain case as depicted in Fig. 2.18.

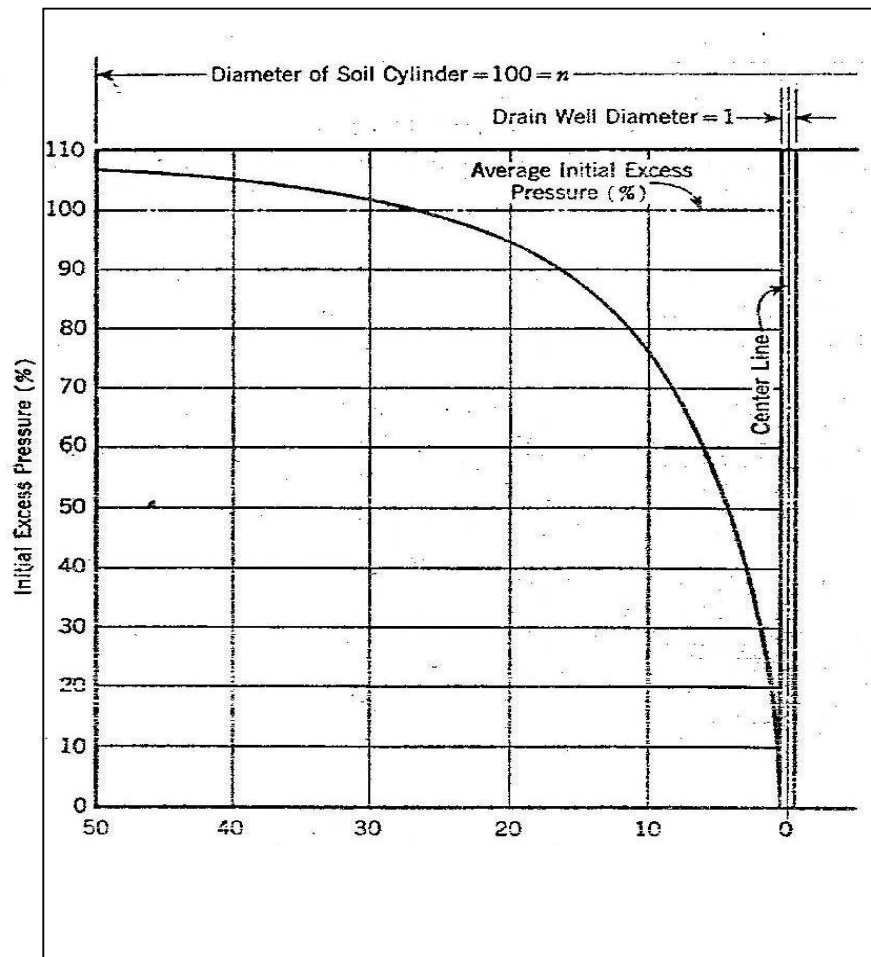


**Fig.2.17** Distribution of initial excess pore water pressure in soil cylinder with  $n = 100$

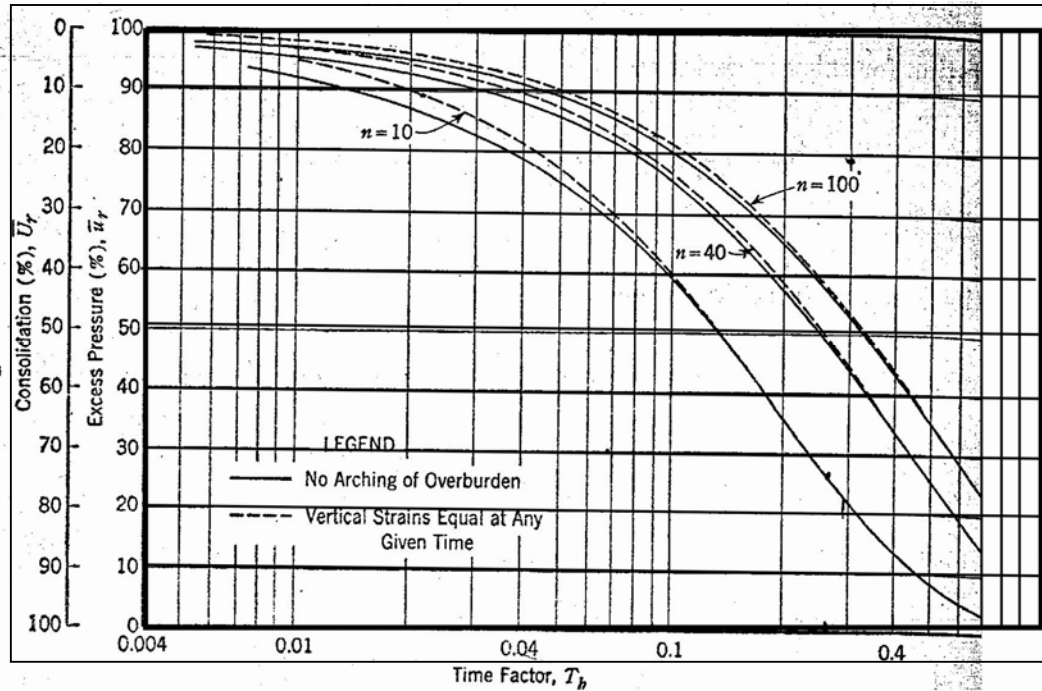


**Fig.2.18** Average degree of consolidation for various values of 'n' under 'equal strain' condition at any given time

### CASE - III : Effect of peripheral smear

Smear is the term used to define the wiping action provided by the casing or hollow mandrel used to form the well as it is driven down into the soil, and then pulled out after it has been filled with sand. The action tends to smear the soil at the well periphery.

#### CASE - III (a): Case of free strain with smear

In this case equation 2.7 reduces to

$$\text{Ch } \left[ \frac{\partial^2 u}{\partial r^2} + \frac{1}{r} \frac{\partial u}{\partial r} \right] = \frac{\partial u}{\partial t} \quad \text{----- 2.13}$$

From which the solution for  $u_r$  for uniform initial excess pore water pressure distribution subject to previously noted boundary conditions is :

$$u_r = u_o \sum \alpha = \frac{-2/S U_1(\alpha S)(U_o(\alpha S/rw)Gu)}{4/\pi^2 \alpha^2 S^2 - U_o^2(\alpha S) - U_1(\alpha S)} \quad \text{----- 2.14}$$

In which

$$U_o = (\alpha S) = J_o(\alpha S) r_1(\alpha n) - J_1(\alpha n) r_o(r, S) \quad \text{----- 2.15}$$

$$U_1 = (\alpha S) = J_1(\alpha S) r_o(\alpha n) - J_1(\alpha n) r_1(\alpha S) \quad \text{----- 2.16}$$

$$U_o(ar/rw)=J_o(ar/rw)r_1(\alpha n)-J_1(\alpha n)r_o(ar/rw) \text{ ----- 2.17}$$

And  $S = r_s/rw$

$$U = -4n^2\alpha^2 T_n \text{ -----2.18}$$

The average excess pore water pressure between  $r_s$  and  $r_e$  is

$$U_r = U_o \sum U_1^2(\alpha S) G\mu / \alpha^2 n^2 - S^2]4/\pi^2 \alpha^2 S^2 - U_o^2(\alpha S) - U_1(\alpha, S)] \text{ ----- 2.19}$$

CASE - III (b) : Case of equal vertical strain with smear

Solution of equation 2.7 for consolidation by radial flow to a central drain well with smeared zone at its periphery is:

$$U_r=U_r [\ln (r/rs)-(r^2-rs^2)/2re] +kh /ks [ (n^2-S^2) /n^2]\ln (S)] /V \text{ -----2.20}$$

in which ,

$$V=[n^2/(n^2-S^2)\ln(n/S)(-3/4) +(S^2/4n^2) + (kh/ks) [(n^2-S^2)/n^2 ] \ln (S)] \text{ -----2.21}$$

$$\text{And } u_r = u_o e \text{ -----2.22}$$

$$\text{In which } \epsilon = -8T_n/V \text{ -----2.23}$$

For combined radial and vertical flow, approximate solution may be obtained using eq.2.7 with  $u_z$  and  $u_z$  obtained as noted previously. The effect of smear is indicated in fig.2.19. for a greater ratio of  $k_h/k_v$  the difference is still large.

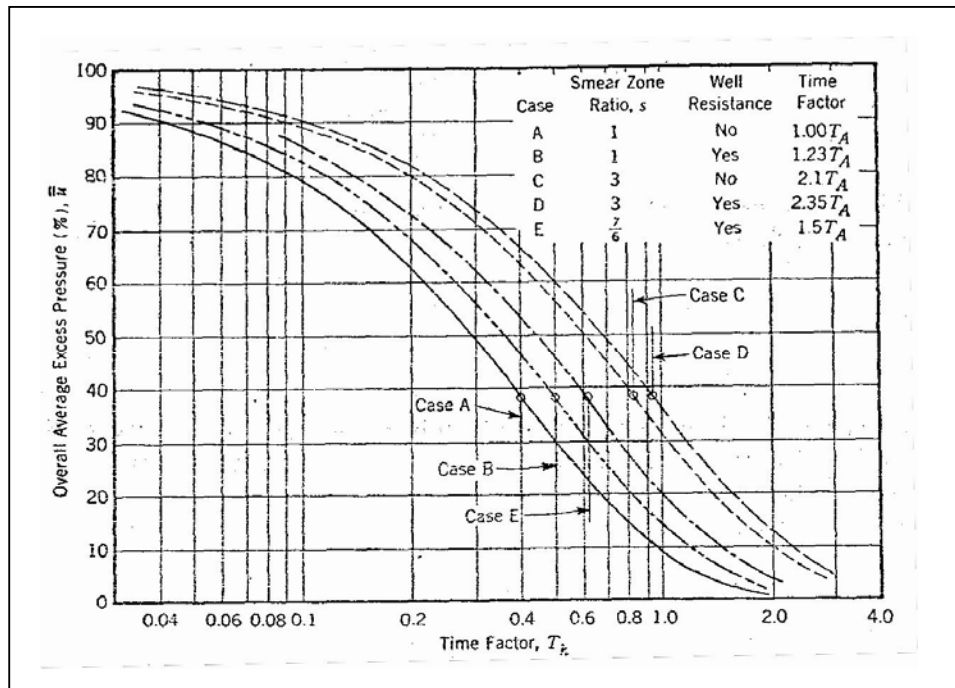


**Fig.2.19** Effect of smear and well resistance on 'equal strain' consolidation by radial flow to drain wells

**CASE – IV : Effect of well resistance**

A solution has been developed for equal vertical strain , with or without smear , where  $k_v$  of the consolidating soil is equal to zero that is  $u/z = 0$ , but because  $k_v = 0$  no vertical flow exists .A solution to equation 2.7 for  $u_{r,z}$  at any point where smear and well resistance are involved is :

$$U_{r,z} = U_z \left[ \frac{f(z)}{\mu} \left[ \ln(r/r_s) - (r^2 - r_s^2)/z^2 r_e^2 + k_h/k_s (n^2 - S^2)/n^2 \ln(S) \right] + (1 - (1_z)) \right] \text{-----2.24}$$

in which  $u_z$  , the average excess pressure between  $r_e$  and  $r_s$  at depth  $z$  , is  $u_z = u_o$

$$e^{y f(z)} \text{-----2.25}$$

$$f(z) = [e^{\beta(z-2H)} + e^{-\beta z}] / 1 + e^{-2\beta h} \text{-----2.26}$$

$$\text{and } \beta = [2kn (n^2 - s^2) / kw r_e^2]^{1/2} \text{-----2.27}$$

in which  $k_w$  is the permeability of well backfill . The overall average excess pressure over the entire soil mass between  $r_e$  and  $r_s$  and between  $O$  and  $Z=H$  is :

$$u = \int_0^H u_z dz \text{-----2.28}$$

**Comparison of free and equal vertical strain theory :**

A comparison between free strain and equal strain solutions indicated that both yield almost equal of consolidation with respect to radial flow for the values of  $n = 5$  and  $T_h > 0.1$ . This justifies the wide use of the simpler equal strain solution for design purposes particularly when one is mainly interested in the evaluation of consolidation with respect to radial flow, Jamiolkowski et al.(1983).

**2.7.6 Kjellman's Theory (1948)**

The theory is based on the 'Equal strain hypotheses' i.e. on the assumption that horizontal section remains horizontal throughout the consolidation process as shown in fig. 2.20

Kjellman's established his solution for radial flow consolidation.

$$2\pi PV_p = (R^2 - j^2) d e/dt \text{-----2.29}$$

where,  $de/dt$  is rate of vertical strain,

From equation 2.29

$$du/dp = r_w/2k_c [(R^2/o) - o] de/dt \text{-----2.30}$$

Integrating equation 2.30 and introducing boundary conditions

$U = 0$  for  $o = r$ , we get :

$$U = r_w / 2k_c [R^2 \log_e o / r - (o^2 - r^2) / 2] de / dt \text{ -----2.31}$$

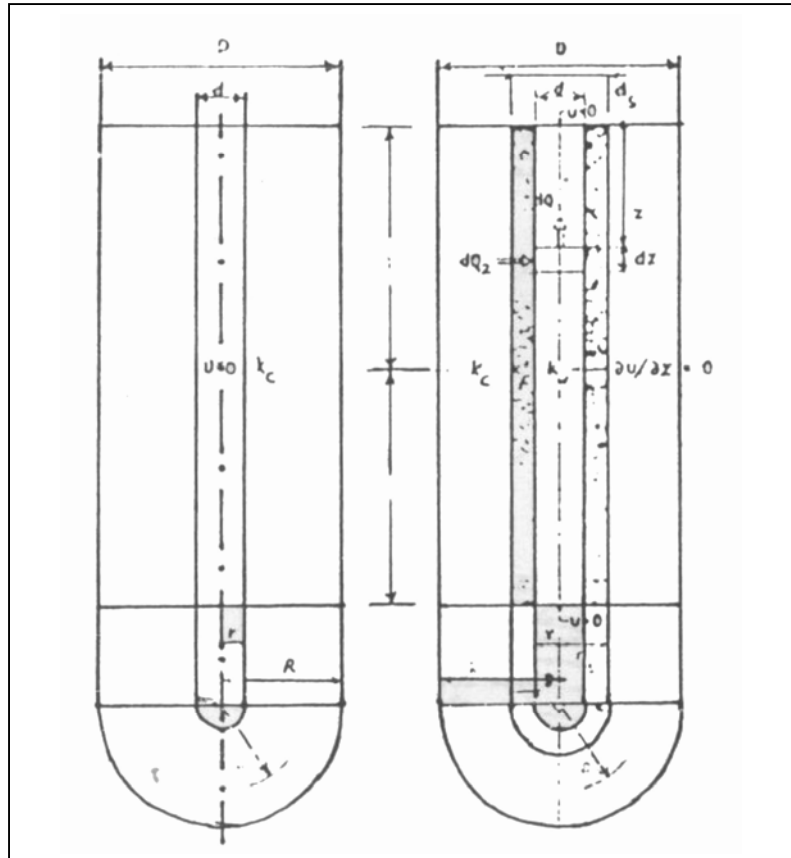


**Fig.2.20** Schematic picture of soil cylinder dewatered by vertical drain (a) idealized case(left) (b) real case influence of smear and well resistance (right)

### 2.7.7 Silveira's Theory (1953)

Silveira (1953) considered the process of consolidation of cylindrical sample with drainage made possible through the external cylindrical surface. He solved classical equation for plane radial flow by Laplace transform and Brom witch Wanger inversion integral and portrayed consolidation chart for a cylindrical sample with external radial flow of water as shown in Fig.2.21.



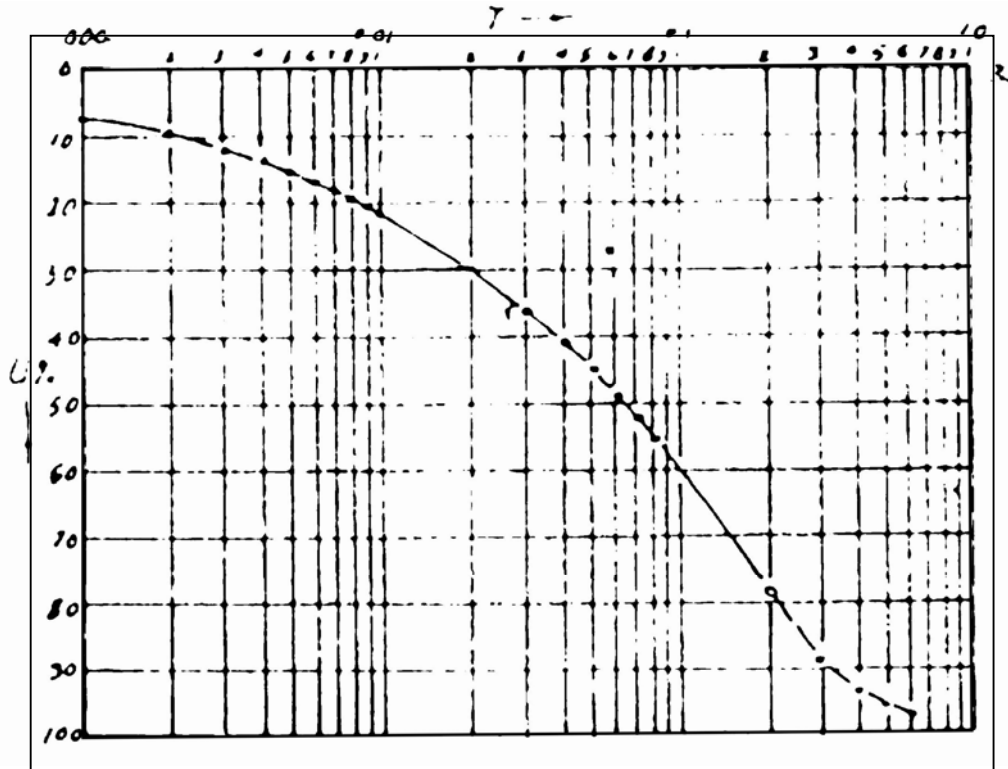


**Fig.2.21** Consolidation chart for cylindrical sample with external radial flow of water (after Silveria, 1953)

### 2.7.8 Richart's Theory (1959)

In this theory critical review for three dimensional consolidation by sand drain is done. Solution for Barron's equation is given and he considered them satisfactory for the analysis of any situation. Fig.2.22, 2.23, 2.24 are given for quantitative evaluation of this relation between behavior of ideal and smeared wells. By interpolating the consolidation behavior, due to an actual well in terms of that of an equivalent ideal well, Fig.2.25, 2.26 proposed by Barron for ideal wells can be used directly in design. Further Richart studied the effect of size of drain well on the time of consolidation for field case as indicated in Fig. 2.27. He suggested to adopt numerical procedures for solving consolidation problems accounting factors such as a variable rate of loading, variable soil properties and layered systems.

The effect of consolidation of the soil cylinder caused by the introduction of smeared zone at the well periphery is identical to the effect caused by reducing the size of the ideal well.

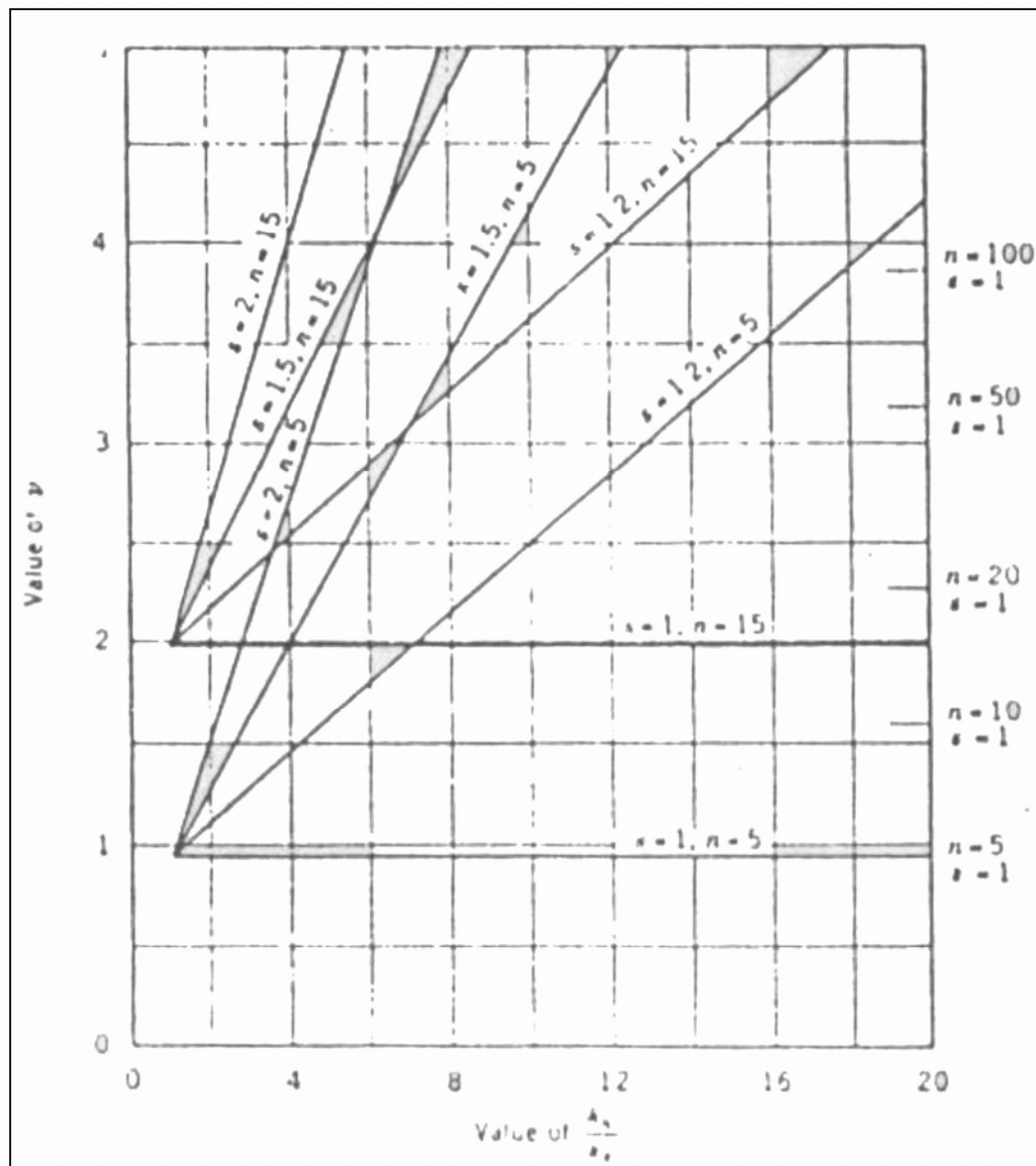


**Fig.2.22** Relationship between  $Kh/K_v$ ,  $u$  and  $r$  for  $n=5$  and  $n=15$  (after Richart, 1957)

**Richart** has also given numerical solution of consolidation by radial flow. Expressing the fundamental equation,

$$\frac{du}{dt} = C_{vr} \left[ \frac{d^2 u}{dr^2} + \left( \frac{1}{r} \right) \left( \frac{du}{dr} \right) \right] \text{-----2.32}$$

By taking the average values of excess pore pressure at only time, a curve of  $U_r$  v/s  $T_h$  can be constructed that corresponds to within a few percentage of the value obtained by Barron's procedure. This procedure is ideally suited for consolidation of qualities that vary with time.

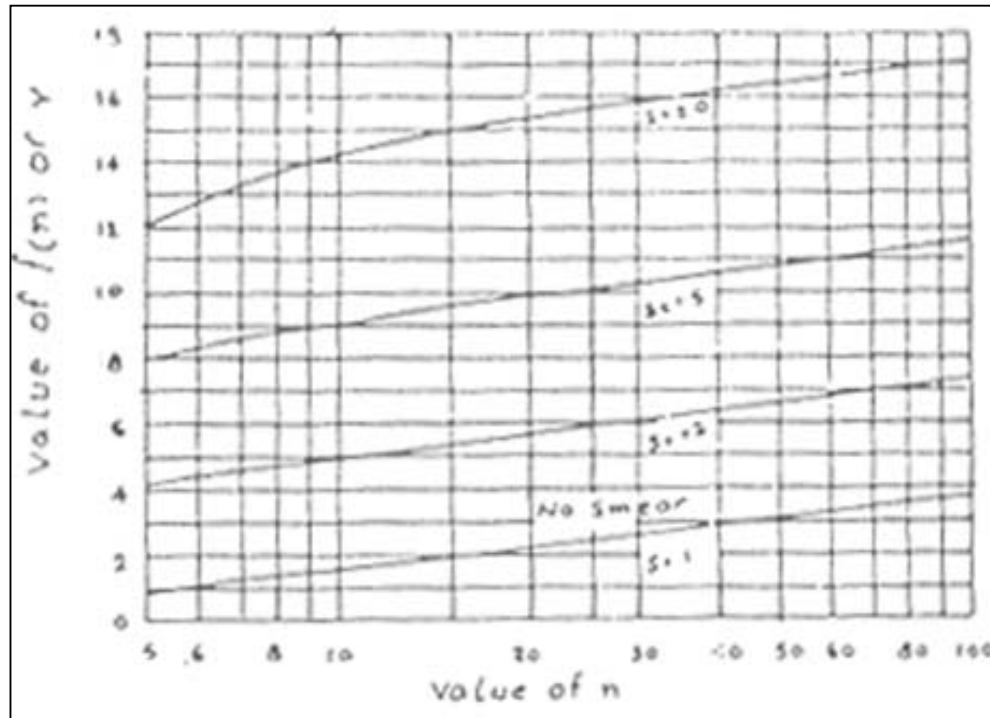


**Fig.2.23:** Relationship between  $n$  and  $f(n)$  or  $v$  for  $\frac{K_h}{K_s} = 20$  (After Richart 1954)

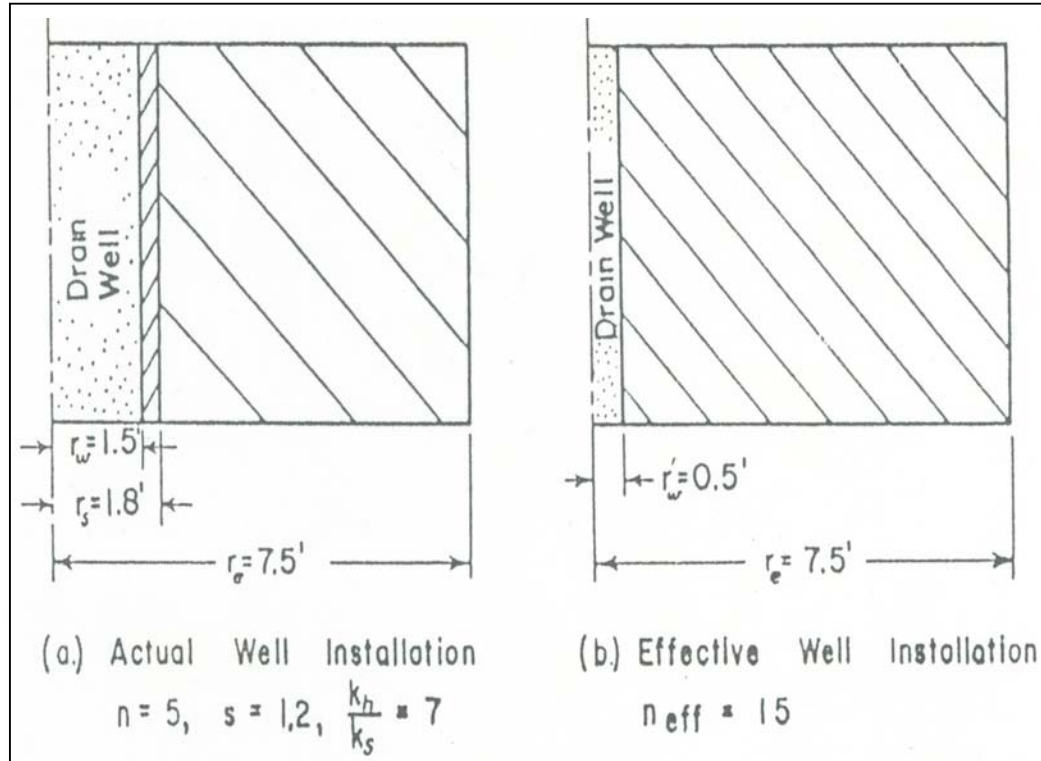


**Fig.2.24** Actual and equivalent well installations (after Richart, 1957)

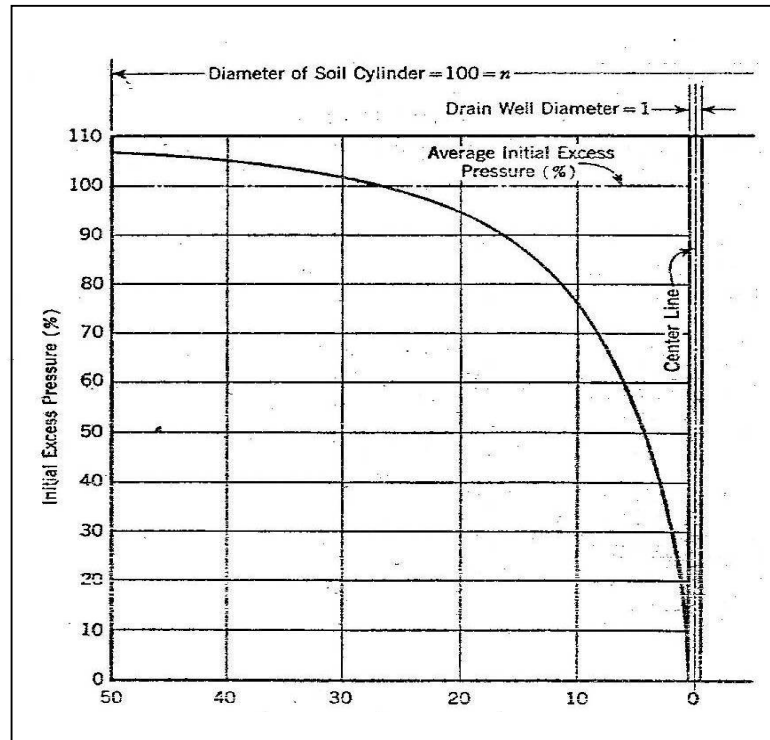


**Fig.2.25** Distribution of initial excess pore water pressure in soil cylinder with  $n = 100$

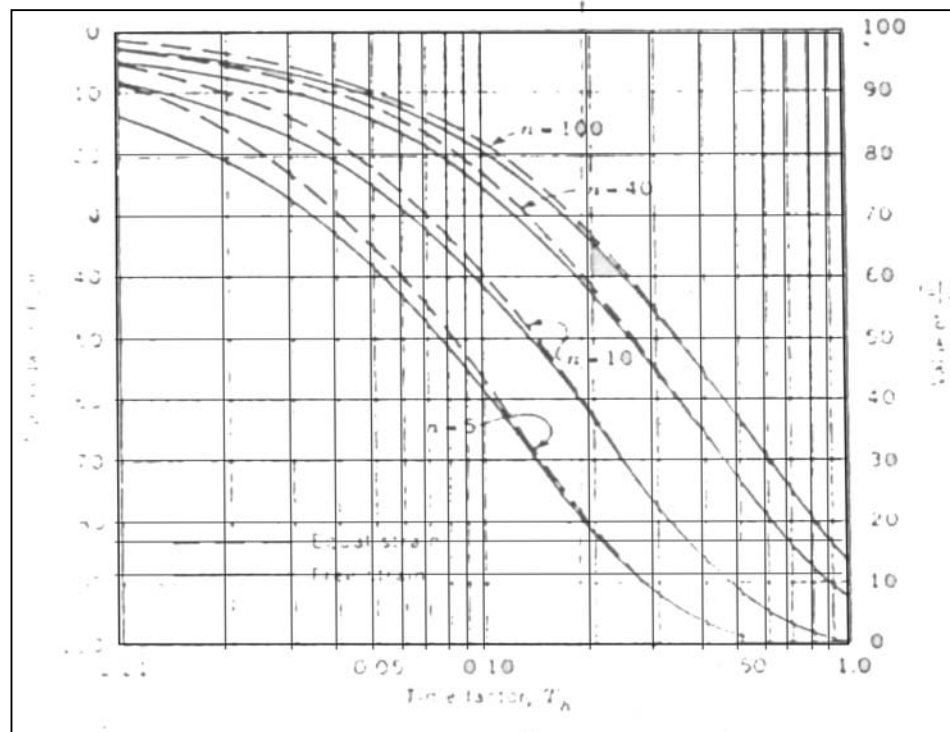


**Fig.2.26** Comparison of average consolidation rates in clay cylinders by radial drainage only for various values of 'n' (after Barron, 1948)

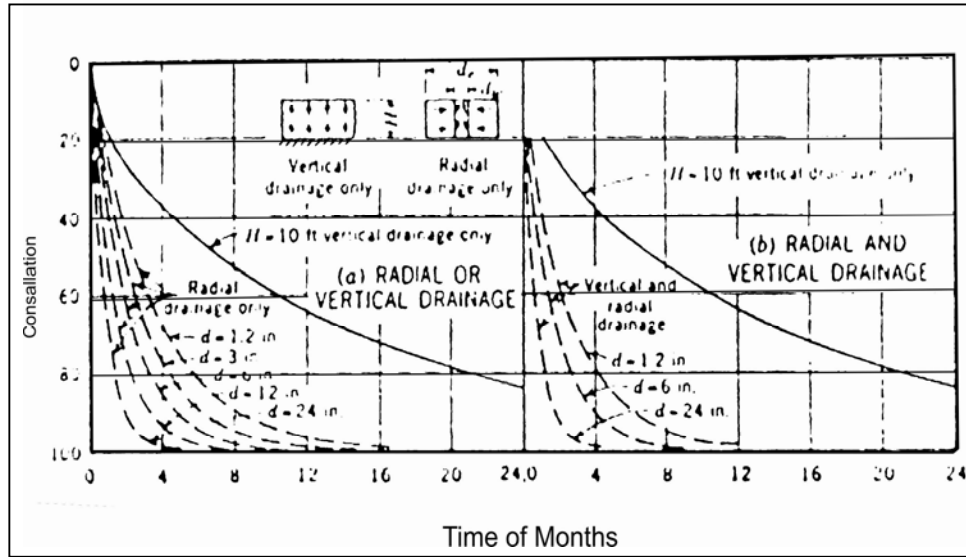


**Fig. 2.27** Effect of size of drain well vs. time for consolidation (after Richart, 1957)

### 2.7.9 Takagi's Theory

Three dimensional theory is presented considering rate of loading variable. The total degree of consolidation at time  $t$ , say  $U(t)$ , is given by sum of the influence caused by the loading prior to time  $t$ ,

$$U(t) = \frac{1}{Q} \int_0^t \frac{u'(t-z)q'(z)dz}{Q} \quad \text{when } 0 < t < z \quad \text{-----2.33}$$

$$= \frac{1}{Q} \int_0^t \frac{u'(t-z)q'(z)dz}{Q} \quad \text{when } 0 < z < t \quad \text{-----2.34}$$

Where  $q'(z)$  is rate of loading at time  $t$ . Fig 2.28 illustrates the isochrones.

### 2.7.10 Schiffman's Theory (1958)

Schiffman extended the theory of Barron and provided solution for problems pertaining to variable loading during the consolidation process. He presented analysis of consolidation of soil by sand drain for free strain and equal strain considerations similar to Barron for

- (i) Constant load – Variable permeability case
- (ii) Variable load – Constant permeability case and
- (iii) Variable load – Variable permeability case.

For peripheral smear and no smear cases for general boundary conditions adopted by Barron (1948), Fig.2.29

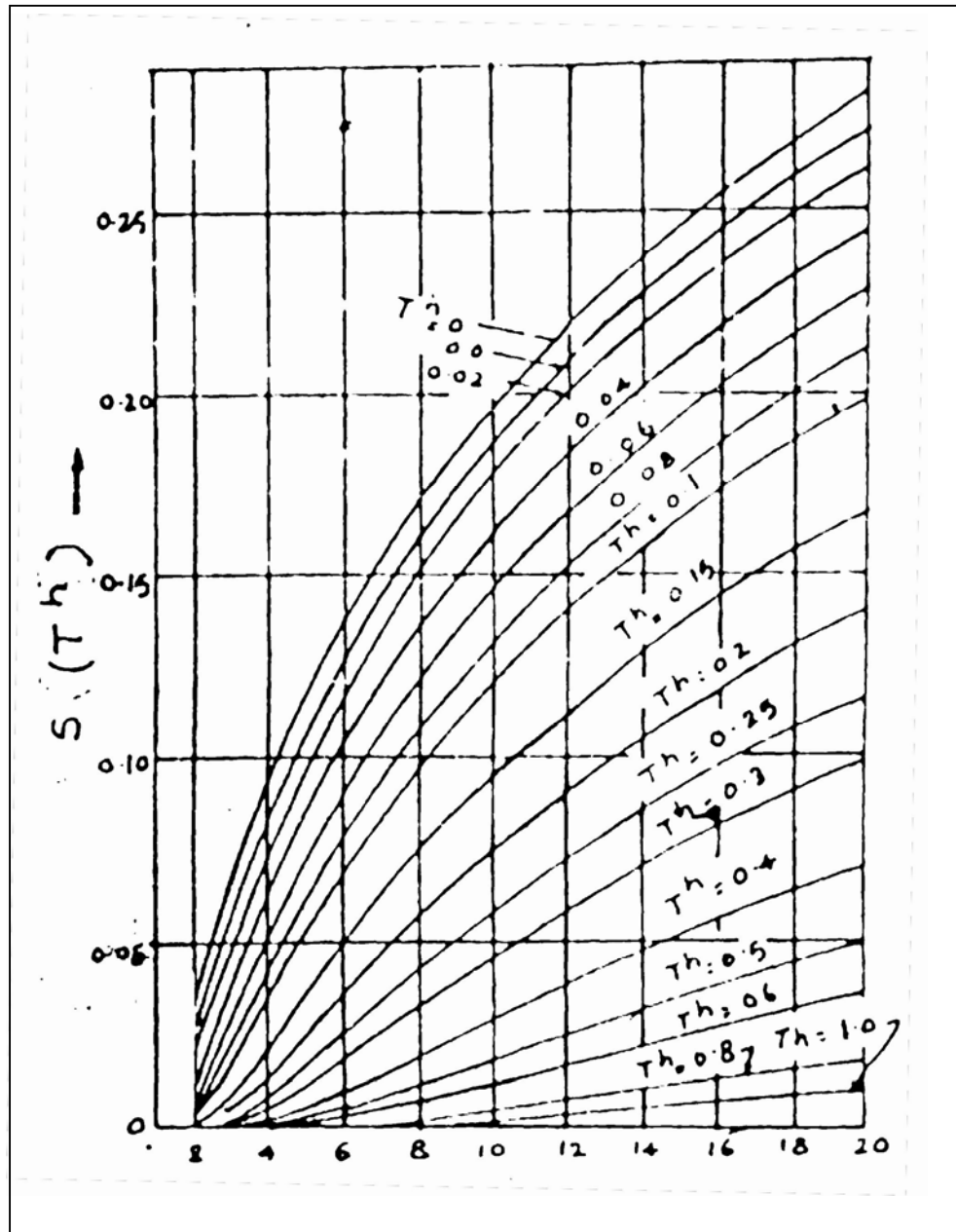
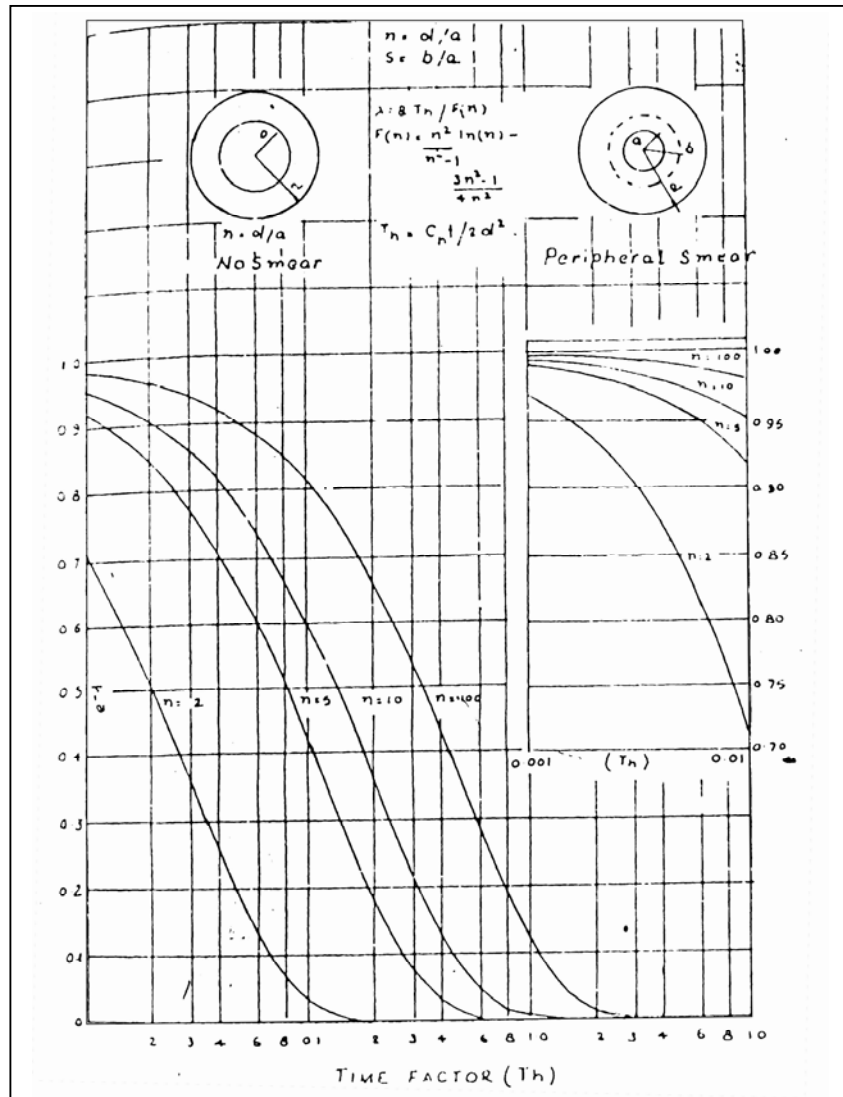


Fig. 2.28 Plot of isochrones (after Takagi, 1957)



**Fig. 2.29** Exponents for equal strain sand drain problem with no smear, radial flow (after Schiffman, 1958)

### 2.7.11 Hansbo Theory (1960)

Hansbo(1960) made extensive sand drain study involving large scale field tests and observations of sand drain in soft clays.(ref fig.2.20) He also evaluated the effect of sand drain on shear strength of clay. While deriving the theory of radial consolidation, most of the workers assumed that the Darcy's law is strictly valid. However, Hansbo (1960) and other workers have shown that this may not be true when the hydraulic gradient is in the range of magnitude prevailing during most consolidation process in practice. Solution for ideal case (with no smear and no well resistance) consider the ideal case of a circular soil cylinder

with impervious boundaries except for the outlets of a central circular drain  
Figure 2.24

The solution yields the average degree of consolidation,  $U_n$  as:

$$U_n = 1 - (u/u_o) = 1 - e^{-8T_n/ur} \text{-----2.35}$$

Where,

$$U = [n^2/(n^2-1)] [\ln(n) - 3/4 + 1/n^2 - 1/4n^4] \text{-----2.36}$$

This solution is similar to Barron's solution for equal vertical strain condition with out smear and well resistance.

#### Effect of well resistance and smear:

Hansbo finally arrived at a solution:

$$\sqrt{n} = 1 - e^{-8T_n/ur} \text{-----2.37}$$

In which,

$$\mu_r = \mu + [(n^2-1)kc/(n^2 q_w)] z (21-z) \text{-----2.38}$$

$$\text{Or, } \mu_r = \mu + \pi z (21-z) [kc/q_w] \text{-----2.39}$$

Where,

$K$  = permeability in horizontal direction of the undisturbed soil

$Q$  = well discharge capacity.

$l$  = characteristic length of the drain, equal to half the drain

Length for fully penetrating drains.

$Z$  = entire length of partially penetrating.

Now considering the effect of smear, the final solutions for  $U_n$  is given by:

$$U_n = 1 - e^{-8T_n/ur} \text{-----2.40}$$

In which,

$$\begin{aligned} \mu_n = [n^2/(n^2-1)] [\ln(n/s) + kc/kc' \ln(s) - 3/4] + [s^2/(n^2-1)] [1-(s^2/4n^2)] \\ + kc/kc' (1/(n^2-1) + \pi z (21-z) (kc/q_w) [1-1/n^2] \text{-----2.41} \end{aligned}$$

or,

$$\mu_s = \ln(n/s) + kc/kc' \ln(s) - 3/4 + \pi z (21-z) (kc/q_w) \text{-----2.42}$$

The last term of equation 3.49 and equation 3.50 obviously represent the influence of well resistance.

Thus rewriting equation 3.50 in the from:

$$\mu_s = V + \pi z (21-z) kc/q_w (1-1/n^2) \text{-----2.43}$$

The new parameter  $u$  can be said to represent the effect of smear only.



$k_c$  = coefficient of horizontal permeability in smeared zone .

These equations were developed by modifying Barron's equations for prefabricated drain applications. Hansbo (1979) studied the consolidation process of clay by band shaped prefabricated drains. He considered the design considerations. Hansbo (1981) developed the simple solution using Kjellman's solution, to account for smear and well resistance effects.

### 2.7.12 Escario-Uriel's Solution

Escario and Uriel (1961) gave solution of Terzaghi's equation for peripheral drain for peripheral drain for consolidation test in a triaxial cell. He made no comments on Barron's theory.

$$U = \frac{2u_0(R^2 - r^2)}{R^2} - \frac{8Kt}{(1+2)\gamma_w R^2 m_v} \text{-----2.44}$$

For the following boundary condition as shown in Fig.2.30

(i) For  $r = R$ ,  $U =$  and for  $r = 0$ ,  $\partial u / \partial r = 0$

(ii) For  $t = 0$ ,  $U_0 = \Delta P$

Also  $C_v = K/m_v \gamma_w$  and  $T_v t = C_v t / R^2$ .

The above equation for  $u$  is expressed as

$$U = 2 U_0 [ \text{Exp} (-8 T_v) / (1 + 2) ] (1 - r^2/R^2) \text{-----2.45}$$

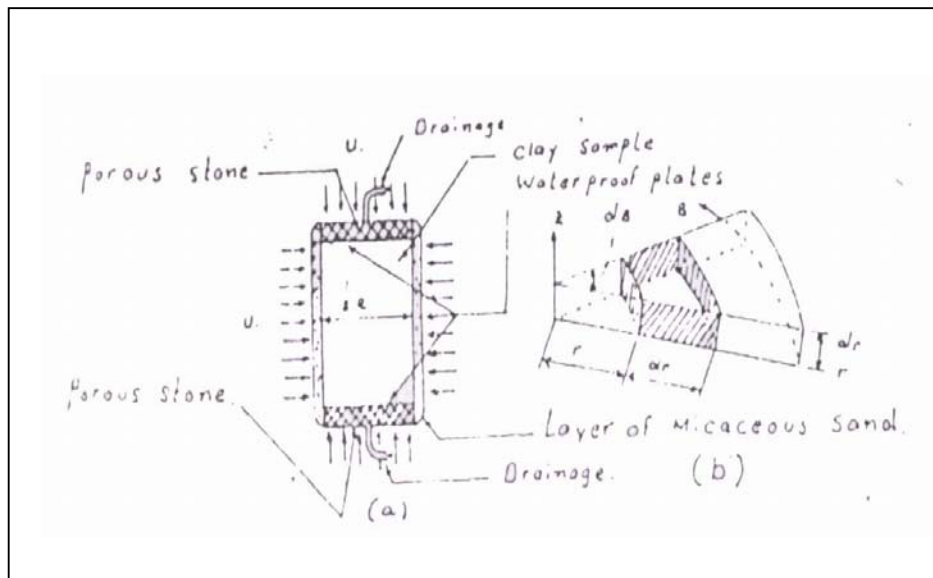


**Fig.2.30 (a)** Scheme of arrangement of the consolidation test in the triaxial apparatus with drainage towards the cylindrical surface (b) cylindrical element of the sample (after Escario et al., 1961)

### 2.7.13 Horne's Solution

Horne (1964) utilized Barron's equation for soils stratified in horizontal layers, with the simultaneous possibility of over all drainage, both vertically to pervious layers above or below the series of strata and horizontally to vertical sand drains. He obtained general solution for any sequence of horizontal strata in which the coefficient of compressibility for horizontal and vertical flow are regarded as arbitrary function of the vertical co-ordinates. For this he presented solutions for both two dimensional and the radially symmetrical cases, and a special treatment is given for equal alternate layers such as clay and silt or clay and sand. He suggested that Carillo's separation of equation into vertical and plane radial flow may also be applied in case of stratified soil to determine the effect of over all vertical drainage. Fig 2.31 illustrates solution for effective coefficient of consolidation with horizontal drainage of soil consisting of horizontal layers of low permeability interposed by thin layers of high permeability.

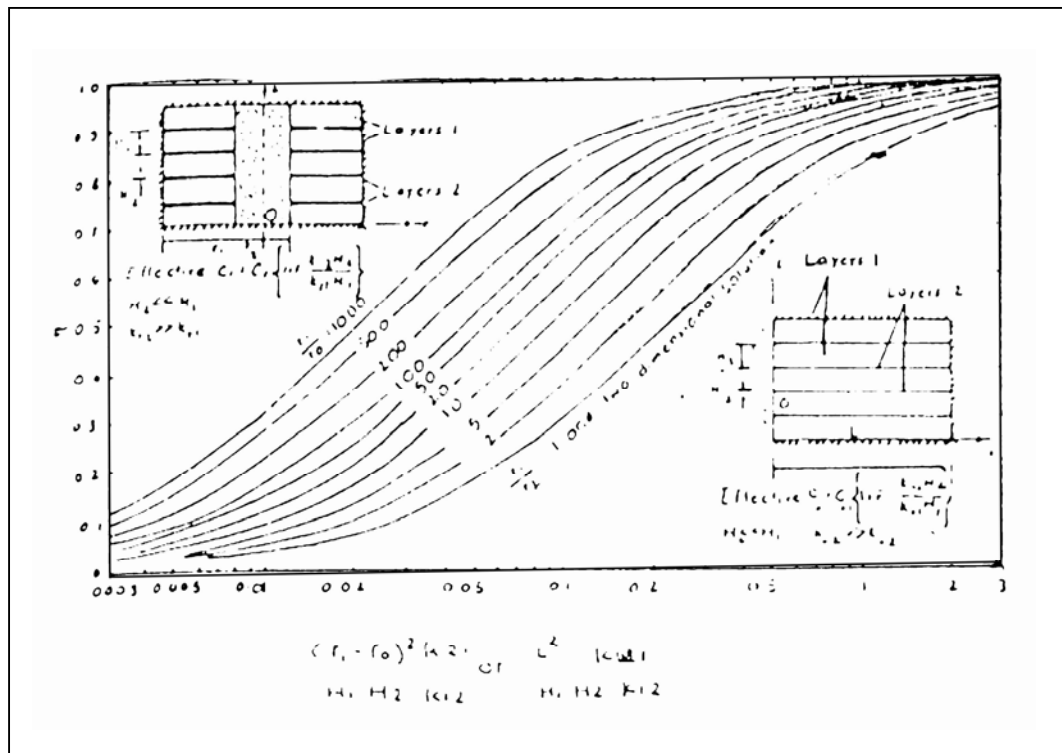


**Fig. 2.31** Approximate solution for effective coefficient of consolidation with horizontal drainage of soil consisting of horizontal permeability (after Horne, 1964)

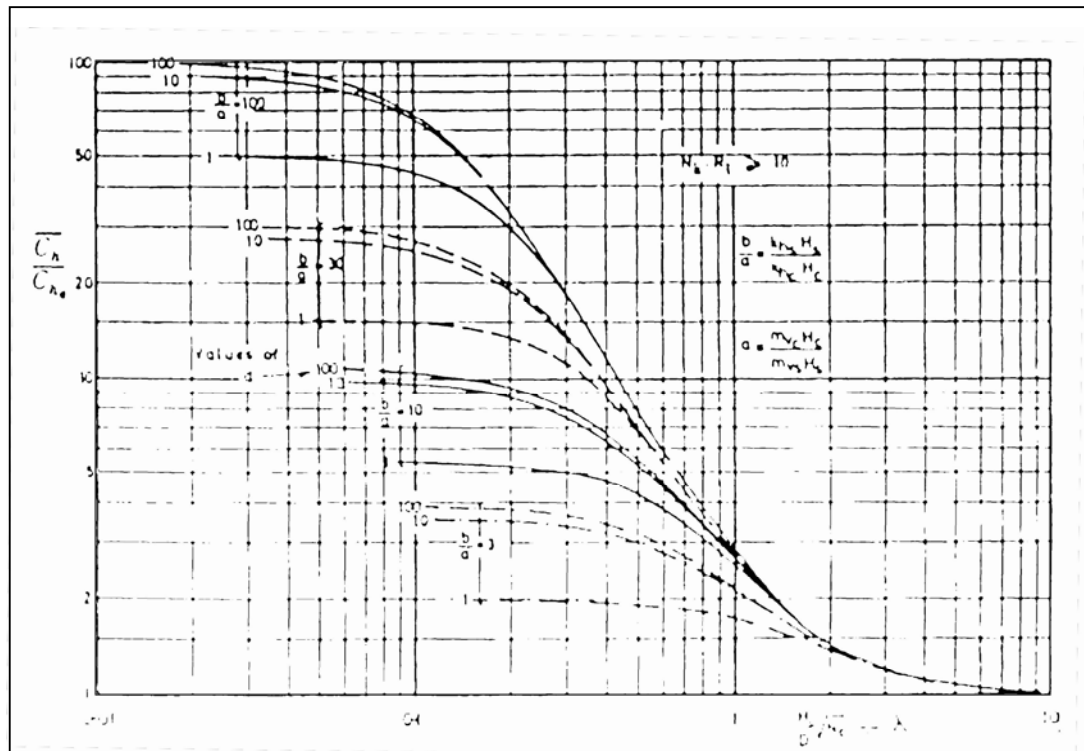


**Fig. 2.32** Theoretical relations between the geometry of the sample and the measured coefficient of consolidation (after Rowe, 1964)

#### 2.7.14 Rowe's Theory (1964)

This theory has been developed from the general mathematical solutions by M.R. Horne (1964) for consolidation rate of statistical soil drainage to a lateral boundary for engineering application. It has been shown that the calculated values of the coefficient of consolidation in the horizontal directions vary widely with structure of the deposit and the size of the sample. Horizontal coefficient of permeability much greater than vertical coefficient of permeability for layered soil.

The average degree of consolidation is given by:

$$\begin{aligned}
 m &= \infty \\
 n &= \infty \\
 U_s &= 1 - \sum_{n=1}^{\infty} \left( \frac{A a^n N m}{F_c} \right) (e^{-b N m} + (a + F_c / F_s) (a+1)) \quad \text{-----2.46} \\
 m &= 1
 \end{aligned}$$

where ,

$$A = [4 U_1 2(\infty n)] / [\infty N^2 (n^2 - 1) (n^2 U_0 (n \infty N) - U_1^2(\infty N))] \quad \text{-----2.47}$$

and

$$(a'N_m)/F_c = [N_{sc} R_t + F_c/F_s] / N_{sc} R + (F_c^2 + B_c^2 + F_c) / 2 + (F_c^2 / F_s^2) (F_s^2 + \theta s^2 + F_s) / 2] \quad \text{--2.48}$$

The ratio  $C_h / C_{he}$  is given by:

$$C_h / C_{he} = (b/a) [(F_c / F_s) + 1] / [(1/a) [(F_c / F_s) + 1]] \quad \text{----- 2.49}$$

and the maximum value ,when  $F_c / F_s = 1$  ,is :

$$C_{h \text{ max}} / C_{he} = [(b/a) + 1] / [(1/a) + 1]$$

Rowe concluded that the measured value of coefficient of consolidation in the horizontal direction of a Laminated, layered or varved clay depends on the relation between the geometry and the properties of the internal structure of deposit and size of the sample. Theoretical relations are given in Fig.2.32 The diagram shows that as the length of drainage ,d, is increased the value of  $C_h$  increases to a maximum .The influence of ratio of  $b/a$  on maximum value of horizontal coefficient of consolidation is theoretically indicated in the Fig. 2.33

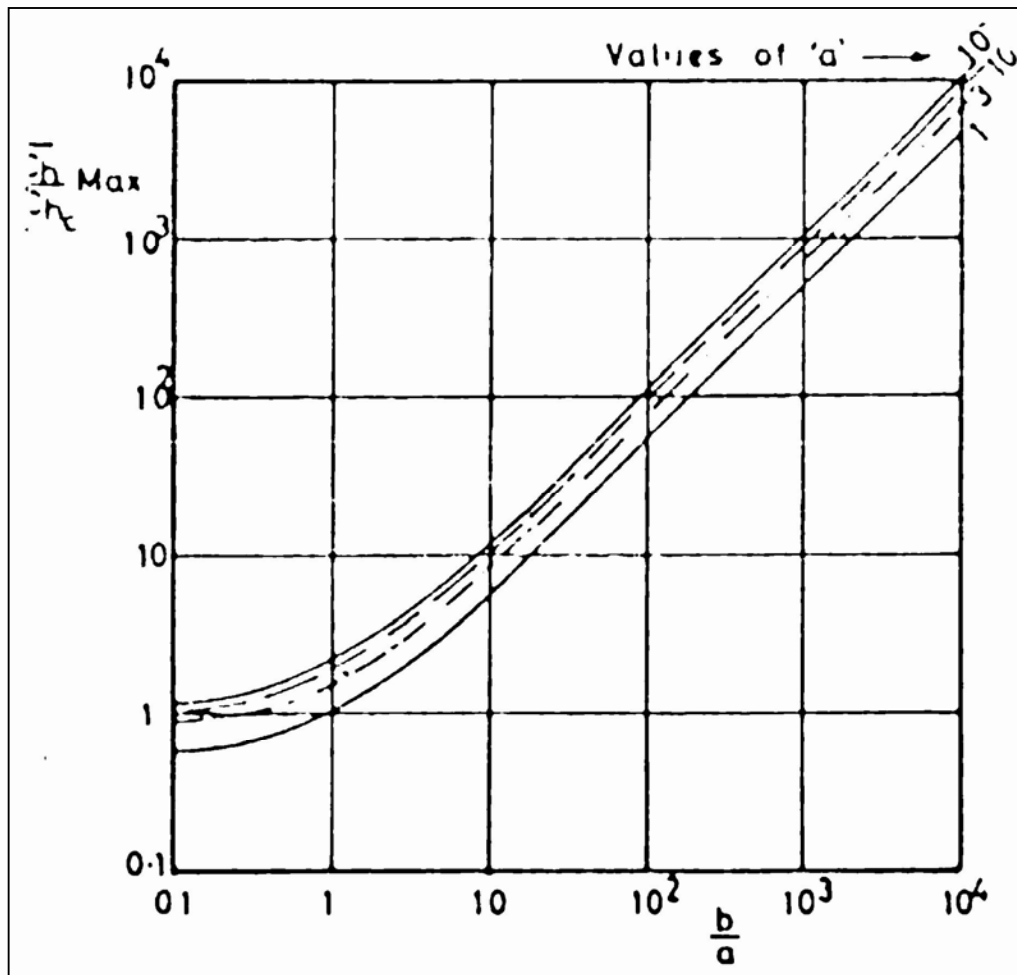
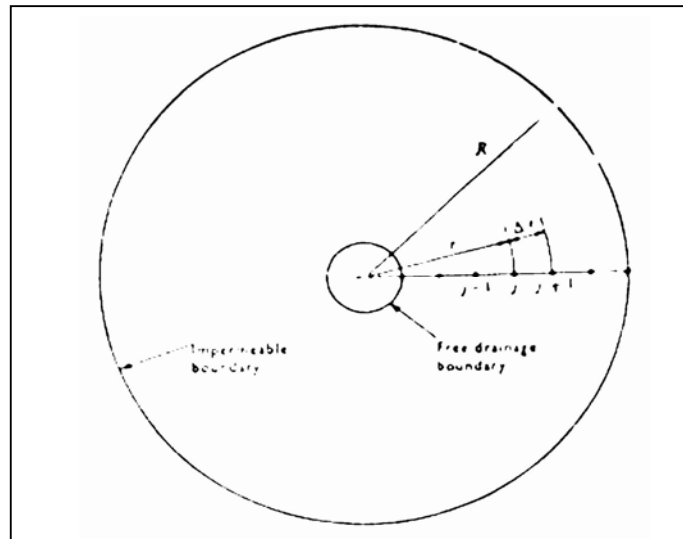


Fig. 2.33: Influence of the ratio  $b/a$  on the maximum value of  $C_h$

### 2.7.15 Christie's Solution (1966)

Christie (1966) solved Terzaghi's equation of consolidation with drainage in 2 and 3 dimensions by the use of electronic analogue computer Fig. 2.34, 2.35 illustrates typical results for the case of cylinder of soil with  $M = 1.43$  (70 % primary and 30 % secondary ) and drain diameter equal to the  $1/10$ th of the diameter of the soil cylinder.



**Fig.2.34:** Plan showing location of discrete points in a cylinder of soil with a central vertical sand drain (after Christie, 1966)

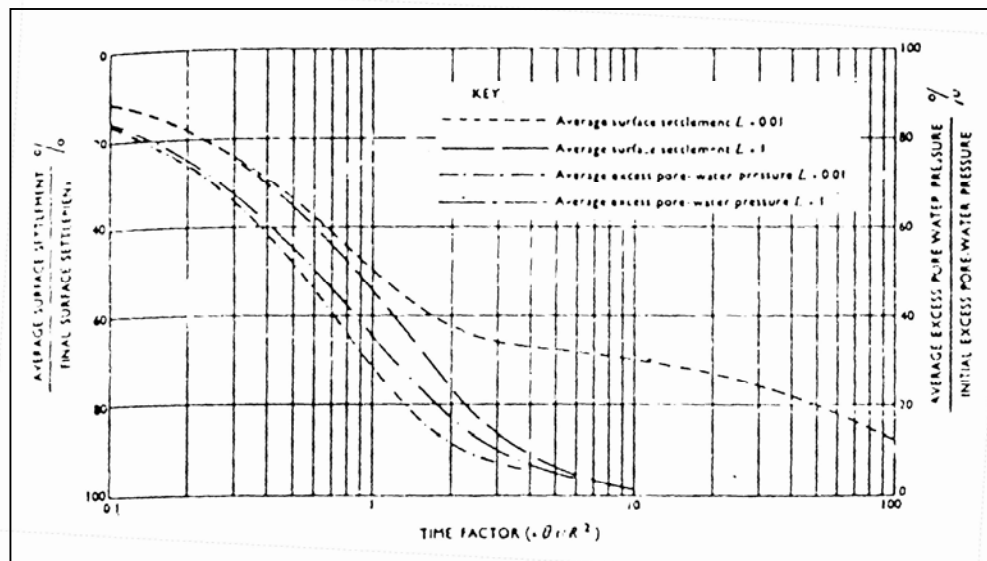


**Fig.2.35:** Consolidation of a cylinder of a soil with 30% secondary compression and radial drainage to a drain of diameter equal to one tenth of the diameter of cylinder (after Christie, 1966)

### 2.7.16 Anandkrishnan-Kappuswamy's Solution

Anandkrishnan and Kappuswamy (1969) studied influence of distributed zone on the consolidation. The values of coefficient of consolidation for disturbed zone may be assumed same as that for parent material. However if there is a pronounced effect on the permeability values and if diameter of smeared zone is more, then they have a pronounced effect on the design of sand drains for construction loading.

### 2.7.17 Siva Reddy – Murty's Solution

Siva Reddy (1969) in his analysis is based on Barron's work, considering the materials in a disturbed zone to be compressible. He suggested Barron's considerations that the thickness of smear is negligible and that the material in the disturbed zone is incompressible because it has consolidated comparatively at faster rate than that of parent material. They considered two different cases with zone of influence of drain well finite and infinite as shown in Fig. 2.36 and Fig. 2.37.

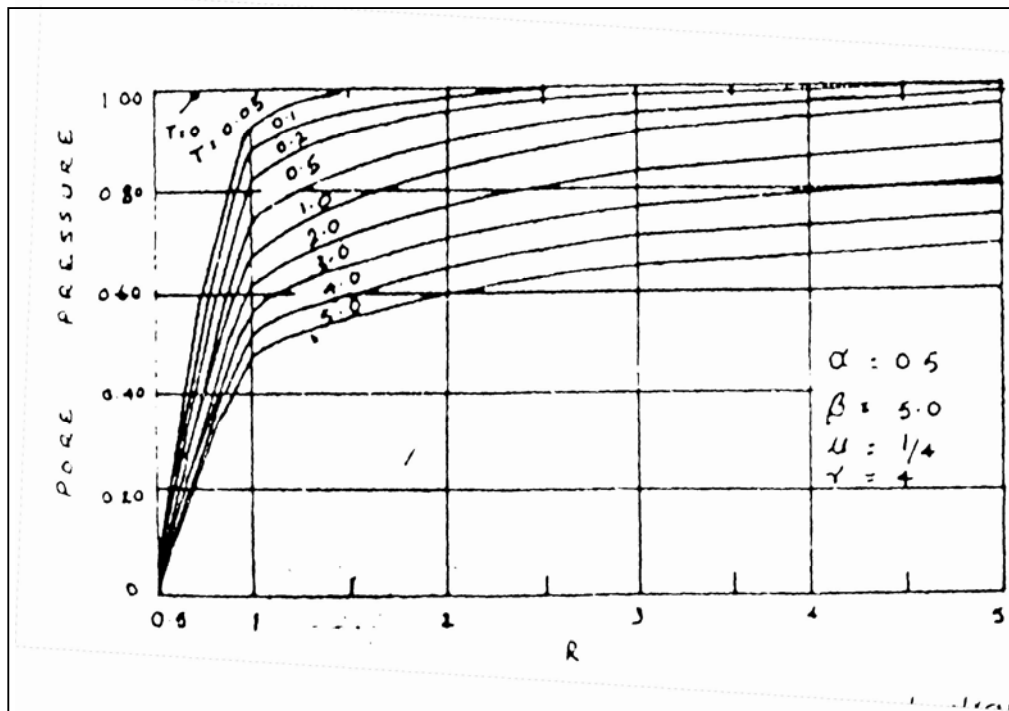


**Fig.2.36:** Pore pressure distribution in a sand drain for case I

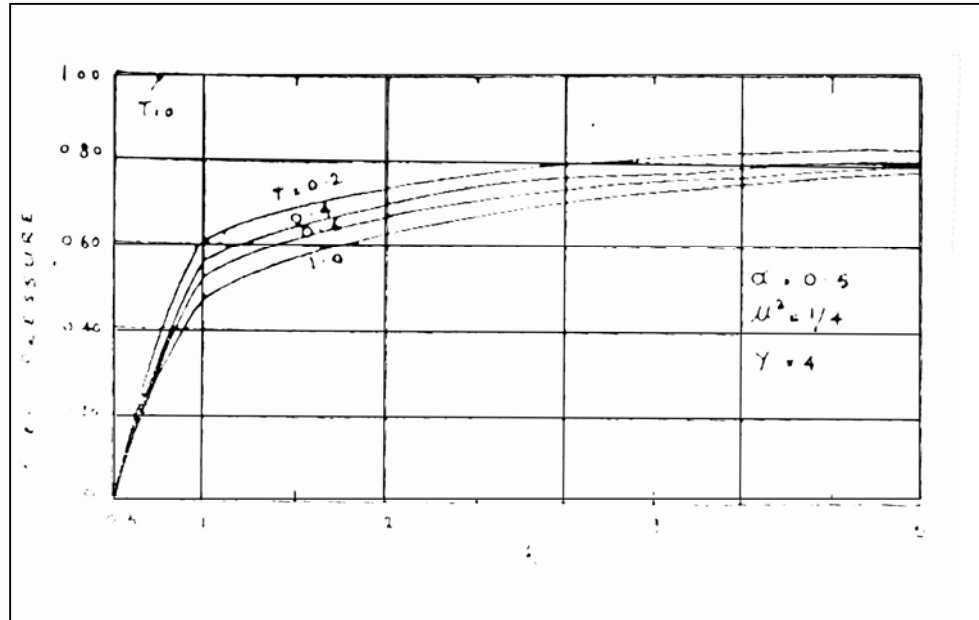


**Fig.2.37:** Pore pressure distribution in a sand drain for case II  
(after Sivareddy, 1969)

#### 2.7.18 Berry and Wilkinson's Theory (1969)

Berry and Wilkinson extended the radial consolidation theory to take account of a varying permeability and compressibility non-linear structural viscosity and also smear at the drainage boundaries. Rheological model is disused for structural viscosity in three dimensional case which reduces to Kelvin spring model and to Barron's equation for  $m=0$ . Though the soil is considered homogeneous anisotropy prevails but the effect is small. Comparison of theoretical analysis of Barron and Wilkinson indicates that no derivation is observed for case of varying coefficient of permeability and coefficient of volume compressibility when ratio of effective pressure at time 't' to initial value of effective pressure is less than or equal to two.

Case –I: Effect of smear adjacent to the drainage boundaries:

The limited number of solution presented by Barron (1948) has been extended to cover a wide range of  $k_h / k_s$  and  $r_e / r_w$  values corresponding to  $n$  values of 10 and 20. Fig.2.38 shows the relationship of average degree of consolidation ' $\mu$ ' against time factor ' $T$ ' for sand drain  $n = 20$  with smear effects for free strain condition and Fig.2.39, 2.40 shows the theoretical solution in terms of  $u$  against  $T_{50}$  and  $(r = 0.55r_e)$  against  $\log T$  for typical values of  $k_u / k_s$ ,  $r_s / r_w$

of 1.1 and  $n$  of 20 . From such solution the ratio of the actual  $C_h$  values of the undisturbed soil to measured  $C_h$  value based on the two fitting methods previously described, may be obtained. Fig. 2.41 shows the ratio  $C_{h \text{ actual}} / C_{h \text{ measured}}$  plotted against  $k_h / k_s$  for various values of  $r_s / r_w$  and  $n$  values of 10 and 20.

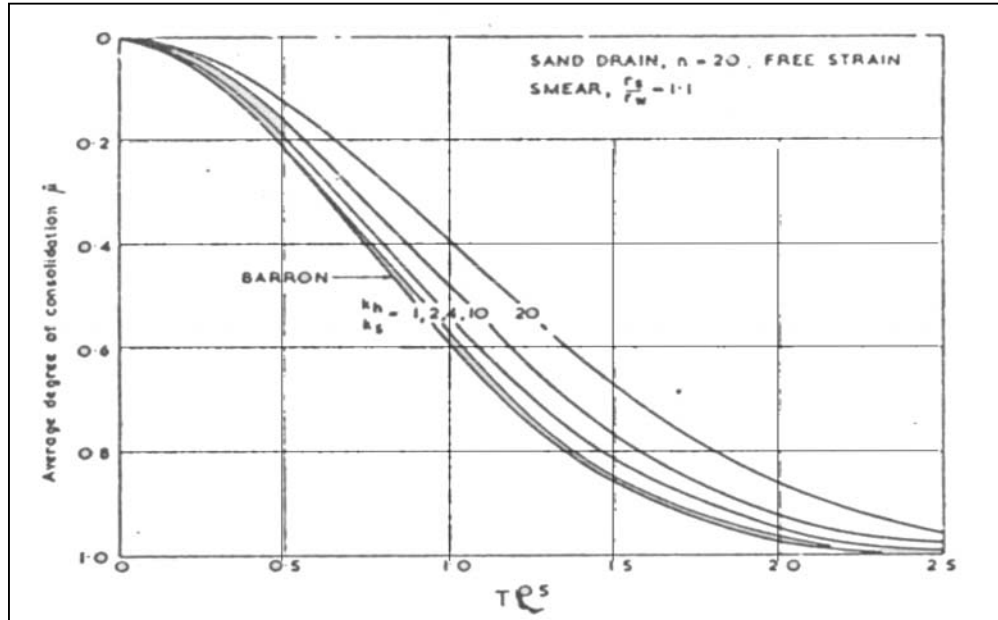


**Fig. 2.38:** Average degree of consolidation  $\bar{u}$  plotted against time factor  $T$  for sand drain  $n=20$  with smear  $s_m = 1.1$ , free strain (after Berry et al., 1969)

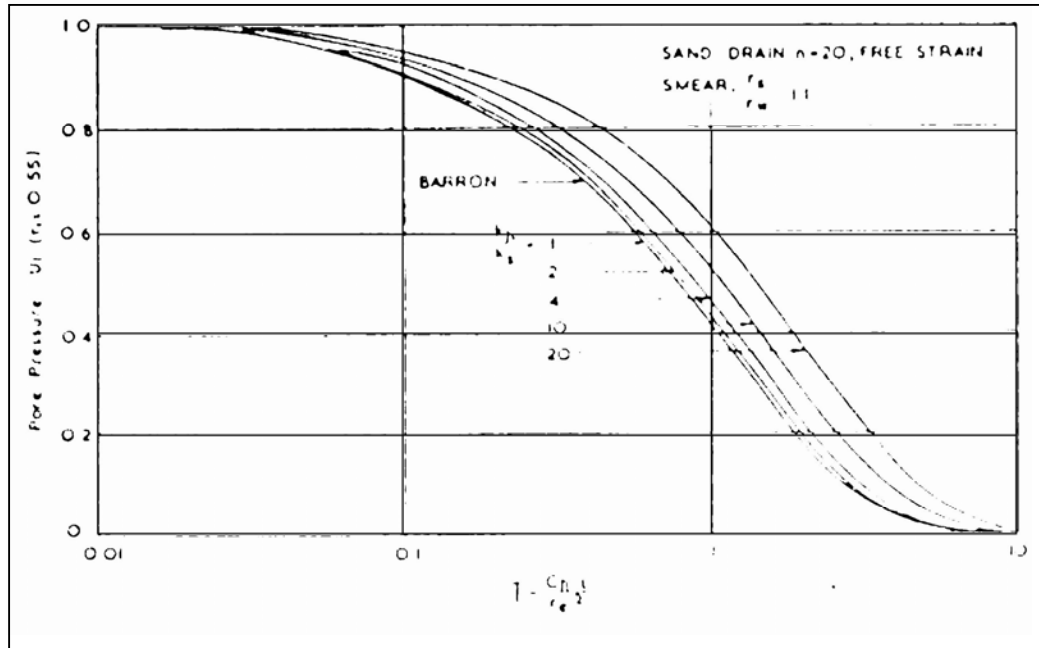


**Fig. 2.39:** Rate of dissipation of pore pressure plotted against time factor  $T$  for sand drain  $n=20$  with smear  $s_m = 1.1$ , free strain (after Berry et.al, 1969)



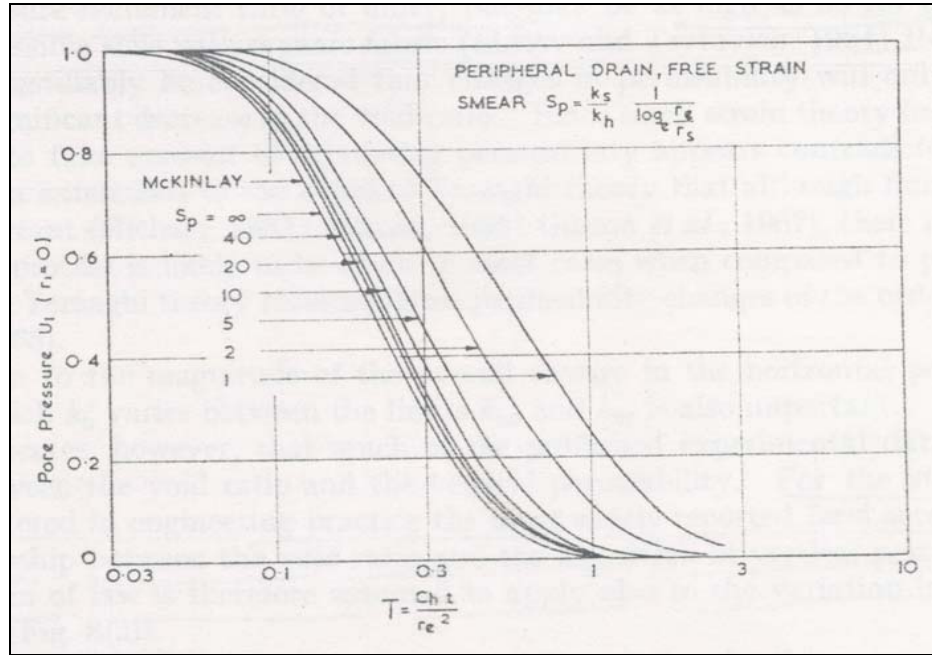


**Fig.2.40:** Rate of dissipation of pore pressure plotted against time factor T for peripheral drain with smear for various values of  $s_p$ , free strain (after Berry et al., 1969)

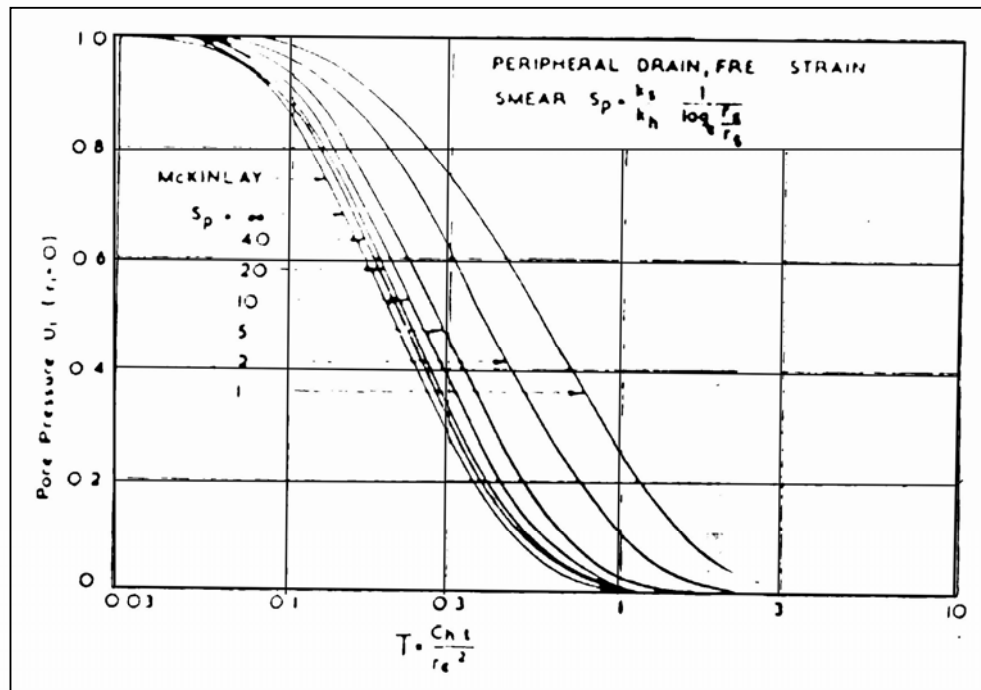


**Fig.2.41:** Boundary conditions for central sand drain and peripheral drain (after Berry et al., 1969)

Case – II: Effect of variable permeability and non linear compressibility

Structural viscosity and not taken into account. Darcy's law is assumed to be valid with respect to the flow of pore water i.e.  $v_n = +k b_i r$  where ' $i_r$ ' is the hydraulic gradient in the radial direction .

As pointed out by Gibson et al. (1967), it is the relative velocity between the soil grains and the pore water that cause a pore pressure gradient. The continuity of volume for radial flow of pore water through an element of soil given:

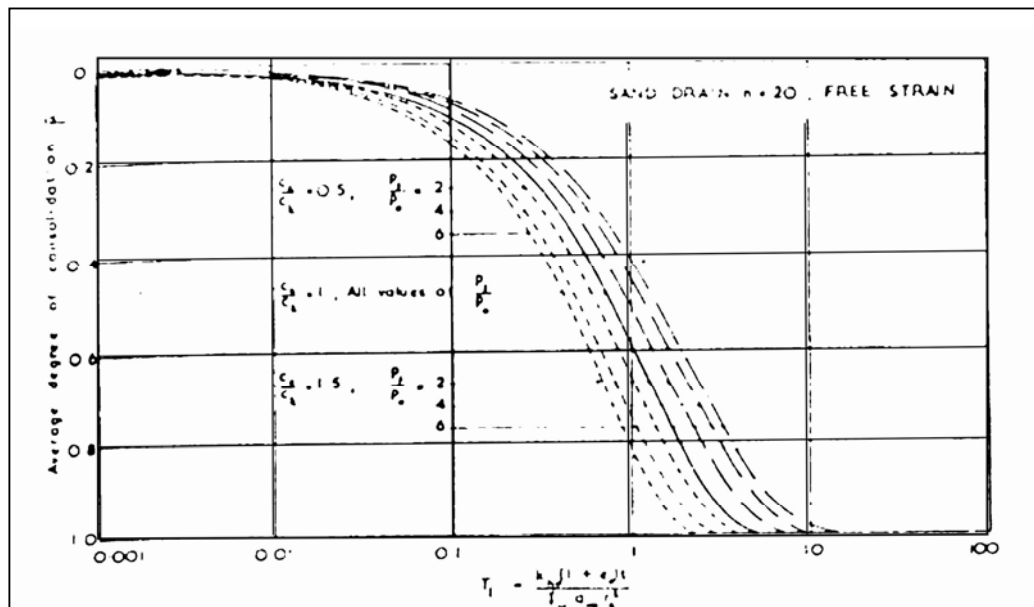
$$\frac{\partial}{\partial r} [k h \frac{\partial u}{\partial r}] + \frac{k h}{r_w r} \frac{\partial u}{\partial r} = \frac{1}{1+e} \frac{\partial e}{\partial t} \quad \text{2.50}$$

Solution of this equation of boundary condition identical to Barron's theory, gives

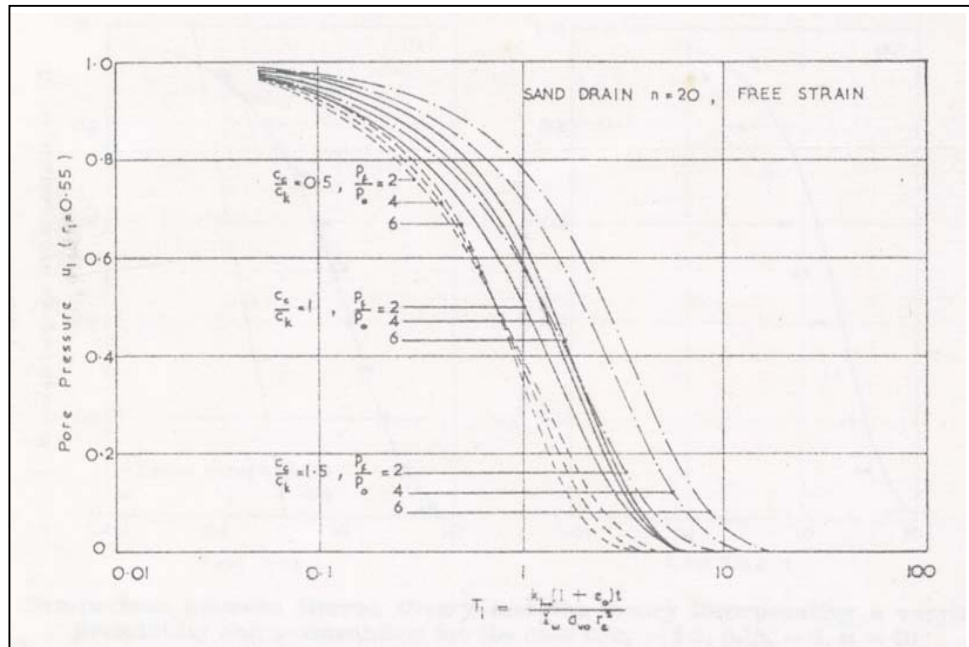
$$\frac{h(1+q)u}{r_1^2} \frac{\partial^2 u}{\partial s^2} + \frac{[\partial u]^2}{\partial s} \frac{1}{h(1-q)} = \frac{\partial u}{\partial T_1} \quad \text{2.51}$$

Figure 2.42(a) , 2.43(a) , 2.44 shows the effect of different values of  $p_1/p_0$  and  $C_c/C_k$  on the  $u \cdot \log T$  , relation for the case of sand drain having  $n$  of 20 and 10 respectively .It can be seen that the rate of settlement is critically dependent on whether  $1 < C_c/C_k < 1$ . The solution is most conveniently explained by the equations:

$$\frac{k n_0}{k n_f} = \left[ \frac{p_f}{p_0} \right]^{C_c/C_k} = \left[ \frac{a v_0}{a v_f} \right]^{C_c/C_k} \quad \text{2.52}$$



**Fig.2.42 (a):** Average degree of consolidation  $u$  plotted against time factor  $T_1$  for a varying compressibility and permeability relationship, sand drain  $n=20$ , free strain (after Berry et al. 1969)



**Fig.2.42 (b):** Rate of dissipation of pore pressure plotted against time factor  $T_1$  for a varying compressibility and permeability relationship, sand drain  $n=20$ , free strain (after Berry et al. 1969)

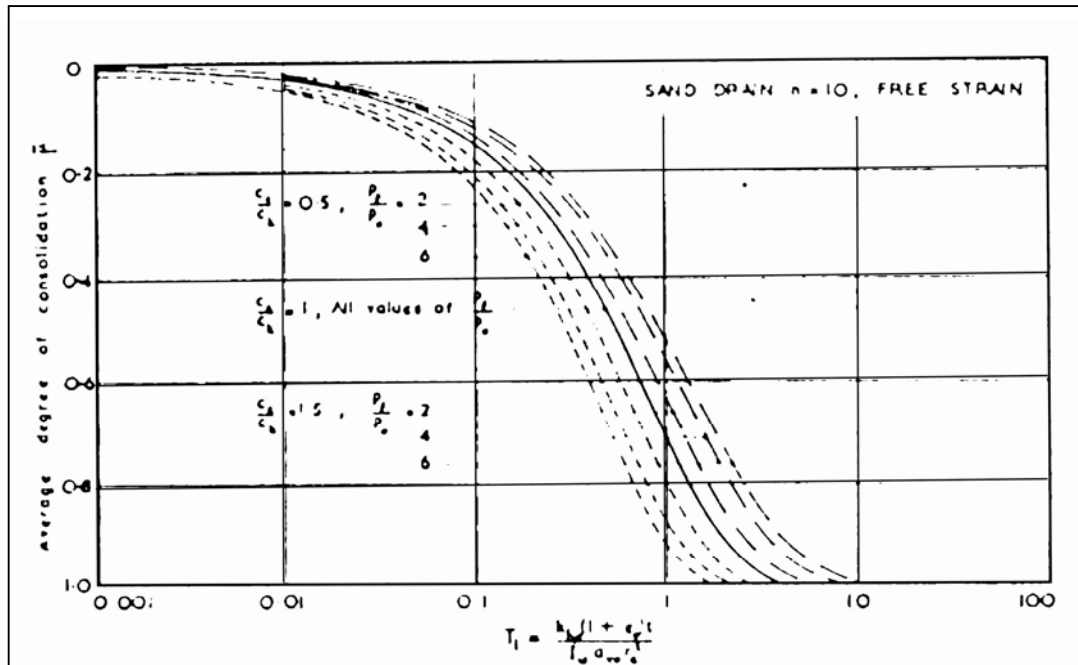


**Fig.2.43(a):** Average degree of consolidation  $U$  plotted against time factor  $T_1$  for a varying compressibility and permeability relationship, sand drain  $n=10$ , free strain (after Berry et al. 1969)

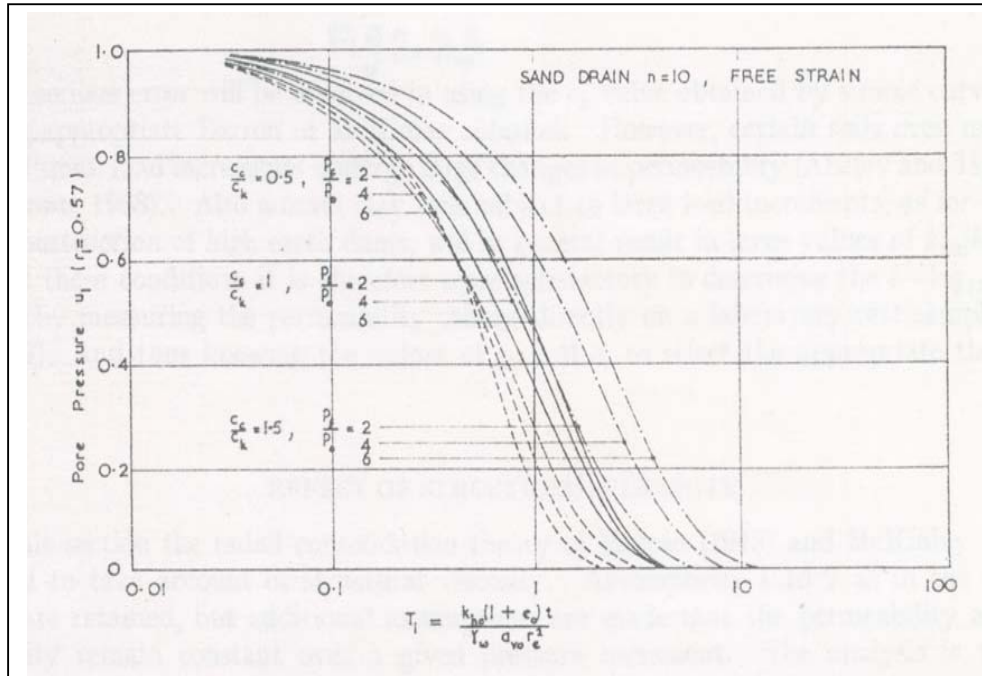


**Fig.2.43 (b):** Rate of dissipation of pore pressure plotted against time factor  $T_1$  for a varying compressibility and permeability relationship, sand drain  $n=10$ , free strain (after Berry et al. 1969)

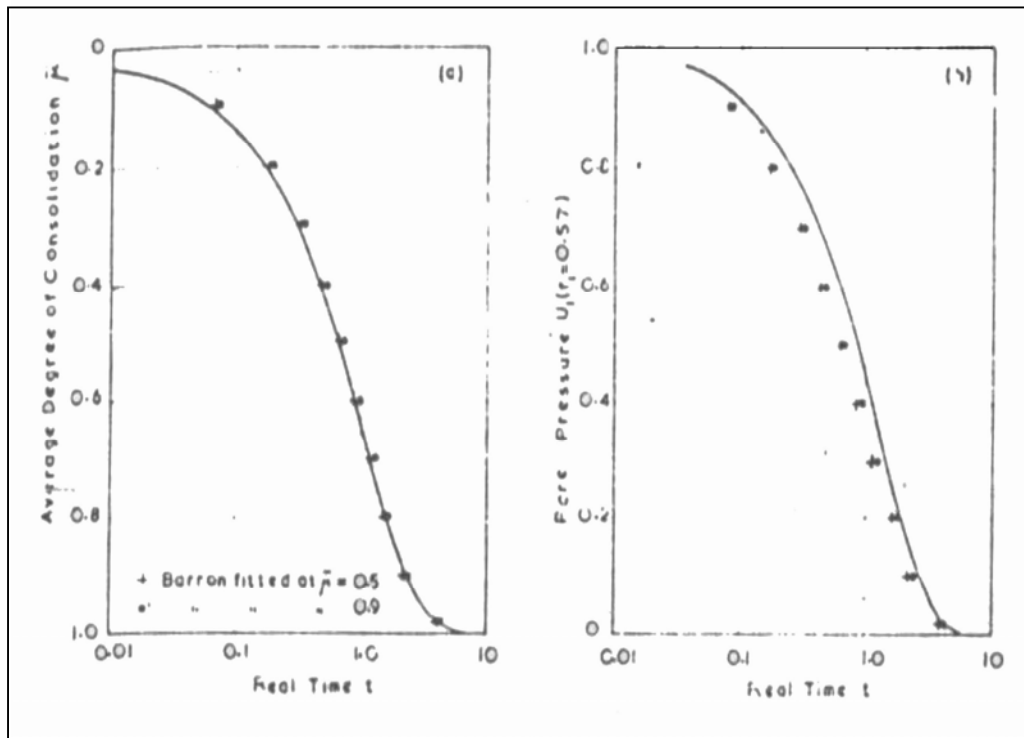


**Fig.2.44 :** Comparison between Barron theory and the theory incorporating a varying compressibility and permeability for the case  $C_c/C_k = 1.5$ ,  $p_i/p_0 = 2$ ,  $n=10$

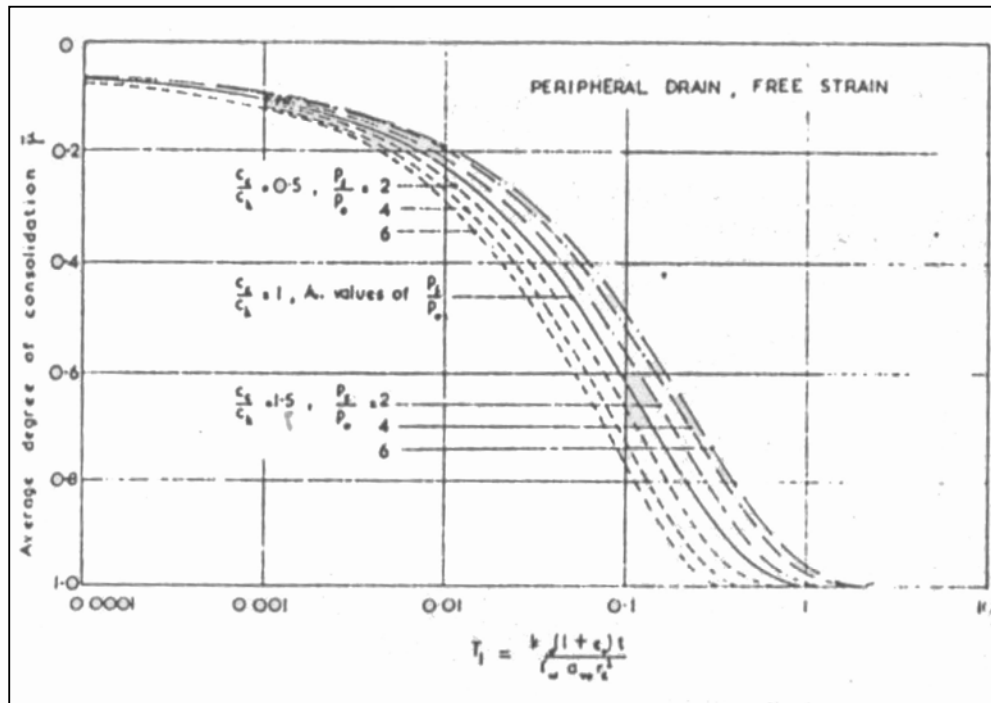


**Fig.2.45:** Average degree of consolidation  $u$  plotted against time factor  $T_1$  for varying compressibility and permeability relationship, peripheral drain, free strain

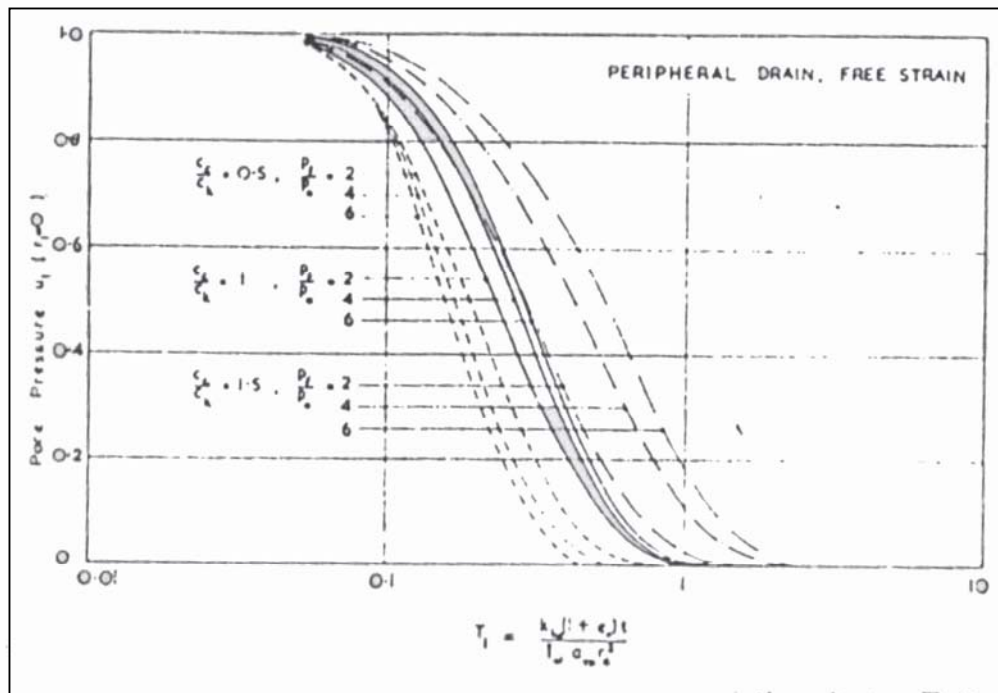


**Fig.2.46:** Rate of dissipation of pore pressure plotted against time factor  $T_1$  for varying compressibility and permeability relationship, peripheral drain, free strain

Case – III: Effect of structural viscosity

Assuming the permeability and compressibility to be constant, the equation for continuity of volume for radial flow of pore water through an element of soil was given as :

$$\frac{\partial u}{\partial r} = \frac{\partial^2 u_1}{\partial r^2} + \frac{1}{r_1} \frac{\partial u_1}{\partial r_1} \text{-----} 2.53$$

If non-linear viscosity is represented by a Kelvin element as shown in Fig.2.47, its void ratio effective pressure relationship will be as shown in Fig.2.47 and another governing equation for radial consolidation of the soil possessing structural viscosity will be

$$\frac{\partial u}{\partial T} = (1/m) (1-u-u_1) m \text{-----} 2.54$$

where,

$$M = T/T_s = [Kh(1+e_o)b_1^m] [r_w r_e^2 (\Delta p)^{m-1}] \text{-----} 2.55$$

Equation 2.54 becomes

$$\partial u / \partial T = [(1/r_1^2) (\partial^2 u_1 / \partial s^2)] \text{-----} 2.56$$

$$\text{Where, } S = \ln (n, r,) \text{-----} 2.57$$

Numerical solution of the two pairs of simultaneous equations 2.54 and 2.56 can be obtained using Barden's method, Barden (1965). The initial distribution of pore pressure for clay with  $m = 5$  and sand drains with  $n = 5, 10$  and  $20$  for a range of values of  $m$  has been computed and shown in Fig. 2.48(a) and 2.49(a). The corresponding plots of average degree of consolidation against  $\log T$  are presented in Fig. 2.48(b) and 2.49(b). These figures show that the effect of  $M$  which is measure of the effective viscous resistance on the soil skeleton to deformation is to retard the rate of consolidation and accelerate the rate of dissipation of pore pressure.

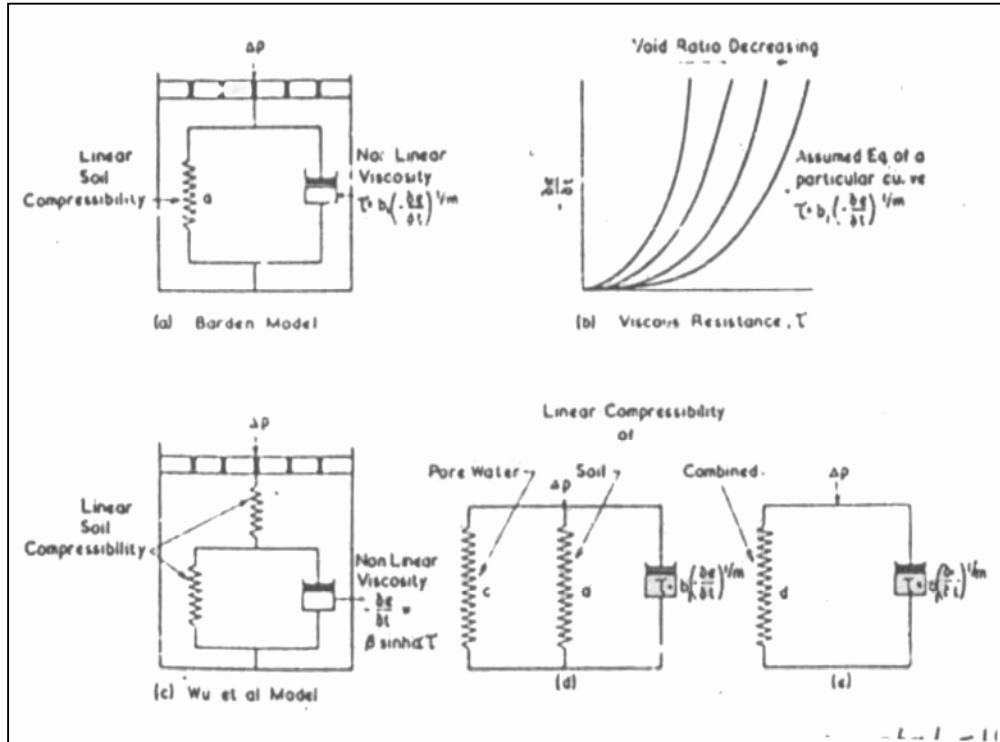


Fig.2.47: Rheological Models (after Berry et al., 1969)

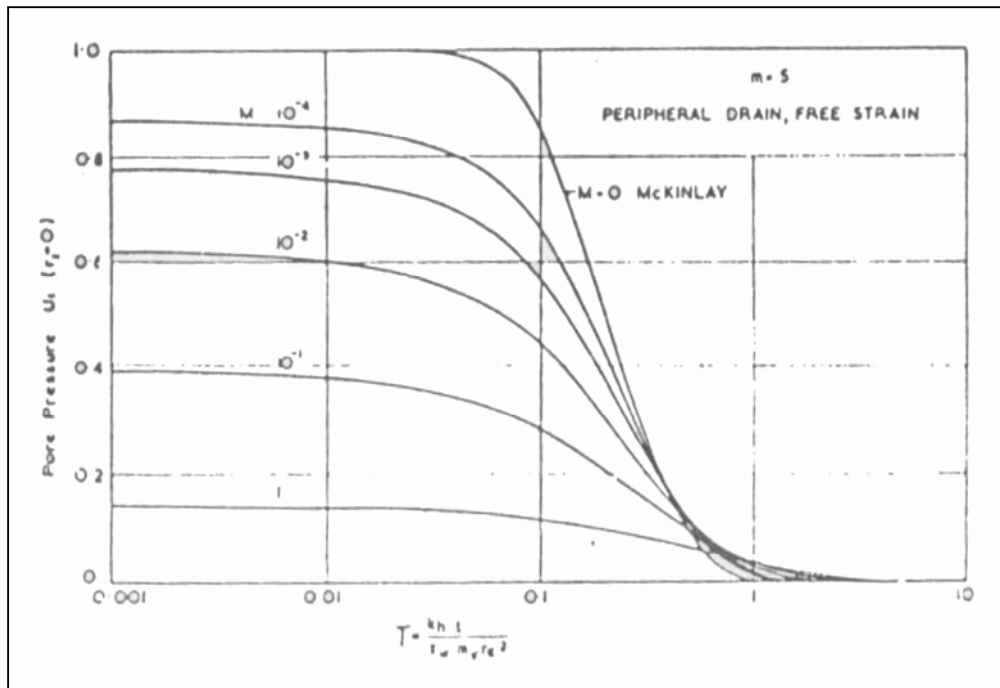
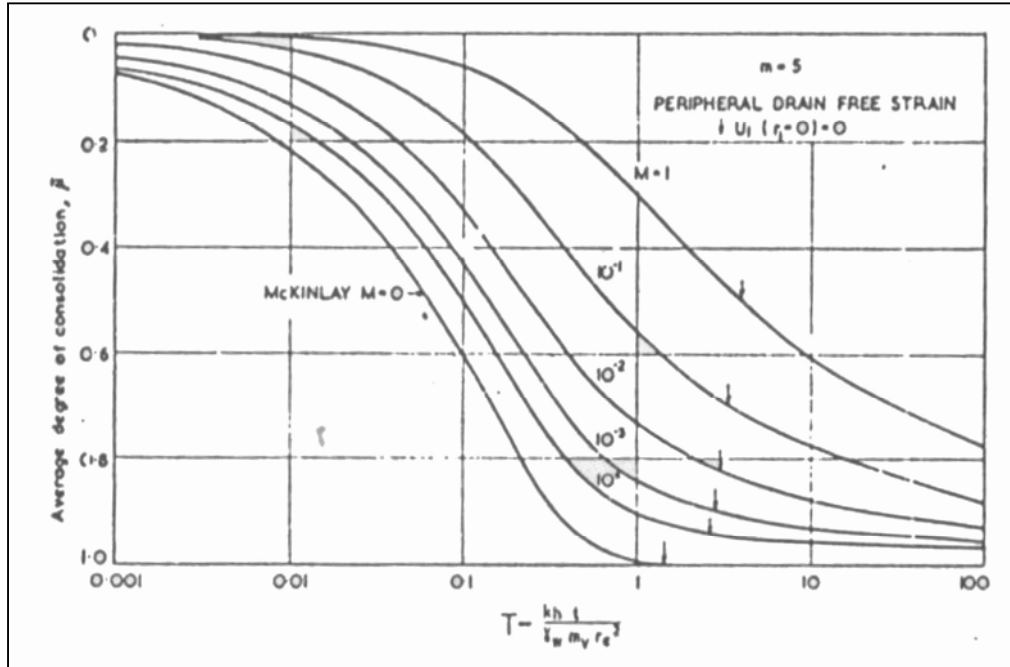
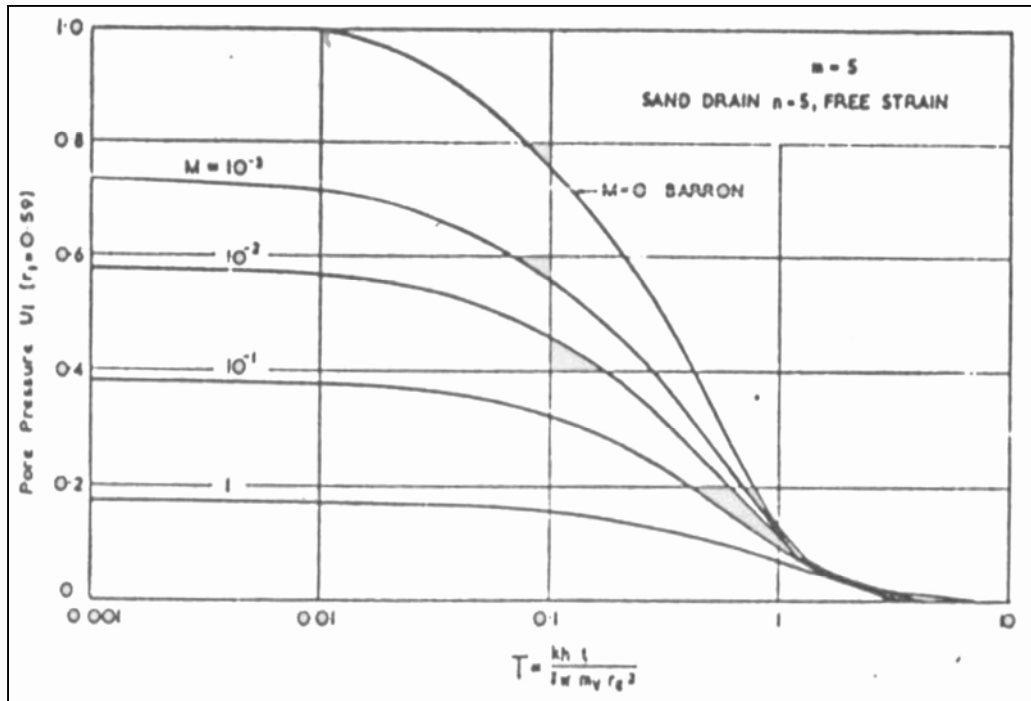


Fig.2.48(a): Rate of dissipation of pore pressure plotted against time factor T for different values of M, peripheral drain, free strain (Berry et al., 1969)



**Fig.2.48 (b):** Average degree of consolidation  $\bar{u}$  plotted against time factor  $T$  for different values of  $M$ , peripheral drain, free strain (Berry et al., 1969)



**Fig. 2.49 (a):** Rate of dissipation of pore pressure plotted against time factor  $T$  for different values of  $M$ , sand drain  $n=5$ , free strain (Berry et al., 1969)



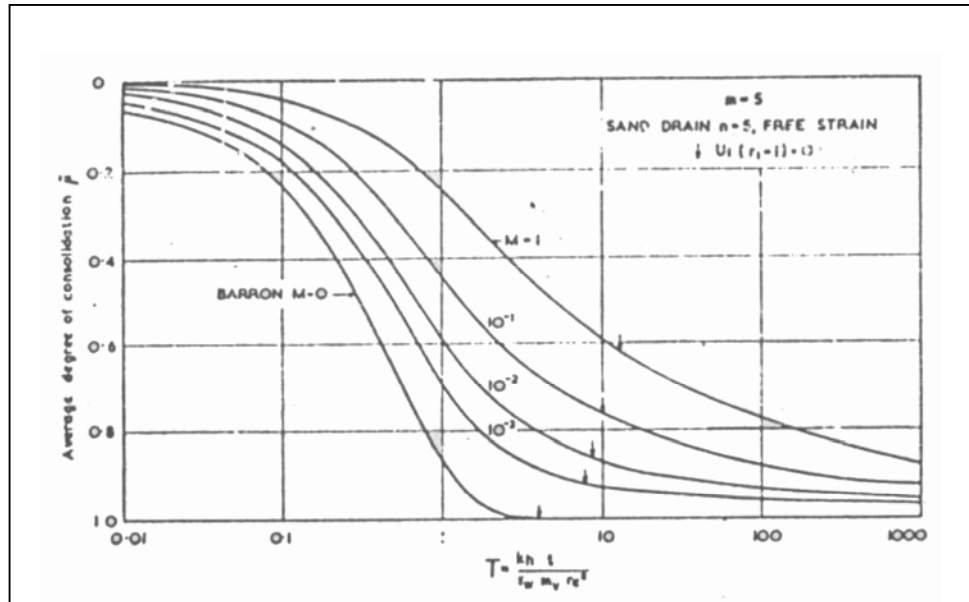


**Fig.2.49 (b):** Average degree of consolidation  $\bar{u}$  plotted against time factor  $T$  for different values of  $M$ , sand drain  $n=5$ , free strain (after Berry, et al., 1969)

### 2.7.19 Simons – Tan Solution (1971)

Simons and Tan (1971) extended the work of Berry-Wilkinson incorporating additional factors namely coefficient of compressibility during consolidation as variable non-linear relationship of void ratio and effective stress and rate of pore water dissipation and magnitude of consolidation as depicted from fig.2.50 and fig.2.51.

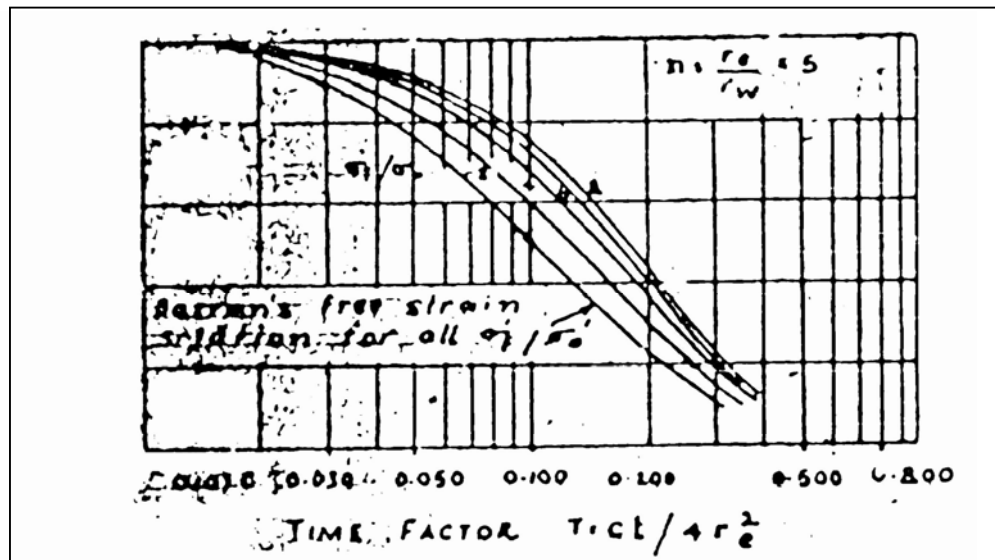


**Fig.2.50:** Comparative plot of ratio  $U/\sigma'_t - \sigma'$  against time factor  $T$  (after Simon-Tan, 1971)

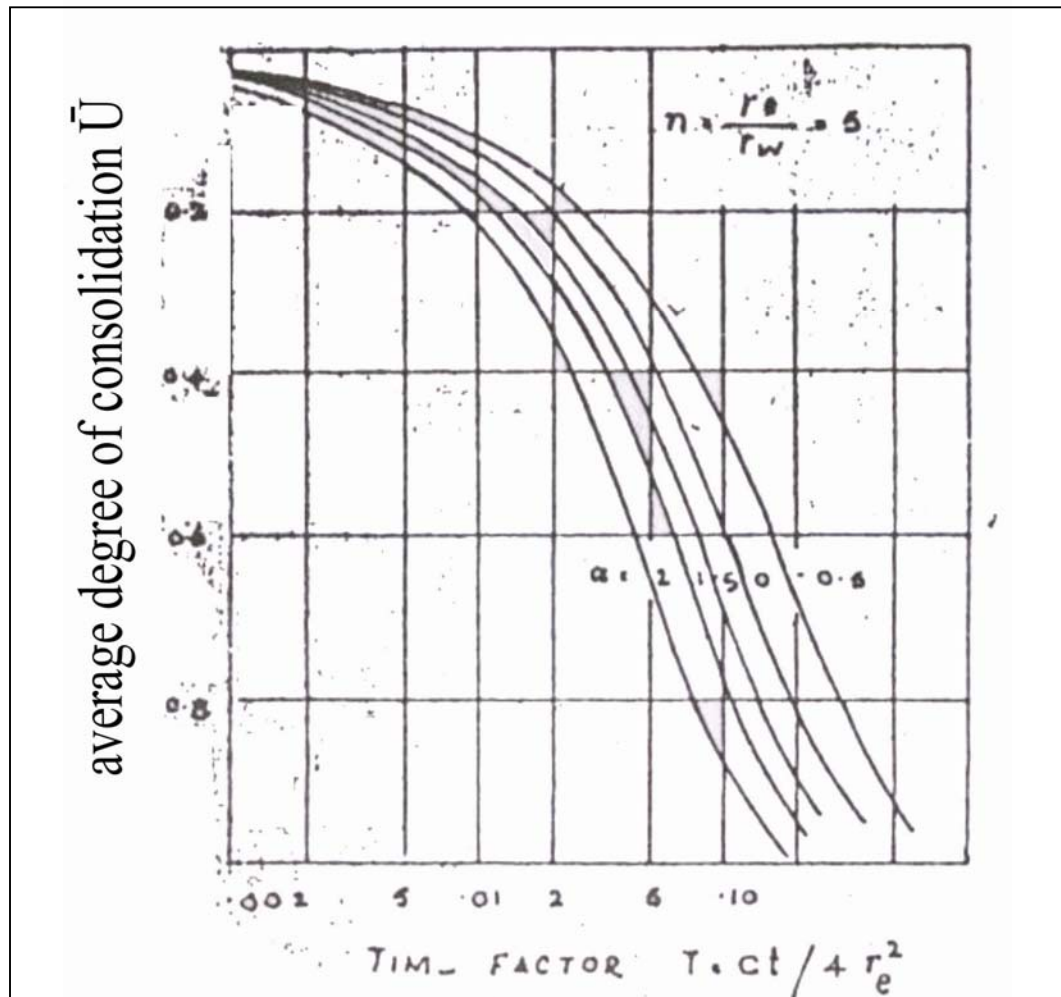


**Fig. 2.51:** Plot of average degree of consolidation  $\bar{U}$  against time factor  $T$  (after Simon-Tan, 1971)

#### 2.7.20 Tsytovinch Martirosyan Kulkarni's Theory (1971)

Tsytovinch et al. (1971) presented solution of several three dimensional problems the consolidation of clayey soils by making use of the concept for consolidation of multiphase soils taking into account the selection creep and the compressibility of the pore fluid , according to the design model of equal deformation (equal vertical strain ) .

The modification accounts for the quantity 'q' termed the coefficient of volume compressibility of the pore fluid. The solution of state of skeleton is presented as an integral equation of the hereditary creep theory, Ter-martirosyan (1965). The equation is expressed as:

$$\frac{\partial e}{\partial t} = e_o q_w \left( \frac{dp}{dt} \right) = k_v [1+e_o] / r_w \left[ \frac{dp^2}{dr^2} + \frac{1}{r} \left( \frac{dp}{dr} \right) \right] + k_v (1+e_o) / r_w \left( \frac{dp^2}{dz^2} \right)$$

2.58

where,

$$q_w = - \left[ \left( \frac{1}{v} \right) \frac{dv}{dp} - (1-l_w)/p_a \right]$$

 $r_w$  = unit weight of pore fluid $v$  = volume of pore fluid $l_w$  = degree of saturations (determined experimentally) $p_a$  = atmospheric pressure $k_v, k_r$  = coefficient of permeability in the vertical and radial direction (determined experimentally)

### 2.7.21 Creyer's Theory

Creyer (1961) considered Biot's equation for a porous isotropic and elastic medium is discussed in details for three dimensional process of consolidation. The solutions of Biot's and Terzaghi's theories are compared for a case of saturated sphere of soil subjected to uniform pressure. In his opinion agreement between Terzaghi's one dimensional theory and the experimental results is not perfect because secondary compression is not accounted for in theory. Three dimensional theories of Terzaghi, Rendulic and Barron are not uniquely defined and several variants are used. Biot's equation is not adopted by any for laboratory analysis. Mathematical theories are in complete state. Biot's and Terzaghi's theories give a complete picture of consolidation. In this theory (1961) the soils is considered as porous skeleton filled with water. Final plots given by Creyer are represented in fig. 2.52 and fig. 2.53.

### 2.7.22 T.K.Tan's Theory

Tan (1961) presented for anisotropic clay strata secondary compression. Stress-strain relationship for clay as a function of time by linear differential equation. Rheological measurements emphasized for secondary compression. The differential equation for displacement and pore water pressure are:

$$-s \frac{d\epsilon}{dt} = K_h \left[ \frac{d^2 \sigma_w}{dx^2} + \frac{d^2 \sigma_w}{dy^2} \right] + K_v \frac{d^2 \sigma_w}{dz^2} \text{-----} 2.59$$

$$C_v = C_h = \frac{3(1-e)}{1+e}$$

Where,  $e$  is a function of  $K_h$ ,  $K_v$  and  $S$ .  $S$  is compression modulus. Tan considered  $e$  as elastic path of lateral expansion as shown in fig. 2.54.

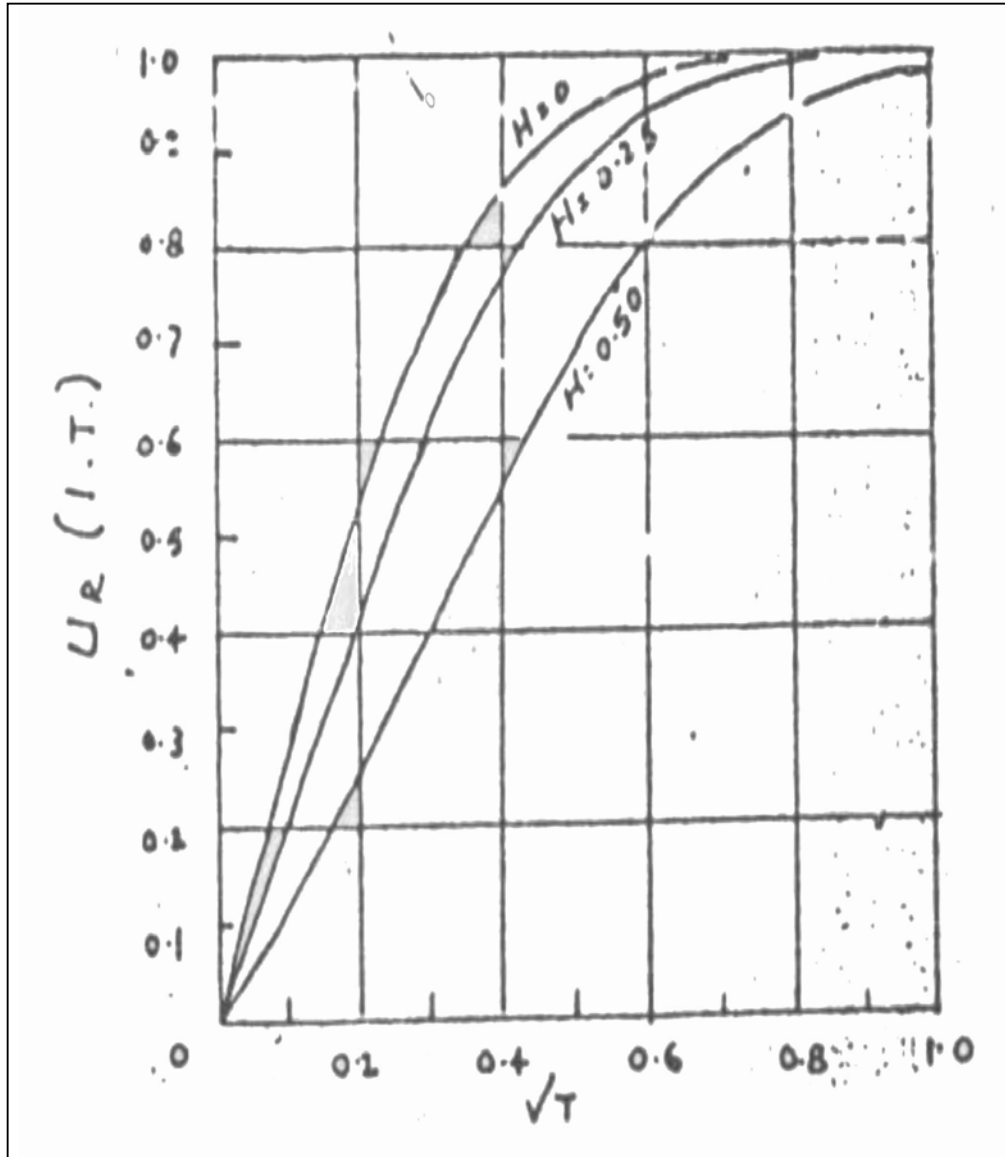


**Fig. 2.52:** Plot of degree of consolidation against under root of time factor  $T$  for  $\mu = 0.25, 0.50$  (after Creyer, 1961)

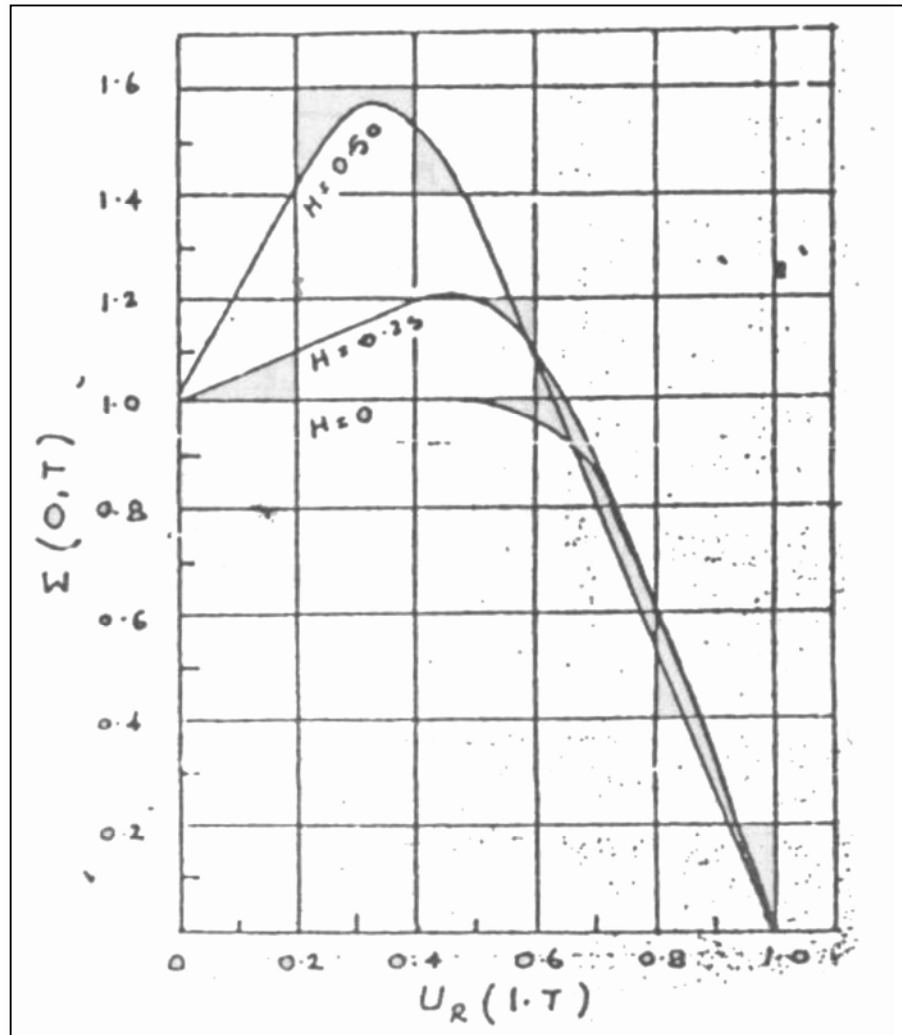


**Fig.2.53:** Plot of  $\Sigma(0, T)$  against  $U_R(1, T)$  for  $\mu = 0.25, 0.50$  (after Creyer, 1961)

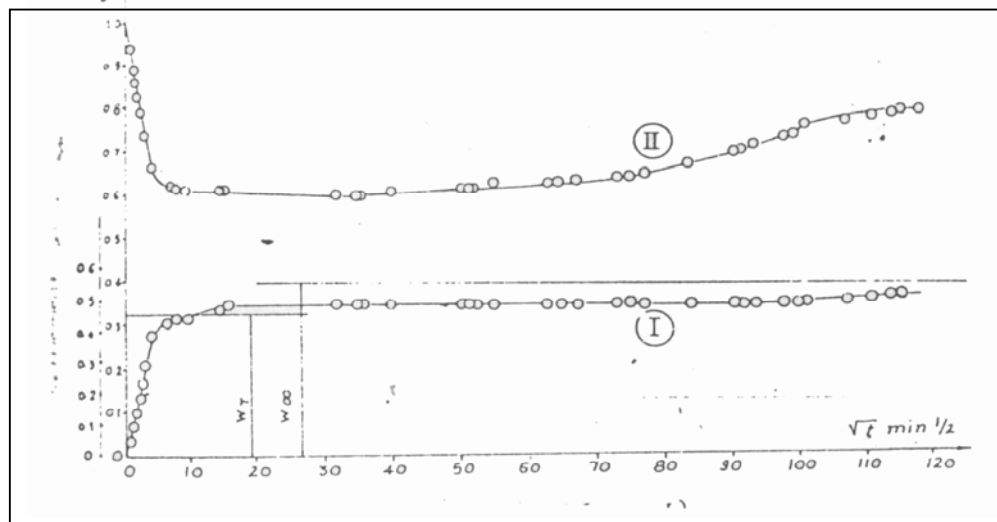


**Fig.2.54:** Settlement as function of  $\sqrt{t}$  (curve I) and Ratio of lateral/vertical pressure  $\delta e/q$  as function of  $\sqrt{t}$  (curve II)

### 2.7.23 Parikh, Verma and Shroff Theory (1975)

Parikh, Verma and Shroff (1975) established a differential equation following the work of Gibson et al. (1967) based on Lagrangian mathematical scheme. The stress strain relationship for clayey minerals, pore fluid and soil skeleton are accounted in a lumped parameter 'p'. For one dimensional consolidation 'p' is considered constant by Shroff (1972). For studying the influence of various physico chemical factor. For a case of pure vertical flow (one way drainage) with equal vertical strain condition of consolidation, the constant parameter 'p' of the equation can be used as a variable. The basic equation is:

$$\partial e / \partial t = [\partial^2 e / \partial z^2 - P (\partial e / \partial z)] \text{-----} 2.60$$

This equation has a form identical to the differential equation for non – steady, one dimensional flow of heat through moving media against the Terzaghi's classical concept of heat flow through isotropic bodies.

### 2.7.24 Sill's Theory (1975)

Sill (1975) compared under certain Biot's equation and Terzaghi's equation. He suggested that Terzaghi's assumed total stress remaining every where constant and change are caused only by change of pore water pressure. Biot considered continuing interaction between skeleton and pore water. If sum of normal total stress is constant these equations are the same. The functions demonstrating these conditions are developed and confronted.

### 2.7.25 Yamaguchi Theory (1976)

Yamaguchi et al. (1976) used Biot's theory for two and three dimensional consolidation of clay layer with finite thickness. Peculiar phenomena that the settlement is more retarded than that of Terzaghi's theory is predicted. He also suggested that behavior of pore water pressure can be satisfactorily predicted by Biot's theory if the dilatancy effect is taken into account.

### 2.7.26 Yoshikuni and Nakanodo Theory (1974)

The resistance offered by the drains to the vertical flow of water affects the rate of consolidation. Barron studied the effect on radial consolidation while

Yoshikuni and Nakanodo (1974) dealt with three dimensional consolidation. Their results are shown in Fig.2.55 and notations are defined in Fig.2.55. The values of  $C_{vr}$  are given for a specific situation as shown in fig.2.55 presents the time required to reach 50% and 80% degree of consolidation for a wide range of situations.

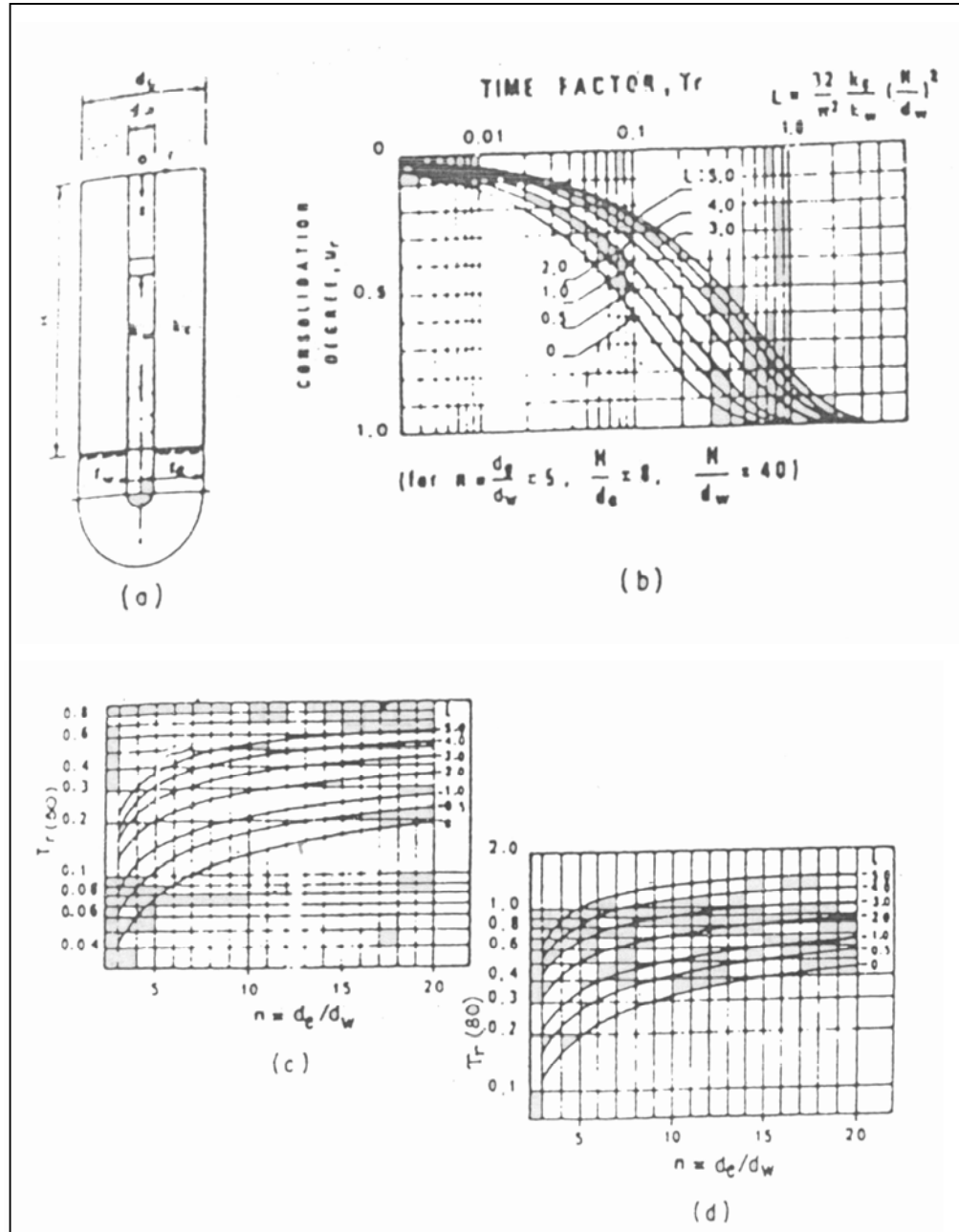


**Fig. 2.55:** Effect of drain resistance on consolidation rate (a) Notation (b) Values of  $U_r$  (c) Values of  $T_r(50)$  (d) Values of  $T_r(80)$   
(After Yoshikuni & Nakanodo, 1974)

### 2.7.27 Lee and Viliappan Theory (1974)

The presence of stratification in the form of thin seams of silt or sand causes consolidation to occur faster than predicted on the basis of laboratory Oedometer tests. In addition to well known papers by Rowe (1964, 1968) which consider the influence of stratification, Lee and Viliappan (1974) produced the Nomo graphs in Fig.2.56 to illustrate these effects.

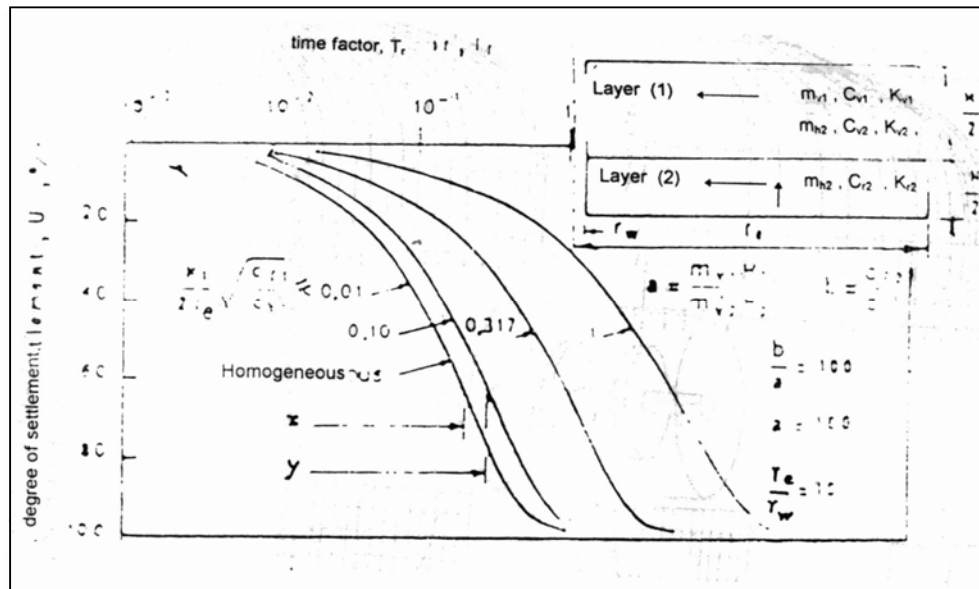


**Fig. 2.56:** Effect of stratification on vertical drain performance  
(Lee & Viliappan, 1974)

### 2.7.28 Chaput and Thomann's Theory (1975)

Early theoretical studies of vertical drains assumed instantaneous loadings, but the practical solution is one of gradual loading, and the prediction of amount of consolidation during the loading stage is of considerable importance. A solution for linearly increasing load has been given by Chaput and Thomann's (1975). If the average degree of consolidation  $u$ , is defined as the ratio of the settlement at time  $t$  when the load reaches from  $p(t)$  Fig.2.57(a) to the ultimate settlement that would result from  $p(t)$  applied instantly, then during the application

$$(0 \leq t \leq t_0) .$$

where ,

$\Delta 1$ ,  $B(n)$ , and  $c$  are given in Figure – 2.57(b),(c) and (d) respectively . Once the total load has been applied.



$$U = B(n) C (\Lambda_1^n n^2 Tr_0, Tv_0) D [\Lambda_1^{-2} n_1^2 (Tr - To)(Tv - Tvo)] \text{ ----- } 2.62$$

D is in the nomogram in Fig.2.57 (e).

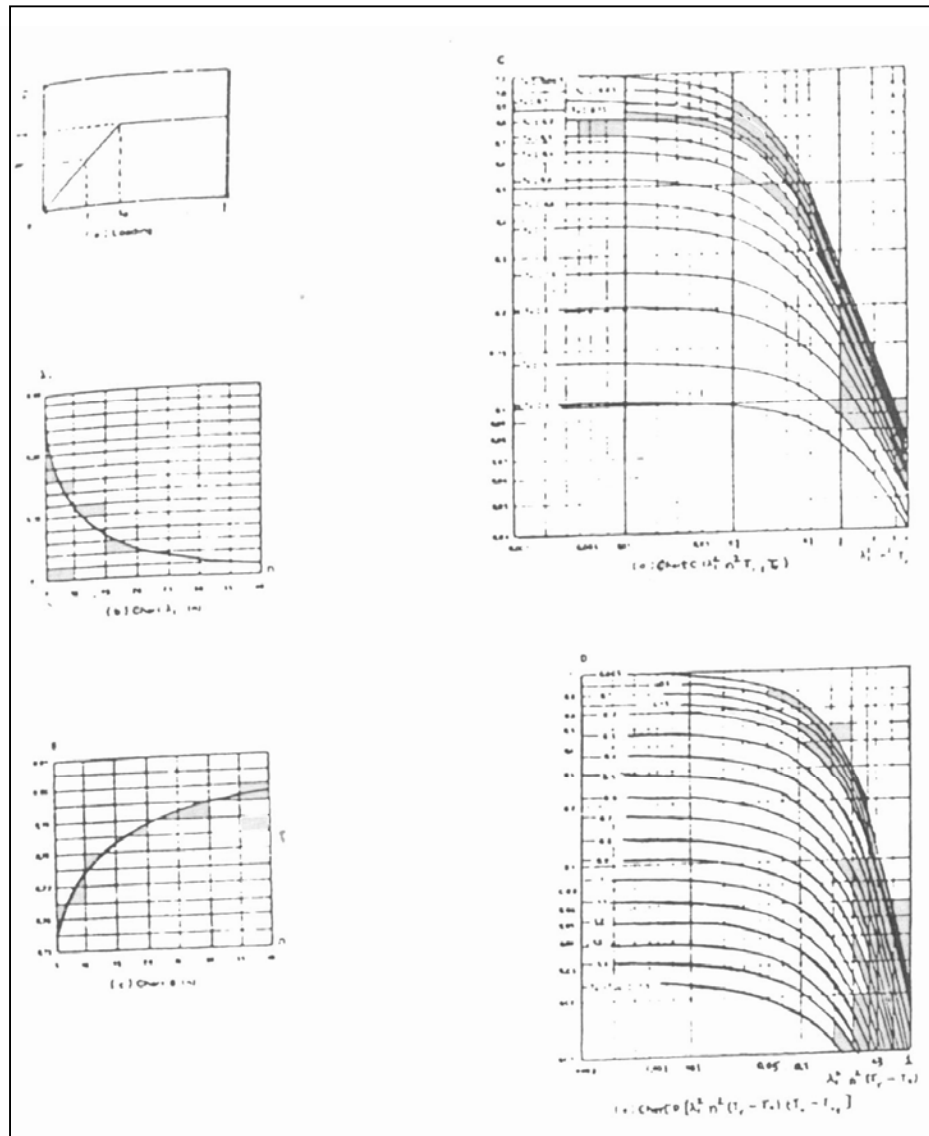


**Fig.2.57:** Nomograms for the function required for the design of vertical drains under progressive loading conditions (Chaput & Thomann, 1975)

### 2.7.29 Brenner and Pbebaharan's Theory (1983)

Brenner and Pbebaharan (1983) develops a finite difference model for prediction of settlement and pore pressure and back calculated consolidation parameters taking into account a layered soil profile , two dimensional water flow time dependent loading , stress distribution varying with depth and undrained

deformations . The finite difference scheme was used for numerical treatment of the pore pressure time variations.

The degree of consolidation  $U$  for instantaneous loading is:

$$U = 1 - [U(t) / U_o] \quad \text{-----} \quad 2.63$$

where ,

$U(t)$  = mean excess pore pressure .

$U_o$  = initial excess pore pressure.

In case of sand drains, the pore pressure dissipates both in vertical and radial direction. The degree of consolidation will be over estimated when  $u_o(t) = p(t)$  .

$$1 - U(t) / U_o(t) \quad \text{for } 0 < t \leq t_o$$

$$U(t) = - U(t) / U_o(t_o) \quad \text{for } t > t_o$$

where ,

$$U_o = B (\Delta o_3 + A (\Delta o_1 - \Delta o_3)) \quad \text{-----} \quad 2.64$$

The degree of consolidation of the sand drain can be written as:

$$U_{jk} = 1/V_j \int u_{i,j} K dv_{i+j}$$

where  $V_j$  is volume of soil below depth  $z = j(z)$  . Neglecting creep settlement the ultimate consolidation ,  $s_{ult,j}$  at depth  $j(z)$  is given by :

$$s_{ult,j} = \sum_{u=j}^N e / (1+e_o) H_u \quad \text{-----} \quad 2.65$$

The total settlement is the sum of initial and the consolidation settlement.

### 2.7.30 Vreeken and Duijn's Theory (1983)

Vreeken and Duijn (1983) presented the numerical solution of the consolidation of heterogeneous soil a by vertical sand drains. They accounted for the heterogeneities in horizontally layered, circular shaped sand lenses surrounded by a low permeable material (clay).

The three dimensional consolidation equations for completely layered, homogenous and isotropic soils described by De Josselin Jong (1983) is:

$$k / r_w \Delta u = \partial e / \partial t \quad \text{-----} \quad 2.66$$

The water pressure  $u$  and the volume dilation of diameter skeleton 'e' can be related as:

$$[k + 4/3G] \Delta e = \Delta u \quad \text{-----} \quad 2.67$$

where,  $k$  and  $G$  do not depend upon the degree of consolidation. By integration of equation 2.67, we get,

$$[k + 4/3 G] e = u + g(x, y, z, t) \quad \text{-----} \quad 2.68$$

where the function 'g' should satisfy  $g = 0$ .

To study the influence of vertical chains in horizontally layered soils, De Leeuw (1965) results were used, which can be written as

$$C = k / r_w (k + 4/3G) = \text{consolidation coefficient.}$$

For heterogeneous case, with  $G$  and  $k$  constant and above equation changes to,

$$(1/r) \partial / \partial r [(C/r) \partial u / \partial r] + \partial / \partial z [C \partial u / \partial z] = \partial u / \partial t \quad \text{-----} \quad 2.69$$

From equation 2.69, exact degree of settlement can be determined

$$Q(t) = \pi (R^2 - r_o^2) [-u_z(H, t) + u_z(o, t)] \quad \text{-----} \quad 2.70$$

where,  $Q(t)$  = total amount of ground water which has been transported through the drain up to time  $t$ ,

$u_z$  = vertical upward displacement.

They concluded that the effect of permeable layers on the consolidation rate in a poorly permeable matrix is strongly determined by the length of the layers. The effect of short permeable layers ( $r_s / R_c - 2$ ) is small even for a high number of layers per meter and for large difference between the permeability of sand and clay.

### 2.7.31 Table for Theoretical Developments

Many research workers other than those discussed in section 2.7.1 to 2.7.30 have also carried out theoretical works on different aspects of consolidation problems like magnitude and rate of loading, permeability with respect to stratification, accounting linear and non-linear behavior with void ratio change, stratification of layers along with numerical simulations using finite element approach, finite difference approach, statistical approach considering with and without smear effects. The summary of these works have been reported in Table no. 2.4.

**Table 2.4:** Summary of various researchers in theoretical development

| Sr.No | Year       | Name of researchers           | Contribution   |
|-------|------------|-------------------------------|--|
| 1.    | 1969       | H.B.Poorooshab                | Proposed a mathematical model on the basis of certain observations of Jarret (1967) according to which the rate of change of void ratio with time is uniquely dependent on the state of the clay element. An approximate technique is used to obtain a solution of the set of differential equation incorporating above form and thus governing the process of consolidation of such a clay layer. |
| 2.    | 1974       | Olson R.E & Daniel D E et al. | Finite difference method (FDM) analysis for sand drains problems.  |
| 3.    | After 1975 | M.S.Atkinson & Eldred         | Consolidations of soil using vertical drains--practical factors are modeled using FDM program for Band shaped drains. -Like theoretical considerations, shape of drain, smear effect, drain resistance, soil drainage parameters, drain spacing)   |
| 4.    | 1979       | Chien-HsinYuan & Yvan Mao     | Primary and secondary plane strain consolidation using FEM approach.   |
| 5.    | 1979       | Bhide                         | Investigated the effects of soil smear and drain resistance.   |
| 6.    | 1985       | Runesson et al.               | FEM for radial consolidation   |
| 7.    | 1987, 1991 | A.Al Tabbaa & D.Muir Wood     | Studied the horizontal drainage during consolidation   |
| 8.    | 1989       | Zeng & Xie                    | Investigated the effects of soil smear and drain resistance  |

|     |            |                                |   |
|-----|------------|--------------------------------|---|
| 9.  | 1993       | Madhav et al.                  | Modeling and study of smear zones around the band shaped drains   |
| 10. | 1994, 2001 | J.C.Chai & N.Miura             | Complete new theoretical solution for unit cell consolidation is derived assuming the permeability in smear zone is linearly varied with radial distance from the drain. (Extension of Hansbo's theory)   |
| 11. | 1992, 1994 | Goughnour.R.R                  | Presented a model in which vertical strains are taken into account but soil properties are assumed to remain constant during consolidation Also presented study on finite strain consolidation for vertical drain.  |
| 12. | 1994       | Mesri et al.                   | Model based on material coordinates was proposed which can account for vertical strain and associated changes in the soil properties during radial consolidation.   |
| 13. | 1997       | H.D. Lin & C.C Wang            | Analysis of axial –strain induced by 3D-consolidation of cohesive soils-FDM approach was performed.   |
| 14. | 1997       | Indraratna B. & Redana .I      | Plane strain modeling of smear effects associated with vertical drains  |
| 15. | 1997       | Chai J.C & Miura. N & Sakajo.S | Theoretical study on smear effects around vertical drain  |
| 16. | 1998, 2000 | GuoFu Zhu, Jian-Hau Yin        | Finite elements procedure for the analysis of consolidation of layered soils with vertical drains using general one dimensional (1D) constitutive model using Newton-Cotes type integration formula. Takes into consideration layered systems, time dependent loading, well resistance, smear effect, inelastic stress-strain behavior. |

|     |               |   |   |
|-----|---------------|---|---|
| 17. | 1998          | Xio-Wu Tang,<br>Katsutada<br>Onitsuka                   | Simultaneous partial differential equation of consolidation considering well resistance and smear action are obtained for arbitrary loading method. Also solutions are obtained for above by the virtue of impulse function method.   |
| 18. | 1999          | W.Zhov,<br>H.P.Hong,<br>J.Q.Shang                       | A probabilistic design method is given taking into account the uncertainty in $C_h$ in the design for the optimum use of PVD for soil improvement. Carillo and Hansbo's theoretical solutions are modified.   |
| 19. | 2000          | Basu & Madhav   | Investigated the effects of soil compressibility and hydraulic conductivity   |
| 20. | 2000,<br>2001 | Tang& Onitsuka  | Worked on time dependent time loading   |
| 21. | 2001          | Xio-Wu Tang,<br>Katsutada<br>Onitsuka                   | Analytical solution for consolidation of double-layered ground with vertical drains under quasi-equal strain condition- Numerical approach was developed.   |
| 22. | 2001          | J.C.Chai,<br>Shui-Long Shen,<br>N.Miura,<br>D.T.Bergado | Approximate method for analyzing PVD improved sub-soil is proposed in this study. In this method the average degree of consolidation is compared with combination of (Terzaghi & Hansbo's) solution. An equivalent hydraulic conductivity is derived for PVD improved sub-soil. |
| 23. | 2001          | Jang et al.   | Investigated the effects of soil smear and drain resistance   |
| 24. | 1997,<br>2002 | Bergado et al.  | Reported that large strains are generally considered for PVD preloading projects  |
| 25. | 2003          | Toyoaki Nogami  | Produced a design method for an   |

|     |      |   |   |
|-----|------|---|---|
|     |      | & Maoxin Li   | optimum drain system and using a powerful transfer matrix method to formulate the consolidation behavior of clay with system of horizontal thin drains and vertical cylindrical drains. (FEM based approach)  |
| 26. | 2003 | Guo-Xiong Mei, Jian-Hua Yin, Jin-Min Zai, Zong-Ze Yin | Finite layer procedure for Biot's consolidation analysis of layered soils using a cross-anisotropic elastic constitutive model was developed.   |
| 27. | 2003 | Patrick Fox & Mario Di Nicolo                         | Piecewise Linear model for large strain radial consolidation (FEM based) was proposed.  |
| 28. | 2004 | Xu-Sheng Wang, Jiu-Jimmy Jiao                         | Analysis of soil consolidation by vertical drain with double porosity model. The horizontal flow under equal strain condition is analyzed with circular or regular polygonal boundary. Developed (one dimensional double porosity model (DPM))-analytical and numerical solutions are obtained.   |
| 29. | 2004 | Chin Jian Leo   | Proposed solution for the equal strain consolidation by considering vertical and radial drainage in a fully coupled fashion. The closed-form solutions are obtained for excess pore pressure and degree of consolidation in the undisturbed soil mass subjected to a step or ramp loading. Mathematical formulation is given for case of 'no smear' and 'well resistance. |
| 30. | 2004 | Leo.C.J   | Equal strain consolidation by vertical drains   |

|     |            |                                       |  |
|-----|------------|---------------------------------------|--|
| 31. | 2005       | Sushil .K. Singh                      | Analytical solutions developed for the one-dimensional consolidation settlement of clay under triangular loading along with two new methods' diagnostic curve and Peak derivative 'for estimation of $C_v$ ' and settlement.   |
| 32. | 2005       | Zhu & Yin                             | Proposed solution for one dimensional consolidation using numerical approach and presented design charts for vertical drainage with two layers.  |
| 33. | 2005, 2008 | B. Indraratna, I .Sathananthan et al. | Analytical and Numerical modeling of soft soil stabilized by PVD with a linearly distributed (Trapezoidal) vacuum pressure for both axisymmetric and plane strain conditions. The plane strain analysis was executed by transferring the actual vertical drains into a system of equivalent parallel drain wells by adjusting the coefficient of permeability of the soil & applied vacuum pressure. Use of FEM code ABAQUS was employed using modified cam-clay theory. Later on they also presented a study to analyze the extent of the smear zone caused by mandrel driven vertical drains, employing the cavity expansion theory for soft clay obeying the modified Cam-clay model. |
| 34. | 2008, 2009 | Rohan Walker, B. Indraratna et al.    | Analytical solutions are presented for vertical and radial consolidation of multilayered soils using spectral method. Combined vertical and radial drainage are considered under instantaneous or single ramp loading ignoring well resistance.  |



|     |      |  |  |
|-----|------|--|--|
| 35. | 2008 | Cholachat Rujikiatkamjorn, B.Indraratna              | Presented three-dimensional 3D and two-dimensional 2D numerical analysis of a case study of a combined vacuum and surcharge preloading project for a storage yard at Tianjin Port, China. In 3D analysis, the actual shape of PVDs and their installation pattern with the in situ soil parameters were simulated. The finite-element code, ABAQUS, using the modified Cam-clay model was used in the numerical analysis.  |
| 36. | 2010 | Ali Ghandeharioon, B. Indraratna et al.              | The installation of mandrel-driven prefabricated vertical drains and resulting disturbance of soft saturated clays are analyzed with a new elliptical cavity expansion theory. This formulated theory accounts for a concentric progression of elliptical cavities in an undrained condition and the large-strain effects in the plastic zone incorporating the modified Cam clay parameters.  |
| 37. | 2010 | Jinsong Huang, D. V. Griffiths, and Gordon A. Fenton | Coupled Biot consolidation theory was combined with the random finite-element method to investigate the consolidation behavior of soil deposits with spatially variable properties in one-dimensional (1D) and two-dimensional (2D) spaces. The generated random variables are mapped onto a finite-element mesh and Monte Carlo finite-element simulations follow. The results of parametric studies describe the effect of the standard deviation, spatial correlation length, and |

|     |      |                                 |   |
|-----|------|---------------------------------|---|
|     |      |                                 | cross correlation coefficient on output statistics relating to the overall “equivalent” coefficient of consolidation.   |
| 38. | 2010 | Deguang Meng,<br>Ying Long      | Three-dimensional finite element model is established on the based of Biot consolidation theory, the model is loaded and calculated on the based of considering lateral deformation and spatial seepage, elasticplasticity character of soil, construction stage loading progress etc. case study is analyzed to obtain the regular of settlement and excess hydrostatic pore pressure. The calculation value of finite element method is reasonable to compare with measured data. The finite element method is used to simulate truly every position and step settlement and excess hydrostatic pore pressure. And reasonable project plan is obtained through the optimization analysis. |
| 39. | 2010 | J. Huang and D.<br>V. Griffiths | Paper presents study on coupled, uncoupled and the Terzaghi 1D consolidation theories have been re-examined using the FE method and it is shown that the Terzaghi FE solutions do not satisfy the flow continuity conditions at the interfaces between soil layers. Numerical results show that applying the Terzaghi FE solution to a layered system can lead to incorrect results. It is also shown that the average degree of consolidation, as defined by settlement  |

|     |      |   |   |
|-----|------|---|---|
|     |      |   | and excess pore pressure, are different for layered systems.  |
| 40. | 2011 | M.R. Madhav et al.  | Proposed non-linear theory of radial consolidation for thick deposit of clays considering linear void ratio-log effective stress relationship and dissipation of pore pressure is much dependant on stress ratio. Theory is very useful to study forensic investigations of embankments constructed rapidly on thick deposits of fine grained soils. Analytical solutions were proposed considering stiffness of the drain. |
| 41. | 2012 | Lu Huang,<br>Cheng-Gang<br>Zhao et al.                          | Study of the influence of barrier consolidation on transport coefficients, and a 3D transport model based on mixture theory is proposed for describing the liners that involve circular defects in the geomembrane. The elastoplastic ALPHA model is revised by using the spatially mobilized plane (SMP) criterion for simulating the deformation of the soils using ABAQUS.   |
| 42. | 2012 | Guan-Bao Ye,<br>Zhen Zhang, Jie<br>Han, Hao-Feng<br>Xing et al. | Combined ground improvement method namely deep mixed columns and vertical drain is adopted to study three-dimensional (3-D) and two-dimensional (2-D) finite-element analyses were conducted to evaluate the performance of an embankment constructed over soft soil improved by the DM columns and PVDs. In the 2-D analysis, a plane-strain conversion method was used to simulate  |

|     |      |                             |  |
|-----|------|-----------------------------|--|
|     |      |                             | the 3-D condition. The finite element software, ABAQUS, was used for these analyses. Good agreements are found between the computed and measured data.   |
| 43. | 2012 | Zhi Yong Ai and Wen Ze Zeng | Biot's theory is extended to study consolidation of multilayered soils subjected to non-axisymmetric loading in arbitrary depth. Governing equations are solved analytically using Laplace–Hankel transform and a Fourier expansion. The analytical layer-element (i.e. a symmetric stiffness matrix) describing the relationship between generalized displacements and stresses of a layer is exactly derived in the transformed domain. Considering the continuity conditions between adjacent layers, the global stiffness matrix of multilayered soils is obtained by assembling the inter-related layer-elements. |

## 2.8 Historical Experimental Developments

Another school of research workers Barden et al.(1960), Aboshi-Monden(1961), Rowe-Shields (1965), Ramanjaneya(1969), Rowe et al.(1970), Escario Uriel (1971), Singh and Hattab (1980), I.Juran (1987), Holtz & Christopher (1987), J.Blewett et al. (2002), S.Hansbo (2004), Indraratna et al. (1998,2005), Shroff-Shah(2006) have developed experimental set-up for the measurement of consolidation of soft clay with and without horizontal top drainage layer, with and without pore pressure measurement, either by using peripheral and central vertical drain in oedometer along with sophisticated instrumentation. Shroff A.V and Shah M.V (2006,2007) modified hydraulically pressurized oedometer for the

study of sequence of consolidation of soft clay through isochrones. They also developed special set-up for measurement of radial permeability of various drains of different diameters.

S.Hansbo (1983), R.Kremer (1983), Jamiolkowski et al. (1984), Bergado et al. (1991), Koerner et al. (1994), G.V.Rao (1994, 1995, 1997, 2004), Chai.J.C. (1999), Sharma et al. (2000), Hird et al. (2000,2002), J.Chu et al. (2003), J.N.Mandal et al. (2003), Indraratna et al. (1998, 2005,2010), Lee et al. (2007) have worked on different shapes of drains, type of drains, method of installation, spacing of drains using synthetic and non-synthetic natural fibers under various types of loading.

### **2.8.1 Contribution by Some of the Research Workers in Experimental and Laboratory Investigations is Discussed Below:-**

Comprehensive study by Moran et al. (1958) shows that the driven closed end mandrel method for installation is most common and used in about 60 percentages of cases. However, use of any method causes some disturbance when drain holes are made. Displacement methods cause most disturbances but they are faster and cheaper than other drains, despite the possibility of being less efficient closed mandrels shows same significance on the efficiency of installation.

The Rowe consolidation cells of three different diameters, as stated, has been used with improvement of adopting clear Perspex for construction of 254 mm diameter cell reinforced by a steel ring. This produced the desired transparent qualities without violating the basic criterion of lateral confinement of the sample (Ko condition) assumed in the Terzaghi's consolidation theory. (Refer fig.2.58). His laboratory scaled models are shown in Fig.2.59 to 2.61 for forming sand drains, which were developed to simulate for various methods of installation. A nominal size of 25.4 mm diameter drain was adopted giving the ratio 'n' as 10 for 254mm diameter cell.

The values of the coefficient of consolidation for various drainage conditions measured by the Rowe consolidation cells found to be within the scatter of the

coefficient of variation of 21% obtained by the tests conducted on the Casagrande oedometer for the vertical flow for the three load increments. The values of the coefficient of permeability for the 254mm diameter are higher by about 39 percentage than those of Casagrande Oedometer. Fig.2.62 to 2.70 shows the graphs of the coefficient of consolidation and permeability for various methods of installation plotted against loading increments. The coefficient of consolidation and permeability are highest for the cross shaped mandrel and lowest for the open mandrel.

The average ratio of ( $C_r/C_v$ ) for the three loading increments, taken for various methods of loading, range from 8.088 for the cross-shaped closed mandrel to 2.2 for the open mandrel in the 254 mm diameter cell (n equal to 10). The ratio ( $C_r/C_v$ ) for the auger and 2.48 for the open mandrel in the 152 mm diameter cell (n equal to 6). In the 76 mm diameter cell (n equal to 3), the ratio is 1.55 for the jetted mandrel and 0.17 for the open mandrel. This should give a clear indication to the erroneous practice of measuring and applying the coefficient of consolidation for vertical flow to the design of sand drains.

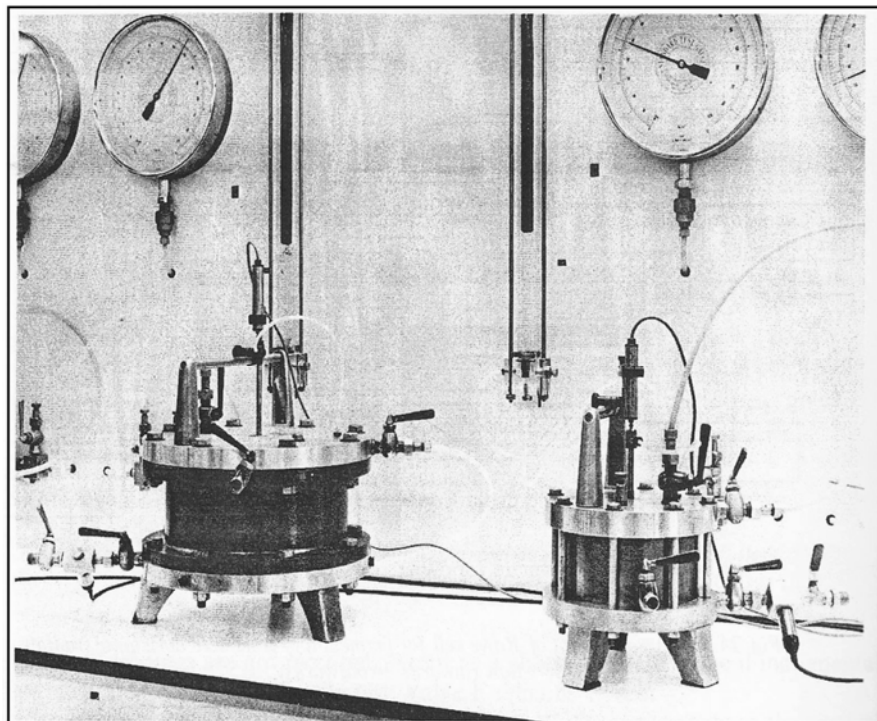
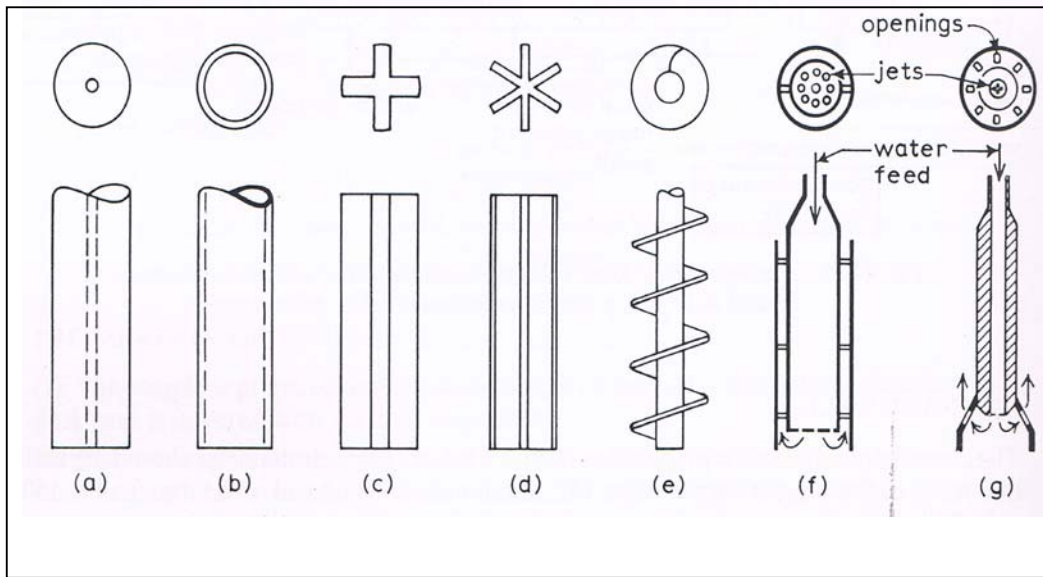
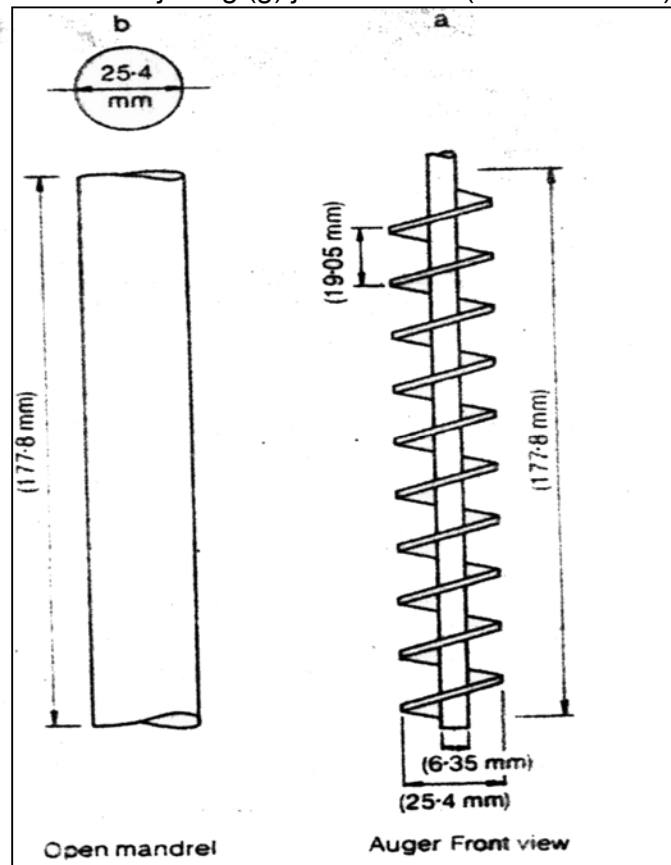


Fig.2.58: General view of 152mm dia. and 254mm dia. consolidation cell



**Fig.2.59:** Laboratory models of sand drain formers (a) closed mandrel (circular shaped); (b) closed mandrel (hollow tube); (c) closed mandrel (cruciform shaped); (d) closed mandrel (star shaped); (e) open mandrel (auger shaped); (f) double wall jetting (g) jetted drains (Dutch method)



**Fig.2.60:** Laboratory model of sand drain formers

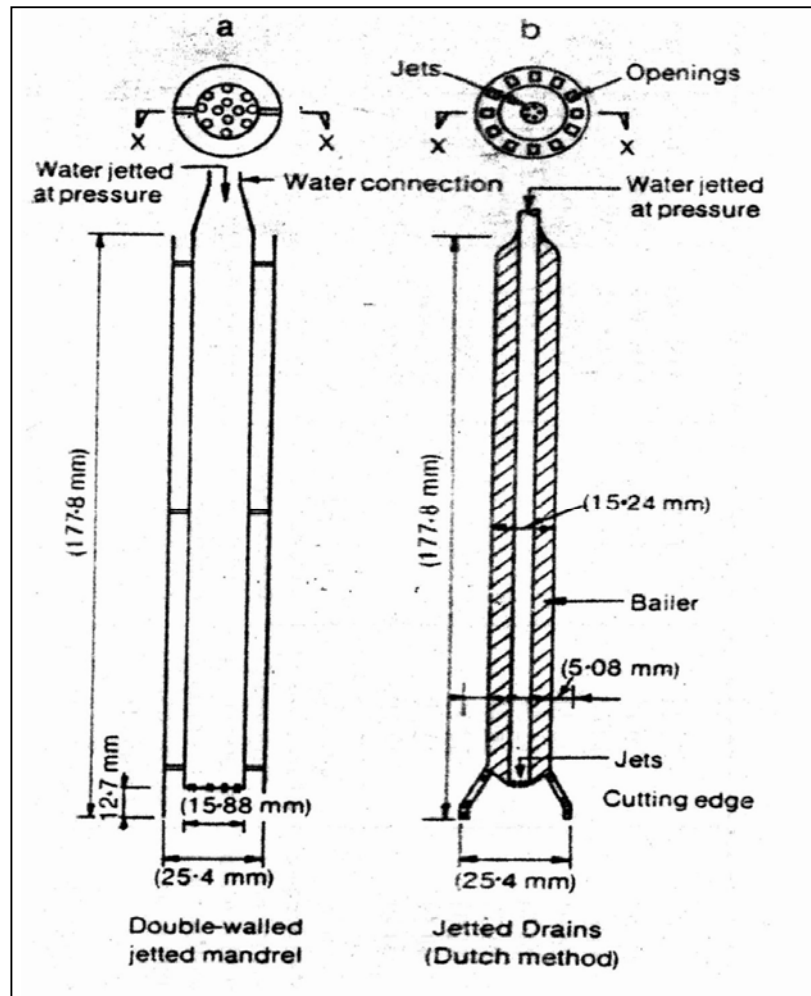
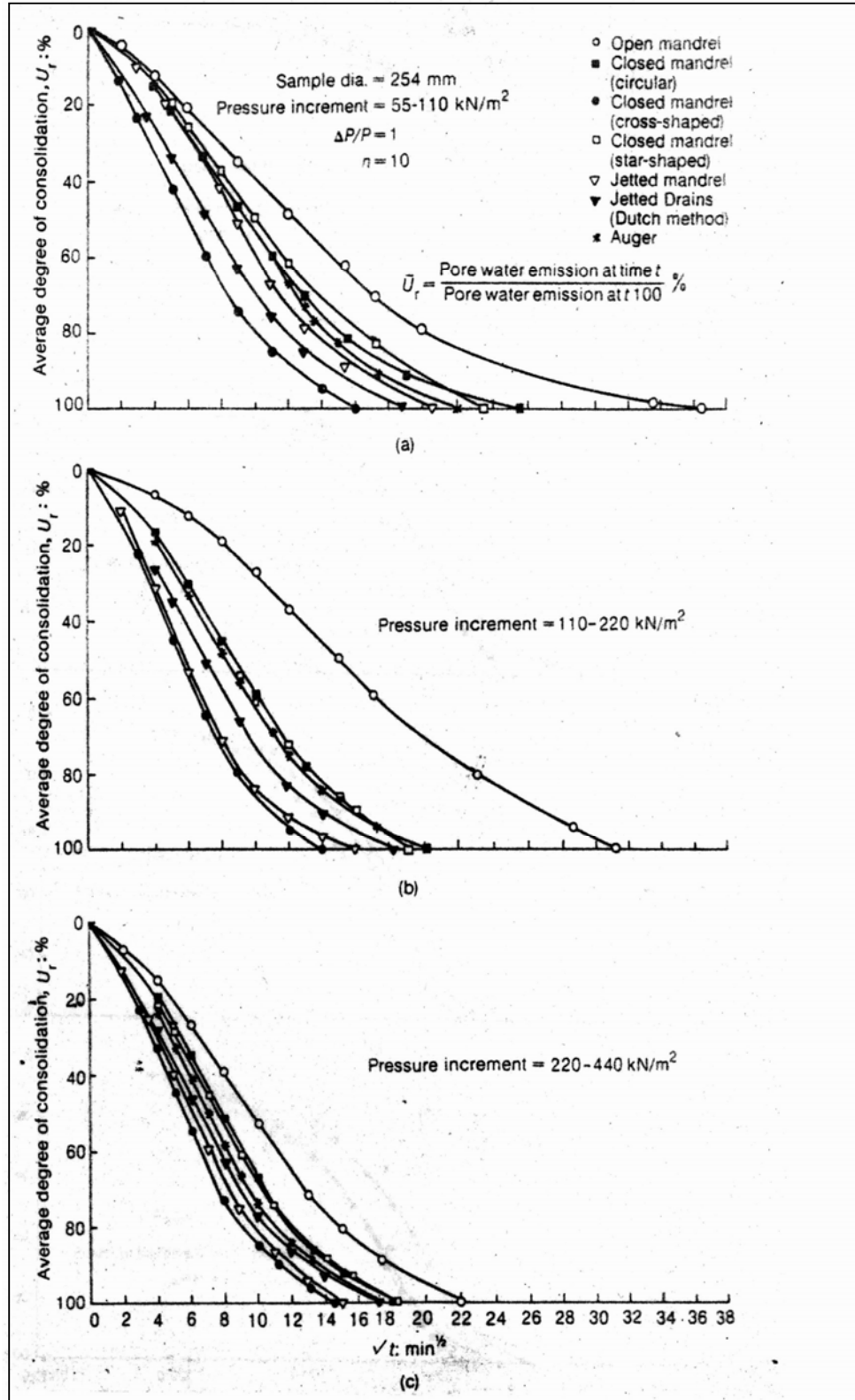
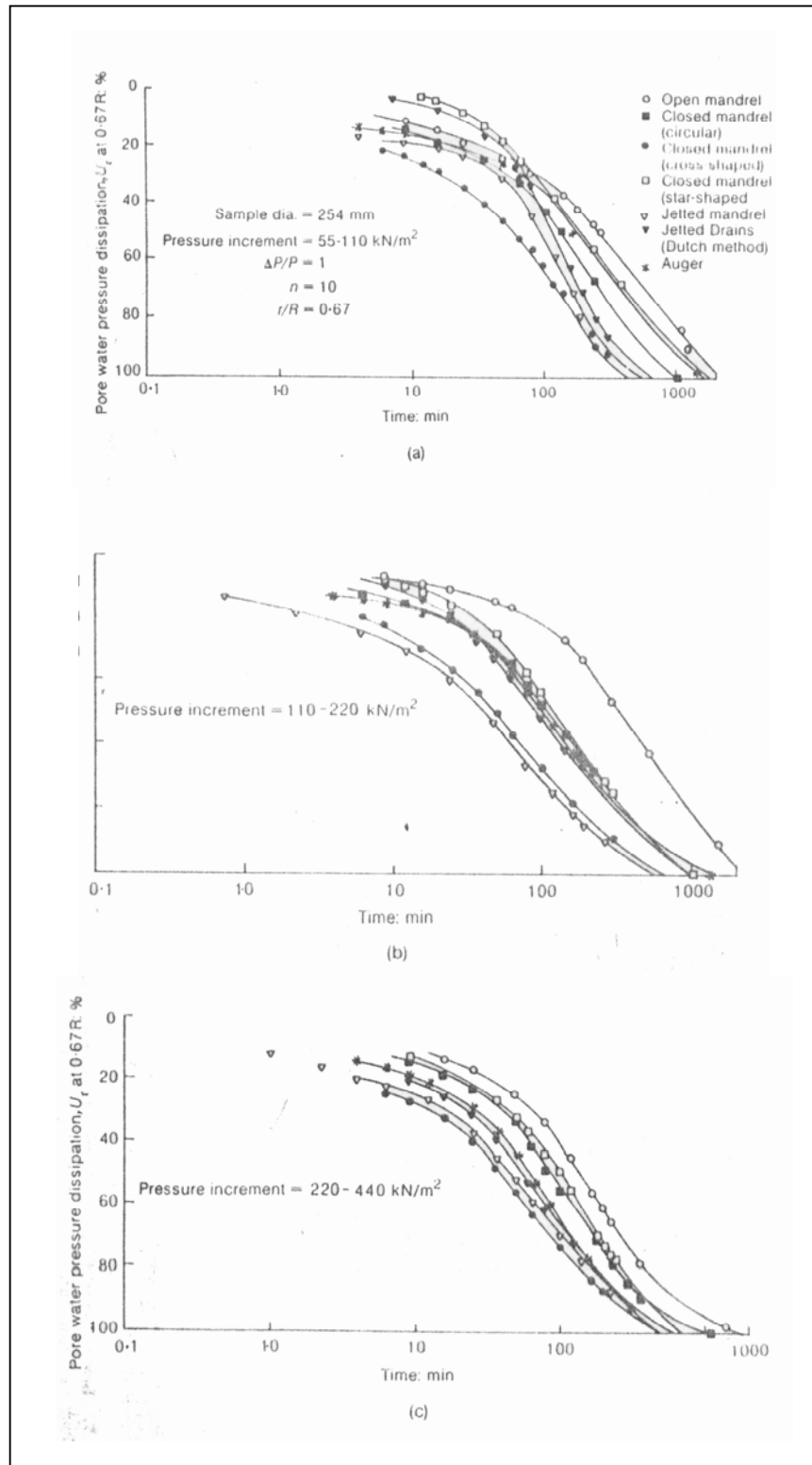


Fig. 2.61: Laboratory model of sand drain formers





**Fig.2.62:** Inward radial flow consolidation tests: percentage consolidation against square root of time for various methods of consolidation



**Fig.2.63:** Inward radial flow consolidation tests: rate of dissipation of pore pressure against time for various methods of consolidation

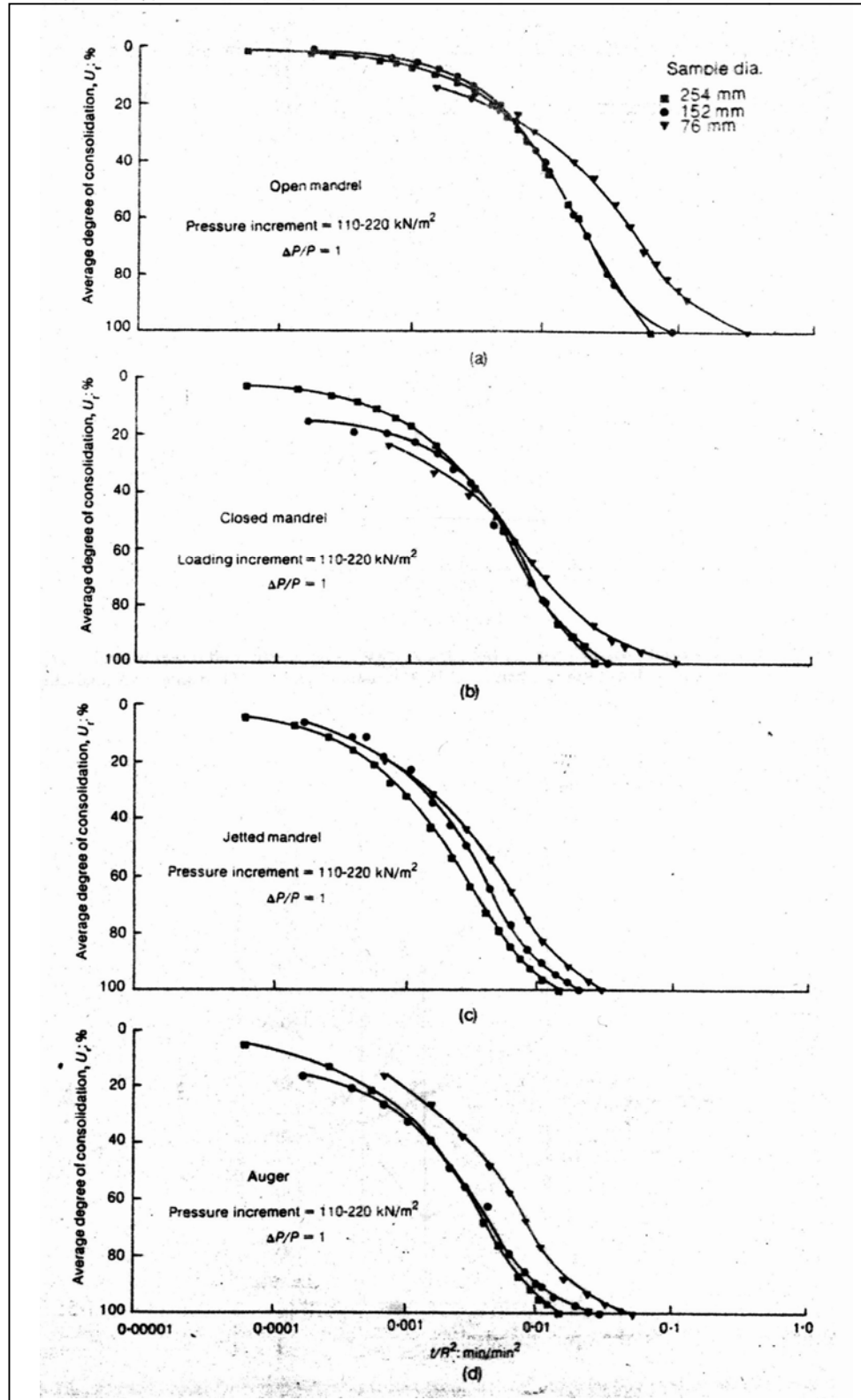
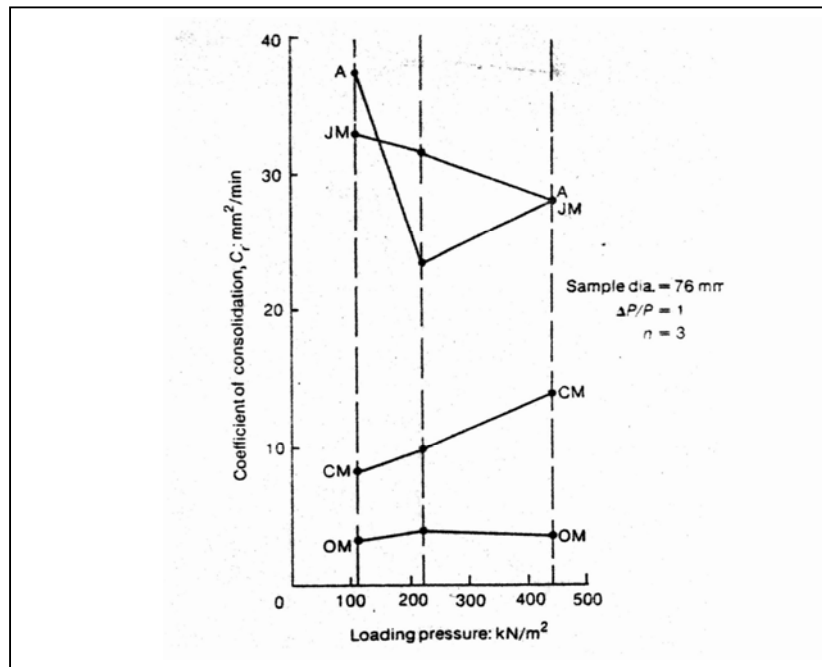
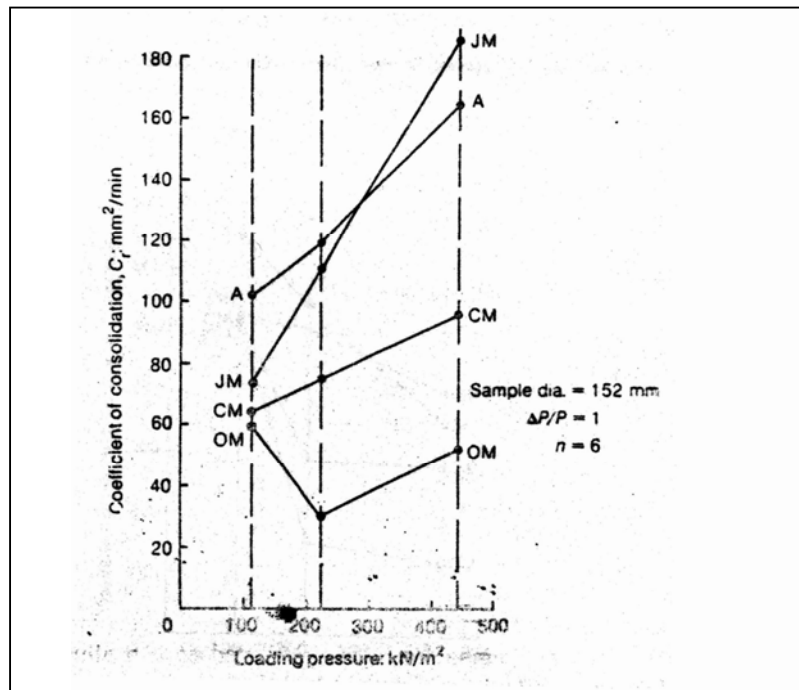


Fig. 2.64: Inward radial flow consolidation test: scale effects for various methods of boring



**Fig.2.65:** Inward radial flow consolidation tests: coefficient of consolidation versus loading for various methods of installation. A= auger, JM = jetted mandrel, CM= closed mandrel, OM = open mandrel



**Fig. 2.66:** Inward radial flow consolidation tests: coefficient of consolidation versus loading for various methods of installation. A= auger, JM = jetted mandrel, CM= closed mandrel, OM = open mandrel

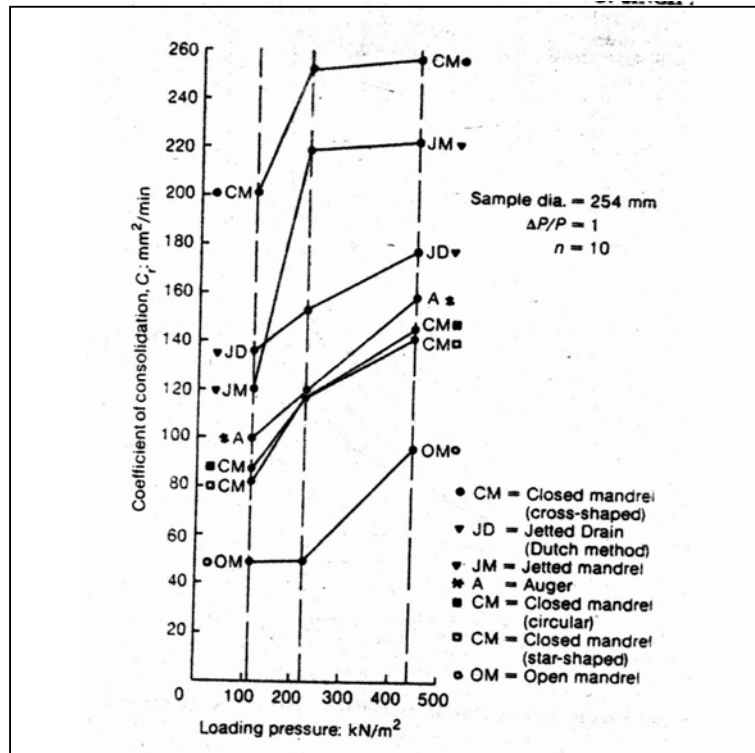


**Fig.2.67:** Inward radial flow condition tests: coefficient of consolidation against loading pressure for various methods of installation

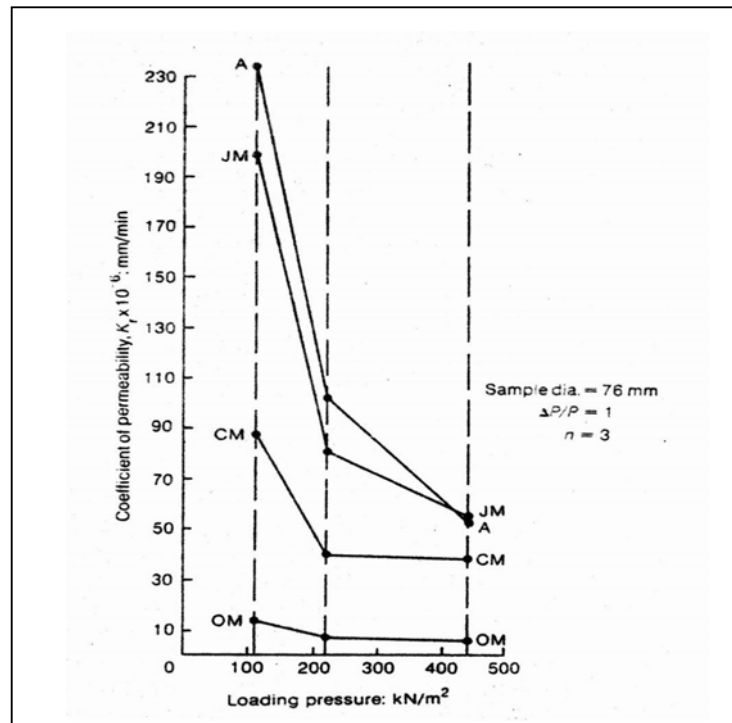


**Fig.2.68:** Inward radial flow consolidation tests: coefficient of permeability against pressure for various methods of installation

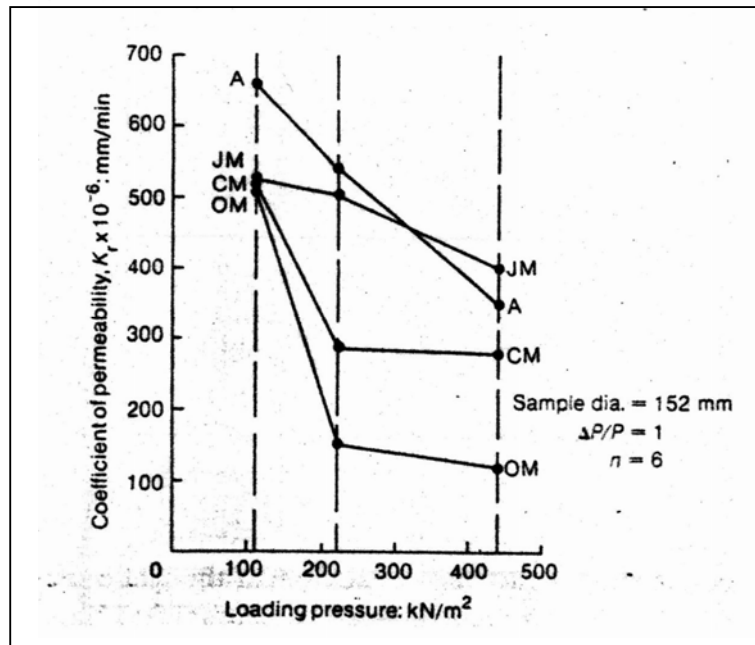


**Fig.2.69:** Inward radial flow consolidation tests: coefficient of consolidation against loading pressure for various methods of installation

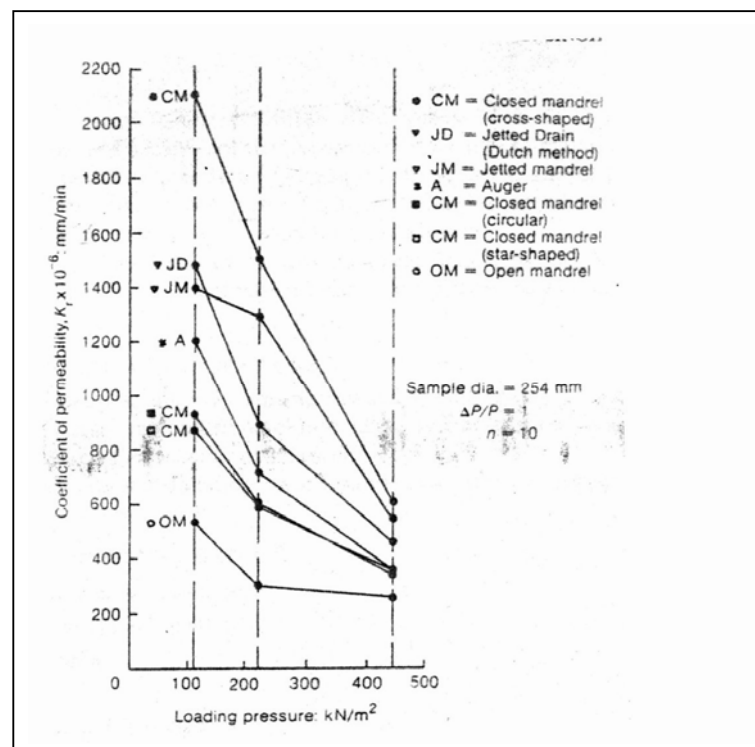


**Fig.2.70:** Inward radial flow consolidation tests: coefficient of permeability against loading pressure for various methods of installation

Rowe (1959) presented results of 230 consolidation tests on lacustrine clays, studying the influence of direction and length of drainage, shape of sample and stress condition of test. He concluded that the coefficient of consolidation of laminated clay increases with the length of drainage along laminations as indicated in. The coefficient of consolidation increases with the ratio of length of drainage boundary to the total perimeter of sample as indicated in Fig 2.71 and 2.72. The empirical coefficient determined from the Oedometer test can exceed than measured value from the triaxial test. Filter paper drains do not provide an effective boundary drain. Rowe (1964) compared the original experimental observation Rowe (1959) on a laminated undisturbed sample of clay with the theoretical analysis of Horne's solution (1964) considering the ratio of overall horizontal coefficient of consolidation of clay layer of a layered deposit.

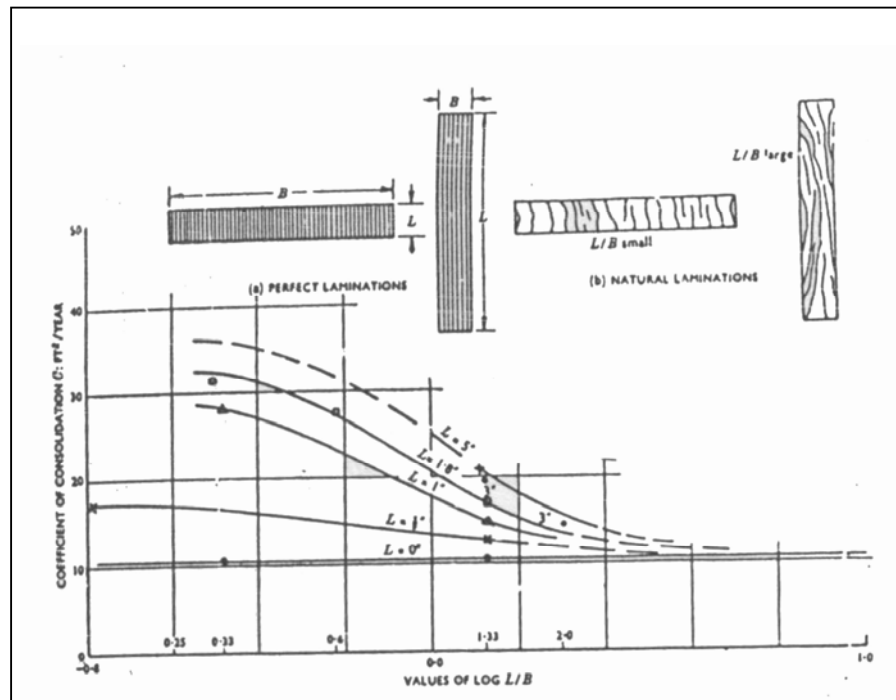


**Fig.2.71:** Influence of geometry of sample on equivalent Oedometer results (after Rowe, 1959)

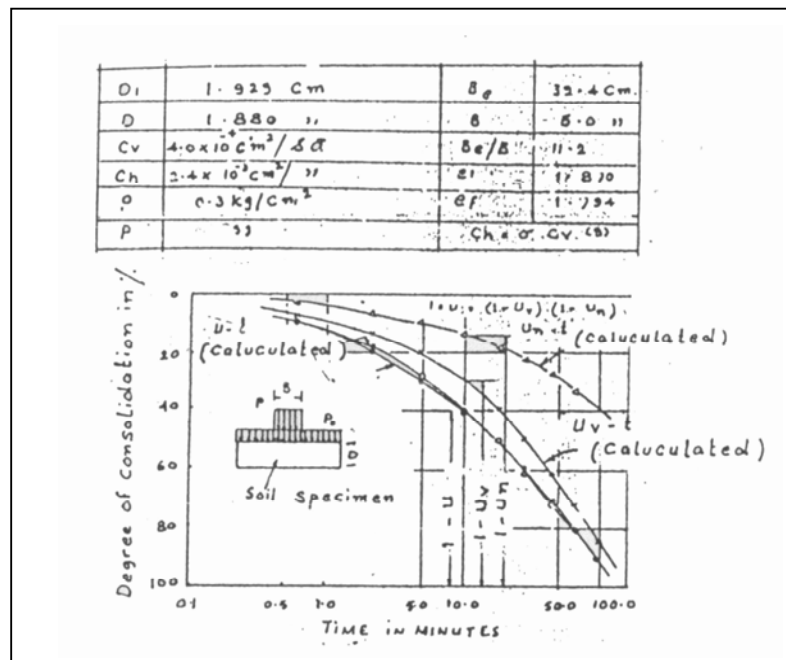


**Fig.2.72:** Summary of consolidation test results (after Rowe, 1959)

Aboshi and Monden (1961) suggested an experimental method for estimating the total settlement and the time-settlement relationship of the three dimensional consolidation of saturated clays, using the results obtained from a series of a laboratory model tests. In estimating the total settlement, it has been suggested that by introducing the concept of “equivalent stress ratio” or “equivalent permeability value”, the 3-D consolidation of a model can be replaced by a triaxial consolidation test having the actual stress ratio,  $K_e$ . He also proposed to use the concept of “equivalent drainage diameter”(Be) in order to approximate more closely to the Carillo’s work (1941) for separating radial and vertical linear flow. This study represents calculated value of degree of consolidation for horizontal and vertical drainage separately and compares the combined effect of horizontal and vertical drainage with observed value as depicted in Fig 2.73.



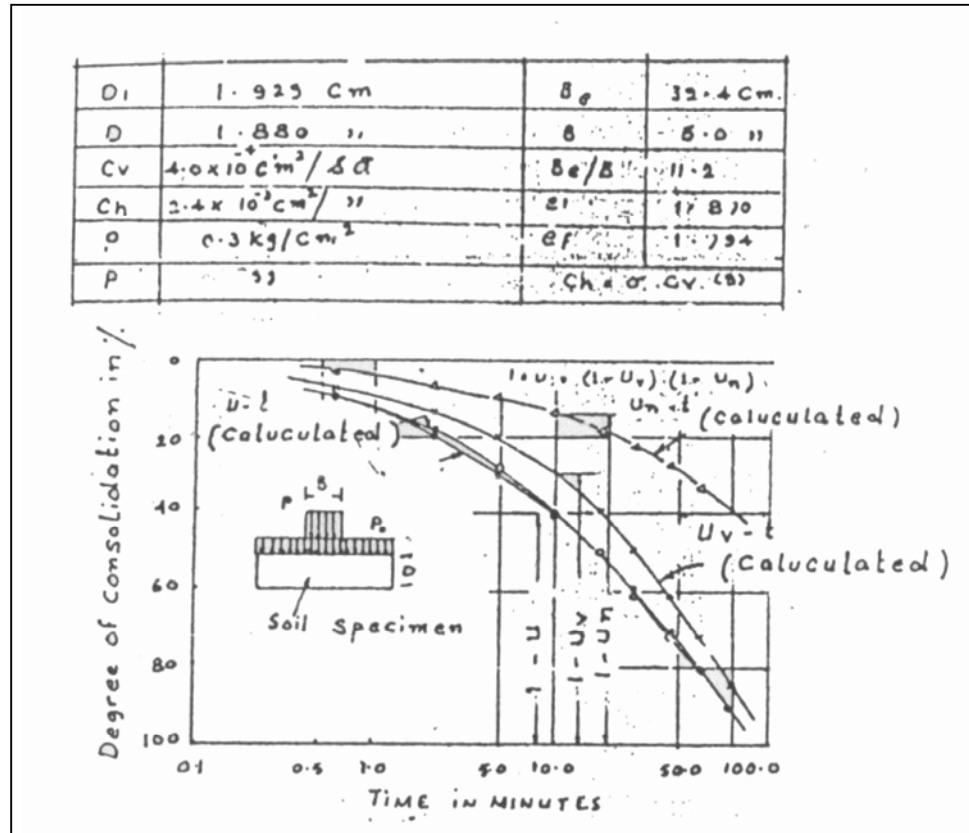


**Fig.2.73:** Three dimensional consolidation curves and its analysis  
(after Aboshi, 1961)

Escario and Uriel (1961) have described radial permeability test on 10 cm diameter soil specimen with various heights in triaxial equipment with drainage only towards the cylindrical surface. He concluded that coefficient of consolidation and permeability in sample with drainage towards the cylindrical surface of sample surround by a layer of micaceous sand has a twin advantage. The values of coefficient of consolidation and lateral stress are presented in Fig.2.74.

Mc Kinlay (1965) after studying the radial consolidation using sand drain proposed a curve fitting procedure for analysis of experimental results. This procedure is similar, uniform to the square root of time fitting method. He also studied the influence of radial flow and vertical flow on coefficient for various effective pressures. (Refer fig.2.75)

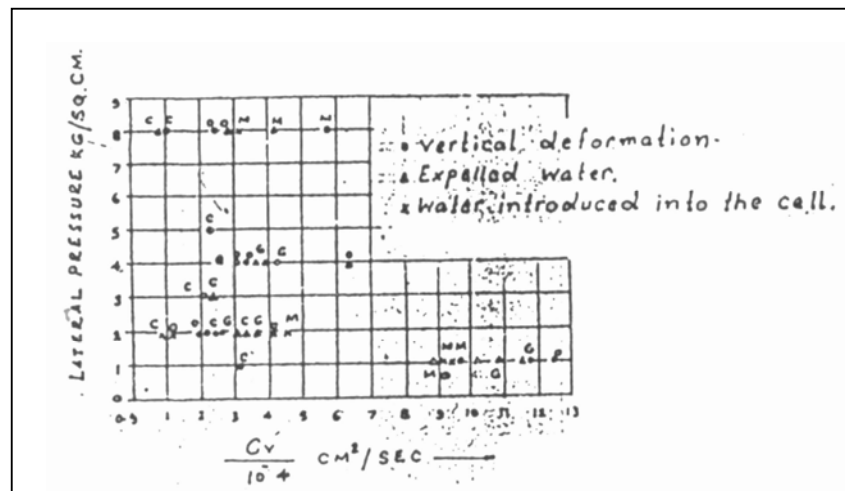


**Fig. 2.74:** Values of the coefficient of consolidation of the blue clays from Huelva obtained by radial permeability test (after Escario et al, 1961)

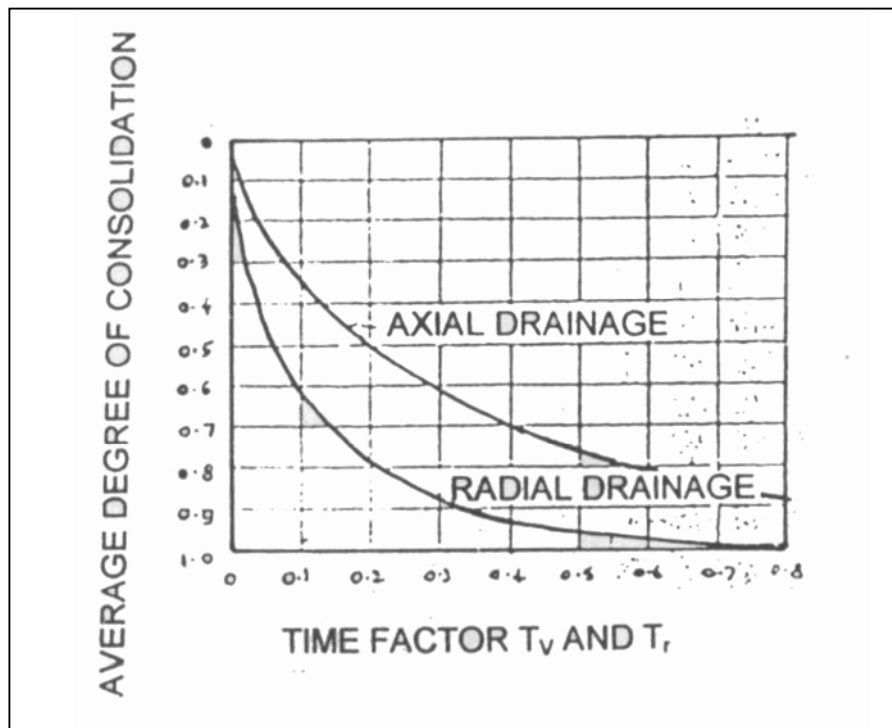


**Fig.2.75:** Theoretical consolidation curves for the axial and radial cases (after Mc Kinlay, 1965)

Rowe Shield (1965) studied the influence of the drain on the settlement and the coefficient of consolidation. He concluded that the model sand drains may be used for accurate measurement of the coefficient of consolidation and settlement of clay sample during radial drainage, where the ratio of oedometer to drain diameter is 20. Fig.2.76 illustrates influence of drain well diameter on

measured value of coefficient of consolidation by a model sand drain experiments. Also Rowe Shield compared the Horne's theoretical analysis (1964) with the experimental results of consolidation of a layered deposit using model sand drain in hydraulically pressurized oedometer Fig. 2.77.

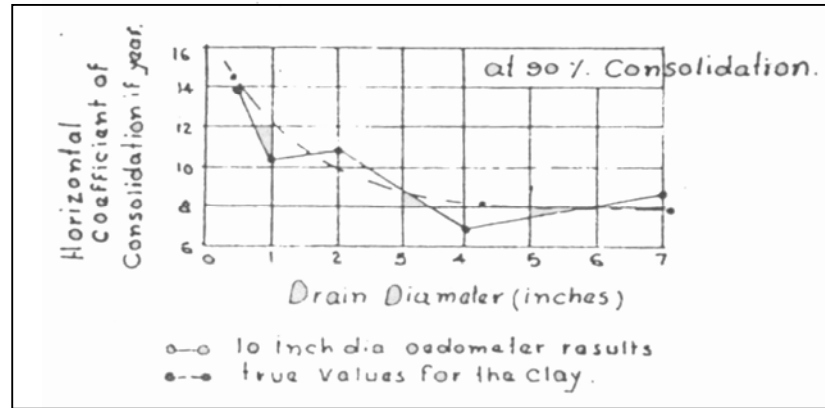


**Fig. 2.76:** Effect of drain diameter on measured coefficient of consolidation

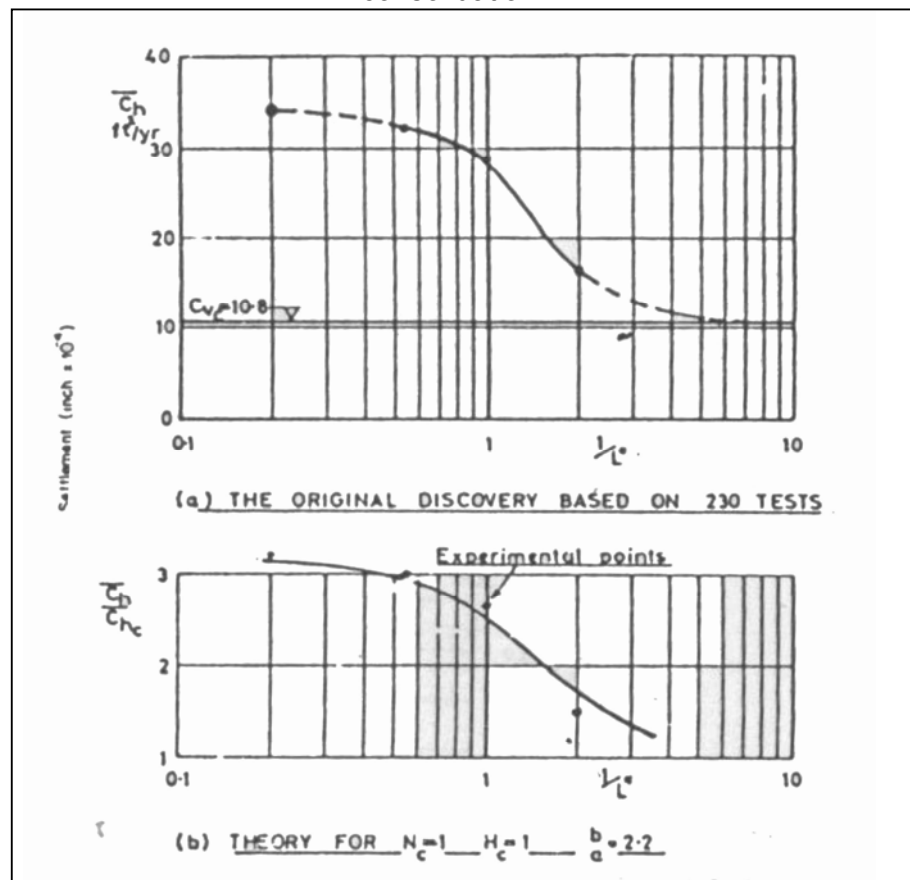


**Fig. 2.77:** Comparison with previous experimental observations (after Rowe)

Singh and Hattab (1980) studied the radial drainage of the remolded clay to a central sand drain to assess the effects of methods of installation and spacing on the consolidation characteristics of soil. Both the displacement and non-displacement methods of installation were studied. They used Rowe consolidation cells of 76, 152 and 254 mm diameter. Improvement was sought by adopting clear perspex for the construction of 254 mm diameter cell reinforced by steel rings. Laboratory scale model for forming the sand drain as shown in Fig. 2.59 to 2.61 were developed for method of installation 'n' value was 10 for 254 mm cell. Fig. 2.62 shows the curves of percentage average degree of consolidation plotted against square root of time for all increments of pressure for 76 mm diameter samples. The performance of the various methods in the 254 mm diameter sample assessed by pore pressure dissipation is shown in Fig. 2.63. The cross shaped closed mandrel reflects a highest consolidation performance. The influence of scale effects for various methods of boring on degree of consolidation for the three cells is illustrated in Fig. 2.64.

S. Prawono (1981) conducted a variety of laboratory tests on the soft clay samples to evaluate the coefficient of vertical consolidation for radial drainage,  $C_{vr}$ . These tests included lever arm and Bishop Oedometer tests on 63.5 mm diameter specimen with central drain as well as tests on 152 mm diameter specimen in a Rowe cell. The  $C_{vr}$  value was evaluated from compression time curves in case of the lever arm and Bishop Oedometer tests and from pore pressure dissipation curves in the case of the Rowe Oedometer tests. In order to compare the test results with the Barron's equal strain solution a Rowe cell was modified by providing its base with four pore pressure measuring points arranged at different distances from drain. Based on the results obtained in the investigation Prawono made concluding remark that  $C_{vr}$  values obtained by different Oedometer differ considerably. However, the values determined from pore pressure curves, as practiced in Rowe's Oedometer test, appears to be more consistent. A fair agreement between measured and predicted values could be obtained as depicted in Fig. 2.78 to Fig. 2.83.

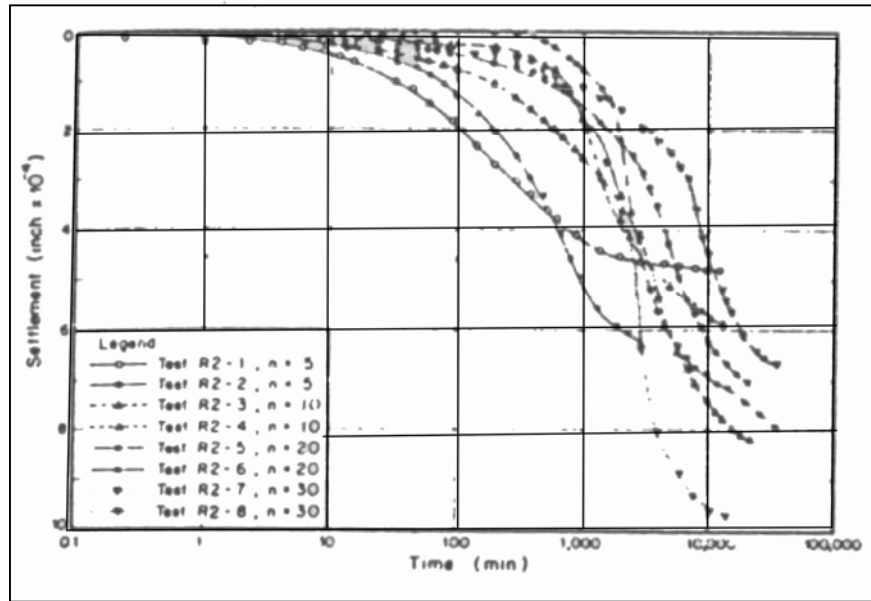


**Fig.2.78:** Compression-Time curves obtained from R2 type tests

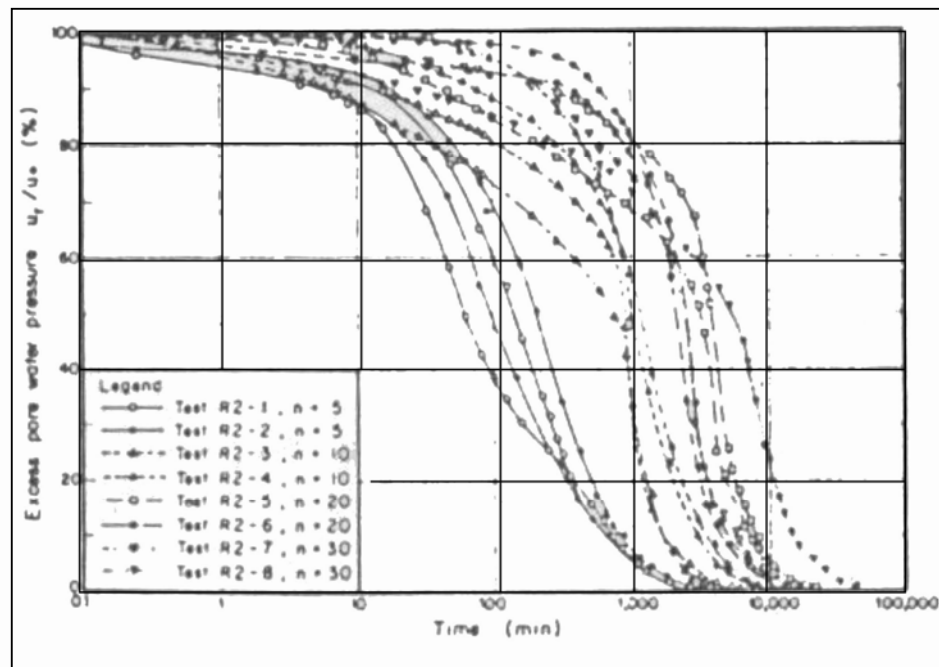


**Fig.2.79:** Pore pressure dissipation curves from R2 type tests

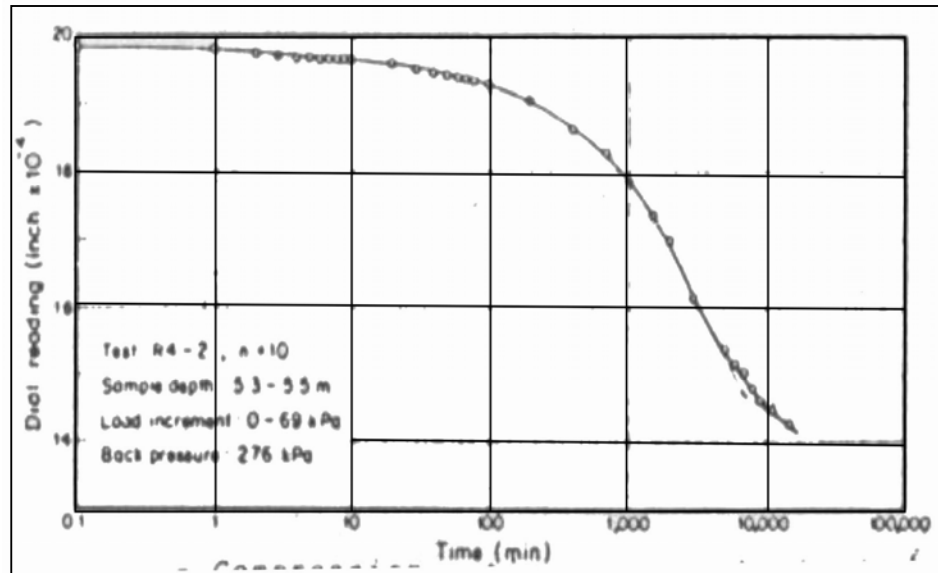


**Fig.2.80:** Compression-Time curves obtained from R4-2 type tests

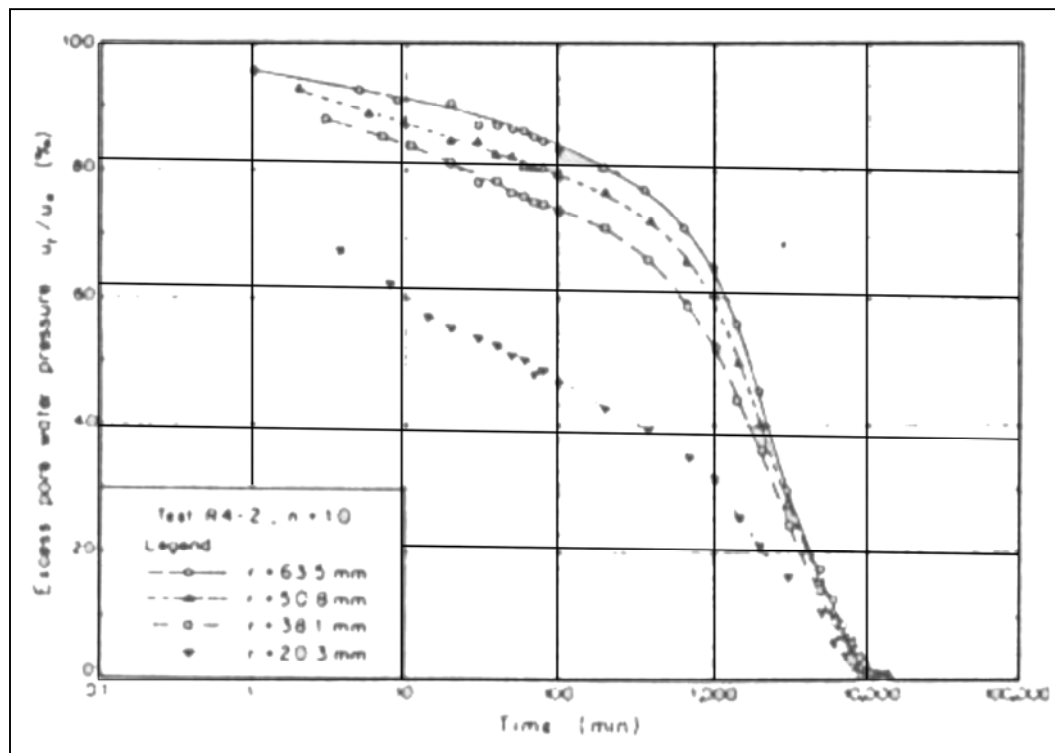


**Fig.2.81:** Pore pressure dissipation curves at various distances from centre of drain as measured from R4-2 type tests

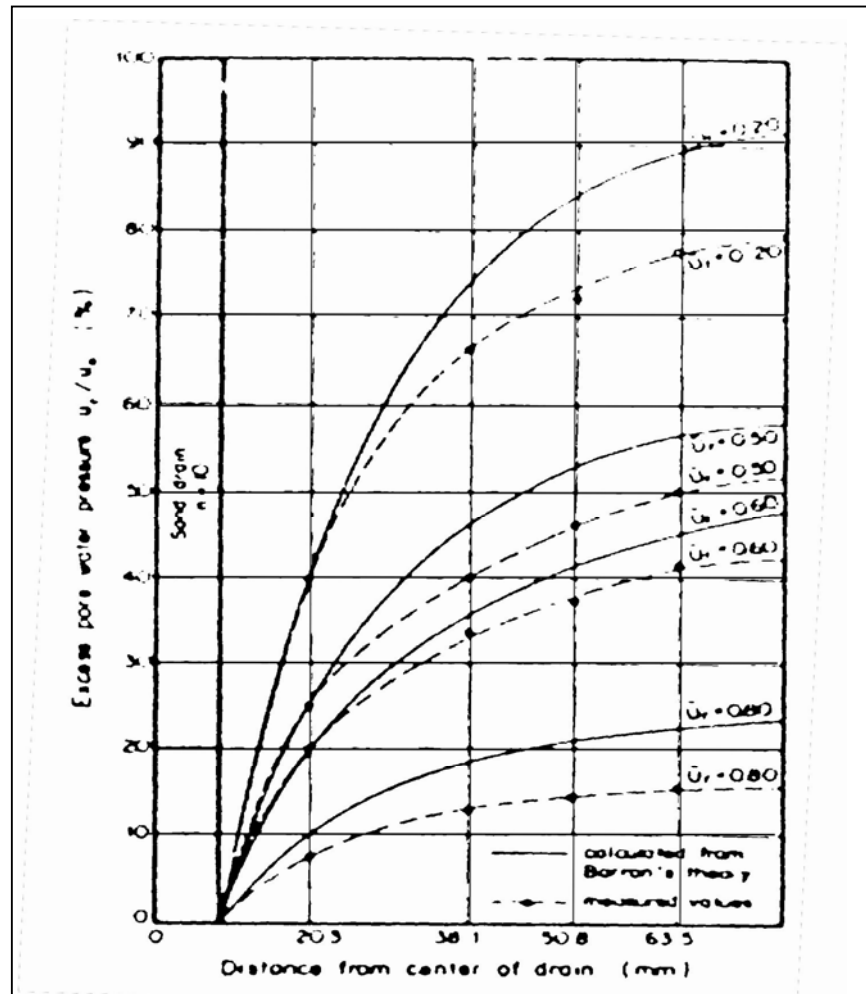


**Fig.2.82:** Comparison of measured and predicted pore pressures for various degrees of consolidation

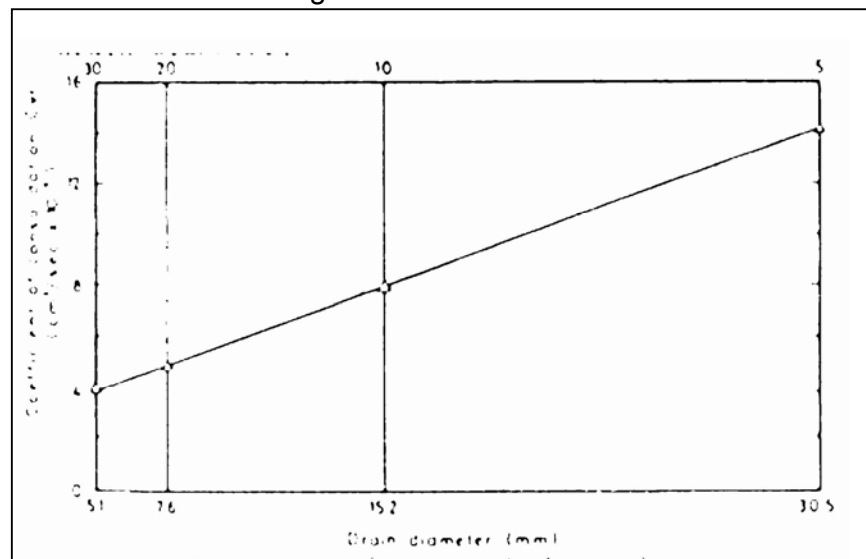


**Fig.2.83:** Variation of  $C_{vr}$  with drain diameter ( $U_r = 90\%$ )

I.Juran (1987) conducted laboratory study to investigate the effect of various parameters on the settlement response of a soft foundation soil reinforced by compacted sand columns. He made triaxial compression tests under different boundary conditions on composite soil specimens made of annular silty soil samples with a central, compacted river sand column. These tests, performed in a specially modified triaxial cell, which shows that the group effect, the replacement factor and the consolidation of the soft soil have a significant effect on the vertical stress concentration on the column and on the settlement reduction of the foundation soil. He used a modified triaxial cell and its instrumentation having four pressure cells at the bottom of the sample to measure the pore water pressures generated in the soft soil and in the column and two load cells at the top of the sample to measure simultaneously the applied total load and the load supported by the soft soil. The radial drainage of the soft soil was realized through the porous stone located at the top of the sand column. This modified cell enabled triaxial compression tests to be performed on composite reinforced soil specimens of 100 mm diameter. This experimental study demonstrates the significant influence of the drainage of the column, the consolidation of the soil, the replacement factor and the group effect on the settlement response of soft foundation soils reinforced by compacted sand columns.

Mandal and Kanagi (1998) conducted centrifuge modeling of drains with flow conditions as only vertical, only radial and combined flow at 120g acceleration at 80 % water content, and concluded that the consolidation theories viz. vertical flow (Terzaghi), radial flow (Barron) and combined flow (Carrillo) are in close agreement with centrifuge results in sand drain case. Smaller 'n' (ratio of influence diameter to drain diameter) values are effective to achieve higher degree of consolidation in short time. The water content in 8 cm mould diameter in radial flow case was predominantly less in a soil section close to sand drain. Fig. 2.84 to Fig. 2.89.



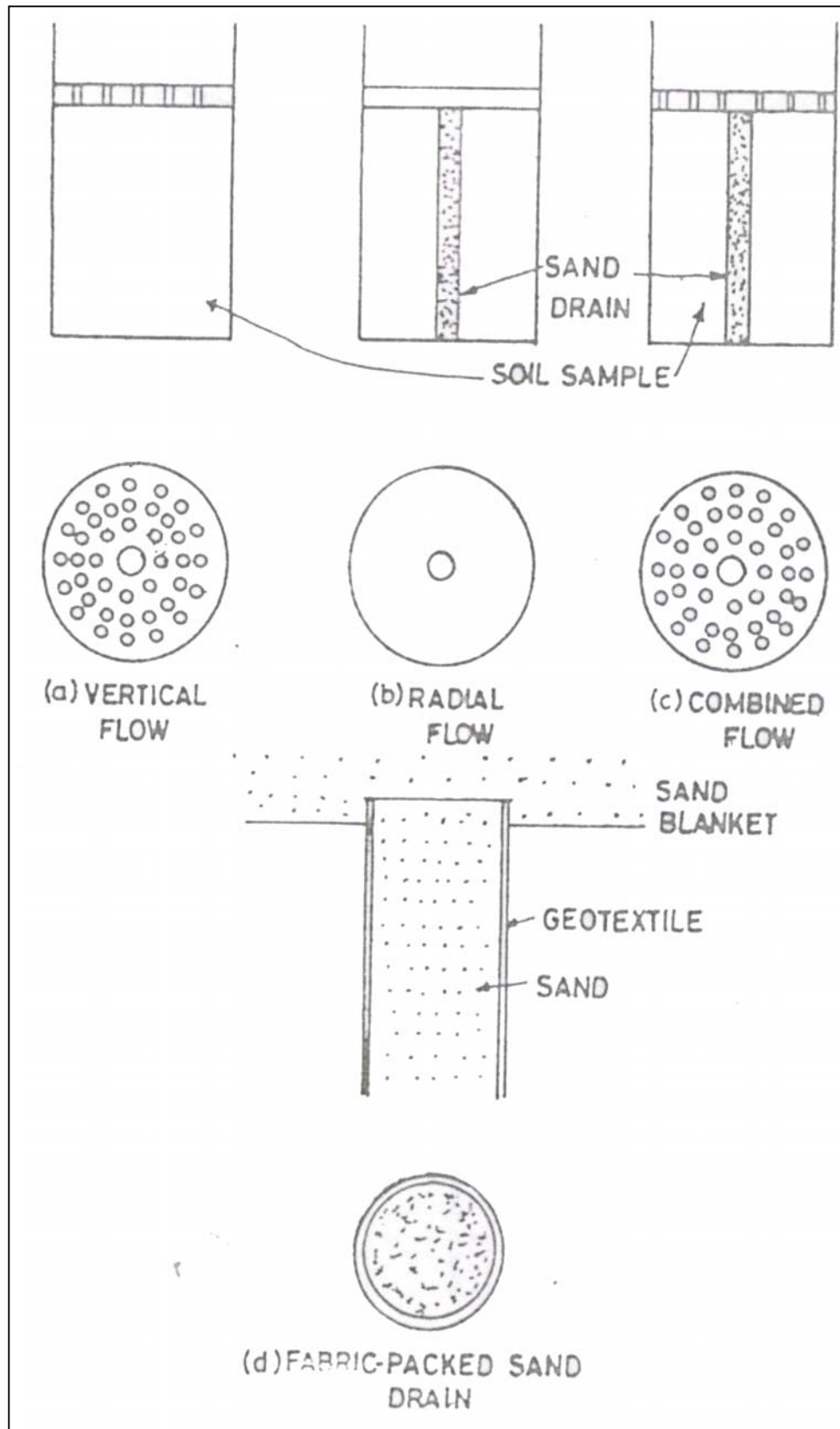


**Fig.2.84:** Model container

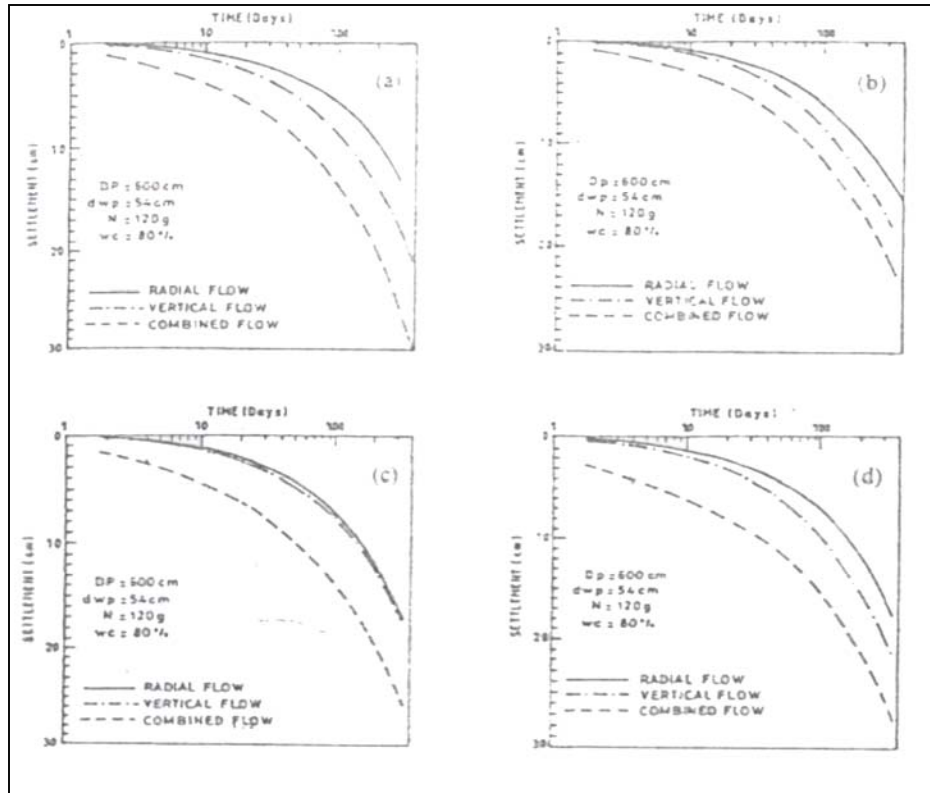


**Fig.2.85:** Time-Settlement curves with vertical sand drain (radial and combined flow) and marine clay (vertical flow) using centrifuge modeling for loading (a) 0.1-0.2kPa (b) 0.2-0.5kPa (c) 0.5-1.0kPa (d) 1.0-2.0kPa

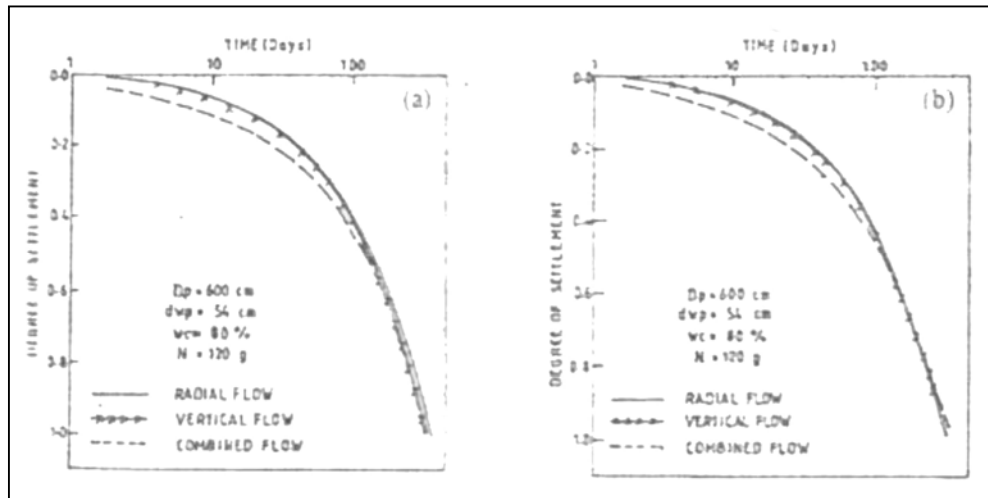


**Fig.2.86:** Time-Degree of settlement curves with vertical sand drain (radial and combined flow) and marine clay (vertical flow) using centrifuge modeling for loading (a) 0.1-0.2kPa (b) 0.2-0.5kPa

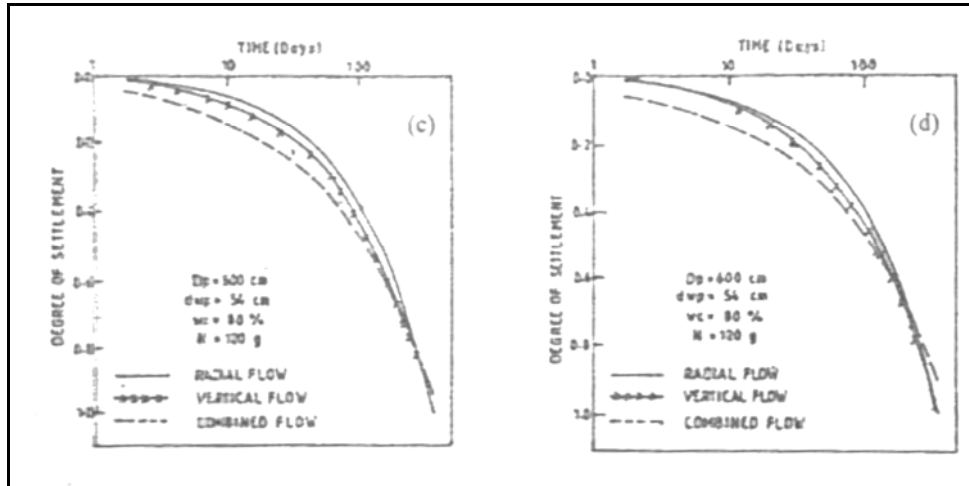


**Fig.2.86:** Time-Degree of settlement curves with vertical sand drain (radial and combined flow) and marine clay (vertical flow) using centrifuge modeling for loading (c) 0.5-1.0kPa (d) 1.0-2.0kPa

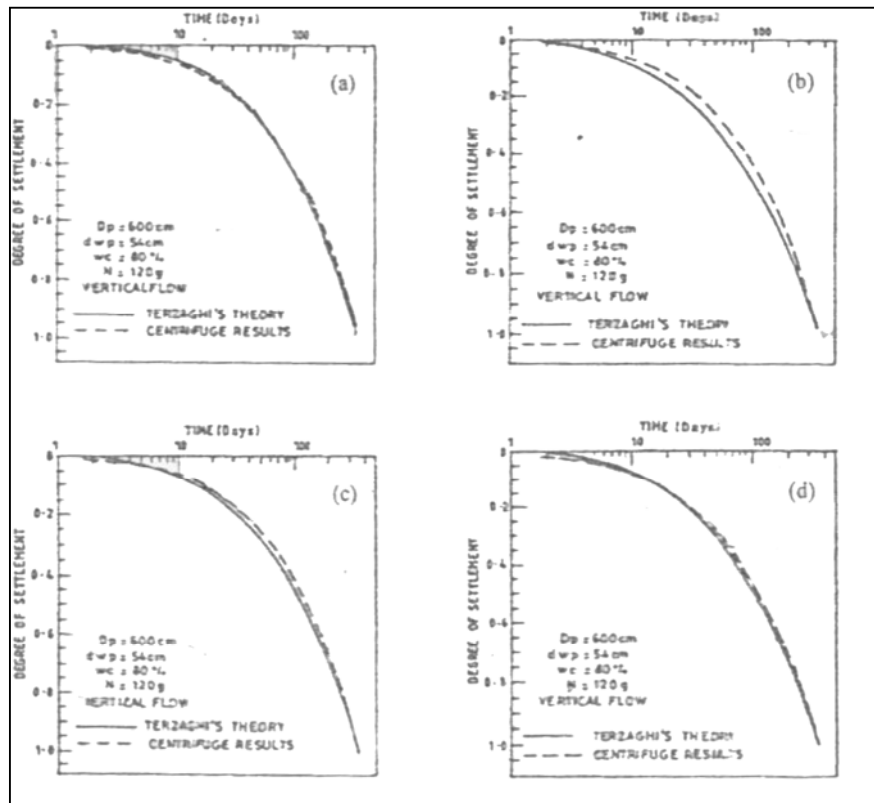


**Fig.2.87:** Time-Degree of settlement curves of marine clay under vertical flow condition (theoretical and experimental) using centrifuge modeling for loading (a) 0.1-0.2kPa (b) 0.2-0.5kPa (c) 0.5-1.0kPa (d) 1.0-2.0kPa

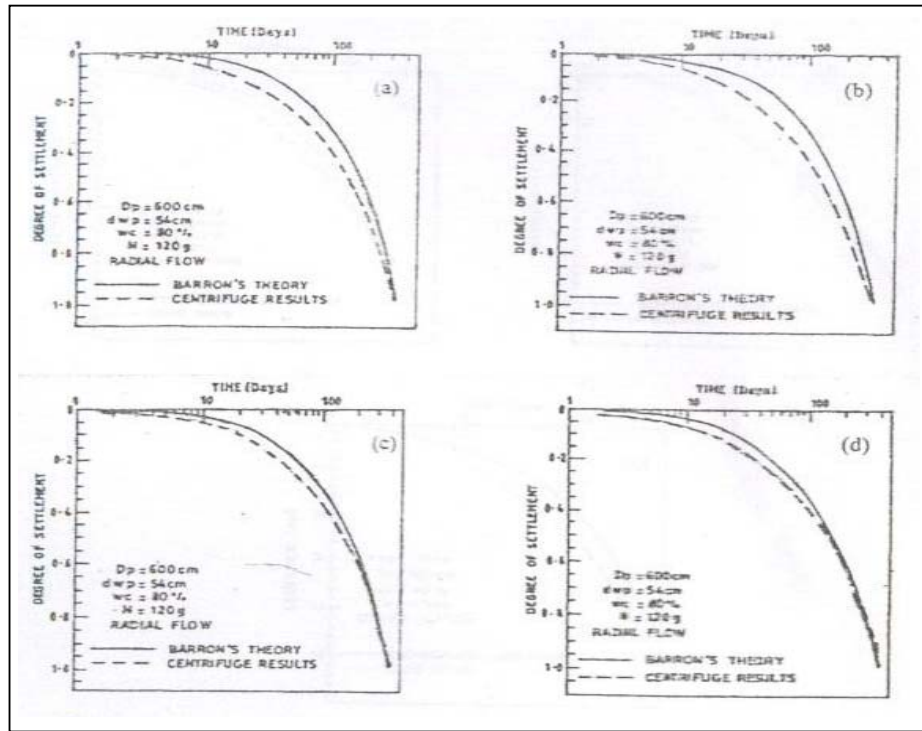


**Fig.2.88:** Time-Degree of settlement curves of marine clay under radial flow condition (theoretical and experimental) using centrifuge modeling for loading (a) 0.1-0.2kPa (b) 0.2-0.5kPa (c) 0.5-1.0kPa (d) 1.0-2.0kPa

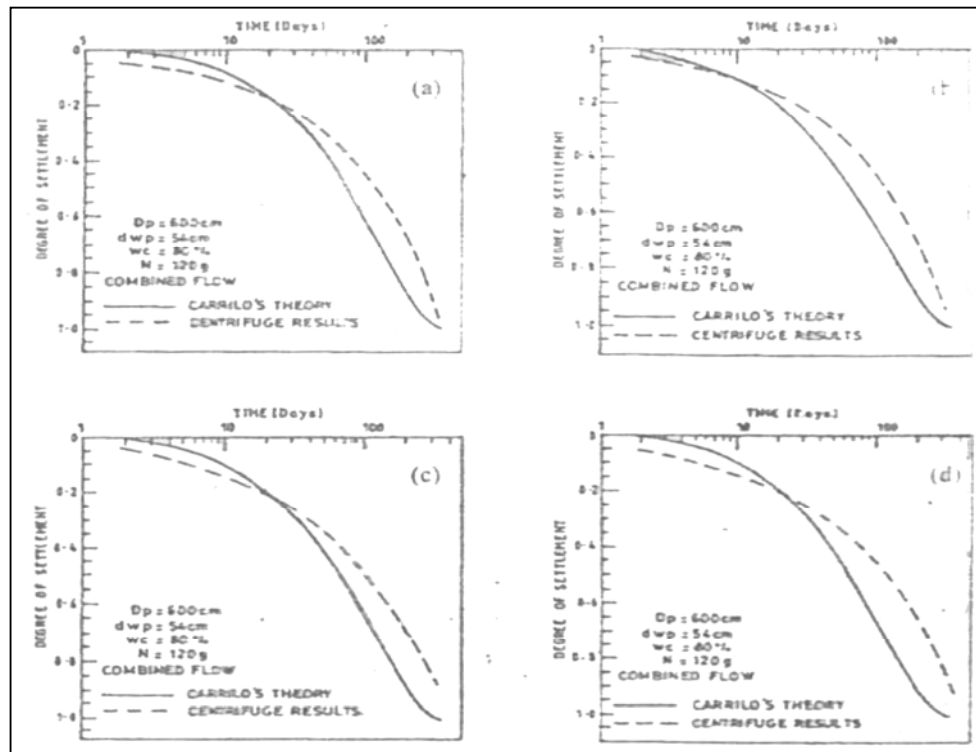


**Fig.2.89:** Time-Degree of settlement curves of marine clay under combined flow condition (theoretical and experimental) using centrifuge modeling for loading (a) 0.1-0.2kPa (b) 0.2-0.5kPa (c) 0.5-1.0kPa (d) 1.0-2.0kPa

### 2.8.2 Table for Laboratory Developments

Though the above para mentions some of the historic laboratory developments in consolidation of soils using various vertical drains either by using conventional Rowe Oedometer or Casagrande Oedometer of various sizes, still there are many researchers who have specifically worked on experimental part of consolidation such as development of large size Oedometer, modeling of vertical drains, drain installation techniques, smear effects, well resistance, discharge capacity of drains, pore pressure measurements, variations in loading the sample, etc either to simulated the field conditions in laboratory as well to justify theoretical approach. Some group of research workers have worked on material section both of soil type and vertical drains. In soil section, soil types are varied along with layered soils, partly saturated soils, variations in horizontal and vertical permeability of soil. While on vertical drain material section it is efficiency of drain material whether synthetic or natural, drain fabrication, drain size and shape, clogging potential of drains and composite vertical drains. The following two tables summarize the list of few contributors who have worked on experimental aspects and material aspects. (Refer table no.2 and 3)

**Table 2.5:** Excerpts based on Experimental set-up

| Sr. No | Year | Name  | Contribution   |
|--------|------|---|--|
| 1      | 1960 | Hisao Aboshi & Hirokazo Monden                  | An experimental method developed to determine the horizontal coefficient of consolidation of fine grained soils. In this work both inward radial and outward radial flow is used with sand drains. Barron's theory is used for analysis. |
| 2      | 1991 | D.T. Beragado, Hiroshi Asakami Alfaro           | Large scale laboratory study on smear effects due to installation of PVD with full scale test embankment was carried out.  |
|        | 2002 | J.Blewett, W.J. Mc Carter, T.M. Chrisp, G.Stars | Automated hydraulic consolidation cell with data acquisition system modified for monitoring the electrical conductivity of soil in conjunction with load deformation characteristics.  |

|   |              |  |   |
|---|--------------|--|---|
| 3 | 2004         | S.Hansbo   | Design of vertical drains carried out as per new theory which incorporates parameters such as vertical discharge capacity, moulding effects during installation and filter resistance supported by case studies.  |
| 4 | 1998<br>2005 | B.Indraratna,<br>Sathananthan<br>& Redana.I.W    | Study of smear zone and reduction of permeability and water content within the smear zone using large-scale consolidometer was performed.   |
| 5 | 2008         | B. Indraratna,<br>I .Sathananthan<br>et al.      | Reported large-scale laboratory tests, where the extent of the smear zone was estimated based on the indications, such as the pore pressure generated during mandrel driving, change in lateral permeability, and the water content reduction. Study reveals that the radius of smear zone is about 4–6 times the equivalent vertical drain radius, and the lateral permeability (inside the smear zone) is 61–92% of that of the outer undisturbed zone. |
| 6 | 2010         | Ali<br>Ghandeharioon,<br>B. Indraratna<br>et al. | The installation of mandrel-driven prefabricated vertical drains and resulting disturbance of soft saturated clays are analyzed with a new elliptical cavity expansion theory. The theoretical variation of excess pore pressure is then compared with the results of large-scale consolidometer tests, which show that the estimated and measured pore pressures are almost the same.  |
| 7 | 2012         | B. Indraratna<br>et al.                          | Reported large scale consolidometer for consolidation of layered soils using vacuum loading method.   |

**Table 2.6:** Excerpts based on Material properties

| <b>Sr. No</b> | <b>Year</b> | <b>Name</b>                                    | <b>Contribution</b>   |
|---------------|-------------|--|---|
| 1             | 1979        | G.Singh & T.N. Hattab                          | Experimental study carried out to assess the effects of the various methods of installation and spacing of sand drains using Rowe consolidation cell of 76,152 & 254mm diameter. (Studied on the various geometrical shapes of mandrels)  |
| 2             | 1979        | A.V. Brednv,<br>E.V.Svtinsky,<br>A.S.Stroganov | Soil consolidation by means of band-shaped drains. Also equations are proposed for calculating the consolidation of soils and to determine the design parameters of drain. Filter paper wrapped geodrain and geodrain with filter of synthetic paper is used.                                     |
| 3             | 1981        | A.Mc Gown & F.H.Hughes                         | Practical aspects of the design and installation of deep vertical drain reported (soil type, type of sampling and testing, type of drain and installation method, diameter of drain, type of analytical method used, cost factors, rate of placement of drain, instrumentation needed for drain). |
| 4             | 1982        | A.G. Dastidar.<br>S.Gupta and<br>T.K. Ghosh    | Field application of sandwich in a housing project, Calcutta is reported.   |
| 5             | 1982        | P.L.Newland & B.H.Allely                       | An experimental study of the consolidation characteristics of clay.   |
| 6             | 1983        | S.Hansbo                                       | Reported methodology to evaluate the properties of prefabricated drain (equivalent diameter of a non-circular drain, discharge capacity and filter criteria)  |

|    |                      |   |   |
|----|----------------------|---|---|
| 7  | 1983                 | R.H.J.Kremer,<br>W.F.J.De Jager<br>et al. | The quality of vertical drainage is discussed—<br>Presents highlights on proper need of quality standards and specification for type of drain.<br>---Like type of loading, method of installation, reliability and durability, discharge capacity, theory used, filter criteria, tensile strength of drain material and elasticity of filter. |
| 8  | 1984<br>1988         | K.Leminen &<br>H.Rathmayer                | Horizontal oedometer tests to determine the parameter $C_h$ is conducted and reported.  |
| 9  | 1984                 | J.P.Magnan,<br>G.Pilot,<br>D.Queyroi      | Back analysis of soil consolidation around vertical drains to check its efficiency is carried out. In this analysis (Asaoka, Magnan, Deroy, 1978, 1980) method is used for settlement analysis.   |
| 10 | 1994                 | Y.Wasti &<br>T.Hergul                     | Laboratory study: on performance of geosynthetic band shaped/strip drains by means of radial consolidation is reported.   |
| 11 | 1994<br>1995<br>1997 | G.V. Rao,<br>R.K. Dutta<br>et al.         | Laboratory testing on Geotextiles, jute-coir, geosynthetics, geogrids carried out.  |
| 12 | 1999                 | J.C.Chai &<br>N.Miura                     | Paper presents the some factors affecting the behavior of vertical drains followed by the back-analyses of test embankments to valuate field performance of PVD as well as sanddrains. Comparison is made between laboratory test data and corresponding back calculated field values of the parameters related to drain behavior.            |
| 13 | 2003                 | J.Chu,<br>M.W.bo & V.Choa                 | A practical consideration in the use of PVDs in soil improvement projects is discussed. (Like quality control tests for PVDs, selection of  |



|    |      |  |   |
|----|------|--|---|
|    |      |  | design parameters and smear effect)   |
| 14 | 2003 | J.N.Mandel,<br>A.Shiv                      | CAD on geocomposite (jute and coir) vertical strip drains used at Haldia in West Bengal and Vashi station complex at Mumbai)  |
| 15 | 2003 | Chai J.C,<br>Miura .N,<br>Nomura .T        | Effect of hydraulic radius on long-term drainage capacity of geosynthetics drains studied by employing rational approach  |
| 16 | 2004 | S.Hansbo                                   | Laboratory-cum-analytical method to analyze consolidation with and without vertical drains is discussed. The classical approach is based on non-darcian flow conditions with assumed effect of creep. Also detail discussions are made on specifications, testing and design of prefabricated vertical drains (PVDs) of band shape along with its installation technique. |
| 17 | 2005 | Balasubramaniam<br>, Oh.Bolton,<br>Bergado | Large field works done for sand drains, sandwicks & PVDs for consolidation are reported.  |
| 18 | 2007 | Lee, Karunaratne                           | Utilization of Jute-coir fiber drains for soft soil improvement is studied.   |
| 20 | 2011 | M.R.Madhav<br>et al.                       | Proposed Granular piles (GPs) instead of PVDs for accelerating rate of consolidation considering stress concentration ratio and stiffness of granular material.   |

## 2.9 Critical Appraisal on Discrepancies and Limitations of Theoretical and Experimental Development till Date:

Looking to the theoretical development done so far in the field of consolidation through radial drainage using various vertical drains almost all research workers have extended one dimensional theory of consolidation into two or three dimensional theories considering various theoretical parameters affecting both process of consolidation and rate of consolidation like magnitude and rate of

loading, permeability with respect to stratification, accounting linear and non-linear behavior with void ratio change, pore pressure distribution and its variation along radial distances, with and without stratification (1936, 1941, 1943, 1958, 1961, 1969, 1975, 1987, 1991, 1992, 1994, 2005). Out of many research workers, some research workers have not considered isotropy of soil mass and its influence on stress distribution and settlement and have established equations while some have extended their solutions for arbitrary loading with time, considering plane radial flow and vertical linear flow, taking non-homogeneity of soil and stress-strain characteristics of soil, for radial flow with peripheral drainage, for variable loading, soil properties and layered system, by accounting variation in rate of loading and coefficient of permeability for inward and peripheral drainage (1942, 1948, 1953, 1957, 1964, 1975, 1989, 1994, 1999, 2004, 2005).

Another group of research workers have extended either Barron's equal strain theory or free strain theory considering the material in disturbed zone to be compressible, for smear zone and well resistance considering effect of permeability around smear zone, taking account structural viscosity for rheological model study, for three dimensional consolidation considering creep and compressibility of pore fluid with equal deformation (1957, 1969, 1971, 1979, 1993, 2000, 2003, 2005).

Some research workers have developed equation by taking help of rheological models to define stress-strain relationships of soil, some have given solutions for consolidation by taking effect of dilatancy of soil mass, solutions for triangular loading, instantaneous loading, arbitrary loading, with and without soil heterogeneity both for two and three dimensional flow using either finite difference method or other numerical approaches including finite element approach using appropriate softwares. (1966, 1975, 1976, 1979, 1985, 1989, 1994, 1997, 1998, 1999, 2000, 2001, 2003, 2004, 2005, 2008, 2009, 2010).

Another school of research workers have developed numerical solutions on consolidation by radial flow assuming variable permeability of smear zone, probabilistic design approach, plane strain modeling with smear effects and soil compressibility, closed form solution for ramp loading, by adopting Finite Element approach for the extension of Hansbo's theoretical aspect for 'no

smearing and well resistance' condition for band shaped drains.(1994, 1997, 1998, 2000, 2001, 2005, 2007, 2008)

Another school of research workers have developed experimental set-up for the measurement of consolidation of soft clay considering with and without horizontal top drainage layer, along with and without pore pressure measurement either by using peripheral and central vertical drain in oedometer along with sophisticated instrumentation. Some have worked on different shapes of drains, type of drains, method of installation, spacing of drains using synthetic and non-synthetic natural fibers using either modified triaxial set up or oedometer or other physical models (1960, 1979, 1981, 1982, 1983, 1984, 1988, 1991, 1994, 1995, 1997, 1998, 2002, 2003, 2004, 2005, 2007). However it has been noted that there has been no effort made by any research workers in measuring the pore water pressure along the various radial distances to account the sequence of consolidation at various time intervals due to radial flow towards central drain incorporating either mechanical pore pressure measuring device like bishop or a electronic data acquisition system interfaced with computer software.

All the above research workers have concentrated on extension of Barron's theory or Hansbo's theory considering its limitations to amalgamate smear effect, well resistance, variable permeability and non-linear behavior of void-ratio by adopting Finite element method, Finite difference method, probabilistic design approach, spectral method and other numerical methods (eigen value or differential quadrature) and have not arrived to one common consensus. Further they could not obtain theoretical formulation of radial pore pressure distribution during process of consolidation (isochrone) from first principle considering non-homogeneity, time effects intrinsic to the soil skeleton and compressibility of the pore fluid and solids along with variation of compressibility and permeability.

Though some of the research workers have attempted in adopting experimental set-up for the measurement of consolidation but only few could measure pore pressure during the process.

They failed to accommodate these measurements at the various sequence of process of consolidation and its effect on effective stress with a use of Isochrones. No researcher could compare theoretical isochrone with experimental one.

Above researchers took pain in attempting in using various synthetics, non-synthetics and natural materials for vertical drain but missed the above measurements and analysis based on physico-chemical aspect of soil structure interaction in clay water system of the saturated soil element.

Looking to the above limitations and deficiencies both in terms of theory and experimental investigations authors decided to extend the theory for one dimensional consolidation, Shroff et al., (1985) of soft soils through inward radial flow using vertical drains with radial pore water pressure dissipation under same magnitude of constant pressure using first principle which is easy to implement for various field conditions.

This theoretical treatment incorporates non-homogeneity, time effects intrinsic to the soil skeleton along with physico-chemical changes, compressibility of pore fluid and solid, variation of compressibility and permeability during consolidation. The lump parameter ( $\lambda$ ) which has been proposed in the current study incorporates above all factors. Further, Darcy's law is assumed to be valid and has been recasted in a form in which it is the relative velocity of the soil skeleton and pore fluid flow with reference to central drain characteristics that is related to the excess pore fluid pressure gradient.

The various experimental factors are treated by using hydraulically pressurized oedometer for the measurement of pore water pressure at various radial points to obtain experimental isochrones that is sequence of consolidation and at various  $r/r_e$  ratio for corresponding concentric planar location for given  $z/h$  at that time with reference to various factors influencing consolidation due to radial dissipation of pore water pressure. Average degree of consolidation is computed from trajectory of isochrones and influence of each parameter is obtained in form of value of lump parameter ( $\lambda$ ). The average degree of consolidation ( $U_R$ ) obtained experimentally for each influencing factor is then compared with theoretical one with respect to time factor ( $T_r$ ), and appropriate lump parameter ' $\lambda$ ' is determined.

## **CHAPTER-3**

### **SCOPE, PROGRAMME AND SCHEME OF INVESTIGATIONS**

---

**B**eginning with the classical work of Terzaghi's on three dimensional consolidation process and thereafter Barron's theory on consolidation due to radial flow which was further extended by Hansbo, numbers of research workers carried out research and focused the attention on various influencing factors of vertical geodrain on consolidation characteristics of clayey soil due to radial flow either by laboratory model or in the field. The objective of the present investigation is to examine the influence of diameter, distinctive material and geometry of vertical drain with soil structure effects on consolidation characteristics of soft clay due to radial drainage from fundamental considerations and aims to propose a unified solution of the phenomenon. An abstract of the work is presented as Appendix A and Synopsis in this Volume. A list of references directly used in this work is given at the end of this Volume.

#### **3.1. SCOPE**

##### **3.1.1. Theoretical Work**

Classical and modern theories of one dimensional consolidation of clays by radial drainage using vertical geodrains are critically appraised in chapter II, to find out their sensitiveness in reflecting the various influencing factors like diameter, distinctive material, and geometry of the vertical drains. Simultaneously, other associated factors like physico-chemical changes, compressibility of pore fluid and soil solids, variation of compressibility and permeability along with soil structure effects are taken into account. The shortcomings arise due to neglecting simultaneous effect of above factors on rate of consolidation and sequence of consolidation at various time intervals and its overall effect on deformation characteristics of clay mass. Earlier studies could neither systematically co-relate the effect of vertical drains on consolidation of clays in the laboratory model nor analyze the effect of geodrains

on the pore pressure dissipation during process of consolidation through radial flow. With an objective to understand above discussed effects, the aim of the present work is to study the one-dimensional consolidation of saturated soft clay with radial pore water pressure dissipation under constant magnitude of constant pressure using central vertical drain of different materials, geometry (shapes) and 'n' value ('n' is the ratio of drain radius to radius of zone of influence of soil sample). In this study, a generalized theory based upon the fundamental considerations is developed by the author's which is described in Chapter IV. In order to utilize the new theory for the analysis of experimental data, the analytical solution of the higher order partial differential equation assuming the lump parameter ' $\lambda$ ' as constant is evaluated using Visual Basic Programme and Curve Expert 3 software on computer. Further lumped parameter ( $\lambda$ ) is the ratio of  $(C_e / C_r) r_e$ , where  $C_r$  is coefficient of consolidation due to radial drainage and  $C_e$  is coefficient due to permeability and porosity which is to some extent due to small magnitude of radial strain which helps in redistributing loads to the surface at interface of drain giving same settlement supporting 'equal strain' condition. In turn  $C_r$  will vary with the drain material reflecting in the values of ( $\lambda$ ). Isochrones and various theoretical relationships between degree of consolidation and time factors are obtained for range of positive and negative ' $\lambda$ ' values.

### **3.1.2. Experimental Work**

Experimental data of variety of tests from number of important research studies are reviewed and discussed in chapter II to determine the major factors that influence the consolidation characteristics of soft clay due to radial flow. In the present work experimental investigation are planned to examine the influence of diameter of drain ('n' value), distinctive material of drain, geometry of drain, variation of water content ratio (WCR), variation of consolidation pressure ratio (CPR), variation of horizontal permeability ( $k_h$ ) to vertical permeability ( $k_v$ ) ratio and orientation of particle (scanning electron microscopy) on the consolidation characteristics of clays using modified hydraulically pressurized Oedometers. In order to conduct these studies, modification of the existing hydraulically pressurized Oedometer is carried out for the measurement of pore water pressure at various radial points to obtain experimental isochrones. It enables to measure sequence of consolidation at various  $r/r_e$  ratio for corresponding

concentric planar location for given  $z/h$  at that time with reference to various factors influencing consolidation due to radial dissipation of pore water pressure.

Further, in order to verify the proposed theory and the lumped parameter ( $\lambda$ ), a series of consolidation tests with radial drainage through vertical geodrain at central location of a cylindrical saturated soil sample along with pore pressure measurements at three radial distances and displacement measurements so as to prove its efficacy against various physical factors namely type of drain material, various shapes of the drain with different geometry of the drain, 'n' values (i.e. different diameters of drain related to influence zone) are carried out. Various derived parameters are evaluated for the above and analysis is carried to access the structural variation with load, tortuosity changes with change in the horizontal permeability and consolidation pressure ratio (CPR). For this assessment the microscopy of several samples collected during the testing of several factors are examined to understand the philosophy of microscopical sequential changes occurred in the clay-water system of soil skeleton.

Prior to planning the actual experimental schedule preliminary experiments are carried out in order to design same initial thickness of sample, same physical properties of the drain, shapes of the drain and installation technique.

A series of consolidation tests considering all the above factors viz. drain material, shape of drain and various 'n' value, are conducted in 254 mm & 152 mm diameter Oedometer by employing system consisting of displacement and pore pressure transducers supplemented with Data Logger System interfaced with computer to measure, record and display with time simultaneously pore pressure and settlement at various radial co-ordinates using LabVIEW-8.2 software along with mechanical system. Sample in the Oedometer is representative of one influence zone (effective zone). The functional details of Data Logger System, LabVIEW-8.2 software and Curve Expert 3 software are given in Appendix B, C and D at the end of this volume.

It is planned to use sand, polypropylene fabric, coir-jute, and polypropylene fibers to fabricate vertical geodrains of different diameters in relation to diameter of Oedometer to achieve various 'n' values.

To assess the influence of various shapes of the drain with different geometry of the drain on consolidation, plus-shaped drain, tripod-shaped drain,

rectangular-stripped drain (band) are adopted. The optimacy of 'n' value dictate the economy and the efficiency of the functioning of the drain. The experiments are designed and conducted for 'n' value equal to 11.04, 16.93 & 21.71 using various drains of above materials.

Further in order to study the structural variation in soil during the consolidation process under different conditions discussed above, (i) the water content ratio (WCR) is evaluated considering the ratio of existing water content at the end of particular load to water content at the end of initial load (10kPa). (ii) consolidation pressure ratio (CPR) is assessed considering load under testing to the load with which sample is preconsolidated initially before the commencement of test. For the analysis CPR as 2, 4, & 16 are accounted. (iii) permeability ratios with variation in horizontal permeability deduced from the above results are utilized to access the effect of tortuosity in the soil structure. Also, the magnitude of the gain in shear strength of clay due to the expulsion of pore water is determined by performing laboratory vane shear tests at the beginning and at the end of the consolidation test. Further an attempt is made to examine the remedial changes which occur due to consolidation due to radial flow by prefabricated vertical geodrains under influence of seismic forces. After consolidation test the sample is subjected to 0.1g acceleration which is equivalent to 6.5 magnitude of Richter scale-(IS: 1893 1984, IS 1893 2002 part 1-4) vibration/seismic forces, by putting the consolidated soil sample on vibration table. Before and after the subjection of seismic forces the remediation achieved is assessed by measuring the shear strength of the soil sample.

The factors affecting measurements such as de-airing of the system, reduce pressure loss through polypropylene pipe (system flexibility), preparation of deaired soft soil sample, smearless vertical drain installation, smooth polished frictionless base plate and middle ring of the oedometer, deairing of the porous stone, frictionless settlement rod are ensured during the experiments to increase perfection and accuracy of the system. A development of special radial and vertical permeability measurement set-up is done to assess the efficacy of the drain by capturing the equivalent pore space and clogging potential of the drain. The stiffness/flexibility of the drain is measured against the load variation in control triaxial compression set-up.



About 50 consolidation tests with radial drainage along with pore pressure and settlement measurements are planned and performed to examine the several factors mentioned earlier. The schedule for the same is illustrated in the **table no.3.1 to 3.8.**

### **3.2. Programme**

#### **3.2.1. Objectives**

It is proposed to keep in view the following specific points while analyzing the experimental data obtained during this investigation:

1. System inadequacies and the compatibility of the pore pressure measuring system.
2. Interaction of radial flow with rate and magnitude of consolidation.
3. Orientation of particles and drainage path.
4. Tortuosity of the flow in radial and vertical path.
5. Soil structural changes along with changes in the soil skeleton, inter molecular water and permeability

#### **3.2.2 Experimental Schedule**

The soil used in the current study is kaolinitic clays. The details of the physical properties of these clays used are given at the end of this chapter under table no. 3.9 and results of various test performed are given in Appendix E. Consolidation tests are conducted on modified hydraulically pressurized Oedometers as described in Chapter 5. Also it describes specifications of various equipments employed during this investigation. The sand used for preparing sand drain and sandwich is described in table no. 3.9 and 3.10 at the end of this chapter and detailed results of test performed are given in Appendix F. The properties of geotextile used for preparing sandwich are described in table no. 3.11 at the end of this chapter. The properties of coir and jute fibers used for fabricating coir-jute drain are described in table no. 3.12 at the end of this chapter. The properties of polypropylene fibers used for fabricating polypropylene fiber drain encapsulated by filter paper is described in table no. 3.13 at the end of this chapter. Table 3.2 to Table 3.8 presents experimental schedule followed for the investigation of various factors.

### 3.3. Scheme

Data collected from the experimental investigations as detailed in Table 3.2 to Table 3.8 are analyzed employing standard parameters and plots. In order to bring out specific points, necessary plots and parameters are chosen, which is further discussed in chapter VII.

#### 3.3.1. Parameters

Parameters as defined in the classical consolidation theory and which have become conventional are adopted in the present work. Some of the other parameters which are adopted according to need of theory and analysis are also mentioned here. These standard parameters are:

1. Coefficients of consolidation due to radial flow,  $C_r$ .
2. Time factor for consolidation due to radial flow,  $T_r$ .
3. Degree of consolidation due to the radial drainage, for settlement reading,  $U_r\%$  and for pore pressure readings,  $(1-u_r/u_o)\%$ .
4. Compression index for consolidation due to radial flow,  $C_{cr}$ .
5. Primary compression ratio for consolidation due to radial flow,  $P_{cr}$ .
6. Pore pressure ratio for radial flow,  $u_r/u_o\%$ .
7. Coefficient of permeability due to vertical flow,  $k_v$ .
8. Coefficient of permeability due to radial flow,  $k_h$ .
9. Coefficient of compressibility due to radial flow,  $a_{vr}$ .
10. Coefficient of volume change due to radial flow,  $m_{vr}$ .
11. Lump parameter,  $\lambda$ .

#### 3.3.2 Plots

Results of experimental investigation are collected for various load intensity with respect to settlement and pore pressure measurements. For 254 mm (10") diameter and 152 mm (6") diameter Oedometer, following graphs are plotted.

#### Consolidation due to Radial Drainage

##### (a) Settlement:

- 1) Degree of consolidation against log of time ( $U_r\%$  v/s  $\log t$ ).
- 2) Coefficient of consolidation against degree of consolidation ( $C_r$  v/s  $U_r\%$ ).

- 3) Coefficient of consolidation against consolidation pressure ( $C_r$  v/s  $P$ ).
- 4) Coefficient of horizontal permeability against consolidation pressure ( $k_h$  v/s  $P$ ).
- 5) Void ratio against log of consolidation pressure ( $e$  v/s  $\log P$ ).
- 6) Primary compression ratio against consolidation pressure ( $P_{cr}$  v/s  $P$ ).
- 7) Coefficient of compressibility against 'n' value ( $C_{cr}$  v/s 'n')
- 8) Coefficient of compressibility against drain material ( $C_{cr}$  v/s 'drain material')
- 9) Coefficient of compressibility against drain geometry ( $C_{cr}$  v/s 'drain geometry')
- 10) Coefficient of compressibility against volumetric water ratio ( $C_{cr}$  v/s VWR)
- 11) Coefficient of compressibility against consolidation pressure ratio  
( $C_{cr}$  v/s CPR)
- 12) Loss in shear strength against 'n' value under constant seismic force  
( $\zeta$  v/s  $n$ )
- 13) Average degree of consolidation against Time factor ( $U_r$  % v/s  $T_r$ ).

(b) Pore pressure:

- 1) Degree of consolidation against log of time ( $(1 - u_r/u_o)$  % v/s  $\log t$ ).
- 2) Coefficient of consolidation against degree of consolidation  
( $C_{vr}$  v/s  $(1 - u_r/u_o)$  %).
- 3) Coefficient of consolidation against consolidation pressure ( $C_{vr}$  v/s  $P$ ).
- 4) Coefficient of horizontal permeability against consolidation pressure  
( $k_h$  v/s  $P$ ).
- 5) Void ratio against log of consolidation pressure ( $e$  v/s  $\log P$ ).
- 6) Experimental and Theoretical Isochrones ( $u_r/u_o$  v/s  $r/r_e$ ).
- 7) Average degree of consolidation against Time factor ( $U_r$  % v/s  $T_r$ ).

(c) From Scanning Electron Microscopy, additional plots are made from the soil micrograph to support the reasoning of pattern of above curves.

- (1) % porosity vs. depth of sample
- (2) % porosity vs. drain material
- (3) % porosity vs. radial distance and 'n' value
- (4) Angle of orientation ( $\beta$ ) vs. drain material
- (5) Angle of orientation ( $\beta$ ) vs. porosity
- (6) Angle of orientation ( $\beta$ ) vs. radial distance
- (7) Tortuosity of flow path vs. drain material

## (8) Tortousity of flow path vs. 'n' value

Note: Results of consolidation due to vertical flow are shown wherever found necessary, with an objective of comparison of results between consolidation through radial flow and consolidation through vertical flow.

### 3.4 Experimental Schedule

The various influencing factors mentioned in table no.3.1 are each analysed in detail as per the list of plots mentioned above in section 3.3.2 which is further presented in chapter VII. For easy understanding and reference the various conventional parameters and derived parameters are assigned by their symbol and respective plots numbers.

**Table 3.1:** Schedule of study parameters and related figure numbers

| Sr. No. | Influencing Factor                              | Parameters analyzed   | Vertical Drain used and corresponding 'n' value | Related figure nos. |
|---------|---|---|---|---------------------|
| 1.      | Type of Drain Material                          | Settlement, Pore pressure and Micro structure characteristics | SD & 11.04                                      | 6.10 to 6.116       |
|         |   |   | SW & 11.04                                      |                     |
|         |   |   | CJ & 11.04                                      |                     |
|         |   |   | PF & 11.04                                      |                     |
| 2.      | Variation of Diameter (n) value                 | Settlement, Pore pressure and Micro structure characteristics | SD & 11.04, 16.93, 21.71                        | 6.117 to 6.259      |
|         |   |   | SW & 11.04, 16.93, 21.71                        |                     |
|         |   |   | CJ & 11.04, 16.93, 21.71                        |                     |
|         |   |   | PF & 11.04, 16.93, 21.71                        |                     |
| 3.      | Various Geometry (shapes) of Drain              | Settlement and Pore pressure                                  | CSSD & 11.04                                    | 6.260 to 6.319      |
|         |   |   | PSSD & 11.04                                    |                     |
|         |   |   | TSSD & 11.04                                    |                     |
|         |   |   | BSSD & 11.04                                    |                     |
| 4.      | Variation of Water Content Ratio (VWR)          | Settlement and Pore pressure                                  | SD & 11.04                                      | 6.320 to 6.322      |
|         |   |   | SW & 11.04                                      |                     |
|         |   |   | CJ & 11.04                                      |                     |
|         |   |   | PF & 11.04                                      |                     |
| 5.      | Variation of Consolidation Pressure Ratio (CPR) | Settlement and Pore pressure                                  | SW & 11.04                                      | ----                |
|         |   |   | CJ & 11.04                                      |                     |
|         |   |   | PF & 11.04                                      |                     |

### 3.4.1 Conventional Parameters

**Table 3.2:** Variation of Vertical Drain Materials

| Type of drain material                   | Type of drain             | 'n' value & Type of drainage | Diameter of Oedometer | Type of measurement              | Diameter of geodrain |
|--|---------------------------|------------------------------|-----------------------|----------------------------------|----------------------|
| Sand                                     | Sand drain (SD)           | Radial                       | 254mm                 | Settlement & Pore water pressure | 23mm                 |
| Sand + polypropylene geotextile          | Sandwick (SW)             | Radial                       | 152mm                 | Settlement & Pore water pressure | 14mm                 |
| Coir fibers + Jute fibers + Filter paper | Coir-Jute (CJ)            | Radial                       | 254mm                 | Settlement & Pore water pressure | 23mm                 |
| Polypropylene fibers + Filter paper      | Polypropylene fibers (PF) | Radial                       | 254mm                 | Settlement & Pore water pressure | 23mm                 |

\* n = ratio of radius of odometer to the radius of drain

Note: study was carried out keeping same initial void ratio and same  $k_h/k_v$

**Table 3.3:** Variation of 'n' values

| 'n' values | Drain type                     | Type of drainage | Size of Oedometer | Type of measurement              | Diameter of geodrain | Aspect ratio |
|------------|--------------------------------|------------------|-------------------|----------------------------------|----------------------|--------------|
| 11.04      | Sand drain (SD)                | Radial           | 254mm             | Settlement & Pore water pressure | 2.3cm                | 2.39         |
| 16.93      |                                | Radial           | 254mm             | Settlement & Pore water pressure | 1.5cm                | 3.67         |
| 21.71      |                                | Radial           | 152mm             | Settlement & Pore water pressure | 0.7cm                | 4.70         |
| 11.04      | Sandwich drain (SW)            | Radial           | 152mm             | Settlement & Pore water pressure | 1.38cm               | 2.39         |
| 16.93      |                                | Radial           | 152mm             | Settlement & Pore water pressure | 0.9cm                | 3.67         |
| 21.71      |                                | Radial           | 254mm             | Settlement & Pore water pressure | 1.17cm               | 4.70         |
| 11.04      | Coir-Jute drain (CJ)           | Radial           | 254mm             | Settlement & Pore water pressure | 2.3cm                | 2.39         |
| 16.93      |                                | Radial           | 152mm             | Settlement & Pore water pressure | 0.9cm                | 3.67         |
| 21.71      |                                | Radial           | 254mm             | Settlement & Pore water pressure | 1.17cm               | 4.70         |
| 11.04      | Polypropylene fiber drain (PF) | Radial           | 254mm             | Settlement & Pore water pressure | 2.3cm                | 2.39         |
| 16.93      |                                | Radial           | 152mm             | Settlement & Pore water pressure | 0.9cm                | 3.67         |
| 21.71      |                                | Radial           | 254mm             | Settlement & Pore water pressure | 1.17cm               | 4.70         |

Where,  $n$  = ratio of radius of oedometer to the radius of drain

Aspect ratio = ratio of height of geodrain sample to diameter of geodrain

**Table 3.4:** Various Geometry (shapes) of Vertical Drain

| Shape of drain     | 'n' value | † Drain-<br>age path<br>ratio | Drainage Path |               | Surface<br>area<br>(Sa) in<br>cm <sup>2</sup> | ** Equivalent<br>diameter of<br>geodrain (De) | Surface<br>area index<br>= Sa/De | * Effective<br>surface<br>area<br>(cm <sup>-1</sup> ) |
|--------------------|-----------|-------------------------------|---------------|---------------|---|---|----------------------------------|---|
|                    |           |                               | d max<br>(cm) | d min<br>(cm) |   |   |                                  |   |
| Circular<br>(CSSD) | 11.04     | 1                             | 11.55         | 11.55         | 41.90   | 2.3cm   | 18.21                            | 0.28  |
| Plus<br>(PSSD)     | 11.04     | 1.04                          | 12.28         | 11.7          | 41.90   | 2.3cm   | 18.21                            | 0.27  |
| Tripod<br>(TSSD)   | 11.04     | 1.17                          | 12.4          | 11.15         | 41.90   | 2.3cm   | 18.21                            | 0.26  |
| Band<br>(BSSD)     | 11.04     | 1.06                          | 12.4          | 11.7          | 41.90   | 2.3cm   | 18.21                            | 0.27  |

Where, †Drainage path ratio= Maximum drainage path/Minimum drainage path

\*Effective surface area = Effective drainage path (d min)/Surface area

\*\*Equivalent diameter for:

(i) Plus shape:  $8B_d + 4T_d$  (ii) Tripod shape:  $6B_d + 3T_d$

(iii) Band shape:  $2(B_d + T_d)/\pi$ ,  $B_d$ = Breadth of drain,  $T_d$ = Thickness of drain

Where, CSSD = Circular shape sand drain, PSSD = Plus shape sand drain, BSSD = Band shape sand drain

TSSD = Tripod/Y shape sand drain

Note: Study was made for same drain material, same void ratio, same  $k_h/k_v$  and to know effect of variation in drainage path versus consolidation parameters (0.26, 0.27, 0.28)

### 3.4.2 Derived Parameters:

**Table 3.5:** Variation of Water Content Ratio (WCR)\*

| Water Content Ratio | Water content      |                    | Drain type                     | 'n' value | End of Load (kPa) | Water content (%) | Cc average from graph | *Cc as per load variation |
|---------------------|--------------------|--------------------|--------------------------------|-----------|-------------------|-------------------|-----------------------|---------------------------|
|                     | W <sub>i</sub> (%) | W <sub>f</sub> (%) |                                |           |                   |                   |                       |                           |
| 0.851               | 91                 | 47.67              | Sand drain (SD)                | 11.04     | 20                | 77.53             | 0.400                 | 0.896                     |
| 0.724               |                    |                    |                                |           | 40                | 65.95             |                       | 0.734                     |
| 0.634               |                    |                    |                                |           | 80                | 57.72             |                       | 0.619                     |
| 0.566               |                    |                    |                                |           | 160               | 51.54             |                       | 0.532                     |
| 0.523               |                    |                    |                                |           | 320               | 47.67             |                       | 0.468                     |
| 0.863               | 91                 | 45.48              | Sandwick drain (SW)            | 11.04     | 20                | 78.58             | 0.315                 | 0.911                     |
| 0.777               |                    |                    |                                |           | 40                | 70.10             |                       | 0.792                     |
| 0.657               |                    |                    |                                |           | 80                | 59.82             |                       | 0.648                     |
| 0.577               |                    |                    |                                |           | 160               | 52.52             |                       | 0.546                     |
| 0.499               |                    |                    |                                |           | 320               | 45.48             |                       | 0.437                     |
| 0.802               | 91                 | 41.52              | Coir-Jute drain (CJ)           | 11.04     | 20                | 73.00             | 0.258                 | 0.833                     |
| 0.717               |                    |                    |                                |           | 40                | 65.26             |                       | 0.724                     |
| 0.638               |                    |                    |                                |           | 80                | 58.10             |                       | 0.624                     |
| 0.531               |                    |                    |                                |           | 160               | 48.38             |                       | 0.488                     |
| 0.456               |                    |                    |                                |           | 320               | 41.52             |                       | 0.370                     |
| 0.847               | 91                 | 47.20              | Polypropylene fiber drain (PF) | 11.04     | 20                | 77.13             | 0.366                 | 0.891                     |
| 0.739               |                    |                    |                                |           | 40                | 67.28             |                       | 0.753                     |
| 0.645               |                    |                    |                                |           | 80                | 58.75             |                       | 0.633                     |
| 0.570               |                    |                    |                                |           | 160               | 51.92             |                       | 0.538                     |
| 0.518               |                    |                    |                                |           | 320               | 47.20             |                       | 0.465                     |

\* Where, Water content ratio is the ratio of existing water content at the end of particular load to water content at the end of initial load (10kPa). W<sub>i</sub> and W<sub>f</sub> = Initial water content and Final water content of clay sample at the end of particular load. \* Cc calculated as per Nishida method



**Table 3.6:** Variation of Consolidation Pressure Ratio (CPR)

| CPR | Drain Type           | 'n' value | Existing load (kPa) | $k_h$ (cm/sec)        | $k_v$ (cm/sec)        | $k_h/k_v$ | Cc value | Diameter of Oedometer |
|-----|----------------------|-----------|---------------------|-----------------------|-----------------------|-----------|----------|-----------------------|
| 2   | Coir-jute fiber (CJ) | 11.04     | 20                  | $3.55 \times 10^{-7}$ | $1.31 \times 10^{-7}$ | 2.71      | 0.227    | 254mm                 |
| 4   |                      | 11.04     | 40                  | $3.05 \times 10^{-7}$ | $4.67 \times 10^{-8}$ | 6.54      | 0.258    |                       |
| 16  |                      | 11.04     | 160                 | $2.17 \times 10^{-7}$ | $8.04 \times 10^{-9}$ | 27.1      | 0.286    |                       |
| 2   | Sandwick (SW)        | 11.04     | 20                  | $1.25 \times 10^{-7}$ | $1.31 \times 10^{-7}$ | 1.00      | 0.308    | 254mm                 |
| 4   |                      | 11.04     | 40                  | $7.81 \times 10^{-8}$ | $4.67 \times 10^{-8}$ | 1.67      | 0.312    |                       |
| 16  |                      | 11.04     | 160                 | $3.36 \times 10^{-8}$ | $8.04 \times 10^{-9}$ | 4.17      | 0.320    |                       |
| 2   | PP drain (PF)        | 11.04     | 20                  | $3.15 \times 10^{-7}$ | $1.31 \times 10^{-7}$ | 2.41      | 0.339    | 254mm                 |
| 4   |                      | 11.04     | 40                  | $2.08 \times 10^{-7}$ | $4.67 \times 10^{-8}$ | 4.46      | 0.353    |                       |
| 16  |                      | 11.04     | 160                 | $6.17 \times 10^{-8}$ | $8.04 \times 10^{-9}$ | 7.67      | 0.380    |                       |
| 2   | Sand drain (SD)      | 11.04     | 20                  | $3.98 \times 10^{-7}$ | $1.31 \times 10^{-7}$ | 3.03      | 0.255    | 254mm                 |
| 4   |                      | 11.04     | 40                  | $3.16 \times 10^{-7}$ | $4.67 \times 10^{-8}$ | 6.76      | 0.555    |                       |
| 16  |                      | 11.04     | 160                 | $7.97 \times 10^{-8}$ | $8.04 \times 10^{-9}$ | 9.91      | 0.928    |                       |

Where, CPR = ratio of existing pressure/initial pressure of 10kPa ,  
Cc = Compression index (slope of e vs.log'p' graph)

Note: Data of Coefficient of vertical permeability of soil ( $k_v$ ) used in this table is obtained from laboratory test data of one-dimensional consolidation experiment.

### 3.4.3 Scanning Electron Microscopy (SEM)

**Table 3.7:** Schedule of SEM of consolidated clay samples with central vertical drain

| Sr.No. | Type of Geodrain | 'n' value | Location  | Magnification Factor |
|--------|------------------|-----------|-----------|----------------------|
| 1.     | Sand drain-SD    | 11.04     | $h_{tr2}$ | 500x                 |
| 2.     | Sand drain-SD    | 11.04     | $h_{tr2}$ | 1000x                |
| 3.     | Sand drain-SD    | 11.04     | $h_{tr2}$ | 1000x                |
| 4.     | Sand drain-SD    | 11.04     | $h_{tr2}$ | 2700x                |
| 5.     | Sand drain-SD    | 11.04     | $h_{cr2}$ | 500x                 |
| 6.     | Sand drain-SD    | 11.04     | $h_{cr2}$ | 1000x                |
| 7.     | Sand drain-SD    | 11.04     | $h_{cr2}$ | 2700x                |
| 8.     | Sand drain-SD    | 11.04     | $h_{cr2}$ | 2700x                |
| 9.     | Sand drain-SD    | 11.04     | $h_{br2}$ | 500x                 |
| 10.    | Sand drain-SD    | 11.04     | $h_{br2}$ | 1000x                |
| 11.    | Sand drain-SD    | 11.04     | $h_{br2}$ | 2700x                |
| 12.    | Sand drain-SD    | 11.04     | $h_{br2}$ | 2700x                |
| 13.    | Sand drain-SD    | 11.04     | $h_{br3}$ | 500x                 |
| 14.    | Sand drain-SD    | 11.04     | $h_{br3}$ | 1000x                |
| 15.    | Sand drain-SD    | 11.04     | $h_{br3}$ | 2700x                |
| 16.    | Sand drain-SD    | 11.04     | $l_{trd}$ | 500x                 |
| 17.    | Sand drain-SD    | 11.04     | $l_{trd}$ | 1000x                |
| 18.    | Sand drain-SD    | 11.04     | $l_{trd}$ | 2700x                |
| 19.    | Sand drain-SD    | 11.04     | $l_{crd}$ | 500x                 |
| 20.    | Sand drain-SD    | 11.04     | $l_{crd}$ | 1000x                |
| 21.    | Sand drain-SD    | 11.04     | $l_{crd}$ | 2700x                |
| 22.    | Sand drain-SD    | 11.04     | $l_{brd}$ | 270x                 |
| 23.    | Sand drain-SD    | 11.04     | $l_{brd}$ | 500x                 |
| 24.    | Coir-Jute-CJ     | 11.04     | $h_{tr2}$ | 1000x                |
| 25.    | Coir-Jute-CJ     | 11.04     | $h_{tr2}$ | 1000x                |
| 26.    | Coir-Jute-CJ     | 11.04     | $h_{tr2}$ | 2700x                |
| 27.    | Coir-Jute-CJ     | 11.04     | $h_{tr2}$ | 2700x                |
| 28.    | Coir-Jute-CJ     | 11.04     | $h_{tr2}$ | 5000x                |
| 29.    | Coir-Jute-CJ     | 11.04     | $h_{tr2}$ | 5500x                |
| 30.    | Coir-Jute-CJ     | 11.04     | $h_{tr2}$ | 10000x               |
| 31.    | Coir-Jute-CJ     | 11.04     | $h_{cr2}$ | 5000x                |
| 32.    | Coir-Jute-CJ     | 11.04     | $h_{cr2}$ | 10000x               |
| 33.    | Coir-Jute-CJ     | 11.04     | $l_{crd}$ | 2700x                |
| 34.    | Coir-Jute-CJ     | 11.04     | $l_{crd}$ | 5000x                |
| 35.    | Coir-Jute-CJ     | 11.04     | $l_{crd}$ | 11000x               |
| 36.    | Coir-Jute-CJ     | 11.04     | $h_{br2}$ | 2700x                |
| 37.    | Coir-Jute-CJ     | 11.04     | $h_{br2}$ | 5500x                |
| 38.    | Coir-Jute-CJ     | 11.04     | $h_{br2}$ | 5500x                |
| 39.    | Coir-Jute-CJ     | 11.04     | $h_{br2}$ | 11000x               |
| 40.    | Coir-Jute-CJ     | 11.04     | $h_{br2}$ | 11000x               |

|     |              |       |           |        |
|-----|--------------|-------|-----------|--------|
| 41. | Coir-Jute-CJ | 11.04 | $l_{tr1}$ | 2700x  |
| 42. | Coir-Jute-CJ | 11.04 | $l_{tr1}$ | 5000x  |
| 43. | Coir-Jute-CJ | 11.04 | $l_{tr1}$ | 5500x  |
| 44. | Coir-Jute-CJ | 11.04 | $l_{tr1}$ | 11000x |
| 45. | Coir-Jute-CJ | 11.04 | $l_{tr1}$ | 11000x |
| 46. | Coir-Jute-CJ | 11.04 | $l_{brd}$ | 500x   |
| 47. | Coir-Jute-CJ | 11.04 | $l_{brd}$ | 2700x  |
| 48. | Coir-Jute-CJ | 11.04 | $l_{brd}$ | 5500x  |
| 49. | Coir-Jute-CJ | 11.04 | $l_{brd}$ | 1100x  |
| 50. | Coir-Jute-CJ | 11.04 | $l_{brd}$ | 11000x |
| 51. | Coir-Jute-CJ | 16.93 | $l_{trd}$ | 2700x  |
| 52. | Coir-Jute-CJ | 16.93 | $l_{trd}$ | 2700x  |
| 53. | Coir-Jute-CJ | 16.93 | $l_{trd}$ | 5500x  |
| 54. | Coir-Jute-CJ | 16.93 | $l_{trd}$ | 5500x  |
| 55. | Coir-Jute-CJ | 16.93 | $l_{trd}$ | 11000x |
| 56. | Coir-Jute-CJ | 16.93 | $l_{trd}$ | 11000x |
| 57. | Coir-Jute-CJ | 16.93 | $l_{brd}$ | 2700x  |
| 58. | Coir-Jute-CJ | 16.93 | $l_{brd}$ | 2700x  |
| 59. | Coir-Jute-CJ | 16.93 | $l_{brd}$ | 5500x  |
| 60. | Coir-Jute-CJ | 16.93 | $l_{brd}$ | 5500x  |
| 61. | Coir-Jute-CJ | 16.93 | $l_{brd}$ | 11000x |
| 62. | Coir-Jute-CJ | 16.93 | $l_{brd}$ | 11000x |
| 63. | Coir-Jute-CJ | 16.93 | $l_{br1}$ | 2700x  |
| 64. | Coir-Jute-CJ | 16.93 | $l_{br1}$ | 2700x  |
| 65. | Coir-Jute-CJ | 16.93 | $l_{br1}$ | 5500x  |
| 66. | Coir-Jute-CJ | 16.93 | $l_{br1}$ | 5500x  |
| 67. | Coir-Jute-CJ | 16.93 | $l_{br1}$ | 5500x  |
| 68. | Coir-Jute-CJ | 16.93 | $l_{br1}$ | 5500x  |
| 69. | Coir-Jute-CJ | 16.93 | $l_{br1}$ | 11000x |
| 70. | Coir-Jute-CJ | 16.93 | $l_{br1}$ | 11000x |
| 71. | Coir-Jute-CJ | 16.93 | $h_{tr2}$ | 2700x  |
| 72. | Coir-Jute-CJ | 16.93 | $h_{tr2}$ | 5000x  |
| 73. | Coir-Jute-CJ | 16.93 | $h_{tr2}$ | 5500x  |
| 74. | Coir-Jute-CJ | 16.93 | $h_{tr2}$ | 11000x |
| 75. | Coir-Jute-CJ | 16.93 | $h_{tr2}$ | 11000x |

Where,

$r$  = radius of clay sample equal to 76mm for 152mm diameter Oedometer  
and 127mm for 254mm diameter Oedometer.

$r_d$  = radius of drain

$r_1$  = first radial point for measurement of pore pressure at a distance of  $r/4$

$r_2$  = second radial point for measurement of pore pressure at a distance of  $r/2$

$r_3$  = third radial point for measurement of pore pressure at a distance of  $3r/4$

$h$  = thickness of final consolidated clay sample

$h_t$  = Top of final consolidated clay sample

$h_c$  = Centre of final consolidated clay sample

$h_b$  = Bottom of final consolidated clay sample  
 $h_{tr1}$  = Top of final consolidated clay sample at near radial point  $r_1$   
 $h_{tr2}$  = Top of final consolidated clay sample at mid radial point  $r_2$   
 $h_{tr3}$  = Top of final consolidated clay sample at farthest radial point  $r_3$   
 $h_{cr1}$  = Centre of final consolidated clay sample at first radial point  $r_1$   
 $h_{cr2}$  = Centre of final consolidated clay sample at mid radial point  $r_2$   
 $h_{cr3}$  = Centre of final consolidated clay sample at farthest radial point  $r_3$   
 $h_{br1}$  = Bottom of final consolidated clay sample at first radial point  $r_1$   
 $h_{br2}$  = Bottom of final consolidated clay sample at mid radial point  $r_2$   
 $h_{br3}$  = Bottom of final consolidated clay sample at farthest radial point  $r_3$   
 $l_{td}$  = Clay-Drain interface at top of final consolidated clay sample at location  $r_d$   
 $l_{cd}$  = Clay-Drain interface at centre of final consolidated clay sample at location  $r_d$   
 $l_{bd}$  = Clay-Drain interface at bottom of final consolidated clay sample at location  $r_d$   
 $l_{tr1}$  = Clay-Drain interface at top of final consolidated clay sample at location  $r_1$   
 $l_{tr2}$  = Clay-Drain interface at top of final consolidated clay sample at location  $r_2$   
 $l_{tr3}$  = Clay-Drain interface at top of final consolidated clay sample at location  $r_3$   
 $l_{cr1}$  = Clay-Drain interface at centre of final consolidated clay sample at location  $r_1$   
 $l_{cr2}$  = Clay-Drain interface at centre of final consolidated clay sample at location  $r_2$   
 $l_{cr3}$  = Clay-Drain interface at centre of final consolidated clay sample at location  $r_3$   
 $l_{br1}$  = Clay-Drain interface at bottom of final consolidated clay sample at location  $r_1$   
 $l_{br2}$  = Clay-Drain interface at bottom of final consolidated clay sample at location  $r_2$

#### 3.4.4 Shear Strength Measurement of the Consolidated Clay Mass under Static and Dynamic Load:

**Table 3.8:** Schedule of measurement of vane shear strength of soil mass

| Sr.No. | Drain Type & Symbol            | 'n' value            | Condition | Period of Vibration (sec) |
|--------|--------------------------------|----------------------|-----------|---------------------------|
| 1.     | Sand Drain (SD)                | 11.04, 16.93 & 21.71 | Static    | -----                     |
| 2.     | Sandwick Drain (SW)            | 11.04, 16.93 & 21.71 | Static    | -----                     |
|        |                                | 16.93 & 21.71        | Dynamic   | 5, 15, 30, 60, 120        |
| 3.     | Coir-Jute Drain (CJ)           | 11.04, 16.93 & 21.71 | Static    | -----                     |
| 4.     | Polypropylene fiber Drain (PF) | 11.04, 16.93 & 21.71 | Static    | -----                     |

### 3.5 Properties of Various Materials Used In Laboratory Investigation

The determination of physical, mechanical and hydraulic properties of various materials (laboratory testing) used in present scheme of investigation was carried out at following places:

- I. Soil Testing: Geotechnical Engineering Laboratory of M.S. University
- II. Geosynthetics Testing: Geotechnical Engineering Laboratory and Textile Engineering Laboratory of M.S. University
- III. Geosynthetics Testing: ATIRA, Ahmedabad
- IV. Scanning Electron Microscopy: Metallurgy Department of M.S. University and TCR Advanced Engg Pvt. Ltd, Vadodara

**Table 3.9:** Properties of Kaolinitic clay used for investigation

|    |                            |                 |
|----|----------------------------|-----------------|
| 1. | Type of clay               | Kaolinitic clay |
| 2. | Specific gravity(G)        | 2.592           |
| 3. | Liquid limit ( $L_L$ )     | 67%             |
| 4. | Plastic Limit ( $P_L$ )    | 33.43%          |
| 5. | Plasticity Index ( $I_p$ ) | 33.57%          |
| 6. | Soil Classification        | CH (as per ISC) |

**Table 3.10:** Properties of sand used in Sand drain, SD

|    |  |                              |
|----|--|------------------------------|
| 1. | Specific gravity(G)  | 2.645                        |
| 2. | Coefficient of permeability (k)  | $8.45 \times 10^{-3}$ cm/sec |
| 3. | Coefficient of uniformity ( $C_u$ ) and Coefficient of curvature ( $C_c$ )   | 2.023 and 1.295              |
| 4. | Fineness Moduli (FM)   | 2.2-2.3                      |
| 5. | According to I.S. 1498-1970:<br>Sand is classified as SW (well graded sands with little or no fines)<br>Field identification: Wide range in grain size and substantial amounts of all intermediate particle sizes.<br>Highly pervious sand. Permeability $k > 10^{-3}$ cm/sec. Unit dry density 1.76-2.08 g/cm <sup>3</sup> . Good bearing value. It is used for u/s blanket and toe drainage wells. |                              |

**Table 3.11:** Properties of sand used in Sandwich drain, SW

| Sr.No. | Mechanical Analysis and Permeability measurements |  |
|--------|---|--|
| 1.     | Size of sand particles                            | Vary between 0.2mm – 0.3mm               |
| 2.     | Coefficient of permeability (k)                   | $1.47 \times 10^{-1}$ cm/sec             |
| 3.     | Size analysis                                     | 100 percent fine sand (uniformly graded) |
| 4.     | Coefficient of uniformity ( $C_u$ )               | 1.08 (uniformly graded)                  |

**Table 3.12(a):** Physical Properties of polypropylene geotextile used for Sandwich drain, SW

|    |   |                                |
|----|---|--------------------------------|
| 1. | Type of fabric  | Multifilament woven fabric     |
| 2. | Type of weave   | Plain                          |
| 3. | Thickness of PP   | 0.74mm                         |
| 4. | Weight per square meter                                       | 2.261N                         |
| 5. | Threads per square inch<br>(a) Longitudinal<br>(b) Transverse | 43/44<br>18/19                 |
| 6. | Denier value<br>(a) Warp<br>(b) Weft                          | (a)8.79 (N/m)<br>(b)8.03 (N/m) |

**Table 3.12(b):** Mechanical and Hydraulic Properties of polypropylene geotextile used for Sandwich drain, SW (photograph 3.1, 3.2, 3.3 and 3.4)

| Sr.No. | Properties   | Range of Values                |
|--------|--|--------------------------------|
| 1.     | Tensile strength of 1cm x 30cm strip<br>(a) Longitudinal<br>(b) Transverse | (a)2.90(N/m)<br>(b)3.71(N/m)   |
| 2.     | Breaking Elongation<br>(a) Longitudinal<br>(b) Transverse                  | 31.00 percent<br>25.00 percent |
| 3.     | Bursting Strength  | > 2.94MN/m <sup>2</sup>        |

|    |  |  |
|----|--|--|
| 4. | Air permeability at 1.27cm water pressure drop                         | 1320 m <sup>3</sup> /m <sup>2</sup> /hr                          |
| 5. | Water permeability<br>(a) PP Geotextile<br>(b) PP Geotextile with sand | 1.07 x 10 <sup>-1</sup> cm/sec<br>1.87 x 10 <sup>-1</sup> cm/sec |

**Table 3.13:** Permittivity and transmissivity of vertical drain of geosynthetics in fabricating the drain (test on special radial permeability set-up, refer chapter 5)

| Drain Type                | Coefficient of vertical permeability<br>'k <sub>v</sub> '(cm/sec) | Coefficient of horizontal permeability<br>'k <sub>h</sub> '(cm/sec) | Permittivity<br>'ψ'= k <sub>v</sub> /h | Transmissivity<br>'θ'= k <sub>h</sub> /h |
|---------------------------|---|---|--|--|
| Sand drain                | 8.45 x 10 <sup>-3</sup>   | 5.48 x 10 <sup>-2</sup>   | -----                                  | -----                                    |
| Sandwich drain            | 1.87 x 10 <sup>-1</sup>   | 0.859   | 3.4 x 10 <sup>-2</sup>                 | 4.724                                    |
| Coir-Jute drain           | 1.35 x 10 <sup>-1</sup>   | 1.446   | 2.45 x 10 <sup>-1</sup>                | 7.953                                    |
| Polypropylene fiber drain | 1.79 x 10 <sup>-1</sup>   | 1.020   | 3.25 x 10 <sup>-1</sup>                | 5.610                                    |



**Photograph 3.1:** Tensile test on geotextile used in fabricating Sandwich



**Photograph 3.2:** Air permeability test on geotextile used in Sandwich

**Table 3.14:** Specific surface area of vertical geodrains used in present investigations

| Sr.No. | Drain Type                | 'n' value | Specific surface area (mm <sup>2</sup> ) |
|--------|---------------------------|-----------|--|
| 1.     | Sand drain                | 11.04     | 3974.11                                  |
|        |                           | 16.93     | 2591.81                                  |
|        |                           | 21.71     | 2021.61                                  |
| 2.     | Sandwick drain            | 11.04     | 3974.11                                  |
|        |                           | 16.93     | 2591.81                                  |
|        |                           | 21.71     | 2021.61                                  |
| 3.     | Coir-jute drain           | 11.04     | 3974.11                                  |
|        |                           | 16.93     | 2591.81                                  |
|        |                           | 21.71     | 2021.61                                  |
| 4.     | Polypropylene fiber drain | 11.04     | 3974.11                                  |
|        |                           | 16.93     | 2591.81                                  |
|        |                           | 21.71     | 2021.61                                  |



**Table 3.15:** Physical, Mechanical and Hydraulic Properties of Jute fibers used in Coir-Jute fiber drain, CJ (photograph 3.5)

| Sr.No. | Properties   | Range of Values  |
|--------|--|--|
| 1.     | Fiber length (mm)  | 120-800  |
| 2.     | Fiber diameter (mm)  | 0.10-0.20  |
| 3.     | Specific gravity   | 1.02-1.04  |
| 4.     | Bulk density ( $\text{kg/m}^3$ )   | 120-150  |
| 5.     | Ultimate tensile strength ( $\text{N/mm}^2$ )  | 250-350  |
| 6.     | Modulus of elasticity ( $\text{kN/mm}^2$ )   | 26-32  |
| 7.     | Elongation at break %  | 2-3  |
| 8.     | Water absorption %   | 25-40  |
| 9.     | Coefficient of vertical permeability ( $k_v$ )<br>(a) 25% coir + 75% jute fibers placed in vertical direction<br>(b) 25% coir + 75% jute fibers placed in radial direction<br>(c) 25% coir + 75% jute fibers placed in partly in vertical and partly in radial direction | $2.10 \times 10^{-1} \text{ cm/sec}$<br><br>$1.81 \times 10^{-1} \text{ cm/sec}$<br><br>$1.35 \times 10^{-1} \text{ cm/sec}$ |

**Table 3.16:** Physical and Mechanical Properties of Coir fibers used in Coir-Jute fiber drain, CJ

| Sr.No. | Properties                        | Range of Values |
|--------|-----------------------------------|-----------------|
| 1.     | Fiber length (mm)                 | 60-200          |
| 2.     | Density ( $\text{kg/m}^3$ )       | 140             |
| 3.     | Tenacity (g/tex)                  | 10.0            |
| 4.     | Breaking elongation (%)           | 30              |
| 5.     | Moisture regained at 65% R.H. (%) | 10.5            |
| 6.     | Swelling in water (diameter) %    | 5.0             |

**Table 3.17:** Properties of Polypropylene fibers used in Polypropylene fiber Drain, PF (photograph 3.6)

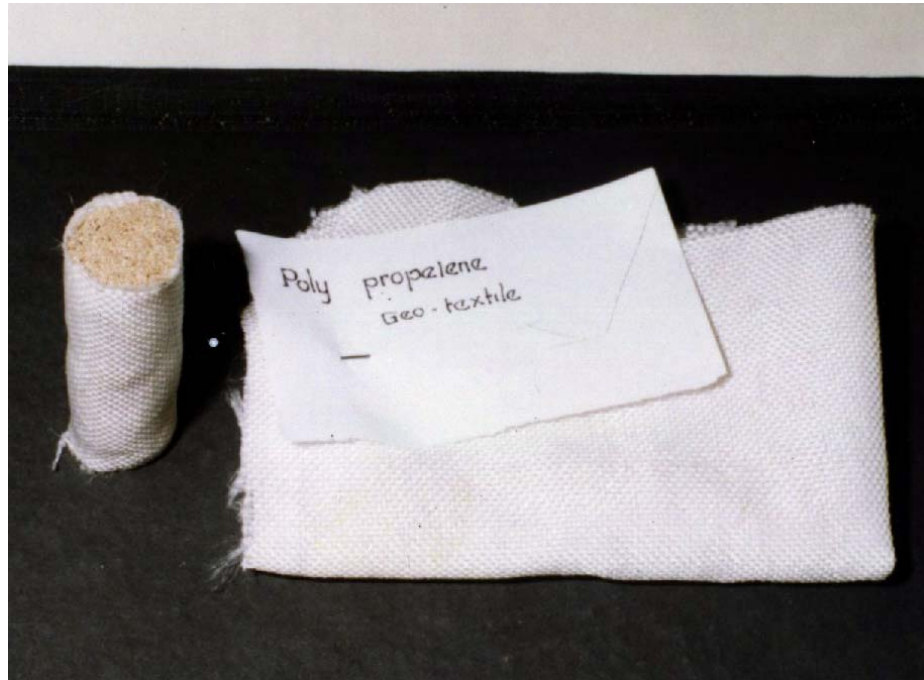
| Sr.No. | Properties                                   | Range of Values |
|--------|--|-----------------|
| 1.     | Fiber length, mm                             | 20-180          |
| 2.     | Fiber diameter, mm                           | 0.1-1.0         |
| 3.     | Specific gravity                             | 0.90-0.95       |
| 4.     | Bulk density, kg/m <sup>3</sup>              | 80-120          |
| 5.     | Ultimate tensile strength, N/mm <sup>2</sup> | 350-800         |
| 6.     | Modulus of elasticity, KN/mm <sup>2</sup>    | 40              |
| 7.     | Elongation at break, percent                 | 33-125          |
| 8.     | Water absorption, percent                    | 1-2             |
| 9.     | Breaking Tenacity (g/denier)                 | 4.8-7.0         |

**Table 3.18:** Stress-Strain characteristics of various vertical geodrains used in laboratory investigations (photograph 3.7)

| Type of Drain           | Stiffness                    |           |            |           |
|-------------------------|------------------------------|-----------|------------|-----------|
|                         | Stress (kg/cm <sup>2</sup> ) |           | Strain (%) |           |
|                         | Dry                          | Saturated | Dry        | Saturated |
| Sandwick(SW)            | ----                         | 2.1       | ----       | 0.16      |
| Coir-Jute(CJ)           | 0.297                        | 0.196     | 0.12       | 0.06      |
| Polypropylene fiber(PF) | 0.672                        | 0.344     | 0.23       | 0.11      |



**Photograph 3.3:** Bursting strength test on Geotextile used in Sandwich



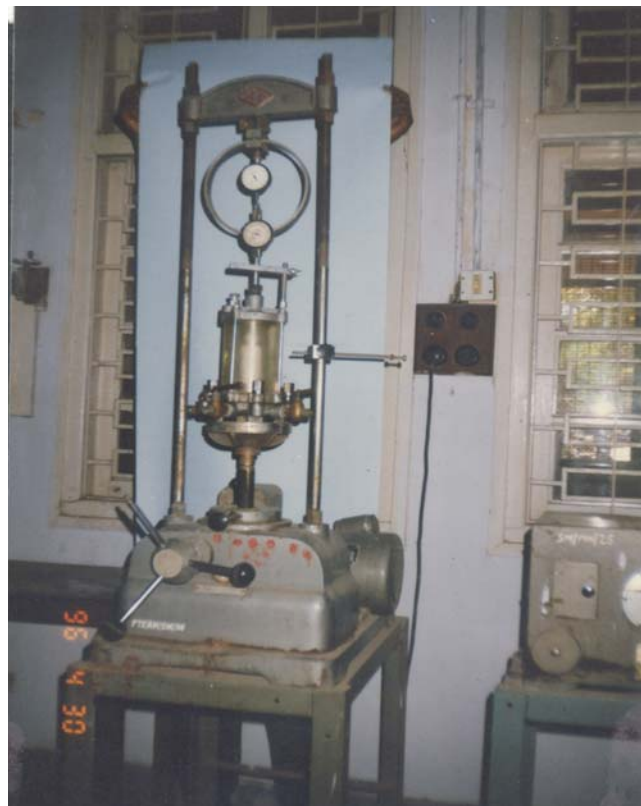
**Photograph 3.4:** Sample of Sandwich drain ('n'11.04) along with polypropylene geotextile



**Photograph 3.5:** Sample of Coir-Jute fibers and Coir-Jute drain ('n'11.04) encapsulated by filter paper



**Photograph 3.6:** Sample of white Polypropylene fibers and Polypropylene fiber drain ('n' 11.04) encapsulated by filter paper



**Photograph 3.7:** Stiffness test on vertical drains

## **CHAPTER - 4**

### **THEORETICAL DEVELOPMENTS**

#### **(ADVANCED THEORY OF CONSOLIDATION THROUGH RADIAL FLOW)**

---

Looking to the theoretical development done so far in the field of consolidation through radial drainage using various vertical drains almost all research workers have extended one dimensional theory of consolidation into two or three dimensional considering various theoretical parameters affecting both process of consolidation and rate of consolidation like magnitude and rate of loading, permeability with respect to stratification, accounting linear and non-linear behavior with void ratio change, pore pressure distribution and its variation along radial distances, with and without stratification (1936, 1941, 1943, 1958, 1961, 1969, 1975, 1987, 1991, 1992, 1994, 2005,2008,2010). Out of many research workers, some research workers have not considered isotropy of soil mass and its influence on stress distribution and settlement and have established equations while some have extended their solutions for arbitrary loading with time, considering plane radial flow and vertical linear flow, taking non-homogeneity of soil and stress-strain characteristics of soil, for radial flow with peripheral drainage, for variable loading, soil properties and layered system, by accounting variation in rate of loading and coefficient of permeability for inward and peripheral drainage (1942, 1948, 1953, 1957, 1964, 1975, 1989, 1994, 1999, 2004, 2005,2008,2009,2010).

Another group of research workers have extended either Barron's equal strain theory or free strain theory considering the material in disturbed zone to be compressible, for smear zone and well resistance considering effect of permeability around smear zone, taking account structural viscosity for rheological model study, for three dimensional consolidation considering creep and compressibility of pore fluid with equal deformation (1957, 1969, 1971, 1979, 1993, 2000, 2003, 2005,2008,2011,2012).

Some research workers have developed equation by taking help of rheological models to define stress-strain relationships of soil, some have given solutions for consolidation

by taking effect of dilatancy of soil mass, solutions for triangular loading, instantaneous loading, arbitrary loading, with and without soil heterogeneity both for two and three dimensional flow using either finite difference method or other numerical approaches including finite element approach using appropriate software's (1966, 1975, 1976, 1979, 1985, 1989, 1994, 1997, 1998, 1999, 2000, 2001, 2003, 2004, 2005, 2008, 2009, 2010, 2011).

Another school of research workers have developed numerical solutions on consolidation by radial flow assuming variable permeability of smear zone, probabilistic design approach, plane strain modeling with smear effects and soil compressibility, closed form solution for ramp loading, by adopting Finite Element approach for the extension of Hansbo's theoretical aspect for 'no smearing and well resistance' condition for band shaped drains (1994, 1997, 1998, 2000, 2001, 2005, 2007, 2008, 2011).

All the above research workers have concentrated on extension of Barron's theory or Hansbo's theory considering its limitations to amalgamate smear effect, well resistance, variable permeability and non-linear behavior of void-ratio by adopting Finite element method, Finite difference method, probabilistic design approach, spectral method and other numerical methods (eigen value or differential quadrature) and have not arrived to one common consensus. Further they could not obtain theoretical formulation of radial pore pressure distribution during process of consolidation (isochrone) from first principle considering non-homogeneity, time effects intrinsic to the soil skeleton and compressibility of the pore fluid and solids along with variation of compressibility and permeability.

Above researchers took pain in attempting in using various synthetics, non-synthetics and natural materials for vertical drain but missed the pore pressure measurements and analysis based on physico-chemical aspect of soil structure interaction in clay water system of the saturated soil element.

Looking to the above limitations and deficiencies both in terms of theory and experimental investigations authors decided to extend the theory for one dimensional consolidation, Shroff et al., (1985) of soft soils through inward radial flow using vertical drains with radial pore water pressure dissipation under same magnitude of constant pressure using first principle which is easy to implement for various field conditions.

This theoretical treatment incorporates non-homogeneity, time effects intrinsic to the soil skeleton along with physico-chemical changes, compressibility of pore fluid and solid, variation of compressibility and permeability during consolidation. The lump parameter ( $\lambda$ ) incorporates above all factors. Further, Darcy's law is assumed to be valid, recasted in a form in which it is the relative velocity of the soil skeleton and pore fluid flow reference to central drain characteristics that is related to the excess pore fluid pressure gradient.

### **A GENERALISED THEORY OF ONE DIMENSIONAL CONSOLIDATION OF SOFT SOILS THROUGH RADIAL DRAINAGE USING VERTICAL GEODRAINS**

The fundamental requirements for a realistic theory of consolidation of clays are (i) consideration of the deformation characteristics of the constituent phases and (ii) application of a consistent mathematical technique. On the basis of the physical and experimental analysis of clays colloid water system due to various workers, it is possible to ascribe the state changes that occur in colloid particle, double layer and clay skeleton configuration consequent upon a consolidating stress. The basic necessity of the mathematical technique for analyzing the deformation of this kind of material is that it should be valid even for large deformation.

#### **4.1. Physical Background**

##### **4.1.1. Nature of change in Clay Colloid**

Grim (1948) argued that the properties of clays are difficult to account for without postulating some changes in the physical state of adsorbed compound in the lattice and surrounding the colloidal particle. On the basis of an analysis of the phase relations of adsorbed water, Winterkorn (1943) showed that the change in state of this water with distance from clay mineral surface is an exponential one. Since the interparticle spacing vary with time under pressure change, a time deformation relationship for the clay colloid could also be represented by an exponential function.

##### **4.1.2. Nature of change in Fabric Structure**

A particular type of contacts forming a structure in clay material is dependent on the net resultant potential at the colloidal surfaces. A change in the contacts occurs as the stress is applied altering the value of the resultant electrical potential. The value of the resultant potential varies exponentially proportional to the applied stress which is gradually acting upon the particles. Hence, it will be reasonable to assume an exponential law for the change in fabric structure with time.

#### 4.1.3. Nature of Radial Flow of Pore Fluid

While considering the radial flow of pore fluid through an element of soil, at least two factors must be appreciated one, the continuous contraction of the pore space in vertical direction and two, the drag forces in radial direction. Gibson et al. (1967) expressed the classical Darcy's law in a more general form conforming to the experimental evidence due to Schiedegger (1957).

#### 4.1.4. Nature of Effective Stress Law

In the Terzaghi (1923) classical principle of effective stress, the compressibility of the individual grains is ignored. Bishop (1963) examined the influence of compressibility of water relative to the soil structure and the soil grains on the effective stress law for consolidation. For compressible grains, there is an excess pore water stress over and above the usual excess pore water stress due to distortion and displacement of individual grains. Thus the volume changes due to compressibility of the soil structure are controlled not by the classical effective stress law  $\sigma' = \sigma - u$  but by:  $\sigma - (1 + a_s)u$  where  $a_s$  denotes the grain area per unit cross sectional area. Lambe and Whitman (1959) suggested that the contact area of an expansive soil is a function of water content and further argued that areas of influence of hydrostatic pore water may overlap the adsorbed pore water particularly when there is air present in the voids. Skempton (1960) reported an expression of effective stress to be used for volume change as  $\sigma = \sigma - \left(1 - \frac{C_s}{C}\right)u$  where  $C_s$  denotes the compressibility of the particle and  $C$  is the compressibility of the soil skeleton. For the specialized case of saturated soils of incompressible grains the equation reduces to the classical one.

## 4.2 Mathematical Formulation

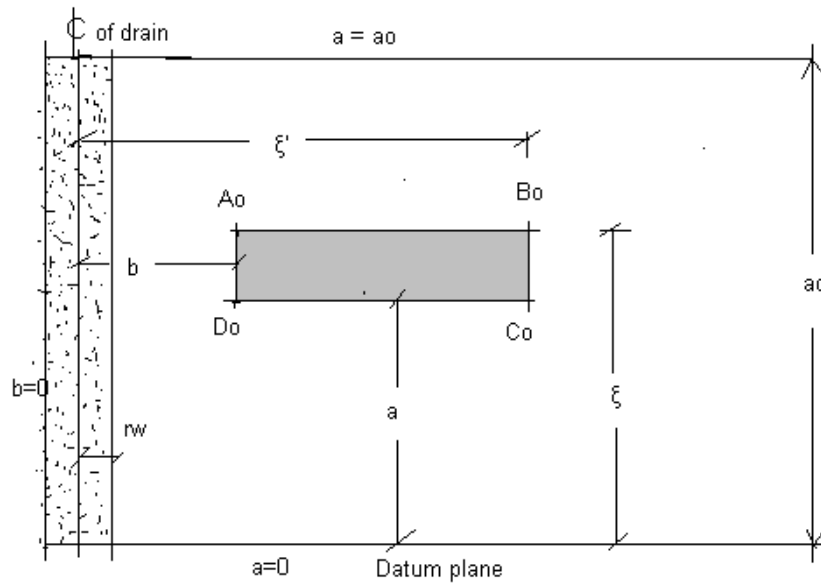


The basic framework adopted for the present mathematical treatment is that of Gibson et al. (1967) and Shroff et al. (1975) and attempts further generalization based on physical consideration.

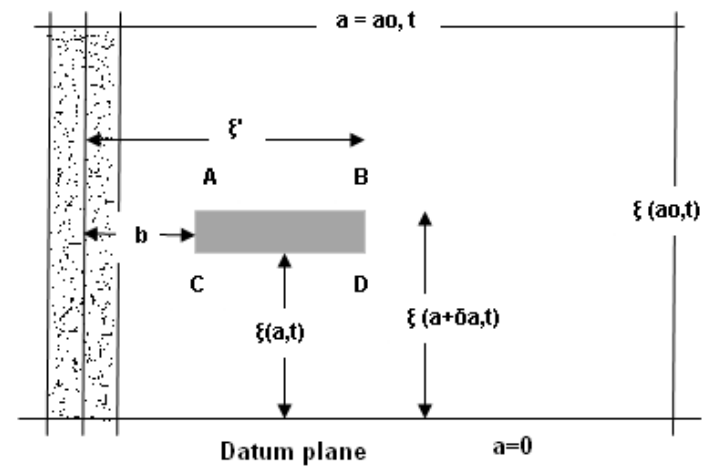
#### 4.2.1 Governing Equations

##### 4.2.1.1. Co-ordinate Scheme:

Since in this problem the exact location in space of the boundary at any time will not be known, the most advantageous choice will be that of the Lagrangian scheme over the Eulerian scheme. The most favorable aspect of Lagrangian method is that the motion and trajectory of each and every particle of fluid is known, so that at any time it is possible to trace history of each fluid particle. In addition, by virtue of the fact that particles are initially identified and traced through their motion, conservation of mass is inherent. We shall follow history of every particle at all instant through coordinates  $x$ ,  $y$ ,  $z$  of any particle which are functions of the independent variables  $a$ ,  $b$ ,  $c$  and  $t$ , Lamb (1932). For the case of one dimensional movement, we may consider an element of the soil skeleton of unit cross sectional area normal to the direction of pore fluid which at time  $t=0$  lies between planes embedded at distances  $a$  and  $(a+\delta a)$  from an embedded datum plane along with distances ' $b$ ' and  $(b+\delta b)$  from the centre line of the drain. At some subsequent time the same planes will be located at unknown distance  $\xi(a, t)$  &  $\xi(a+\delta a, t)$  from this datum plane along with unknown distances  $\xi'(b, t)$  &  $\xi'(b+\delta b, t)$  from the centre line of the drain. As per Lagrange co-ordinates each plane of particles shall be labeled throughout its subsequent motion by its initial distance ' $a$ ' from the datum plane and distance ' $b$ ' from centre line of drain ; for example the upper boundary of the layer is always at  $a=a_0$ . (Refer Fig. 4.1(a) & 4.1(b))



**(a)** Initial Configuration  $t = 0$



**(b)** Current Configuration at time =  $t$

**Fig. 4.1:** Configuration of clay element



#### 4.2.1.2 Equilibrium Equation:

The vertical equilibrium equations of the solid grains and fluid are established by considering an elemental cylinder ABCD as shown in above fig. Neglecting the inertia terms, Mandel (1953) the equilibrium equation is:

$$\frac{\partial \sigma}{\partial a} \pm [\eta \rho_f + (1 - \eta) \rho_s] \frac{\partial \xi}{\partial a} = 0 \quad \text{----- (4.1)}$$

Where,

$\sigma$  = the vertical total stress

$\eta$  = the initial volume porosity

$\rho_f, \rho_s$  = weights per unit volume of fluid and solid phases and are functions of  $a$  and  $t$  ( $a$  has positive sign if measured against gravity)

#### 4.2.1.3. Equation of Continuity:

In consideration of the volume changes occurring in the clay colloid and clay skeleton the equation of continuity for the solid phase will be written as:

$$\rho_{s(b,0)} \{1 - \eta_{(b,0)}\} = \rho_{s(b,t)} \{1 - \eta_{(b,t)}\} \frac{\partial \xi'}{\partial b} * \exp(-\beta \tanh t) \quad \text{----- (4.2)}$$

where the unit weight of the clay colloid changes with time as:

$$\rho_{s(b,t)} = \rho_{s(b,0)} * \exp(\alpha \tanh t) \quad \text{----- (4.3)}$$

To determine the equation of continuity of fluid phase, the concept of relative velocity between solid phase  $V_s$  and that of pore fluid  $V_f$  will be used to eliminate the limitation imposed from continuous contraction of the pore space. Thus the rate of weight in flow of fluid into the element ABCD will be equal to  $\eta(V_f - V_s) \delta a$  if we assume equality of area and volume porosities, while the rate of weight outflow of fluid will be:

$$\frac{\partial}{\partial b} [\eta \rho_f (V_f - V_s)] \delta b \quad \text{----- (4.4)}$$

Since then the rate of weight outflow of fluid equals the rate of change of fluid in the element,

$$\frac{\partial}{\partial b} [\eta \rho_f (V_f - V_s)] + \frac{\partial}{\partial t} \left[ \eta \rho_f \frac{\partial \xi'}{\partial b} \right] = 0 \quad \text{----- (4.5)}$$

#### 4.2.1.4. Flow Equation:

The flow of pore fluid through soil skeleton is in accordance with Darcy's law,

$$V = ki \quad \text{----- (4.6)}$$

but it is expressed in a general form to be consonant with the physics of the problem.

Gibson et al. (1967) proposed a following expression:

$$\eta(V_f - V_s) = \frac{-k_h}{\rho_f} \frac{\partial u}{\partial \xi'} \quad \text{----- (4.7)}$$

The influence of compressibility of space and drag forces does not invalidate the above expression keeping 'equal strain' condition. Introducing parameter coefficient of permeability due to radial drainage at rest ( $k_o$ ) as the flow of fluid is in radial (horizontal) direction, the excess fluid pressure gradient could be expressed as

$$\eta(V_f - V_s) = \frac{-k_h}{\rho_f} \left[ k_o \frac{\partial p}{\partial \xi'} \pm \rho_f \right] \quad \text{----- (4.8)}$$

$$\rightarrow \left\langle \frac{\partial u}{\partial \xi'} = k_o \frac{\partial p}{\partial \xi'} \pm \rho_f \right\rangle \quad \text{----- (4.9)}$$

(Eqn.9 is substituted in eqn.7 to get eqn.8)

→ Eqn.8 becomes

$$\eta(V_f - V_s) = \frac{-k_h k_o}{\rho_f} \frac{\partial p}{\partial \xi'} \mp k_h \quad \text{----- (4.10)}$$

where  $p$  is the fluid pressure and the positive sign is taken if  $\xi'$  is measured against gravity. Since  $\xi'$  is a dependant variable of 'b', we will use the relation:

$$\text{@ Chain rule: } k_o \frac{\partial p}{\partial b} = k_o \frac{\partial p}{\partial \xi'} * \frac{\partial \xi'}{\partial b} \quad \text{-----(4.11)}$$

Thus uniting equations eqn.7 and eqn.8 to be consistent with our frame work, we get,

Multiply eqn. 10 with  $\frac{\partial \xi'}{\partial b}$ ,

$$\eta(V_f - V_s) \frac{\partial \xi'}{\partial b} = -\frac{k_h k_o}{\rho_f} \frac{\partial p}{\partial \xi'} * \frac{\partial \xi'}{\partial b} \mp k_h \frac{\partial \xi'}{\partial b} \quad \text{-----(4.12)}$$

Substituting chain rule,

$$\eta(V_f - V_s) \frac{\partial \xi'}{\partial b} = -\frac{k_h k_o}{\rho_f} \frac{\partial p}{\partial b} \mp k_h \frac{\partial \xi'}{\partial b}$$

$$\eta(V_f - V_s) \frac{\partial \xi'}{\partial b} = -\frac{k_h}{\rho_f} \left[ k_o \frac{\partial p}{\partial b} \pm \rho_f \frac{\partial \xi'}{\partial b} \right] \quad \text{-----(4.13)}$$

This equation is w.r.t 'b' only.

#### 4.2.1.5. Effective Stress Law:

The classical effective stress law need be rigoursly expressed in consideration of the variations in clay colloid and clay skeleton. The expression given by Gibson et al. (1967) is of similar type to that of Skempton (1960) which is adopted in this treatment. The effective stress law used in the present approach is:

$$\sigma' = \sigma - \eta u$$

in which,  $\eta$  is viscosity of water, taking  $\eta = 1$  when the solid phase is of constant density and soil is completely saturated, otherwise it could be a function of 'a' and 't'.

#### 4.2.1.6. Permeability, Porosity and Fluid Density relationship:

In regard to the physical considerations discussed in eqn.1 the physical quantities, such as coefficient of permeability, porosity or void ratio and fluid density need to be defined and given mathematical qualification.

$k$  will be a function both of the porosity  $\eta$  or void ratio  $e$  and the location of the particular portion of the soil skeleton to account for possible non-homogeneity. Therefore,

$$k = k(\eta, b) \text{ -----(4.14)}$$

$\eta$  will be a function of factors for non-homogeneity, stress history and time effects.

Thus

$$\rightarrow \eta = \oint(\sigma', b, t) \text{ -----(4.15)}$$

where  $\oint$  is a functional.

We shall consider valid the isothermal equation of state for the physical quantity

$\rho_f$ , thus

$$\rho_f = \rho_f(p) \text{ ----- (4.16)}$$

#### 4.3 Transformed Equations

For convenience we shall now resort to transformation to a new independent variable 'r' to replace 'b' and 'a' to replace 'z'

$$r(b) = \int_o^b [1 - \eta(b', o)] db' \text{ -----(4.17)}$$

$$\therefore \frac{\partial r}{\partial b} = 1 - \eta_{(b,o)}$$

This means that at any point of the soil skeleton is now identified by the volume of solids 'z' in a prism of unit cross-sectional area lying between the datum plane and the point. This new variable 'z' is independent of 't'. Further, if we substitute the porosity by void ratio, simplified forms of the governing equations are possible.

→ **Writing Equilibrium Equations again,**

$$\frac{\partial \sigma}{\partial a} \pm [\eta \rho_f + (1 - \eta) \rho_s] \frac{\partial \xi}{\partial a} = 0$$

$$\therefore \frac{\partial \sigma}{\partial a} \pm \left[ \frac{e}{1+e} \rho_f + \frac{1}{1+e} \rho_s \right] \frac{\partial \xi}{\partial a} = 0$$

$$\therefore \frac{\partial \xi}{\partial a} \pm \left[ \frac{e}{1+e} \rho_f + \frac{1}{1+e} \rho_s \right] \frac{\partial \xi}{\partial a} = 0 \quad \text{-----(4.18)}$$

→ From Equation of Continuity

$$\frac{\partial \xi}{\partial a} = (1 + e) \exp[(\beta - \alpha) \tanh t] \quad \text{-----(4.19)}$$

→ From equation -8

$$\frac{\partial}{\partial b} \left[ \frac{e}{1+e} \rho_f (V_f - V_s) \right] + \frac{\partial}{\partial t} \left[ \frac{e}{1+e} \rho_s * \frac{\partial \xi'}{\partial b} \right] = 0 \quad \text{-----(4.20)}$$

→ Dividing eqn. 13 by  $k_h$  and substituting  $\eta = \frac{e}{1+e}$

$$\frac{e}{1+e} \frac{(V_f - V_s)}{k_h} \frac{\partial \xi'}{\partial b} = - \frac{k_o}{\rho_f} \frac{\partial p}{\partial b} \mp \frac{\partial \xi'}{\partial b} \quad \text{-----(4.21)}$$



$$\therefore \left[ \frac{e}{1+e} \frac{(V_f - V_s)}{k_h} \pm 1 \right] \frac{\partial \xi'}{\partial b} + \frac{k_o}{\rho_f} \frac{\partial p}{\partial b} = 0 \quad \text{-----(4.22)}$$

→ substituting eqn.19 in eqn.18

$$\frac{\partial \sigma}{\partial a} \pm \left[ \frac{e \rho_f + \rho_s}{1+e} \right] * (1+e) \exp(\beta - \alpha) \tanh t = 0$$

$$\therefore \frac{\partial \sigma}{\partial a} \pm (e \rho_f + \rho_s) \exp(\beta - \alpha) \tanh t = 0 \quad \text{-----(4.23)}$$

From eqn. -4.19

$$\frac{1}{1+e} = \frac{\exp(\beta - \alpha) \tanh t}{\frac{\partial \xi}{\partial a}} \quad \text{-----(4.19A)}$$

Substituting the values of eqn.19A in eqn. 20 of 2<sup>nd</sup> term only.

$$\frac{\partial}{\partial b} \left[ \frac{e}{1+e} \rho_f (V_f - V_s) \right] + \frac{\partial}{\partial t} \left[ \frac{e \rho_f * \exp(\beta - \alpha) \tanh t}{\frac{\partial \xi}{\partial a}} * \frac{\partial \xi'}{\partial b} \right] = 0 \quad \text{----- (4.24)}$$

→ substituting equation. 4.19A in 4.22

$$e * \frac{\exp(\beta - \alpha) \tanh t}{\frac{\partial \xi}{\partial a}} * \frac{(V_f - V_s)}{k_h} \pm 1 \left( \frac{\partial \xi'}{\partial b} \right) + \frac{k_o}{\rho_f} \frac{\partial p}{\partial b} = 0$$

multiply by '  $\rho_f$  ',

$$\therefore \frac{e\rho_f(V_f - V_s)}{k_h} * \frac{\exp(\beta - \alpha) \tanh t}{\frac{\partial \xi}{\partial a}} * \frac{\partial \xi'}{\partial b} \pm \rho_f * \frac{\partial \xi'}{\partial b} + k_o \frac{\partial p}{\partial b} = 0 \quad \text{----- (4.25)}$$

Therefore main equations are – 4.23, 4.24, and 4.25

*Taking  $\exp(\beta - \alpha) \tanh t = \text{unity}$  (1)*

Rewriting above equations,

$$\frac{\partial \sigma}{\partial a} \pm (e\rho_f + \rho_s) = 0 \quad \text{----- (A)}$$

$$\frac{\partial}{\partial b} \left[ \frac{e}{1+e} \rho_f (V_F - V_s) \right] + \frac{\partial}{\partial t} \left[ \frac{e \rho_f}{\frac{\partial \sigma}{\partial a}} * \frac{\partial \xi'}{\partial b} \right] = 0 \quad \text{----- (B)}$$

$$\frac{e \rho_f (V_f - V_s)}{k_h} * \frac{\frac{\partial \xi'}{\partial b}}{\frac{\partial \xi}{\partial a}} \pm \rho_f \frac{\partial \xi'}{\partial b} + k_o \frac{\partial p}{\partial b} = 0 \quad \text{----- (C)}$$

**Again the same equations:**

$$\frac{\partial \sigma'}{\partial a} + \frac{\partial p}{\partial a} \pm (e\rho_f + \rho_s) = 0 \Rightarrow \frac{\partial p}{\partial a} \mp (e\rho_f + \rho_s) - \frac{\partial \sigma'}{\partial a} \quad \text{----- (A)}$$

Now,

$$\frac{\partial}{\partial b} \left[ \frac{e}{1+e} (V_f - V_s) \right] + \frac{\partial}{\partial t} \left[ e * \frac{\frac{\partial \xi'}{\partial b}}{\frac{\partial \xi}{\partial a}} \right] = 0 \text{ -----(B)}$$

$$\frac{e \rho_f (V_f - V_s)}{k_h} * \frac{\partial \xi'}{\partial b} \pm \rho_f \frac{\partial \xi'}{\partial b} * \frac{\partial \xi}{\partial a} + k_o \frac{\partial p}{\partial b} * \frac{\partial \xi}{\partial a} = 0 \text{ ----- (c)}$$

Multiply equation (C) by  $\frac{k_h}{\rho_f (1+e)}$

$$\frac{e}{1+e} (V_f - V_s) \frac{\partial \xi'}{\partial b} \pm \frac{k_h}{1+e} \frac{\partial \xi}{\partial a} * \frac{\partial \xi'}{\partial b} + \frac{k_o k_h}{\rho_f (1+e)} * \frac{\partial p}{\partial b} * \frac{\partial \xi}{\partial a} = 0$$

Dividing by  $\frac{\partial \xi'}{\partial b}$ ,

$$\frac{e}{1+e} (V_f - V_s) \pm \frac{k_h}{1+e} * \frac{\partial \xi}{\partial a} + \frac{k_o k_h}{\rho_f (1+e)} * \frac{\partial p}{\partial b} * \frac{\frac{\partial \xi}{\partial a}}{\frac{\partial \xi'}{\partial b}} = 0$$

Substituting this value in equation – (B)

$$\frac{\partial}{\partial b} \left[ \mp \frac{k_h}{1+e} \frac{\partial \xi}{\partial a} - \frac{k_h k_o}{\rho_f (1+e)} * \frac{\partial p}{\partial b} * \frac{\frac{\partial \xi}{\partial a}}{\frac{\partial \xi'}{\partial b}} \right] + \frac{\partial}{\partial t} \left[ e \frac{\frac{\partial \xi'}{\partial b}}{\frac{\partial \xi}{\partial a}} \right] = 0$$

$$\frac{\partial}{\partial b} \left[ \mp \frac{k_h}{1+e} \frac{\partial \xi}{\partial a} - \frac{k_h k_o}{\rho_f (1+e)} * \frac{\frac{\partial \xi}{\partial a}}{\frac{\partial \xi'}{\partial b}} * \frac{\partial a}{\partial b} * \left\{ \mp (e \rho_f + \rho_s) - \frac{\partial \sigma'}{\partial a} \right\} \right] + \frac{\partial}{\partial t} \left[ e \frac{\frac{\partial \xi'}{\partial b}}{\frac{\partial \xi}{\partial a}} \right] = 0$$

$$\Rightarrow$$

$$\frac{\partial}{\partial b} \left[ \mp \frac{k_h \rho_f}{\rho_f (1+e)} * \frac{\partial \xi}{\partial a} \pm \frac{k_h k_o (e \rho_f + \rho_s)}{\rho_f (1+e)} * \frac{\partial \xi}{\partial \xi'} + \frac{k_h k_o}{\rho_f (1+e)} * \frac{\partial \sigma'}{\partial a} * \frac{\partial \xi}{\partial \xi'} \right] + \frac{\partial}{\partial t} \left[ e \frac{\frac{\partial \xi'}{\partial b}}{\frac{\partial \xi}{\partial a}} \right] = 0$$

$$\therefore \frac{\partial}{\partial b} \left[ \mp \frac{k_h \rho_f \frac{\partial \xi}{\partial a} \pm k_h k_o (e \rho_f + \rho_s) \frac{\partial \xi}{\partial \xi'} + k_h k_o \frac{\partial \sigma'}{\partial a} * \frac{\partial \xi}{\partial \xi'}}{\rho_f (1+e)} \right] + \frac{\partial}{\partial t} \left[ e \frac{\frac{\partial \xi'}{\partial b}}{\frac{\partial \xi}{\partial a}} \right] = 0$$

$$\therefore \frac{\partial}{\partial b} \left[ \frac{k_h k_o}{\rho_f (1+e)} * \frac{\partial \sigma'}{\partial a} * \frac{\partial a}{\partial \xi} * \frac{\partial \xi}{\partial \xi'} \right] \pm \frac{\partial}{\partial b} \left[ k_h \left\{ \frac{k_o (e \rho_f + \rho_s)}{\rho_f (1+e)} * \frac{\partial \xi}{\partial \xi'} \right\} - k_h \frac{\frac{\partial \xi}{\partial a}}{1+e} \right] + \frac{\partial}{\partial t} \left[ e \frac{\frac{\partial \xi'}{\partial b}}{\frac{\partial \xi}{\partial a}} \right] = 0$$

$$\therefore \frac{\partial}{\partial b} \left[ \frac{k_h k_o}{\rho_f (1+e)} * \frac{\partial \sigma'}{\partial a} * \frac{\partial a}{\partial \xi} * \frac{\partial \xi}{\partial \xi'} \right] \pm \frac{\partial}{\partial b} \left[ k_h \left\{ \frac{k_o (e \rho_f + \rho_s)}{\rho_f (1+e)} * \frac{\partial \xi}{\partial \xi'} \right\} - k_h \right] + \frac{\partial}{\partial t} \left[ e \frac{\frac{\partial \xi'}{\partial b}}{\frac{\partial \xi}{\partial a}} \right] = 0$$

$$\left\langle \because \frac{\partial \xi}{\partial a} = (1+e) \exp(\beta - \alpha) \tanh t \right\rangle \Rightarrow \frac{\frac{\partial \xi}{\partial a}}{1+e} = 1$$

Replacing the following terms: 'r' to replace 'b' & 'a' to replace 'z'

$$\therefore \frac{\partial}{\partial r} \left[ \frac{k_h k_o}{\rho_f (1+e)} \frac{\partial \sigma'}{\partial e} * \frac{\partial e}{\partial z} * \frac{\partial \xi}{\partial \xi'} \right] \pm \frac{\partial}{\partial r} \left[ k_h \left\{ \frac{k_o (e \rho_f + \rho_s)}{\rho_f (1+e)} * \frac{\partial \xi}{\partial \xi'} \right\} - k_h \right] + \frac{\partial}{\partial t} \left[ e \frac{\frac{\partial \xi}{\partial r}}{\frac{\partial \xi}{\partial z}} \right] = 0$$

$\downarrow$   
**C<sub>r</sub>**  
 (Coefficient of consolidation  
due to radial drainage)

$\downarrow$   
**C<sub>e</sub>**  
 (Coefficient due to  
permeability & porosity)

**Final Form of General Differential Equation:**

$$\therefore \frac{\partial}{\partial r} \left[ \frac{k_h k_o}{\rho_f (1+e)} \frac{\partial \sigma'}{\partial e} * \frac{\partial e}{\partial z} * \frac{\partial \xi}{\partial \xi'} \right] \pm \frac{\partial}{\partial r} \left[ k_h \left\{ \frac{k_o (e \rho_f + \rho_s)}{\rho_f (1+e)} * \frac{\partial \xi}{\partial \xi'} \right\} - k_h \right] + \frac{\partial}{\partial t} \left[ e \frac{\frac{\partial \xi}{\partial r}}{\frac{\partial \xi}{\partial z}} \right] = 0$$

$\downarrow$   
**C<sub>r</sub>**  
 (Coefficient of consolidation  
due to radial drainage)

$\downarrow$   
**C<sub>e</sub>**  
 (Coefficient due to  
permeability & porosity)

Now we know that,

$$C_v = \frac{k}{m_v \gamma_w} = \frac{k_h k_o}{m_v \gamma_w} \quad \text{-----(4.26)}$$

$$\text{Taking } m_v = \frac{a_v}{1+e_o} \text{ but } a_v = \frac{\Delta e}{\Delta \sigma'} = \frac{e_o - e}{d\sigma'} = \frac{de}{d\sigma'}$$

$$\therefore m_v = \frac{e_o - e}{(1+e_o)d\sigma'} \Rightarrow \therefore C_v = \frac{k}{\frac{e_o - e \rho_f}{(1+e_o)d\sigma'}} = \frac{k_h k_o (1+e_o)}{\rho_f} \frac{d\sigma'}{de}$$

Using the relation (as given by Gibson) for radial drainage,

$$C_r = \frac{(1+e_o)C_v}{1+e}$$

$$\therefore C_r = \left[ \frac{(1+e_o)}{(1+e)} * \frac{k_h k_o (1+e_o)}{\rho_f} * \frac{d\sigma'}{de} \right] * \frac{\partial \xi}{\partial \xi'} \quad \text{-----(4.27)}$$

$$\therefore C_r = \left[ \frac{(1+e_o)^2}{(1+e)} * \frac{k_h k_o}{\rho_f} * \frac{d\sigma'}{de} \right] \frac{\partial \xi}{\partial \xi'} \quad \text{-----(4.27A)}$$

Now,  $C_e$  = Coefficient of permeability in terms of void ratio,

$$C_e = k_h k_o (1+e_o) \left\{ \frac{\frac{\rho_s}{1+e} + e}{1+e} - \eta \right\} \quad \text{Here } \eta = 1 \text{ assumed}$$

$$C_e = k_h k_o (1 + e_o) \left\{ \left( \frac{\rho_s}{\rho_f} + e \right) \frac{\partial \xi}{\partial \xi'} - \eta \right\} \text{-----(4.28)}$$

⇒ Using the standard equation of conduction of heat in a moving medium

$$\frac{\partial \theta}{\partial t} = \kappa \frac{\partial^2 \theta}{\partial Y^2} - \mathcal{G} \frac{\partial \theta}{\partial Y} \text{-----(4.29)}$$

The above equation can now be represented in the form:

$$\frac{\partial e}{\partial t} = C_r \left( \frac{\partial^2 e}{\partial b \partial a} \right) \mp C_e \left( \frac{\partial e}{\partial b} \right) \text{-----(4.30)}$$

'r' to replace 'b' and 'z' to replace 'a'

$$\frac{\partial e}{\partial t} = C_r \left( \frac{\partial^2 e}{\partial r \partial z} \right) \mp C_e \left( \frac{\partial e}{\partial r} \right) \text{-----(4.31)}$$

By putting,  $Z = \frac{z}{h}$ ,  $R = \frac{r}{r_e}$ ,  $T = \frac{C_r t}{r_e^2}$ ,  $\lambda = r_e \frac{C_e}{C_r}$

$$\therefore r = R * r_e, z = Z * h, t = \frac{T * r_e^2}{C_r}, C_e = \lambda \frac{C_r}{r_e}$$

Putting the above values in eqn. 31,

$$\frac{\partial e}{\partial \left( \frac{T * r_e^2}{C_f} \right)} = C_r \frac{\partial^2 e}{\partial (Zh) \partial (R * r_e)} \mp C_r \frac{\partial e * \lambda}{\partial R * r_e^2}$$

$$\frac{\partial e}{\partial T} \left( \frac{C_r}{r_e^2} \right) = C_r \left( \frac{\partial^2 e}{h r_e \partial Z \partial R} \right) \mp C_r \frac{\lambda}{r_e^2} \frac{\partial e}{\partial R}$$

$$\frac{\partial e}{\partial T} = \left( \frac{r_e}{h} \right) \frac{\partial^2 e}{\partial Z \partial R} \mp \lambda \frac{\partial e}{\partial R} \quad (\lambda = \text{lumped parameter}) \text{-----}(4.32)$$

This is the *general differential equation* for consolidation through radial drainage using vertical drains, where the flow of water through soil void under pressure is radial while strain of the element is in vertical direction.

This equation is further simplified in the form:

$$\text{Putting } Z = R = m \text{ as taking } r/r_e = z/h = m,$$

$$r = m r_e \text{ -----(i), \quad or \quad } z = m h \text{ -----(ii), \quad -----(4.33)}$$

$$\frac{\partial e}{\partial T} = \left( \frac{r_e}{h} \right) \frac{\partial^2 e}{\partial m^2} \mp \lambda \frac{\partial e}{\partial m}$$

Rewriting in the form of 'R'

$$\frac{\partial e}{\partial T} = \left( \frac{r_e}{h} \right) \frac{\partial^2 e}{\partial R^2} \mp \lambda \frac{\partial e}{\partial R} \text{-----}(4.34)$$

We shall regard  $\lambda$  as a constant in which all the factors causing deviation of the experimental observations from the classical Terzaghi theory and Barron's equal strain theory for radial drainage are taken in to account. The assumption of regarding ' $\lambda$ ' as a constant is purely from the considerations of mathematical simplicity but it may prove as well as to be so for most soils. Referring to publications of mathematical physics it



may be noted that it has an identical form to that of a differential equation for non-steady radial conduction of heat in a moving medium through vertical central heat dissipater, Bateman (1964).

#### 4.4 Analytical Solutions

Verma, Parikh & Shroff (1969) published a Laplace Transform solution of a one dimensional groundwater recharge. This technique is employed in the solution of the above equation for the boundary conditions of standard one dimensional consolidation through radial drainage for soft clays.

##### 4.4.1. Boundary conditions

$$\begin{aligned} e(0, T) &= e_1, \quad (T > 0); \\ e(1, T) &= e_1, \quad (T > 0); \\ e(R, 0) &= e_o, \quad (T = 0, 0 < R < 1) \end{aligned}$$

##### 4.4.2. Mathematical treatment

On multiplying each term of standard eqn.-17 by  $\exp\{- (ST)\}dT$  and integrating the result from zero to infinity, and using condition  $e(R, 0) = e_o$  we obtain

$$\frac{d^2 e}{dR^2} - \frac{de}{dR} - Se = -e_o \quad \text{----- (4.35)}$$

$$\text{where, } e(R, S) = \int_0^\infty \exp\{- (ST)\}dT * e(R, T) \quad \text{----- (4.36)}$$

represents the Laplace transform of  $e(R, T)$ . The Laplace transformation of boundary

$$\text{condition yields } \bar{e}(0, S) = \frac{e_1}{S}, \quad \bar{e}(1, S) = \frac{e_1}{S}$$

Since equation-35 is a linear equation with constant coefficient, we may write its general solution as

$$e(R, S) = \left[ M \cos \left( R \sqrt{\lambda^2/4 + S} \right) + N \sin \left( R \sqrt{\lambda^2/4 + S} \right) \right] \exp \left\{ \left( \frac{\lambda}{2} \right) R \right\} \quad (4.37)$$

Where, M and N are constants of integration.

For evaluating M and N, we apply condition eqn.-36, so that after simplification, we have

$$M = \frac{e_1 - e_o}{S}, \quad N = \frac{\frac{1}{S} \exp \left\{ - \left( \frac{\lambda}{2} \right) \right\} - \frac{e_1 - e_o}{S} \cosh \left( \sqrt{\lambda^2/4 + S} \right)}{\sinh \left( \sqrt{\lambda^2/4 + S} \right)} \quad (4.38)$$

Substituting these values in eqn.-37, we have

$$\begin{aligned} \bar{e}(R, S) = & \exp \left\{ \left( \frac{\lambda}{2} \right) R \right\} \frac{e_1 - e_o}{S} \left[ \frac{\sinh \left( (1-R) \sqrt{\lambda^2/4 + S} \right)}{\sinh \sqrt{\lambda^2/4 + S}} \right] + \\ & \dots \exp \left\{ - \left( \frac{\lambda}{2} \right) (1-R) \right\} \frac{e_1 - e_o}{S} \left[ \frac{\sinh R \sqrt{\lambda^2/4 + S}}{\sinh \sqrt{\lambda^2/4 + S}} + \frac{e_o}{\lambda} \right] \quad (4.39) \end{aligned}$$

The inverse transform  $(L^{-1})$  of the right hand side terms in eqn.-39 may be determined by recalling a standard result, Mickley et al., (1957) viz;

$$L^{-1} \left| \frac{\mathfrak{I}(S)}{\eta(S)} \right| = \sum_{n=0}^{\infty} \frac{\mathfrak{I}(Sn)}{\eta(Sn)} \exp(SnT) \quad (4.40)$$

where  $\mathfrak{I}(S)$  and  $\eta(S)$  represents two entire transcendental functions such that degree of  $\eta(S)$  is at least one greater in  $S$  (when expressed as power series) than

that of  $\Im(S)$ ,  $S_n$  is a simple pole of  $\frac{\Im(S)}{\eta(S)}$ , &  $\eta'(S_n)$  denotes the value of

$$\frac{d\eta(S)}{dS} \text{ at } S = S_n$$

Putting

$$\frac{\Im(S)}{\eta(S)} = \frac{\text{Sinh}\left(R\sqrt{\lambda^2/4 + S}\right)}{S \text{Sinh}\left(\sqrt{\lambda^2/4 + S}\right)} = \frac{\text{Sinh}\left(iR\sqrt{\lambda^2/4 + S}\right)}{\text{Sinh}\left(i\sqrt{\lambda^2/4 + S}\right)} \quad \text{-----(4.41)}$$

and noting that the roots of equation  $\text{Sinh}\left(\sqrt{\lambda^2/4 + S}\right) = 0$  are given by

$$S_n = -\lambda^2/4 - n^2\pi^2$$

We may write:  $\Im(S_n) = \text{Sin}(n\pi R)$ ,  $\Im(0) = i \text{Sinh}(\lambda/2)R$

$$\eta^1(S_n) = \frac{\left((-1)^n \left(\lambda^2/4 + n^2\pi^2\right)\right)}{2n\pi}, \quad \eta^1(0) = i \text{Sinh}(\lambda/2) \quad \text{----- (4.42)}$$

From equations-4.40, 4.41 and 4.42, we get,

$$L^{-1} \frac{\text{Sinh}R\sqrt{\lambda^2/4 + S}}{S \text{Sinh}\sqrt{\lambda^2/4 + S}} = \frac{\text{Sinh}\lambda/2 R}{\text{Sinh}\lambda/2} + 2\pi \sum_{n=1}^{\infty} \frac{(-1)^n n \text{Sin}(n\pi R)}{\lambda^2/4 + n^2\pi^2} \exp\left\{-\left(\lambda^2/4 + n^2\pi^2\right)\right\} \quad \text{----- (4.43)}$$

Similarly, we have:

$$L^{-1} \left[ \frac{\text{Sinh}(1-R) \sqrt{\lambda^2/4 + S}}{S \text{Sinh} \sqrt{\lambda^2/4 + S}} \right] =$$

$$\frac{\text{Sinh} \lambda/2 (1-R)}{\text{Sinh}(\lambda/2)} - 2\pi \sum_{n=1}^{\infty} \frac{n \text{Sin}(n\pi R)}{\lambda^2/4 + n^2 \pi^2} \exp \left\{ - \left( \lambda^2/4 + n^2 \pi^2 \right) T \right\}$$

-----(4.44)

The inverse transformation of eqn.-39 with the help of eqn.-43 & 44 yields:

$$e(R, T) = (e_1 - e_o) \exp \left\{ \left( \lambda/2 \right) R \right\} *$$

$$\left[ \frac{\text{Sinh} \lambda/2 R}{\text{Sinh} \lambda/2} + 2\pi \sum_{n=1}^{\infty} \frac{(-1)^n n \text{Sin}(n\pi R)}{\lambda^2/4 + n^2 \pi^2} \exp \left\{ - \left( \lambda^2/4 + n^2 \pi^2 \right) T \right\} \right] +$$

$$(e_1 - e_o) \exp \left\{ - \left( \lambda/2 \right) (1-R) \right\} *$$

$$\left[ \frac{\text{Sinh} \lambda/2 (1-R)}{\text{Sinh}(\lambda/2)} - 2\pi \sum_{n=1}^{\infty} \frac{n \text{Sin}(n\pi R)}{\lambda^2/4 + n^2 \pi^2} \exp \left\{ - \left( \lambda^2/4 + n^2 \pi^2 \right) T \right\} \right] + e_o$$

----- (4.45)

$$\text{As } L^{-1} \left( \frac{1}{\lambda} \right) = 1$$

$$\begin{aligned}
U_R &= \frac{e - e_o}{e_1 - e_o} \\
&= \exp\left\{\left(\lambda/2\right)\right\} \\
&\quad \left[ \frac{\text{Sinh} \lambda/2 R}{\text{Sinh} \lambda/2} + 2\pi \sum_{n=1}^{\infty} \frac{(-1)^n \cdot n \text{Sin}(n\pi R)}{\lambda^2/4 + n^2 \pi^2} \exp\left\{-\left(\lambda^2/4 + n^2 \pi^2\right) T\right\} \right] + \\
&\quad \exp\left\{-\left(\lambda/2\right)\right\} \\
&\quad \left[ \frac{\text{Sinh} \lambda/2 (1-R)}{\text{Sinh}(\lambda/2)} - 2\pi \sum_{n=1}^{\infty} \frac{n \text{Sin}(n\pi R)}{\lambda^2/4 + n^2 \pi^2} \exp\left\{-\left(\lambda^2/4 + n^2 \pi^2\right) T\right\} \right] \\
&\quad \text{-----}(4.46)
\end{aligned}$$

when  $\lambda = 0$

$$\lim_{\lambda \rightarrow 0} \frac{\text{Sinh} \lambda/2 R}{\text{Sinh} \lambda/2} \Rightarrow R$$

and

$$\lim_{\lambda \rightarrow 0} \frac{\text{Sinh} \lambda/2 (1-R)}{\text{Sinh} \lambda/2} \Rightarrow 1-R$$

$$= 1 - 4\pi \sum_{n=1,3,5}^{\infty} \frac{n \text{Sin} n\pi R}{n^2 \pi^2} \exp\left\{-\left(n^2 \pi^2 T\right)\right\} \text{-----}(4.47)$$

Replacing the above eqn. by eqn.33, above eqn. will be changed to solution of Terzaghi one dimensional theory of consolidation.

#### 4.4.3. Theoretical Relationships

To obtain theoretical relationships for the process of consolidation a Visual Basic (VB) programme for the expression (4.46) of the previous section was run on PC. Isochrones for various values of parameter ' $\lambda$ ' is shown from figures 4.4 to 4.22 which represents the degree of consolidation at various radial distances against the time factor from which the pore pressure dissipation at various radial distance is possible to deduce by the expression:  $U_R = 1 - u_r/u_i$  where ' $u_r$ ' denotes the pore water pressure at any radial distance ' $r$ ' and ' $u_i$ ' is the initial value of pore pressure while in experimental studies will be the value of increment of pressure applied. Fig. 4.11 shows the theoretical relationship between the average degree of consolidation and Time factor generally used for comparing the experimental results. The value of average degree of consolidation is computed using Simpson's rule as explained in Taylor (1948) and Lambe-Whitman (1969).

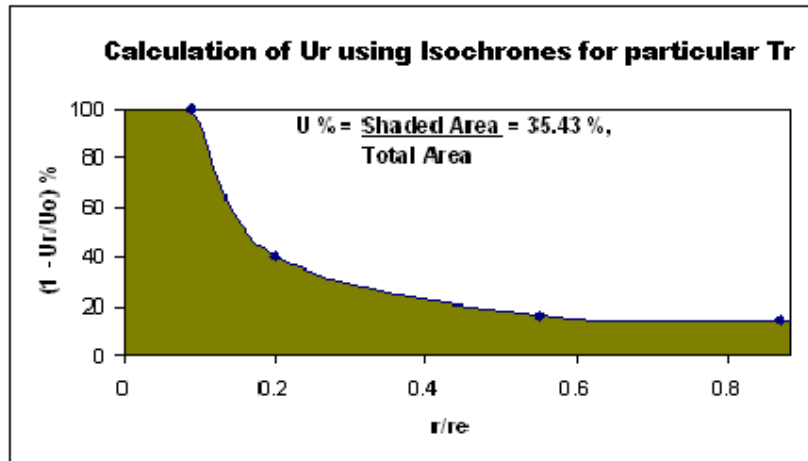


**Figure 4.2:** Simpsons rule to estimate degree of consolidation

Experimental data obtained from the laboratory studies to investigate the influence of various factors affecting the consolidation characteristics of clays by radial flow are analyzed using these theoretical relationships.

Curve expert software is used to compute theoretical relationships. From the data of consolidation ratio ( $U_r$ ) versus  $r/r_e$ , isochrone is drawn for particular value of  $T_r$  and further average degree of consolidation ( $U_{avg}$ ) for a given  $T_r$  is computed by ratio of

area outside particular isochrone over total area. From the data of  $U_{\text{avg}}$  versus  $T_r$ , degree of consolidation versus  $T_r$  for a particular ( $\lambda$ ) parameter is presented. Similarly for various positive and negative values of ( $\lambda$ ) the trajectory of the curves can be obtained.

Pore pressures are measured at the three radial points located at 120 degree each with  $r/r_e$  distances as  $r/4$ ,  $r/2$  and  $3r/4$  respectively where ' $r$ ' is the radius of Oedometer which is also known as radius of influence ( $r_e$ ). According to proposed theory, for plotting isochrones as per size of Oedometer used, the values of ' $R$ ' are 0.001, 0.1, 0.275, 0.435, 0.5. In experimental programme the thickness of sample is  $R$ , the distance ' $R$ ' being the length of longest drainage path, while comparing experimental isochrones and theoretical isochrones, value of ' $R$ ' is modified to ' $R/2$ ' and considered accordingly. As per radial distances the ratio of radius (distance) of radial points to the radius of influence is shown below.

| Diameter of Oedometer (mm) | Radius of Oedometer (mm) | $r/4$ distance (mm) | Ratio $r/4 r_e$ | $r/2$ distance (mm) | Ratio $r/2 r_e$ | $3r/4$ distance (mm) | Ratio $3r/4 r_e$ |
|----------------------------|--------------------------|---------------------|-----------------|---------------------|-----------------|----------------------|------------------|
| 254                        | 127                      | 25.4                | 0.2             | 71                  | 0.55            | 110                  | 0.87             |
| 152                        | 76                       | 26                  | 0.2             | 44                  | 0.55            | 60                   | 0.87             |

For example, let us take case of ' $\lambda$ ' = +0.7

Step 1: Assuming various value of  $T_r$  ranging from 0.02, 0.04, 0.06.....0.34 for particular value of ' $\lambda$ ' = +0.7.

Step 2: Now using equation no. 46, and substituting values of  $T_r$  say 0.02, values of consolidation ratio ( $U_r$ ) are determined at various ' $R$ ' mentioned earlier and isochrone for  $T_r = 0.02$  is plotted, similarly, say for  $T_r = 0.04$  is taken, radial values of consolidation ratio ( $U_r$ ) are determined at various ' $R$ ' mentioned earlier and isochrone for  $T_r = 0.04$  is plotted and similarly trajectory of curves for various  $T_r$  are obtained.

Step 3: From the data of consolidation ratio ( $U_r$ ) versus  $R$  ( $r/r_e$ ), isochrone is plotted for particular ' $T_r$ ' and then average degree of consolidation ( $U_{\text{avg}}$ ) for given ' $T_r$ ' is computed by ratio of area outside particular isochrone over total area as shown below.

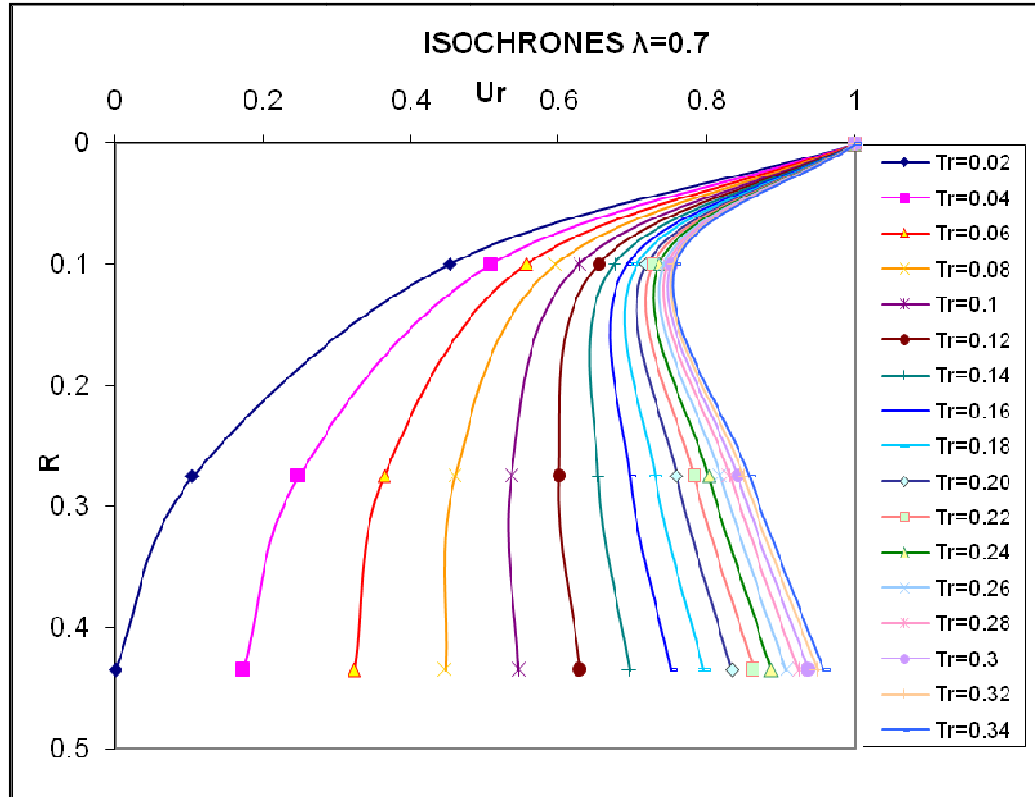


**Fig.4.3:** Consolidation ratio ( $U_r$ ) vs. Ratio of radial distance ( $R$ ) for  $\lambda = 0.7$

Table representing sample calculation for  $\lambda = +0.7$  using isochrones

| $\lambda$ | $T_r$ | $R=0.001$ | $R=0.1$ | $R=0.275$ | $R=0.435$ | $R=0.5$ | Shaded Area | Total Area | $U_R$ (%) |
|-----------|-------|-----------|---------|-----------|-----------|---------|-------------|------------|-----------|
| 0.7       | 0.02  | 1         | 0.453   | 0.106     | 0.001     | 0.001   | 0.118       | 0.499      | 23.65     |
| 0.7       | 0.04  | 1         | 0.510   | 0.248     | 0.174     | 0.202   | 0.179       | 0.499      | 35.87     |
| 0.7       | 0.06  | 1         | 0.557   | 0.364     | 0.324     | 0.355   | 0.224       | 0.499      | 44.89     |
| 0.7       | 0.08  | 1         | 0.596   | 0.459     | 0.446     | 0.480   | 0.265       | 0.499      | 53.11     |
| 0.7       | 0.1   | 1         | 0.628   | 0.537     | 0.546     | 0.582   | 0.296       | 0.499      | 59.32     |
| 0.7       | 0.12  | 1         | 0.654   | 0.601     | 0.629     | 0.667   | 0.323       | 0.499      | 64.73     |
| 0.7       | 0.14  | 1         | 0.675   | 0.653     | 0.696     | 0.735   | 0.344       | 0.499      | 68.94     |
| 0.7       | 0.16  | 1         | 0.692   | 0.696     | 0.751     | 0.791   | 0.361       | 0.499      | 72.34     |
| 0.7       | 0.18  | 1         | 0.707   | 0.731     | 0.796     | 0.837   | 0.375       | 0.499      | 75.15     |
| 0.7       | 0.2   | 1         | 0.718   | 0.759     | 0.833     | 0.875   | 0.386       | 0.499      | 77.35     |
| 0.7       | 0.22  | 1         | 0.728   | 0.783     | 0.863     | 0.906   | 0.395       | 0.499      | 79.16     |
| 0.7       | 0.24  | 1         | 0.736   | 0.802     | 0.888     | 0.931   | 0.402       | 0.499      | 80.56     |
| 0.7       | 0.26  | 1         | 0.742   | 0.818     | 0.908     | 0.952   | 0.408       | 0.499      | 81.76     |
| 0.7       | 0.28  | 1         | 0.747   | 0.831     | 0.925     | 0.969   | 0.414       | 0.499      | 82.97     |
| 0.7       | 0.3   | 1         | 0.751   | 0.841     | 0.938     | 0.983   | 0.418       | 0.499      | 83.77     |
| 0.7       | 0.32  | 1         | 0.755   | 0.850     | 0.950     | 0.994   | 0.422       | 0.499      | 84.57     |
| 0.7       | 0.34  | 1         | 0.758   | 0.857     | 0.959     | 1.003   | 0.425       | 0.499      | 85.17     |



4.4.4 Plots 4.4 to 4.22 show the relationship between Consolidation ratio ( $U_r$ ) through radial drainage, Time factor ( $T_r$ ) and Lump parameter ( $\lambda$ ):

Isochrones for  $\lambda = 0.7, 0.6, 0.5, 0.4, 0.3, 0.2, 0.1, 0.05, 0.01, 0, -0.01, -0.05, -0.1, -0.2, -0.3, -0.4, -0.5, -0.6, -0.7$

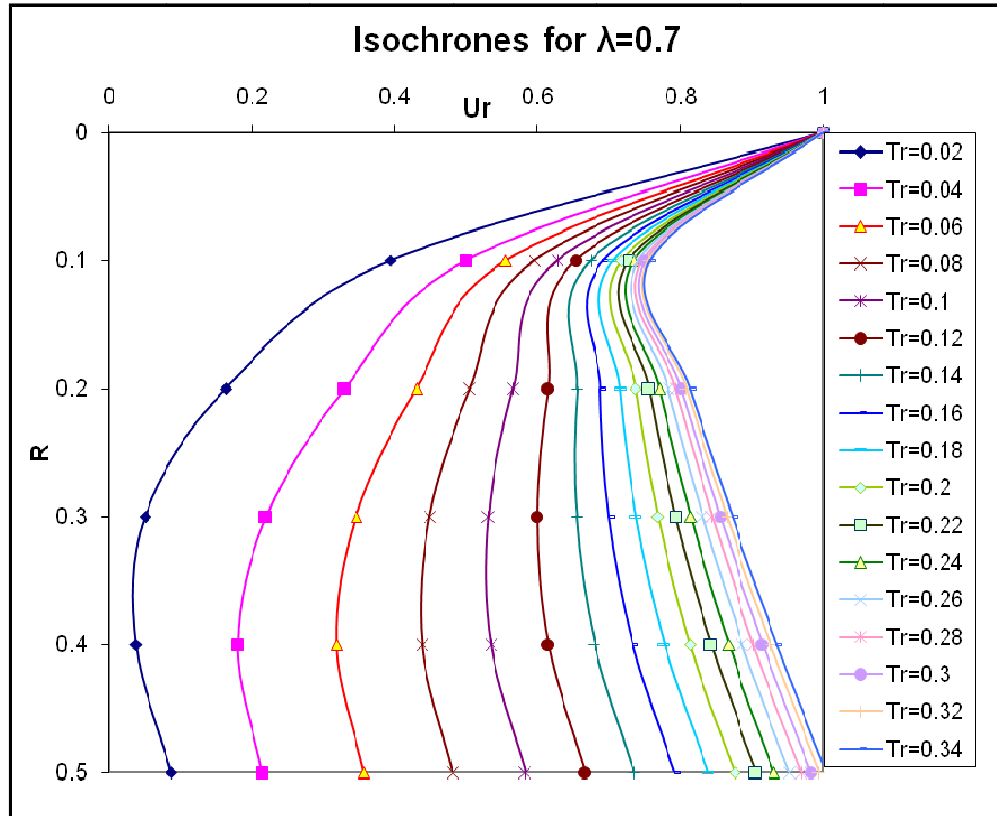


**Fig.4.4:** Consolidation ratio ( $U_r$ ) against ratio of radial distance ( $R$ ) for various time factor ( $T_r$ ) for  $\lambda = 0.7$

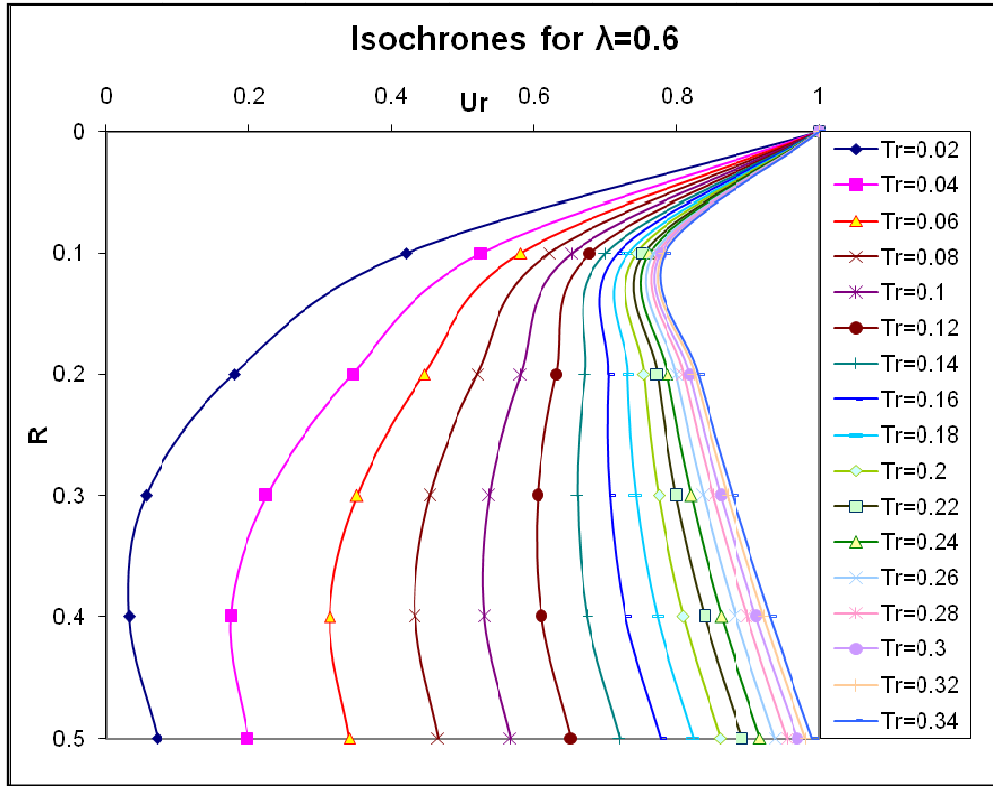


**Fig.4.5:** Consolidation ratio ( $U_r$ ) against ratio of radial distance ( $R$ ) for various time factor ( $T_r$ ) for  $\lambda = 0.6$

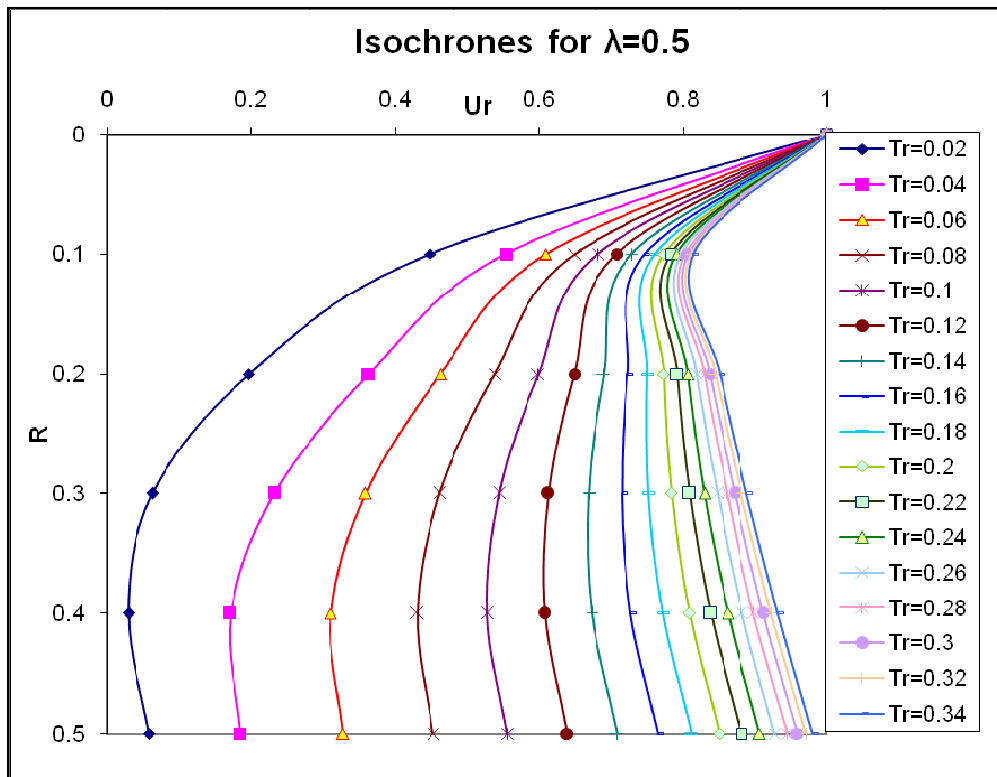


**Fig.4.6:** Consolidation ratio ( $U_r$ ) against ratio of radial distance ( $R$ ) for various time factor ( $T_r$ ) for  $\lambda = 0.5$

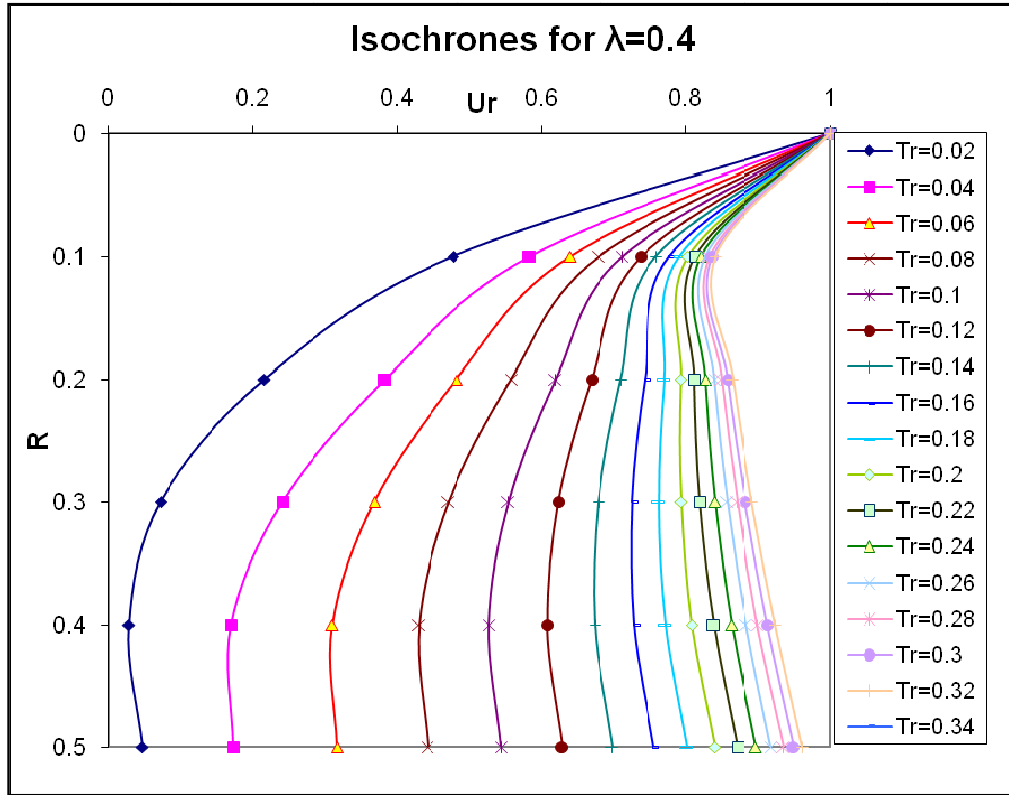


**Fig.4.7:** Consolidation ratio ( $U_r$ ) against ratio of radial distance ( $R$ ) for various time factor ( $T_r$ ) for  $\lambda = 0.4$

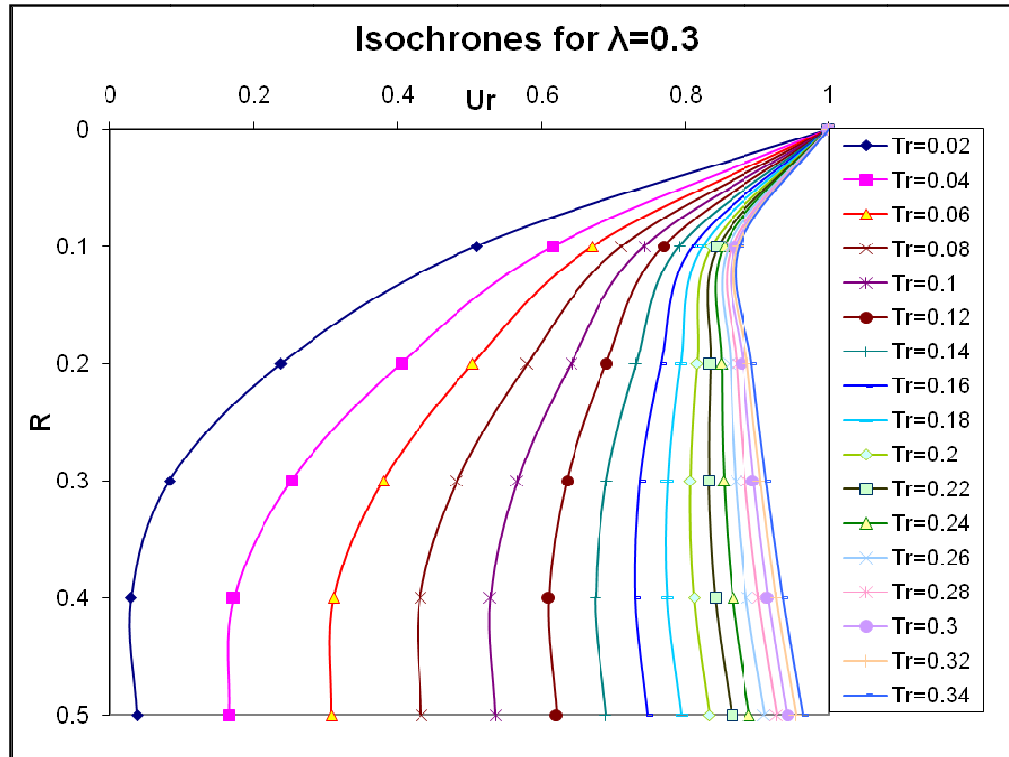


**Fig.4.8:** Consolidation ratio ( $U_r$ ) against ratio of radial distance ( $R$ ) for various time factor ( $T_r$ ) for  $\lambda = 0.3$

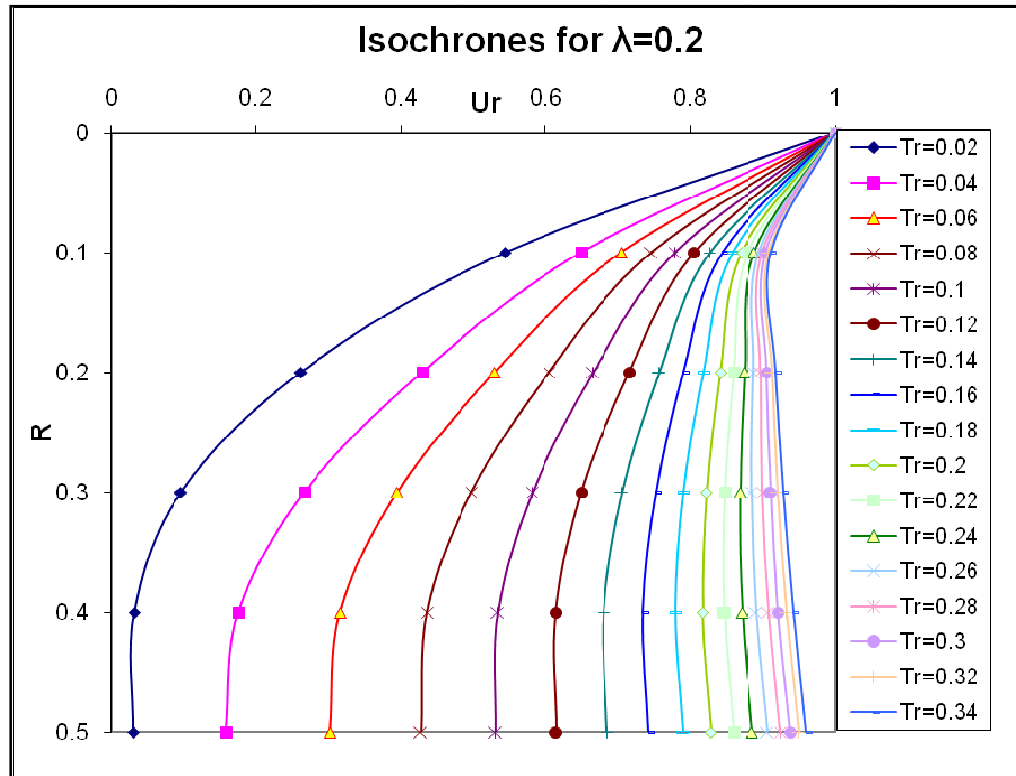


**Fig.4.9:** Consolidation ratio ( $U_r$ ) against ratio of radial distance ( $R$ ) for various time factor ( $T_r$ ) for  $\lambda=0.2$

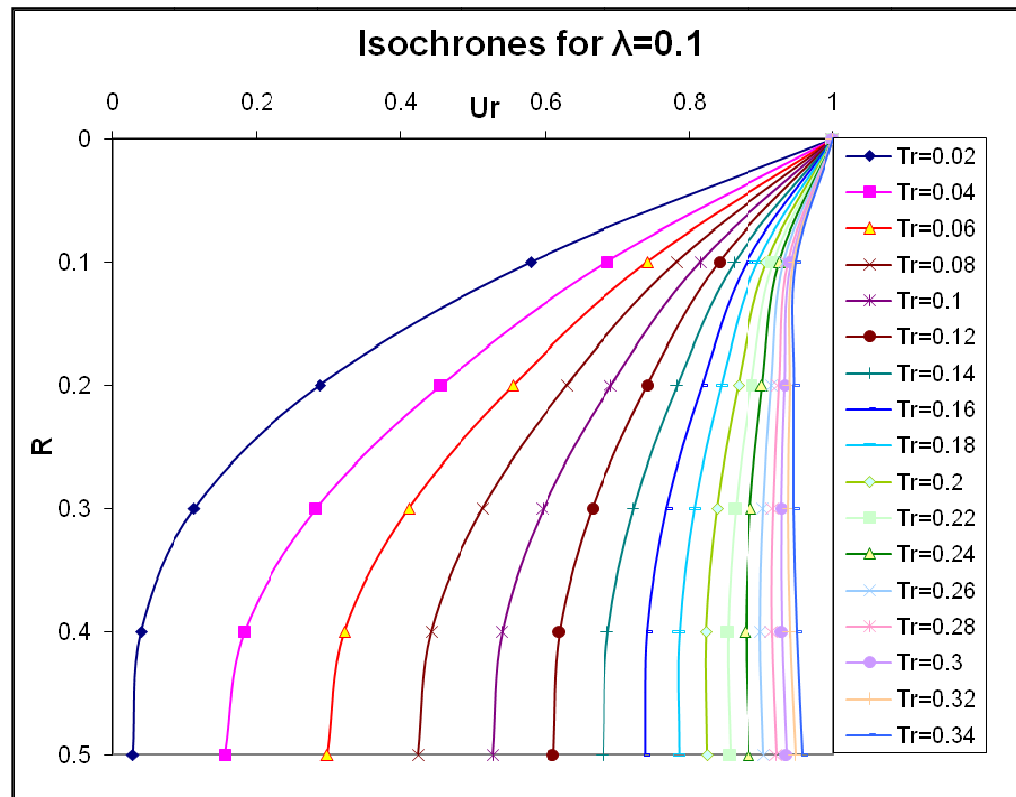


**Fig.4.10:** Consolidation ratio ( $U_r$ ) against ratio of radial distance ( $R$ ) for various time factor ( $T_r$ ) for  $\lambda = 0.1$

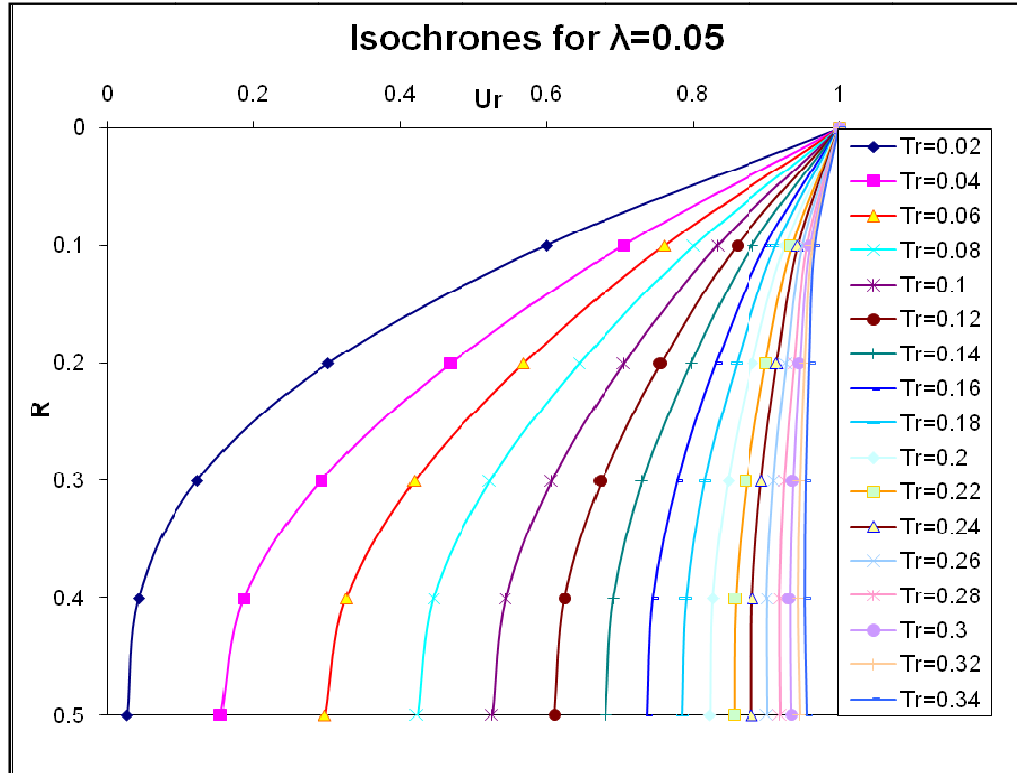


**Fig.4.11:** Consolidation ratio ( $U_r$ ) against ratio of radial distance ( $R$ ) for various time factor ( $T_r$ ) for  $\lambda = 0.05$

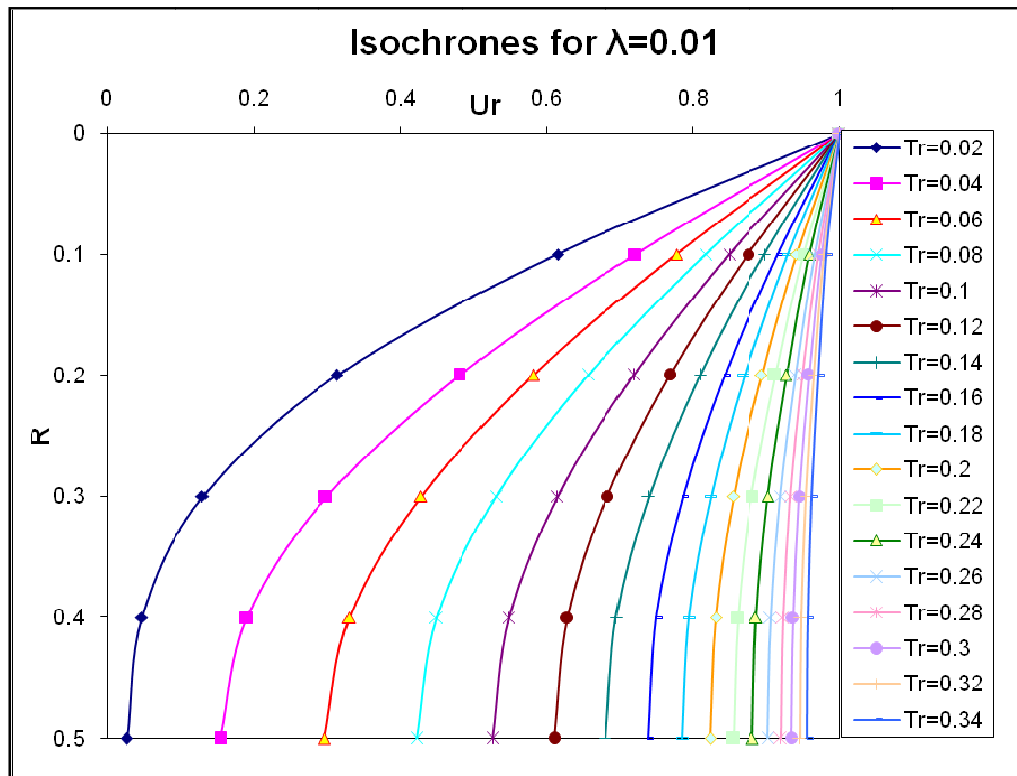


**Fig.4.12:** Consolidation ratio ( $U_r$ ) against ratio of radial distance ( $R$ ) for various time factor ( $T_r$ ) for  $\lambda = 0.01$

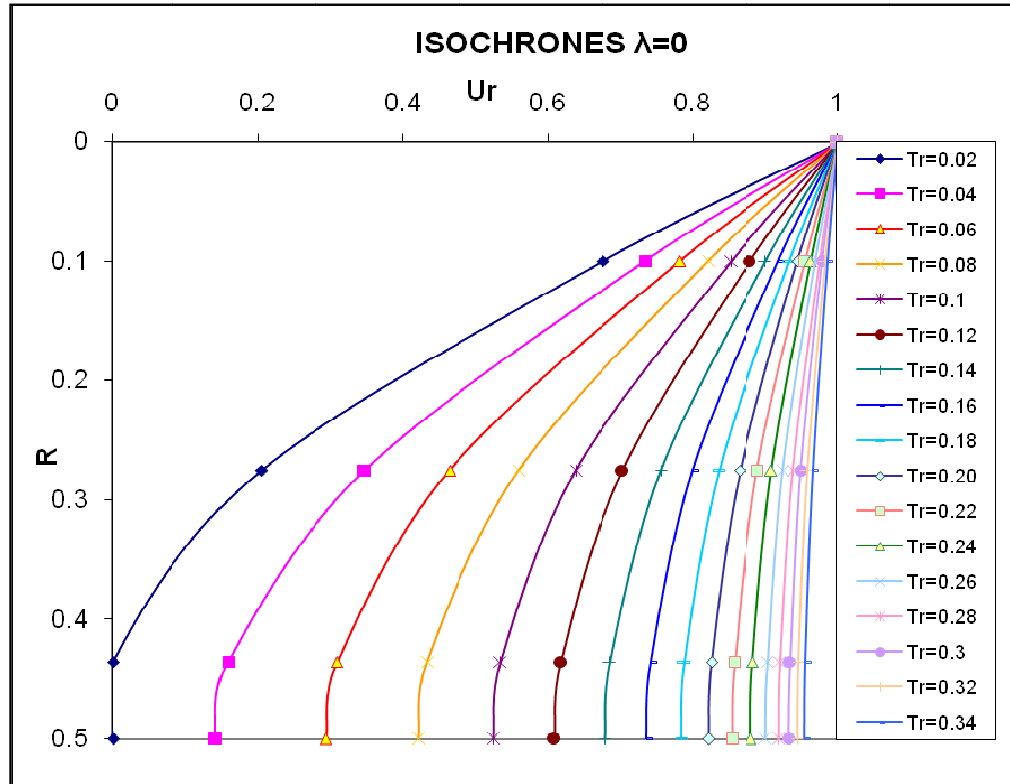


**Fig.4.13:** Consolidation ratio ( $U_r$ ) against ratio of radial distance ( $R$ ) for various time factor ( $T_r$ ) for  $\lambda = 0$

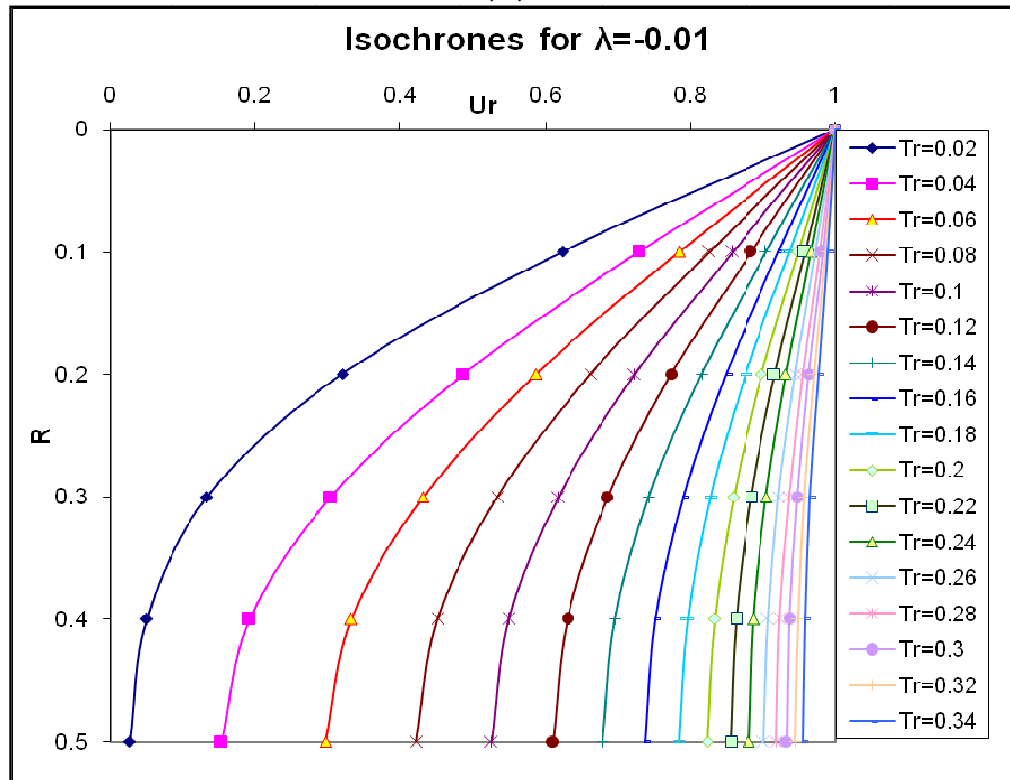


**Fig.4.14:** Consolidation ratio ( $U_r$ ) against ratio of radial distance ( $R$ ) for various time factor ( $T_r$ ) for  $\lambda = -0.01$

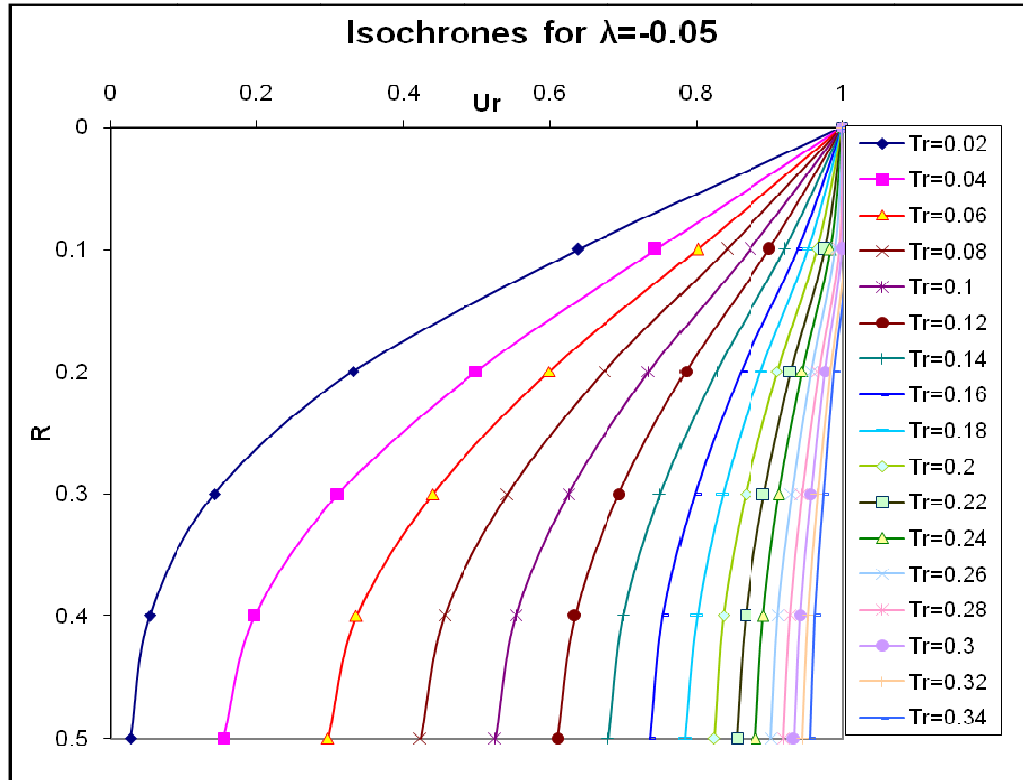


**Fig.4.15:** Consolidation ratio ( $U_r$ ) against ratio of radial distance ( $R$ ) for various time factor ( $T_r$ ) for  $\lambda = -0.05$

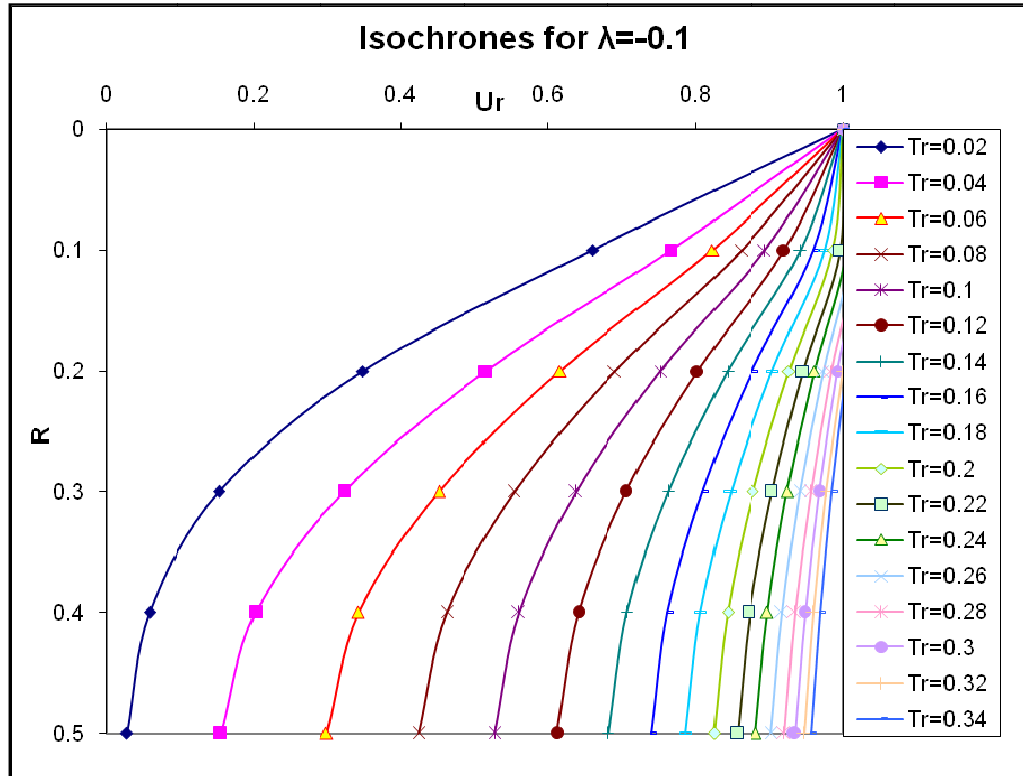


**Fig.4.16:** Consolidation ratio ( $U_r$ ) against ratio of radial distance ( $R$ ) for various time factor ( $T_r$ ) for  $\lambda = -0.01$

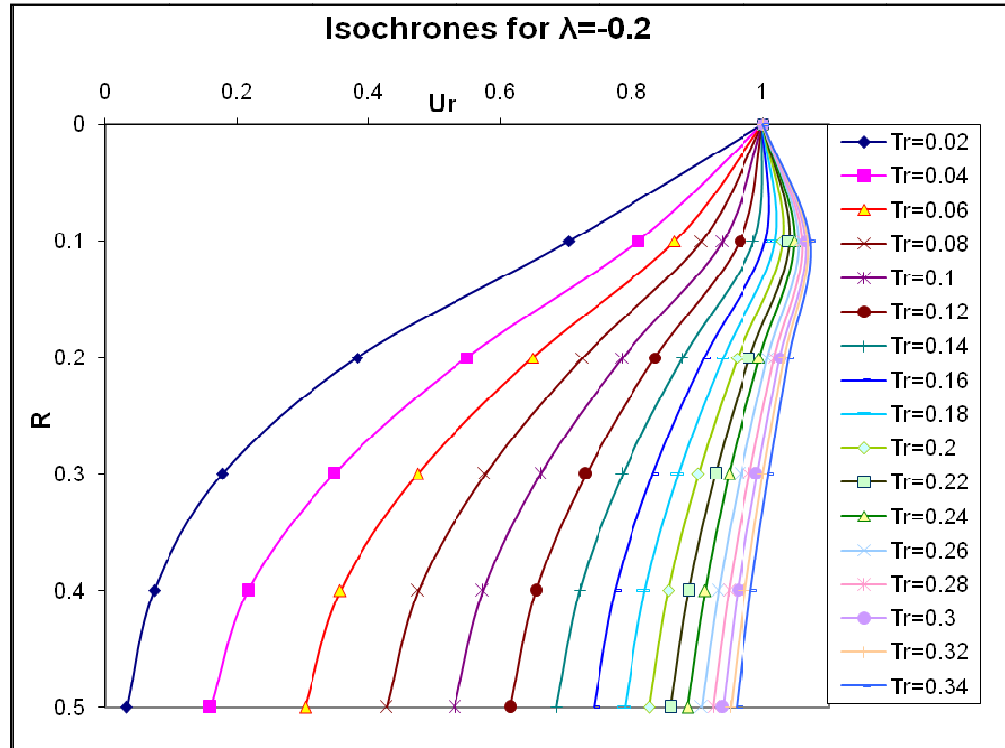


**Fig.4.17:** Consolidation ratio ( $U_r$ ) against ratio of radial distance ( $R$ ) for various time factor ( $T_r$ ) for  $\lambda = -0.2$



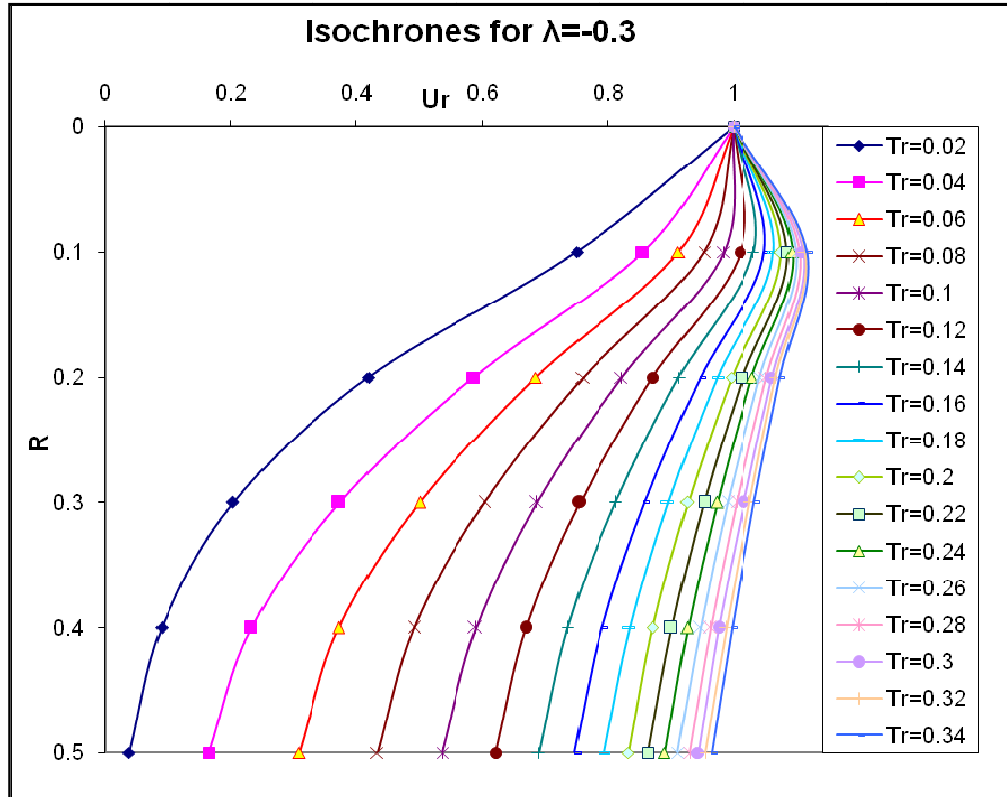


**Fig.4.18:** Consolidation ratio ( $U_r$ ) against ratio of radial distance ( $R$ ) for various time factor ( $T_r$ ) for  $\lambda = -0.3$

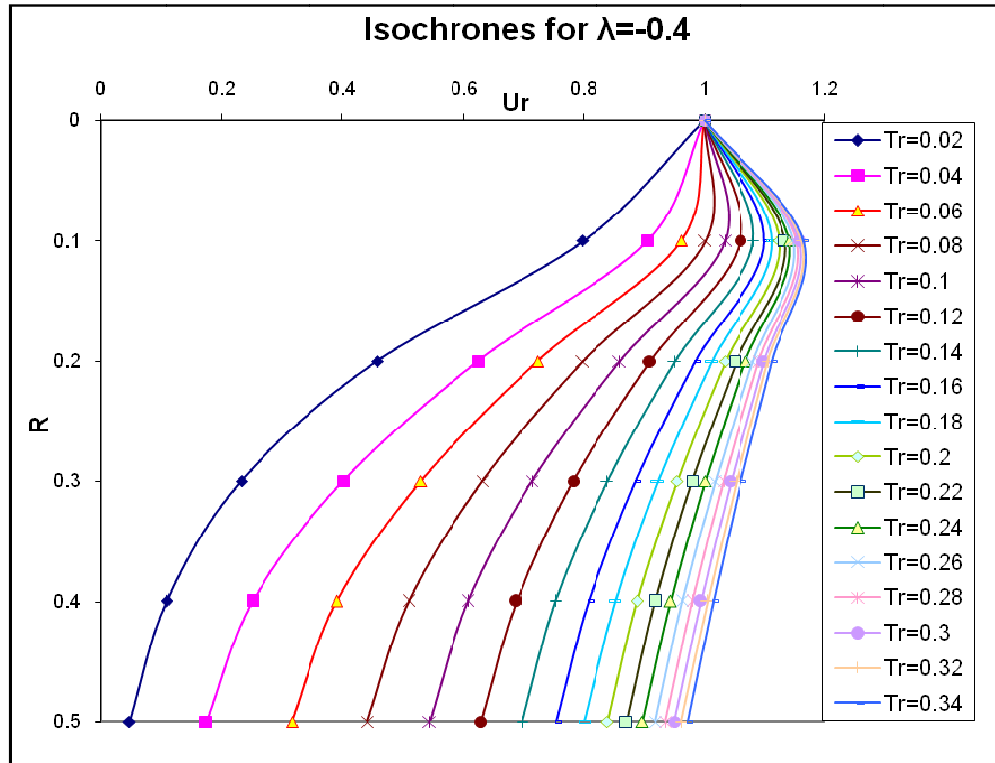


**Fig.4.19:** Consolidation ratio ( $U_r$ ) against ratio of radial distance ( $R$ ) for various time factor ( $T_r$ ) for  $\lambda = -0.4$

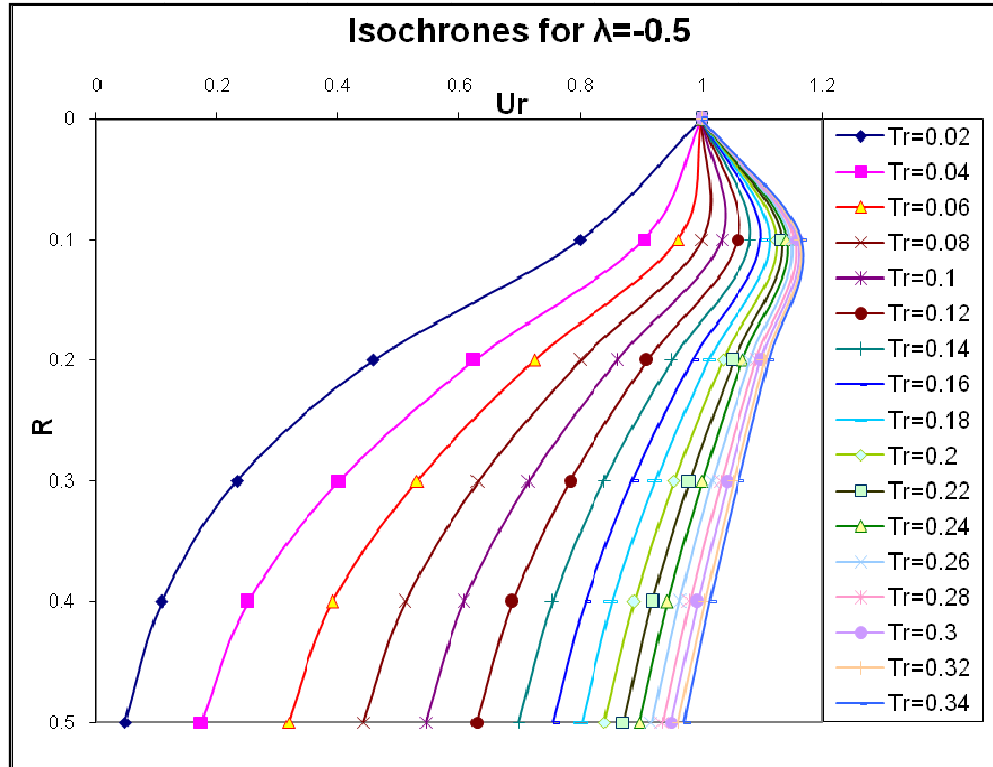


**Fig.4.20:** Consolidation ratio ( $U_r$ ) against ratio of radial distance ( $R$ ) for various time factor ( $T_r$ ) for  $\lambda = -0.5$

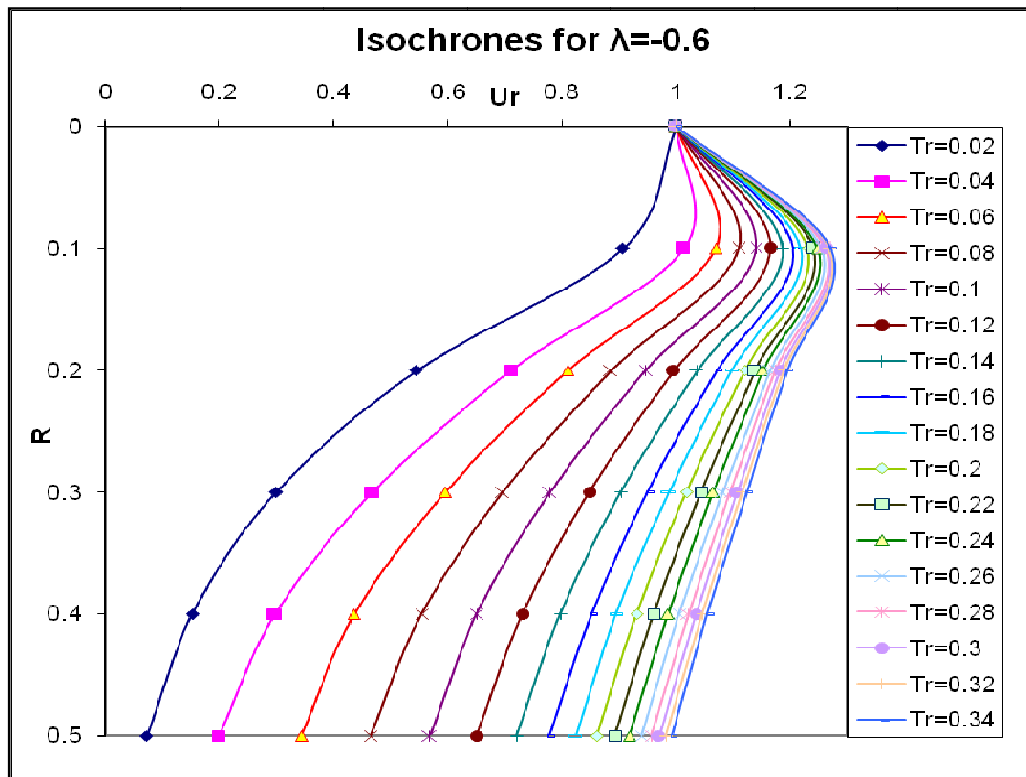


**Fig.4.21:** Consolidation ratio ( $U_r$ ) against ratio of radial distance ( $R$ ) for various time factor ( $T_r$ ) for  $\lambda = -0.6$

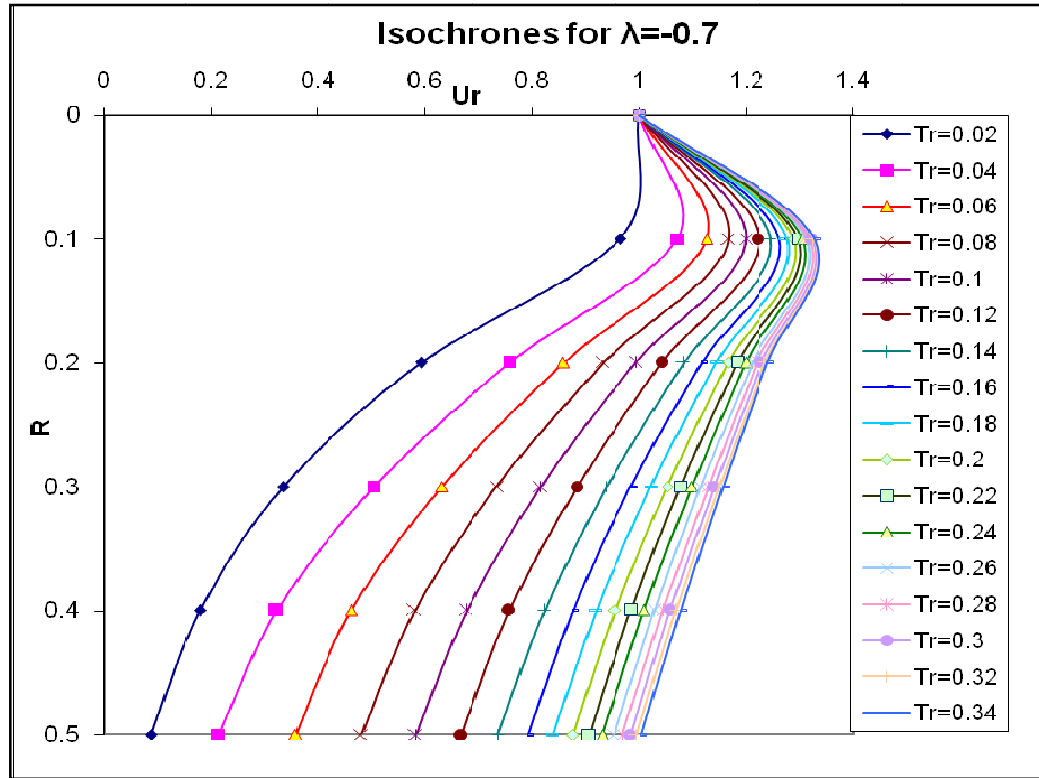


**Fig.4.22:** Consolidation ratio ( $U_r$ ) against ratio of radial distance ( $R$ ) for various time factor ( $T_r$ ) for  $\lambda = -0.7$

**4.4.5 Table showing the relationship between Average Degrees of Consolidation ( $U_R$ ) through radial drainage, Time factor ( $T_r$ ) and Lump parameter ( $\lambda$ ):**

| $T_r$ | $\lambda = 0.7$ | $\lambda = 0.6$ | $\lambda = 0.5$ | $\lambda = 0.4$ | $\lambda = 0.3$ | $\lambda = 0.25$ |
|-------|-----------------|-----------------|-----------------|-----------------|-----------------|------------------|
|       | $U_R$ (%)       | $U_R$ (%)       | $U_R$ (%)       | $U_R$ (%)       | $U_R$ (%)       | $U_R$ (%)        |
| 0.02  | 23.65           | 24.65           | 25.85           | 27.25           | 28.86           | 29.66            |
| 0.04  | 35.87           | 36.67           | 37.68           | 38.68           | 39.88           | 40.68            |
| 0.06  | 44.89           | 45.89           | 47.09           | 48.30           | 49.90           | 50.50            |
| 0.08  | 53.11           | 53.51           | 54.71           | 56.11           | 57.52           | 58.32            |
| 0.1   | 59.32           | 60.32           | 60.92           | 62.73           | 63.93           | 64.93            |
| 0.12  | 64.73           | 65.53           | 66.73           | 67.74           | 69.54           | 70.34            |
| 0.14  | 68.94           | 69.94           | 70.94           | 72.34           | 73.95           | 74.75            |
| 0.16  | 72.34           | 73.35           | 74.55           | 75.95           | 77.56           | 78.36            |
| 0.18  | 75.15           | 76.35           | 77.56           | 78.96           | 80.36           | 81.56            |
| 0.2   | 77.35           | 78.56           | 79.96           | 81.36           | 82.97           | 83.77            |
| 0.22  | 79.16           | 80.16           | 81.76           | 83.17           | 84.77           | 85.77            |
| 0.24  | 80.56           | 81.96           | 83.17           | 84.77           | 86.37           | 87.37            |
| 0.26  | 81.76           | 83.17           | 84.57           | 85.77           | 87.78           | 88.78            |
| 0.28  | 82.97           | 83.97           | 85.57           | 87.17           | 88.58           | 89.78            |
| 0.3   | 83.77           | 84.97           | 86.37           | 87.98           | 89.58           | 90.38            |
| 0.32  | 84.57           | 85.77           | 86.77           | 88.58           | 90.38           | 91.18            |

|      |       |       |       |       |       |       |
|------|-------|-------|-------|-------|-------|-------|
| 0.34 | 85.17 | 86.37 | 87.17 | 89.18 | 90.98 | 91.78 |
|------|-------|-------|-------|-------|-------|-------|

Continue.....

| Tr   | $\lambda = 0.2$ | $\lambda = 0.175$ | $\lambda = 0.15$ | $\lambda = 0.125$ | $\lambda = 0.1$ | $\lambda = 0.09$ |
|------|-----------------|-------------------|------------------|-------------------|-----------------|------------------|
|      | $U_R(\%)$       | $U_R(\%)$         | $U_R(\%)$        | $U_R(\%)$         | $U_R(\%)$       | $U_R(\%)$        |
| 0.02 | 30.46           | 30.86             | 31.26            | 31.86             | 32.26           | 32.26            |
| 0.04 | 41.28           | 41.68             | 42.28            | 42.69             | 43.09           | 43.29            |
| 0.06 | 51.10           | 51.50             | 51.90            | 52.51             | 52.91           | 53.11            |
| 0.08 | 59.32           | 59.72             | 60.12            | 60.52             | 60.92           | 61.12            |
| 0.1  | 65.73           | 66.13             | 66.53            | 67.13             | 67.54           | 67.74            |
| 0.12 | 71.14           | 71.54             | 72.14            | 72.55             | 72.95           | 73.15            |
| 0.14 | 75.55           | 76.15             | 76.55            | 76.95             | 77.35           | 77.76            |
| 0.16 | 79.16           | 79.76             | 80.16            | 80.56             | 81.16           | 81.36            |
| 0.18 | 82.16           | 82.77             | 83.17            | 83.57             | 84.17           | 84.37            |
| 0.2  | 84.57           | 85.17             | 85.77            | 86.17             | 86.57           | 86.77            |
| 0.22 | 86.57           | 87.17             | 87.58            | 88.18             | 88.58           | 88.78            |
| 0.24 | 88.18           | 88.78             | 89.18            | 89.78             | 90.18           | 90.38            |
| 0.26 | 89.58           | 89.98             | 90.58            | 90.98             | 91.58           | 91.78            |
| 0.28 | 90.78           | 91.18             | 91.78            | 92.18             | 92.59           | 92.99            |
| 0.3  | 91.38           | 91.98             | 92.59            | 92.99             | 93.59           | 93.79            |
| 0.32 | 92.18           | 92.59             | 93.39            | 93.79             | 94.39           | 94.59            |
| 0.34 | 92.79           | 93.19             | 93.79            | 94.39             | 94.99           | 95.19            |

Continue .....

| Tr   | $\lambda = 0.08$ | $\lambda = 0.07$ | $\lambda = 0.06$ | $\lambda = 0.05$ | $\lambda = 0.04$ | $\lambda = 0.03$ |
|------|------------------|------------------|------------------|------------------|------------------|------------------|
|      | $U_R(\%)$        | $U_R(\%)$        | $U_R(\%)$        | $U_R(\%)$        | $U_R(\%)$        | $U_R(\%)$        |
| 0.02 | 32.67            | 32.67            | 33.07            | 33.27            | 33.47            | 33.67            |
| 0.04 | 43.49            | 43.69            | 43.89            | 44.09            | 44.29            | 44.49            |
| 0.06 | 53.31            | 53.51            | 53.71            | 53.91            | 54.11            | 54.31            |
| 0.08 | 61.32            | 61.52            | 61.72            | 61.92            | 62.12            | 62.32            |
| 0.1  | 67.94            | 68.14            | 68.34            | 68.54            | 68.74            | 68.94            |
| 0.12 | 73.35            | 73.55            | 73.75            | 73.95            | 74.15            | 74.35            |
| 0.14 | 77.76            | 77.96            | 78.16            | 78.36            | 78.56            | 78.76            |
| 0.16 | 81.56            | 81.76            | 81.96            | 82.16            | 82.36            | 82.57            |
| 0.18 | 84.57            | 84.77            | 84.97            | 85.17            | 85.37            | 85.57            |
| 0.2  | 86.97            | 87.17            | 87.37            | 87.58            | 87.78            | 87.98            |
| 0.22 | 88.98            | 89.18            | 89.38            | 89.58            | 89.78            | 89.98            |
| 0.24 | 90.58            | 90.78            | 90.98            | 91.18            | 91.38            | 91.58            |
| 0.26 | 91.98            | 92.18            | 92.38            | 92.59            | 92.79            | 92.99            |
| 0.28 | 93.19            | 93.39            | 93.59            | 93.79            | 93.99            | 94.19            |
| 0.3  | 93.99            | 94.19            | 94.39            | 94.59            | 94.79            | 94.99            |
| 0.32 | 94.79            | 94.99            | 95.19            | 95.39            | 95.59            | 95.79            |

|      |       |       |       |       |       |       |
|------|-------|-------|-------|-------|-------|-------|
| 0.34 | 95.39 | 95.59 | 95.79 | 95.99 | 96.19 | 96.39 |
|------|-------|-------|-------|-------|-------|-------|

Continue .....

| Tr   | $\lambda = 0.02$ | $\lambda = 0.01$ | $\lambda = 0$ | $\lambda = -0.01$ | $\lambda = -0.02$ | $\lambda = -0.03$ |
|------|------------------|------------------|---------------|-------------------|-------------------|-------------------|
|      | $U_R(\%)$        | $U_R(\%)$        | $U_R(\%)$     | $U_R(\%)$         | $U_R(\%)$         | $U_R(\%)$         |
| 0.02 | 33.67            | 33.67            | 33.87         | 34.27             | 34.47             | 34.67             |
| 0.04 | 44.89            | 44.89            | 45.09         | 45.49             | 45.69             | 45.89             |
| 0.06 | 54.51            | 54.71            | 54.91         | 55.11             | 55.31             | 55.51             |
| 0.08 | 62.53            | 62.73            | 62.93         | 63.33             | 63.53             | 63.73             |
| 0.1  | 69.14            | 69.34            | 69.54         | 69.74             | 70.14             | 70.14             |
| 0.12 | 74.55            | 74.95            | 74.95         | 75.35             | 75.55             | 75.75             |
| 0.14 | 79.16            | 79.36            | 79.56         | 79.76             | 79.96             | 80.16             |
| 0.16 | 82.77            | 82.97            | 83.17         | 83.37             | 83.57             | 83.77             |
| 0.18 | 85.77            | 85.97            | 86.17         | 86.37             | 86.57             | 86.77             |
| 0.2  | 88.18            | 88.38            | 88.58         | 88.78             | 88.98             | 89.18             |
| 0.22 | 90.18            | 90.38            | 90.58         | 90.78             | 90.98             | 92.18             |
| 0.24 | 91.78            | 91.98            | 92.18         | 92.59             | 93.39             | 93.59             |
| 0.26 | 93.19            | 93.39            | 93.59         | 93.99             | 94.59             | 94.99             |
| 0.28 | 94.39            | 94.59            | 94.79         | 95.39             | 95.59             | 95.99             |
| 0.3  | 95.19            | 95.59            | 95.59         | 95.99             | 96.59             | 96.79             |
| 0.32 | 95.99            | 96.19            | 96.39         | 96.99             | 97.19             | 97.39             |
| 0.34 | 96.59            | 96.79            | 96.99         | 97.39             | 97.80             | 98.00             |

Continue .....

| Tr   | $\lambda = -0.04$ | $\lambda = -0.05$ | $\lambda = -0.06$ | $\lambda = -0.07$ | $\lambda = -0.08$ | $\lambda = -0.09$ |
|------|-------------------|-------------------|-------------------|-------------------|-------------------|-------------------|
|      | $U_R(\%)$         | $U_R(\%)$         | $U_R(\%)$         | $U_R(\%)$         | $U_R(\%)$         | $U_R(\%)$         |
| 0.02 | 34.87             | 35.07             | 35.27             | 35.47             | 35.67             | 35.87             |
| 0.04 | 46.09             | 45.69             | 46.49             | 46.69             | 46.89             | 47.29             |
| 0.06 | 55.91             | 55.91             | 56.31             | 56.51             | 56.71             | 57.11             |
| 0.08 | 63.93             | 64.13             | 64.33             | 64.53             | 64.73             | 65.13             |
| 0.1  | 70.54             | 70.74             | 70.94             | 71.14             | 71.34             | 71.54             |
| 0.12 | 75.95             | 76.15             | 76.35             | 76.55             | 76.75             | 77.15             |
| 0.14 | 80.36             | 80.56             | 80.76             | 81.16             | 81.36             | 83.97             |
| 0.16 | 83.97             | 84.17             | 84.37             | 84.77             | 86.77             | 87.17             |
| 0.18 | 86.97             | 88.58             | 88.98             | 89.18             | 89.38             | 89.78             |
| 0.2  | 89.58             | 90.78             | 91.18             | 91.38             | 91.58             | 91.98             |
| 0.22 | 92.38             | 92.59             | 92.99             | 93.19             | 93.59             | 93.79             |
| 0.24 | 93.99             | 94.19             | 94.39             | 94.79             | 94.99             | 95.39             |
| 0.26 | 95.19             | 95.39             | 95.59             | 95.99             | 96.19             | 96.59             |
| 0.28 | 96.19             | 96.39             | 96.79             | 96.99             | 97.39             | 97.60             |

|      |       |       |       |       |       |       |
|------|-------|-------|-------|-------|-------|-------|
| 0.3  | 96.99 | 97.39 | 97.60 | 97.80 | 98.20 | 98.40 |
| 0.32 | 97.80 | 98.00 | 98.40 | 98.60 | 98.80 | 99.20 |
| 0.34 | 98.20 | 98.60 | 98.80 | 99.20 | 99.40 | 99.60 |

Continue .....

| Tr   | $\lambda = -0.1$ | $\lambda = -0.11$ | $\lambda = -0.12$ | $\lambda = -0.125$ | $\lambda = -0.13$ | $\lambda = -0.14$ |
|------|------------------|-------------------|-------------------|--------------------|-------------------|-------------------|
|      | $U_R(\%)$        | $U_R(\%)$         | $U_R(\%)$         | $U_R(\%)$          | $U_R(\%)$         | $U_R(\%)$         |
| 0.02 | 36.07            | 36.47             | 36.67             | 36.87              | 37.07             | 37.27             |
| 0.04 | 47.49            | 47.70             | 47.90             | 48.10              | 48.10             | 48.50             |
| 0.06 | 57.31            | 57.52             | 57.72             | 57.92              | 57.92             | 58.32             |
| 0.08 | 65.33            | 65.53             | 65.73             | 65.93              | 65.93             | 66.33             |
| 0.1  | 71.94            | 72.14             | 72.55             | 72.55              | 72.55             | 72.95             |
| 0.12 | 77.35            | 77.56             | 77.76             | 77.96              | 77.96             | 78.36             |
| 0.14 | 84.17            | 84.57             | 84.77             | 84.97              | 85.17             | 85.37             |
| 0.16 | 87.37            | 87.78             | 87.98             | 88.18              | 88.38             | 88.58             |
| 0.18 | 89.98            | 90.38             | 90.58             | 90.78              | 90.98             | 91.18             |
| 0.2  | 92.18            | 92.59             | 91.38             | 92.99              | 93.19             | 93.39             |
| 0.22 | 93.99            | 93.19             | 94.59             | 94.59              | 94.99             | 95.19             |
| 0.24 | 95.59            | 95.79             | 96.19             | 96.39              | 96.39             | 96.79             |
| 0.26 | 96.79            | 97.19             | 97.39             | 97.60              | 97.80             | 98.00             |
| 0.28 | 97.80            | 98.20             | 98.40             | 98.60              | 98.80             | 99.00             |
| 0.3  | 98.80            | 99.00             | 99.20             | 99.40              | 99.60             | 99.80             |
| 0.32 | 99.40            | 99.80             | 100.00            | 99.80              | 99.80             | 100.20            |
| 0.34 | 100.00           | 100.20            | 100.60            | 100.40             | 100.60            | 100.80            |

Continue .....

| Tr   | $\lambda = -0.15$ | $\lambda = -0.16$ | $\lambda = -0.17$ | $\lambda = -0.175$ | $\lambda = -0.18$ | $\lambda = -0.19$ |
|------|-------------------|-------------------|-------------------|--------------------|-------------------|-------------------|
|      | $U_R(\%)$         | $U_R(\%)$         | $U_R(\%)$         | $U_R(\%)$          | $U_R(\%)$         | $U_R(\%)$         |
| 0.02 | 37.47             | 37.68             | 37.88             | 38.08              | 38.08             | 38.28             |
| 0.04 | 48.70             | 48.90             | 49.10             | 49.50              | 49.50             | 49.90             |
| 0.06 | 58.52             | 58.72             | 58.92             | 59.32              | 59.52             | 59.72             |
| 0.08 | 66.53             | 66.73             | 66.93             | 67.54              | 67.33             | 67.54             |
| 0.1  | 73.15             | 73.35             | 73.55             | 74.95              | 73.95             | 75.35             |
| 0.12 | 78.56             | 78.76             | 78.96             | 79.16              | 79.36             | 79.56             |
| 0.14 | 85.77             | 85.97             | 86.37             | 86.57              | 86.57             | 86.97             |
| 0.16 | 88.98             | 89.18             | 89.58             | 89.78              | 89.78             | 90.18             |
| 0.18 | 91.58             | 91.78             | 92.18             | 92.38              | 92.38             | 92.79             |
| 0.2  | 93.79             | 93.99             | 94.39             | 94.59              | 94.59             | 94.99             |
| 0.22 | 95.59             | 95.79             | 96.19             | 96.39              | 96.39             | 96.79             |
| 0.24 | 96.99             | 97.39             | 97.60             | 97.80              | 98.00             | 98.20             |

|      |        |        |        |        |        |        |
|------|--------|--------|--------|--------|--------|--------|
| 0.26 | 98.20  | 98.60  | 99.00  | 99.00  | 99.20  | 98.80  |
| 0.28 | 99.40  | 99.60  | 99.40  | 99.60  | 99.60  | 100.00 |
| 0.3  | 99.60  | 100.00 | 100.80 | 100.40 | 100.60 | 100.80 |
| 0.32 | 100.40 | 100.80 | 101.00 | 101.20 | 101.40 | 101.60 |
| 0.34 | 101.00 | 101.40 | 101.60 | 101.80 | 102.00 | 102.20 |

Continue .....

| Tr   | $\lambda = -0.2$ | $\lambda = -0.3$ | $\lambda = -0.4$ | $\lambda = -0.5$ | $\lambda = -0.6$ | $\lambda = -0.7$ |
|------|------------------|------------------|------------------|------------------|------------------|------------------|
|      | $U_R(\%)$        | $U_R(\%)$        | $U_R(\%)$        | $U_R(\%)$        | $U_R(\%)$        | $U_R(\%)$        |
| 0.02 | 38.48            | 40.88            | 43.89            | 47.70            | 52.10            | 56.51            |
| 0.04 | 50.10            | 52.91            | 55.91            | 59.12            | 62.73            | 66.33            |
| 0.06 | 59.92            | 62.93            | 65.73            | 69.34            | 72.95            | 79.36            |
| 0.08 | 68.14            | 70.94            | 73.75            | 79.16            | 83.17            | 87.37            |
| 0.1  | 75.55            | 77.35            | 82.16            | 85.57            | 89.58            | 93.59            |
| 0.12 | 79.76            | 83.97            | 87.37            | 90.98            | 94.79            | 99.00            |
| 0.14 | 85.37            | 87.98            | 91.78            | 95.39            | 99.20            | 103.21           |
| 0.16 | 90.38            | 91.78            | 95.19            | 98.80            | 102.61           | 106.81           |
| 0.18 | 92.99            | 94.79            | 98.00            | 101.60           | 105.61           | 109.62           |
| 0.2  | 95.19            | 97.19            | 100.60           | 104.01           | 108.02           | 112.02           |
| 0.22 | 97.19            | 99.20            | 102.40           | 105.81           | 109.82           | 114.03           |
| 0.24 | 98.60            | 100.80           | 104.01           | 107.82           | 111.62           | 115.63           |
| 0.26 | 99.80            | 103.01           | 105.41           | 109.02           | 112.83           | 116.83           |
| 0.28 | 100.80           | 104.01           | 106.61           | 110.22           | 113.83           | 118.04           |
| 0.3  | 101.60           | 104.81           | 107.41           | 111.02           | 114.83           | 118.84           |
| 0.32 | 102.40           | 105.61           | 108.22           | 111.82           | 115.43           | 119.44           |
| 0.34 | 103.01           | 106.21           | 108.82           | 112.42           | 116.03           | 120.04           |

#### 4.4.6 Trajectory of Curves representing relation between Average Degree of Consolidation through radial flow ( $U_R$ ) % and Time factor ( $T_r$ ) for various values of lump parameter ( $\lambda$ ):

For the various positive and negative values of ' $\lambda$ ' the trajectory of curves are drawn showing relationship between degree of consolidation ( $U_R$ ) % and Time factor ( $T_r$ ). After obtaining experimental curve for degree of consolidation, this curve is super-imposed with theoretical curves to find out appropriate value of ' $\lambda$ '. With respect to field problem it can be said that knowing soil properties and consolidation parameters, suitable ' $\lambda$ ' can be proposed on the basis of which most efficient vertical drain can be selected and applied. With this trajectory of curves, the curve of 'Barron's equal strain'

for 'n' value equal to 5, 10, 20 and 30 and curve of Terzaghi's one dimensional consolidation due to vertical flow is shown for comparison.

- a) On Semi-log Graph- Refer fig.4.23
- b) On Natural Graph- Refer fig.4.24



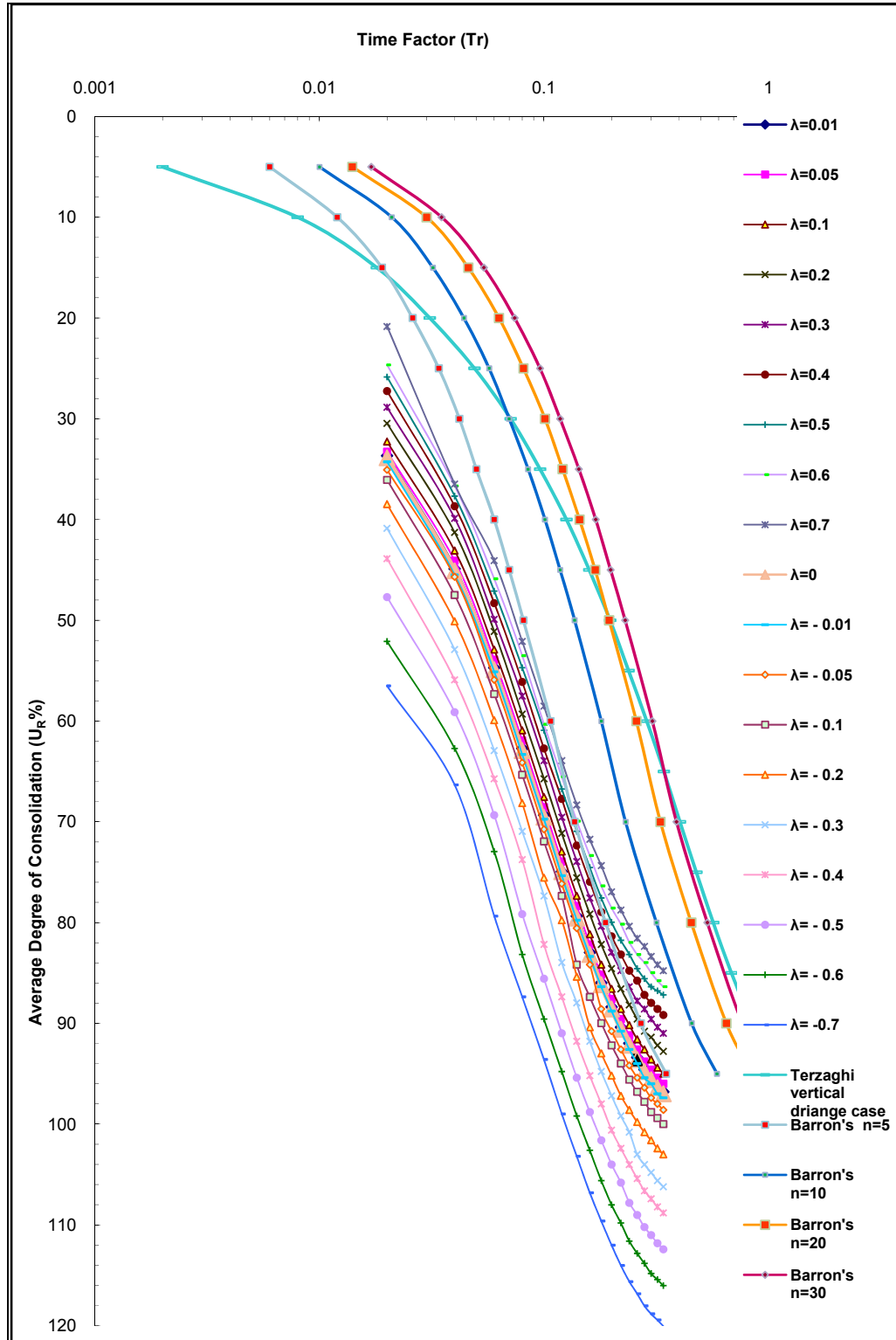


**Fig.4.23:** Average degree of consolidation( $U_r$ ) vs. Time factor ( $T_r$ ) for various values of ' $\lambda$ '

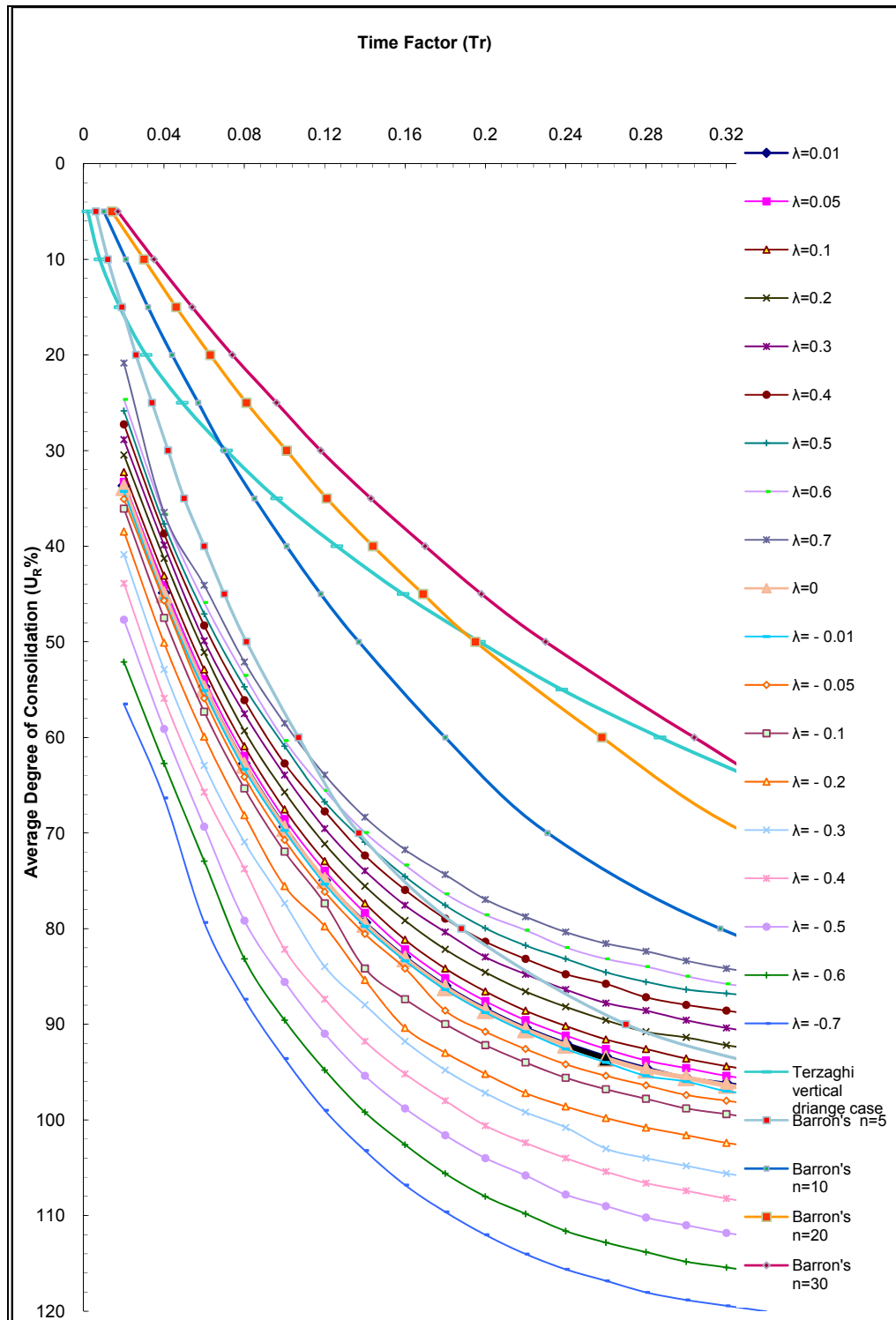


**Fig.4.24:** Average degree of consolidation( $U_r$ ) vs. Time factor ( $T_r$ ) for various values of ' $\lambda$ ' on natural scale

**Comparison of Proposed theory with Barron's Equal strain theory for radial flow:**

| Proposed Theory  | Barron's Theory   |
|--|---|
| Darcy law is valid and is but has been put in the theory in a form which relates the relative velocity of soil skeleton and pore fluid to the excess pore pressure gradient. | Darcy law is valid and 'Equal strain' and 'Free strain' assumption (small strain) are made and validated.   |
| Non-homogeneity, time-effects intrinsic in soil skeleton and compressibility of pore fluids and solids are considered in theory.   | Only vertical strains are allowed.  |
| Like Terzaghi's here also a soil element is considered and equilibrium conditions are applied.   | The soil is fully saturated, and the permeability of the soil is assumed to be constant during consolidation.   |
| Self weight of element is considered in derivation.  | Well resistance is neglected due to the sufficient discharge capacity of the drain, thereby the pore pressure at the drain interface is assumed to be zero. |
| Assuming coefficient of permeability as a function of both porosity and position of element.   | Problem is modeled as axisymmetric and continuity of cylindrical well is considered.  |
| Effective stress law is valid. Only radial flow is considered. Equal strain condition is valid.  | It is assumed that the cylindrical drain wall has a negligible thickness.   |
| Theory considers effect of 'n' value and effect of various physico-chemical factors.   | Only radial flow is permitted, load distribution is uniform over this area.   |
| Single Lump parameter ' $\lambda$ ' covers effect of drain material, size of drain and geometry of drain simultaneously.   | Theory is dependent on 'n' value (size of drain) and assumes constant permeability throughout.  |

**NOTATIONS**

| Symbol    | Meaning  | Dimensions  |
|-----------|--|-------------|
| $\sigma$  | Total stress   | $FL^{-2}$   |
| $\sigma'$ | Effective stress                                       | $FL^{-2}$   |
| $u$       | Pore water pressure                                    | $FL^{-2}$   |
| $a_s$     | Contact area per unit cross section                    | $L^2$       |
| $a$       | Independent variable                                   | $L$         |
| $a_o$     | Initial height of the soil element                     | $L$         |
| $b$       | Independent variable                                   | $L$         |
| $b_o$     | Initial radius of soil element                         | $L$         |
| $\xi$     | Unknown distance from datum plane at any time          | $L$         |
| $\xi'$    | Unknown distance from centre line of drain at any time | $L$         |
| $r_w$     | Radius of drain  | $L$         |
| $r$       | Unknown radial distance at any time                    | $L$         |
| $r_e$     | Radius of influence/Radius of soil sample              | $L$         |
| $t$       | Time   | $T$         |
| $C_s$     | Compressibility of particle                            | $F^{-1}L^2$ |
| $C$       | Compressibility of soil skeleton                       | $F^{-1}L^2$ |
| $n$       | Initial volume porosity                                | $L^3$       |
| $\rho_f$  | Weight per unit volume of fluid                        | $FL^{-3}$   |
| $\rho_s$  | Weight per unit volume of solid                        | $FL^{-3}$   |
| $\alpha$  | Constant   | ---         |
| $V_f$     | Velocity of soil solid                                 | $LT^{-2}$   |
| $V_s$     | Velocity of pore fluid                                 | $LT^{-2}$   |
| $k_o$     | Coefficient of permeability at rest                    | $LT^{-1}$   |
| $k_h$     | Coefficient of horizontal permeability                 | $LT^{-1}$   |
| $p$       | Fluid pressure (above atmospheric)                     | $FL^{-2}$   |
| $\eta$    | Pore water coefficient                                 | ---         |
| $z$       | Volume of solids                                       | $L^3$       |
| $\beta$   | Constant   | ---         |
| $e_o$     | Initial void ratio                                     | ---         |

|                   |   |                 |
|-------------------|---|-----------------|
| e                 | Void ratio at any time                                | ---             |
| Z                 | Depth dimension                                       | Non-dimensional |
| R                 | Radius dimension                                      | Non-dimensional |
| $C_r$             | Coefficient of consolidation due to radial drainage   | $LT^{-2}$       |
| $C_v$             | Coefficient of consolidation as per Terzaghi's theory | $LT^{-2}$       |
| $C_e$             | Coefficient due to porosity and permeability          | $LT^{-2}$       |
| $\lambda$         | Lumped parameter                                      | Non-dimensional |
| $T_r$             | Time factor due to radial drainage                    | Non-dimensional |
| h                 | Thickness   | L               |
| M                 | Constant of integration                               | ---             |
| N                 | Constant of integration                               | ---             |
| $\mathfrak{I}(S)$ | Entire transcendental function                        | ---             |
| $\eta(S)$         | Entire transcendental function                        | ---             |
| $S_n$             | Simple pole   |                 |
| $U_R$             | Average degree of consolidation at radius dimension   | ---             |
| $u_i$             | Initial pore water pressure                           | $FL^{-2}$       |
| $u_r$             | Pore water pressure at any radius at any time         | $FL^{-2}$       |

## **CHAPTER-5**

### **MEASUREMENT FACTORS AND EXPERIMENTAL SET-UP**

---

Different investigators studied the two and three dimensional process of consolidation through radial flow by providing various types of vertical geodrains and put forth their observations and remarks on various factors affecting the process of consolidation. These factors are very important during laboratory study and have to be critically examined. This chapter deals with various factors associated with experimental set-up along with drain selection, drain fabrication, drain installation and measurement of experimental parameters. This chapter applies the theoretical development discussed in the previous chapter to laboratory experiments performed at Geotechnical Engineering Laboratory, The Maharaja Sayajirao University of Baroda. Chapter focuses on modification of hydraulically pressurised Oedometer for consolidation of soft clay through radial flow for measurements of pore water pressure and settlement under various loads. The following are the list of factors examined and studied in detail for present laboratory investigation:

1. Factors affecting measurement
2. Experimental set-up
3. Vertical drain design, selection, fabrication and testing
  - 3.1 Development of radial permeability test set-up of vertical drains
4. Soil sample preparation
5. Drain installation
6. Testing methodology
  - 6.1 Vane shear test of consolidated clay samples under dynamic conditions
7. Scanning electron microscopy of consolidated samples

#### **5.1 Factors Affecting Measurement**

Following are the major factors which are of prime importance while performing one dimensional consolidation test through radial flow using vertical drains.

### 5.1.1 Drain Stiffness

Rowe-Shield (1965) studied the diameter of the drain and the variation in the relative stiffness of the sand drain and the clay to ascertain the effect of these variables on the apparent compressibility of the clay-sand drain system as a whole. With the increase in drain diameter or decrease in ratio of Oedometer diameter ( $d_e$ ) to drain diameter ( $d_w$ ),  $n$  ( $d_e/d_w$ ) the relative stiffness increases in a stiff clay and soft clay as shown in fig.5.1. In case of field sand drain installation where the drain spacing to drain diameter ratio,  $n$ , generally exceeds a factor of 10, the stiffness of the sand drain increases the stiffness of installation by no more than 10 per cent.

In the present investigation four types of vertical drains were considered namely, Sand drain (SD), Sandwich drain (SW), Coir-Jute drain (CJ), Polypropylene fiber drain (PF) of 'n' value as 11.04, 16.93 and 21.71.

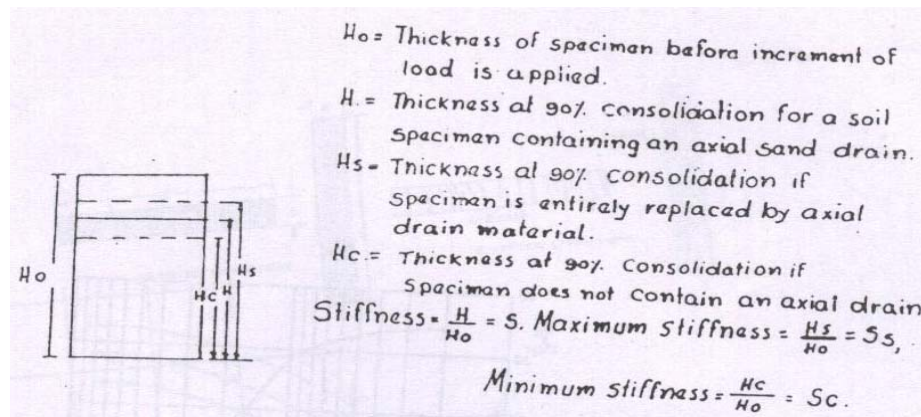


Fig.5.1 (a) Stiffness of sand drain installation

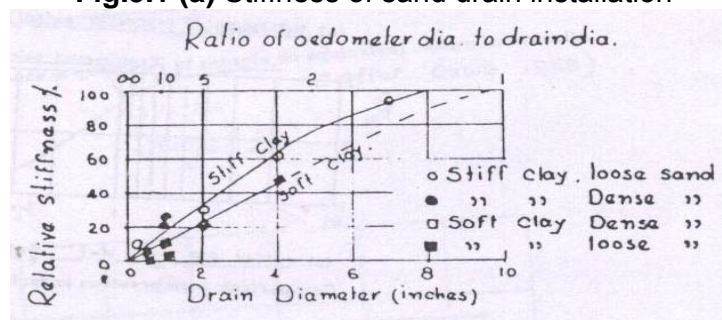


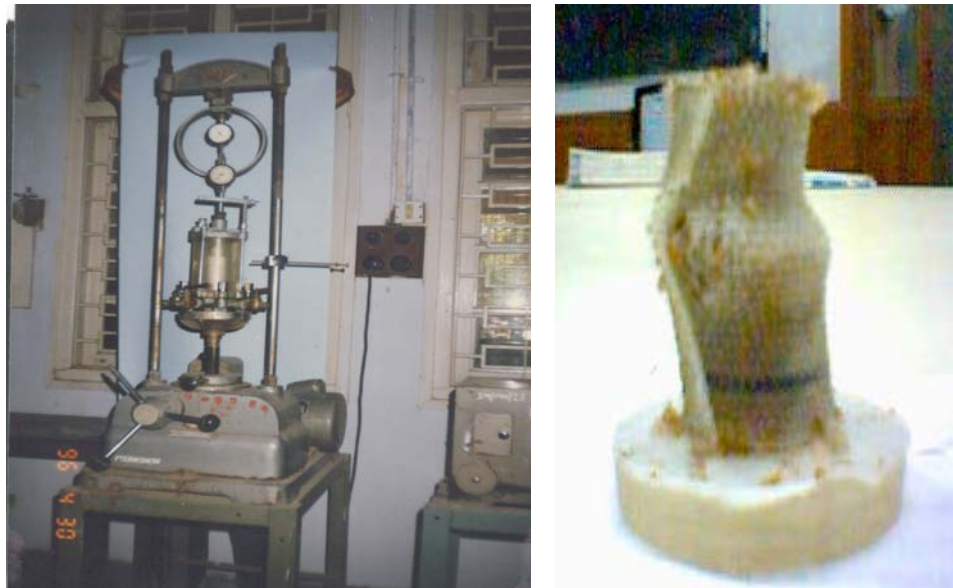
Fig. 5.1(b) Effect of sand drain on relative stiffness of a clay foundation

### Stiffness Test

The stiffness of drains is tested by uni-axial compression test using triaxial set-up. The triaxial set-up (photograph 5.1) uses high pressure cylindrical cell made of Perspex or other transparent material fitted between the base and top cap. A

stainless steel piston running through the centre of the top applies the vertical compressive load on the specimen under test. The load is applied through proving ring of capacity 230kg and sensitivity 230/2050 with the help of mechanically separated frame. Two porous discs are placed at the top and the bottom of the drain. Height to diameter(aspect) ratio is kept equal to 2.0. A constant rate of strain is applied and corresponding stress is recorded using mechanical dial gauge of sensitivity of 0.001mm. The stiffness of vertical drain should be compatible to the compressibility of soil. The stress carrying capacity of Sandwick (SW) is more compare to Coir-Jute fiber drain (CJ) and Polypropylene fiber drain (PF) under saturated coniditions while stress carrying capacity of PF is more in dry condition comapre to CJ. The strain carrying capacity in saturated condition, Sandwick (SW) exhibit more strain compare to CJ & PF. Under dry condition strain carrying capacity of PF is compare to CJ as depicted from fig.5.2 .

| Type of Drain           | Stiffness                    |           |            |           |
|-------------------------|------------------------------|-----------|------------|-----------|
|                         | Stress (kg/cm <sup>2</sup> ) |           | Strain (%) |           |
|                         | Dry                          | Saturated | Dry        | Saturated |
| Sandwick(SW)            | ----                         | 2.1       | ----       | 0.16      |
| Coir-Jute(CJ)           | 0.297                        | 0.196     | 0.12       | 0.06      |
| Polypropylene fiber(PF) | 0.672                        | 0.344     | 0.23       | 0.11      |



**Photograph 5.1:** View of complete tri-axial set-up for stiffness test and sample of sandwick (n=11.04) after failure



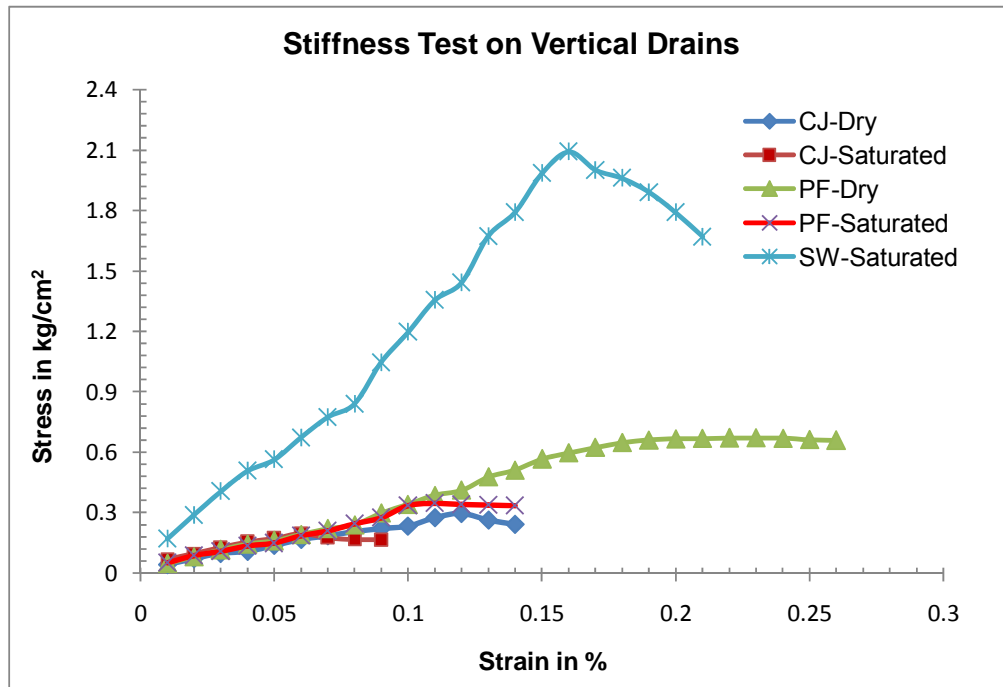


**Fig.5.2:** Stress-Strain nature of various vertical geodrains

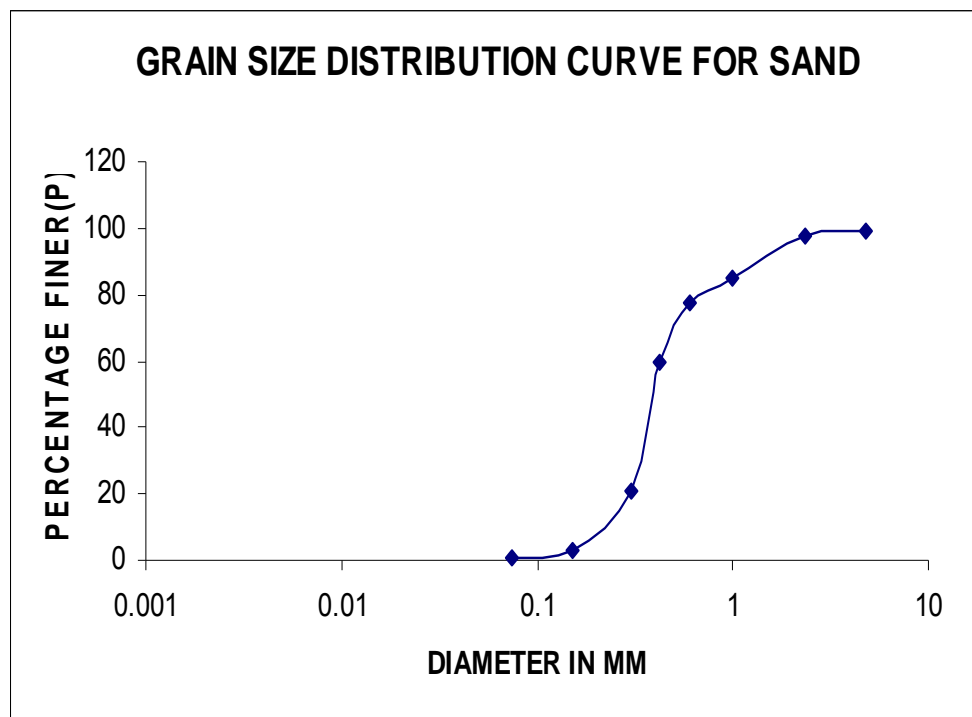


**Fig.5.3:** Standard gradation curve of sand

### 5.1.2 Selection of Gradation of Sand

The choice of sand for the sand drain and sandwick is desired to be such that no penetration through the perforations of the geotextile should occur. The sand shall conform to filter requirements if silt soils are being tested. The maximum size of the particles of sand shall be of the order of  $1/20^{\text{th}}$  the diameter of the drain and the sand must be clean and free draining, Rowe-Shield (1965). The selection of the geotextile is based on the gradation of sand used as shown in fig.5.3 in the present investigation.

With the above considerations, in the present work, it is therefore decided to select Oedometer to drain diameter ratio ( $n$ ) equal to 11.04, 16.93 and 21.71.

### 5.1.3 Smear and Well Resistance

Hansbo (1981) suggested that the influence of smear on consolidation process increases with increase in diameter of the drain and well resistance increases with increase in length of the drain. He suggested that a thin walled mandrel should be used to drill axial drain hole to avoid disturbance to the soil. Rowe-Shield (1965) mentioned that a thin walled mandrel causes little disturbance compared to that due to a 10cm diameter sampling tube. Richart (1959) mentioned that a considerable difference may occur between the geometrical value of ' $n$ ' and the effective value of the ratio ' $n$ ', it is a good evaluation of radius of smeared zone at the well periphery and the coefficient of the permeability within the smeared zone are not obtained. These leads to an appreciable variation in the predicted exceed pore pressure against time relationship. The effect of smear is to retard the flow of pore water from the sample during consolidation test. So that the measured horizontal coefficient of consolidation is lower than that of the undisturbed sample.

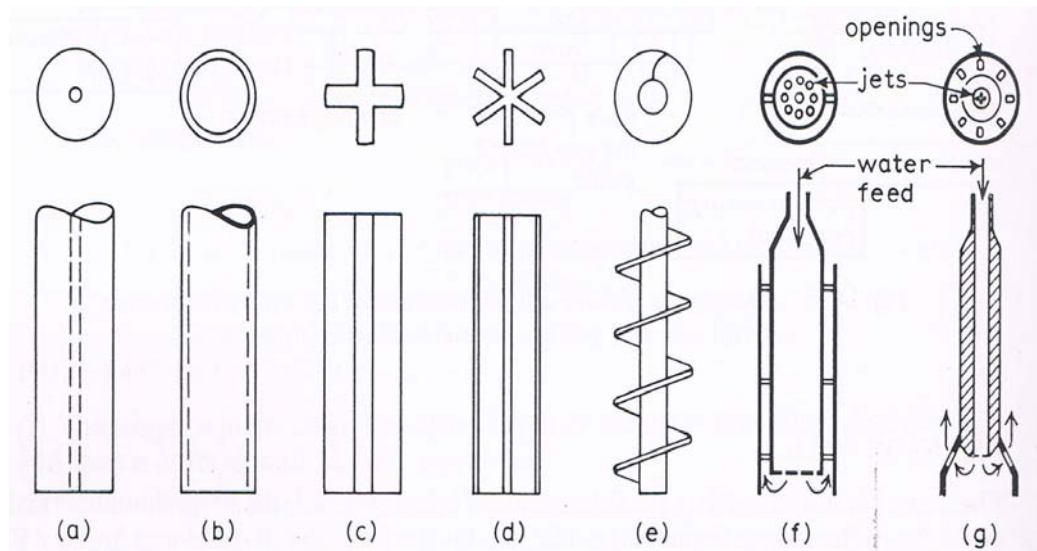


**Fig.5.4:** Types of mandrel for forming drainage well: (a) solid (b) hollow tube (c) cruciform (d) star (e) auger (f) double-wall jetting (g) dutch type jetting

Generally disturbance increases with larger total mandrel cross sectional area. The mandrel cross sectional area should be as close to that of the drain as possible to minimize displacement; while at the same time, adequate stiffness of the mandrel (dependent on cross sectional area and shape) is required to maintain vertical alignment. Although little data are available to assess shape effects (fig.5.4), it is believed that the shape of the mandrel tip and anchor should be as tapered as possible. While working on the effect of mandrel driven drains on soft clays, Akagi (1977, 1985), observed that when a closed-end mandrel is driven into saturated clay, the clay will suffer large excess pore water pressure, associated with ground heave and lateral displacement. The strength and coefficient of consolidation of the surrounding soil can then decrease rapidly. In our case thin wall mandrel were used so as to have minimal disturbance to the soil sample with little regard for the effect of smear while formation of drainage well.

### 5.1.5 Side Friction

One of the striking experimental factor that affects the results is the side friction. The side friction decreases the one dimensional state of strain and prevents some of the axial faces reaching the bottom portion of the specimen. Taylor (1942) first reported the effect of side friction state of strain in soil sample.

According to him, the vertical pressure-void ratio curve was falling off the true one, in the direction of the larger pressure, the value of coefficient of consolidation was, however, not much affected. Aial (1955) and Leonard et al. (1961) reported that the side friction affects pore pressure measurement and indicates that the measured value comes to be considerably smaller than the incremental applied load.

In order to minimize this side friction, it is intended to keep the thickness diameter ratio of specimen as smaller as possible, because smaller the contact area lesser will be the side friction. Results of various investigators, Tschebotariff (1953), Aomaya (1957); Newland (1960), Raymond et al., (1965); Rosco et al., (1969); and Trautwein et al., (1981) indicated that coating the inside well with thin film of silicon grease, side friction can be reduced to small magnitude even for high thickness diameter ratio. Parikh and Shroff (1972) concluded from their comparative study that the influence of the side friction on pore pressure measured, it is advisable to measure pore pressure at point away from the edge of the Oedometer.

#### **5.1.6 System Inadequacies**

Measurement of every parameter is affected by the inadequacies in the test arrangement at a certain extent. It is a common practice that in Rowe type Oedometer, load is applied through convoluted rubber jacket. The load is transferred to sample through a stiff plate to get equal strain compression to stimulate actual field conditions more closely. Stress distribution, hence may be non uniform due to improper seating of plate. Improper bedding may also induce error in settlement observations. The measurement of pore water pressure during test either by conventional Bishop type null indicator or electric transducers, show time lag due to system flexibility. The response of pore pressure measuring system to a change of total stress in the soil is usually delayed since pore water must enter the instrument. Gibson (1963) studied the relation between the time lag, the permeability and compressibility of the soil. In the hydraulically pressurized Oedometer, initial pore water pressure ( $\Delta u$ ) must be equal to applied incremental stress ( $\Delta P$ ), but due to system flexibility, this value of initial pore water pressure ( $\Delta u$ ) is affected. Shroff et al. (1965), Thomas (1965), Wissa (1969), Bruhn (1972), Bishop (1973), Mesri (1976), and Bishop

(1976) demonstrated the importance of influence of system flexibility on the observed pore pressure response in saturated soil to an undrained change in stress. They emphasized on important factor like:

- i. Compressibility of soil and water
- ii. Equivalent compressibility of pore water line and connection ( $C_e$ )
- iii. Compressibility of pore pressure measuring element ( $C_m$ )
- iv. Compressibility of soil skeleton ( $C_s$ )

Whitman et al. (1961) pointed out the discrepancy in the pore pressure measurement by electrical appliances. The general null balance deficiencies also influence the measurements.

In view of the above facts, proper care is taken to avoid system inadequacies in present investigation. To avoid error of the hydraulic pressure system, pressure was recorded very near to the Oedometer, also to measure the pore water pressure the length of the polyethylene drain tube connecting the Bishops set up was kept as short as possible. To avoid error, pore pressure measurements are compared with electronic transducer system where system flexibility effect is negligible.

#### **5.1.7 Shape of Porous Stone**

The porous stone in the bottom plate used for passing the pore water to the Bishop's apparatus is also affecting the rate of consolidation. This porous stone should be of radial shape in the form of arc of the circular central sand drain or other circular geodrain so as the cylindrical element of flow is small and is towards the cylindrical surface of the central sand drain or geodrain. The porous stones are boiled using distilled water for at least 30minutes for deairing so as to achieve zero air entry value. The porous stones were boiled every time before commencement of test.

#### **5.1.8 Radial co-ordinates and pore pressure**

As per suggestion of Berry et.al (1969) in the sand drain problem under free strain consolidation, the theoretical curve of pore water pressure against time factor ( $T_r$ ) for  $r/r_e$  of 0.55, 0.57 and 0.59 for 'n' ( $d_e/d_w$  or  $r/r_e$ ) value 20, 10 and 5 respectively corresponds closely, although not exactly, to U- $T_r$  relationship (U

equal to 10 percentage) and therefore, these radii are often chosen as the point at which pore pressure measurement are made. In the equal strain condition, it may be noted that there is an agreement between  $U_r$ -T and  $U_o$ -T relationship at specified radii. In our case the alignment of porous stone is kept at 120 degree each with central porous stone so as to cover complete plain of radii of sample as radii of sample represents thickness of sample in vertical direction. If 'r' is radius of oedometer/radius of influence, the three porous stones are located at a distance of  $r/4$ ,  $r/2$  and  $3r/4$  at 120 degree each.

In the present work, pore water pressures are measure at all three radial points  $r_1$ ,  $r_2$  and  $r_3$  from centre while comparison is made for middle radial point  $r_2$  located at a distance of  $0.55r$ .

## **5.2 EXPERIMENTAL SETUPS**

### **5.2.1 Review of experimental set-up**

Rowe (1965) first developed the Oedometer for study of consolidation behavior of soils and all later developments were more or less similar. The typical Rowe type Oedometers are of diameter 76 mm, 152 mm, 254 mm. The use of this type of Oedometer made possible to study the three dimensional process of consolidation, Terzaghi (1943) in a better manner with conventional pore pressure measuring system of Bishop. It was the solution of the ordinary consolidation test having number of limitations and made it possible to get time-pore pressure dissipation characteristics of the soil during consolidation process. Number of ground improvement techniques is based on the laboratory testing with Rowe type Oedometer.

Parikh and Shroff (1972) and Shroff and Tamakuwala (1975) used Rowe type Oedometer of 76 mm, 152 mm, 254 mm diameter for various tests on clay. The parameters included the influence of mineral type, degree of saturation, fabric structure, stress history and drainage path on consolidation characteristics of Kaolinite clay.

Shah and Shroff (1978) used Rowe type, hydraulically pressurized Oedometers to study the nature of isochrones in radial consolidation of clays.

Singh and Hattab (1979) performed an experimental study of the inward radial drainage of remolded Kaolinite clay to central model and drain to assess the

effects of various methods of installation and spacing on the consolidation characteristics of the soil by using 76 mm, 152 mm, 254 mm diameter Rowe type Oedometers. In this case improvement over Rowe type Oedometers was brought by adopting clear Perspex for the construction of the 254 mm diameter cell reinforced by a steel ring. This produced the desired transparency qualities without violating the basic orientation of lateral confinement of the sample ( $K_0$  condition) assumed in the solution of the Terzaghi's consolidation theory.

S. Prowono (1981) carried out three types of Oedometer tests.

Lever arm Type Oedometer Tests :

These were conventional lever-arm Oedometer tests on specimens of 63.5 mm diameter and 19.1 mm thickness containing a central sand drain. The porous strains on both sides of the specimen were replaced by annular steel plates having a central hole of the same diameter as the drain. The load increments applied were 0.25, 1, 2, 4, 8, with load increment duration of 24 hours.

Bishop Hydraulic Type Oedometer Tests :

In order to ensure only radial drainage to occur during consolidation a piece of thin plastic having a central hole of same diameter as the central drain was placed between specimen and bottom porous plate. The specimen was consolidated under a back pressure of 276 KPa. Pore pressure measurements were taken during the test due to the limited size of the specimen.

Rowe type Oedometer Tests :

In this type of Oedometer, the specimens had a diameter of 152 mm and a thickness of 25 mm. Sarnzo (1983) conducted triaxial consolidation and piezometer probe tests to determine the coefficient of permeability at harbour of Sybarin. He used conventional rigid ring Oedometer and triaxial cell for these experiments. Shroff and Parikh used 152 mm and 254 mm diameter Rowe type Oedometer to study the nature of isochrones in radial consolidation of clays. Shroff and Rana (1994) and Shroff and Bhatt (1995) studied the influence of various geodrains on the consolidation characteristics of Kaolinite clays. They used 152 mm and 254 mm diameter Rowe type Oedometer with hydraulic pressure system controlled by self compensating mercury apparatus. To record and monitor the measurement, pore pressure transducers, displacement

transducers and data acquisition system were used. Data acquisition system was attached to printer and PC to ensure the printing and storing of the data.

### 5.3 DESCRIPTION OF PRESENT SETUP

The experimental setup used in the present investigation is shown in the Photo- and Fig-

The complete setup consists of:

1. Hydraulic Pressure System.
2. Oedometer.
3. Pore pressure measurement system.
4. Settlement measurement system.

#### 5.3.1 Hydraulic Pressure System

The system to apply pressure on the soil specimen is a self compensating mercury control pressure system as shown in Photograph- 5.2. The volume change self compensating mercury control unit is based on the principles outlined by Bishop and Henkel. The pressure of the water is the rubber jacket at the top of the soil sample in the Oedometer results from the difference in the levels of mercury in the two cylinders, one at some height and another at bottom, connected by a thin flexible Polypropylene pressure tube.

If  $h_1$  and  $h_2$  are the initial levels of the two mercury surfaces, and  $h_3$  is the level of the sample, measured above same datum, then the water pressure at the level  $h_3$  is ' $\sigma$ ', where,  $\sigma = (h_1 - h_2)\gamma_m + (h_2 - h_3)\gamma_w$ ,

$\gamma_m$  = Unit weight of mercury,

$\gamma_w$  = Unit weight of water

If a volume decrease occurs in the sample due to consolidation or if leakage takes place from jacket etc. water will be lost from the bottom cylinder no.2 and the mercury level will rise in the cylinder by  $\Delta h_2$ , resulting in a corresponding drop of mercury level in the upper cylinder no.1 if the cylinders are of same diameter. It follows that

$$-\Delta h_1 = \Delta h_2 = \Delta h$$

If both cylinders remained stationary, fig. 5.5, pressure will change to  $\sigma + \Delta\sigma$ ,

Where  $\sigma + \Delta\sigma = (h_1 - \Delta h - h_2 - \Delta h)\gamma_m + (h_2 + \Delta h - h_3)\gamma_w$



That is  $\Delta\sigma = -(2 \gamma_m - \gamma_w) \Delta h$

If however, the level of the upper cylinder is raised by a distance  $\Delta l$ , fig. 5.5, the value of

$\sigma + \Delta\sigma$  becomes

$$\sigma + \Delta\sigma = (h_1 + L - h - h_2 - h) \gamma_m + (h_2 + h - h_3) \gamma_w,$$

$$\text{that is} \quad \Delta l = (2 - \gamma_w / \gamma_m) \Delta h$$

Since the drop in mercury level,  $h$  in the upper cylinder reduces its weight, the cylinder can be made to adjust its own level automatically if it is hung on a spring of the appropriate stiffness.

The decrease in weight due to drop in mercury level  $\Delta h$  is  $A \cdot \gamma_w \cdot \Delta h$ , where 'A' is the cross sectional area of the cylinder. The shortening of the spring  $\Delta L$ , must correspond to this reduction in weight and also allow for the additional length  $\Delta L$  of the flexible tube filled with mercury which is lifted from the floor. If 'w' is the weight of unit length of this tubing. Then the necessary spring stiffness is 'K' kg per cm extension, where,

$$K \cdot \Delta L = A \cdot \gamma_w \cdot \Delta h - w \Delta L$$

$$\text{Now } \Delta L = (2 - \gamma_w / \gamma_m) \Delta h$$

$$\text{Therefore, } K = A \cdot \gamma_w / (2 - \gamma_w / \gamma_m) - w$$

No change in hydraulic pressure will be observed even if consolidation takes place or leakage through the jacket takes place.

The basic layout of the pressure system is illustrated in fig. 5.5 and the procedure for routine testing is as follows:

- Check that the mercury can be admitted to cylinder No.1 by opening valves of C,D and G and applying pressure from the screw controlled pressure piston.
- Open valve A, and raise the cylinder No.1 until the pressure gauge shown the required pressure to be applied on the Oedometer.
- Close valve G and open valve B and E to admit water into the rubber jacket.
- Raise the pressure in the rubber jacket to the required level by opening the valve C and displacing water from screw controlled pressure piston. Valve C is closed and valve G is opened.

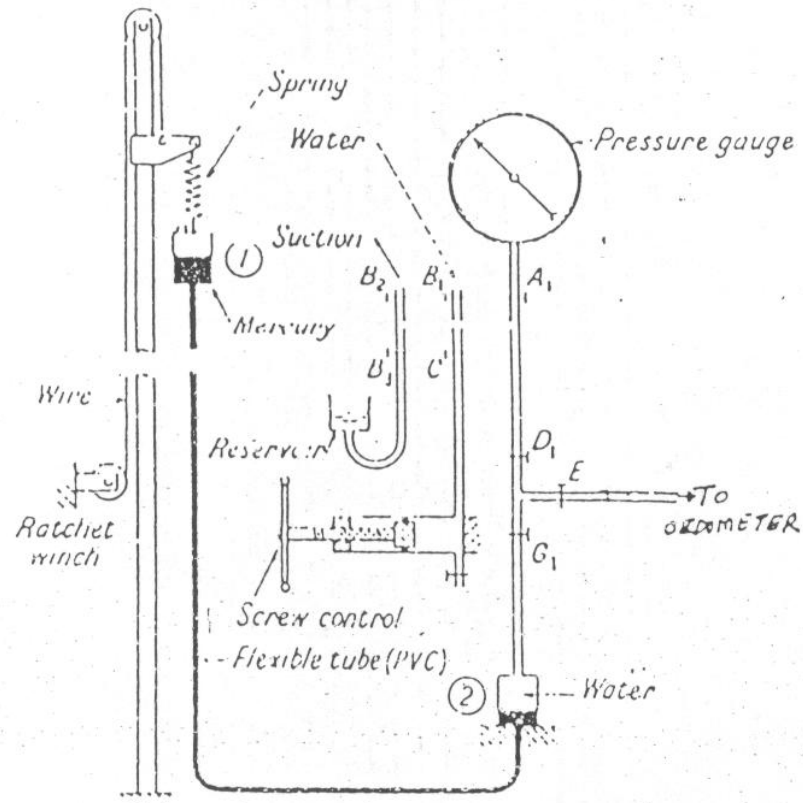


**Fig.5.5:** Basic layout of pressure system

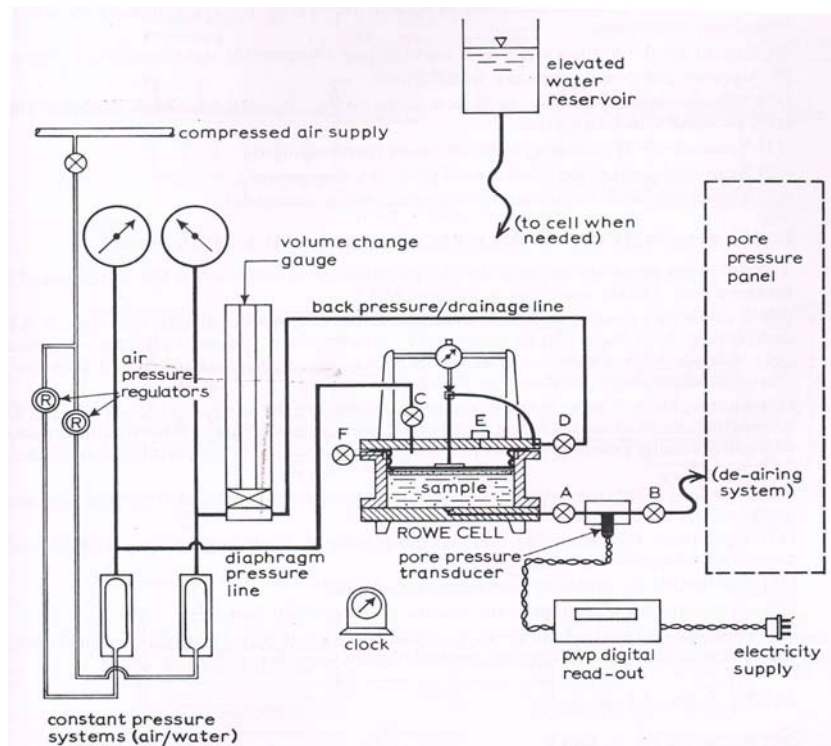
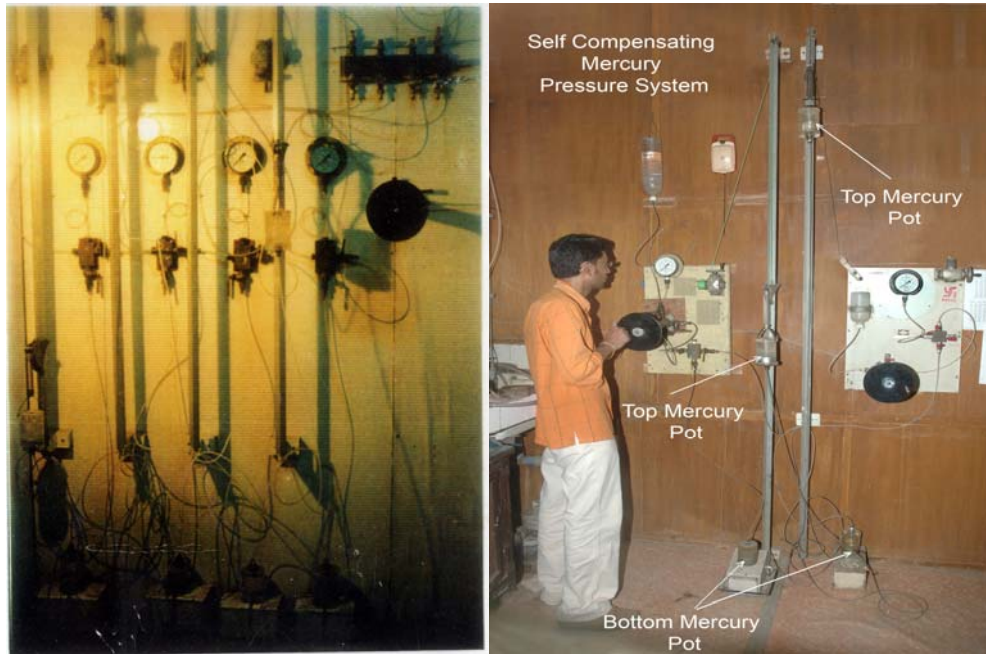


**Fig.5.6:** General arrangement of ancillary equipment used with the Rowe cell

- Pressure measuring system consisted of Bourdon pressure gauge of range  $0-10.6\text{kg/cm}^2$ . With least count of  $0.1\text{kg/cm}^2$ . In present investigation the calibration and repair of the pressure gauge was carried done. Photograph 5.2 and fig.5.6 shows such a self compensating mercury control pressure system used in the present testing.



**Photograph 5.2:** Self compensating mercury pressure system

### 5.3.2 Modified Hydraulically Pressurised Oedometer

In the present experimental investigation Rowe type Oedometer of 254 mm (10") diameter and 152mm (6") is modified for the measurement of pore water pressure at various sequences of consolidation. Modified Oedometer consists of the following parts:

- i. Top Plate.
- ii. Middle Ring.
- iii. Bottom plate.
- iv. Convoluted rubber jack

#### Top Plate :

It is made of aluminum and is 20 mm thick with central hole to convey brass rod for the drainage from the soil sample through central washer of the rubber jacket.

It has the following connections. Valve at the top surface to receive pressure line from hydraulic pressure system. Air valve at the top surface to fill water into the jacket and to release air from the jacket. Drainage hole at the top surface leading to settlement valve. The settlement valve is provided at the periphery of the plate to regulate the consolidation process. The drainage hole has threading for nut, which allows the hollow brass rod which in turn carries elbow at the top for installing extensometer or displacement transducer on it. The rod can move up and down against 'O' ring fitted in nut. A cast iron frame is required for fixing the dial gauge and displacement transducer. Rubber jacket is fitted at the bottom end at the brass rod through washer which seats on middle ring during assembling for providing the hydraulic pressure on the soil sample and sealing the space between the top plate and middle ring.

The Middle Ring :

It is the middle portion of the oedometer, made up of brass and has an internal diameter of 254mm; it contains the soil sample to be tested. The middle ring fits on the base plate of the Oedometer against a 'O' ring positioned in a circular slit of base plate. The peripheral bolts, when fixed between top and bottom plates, holds the ring into its position and at the same time removes possibilities of any leakage.

The Bottom Plate :

There are two bottom plates due to two sets of Oedometer. It is made up of brass and 254 mm size Oedometer has thickness of base plate as 25 mm and that of 152 mm has thickness of 20 mm. It has following features:

Both bottom plates have a central circular housing for receiving central porous stone to allow pore water from the sample through drain well. Bishop pore pressure measuring system is connected to it through a valve to regulate and measure the pore pressure developed and dissipated during testing. In case of 152 mm (6") diameter, base plate has radial housing at three radial distances located at 120 degree to each other with  $(r/r_e)$  equal to 0.362, 0.566 and 0.776 with the distances of 27.5 mm, 43 mm and 59 mm from the center. While in case of 254 mm (10") diameter, bottom plate has radial housing at three radial distances located at 120 degree to each other with  $(r/r_e)$  equal to 0.20, 0.55, and

0.87 with the distances of 25.4 mm, 71.0 mm and 110.0 mm from the centre and are provided to measure the pore water pressure at three locations to obtain the radial distribution of pore pressure for respective loading condition. Valves connected to these location leads to Bishop pore pressure measuring apparatus and pore pressure transducer for simultaneous measurements connected to Data logger system interfaced with PC.

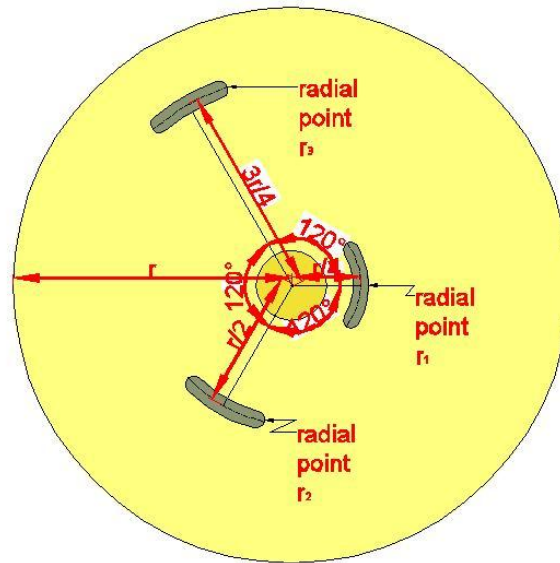


Fig.5.7: Bottom plate with measurement points and location

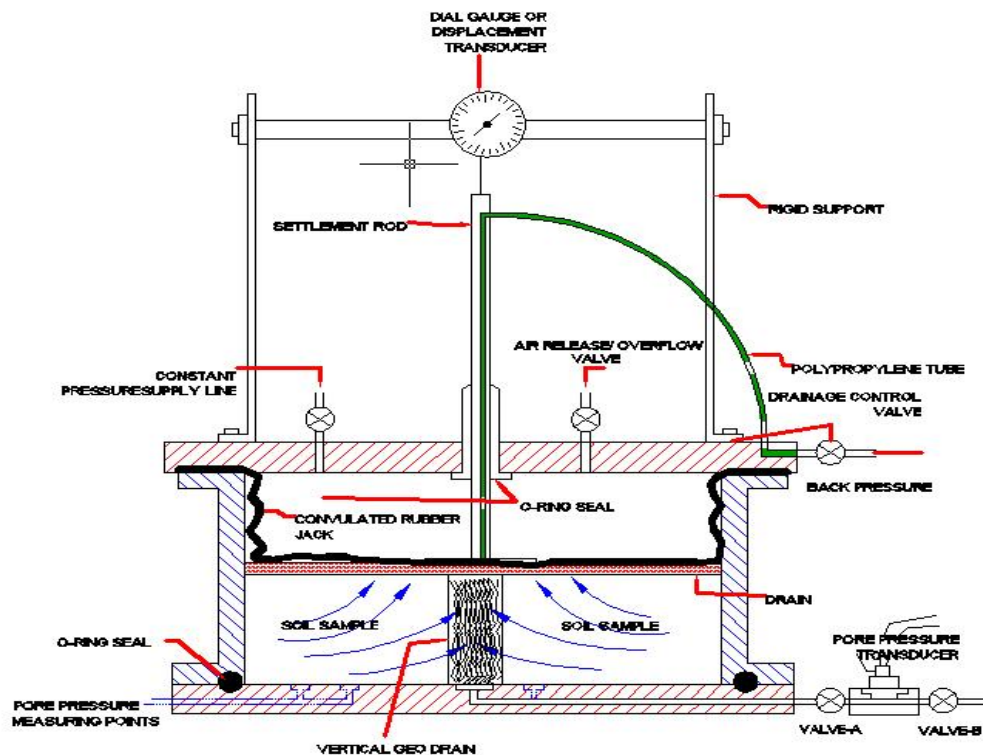


Fig.5.8: Sectional view of Oedometer with measurement points

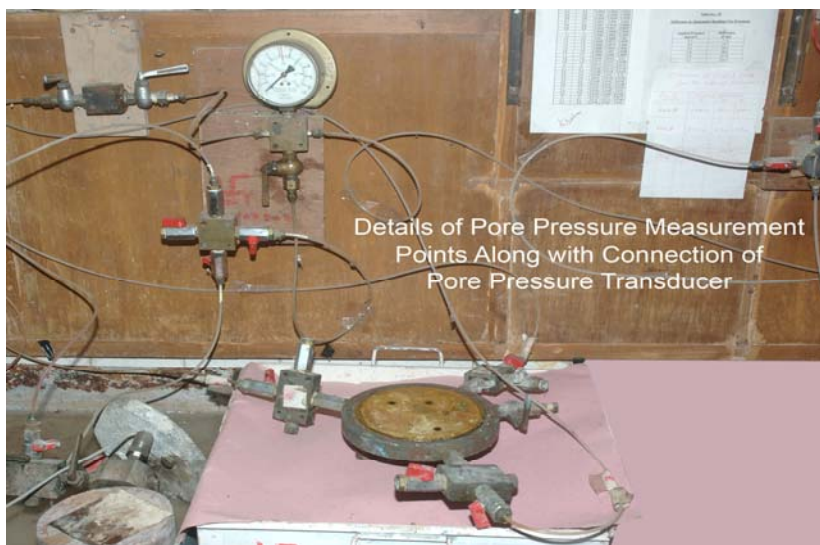


Convuluted Rubber Jack:

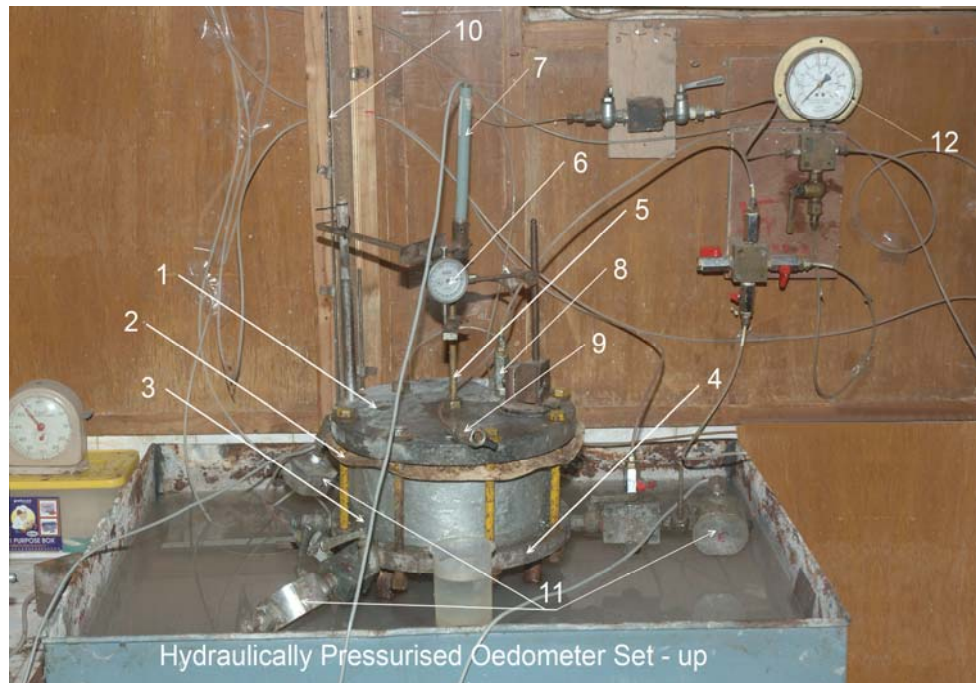
Convuluted rubber jack is made from 0.07 inch thick white rubber (M/S Franklin ltd, England) is used to transmit equal pressure at all the corners and coordinates of the sample with respect to horizontal plane. It can transmit maximum pressure without losing the inherent elasticity of material. A stiff top plate is introduced between the rubber jacket and the sample to simulate equal strain condition in the test it allows drainage during consolidation through porous stone provided. The complete Oedometer assembly is shown in Fig. 5.7 and Fig.5.8. The different components of Oedometer and complete set-up of Oedometer is shown in Photograph.5.3, 5.4 and 5.5 respectively.



**Photograph 5.3:** Complete Oedometer assembly with its components



**Photograph 5.4:** Bottom plate with connections to pore pressure measuring points at 120° each



**Photograph 5.5:** Complete hydraulically pressurized Oedometer set-up

- |                          |                               |
|--------------------------|-------------------------------|
| 1) Top plate             | 7) Displacement transducer    |
| 2) Convolute rubber jack | 8) Pressure inlet             |
| 3) Middle ring           | 9) Drainage valve             |
| 4) Bottom plate          | 10) Mercury manometer U tube  |
| 5) Brass settlement rod  | 11) Pore pressure transducers |
| 6) Dial guage            | 12) Pressure meter            |

The conventional compression not machine is used for measurement as it has following limitations.

1. It does not give the measurement of pore pressure during consolidation.
2. The point load given to it distributes the soil pressure.
3. Stress distribution is not better in the soil.

### 5.3.3 Settlement Measurement System

Settlement is recorded by following method conventional System:

It is mechanical mode of measurement and a dial gauge of least count 0.002 mm is used, fixed at position as shown in the photo. It is held in convenient position with the help of frame work fixed on the top plate of the Oedometer. In the present set-up LVDT (linear variable differential transformer) based displacement transducers were used, interfaced with 16 channel data acquisition

system connected to PC and Printer. This data logger system was synchronized with LabVIEW 8.2 software for continuous measurement of compressibility (settlement). The only disadvantage of this software was that it requires continuous power supply.

#### **5.3.4 Pore Pressure Measurement System**

It is possible to measure pore water pressure developed in the soil by different techniques.

##### **5.3.4.1 Bishop's Pore pressure measuring system**

It is the conventional mechanical system, developed by Bishop for measurement of pore water pressure. Photograph 5.4 shows the layout of Bishop's pore pressure apparatus. It is mainly consisting of following:

- a. The Null Indicator
- b. The Screw pump
- c. Pressure Gauge
- d. Mercury manometer
- e. Burette

The null indicator consists of perspex prism having 'U' shaped mercury capillary connected to mercury reservoir. Other components are connected as shown in photograph 5.4. An increase in pore pressure in the sample during the initial increase of pressure will tend to depress the mercury level in the limb of the null indicator, which is preadjusted at some particular height before application of pressure. This depression can be immediately balanced by adjusting the piston of screw pump to increase the pressure in the capillary by an equal amount, which can be read in the pressure gauge. During the measurement of dissipation of pore pressure during the consolidation, vice a versa measurements are required to be carried out. Valves connected with manometer, reservoir and burette are kept closed during this measurement.

A peculiar behavior of the null indicator was observed during this investigation. Null indicator does not act as a trap if the water pressure coming to it is sudden and fast. The mercury though heavier than water 13.6 times will give space to the sudden water flow and water over passes the mercury by making side paths. This phenomenon was observed when calibration test was done on water



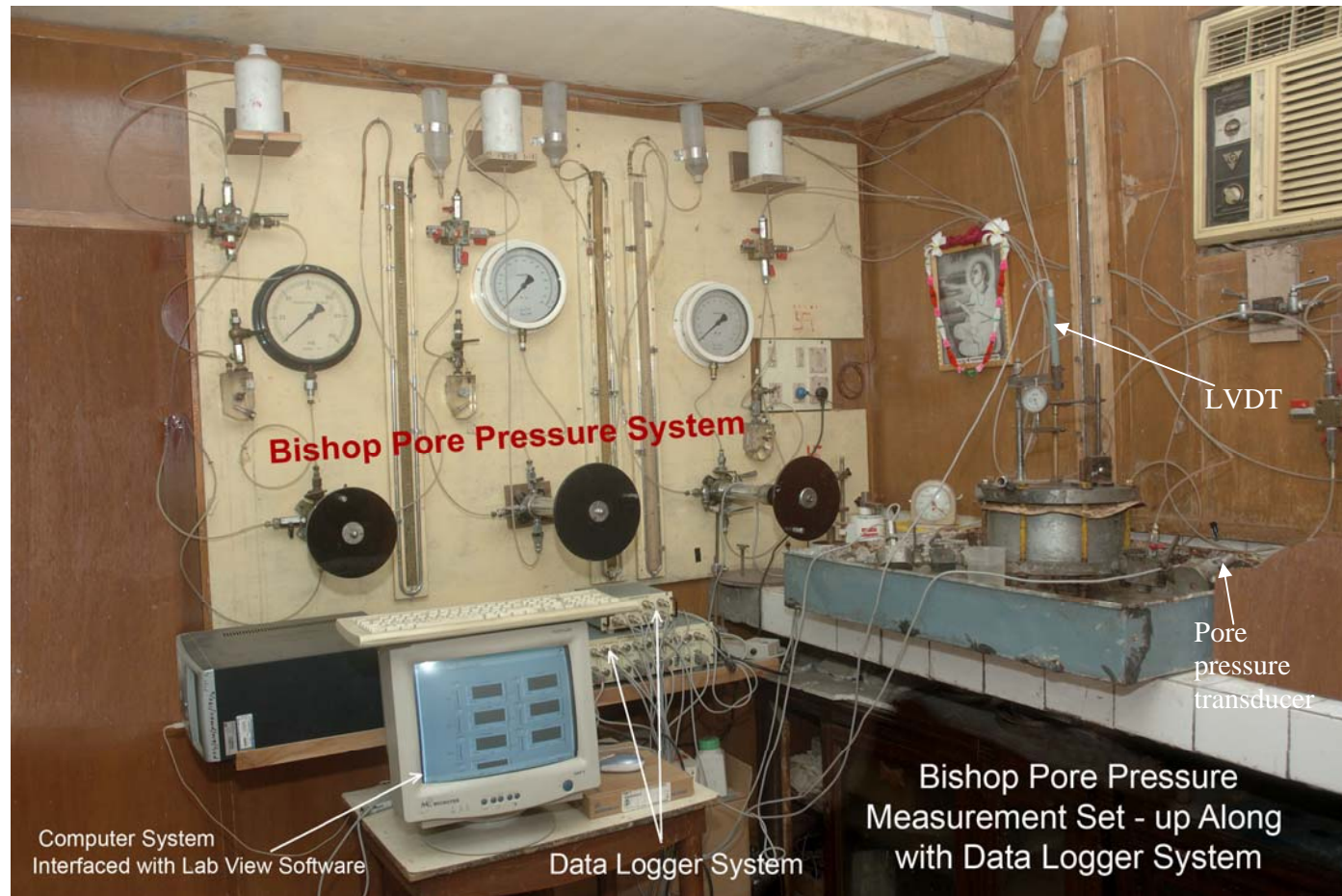
sample instead of soil sample. But however as the flow of pore water pressure is slow in consolidation test the null indicator behaves as a trap for this case.

#### **5.3.4.2 Transducers and Data Acquisition System**

For immediate response of pore pressure measurement the use of electronic pore pressure transducers is desirable, which converts mechanical pressure to millivolt, amplifying to volt through amplifier and read on DVM (Digital Volt Meter) in digits. The conventional method of pore pressure measurement shows time-lag due to system flexibility. To avoid this problem in our case, all the three manometer 'U' tubes along with pressure pump and pressure gauge were connected very nearer to each other.

Gibson (1963) investigated the relation between this time lag, permeability and compressibility of soil and the compliance of the measuring system. Northey-Thomas (1965), Perloff et al. (1965), Wissa (1969), Bruhn (1972), Bishop (1973), Mesri (1976) and Bishop (1976) demonstrated the importance of the influence of system flexibility on the observed pore water pressure response in saturated soil to an undrained change in stress. Transducers used for pore pressure measurement in the system are of spring loaded LVDT type. Internally, the sensor consists of a spring loaded probe/shaft assembly (force of 6 to 20 ounces, model dependant), which runs along two precision sleeve bearings. The end of the shaft is connected to the core of an LVDT. The coil of the LVDT is located inside the body. As the probe is depressed, the relative position of the core to the coil changes, thereby increasing the output of the LVDT. The output can then be connected to any standard (differential input) LVDT signal conditioner to create a variety of analog or digital outputs, or directly to the data acquisition system.

Data Acquisition System used in the present work is 8 channel based latest in technology for measurement of pore water pressure, and settlement at different time interval, simultaneous channelizing and recording the data during consolidation process. The system is connected with LabVIEW 8.2 software for recording measurements and analysis purpose. The complete set-up of Oedometer with data acquisition system, conventional Bishop mercury pressure system, displacement transducers, pore pressure transducers is shown in photograph 5.6.



**Photograph 5.6:** Complete view of laboratory of Consolidation of soft clays through radial flow

## 5.4 METHOD OF SOIL SAMPLE PREPARATION

The soil used for this investigation was clay mineral Kaolinite obtained commercially in the form of powder with the properties already mentioned in Table-3.9. of chapter 3. To ensure full maturation of the sample the clay was mixed to form slurry with twice the liquid limit using de-aired distilled water. Density was sufficiently low to allow the removal of entrapped air when the sample in the consolidation cell was vibrated.

The slurry was transferred into the Oedometer after the cell body had been lightly coated with a thin layer of silicon grease to minimize side friction; the Oedometer was then placed on a handle operated vibrator and was vibrated for approximately one hour after which only occasional air bubbles could be seen on the surface. The clay was then scribed level, thereafter filter paper followed by a porous stone was placed at the top.

The sample was then preconsolidated under a gradually applied static load of 8 kPa, with  $\Delta p/p = 1$ , (1kPa, 2kPa, 4kPa, 8kPa) so that the consolidation occurring is normal (Normal consolidated soil is one which has been never subjected to an effective pressure greater than the existing pressure nor greater than the existing overburden pressure and which can also be completely consolidated by the existing overburden). In this normal consolidation case virgin compression curve gives a straight line. Terzaghi in his basic theory explained by spring analogy which gives that within elastic limit load deflection curve may be assumed to be straight this is a case of normal consolidation. These increments are given by means of dead load with porous stone on the top of the clay sample topped by filter paper so that sample during consolidation water gets removed through porous stone. These increments of static loads are to be kept for a longer period of time (at least 48 hours). Increments are calculated as shown below

$$\begin{aligned}\text{Area of Oedometer} &= \pi/4 \times d^2 \\ &= \pi/4 \times (25.4)^2 \\ &= 506.708 \text{ cm}^2\end{aligned}$$

$$\begin{aligned}\text{For 8 kPa, load} &= 506.708 \times 8 \\ &= 40.53 \text{ KN}\end{aligned}$$

The porous stone was then removed and the shear strength of the sample was then measured by vane shear apparatus as shown in Photograph-5.7. and representative sample for the determination of water content was taken. The porous stone was then replaced. Height of the sample is measured after scribing, from top of Oedometer with respect to total inner height of Oedometer. Filter paper is kept on the clay sample and then acrylic plate with a housing of porous stone topped over it to have equal strain condition throughout the consolidation test.

De-aired distilled water was poured into the rubber jacket already filled with desired distilled water was lowered into position through the water to exclude trapped air pockets. The cell cover was next sealed into position and an initial consolidation pressure of 10 kPa was applied from the hydraulic pressure system then built gradually to 20 kPa on the next day to avoid passage of slurry around the porous stone. When the sample was fully consolidated as indicated by the zero excess pore water pressure on the Bishop pore pressure measuring apparatus, the cell cover and the porous stone was removed and the sample scribed level to the required thickness using a specimen height trimmer.



**Photograph 5.7:** Vane shear set-up with soil sample

## **5.5 VERTICAL DRAIN DESIGN, SELECTION, FABRICATION, TESTING & INSTALLATION**

Numbers of vertical drains are now available in the market under various commercial names, but most of them are prefabricated vertical drain (PVD) of band shape.

In the present investigation, emphasis was put on to explore the both natural and artificial (synthetic and non- synthetic) and easily available materials which can simulate prototype behavior of soft soil in laboratory. These materials include sand, polypropylene fibers, woven and non-woven geotextiles, coir fibers, jute fibers, filter paper and other synthetic fabrics.

Vertical drains are artificially-created drainage paths which can be installed by one of several methods and which can have a variety of physical characteristics. The principal benefits of a vertical drain system (i.e., of accelerated consolidation) are:

- To decrease the overall time required for completion of primary consolidation due to preloading,
- To decrease the amount of surcharge required to achieve the desired amount of precompression in the given time,
- To increase the rate of strength gain due to consolidation of soft soils when stability is of concern.
- Vertical drains can also be used as pressure relief wells to reduce pore pressures due to seepage, such as below natural slopes, and to improve the effectiveness of natural drainage layers below loaded areas.

### **5.5.1 Vertical drains classification**

- 1) Sand drains
- 2) Geocomposite vertical drains
- 3) Prefabricated vertical drains

In the present research, the combination of all the above mentioned three types of vertical drains is considered:

- (1) Sand drains (SD): Further classified as
  - (a) Conventional circular shape sand drain (CSD)
  - (b) Geometrical shape sand drain: (i) Plus shape sand drain (PSD)
    - (ii) Tripod shape sand drain (TSD)
    - (iii) Band shape sand drain (BSD)
- (2) Sandwicks (SW)
- (3) Coir-Jute drain (CJ)
- (4) Polypropylene fiber drain (PF)

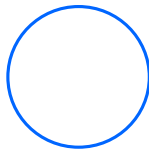
### 5.5.2 Drain design and guidelines

Vertical Drain designs were done on the basis of 'n' value (ratio of drain diameter to soil sample diameter) as dictate in chapter 3. All the mentioned above vertical drains were circular in cross-section and cylindrical shape unless specified. The design of various drains is as follows:

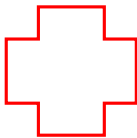
#### 5.5.2.1 Design of sand drain

| Sr.No | 'n' value | Diameter of Oedometer (mm) | Diameter of drain(mm) | Type of mandrel used | Area ratio (%)and thickness of mandrel (mm) |
|-------|-----------|----------------------------|-----------------------|----------------------|---|
| 1     | 11.04     | 254 &152                   | 23 & 13.77            | Open end thin wall   | 1.6 & 0.55                                  |
| 2     | 16.93     | 254 &152                   | 15 & 8.97             | Open end thin wall   | 1.6 & 0.55                                  |
| 3     | 21.71     | 254 &152                   | 11.70 & 7             | Open end thin wall   | 1.6 & 0.55                                  |

#### 5.5.2.2 Design of Geometrical Sand drains



Circular



Plus



Tripod



Band

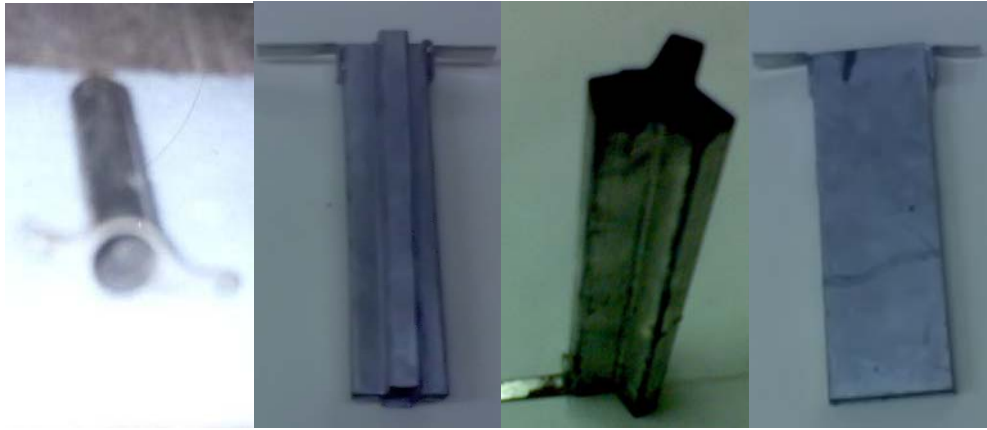
| Sr. No | Geometrical shape | 'n' value | Diameter of Oedometer (mm) | Equivalent Diameter of drain (mm) | Type of mandrel used | Area ratio (%) and thickness of mandrel (mm) | Breadth of drain ( $B_d$ ) and thickness of drain |
|--------|-------------------|-----------|----------------------------|-----------------------------------|----------------------|--|---|
| 1      | Circular (CSSD)   | 11.04     | 254 & 152                  | 23 & 13.77                        | Open end thin wall   | 5 & 0.55                                     | ----  |
| 2      | Plus (PSSD)       | 11.04     | 254 & 152                  | 23 & 13.77                        | Open end thin wall   | 5 & 0.55                                     | $8B_d + 4T_d$                                     |
| 3      | Tripod (TSSD)     | 11.04     | 254 & 152                  | 23 & 13.77                        | Open end thin wall   | 5 & 0.55                                     | $6B_d + 3T_d$                                     |
| 4      | Band (BSSD)       | 11.04     | 254 & 152                  | 23 & 13.77                        | Open end thin wall   | 5 & 0.55                                     | $\frac{2(B_d + T_d)}{\pi}$                        |

#### Selection, Formation and Installation of sand drains:

After trimming the surface, the axial hole was formed with a thin walled mandrel, having area ratio of 0.8 to 1.6 attached with template and guide frame. A drain hole was then flooded with water from the central connection to the reservoir. The drain was filled with de-aired saturated sand (as per gradation) with the aid of small diameter flexible tubing by syphonic action to cause little smear. With least possible time gap a top rigid plate with a porous stone at the centre was placed. The top cover is then seated into position. A proper care of the complete removal of the clay from the bore hole is to be assured so as the clay does not fill the sand drain and block the drainage path during consolidation. The same above procedure is also followed for geometrical sand drains. While during design of geometrical sand drains for 'n' value of 11.04, the specific surface area is kept constant for circular, plus, tripod and band shape, that is equivalent diameter of all four drains is kept same. Regarding the physical and index properties of sand materials determined in laboratory and used in drain fabrication is already mentioned in table no. 3.10 of chapter 3 and fig.5.3. The types of mandrels used for installation of sand drains is shown in photograph 5.8. The formation of bore hole using mandrel and installation of sand drain and



geometrical shape sand drains in sequential form is shown in photograph 5.9 & 5.10.



**Photograph.5.8:** Mandrel of plus shape, circular shape, band shape & tripod shape



**Photograph.5.9:** Top platen installation, bore hole formation using circular mandrel and clay sample with central vertical sand drain ready for testing



**Photograph.5.10:** Formation of plus shape , tripod shape and band shape bore hole using mandrel for geometrical shape sand drains



### 5.5.2.3 Design of Sandwichs (SW)

| Sr.No | 'n' value | Diameter of Oedometer (mm) | Diameter of drain(mm) | Type of mandrel used | Area ratio (%) and thickness of mandrel(mm) |
|-------|-----------|----------------------------|-----------------------|----------------------|---|
| 1     | 11.04     | 254 & 152                  | 23 & 13.77            | Open end thin wall   | 1.6 & 0.55                                  |
| 2     | 16.93     | 254 & 152                  | 15 & 8.97             | Open end thin wall   | 1.6 & 0.55                                  |
| 3     | 21.71     | 254 & 152                  | 11.70 & 7             | Open end thin wall   | 1.6 & 0.55                                  |

The sandwich consist of prepacked geotextile cylindrical bag having diamter as per 'n' value. The polypropylene geotextile bag prepared before the test with height equal to that of sample. The sand and bag are deaired in warm water. The detail properties of sand used as filler and geotextile as outside cover are mentined in table no.3.11, 3.12(a) and 3.12(b) of chapter 3. The outside cover that is polypropylene geotextile bag is fabricated indigeneously at the Geotechnical Engineering laboratory in association with Textile Engineering Laboratory of the M.S University of Baroda. Saturated sand was filled in the bag under syphonic action with sufficient head to fill the sand in the bag with pressure. The wick thus prepared is inserted (placed) in the predrilled hole, formed by thin mandrel at centre of the soil sample in the Oedometer with sufficient care so that no smearing occurs to the wall of the predrilled hole. A photograph 5.11 shows the prepared sandwich used in present testing. A very important tests was developed to determine coefficient of radial permeability of complete composite vertical drain under constant head for any diamter of drain so as to get true discharge capacity of drain as a whole. The detail description of this test is mentioned later on in this chapter.

#### Selection, Formation and Installtion of Sandwich:

In general thermoplastics are durable in most soil conditions. It has made possible the use of fabrics in Civil Engineering because natural fibers do not remain stable for long in a soil environment. These polymer based fabrics are not affected by normally occuring alkalis and acids, and they are resistant to bio-

degradation. They do not, of themselves, provide nourishment for rodents or micro-organisms. Amongst all the thermoplastic materials like polyester, polyamide, polyethylene, polypropylene, acrylic, steam etc. Therefore, in present investigation for preparing prepacked geotextile sandwich, polypropylene geotextile is used.

*Advantages of present fabrics:*

- i. Multifilament fabrics are flexible, compared to mono filament fabrics. Mono filament fabrics are stiff.
- ii. Spun yarn of same denier and some construction will have lower strength compared to multi and mono filament fabrics of some construction. The idea of selecting multi-filament fabrics is to get flexible cloth so that it can bend under compression and do not get burst.
- iii. As polypropylene fabric has more extension, compared to other synthetic fabrics, it is more advantageous as it will burst at much latter stage compared to low extension fabrics.
- iv. Plain weave fabrics is selected to get maximum stability and highest abrasion resistance compared to any other weave.
- v. The air permeability is selected little higher then required, with precaution that even if the compression is of the order of 30%, the permeability would not be lower than minimum required for draining water.
- vi. The bursting strength of the fabrics is very high so that it can resist multi-directional force caused by soil or sand.
- vii. Multifilament fabric has high capillary action, compared to monofilament and spun fabric.
- viii. For the same weight of fabric woven fabrics has higher strength compared to non-woven fabrics.

The laboratory model of sandwich prepared as above procedure is to be installed in its position in predilled hole using mandrel of exactly same outer diameter as that of the sandwich. Important precaution is taken for the height of sandwich that should correspond exactly with the height of sample. During this installation, care is taken for the saturation of the sandwich. Water sprinkling is done to ensure water continuity with porous stone. Immediately after installation, top rigid plate is placed on the sample.



**Photograph.5.11:** Sandwich ('n'11.04) ready for installation and clay sample with central sandwich

#### 5.5.2.4 Design of Coir-Jute drain (CJ)

| Sr.No | 'n' value | Diameter of Oedometer (mm) | Diameter of drain(mm) | Type of mandrel used | Area ratio (%) and thickness of mandrel(mm) |
|-------|-----------|----------------------------|-----------------------|----------------------|---|
| 1     | 11.04     | 254 & 152                  | 23 & 13.77            | Open end thin wall   | 1.6 & 0.55                                  |
| 2     | 16.93     | 254 & 152                  | 15 & 8.97             | Open end thin wall   | 1.6 & 0.55                                  |
| 3     | 21.71     | 254 & 152                  | 11.70 & 7             | Open end thin wall   | 1.6 & 0.55                                  |

Coir-jute vertical drain consist of 75% jute fiber + 25% coir fiber encapsulated by filter paper (Whatman-Grade 591) in form of cylinder as per 'n' value. The jute fibers are almost straight and are arranged in a form of bunch of fibers, while coir fibers are either twisted or little bit circular in nature are mixed and placed in three ways: (i) Coir-jute fibers are placed only vertically (ii) Coir-jute fibers are placed only radially (iii) Coir-jute fibers are placed partially vertical and partially radial. Out of these this arrangements the fibers placed partialy vertical and radial was used as it gives more permeability and also showed more % strain compare to above two cases. The properties of coir and jute fibers used in present investigtion is mentioned in table no. 3.15 and 3.16 in chapter 3.

#### **Selection, Formation and Installtion of Coir-Jute drain:**

Geotextiles are of two types: synthetic and natural. Natural geotextiles include jute burlaps, jute meshes, jute nets, jute mats and other natural jute

fabrics. Before using jute and coir fibers as vertical drain, detail experimental investigations were carried out on jute fibers and coir fibers in order to study their physical and strength properties and performance characteristics. From these investigations, the typical properties of jute and coir fibers were fairly established. (refer table no. 5.1)

Various tests that were conducted to evaluate the performance of jute fibers and coir fibers (twisted coconut fiber threads) include sustained load test, rutting test and dynamic load test. Also the detail properties of coir and jute fiber used in present investigation are mentioned in table no. 3.15, 3.16 and 3.18 in chapter 4. The coir fibers is found to last at least four times longer than the jute fabric itself, in any given environment. It is found to assist by its strong reinforcing effect not only when the jute fiber is functioning, but also continues to contribute as a reinforcing net left underneath the deteriorated jute fibers. To reduce the microbial attack and faster degradation, jute can be treated with chemical agents like phenol, tri-cisly phosphate/tri-tolyl phosphate etc. A few other antimicrobial agents are:

- i) organomercuric compounds
- ii) copper compounds: a) copper 8-hydroxy quinoline    b) copper pentachlore phenolate    c) organo Tin and Zinc compounds
- iii) Quaternary ammonium compounds
- iv) Dodecyl guanidine chloride
- v) Mercapto benzthiazol

**Table.5.1:** Typical chemical composition and physical properties of Coir fibers:

| Sr.No. | Properties                    | Range of Values             |
|--------|-------------------------------|-----------------------------|
| 1      | Lignin                        | 45.84%                      |
| 2      | Cellulose                     | 43.44%                      |
| 3      | Hemi-Cellulose                | 0.25%                       |
| 4      | Pectin's and related Compound | 3.0%                        |
| 5      | Water soluble                 | 5.25%                       |
| 6      | Length in inches              | 6-8                         |
| 7      | Diameter in mm                | 0.1-1.5                     |
| 8      | Density (g/cc)                | 1.4                         |
| 9      | Tenacity (g/Tex)              | 10.0                        |
| 10     | Breaking elongation           | 30%                         |
| 11     | Rigidity of Modulus           | 1.8924 dyne/cm <sup>2</sup> |
| 12     | Swelling in water (diameter)  | 5%                          |
| 13     | Moisture at 65%RH             | 10.5%                       |

Coir is a versatile hard fibre obtained from the husks of coconut. Coir is a natural biodegradable organic fiber material containing cellulose (nearly 54%) and lignin (nearly 46%). The rate of decomposition of coir fiber is generally known to be less than that of any other natural fibers, such as jute, cotton, and others, due to the high lignin content. Coir retains 20% of its strength even after one year. Coir is abundantly available in most parts of south and coastal India, Sri Lanka, Philippines, Indonesia, Malaysia, Brazil, and others. Rao and Balan (2000) compiled considerable information on the properties of coir fiber and its uses in engineering applications. The main advantages of coir fibers compared to other natural fibers are its high initial strength, stiffness, and hydraulic properties. If the requirement is for a shorter period, then coir is the best choice due its biodegradability compared to synthetic fibers. If it has to be used for longer period, then chemical treatment and polymer coating will improve the life of the coir product. Of all natural fibers coir processes the greatest tearing strength, retained as such even in very wet conditions.

Coir is a sufficiently Eco-friendly product and so its application will never sustain any damages to environment and so is far free from resentments. Coir fiber act both as filler and filter when fabricated as vertical drain. Coir fibers differ from jute fibers in another aspect as well, jute fibers exhibit moderately high modulus as well as high tenacity and very low elongation at break whereas coir fibers behave exactly in the opposite manner, namely moderately low modulus, low tenacity and very high elongation at break (Guha, 1995). So logically bending of these two fibers forms ideal partners. Hence in present investigation we propose to use mixture of coir and jute fibers placed radially wrapped (encapsulated) by filter paper to accelerate rate of consolidation of soft soil.

Jute fibers being hydrophilic absorb a high amount of water causing swelling of fibers. They suggested that swelling of jute fibers in a composite material can have positive effects on mechanical properties, Karmaker Hoffmann et al., (1994).

#### Effect of fiber diameter

Stress–strain curves for fibers of different diameters were obtained. Fig. 5.9a shows a typical stress–strain curve of a Brazilian coir fiber of 0.131 mm diameter and gauge length of 20 mm, tested at a strain rate of 5 mm/min. For comparison,

that for an Indian coir fiber of diameter 0.250 mm and 50 mm test length, tested at 20 mm/min, is shown in Fig. 5.9b. The strength properties thus evaluated are presented as a function of diameter in Fig. 5.10. It can be seen that both tensile strength and elastic modulus of fibers decrease with increasing diameter within the range studied (0.04–0.40 mm) but contrary to the values observed for Indian coir fibers. On the other hand, the strain at failure, although showing some variation, may be considered as roughly constant at around 30%, which is again opposite to that observed in the case of Indian coir fibers.

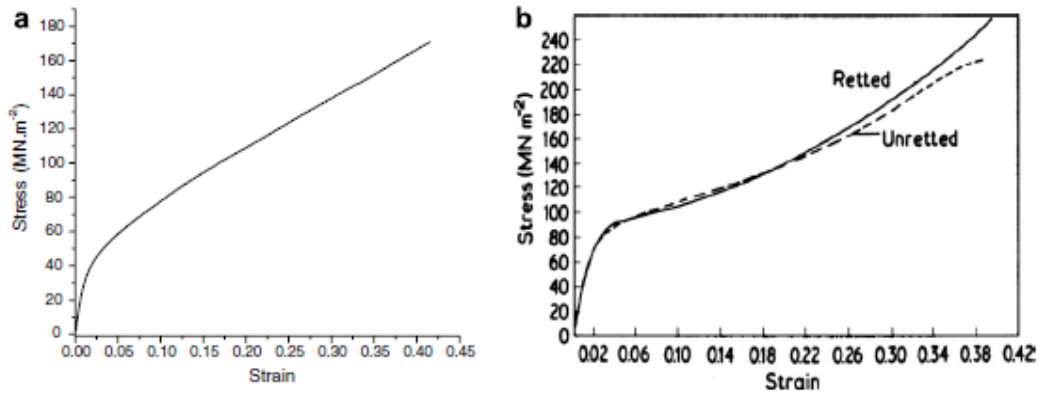


**Fig.5.9:** Typical stress – strain curve of coir fiber  
(Kulkarni, Satyanarayana et al., 1981)

The decrease in tensile strength and initial modulus and constant strain at break with increasing fiber diameter can be understood from the fact that as the diameter of the lignocellulosic fibers changes, the other structural parameters, such as microfibrillar angle, volume of strength rendering cells in the fiber and density of weak-links or flaws, also behave the same manner as reported elsewhere. The changes in these parameters in turn affect the strength properties. As reported elsewhere, both the tensile strength and Young's modulus of lignocellulosic fibers decrease with microfibrillar angle, McLaughlin (1980).

#### Effect of test length

It can be seen that the tensile strength and strain at break both decrease with increasing test length, while the Young's modulus increases with the test length as shown in table.5.2. Longer the fiber's length, the higher will be its lignin

content, and hence the higher will be its resistance to applied stress (higher stiffness or modulus). This in turn results in lower elongation..

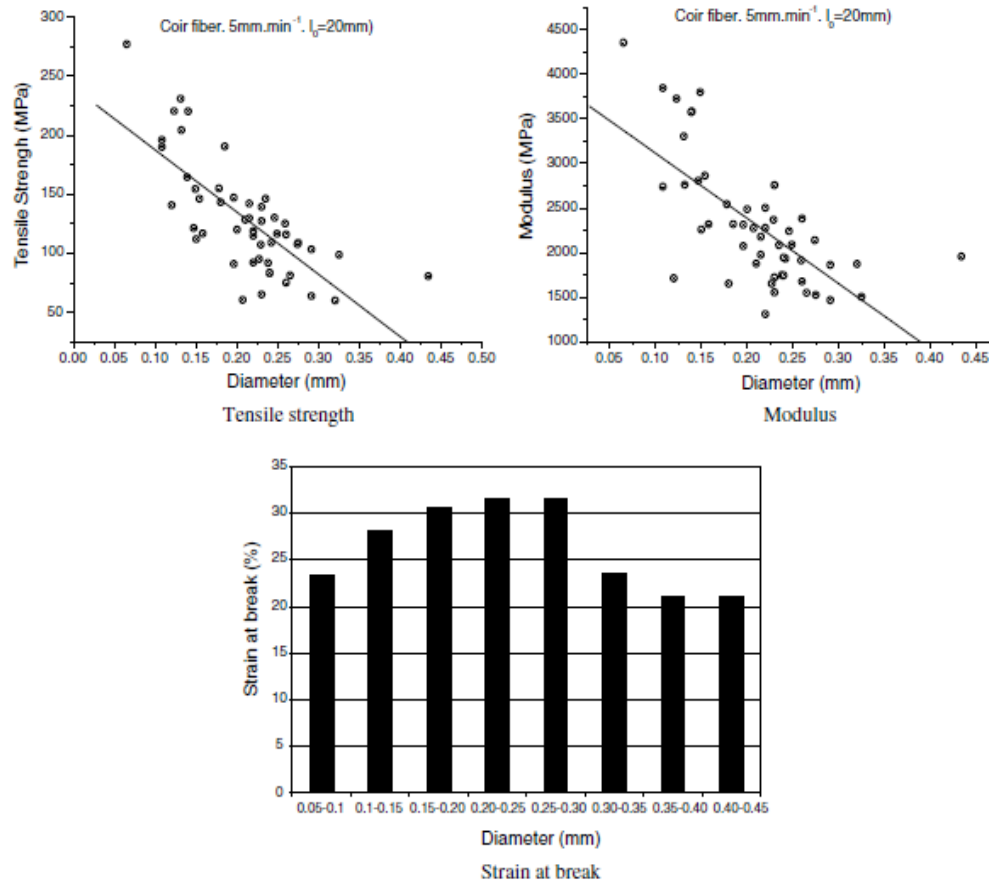


**Fig.5.10:** Influence of diameter on mechanical properties on coir fibers (Tomczak, Satyanarayana et al., 2007)

**Table.5.2:** Tensile properties of coir fibers at different strain rate (Mukherjee, Satyanarayana et al., 1984)

| Gauge length, $L_0$<br>(mm) | Mean tensile strength<br>(MPa) | SD tensile strength<br>(MPa) | Mean modulus<br>(GPa) | SD modulus<br>(GPa) | Mean strain at<br>break (%) | SD strain at break<br>(%) |
|-----------------------------|--------------------------------|------------------------------|-----------------------|---------------------|-----------------------------|---------------------------|
| 5                           | 142.6                          | 53.26                        | 1.269                 | 0.386               | 59.87                       | 23.80                     |
| 10                          | 135.4                          | 44.8                         | 1.966                 | 0.393               | 34.04                       | 15.86                     |
| 20                          | 128.7                          | 47.4                         | 2.302                 | 0.707               | 29.91                       | 12.09                     |
| 25                          | 118.3                          | 35.56                        | 2.734                 | 0.912               | 25.01                       | 12.50                     |

SD—standard deviation.

#### Effect of strain rate:

The increase in tensile strength and unchanged initial modulus and strain at break with increasing strain rate observed in the present study can be explained

in terms of the viscoelastic model of cellulose fibers. In short, the lignocellulosic fibers such as coir, when subjected to mechanical testing, behave as an elastic body at higher speeds, with the crystalline region sharing most of the applied stress/load. This results in increased tensile strength and Young's modulus. But at lower test speeds the fiber behaves like a viscous liquid and hence the applied load is shared mostly by the amorphous region, resulting in a low modulus Tomczak & Satyanarayana et al., (2007). Some surface defects are visible (Fig. 5.11a), while the fracture surfaces (Fig. 5.11b and 5.11c) reveal ductile fracture. Such fracture surfaces are similar to those observed earlier Kulkarni & Satyanarayana et al., (1981). Also, similar surfaces were observed with fibers tested at different strain rates, suggesting that the strain rate does not have any effect on the fiber's fracture mode.

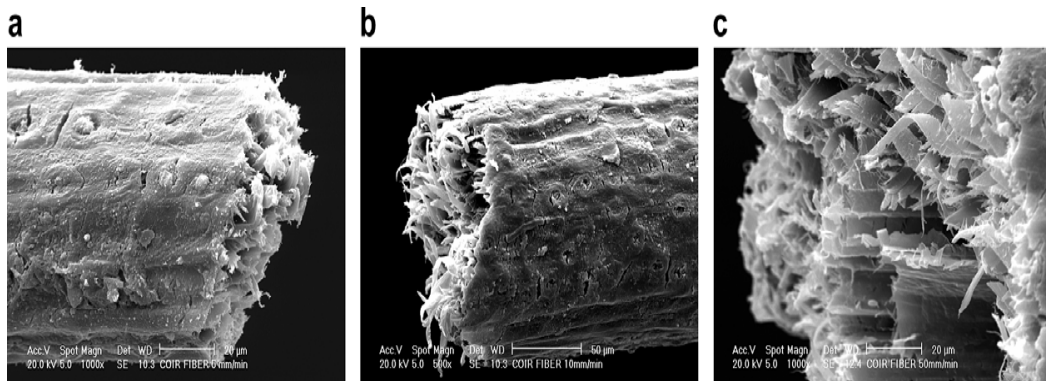


**Fig.5.11:** Scanning electron micrographs of coir fiber at different strain rates (a) and micrograph showing the end of fiber with pull out of microfibrils (b&c)



**Photograph 5.12:** Coir fibers, Bunch of coir and jute fibers of required length and coir-jute drain (CJ) of 'n'11.04



### 5.5.2.5 Design of Polypropylene fiber drain (PF)

| Sr.No | 'n' value | Diameter of Oedometer (mm) | Diameter of drain(mm) | Type of mandrel used | Area ratio (%) and thickness of mandrel (mm) |
|-------|-----------|----------------------------|-----------------------|----------------------|--|
| 1     | 11.04     | 254 & 152                  | 23 & 13.77            | Open end thin wall   | 1.6 & 0.55                                   |
| 2     | 16.93     | 254 & 152                  | 15 & 8.97             | Open end thin wall   | 1.6 & 0.55                                   |
| 3     | 21.71     | 254 & 152                  | 11.70 & 7             | Open end thin wall   | 1.6 & 0.55                                   |

Polypropylene fiber drain is fabricated indigenously in the laboratory as per drain diameter and consists of twisted and straight white polypropylene fibers and filter paper (Whatman Grade 591) whose properties are mentioned in table no.3.17. These fibers are now blended together in a form of rope (bunched) which is then wrapped by filter paper. Photograph.5.13 shows polypropylene fiber drain (PF) for 'n' equal to 11.04 ready for installation and testing.

#### **Selection, Formation and Installation of Polypropylene fiber drain:**

Nowadays, textiles are passive, mostly mono-functional and single-dimensional products, but according to the prognosis, they are going to be active, multifunctional, interactive and multi-dimensional in the near future. Today's complex and highly demanding market is looking for textile end products, which are multipurpose or have specific or desired properties. Consumers need and require active, smart textiles, which combine many various properties. The group of smart textiles includes smart fibres with various other materials or composites to get into a better matrix. The selection of composites depends on the fibres end-use and applicability. Most of the geotextiles used in fabrication of vertical drains are based either on polypropylene, polyester, polyethylene, polyvinylchloride, glass, nylon, polyamide, etc which have good physical, mechanical, hydraulic, survivability and durability properties supported by easy implementation. Considering present scenario, polypropylene fibers along with filter paper is used in present investigation whose properties are mentioned in table no.3.17 of chapter 3. Also very less literature is available regarding the use of polypropylene fibers as vertical drain for accelerating rate of consolidation for

soft soils. The stiffness result (table. no.3.18) of polypropylene fiber drain(PF) indicate that the % strain carrying capacity of polypropylene fiber is more because of more tenacity and more load carrying capacity, but have less capillary capacity to pass water compare to coir-jute fibers.



**Photograph 5.13:** Polypropylene fiber drain (PF) ready for installation and clay sample with central PF drain ready for testing

## 5.6 TESTING PROCEDURE

After the consolidation by static load cell was sealed, settlement dial gauge and Bishop Pore pressure measuring apparatus were connected at their respective location.

Excess pore pressure or excess hydrostatic pressure or hydrodynamic pressure of 10 kPa (excess of initial pressure 8 kPa) is applied by help of screw pump and hydraulic system, keeping the pressure valve on Oedometer and settlement valve (drainage valve) closed (7.35 cm).

Now at this stage after this load (10 kPa) is allowed to enter the Oedometer keeping the settlement valve closed it may occur that a (-ve pressure) may be developed due to following reasons.

- (1) Transfer of load does not occur from rubber jacket to clay sample due to partial air in it or due to insufficient water in it.
- (2) Due to stretching of rubber under pressure.
- (3) Due to adjusting of water and/or air in convolutions of the rubber jacket.
- (4) Due to leakage in rubber jacket, so check it outside before sealing it in the cell for leakage.
- (5) Due to leak in top plate. In the present investigation metal bracing(polishing) was done of the aluminum top plate so as to stop the water leaks from the top

plate in pressurized condition. High vacuum silicon grease applied on the connection between top plate and settlement rod. Also a thin film of coating of grease is done on the entire length of settlement rod before sealing the Oedometer.

(6) It may occur that this –ve pressure condition may occur for small load ranges because according to Henry's law under constant high pressure gas may change to liquid and this condition may not arise.

The behavior of rubber jacket is very important to check as it transfer load to clay sample by Pascal's law. A pressure of 10 kPpa is again maintained in manometer  $[(h_2 - h_1) \times 13.6 \text{ gm/cm}^3 = 0.1 \text{ kg/cm}^2, h = 7.35\text{cm}]$  and open both Oedometer and settlement(drainage) valve.

Let the drainage occur till the pressure 10 kPa is dissipated in manometer. When this stage of primary consolidation( the reduction in volume of soil which is due to principally to squeezing out of water from the voids is termed primary consolidation, primary compression or primary time effect) completes i.e. water has stopped coming out of the drainage valve and manometer pressure excess hydrostatic pressure is zero.

Now in this drainage valve open condition the pressure of 7.35 cm head is again rising up in manometer automatically. In the case of pressure not rising check the mercury level of the pots in hydraulic pressure system.

The consolidation occurring after the primary consolidation has stopped is due to secondary consolidation. Some of the highly viscous water , adsorbed water between the points of contact is forced out between the points of contact is forced out between the particles. After the secondary consolidation is stopped take the final reading of dial gauge . The total settlement occurred during this stage is calculated and this is considered as the initial height of sample for change of ratio method.

Apply the load of 20 kPa by following process now :

- (1) Close the drainage valve and valve going to the Oedometer from the Hydraulic pressure system.
- (2) Adjust the mercury pot to a level of 20 kPa.
- (3) See this level is obtained in to manometer and pressure gauge near to Oedometer.

(4) After 20 kPa is completely developed open the Oedometer valve and wait and see the level is maintained in manometer.

(5) Then open the pore pressure valve and the pore pressure was allowed to develop for sufficient time. The pore pressure is raised more or less equal to the incremental pressure,  $P$ . 10 kPa be developed in the Bishop's apparatus.

(6) Read the datum of pore pressure in Bishop's apparatus after entire 10 kPa is developed. Consolidation was started by opening the drainage control valve (settlement valve) and reading of settlement dial gauge and Bishop's pore pressure measuring apparatus were taken at suitable intervals of time.

After the completion of consolidation process drainage control valve was closed then the next increment of load is applied and the same process is repeated for a series of various pressure increments, with  $\Delta p/p = 1.0$ .

The loading was done in the increment of 10,20,40,80,160 and 320 kPa, keeping  $\Delta p/p = 1.0$ . After the completion of the test, vane shear test was performed at three locations( at radial points  $r_1$ ,  $r_2$  and  $r_3$ ) to determine the gain in shear strength due to dissipation of water as shown in photograph 5.7. Representative sample is sectioned to study the behavior of the geodrain and drain-soil interface study after the test using scanning electron microscopy (SEM) which is presented in chapter 6 along with photographs of consolidated clay samples with various geodrain after the test.

### **5.7 Problems and their Remedial Measures**

Numerous precautions are necessary throughout the test for correct assessment of the consolidation parameters. Some of the most obvious are as follows:

- The complete setup should be leak proof. This should be checked before the actual testing by maintaining some constant pressure in the pressure lines for a period of, say, 48 hours. All connections shall be checked before application of each pressure increment. To prevent the entry of air at the connection of base plate valve, the whole base plate must be immersed in water.
- Porous stone should be boiled in water for about four to eight hours for complete de-airing.

- Drainage line through the porous stone in the base plate should be clear other wise rusting of plate may cause clogging problem and obstruct the development of pore pressure.
- Trimming of the sample should be uniform through out the surface otherwise equal strain condition may not be obtained.
- Care should be taken so that withdrawal of the mandrel does not cause smear on the inside wall of the hole to maintain constant horizontal permeability.
- Additional pressure gauge should be provided near the Oedometer to avoid system flexibility.

**Problems faced in present investigation and their remedial measures:**

(1) The Bourdon pressure gauges of range 0-10.6 kg/cm<sup>2</sup> were used. During the test one of them stopped working due to Bourdon tube being damaged at high pressure. In present investigation the calibration and repair of the pressure gauge was carried done at Process instrument calibration centre, GIDC, Vadodara.

(2) The stud in the top plate has a groove in which a rubber o-ring is placed which keeps the settlement rod fit during the pressure condition. This setting should be such that the settlement rod is flexible to move. This problem was solved by rubbing the rod through entire length by ambry paper and taking an appropriate thickness of o-ring. Also the groove in the stud was increased for its inner dia.

(3) It may occur in initial low pressure that some amount of clay may come out with drainage water because the soft clay with less shear strength initially in this stage is squeezed under pressure and comes out from the annular space but after some time the water starts coming clear.

(4) A bypass block was provided between the hydraulic pressure and the screw pump so that the pressure of hydraulic pressure may not be disturbed by the interference of screw pump (leak of air or water).

(5) The housing well arrangement was made in the base plate to hold the porous stone so that the well of water is filled below porous stone which will not allow to

pass air through the Bishop's apparatus to enter the sample and it will provide a continuity with water in the line going to Bishop's apparatus from Oedometer.

(6) Under different applied pressures, soil attains different equilibrium or final void ratio and under each equilibrium condition the whole of the applied pressure is carried by the solids as an effective pressure. The delay caused in consolidation by the slow drainage of water out of a saturated soil mass is called hydrodynamic lag this occurs more if the pressure lines are long. Thus to decrease the system complexities and hydrodynamic lag the length of the tubes in the present investigation was kept as less as possible.

(7) Use of boiled sand and boiled porous stone is done so that air does not block the pressure lines and measurements are not affected.

(8) The interaction of particles through bonded water in clayey soils promotes the formation of a coagulation bond which is mobile and is easily restored after disturbance. These bonds are known as coagulation Thixotropic bonds. Due to their restored structure the flow path of water in consolidating clay is altered so the consolidation once started has to be continued in progress continuously without break (stopping the drainage) in between until the completion of consolidation for that applied pressure.

### 5.8 De-Airing the Entire System

The process of de-airing is carried out in a similar way as described in IS: 2720 (PART XII) – 1981.(refer fig.5.12)

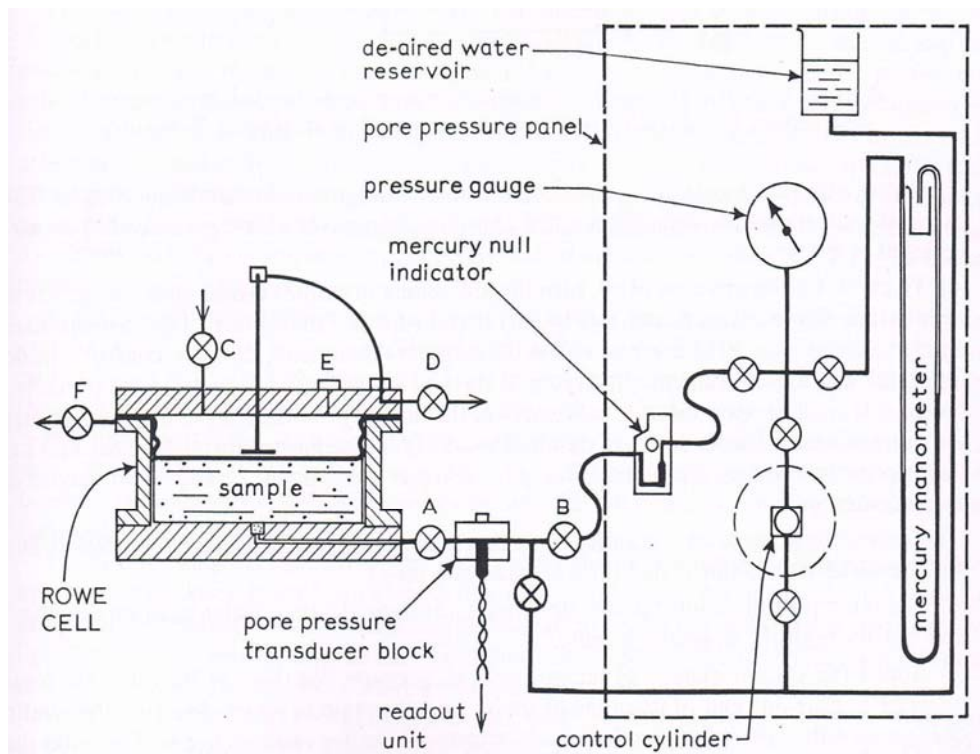


**Fig.5.12:** Rowe cell connected to pore pressure panel for flushing and initial checks

### 5.9 SPECIAL APPARATUS DEVELOPED TO MEASURE COEFFICIENT OF RADIAL PERMEABILITY OF SOIL AND VERTICAL DRAIN

#### Introduction:

Routine falling head and constant head tests to determine coefficient of permeability of soils for horizontal and vertical flow have many limitations. Generally in case of one dimensional consolidation by radial flow using central vertical drain we know that due to vertical stresses the pore water from the soil mass travels radially towards the centre and then water gets squeezed out vertically. This phenomenon was simulated in laboratory by developing a set-up to determine coefficient of radial permeability of either soil or geodrain both by falling head and constant head test method.

**Scope:**

The test method includes the determination of the coefficient of radial permeability of soil and composite vertical drain(as per diameter) to be used in present experiments.

**Test conditions:**

The conditions and assumptions defined in IS 2720 part 17 holds true for constant head test method and falling head test method.

**Test setup:**

The test setup consists of overhead tank, sampler and drain collection system as depicted in Photograph 5.14(d). The overhead tank is connected to a flexible tube for filling it with water. The water flows from the overhead tank to the sample chamber by vertical flow. For constant head test, a continuous supply of water is ensured into the overhead tank to maintain level of water head in the tank. For falling head test, the decrease in water level during the test is measured by determining the water level.

The sampler is fixed below the overhead tank and consists of a perforated cylinder made of PVC material with an outside chamber for collection of water from the overhead tank (refer photograph 5.14(a)). The sample (soil sample or vertical drain material) is placed inside the sampler. The water from the overhead tank flows into the outside chamber of the sampler, and water flows into the sample in the cylinder by radial flow through the perforations. The sampler is provided with top cap to avoid vertical flow of water into the sample (refer photograph 5.14(b)). The bottom portion of the perforated cylinder is connected to a drain valve to collect the flowing water into a measuring container refer photograph 5.14(d).

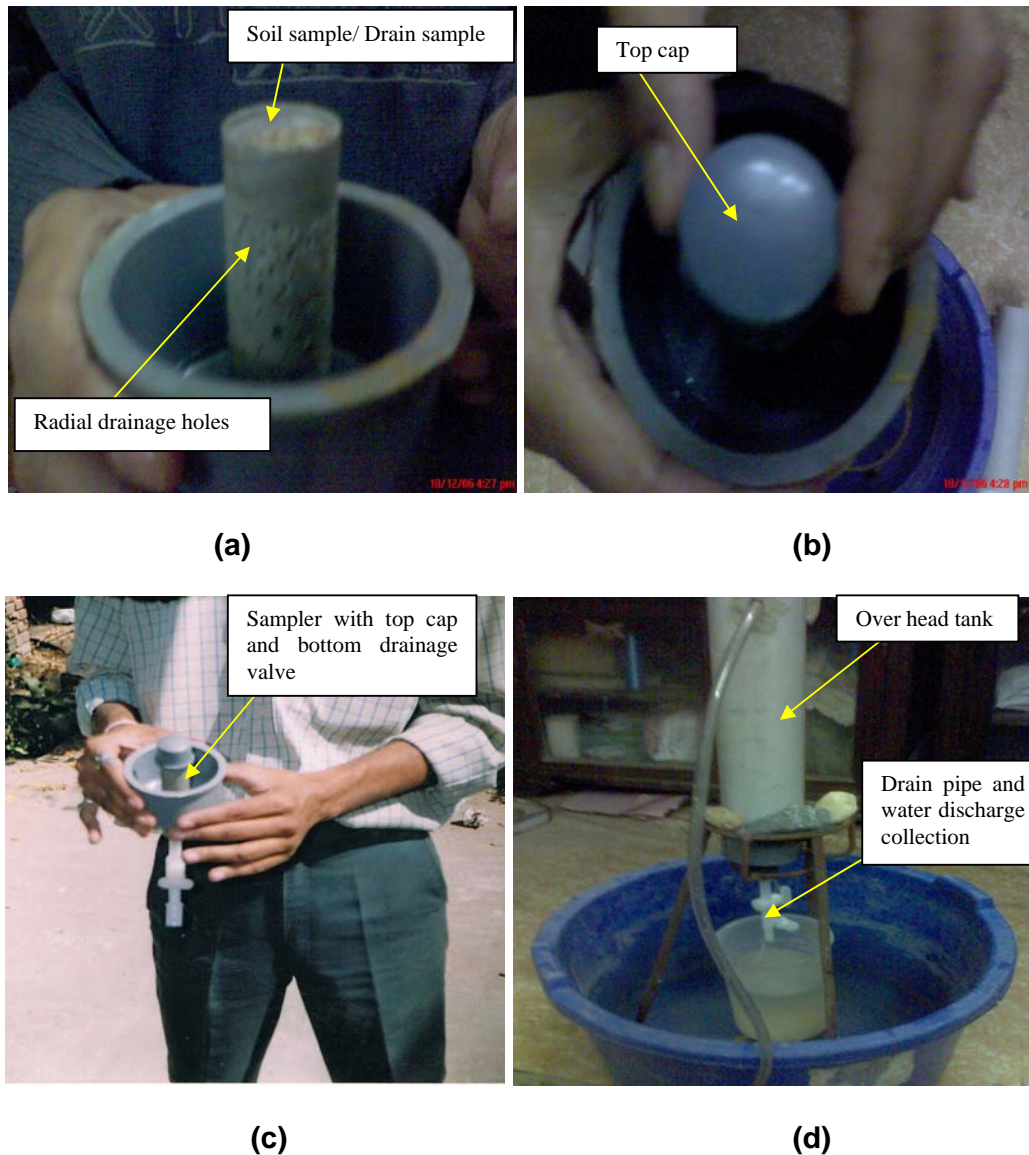
**Sample preparation:**

The sample preparation was done in line with IS 2720 part 17. The sample was wrapped with filter paper and placed into the perforated cylinder of the sampler. Bottom porous stone was placed below the sample. The water flowing through the material by vertical flow was collected through the drain provided at the bottom.



### Calculations:

The quantity of water flowing through the sample was collected through the bottom drain into a measuring cylinder, and coefficient of permeability was calculated as per guidelines of IS 2720 part 17.



**Photograph 5.14:** (a) Sampler with radial drianage (b) Sampler with top cap (c) Set-up of sampler with top cap, centrally placed sample and bottom drainage valve (d) Complete radial permeability set-up

### **5.10 SCANNING ELECTRON MICROSCOPY OF CONSOLIDATED SAMPLES**

To study clay-drain interface, orientation of particles, clay-drain interaction, deformation and failure pattern of vertical drains at the end of consolidation test, scanning electron microscopy(SEM) was carried out for various consolidated clay samples of different 'n' values and different vertical drains whose detail schedule is mentioned in table no.3.7 of chapter 3. Scanning electron microscopy was carried out at SEM laboratory, Metallurgy Department, Faculty of Technology & Engineering, M.S. University of Baroda. The sections of soil samples were taken from different locations and tested as mentioned in table no.3.7 of chapter 3.

The micrographs obtained from SEM were further analysed to study anisotropic behavior of soil mass under stress levels using nano technology of scanning electron microscopy adopting Quanti-image analyzer with system of micro structure characterization (MIC) software based on ASTM method (M/s.TCR Advanced Engineering Pvt. Ltd, Appendix-E). SEM analyses were carried out at different levels of thickness of clay samples. Aim was also to determine percentage of pore space remaining at the end of consolidation under various drains and to know angle of orientation of clay particle at edge-to-edge and face-to-face with respect to horizontal. Also horizontal tortuosity and vertical tortuosity were evaluated using above micrographs.

Further selected micrographs of clay samples consolidated at 320kPa pressure with central vertical drain viz. sand drain and coir-jute fiber drain of 'n' value equal to 11.04 and 16.93 were taken for study to determine % porosity, angle of orientation of clay particle and tortuosity. The following table 5.3 illustrates the detail of selected micrographs which were further analysed using micro structure characterization (MIC) software based on ASTM method. Clay samples consolidated at 320kPa pressure with central vertical drain viz. sand drain and coir-jute fiber drain of various locations were selected. The selection of micrographs were done in a such way so as to cover the influence of drain material, 'n' value and orientation of particles. Using MIC software % porosity, angle of orientation and tortuosity measurements were carried out from micrographs.

**Table. 5.3:** Schedule of Micrographs for MIC

| Factor                           | Type of Geodrain | 'n' value | location  | Magnification factor |
|----------------------------------|------------------|-----------|-----------|----------------------|
| Drain Material                   | SD               | 11.04     | $h_{tr2}$ | X2700                |
|                                  | CJ               | 11.04     | $h_{tr2}$ | X2700                |
|                                  | SD               | 11.04     | $h_{cr2}$ | X2700                |
|                                  | CJ               | 11.04     | $h_{cr2}$ | X2700                |
|                                  | SD               | 11.04     | $h_{br2}$ | X2700                |
|                                  | CJ               | 11.04     | $h_{br2}$ | X2700                |
| 'n' value<br>(diameter of drain) | SD               | 11.04     | $l_{brd}$ | X2700                |
|                                  | SD               | 16.93     | $l_{brd}$ | X2700                |
|                                  | SD               | 21.71     | $l_{brd}$ | X2700                |
|                                  | CJ               | 11.04     | $l_{brd}$ | X2700                |
|                                  | CJ               | 16.93     | $l_{brd}$ | X2700                |
|                                  | CJ               | 21.71     | $l_{brd}$ | X2700                |

Where,

$r_d$  = radius of drain

$r_1$  = first radial point for measurement of pore pressure at a distance of  $r/4$

$r_2$  = second radial point for measurement of pore pressure at a distance of  $r/2$

$r_3$  = third radial point for measurement of pore pressure at a distance of  $3r/4$

$h$  = thickness of final consolidated clay sample

$h_t$  = Top of final consolidated clay sample

$h_c$  = Centre of final consolidated clay sample

$h_{cr2}$  = Centre of final consolidated clay sample at mid radial point  $r_2$

$h_{br2}$  = Bottom of final consolidated clay sample at mid radial point  $r_2$

$l_{tr2}$  = Clay-Drain interface at top of final consolidated clay sample at location  $r_2$

$l_{brd}$  = Clay-Drain interface at bottom of final consolidated clay sample at location  $r_d$

## CHAPTER-6

### RESULTS, ANALYSIS AND DISCUSSION

---

#### 6.1 Presentation of Results

Experimental schedule prepared as given in Table 3.2 to 3.7 has been followed for the investigation of the influence of various factors on the consolidation characteristics of clays through inward radial flow. It is proposed to present the data, observations and results according to the following scheme. The scheme to verify the proposed theory and the lumped parameter ( $\lambda$ ) by conducting a series of consolidation tests with radial drainage through vertical geodrain at central location of a cylindrical saturated soil sample along with pore pressure measurements so as to prove its efficacy against various physical factors namely type of drain, various shapes of the drain with different geometry of the drain, 'n' value (i.e. different diameters of drain related to influence zone). Various derived parameters are evaluated for the above and analysis was carried to structural variation with load, tortousity changes with change of horizontal permeability and consolidation pressure ratio (CPR). For study of structural variation in soil, (i) the volumetric water ratio (VWR) is evaluated considering the ratio of existing weight of water at particular load to weight of water at initial load (10kPa) for same weight of soil solid. (ii) consolidation pressure ratio (CPR) assessed considering load under testing to the load with which sample is preconsolidated initially before the commencement of test. For the analysis CPR as 2, 4 and 16 are accounted. (iii) permeability ratios with variation in horizontal permeability deduced from the above results are utilized to access the effect of tortousity in the soil structure. Permeability ratio as 4.5, 9, 18 and 36 are accounted.

These experimental observations are proposed to be analyzed and discussed from fundamental considerations. It is proposed to compare these experimental results with those from theory discussed in chapter III.

## 6.2 Method of Analysis/Determination of Parameters

The following parameters are determined from settlement measurements and pore water pressure measurements.

### Conventional parameters:

1. Coefficient of consolidation due to radial drainage,  $C_r$
2. Time factor for consolidation due to radial flow,  $T_r$ .
3. Degree of consolidation due to the radial drainage, for settlement reading,  $U_r\%$  and for pore pressure readings,  $(1-u_r/u_o)\%$ .
4. Compression index for consolidation due to radial flow,  $C_{cr}$ .
5. Pore pressure ratio for radial flow,  $u_r/u_o\%$ .
6. Coefficient of permeability due to radial flow,  $k_h$ .
7. Coefficient of compressibility due to radial flow,  $a_{vr}$
8. Coefficient of volume change due to radial flow,  $m_{vr}$ .
9. Lumped parameter,  $\lambda$

### Derived parameters

1. Volumetric water ratio
2. Permeability ratio
3. Consolidation pressure ratio

**6.2.1. Determination of Coefficient of consolidation due to radial drainage ( $C_r$ ), Time factor for consolidation due to radial flow ( $T_r$ ), Degree of consolidation due to the radial drainage, for settlement reading,  $U_r\%$  and for pore pressure readings  $(1-u_r/u_o\%)$ , Pore pressure ratio for radial flow ( $u_r/u_o\%$ ).**

(i) Based on settlement measurements

In the present work the log time method (Casagrande 1936) curve fitting method is employed to determine the coefficient of consolidation due to radial drainage ( $C_r$ ). In the present work coefficient of consolidation due to radial drainage ( $C_r$ ) is computed for 50% and 80% consolidation.

A stepwise procedure for the determination of coefficient of consolidation due to radial drainage ( $C_r$ ) is explained below with example.

**Procedure:**

- i. First of all dial guage reading (dgr) vs time are noted for applied pressures of 20, 40, 80, 160, 320kPa.
- ii. From settlement readings, consolidation curve is plotted as per casagrande method applying necessary corrections. From this curve (refer fig.6.1) degree of consolidation of  $U_r = 0\%$  (denoted by  $d_0$ ) and  $U_r = 100\%$  (denoted by  $d_{100}$ ) and termination of load increment, the final reading for the increment is denoted by ' $d_f$ '. The point of inflexion of the log-time.settlement graph is the point at which the curvature changes, and is the steepest part of the curve. The intersection of the tangent at this point with backward extension of the secondary compression line defines the  $U_r = 100\%$  abscissa as shown in fig. 6.1.
- iii. Now using the formula to get  $C_r = T_r * r_e^2 / t * 60 = \text{cm}^2/\text{sec}$ , where  $r_e$  is radius of influence depend upon radius of oedometer and  $T_r$  is theoretical time factor as per consolidation theory (taken for 80% consolidation) mentioned in chapter 4. Here value of  $T_r$  will depend upon selection of particular lump parameter ' $\lambda$ '.
- iv. Now to determine  $C_{r80}$  (degree of consolidation equal to 80%) the theoretical time factors for each lump parameter  $\lambda$  is determined ( $T_{r80}$  at  $U_r = 80\%$ ) and  $C_{r80}$  is found out using following formulas:  $C_{r80} = T_{r80} * r_e^2 / t * 60 = \text{cm}^2/\text{sec}$ , where  $r_e$  is radius of influence as per radius of oedometer used for that particular ' $n$ ' value.
- v. Now to determine experimental time factor for different degree of consolidation, the formula  $T_r = C_{r80} * t * 60 / r_e^2$  is used and this excersie is repeated for all values of lump parameter  $\lambda$  and for all applied pressures using Excel-macro program.
- vi. Now comparative tables are made for each lump parameter  $\lambda$  between Degree of consolidation, theoretical time factor and experimental time factor. Thereafter degree of error using regression analysis is determined.

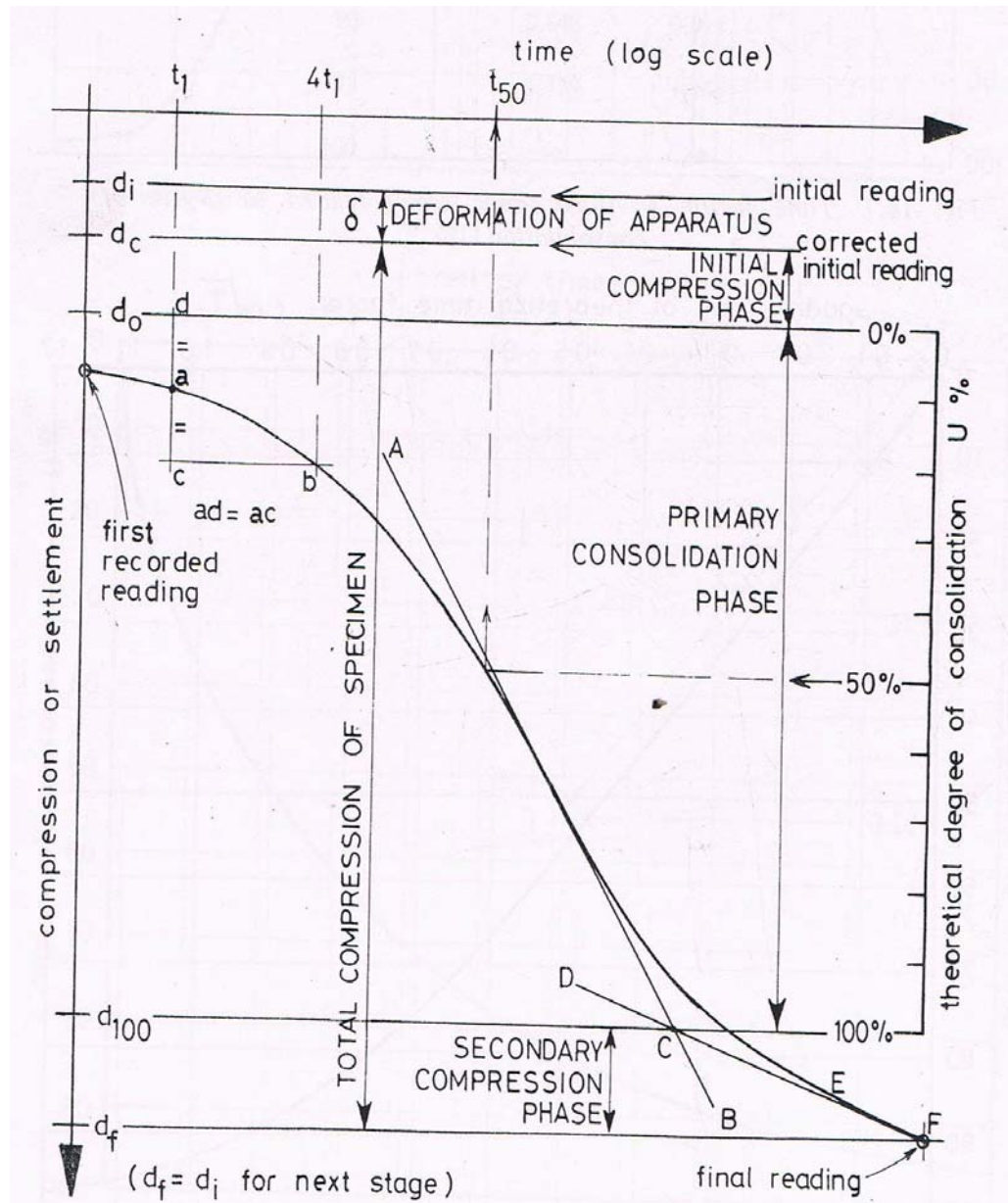


**Fig.6.1:** Stages of consolidation and analysis of log-time/settlement curve

**Example:**

Type of Drain = Coir-Jute fiber drain (CJ), 'n' value = 11.04,

Diameter of Oedometer = 254mm

Type of drainage: Radial drainage

Radial points and location:  $r_1$  @  $r/4$ ,  $r_2$  @  $r/2$  and  $r_3$  @  $3r/4$

Applied pressure = 160kPa

Dial gauge L.C. = 0.002mm

Step 1

| Log't' min | dgr  | thks(mm) | $C_r(\text{cm}^2/\text{sec})$<br>( $\lambda = -0.175$ ) | $U_r(\%)$ |
|------------|------|----------|---|-----------|
| 0          | 2790 | 5.580    | ---   | ---       |
| 0.25       | 2770 | 5.540    | 1.315051  | 0.79      |
| 1          | 2750 | 5.500    | 0.328763  | 1.59      |
| 2.25       | 2724 | 5.448    | 0.146117  | 2.62      |
| 4          | 2685 | 5.370    | 0.082191  | 4.17      |
| 6.25       | 2666 | 5.332    | 0.052602  | 4.93      |
| 9          | 2638 | 5.276    | 0.036529  | 6.04      |
| 12.25      | 2600 | 5.200    | 0.026838  | 7.55      |
| 16         | 2560 | 5.120    | 0.020548  | 9.14      |
| 20.25      | 2525 | 5.050    | 0.016235  | 10.53     |
| 25         | 2486 | 4.972    | 0.013151  | 12.08     |
| 36         | 2411 | 4.822    | 0.009132  | 15.06     |
| 49         | 2330 | 4.660    | 0.006709  | 18.28     |
| 64         | 2240 | 4.480    | 0.005137  | 21.86     |
| 81         | 2111 | 4.222    | 0.004059  | 26.99     |
| 100        | 1980 | 3.960    | 0.003288  | 32.19     |
| 121        | 1830 | 3.660    | 0.002717  | 38.16     |
| 144        | 1745 | 3.490    | 0.002283  | 41.53     |
| 169        | 1662 | 3.324    | 0.001945  | 44.83     |
| 196        | 1550 | 3.100    | 0.001677  | 49.28     |
| 225        | 1460 | 2.920    | 0.001461  | 52.86     |
| 256        | 1381 | 2.762    | 0.001284  | 56.00     |
| 289        | 1300 | 2.600    | 0.001138  | 59.22     |
| 324        | 1225 | 2.450    | 0.001015  | 62.20     |
| 361        | 1160 | 2.320    | 0.000911  | 64.79     |
| 1440       | 420  | 0.840    | 0.000228  | 94.20     |
| 2880       | 313  | 0.626    | 0.000114  | 98.45     |
| 4320       | 274  | 0.548    | 7.61E-05  | 100.00    |

Step 2



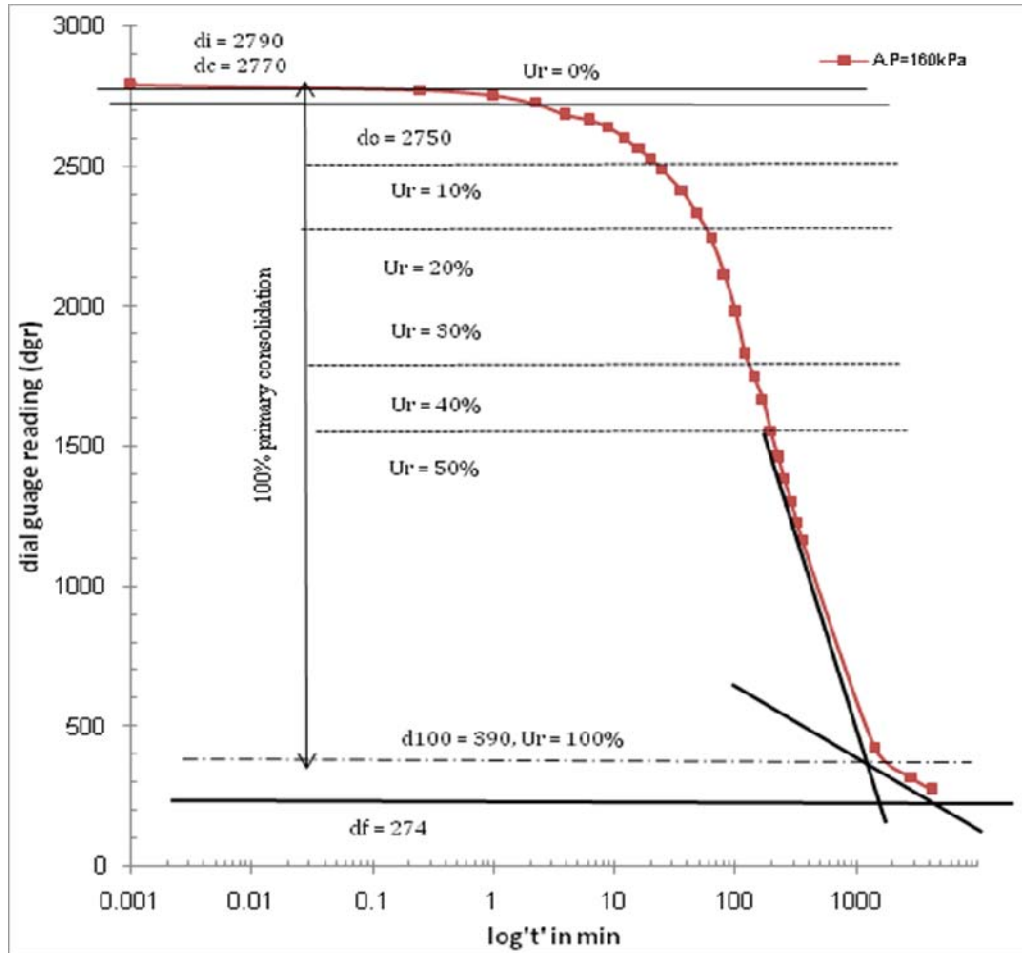


**Fig.6.2:** Plot of dial gauge reading vs.  $\log't'$  and stages of consolidation

### Step 3

Determination of  $T_r$  (theoretical) for 80% consolidation for various positive and negative values of ' $\lambda$ '

| $\lambda$ | $T_{r80}$ | $\lambda$ | $T_{r80}$ | $\lambda$ | $T_{r80}$ |
|-----------|-----------|-----------|-----------|-----------|-----------|
| +0.7      | 0.232     | +0.05     | 0.149     | -0.1      | 0.128     |
| +0.6      | 0.218     | +0.03     | 0.147     | -0.11     | 0.127     |
| +0.5      | 0.200     | +0.01     | 0.144     | -0.12     | 0.126     |
| +0.4      | 0.189     | 0         | 0.142     | -0.125    | 0.126     |
| +0.3      | 0.177     | -0.01     | 0.141     | -0.13     | 0.126     |
| +0.25     | 0.170     | -0.02     | 0.14      | -0.14     | 0.125     |

|        |       |       |       |        |       |
|--------|-------|-------|-------|--------|-------|
| +0.2   | 0.166 | -0.03 | 0.139 | -0.15  | 0.124 |
| +0.175 | 0.161 | -0.04 | 0.138 | -0.16  | 0.123 |
| +0.15  | 0.159 | -0.05 | 0.137 | -0.17  | 0.123 |
| +0.125 | 0.156 | -0.06 | 0.136 | -0.175 | 0.122 |
| +0.1   | 0.154 | -0.07 | 0.135 | -0.18  | 0.122 |
| +0.08  | 0.152 | -0.08 | 0.134 | -0.19  | 0.121 |
| +0.07  | 0.151 | -0.09 | 0.128 | -0.2   | 0.121 |

**Step 4**

Determination of  $T_r$  (experimental) for various positive and negative values of ' $\lambda$ '

|     |      | $\lambda=+0.7$ |                                     |                    | $\lambda=+0.6$ |                                     |                    |
|-----|------|----------------|-------------------------------------|--------------------|----------------|-------------------------------------|--------------------|
| Ur% | t    | $T_{r80}$      | $C_{r80}$<br>(cm <sup>2</sup> /sec) | $T_{r\text{ exp}}$ | $T_{r80}$      | $C_{r80}$<br>(cm <sup>2</sup> /sec) | $T_{r\text{ exp}}$ |
| 10  | 23   | 0.232          | 0.001134                            | 0.010              | 0.218          | 0.001065                            | 0.009              |
| 20  | 54   | 0.232          | 0.001134                            | 0.023              | 0.218          | 0.001065                            | 0.021              |
| 30  | 88   | 0.232          | 0.001134                            | 0.037              | 0.218          | 0.001065                            | 0.035              |
| 40  | 125  | 0.232          | 0.001134                            | 0.053              | 0.218          | 0.001065                            | 0.050              |
| 50  | 185  | 0.232          | 0.001134                            | 0.078              | 0.218          | 0.001065                            | 0.073              |
| 60  | 280  | 0.232          | 0.001134                            | 0.118              | 0.218          | 0.001065                            | 0.111              |
| 70  | 410  | 0.232          | 0.001134                            | 0.173              | 0.218          | 0.001065                            | 0.163              |
| 80  | 550  | 0.232          | 0.001134                            | 0.232              | 0.218          | 0.001065                            | 0.218              |
| 90  | 900  | 0.232          | 0.001134                            | 0.380              | 0.218          | 0.001065                            | 0.357              |
| 100 | 1800 | 0.232          | 0.001134                            | 0.759              | 0.218          | 0.001065                            | 0.713              |

Tables prepared in a similar form for other ' $\lambda$ ' values-----.

| $\lambda = -0.175$ |                                     |                     | $\lambda = -0.19$ |                                     |                     |
|--------------------|-------------------------------------|---------------------|-------------------|-------------------------------------|---------------------|
| $T_{r80}$          | $C_{r80}$<br>(cm <sup>2</sup> /sec) | $T_{r \text{ exp}}$ | $T_{r80}$         | $C_{r80}$<br>(cm <sup>2</sup> /sec) | $T_{r \text{ exp}}$ |
| 0.122              | 0.000596                            | 0.005               | 0.121             | 0.000591                            | 0.005               |
| 0.122              | 0.000596                            | 0.012               | 0.121             | 0.000591                            | 0.012               |
| 0.122              | 0.000596                            | 0.020               | 0.121             | 0.000591                            | 0.019               |
| 0.122              | 0.000596                            | 0.028               | 0.121             | 0.000591                            | 0.028               |
| 0.122              | 0.000596                            | 0.041               | 0.121             | 0.000591                            | 0.041               |
| 0.122              | 0.000596                            | 0.062               | 0.121             | 0.000591                            | 0.062               |
| 0.122              | 0.000596                            | 0.091               | 0.121             | 0.000591                            | 0.090               |
| 0.122              | 0.000596                            | 0.122               | 0.121             | 0.000591                            | 0.121               |
| 0.122              | 0.000596                            | 0.200               | 0.121             | 0.000591                            | 0.198               |
| 0.122              | 0.000596                            | 0.399               | 0.121             | 0.000591                            | 0.396               |

**Step 5**

Transferring above values in EXCEL Macro program to obtain experimental values of Time factor ( $T_r$ ) for all values of ' $\lambda$ ' for given degree of consolidation ( $U_r$ )

Final solution is obtained in following form:

| $T_{r(e)}$ | $U_r(\%)$<br>$\lambda = 0.7$ | $T_{r(t)}$ | % Diff | $T_{r(e)}$ | $U_r(\%)$<br>$\lambda = 0.6$ | $T_{r(t)}$ | % Diff |
|------------|------------------------------|------------|--------|------------|------------------------------|------------|--------|
| 0.028      | 23.65                        | 0.02       | 40.05  | 0.028      | 24.65                        | 0.02       | 38.35  |
| 0.046      | 35.87                        | 0.04       | 15.71  | 0.045      | 36.67                        | 0.04       | 11.67  |
| 0.065      | 44.89                        | 0.06       | 8.50   | 0.064      | 45.89                        | 0.06       | 5.93   |
| 0.090      | 53.11                        | 0.08       | 13.10  | 0.087      | 53.51                        | 0.08       | 8.17   |

|       |       |      |       |       |       |      |       |
|-------|-------|------|-------|-------|-------|------|-------|
| 0.115 | 59.32 | 0.1  | 15.38 | 0.113 | 60.32 | 0.1  | 12.63 |
| 0.144 | 64.73 | 0.12 | 20.04 | 0.139 | 65.53 | 0.12 | 16.23 |
| 0.167 | 68.94 | 0.14 | 19.37 | 0.162 | 69.94 | 0.14 | 15.86 |
| 0.187 | 72.34 | 0.16 | 16.74 | 0.181 | 73.35 | 0.16 | 13.18 |
| 0.203 | 75.15 | 0.18 | 12.98 | 0.198 | 76.35 | 0.18 | 9.87  |
| 0.216 | 77.35 | 0.2  | 8.19  | 0.210 | 78.56 | 0.2  | 5.00  |
| 0.227 | 79.16 | 0.22 | 3.20  | 0.220 | 80.16 | 0.22 | 0.10  |
| 0.240 | 80.56 | 0.24 | 0.12  | 0.245 | 81.96 | 0.24 | 2.19  |
| 0.258 | 81.76 | 0.26 | 0.76  | 0.262 | 83.17 | 0.26 | 0.74  |
| 0.276 | 82.97 | 0.28 | 1.50  | 0.273 | 83.97 | 0.28 | 2.48  |
| 0.288 | 83.77 | 0.3  | 4.13  | 0.287 | 84.97 | 0.3  | 4.35  |
| 0.299 | 84.57 | 0.32 | 6.42  | 0.298 | 85.77 | 0.32 | 6.85  |
| 0.308 | 85.17 | 0.34 | 9.31  | 0.306 | 86.37 | 0.34 | 9.88  |

Tables are prepared in a similar form for all **values of ' $\lambda$ '** as mentioned in Step 4.

| $T_{r(e)}$ | $U_r(\%)$<br>$\lambda = -0.175$ | $T_{r(t)}$ | % Diff |
|------------|---------------------------------|------------|--------|
| 0.026      | 38.08                           | 0.02       | 30.74  |
| 0.040      | 49.50                           | 0.04       | 0.92   |
| 0.061      | 59.32                           | 0.06       | 1.12   |
| 0.084      | 67.54                           | 0.08       | 4.80   |
| 0.106      | 74.95                           | 0.1        | 6.32   |
| 0.119      | 79.16                           | 0.12       | 0.51   |

|       |        |      |       |
|-------|--------|------|-------|
| 0.173 | 86.57  | 0.14 | 23.59 |
| 0.179 | 87.37  | 0.16 | 12.03 |
| 0.207 | 90.38  | 0.18 | 15.13 |
| 0.291 | 94.59  | 0.2  | 45.63 |
| 0.327 | 96.39  | 0.22 | 48.75 |
| 0.355 | 97.80  | 0.24 | 48.03 |
| 0.379 | 99.00  | 0.26 | 45.87 |
| 0.391 | 99.60  | 0.28 | 39.74 |
| 0.395 | 99.80  | 0.3  | 31.76 |
| 0.397 | 99.90  | 0.32 | 24.15 |
| 0.399 | 100.00 | 0.34 | 17.43 |

#### Step 6

Now curve fitting process is carried out on the basis of regression analysis done for % difference between theoretical Time factor and experimental Time factor for given values of ' $\lambda$ ' so as to get most appropriate value of ' $\lambda$ ' for that particular drain and for particular ' $n$ ' value. In this example for coir-jute fiber drain (CJ), curve of  $\lambda = -0.2$  fits with experimental curve as shown in fig. 6.3

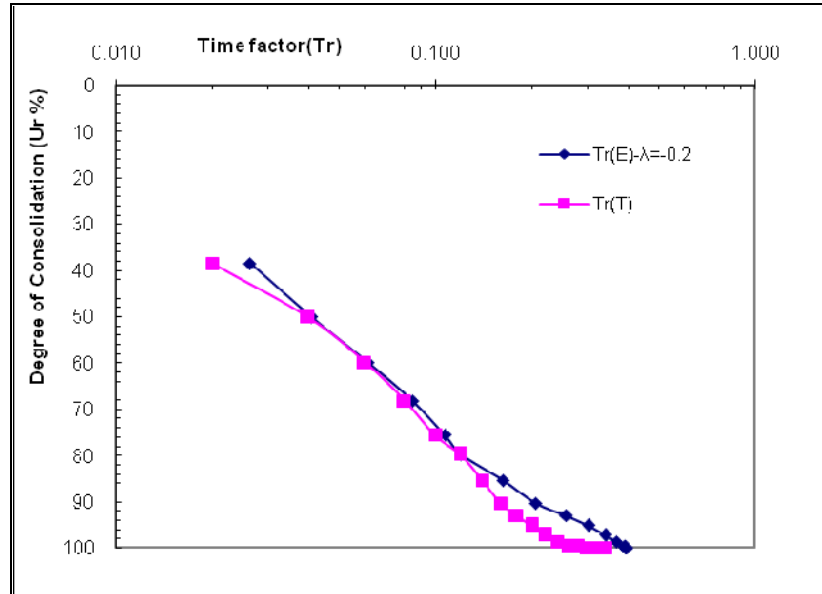


**Fig. 6.3:** Comparison of theoretical and experimental Degree of consolidation and fitting of experimental curve for  $\lambda = -0.2$

(ii) Based on pore water pressure measurements

In the present work coefficient of consolidation due to radial drainage ( $C_r$ ) is computed for 50% and 80% consolidation at three radial points'  $r_1$ ,  $r_2$  and  $r_3$ . While detail analysis is done considering 80% consolidation based on isochrones.

A stepwise procedure for the determination of coefficient of consolidation due to radial drainage at mid plane radial point  $r_2$  i.e. ( $C_{r2}$ ) is explained below with example.

**Procedure:**

- i. First of all dissipation of excess hydrostatic pore water pressure ( $1 - U_r/U_0$ )% vs time are noted at three radial points  $r_1$ ,  $r_2$  and  $r_3$  located at distance of  $r/4$ ,  $r/2$  and  $3r/4$  for applied pressures of 20, 40, 80, 160, 320 kPa respectively. Here  $U_r$  is excess pore water pressure at time 't' from start of consolidation test (difference of mercury in two limbs of manometer 'U' tube) and  $U_0$  is initial excess pore pressure (applied pressure).

- ii. From pore pressure readings, consolidation curve is plotted. From this curve (refer fig.6.4) the time for 50% and 80% consolidation are determined for all three radial points.
- iii. Now using the formula to get  $C_r = T_r \cdot r_e^2 / t \cdot 60 = \text{cm}^2/\text{sec}$ , where  $r_e$  is radius of influence depend upon radius of oedometer/influence ( $r_e$ ) and is taken as net distance between boundary of drain to particular radial point ( $r_1 - r_d$ ), ( $r_2 - r_d$ ), ( $r_3 - r_d$ ) and  $T_r$  is theoretical time factor as per consolidation theory (taken for 80% consolidation) mentioned in chapter 4. Here value of  $T_r$  will depend upon selection of particular lump parameter ' $\lambda$ '. Thus  $C_{r1}$ ,  $C_{r2}$ ,  $C_{r3}$  are computed for 50% and 80% consolidation using above formula.
- iv. Now experimental isochrones are plotted with respect to time for all applied pressures, and from these isochrones the average degree of consolidation for given time is computed using Simpsons rule (area under isochrones divided by total area). Using above  $C_{r2,80}$  of mid radial point ' $r_2$ ' (degree of consolidation equal to 80%) the theoretical time factors for each lump parameter  $\lambda$  is determined ( $T_{r80}$  at  $U_r = 80\%$ ). This step is repeated for all values of ' $\lambda$ '.
- v. After computing  $C_{r2,80}$  the experimental time factor ( $T_r$ ) is obtained using formula for various values of ' $\lambda$ '. This step is repeated for all applied pressures. Now to determine experimental time factor for different degree of consolidation for range of ' $\lambda$ ', the formula  $T_r = C_{r2,80} \cdot t \cdot 60 / r_e^2$  is used and this exercise is repeated for all values of lump parameter  $\lambda$  and for all applied pressures using Excel-macro program.
- vi. Now comparative tables are made for each lump parameter  $\lambda$  between Degree of consolidation, theoretical time factor and experimental time factor. Thereafter degree of error using regression analysis is determined.

### Example:

Type of Drain = CJ, ' $n$ ' value = 11.04

Diameter of Oedometer = 254mm, Diameter of drain = 23mm

Distance of mid radial point  $r_2$  from centre = 71mm

Net distance  $r_2$  from drain boundary ( $r_2 - r_d$ ) = (71-11.5) = 59.5mm = 5.95cm

Type of drainage = Radial drainage

**Step 1**

Applied pressure = 160kPa

| Radial point 'r1' |        |           |           | Radial point 'r2' |        |       |            | Radial point 'r3' |        |       |            |
|-------------------|--------|-----------|-----------|-------------------|--------|-------|------------|-------------------|--------|-------|------------|
| Log't'min         | Ur     | Ur/Uo (%) | 1-Ur/Uo)% | Log't'min         | Ur     | Ur/Uo | (1-Ur/Uo)% | Log't'min         | Ur     | Ur/Uo | (1-Ur/Uo)% |
| 0                 |        |           |           | 0                 |        |       |            | 0                 |        |       |            |
| 0.25              | 0.7264 | 90.80     | 9.20      | 0.25              | 0.7552 | 94.40 | 94.40      | 0.25              | 0.7552 | 94.40 | 5.60       |
| 1                 | 0.7200 | 90.00     | 10.00     | 1                 | 0.7552 | 94.40 | 94.40      | 1                 | 0.7552 | 94.40 | 5.60       |
| 2.25              | 0.6960 | 87.00     | 13.00     | 2.25              | 0.7520 | 94.00 | 94.00      | 2.25              | 0.7520 | 94.00 | 6.00       |
| 4                 | 0.6784 | 84.80     | 15.20     | 4                 | 0.7440 | 93.00 | 93.00      | 4                 | 0.7440 | 93.00 | 7.00       |
| 6.25              | 0.6600 | 82.50     | 17.50     | 6.25              | 0.7376 | 92.20 | 92.20      | 6.25              | 0.7376 | 92.20 | 7.80       |
| 9                 | 0.6400 | 80.00     | 20.00     | 9                 | 0.7328 | 91.60 | 91.60      | 9                 | 0.7328 | 91.60 | 8.40       |
| 12.25             | 0.6216 | 77.70     | 22.30     | 12.25             | 0.7272 | 90.90 | 90.90      | 12.25             | 0.7272 | 90.90 | 9.10       |
| 16                | 0.6048 | 75.60     | 24.40     | 16                | 0.7160 | 89.50 | 89.50      | 16                | 0.7160 | 89.50 | 10.50      |
| 20.25             | 0.5920 | 74.00     | 26.00     | 20.25             | 0.7056 | 88.20 | 88.20      | 20.25             | 0.7056 | 88.20 | 11.80      |
| 25                | 0.5760 | 72.00     | 28.00     | 25                | 0.6944 | 86.80 | 86.80      | 25                | 0.6944 | 86.80 | 13.20      |
| 36                | 0.5384 | 67.30     | 32.70     | 36                | 0.6784 | 84.80 | 84.80      | 36                | 0.6784 | 84.80 | 15.20      |
| 49                | 0.4936 | 61.70     | 38.30     | 49                | 0.6568 | 82.10 | 82.10      | 49                | 0.6568 | 82.10 | 17.90      |
| 64                | 0.4480 | 56.00     | 44.00     | 64                | 0.6400 | 80.00 | 80.00      | 64                | 0.6400 | 80.00 | 20.00      |
| 81                | 0.3872 | 48.40     | 51.60     | 81                | 0.6184 | 77.30 | 77.30      | 81                | 0.6184 | 77.30 | 22.70      |
| 100               | 0.3080 | 38.50     | 61.50     | 100               | 0.5920 | 74.00 | 74.00      | 100               | 0.5920 | 74.00 | 26.00      |
| 121               | 0.2288 | 28.60     | 71.40     | 121               | 0.5600 | 70.00 | 70.00      | 121               | 0.5600 | 70.00 | 30.00      |
| 144               | 0.1848 | 23.10     | 76.90     | 144               | 0.5264 | 65.80 | 65.80      | 144               | 0.5264 | 65.80 | 34.20      |
| 169               | 0.1600 | 20.00     | 80.00     | 169               | 0.5040 | 63.00 | 63.00      | 169               | 0.5040 | 63.00 | 37.00      |
| 196               | 0.1456 | 18.20     | 81.80     | 196               | 0.4712 | 58.90 | 58.90      | 196               | 0.4712 | 58.90 | 41.10      |
| 225               | 0.1288 | 16.10     | 83.90     | 225               | 0.4320 | 54.00 | 54.00      | 225               | 0.4320 | 54.00 | 46.00      |
| 256               | 0.1136 | 14.20     | 85.80     | 256               | 0.4000 | 50.00 | 50.00      | 256               | 0.4000 | 50.00 | 50.00      |
| 289               | 0.1040 | 13.00     | 87.00     | 289               | 0.3656 | 45.70 | 45.70      | 289               | 0.3656 | 45.70 | 54.30      |
| 324               | 0.0888 | 11.10     | 88.90     | 324               | 0.3440 | 43.00 | 43.00      | 324               | 0.3440 | 43.00 | 57.00      |
| 361               | 0.0760 | 9.50      | 90.50     | 361               | 0.3192 | 39.90 | 39.90      | 361               | 0.3192 | 39.90 | 60.10      |
| 1440              | 0.0000 | 0.00      | 100.00    | 1440              | 0.0800 | 10.00 | 10.00      | 1440              | 0.0800 | 10.00 | 90.00      |
| -----             | -----  | -----     | -----     | 2880              | 0.0000 | 0.00  | 0.00       | 2880              | 0.0000 | 0.00  | 100.00     |



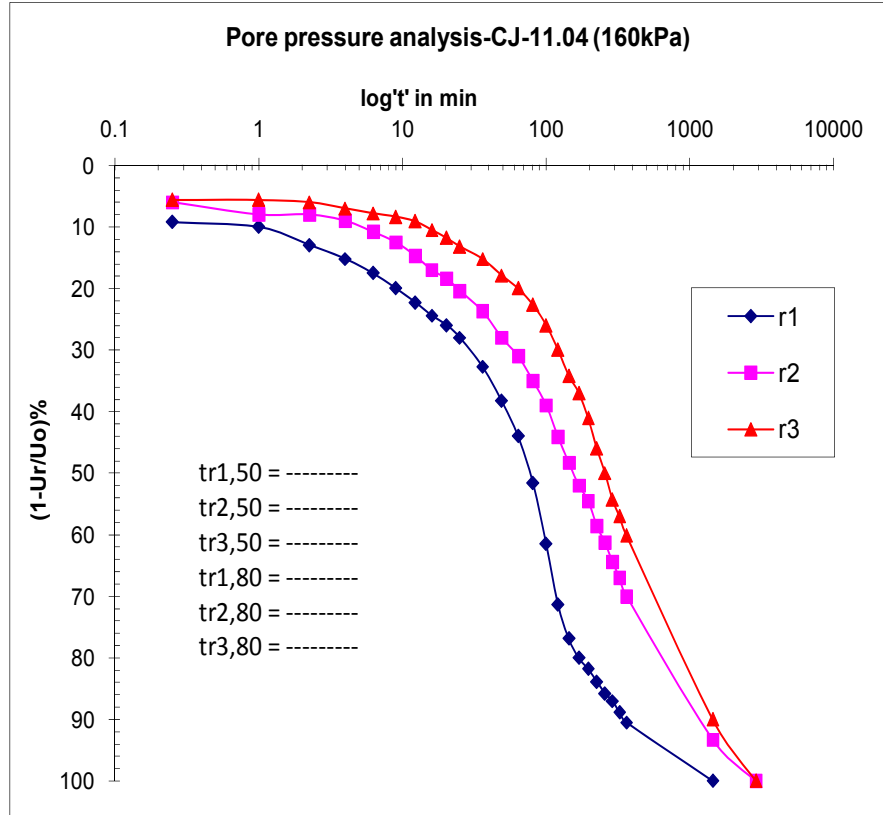


**Fig 6.4:** Dissipation of pore water pressure (degree of consolidation) vs. log't' for CJ drain of 'n'11.04 at three radial points at 160kPa

### Step 2

After obtaining time for 50% and 80% consolidation at three radial points r1, r2 and r3, the mid radial point 'r2' is selected for getting coefficient of consolidation through radial drainage ( $C_r$ ) for various range of values of lump parameter ' $\lambda$ ' i.e. from +0.7 to -0.7, which is represented here. To calculate  $C_r$  for  $U_r = 50\%$  and  $U_r = 80\%$ , the time factor ( $T_r$ ) is taken from theoretical table and is assigned as  $T_{r,50}$  and  $T_{r,80}$ . This exercise is done using excel program. This step is repeated for all applied pressures. Here  $C_r$  is also calculated for various degrees of consolidation.

Results, Analysis and Discussion

| Log't<br>in min | Theo Tr(80) | 0.232     | 0.218     | 0.2004    | 0.1886    | 0.1774    | 0.17      | 0.1656    | 0.161     | 0.159     |
|-----------------|-------------|-----------|-----------|-----------|-----------|-----------|-----------|-----------|-----------|-----------|
|                 | λ           | 0.7       | 0.6       | 0.5       | 0.4       | 0.3       | 0.25      | 0.2       | 0.175     | 0.15      |
|                 | A.P         | 160       | 160       | 160       | 160       | 160       | 160       | 160       | 160       | 160       |
|                 | Time(r2)80  | 575       | 575       | 575       | 575       | 575       | 575       | 575       | 575       | 575       |
|                 | Cr          | 0.0002381 | 0.0002237 | 0.0002056 | 0.0001935 | 0.0001820 | 0.0001744 | 0.0001699 | 0.000165  | 0.000163  |
|                 | Ur%         | Tr(E)     | Tr(E)     | Tr(E)     | Tr(E)     | Tr(E)     | Tr(E)     | Tr(E)     | Tr(E)     | Tr(E)     |
| 0.25            | 9.50        | 0.0001009 | 0.0000948 | 0.0000871 | 0.0000820 | 0.0000771 | 0.0000739 | 0.0000720 | 0.0000700 | 0.0000691 |
| 1               | 10.42       | 0.0004035 | 0.0003791 | 0.0003485 | 0.0003280 | 0.0003085 | 0.0002957 | 0.0002880 | 0.0002800 | 0.0002765 |
| 4               | 12.85       | 0.0016139 | 0.0015165 | 0.0013941 | 0.0013120 | 0.0012341 | 0.0011826 | 0.0011520 | 0.0011200 | 0.0011061 |
| 9               | 15.99       | 0.0036313 | 0.0034122 | 0.0031367 | 0.0029520 | 0.0027767 | 0.0026609 | 0.0025920 | 0.0025200 | 0.0024887 |
| 16              | 19.50       | 0.0064557 | 0.0060661 | 0.0055763 | 0.0052480 | 0.0049363 | 0.0047304 | 0.0046080 | 0.0044800 | 0.0044243 |
| 25              | 22.63       | 0.0100870 | 0.0094783 | 0.0087130 | 0.0082000 | 0.0077130 | 0.0073913 | 0.0072000 | 0.0070000 | 0.0069130 |
| 49              | 29.92       | 0.0197704 | 0.0185774 | 0.0170776 | 0.0160720 | 0.0151176 | 0.0144870 | 0.0141120 | 0.0137200 | 0.0135496 |
| 81              | 39.44       | 0.0326817 | 0.0307096 | 0.0282303 | 0.0265680 | 0.0249903 | 0.0239478 | 0.0233280 | 0.0226800 | 0.0223983 |
| 100             | 44.36       | 0.0403478 | 0.0379130 | 0.0348522 | 0.0328000 | 0.0308522 | 0.0295652 | 0.0288000 | 0.0280000 | 0.0276522 |
| 144             | 55.91       | 0.0581009 | 0.0545948 | 0.0501871 | 0.0472320 | 0.0444271 | 0.0425739 | 0.0414720 | 0.0403200 | 0.0398191 |
| 196             | 61.79       | 0.0790817 | 0.0743096 | 0.0683103 | 0.0642880 | 0.0604703 | 0.0579478 | 0.0564480 | 0.0548800 | 0.0541983 |
| 256             | 67.88       | 0.1032904 | 0.0970574 | 0.0892216 | 0.0839680 | 0.0789816 | 0.0756870 | 0.0737280 | 0.0716800 | 0.0707896 |
| 324             | 72.86       | 0.1307270 | 0.1228383 | 0.1129210 | 0.1062720 | 0.0999610 | 0.0957913 | 0.0933120 | 0.0907200 | 0.0895930 |
| 361             | 75.38       | 0.1456557 | 0.1368661 | 0.1258163 | 0.1184080 | 0.1113763 | 0.1067304 | 0.1039680 | 0.1010800 | 0.0998243 |
| 1440            | 95.36       | 0.5810087 | 0.5459478 | 0.5018713 | 0.4723200 | 0.4442713 | 0.4257391 | 0.4147200 | 0.4032000 | 0.3981913 |
| 2880            | 100.00      | 1.1620174 | 1.0918957 | 1.0037426 | 0.9446400 | 0.8885426 | 0.8514783 | 0.8294400 | 0.8064000 | 0.7963826 |

*Results, Analysis and Discussion*

Continue-----

|              |              |              |              |              |              |              |              |              |              |              |              |              |
|--------------|--------------|--------------|--------------|--------------|--------------|--------------|--------------|--------------|--------------|--------------|--------------|--------------|
| <b>0.156</b> | <b>0.154</b> | <b>0.152</b> | <b>0.151</b> | <b>0.149</b> | <b>0.147</b> | <b>0.144</b> | <b>0.142</b> | <b>0.141</b> | <b>0.14</b>  | <b>0.139</b> | <b>0.138</b> | <b>0.137</b> |
| <b>0.125</b> | <b>0.1</b>   | <b>0.08</b>  | <b>0.07</b>  | <b>0.05</b>  | <b>0.03</b>  | <b>0.01</b>  | <b>0</b>     | <b>-0.01</b> | <b>-0.02</b> | <b>-0.03</b> | <b>-0.04</b> | <b>-0.05</b> |
| 160          | 160          | 160          | 160          | 160          | 160          | 160          | 160          | 160          | 160          | 160          | 160          | 160          |
| 575          | 575          | 575          | 575          | 575          | 575          | 575          | 575          | 575          | 575          | 575          | 575          | 575          |
| 0.000160     | 0.000158     | 0.000156     | 0.000155     | 0.000153     | 0.000151     | 0.000148     | 0.000146     | 0.000145     | 0.000144     | 0.000143     | 0.000142     | 0.000141     |
| <b>Tr(E)</b> | <b>Tr(E)</b> | <b>Tr(E)</b> | <b>Tr(E)</b> | <b>Tr(E)</b> | <b>Tr(E)</b> | <b>Tr(E)</b> | <b>Tr(E)</b> | <b>Tr(E)</b> | <b>Tr(E)</b> | <b>Tr(E)</b> | <b>Tr(E)</b> | <b>Tr(E)</b> |
| 0.000068     | 0.000067     | 0.000066     | 0.000066     | 0.000065     | 0.000064     | 0.000063     | 0.000062     | 0.000061     | 0.000061     | 0.000060     | 0.000060     | 0.000060     |
| 0.000271     | 0.000268     | 0.000264     | 0.000263     | 0.000259     | 0.000256     | 0.000250     | 0.000247     | 0.000245     | 0.000243     | 0.000242     | 0.000240     | 0.000238     |
| 0.001085     | 0.001071     | 0.001057     | 0.001050     | 0.001037     | 0.001023     | 0.001002     | 0.000988     | 0.000981     | 0.000974     | 0.000967     | 0.000960     | 0.000953     |
| 0.002442     | 0.002410     | 0.002379     | 0.002363     | 0.002332     | 0.002301     | 0.002254     | 0.002223     | 0.002207     | 0.002191     | 0.002176     | 0.002160     | 0.002144     |
| 0.004341     | 0.004285     | 0.004230     | 0.004202     | 0.004146     | 0.004090     | 0.004007     | 0.003951     | 0.003923     | 0.003896     | 0.003868     | 0.003840     | 0.003812     |
| 0.006783     | 0.006696     | 0.006609     | 0.006565     | 0.006478     | 0.006391     | 0.006261     | 0.006174     | 0.006130     | 0.006087     | 0.006043     | 0.006000     | 0.005957     |
| 0.013294     | 0.013123     | 0.012953     | 0.012868     | 0.012697     | 0.012527     | 0.012271     | 0.012101     | 0.012016     | 0.011930     | 0.011845     | 0.011760     | 0.011675     |
| 0.021976     | 0.021694     | 0.021412     | 0.021271     | 0.020990     | 0.020708     | 0.020285     | 0.020003     | 0.019863     | 0.019722     | 0.019581     | 0.019440     | 0.019299     |
| 0.027130     | 0.026783     | 0.026435     | 0.026261     | 0.025913     | 0.025565     | 0.025043     | 0.024696     | 0.024522     | 0.024348     | 0.024174     | 0.024000     | 0.023826     |
| 0.039068     | 0.038567     | 0.038066     | 0.037816     | 0.037315     | 0.036814     | 0.036063     | 0.035562     | 0.035311     | 0.035061     | 0.034810     | 0.034560     | 0.034310     |
| 0.053176     | 0.052494     | 0.051812     | 0.051471     | 0.050790     | 0.050108     | 0.049085     | 0.048403     | 0.048063     | 0.047722     | 0.047381     | 0.047040     | 0.046699     |
| 0.069454     | 0.068563     | 0.067673     | 0.067228     | 0.066337     | 0.065447     | 0.064111     | 0.063221     | 0.062776     | 0.062330     | 0.061885     | 0.061440     | 0.060995     |
| 0.087903     | 0.086776     | 0.085649     | 0.085085     | 0.083958     | 0.082831     | 0.081141     | 0.080014     | 0.079450     | 0.078887     | 0.078323     | 0.077760     | 0.077197     |
| 0.097941     | 0.096685     | 0.095430     | 0.094802     | 0.093546     | 0.092290     | 0.090407     | 0.089151     | 0.088523     | 0.087896     | 0.087268     | 0.086640     | 0.086012     |
| 0.390678     | 0.385670     | 0.380661     | 0.378157     | 0.373148     | 0.368139     | 0.360626     | 0.355617     | 0.353113     | 0.350609     | 0.348104     | 0.345600     | 0.343096     |
| 0.781357     | 0.771339     | 0.761322     | 0.756313     | 0.746296     | 0.736278     | 0.721252     | 0.711235     | 0.706226     | 0.701217     | 0.696209     | 0.691200     | 0.686191     |

Continue-----

| <b>0.136</b> | <b>0.135</b> | <b>0.134</b> | <b>0.128</b> | <b>0.128</b> | <b>0.127</b> | <b>0.126</b> | <b>0.126</b>  | <b>0.126</b> | <b>0.125</b> | <b>0.124</b> |
|--------------|--------------|--------------|--------------|--------------|--------------|--------------|---------------|--------------|--------------|--------------|
| <b>-0.06</b> | <b>-0.07</b> | <b>-0.08</b> | <b>-0.09</b> | <b>-0.1</b>  | <b>-0.11</b> | <b>-0.12</b> | <b>-0.125</b> | <b>-0.13</b> | <b>-0.14</b> | <b>-0.15</b> |
| 160          | 160          | 160          | 160          | 160          | 160          | 160          | 160           | 160          | 160          | 160          |
| 575          | 575          | 575          | 575          | 575          | 575          | 575          | 575           | 575          | 575          | 575          |
| 0.000140     | 0.000139     | 0.000138     | 0.000131     | 0.000131     | 0.000130     | 0.000129     | 0.000129      | 0.000129     | 0.000128     | 0.000127     |
| <b>Tr(E)</b> | <b>Tr(E)</b> | <b>Tr(E)</b> | <b>Tr(E)</b> | <b>Tr(E)</b> | <b>Tr(E)</b> | <b>Tr(E)</b> | <b>Tr(E)</b>  | <b>Tr(E)</b> | <b>Tr(E)</b> | <b>Tr(E)</b> |
| 0.000059     | 0.000059     | 0.000058     | 0.000056     | 0.000056     | 0.000055     | 0.000055     | 0.000055      | 0.000055     | 0.000054     | 0.000054     |
| 0.000237     | 0.000235     | 0.000233     | 0.000223     | 0.000223     | 0.000221     | 0.000219     | 0.000219      | 0.000219     | 0.000217     | 0.000216     |
| 0.000946     | 0.000939     | 0.000932     | 0.000890     | 0.000890     | 0.000883     | 0.000877     | 0.000877      | 0.000877     | 0.000870     | 0.000863     |
| 0.002129     | 0.002113     | 0.002097     | 0.002003     | 0.002003     | 0.001988     | 0.001972     | 0.001972      | 0.001972     | 0.001957     | 0.001941     |
| 0.003784     | 0.003757     | 0.003729     | 0.003562     | 0.003562     | 0.003534     | 0.003506     | 0.003506      | 0.003506     | 0.003478     | 0.003450     |
| 0.005913     | 0.005870     | 0.005826     | 0.005565     | 0.005565     | 0.005522     | 0.005478     | 0.005478      | 0.005478     | 0.005435     | 0.005391     |
| 0.011590     | 0.011504     | 0.011419     | 0.010908     | 0.010908     | 0.010823     | 0.010737     | 0.010737      | 0.010737     | 0.010652     | 0.010567     |
| 0.019158     | 0.019017     | 0.018877     | 0.018031     | 0.018031     | 0.017890     | 0.017750     | 0.017750      | 0.017750     | 0.017609     | 0.017468     |
| 0.023652     | 0.023478     | 0.023304     | 0.022261     | 0.022261     | 0.022087     | 0.021913     | 0.021913      | 0.021913     | 0.021739     | 0.021565     |
| 0.034059     | 0.033809     | 0.033558     | 0.032056     | 0.032056     | 0.031805     | 0.031555     | 0.031555      | 0.031555     | 0.031304     | 0.031054     |
| 0.046358     | 0.046017     | 0.045677     | 0.043631     | 0.043631     | 0.043290     | 0.042950     | 0.042950      | 0.042950     | 0.042609     | 0.042268     |
| 0.060550     | 0.060104     | 0.059659     | 0.056988     | 0.056988     | 0.056543     | 0.056097     | 0.056097      | 0.056097     | 0.055652     | 0.055207     |
| 0.076633     | 0.076070     | 0.075506     | 0.072125     | 0.072125     | 0.071562     | 0.070998     | 0.070998      | 0.070998     | 0.070435     | 0.069871     |
| 0.085384     | 0.084757     | 0.084129     | 0.080362     | 0.080362     | 0.079734     | 0.079106     | 0.079106      | 0.079106     | 0.078478     | 0.077850     |
| 0.340591     | 0.338087     | 0.335583     | 0.320557     | 0.320557     | 0.318052     | 0.315548     | 0.315548      | 0.315548     | 0.313043     | 0.310539     |
| 0.681183     | 0.676174     | 0.671165     | 0.641113     | 0.641113     | 0.636104     | 0.631096     | 0.631096      | 0.631096     | 0.626087     | 0.621078     |

Continue-----

|              |              |               |              |              |              |
|--------------|--------------|---------------|--------------|--------------|--------------|
| <b>0.123</b> | <b>0.123</b> | <b>0.122</b>  | <b>0.122</b> | <b>0.121</b> | <b>0.121</b> |
| <b>-0.16</b> | <b>-0.17</b> | <b>-0.175</b> | <b>-0.18</b> | <b>-0.19</b> | <b>-0.2</b>  |
| 160          | 160          | 160           | 160          | 160          | 160          |
| 575          | 575          | 575           | 575          | 575          | 575          |
| 0.000126     | 0.000126     | 0.000125      | 0.000125     | 0.000124     | 0.000124     |
| <b>Tr(E)</b> | <b>Tr(E)</b> | <b>Tr(E)</b>  | <b>Tr(E)</b> | <b>Tr(E)</b> | <b>Tr(E)</b> |
| 0.000053     | 0.000053     | 0.000053      | 0.000053     | 0.000053     | 0.000053     |
| 0.000214     | 0.000214     | 0.000212      | 0.000212     | 0.000210     | 0.000210     |
| 0.000856     | 0.000856     | 0.000849      | 0.000849     | 0.000842     | 0.000842     |
| 0.001925     | 0.001925     | 0.001910      | 0.001910     | 0.001894     | 0.001894     |
| 0.003423     | 0.003423     | 0.003395      | 0.003395     | 0.003367     | 0.003367     |
| 0.005348     | 0.005348     | 0.005304      | 0.005304     | 0.005261     | 0.005261     |
| 0.010482     | 0.010482     | 0.010397      | 0.010397     | 0.010311     | 0.010311     |
| 0.017327     | 0.017327     | 0.017186      | 0.017186     | 0.017045     | 0.017045     |
| 0.021391     | 0.021391     | 0.021217      | 0.021217     | 0.021043     | 0.021043     |
| 0.030803     | 0.030803     | 0.030553      | 0.030553     | 0.030303     | 0.030303     |
| 0.041927     | 0.041927     | 0.041586      | 0.041586     | 0.041245     | 0.041245     |
| 0.054762     | 0.054762     | 0.054317      | 0.054317     | 0.053871     | 0.053871     |
| 0.069308     | 0.069308     | 0.068744      | 0.068744     | 0.068181     | 0.068181     |
| 0.077223     | 0.077223     | 0.076595      | 0.076595     | 0.075967     | 0.075967     |
| 0.308035     | 0.308035     | 0.305530      | 0.305530     | 0.303026     | 0.303026     |
| 0.616070     | 0.616070     | 0.611061      | 0.611061     | 0.606052     | 0.606052     |

**Step 3**

After getting experimental time factor ( $T_r(E)$ ) for various degree of consolidation and time for that degree of consolidation, this complete data sheet is transferred to excel macro program to interpolate and compare with theoretical time factors. For doing this same degree of consolidation is kept constant and experimental time factors are generated along with % error column (difference between theoretical and experimental time factors). Simultaneously isochrones are plotted with respect to time and time factor ( $T_r$ ) both theoretically and experimentally.

The sheet below represents how isochrones are drawn:

| Isochrones with respect to time (applied pressure =160kPa) |      |      |      |      |      |      |      |      |      |      |      |      |      |      |      |
|--|------|------|------|------|------|------|------|------|------|------|------|------|------|------|------|
| CJ-11.04   |      |      |      |      |      |      |      |      |      |      |      |      |      |      |      |
| (Ur/Uo)%   |      |      |      |      |      |      |      |      |      |      |      |      |      |      |      |
| Log't'   |      |      |      |      |      |      |      |      |      |      |      |      |      |      |      |
| min  | 0.25 | 1    | 4    | 9    | 16   | 25   | 49   | 81   | 100  | 144  | 196  | 256  | 324  | 361  | 1440 |
| r/re   |      |      |      |      |      |      |      |      |      |      |      |      |      |      |      |
| 0.09   | 0    | 0    | 0    | 0    | 0    | 0    | 0    | 0    | 0    | 0    | 0    | 0    | 0    | 0    | 0    |
| 0.2  | 90.8 | 90   | 84.8 | 80   | 75.6 | 72   | 61.7 | 48.4 | 38.5 | 23.1 | 18.2 | 14.2 | 11.1 | 9.5  | 0    |
| 0.55   | 94   | 92   | 91   | 87.5 | 83   | 79.6 | 72   | 65   | 61   | 51.7 | 45.5 | 38.7 | 33   | 30   | 6.7  |
| 0.87   | 94.4 | 94.4 | 93   | 91.6 | 89.5 | 86.8 | 82.1 | 77.3 | 74   | 65.8 | 58.9 | 50   | 43   | 39.9 | 10   |

**Step 4:** The figure 6.5 shows isochrones (degree of dissipation of hydrostatic pore water pressure,  $U_r/U_o$ ) drawn with respect to time obtained from pore pressure measurements at three radial points.

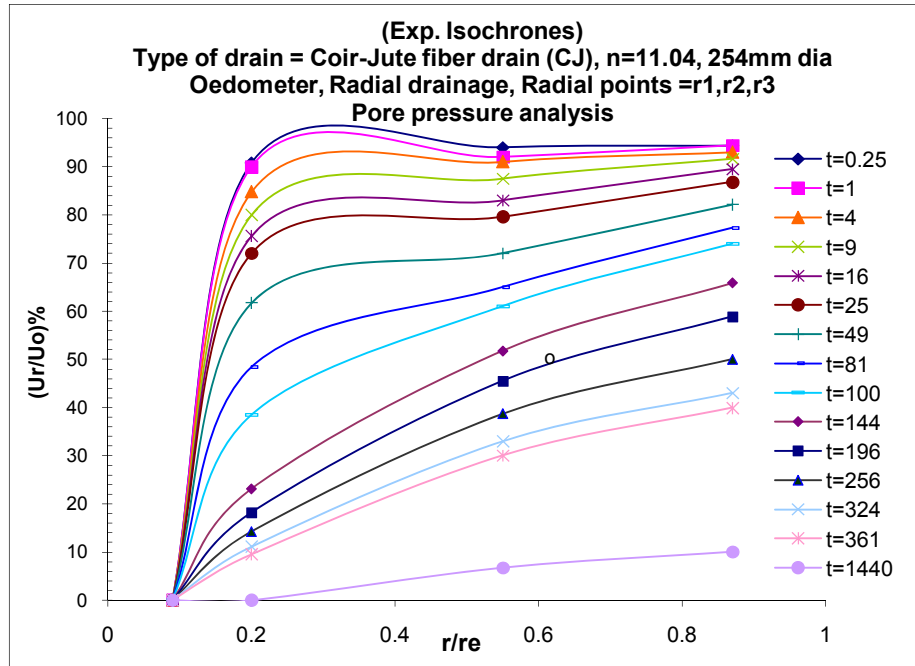


**Fig.6.5:** Experimental isochrones with respect to time for CJ of 'n'11.04

#### Step 5

After drawing isochrones for each pressures next step is to find out average degree of consolidation ( $U_r$ ) as per Simpsons rule, i.e. area under isochrones(shaded area) divided by total area of isochrones. The determination of area under isochrones was done using method of integration using software CURVE EXPERT 3.0. The table below is an example of this,

| Time in min | Shaded area | Total area | $U_r$  | $U_r\%$ |
|-------------|-------------|------------|--------|---------|
| 0.25        | 7.41        | 78         | 0.0950 | 9.50    |
| 1           | 8.13        | 78         | 0.1042 | 10.42   |
| 4           | 10.02       | 78         | 0.1285 | 12.85   |
| 9           | 12.47       | 78         | 0.1599 | 15.99   |
| 16          | 15.21       | 78         | 0.1950 | 19.50   |
| 25          | 17.65       | 78         | 0.2263 | 22.63   |
| 49          | 23.34       | 78         | 0.2992 | 29.92   |
| 81          | 30.76       | 78         | 0.3944 | 39.44   |
| 100         | 34.6        | 78         | 0.4436 | 44.36   |
| 144         | 43.61       | 78         | 0.5591 | 55.91   |
| 196         | 48.2        | 78         | 0.6179 | 61.79   |
| 256         | 52.95       | 78         | 0.6788 | 67.88   |
| 324         | 56.83       | 78         | 0.7286 | 72.86   |
| 361         | 58.8        | 78         | 0.7538 | 75.38   |
| 1440        | 74.38       | 78         | 0.9536 | 95.36   |

**Step 6**

Now comparison of experimental isochrones with theoretical isochrones is done in following way:

- After fitting appropriate lump parameter ' $\lambda$ ' for obtained average degree of consolidation, theoretical table for dissipation of excess hydrostatic pore water pressure ( $U_r/U_o$ ) is obtained theoretically (from proposed theory, chapter 4) for each radial point  $r_1$ ,  $r_2$  and  $r_3$  as shown in form  $U_{r1}/U_o$ ,  $U_{r2}/U_o$ , and  $U_{r3}/U_o$ .

| $\lambda = -0.175$ |              |        |        |        |        |        |         |
|--------------------|--------------|--------|--------|--------|--------|--------|---------|
| Avg<br>Ur%         | Tr<br>(theo) | Ur1/Uo | %      | Ur2/Uo | %      | Ur3/Uo | %       |
| 38.08              | 0.02         | 0.249  | 24.911 | 0.752  | 75.153 | 1.008  | 100.822 |
| 49.50              | 0.04         | 0.191  | 19.127 | 0.609  | 60.920 | 0.825  | 82.493  |
| 59.32              | 0.06         | 0.144  | 14.379 | 0.492  | 49.238 | 0.675  | 67.450  |
| 67.54              | 0.08         | 0.105  | 10.483 | 0.397  | 39.650 | 0.551  | 55.103  |
| 74.95              | 0.10         | 0.073  | 7.285  | 0.318  | 31.781 | 0.450  | 44.970  |
| 79.16              | 0.12         | 0.047  | 4.660  | 0.253  | 25.323 | 0.367  | 36.653  |
| 86.57              | 0.14         | 0.025  | 2.506  | 0.200  | 20.022 | 0.298  | 29.827  |
| 89.78              | 0.16         | 0.007  | 0.738  | 0.157  | 15.671 | 0.242  | 24.224  |
| 92.38              | 0.18         | -0.007 | 0.000  | 0.121  | 12.101 | 0.196  | 19.626  |
| 94.59              | 0.20         | -0.019 | 0.000  | 0.092  | 9.170  | 0.159  | 15.852  |
| 96.39              | 0.22         | -0.029 | 0.000  | 0.068  | 6.765  | 0.128  | 12.755  |
| 97.80              | 0.24         | -0.037 | 0.000  | 0.048  | 4.791  | 0.102  | 10.212  |
| 99.00              | 0.26         | -0.043 | 0.000  | 0.032  | 3.170  | 0.081  | 8.126   |
| 99.60              | 0.28         | -0.049 | 0.000  | 0.018  | 1.841  | 0.064  | 6.413   |
| 100.40             | 0.30         | -0.053 | 0.000  | 0.007  | 0.749  | 0.050  | 5.008   |
| 101.20             | 0.32         | -0.057 | 0.000  | -0.001 | -0.147 | 0.039  | 3.854   |
| 101.80             | 0.34         | -0.060 | 0.000  | -0.009 | -0.882 | 0.029  | 2.908   |

- Now comparative table is made between theoretical and experimental isochrones for each time factor ( $T_r$ ), this is done by interpolation as mid radial point  $r_2$  is selected for analysis as shown.
- In experimental programme the thickness of sample is  $R$ , the distance ' $R$ ' being the length of longest drainage path, while comparing experimental isochrones and theoretical isochrones, value of ' $R$ ' is modified to ' $R/2$ ' and considered accordingly.



| n=11.04, 160kPa, CJ drain |          |       |        |      |        |       |        |       |        |       |        |       |        |       |
|---------------------------|----------|-------|--------|------|--------|-------|--------|-------|--------|-------|--------|-------|--------|-------|
| r/re                      | Ur/Uo(%) |       |        |      |        |       |        |       |        |       |        |       |        |       |
|                           | T        | E     | T      | E    | T      | E     | T      | E     | T      | E     | T      | E     | T      | E     |
|                           | Tr       |       | Tr     |      | Tr     |       | Tr     |       | Tr     |       | Tr     |       | Tr     |       |
|                           | 0.02     |       | 0.04   |      | 0.06   |       | 0.08   |       | 0.1    |       | 0.12   |       | 0.14   |       |
| 0.09                      | 0        | 0     | 0      | 0    | 0      | 0     | 0      | 0     | 0      | 0     | 0      | 0     | 0      | 0     |
| 0.20                      | 24.91    | 25.04 | 19.127 | 19.1 | 14.379 | 14.42 | 10.483 | 10.46 | 7.285  | 7.91  | 4.660  | 5.65  | 2.506  | 3.39  |
| 0.56                      | 75.15    | 74.87 | 60.920 | 61   | 49.238 | 49.05 | 39.650 | 39.6  | 31.781 | 31.87 | 25.323 | 26.9  | 20.022 | 22.9  |
| 0.87                      | 100.82   | 99.8  | 82.493 | 82.1 | 67.450 | 67.2  | 55.103 | 55.08 | 44.970 | 44.8  | 36.653 | 38.06 | 29.827 | 33.46 |

Continue-----

| Ur/Uo(%) |       |        |       |       |       |        |       |        |       |       |      |       |      |
|----------|-------|--------|-------|-------|-------|--------|-------|--------|-------|-------|------|-------|------|
| T        | E     | T      | E     | T     | E     | T      | E     | T      | E     | T     | E    | T     | E    |
| Tr       |       | Tr     |       | Tr    |       | Tr     |       | Tr     |       | Tr    |      | Tr    |      |
| 0.16     |       | 0.18   |       | 0.2   |       | 0.22   |       | 0.24   |       | 0.26  |      | 0.28  |      |
| 0        | 0     | 0      | 0     | 0     | 0     | 0      | 0     | 0      | 0     | 0     | 0    | 0     | 0    |
| 0.7383   | 1.13  | 0      | 0     | 0     | 0     | 0      | 0     | 0      | 0     | 0     | 0    | 0     | 0    |
| 15.6714  | 18.85 | 12.101 | 14.8  | 9.17  | 10.75 | 6.765  | 6.7   | 4.791  | 5.3   | 3.170 | 3.9  | 1.841 | 2.51 |
| 24.2242  | 28.86 | 19.626 | 24.26 | 15.85 | 19.66 | 12.755 | 15.06 | 10.212 | 10.46 | 8.126 | 9.14 | 6.413 | 8.19 |

Note: Tr = Time factor, E = Experimental readings, T = Theoretical readings

➤ Now isochrones are plotted as shown in fig 6.6,

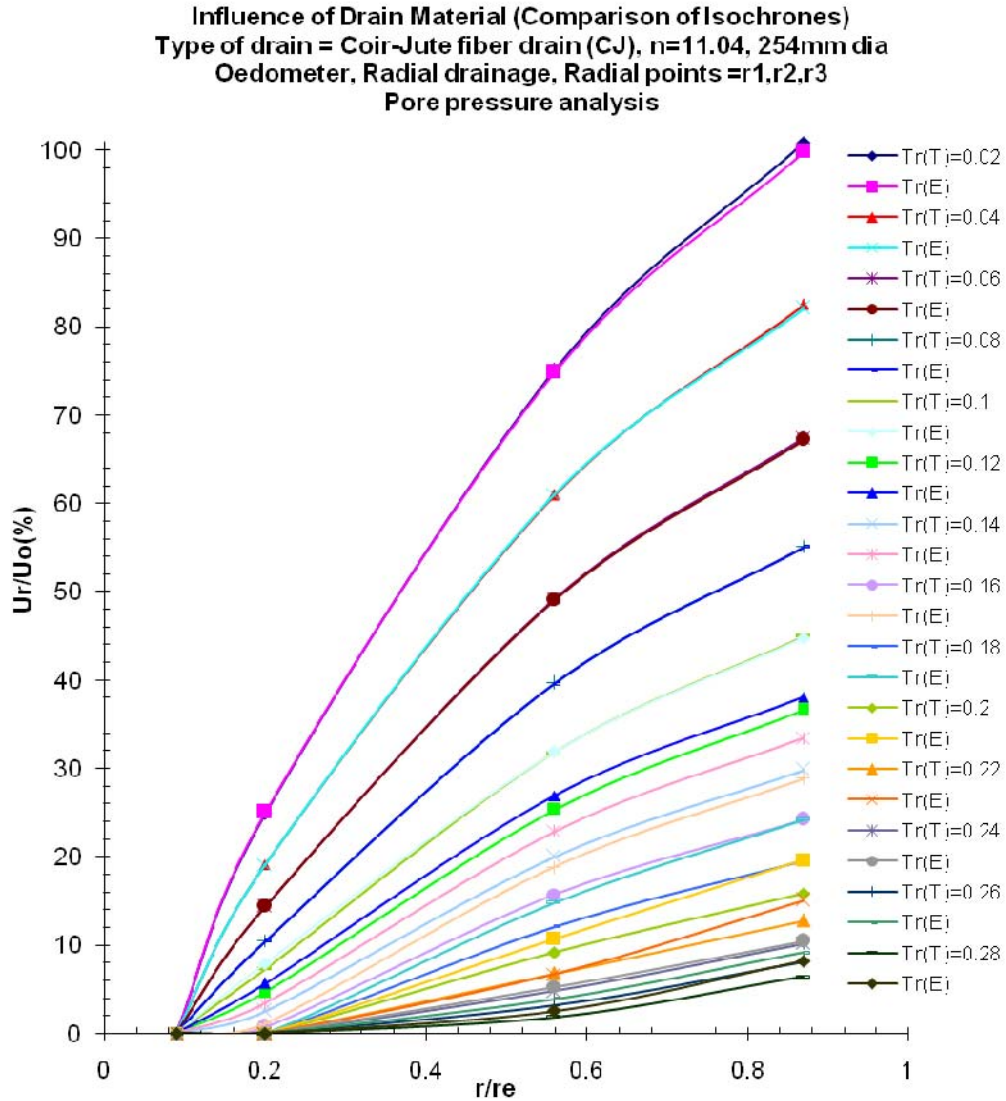


**Fig. 6.6:** Comparison of theoretical and experimental isochrones

- After plotting isochrones, the last step is to interpolate experimental time factor ( $Tr(E)$ ) with theoretical time factor ( $Tr(T)$ ) for same degree of consolidation ( $U_r$ ), this exercise is done using excel macro program, the final table (solution) is represented in form of table below. On the basis of % error calculated the most appropriate lump parameter is obtained and curve of degree of consolidation vs. time factor is plotted at last as shown in fig. 6.7. Similarly final plot is also shown here for sand drain (SD), sandwich drain (SW) for reference.
- Thus above mentioned all steps are repeated for all pressures.

**Coir-Jute fiber drain (CJ), n =11.04, 160kPa, 254mm diameter Oedometer**

| $\lambda=0.7$ |        |       |          | $\lambda=0.6$ |        |       |          | $\lambda=0.5$ |        |       |          |
|---------------|--------|-------|----------|---------------|--------|-------|----------|---------------|--------|-------|----------|
| Tr(E)         | Ur%    | Tr(T) | %        | Tr(E)         | Ur%    | Tr(T) | %        | Tr(E)         | Ur%    | Tr(T) | %        |
| 0.011         | 23.647 | 0.020 | 42.801   | 0.012         | 24.649 | 0.020 | 40.004   | 0.012         | 25.852 | 0.020 | 37.954   |
| 0.028         | 35.872 | 0.040 | 30.389   | 0.027         | 36.673 | 0.040 | 32.034   | 0.026         | 37.675 | 0.040 | 34.584   |
| 0.041         | 44.890 | 0.060 | 31.394   | 0.040         | 45.892 | 0.060 | 33.122   | 0.038         | 47.094 | 0.060 | 35.861   |
| 0.054         | 53.106 | 0.080 | 32.761   | 0.051         | 53.507 | 0.080 | 36.095   | 0.049         | 54.709 | 0.080 | 39.259   |
| 0.070         | 59.319 | 0.100 | 29.747   | 0.069         | 60.321 | 0.100 | 30.629   | 0.066         | 60.922 | 0.100 | 34.378   |
| 0.091         | 64.729 | 0.120 | 24.377   | 0.088         | 65.531 | 0.120 | 26.445   | 0.085         | 66.733 | 0.120 | 28.943   |
| 0.109         | 68.938 | 0.140 | 22.072   | 0.108         | 69.940 | 0.140 | 23.065   | 0.104         | 70.942 | 0.140 | 25.866   |
| 0.128         | 72.345 | 0.160 | 20.069   | 0.126         | 73.347 | 0.160 | 21.533   | 0.122         | 74.549 | 0.160 | 24.031   |
| 0.144         | 75.150 | 0.180 | 19.850   | 0.157         | 76.353 | 0.180 | 12.948   | 0.167         | 77.555 | 0.180 | 7.400    |
| 0.189         | 77.355 | 0.200 | 5.702    | 0.202         | 78.557 | 0.200 | 0.920    | 0.212         | 79.960 | 0.200 | 5.978    |
| 0.228         | 79.158 | 0.220 | 3.594    | 0.235         | 80.160 | 0.220 | 6.670    | 0.246         | 81.764 | 0.220 | 11.778   |
| 0.258         | 80.561 | 0.240 | 7.700    | 0.272         | 81.964 | 0.240 | 13.172   | 0.272         | 83.166 | 0.240 | 13.467   |
| 0.285         | 81.764 | 0.260 | 9.495    | 0.296         | 83.166 | 0.260 | 13.938   | 0.299         | 84.569 | 0.260 | 14.897   |
| 0.311         | 82.966 | 0.280 | 11.034   | 0.313         | 83.968 | 0.280 | 11.663   | 0.318         | 85.571 | 0.280 | 13.427   |
| 0.328         | 83.768 | 0.300 | 9.455    | 0.333         | 84.970 | 0.300 | 11.059   | 0.333         | 86.373 | 0.300 | 10.896   |
| 0.346         | 84.569 | 0.320 | 8.074    | 0.350         | 85.772 | 0.320 | 9.248    | 0.340         | 86.774 | 0.320 | 6.323    |
| 0.359         | 85.170 | 0.340 | 5.571    | 0.362         | 86.373 | 0.340 | 6.443    | 0.348         | 87.174 | 0.340 | 2.288    |
|               |        |       | 314.0853 |               |        |       | 328.9885 |               |        |       | 347.3319 |

Continue-----

## Coir-Jute fiber drain (CJ), n =11.04, 160kPa, 254mm diameter Oedometer

| $\lambda=0.4$ |        |       |          | $\lambda=0.3$ |        |       |          | $\lambda=0.25$ |        |       |          |
|---------------|--------|-------|----------|---------------|--------|-------|----------|----------------|--------|-------|----------|
| Tr(E)         | Ur%    | Tr(T) | %        | Tr(E)         | Ur%    | Tr(T) | %        | Tr(E)          | Ur%    | Tr(T) | %        |
| 0.013         | 27.255 | 0.020 | 34.038   | 0.014         | 28.858 | 0.020 | 29.819   | 0.014          | 29.659 | 0.020 | 28.848   |
| 0.026         | 38.677 | 0.040 | 35.672   | 0.026         | 39.880 | 0.040 | 36.203   | 0.025          | 40.681 | 0.040 | 36.578   |
| 0.038         | 48.297 | 0.060 | 37.134   | 0.037         | 49.900 | 0.060 | 37.727   | 0.036          | 50.501 | 0.060 | 39.196   |
| 0.048         | 56.112 | 0.080 | 40.228   | 0.049         | 57.515 | 0.080 | 38.997   | 0.049          | 58.317 | 0.080 | 38.924   |
| 0.067         | 62.725 | 0.100 | 32.705   | 0.067         | 63.928 | 0.100 | 33.046   | 0.067          | 64.930 | 0.100 | 32.920   |
| 0.083         | 67.735 | 0.120 | 30.428   | 0.086         | 69.539 | 0.120 | 28.367   | 0.086          | 70.341 | 0.120 | 28.656   |
| 0.104         | 72.345 | 0.140 | 25.739   | 0.105         | 73.948 | 0.140 | 25.084   | 0.104          | 74.749 | 0.140 | 25.729   |
| 0.128         | 75.952 | 0.160 | 19.713   | 0.148         | 77.555 | 0.160 | 7.781    | 0.154          | 78.357 | 0.160 | 3.627    |
| 0.182         | 78.958 | 0.180 | 0.956    | 0.194         | 80.361 | 0.180 | 7.949    | 0.205          | 81.563 | 0.180 | 14.115   |
| 0.224         | 81.363 | 0.200 | 12.165   | 0.238         | 82.966 | 0.200 | 18.864   | 0.241          | 83.768 | 0.200 | 20.307   |
| 0.256         | 83.166 | 0.220 | 16.494   | 0.268         | 84.770 | 0.220 | 21.721   | 0.273          | 85.772 | 0.220 | 23.918   |
| 0.285         | 84.770 | 0.240 | 18.622   | 0.295         | 86.373 | 0.240 | 22.711   | 0.298          | 87.375 | 0.240 | 24.260   |
| 0.302         | 85.772 | 0.260 | 16.326   | 0.318         | 87.776 | 0.260 | 22.264   | 0.321          | 88.778 | 0.260 | 23.318   |
| 0.327         | 87.174 | 0.280 | 16.894   | 0.331         | 88.577 | 0.280 | 18.302   | 0.337          | 89.780 | 0.280 | 20.225   |
| 0.342         | 87.976 | 0.300 | 13.835   | 0.348         | 89.579 | 0.300 | 15.981   | 0.346          | 90.381 | 0.300 | 15.411   |
| 0.352         | 88.577 | 0.320 | 10.049   | 0.361         | 90.381 | 0.320 | 12.907   | 0.359          | 91.182 | 0.320 | 12.198   |
| 0.363         | 89.178 | 0.340 | 6.709    | 0.371         | 90.982 | 0.340 | 9.213    | 0.369          | 91.784 | 0.340 | 8.423    |
|               |        |       | 367.7072 |               |        |       | 386.9365 |                |        |       | 396.6519 |

Continue-----

## Coir-Jute fiber drain (CJ), n =11.04, 160kPa, 254mm diameter Oedometer

| $\lambda=0.2$ |        |       |          | $\lambda=0.175$ |        |       |          | $\lambda=0.15$ |        |       |          |
|---------------|--------|-------|----------|-----------------|--------|-------|----------|----------------|--------|-------|----------|
| Tr(E)         | Ur%    | Tr(T) | %        | Tr(E)           | Ur%    | Tr(T) | %        | Tr(E)          | Ur%    | Tr(T) | %        |
| 0.015         | 30.461 | 0.020 | 26.835   | 0.015           | 30.862 | 0.020 | 26.980   | 0.015          | 31.263 | 0.020 | 26.022   |
| 0.025         | 41.283 | 0.040 | 36.549   | 0.025           | 41.683 | 0.040 | 37.228   | 0.025          | 42.285 | 0.040 | 36.404   |
| 0.036         | 51.102 | 0.060 | 39.671   | 0.036           | 51.503 | 0.060 | 40.634   | 0.036          | 51.904 | 0.060 | 40.668   |
| 0.050         | 59.319 | 0.080 | 37.317   | 0.050           | 59.719 | 0.080 | 37.819   | 0.050          | 60.120 | 0.080 | 37.367   |
| 0.068         | 65.731 | 0.100 | 32.382   | 0.067           | 66.132 | 0.100 | 33.154   | 0.067          | 66.533 | 0.100 | 32.893   |
| 0.087         | 71.142 | 0.120 | 27.872   | 0.086           | 71.543 | 0.120 | 28.597   | 0.087          | 72.144 | 0.120 | 27.590   |
| 0.107         | 75.551 | 0.140 | 23.887   | 0.113           | 76.152 | 0.140 | 19.506   | 0.117          | 76.553 | 0.140 | 16.230   |
| 0.163         | 79.158 | 0.160 | 1.673    | 0.167           | 79.760 | 0.160 | 4.533    | 0.171          | 80.160 | 0.160 | 6.976    |
| 0.209         | 82.164 | 0.180 | 16.358   | 0.213           | 82.766 | 0.180 | 18.177   | 0.216          | 83.166 | 0.180 | 20.035   |
| 0.247         | 84.569 | 0.200 | 23.428   | 0.249           | 85.170 | 0.200 | 24.546   | 0.255          | 85.772 | 0.200 | 27.490   |
| 0.278         | 86.573 | 0.220 | 26.379   | 0.279           | 87.174 | 0.220 | 27.002   | 0.282          | 87.575 | 0.220 | 28.146   |
| 0.303         | 88.176 | 0.240 | 26.240   | 0.304           | 88.778 | 0.240 | 26.522   | 0.306          | 89.178 | 0.240 | 27.445   |
| 0.325         | 89.579 | 0.260 | 24.923   | 0.322           | 89.980 | 0.260 | 23.785   | 0.327          | 90.581 | 0.260 | 25.701   |
| 0.344         | 90.782 | 0.280 | 22.681   | 0.340           | 91.182 | 0.280 | 21.438   | 0.345          | 91.784 | 0.280 | 23.137   |
| 0.353         | 91.383 | 0.300 | 17.620   | 0.352           | 91.984 | 0.300 | 17.384   | 0.357          | 92.585 | 0.300 | 18.919   |
| 0.365         | 92.184 | 0.320 | 14.166   | 0.361           | 92.585 | 0.320 | 12.889   | 0.369          | 93.387 | 0.320 | 15.229   |
| 0.375         | 92.786 | 0.340 | 10.201   | 0.370           | 93.186 | 0.340 | 8.923    | 0.375          | 93.788 | 0.340 | 10.211   |
|               |        |       | 408.1822 |                 |        |       | 409.1183 |                |        |       | 420.4633 |

Cointinue-----

Similar way results are obtained for various positive and negative values of lump parameter ' $\lambda$ ' and results are presented in form of tables. Here only some part of results are displayed.

| Coir-Jute fiber drain (CJ), $n = 11.04$ , 160kPa, 254mm diameter Oedometer |         |       |          |                    |         |       |          |                   |         |       |          |
|--|---------|-------|----------|--------------------|---------|-------|----------|-------------------|---------|-------|----------|
| $\lambda = -0.17$  |         |       |          | $\lambda = -0.175$ |         |       |          | $\lambda = -0.18$ |         |       |          |
| Tr(E)  | Ur%     | Tr(T) | %        | Tr(E)              | Ur%     | Tr(T) | %        | Tr(E)             | Ur%     | Tr(T) | %        |
| 0.016  | 37.876  | 0.020 | 18.978   | 0.016              | 38.076  | 0.020 | 18.922   | 0.016             | 38.076  | 0.020 | 18.922   |
| 0.025  | 49.098  | 0.040 | 36.868   | 0.025              | 49.499  | 0.040 | 36.571   | 0.025             | 49.499  | 0.040 | 36.571   |
| 0.036  | 58.918  | 0.060 | 39.186   | 0.037              | 59.319  | 0.060 | 38.428   | 0.037             | 59.519  | 0.060 | 37.801   |
| 0.053  | 66.934  | 0.080 | 34.053   | 0.054              | 67.535  | 0.080 | 33.018   | 0.053             | 67.335  | 0.080 | 33.541   |
| 0.071  | 73.547  | 0.100 | 28.536   | 0.075              | 74.950  | 0.100 | 24.756   | 0.072             | 73.948  | 0.100 | 27.871   |
| 0.119  | 78.958  | 0.120 | 1.239    | 0.120              | 79.158  | 0.120 | 0.128    | 0.122             | 79.359  | 0.120 | 1.787    |
| 0.204  | 86.373  | 0.140 | 45.854   | 0.205              | 86.573  | 0.140 | 46.308   | 0.205             | 86.573  | 0.140 | 46.308   |
| 0.241  | 89.579  | 0.160 | 50.779   | 0.214              | 87.375  | 0.160 | 33.762   | 0.242             | 89.780  | 0.160 | 50.992   |
| 0.271  | 92.180  | 0.180 | 50.722   | 0.248              | 90.381  | 0.180 | 38.040   | 0.271             | 92.385  | 0.180 | 50.801   |
| 0.297  | 94.389  | 0.200 | 48.412   | 0.297              | 94.589  | 0.200 | 48.354   | 0.297             | 94.589  | 0.200 | 48.354   |
| 0.363  | 96.192  | 0.220 | 65.159   | 0.374              | 96.393  | 0.220 | 69.813   | 0.374             | 96.393  | 0.220 | 69.813   |
| 0.456  | 97.595  | 0.240 | 90.191   | 0.466              | 97.796  | 0.240 | 94.141   | 0.479             | 97.996  | 0.240 | 99.638   |
| 0.550  | 98.998  | 0.260 | 111.371  | 0.545              | 98.998  | 0.260 | 109.652  | 0.558             | 99.198  | 0.260 | 114.727  |
| 0.576  | 99.399  | 0.280 | 105.774  | 0.585              | 99.599  | 0.280 | 108.813  | 0.572             | 99.400  | 0.280 | 104.129  |
| 0.590  | 99.600  | 0.300 | 96.507   | 0.598              | 99.800  | 0.300 | 99.298   | 0.585             | 99.600  | 0.300 | 94.909   |
| 0.603  | 99.800  | 0.320 | 88.373   | 0.604              | 99.900  | 0.320 | 88.899   | 0.598             | 99.800  | 0.320 | 86.842   |
| 0.616  | 100.000 | 0.340 | 81.197   | 0.611              | 100.000 | 0.340 | 79.724   | 0.611             | 100.000 | 0.340 | 79.724   |
|  |         |       | 993.1975 |                    |         |       | 968.6279 |                   |         |       | 1002.731 |

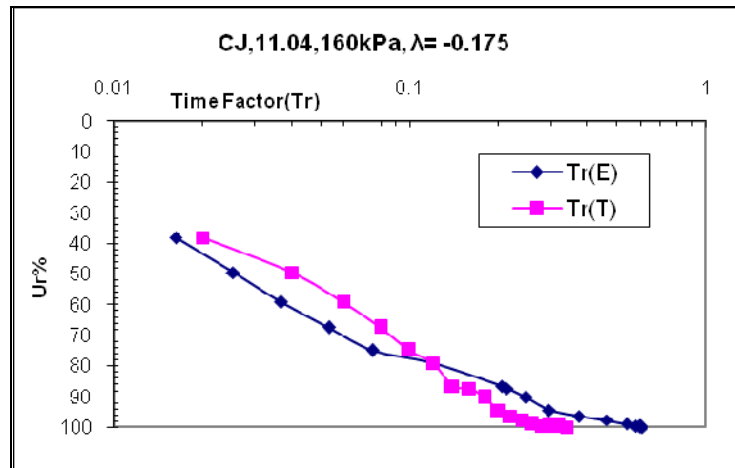


**Fig.6.7:** Comparison of degree of consolidation vs. experimental and theoretical time factor ( $Tr$ ) for CJ of 'n'11.04

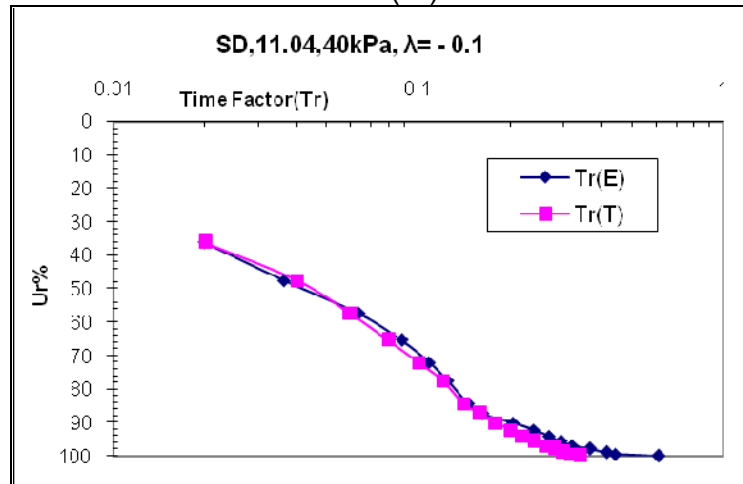


**Fig.6.8:** Comparison of degree of consolidation vs. experimental and theoretical time factor ( $Tr$ ) for SD of 'n'11.04

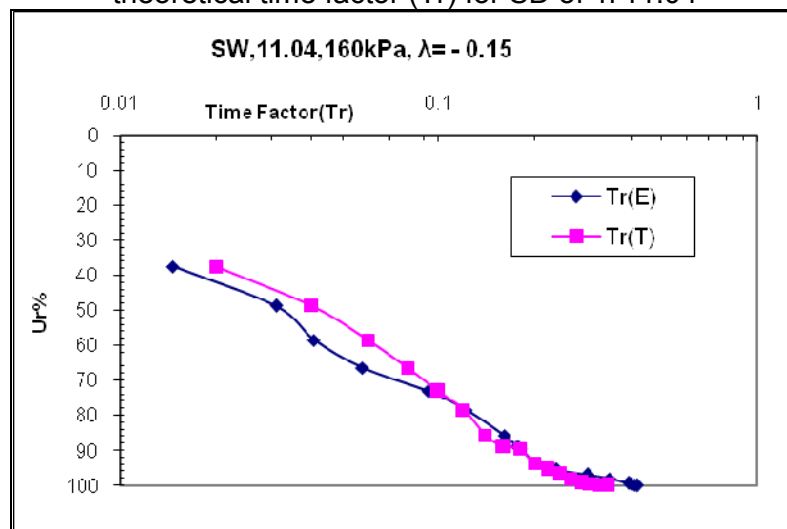


**Fig.6.9:** Comparison of degree of consolidation vs. experimental and theoretical time factor ( $Tr$ ) for SW of 'n'11.04

### 6.3. Analysis and Discussion: Consolidation due to radial drainage

Following factors are considered for analysis:

#### **Conventional Factors**

- 6.3.1 Type of drain materials
- 6.3.2 Influence of diameter('n' value)
- 6.3.3 Geometry (shape) of drain

#### **Derived Factors:**

- 6.3.4 Volumetric water ratio
- 6.3.5 Consolidation pressure ratio

The experimental data from a variety of test performed during these investigations are examined critically and discussed from fundamental considerations.

- From basic measurements of settlement for various interval of time the basic plot of dial gauge reading (dgr) vs.  $\log t$  for particular intensity of load are obtained for various factors influencing the consolidation due to only radial drainage. Similarly measurement of pore pressure at various radial points under particular intensity of pressure at different interval of time the basic plots of consolidation ratio versus log time and for different  $r/r_e$  are obtained.
- From basic settlement plots the coefficient of consolidation due to radial drainage( $C_r$ ) is deduced for various average degree of consolidation( $U_{avg}$ ) under various different pressures for appropriate lumped parameter ' $\lambda$ ' fitting to the theoretical and experimental curve. Consequently pore pressure basic plots are utilized to access average degree of consolidation from experimental isochrones for various experimental time factors. Simultaneously coefficient of consolidation is computed from consolidation ratio vs.  $\log t$  for various pore pressure measurement points.
- Void ratio computed at the end of every increment of pressure is plotted against effective log pressure from which compression index is



calculated. Pattern of  $C_c$  values versus pressure is ascertained by  $C_c$  vs. pressure plot for various influencing factors.

- While deciding various influencing factors some of the specific parameters are derived such as volumetric water ratio, drainage path ratio, permeability ratio, consolidation pressure ratio. The influence of these parameters on consolidation due to radial flow is analyzed critically. Also the experimental isochrone for above each parameter is compared with theoretical one along with comparison of theoretical ( $\lambda$ ) value with average degree of consolidation vs. time factor. Further in analysis, the terms average degree of consolidation ( $U_{Ravg}$ ) and  $U_r$  has the same means unless specified.

### 6.3.1: Type of Drain Material

Refer **figures 6.10 to 6.110** which are obtained from the settlement measurements and pore water pressure measurements.

- Sand drain-SD
- sandwich-polypropylene bags with sand as filler material-SW
- coir-jute fibers with outer cover of filter paper-CJ
- polypropylene fibers with outer cover of filter paper-PF

#### 1) Degree of consolidation $U_r$ vs. Time: Figures 6.10 to 6.26

**a) Settlement analysis:** Fig.6.10 to Fig.6.14 shows the plots of degree of consolidation versus time for various drain materials for all pressures ranging from 20kPa, 40kPa, 80kPa, 160kPa and 320kPa as and following observations are noted and discussed:

- The time required for 50 % consolidation using sand as drain material for  $n=11.04$  at 20kPa, 40kPa, 80kPa, 160kPa and 320kPa are 600min, 500min, 400min, 310min and 260min respectively while time required for 80% consolidation is 1300min, 980min, 840min, 760min and 580min respectively as shown in fig.6.10.
- The time required for 50 % consolidation using sandwich as drain material for  $n=11.04$  at 20kPa, 40kPa, 80kPa, 160kPa and 320kPa are

560min,500min,380min,300min and 200min respectively while time required for 80% consolidation is 1100min,950min,800min,720min and 540min respectively as shown in fig.6.11.

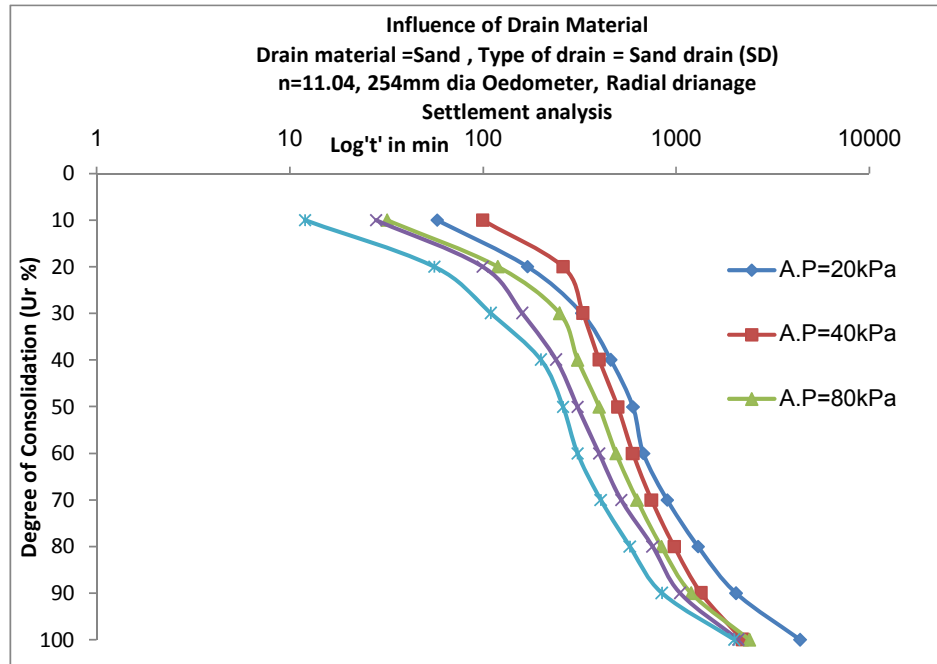


**Fig.6.10:** Degree of consolidation ( $U_r$ ) vs.  $\log't'$  in min for SD

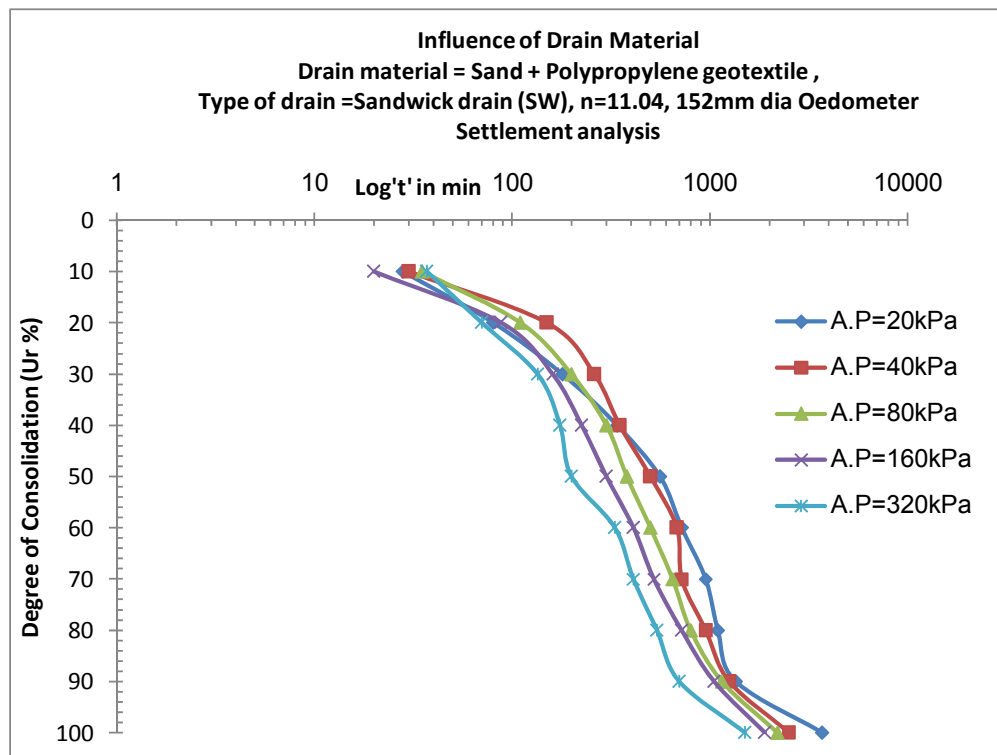


**Fig.6.11:** Degree of consolidation ( $U_r$ ) vs.  $\log't'$  in min for SW

- The time required for 50 % consolidation using coir-jute fiber as drain material for  $n=11.04$  at 20kPa, 40kPa, 80kPa, 160kPa and 320kPa are 425min, 330min, 240min, 185min and 140min respectively while time required for 80 % consolidation is 880min, 750min, 620min, 550min and 380min respectively.
- The time required for 50 % consolidation using polypropylene fiber as drain material for  $n=11.04$  at 20kPa, 40kPa, 80kPa, 160kPa and 320kPa are 700min, 630min, 500min, 425min and 300min respectively while time required for 80 % consolidation is 1070min, 1250min, 1000min, 940min and 560min respectively.

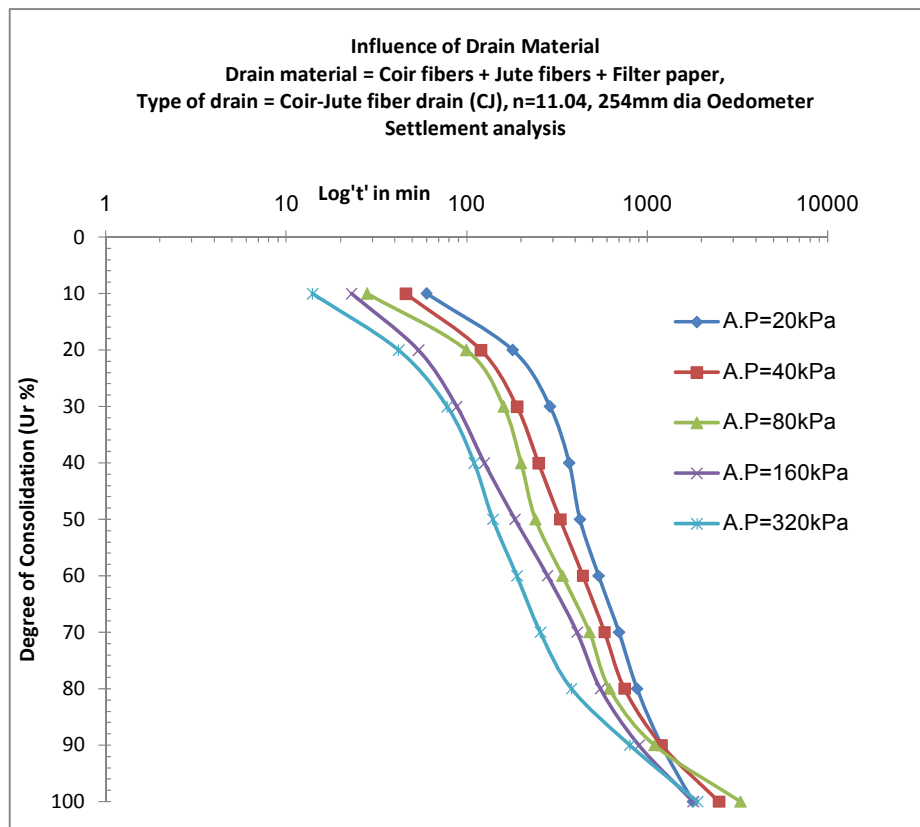


**Fig.6.12:** Degree of consolidation ( $U_r$ ) vs.  $\log't'$  in min for CJ

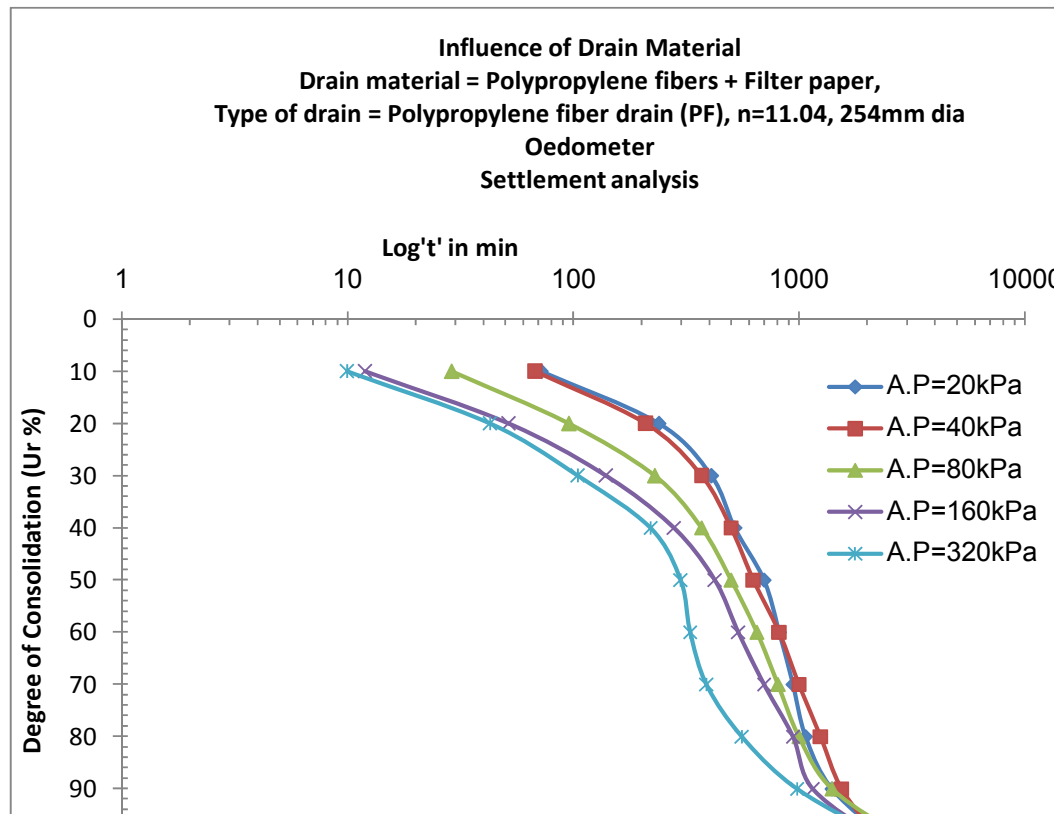


**Fig.6.13:** Degree of consolidation ( $U_r$ ) vs.  $\log't'$  in min for PF

- Comparing all four drain materials CJ takes lowest time both in terms of 50% and 80% consolidation. For 40kPa and for 50% consolidation CJ takes 51% less time in compare to SD & SW, 90% in compare to PF, while for 80% consolidation CJ takes 26.6% less time in compare to SW, 66.7% in compare to PF and 30.6% in compare to SD as depicted from fig.6.14 and table 6.1. (for same 'n' value and for same pressure)
- For 160kPa and for 50% consolidation CJ takes 67.5% less time in compare to SD, 62.2% less time in compare to SW, 129.7% in compare to PF, while for 80% consolidation CJ takes 30.9% less time in compare to SW, 70.9% in compare to PF and 38.1% in compare to SD as depicted from fig.6.14 and table 6.1. (for same 'n' value and for same pressure)
- From the above observations it is clear that CJ is most efficient drain material as it shows higher rate of compressibility (settlement) both for 50% and 80% consolidation.

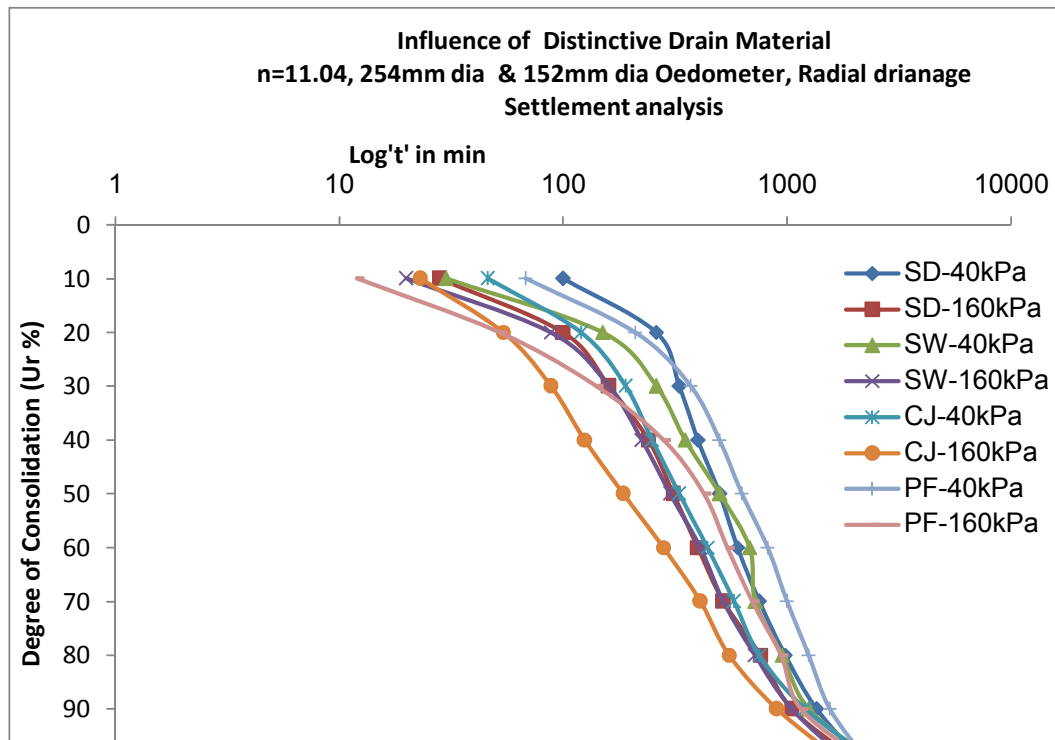


**Fig.6.14:** Comparison of Degree of consolidation of various drain materials w.r.t 40kPa and 160kPa applied pressure

**Table 6.1:** Comparison of time taken for 50% and 80% degree of consolidation of drain material based on settlement and pore pressure measurements

| Drain material | Settlement based     |                      | Pore pressure based  |                      |
|----------------|----------------------|----------------------|----------------------|----------------------|
|                | Time for 50%Ur-40kPa | Time for 80%Ur-40kPa | Time for 50%Ur-40kPa | Time for 80%Ur-40kPa |
| SD             | 490                  | 1200                 | 500                  | 980                  |
| SW             | 500                  | 950                  | 250                  | 740                  |
| CJ             | 330                  | 750                  | 125                  | 580                  |
| PF             | 630                  | 1250                 | 215                  | 650                  |

| Drain material | Settlement based      |                       | Pore pressure based   |                       |
|----------------|-----------------------|-----------------------|-----------------------|-----------------------|
|                | Time for 50%Ur-160kPa | Time for 80%Ur-160kPa | Time for 50%Ur-160kPa | Time for 80%Ur-160kPa |
| SD             | 310                   | 760                   | 640                   | 1500                  |
| SW             | 300                   | 720                   | 385                   | 850                   |
| CJ             | 185                   | 550                   | 160                   | 575                   |
| PF             | 425                   | 940                   | 361                   | 780                   |

**b) Pore pressure analysis-** Fig.6.11 to Fig.6.24 shows plots of degree of consolidation (dissipation of excess pore water pressure) versus time for various drain materials for all pressures ranging from 20kPa, 40kPa, 80kPa, 160kPa and 320kPa at three radial points  $r_1$ ,  $r_2$ ,  $r_3$  and following observations are noted and discussed as follows:

- The time required for 50 % consolidation using sand as drain material (sand drain) for  $n=11.04$  at 40kPa for radial point  $r_1, r_2$  &  $r_3$  is 245min, 490min, 760min while for 160kPa for radial point  $r_1, r_2$  &  $r_3$  is 400min, 640min, 950min respectively and time required for 80 % consolidation at 40kPa for radial point  $r_1, r_2$  &  $r_3$  is 600min, 1200min, 1800min while for 160kPa for radial point  $r_1, r_2$  &  $r_3$  is 750min, 1500min, 2100min respectively as shown in fig.6.15.
- The time required for 50 % consolidation using sand wrapped by polypropylene geotextile cover (sandwich) as drain material for  $n=11.04$  at 40kPa for radial point  $r_1, r_2$  &  $r_3$  is 160min, 250min, 400min while for 160kPa for radial point  $r_1, r_2$  &  $r_3$  is 220min, 385min, 570min respectively and time required for 80 % consolidation at 40kPa for radial point  $r_1, r_2$  &  $r_3$  is 350min, 740min, 950min while for 160kPa for radial point  $r_1, r_2$  &  $r_3$  is 440min, 850min, 1200min respectively as shown in fig.6.16.
- The time required for 50 % consolidation using coir-jute fiber wrapped by filter paper (coir-jute drain) as drain material for  $n=11.04$  at 40kPa for radial point  $r_1, r_2$  &  $r_3$  is 39min, 125min, 220min while for 160kPa for radial point  $r_1, r_2$  &  $r_3$  is 80min, 160min, 256min min respectively and time required for 80 % consolidation at 40kPa for radial point  $r_1, r_2$  &  $r_3$  is 105min, 580min, 680min while for 160kPa for radial point  $r_1, r_2$  &  $r_3$  is 160min, 575min, 920min respectively as shown in fig.6.17.
- The time required for 50 % consolidation using polypropylene fiber wrapped by filter paper (polypropylene fiber drain) as drain material for  $n=11.04$  at 40kPa for radial point  $r_1, r_2$  &  $r_3$  is 135min, 215min, 350min while for 160kPa for radial point  $r_1, r_2$  &  $r_3$  is 170min, 361min, 520min respectively and time required for 80 % consolidation at 40kPa for radial point  $r_1, r_2$  &  $r_3$  is 300min, 650min, 800min while for 160kPa for radial point  $r_1, r_2$  &  $r_3$  is 360min, 780min, 1100min respectively as shown in fig.6.18.

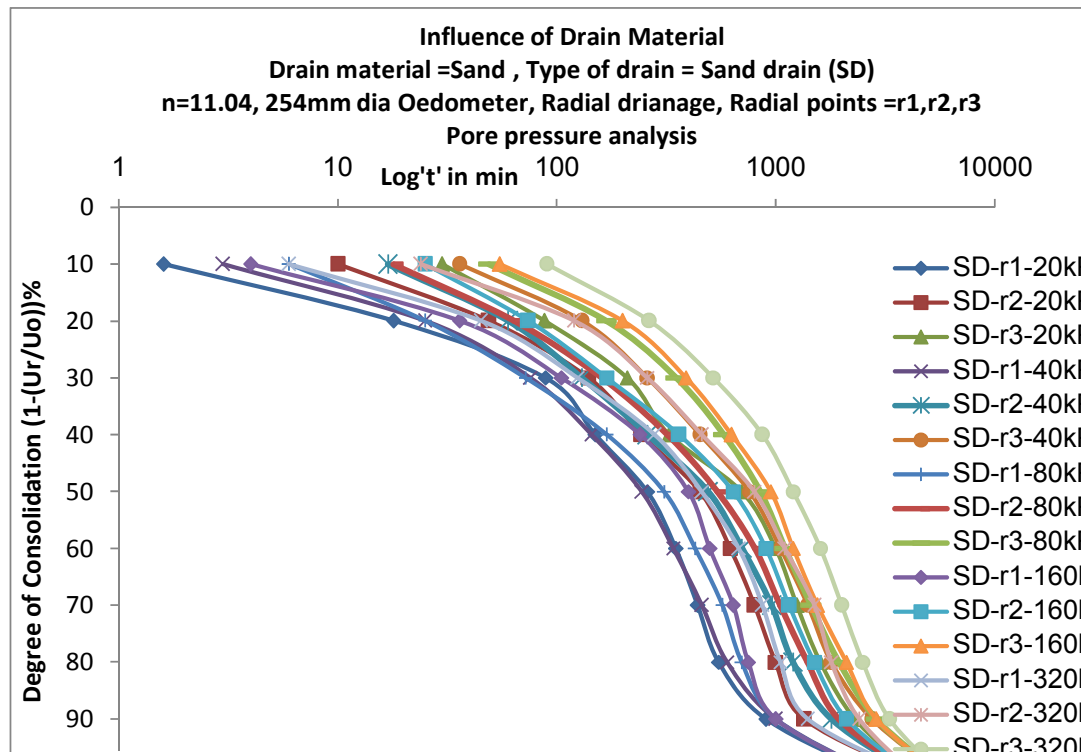


**Fig.6.15:** Degree of consolidation based on dissipation of excess hydrostatic pore water pressure vs.  $\log't'$  in min

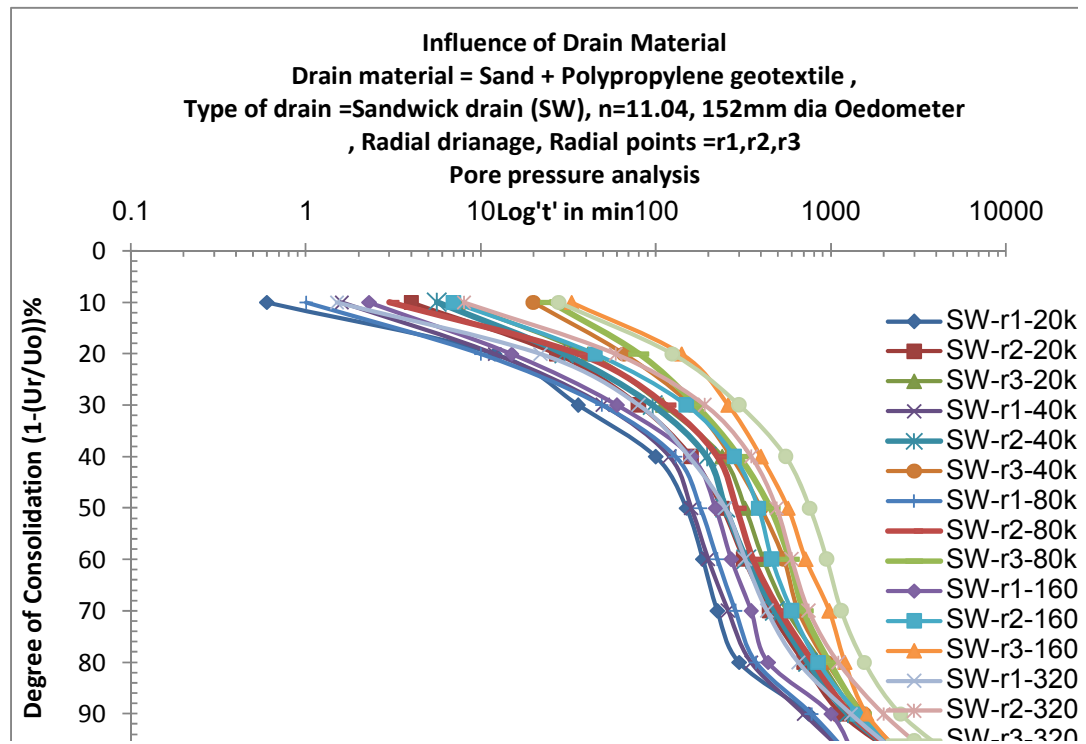


**Fig.6.16:** Degree of consolidation based on dissipation of excess hydrostatic pore water pressure vs.  $\log't'$  in min

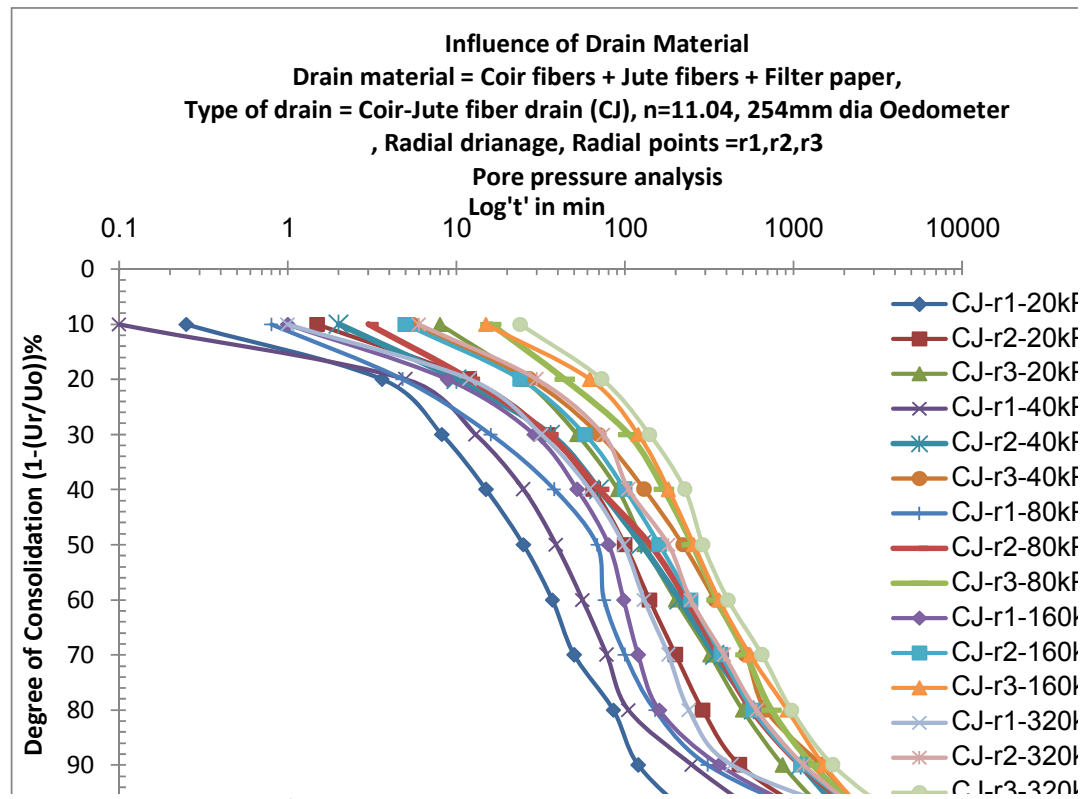


**Fig.6.17:** Degree of consolidation based on dissipation of excess hydrostatic pore water pressure vs.  $\log't'$  in min

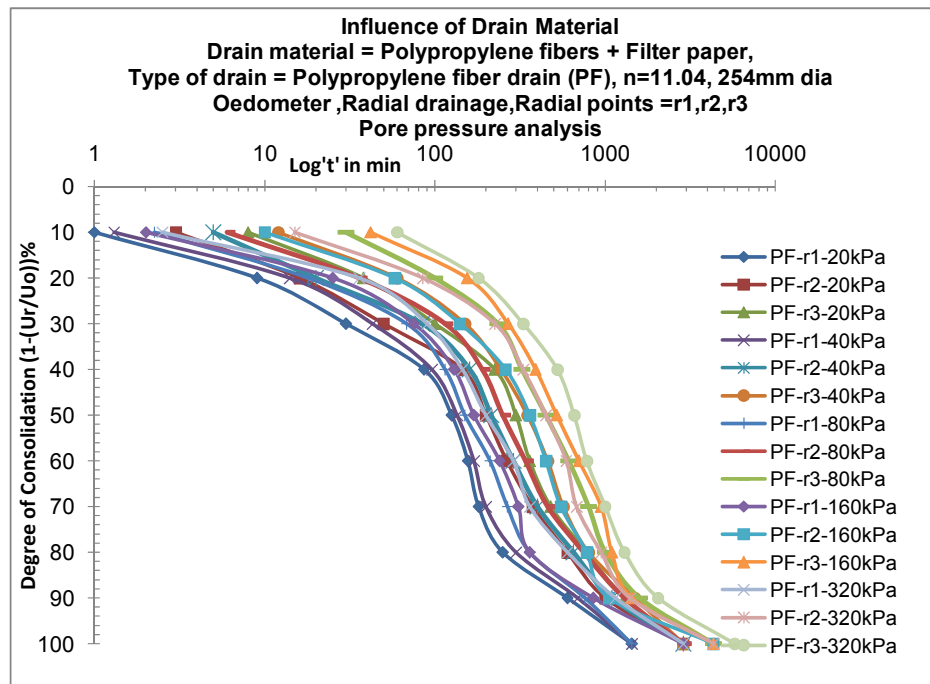


**Fig.6.18:** Degree of consolidation based on dissipation of excess hydrostatic pore water pressure vs.  $\log't'$  in min



- Comparing all four drain materials CJ takes lowest time both in terms of 50% and 80% consolidation at three radial points' r1, r2 and r3. For 40kPa and for 50% consolidation for radial points r1, CJ takes 528% less time in compare to SD, 310% less time in compare to SW, 246% less time in compare to PF,while for 80% consolidation, CJ takes 471% less time in compare to SD, 233% less time in compare to SW, 185% less time in compare to PF.
- For 40kPa and for 50% consolidation for radial points r2, CJ takes 292% less time in compare to SD, 100% less time in compare to SW, 72% less time in compare to PF,while for 80% consolidation, CJ takes 106% less time in compare to SD, 27.5% less time in compare to SW, 12.1% less time in compare to PF.
- For 40kPa and for 50% consolidation for radial points r3, CJ takes 245% less time in compare to SD, 81.8% less time in compare to SW, 59% less time in compare to PF,while for 80% consolidation, CJD takes 164% less time in compare to SD, 39.7% less time in compare to SW, 17.6% less time in compare to PF.
- For 160kPa and for 50% consolidation for radial points r1, CJ takes 400% less time in compare to SD, 175% less time in compare to SWD, 112.5% less time in compare to PF,while for 80% consolidation, CJ takes 368% less time in compare to SD, 175% less time in compare to SW, 125% less time in compare to PF.
- For 160kPa and for 50% consolidation for radial points r2, CJ takes 292% less time in compare to SD, 100% less time in compare to SW, 72% less time in compare to PF,while for 80% consolidation, CJ takes 160% less time in compare to SD, 47.8% less time in compare to SW, 35.6% less time in compare to PF.
- For 160kPa and for 50% consolidation for radial points r3, CJ takes 271% less time in compare to SD, 122% less time in compare to SW, 103% less time in compare to PF,while for 80% consolidation, CJ takes 128% less time in compare to SD, 30.4% less time in compare to SW, 19.5% less time in compare to PF.

From the above observations it is clear that CJ is most efficient drain material as it shows higher rate of dissipation of excess pore water pressure both for 50% and 80% consolidation at three radial points' r1, r2 and r3.

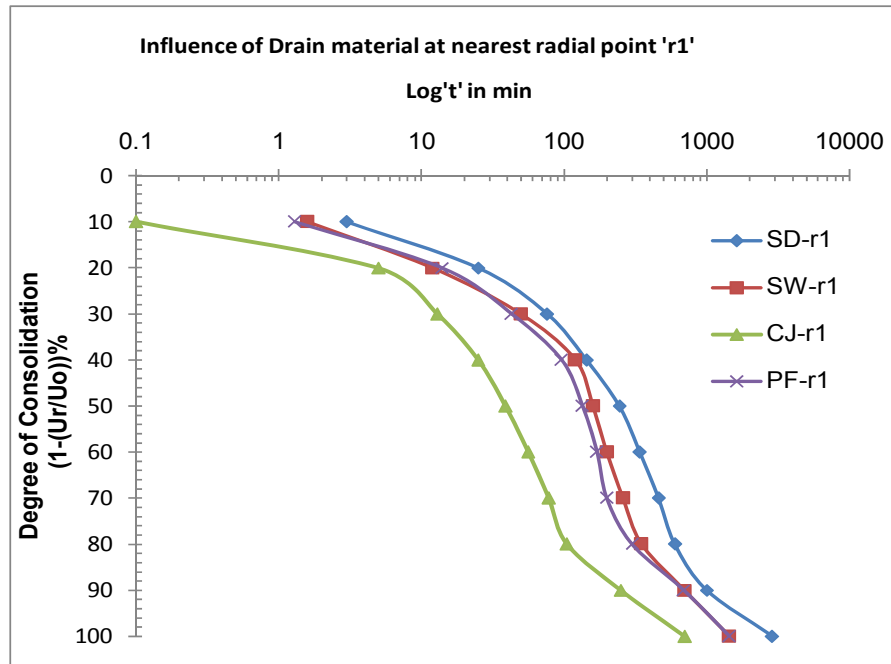


**Fig.6.19:** Comparison of drain material w.r.t radial point 'r1' at 40kPa pressure

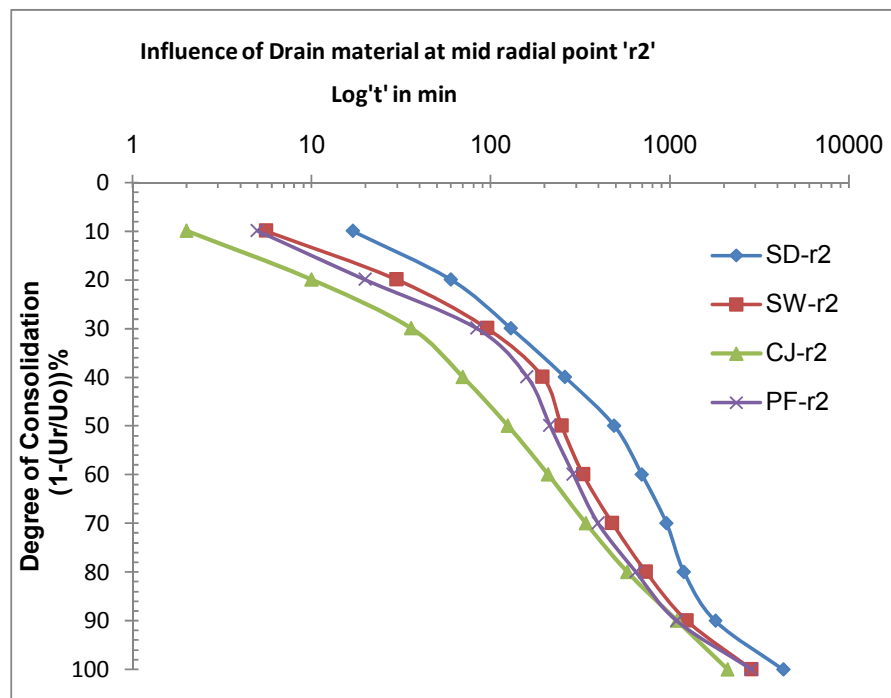


**Fig.6.20:** Comparison of drain material w.r.t radial point 'r2' at 40kPa pressure

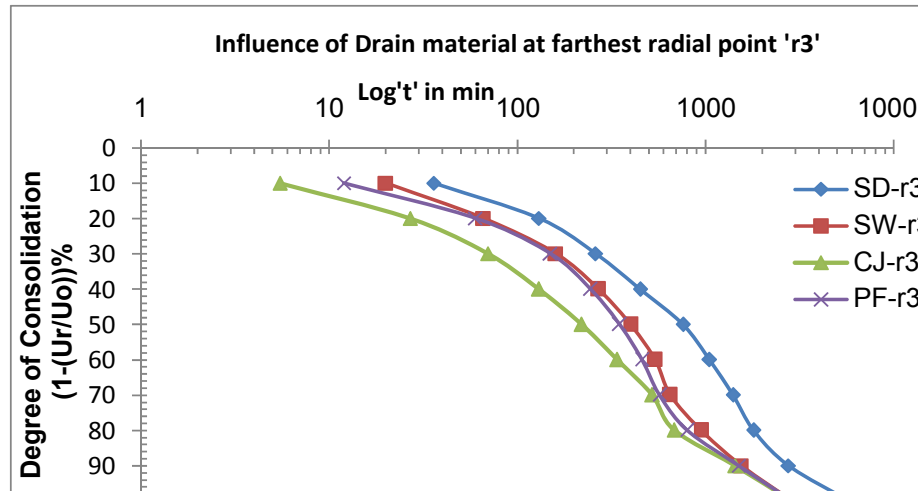


**Fig.6.21:** Comparison of drain material w.r.t radial point 'r3' at 40kPa pressure

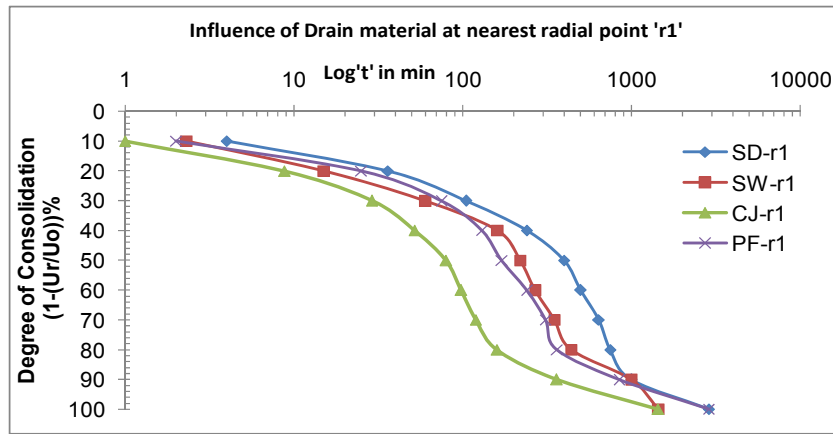


**Fig.6.22:** Comparison of drain material w.r.t radial point 'r1' at 160kPa pressure

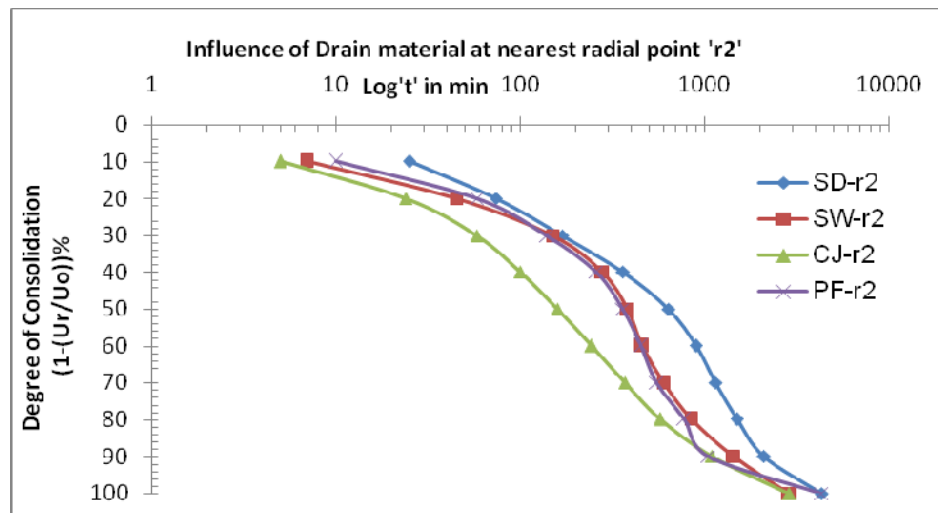


**Fig.6.23:** Comparison of drain material w.r.t radial point 'r2' at 160kPa pressure

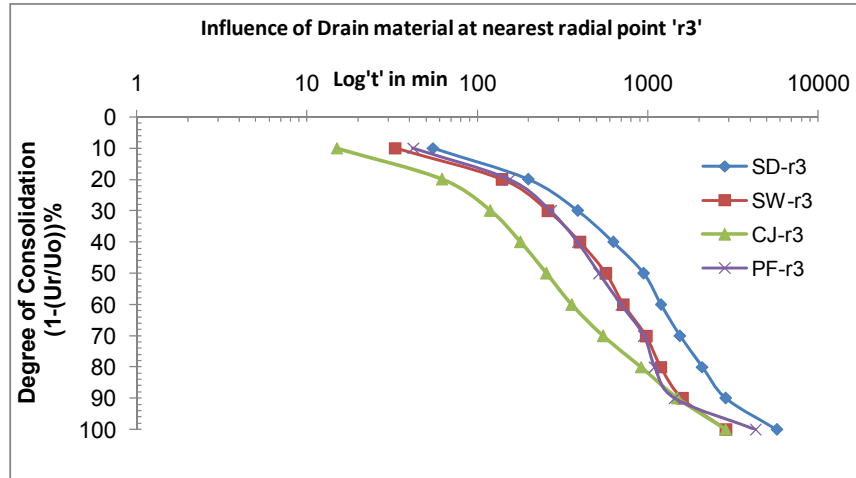


**Fig.6.24:** Comparison of drain material w.r.t radial point 'r3' at 160kPa pressure

**Discussion:** (Refer figures 6.25 to 6.26 and table 6.1)

It is observed that time taken for 50% and 80% consolidation based on pore pressure measurements is less compare to time taken by settlement measurements for any 'n' value and for any drain material.

- From settlement and pore pressure measurement considerations it infers that for 50% consolidation, CJ under light loading takes 46% less time in compare to SW, 49% in compare to PF, 56% in compare to SD, while for 80% consolidation, CJ takes 31% less time in compare to SW, 35% in compare to PF and 44% in compare to SD and under constructional loading CJ takes 45% less time in compare to SW, 58% less time in compare to PF, 58% in compare to SD, while for 80% consolidation CJ takes 29% less time in compare to SW, 41% in compare to PF and 47% in compare to SD for same 'n' value and permeability ratio.
- Under light loading for 50% consolidation SW takes 26% less time in compare to PF while it takes 0% against SD while SD takes 26% less time compare to PF but 34% more time compare to CJ. Similarly under constructional loading SW takes 41% & 3% less time in compare to PF & SD. Also SD takes 37% lesser time in compare to PF while SD takes 3% & 40% more time compare to SW and CJ.

- Under light loading for 80% consolidation SW takes 31% less time in compare to PF while it takes 3% against SD while SD takes 27% less time compare to PF but 23% more time compare to CJ. Similarly under constructional loading SW takes 30% & 5% less time in compare to PF & SD. Also SD takes 23% lesser time in compare to PF while SD takes 5% & 27% more time compare to SW and CJ.
- Time-deformation curve with respect to pore pressure dissipation and settlement follow a general trend of transmission of particle orientation from one stage to another against several physico-chemical forces initially and then thereafter achieving randomly oriented or parallel oriented soil structure. The quantum of initial resistance will depend on magnitude of load, characteristics of drain material and the 'n' value (particularly when consolidation by radial drainage is considered) and horizontal permeability that is tortuosity in horizontal direction. The initial flocculated structure of soil bed has edge to surface or edge to edge link bonds. When load is applied some resistance is offered by this link bond. Load has to overcome the edge to edge or edge to face attraction to alter the packing geometry. During this resistance the stage can be regarded as 'microcompressibility', Shroff (1972) and specific deformation can be expressed as slow decay as soon as local breakdown commences, the initial resistance to compression diminishes and the rate of consolidation increases to some extent. Progressive deformation can be visualised as 'macro compressibility', Shroff (1972) in which deformation is caused by sliding and lifting of plate shape particles, pressing out the pore water, at the same time it loosens the 'interfacial grip' of adsorbed water at links of plate shape particles. Under high loading microcompressibility and interfacial grip at links of plate shape clay particle have little relevance.
- For any load intensity and drain material, the time deformation curve with respect to pore pressure dissipation remain towards the vertical axis compare to curve of settlement, that is time require for 50% or 80% consolidation is less compare to settlement curve which also reflects in isochrones curves. This is because of direction of flow from the void space is radial which allows early dissipation compare to particle reorientation achieving same degree of

consolidation. The role played here is by 'macrocompressibility' in settlement case while 'microcompressibility' in pore pressure case.

- Rate of drainage of a radial points nearer to drainage being faster the time taken for particular % of consolidation is less in compare to radial points farther away, it also reflects this observation in settlement measurements to some extent showing more compressibility gradient towards central drain. It seems from the micrograph (photograph 6.1 & 6.2) of several drains the pore space in terms of nanomeasurement is larger compare to other drains. This reflects the efficiency of CJ with respect to micro structure opening even under light and heavy constructional loading.
- The gradient of radial flow is also facilitated by type of drain material, CJ drain may facilitate easy dissipation compare to other drain material, because of more percentage of microporosity in CJ drain compare to others which is also mentioned earlier in chapter 3 in para drain characteristics which also explains describes 'permeability' and 'transmissivity' of various drain material used in fabricating the circular drain. Further this data indicate the gradient of water formed because of the higher or lower transmissivity of geosynthetic material used in the present investigation. Inplane permeability data also confirms the above reasoning.

Because of the above reasonings the time-deformation curve and isochrones indicate early dissipation and early deformation as well as the magnitude of vertical consolidation in CJ drain compare to other drains.

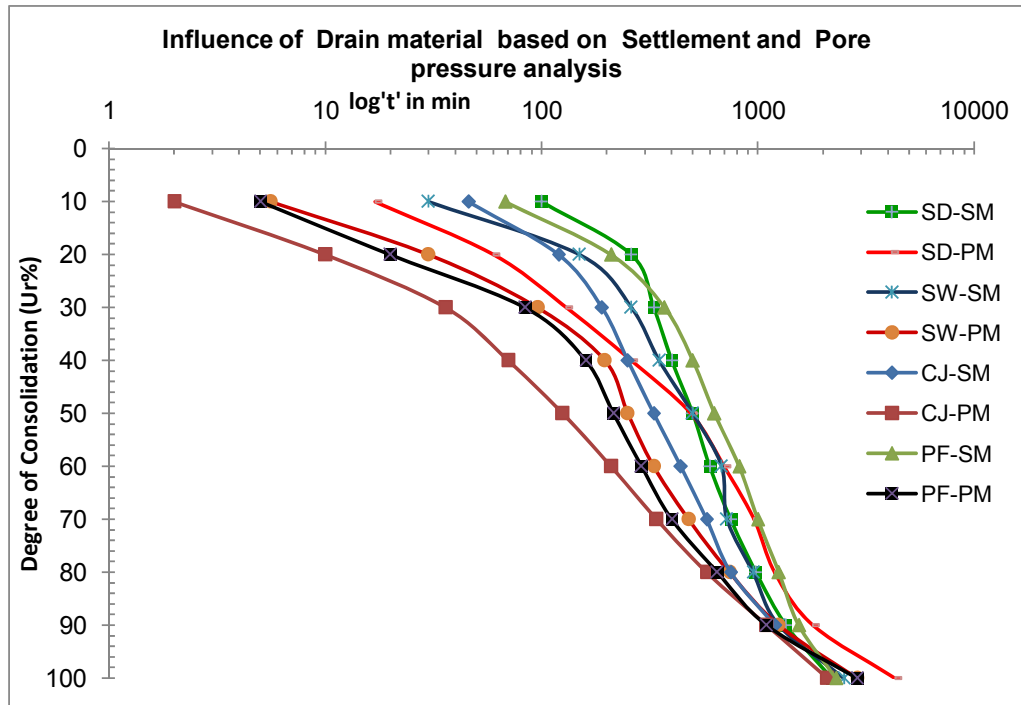


**Fig.6.25:** Comparison of Degree of consolidation against drain material based on settlement and pore pressure measurements at 40kPa pressure

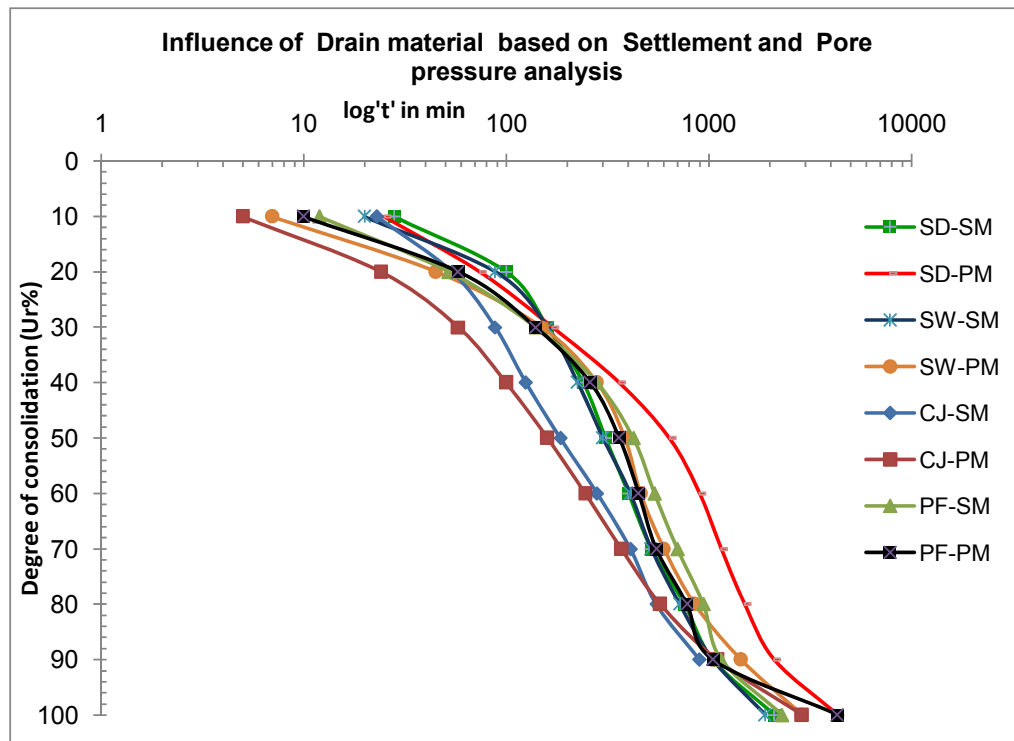
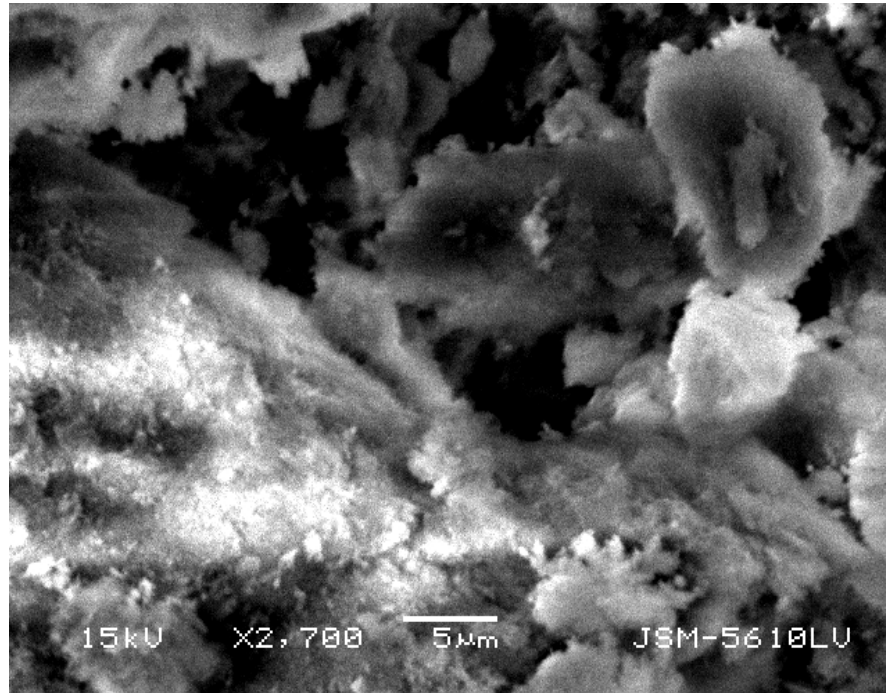
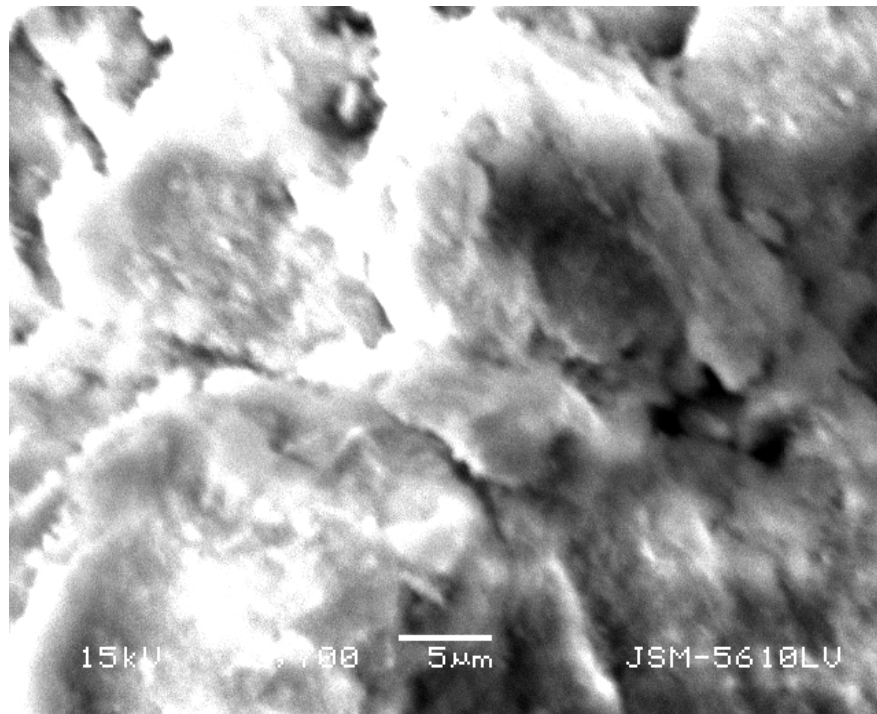


**Fig.6.26:** Comparison of drain material based on settlement and pore pressure measurements at 160kPa pressure

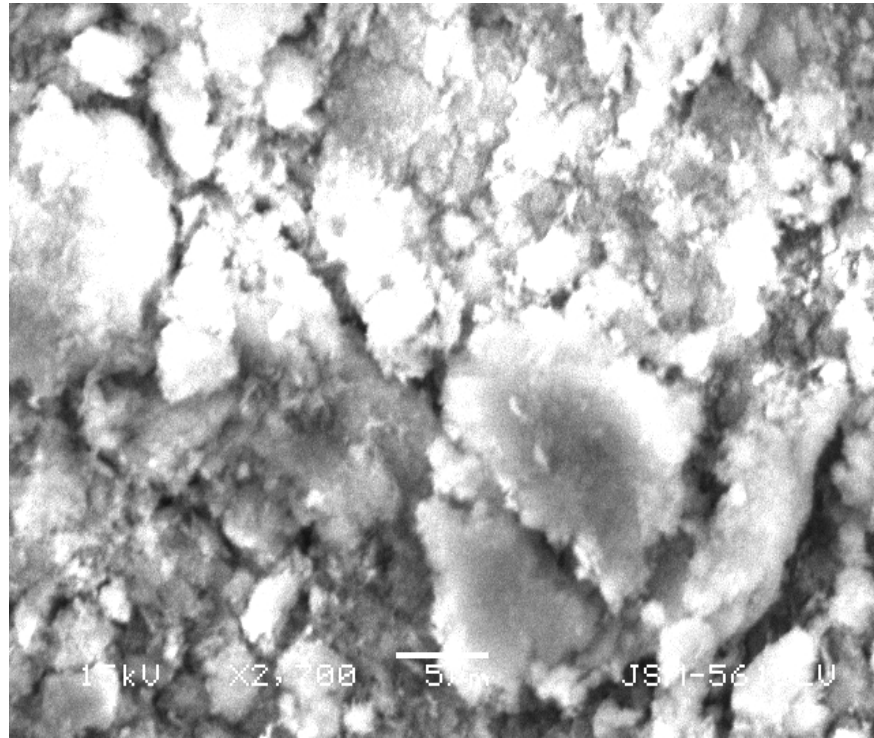


**Photograph 6.1(a):** Micrographs of Sand drain (SD) of 'n'11.04 at locations  $h_{tr2}$ ,  $h_{cr2}$ ,  $h_{br2}$

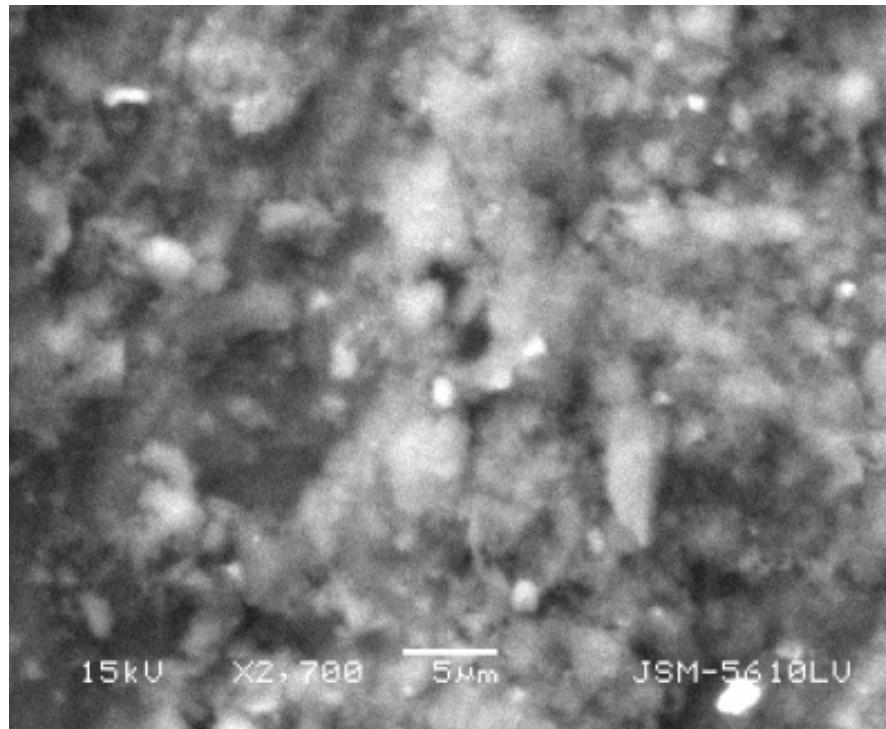


**Photograph 6.1(b):** Micrographs of Sand drain (SD) of 'n'11.04 at locations  $h_{cr2}$ ,

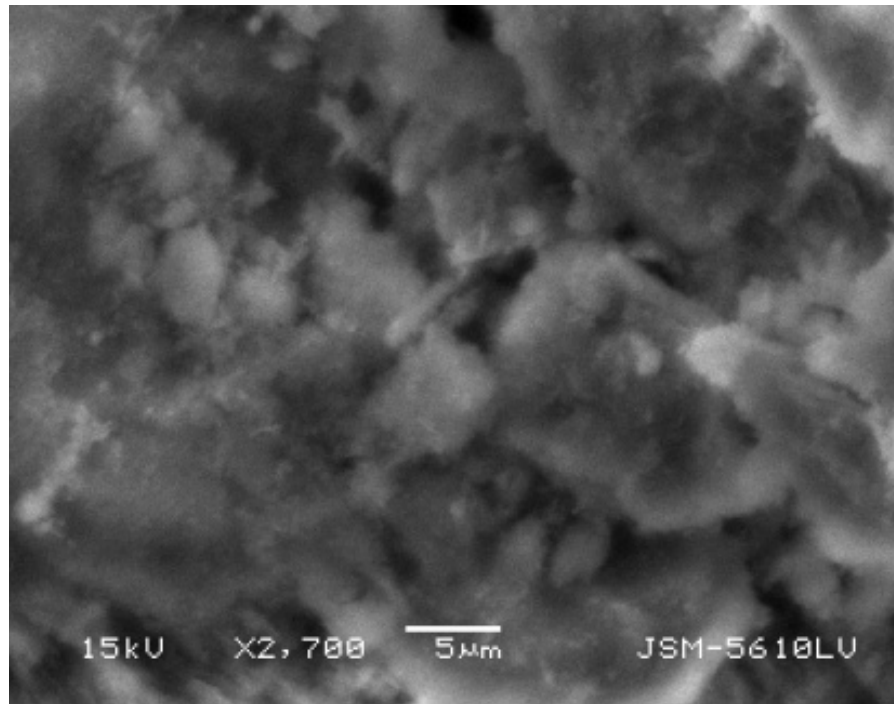




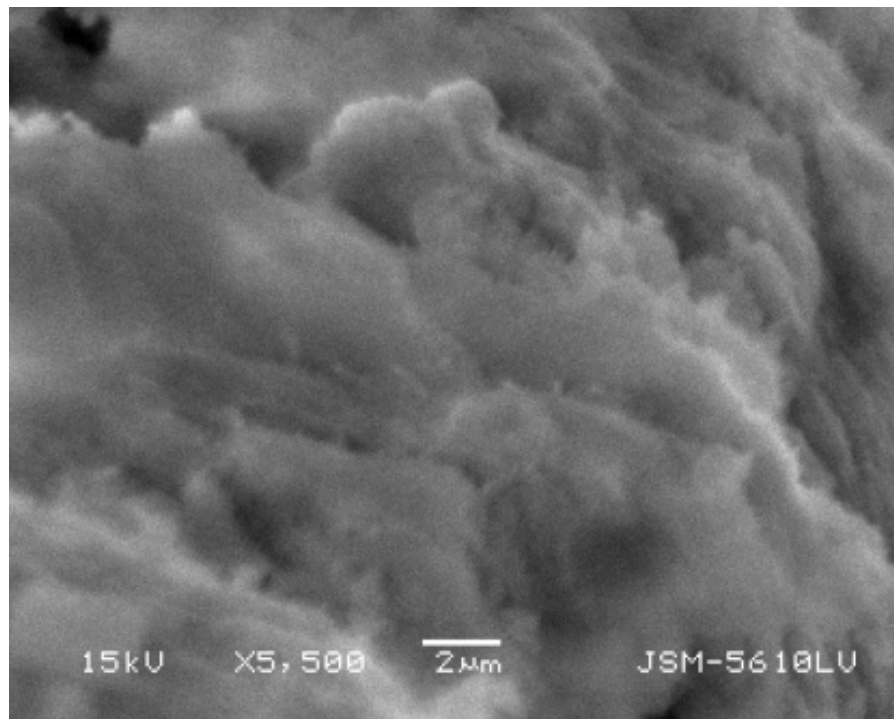
**Photograph 6.1(c):**Micrographs of Sand drain (SD) of 'n'11.04 at locations  $h_{br2}$



**Photograph 6.2(a):** Micrographs of Coir-Jute drain (CJ) of 'n'11.04 at locations  $h_{tr2}$



**Photograph 6.2(b):** Micrographs of Coir-Jute drain (CJ) of 'n'11.04 at locations  $h_{cr2}$



**Photograph 6.2(c):** Micrographs of Coir-Jute drain (CJ) of 'n'11.04 at locations  $h_{br2}$

**2) Coefficient of consolidation (Cr) vs. Degree of consolidation (Ur):  
Figures 6.27 to 6.44**

**a) Settlement analysis:** Fig.6.27 to Fig.6.31 shows the characteristic exponential curves of coefficient of consolidation versus degree of consolidation for all drain materials viz. SD, SW, CJ and PF for different values of effective pressures. Rate of decrease of coefficient of consolidation is faster up to 40%, thereafter the rate decreases slowly leading to asymptotic to x-axis for the case of radial drainage. For lower pressures ranging from 20 kPa to 80 kPa the value of Coefficient of consolidation decreases with average degree of consolidation. Thereafter the value of  $C_r$  becomes more or less constant with degree of consolidation at higher pressure from 160 to 320 kPa.

- The average values of  $C_{r50}$  and  $C_{r80}$  for all applied pressures for sand as drain material are  $7.42 \times 10^{-4} \text{cm}^2/\text{sec}$  &  $3.37 \times 10^{-4} \text{cm}^2/\text{sec}$  respectively.
- The average values of  $C_{r50}$  and  $C_{r80}$  for all applied pressures for sandwich as drain material are  $2.9 \times 10^{-4} \text{cm}^2/\text{sec}$  &  $1.27 \times 10^{-4} \text{cm}^2/\text{sec}$  respectively.
- The average values of  $C_{r50}$  and  $C_{r80}$  for all applied pressures for coir-jute fiber as drain material are  $1.17 \times 10^{-3} \text{cm}^2/\text{sec}$  &  $4.55 \times 10^{-4} \text{cm}^2/\text{sec}$  respectively.
- The average values of  $C_{r50}$  and  $C_{r80}$  for all applied pressures for polypropylene fiber as drain material are  $5.82 \times 10^{-4} \text{cm}^2/\text{sec}$  &  $3.04 \times 10^{-4} \text{cm}^2/\text{sec}$  respectively.

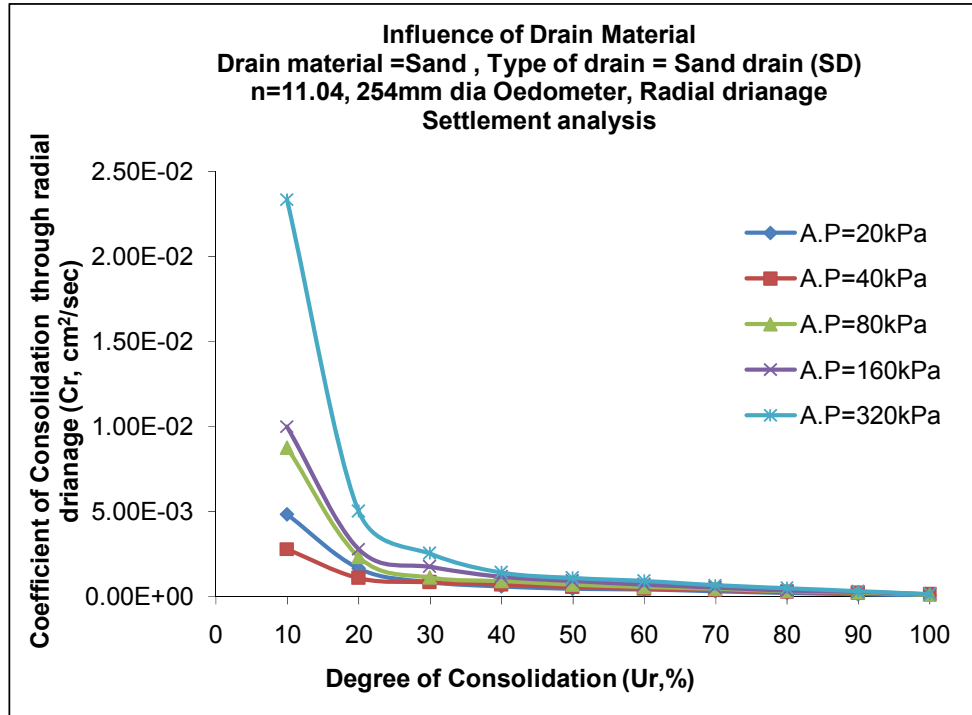


**Fig.6.27:** Coefficient of consolidation through radial drainage (Cr) vs. Degree of consolidation (Ur) for SD

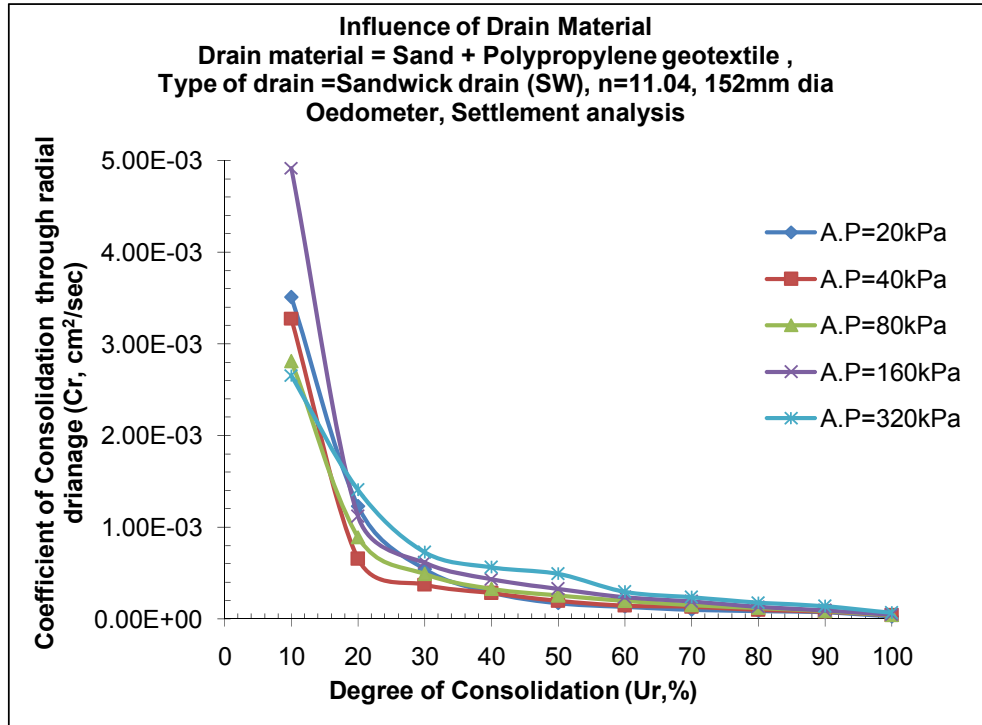


**Fig.6.28:** Coefficient of consolidation through radial drainage (Cr) vs. Degree of consolidation (Ur) for SW

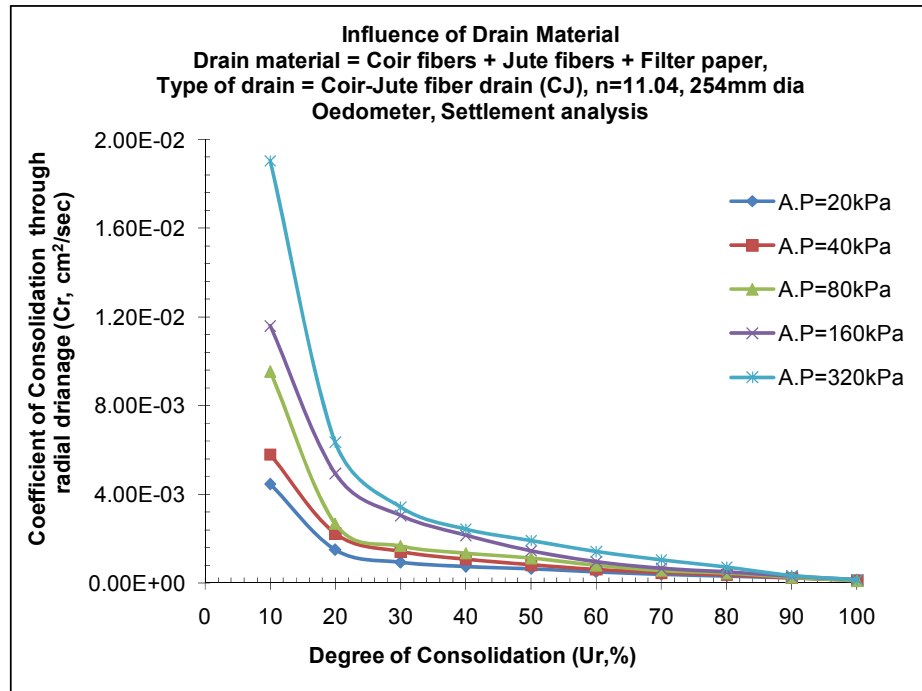


**Fig.6.29:** Coefficient of consolidation through radial drainage ( $C_r$ ) vs. Degree of consolidation ( $U_r$ ) for CJ

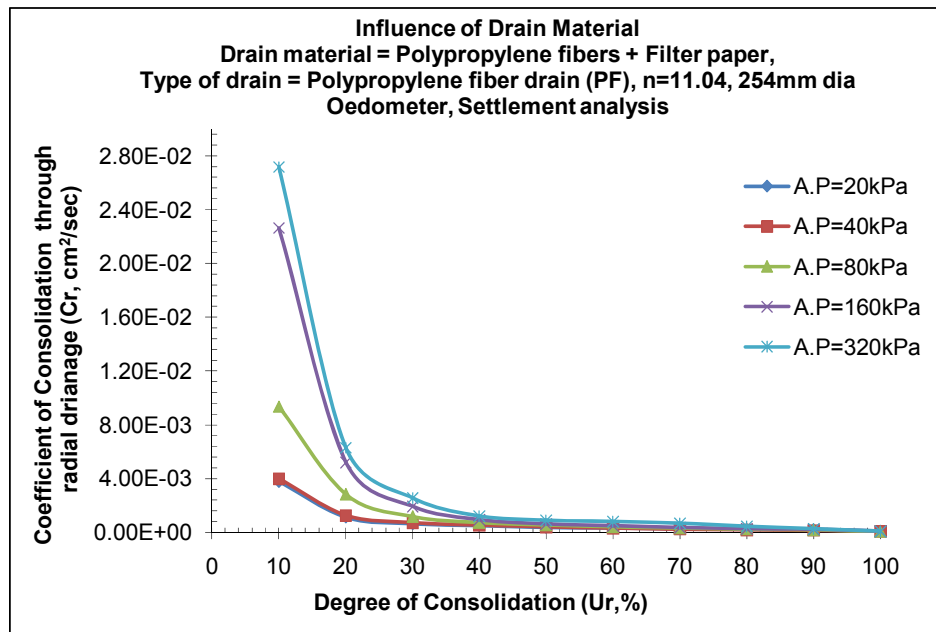


**Fig.6.30:** Coefficient of consolidation through radial drainage ( $C_r$ ) vs. Degree of consolidation ( $U_r$ ) for PF

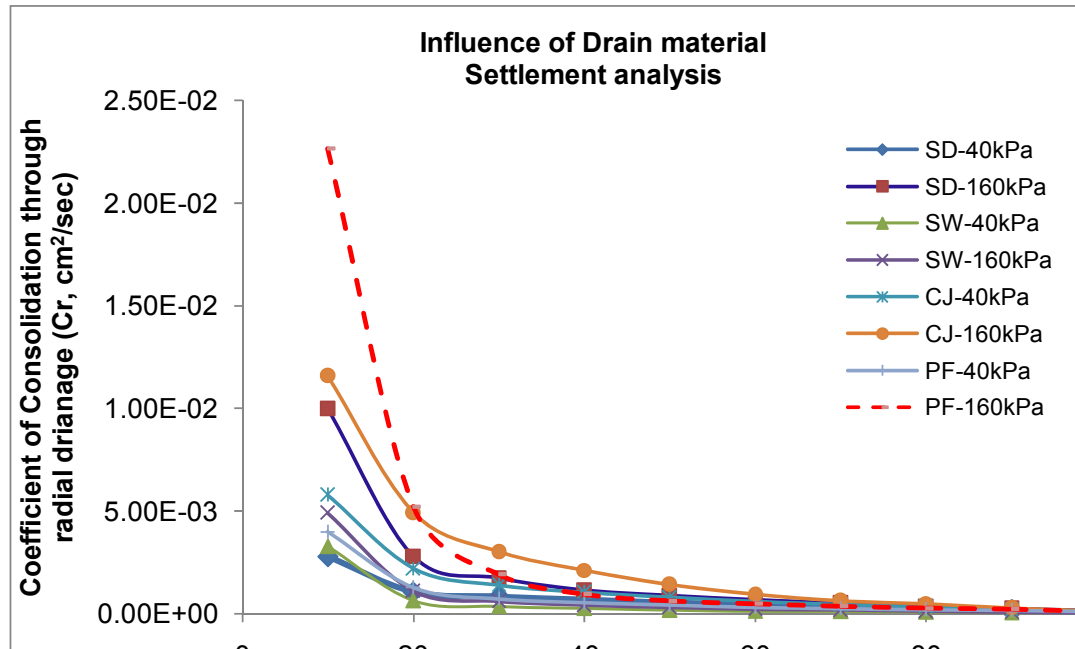


**Fig.6.31:** Comparison of drain material for coefficient of consolidation through radial flow for various degree of consolidation at low and high pressure using settlement analysis

**Table 6.2:** Comparison of  $C_r$  values for various drain materials based on settlement and pore pressure analysis

| Drain material | Settlement based              |                       | Pore pressure based- $r_2$    |                       |
|----------------|-------------------------------|-----------------------|-------------------------------|-----------------------|
|                | $C_r(\text{cm}^2/\text{sec})$ |                       | $C_r(\text{cm}^2/\text{sec})$ |                       |
|                | Ur (50%)-40kPa                | Ur (80%)-40kPa        | Ur (50%)-40kPa                | Ur (80%)-40kPa        |
| SD             | $5.6 \times 10^{-4}$          | $2.86 \times 10^{-4}$ | $1.54 \times 10^{-4}$         | $6.29 \times 10^{-5}$ |
| SW             | $1.97 \times 10^{-4}$         | $1.04 \times 10^{-4}$ | $1.29 \times 10^{-4}$         | $4.36 \times 10^{-5}$ |
| CJ             | $8.09 \times 10^{-4}$         | $3.56 \times 10^{-4}$ | $5.77 \times 10^{-4}$         | $1.24 \times 10^{-4}$ |
| PF             | $4.32 \times 10^{-4}$         | $2.18 \times 10^{-4}$ | $3.46 \times 10^{-4}$         | $1.14 \times 10^{-4}$ |
| Drain material | Settlement based              |                       | Pore pressure based- $r_2$    |                       |
|                | $C_r(\text{cm}^2/\text{sec})$ |                       | $C_r(\text{cm}^2/\text{sec})$ |                       |
|                | Ur (50%)-160kPa               | Ur (80%)-160kPa       | Ur (50%)-160kPa               | Ur (80%)-160kPa       |
| SD             | $9.04 \times 10^{-4}$         | $3.69 \times 10^{-4}$ | $1.18 \times 10^{-4}$         | $5.04 \times 10^{-5}$ |
| SW             | $3.28 \times 10^{-4}$         | $1.37 \times 10^{-4}$ | $8.36 \times 10^{-5}$         | $3.79 \times 10^{-5}$ |
| CJ             | $1.44 \times 10^{-3}$         | $4.85 \times 10^{-4}$ | $4.51 \times 10^{-4}$         | $1.25 \times 10^{-4}$ |
| PF             | $6.4 \times 10^{-4}$          | $2.89 \times 10^{-4}$ | $2.06 \times 10^{-4}$         | $9.53 \times 10^{-5}$ |

**b) Pore pressure analysis:-** Fig.6.32 to Fig.6.43 shows the characteristic exponential curves of coefficient of consolidation ( $C_r$ ) versus degree of consolidation ( $U_r$ ) for all drain materials viz. SD, SW, CJ & PF at three radial point's  $r_1$ ,  $r_2$ ,  $r_3$  for effective pressures of 40kPa and 160kPa for  $n=11.04$ . Higher rate of consolidation is observed for nearest radial point  $r_1$  in compare to  $r_2$  &  $r_3$ . Rate of decrease of coefficient of consolidation is faster up to 20 %, thereafter the rate decreases slowly leading to asymptotic to x-axis for the case of radial drainage for radial points  $r_2$  &  $r_3$ . Nature of plot of  $C_r$  remains nearly constant for particular applied pressures at three radial points and this is true for all drain materials.

- The average values of  $C_{r50}$  and  $C_{r80}$  at radial point's  $r_1$ ,  $r_2$ ,  $r_3$  for all applied pressures using sand as drain material are  $1.3 \times 10^{-5} \text{cm}^2/\text{sec}$ ,  $1.35 \times 10^{-4} \text{cm}^2/\text{sec}$ ,  $2.4 \times 10^{-4} \text{cm}^2/\text{sec}$  &  $5.93 \times 10^{-6} \text{cm}^2/\text{sec}$ ,  $5.69 \times 10^{-5} \text{cm}^2/\text{sec}$ ,  $1.06 \times 10^{-4} \text{cm}^2/\text{sec}$  respectively.
- The average values of  $C_{r50}$  and  $C_{r80}$  at radial point's  $r_1$ ,  $r_2$ ,  $r_3$  for all applied pressures using sandwich as drain material are  $6.17 \times 10^{-5} \text{cm}^2/\text{sec}$ ,  $1.05 \times 10^{-4} \text{cm}^2/\text{sec}$ ,  $1.33 \times 10^{-4} \text{cm}^2/\text{sec}$  &  $2.89 \times 10^{-5} \text{cm}^2/\text{sec}$ ,  $3.95 \times 10^{-5} \text{cm}^2/\text{sec}$ ,  $5.76 \times 10^{-5} \text{cm}^2/\text{sec}$  respectively.
- The average values of  $C_{r50}$  and  $C_{r80}$  at radial point's  $r_1$ ,  $r_2$ ,  $r_3$  for all applied pressures using coir-jute fiber as drain material are  $8.12 \times 10^{-5} \text{cm}^2/\text{sec}$ ,  $5.33 \times 10^{-4} \text{cm}^2/\text{sec}$ ,  $9.33 \times 10^{-4} \text{cm}^2/\text{sec}$  &  $3.02 \times 10^{-5} \text{cm}^2/\text{sec}$ ,  $1.5 \times 10^{-4} \text{cm}^2/\text{sec}$ ,  $2.74 \times 10^{-4} \text{cm}^2/\text{sec}$  respectively.
- The average values of  $C_{r50}$  and  $C_{r80}$  at radial point's  $r_1$ ,  $r_2$ ,  $r_3$  for all applied pressures using polypropylene fiber as drain material are  $2.67 \times 10^{-5} \text{cm}^2/\text{sec}$ ,  $2.77 \times 10^{-4} \text{cm}^2/\text{sec}$ ,  $4.83 \times 10^{-4} \text{cm}^2/\text{sec}$  &  $1.18 \times 10^{-5} \text{cm}^2/\text{sec}$ ,  $1.02 \times 10^{-4} \text{cm}^2/\text{sec}$ ,  $2.12 \times 10^{-4} \text{cm}^2/\text{sec}$  respectively.

**Discussion:** Looking to above inferences it is clear that CJ shows more rate of consolidation both at low and high pressures in compare to other drain materials from settlement and pore pressure measurement (**refer figure 6.44 and table 6.2**) considerations because of higher horizontal permeability of drain of CJ.

- $C_r$  for CJD for 50% consolidation from settlement readings work out to be averagely 73% & 78% more compare to other drain materials under light and

heavy construction loading. Similarly for 80% consolidation it is averagely 63% & 66% more. This observation satisfies that higher horizontal permeability of CJD compare to other drain materials under light and heavy construction loading.

- $C_r$  for CJD from mid plane pore pressure measurements for 50% consolidation work out to be averagely 154% & 155% more compare to other drain materials under light and heavy construction loading. Similarly for 80% consolidation it is averagely 48% & 81% more.
- Effectiveness of PF seems too remote from really compare to functioning of other drains. While effectiveness of SW is less than CJ but higher then SD.
- The gradient of radial flow is also facilitated by type of drain material, CJ drain may facilitate easy dissipation compare to other drain material, because of more percentage of microporosity in CJ drain compare to others. (refer figure 6.64, 6.65 and 6.66)

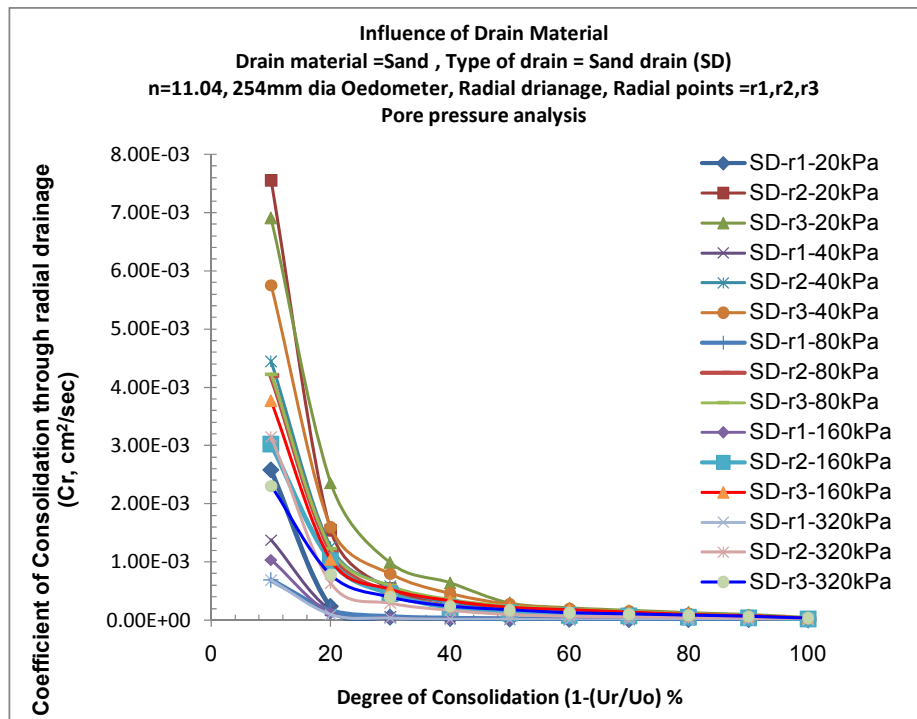


**Fig.6.32:** Coefficient of consolidation through radial drainage ( $C_r$ ) vs. Degree of consolidation ( $U_r$ ) at radial point's r1, r2 and r3 for SD at all pressures



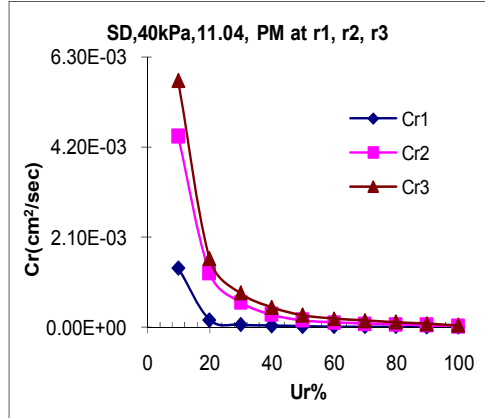


**Fig.6.33:** Cr vs. Ur for SD at radial points r1, r2, r3 at 40kPa pressure

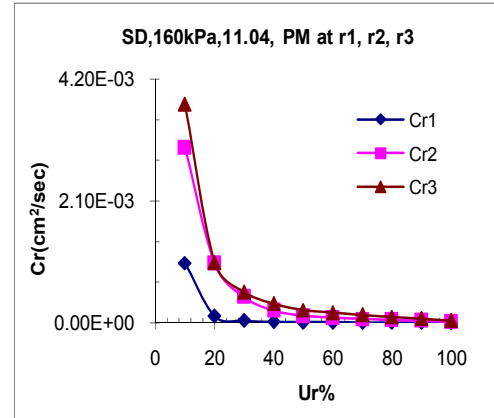


**Fig.6.34:** Cr vs. Ur for SD at radial points r1, r2, r3 at 160kPa pressure

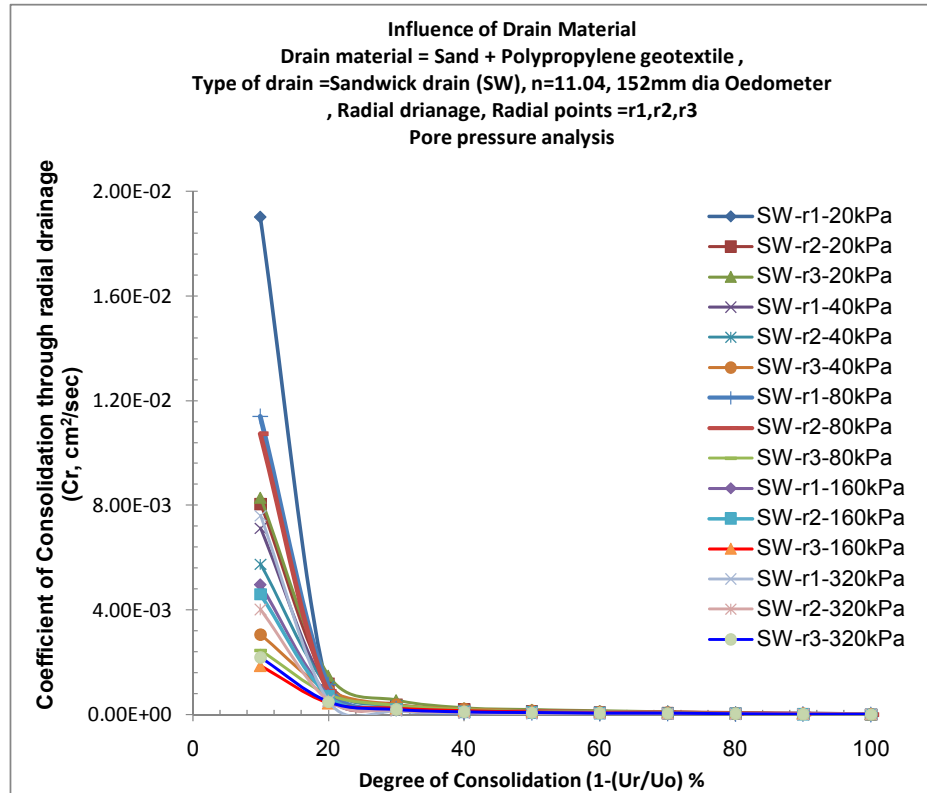


**Fig.6.35:** Coefficient of consolidation through radial drainage (Cr) vs. Degree of consolidation (Ur) at radial points r1, r2 and r3 for SW at all pressures

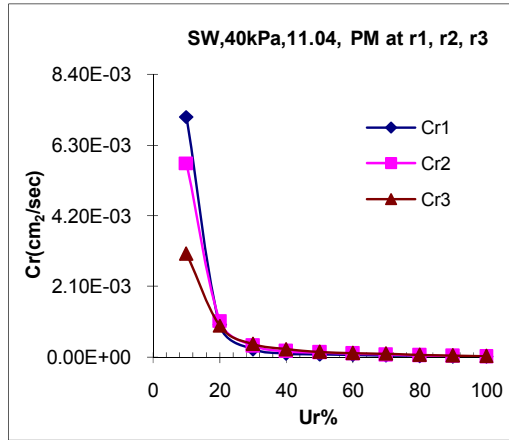


**Fig.6.36:** Cr vs. Ur for SW at radial points r1, r2, r3 at 40kPa pressure

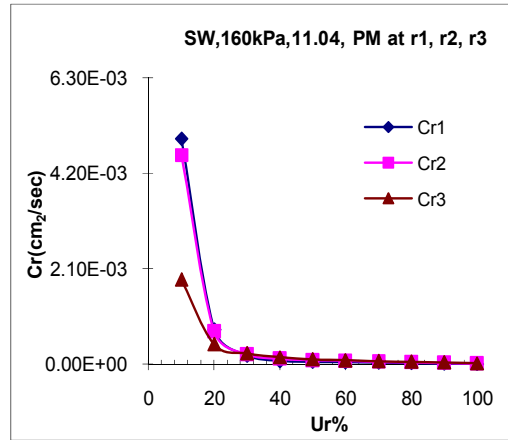


**Fig.6.37:** Cr vs. Ur for SW at radial points r1, r2, r3 at 160kPa pressure

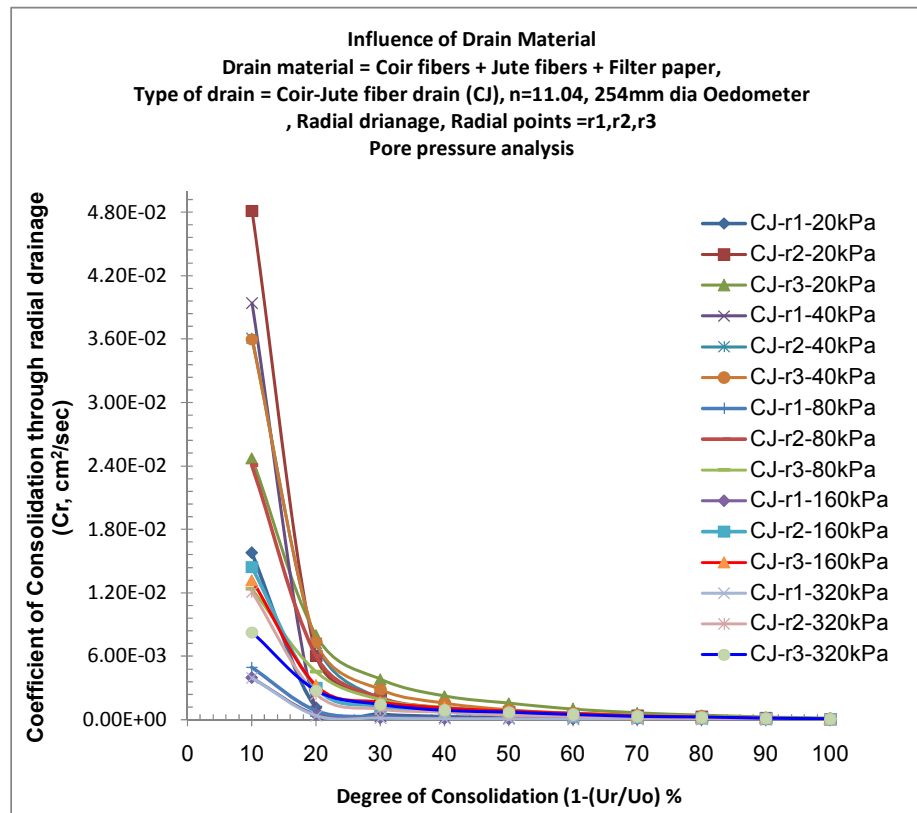


**Fig.6.38:** Coefficient of consolidation through radial drainage (Cr) vs. Degree of consolidation (Ur) at radial points r1, r2 and r3 for CJ at all pressures

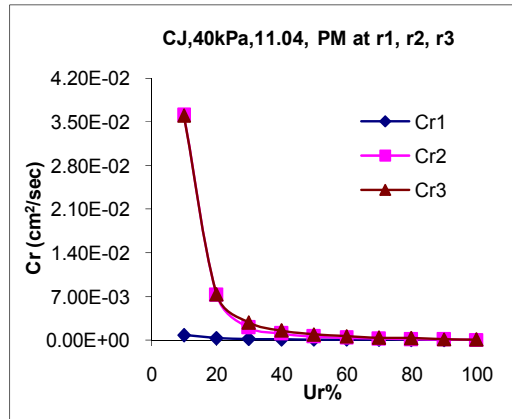


**Fig.6.39:** Cr vs. Ur for CJ at radial points r1, r2, r3 at 40kPa pressure

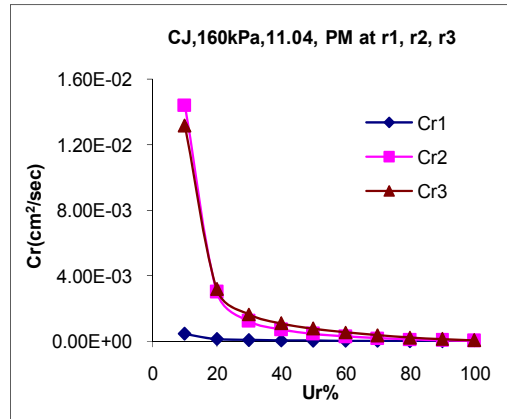


**Fig.6.40:** Cr vs. Ur for CJ at radial points r1, r2, r3 at 160kPa pressure

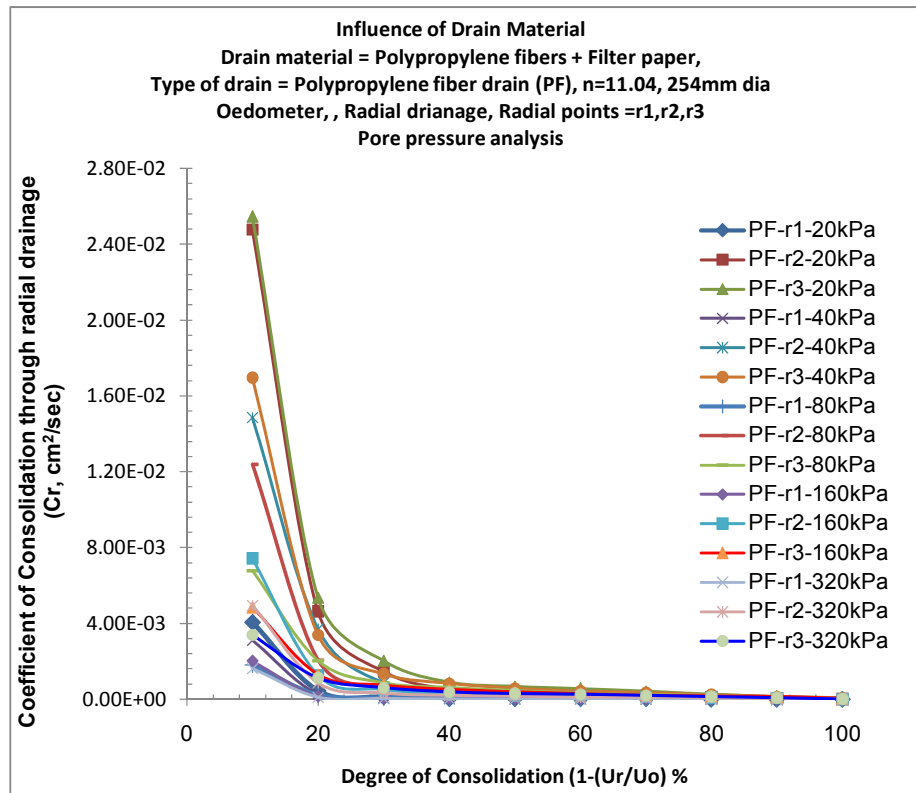


**Fig.6.41:** Coefficient of consolidation through radial drainage (Cr) vs. Degree of consolidation (Ur) at radial points r1, r2 and r3 for PF at all pressures

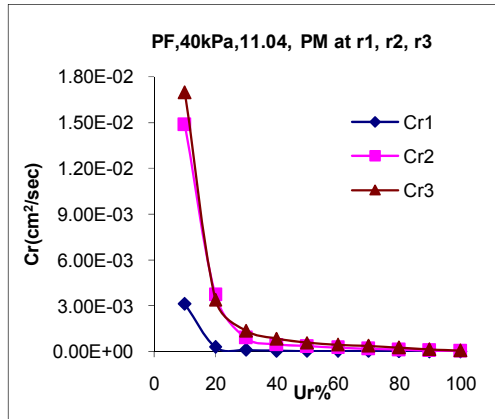


**Fig.6.42:** Cr vs. Ur for PF at radial points r1, r2, r3 at 40kPa pressure

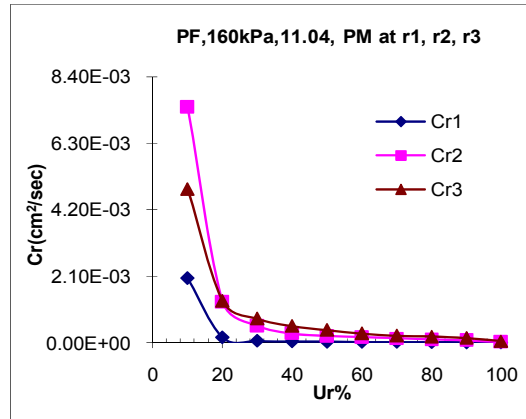


**Fig.6.43:** Cr vs. Ur for PF at radial points r1, r2, r3 at 160kPa pressure

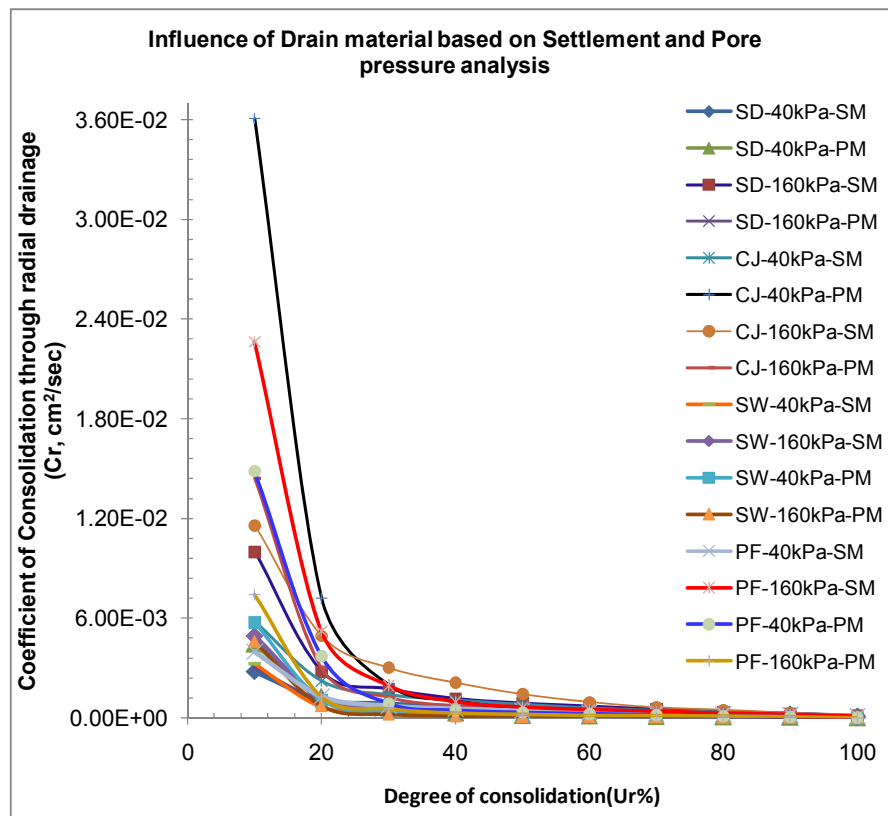


**Fig.6.44:** Comparison of Coefficient of consolidation through radial flow against drain material based on settlement and pore pressure measurements at 40kPa and 160kPa pressure

### 3) Coefficient of consolidation (Cr) vs. applied pressure: Figures 6.45 to 6.57

**a) Settlement analysis:** Fig.6.45 to Fig.6.50 shows the plots of coefficient of consolidation due to radial drainage ( $C_r$ ) versus applied pressure for various drain materials i.e. SD, SW, CJ & PF for 'n' values of 11.04. Here for analysis time required for 50% ( $T_{50}$ ) consolidation and time required for 80% ( $T_{80}$ ) consolidation are taken for all applied pressures. From the plots it is very clear that the nature of  $T_{80}$  graph remains same that is nearly constant or say linear increasing, while  $T_{50}$  graph has much variation in initial pressures and thereafter  $C_r$  values increases rapidly for later higher pressures. This is true almost for all drain materials. There is no much variation in the value of  $C_r$  up to 50 kPa, change of  $C_r$  value indicate the initial structural resistance existing in the clay water structure in the Kaolinite clay.

- The average value of  $C_{r50}$  was found to be  $7.42 \times 10^{-4}$  cm<sup>2</sup>/sec and  $C_{r80}$  was found as  $3.37 \times 10^{-4}$  cm<sup>2</sup>/sec using sand as drain material. For lower stress of 40kPa the  $C_{r50}$  &  $C_{r80}$  was determined as  $5.6 \times 10^{-4}$  cm<sup>2</sup>/sec &  $2.86 \times 10^{-4}$  cm<sup>2</sup>/sec respectively, while for higher engineering stress of 160kPa the  $C_{r50}$  &  $C_{r80}$  was determined as  $9.04 \times 10^{-4}$  cm<sup>2</sup>/sec &  $3.69 \times 10^{-4}$  cm<sup>2</sup>/sec respectively as shown in fig.6.45.
- The average value of  $C_{r50}$  was found to be  $2.90 \times 10^{-4}$  cm<sup>2</sup>/sec and  $C_{r80}$  was found as  $1.27 \times 10^{-4}$  cm<sup>2</sup>/sec using sandwick as drain material. For lower stress of 40kPa the  $C_{r50}$  &  $C_{r80}$  was determined as  $1.97 \times 10^{-4}$  cm<sup>2</sup>/sec &  $1.04 \times 10^{-4}$  cm<sup>2</sup>/sec respectively, while for higher engineering stress of 160kPa the  $C_{r50}$  &  $C_{r80}$  was determined as  $3.28 \times 10^{-4}$  cm<sup>2</sup>/sec &  $1.37 \times 10^{-4}$  cm<sup>2</sup>/sec respectively as shown in fig.6.46.
- The average value of  $C_{r50}$  was found to be  $1.17 \times 10^{-3}$  cm<sup>2</sup>/sec and  $C_{r80}$  was found as  $4.55 \times 10^{-4}$  cm<sup>2</sup>/sec using coir-jute fiber as drain material. For lower stress of 40kPa the  $C_{r50}$  &  $C_{r80}$  was determined as  $8.09 \times 10^{-4}$  cm<sup>2</sup>/sec &  $3.56 \times 10^{-4}$  cm<sup>2</sup>/sec respectively, while for higher engineering stress of 160kPa the  $C_{r50}$  &  $C_{r80}$  was determined as  $1.44 \times 10^{-3}$  cm<sup>2</sup>/sec &  $4.85 \times 10^{-4}$  cm<sup>2</sup>/sec respectively as shown in fig.6.47.

- The average value of  $C_{r50}$  was found to be  $5.82 \times 10^{-4} \text{ cm}^2/\text{sec}$  and  $C_{r80}$  was found as  $3.04 \times 10^{-4} \text{ cm}^2/\text{sec}$  using polypropylene fiber as drain material. For lower stress of 40kPa the  $C_{r50}$  &  $C_{r80}$  was determined as  $4.32 \times 10^{-4} \text{ cm}^2/\text{sec}$  &  $2.18 \times 10^{-4} \text{ cm}^2/\text{sec}$  respectively, while for higher engineering stress of 160kPa the  $C_{r50}$  &  $C_{r80}$  was determined as  $6.4 \times 10^{-4} \text{ cm}^2/\text{sec}$  &  $2.89 \times 10^{-4} \text{ cm}^2/\text{sec}$  respectively as shown in fig.6.48.
- Looking to above plots and values it is clear that CJ shows more rate of consolidation both at low and high pressures in compare to other drain materials. Also it is observed that variation in value of  $C_{r50}$  and  $C_{r80}$  between various pressures is very high in case of CJ i.e. 43.3% and 26.6% while PF shows 32.5% & 24.8%. So it can be said that CJ shows more inter-rate of compressibility even at following pressures in compare to other drain materials as depicted from fig.6.49 and fig.6.50.

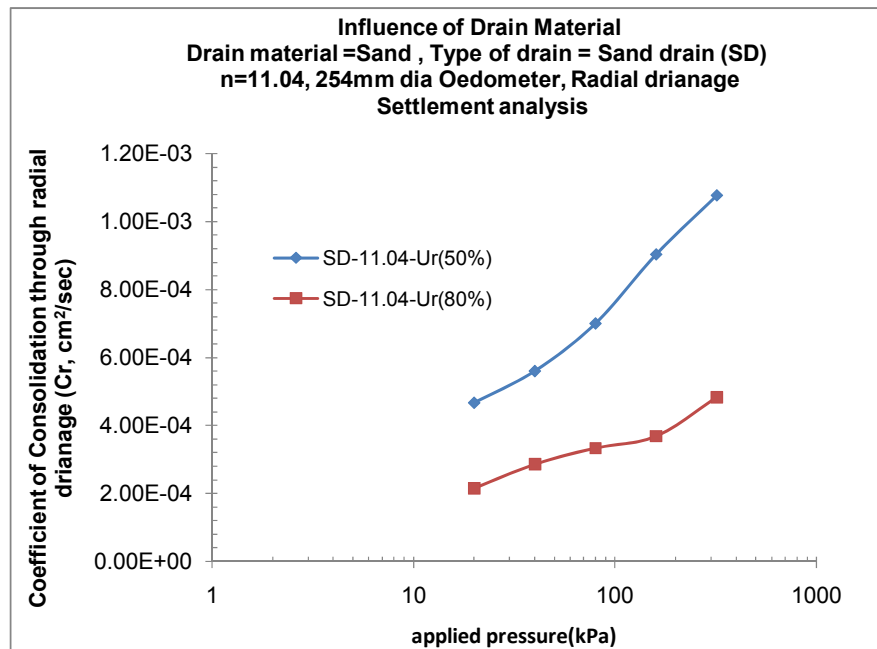


**Fig.6.45:** Coefficient of consolidation through radial drainage( $C_r$ ) vs. Applied pressure for SD at 50% and 80% degree of consolidation (Ur)

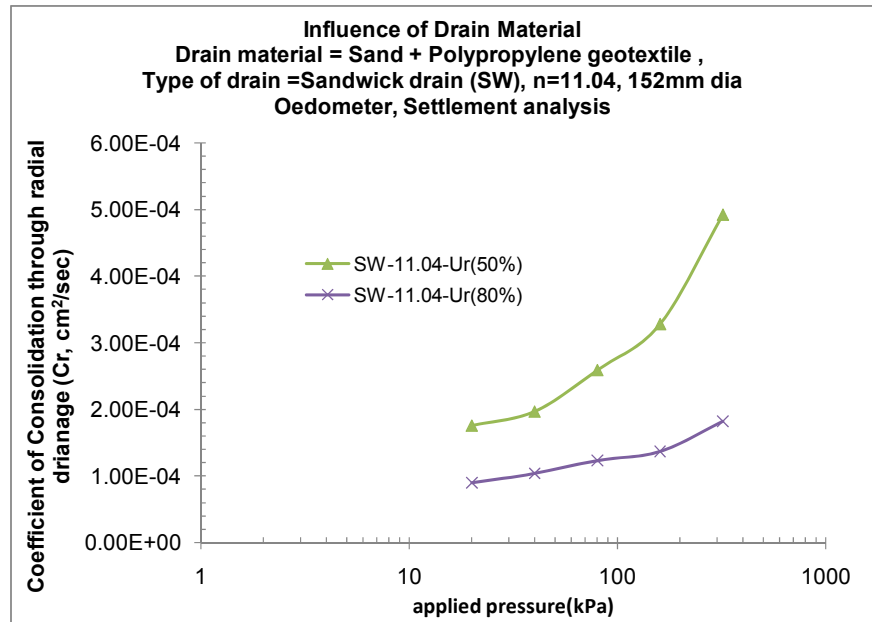


**Fig.6.46:** Coefficient of consolidation through radial drainage( $C_r$ ) vs. Applied pressure for SW at 50% and 80% degree of consolidation ( $U_r$ )

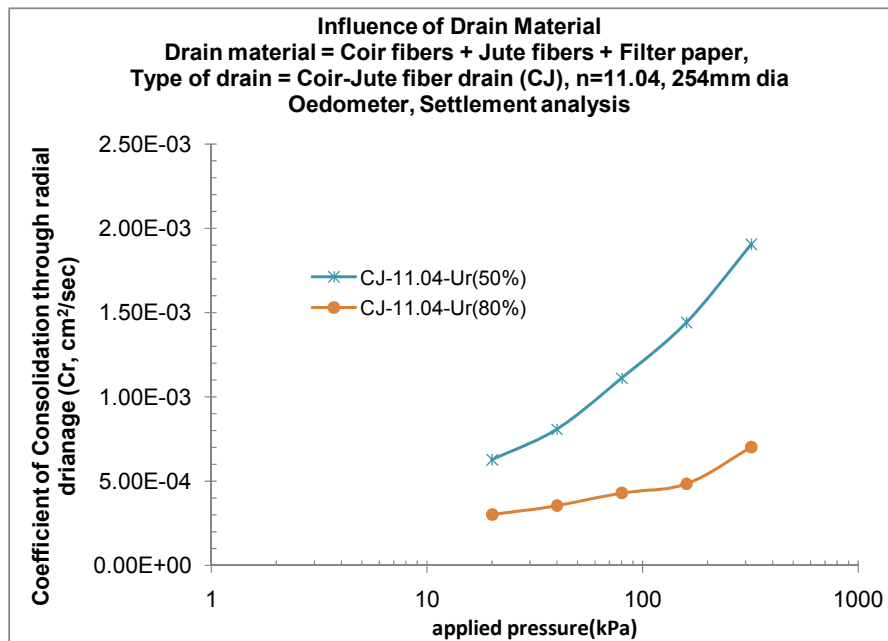


**Fig.6.47:** Coefficient of consolidation through radial drainage( $C_r$ ) vs. Applied pressure for CJ at 50% and 80% degree of consolidation ( $U_r$ )

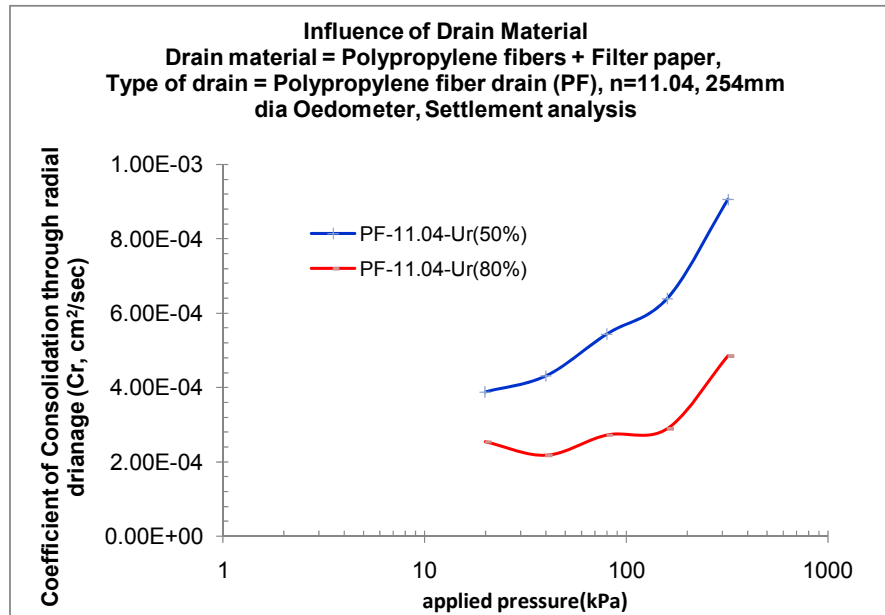


**Fig.6.48:** Coefficient of consolidation through radial drainage( $C_r$ ) vs. Applied pressure for PF at 50% and 80% degree of consolidation (Ur)

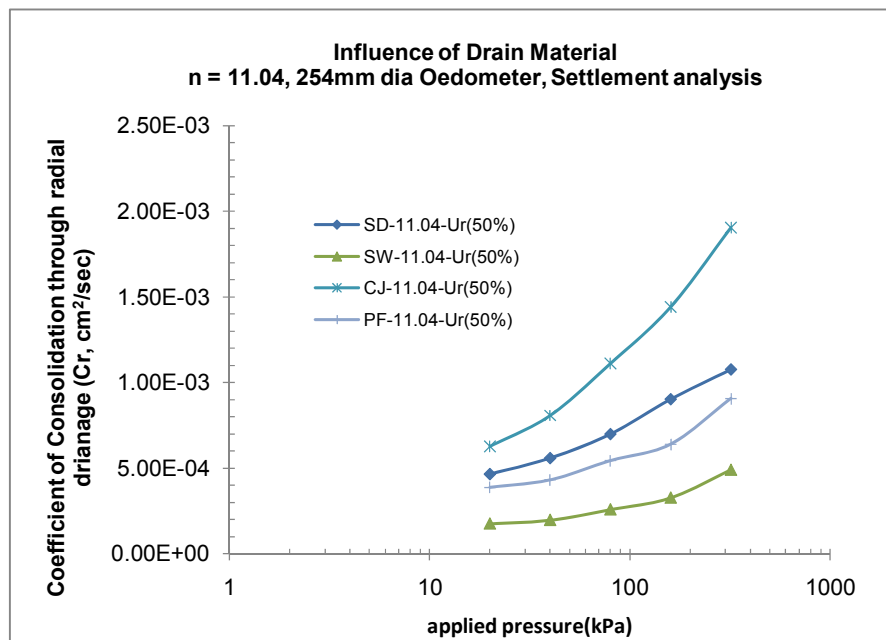


**Fig.6.49:** Comparison of Drain material w.r.t coefficient of consolidation through radial drainage( $C_r$ ) against applied pressure at 50% degree of consolidation (Ur)



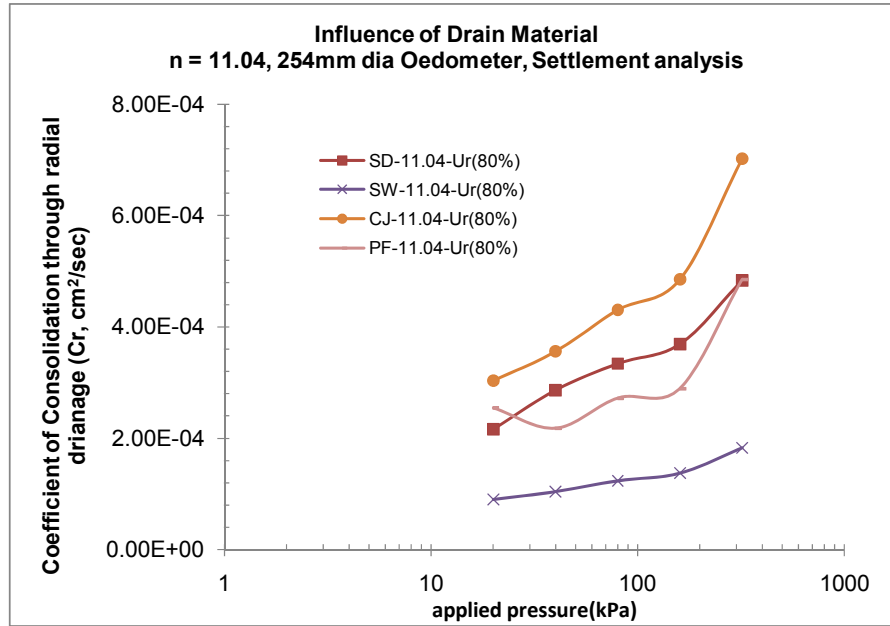


**Fig.6.50:** Comparison of Drain material w.r.t coefficient of consolidation through radial drainage( $C_r$ ) against applied pressure at 80% degree of consolidation ( $U_r$ )

**b) Pore pressure analysis-** Fig.6.51 to Fig.6.56 shows the plots of coefficient of consolidation due to radial drainage ( $C_r$ ) versus applied pressure for various drain materials like SD, SW, CJ, PF for 'n' values of 11.04 at three radial points'  $r_1$ ,  $r_2$  and  $r_3$ . Here for analysis time required for 50 %( $T_{50}$ ) consolidation and time required for 80% ( $T_{80}$ ) consolidation are taken for all 40kPa and 160kPa pressures. From the plots it is very clear that for all drain materials the initial nature of  $T_{80}$  graph &  $T_{50}$  graph decreases with initial applied pressure and at higher pressures it remains same that is nearly constant. There is much variation in the value of  $C_r$  up to 50 kPa, change of  $C_r$  value indicate the initial structural resistance existing in the clay water structure in the Kaolinite clay. Lesser variation in  $C_r$  value is observed for radial point's  $r_2$  and  $r_3$  for all drain materials and for all applied pressures.

- The average value of  $C_{r1,50}$  found to be  $1.3 \times 10^{-5} \text{ cm}^2/\text{sec}$  while average value of  $C_{r1,80}$  found to be  $5.93 \times 10^{-6} \text{ cm}^2/\text{sec}$  for SD.
- The average value of  $C_{r2,50}$  found to be  $1.35 \times 10^{-4} \text{ cm}^2/\text{sec}$  while average value of  $C_{r2,80}$  found to be  $5.69 \times 10^{-5} \text{ cm}^2/\text{sec}$  for SD.

- The average value of  $C_{r3,50}$  found to be  $2.4 \times 10^{-4} \text{ cm}^2/\text{sec}$  while average value of  $C_{r3,80}$  found to be  $1.06 \times 10^{-4} \text{ cm}^2/\text{sec}$  for SD.
- The average value of  $C_{r1,50}$  found to be  $6.17 \times 10^{-5} \text{ cm}^2/\text{sec}$  while average value of  $C_{r1,80}$  found to be  $2.89 \times 10^{-5} \text{ cm}^2/\text{sec}$  for SW.
- The average value of  $C_{r2,50}$  found to be  $1.05 \times 10^{-4} \text{ cm}^2/\text{sec}$  while average value of  $C_{r2,80}$  found to be  $3.95 \times 10^{-5} \text{ cm}^2/\text{sec}$  for SW.
- The average value of  $C_{r3,50}$  found to be  $1.33 \times 10^{-4} \text{ cm}^2/\text{sec}$  while average value of  $C_{r3,80}$  found to be  $5.76 \times 10^{-5} \text{ cm}^2/\text{sec}$  for SW.
- The average value of  $C_{r1,50}$  found to be  $8.12 \times 10^{-5} \text{ cm}^2/\text{sec}$  while average value of  $C_{r1,80}$  found to be  $3.02 \times 10^{-5} \text{ cm}^2/\text{sec}$  for CJ.
- The average value of  $C_{r2,50}$  found to be  $5.33 \times 10^{-4} \text{ cm}^2/\text{sec}$  while average value of  $C_{r2,80}$  found to be  $1.5 \times 10^{-4} \text{ cm}^2/\text{sec}$  for CJ.
- The average value of  $C_{r3,50}$  found to be  $9.33 \times 10^{-4} \text{ cm}^2/\text{sec}$  while average value of  $C_{r3,80}$  found to be  $2.74 \times 10^{-4} \text{ cm}^2/\text{sec}$  for CJ.
- The average value of  $C_{r1,50}$  found to be  $2.67 \times 10^{-5} \text{ cm}^2/\text{sec}$  while average value of  $C_{r1,80}$  found to be  $1.81 \times 10^{-5} \text{ cm}^2/\text{sec}$  for PF.
- The average value of  $C_{r2,50}$  found to be  $2.77 \times 10^{-4} \text{ cm}^2/\text{sec}$  while average value of  $C_{r2,80}$  found to be  $1.02 \times 10^{-4} \text{ cm}^2/\text{sec}$  for PF.
- The average value of  $C_{r3,50}$  found to be  $4.83 \times 10^{-4} \text{ cm}^2/\text{sec}$  while average value of  $C_{r3,80}$  found to be  $2.12 \times 10^{-4} \text{ cm}^2/\text{sec}$  for PF.
- The value of  $C_{r1,50}$  &  $C_{r1,80}$  at 40kPa for SD is  $1.7 \times 10^{-5} \text{ cm}^2/\text{sec}$  &  $6.87 \times 10^{-6} \text{ cm}^2/\text{sec}$ , while for 160kPa it was found to be  $1 \times 10^{-5} \text{ cm}^2/\text{sec}$  &  $5.5 \times 10^{-6} \text{ cm}^2/\text{sec}$ .
- The value of  $C_{r2,50}$  &  $C_{r2,80}$  at 40kPa for SD is  $1.54 \times 10^{-4} \text{ cm}^2/\text{sec}$  &  $6.3 \times 10^{-5} \text{ cm}^2/\text{sec}$ , while for 160kPa it was found to be  $1.18 \times 10^{-4} \text{ cm}^2/\text{sec}$  &  $5 \times 10^{-5} \text{ cm}^2/\text{sec}$ .
- The value of  $C_{r3,50}$  &  $C_{r3,80}$  at 40kPa for SD is  $2.72 \times 10^{-4} \text{ cm}^2/\text{sec}$  &  $1.15 \times 10^{-4} \text{ cm}^2/\text{sec}$ , while for 160kPa it was found to be  $2.18 \times 10^{-4} \text{ cm}^2/\text{sec}$  &  $9.86 \times 10^{-5} \text{ cm}^2/\text{sec}$ .
- The value of  $C_{r1,50}$  &  $C_{r1,80}$  at 40kPa for SW is  $7.13 \times 10^{-5} \text{ cm}^2/\text{sec}$  &  $3.26 \times 10^{-5} \text{ cm}^2/\text{sec}$ , while for 160kPa it was found to be  $5.19 \times 10^{-5} \text{ cm}^2/\text{sec}$  &  $2.59 \times 10^{-5} \text{ cm}^2/\text{sec}$ .

- The value of  $C_{r2,50}$  &  $C_{r2,80}$  at 40kPa for SW is  $1.29 \times 10^{-4} \text{ cm}^2/\text{sec}$  &  $4.4 \times 10^{-5} \text{ cm}^2/\text{sec}$ , while for 160kPa it was found to be  $8.38 \times 10^{-5} \text{ cm}^2/\text{sec}$  &  $3.8 \times 10^{-5} \text{ cm}^2/\text{sec}$ .
- The value of  $C_{r3,50}$  &  $C_{r3,80}$  at 40kPa for SW is  $1.53 \times 10^{-4} \text{ cm}^2/\text{sec}$  &  $6.46 \times 10^{-5} \text{ cm}^2/\text{sec}$ , while for 160kPa it was found to be  $1.08 \times 10^{-4} \text{ cm}^2/\text{sec}$  &  $5.12 \times 10^{-5} \text{ cm}^2/\text{sec}$ .
- The value of  $C_{r1,50}$  &  $C_{r1,80}$  at 40kPa for CJ is  $1.01 \times 10^{-4} \text{ cm}^2/\text{sec}$  &  $3.75 \times 10^{-5} \text{ cm}^2/\text{sec}$ , while for 160kPa it was found to be  $4.92 \times 10^{-5} \text{ cm}^2/\text{sec}$  &  $2.46 \times 10^{-5} \text{ cm}^2/\text{sec}$ .
- The value of  $C_{r2,50}$  &  $C_{r2,80}$  at 40kPa for CJ is  $5.77 \times 10^{-4} \text{ cm}^2/\text{sec}$  &  $1.24 \times 10^{-4} \text{ cm}^2/\text{sec}$ , while for 160kPa it was found to be  $4.51 \times 10^{-4} \text{ cm}^2/\text{sec}$  &  $1.25 \times 10^{-4} \text{ cm}^2/\text{sec}$ .
- The value of  $C_{r3,50}$  &  $C_{r3,80}$  at 40kPa for CJ is  $8.99 \times 10^{-4} \text{ cm}^2/\text{sec}$  &  $2.9 \times 10^{-4} \text{ cm}^2/\text{sec}$ , while for 160kPa it was found to be  $7.73 \times 10^{-4} \text{ cm}^2/\text{sec}$  &  $2.15 \times 10^{-4} \text{ cm}^2/\text{sec}$ .
- The value of  $C_{r1,50}$  &  $C_{r1,80}$  at 40kPa for PF is  $3.01 \times 10^{-5} \text{ cm}^2/\text{sec}$  &  $1.35 \times 10^{-5} \text{ cm}^2/\text{sec}$ , while for 160kPa it was found to be  $2.39 \times 10^{-5} \text{ cm}^2/\text{sec}$  &  $1.13 \times 10^{-5} \text{ cm}^2/\text{sec}$ .
- The value of  $C_{r2,50}$  &  $C_{r2,80}$  at 40kPa for PF is  $3.46 \times 10^{-4} \text{ cm}^2/\text{sec}$  &  $1.14 \times 10^{-4} \text{ cm}^2/\text{sec}$ , while for 160kPa it was found to be  $2.06 \times 10^{-4} \text{ cm}^2/\text{sec}$  &  $9.5 \times 10^{-5} \text{ cm}^2/\text{sec}$ .
- The value of  $C_{r3,50}$  &  $C_{r3,80}$  at 40kPa for PF is  $5.82 \times 10^{-4} \text{ cm}^2/\text{sec}$  &  $2.55 \times 10^{-4} \text{ cm}^2/\text{sec}$ , while for 160kPa it was found to be  $3.92 \times 10^{-4} \text{ cm}^2/\text{sec}$  &  $1.85 \times 10^{-4} \text{ cm}^2/\text{sec}$ .
- Looking to above plots and values it is clear that CJ shows more rate of consolidation both at low and high pressures in compare to other drain materials at all three radial points. Also it is observed that variation in value of  $C_{r50}$  and  $C_{r80}$  between various pressures at three radial points is very high in case of CJ i.e. 28% and 8% at middle radial point 'r2' while PF shows 67% & 20%. So it can be said that CJ shows more inter-rate of dissipation of excess hydrostatic pore water pressure even at following pressures in compare to other drain materials. At higher pressures though dissipation is fast at nearest radial point 'r1' during initial time but it ceases as consolidation proceeds and

so middle radial point is taken for comparison as no much variation is observed in value of  $C_r$  at all pressures.

**Discussion:** Under any strain condition because of the flexibility CJ drain shows higher horizontal permeability compare to others.

- From the plots it is very clear that for all drain materials the initial nature of  $T_{r80}$  graph &  $T_{r50}$  graph decreases with initial applied pressure and at higher pressures it remains same that is nearly constant. It is because of the initial structural resistance existing in the clay water structure of the Kaolinite clay. (refer figure 6.57)
- Lesser variation in  $C_r$  value is observed for radial point's  $r_2$  and  $r_3$  for all drain materials and for all applied pressures. Though CJ shows more inter-rate of dissipation of excess hydrostatic pore water pressure even at successive pressures in compare to other drain materials.

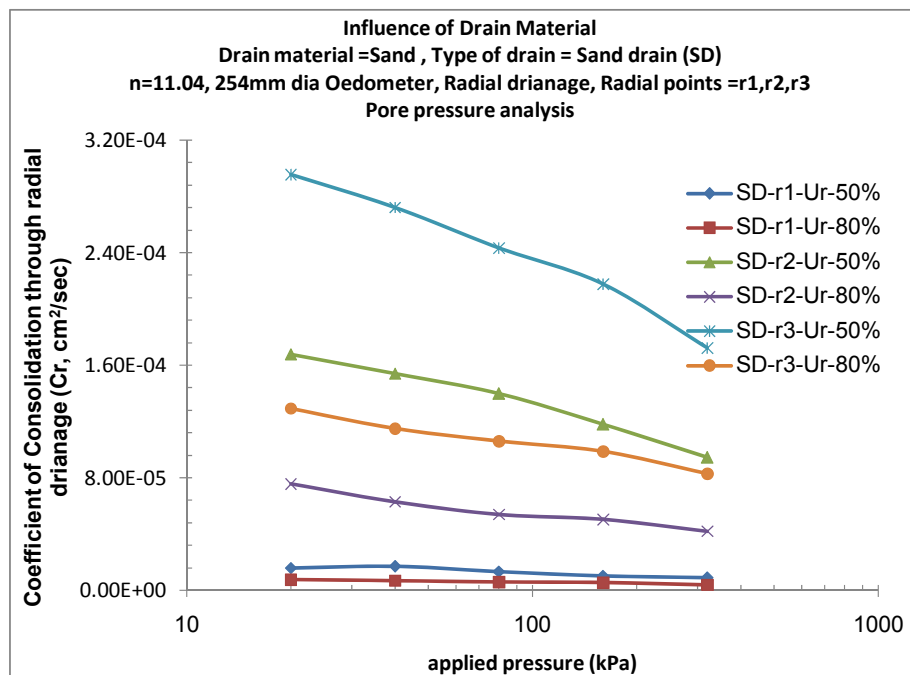


**Fig.6.51:** Coefficient of consolidation through radial drainage( $C_r$ ) vs. Applied pressure for SD at 50% and 80% degree of consolidation (Ur) at radial points r1, r2, r3

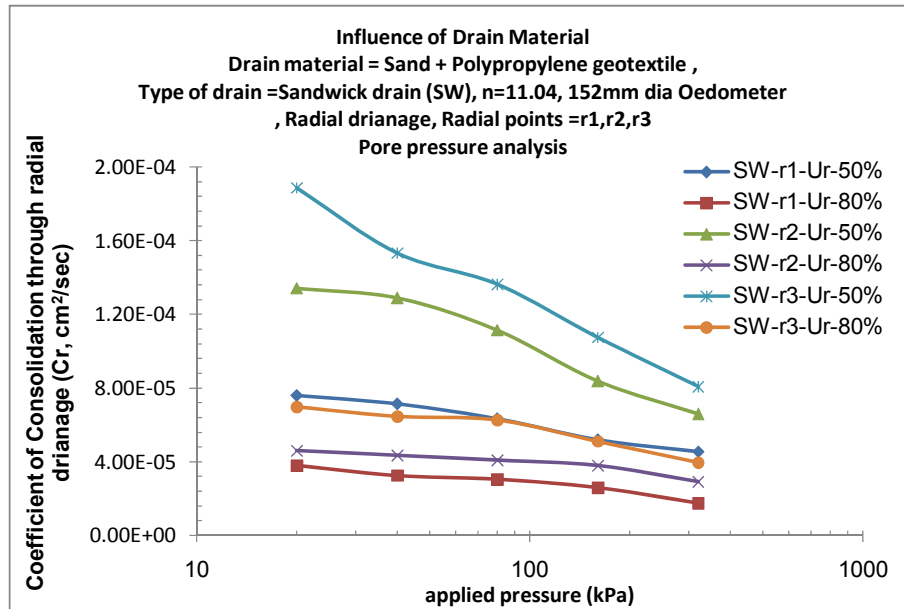


**Fig.6.52:** Coefficient of consolidation through radial drainage( $C_r$ ) vs. Applied pressure for SW at 50% and 80% degree of consolidation ( $U_r$ ) at radial points r1, r2, r3

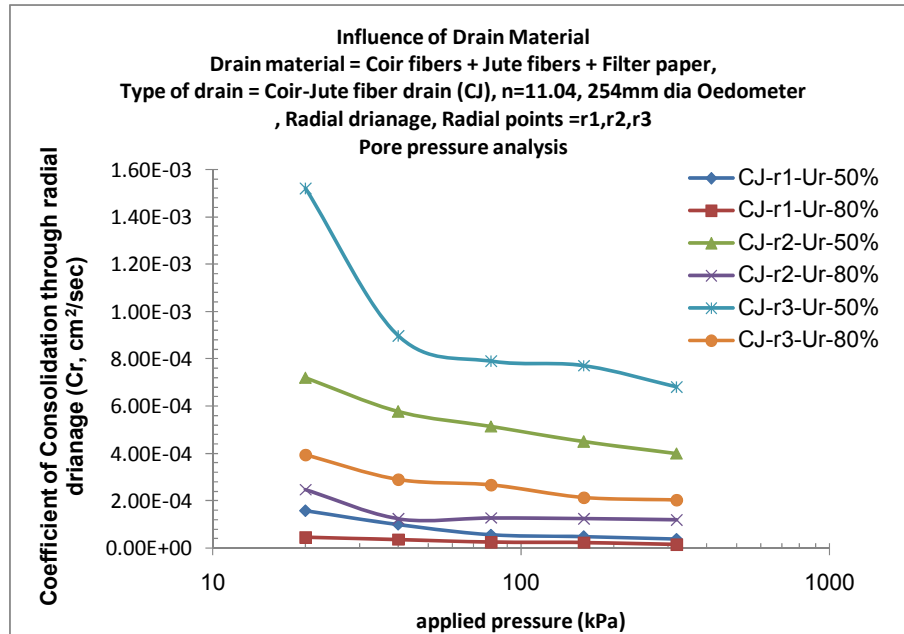


**Fig.6.53:** Coefficient of consolidation through radial drainage( $C_r$ ) vs. Applied pressure for CJ at 50% and 80% degree of consolidation ( $U_r$ ) at radial points r1, r2, r3

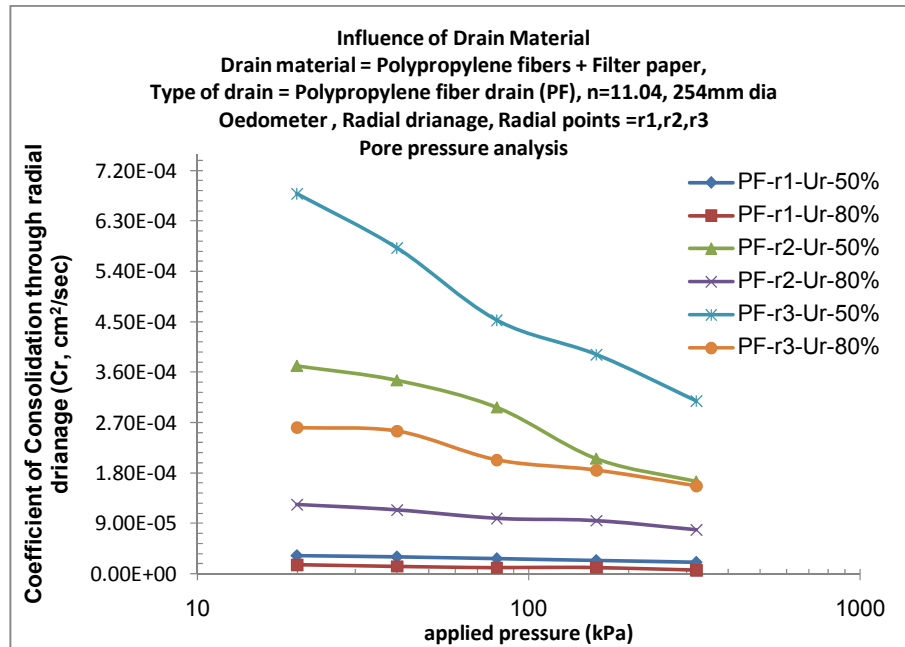


**Fig.6.54:** Coefficient of consolidation through radial drainage( $C_r$ ) vs. Applied pressure for PF at 50% and 80% degree of consolidation ( $U_r$ ) at radial points r1, r2, r3

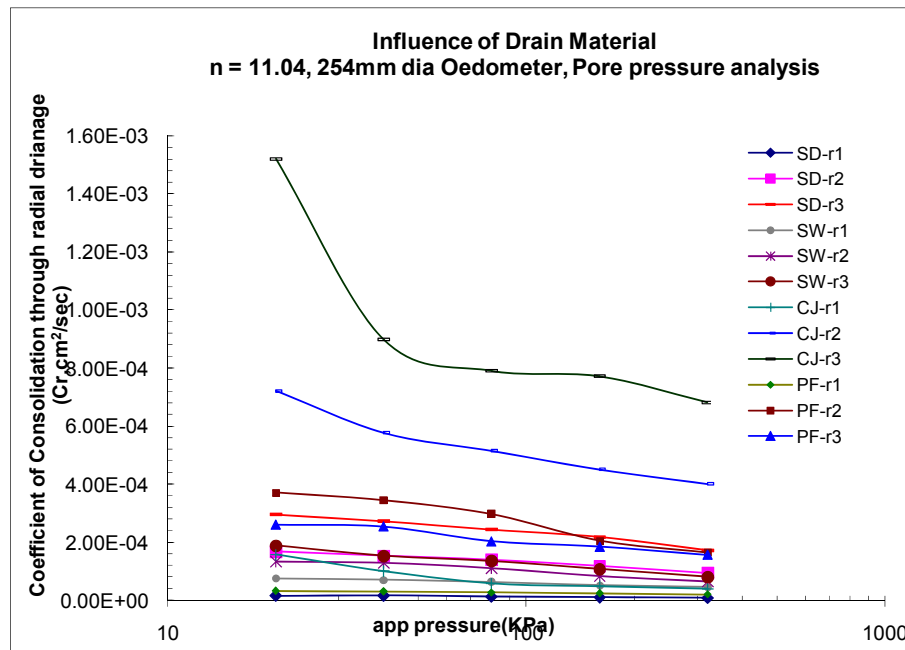


**Fig.6.55:** Comparison of Drain material w.r.t coefficient of consolidation through radial drainage( $C_r$ ) against applied pressure at 50%  $U_r$  at radial points r1, r2, r3

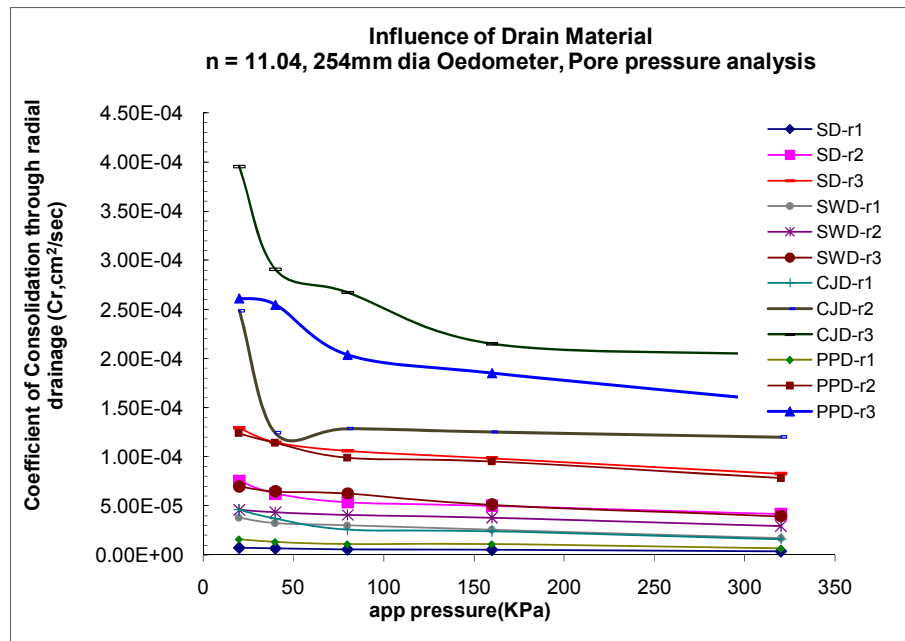


**Fig.6.56:** Comparison of Drain material w.r.t coefficient of consolidation through radial drainage( $C_r$ ) against applied pressure at 80%  $U_r$  at radial points r1, r2, r3

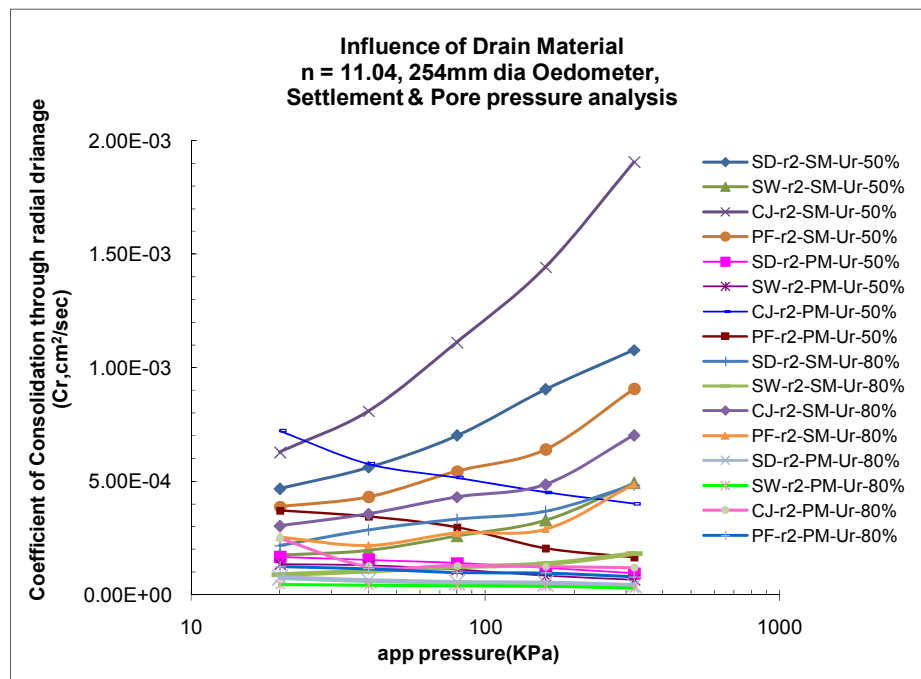


**Fig.6.57:** Comparison of Drain material w.r.t  $C_r$  against applied pressure for 50% & 80%  $U_r$  based on settlement and pore pressure analysis

#### 4) Void ratio (e) vs. applied pressure: Figures 6.58 to 6.63

**a) Settlement analysis-** Fig.6.58 to Fig.6.63 shows a characteristic curve of normally consolidation soil for 'n' value equal to 11.04 and for various drain materials like SD, SW, CJ & PF. The value of coefficient of compression ( $C_c$ ) for various drain materials is 0.400 for SD, 0.315 for SW, 0.258 for CJ and 0.366 for PF. Amongst the various drains CJ shows lower  $C_c$  value indicating 100% dissipation of pore water pressure at early time and thus showing more compressibility of clay mass also indicating achievement of higher vane shear strength of magnitude 150kPa.

#### **Discussion:**

- Amongst various drain material fibers of CJ orient in such a way that the rate of dissipation remain faster in spite of pressure increase though pressure effects their orientation but compare to other drains it maintains its efficaciousness. These reflect in the value of  $C_c$  of SW and CJ which results into effective compressibility of soil.
- The e vs. log p relationship and  $C_c$  vs. pressure indicate that because of effectiveness of CJ drain the compression index under lighter loading remains in the range of such a value that soil structure follow easy rate of dissipation showing low porosity compare to SD.
- Initial curvature portion of e vs. log p relationship interpret soil structural resistance that is hydrodynamic lag against compressive load which giving resistance to deformation as mentioned earlier. This structural resistance or hydrodynamic lag against compression is more pronounced in SW and SD compare to PF and CJ drain. CJ or PF allows higher gradient of radial flow forming structural orientation of particle accordingly pushing the particles against face to edge bonds of random orientation bringing close to each other in a parallel orientation (refer photos 6.3 to 6.8) cultivating face to face bonds showing more shear strength of a consolidated mass. The same thing is reflected in values of compression index of the soil structure produced by various drains. In micrographs of sample collected after loading of 320kPa exhibit the same thing of above materials. (refer fig. 6.64, 6.65 & 6.66)



- For any depth the % porosity remains less at any consolidation pressure with coir-jute drain compare to sand drain exhibiting effective consolidation.
- In general the degree of orientation(decrease of angle between particles) of particles in the soil structure undergoing consolidation indicate comparatively more face-to-face contact towards drain. Also this pattern is exhibited depth wise for any radial distance and drain material.
- In case of SD the degree of orientation during consolidation is more near the drain (radial point r1) compare to CJ, while more degree of orientation is observed in CJ at middle radial point r2 compare to SD, and almost same degree of orientation is observed in CJ & SD at farthest radial point r3.
- This is because of in case of SD consolidation proceeds faster near the drain thereby causing comparatively more surface settlement in that region, it could very well cause a redistribution of surface loading. While in case of CJ the condition of free strain develops which is implied that the settlement at the surface did not change the distribution of load to the soil at any location. At mid radial distance r2, the plot indicates effectiveness of CJ drain in early achievement of face-to-face orientation of particle.

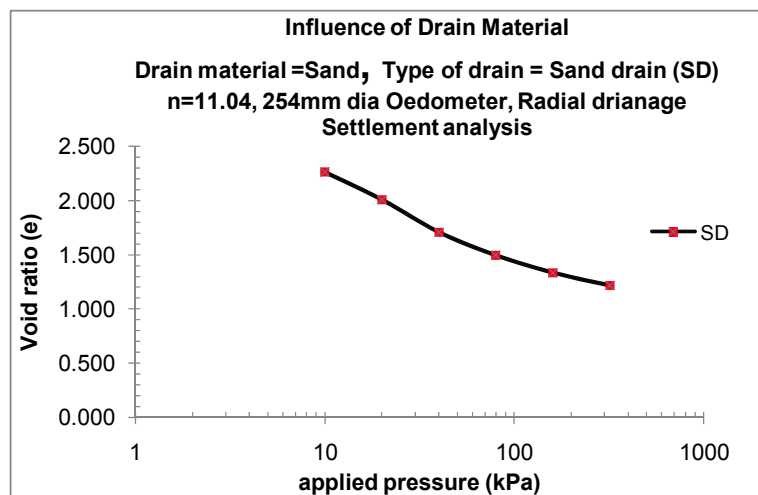


**Fig.6.58:** Void ratio vs. Applied pressure for SD

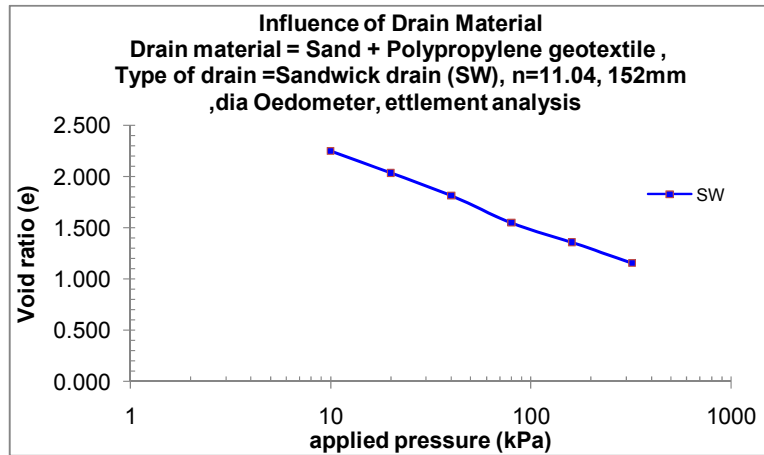


Fig.6.59: Void ratio vs. Applied pressure for SW

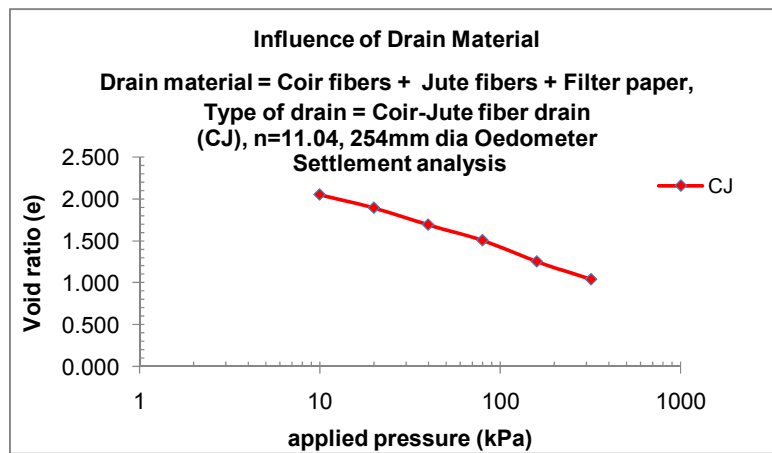


Fig.6.60: Void ratio vs. Applied pressure for CJ

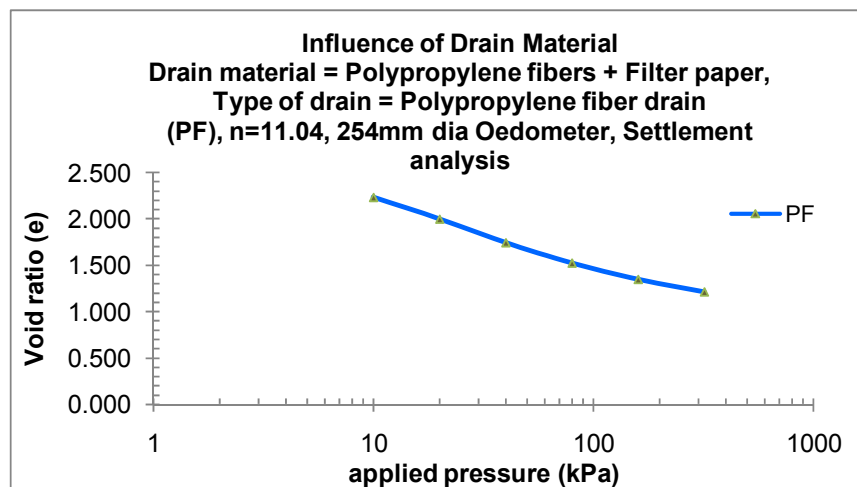
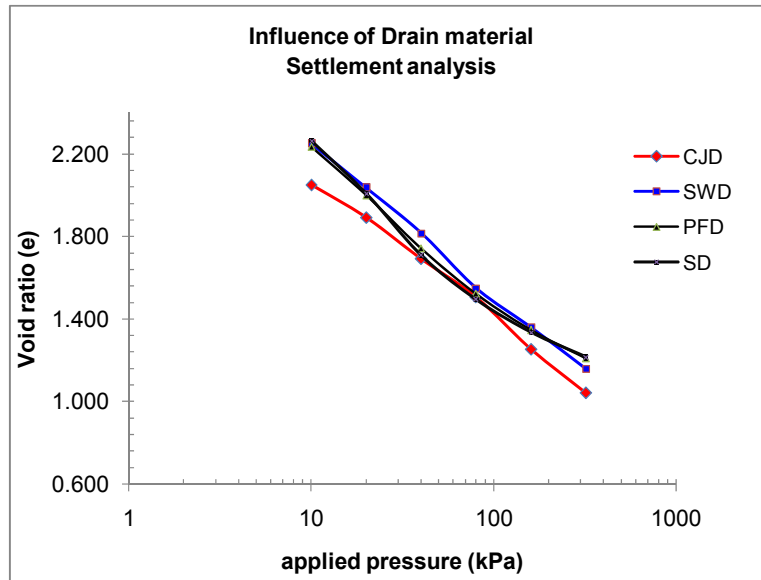
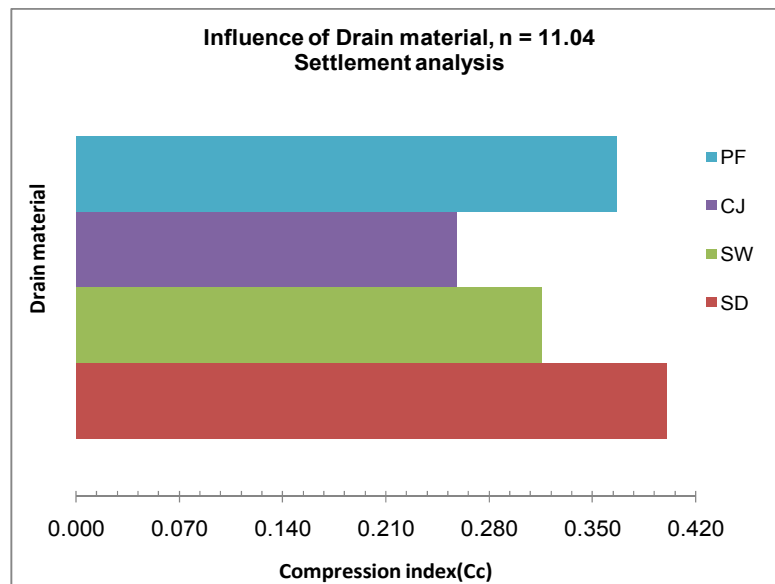


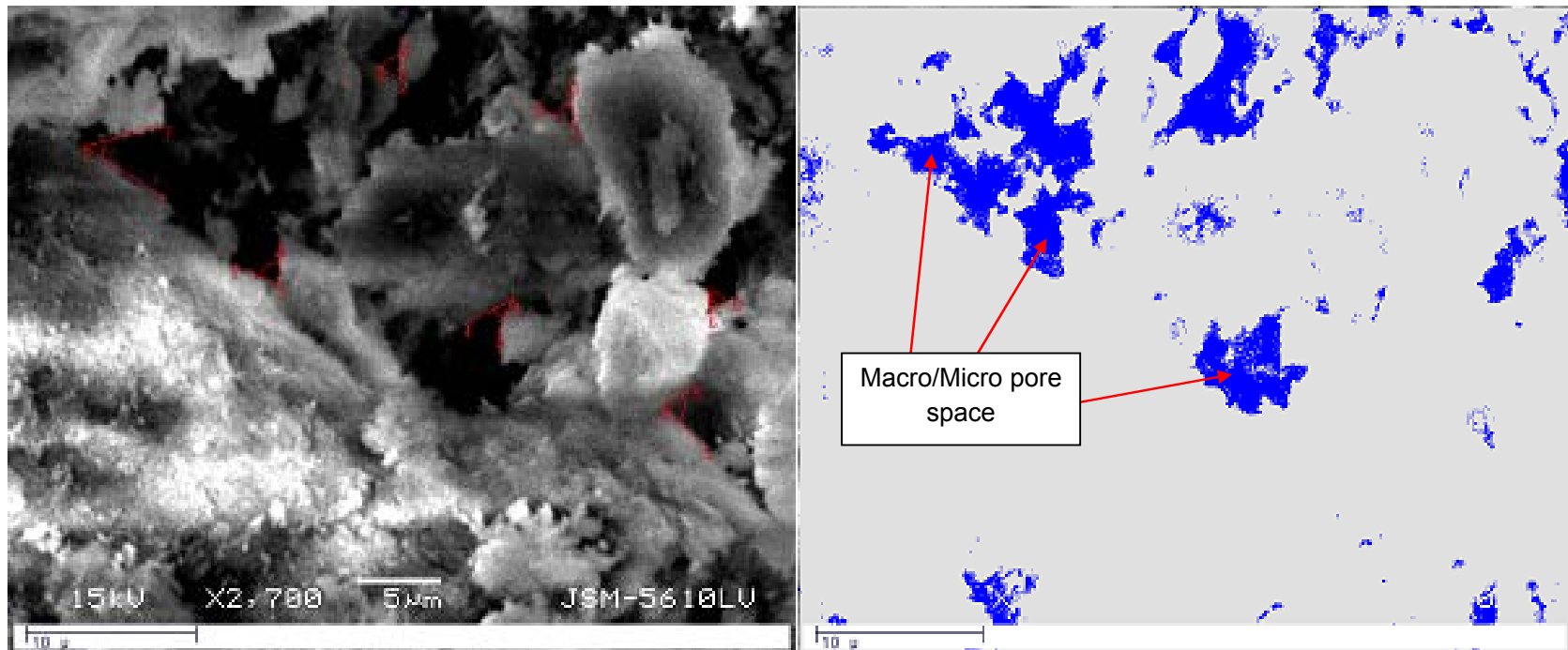
Fig.6.61: Void ratio vs. Applied pressure for PF



**Fig.6.62:** Comparison of Drain materials w.r.t void ratio( $e$ ) against applied pressure for  $n=11.04$ (same 'n' value)

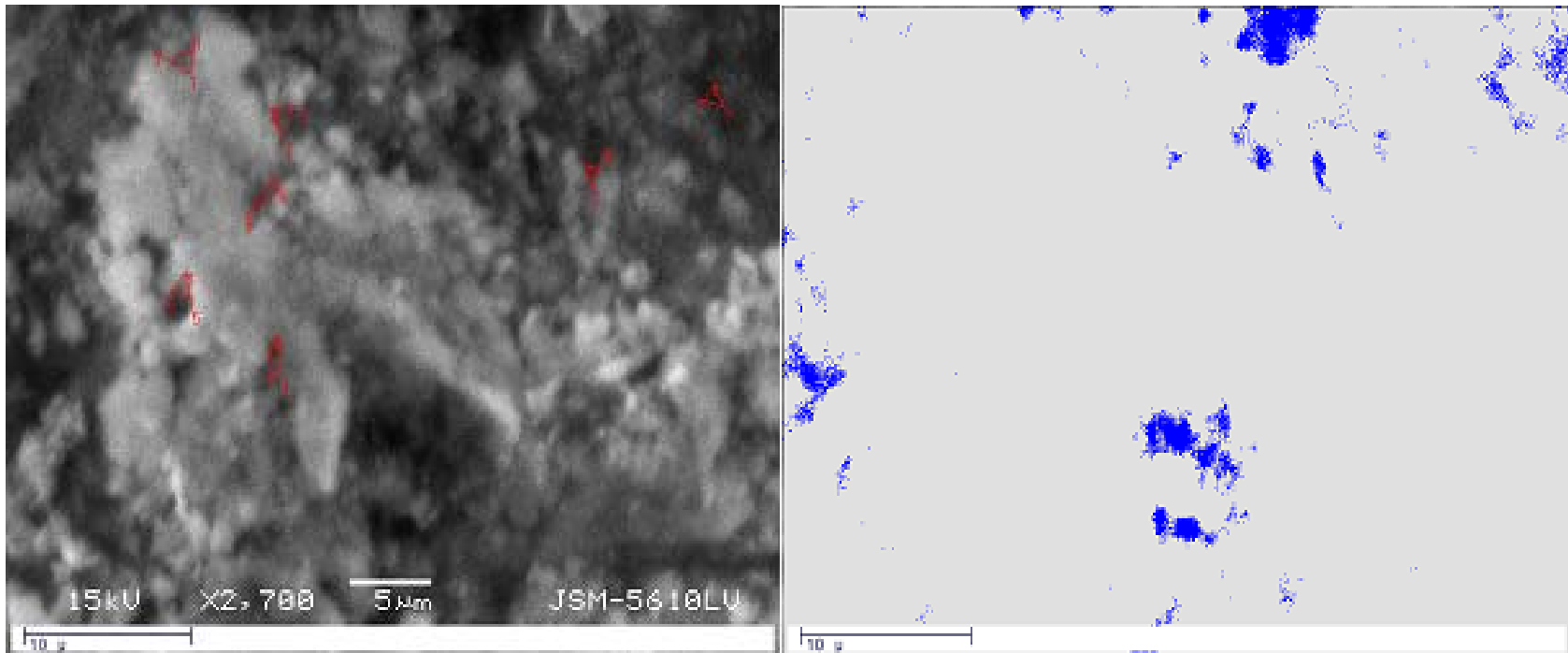


**Fig.6.63** Comparison of compression index ( $C_c$ ) with drain material for  $n=11.04$



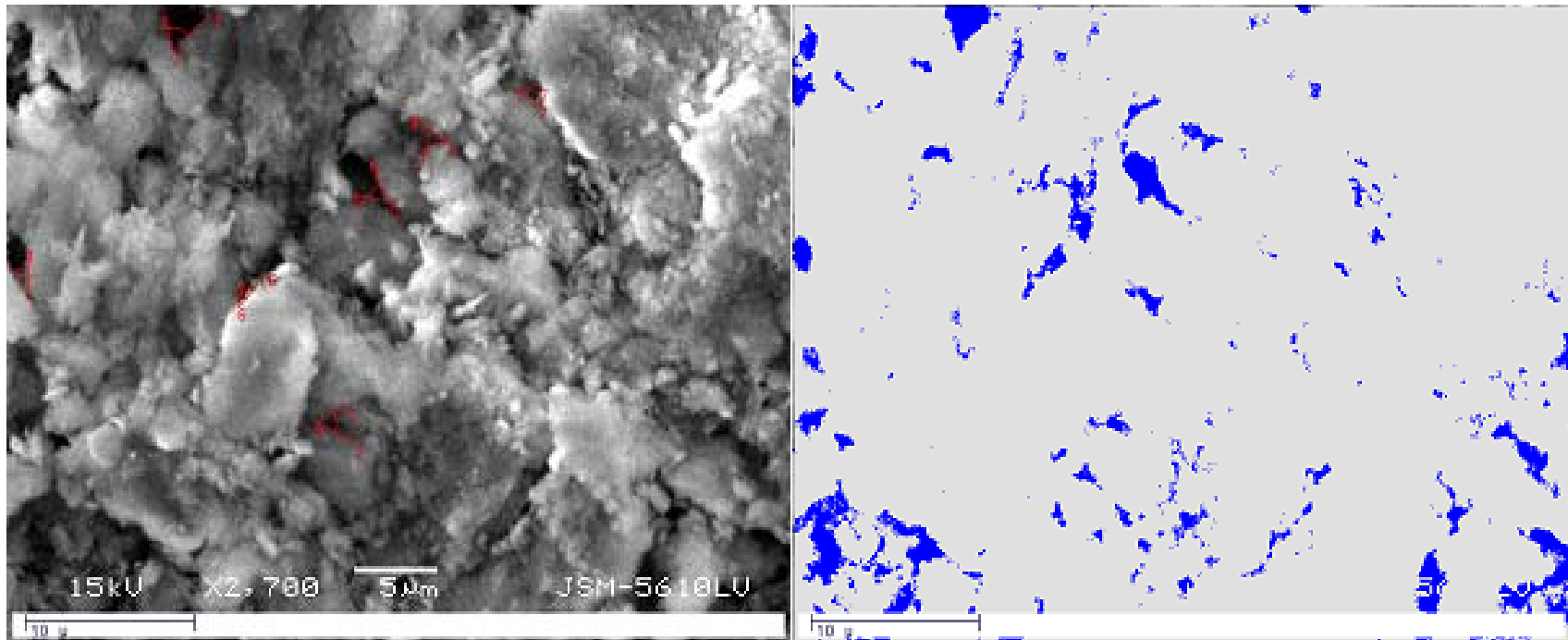
**Photograph 6.3:** Microscopic image of soil consolidated by Sand drain (SD) at location  $h_{tr2}$  and measurement of % porosity and angle of orientation ( $\beta$ ) using MIC software

Note: First image shows particle orientation(red mark) and second image shows porosity(blue mark)



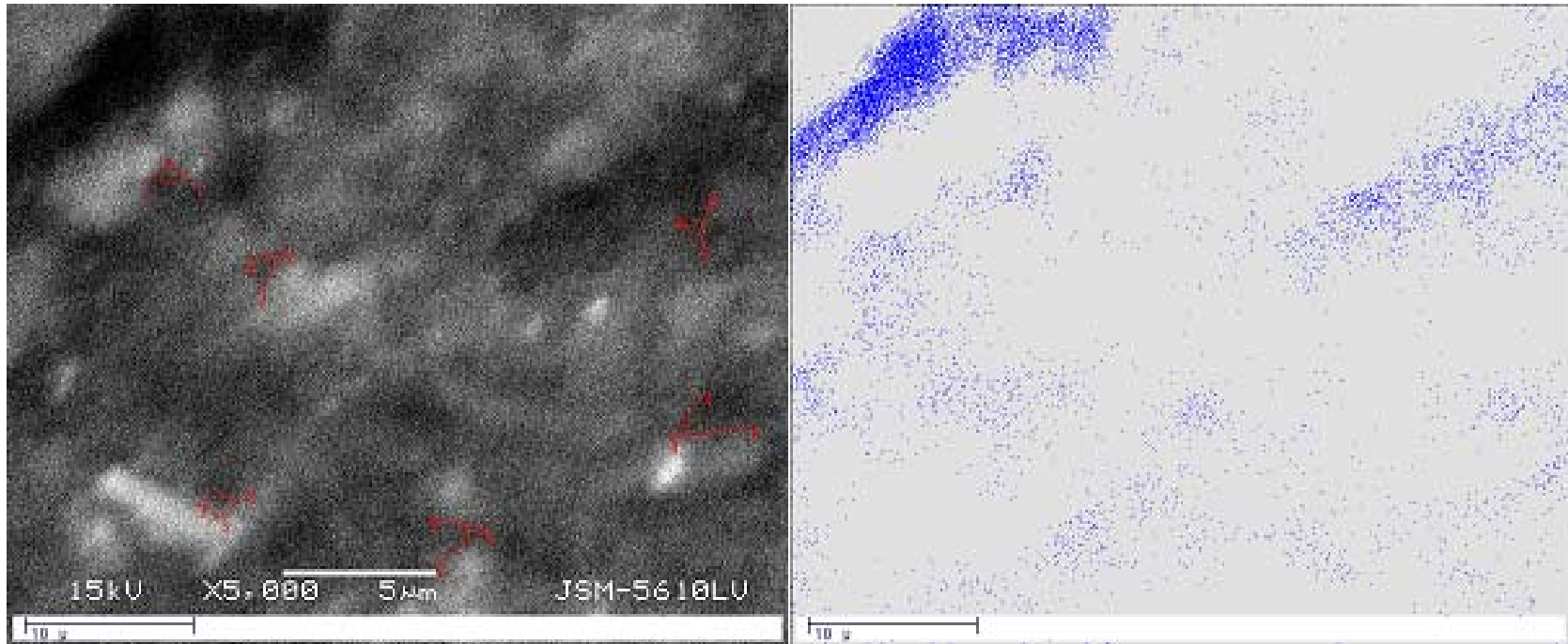
**Photograph 6.4:** Microscopic image of soil consolidated by Coir-Jute fiber drain (CJ) at location  $h_{tr2}$  and measurement of % porosity and angle of orientation ( $\beta$ ) using MIC software

Note: First image shows particle orientation(red mark) and second image shows porosity(blue mark)



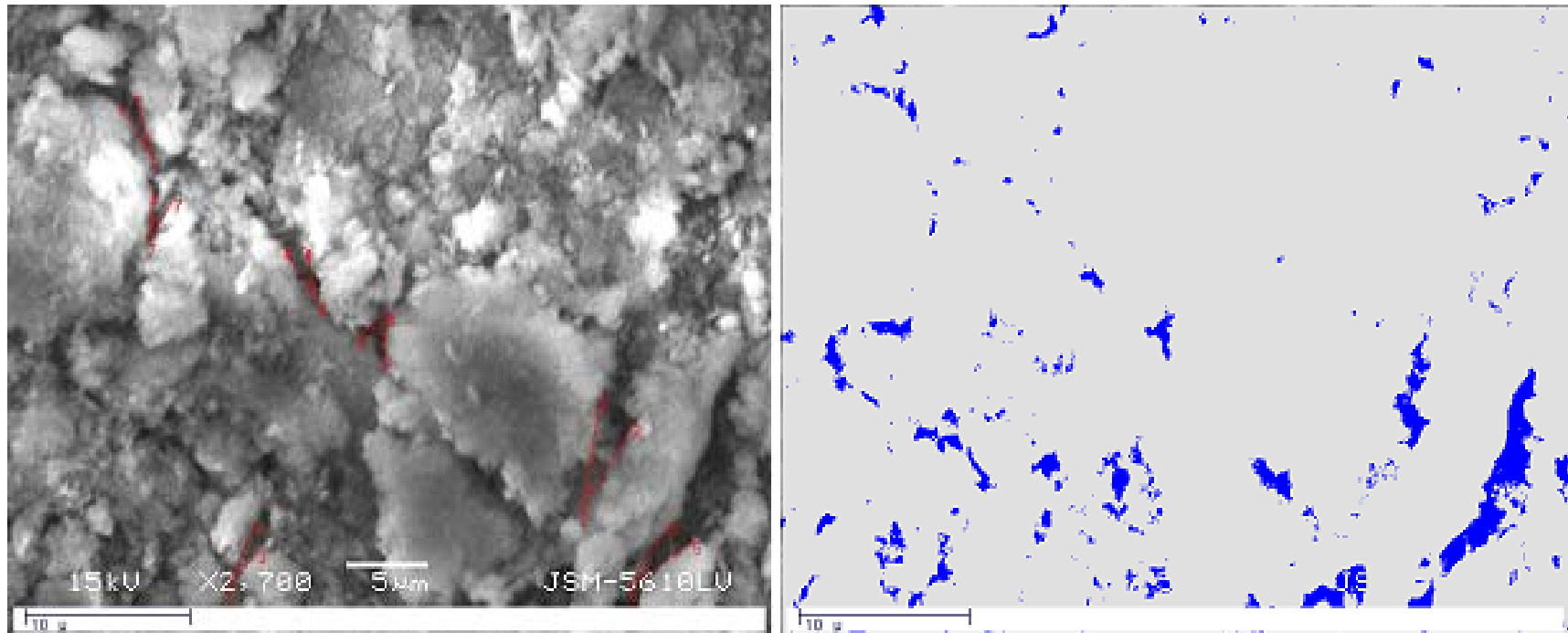
**Photograph 6.5:** Microscopic image of soil consolidated by Sand drain (SD) at location  $h_{cr2}$  and measurement of % porosity and angle of orientation ( $\beta$ ) using MIC software

Note: First image shows particle orientation(red mark) and second image shows porosity(blue mark)



**Photograph 6.6:** Microscopic image of soil consolidated by Coir-Jute drain (CJ) at location  $h_{cr2}$  and measurement of % porosity and angle of orientation ( $\beta$ ) using MIC software

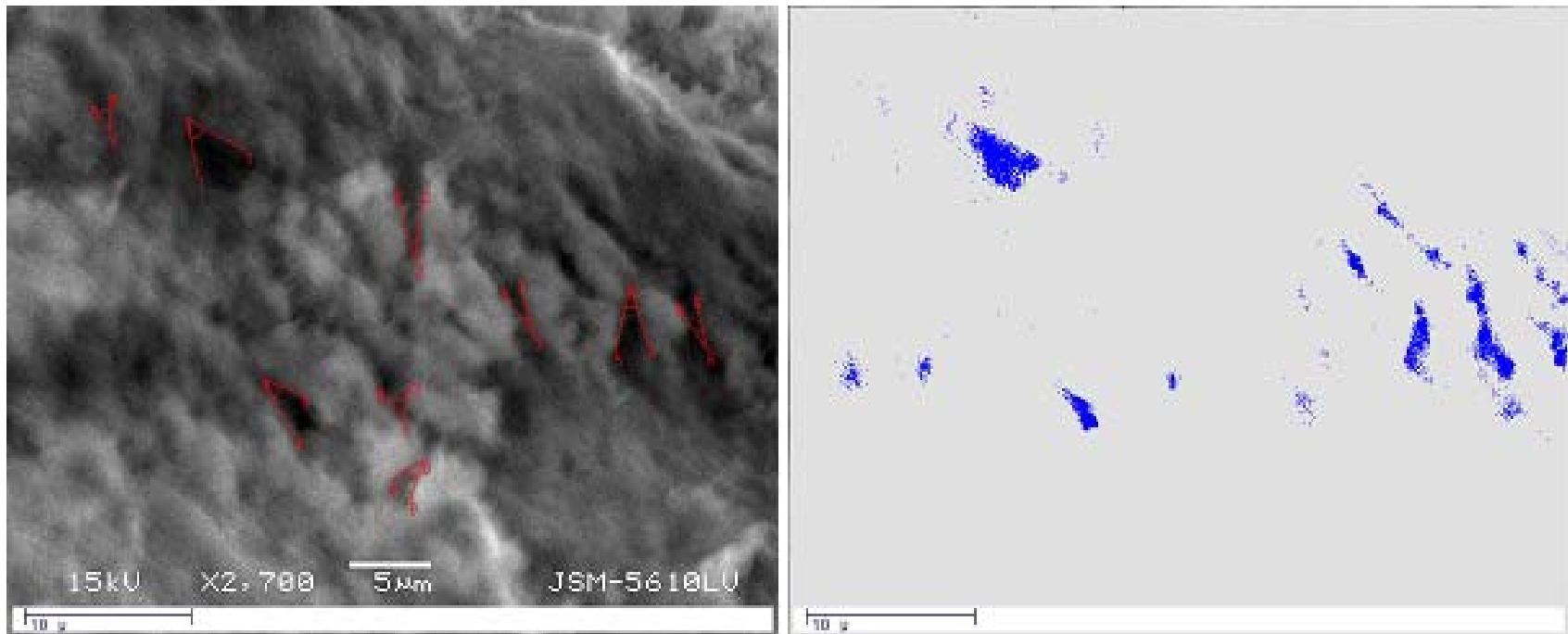
Note: First image shows particle orientation(red mark) and second image shows porosity(blue mark)



**Photograph 6.7:** Microscopic image of soil consolidated by Sand drain (SD) at location  $h_{br2}$  and measurement of % porosity and angle of orientation ( $\beta$ ) using MIC software

Note: First image shows particle orientation(red mark) and second image shows porosity(blue mark)





**Photograph 6.8:** Microscopic image of soil consolidated by Coir-Jute drain (CJ) at location  $h_{br2}$  and measurement of % porosity and angle of orientation ( $\beta$ ) using MIC software

Note: First image shows particle orientation(red mark) and second image shows porosity(blue mark)

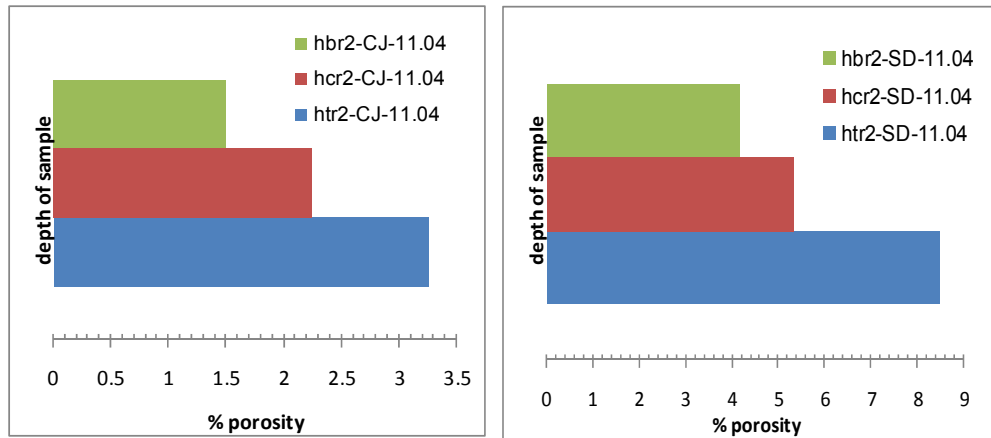


**Fig.6.64:** Comparison of % microporosity of CJ and SD ('n'11.04) at various locations (Influence of drain material)

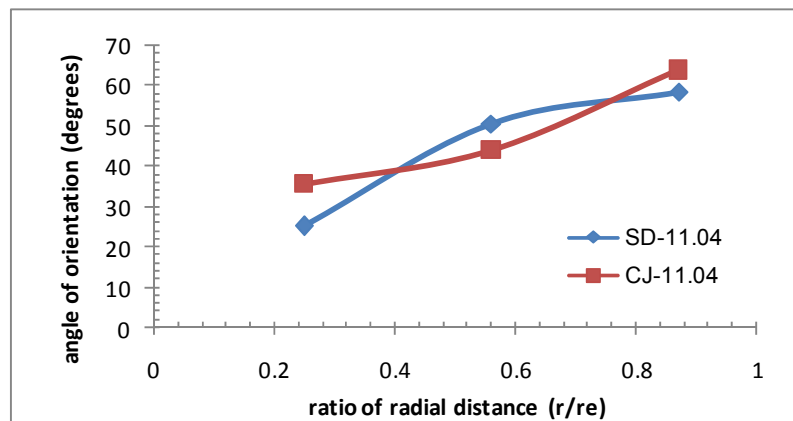


**Fig.6.65:** Comparison of angle of orientation ( $\beta$ ) against ratio of radial distance ( $r/re$ ) of CJ and SD of 'n'11.04 (Influence of drain material)

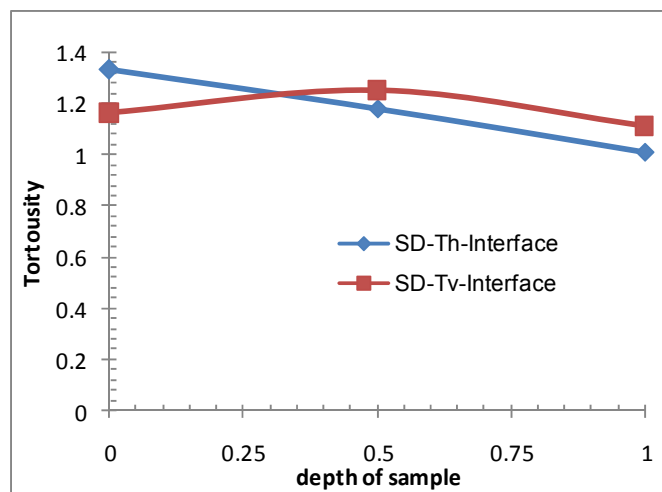


**Fig.6.66:** Comparison of horizontal tortuosity (Th) and vertical tortuosity (Tv) against depth of sample for CJ and SD of 'n'11.04 (Influence of drain material)

### 5) Coefficient of horizontal permeability ( $k_h$ ) vs. applied pressure: Figures 6.67 to 6.79

**a) Settlement analysis:-** Fig.6.67 to Fig.6.72 shows the plots of coefficient of horizontal permeability ( $k_h$ ) versus applied pressure for various drain materials like SD, SW, CJ and PF 'n' value of 11.04 at all applied pressures. Here for analysis time required for 50% ( $T_{50}$ ) consolidation and time required for 80% ( $T_{80}$ ) consolidation are taken for all pressures and all 'n' values to get  $k_{h50}$  and  $k_{h80}$ .

- The horizontal permeability ( $k_{h50}$ ) obtained by settlement decreases with increase in the pressure from  $3.98 \times 10^{-7}$  cm/sec at 20 kPa to  $3.75 \times 10^{-8}$  cm/sec at 320 kPa for SD.
- The horizontal permeability ( $k_{h80}$ ) obtained by settlement decreases with increase in the pressure from  $1.84 \times 10^{-7}$  cm/sec at 20 kPa to  $1.68 \times 10^{-8}$  cm/sec at 320 kPa for SD.
- The horizontal permeability ( $k_{h50}$ ) obtained by settlement decreases with increase in the pressure from  $1.25 \times 10^{-7}$  cm/sec at 20 kPa to  $2.97 \times 10^{-8}$  cm/sec at 320 kPa for SW.
- The horizontal permeability ( $k_{h80}$ ) obtained by settlement decreases with increase in the pressure from  $6.36 \times 10^{-8}$  cm/sec at 20 kPa to  $1.10 \times 10^{-8}$  cm/sec at 320 kPa for SW.
- The horizontal permeability ( $k_{h50}$ ) obtained by settlement decreases with increase in the pressure from  $3.55 \times 10^{-7}$  cm/sec at 20 kPa to  $1.08 \times 10^{-7}$  cm/sec at 320 kPa for CJ.
- The horizontal permeability ( $k_{h80}$ ) obtained by settlement decreases with increase in the pressure from  $1.72 \times 10^{-7}$  cm/sec at 20 kPa to  $3.97 \times 10^{-8}$  cm/sec at 320 kPa for CJ.
- The horizontal permeability ( $k_{h50}$ ) obtained by settlement decreases with increase in the pressure from  $3.15 \times 10^{-7}$  cm/sec at 20 kPa to  $3.55 \times 10^{-8}$  cm/sec at 320 kPa for PF.
- The horizontal permeability ( $k_{h80}$ ) obtained by settlement decreases with increase in the pressure from  $2.06 \times 10^{-7}$  cm/sec at 20 kPa to  $1.90 \times 10^{-8}$  cm/sec at 320 kPa for PF.

- The  $k_{h50}$  and  $k_{h80}$  both decreases with increase in pressure for all drain materials.  $k_{h50}$  &  $k_{h80}$  for CJ is 26% and 9% more in compare to SD, while 40%.and 24% more in compare to PF.This clearly shows that CJ has higher rate permeability in compare to other drain materials.

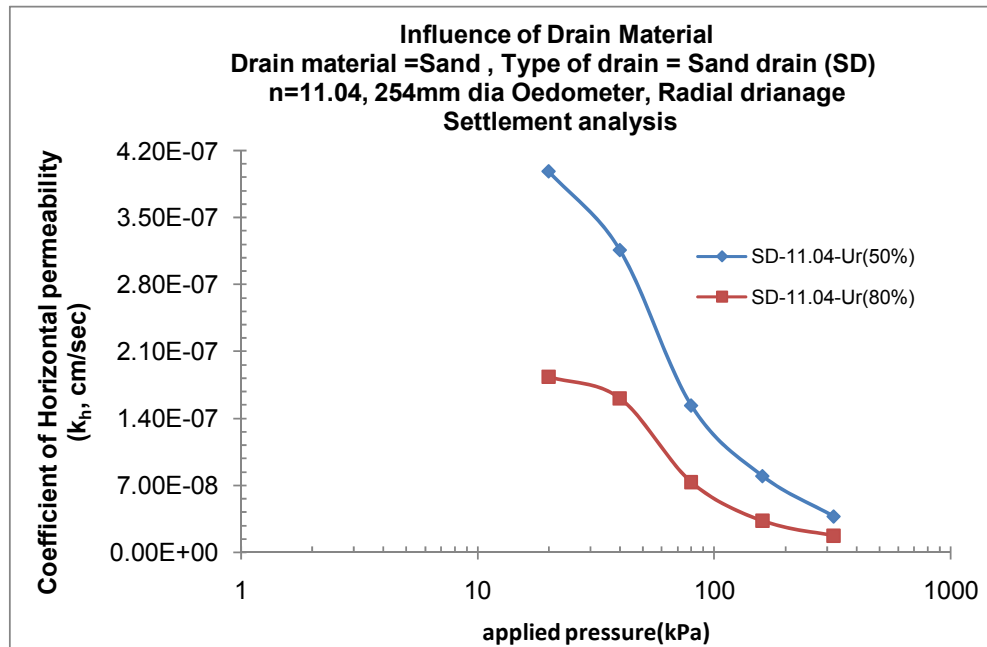


**Fig.6.67:** Coefficient of consolidation through radial drainage( $C_r$ ) vs. Applied pressure for SD at 50% and 80% degree of consolidation ( $U_r$ )

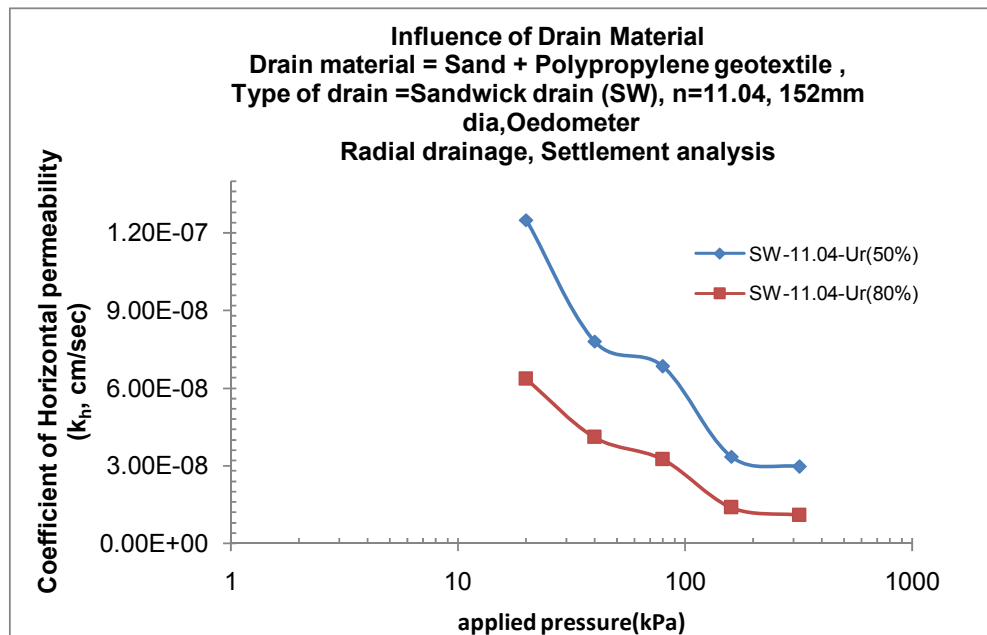


**Fig.6.68:** Coefficient of consolidation through radial drainage( $C_r$ ) vs. Applied pressure for SD at 50% and 80% degree of consolidation ( $U_r$ )

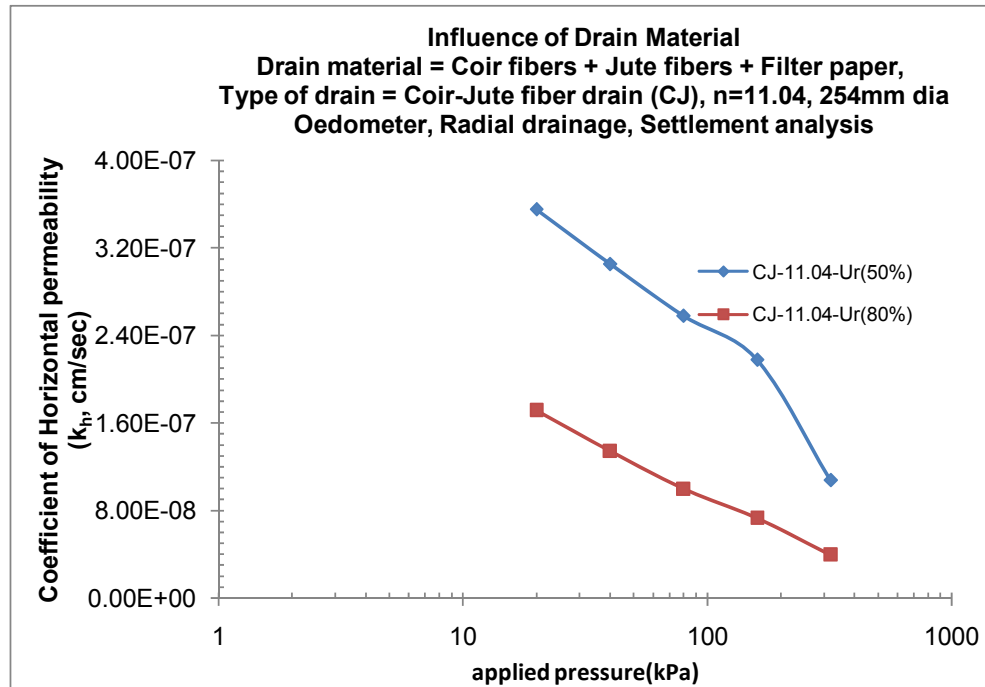


**Fig.6.69:** Coefficient of consolidation through radial drainage( $C_r$ ) vs. Applied pressure for CJ at 50% and 80% degree of consolidation ( $U_r$ )

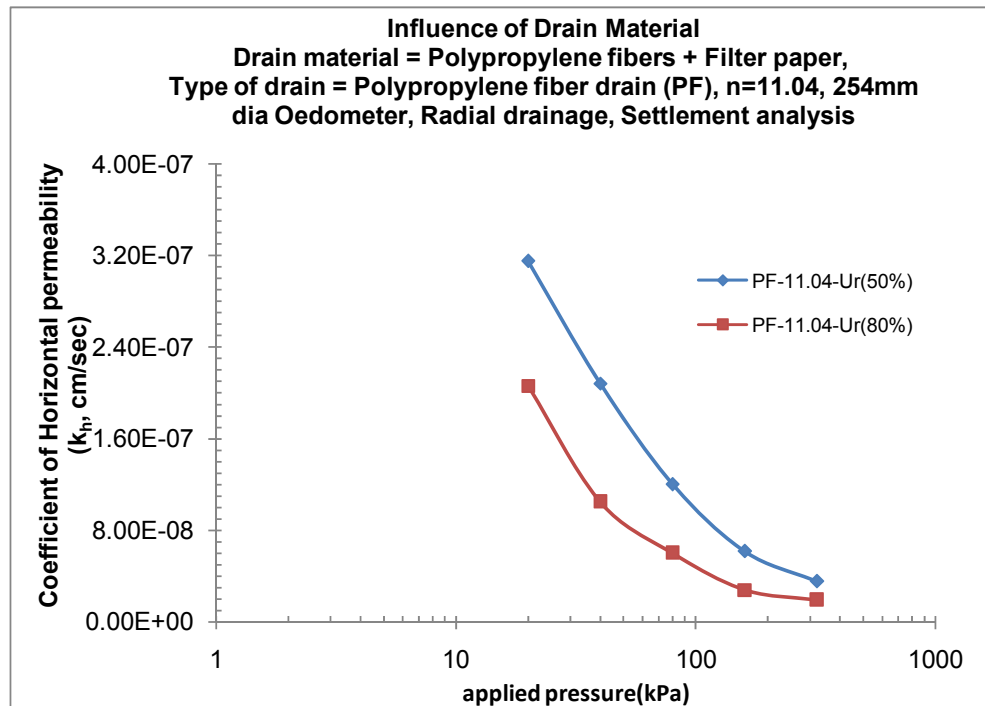


**Fig.6.70:** Coefficient of consolidation through radial drainage( $C_r$ ) vs. Applied pressure for PF at 50% and 80% degree of consolidation ( $U_r$ )

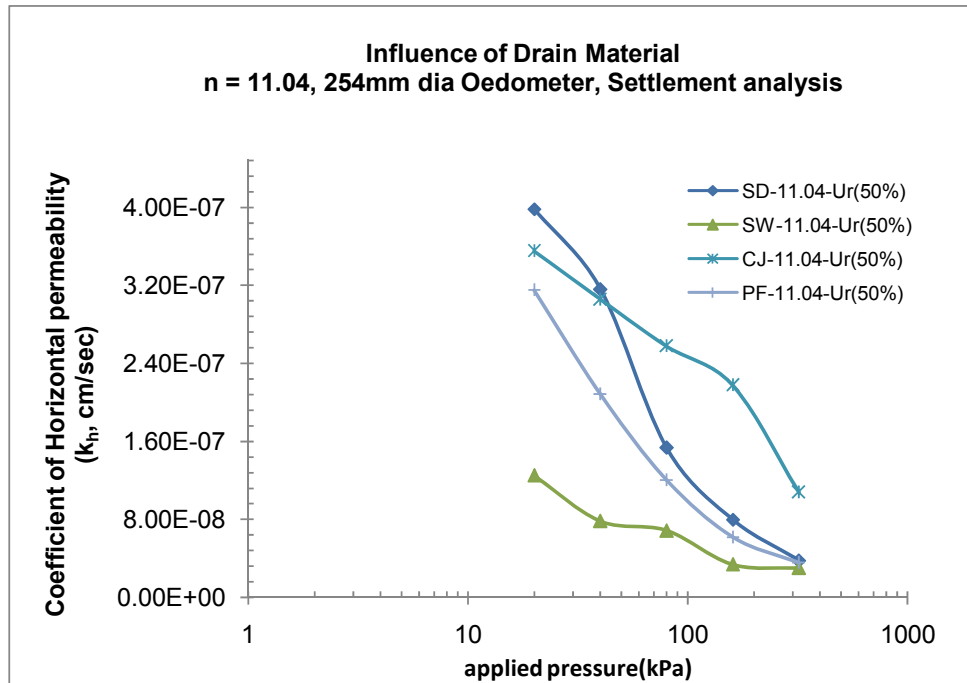


**Fig.6.71:** Comparison of Drain material w.r.t coefficient of horizontal permeability ( $k_h$ ) against applied pressure at 50% degree of consolidation ( $U_r$ )

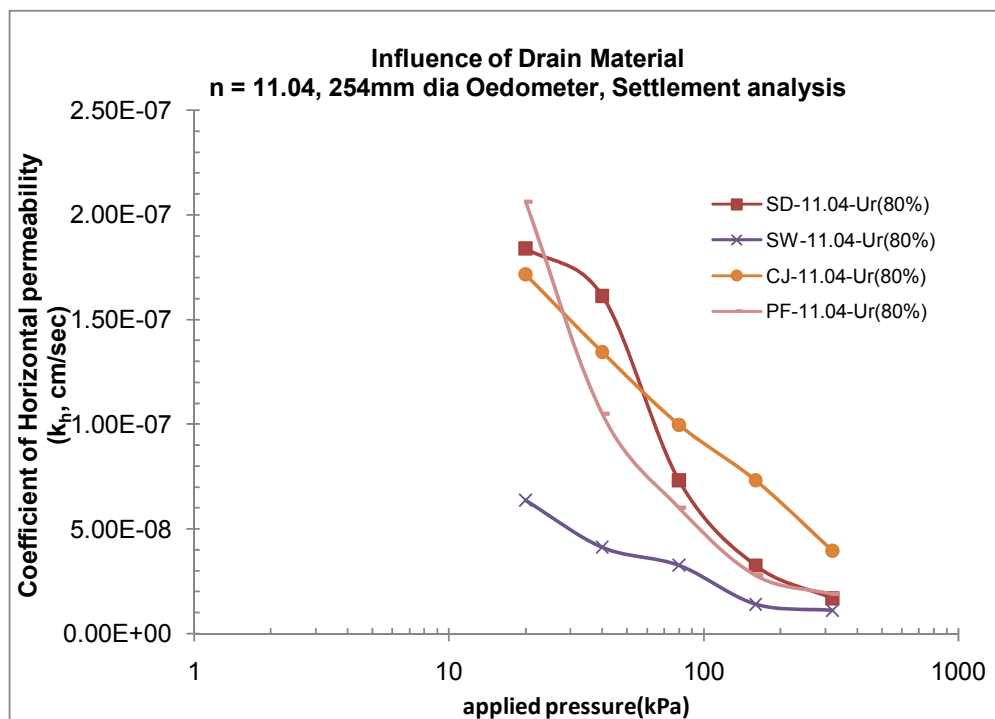


**Fig.6.72:** Comparison of Drain material w.r.t coefficient of horizontal permeability ( $k_h$ ) against applied pressure at 80% degree of consolidation ( $U_r$ )

**b) Pore pressure analysis:-** Fig.6.73 to Fig.6.78 shows the plots of coefficient of horizontal permeability ( $k_h$ ) versus applied pressure for various drain materials like SD, SW, CJ & PF for all 'n' values of 11.04 for three radial points' r1, r2 & r3. Here for analysis time required for 50% ( $T_{50}$ ) consolidation and time required for 80% ( $T_{80}$ ) consolidation are taken for all pressures and all 'n' values to get  $k_{h50}$  and  $k_{h80}$ . The horizontal permeability at three different radial points' r1, r2 and r3 for 50% consolidation obtained by pore pressure readings decreases with increase in the pressure.

- For SD as drain material at 20kPa pressure at nearest radial point (r1),  $k_{h150}$  is  $1.35 \times 10^{-8}$  to  $3.12 \times 10^{-10}$  cm/sec at 320 kPa, while  $k_{h180}$  for 20kPa it is  $6.39 \times 10^{-9}$ cm/sec to  $1.37 \times 10^{-10}$ cm/sec at 320 kPa respectively.
- For SD as drain material at 20kPa pressure at middle radial point (r2),  $k_{h250}$  is  $1.43 \times 10^{-7}$  to  $3.29 \times 10^{-9}$  cm/sec at 320 kPa, while  $k_{h180}$  for 20kPa it is  $6.44 \times 10^{-8}$ cm/sec to  $1.46 \times 10^{-9}$ cm/sec at 320 kPa respectively.
- For SD as drain material at 20 kPa pressure at farthest radial point (r3)  $k_{h350}$  is  $2.52 \times 10^{-7}$  to  $6 \times 10^{-9}$  cm/sec at 320 kPa, while  $k_{h380}$  for 20kPa it is  $1.01 \times 10^{-7}$ cm/sec to  $2.88 \times 10^{-9}$ cm/sec at 320 kPa respectively.
- For SW as drain material at 20 kPa pressure at nearest radial point (r1),  $k_{h150}$  is  $5.41 \times 10^{-8}$  to  $2.76 \times 10^{-9}$ cm/sec at 320 kPa, while  $k_{h180}$  for 20kPa it is  $2.71 \times 10^{-8}$ cm/sec to  $1.06 \times 10^{-9}$ cm/sec at 320 kPa respectively.
- For SW as drain material at 20 kPa pressure at middle radial point (r2),  $k_{h250}$  is  $9.56 \times 10^{-8}$  to  $3.89 \times 10^{-9}$  cm/sec at 320 kPa, while  $k_{h180}$  for 20kPa it is  $3.28 \times 10^{-8}$ cm/sec to  $1.77 \times 10^{-9}$ cm/sec at 320 kPa respectively.
- For SW as drain material at 20 kPa pressure at farthest radial point (r3)  $k_{h350}$  is  $1.34 \times 10^{-7}$  to  $4.88 \times 10^{-9}$  cm/sec at 320 kPa, while  $k_{h380}$  for 20kPa it is  $4.96 \times 10^{-8}$ cm/sec to  $2.39 \times 10^{-9}$ cm/sec at 320 kPa respectively.
- For CJ as drain material at 20kPa pressure at nearest radial point (r1),  $k_{h150}$  is  $8.91 \times 10^{-8}$  to  $2.27 \times 10^{-9}$  cm/sec at 320 kPa, while  $k_{h180}$  for 20kPa it is  $2.62 \times 10^{-8}$ cm/sec to  $9.27 \times 10^{-10}$ cm/sec at 320 kPa respectively.
- For CJ as drain material at 20 kPa pressure at middle radial point (r2),  $k_{h250}$  is  $4.08 \times 10^{-7}$  to  $2.27 \times 10^{-8}$  cm/sec at 320 kPa, while  $k_{h180}$  for 20kPa it is  $1.41 \times 10^{-7}$ cm/sec to  $6.8 \times 10^{-9}$ cm/sec at 320 kPa respectively.

- For CJ as drain material at 20 kPa pressure at farthest radial point (r3)  $k_{h350}$  is  $8.61 \times 10^{-7}$  to  $3.58 \times 10^{-8}$  cm/sec at 320 kPa, while  $k_{h380}$  for 20kPa it is  $2.24 \times 10^{-7}$ cm/sec to  $1.15 \times 10^{-8}$ cm/sec at 320 kPa respectively.
- For PF as drain material at 20 kPa pressure at farthest radial point (r1)  $k_{h150}$  is  $2.63 \times 10^{-8}$  to  $7.94 \times 10^{-10}$  cm/sec at 320 kPa, while  $k_{h180}$  for 20kPa it is  $1.32 \times 10^{-8}$ cm/sec to  $2.65 \times 10^{-10}$  cm/sec at 320 kPa respectively.
- For PF as drain material at 20 kPa pressure at middle radial point (r2),  $k_{h250}$  is  $3.02 \times 10^{-7}$  to  $6.47 \times 10^{-9}$  cm/sec at 320 kPa, while  $k_{h180}$  for 20kPa it is  $1.01 \times 10^{-7}$ cm/sec to  $3.06 \times 10^{-9}$ cm/sec at 320 kPa respectively.
- For PF as drain material at 20 kPa pressure at farthest radial point (r3)  $k_{h350}$  is  $5.51 \times 10^{-7}$  to  $1.21 \times 10^{-8}$  cm/sec at 320 kPa, while  $k_{h380}$  for 20kPa it is  $2.12 \times 10^{-7}$ cm/sec to  $6.14 \times 10^{-9}$ cm/sec at 320 kPa respectively.
- It is also concluded that coefficient of permeability ( $k_h$ ) for CJ material is highest in compare to other drain materials.  $k_{h150}$  &  $k_{h180}$  for CJ is 28% and 0.1% more in compare to SW,  $k_{h250}$  &  $k_{h280}$  is 77% and 72% more in compare to SW,  $k_{h350}$  &  $k_{h380}$  is 83% and 77% more in compare to SW. Also  $k_{h150}$  &  $k_{h180}$  in compare to SD it is 81% and 76% more in compare to SD,  $k_{h250}$  &  $k_{h280}$  is 67% and 51% more in compare to SD,  $k_{h350}$  &  $k_{h380}$  is 68% and 52% more in compare to SD.

**Discussion:** (Refer fig. 6.79)

- From the above analysis it indicates that  $k_h$  value of drain increases the efficacy of rate of drainage through soil thereby it reflects coefficient of transmissivity of water through soil. For any pressure the  $k_h$  value of CJ remains efficient compare to others when compared either with settlement analysis or pore pressure analysis. The value of coefficient of horizontal permeability ( $k_h$ ) remains higher for CJ both for 50% and 80% consolidation compare to drain materials viz. SD, SW and PF. Reason of higher permeability is because of more porous structure of CJ drain and specifically due to high capillary action of coir-jute fibers compare to other drain materials. Secondly coir-jute fiber has more wetting capacity under longer duration because complete specific surface area of each fiber gets wet and helps to migrate water at faster rate.



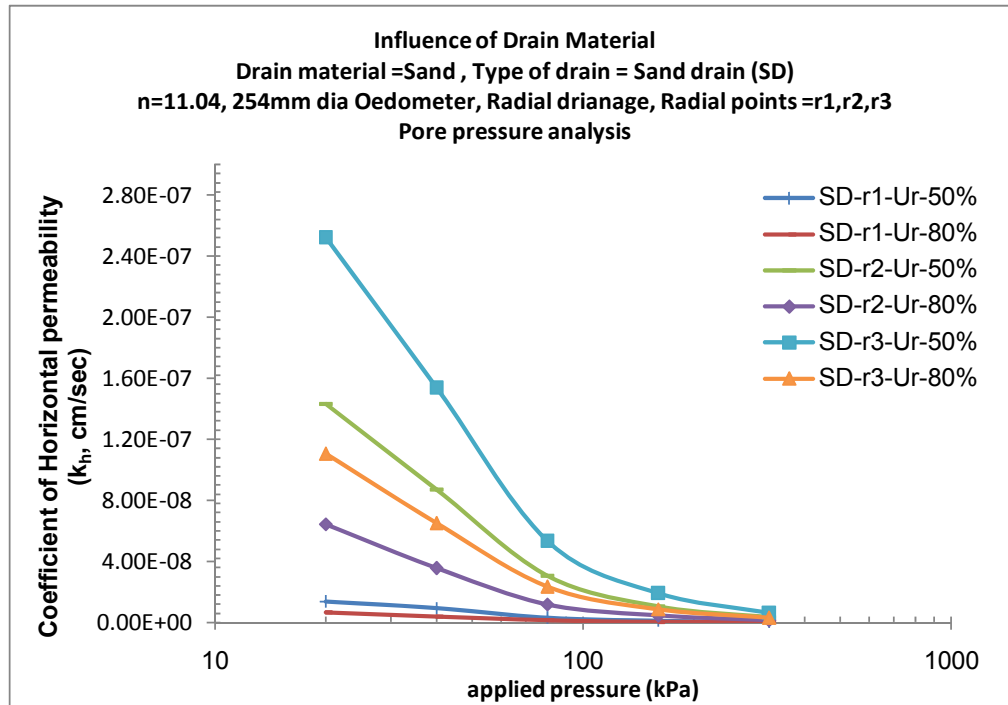


**Fig.6.73:** Coefficient of consolidation through radial drainage( $C_r$ ) vs. Applied pressure for SD at 50% and 80% degree of consolidation ( $U_r$ ) at radial points r1, r2, r3

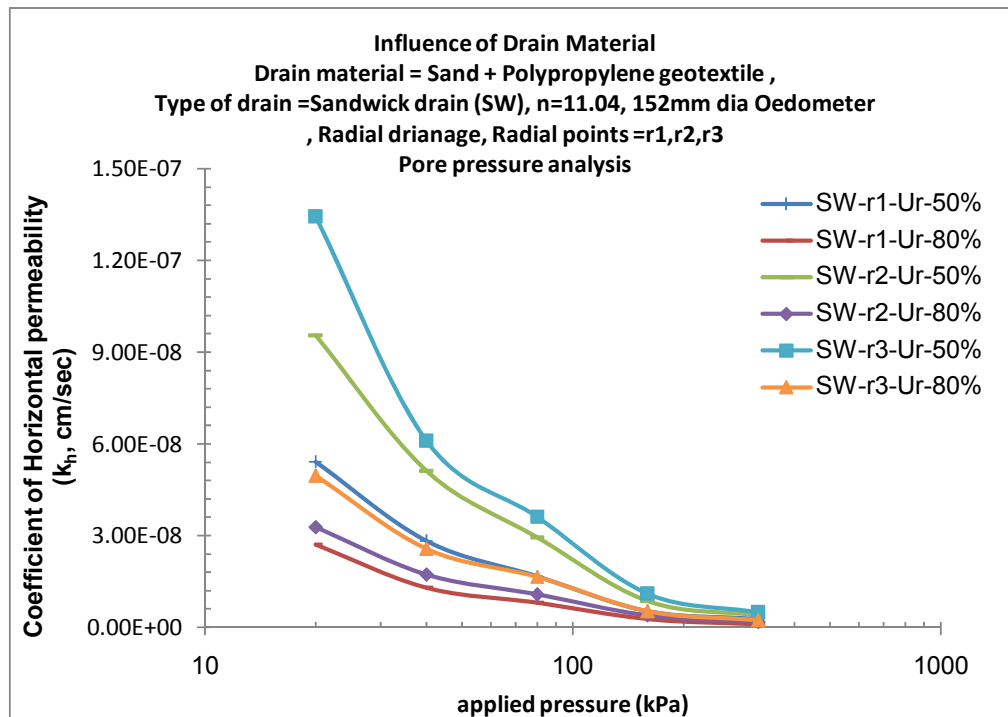


**Fig.6.74:** Coefficient of consolidation through radial drainage( $C_r$ ) vs. Applied pressure for SW at 50% and 80% degree of consolidation ( $U_r$ ) at radial points r1, r2, r3

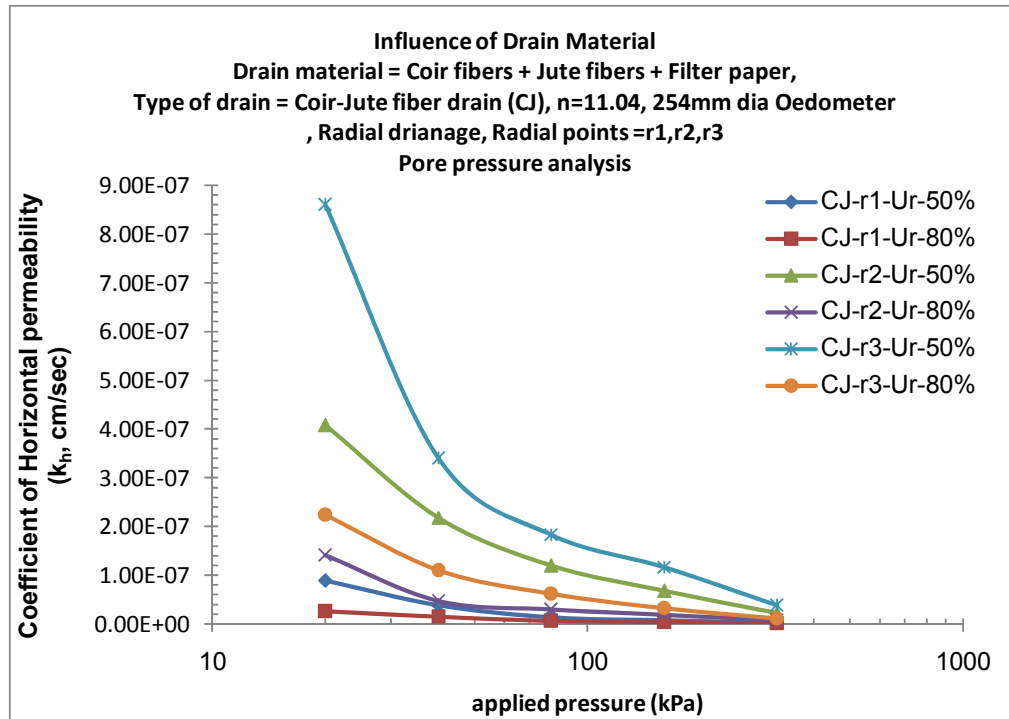


**Fig.6.75:** Coefficient of consolidation through radial drainage( $C_r$ ) vs. Applied pressure for CJ at 50% and 80% degree of consolidation ( $U_r$ ) at radial points  $r_1$ ,  $r_2$ ,  $r_3$

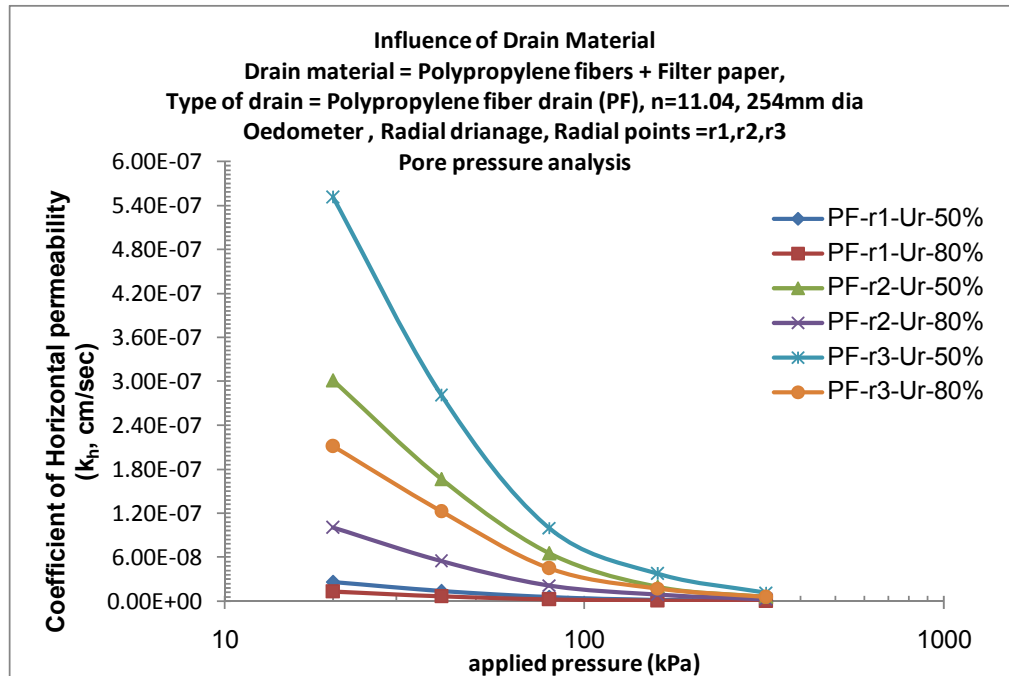


**Fig.6.76:** Coefficient of consolidation through radial drainage( $C_r$ ) vs. Applied pressure for PF at 50% and 80% degree of consolidation ( $U_r$ ) at radial points  $r_1$ ,  $r_2$ ,  $r_3$

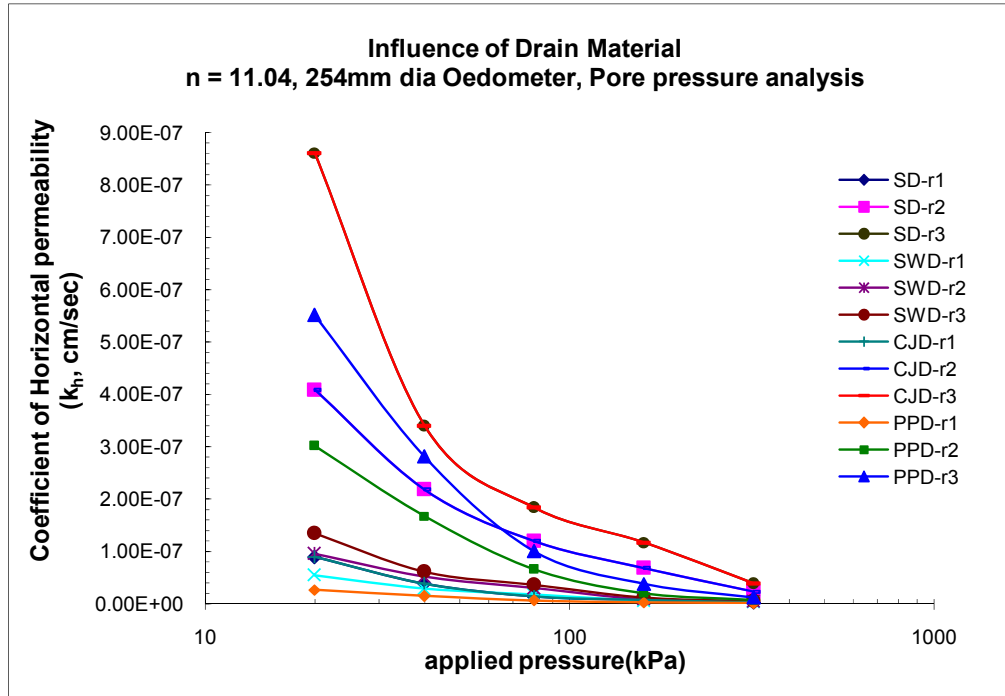


**Fig.6.77:** Comparison of Drain material w.r.t coefficient of horizontal permeability ( $k_h$ ) against applied pressure at 50%  $U_r$  at radial points r1, r2, r3

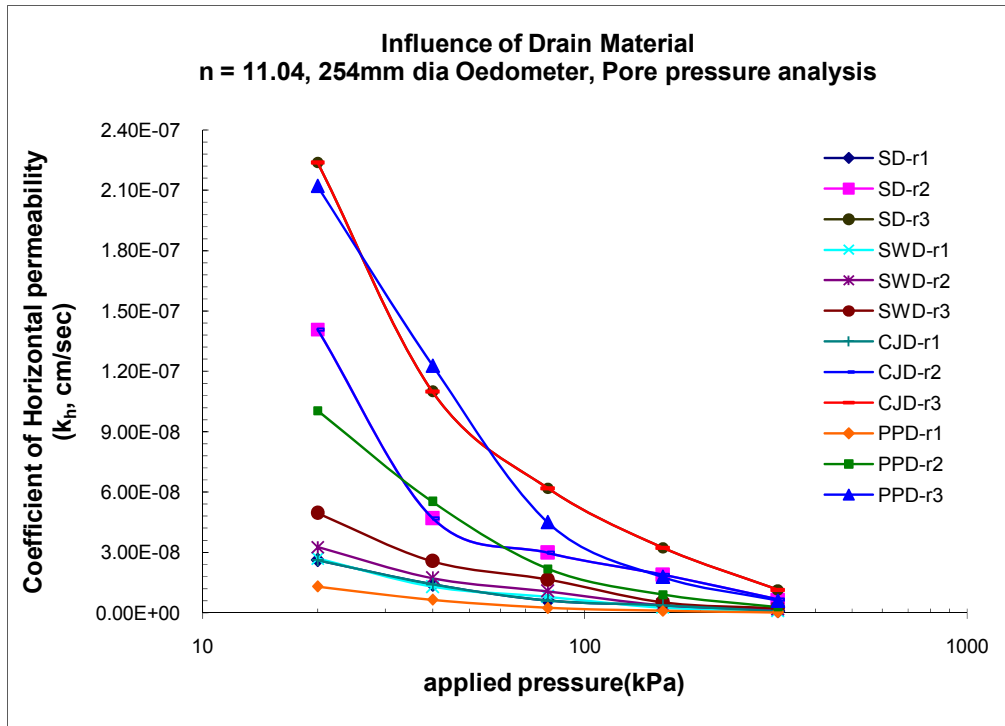


**Fig.6.78:** Comparison of Drain material w.r.t coefficient of horizontal permeability ( $k_h$ ) against applied pressure at 80%  $U_r$  at radial points r1, r2, r3

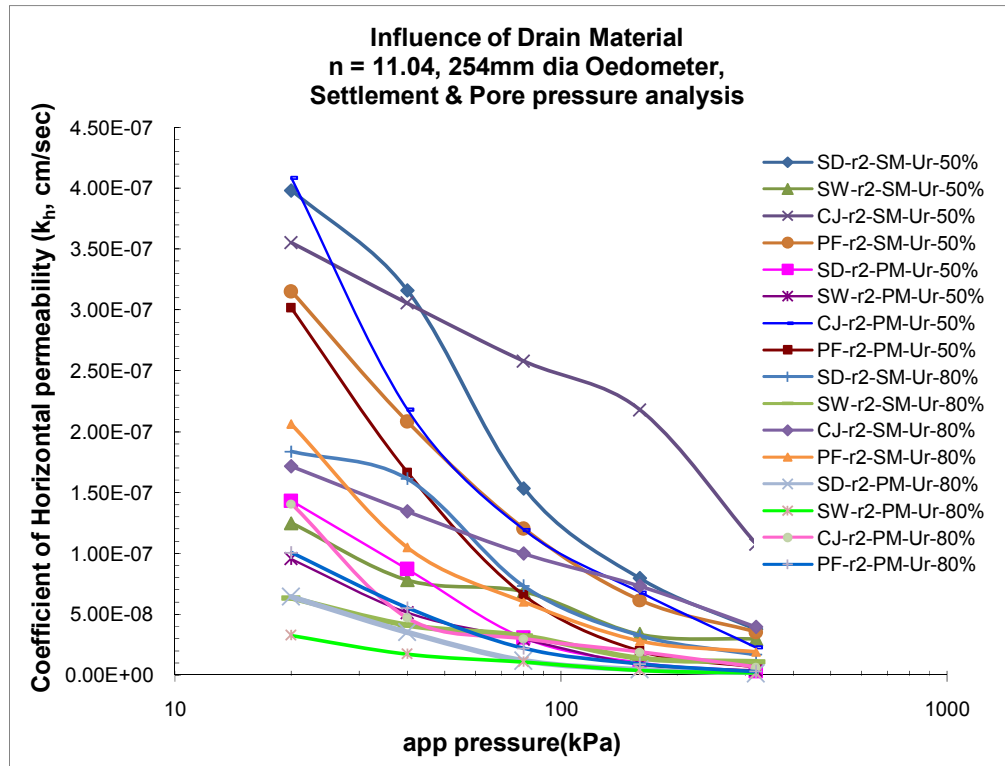


**Fig.6.79:** Comparison of Drain material w.r.t  $k_h$  against applied pressure for 50% & 80% Ur based on settlement and pore pressure analysis

## 6) Isochrones: Figures 6.80 to 6.94

**Pore Pressure analysis:** Fig.6.80 to Fig.6.94 shows the plots of isochrones with respect to time (fig.6.80 to 6.87) and comparison of isochrones with respect to Time factor,  $Tr$  (fig.6.88 to 6.94) for various drain material viz. SD, SW, CJ and PF. Comparing initial slope of isochrones for various drain material it interprets that CJ shows more rate of dissipation at any time (initial linear portion of graph) compare to SW, SD and PF. Also it is observed that PF shows better rate of dissipation at all three radial points  $r_1$ ,  $r_2$  and  $r_3$  at all applied pressures. Almost for all drain materials nature of isochrones were similar except SW. Comparing theoretical and experimental isochrones using proposed theory it interprets that experimental isochrones matches very well with theoretical isochrones for various time factors ( $Tr$ ). This is well observed for all drain materials viz. SD, SW, CJ and PF at all pressures. For initial low value of time factors the theoretical isochrones mostly super-imposes with

theoretical isochrones while some variation of about 8-14% is observed for higher values of time factors ( $T_r$  greater than 0.16). It is also observed that irrespective of pressure and drain material experimental isochrones exhibits real picture of consolidation phenomena under influence of that drain material as dissipation of pore water pressure and drainage path travel by water particle is very much dependant on drain material hydraulic properties and response behavior of drain material under saturated loading conditions.

For all drain material experimental time factor more than 0.24 exhibit concave shapes initially, while  $T_r$  less than 0.24 shows convex towards vertical axis. Comparing isochrones for various drain materials it indicates that CJ shows more magnitude of dissipation at same time factor for almost all pressures. Initial slope of SD and PF drain indicates that their initial capacity of dissipation of pore water is faster up to 15% consolidation but thereafter its rate retard consistently, while CJ though not showing fast rate of dissipation during initial stage of consolidation but its performance is consistent and shows more degree of consolidation at less time factor. Reverse is the behavior of SW for pore pressure dissipation either at low value of time factor at high value of time factor. Comparing groups of all the isochrones of various time factor of drain materials, SW curve are distinctly showing initial concave curve.

### **Discussion:**

The micro pore structures of the SW drain and other drains are quite distinct that is initial micro porosity of SW is less compare to other drains which reflects in isochrones characteristics. Other drains shows more or less same micro porosity that wise initial slope of isochrones is same to some extent, but with increase of time factor micro-porosity decreases in other drains while in CJ drain micro porosity remains almost same being the flexible nature of jute and coir fibers which helps in more dissipation of pore pressure indicating more percentage of consolidation.

## a) Experimental Isochrones with respect to time: Figures 6.80 to 6.87

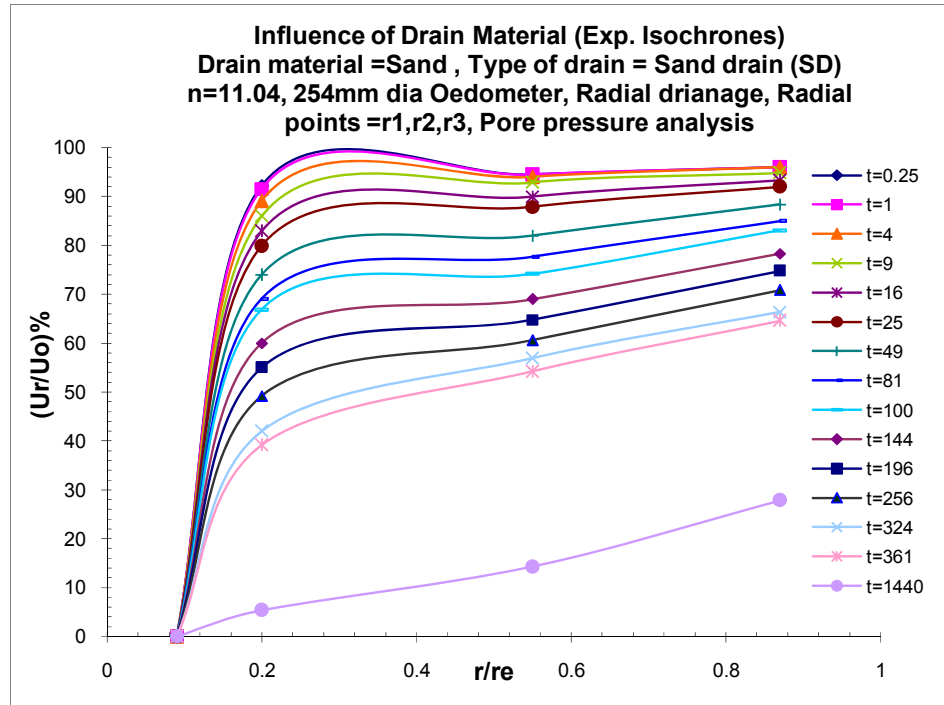


**Fig.6.80:** Dissipation of hydrostatic excess pore water pressure ( $U_r/U_o$ ) vs. ratio of radial distance ( $r/r_e$ ) with respect to time for SD at 40kPa

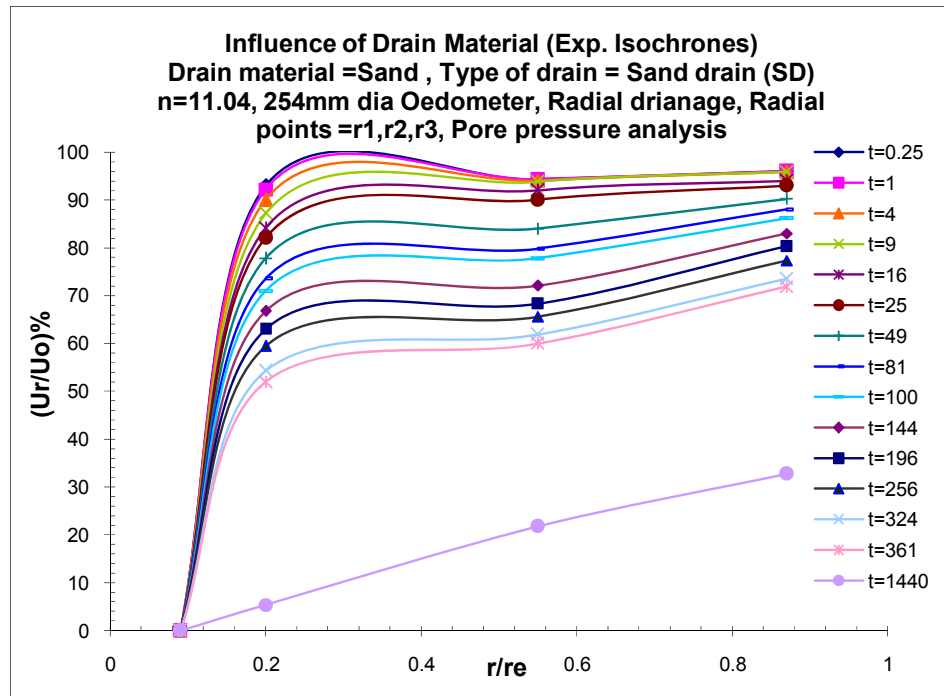


**Fig.6.81:** Dissipation of hydrostatic excess pore water pressure ( $U_r/U_o$ ) vs. ratio of radial distance ( $r/r_e$ ) with respect to time for SD at 160kPa

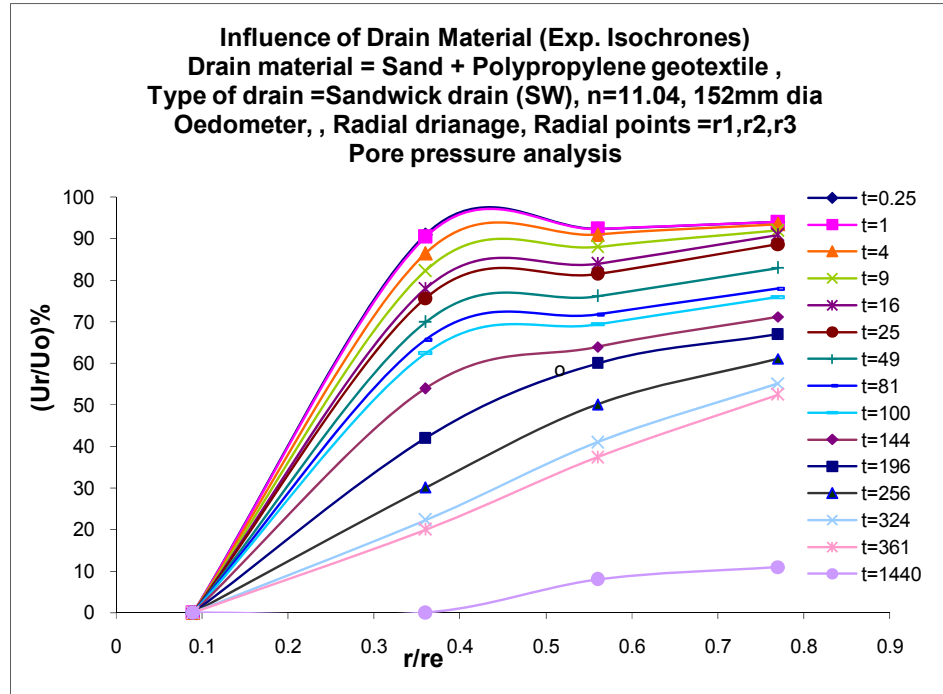


**Fig.6.82:** Dissipation of hydrostatic excess pore water pressure ( $U_r/U_o$ ) vs. ratio of radial distance ( $r/r_e$ ) with respect to time for SW at 40kPa

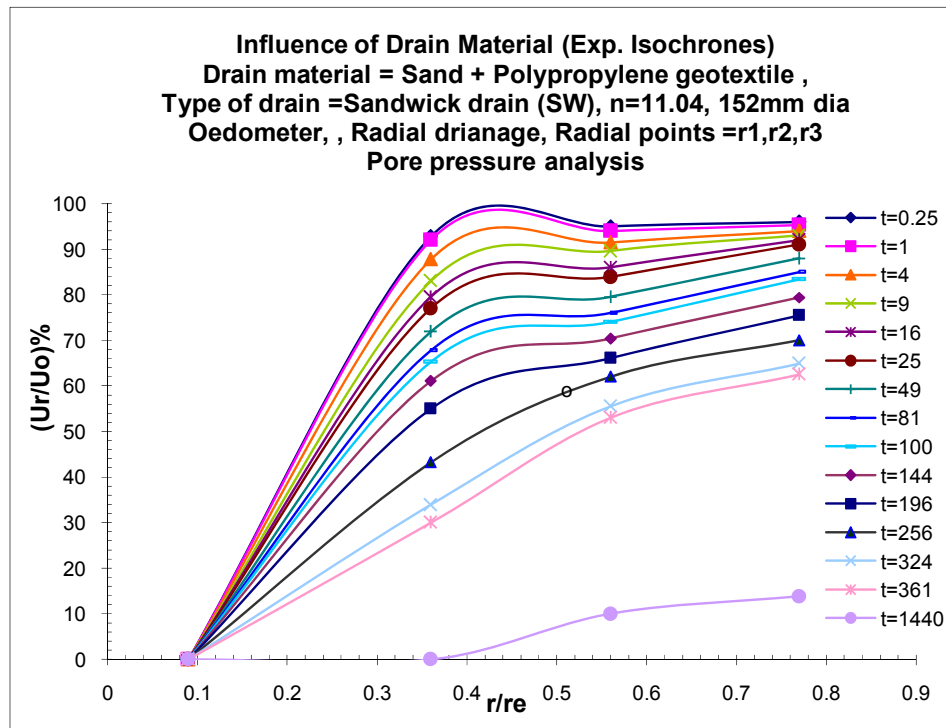


**Fig.6.83:** Dissipation of hydrostatic excess pore water pressure ( $U_r/U_o$ ) vs. ratio of radial distance ( $r/r_e$ ) with respect to time for SW at 160kPa

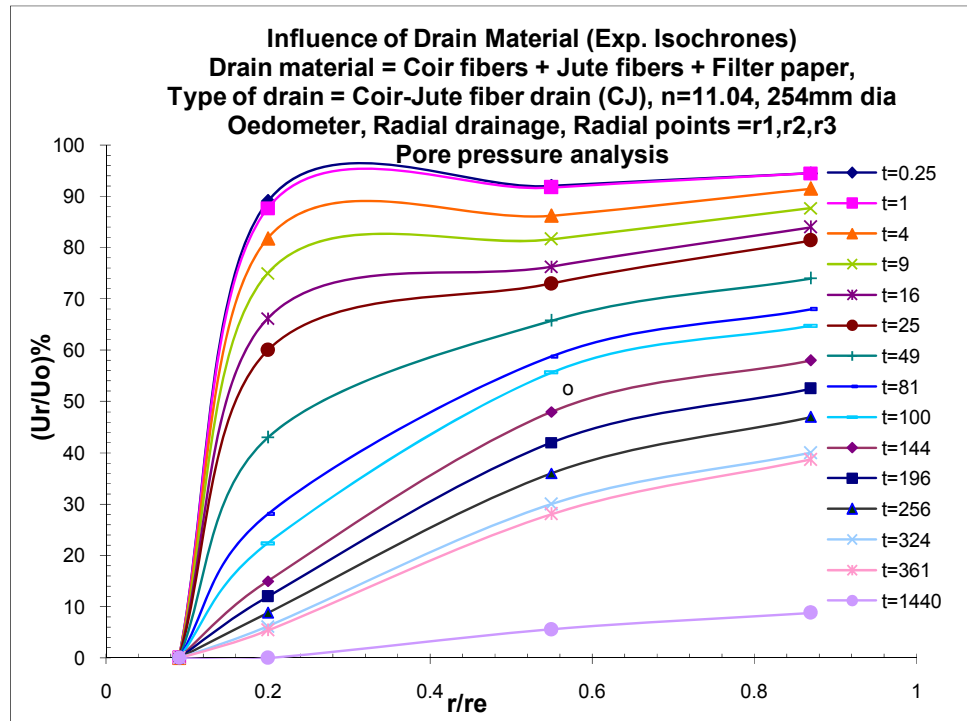


**Fig.6.84:** Dissipation of hydrostatic excess pore water pressure ( $U_r/U_o$ ) vs. ratio of radial distance ( $r/r_e$ ) with respect to time for CJ at 40kPa

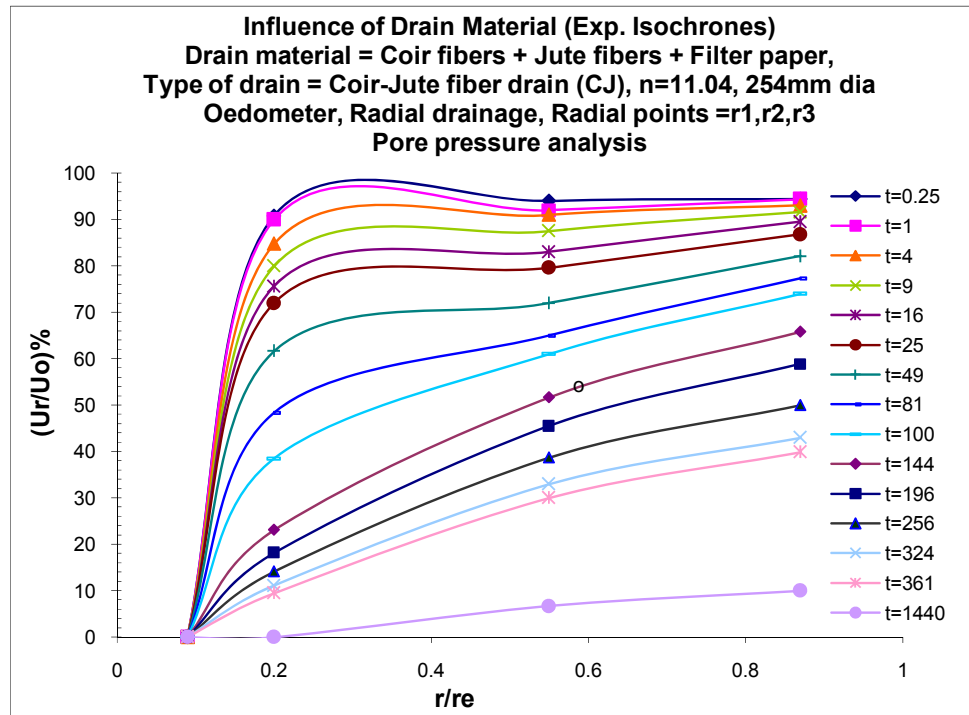


**Fig.6.85:** Dissipation of hydrostatic excess pore water pressure ( $U_r/U_o$ ) vs. ratio of radial distance ( $r/r_e$ ) with respect to time for CJ at 160kPa



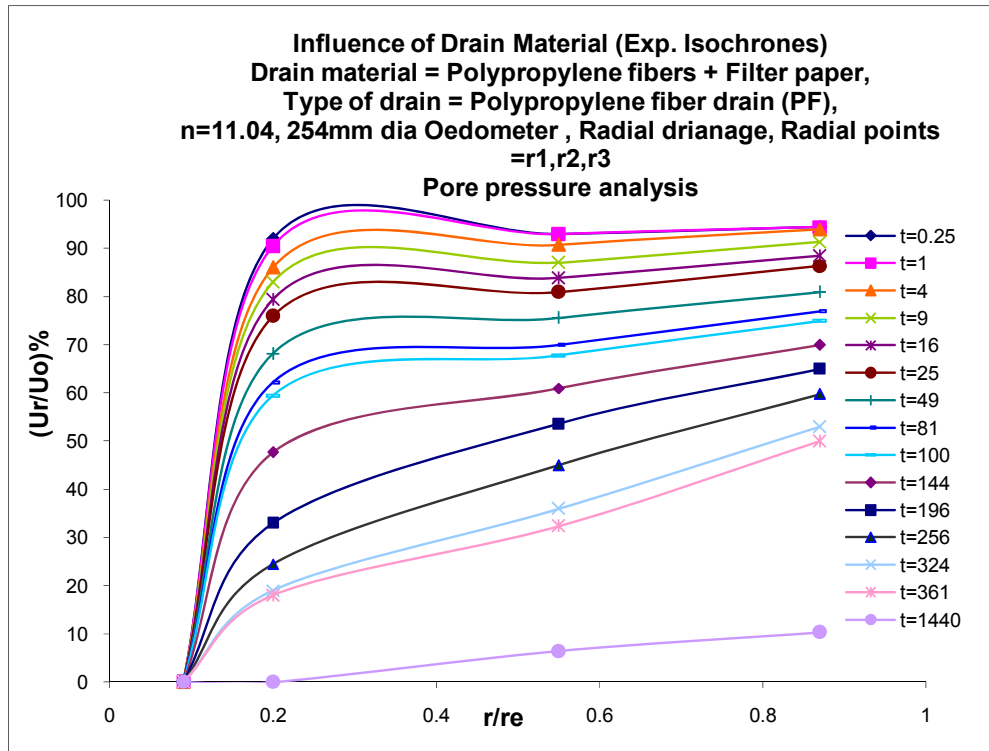


**Fig.6.86:** Dissipation of hydrostatic excess pore water pressure ( $U_r/U_o$ ) vs. ratio of radial distance ( $r/re$ ) with respect to time for PF at 40kPa

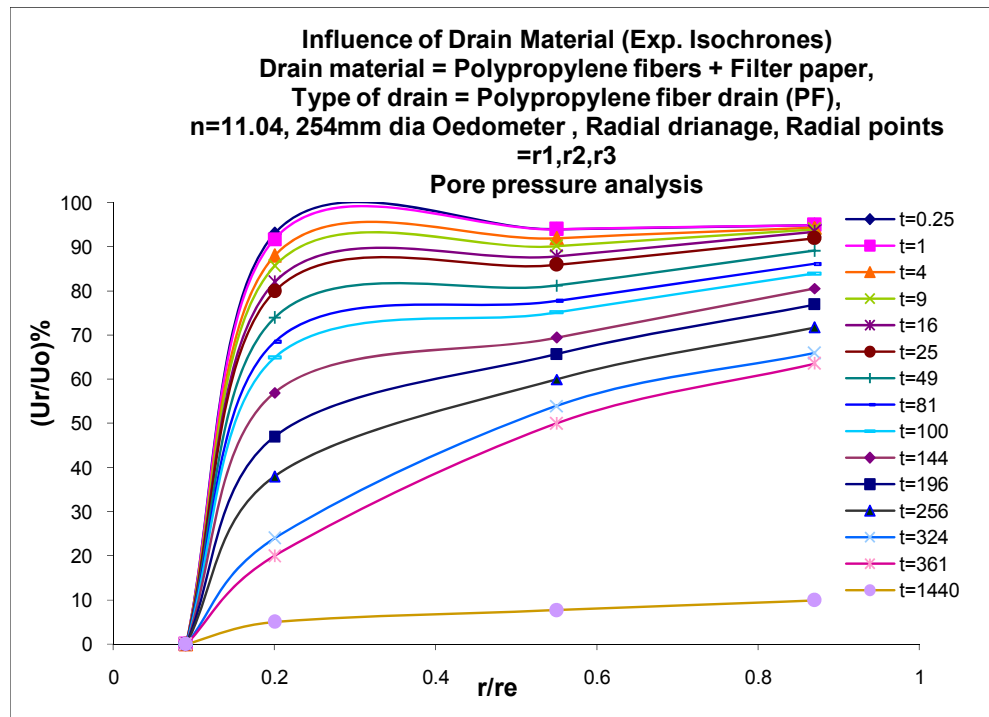


**Fig.6.87:** Dissipation of hydrostatic excess pore water pressure ( $U_r/U_o$ ) vs. ratio of radial distance ( $r/re$ ) with respect to time for PF at 160kPa

**b) Comparison of Theoretical and Experimental Isochrones with Time factor ( $T_r$ ): Figures 6.88 to 6.94**

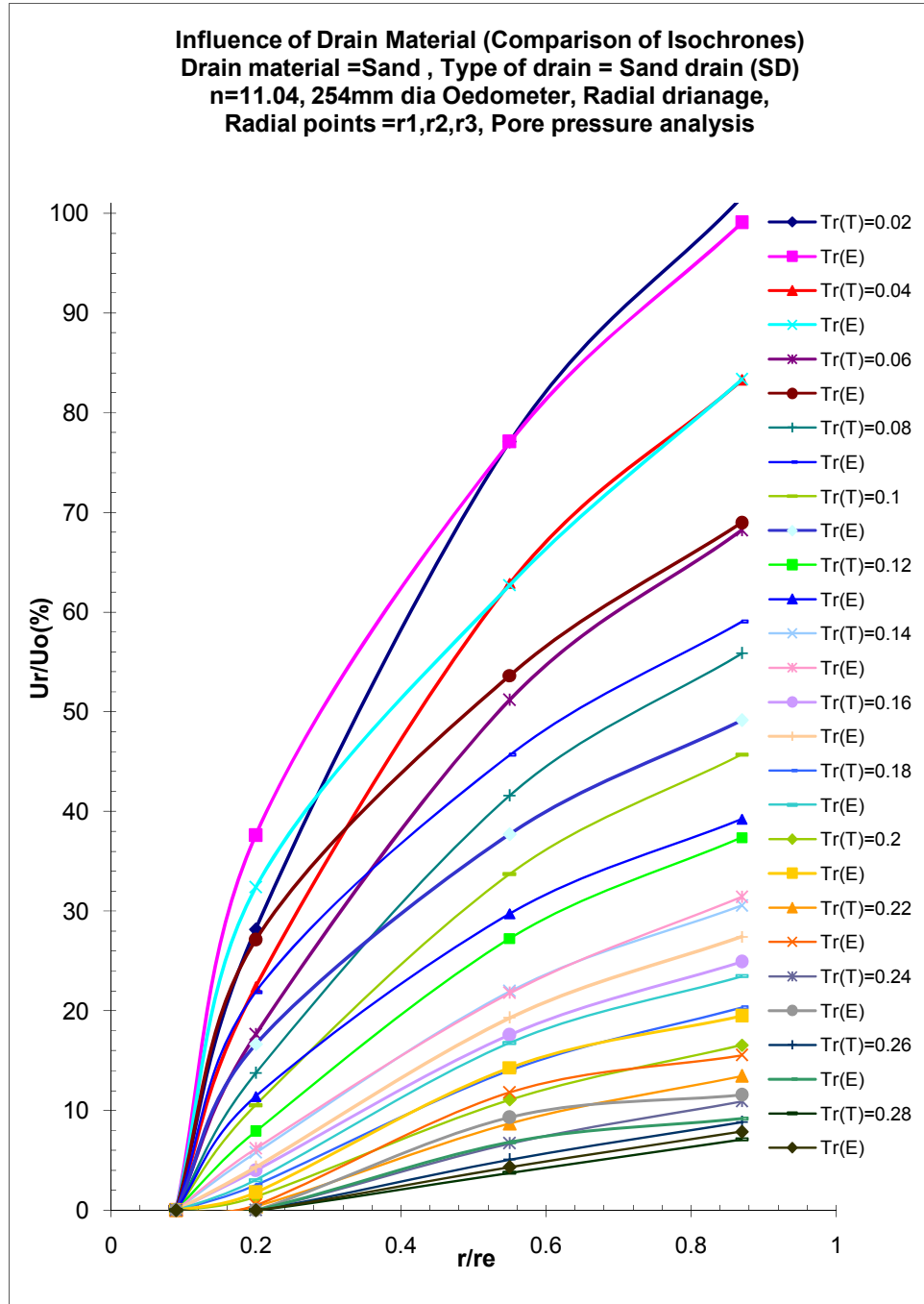


**Fig.6.88:** Comparison of theoretical isochrones and experimental isochrones with respect to time factor ( $T_r$ ) for SD at 160kPa pressure

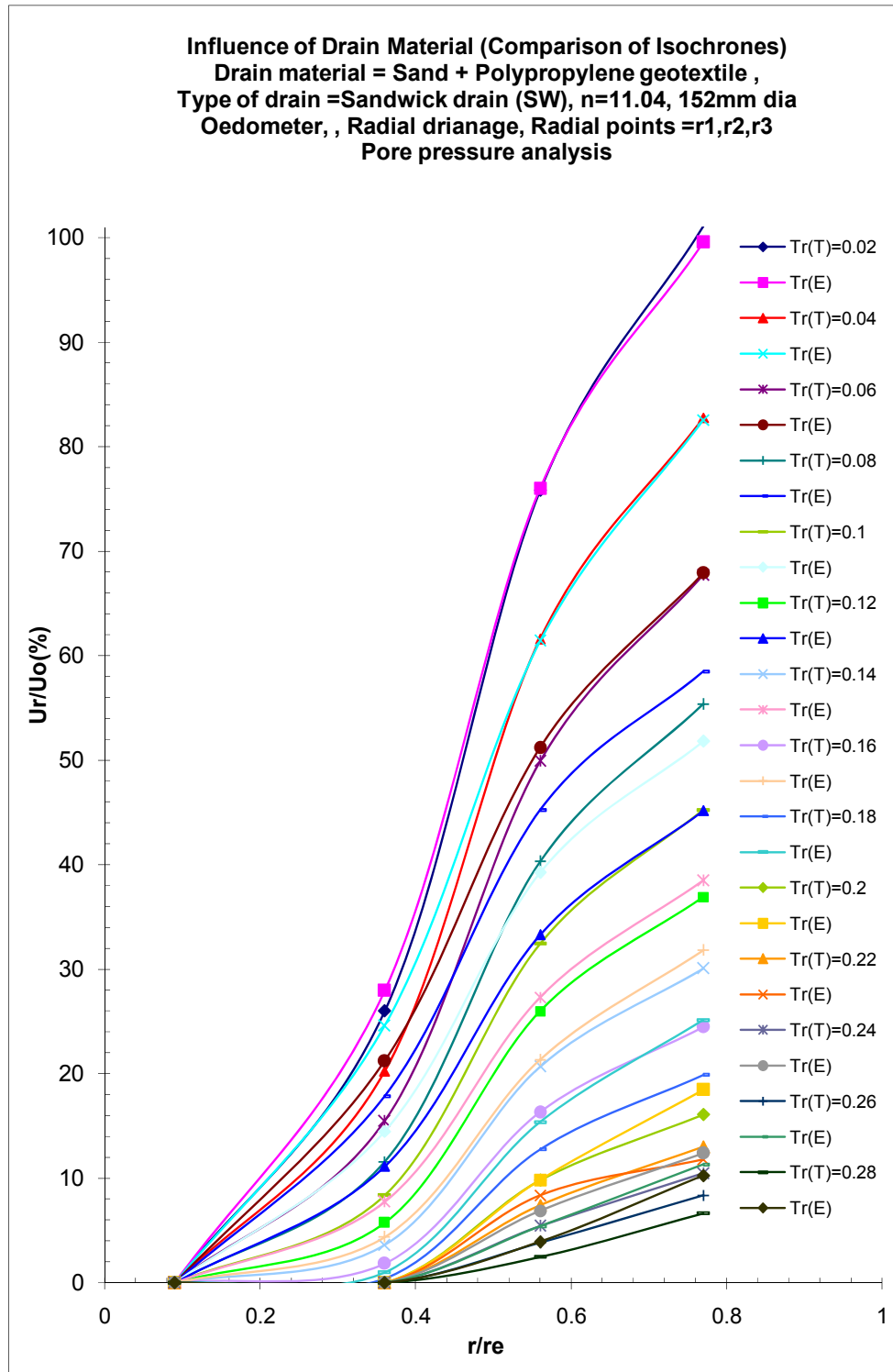


**Fig.6.89:** Comparison of theoretical isochrones and experimental isochrones with respect to time factor (Tr) for SW at 160kPa pressure

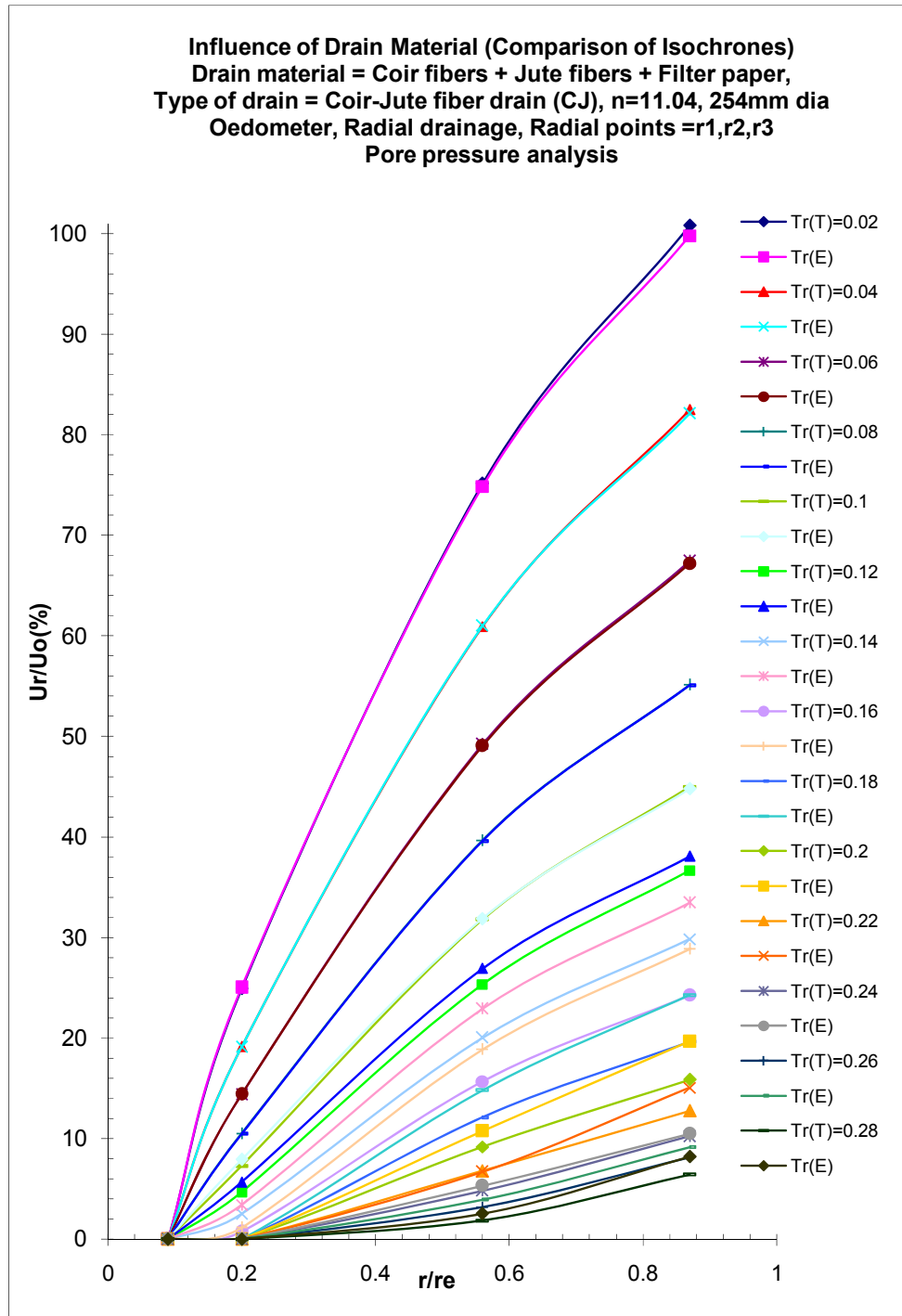


**Fig.6.90:** Comparison of theoretical isochrones and experimental isochrones with respect to time factor ( $Tr$ ) for CJ at 160kPa pressure

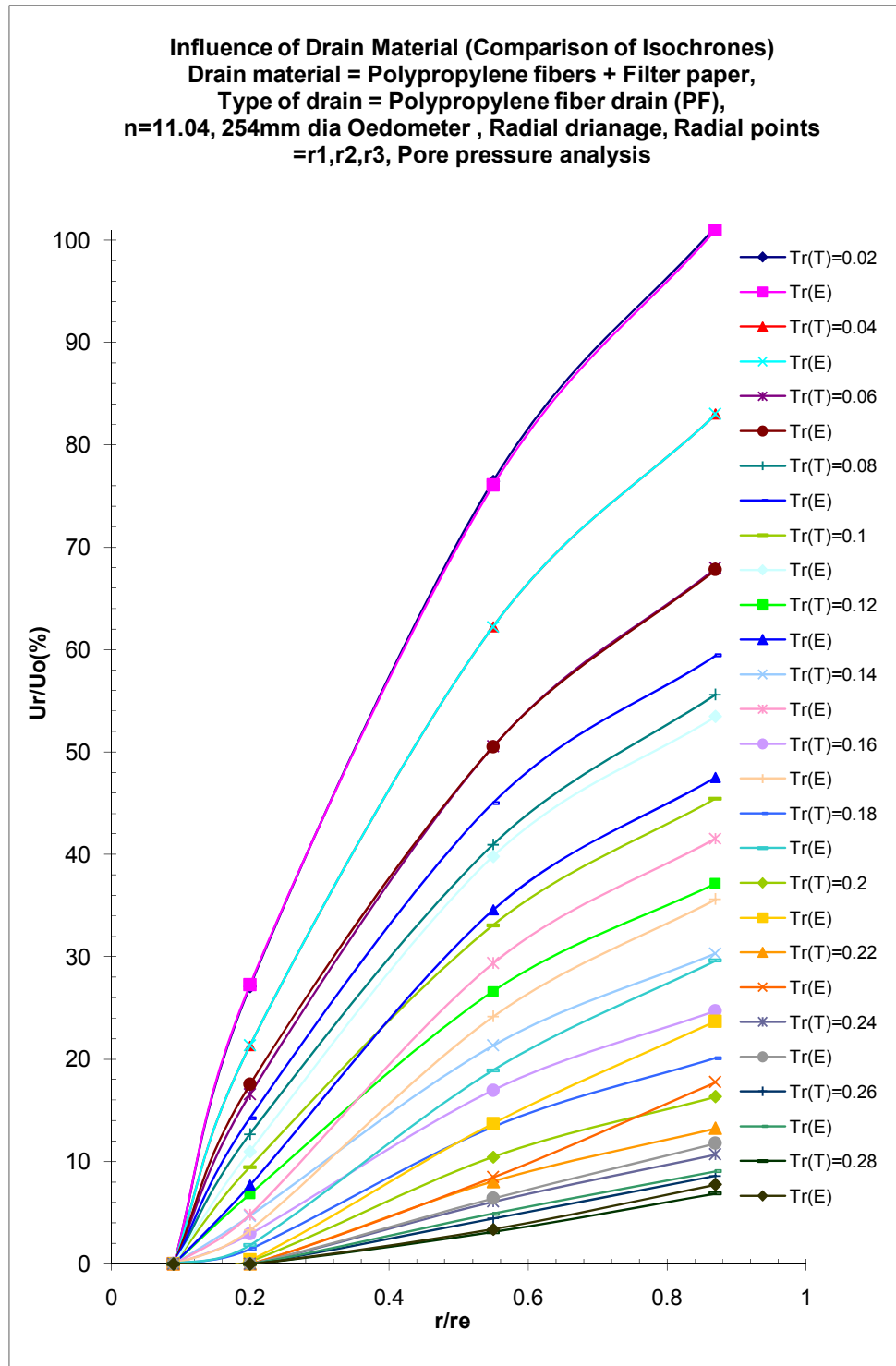


**Fig.6.91:** Comparison of theoretical isochrones and experimental isochrones with respect to time factor ( $Tr$ ) for PF at 160kPa pressure

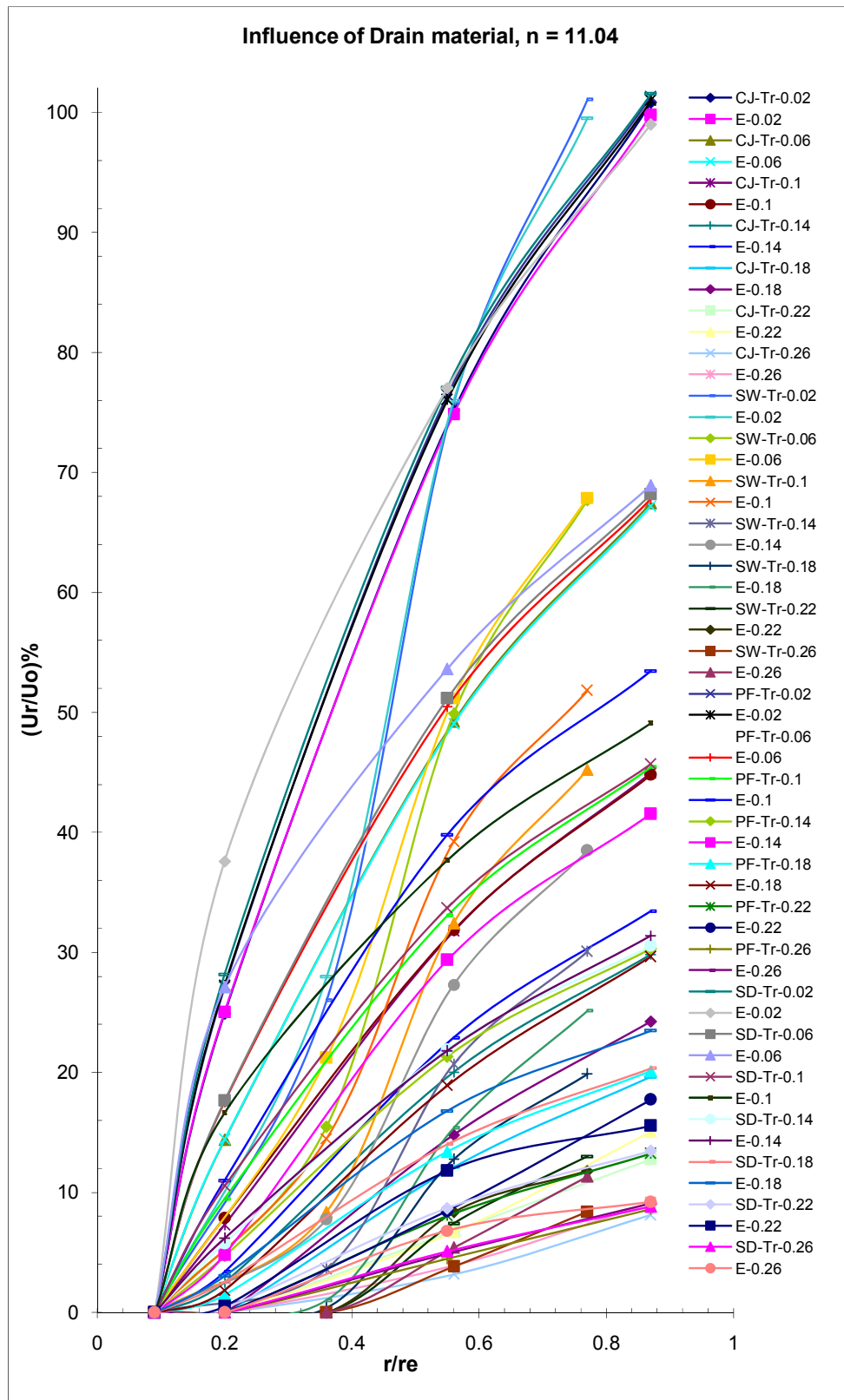


**Fig.6.92:** Comparison of Drain materials with respect to isochrones for time factors ( $Tr$ ) at 160kPa pressure

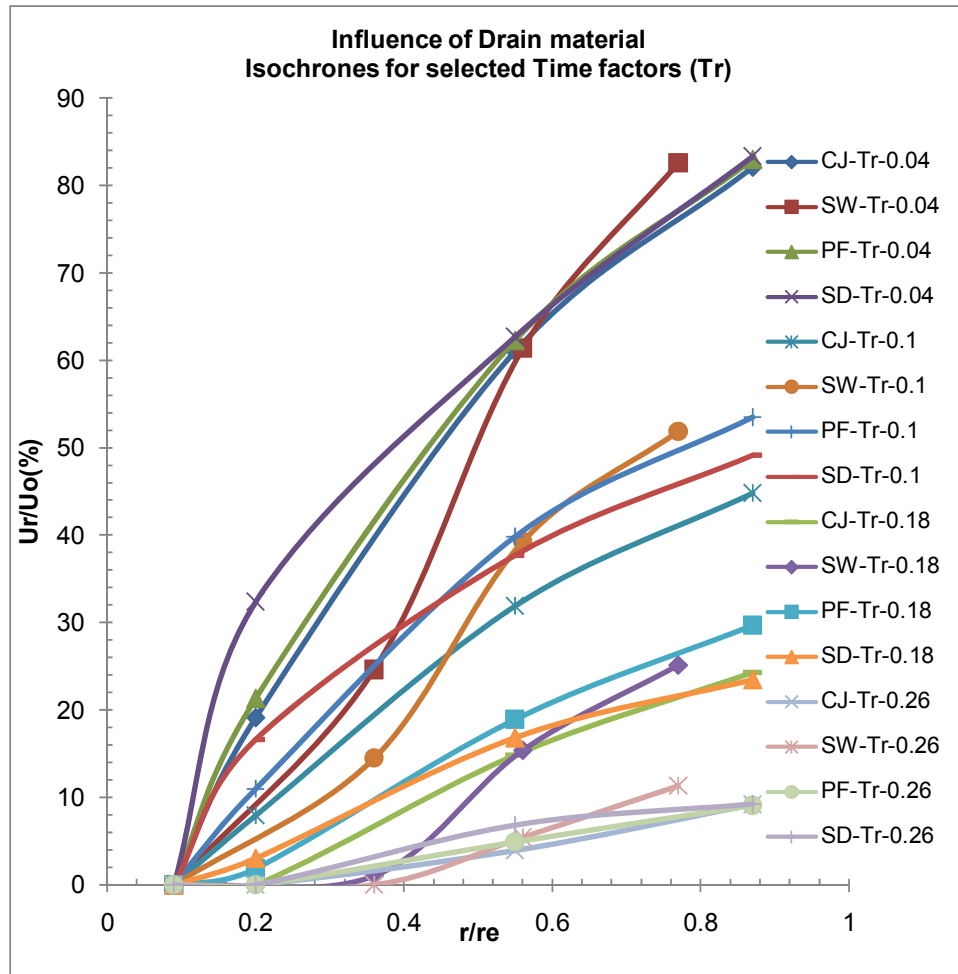
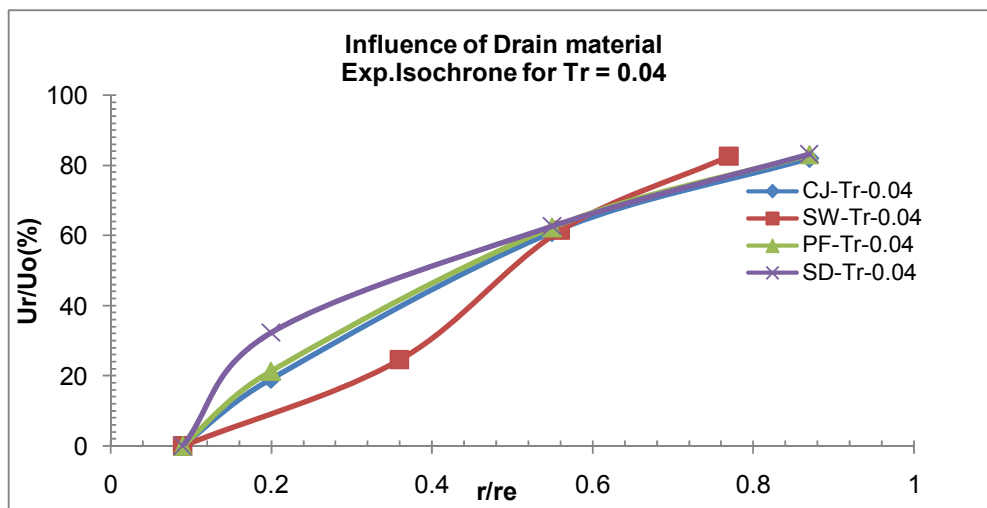


Fig.

**6.93:** Comparison of Drain materials with respect to isochrones for selected time factors ( $T_r$ ) at 160kPa pressure



**Fig.6.94:** Comparison of Drain materials with respect to experimental isochrones for  $T_r = 0.04$  time at 160kPa pressure

## 7) Degree of consolidation ( $U_r$ ) vs. Time factor ( $T_r$ ): Figures 6.95 to 6.115

**a) Settlement analysis:-** Fig.6.95 to Fig.6.104 shows the comparative plots of various drain materials for degree of consolidation ( $U_r$ ) versus time factor ( $T_r$ ) for 'n' value 11.04. For comparison between theoretical ( $T_r(T)$ ) and experimental ( $T_r(E)$ ) values two applied pressure of 40kPa and 160kPa are selected. The lumped parameter ' $\lambda$ ' is appropriately fitted for each drain with respect to time factors so as to study the influence of distinctive material on vertical drain performance. Here it is determined that for CJ, PF, SW and SD the lumped parameter ' $\lambda$ ' is equal to -0.2, -0.175, -0.15 and -0.125 fits respectively. It is observed that ' $\lambda$ ' value of -0.2 is having maximum efficiency and as ' $\lambda$ ' value decreases efficiency of drain material decreases. It is also observed that the value of lump parameter ' $\lambda$ ' remains nearly same under pressure variations, and this is true for all drain materials, even though some variation is observed in case of light loading and constructional loading in case of CJ and SD the overall nature of plot is not changing. The reason of getting appropriate lump parameter for particular drain material is because that all values of lump parameter (positive or negative) are checked and matched with experimental results and the lump parameter which gives less error and best super-imposition with theoretical curve is selected. It is observed from the above graphs that experimental results almost matches with theoretical results and this is true for all drain materials and for all applied pressures. Table shows the value of lumped parameter ' $\lambda$ ' fitted to each drain material.

**Table:** Lump parameter ' $\lambda$ ' against various Drain materials based on Settlement analysis

| Sr.No. | Drain Material  | Drain Type | 'n' value | Lumped Parameter ' $\lambda$ ' |
|--------|---|------------|-----------|--------------------------------|
| 1.     | Sand  | SD         | 11.04     | $\lambda = -0.125$             |
| 2.     | Prepacked sandwich with polypropylene with sand as filler | SW         | 11.04     | $\lambda = -0.15$              |
| 3.     | Coir-Jute fibers wrapped by filter paper                  | CJ         | 11.04     | $\lambda = -0.2$               |
| 4.     | White Polypropylene fibers wrapped by filter paper        | PF         | 11.04     | $\lambda = -0.175$             |



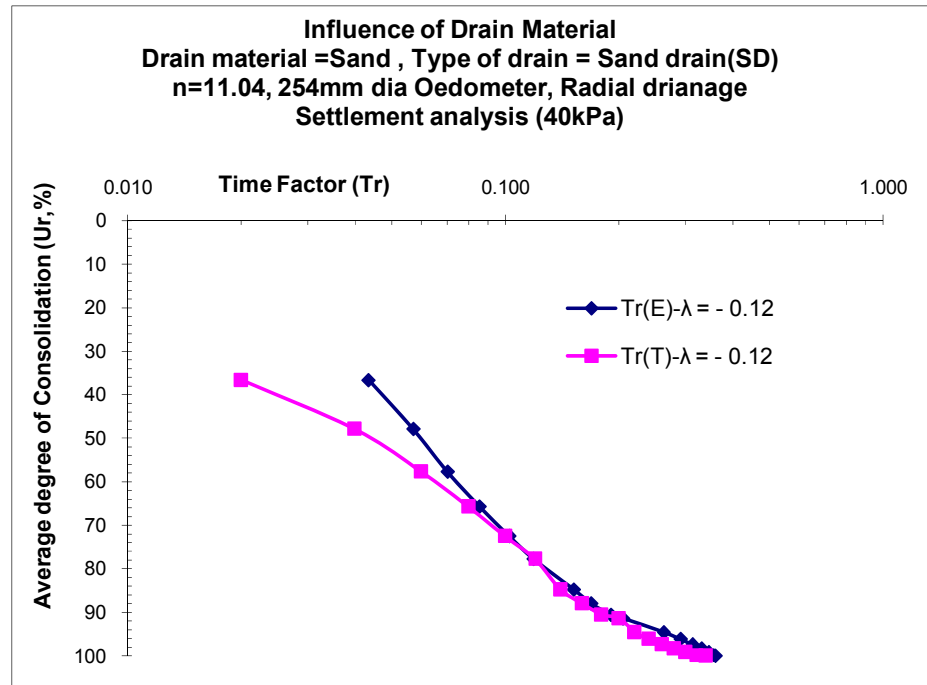


**Fig.6.95:** Comparison of average degree of consolidation ( $U_r$ ) against theoretical and experimental Time factor ( $Tr$ ) for SD at 40kPa

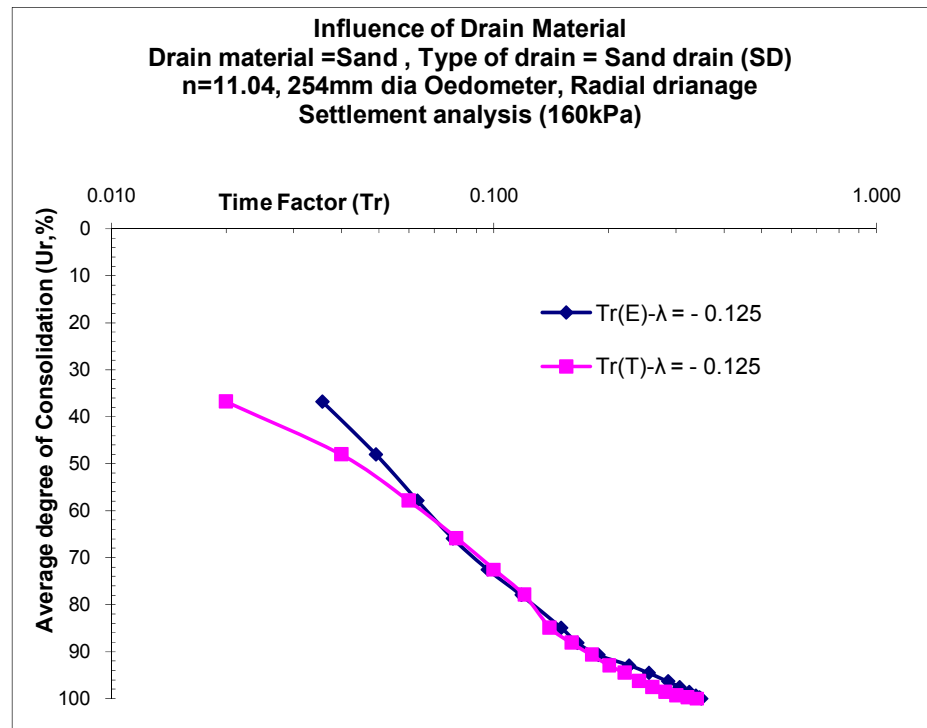


**Fig.6.96:** Comparison of average degree of consolidation ( $U_r$ ) against theoretical and experimental Time factor ( $Tr$ ) for SD at 160kPa

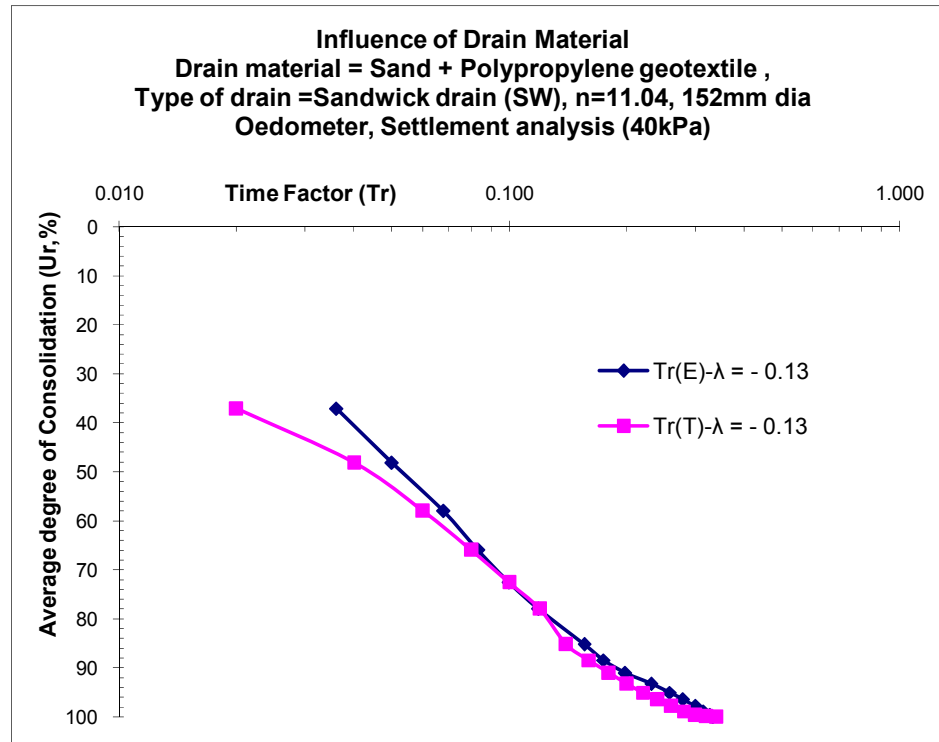


**Fig.6.97:** Comparison of average degree of consolidation ( $U_r$ ) against theoretical and experimental Time factor ( $Tr$ ) for SW at 40kPa

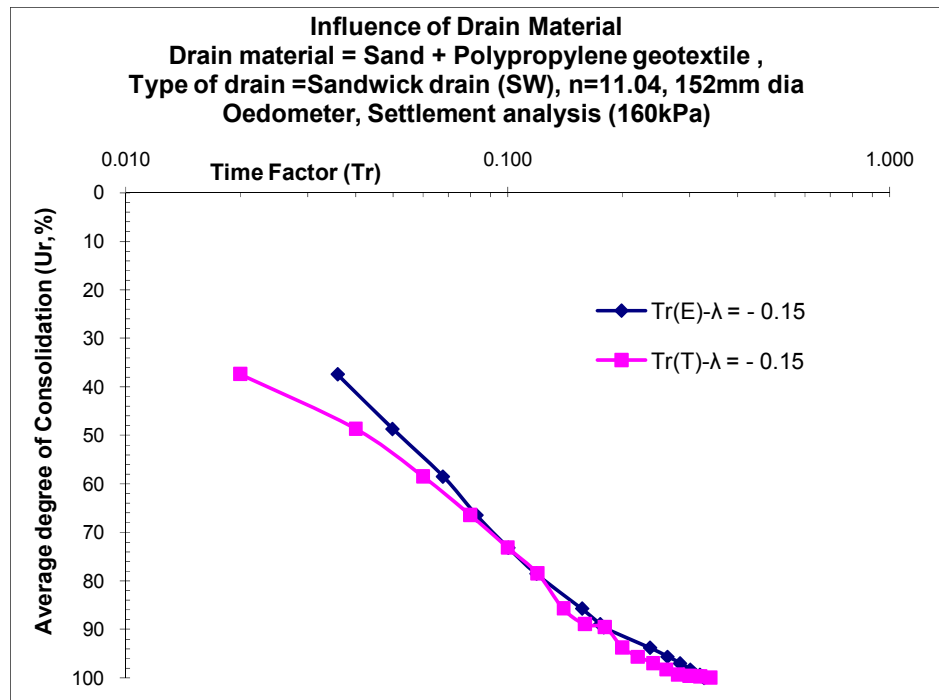


**Fig.6.98:** Comparison of average degree of consolidation ( $U_r$ ) against theoretical and experimental Time factor ( $Tr$ ) for SW at 160kPa

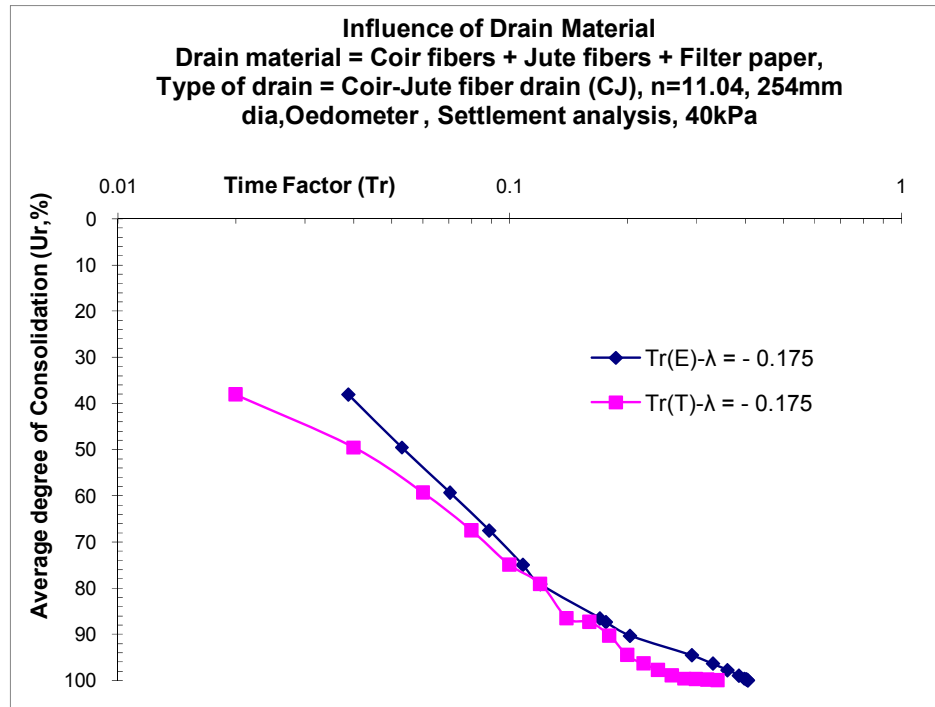


**Fig.6.99:** Comparison of average degree of consolidation ( $U_r$ ) against theoretical and experimental Time factor ( $Tr$ ) for CJ at 40kPa

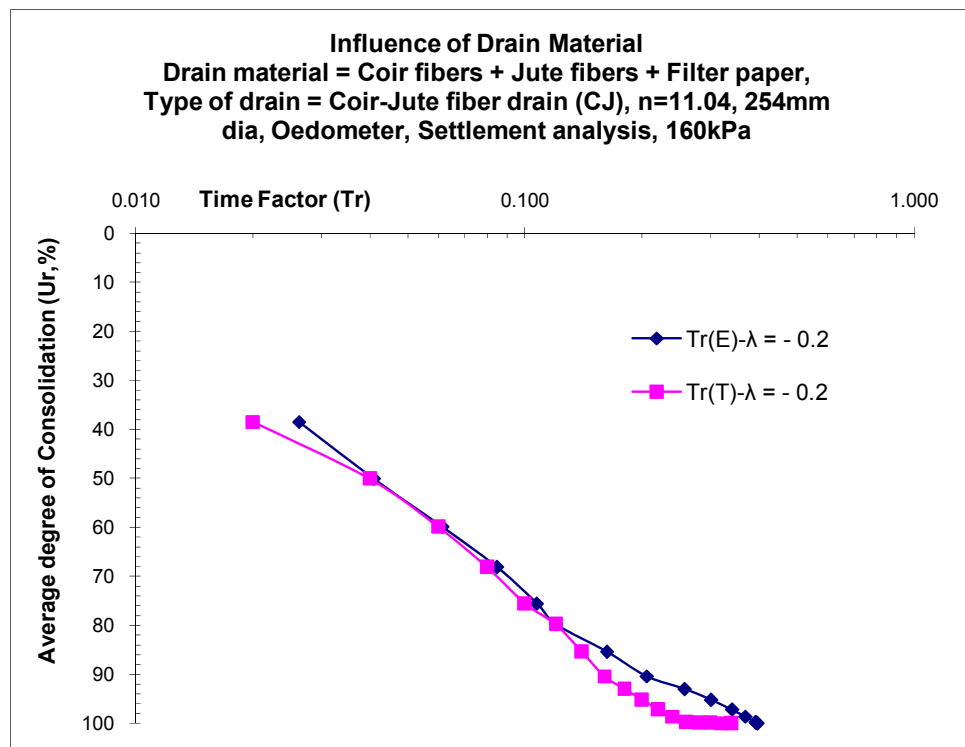


**Fig.6.100:** Comparison of average degree of consolidation ( $U_r$ ) against theoretical and experimental Time factor ( $Tr$ ) for CJ at 160kPa

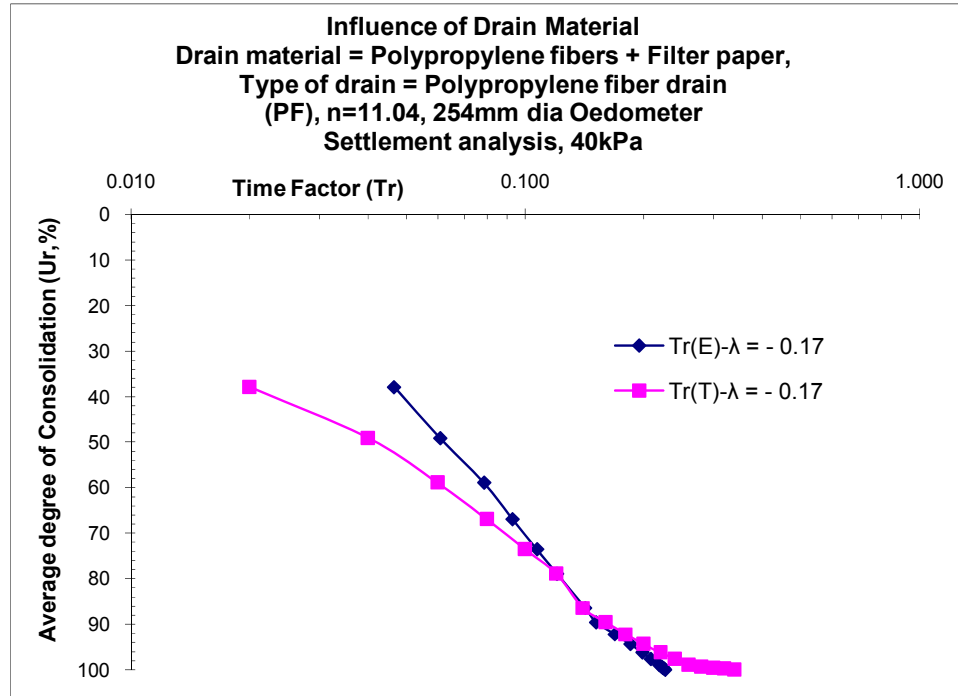


**Fig.6.101:** Comparison of average degree of consolidation ( $U_r$ ) against theoretical and experimental Time factor ( $Tr$ ) for PF at 40kPa

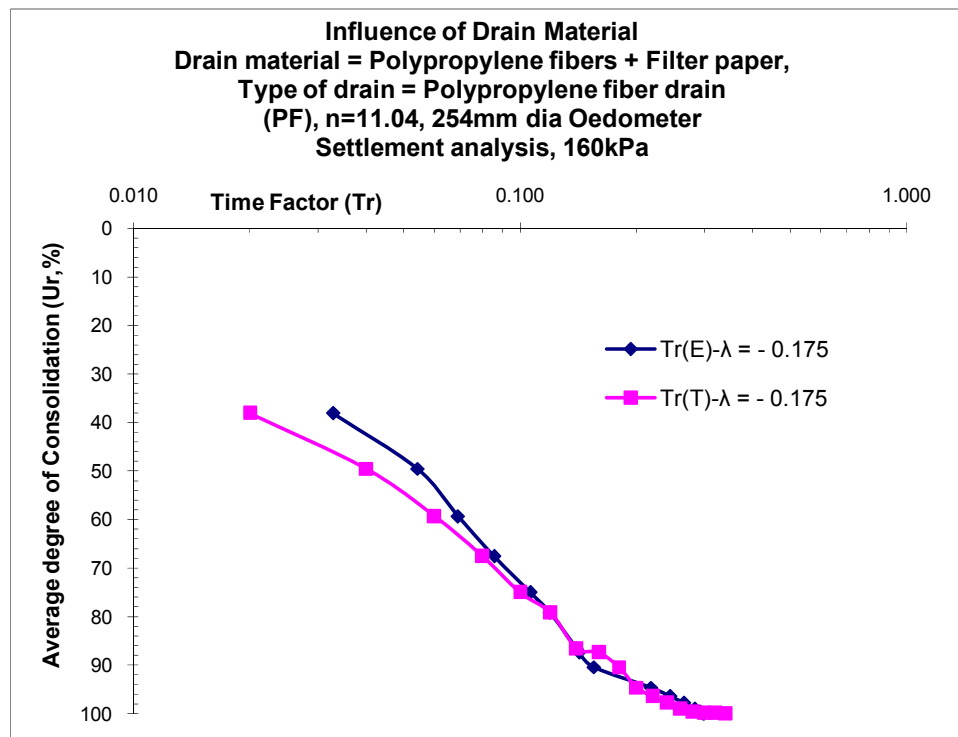


**Fig.6.102:** Comparison of average degree of consolidation ( $U_r$ ) against theoretical and experimental Time factor ( $Tr$ ) for PF at 160kPa

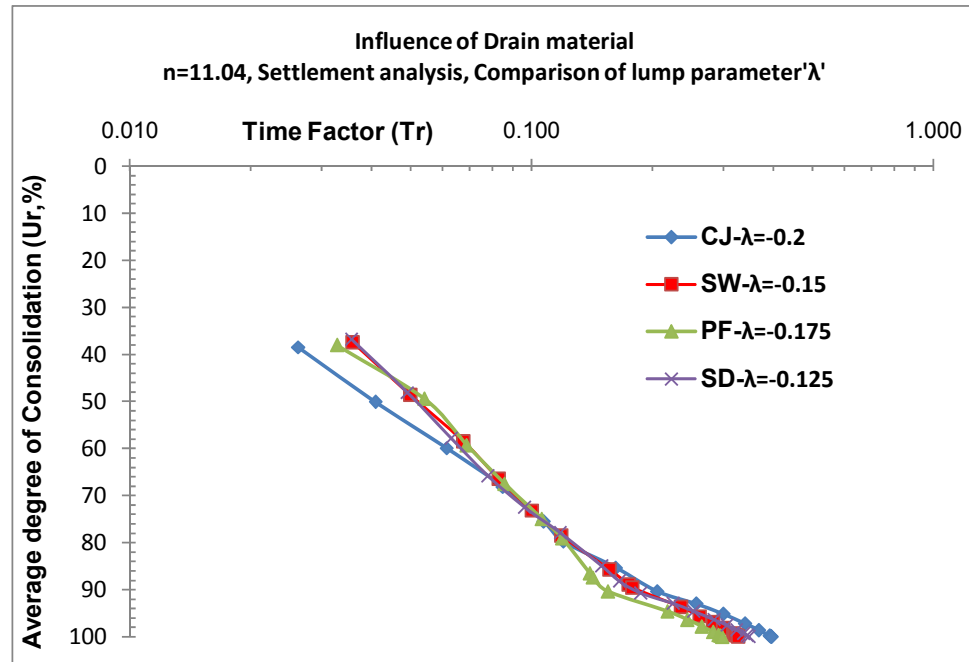


**Fig.6.103:** Comparison of average degree of consolidation ( $U_r$ ) against experimental Time factor ( $T_r$ ) for various Drain materials with lump parameter ' $\lambda$ '

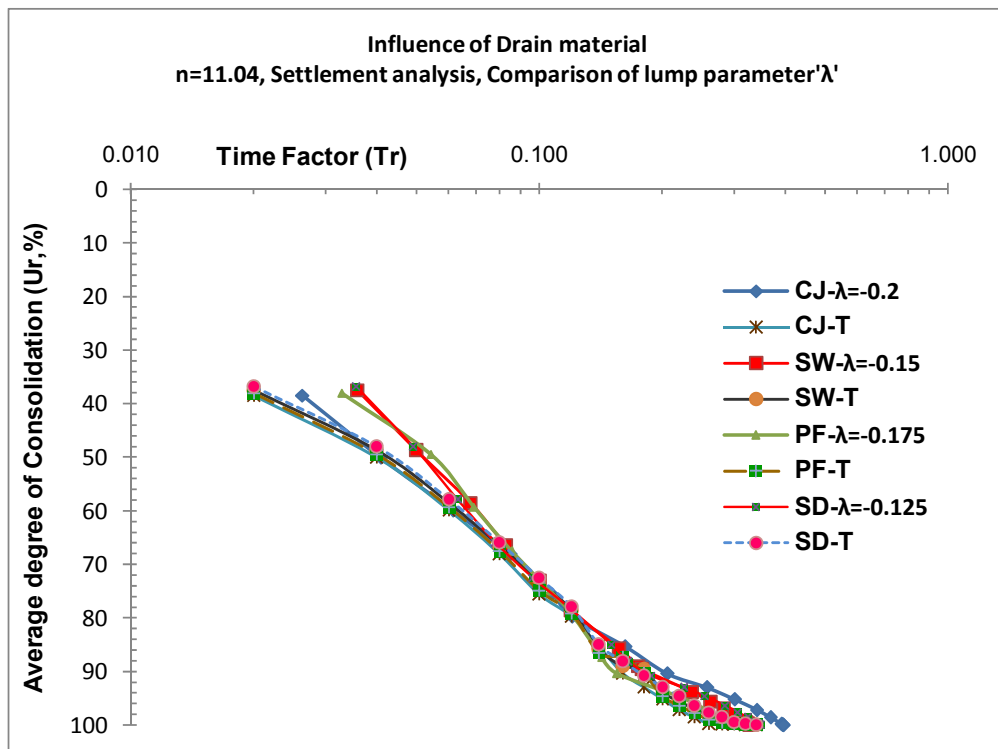


**Fig.6.104:** Comparison of average degree of consolidation ( $U_r$ ) against theoretical and experimental Time factors ( $T_r$ ) for various Drain materials with lump parameter ' $\lambda$ '

**b) Pore pressure analysis:-** Fig.6.105 to Fig.6.114 shows the comparative plots of various drain materials for degree of consolidation ( $U_r$ ) versus time factor ( $T_r$ ) for 'n' value 11.04. For comparison between theoretical and experimental values two applied pressure of 40kPa and 160kPa are selected. The lumped parameter ' $\lambda$ ' is appropriately fitted for each drain material with respect to time factors so as to study the influence of distinctive material on vertical drain performance. Here it is determined that for CJ, PF, SW and SD the lumped parameter ' $\lambda$ ' is equal to -0.175, -0.125, -0.15 and -0.1 fits respectively. It is observed that ' $\lambda$ ' value of -0.175 is having maximum efficiency and as ' $\lambda$ ' value decreases efficiency of drain material decreases. It is observed from the above graphs that experimental results almost matches with theoretical results and this is true for all drain materials and for all applied pressures. Table shows the value of lumped parameter ' $\lambda$ ' fitted to each drain material. It is observed that degree of consolidation determined from pore pressure readings suggest that SW is more efficient in compare to PF while settlement readings suggest that PF is more efficient in compare to SW.

**Discussion:** (refer fig. 6.115)

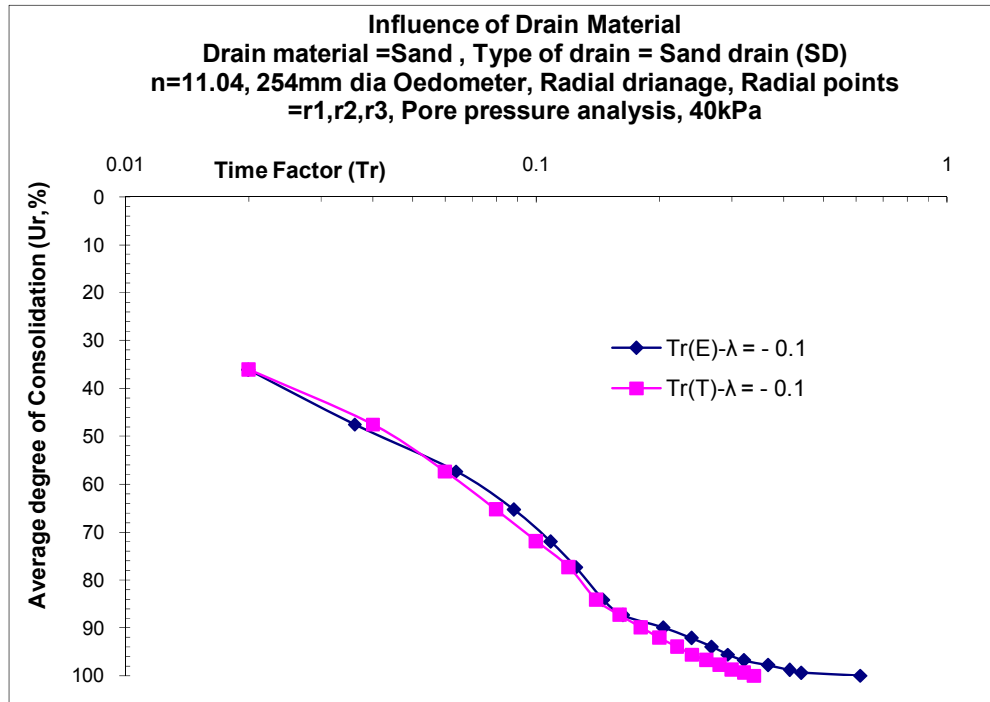
- The discussion for above pattern of curves are reasoned on the basis of scanning micrographs that is micro-porosity, degree of orientation of particle, tortuosity; physico-chemical changes in the clay water system during initial and final stages of consolidation for a particular load and structural changes in the soil structure with increase of load with respect to various types of drain material.
- Void ratio-effective pressure relationship: Void ratio-pressure relationship can be of initial flocculated structure or random type of structure. The magnitude of the bonding force defining the flocculated state will control the curvature middle region. This critical region is not well defined for the random structure clay, since the bonding forces are smaller than the flocculated structure. Our is the intermediate stage of flocculated and random soil structure. The critical region is defined to some extent exhibiting some bonding forces are prevalent edge to face bonds which is illustrated in micrograph (photos. 6.3 to 6.9) the resistance during 'microcompressibility' occurring under lighter load

is clearly reflected in the critical zone. Viewed microscopically, particles in a randomly oriented particles sample are rotated into more parallel orientation and then pushed closed together. These two actions probably occur simultaneously. Pushing particles closer together involves action against interparticle forces of repulsion, but particle rotation must also be considered as an integral part of compression. After critical region of curve, the fall down of curve indicates structural breakdown that occurs under consolidation pressure sufficient large to disrupt the bonds formed in the soil structure as shown in figure 6.64, 6.65 and 6.66. The abrupt change in slope beyond preconsolidation pressure in the latter zone of curve might be viewed as the collapse of matrix. Degree of structural collapse has been evaluated in the present investigation by means of measuring the angle between particle orientation and microporosity of the sample at the final load as shown in figure 6.64, 6.65 and 6.66 supported by photos (micrograph) 6.3 to 6.9. Tortuosity with respect to actual flow path and thickness of sample works out to tend towards unity from analysis of micrographs indicating soil particles more oriented having face to face configuration.

- Tortuosity is a real measure of actual flow path towards radial direction towards central drain during consolidation process. Tortuosity tends to unity in case of CJ drain compare to SD as mentioned earlier. Soil structure because of the gradient of flow in horizontal direction and vertical load help causes more quantum of face-to-face contact in the former case. For the same drain the depth wise tortuosity also indicates the effect of overburden to some extent. In case of coir-jute drain the tortuosity at interface and at mid radial point are almost same indicating uniform surface settlement unlike sand drain.

**Table:** Lump parameter ' $\lambda$ ' against various Drain materials based on Pore pressure analysis

| Sr.No. | Drain Material  | Drain Type | 'n' value | Lumped Parameter ' $\lambda$ ' |
|--------|---|------------|-----------|--------------------------------|
| 1.     | Sand  | SD         | 11.04     | $\lambda = -0.1$               |
| 2.     | Prepacked sandwich with polypropylene with sand as filler | SW         | 11.04     | $\lambda = -0.15$              |
| 3.     | Coir-Jute fibers wrapped by filter paper                  | CJ         | 11.04     | $\lambda = -0.175$             |
| 4.     | White Polypropylene fibers wrapped by filter paper        | PF         | 11.04     | $\lambda = -0.125$             |

**Fig.6.105:** Comparison of average degree of consolidation ( $U_r$ ) against theoretical and experimental Time factor ( $Tr$ ) for SD at 40kPa



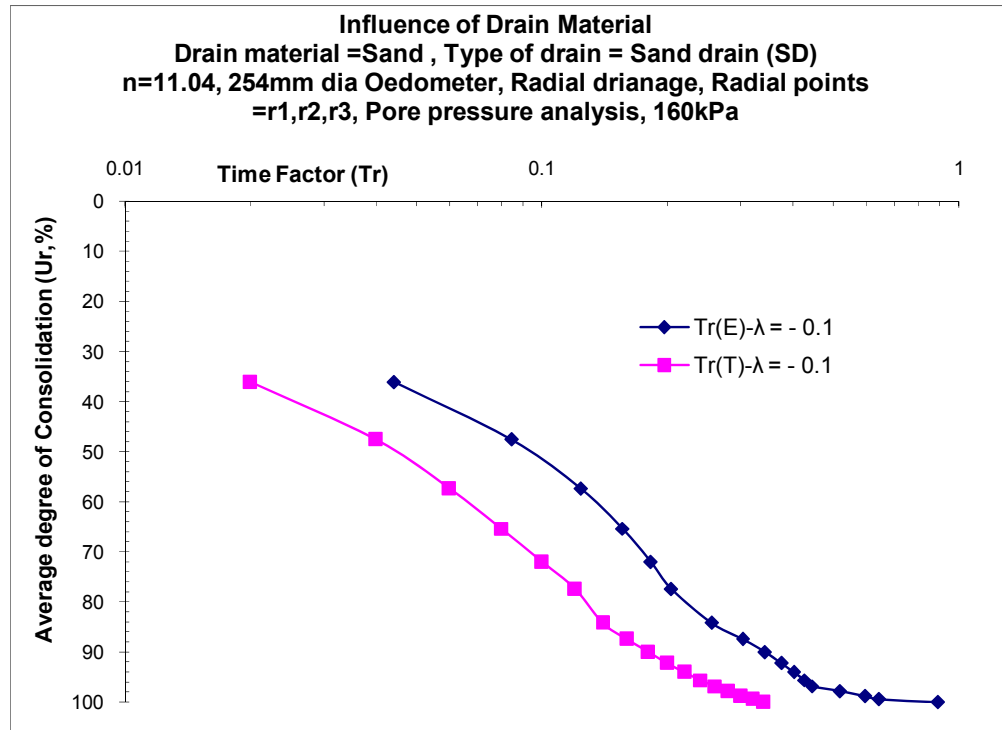


**Fig.6.106:** Comparison of average degree of consolidation ( $U_r$ ) against theoretical and experimental Time factor ( $Tr$ ) for SD at 160kPa

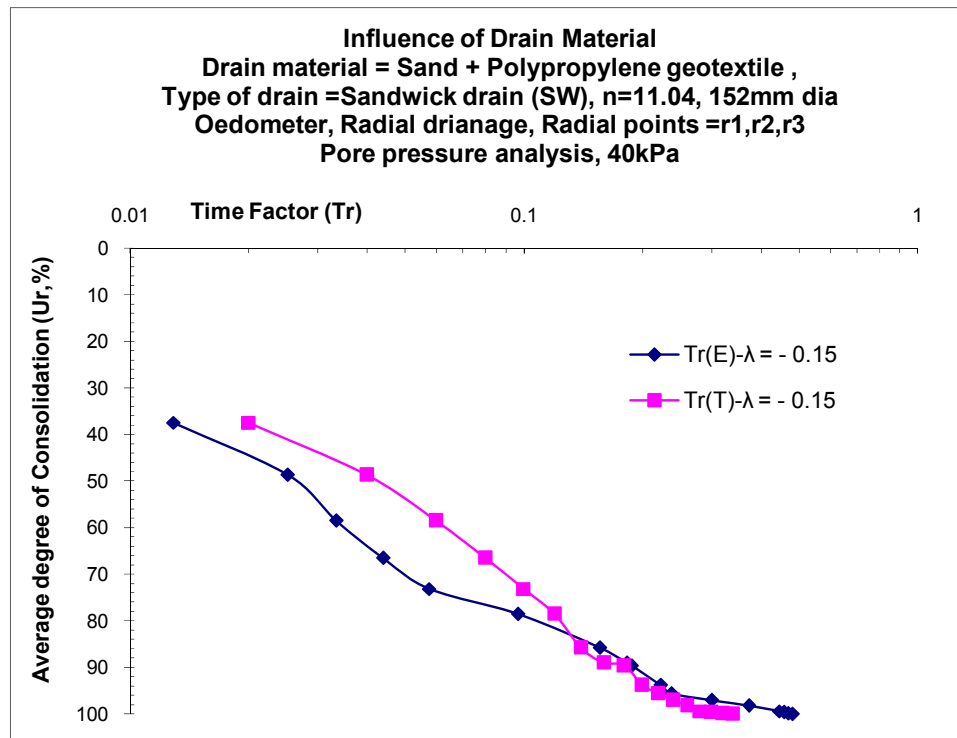


**Fig.6.107:** Comparison of average degree of consolidation ( $U_r$ ) against theoretical and experimental Time factor ( $Tr$ ) for SW at 40kPa

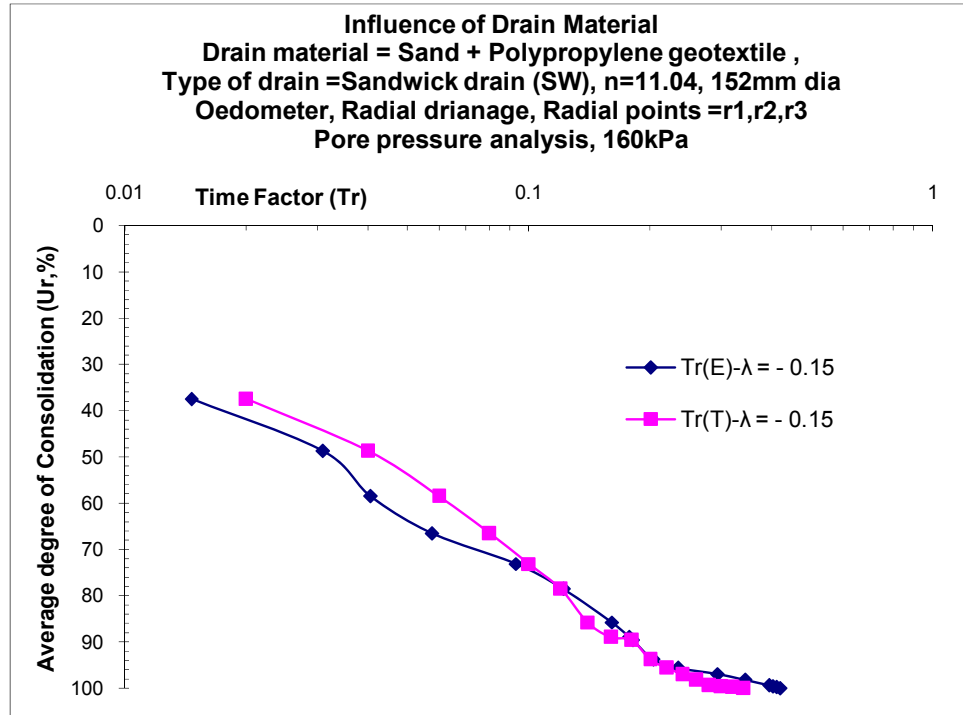


**Fig.6.108:** Comparison of average degree of consolidation ( $U_r$ ) against theoretical and experimental Time factor ( $Tr$ ) for SW at 160kPa

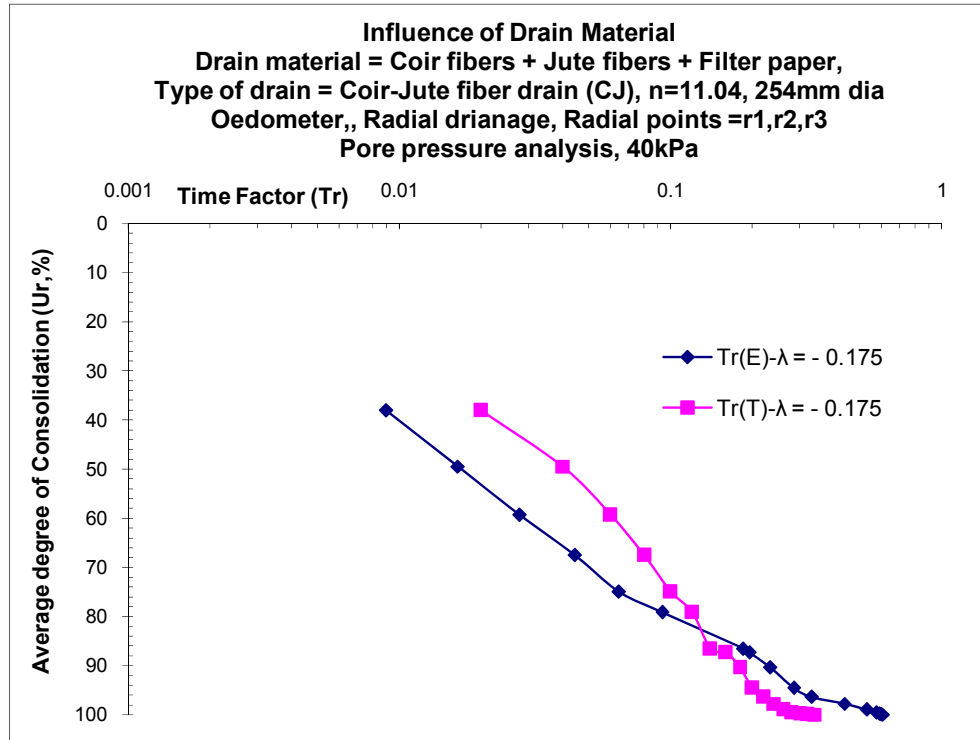


**Fig.6.109:** Comparison of average degree of consolidation ( $U_r$ ) against theoretical and experimental Time factor ( $Tr$ ) for CJ at 40kPa

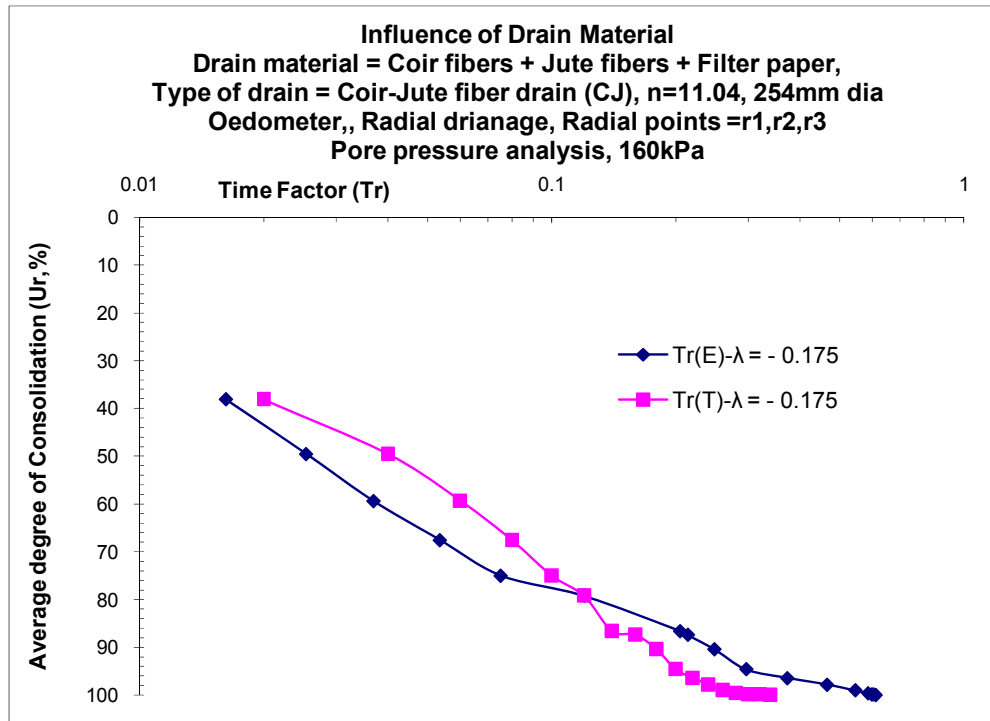


**Fig.6.110:** Comparison of average degree of consolidation ( $U_r$ ) against theoretical and experimental Time factor ( $Tr$ ) for CJ at 160kPa

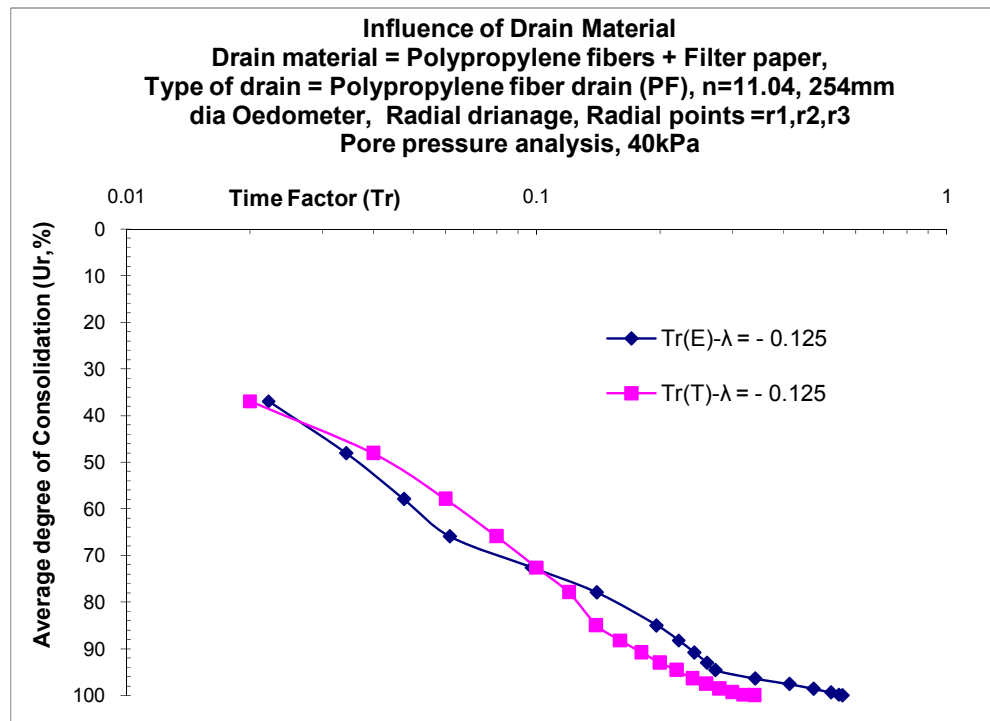


**Fig.6.111:** Comparison of average degree of consolidation ( $U_r$ ) against theoretical and experimental Time factor ( $Tr$ ) for PFat 40kPa

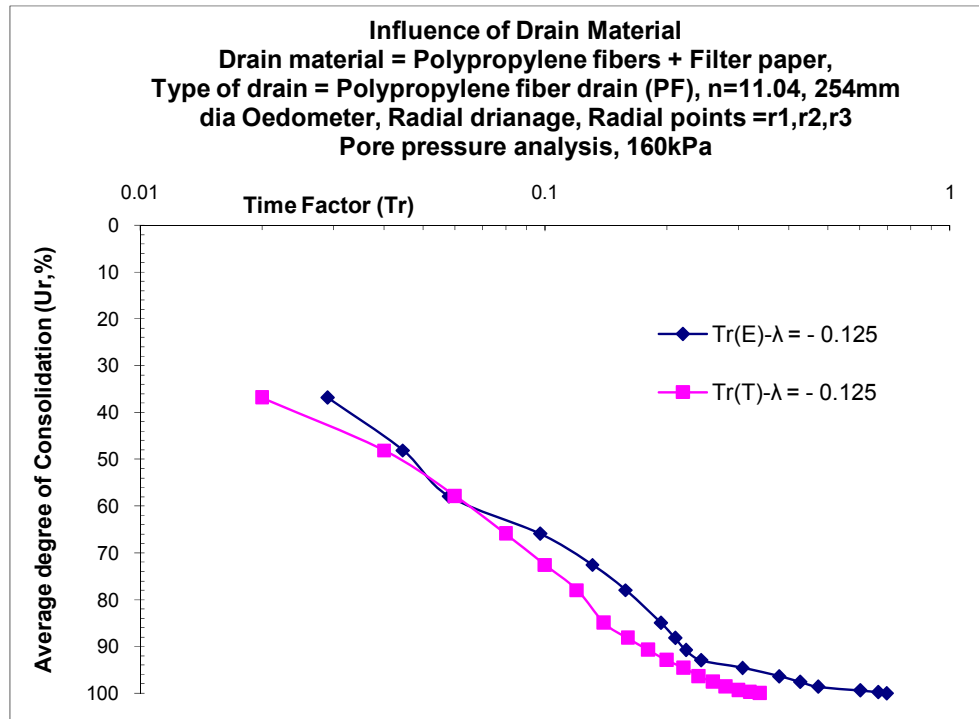


**Fig.6.112:** Comparison of average degree of consolidation ( $U_r$ ) against theoretical and experimental Time factor ( $T_r$ ) for PF at 160kPa

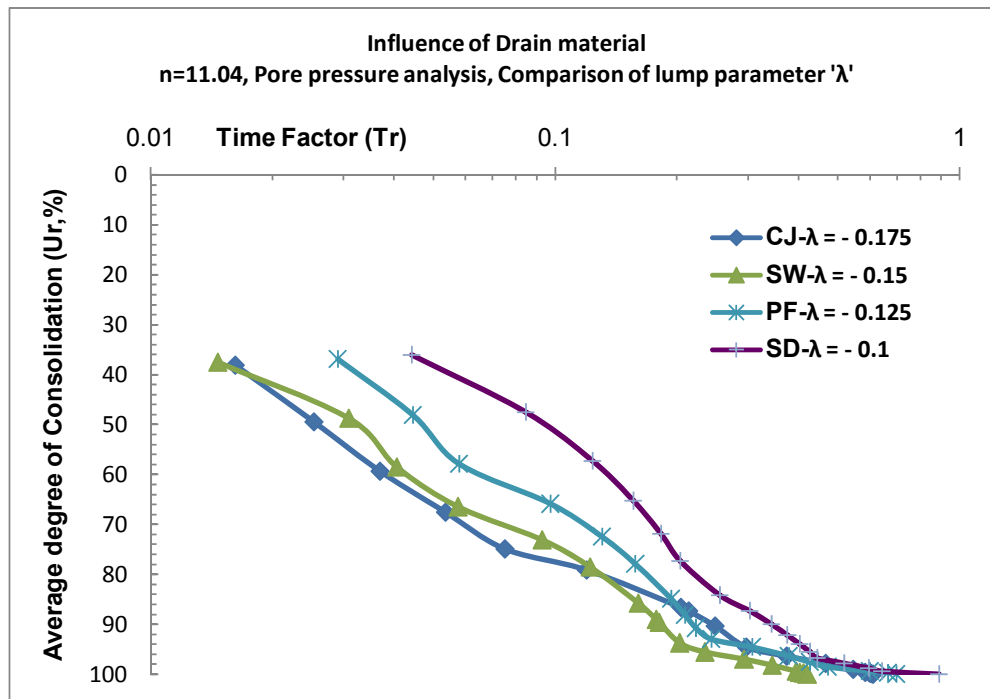


**Fig.6.113:** Comparison of average degree of consolidation ( $U_r$ ) against experimental Time factor ( $T_r$ ) for various Drain materials with lump parameter ' $\lambda$ '

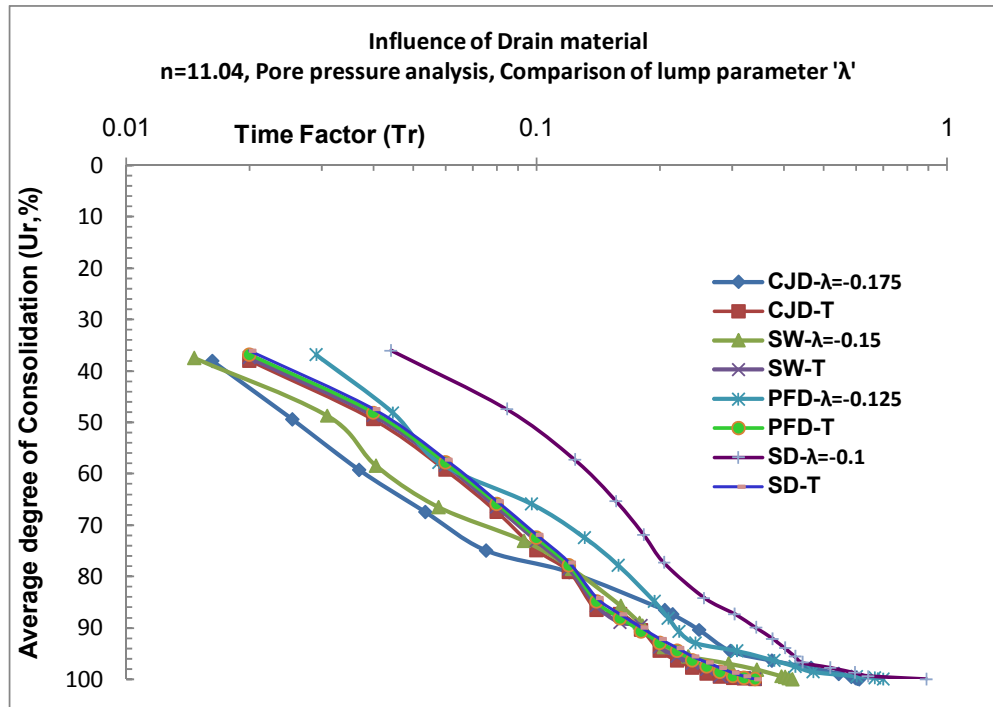


**Fig.6.114:** Comparison of average degree of consolidation ( $U_r$ ) against theoretical and experimental Time factors ( $Tr$ ) for various Drain materials with lump parameter ' $\lambda$ '

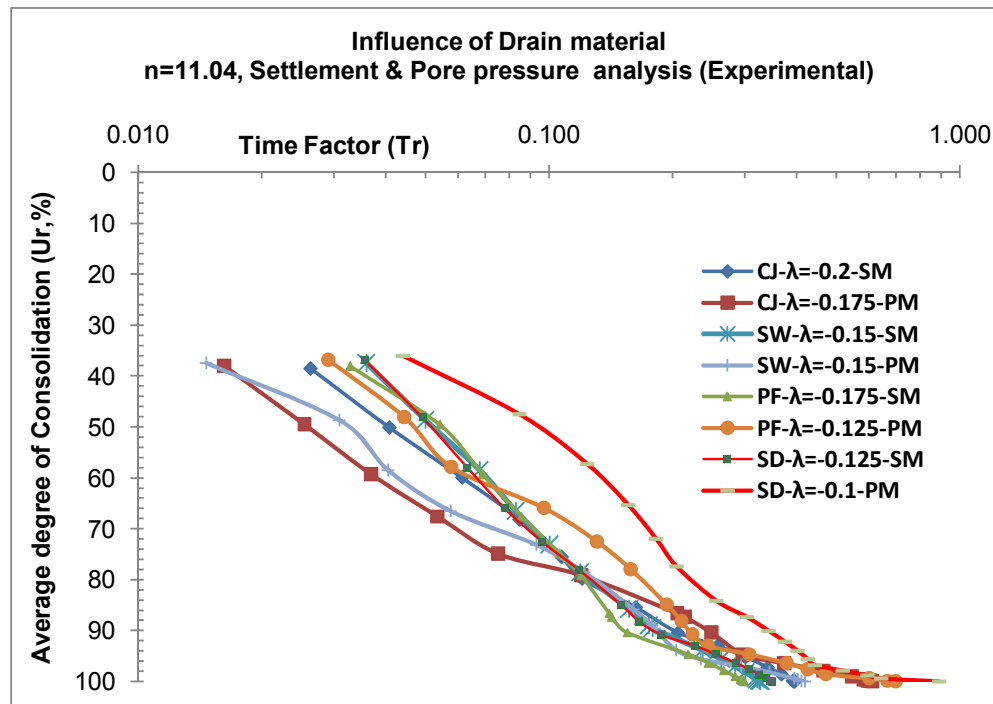


**Fig.6.115:** Comparison  $U_r$  vs.  $Tr$  for various Drain materials with lump parameter ' $\lambda$ ' on the basis of settlement and pore pressure analysis

### 8) Vane Shear Strength (Fig. 6.116) and Images of Consolidated clay samples (end of 320kPa pressure) with central vertical drains

**Discussion:** Shear strength increases to some extent towards drain for any drain material. Comparing effect of various drain materials, the shear strength achieved at end of consolidation it is observed that CJ gains highest shear strength compare to SW, SD, PF. Soft clay consolidated by CJ gained a shear strength of 153kPa compare to shear strength gained by SW, PF, SD as 120kPa, 118kPa and 100kPa respectively. The curve of CJ lies on the top for all three radial distances while curve of SW and PF are nearly at same level indicating similar strength and curve of SD lies below the curve of PF indicating achievement of lowest shear strength.

Macro porous structure of CJ drain invite dissipation of pore water pressure at faster rate for any radial distance which reflects into orientation of face-to-face particle of minimum void ratio.

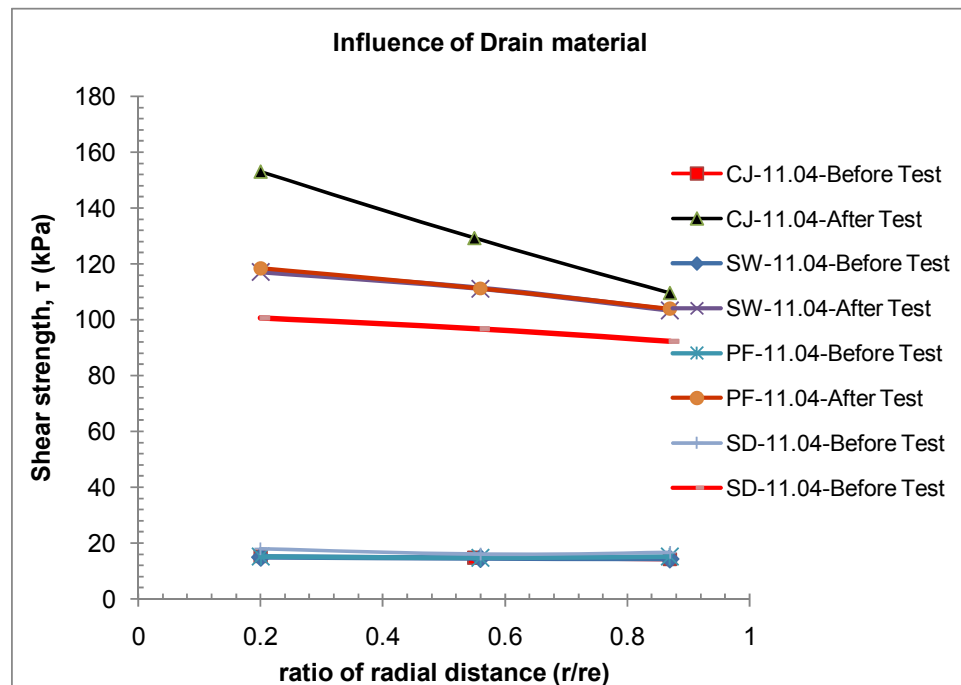
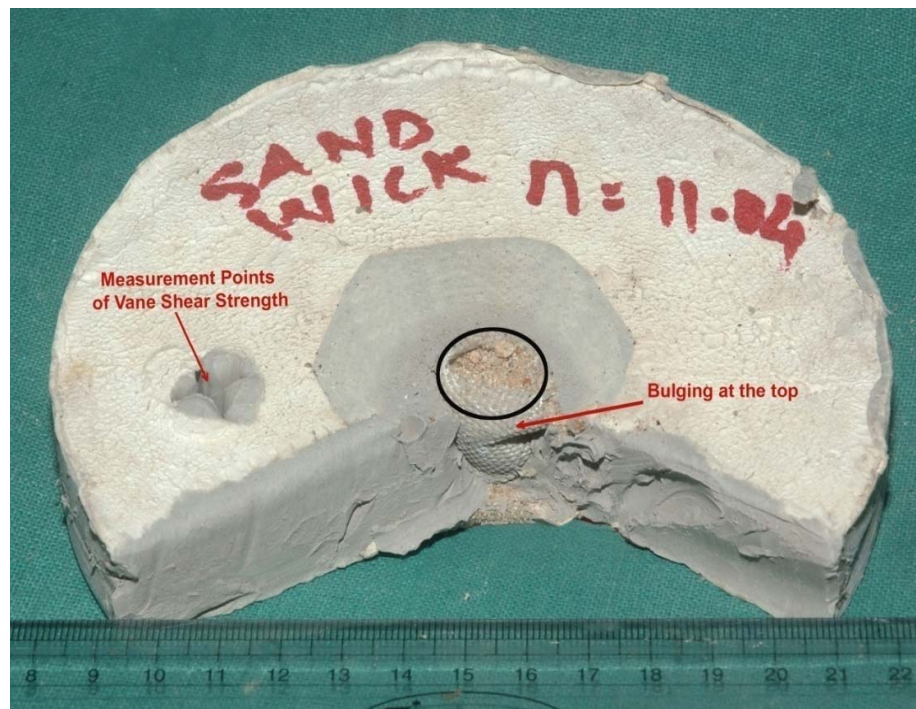


**Fig.6.116:** Comparison of vane shear strength of clay samples consolidated by various Drain materials

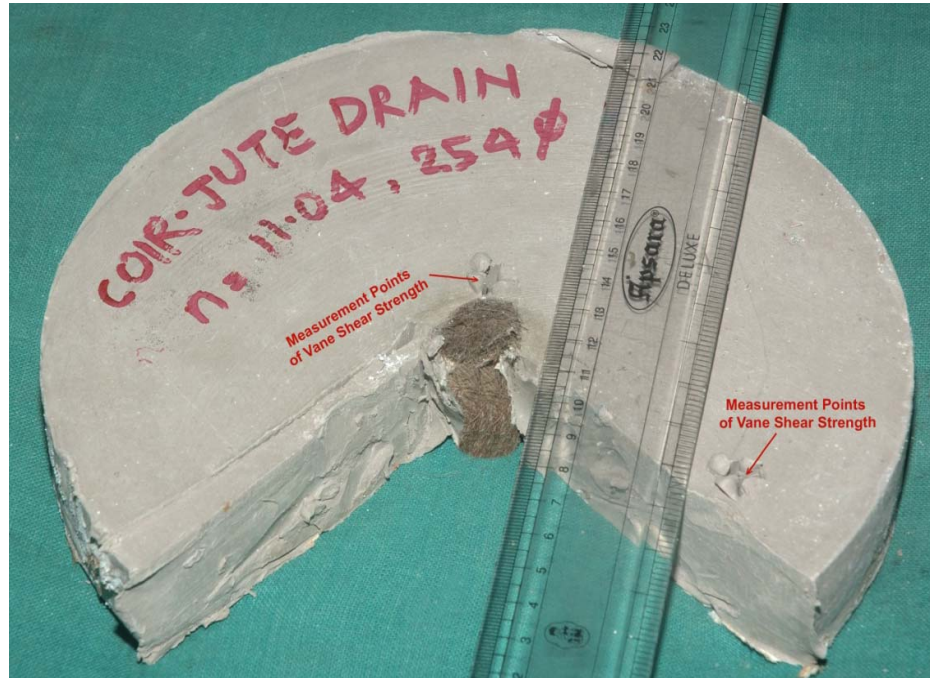


**Photograph 6.9:** Sectional view of consolidated clay sample (end of 320kPa pressure) with central vertical sand drain (SD) of  $n = 11.04$



**Photograph 6.10:** Sectional view of consolidated clay sample (end of 320kPa pressure) with central vertical sandwich drain (SW) of  $n = 11.04$





**Photograph 6.11:** Sectional view of consolidated clay sample (end of 320kPa pressure) with central vertical coir-jute drain (CJ) of  $n = 11.04$



**Photograph 6.12:** Sectional view of consolidated clay sample (end of 320kPa pressure) with central vertical polypropylene fiber drain (PF) of  $n = 11.04$



### 6.3.2) Diameter (size) of vertical drain – ‘n’ value

Refer **figures 6.117 to 6.259** which are derived from the settlement measurements and pore water pressure measurements.

- i. Sand-SD with ‘n’ values -11.04, 16.93, 21.71
- ii. sandwich-polypropylene bags with sand as filler material-SW with ‘n’ values -11.04, 16.93, 21.71
- iii. coir-jute fibers with outer cover of filter paper-CJ with ‘n’ values -11.04, 16.93, 21.71
- iv. polypropylene fibers with outer cover of filter paper-PF with ‘n’ values -11.04, 16.93, 21.71

### 1) Degree of consolidation $U_r$ vs. Time: Figures 6.117 to 6.137

**a) Settlement analysis:-** Fig.6.117 to Fig.6.126 shows comparison plots of degree of consolidation versus time for three ‘n’ values of 11.04, 16.93 and 21.71 for various vertical drains i.e.CJ, PF, SW &SD at all pressures and comparative plots are given for 40kPa and 160kPa applied pressures.

#### CJ

- The time required for 50% consolidation for CJ for  $n=11.04$  at 40kPa & 160kPa are 330min & 185min respectively while time required for 80% consolidation is 750min & 550min respectively.
- The time required for 50% consolidation for CJ for  $n=16.93$  at 40kPa & 160kPa are 580min & 325min respectively while time required for 80% consolidation is 1000min & 760min respectively.
- The time required for 50% consolidation for CJ for  $n=21.71$  at 40kPa & 160kPa are 720min & 480min respectively while time required for 80% consolidation is 1300min & 1050min respectively.

#### SW

- The time required for 50% consolidation for SW for  $n=11.04$  at 40kPa & 160kPa are 500min & 300min respectively while time required for 80% consolidation is 950min & 720min respectively.
- The time required for 50% consolidation for SW for  $n=16.93$  at 40kPa & 160kPa are 740min & 520min respectively while time required for 80% consolidation is 1400min & 1150min respectively.

- The time required for 50% consolidation for SW for  $n=21.71$  at 40kPa & 160kPa are 1650min & 1200min respectively while time required for 80% consolidation is 2700min & 2000min respectively.

#### **PF**

- The time required for 50% consolidation for PF for  $n=11.04$  at 40kPa & 160kPa are 630min & 425min respectively while time required for 80% consolidation is 1250min & 940min respectively.
- The time required for 50% consolidation for PF for  $n=16.93$  at 40kPa & 160kPa are 740min & 580min respectively while time required for 80% consolidation is 1300min & 1000min respectively.
- The time required for 50% consolidation for PF for  $n=21.71$  at 40kPa & 160kPa are 960min & 620min respectively while time required for 80% consolidation is 1600min & 1300min respectively.

#### **SD**

- The time required for 50% consolidation for SD for  $n=11.04$  at 40kPa & 160kPa are 500min & 310min respectively while time required for 80% consolidation is 980min & 760min respectively.
- The time required for 50% consolidation for SD for  $n=16.93$  at 40kPa & 160kPa are 1050min & 820min respectively while time required for 80% consolidation is 1500min & 1200min respectively.
- The time required for 50% consolidation for SD for  $n=21.71$  at 40kPa & 160kPa are 1950min & 1500min respectively while time required for 80% consolidation is 3500min & 2800min respectively.
- Comparing all four types of vertical drains and their diameters(size) it is observed that, for 50% consolidation  $n=11.04$  for 40kPa CJ takes 54% less time in compare to  $n=21.71$  and 43.1% in compare to  $n=16.93$ . For engineering stress of 160kPa for 50% consolidation  $n=11.04$  for CJ takes 61.4% less time in compare to  $n=21.71$  and 43% in compare to  $n=16.93$ . Similarly for 80% consolidation  $n=11.04$  for 40kPa CJ takes 42.3% less time in compare to  $n=21.71$  and 25% in compare to  $n=16.93$  for 40kPa pressure.
- For 50% consolidation,  $n=11.04$  & 40kPa CJ takes 51%, 90%, 51% less time in compare to SW, PF & SD respectively.

- For 80% consolidation,  $n=11.04$  & 40kPa CJ takes 26.7%, 66.7%, 30.6% less time in compare to SW, PF & SD respectively.
- For 50% consolidation,  $n=11.04$  & 160kPa CJ takes 62%, 129.7%, 67.5% less time in compare to SW, PF & SD respectively.
- For 80% consolidation,  $n=11.04$  & 160kPa CJ takes 30.9%, 70.9%, 38.2% less time in compare to SW, PF & SD respectively.
- For 50% consolidation,  $n=16.93$  & 40kPa CJ takes 27.5%, 26.5%, 81% less time in compare to SW, PF & SD respectively.
- For 80% consolidation,  $n=16.93$  & 40kPa CJ takes 40%, 30%, 50% less time in compare to SW, PF & SD respectively.
- For 50% consolidation,  $n=16.93$  & 160kPa CJ takes 60%, 78.4%, 152% less time in compare to SW, PF & SD respectively.
- For 80% consolidation,  $n=16.93$  & 160kPa CJ takes 51.3%, 31.5%, 57.9% less time in compare to SW, PF & SD respectively.
- For 50% consolidation,  $n=21.71$  & 40kPa CJ takes 66.7%, 33.3%, 170% less time in compare to SW, PF & SD respectively.
- For 80% consolidation,  $n=21.71$  & 40kPa CJ takes 107%, 23%, 169% less time in compare to SW, PF & SD respectively.
- For 50% consolidation,  $n=21.71$  & 160kPa CJ takes 150%, 29.1%, 212% less time in compare to SW, PF & SD respectively.
- For 80% consolidation,  $n=21.71$  & 160kPa CJ takes 90.5%, 23.8%, 166% less time in compare to SW, PF & SD respectively.
- Graphs of higher pressures value falls above the graphs of lower pressures for all three 'n' values. This is true for all individual applied pressures. This reflects higher rate of consolidation at less 'n' value. This is occurring so as the 'n' value increases the surface area of drain gets smaller then the effect of tortousity increases.
- Above discussion clearly indicates that CJ of  $n=11.04$  is most efficient drain. Also  $n=16.93$  is better in compare to  $n=21.71$ .

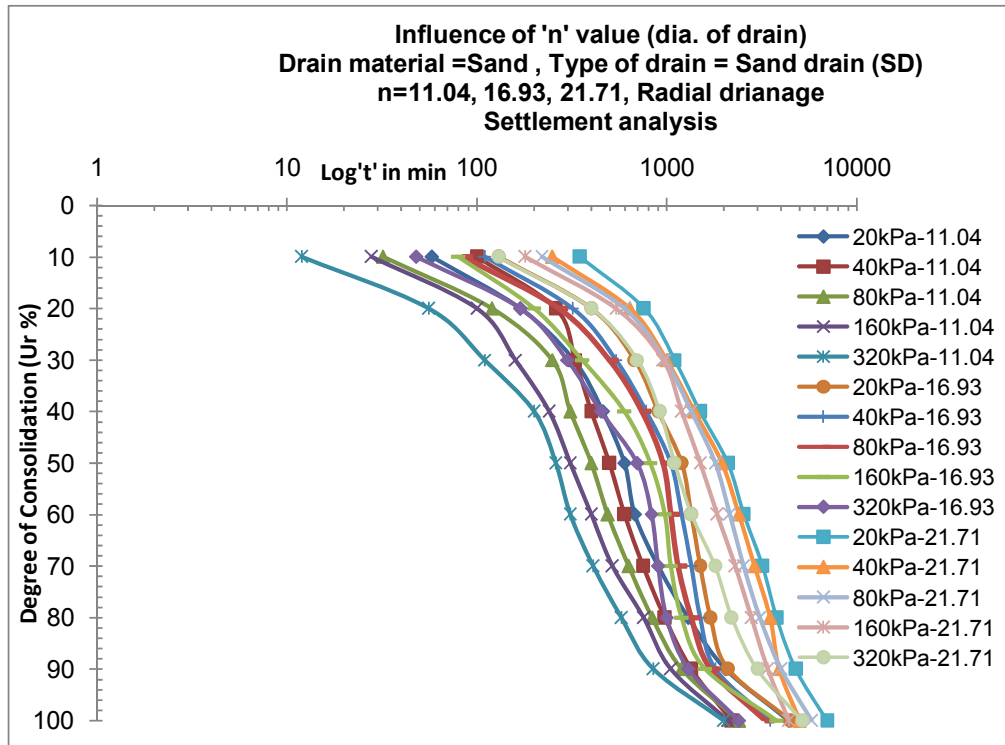


**Fig. 6.117:** Degree of consolidation ( $U_r$ ) vs.  $\log't'$  in min for SD

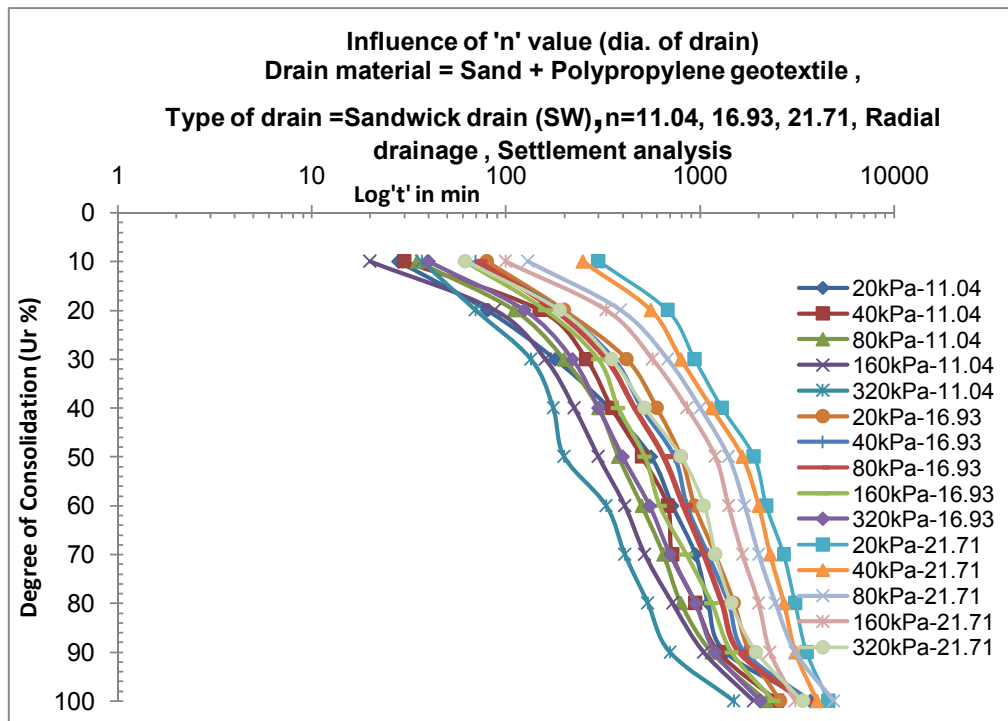


**Fig. 6.118:** Degree of consolidation ( $U_r$ ) vs.  $\log't'$  in min for SW

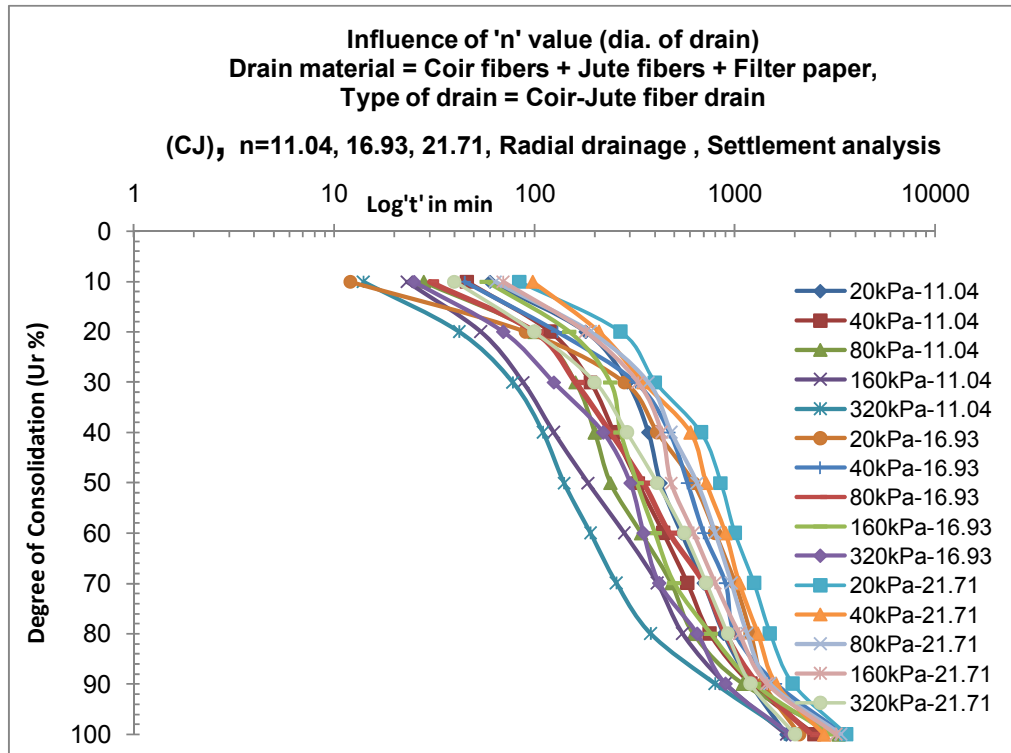


**Fig. 6.119:** Degree of consolidation ( $U_r$ ) vs.  $\log't'$  in min for CJ

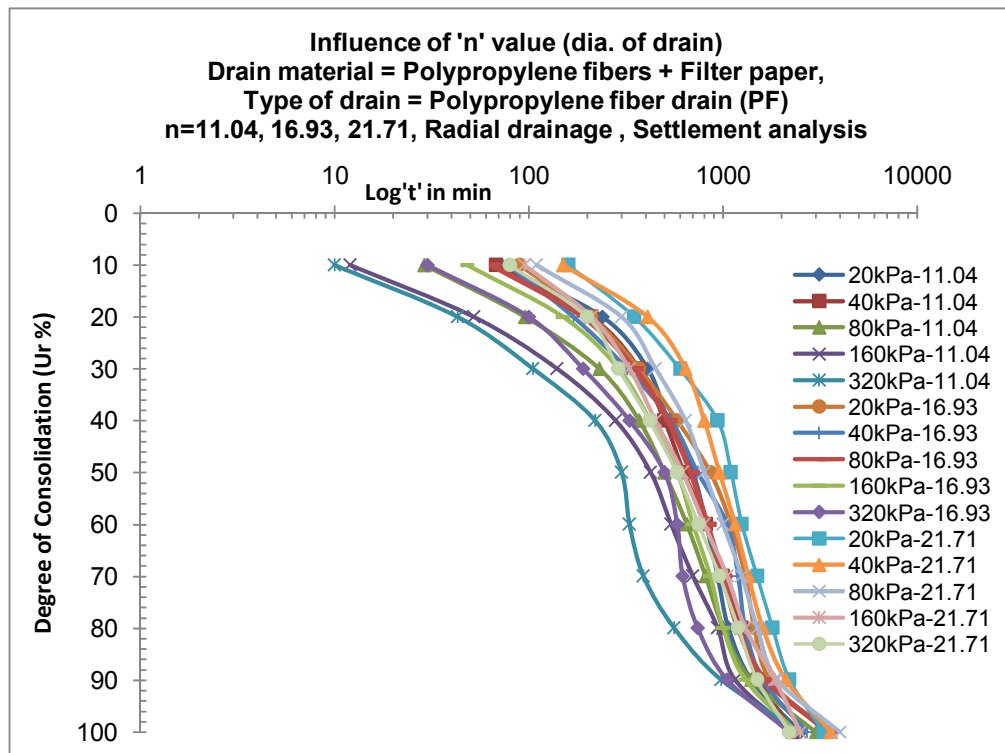


**Fig. 6.120:** Degree of consolidation ( $U_r$ ) vs.  $\log't'$  in min for PF

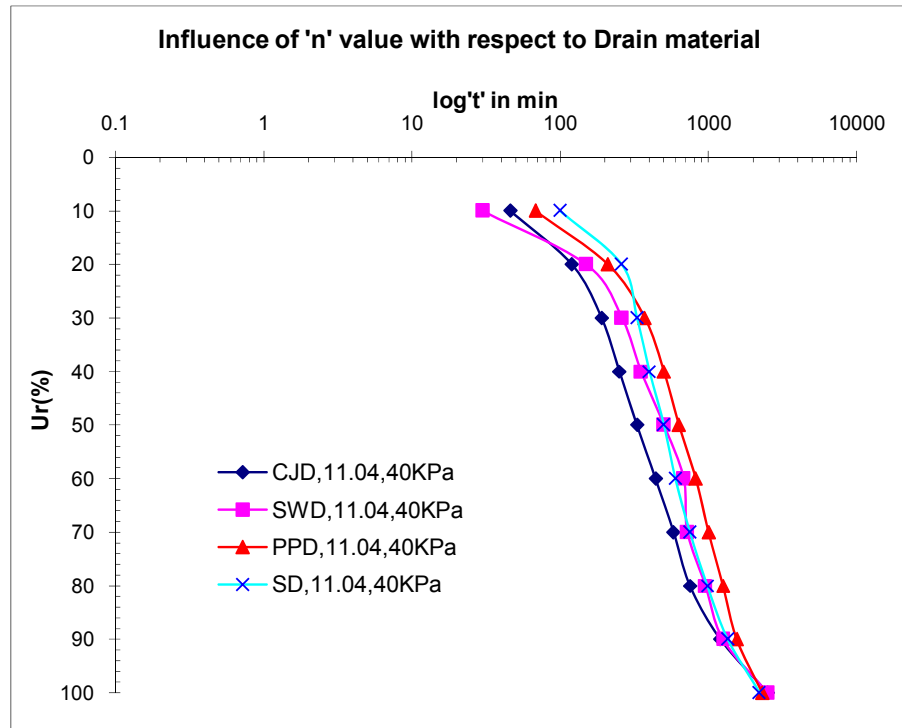


**Fig. 6.121:** Comparison of degree of consolidation ( $U_r$ ) vs.  $\log't'$  in min for 'n' value with respect to drain material at 40kPa pressure

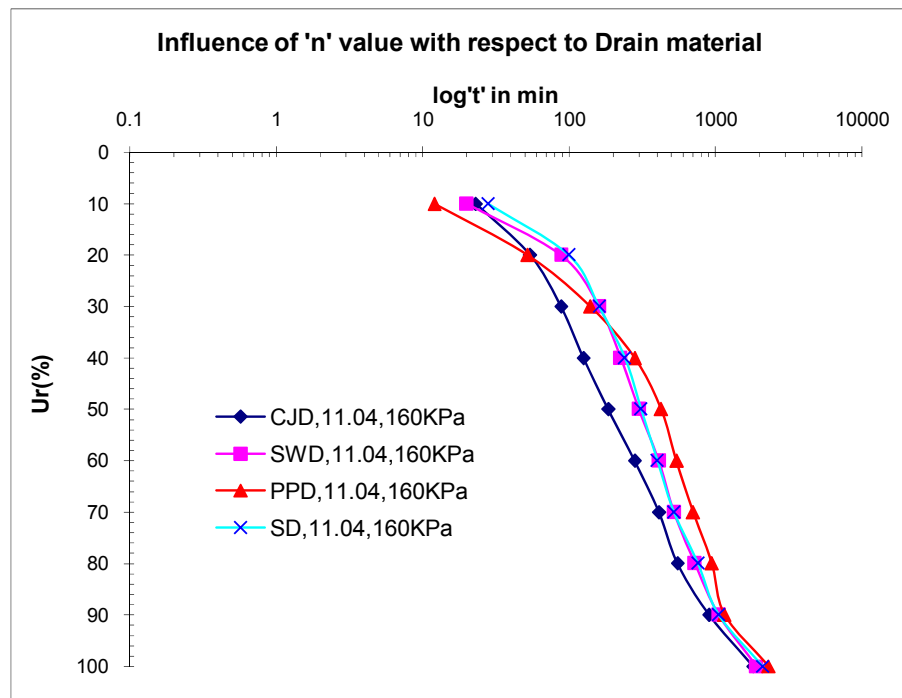


**Fig. 6.122:** Comparison of degree of consolidation ( $U_r$ ) vs.  $\log't'$  in min for 'n' 11.04 with respect to drain material at 160kPa pressure

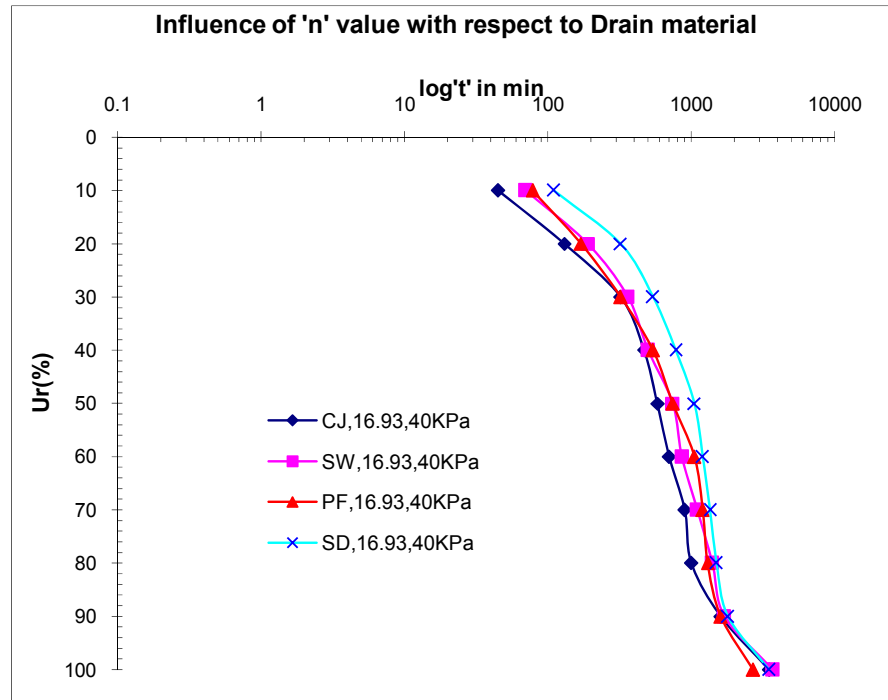


**Fig. 6.123:** Comparison of degree of consolidation ( $U_r$ ) vs.  $\log t'$  in min for 'n' 16.93 with respect to drain material at 40kPa pressure

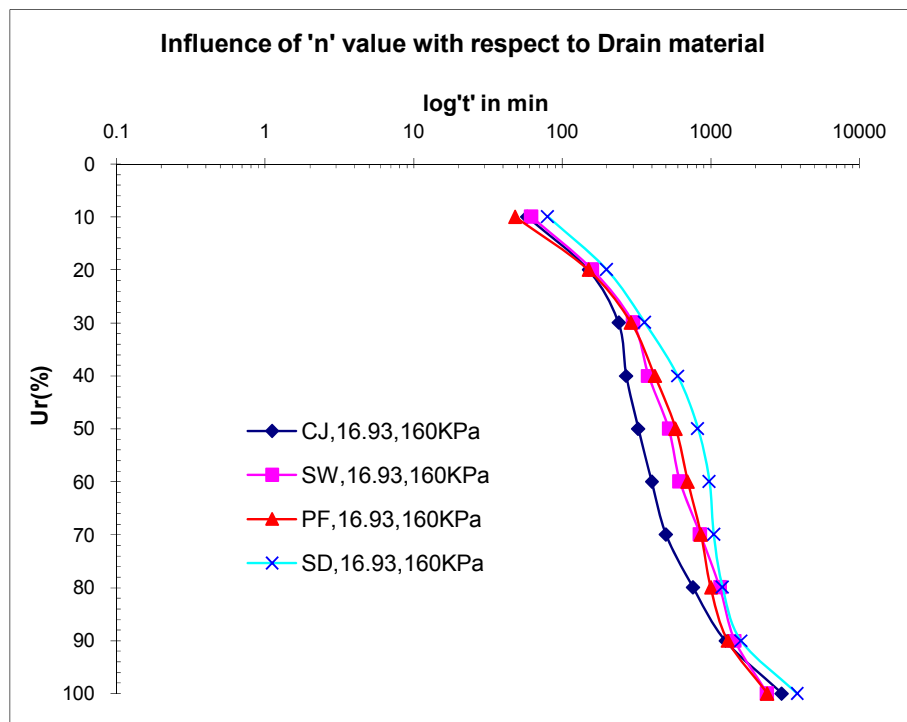


**Fig. 6.124:** Comparison of degree of consolidation ( $U_r$ ) vs.  $\log t'$  in min for 'n' 16.93 with respect to drain material at 160kPa pressure

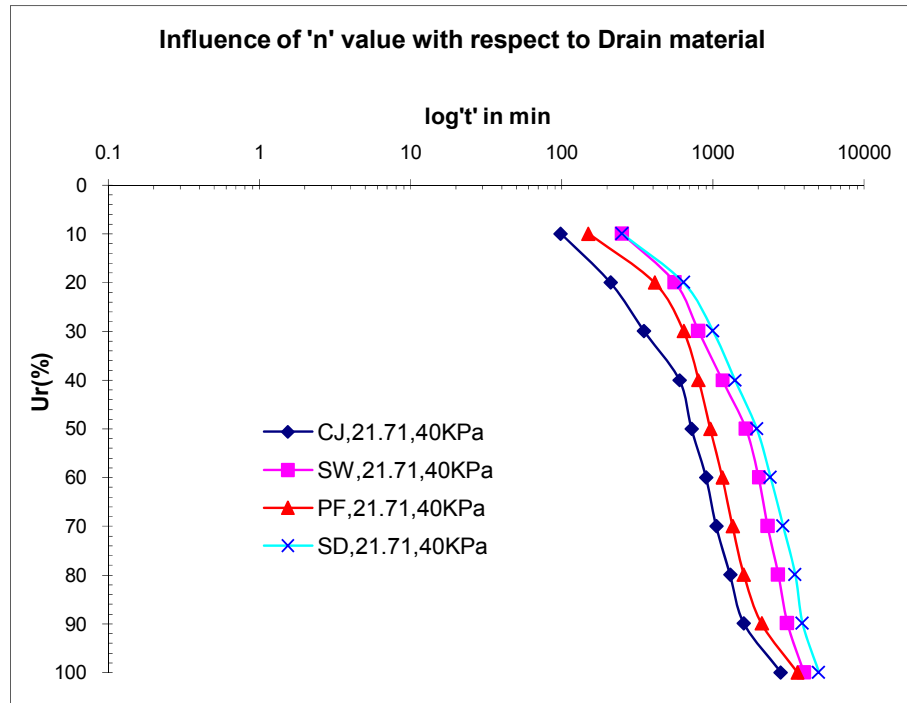


**Fig. 6.125:** Comparison of degree of consolidation ( $U_r$ ) vs.  $\log t$  in min for 'n'21.71 with respect to drain material at 40kPa pressure

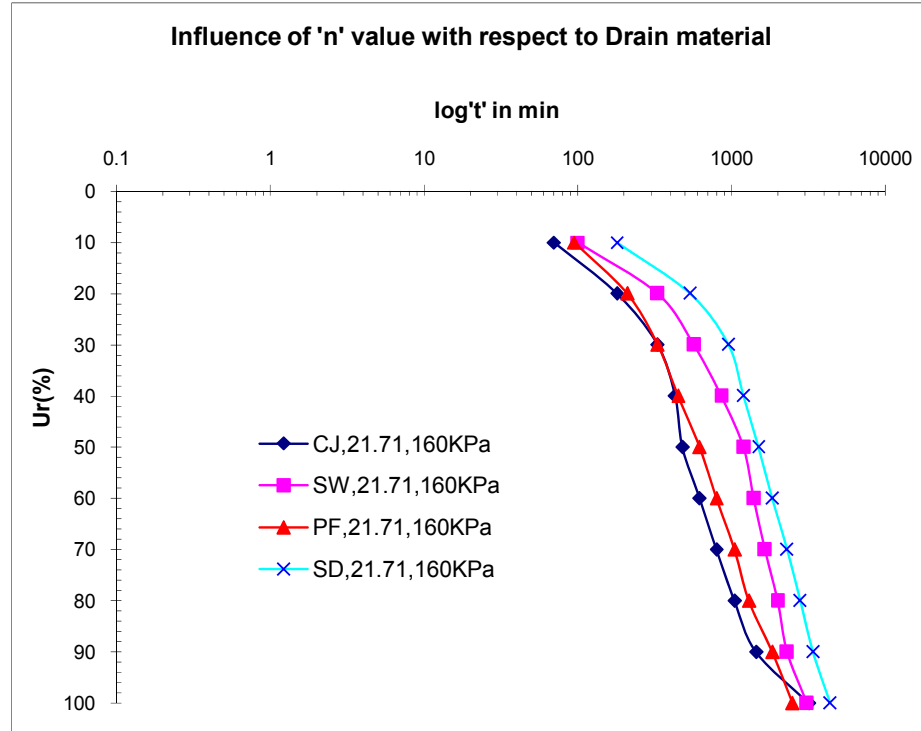


**Fig. 6.126:** Comparison of degree of consolidation ( $U_r$ ) vs.  $\log t$  in min for 'n'21.71 with respect to drain material at 160kPa pressure



**Table 6.3:** Comparison of time taken for 50% and 80% degree of consolidation for various 'n' value based on settlement and pore pressure measurements

| Drain material | 'n' value | Settlement based     |                      | Pore pressure based  |                      |
|----------------|-----------|----------------------|----------------------|----------------------|----------------------|
|                |           | Time for 50%Ur-40kPa | Time for 80%Ur-40kPa | Time for 50%Ur-40kPa | Time for 80%Ur-40kPa |
| SD             | 11.04     | 500                  | 980                  | 640                  | 1500                 |
|                | 16.93     | 1050                 | 1500                 | 850                  | 1800                 |
|                | 21.71     | 1950                 | 3500                 | 1440                 | 2700                 |
| SW             | 11.04     | 500                  | 950                  | 250                  | 740                  |
|                | 16.93     | 740                  | 1400                 | 340                  | 980                  |
|                | 21.71     | 1650                 | 2700                 | 550                  | 1550                 |
| CJ             | 11.04     | 330                  | 750                  | 125                  | 580                  |
|                | 16.93     | 580                  | 1000                 | 175                  | 750                  |
|                | 21.71     | 720                  | 1300                 | 320                  | 1000                 |
| PF             | 11.04     | 630                  | 1250                 | 215                  | 650                  |
|                | 16.93     | 740                  | 1300                 | 370                  | 1050                 |
|                | 21.71     | 960                  | 1600                 | 580                  | 1650                 |

| Drain material | 'n' value | Settlement based      |                       | Pore pressure based   |                       |
|----------------|-----------|-----------------------|-----------------------|-----------------------|-----------------------|
|                |           | Time for 50%Ur-160kPa | Time for 80%Ur-160kPa | Time for 50%Ur-160kPa | Time for 80%Ur-160kPa |
| SD             | 11.04     | 310                   | 760                   | 640                   | 1500                  |
|                | 16.93     | 820                   | 1200                  | 850                   | 1800                  |
|                | 21.71     | 1500                  | 2800                  | 1440                  | 2700                  |
| SW             | 11.04     | 300                   | 720                   | 385                   | 850                   |
|                | 16.93     | 520                   | 1150                  | 460                   | 1200                  |
|                | 21.71     | 1200                  | 2000                  | 750                   | 1800                  |
| CJ             | 11.04     | 185                   | 550                   | 160                   | 575                   |
|                | 16.93     | 325                   | 760                   | 280                   | 800                   |
|                | 21.71     | 480                   | 1050                  | 400                   | 1200                  |
| PF             | 11.04     | 425                   | 940                   | 361                   | 780                   |
|                | 16.93     | 580                   | 1000                  | 580                   | 1250                  |
|                | 21.71     | 620                   | 1300                  | 760                   | 1850                  |

**b) Pore pressure analysis:-** Fig.6.127 to Fig.6.136 shows the plots of dissipation of excess hydrostatic pore water pressure (degree of consolidation) versus logarithm of time at three radial points  $r_1$ ,  $r_2$ ,  $r_3$  for vertical drains i.e. CJ,

SW, PF, SD & analysis is carried out for all three 'n' values .i.e. 11.04, 16.93 and 21.71 for all pressures. Here results are presented for all pressures and comparative plots are shown for 40kPa & 160kPa pressures for all three radial points.

- The time required for 50% consolidation for CJ for  $n=11.04$  at 40kPa for radial point r1, r2 & r3 is 39min,125min,220min while for 160kPa for radial point r1, r2 & r3 is 80min,160min,256min min respectively and time required for 80% consolidation at 40kPa for radial point r1, r2 & r3 is 105min,580min,680min while for 160kPa for radial point r1, r2 & r3 is 160min,575min,920min respectively.
- The time required for 50% consolidation for CJ for  $n=16.93$  at 40kPa for radial point r1, r2 & r3 is 49min,105min,160min while for 160kPa for radial point r1, r2 & r3 is 115min,280min,315min respectively and time required for 80% consolidation at 40kPa for radial point r1, r2 & r3 is 210min,750min,900min while for 160kPa for radial point r1, r2 & r3 is 300min,800min,1150min respectively.
- The time required for 50% consolidation for CJ for  $n=21.71$  at 40kPa for radial point r1, r2 & r3 is 150min,320min,650min while for 160kPa for radial point r1, r2 & r3 is 240min,400min,950min respectively and time required for 80% consolidation at 40kPa for radial point r1, r2 & r3 is 380min,1000min,1600min while for 160kPa for radial point r1, r2 & r3 is 540min,1200min,1950min respectively.
- The time required for 50% consolidation for SW for  $n=11.04$  at 40kPa for radial point r1, r2 & r3 is 160min,250min,400min while for 160kPa for radial point r1, r2 & r3 is 220min,385min,570min respectively and time required for 80% consolidation at 40kPa for radial point r1, r2 & r3 is 350min,740min,950min while for 160kPa for radial point r1, r2 & r3 is 440min,850min,1200min respectively.
- The time required for 50% consolidation for SW for  $n=16.93$  at 40kPa for radial point r1, r2 & r3 is 200min,340min,550min while for 160kPa for radial point r1, r2 & r3 is 280min,460min,780min respectively and time required for 80% consolidation at 40kPa for radial point r1, r2 & r3 is 430min,980min,1350min while for 160kPa for radial point r1, r2 & r3 is 680min,1200min,1550min respectively.

- The time required for 50% consolidation for SW for  $n=21.71$  at 40kPa for radial point r1, r2 & r3 is 350min,550min,850min while for 160kPa for radial point r1, r2 & r3 is 450min,750min,960min respectively and time required for 80% consolidation at 40kPa for radial point r1, r2 & r3 is 980min,1550min,2000min while for 160kPa for radial point r1, r2 & r3 is 1200min,1800min,2500min respectively.
- The time required for 50 % consolidation for PF for  $n=11.04$  at 40kPa for radial point r1,r2 & r3 is 135min,215min,350min while for 160kPa for radial point r1,r2 & r3 is 170min,361min,520min respectively and time required for 80% consolidation at 40kPa for radial point r1, r2 & r3 is 300min,650min,800min while for 160kPa for radial point r1, r2 & r3 is 360min,780min,1100min respectively.
- The time required for 50% consolidation for PF for  $n=16.93$  at 40kPa for radial point r1,r2 & r3 is 240min,370min,580min while for 160kPa for radial point r1, r2 & r3 is 325min,580min,900min respectively and time required for 80% consolidation at 40kPa for radial point r1, r2 & r3 is 450min,1050min,1440min while for 160kPa for radial point r1, r2 & r3 is 750min,1250min,1700min respectively.
- The time required for 50% consolidation for PF for  $n=21.71$  at 40kPa for radial point r1, r2 & r3 is 361min,580min,880min while for 160kPa for radial point r1, r2 & r3 is 480min,760min,1000min respectively and time required for 80% consolidation at 40kPa for radial point r1, r2 & r3 is 1000min,1650min,2100min while for 160kPa for radial point r1, r2 & r3 is 1300min,1850min,2600min respectively.
- The time required for 50 % consolidation for SD for  $n=11.04$  at 40kPa for radial point r1, r2 & r3 is 245min,490min,760min while for 160kPa for radial point r1, r2 & r3 is 400min,640min,950min respectively and time required for 80% consolidation at 40kPa for radial point r1, r2 & r3 is 600min,1200min,1800min while for 160kPa for radial point r1, r2 & r3 is 750min,1500min,2100min respectively.
- The time required for 50 % consolidation for SD for  $n=16.93$  at 40kPa for radial point r1, r2 & r3 is 325min,600min,920min while for 160kPa for radial point r1, r2 & r3 is 430min,850min,1400min respectively and time required for 80 % consolidation at 40kPa for radial point r1, r2 & r3 is

750min,1440min,2000min while for 160kPa for radial point r1, r2 & r3 is 1150min,1800min,2700min respectively.

- The time required for 50 % consolidation for SD for  $n=21.71$  at 40kPa for radial point r1, r2 & r3 is 700min,1150min,1500min while for 160kPa for radial point r1, r2 & r3 is 1000min,1440min,2100min respectively and time required for 80% consolidation at 40kPa for radial point r1, r2 & r3 is 1440min,2300min,3300min while for 160kPa for radial point r1, r2 & r3 is 1850min,2700min,4100min respectively.
- For engineering stress of 160kPa for 50% consolidation  $n=11.04$  for CJ takes 66.67%,60%,73.05% less time for radial points r1,r2,r3 in compare to  $n=16.93$  &  $n=21.71$ , while for 80% consolidation  $n=11.04$  for CJ takes 70.3%,52.08%,52.81% less time for radial points r1,r2,r3 in compare to  $n=21.71$  and  $n=16.93$  takes 44.4%,33.3%,41% less time for radial points r1,r2,r3 in compare to  $n=21.71$ .
- For engineering stress of 160kPa for 50% consolidation  $n=11.04$  for SW takes 51.1%,48.7%,40.6% less time in compare to  $n=21.71$ , while for  $n=16.93$  it takes 37.8%,38.7%,18.8% less time in compare to  $n=21.71$ . For 80% consolidation  $n=11.04$  for SW takes 63.3%,52.8%,52% less time in compare to  $n=21.71$  while  $n=16.93$  takes 43.3%,33.3%,38% less time in compare to  $n=21.71$ .
- For engineering stress of 160kPa for 50% consolidation  $n=11.04$  for PF takes 64.5%,52.5%,48% less time in compare to  $n=21.71$ , while for  $n=16.93$  it takes 32.3%,23.7%,10% less time in compare to  $n=21.71$ . For 80% consolidation  $n=11.04$  for PF takes 72.3%,57.8%,57.7% less time in compare to  $n=21.71$  while  $n=16.93$  takes 42.3%,32.4%,34.6% less time in compare to  $n=21.71$ .
- For engineering stress of 160kPa for 50% consolidation  $n=11.04$  for SD takes 60%,55.5%,54.8% less time in compare to  $n=21.71$ , while for  $n=16.93$  it takes 57%,41%,33.3% less time in compare to  $n=21.71$ . For 80% consolidation  $n=11.04$  for SD takes 59.5%,44.4%,48.7% less time in compare to  $n=21.71$  while  $n=16.93$  takes 37.8%,33.3%,34.1% less time in compare to  $n=21.71$ .
- From the above discussions it is clear that out of three 'n' values, the  $n=11.04$  is more efficient in compare to  $n=16.93$  and  $n=21.71$  for all four drains and at

all pressures. Dissipation rate of pore pressure is faster in case of radial point 'r1' for all 'n' values for all pressures for all vertical geodrains. r1 shows faster rate of dissipation in compare to r2 and r3 while r2 shows faster rate of dissipation in compare to r3 for all pressures. Graphs of higher pressures value falls above the graphs of lower pressures for all three 'n' values. This is true for all individual applied pressures. This reflects higher rate of consolidation at less 'n' value.

**Discussion:** (Refer figure 6.137 and table 6.3)

- It concludes that for 50% consolidation,  $n=11.04$  takes 48% and 71% less time compared to  $n=16.93$  and 21.71 for any drain material under light loading (upto 40kPa) and 53%, 63%, under constructional loading (160kPa and greater). Similarly for 80% consolidation,  $n=11.04$  takes 35% and 61% less time compared to  $n=16.93$  and 21.71 for any drain material under light loading and 37%, 54% under constructional loading.
- From pore pressure measurements, it infers that for 50% consolidation and mid plane radial point  $r_2$ ,  $n=11.04$  takes 59% and 76% less time compared to  $n=16.93$  and 21.71 for any drain material under light loading and 65%, 77%, under constructional loading. Similarly for 80% consolidation,  $n=11.04$  takes 42% and 61% less time compared to  $n=16.93$  and 21.71 for any drain material under light loading and 51%, 67% under constructional loading.
- In case of coir-jute drain(CJ) at 50% consolidation,  $n=11.04$  takes lowest time of 330min & 185min amongst other drains under light and construction loadings respectively. Also for 80% consolidation CJ and  $n=11.04$  remain effective exhibiting lowest time of 750min & 550min time under light and constructional loading respectively as discussed earlier.
- It concludes that for 50% consolidation,  $n=11.04$  takes 135% and 300% less time compared to  $n=16.93$  and 21.71 for any drain material under light loading and 203%, 413%, under constructional loading. Similarly for 80% consolidation,  $n=11.04$  takes 73% and 203% less time compared to  $n=16.93$  and 21.71 for any drain material under light loading and 86%, 225% under constructional loading.

- From pore pressure measurements, it infers that for 50% consolidation and mid plane radial point  $r_2$ ,  $n=11.04$  takes 197% and 420% less time compared to  $n=16.93$  and  $21.71$  for any drain material under light loading and 239%,423%, under constructional loading. Similarly for 80% consolidation,  $n=11.04$  takes 81% and 180% less time compared to  $n=16.93$  and  $21.71$  for any drain material under light loading and 119%,228% under constructional loading.
- For any load intensity and 'n' value of any drain material, the time deformation curve with respect to pore pressure dissipation remain towards the vertical axis compare to curve of settlement, that is time require for 50% or 80% consolidation is less compare to settlement curve which also reflects in isochrones curves. The curve of pore pressure for 'n' equal to 11.04 shifts towards vertical axis compare to 'n' equal to 16.93 and 21.71 for any drain material and for any pressure. While curve of pore pressure of 'n' equal to 16.93 align left of 'n'21.71 for any drain material. The reasons for this is the specific surface area of drain which gives direct flow path to water particle for dissipation of pore water. More the specific surface area, more the discharge and higher the compressibility of soil mass. The above reason can be justified by the microporosity measured and angle of orientation measured for sand drains (SD) and coir-jute drain (CJ) of different 'n' values which is presented in photographs 6.13 to 6.18 and figures 6.138 to 6.140 which represents porosity, angle of orientation and tortousity (horizontal and vertical) variation with 'n' value.
- Tortousity tends to unity in case of 'n'11.04 and increases as 'n' increases. Lowest tortousity is found in CJ drain of 'n'11.04 compare to SD drain of 'n'11.04 as mentioned earlier. Soil structure because of the gradient of flow in horizontal direction and vertical load help causes more quantum of face-to-face contact in the former case. For the same 'n' value of different vertical drains the depth wise tortousity also indicate the effect of over burden to some extent and nature of dissipation of pore water along the macrochannels and tubular pores which are formed under various loads. In case of coir-jute drain the tortouisty at interface and at mid radial point are almost same indicating uniform surface settlment unlike sand drain.

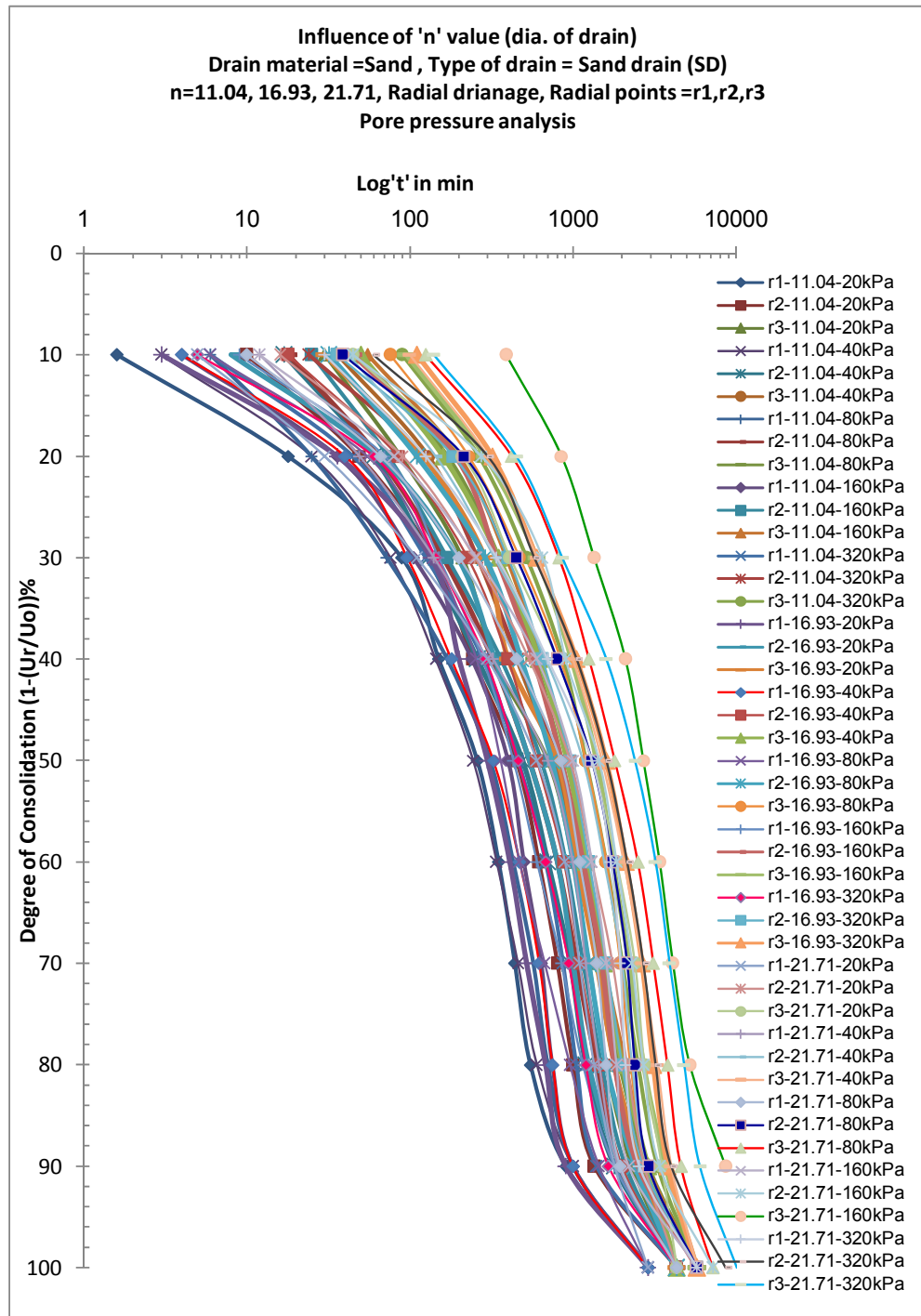


**Fig. 6.127:** Comparison of dissipation of pore water pressure against log't' w.r.t 'n' value for SD at all pressures

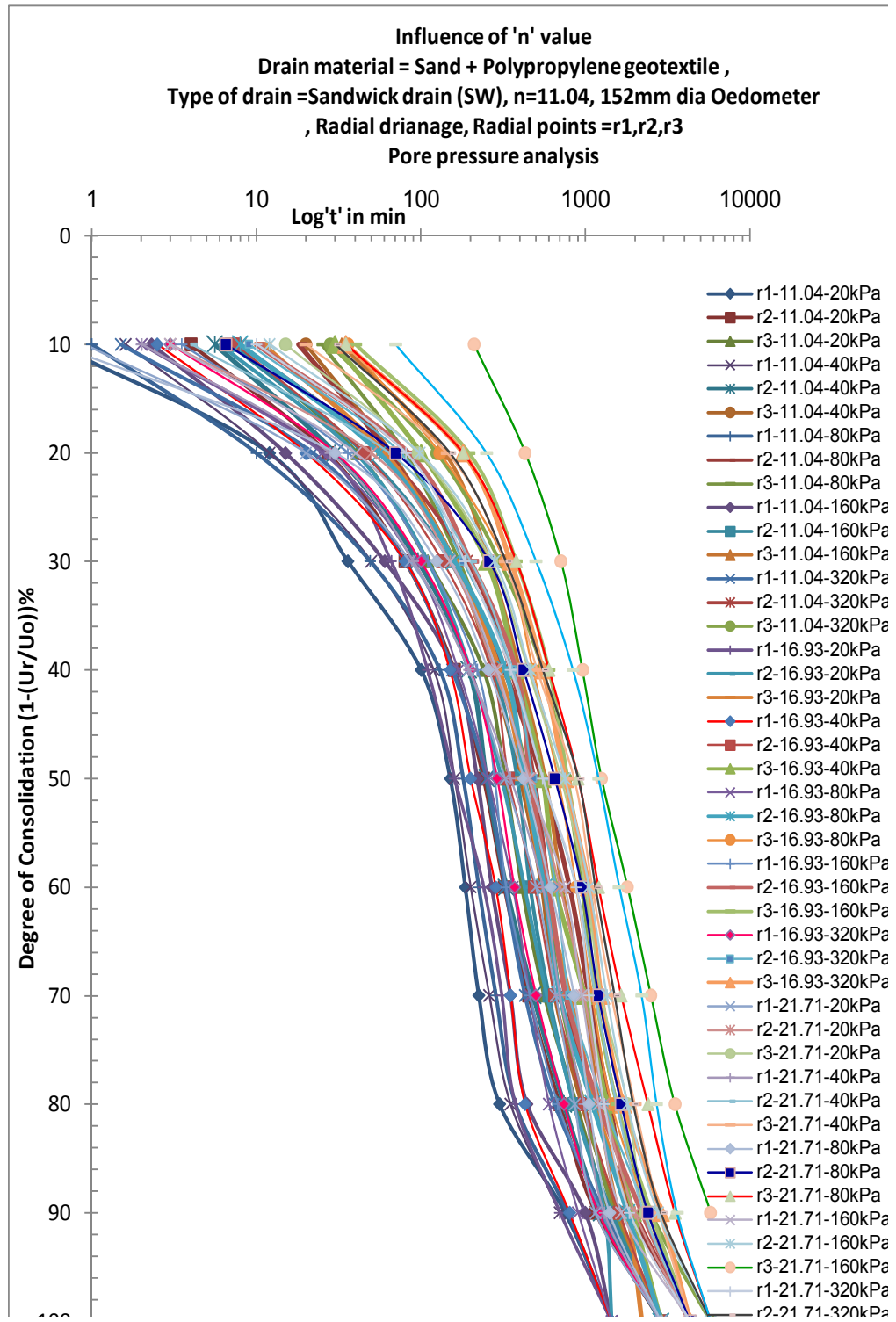


**Fig. 6.128:** Comparison of dissipation of pore water pressure against log't' w.r.t 'n' value for SW at all pressures



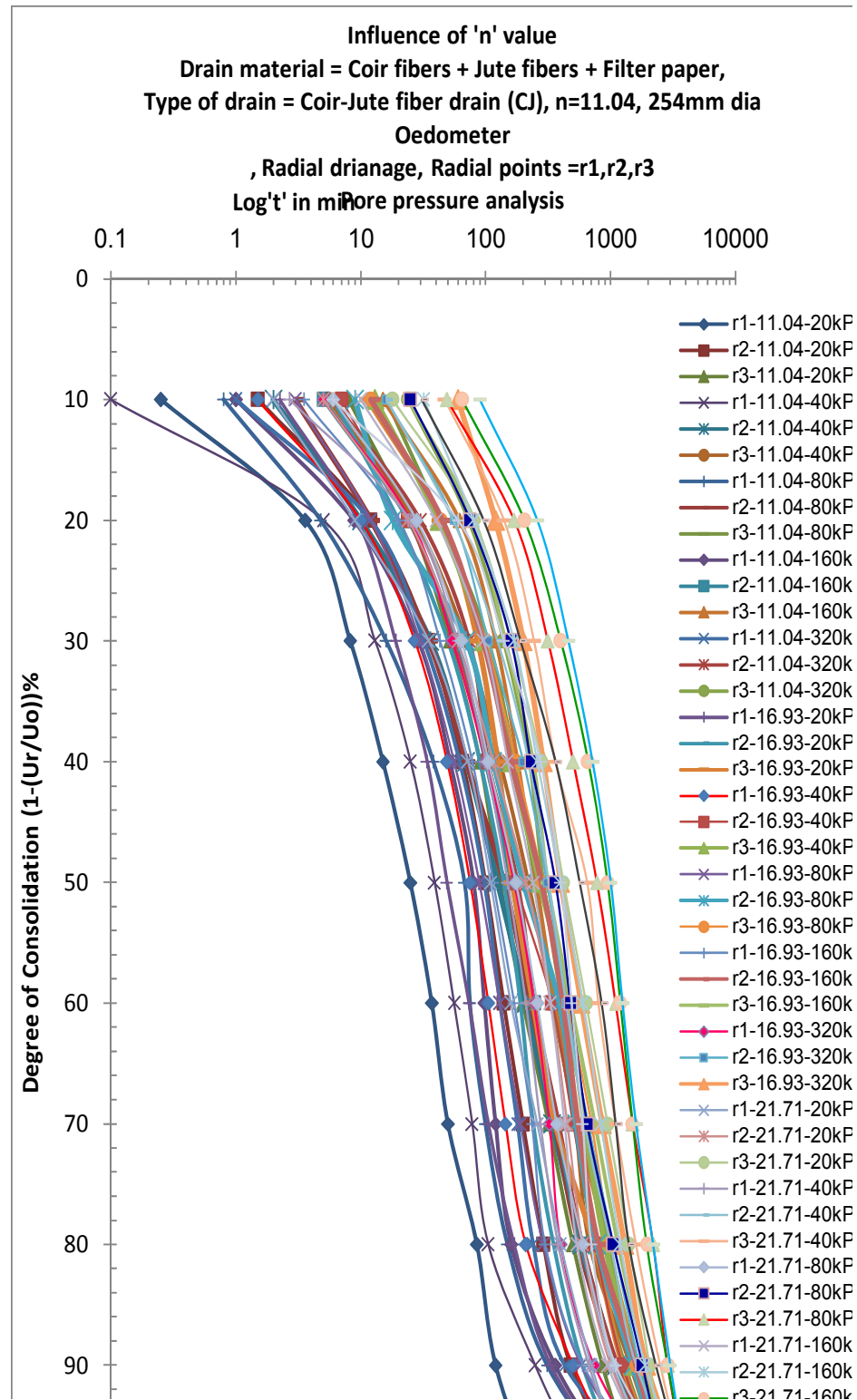


**Fig. 6.129:** Comparison of dissipation of pore water pressure against log't' w.r.t 'n' value for CJ at all pressures

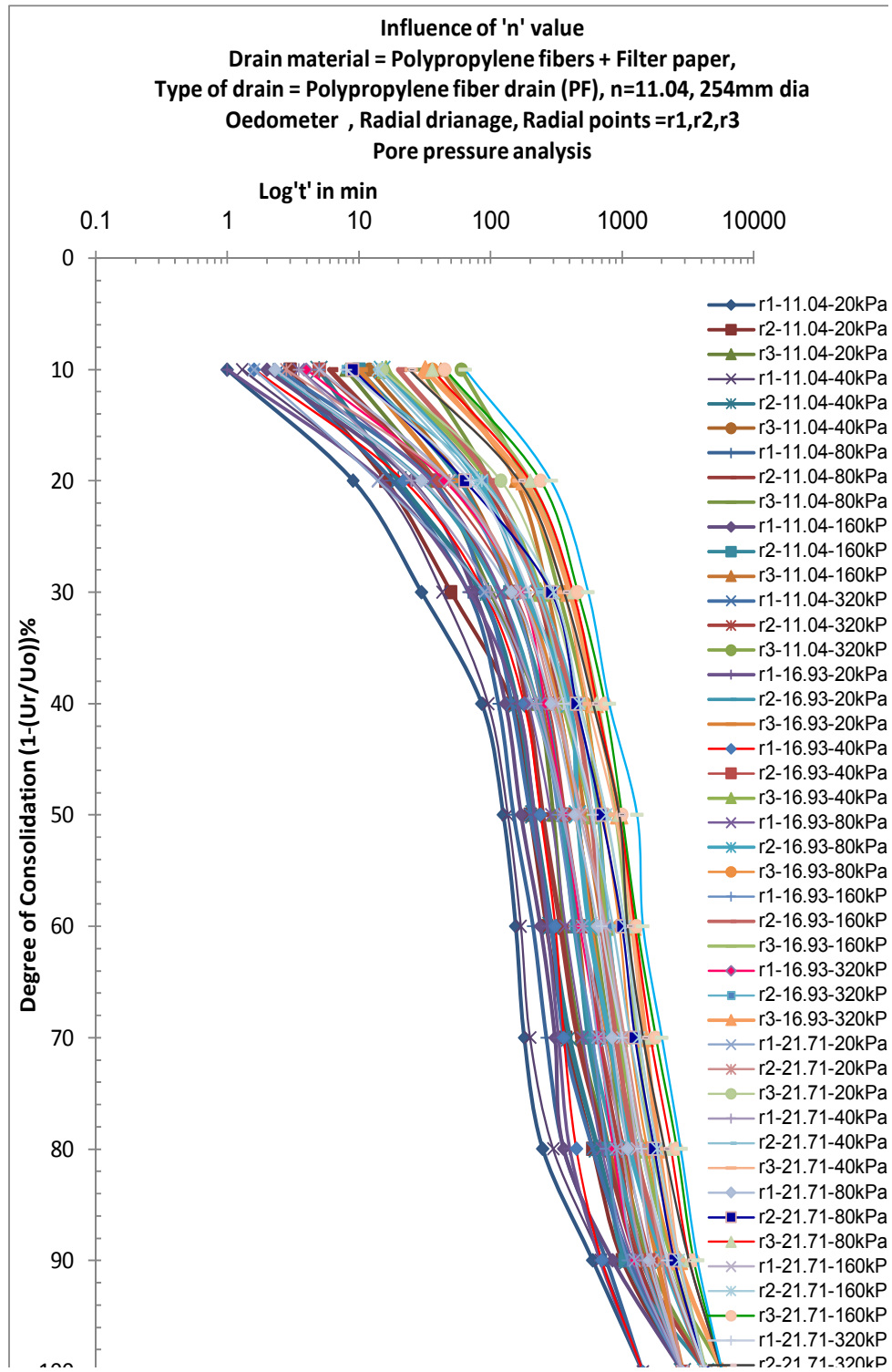


**Fig. 6.130:** Comparison of dissipation of pore water pressure against log't' w.r.t 'n' value for PF at all pressures

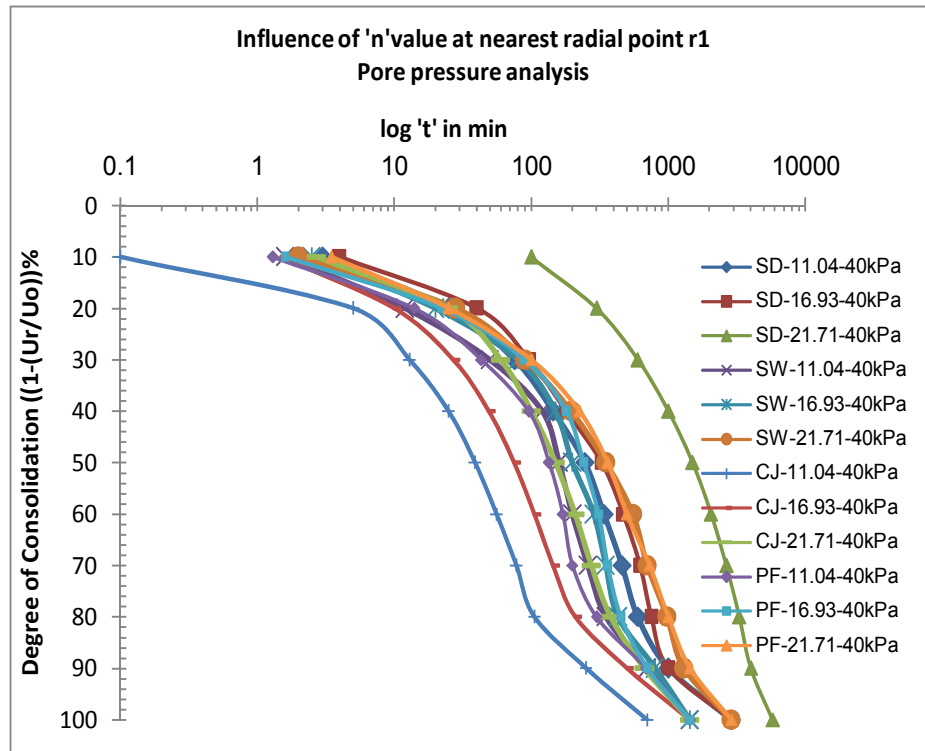


**Fig. 6.131:** Comparison of dissipation of pore water pressure for 'n' values at nearest radial point 'r1' for various vertical drains

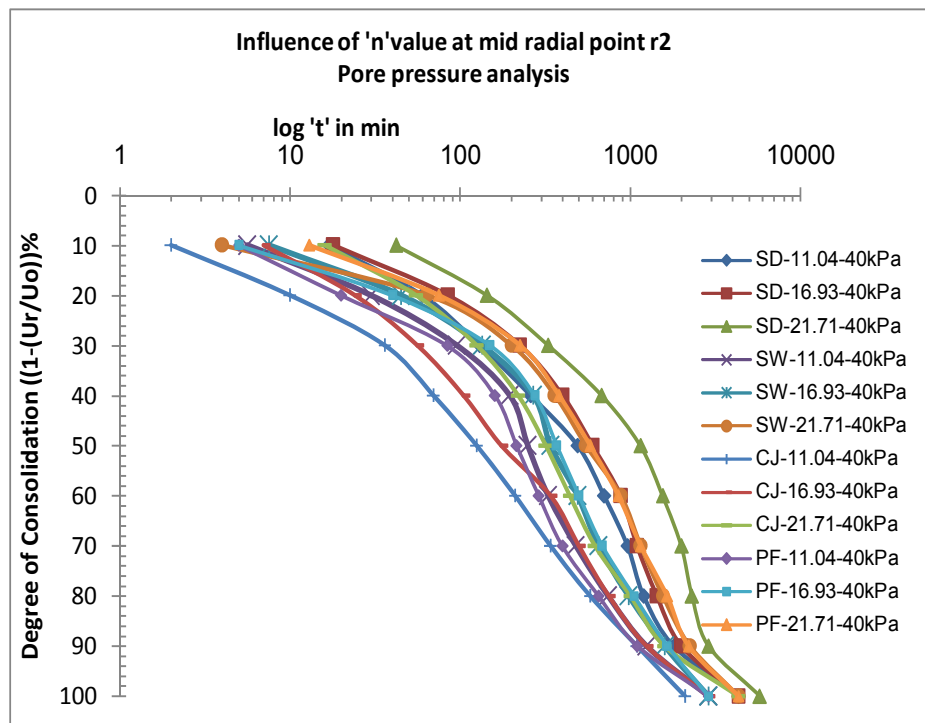


**Fig. 6.132:** Comparison of dissipation of pore water pressure for 'n' values at mid radial point 'r2' for various vertical drains

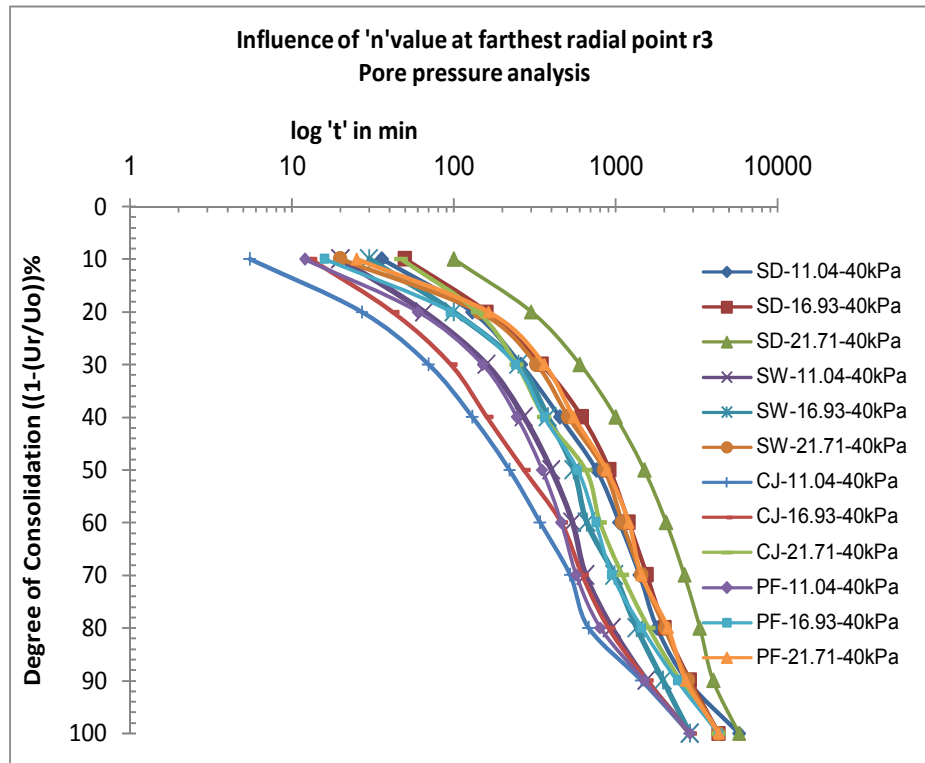


**Fig. 6.133:** Comparison of dissipation of pore water pressure for 'n' values at farthest radial point 'r3' for various vertical drains

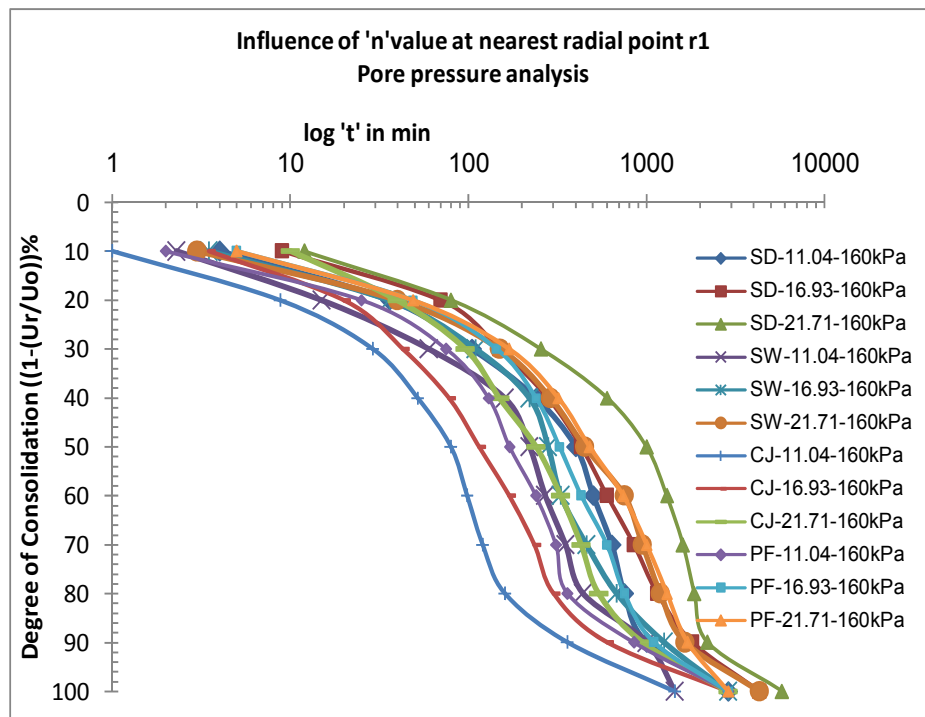


**Fig. 6.134:** Comparison of dissipation of pore water pressure for 'n' values at nearest radial point 'r1' for various vertical drains

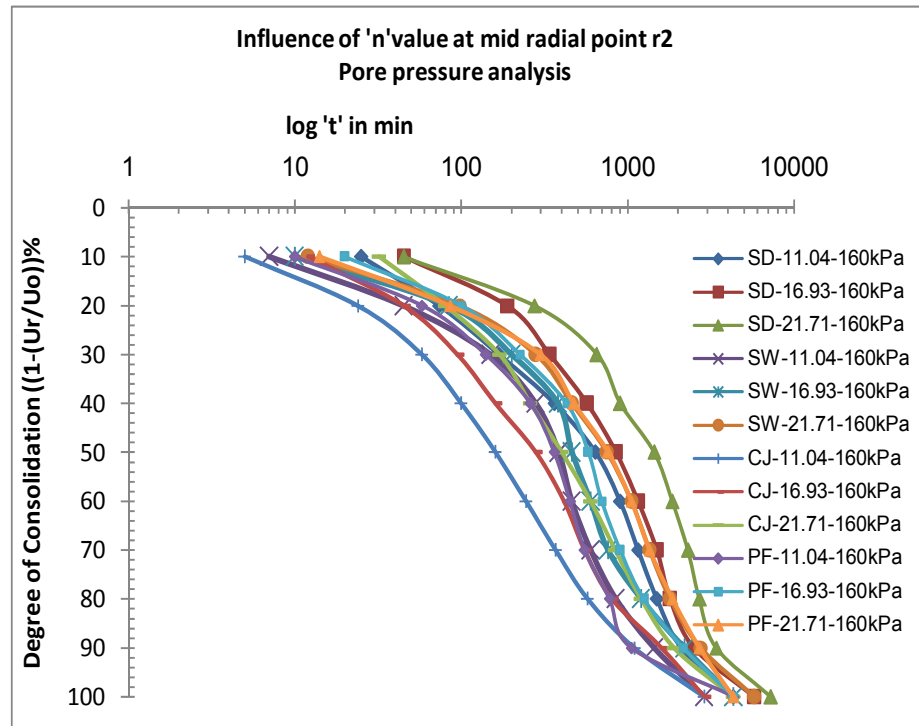


**Fig. 6.135:** Comparison of dissipation of pore water pressure for 'n' values at mid radial point 'r2' for various vertical drains

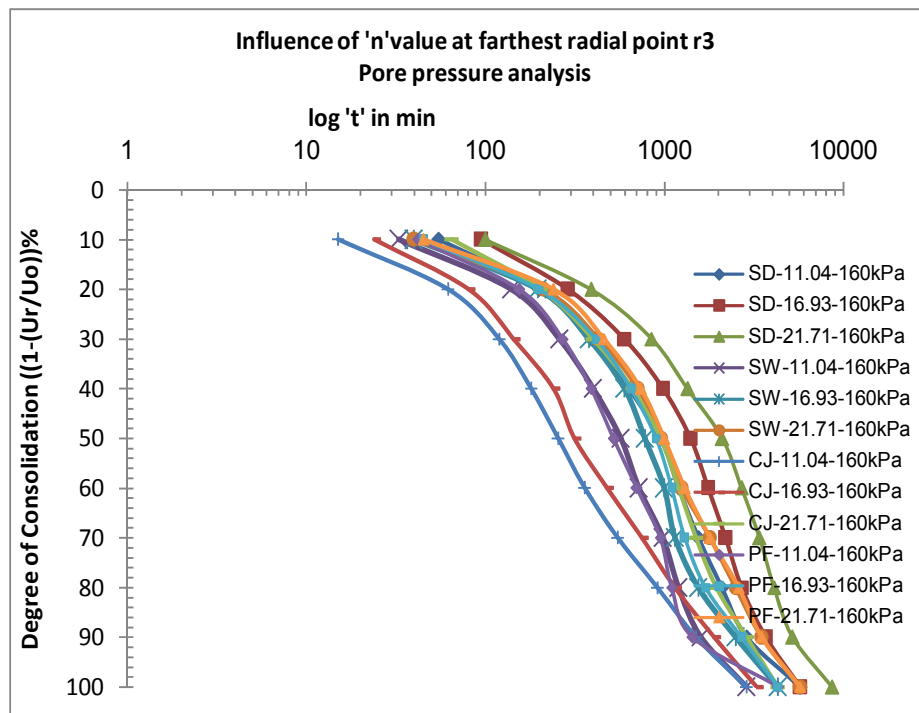


**Fig. 6.136:** Comparison of dissipation of pore water pressure for 'n' values at mid radial point 'r3' for various vertical drains

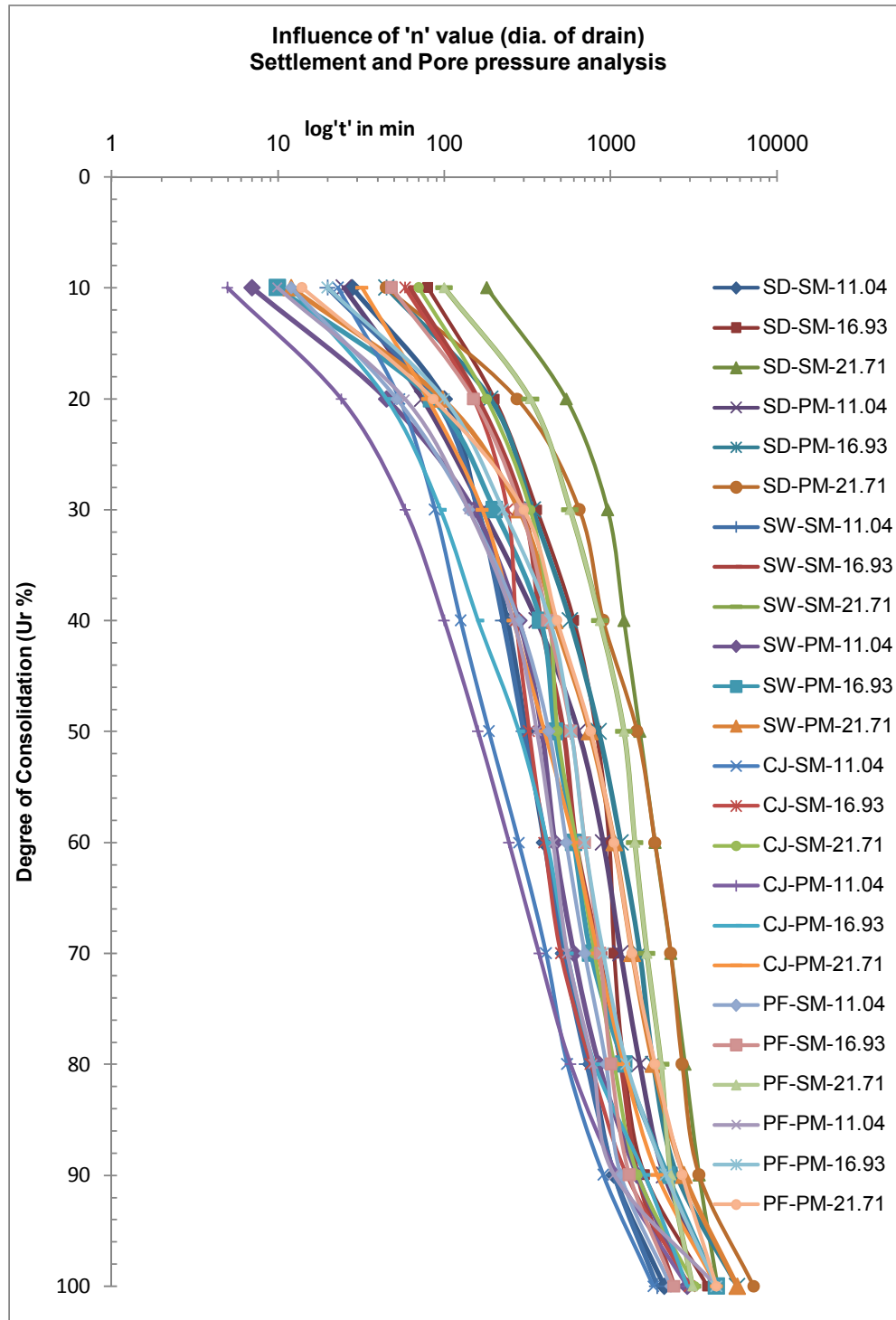
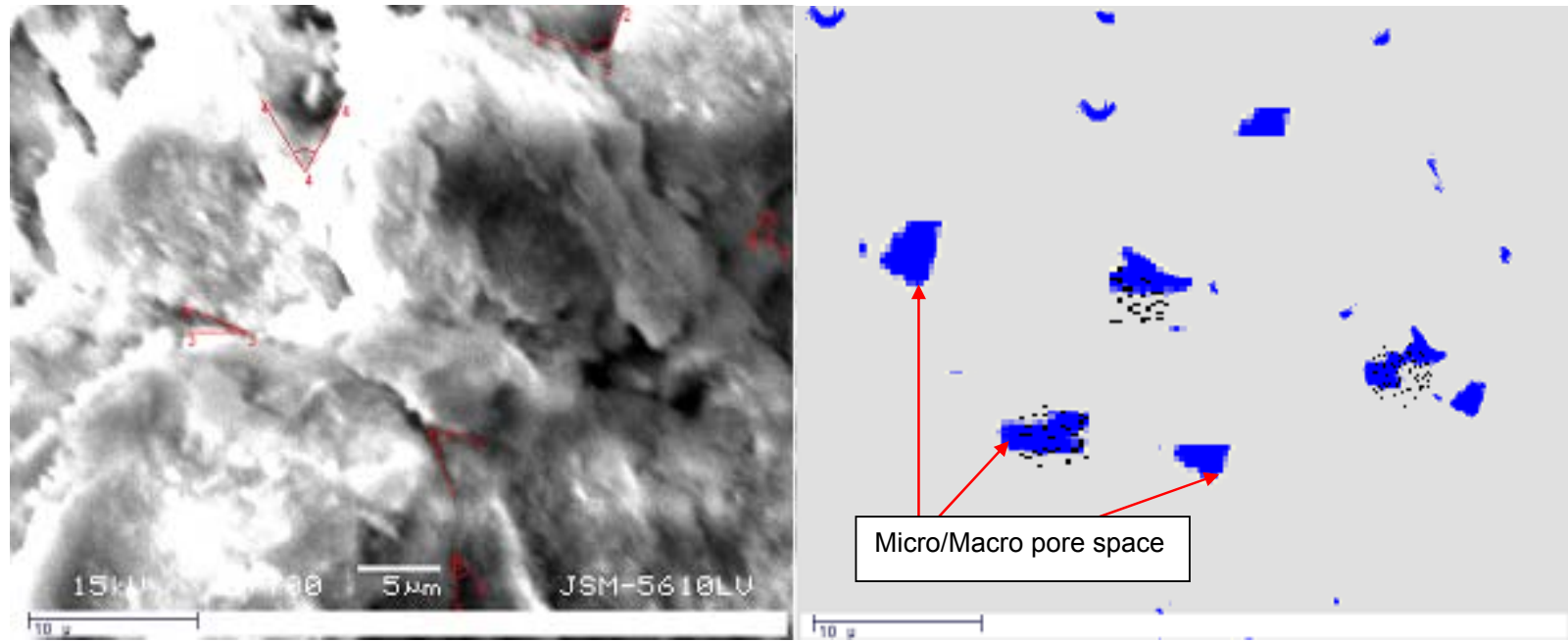


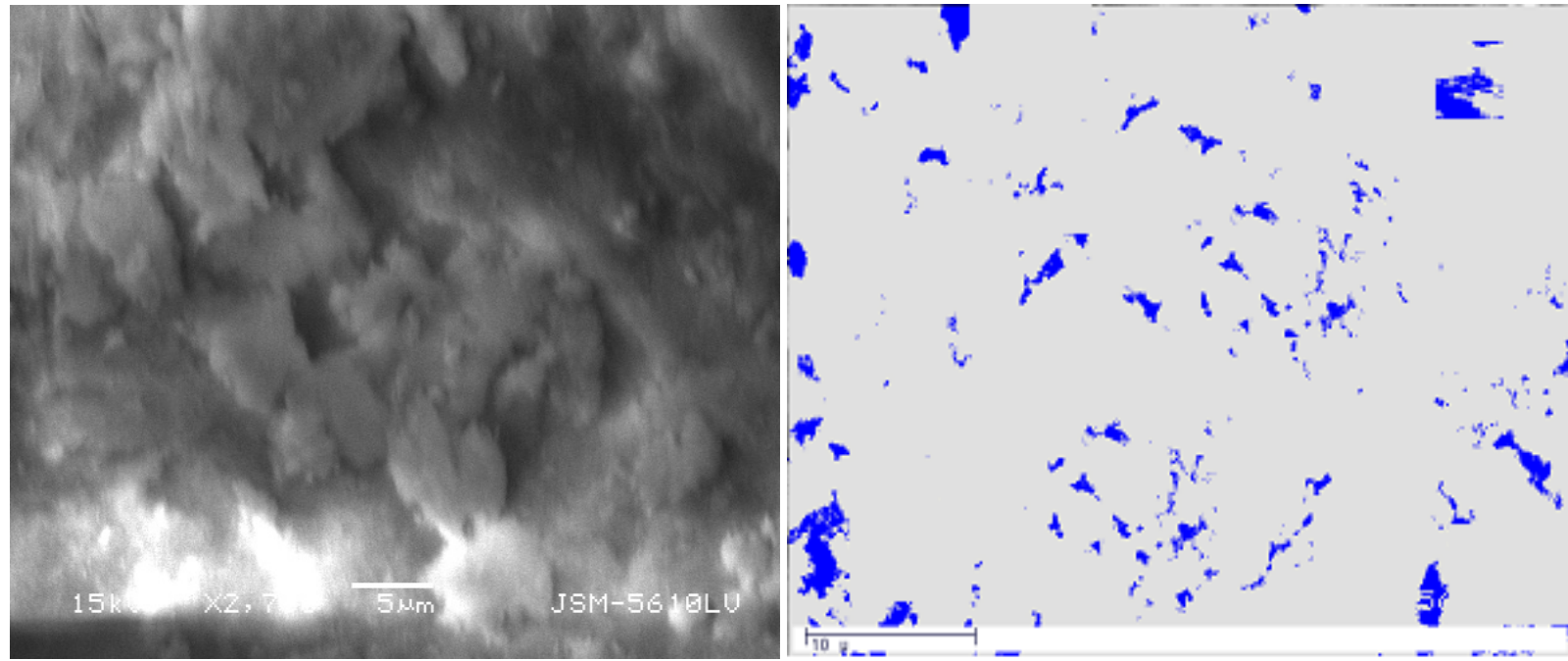
**Fig. 6.137:** Comparison of degree of consolidation vs. time based on settlement analysis and pore pressure analysis at 160kPa pressure



**Photograph 6.13:** Microscopic image of soil consolidated by Sand drain (SD,'n'11.04) at location  $I_{brd}$  and measurement of % porosity and angle of orientation ( $\beta$ ) using MIC software

Note: First image shows particle orientation(red mark) and second image shows porosity(blue mark)

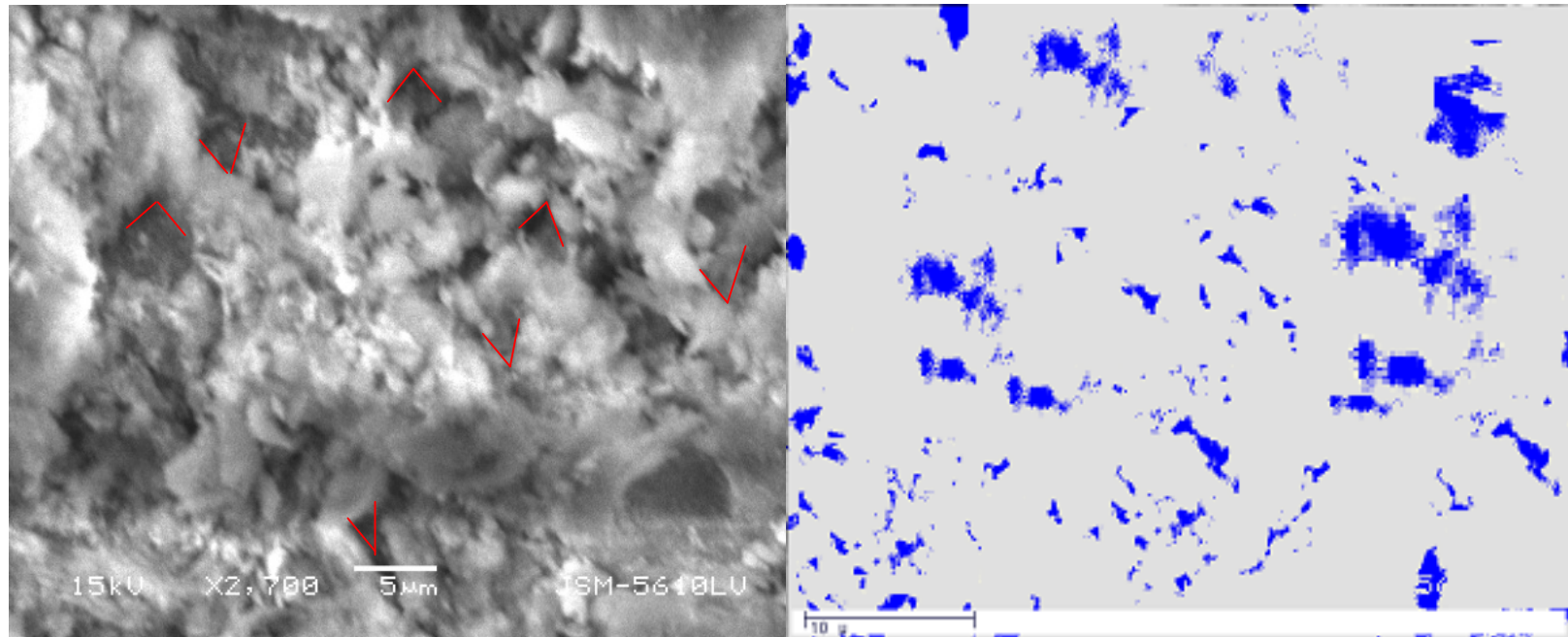




**Photograph 6.14:** Microscopic image of soil consolidated by Sand drain (SD,'n'16.93) at location  $I_{brd}$  and measurement of % porosity and angle of orientation ( $\beta$ ) using MIC software

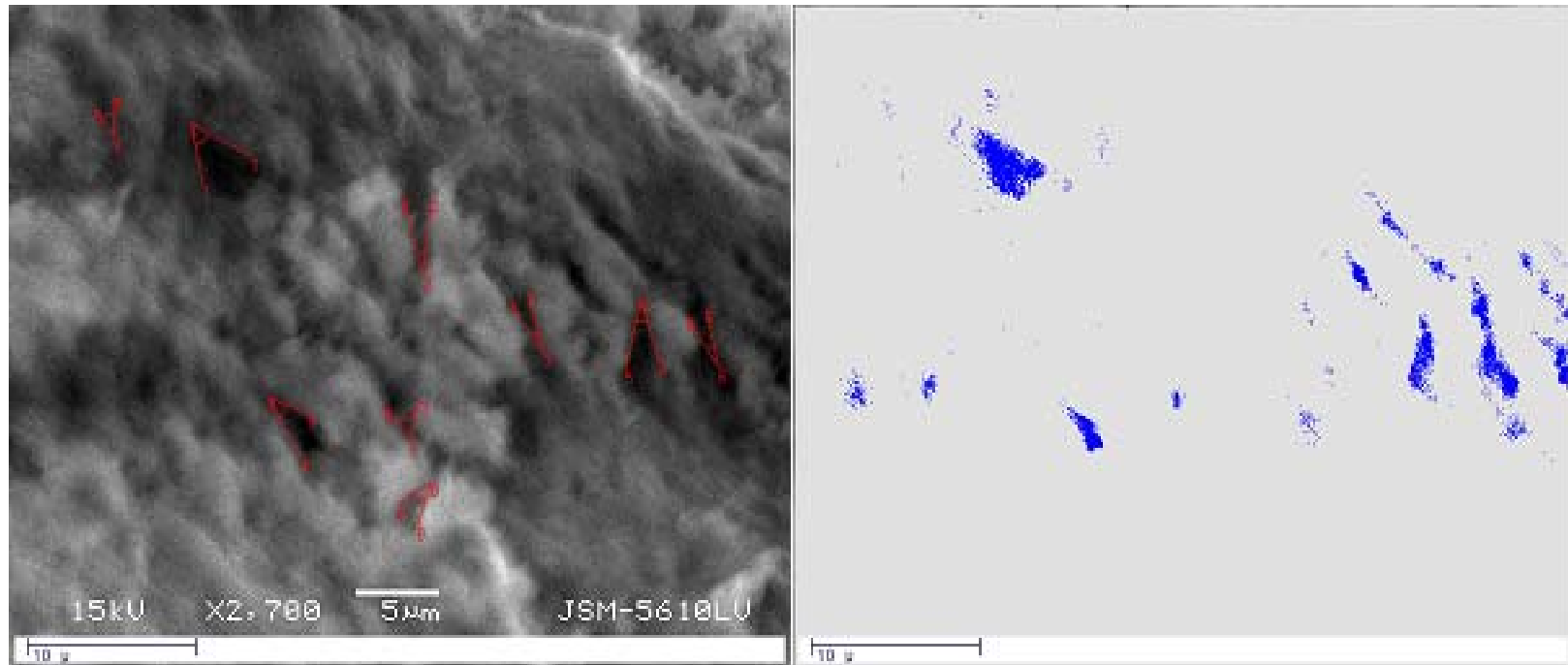
Note: First image shows particle orientation(red mark) and second image shows porosity(blue mark)





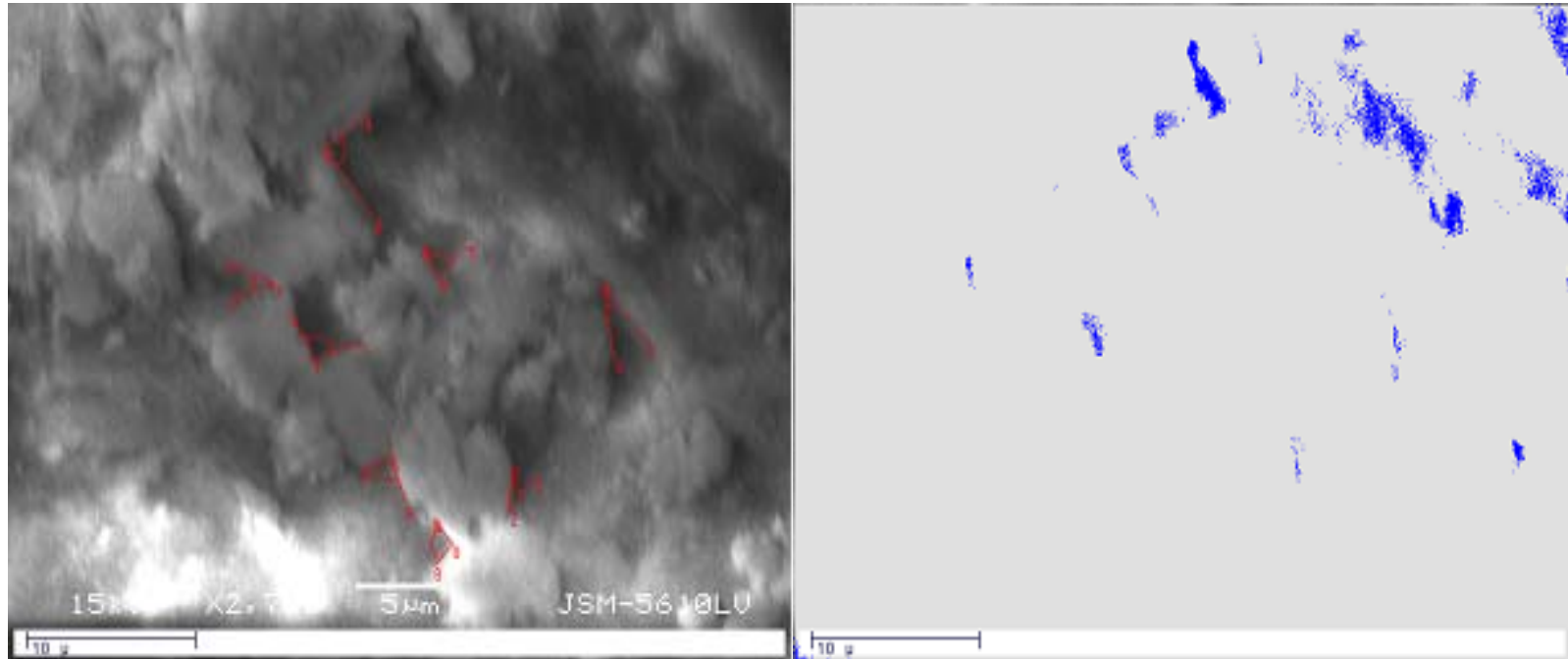
**Photograph 6.15:** Microscopic image of soil consolidated by Sand drain (SD,'n'21.71) at location  $I_{brd}$  and measurement of % porosity and angle of orientation ( $\beta$ ) using MIC software

Note: First image shows particle orientation(red mark) and second image shows porosity(blue mark)



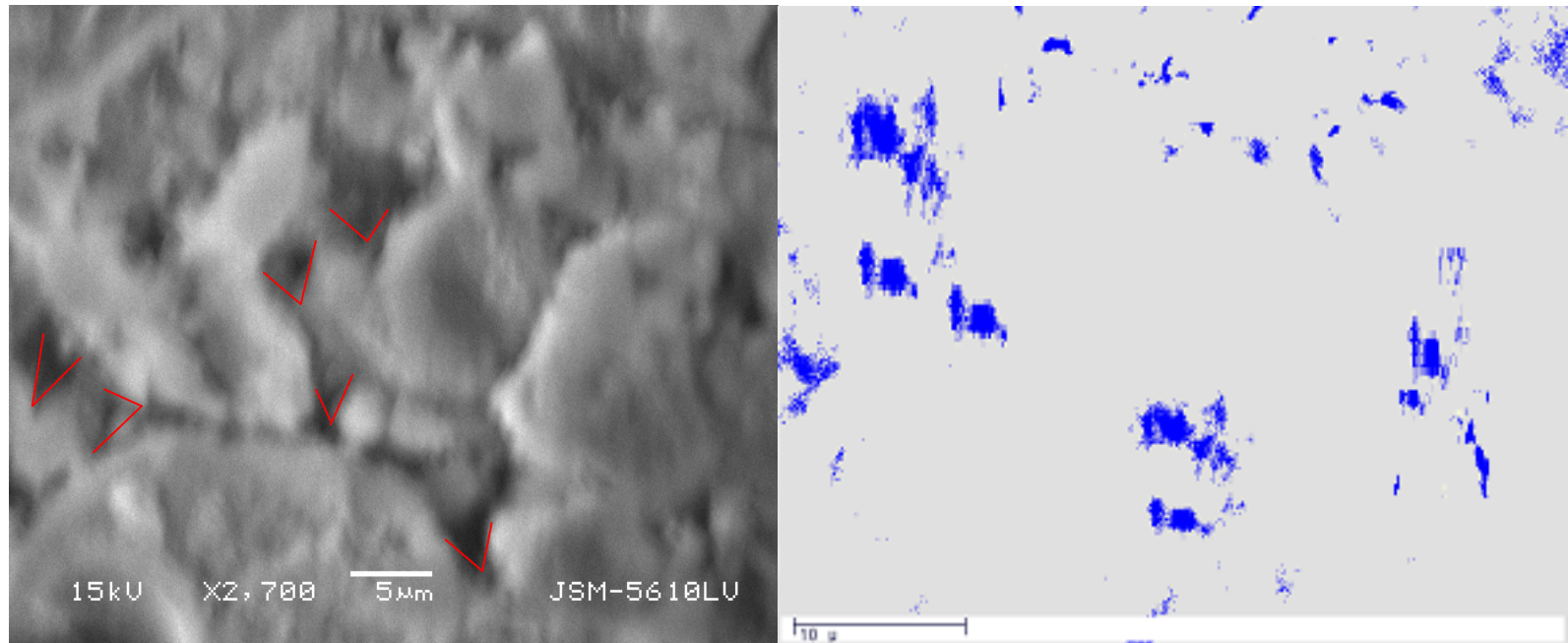
**Photograph 6.16:** Microscopic image of soil consolidated by Coir-Jute fiber drain (CJ,'n'11.04) at location  $I_{brd}$  and measurement of % porosity and angle of orientation ( $\beta$ ) using MIC software

Note: First image shows particle orientation(red mark) and second image shows porosity(blue mark)



**Photograph 6.17:** Microscopic image of soil consolidated by Coir-Jute fiber drain (CJ,'n'16.93) at location  $I_{brd}$  and measurement of % porosity and angle of orientation ( $\beta$ ) using MIC software

Note: First image shows particle orientation(red mark) and second image shows porosity(blue mark)



**Photograph 6.18:** Microscopic image of soil consolidated by Coir-Jute fiber drain (CJ,'n'21.71) at location  $I_{brd}$  and measurement of % porosity and angle of orientation ( $\beta$ ) using MIC software

Note: First image shows particle orientation(red mark) and second image shows porosity(blue mark)

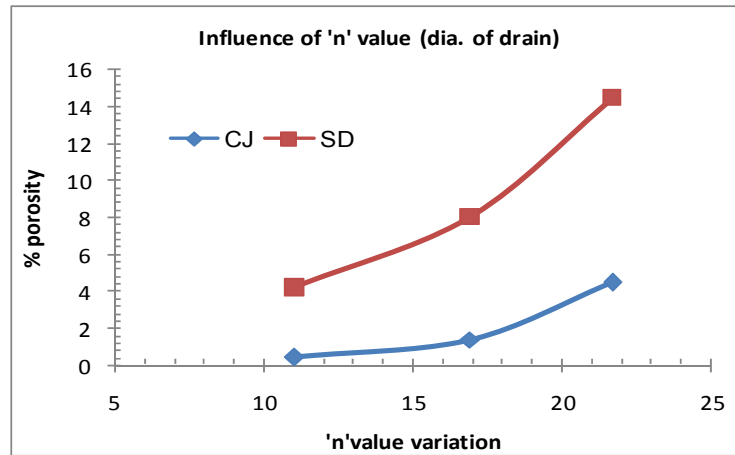


**Fig. 6.138:** Comparison of % porosity on 'n' value using MIC software

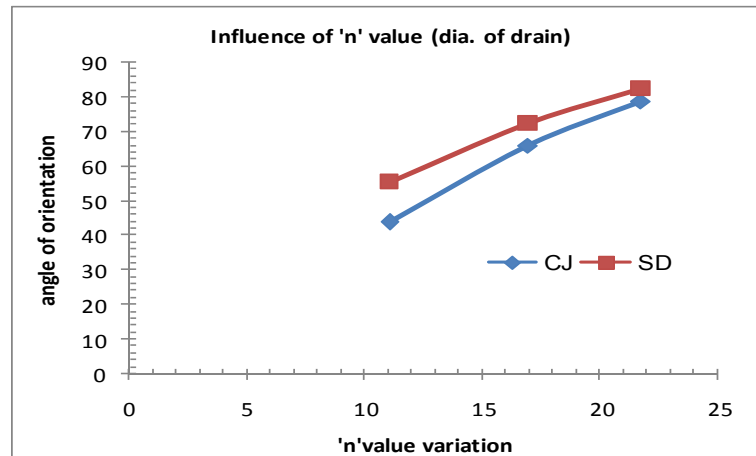


**Fig. 6.139:** Comparison of angle of orientation ( $\beta$ ) on 'n' value using MIC software

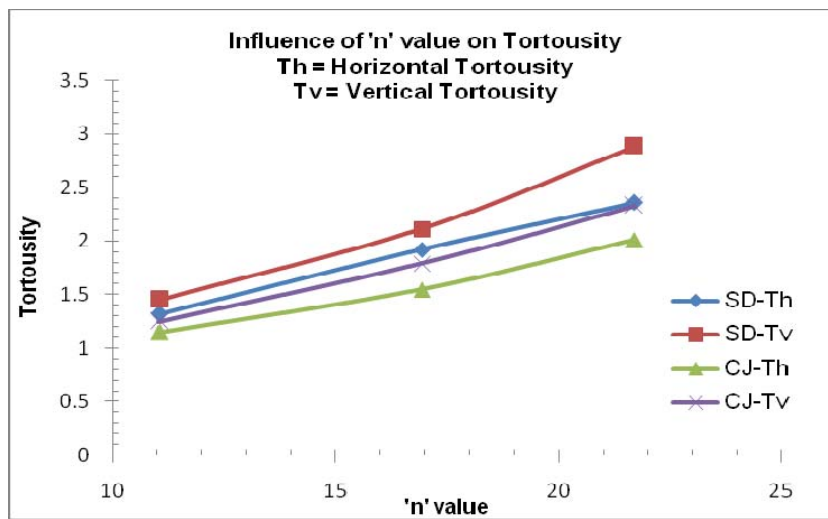


**Fig. 6.140:** Comparison of horizontal and vertical tortuosity on 'n' value using MIC software

**2) Coefficient of consolidation (Cr) vs. Degree of consolidation (Ur) :  
Figures 6.141 to 6.176**

**a) Settlement analysis:-** Fig.6.141 to Fig.6.154 shows comparison plots of Coefficient of consolidation versus degree of consolidation for three 'n' values of 11.04, 16.93 and 21.71 for various vertical drains i.e.CJ, PF, SW & SD at all pressures and also comparative plots are made for 40kPa and 160kPa applied pressures.

- n=11.04, for 50% consolidation CJ shows 78% and 48% higher Cr value in compare to n=16.93 and n=21.71 for 40kPa pressure, while n=11.04 for 80% consolidation CJ shows 71% and 35% higher Cr value in compare to n=16.93 and n=21.71 for 40kPa pressure.
- n=11.04, for 50% consolidation CJ shows 71% and 56% higher Cr value in compare to n=16.93 and n=21.71 for 160kPa pressure, while n=11.04 for 80% consolidation CJ shows 72% and 41% higher Cr value in compare to n=16.93 and n=21.71 for 160kPa pressure.
- n=11.04, for 50% consolidation PF shows 67% and 27% higher Cr value in compare to n=16.93 and n=21.71 for 40kPa pressure, while n=11.04 for 80% consolidation CJ shows 63% and 13% higher Cr value in compare to n=16.93 and n=21.71 for 40kPa pressure.
- n=11.04, for 50% consolidation PF shows 71% and 23% higher Cr value in compare to n=16.93 and n=21.71 for 160kPa pressure, while n=11.04 for 80% consolidation CJ shows 63% and 19% higher Cr value in compare to n=16.93 and n=21.71 for 160kPa pressure.
- n=11.04, for 50% consolidation SW shows 26% and 5% higher Cr value in compare to n=16.93 and n=21.71 for 40kPa pressure, while n=11.04 for 80% consolidation CJ shows 26% and -9% higher Cr value in compare to n=16.93 and n=21.71 for 40kPa pressure.
- n=11.04, for 50% consolidation SW shows 37% and 21% higher Cr value in compare to n=16.93 and n=21.71 for 40kPa pressure, while n=11.04 for 80% consolidation CJ shows 32% and -12% higher Cr value in compare to n=16.93 and n=21.71 for 160kPa pressure.

- $n=11.04$ , for 50% consolidation SD shows 48% and 89% higher  $C_r$  value in compare to  $n=16.93$  and  $n=21.71$  for 40kPa pressure, while  $n=11.04$  for 80% consolidation CJ shows 29% and 88% higher  $C_r$  value in compare to  $n=16.93$  and  $n=21.71$  for 160kPa pressure.
- $n=11.04$ , for 50% consolidation SD shows 59% and 91% higher  $C_r$  value in compare to  $n=16.93$  and  $n=21.71$  for 160kPa pressure, while  $n=11.04$  for 80% consolidation CJ shows 31% and 89% higher  $C_r$  value in compare to  $n=16.93$  and  $n=21.71$  for 160kPa pressure.
- From the above discussions it is clear that out of three 'n' values, the  $n=11.04$  is more efficient in compare to  $n=16.93$  and  $n=21.71$  for all four drains and at all pressures.  $n=11.04$  shows more rate of compressibility in compare to  $n=16.93$  & 21.71.

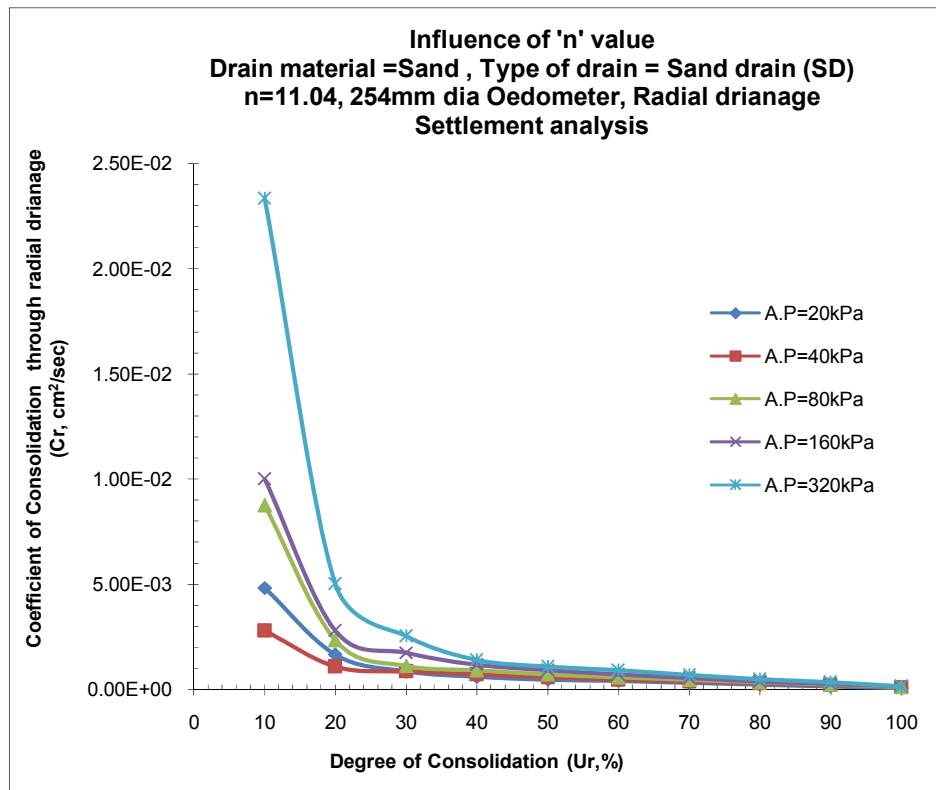


**Fig. 6.141:** Comparison of  $C_r$  against  $U_r$  for SD of 'n'11.04 at all applied pressures

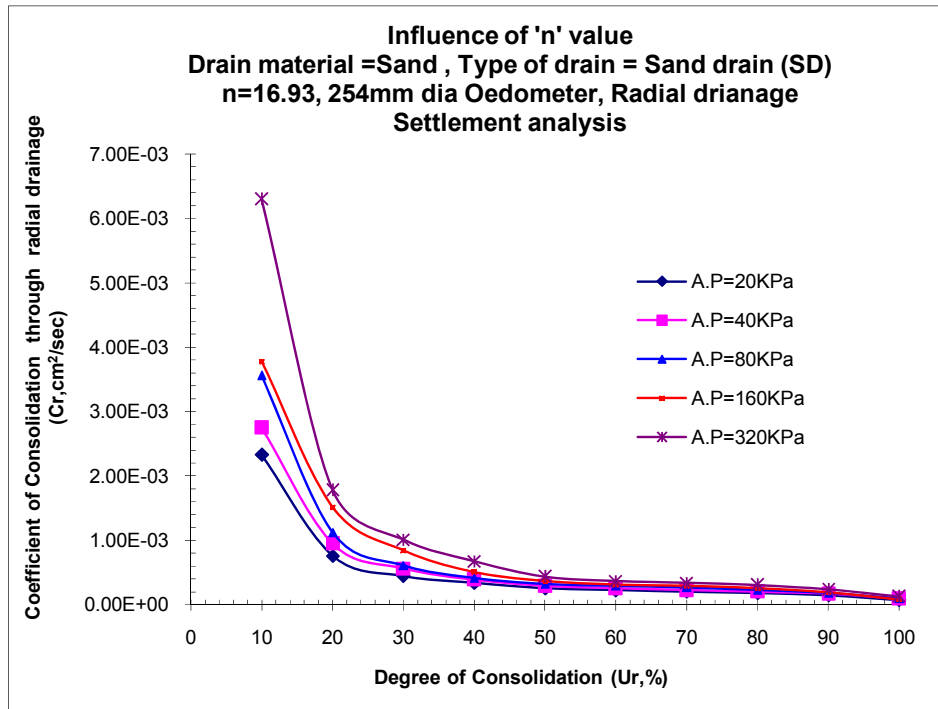


**Fig. 6.142:** Comparison of Cr against Ur for SD of 'n'16.93 at all applied pressures

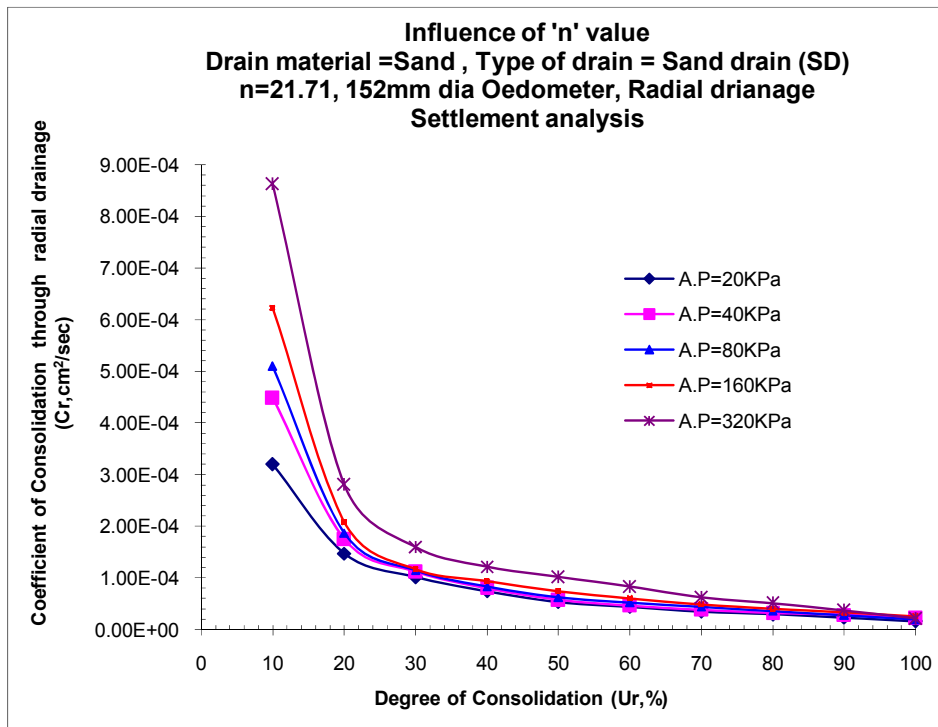


**Fig. 6.143:** Comparison of Cr against Ur for SD of 'n'21.71 at all applied pressures



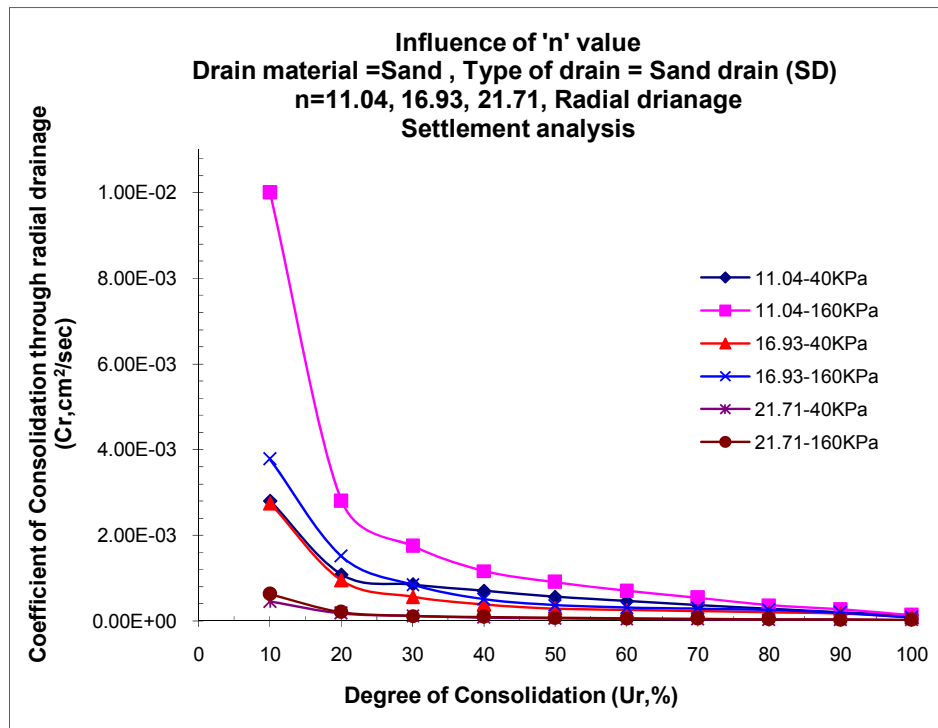


**Fig. 6.144:** Influence of 'n' value on Cr vs. Ur for SD at 40kPa and 160kPa

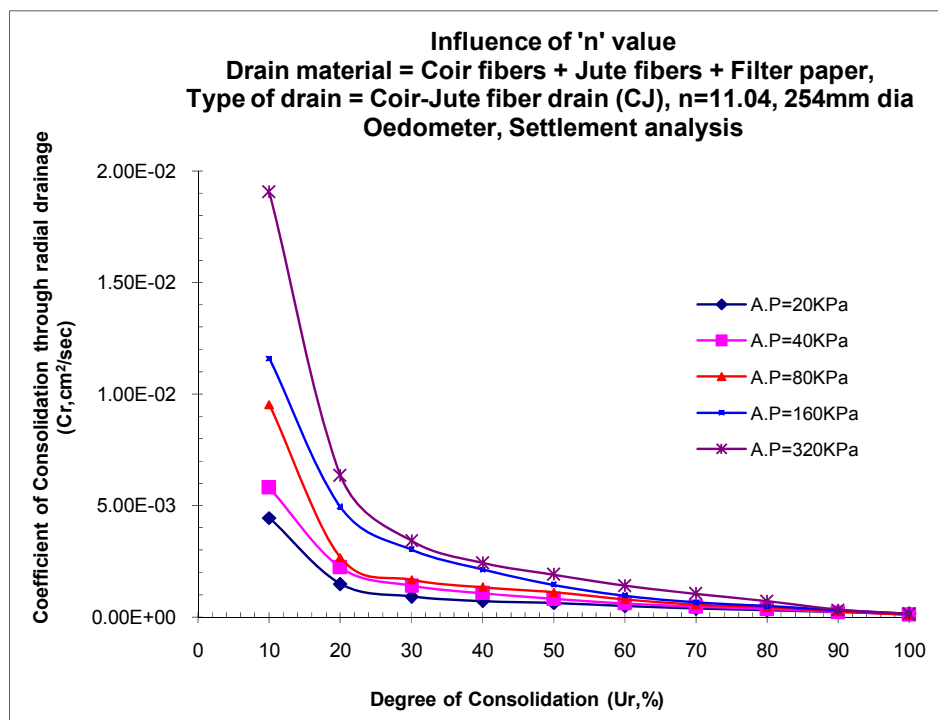


**Fig. 6.145:** Comparison of Cr against Ur for CJ of 'n'11.04 at all applied pressures

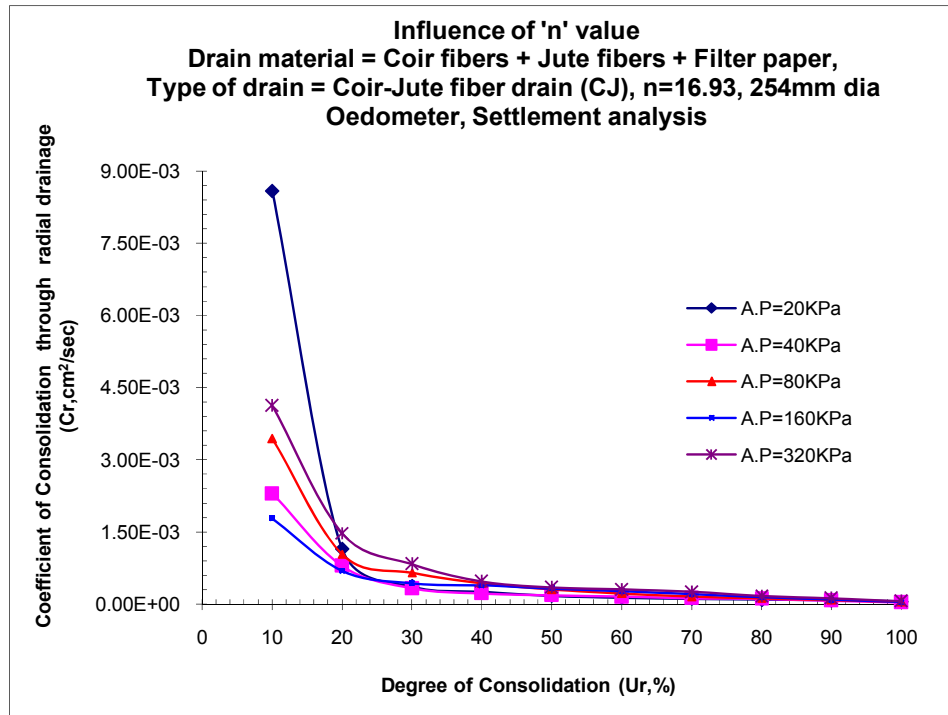


**Fig. 6.146:** Comparison of  $C_r$  against  $U_r$  for CJ of 'n'16.93 at all applied pressures

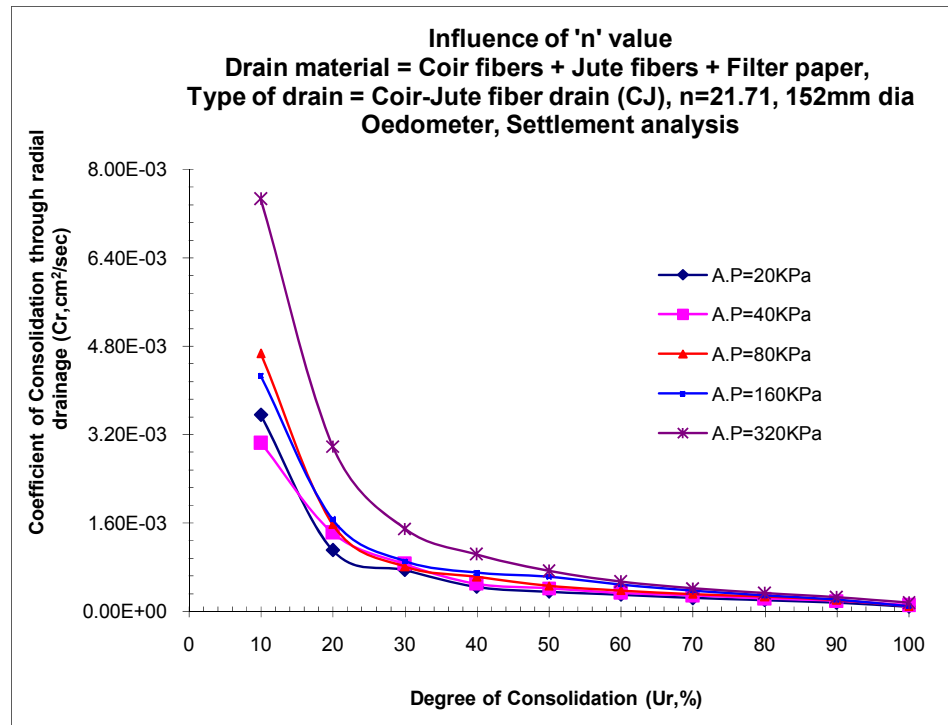


**Fig. 6.147:** Comparison of  $C_r$  against  $U_r$  for CJ of 'n'21.71 at all applied pressures

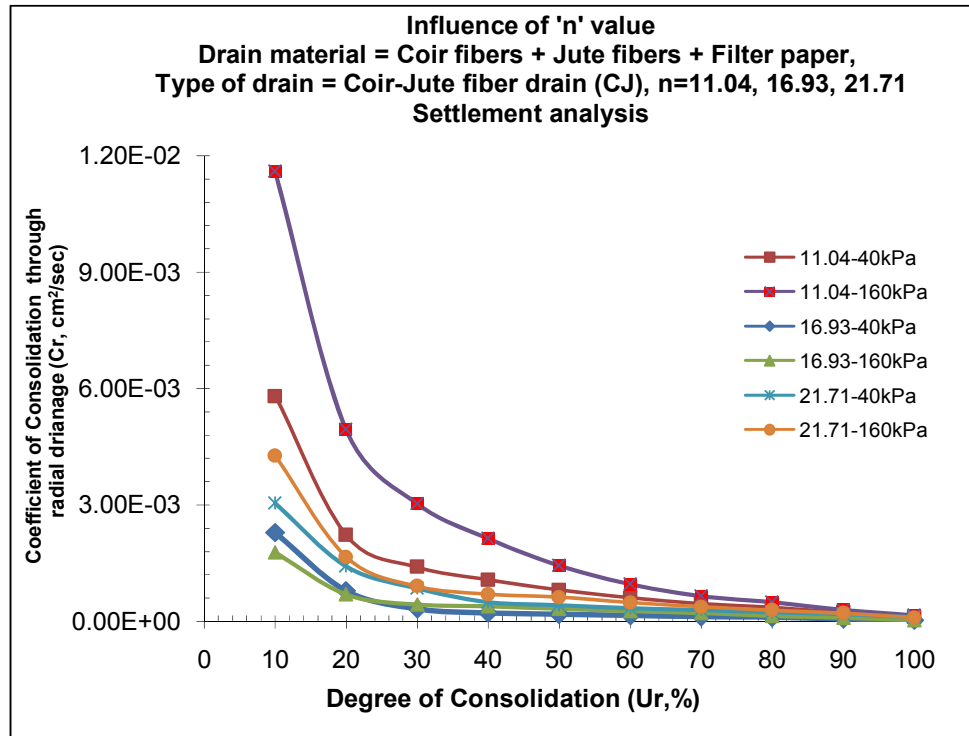


**Fig. 6.148:** Influence of 'n' value on  $C_r$  vs.  $U_r$  for CJ at 40kPa and 160kPa

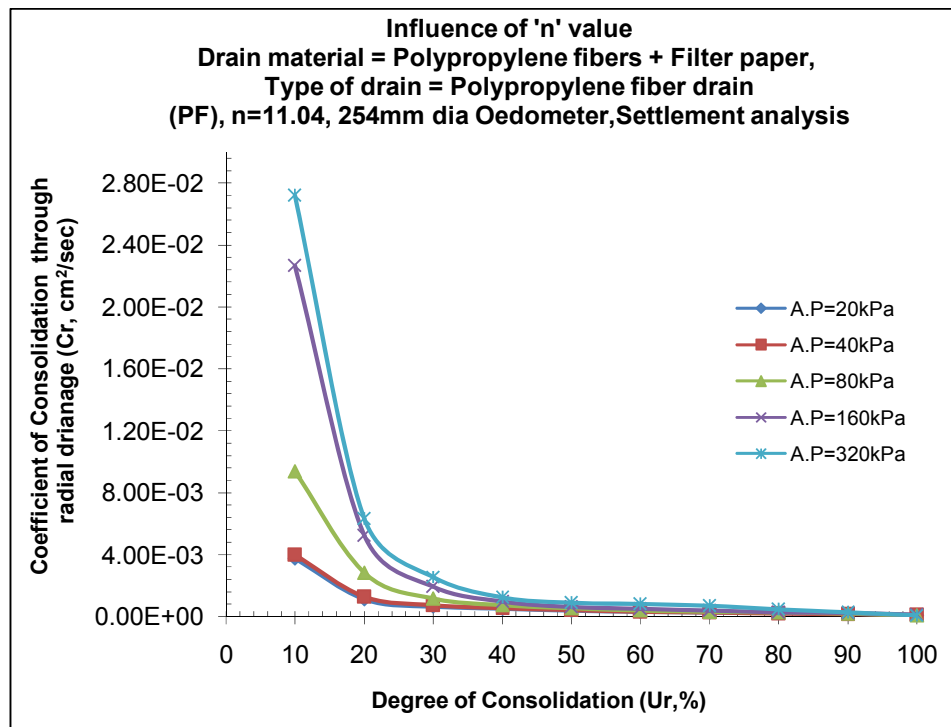


**Fig. 6.149:** Comparison of  $C_r$  against  $U_r$  for PF of 'n'11.04 at all applied pressures

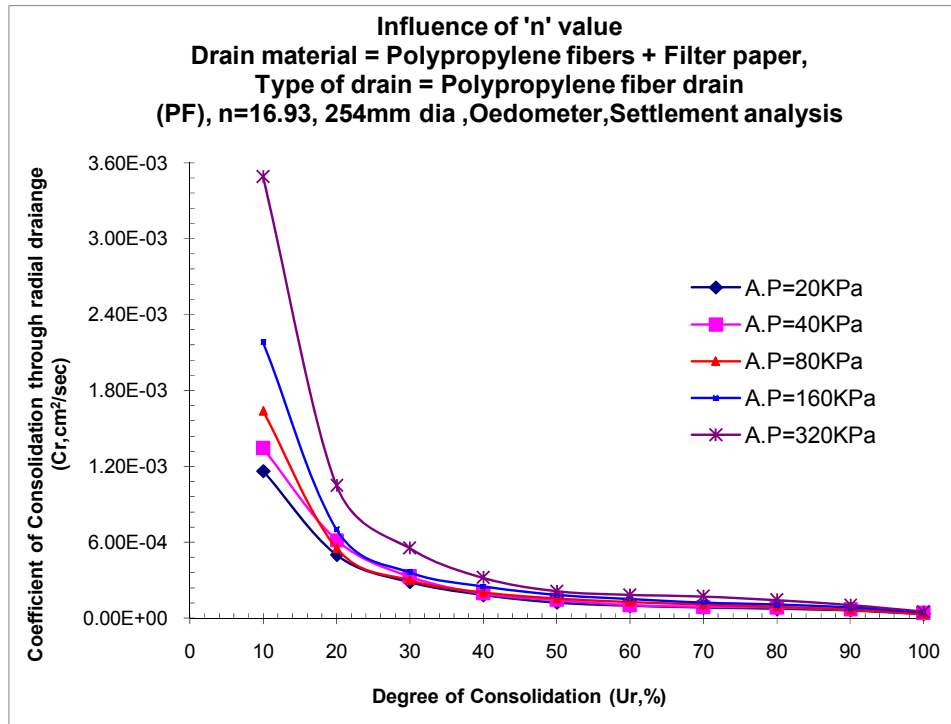


**Fig. 6.150:** Comparison of  $C_r$  against  $U_r$  for PF of ' $n$ '16.93 at all applied pressures

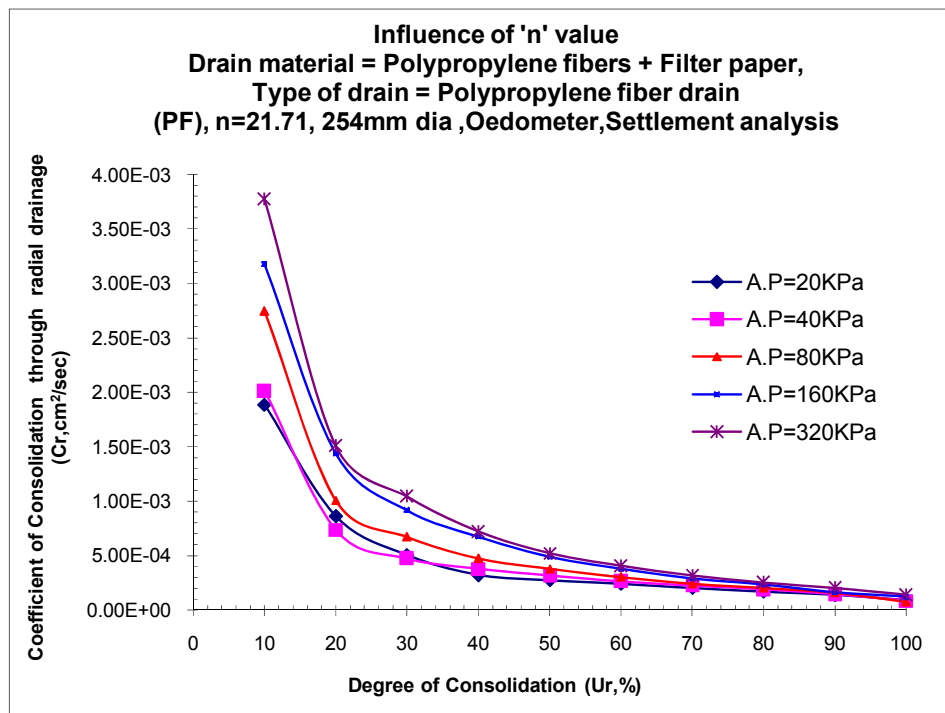


**Fig. 6.151:** Comparison of  $C_r$  against  $U_r$  for PF of ' $n$ '21.71 at all applied pressures

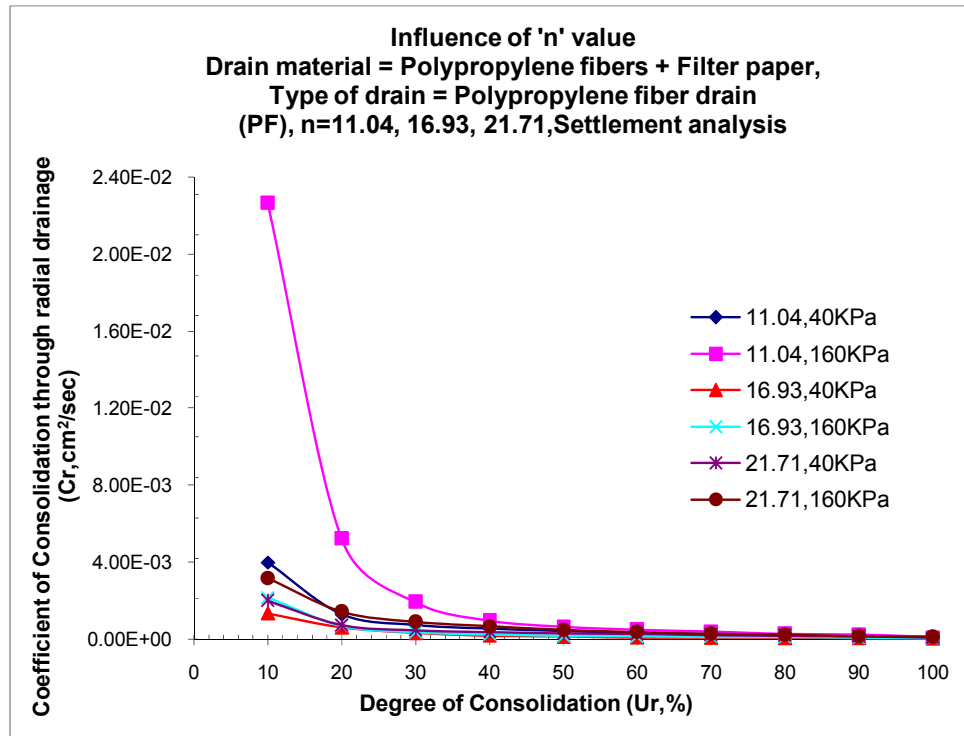


**Fig. 6.152:** Influence of 'n' value on Cr vs. Ur for PF at 40kPa and 160kPa

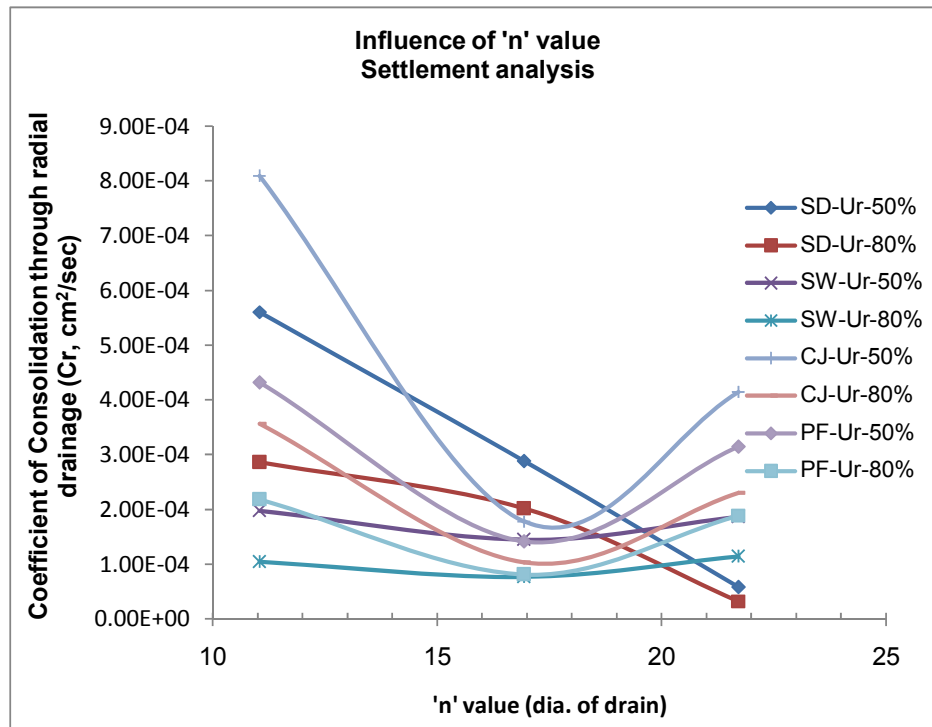


**Fig. 6.153:** Comparison of Cr vs. 'n' value at Ur50% and Ur80% at 40kPa

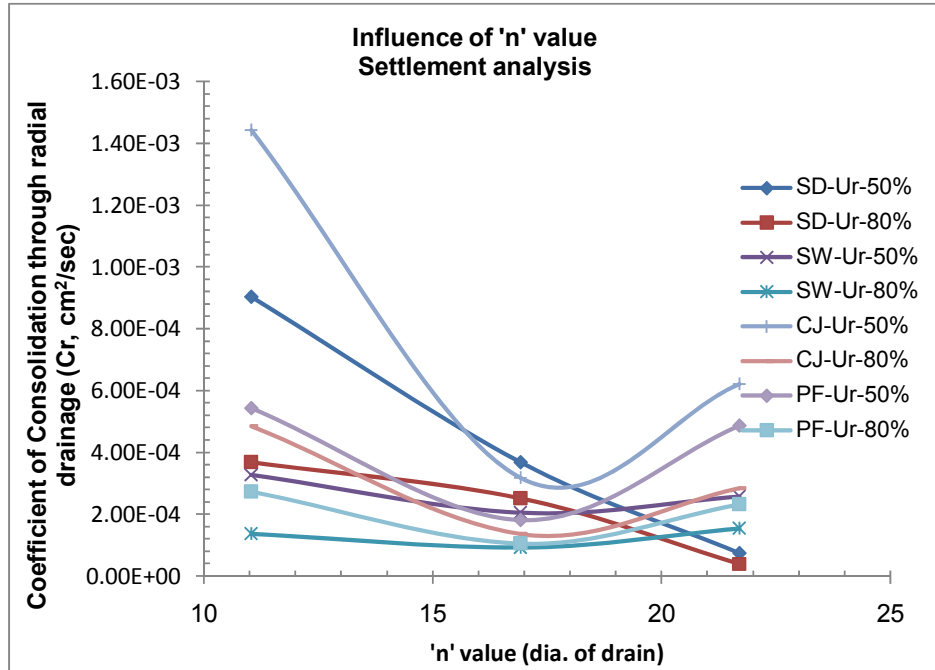


**Fig. 6.154:** Comparison of  $C_r$  vs. 'n' value at Ur50% and Ur80% at 160kPa

**Table 6.4:** Comparison of  $C_r$  values for various drain materials based on settlement and pore pressure analysis

| Drain Type | 'n' value | Settlement based              |                       | Pore pressure based- $r_2$    |                       |
|------------|-----------|-------------------------------|-----------------------|-------------------------------|-----------------------|
|            |           | $C_r(\text{cm}^2/\text{sec})$ |                       | $C_r(\text{cm}^2/\text{sec})$ |                       |
|            |           | Ur (50%)-40kPa                | Ur (80%)-40kPa        | Ur (50%)-40kPa                | Ur (80%)-40kPa        |
| SD         | 11.04     | $5.60 \times 10^{-4}$         | $2.86 \times 10^{-4}$ | $1.54 \times 10^{-4}$         | $6.29 \times 10^{-5}$ |
|            | 16.93     | $2.88 \times 10^{-4}$         | $2.02 \times 10^{-4}$ | $1.51 \times 10^{-4}$         | $6.30 \times 10^{-5}$ |
|            | 21.71     | $5.75 \times 10^{-5}$         | $3.20 \times 10^{-5}$ | $3.17 \times 10^{-5}$         | $1.59 \times 10^{-5}$ |
| SW         | 11.04     | $1.97 \times 10^{-4}$         | $1.04 \times 10^{-4}$ | $1.29 \times 10^{-4}$         | $4.36 \times 10^{-5}$ |
|            | 16.93     | $1.44 \times 10^{-4}$         | $7.61 \times 10^{-5}$ | $9.08 \times 10^{-5}$         | $3.15 \times 10^{-5}$ |
|            | 21.71     | $1.86 \times 10^{-4}$         | $1.14 \times 10^{-4}$ | $1.61 \times 10^{-4}$         | $5.72 \times 10^{-5}$ |
| CJ         | 11.04     | $8.09 \times 10^{-4}$         | $3.56 \times 10^{-4}$ | $5.77 \times 10^{-4}$         | $1.24 \times 10^{-4}$ |
|            | 16.93     | $1.78 \times 10^{-4}$         | $1.03 \times 10^{-4}$ | $1.74 \times 10^{-4}$         | $4.06 \times 10^{-5}$ |
|            | 21.71     | $4.14 \times 10^{-4}$         | $2.30 \times 10^{-4}$ | $2.71 \times 10^{-4}$         | $8.77 \times 10^{-5}$ |
| PF         | 11.04     | $4.32 \times 10^{-4}$         | $2.18 \times 10^{-4}$ | $3.46 \times 10^{-4}$         | $1.14 \times 10^{-4}$ |
|            | 16.93     | $1.41 \times 10^{-4}$         | $8.05 \times 10^{-5}$ | $8.57 \times 10^{-5}$         | $3.02 \times 10^{-5}$ |
|            | 21.71     | $3.14 \times 10^{-4}$         | $1.89 \times 10^{-4}$ | $1.67 \times 10^{-4}$         | $5.86 \times 10^{-5}$ |

| Drain Type | 'n' value | Settlement based         |                         | Pore pressure based-r <sub>2</sub> |                         |
|------------|-----------|--------------------------|-------------------------|------------------------------------|-------------------------|
|            |           | Cr(cm <sup>2</sup> /sec) |                         | Cr(cm <sup>2</sup> /sec)           |                         |
|            |           | Ur (50%)-160kPa          | Ur (80%)-160kPa         | Ur (50%)-160kPa                    | Ur (80%)-160kPa         |
| SD         | 11.04     | 9.04 x 10 <sup>-4</sup>  | 3.69 x 10 <sup>-4</sup> | 1.18 x 10 <sup>-4</sup>            | 5.04 x 10 <sup>-5</sup> |
|            | 16.93     | 3.69 x 10 <sup>-4</sup>  | 2.52 x 10 <sup>-4</sup> | 1.07 x 10 <sup>-4</sup>            | 5.04 x 10 <sup>-5</sup> |
|            | 21.71     | 7.48 x 10 <sup>-5</sup>  | 4.00 x 10 <sup>-5</sup> | 2.53 x 10 <sup>-5</sup>            | 1.35 x 10 <sup>-5</sup> |
| SW         | 11.04     | 3.28 x 10 <sup>-4</sup>  | 1.37 x 10 <sup>-4</sup> | 8.38 x 10 <sup>-5</sup>            | 3.79 x 10 <sup>-5</sup> |
|            | 16.93     | 2.05 x 10 <sup>-4</sup>  | 9.26 x 10 <sup>-5</sup> | 6.71 x 10 <sup>-5</sup>            | 2.57 x 10 <sup>-5</sup> |
|            | 21.71     | 2.56 x 10 <sup>-4</sup>  | 1.54 x 10 <sup>-4</sup> | 1.18 x 10 <sup>-4</sup>            | 4.93 x 10 <sup>-5</sup> |
| CJ         | 11.04     | 1.44 x 10 <sup>-3</sup>  | 4.85 x 10 <sup>-4</sup> | 4.51 x 10 <sup>-4</sup>            | 1.25 x 10 <sup>-4</sup> |
|            | 16.93     | 3.17 x 10 <sup>-4</sup>  | 4.85 x 10 <sup>-4</sup> | 1.09 x 10 <sup>-4</sup>            | 3.81 x 10 <sup>-5</sup> |
|            | 21.71     | 6.22 x 10 <sup>-4</sup>  | 4.85 x 10 <sup>-4</sup> | 2.19 x 10 <sup>-4</sup>            | 7.31 x 10 <sup>-5</sup> |
| PF         | 11.04     | 5.44 x 10 <sup>-4</sup>  | 2.72 x 10 <sup>-4</sup> | 2.06 x 10 <sup>-4</sup>            | 9.53 x 10 <sup>-5</sup> |
|            | 16.93     | 1.80 x 10 <sup>-4</sup>  | 1.05 x 10 <sup>-4</sup> | 5.46 x 10 <sup>-5</sup>            | 2.54 x 10 <sup>-5</sup> |
|            | 21.71     | 4.87 x 10 <sup>-4</sup>  | 2.32 x 10 <sup>-4</sup> | 1.27 x 10 <sup>-4</sup>            | 5.23 x 10 <sup>-5</sup> |

**b) Pore pressure analysis:-** Fig.6.155 to Fig.6.176 shows the comparison plots of Coefficient of consolidation versus degree of consolidation at three radial points' r<sub>1</sub>, r<sub>2</sub>, r<sub>3</sub> for vertical drains i.e. CJ, SW, PF, SD & analysis is carried out for all three 'n' values i.e. 11.04, 16.93 and 21.71 for all pressures. Here results are presented for all pressures and comparative plots are also presented for 40kPa & 160kPa pressures.

- n=11.04, for 50% consolidation, for radial point r<sub>1</sub>, CJ shows -37% and 47% higher Cr value in compare to n=16.93 and n=21.71 for 40kPa pressure, while n=11.04 for 80% consolidation CJ shows -32% and 44% higher Cr value in compare to n=16.93 and n=21.71 for 40kPa pressure. Similarly for radial point r<sub>2</sub>, CJ shows 69% and 52% higher Cr value in compare to n=16.93 and n=21.71 for 40kPa pressure, while n=11.04 for 80% consolidation CJ shows 67% and 29% higher Cr value in compare to n=16.93 and n=21.71 for 40kPa pressure. Similarly for radial point r<sub>3</sub>, CJ shows 75% and 61% higher Cr value in compare to n=16.93 and n=21.71 for 40kPa pressure, while n=11.04 for 80% consolidation CJ shows 77% and 51% higher Cr value in compare to n=16.93 and n=21.71 for 40kPa pressure.
- n=11.04, for 50% consolidation, for radial point r<sub>1</sub>, SW shows 26% and 68% higher Cr value in compare to n=16.93 and n=21.71 for 40kPa pressure,

while  $n=11.04$  for 80% consolidation SW shows 24% and 75% higher Cr value in compare to  $n=16.93$  and  $n=21.71$  for 40kPa pressure. Similarly for radial point r2, SW shows 29% and -25% higher Cr value in compare to  $n=16.93$  and  $n=21.71$  for 40kPa pressure, while  $n=11.04$  for 80% consolidation SW shows 27% and -31% higher Cr value in compare to  $n=16.93$  and  $n=21.71$  for 40kPa pressure. Similarly for radial point r3, SW shows 29% and -74% higher Cr value in compare to  $n=16.93$  and  $n=21.71$  for 40kPa pressure, while  $n=11.04$  for 80% consolidation SW shows 31% and -75% higher Cr value in compare to  $n=16.93$  and  $n=21.71$  for 40kPa pressure.

- $n=11.04$ , for 50% consolidation, for radial point r1, PF shows -50% and 26% higher Cr value in compare to  $n=16.93$  and  $n=21.71$  for 40kPa pressure, while  $n=11.04$  for 80% consolidation PF shows -77% and 36% higher Cr value in compare to  $n=16.93$  and  $n=21.71$  for 40kPa pressure. Similarly for radial point r2, PF shows 75% and 51% higher Cr value in compare to  $n=16.93$  and  $n=21.71$  for 40kPa pressure, while  $n=11.04$  for 80% consolidation PF shows 73% and 48% higher Cr value in compare to  $n=16.93$  and  $n=21.71$  for 40kPa pressure. Similarly for radial point r3, PF shows 81% and 51% higher Cr value in compare to  $n=16.93$  and  $n=21.71$  for 40kPa pressure, while  $n=11.04$  for 80% consolidation PF shows 83% and 53% higher Cr value in compare to  $n=16.93$  and  $n=21.71$  for 40kPa pressure.
- $n=11.04$ , for 50% consolidation, for radial point r1, SD shows -31% and -9% higher Cr value in compare to  $n=16.93$  and  $n=21.71$  for 40kPa pressure, while  $n=11.04$  for 80% consolidation SD shows -39% and -30% higher Cr value in compare to  $n=16.93$  and  $n=21.71$  for 40kPa pressure. Similarly for radial point r2, SD shows 2% and 79% higher Cr value in compare to  $n=16.93$  and  $n=21.71$  for 40kPa pressure, while  $n=11.04$  for 80% consolidation SD shows 0% and 74% higher Cr value in compare to  $n=16.93$  and  $n=21.71$  for 40kPa pressure. Similarly for radial point r3, SD shows 5% and 83% higher Cr value in compare to  $n=16.93$  and  $n=21.71$  for 40kPa pressure, while  $n=11.04$  for 80% consolidation SD shows -3% and 81% higher Cr value in compare to  $n=16.93$  and  $n=21.71$  for 40kPa pressure.
- $n=11.04$ , for 50% consolidation, for radial point r1, CJ shows -83% and 33% higher Cr value in compare to  $n=16.93$  and  $n=21.71$  for 160kPa



pressure, while  $n=11.04$  for 80% consolidation CJ shows -41% and 40% higher  $C_r$  value in compare to  $n=16.93$  and  $n=21.71$  for 160kPa pressure. Similarly for radial point r<sub>2</sub>, CJ shows 75% and 51% higher  $C_r$  value in compare to  $n=16.93$  and  $n=21.71$  for 160kPa pressure, while  $n=11.04$  for 80% consolidation CJ shows 69% and 41% higher  $C_r$  value in compare to  $n=16.93$  and  $n=21.71$  for 160kPa pressure. Similarly for radial point r<sub>3</sub>, CJ shows 75% and 69% higher  $C_r$  value in compare to  $n=16.93$  and  $n=21.71$  for 160kPa pressure, while  $n=11.04$  for 80% consolidation CJ shows 76% and 46% higher  $C_r$  value in compare to  $n=16.93$  and  $n=21.71$  for 160kPa pressure.

- $n=11.04$ , for 50% consolidation, for radial point r<sub>1</sub>, SW shows 27% and 66% higher  $C_r$  value in compare to  $n=16.93$  and  $n=21.71$  for 160kPa pressure, while  $n=11.04$  for 80% consolidation SW shows 40% and 74% higher  $C_r$  value in compare to  $n=16.93$  and  $n=21.71$  for 160kPa pressure. Similarly for radial point r<sub>2</sub>, SW shows 19% and -41% higher  $C_r$  value in compare to  $n=16.93$  and  $n=21.71$  for 160kPa pressure, while  $n=11.04$  for 80% consolidation SW shows 32% and -29% higher  $C_r$  value in compare to  $n=16.93$  and  $n=21.71$  for 160kPa pressure. Similarly for radial point r<sub>3</sub>, SW shows 29% and -119% higher  $C_r$  value in compare to  $n=16.93$  and  $n=21.71$  for 160kPa pressure, while  $n=11.04$  for 80% consolidation SW shows 24% and -77% higher  $C_r$  value in compare to  $n=16.93$  and  $n=21.71$  for 160kPa pressure.

**Discussion:** (refer table 6.4)

- During settlement measurements it concludes that  $n=11.04$  for 50% consolidation shows 76% and 69% higher  $C_r$  value compare to  $n=16.93$  and 21.71 for any drain material under light loading and 81% and 75% under constructional loading. Similarly for 80% consolidation shows 67% and 60% higher  $C_r$  value compare to  $n=16.93$  and 21.71 for any drain material under light loading and 69% and 63% under constructional loading.
- During pore pressure measurements for middle radial point r<sub>2</sub> it concludes that  $n=11.04$  for 50% consolidation shows 405% and 583% higher  $C_r$  value compare to  $n=16.93$  and 21.71 for any drain material under light loading and

483% and 580% under constructional loading. Similarly for 80% consolidation shows 227% and 239% higher  $C_r$  value compare to  $n=16.93$  and 21.71 for any drain material under light loading and 290% and 298% under constructional loading.

- $n=16.93$  is found to be more efficient then  $n=21.71$  under both light and constructional loadings.  $n=16.93$  shows averagely 92% higher  $C_r$  value under light loading while 60% higher under constructional loading compare to  $n=21.71$  but 61% lower compare to  $n=11.04$  under light loading and 56% lower under constructional loading.
- The general pattern of  $C_r$  vs. pressure for any 'n' value indicates that it increases with pressure, but at 50% consolidation variation in  $C_r$  value is higher compare to 80% consolidation. In pore pressure measurement under lighter loading there is variation in  $C_r$  value, but constancy is maintained after 50kPa for any 'n' value.
- For  $n=11.04$  the maximum value of  $C_r$  is  $8.09 \times 10^{-4} \text{ cm}^2/\text{sec}$  &  $7.02 \times 10^{-4} \text{ cm}^2/\text{sec}$  at 50% and 80% consolidation for CJ from settlement consideration.
- For  $n=16.93$  average  $C_r$  value ranges from  $1.46 \times 10^{-4} \text{ cm}^2/\text{sec}$  &  $3.49 \times 10^{-5} \text{ cm}^2/\text{sec}$  for 80% consolidation for constructional loading from settlement and pore pressure measurements respectively.
- For  $n=21.71$  average  $C_r$  value ranges from  $1.78 \times 10^{-4} \text{ cm}^2/\text{sec}$  &  $4.7 \times 10^{-5} \text{ cm}^2/\text{sec}$  for 80% consolidation for constructional loading from settlement and pore pressure measurements respectively.
- Average  $C_r$  value for  $n=16.93$  remain in between  $n=11.04$  and  $n=21.71$ . The lowest average value of  $n=21.71$  signifies inefficiency of the drains of any material compare to drains of other 'n' value.

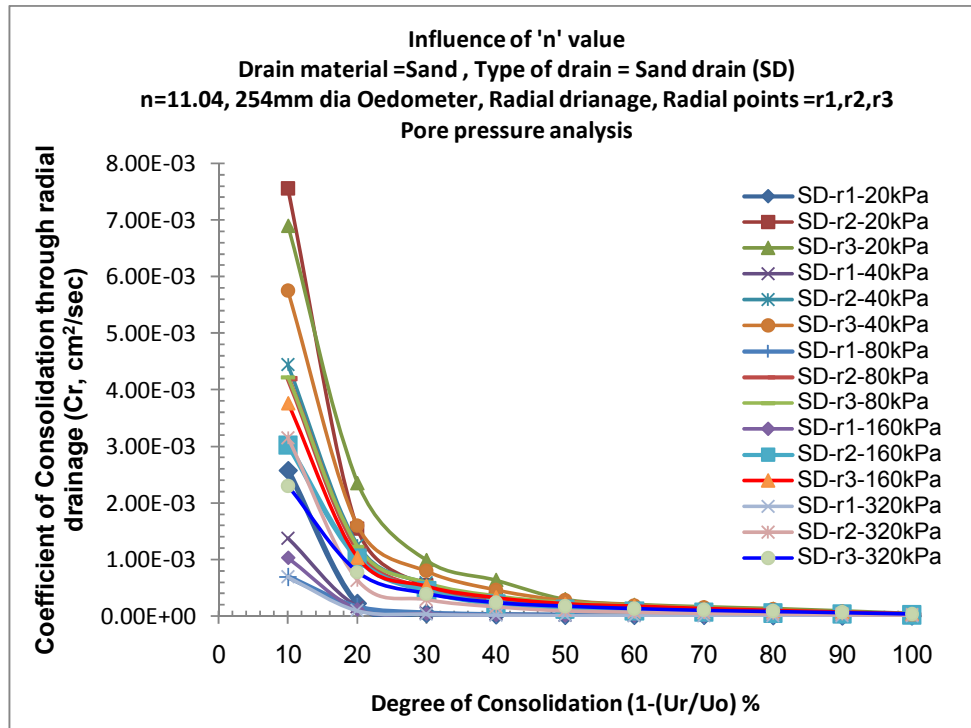


**Fig. 6.155:** Coefficient of consolidation through radial drainage against Degree of consolidation for SD of 'n'11.04 at radial points for all pressures

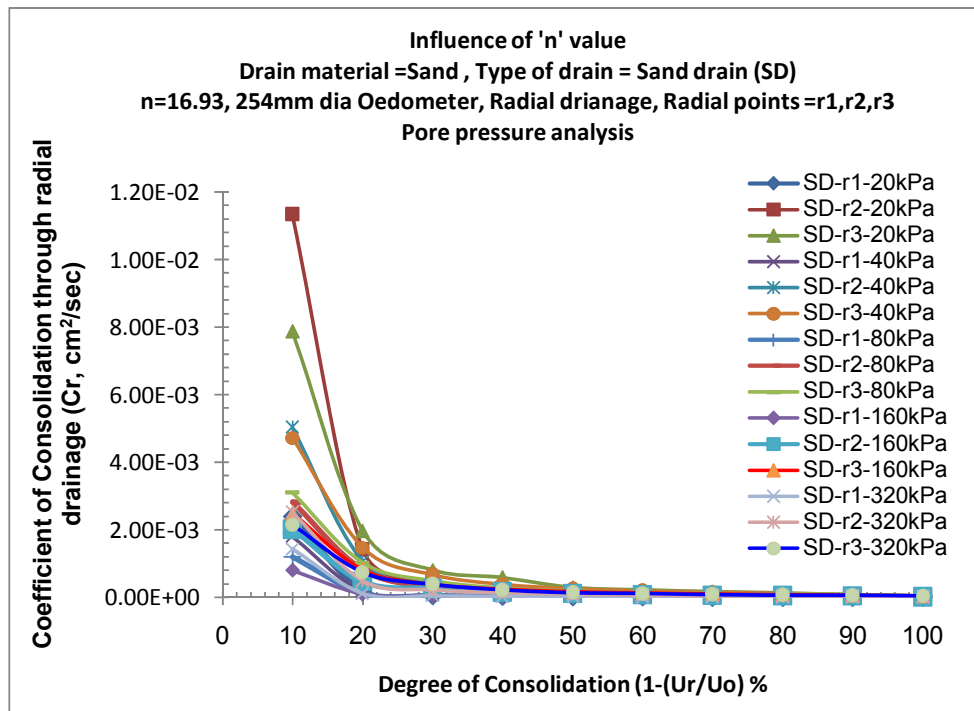


**Fig. 6.156:** Coefficient of consolidation through radial drainage against Degree of consolidation for SD of 'n'16.93 at radial points for all pressures

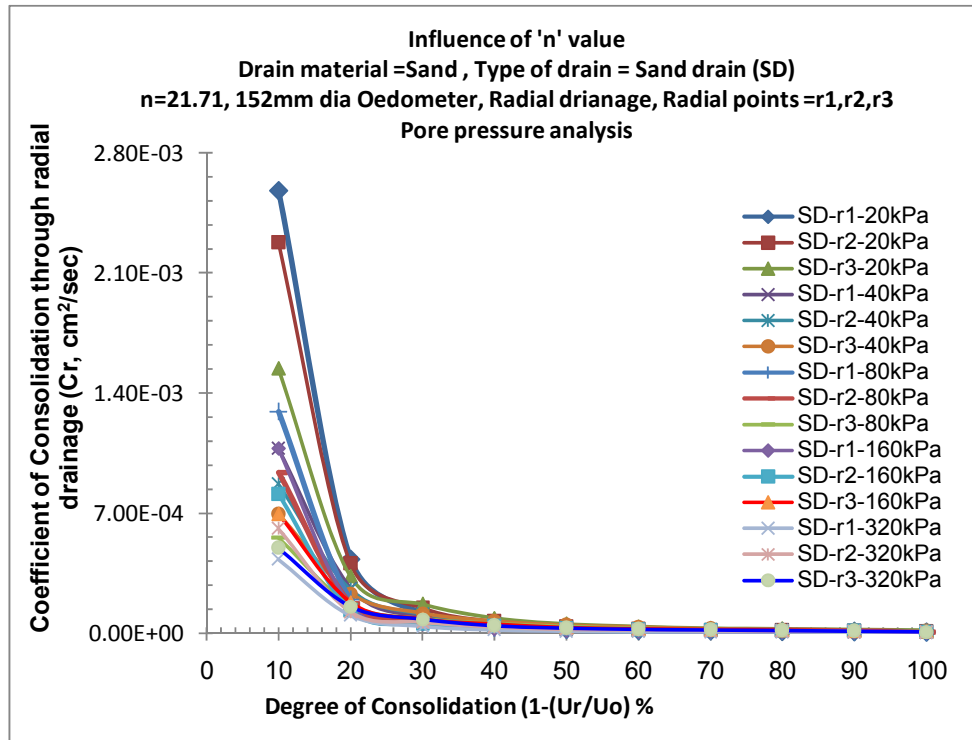


**Fig. 6.157:** Coefficient of consolidation through radial drainage against Degree of consolidation for SD of 'n'21.71 at radial points for all pressures

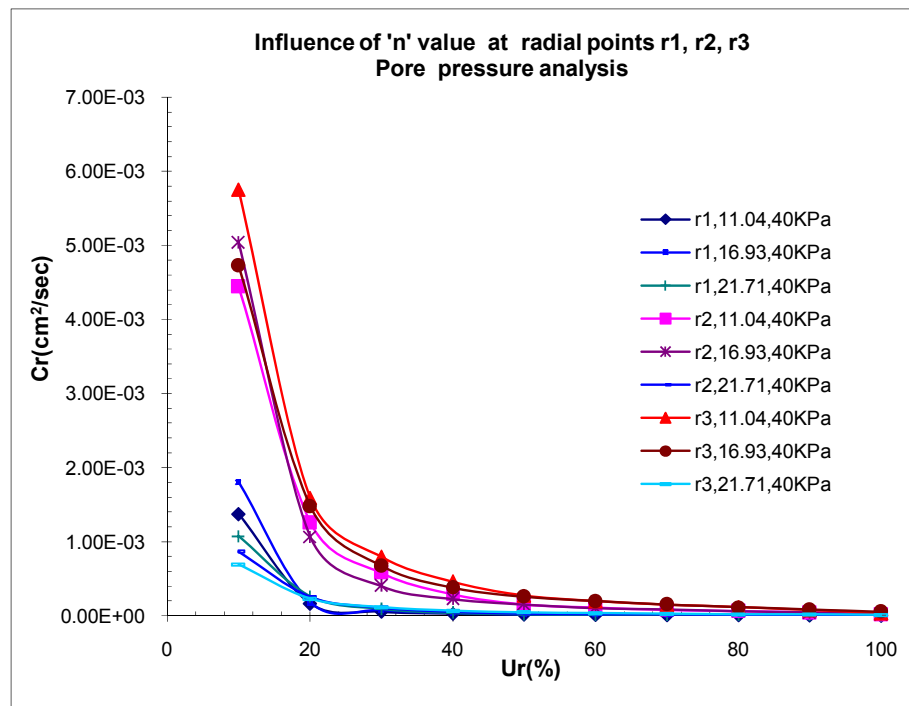


**Fig. 6.158:** Comparison of  $C_r$  vs.  $U_r$  for various 'n' values of SD at radial points

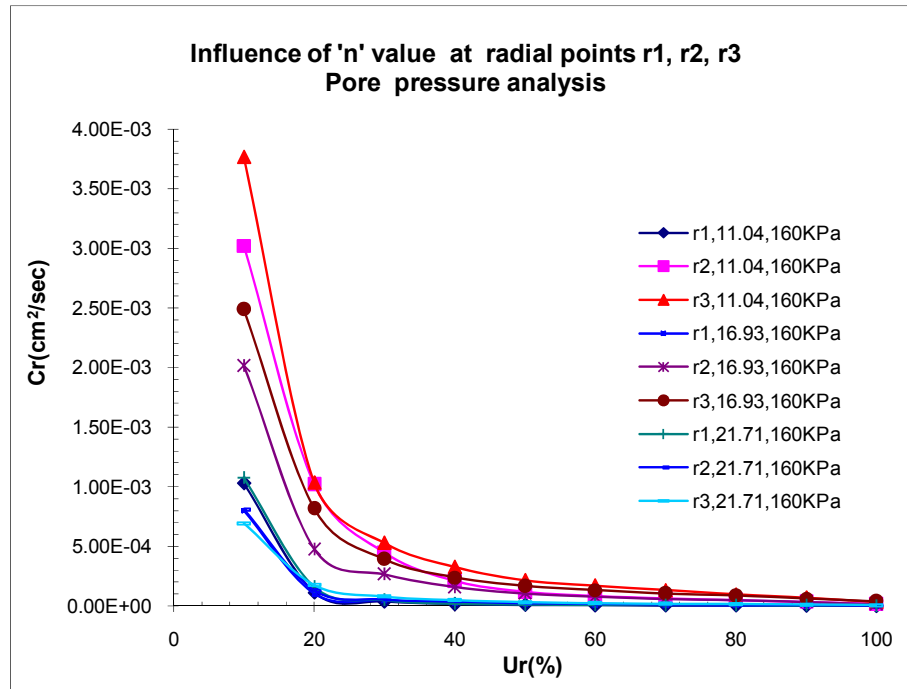


**Fig. 6.159:** Comparison of  $Cr$  vs.  $Ur$  for various 'n' values of SD at radial points

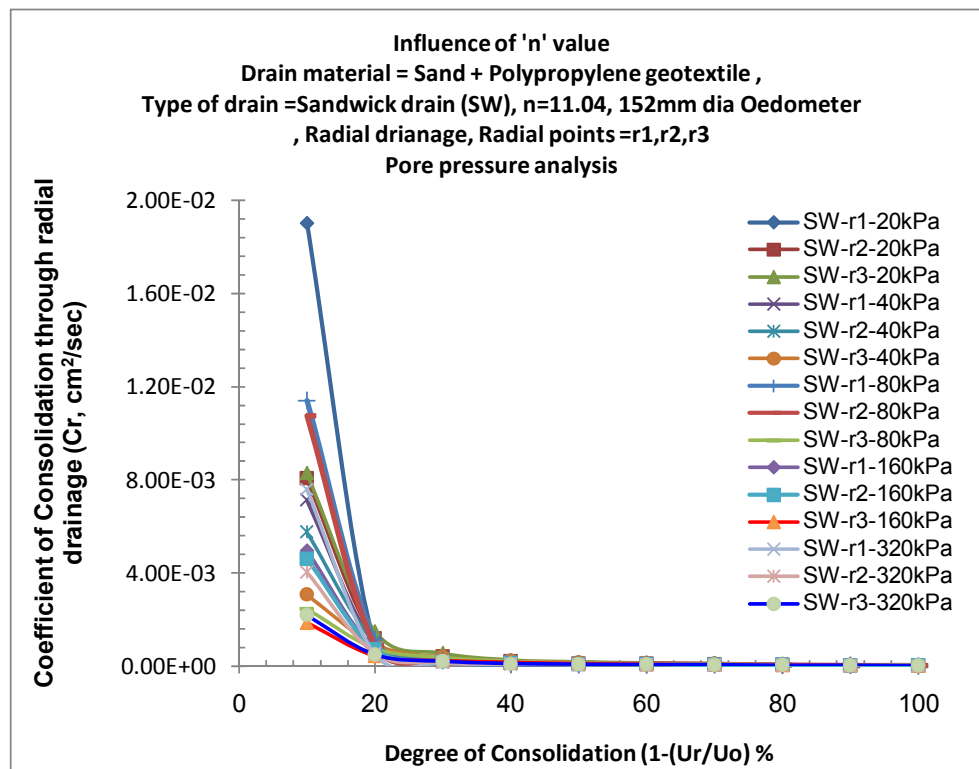


**Fig. 6.160:** Coefficient of consolidation through radial drainage against Degree of consolidation for SW of 'n'11.04 at radial points for all pressures

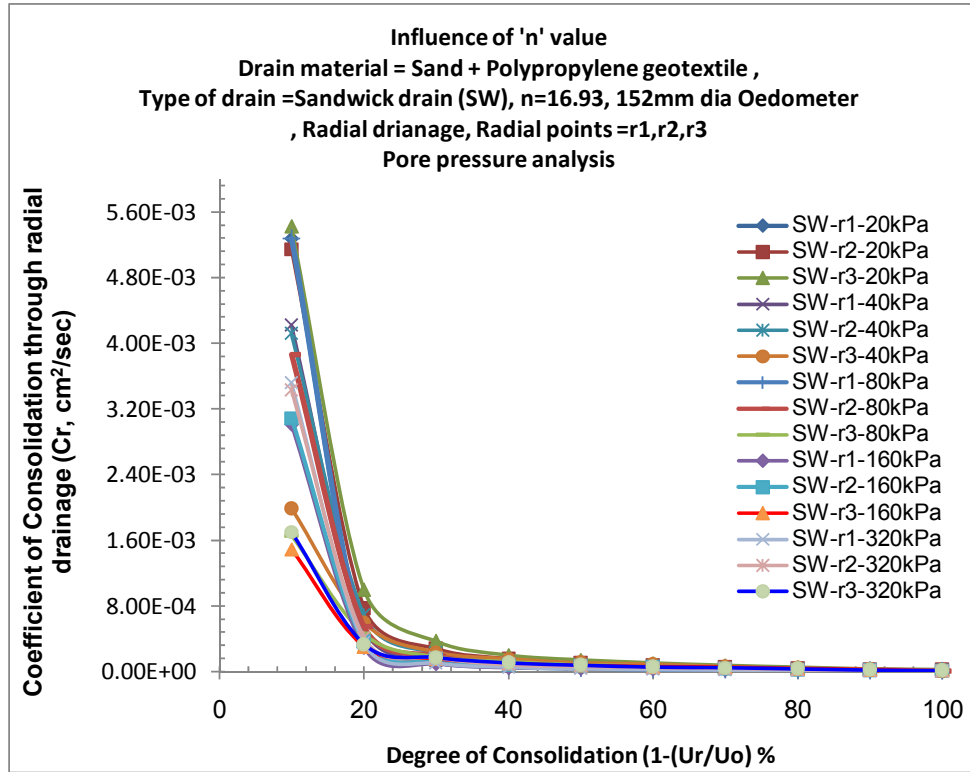


**Fig. 6.161:** Coefficient of consolidation through radial drainage against Degree of consolidation for SW of 'n'16.93 at radial points for all pressures

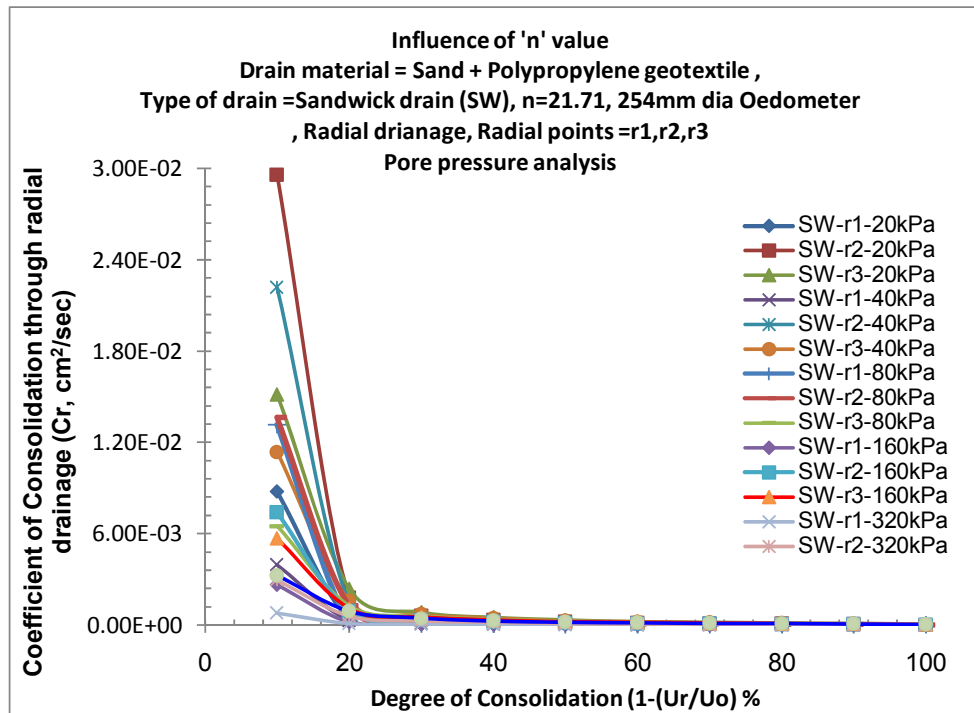


**Fig. 6.162:** Coefficient of consolidation through radial drainage against Degree of consolidation for SW of 'n'21.71 at radial points for all pressures

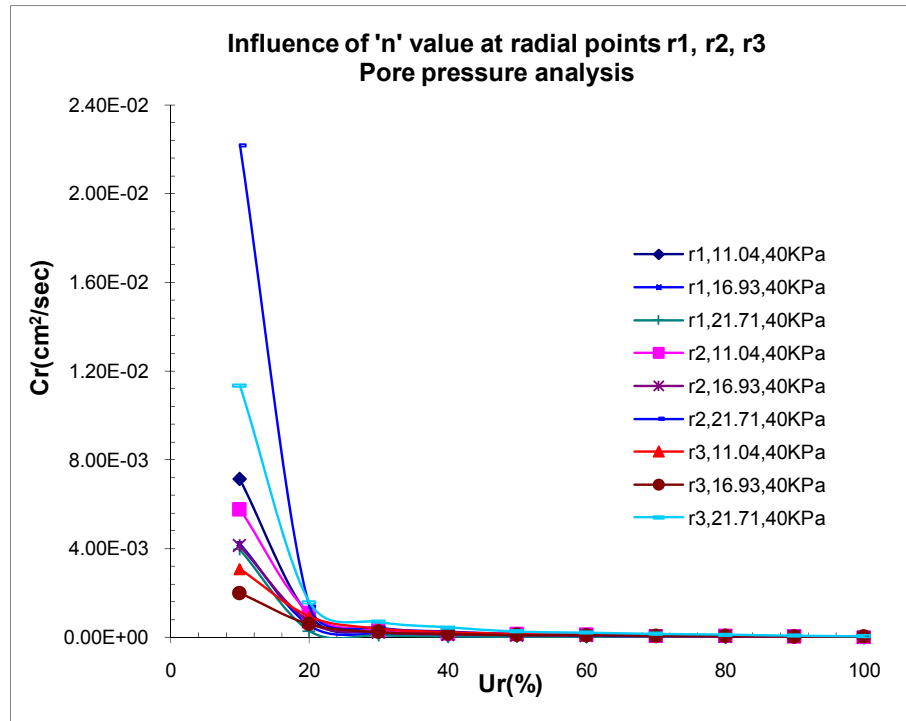


**Fig. 6.163:** Comparison of Cr vs. Ur for various 'n' values of SW at radial points

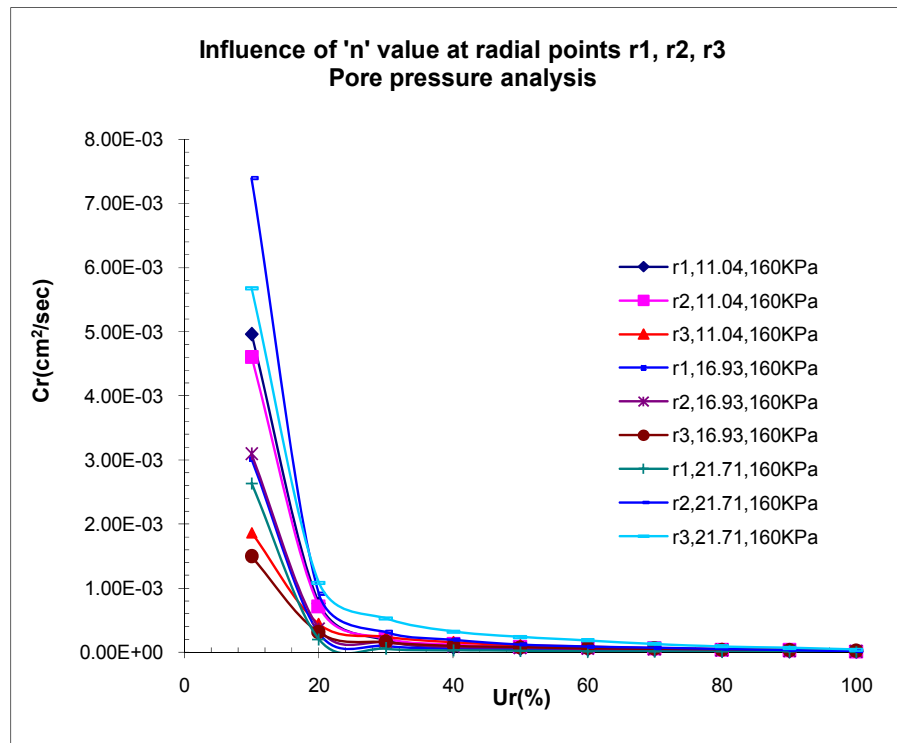


**Fig. 6.164:** Comparison of Cr vs. Ur for various 'n' values of SW at radial points

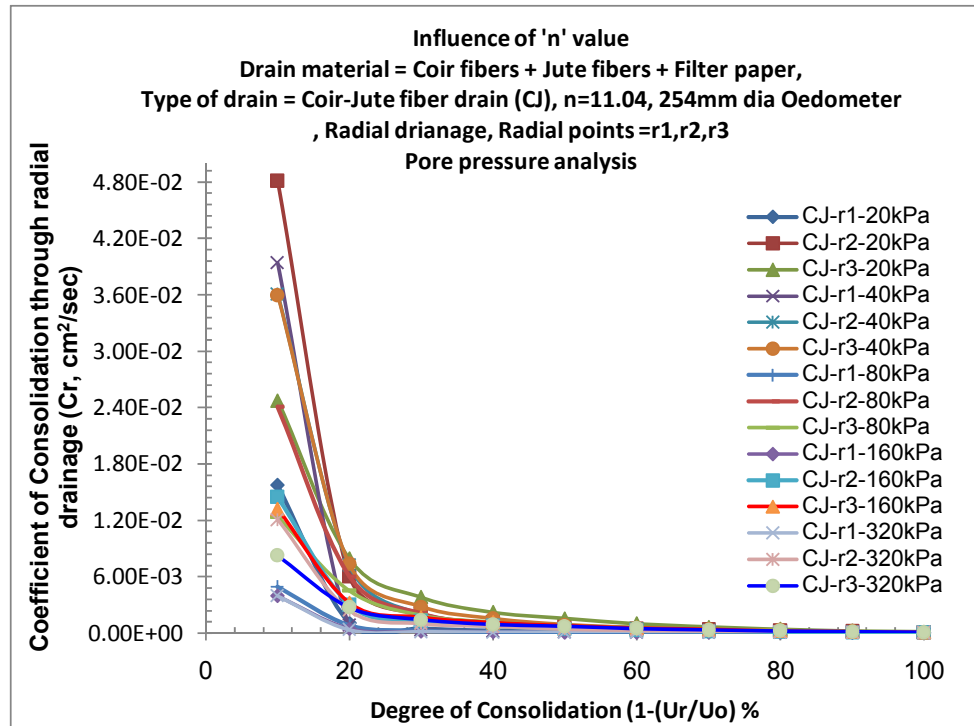


**Fig. 6.165:** Coefficient of consolidation through radial drainage against Degree of consolidation for CJ of 'n'11.04 at radial points for all pressures

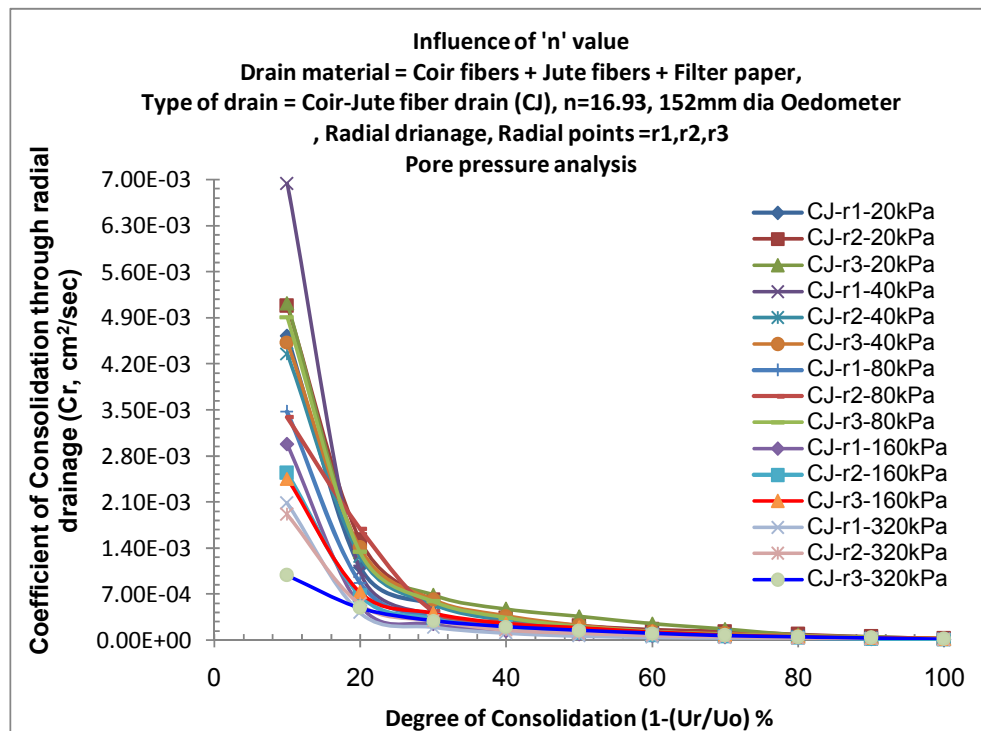


**Fig. 6.166:** Coefficient of consolidation through radial drainage against Degree of consolidation for CJ of 'n'16.93 at radial points for all pressures



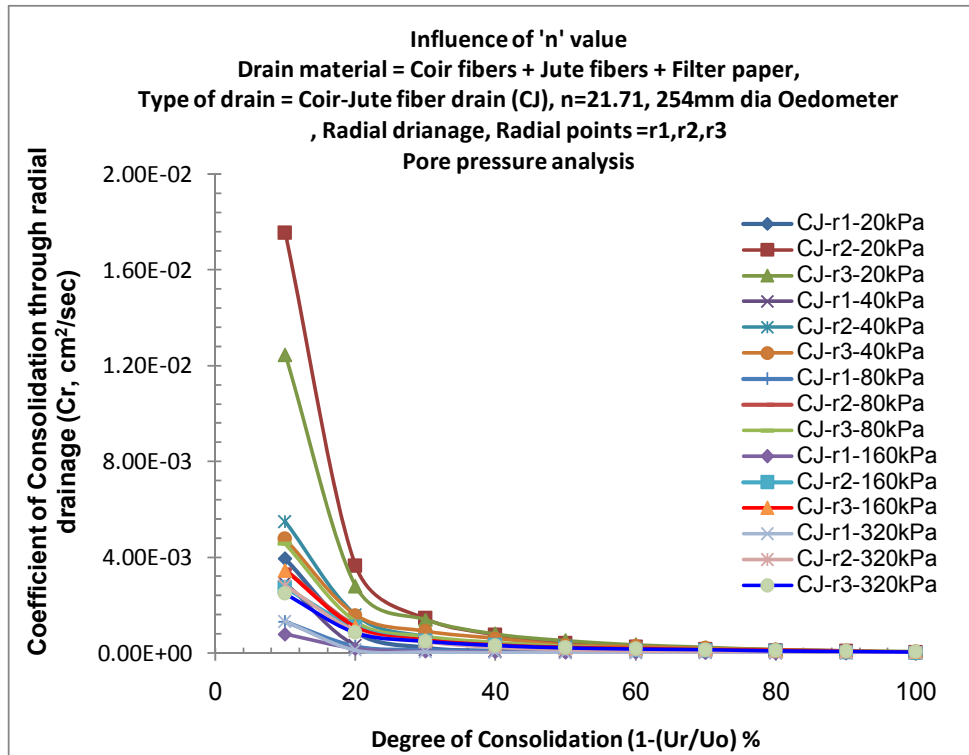


**Fig. 6.167:** Coefficient of consolidation through radial drainage against Degree of consolidation for CJ of 'n'21.71 at radial points for all pressures

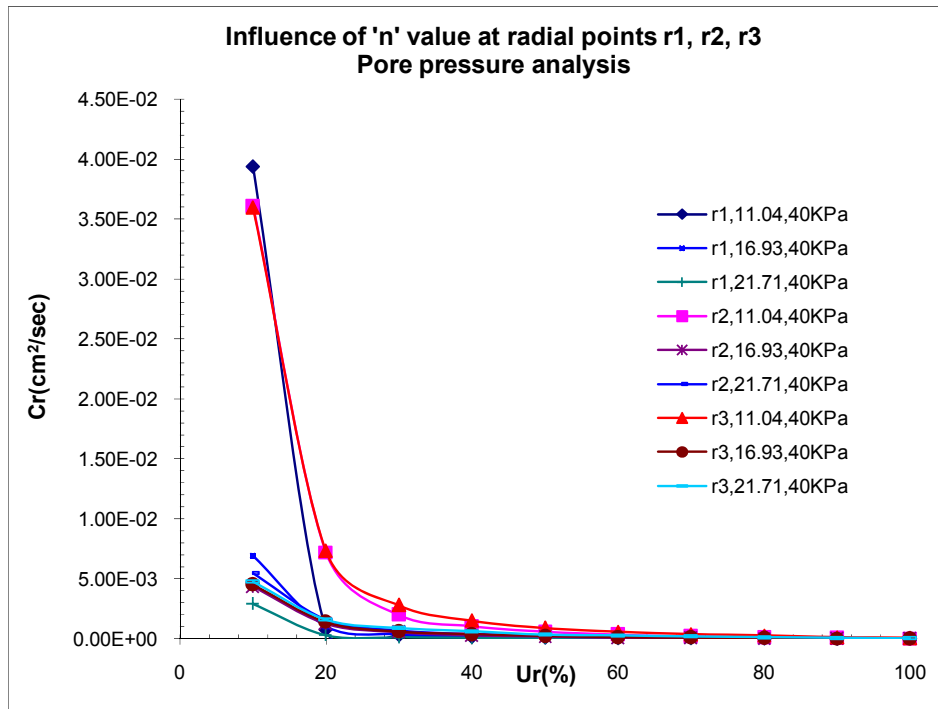


**Fig. 6.168:** Comparison of Cr vs. Ur for various 'n' values of CJ at radial points

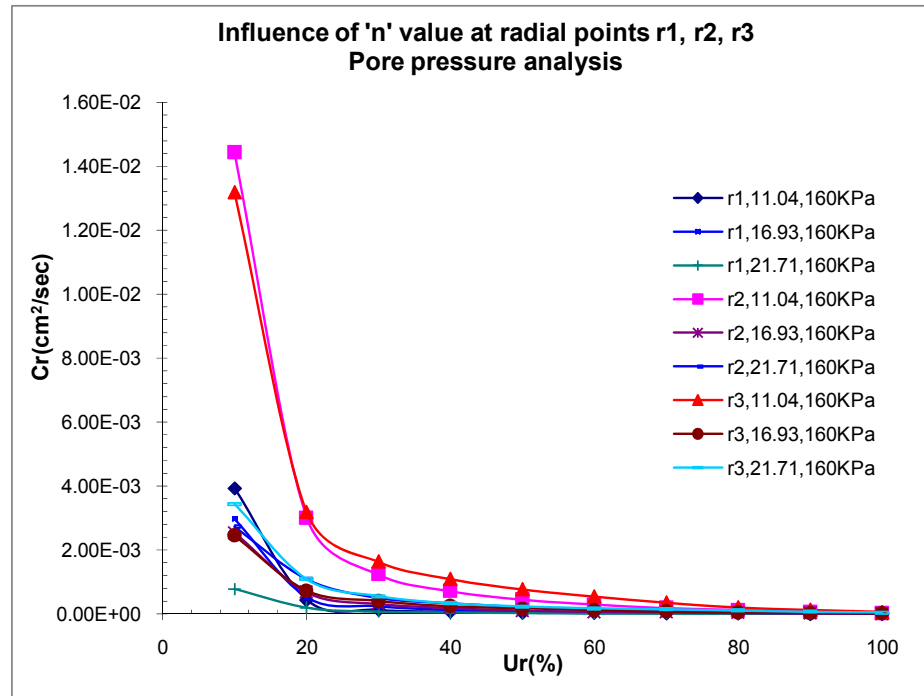


**Fig. 6.169:** Comparison of Cr vs. Ur for various 'n' values of CJ at radial points

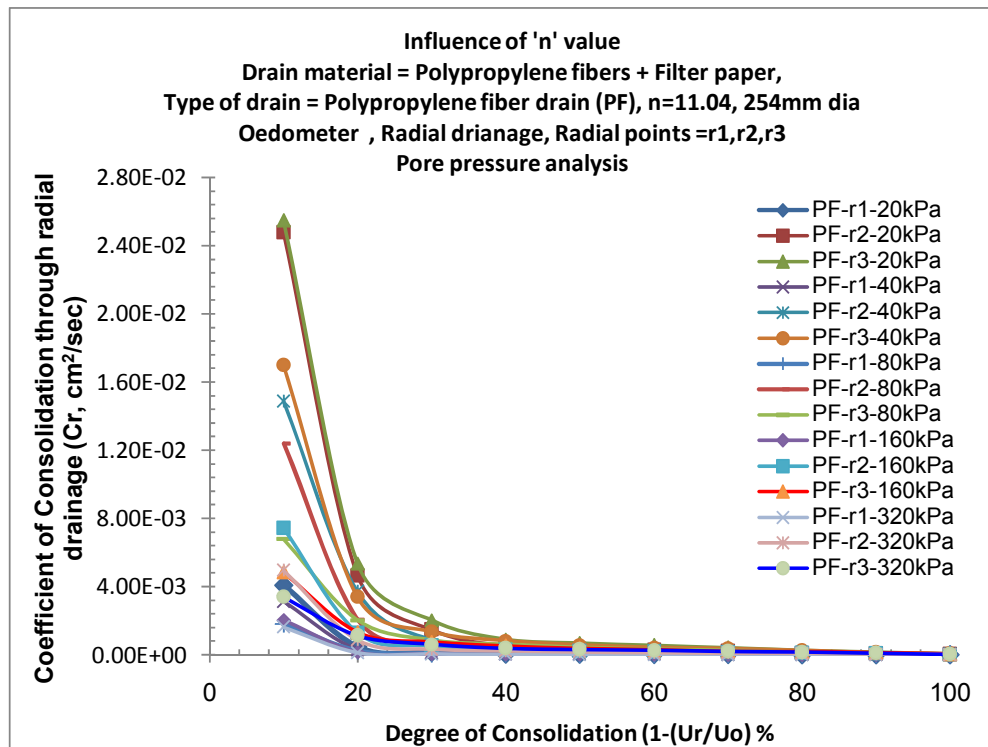


**Fig. 6.170:** Coefficient of consolidation through radial drainage against Degree of consolidation for PF of 'n'11.04 at radial points for all pressures

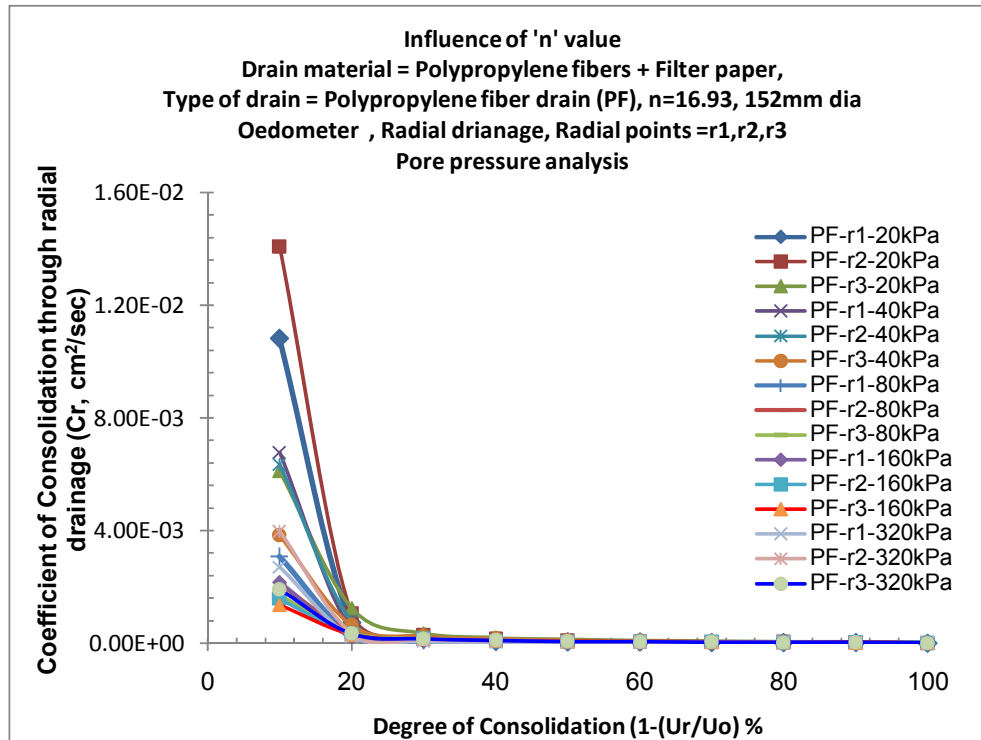


**Fig. 6.171:** Coefficient of consolidation through radial drainage against Degree of consolidation for PF of 'n'16.93 at radial points for all pressures

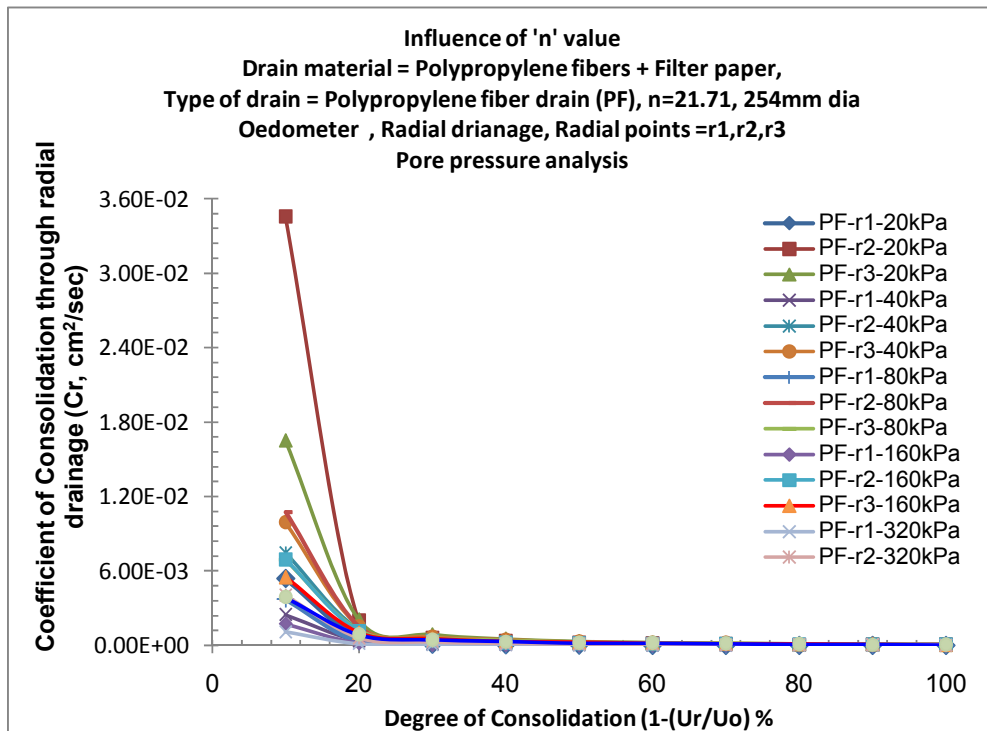


**Fig. 6.172:** Coefficient of consolidation through radial drainage against Degree of consolidation for PF of 'n'21.71 at radial points for all pressures

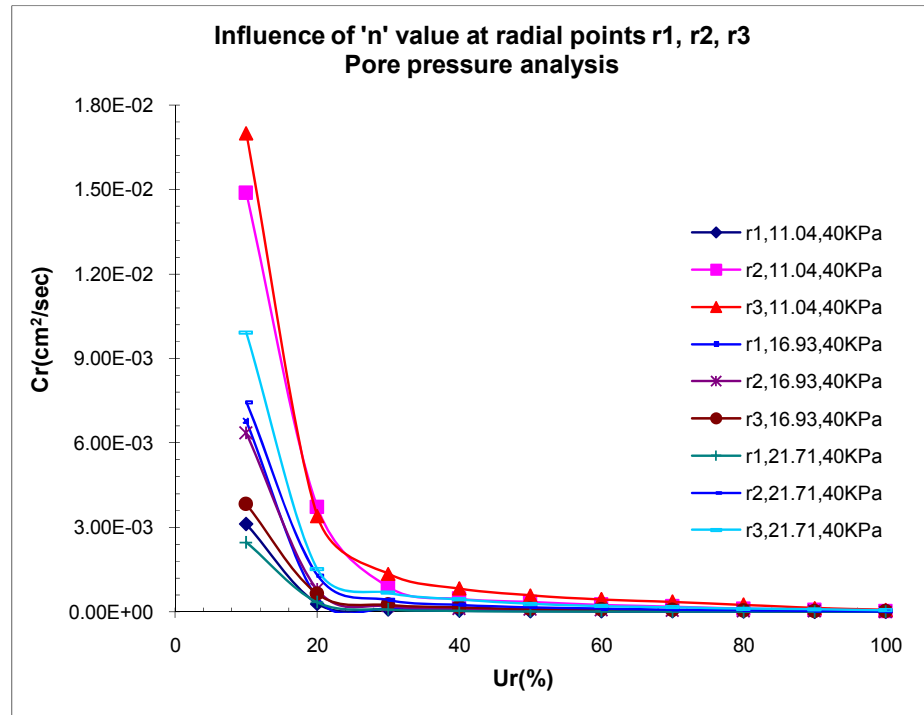


**Fig. 6.173:** Comparison of  $C_r$  vs.  $U_r$  for various 'n' values of PF at radial points

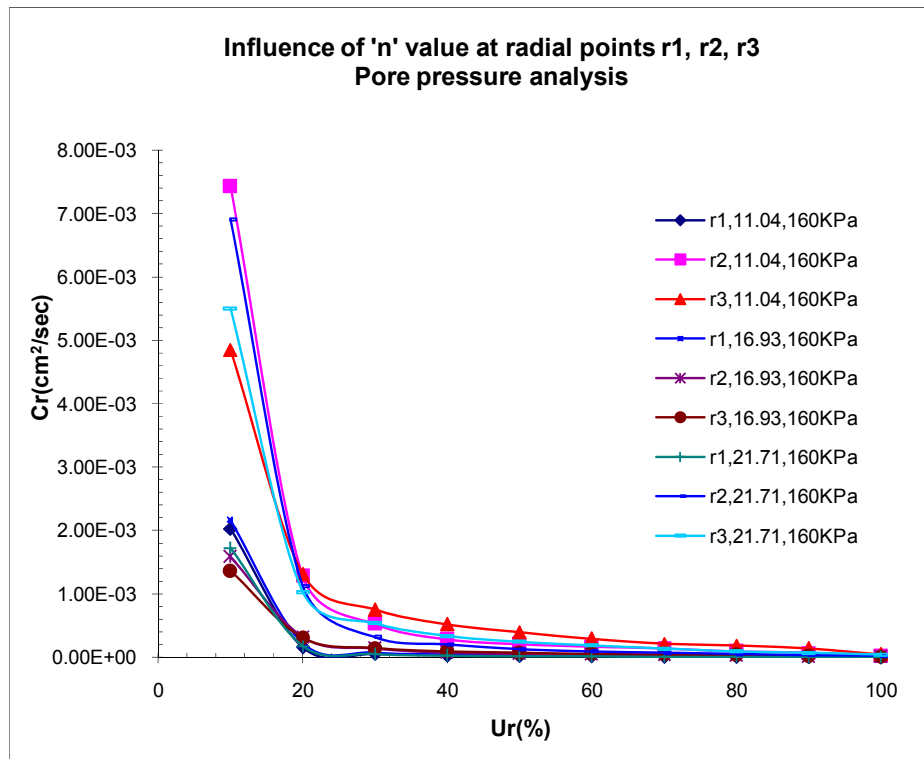


**Fig. 6.174:** Comparison of  $C_r$  vs.  $U_r$  for various 'n' values of PF at radial points

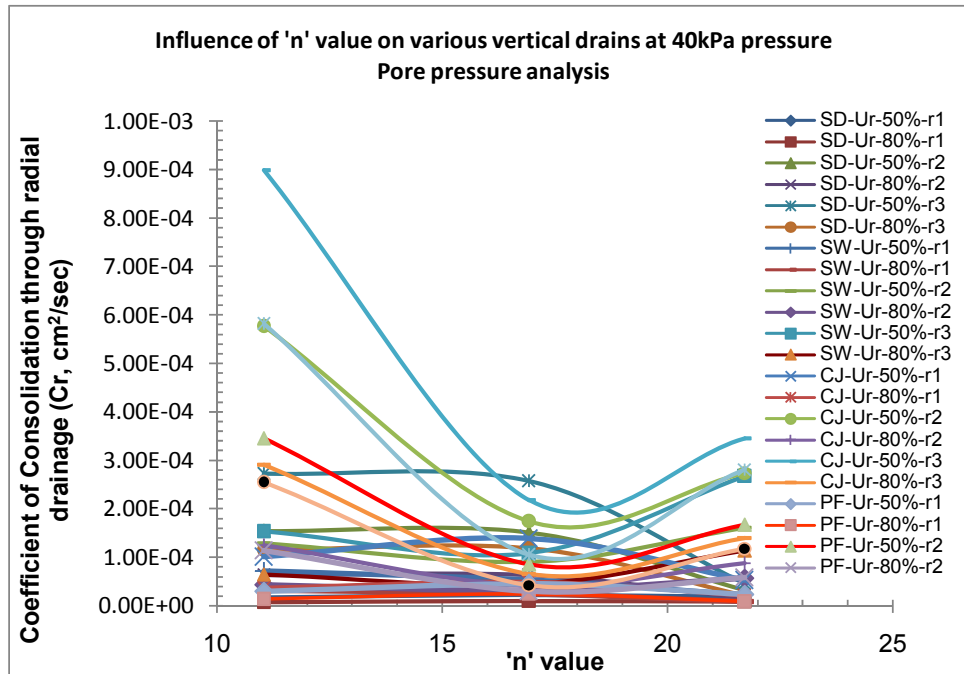


**Fig. 6.175:** Comparison of  $C_r$  value against 'n' values for various vertical drains at 40kPa applied pressure

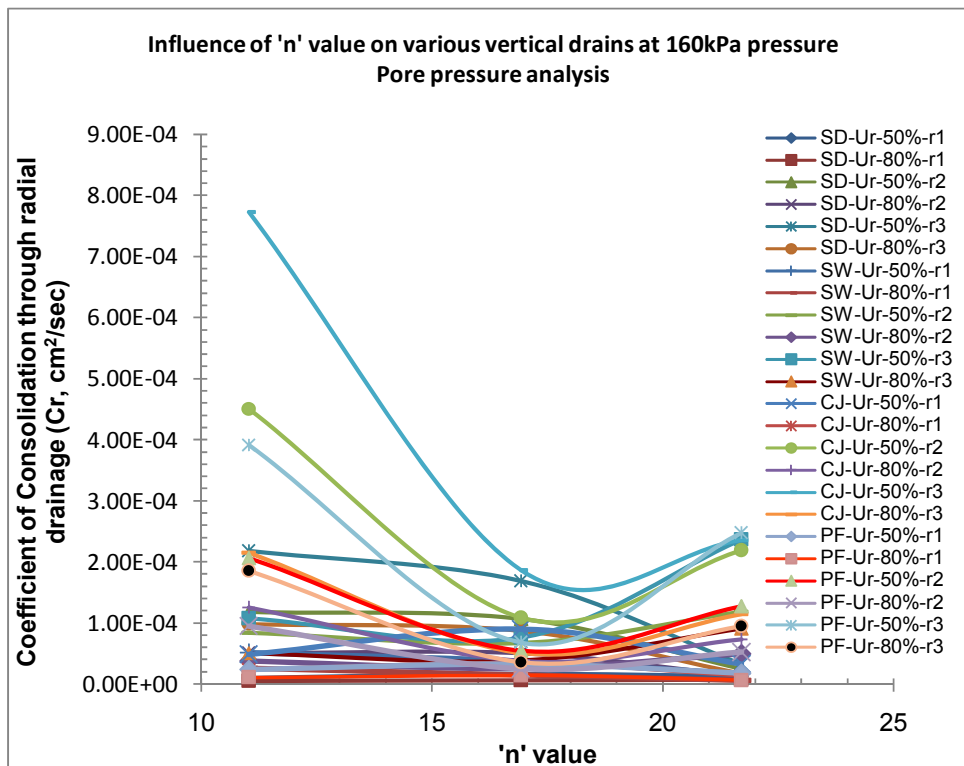


**Fig. 6.176:** Comparison of  $C_r$  value against 'n' values for various vertical drains at 160kPa applied pressure

### 3) Coefficient of consolidation (Cr) vs. applied pressure: Figures 6.177 to 6.196

**a) Settlement analysis:-** Fig.6.177 to Fig.6.186 shows the plots of coefficient of consolidation due to radial drainage (Cr) versus applied pressure for various drains i.e. SD,SW,CJ & PF for three 'n' values of 11.04,16.93 and 21.71. Here for analysis time required for 50% ( $T_{50}$ ) consolidation and time required for 80% ( $T_{80}$ ) consolidation are taken for all applied pressures. From the plots it is very clear that the nature of  $T_{80}$  graph remains same that is nearly constant or say linear increasing, while  $T_{50}$  graph has much variation in initial pressures and thereafter Cr values increase rapidly for later higher pressures. This is true almost for all drains. There is no much variation in the value of Cr up to 50 kPa, change of Cr value indicates the initial structural resistance existing in the clay water structure in the Kaolinite clay.

- The value of  $C_{r50}$  for CJ for 'n' equal to 11.04, 16.93 and 21.71 and for 40kPa was found to be  $8.09 \times 10^{-4} \text{ cm}^2/\text{sec}$ ,  $1.78 \times 10^{-4} \text{ cm}^2/\text{sec}$ ,  $4.14 \times 10^{-4} \text{ cm}^2/\text{sec}$  and  $C_{r80}$  was found as  $3.56 \times 10^{-4} \text{ cm}^2/\text{sec}$ ,  $1.03 \times 10^{-4} \text{ cm}^2/\text{sec}$ ,  $2.3 \times 10^{-4} \text{ cm}^2/\text{sec}$  respectively. For higher engineering stress of 160kPa the  $C_{r50}$  for all three 'n' values was determined as  $1.44 \times 10^{-3} \text{ cm}^2/\text{sec}$ ,  $3.17 \times 10^{-4} \text{ cm}^2/\text{sec}$ ,  $6.22 \times 10^{-4} \text{ cm}^2/\text{sec}$  and  $C_{r80}$  was found as  $4.85 \times 10^{-4} \text{ cm}^2/\text{sec}$ ,  $1.36 \times 10^{-4} \text{ cm}^2/\text{sec}$ ,  $2.84 \times 10^{-4} \text{ cm}^2/\text{sec}$  respectively.
- The value of  $C_{r50}$  for SW for 'n' equal to 11.04, 16.93 and 21.71 and for 40kPa was found to be  $1.97 \times 10^{-4} \text{ cm}^2/\text{sec}$ ,  $1.44 \times 10^{-4} \text{ cm}^2/\text{sec}$ ,  $1.86 \times 10^{-4} \text{ cm}^2/\text{sec}$  and  $C_{r80}$  was found as  $1.04 \times 10^{-4} \text{ cm}^2/\text{sec}$ ,  $7.61 \times 10^{-5} \text{ cm}^2/\text{sec}$ , and  $1.14 \times 10^{-4} \text{ cm}^2/\text{sec}$  respectively. For higher engineering stress of 160kPa the  $C_{r50}$  for all three 'n' values was determined as  $3.28 \times 10^{-4} \text{ cm}^2/\text{sec}$ ,  $2.05 \times 10^{-4} \text{ cm}^2/\text{sec}$ ,  $2.56 \times 10^{-4} \text{ cm}^2/\text{sec}$  and  $C_{r80}$  was found as  $1.37 \times 10^{-4} \text{ cm}^2/\text{sec}$ ,  $9.26 \times 10^{-5} \text{ cm}^2/\text{sec}$ ,  $1.54 \times 10^{-4} \text{ cm}^2/\text{sec}$  respectively.
- The value of  $C_{r50}$  for PF for 'n' equal to 11.04, 16.93 and 21.71 and for 40kPa was found to be  $4.32 \times 10^{-4} \text{ cm}^2/\text{sec}$ ,  $1.41 \times 10^{-4} \text{ cm}^2/\text{sec}$ ,  $3.14 \times 10^{-4} \text{ cm}^2/\text{sec}$  and  $C_{r80}$  was found as  $2.18 \times 10^{-4} \text{ cm}^2/\text{sec}$ ,  $8.05 \times 10^{-5} \text{ cm}^2/\text{sec}$ , and  $1.89 \times 10^{-4} \text{ cm}^2/\text{sec}$  respectively. For higher engineering stress of 160kPa the  $C_{r50}$  for all three 'n' values was determined as  $6.4 \times 10^{-4} \text{ cm}^2/\text{sec}$ ,  $1.89 \times 10^{-4} \text{ cm}^2/\text{sec}$

$\text{cm}^2/\text{sec}$ ,  $4.87 \times 10^{-4} \text{ cm}^2/\text{sec}$  and  $C_{r80}$  was found as  $2.89 \times 10^{-4} \text{ cm}^2/\text{sec}$ ,  $1.05 \times 10^{-4} \text{ cm}^2/\text{sec}$ ,  $2.32 \times 10^{-4} \text{ cm}^2/\text{sec}$  respectively.

- The value of  $C_{r50}$  for SD for 'n' equal to 11.04, 16.93 and 21.71 and for 40kPa was found to be  $5.6 \times 10^{-4} \text{ cm}^2/\text{sec}$ ,  $2.88 \times 10^{-4} \text{ cm}^2/\text{sec}$ ,  $5.75 \times 10^{-5} \text{ cm}^2/\text{sec}$  and  $C_{r80}$  was found as  $2.86 \times 10^{-4} \text{ cm}^2/\text{sec}$ ,  $2.02 \times 10^{-4} \text{ cm}^2/\text{sec}$ , and  $3.2 \times 10^{-4} \text{ cm}^2/\text{sec}$  respectively. For higher engineering stress of 160kPa the  $C_{r50}$  for all three 'n' values was determined as  $9.04 \times 10^{-4} \text{ cm}^2/\text{sec}$ ,  $3.69 \times 10^{-4} \text{ cm}^2/\text{sec}$ ,  $7.48 \times 10^{-5} \text{ cm}^2/\text{sec}$  and  $C_{r80}$  was found as  $3.69 \times 10^{-4} \text{ cm}^2/\text{sec}$ ,  $2.52 \times 10^{-4} \text{ cm}^2/\text{sec}$ ,  $4 \times 10^{-5} \text{ cm}^2/\text{sec}$  respectively.
- Looking to given plots and values it is clear that of all three 'n' values the  $n=11.04$  proves to be most economical diameter of vertical drain and this is true for all types of drains. Also  $n=16.93$  is more superior in compare to  $n=21.71$  for all drain's= $21.71$  shows slowest rate of compressibility for all pressures. Out of all drains CJ shows more rate of consolidation both at low and high pressures in compare to other drains. So it can be said that CJ shows more inter-rate of compressibility even at following pressures in compare to other drains for  $n=11.04$ .

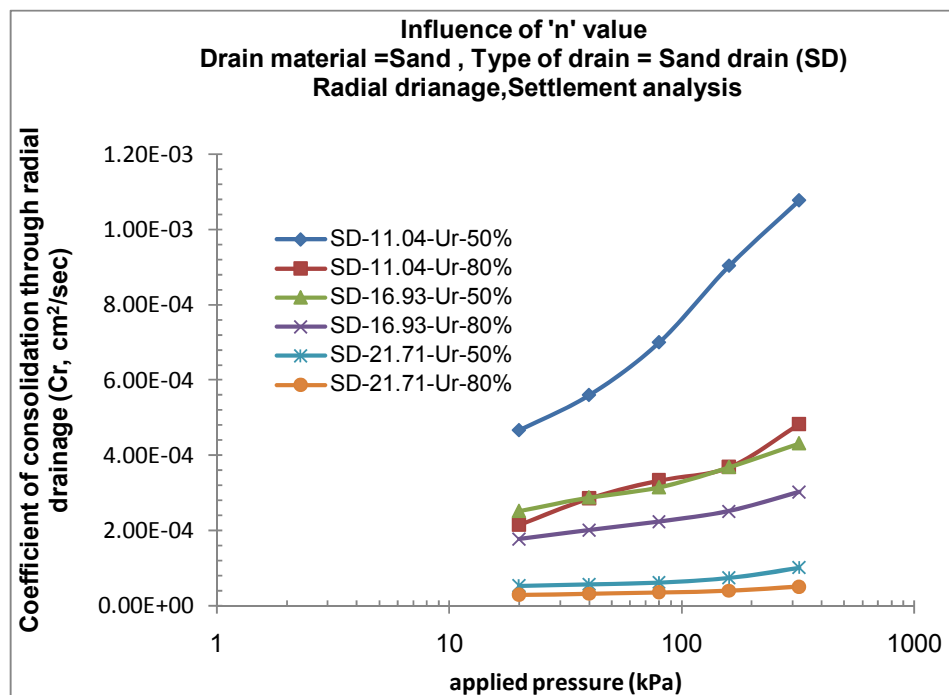


**Fig. 6.177:** Comparison of  $C_r$  against applied pressure for SD at 50% and 80% degree of consolidation

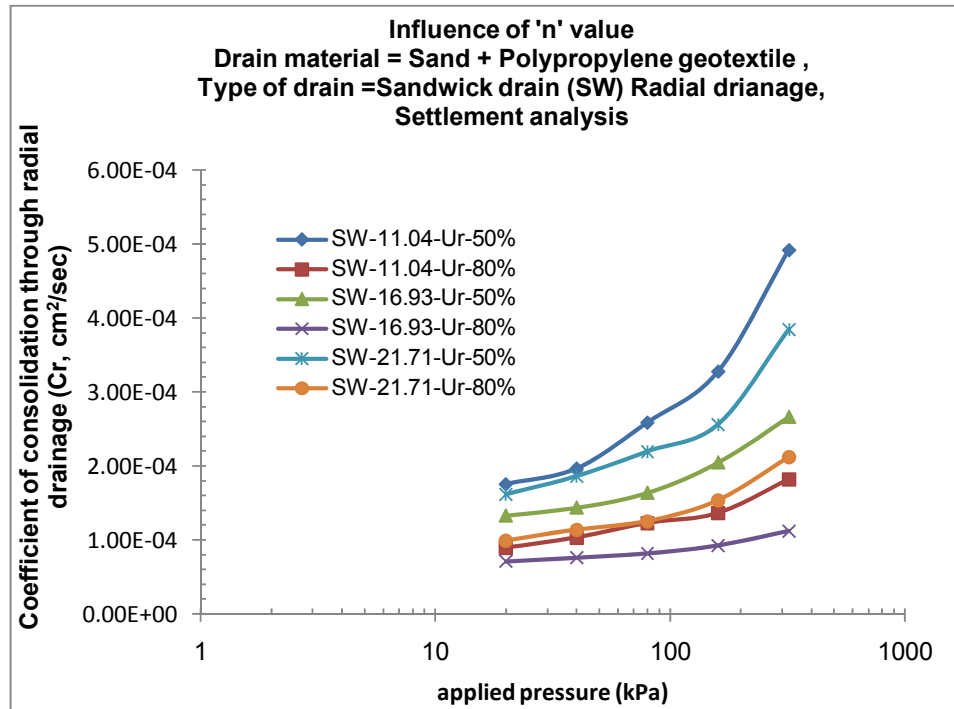


**Fig. 6.178:** Comparison of  $C_r$  against applied pressure for SW of various 'n' values at 50% and 80% degree of consolidation

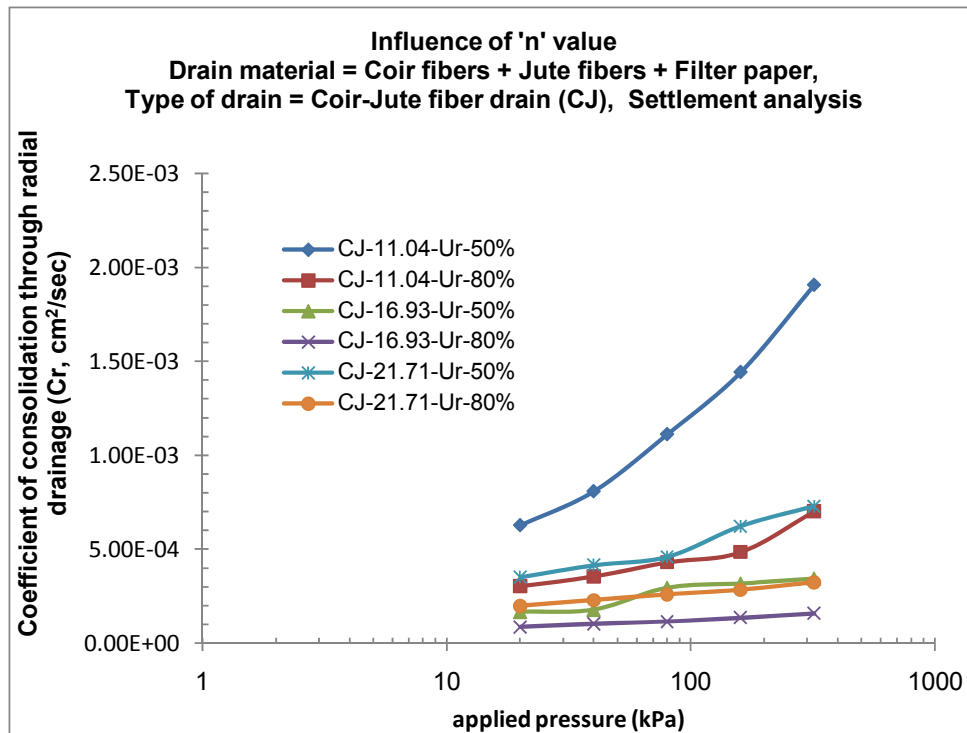


**Fig. 6.179:** Comparison of  $C_r$  against applied pressure for CJ of various 'n' values at 50% and 80% degree of consolidation



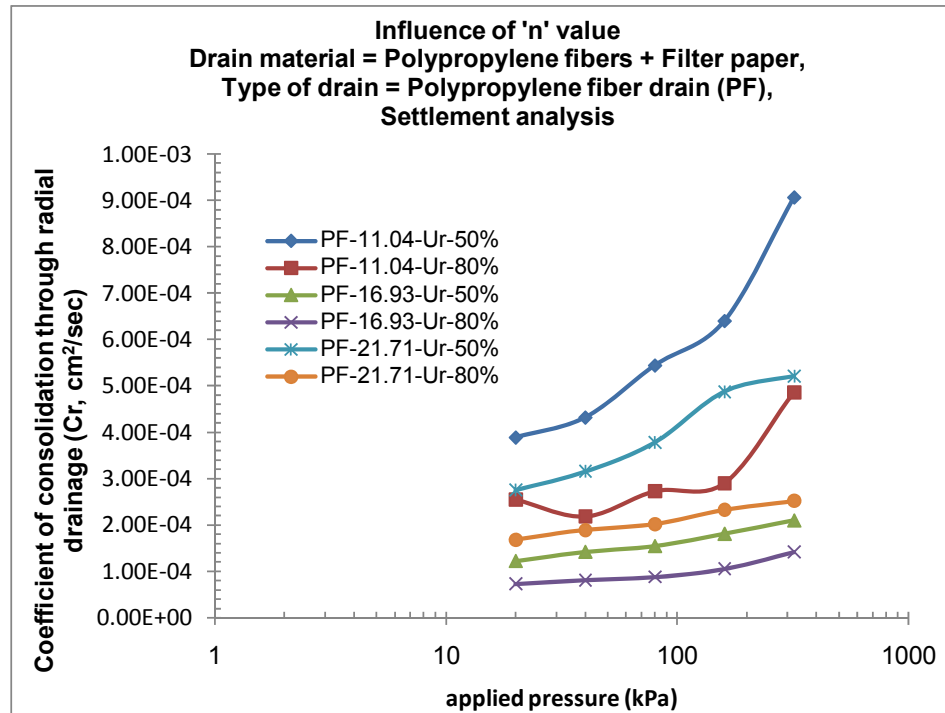


**Fig. 6.180:** Comparison of  $C_r$  against applied pressure for PF of various 'n' values at 50% and 80% degree of consolidation

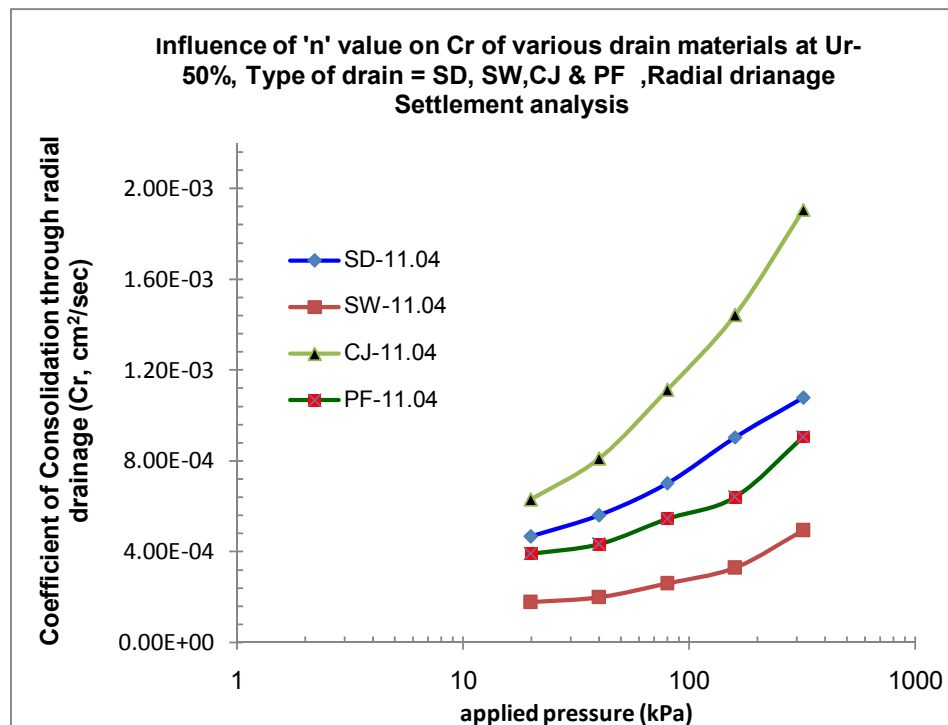


**Fig. 6.181:** Comparison of  $C_r$  value on drain material for same 'n' 11.04 at Ur = 50%

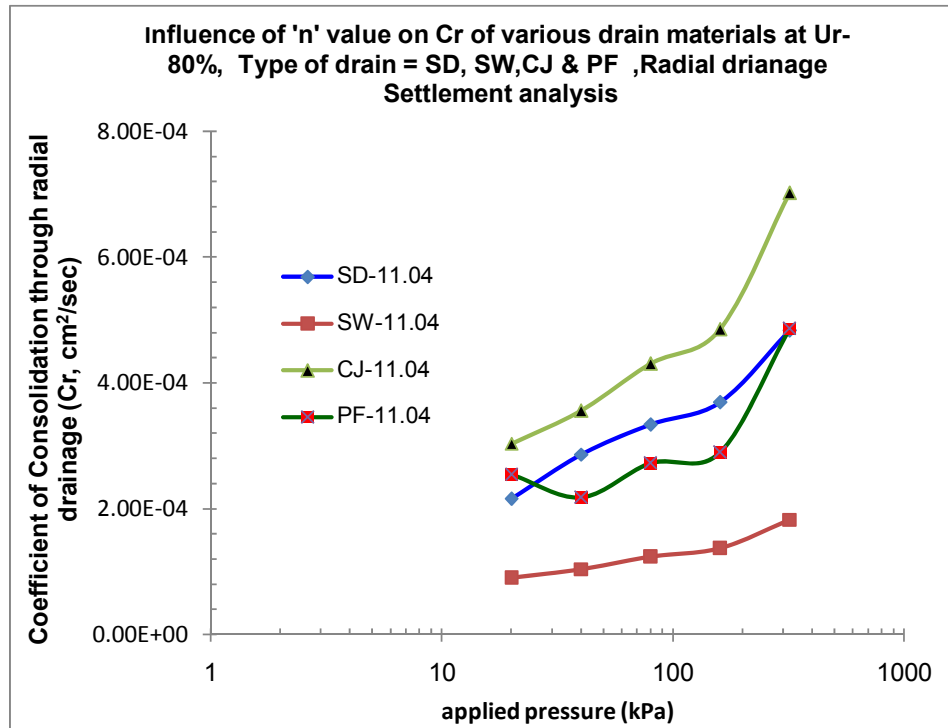


**Fig. 6.182:** Comparison of Cr value on drain material for same 'n' 11.04 at Ur =80%

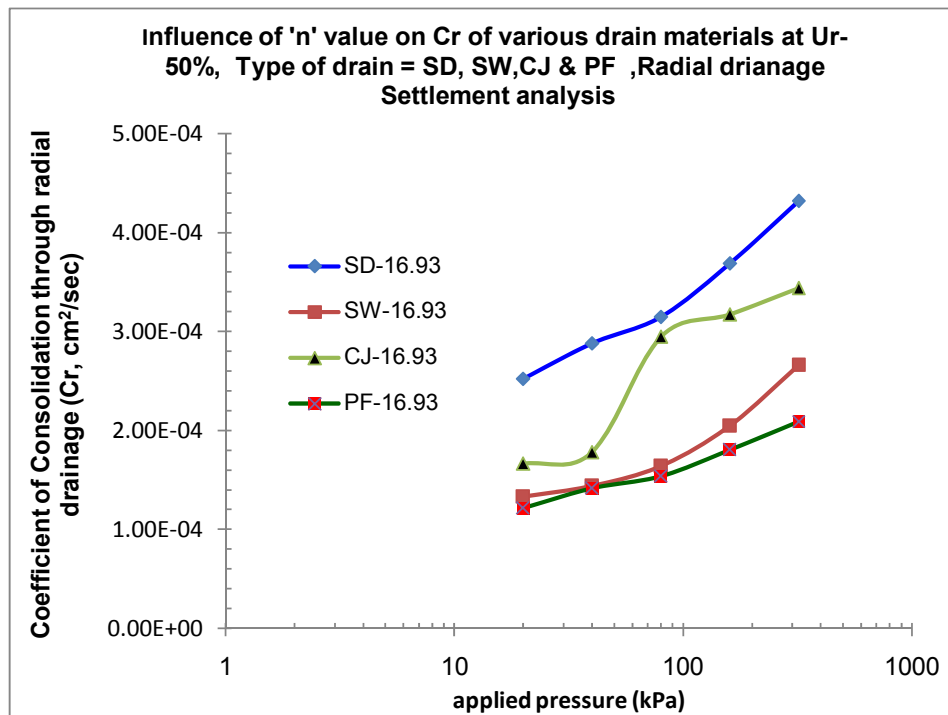


**Fig. 6.183:** Comparison of Cr value on drain material for same 'n' 16.93 at Ur =50%

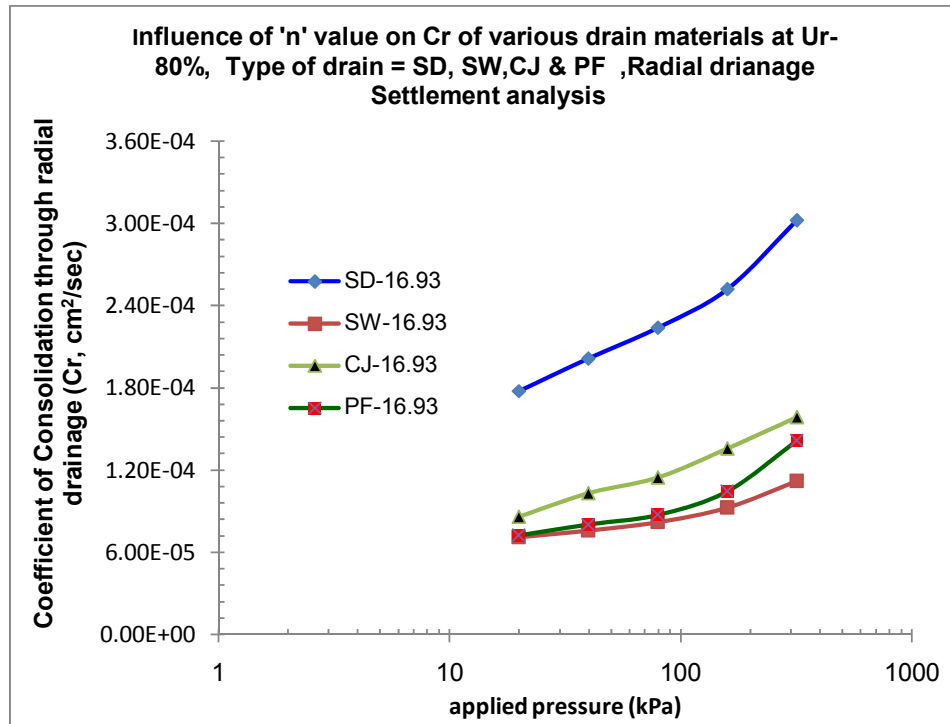


**Fig. 6.184:** Comparison of Cr value on drain material for same 'n' 16.93 at Ur =80%

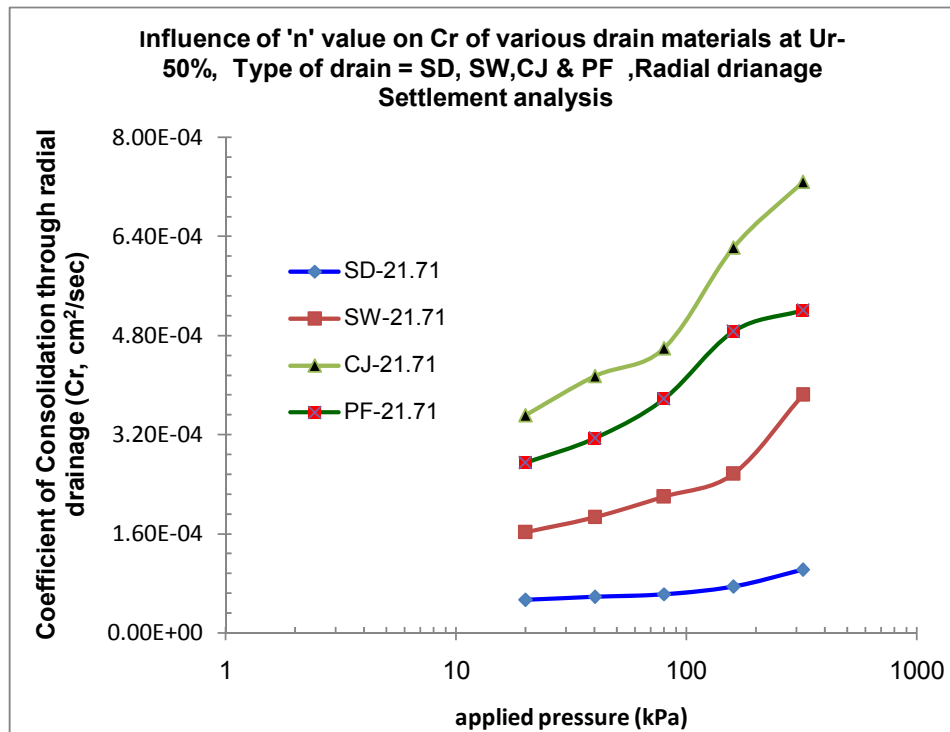


**Fig. 6.185:** Comparison of Cr value on drain material for same 'n' 21.71 at Ur =50%

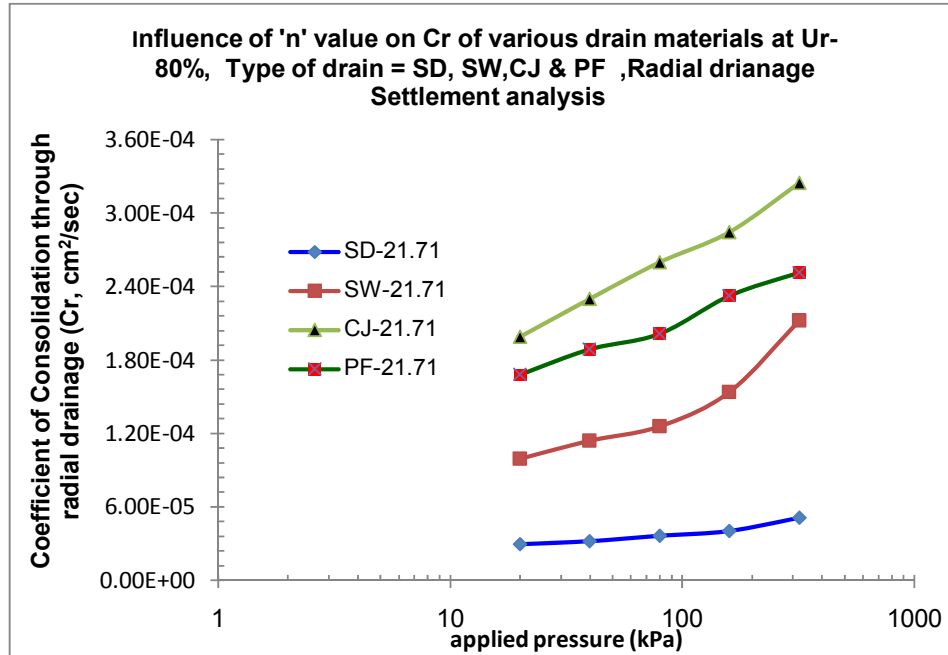


**Fig. 6.186:** Comparison of Cr value on drain material for same 'n' 21.71 at Ur =50%

**b) Pore pressure analysis:-** Fig.6.187 to Fig.6.196 shows the plots of coefficient of consolidation due to radial drainage (Cr) versus applied pressure for various drains like SD, SW, CJ, PF for 'n' values of 11.04, 16.93, and 21.71 at three radial points' r1, r2 and r3. Here for analysis time required for 50 % ( $T_{50}$ ) consolidation and time required for 80% ( $T_{80}$ ) consolidation are taken for all 40kPa and 160kPa pressures. From the plots it is very clear that for all drain materials the initial nature of  $T_{80}$  graph &  $T_{50}$  graph decreases with initial applied pressure and at higher pressures it remains same that is nearly constant. This is true for all 'n' values. There is much variation in the value of Cr up to 50 kPa, change of Cr value indicate the initial structural resistance existing in the clay water structure in the Kaolinite clay. Lesser variation in Cr value is observed for radial point's r2 and r3 for all 'n' values, for all drains and for all applied pressures.

- The value of  $C_{r1,50}$  at 40KPa for CJ for 'n' equal to 11.04, 16.93 and 21.71 is  $1.01 \times 10^{-4}$  cm<sup>2</sup>/sec,  $1.39 \times 10^{-4}$  cm<sup>2</sup>/sec, and  $5.27 \times 10^{-5}$  cm<sup>2</sup>/sec while for 160kPa it was found to be  $4.92 \times 10^{-5}$  cm<sup>2</sup>/sec,  $9.05 \times 10^{-5}$  cm<sup>2</sup>/sec and  $3.29 \times 10^{-5}$  cm<sup>2</sup>/sec respectively. Similarly value of  $C_{r2,50}$  is  $5.77 \times 10^{-4}$  cm<sup>2</sup>/sec,  $1.74 \times 10^{-4}$  cm<sup>2</sup>/sec, and  $2.74 \times 10^{-4}$  cm<sup>2</sup>/sec while for 160kPa it was found to

be  $4.5 \times 10^{-4} \text{ cm}^2/\text{sec}$ ,  $1.08 \times 10^{-4} \text{ cm}^2/\text{sec}$  and  $2.19 \times 10^{-4} \text{ cm}^2/\text{sec}$  respectively. Similarly value of  $C_{r3,50}$  is  $5.77 \times 10^{-4} \text{ cm}^2/\text{sec}$ ,  $1.74 \times 10^{-4} \text{ cm}^2/\text{sec}$ , and  $2.74 \times 10^{-4} \text{ cm}^2/\text{sec}$  while for 160kPa it was found to be  $4.5 \times 10^{-4} \text{ cm}^2/\text{sec}$ ,  $1.08 \times 10^{-4} \text{ cm}^2/\text{sec}$  and  $2.19 \times 10^{-4} \text{ cm}^2/\text{sec}$  respectively.

- The value of  $C_{r1,50}$  at 40kPa for SW for 'n' equal to 11.04, 16.93 and 21.71 is  $7.13 \times 10^{-5} \text{ cm}^2/\text{sec}$ ,  $5.27 \times 10^{-5} \text{ cm}^2/\text{sec}$ , and  $2.25 \times 10^{-5} \text{ cm}^2/\text{sec}$  while for 160kPa it was found to be  $5.19 \times 10^{-5} \text{ cm}^2/\text{sec}$ ,  $3.76 \times 10^{-5} \text{ cm}^2/\text{sec}$  and  $1.75 \times 10^{-5} \text{ cm}^2/\text{sec}$  respectively. Similarly value of  $C_{r2,50}$  is  $1.29 \times 10^{-4} \text{ cm}^2/\text{sec}$ ,  $9.08 \times 10^{-5} \text{ cm}^2/\text{sec}$ , and  $1.61 \times 10^{-4} \text{ cm}^2/\text{sec}$  while for 160kPa it was found to be  $8.38 \times 10^{-5} \text{ cm}^2/\text{sec}$ ,  $6.71 \times 10^{-5} \text{ cm}^2/\text{sec}$  and  $1.18 \times 10^{-4} \text{ cm}^2/\text{sec}$  respectively. Similarly value of  $C_{r3,50}$  is  $1.53 \times 10^{-4} \text{ cm}^2/\text{sec}$ ,  $1.08 \times 10^{-4} \text{ cm}^2/\text{sec}$ , and  $2.67 \times 10^{-4} \text{ cm}^2/\text{sec}$  while for 160kPa it was found to be  $1.08 \times 10^{-4} \text{ cm}^2/\text{sec}$ ,  $7.64 \times 10^{-5} \text{ cm}^2/\text{sec}$  and  $2.37 \times 10^{-4} \text{ cm}^2/\text{sec}$  respectively.
- The value of  $C_{r1,80}$  at 160kPa for CJ for 'n' equal to 11.04, 16.93 and 21.71 is  $2.46 \times 10^{-5} \text{ cm}^2/\text{sec}$ ,  $3.47 \times 10^{-5} \text{ cm}^2/\text{sec}$ , and  $1.46 \times 10^{-5} \text{ cm}^2/\text{sec}$  respectively. Similarly value of  $C_{r2,80}$  is  $1.25 \times 10^{-4} \text{ cm}^2/\text{sec}$ ,  $3.81 \times 10^{-5} \text{ cm}^2/\text{sec}$ , and  $7.31 \times 10^{-5} \text{ cm}^2/\text{sec}$  respectively. Similarly value of  $C_{r3,80}$  is  $2.15 \times 10^{-4} \text{ cm}^2/\text{sec}$ ,  $5.11 \times 10^{-5} \text{ cm}^2/\text{sec}$ , and  $1.15 \times 10^{-4} \text{ cm}^2/\text{sec}$  respectively.
- The value of  $C_{r1,80}$  at 160kPa for PF for 'n' equal to 11.04, 16.93 and 21.71 is  $1.13 \times 10^{-5} \text{ cm}^2/\text{sec}$ ,  $1.44 \times 10^{-5} \text{ cm}^2/\text{sec}$ , and  $6.63 \times 10^{-6} \text{ cm}^2/\text{sec}$  respectively. Similarly value of  $C_{r2,80}$  is  $9.5 \times 10^{-5} \text{ cm}^2/\text{sec}$ ,  $2.54 \times 10^{-5} \text{ cm}^2/\text{sec}$ , and  $5.23 \times 10^{-5} \text{ cm}^2/\text{sec}$  respectively. Similarly value of  $C_{r3,80}$  is  $1.85 \times 10^{-4} \text{ cm}^2/\text{sec}$ ,  $3.6 \times 10^{-5} \text{ cm}^2/\text{sec}$ , and  $9.53 \times 10^{-5} \text{ cm}^2/\text{sec}$  respectively.
- The value of  $C_{r1,80}$  at 160kPa for SD for 'n' equal to 11.04, 16.93 and 21.71 is  $5.5 \times 10^{-6} \text{ cm}^2/\text{sec}$ ,  $6.27 \times 10^{-6} \text{ cm}^2/\text{sec}$ , and  $6.98 \times 10^{-6} \text{ cm}^2/\text{sec}$  respectively. Similarly value of  $C_{r2,80}$  is  $5 \times 10^{-5} \text{ cm}^2/\text{sec}$ ,  $5.04 \times 10^{-5} \text{ cm}^2/\text{sec}$ , and  $1.35 \times 10^{-5} \text{ cm}^2/\text{sec}$  respectively. Similarly value of  $C_{r3,80}$  is  $9.86 \times 10^{-5} \text{ cm}^2/\text{sec}$ ,  $8.76 \times 10^{-5} \text{ cm}^2/\text{sec}$ , and  $1.69 \times 10^{-5} \text{ cm}^2/\text{sec}$  respectively.
- Looking to above plots and values it is clear that out of all three 'n' values the 'n' 11.04 shows more rate of consolidation both at low and high pressures at all three radial points for all drains. The 'n' equal to 16.93 is better in compare to 21.71 for all pressures. 'n' equal to 21.71 is not much efficient in dissipation pore water pressure because of smaller diameter and clogging problems. Out of all drains CJ shows more rate of consolidation both at low and high

pressures in compare to other drains. So it can be said that CJ shows more inter-rate of dissipation of excess hydrostatic pore water pressure even at following pressures in compare to other drains for same 'n' value. At higher pressures though dissipation is fast at nearest radial point 'r1' during initial time but it ceases as consolidation proceeds and so middle radial point is taken for comparison as no much variation is observed in value of  $C_r$  at all pressures. This is true for all 'n' values.

### **Discussion:**

Under any strain condition because of the more surface area, higher radial permeability (discharge capacity) and flexibility CJ drain of 'n' equal to 11.04 shows more efficiency in rate of consolidation compare to other 'n' equal to 16.93 and 21.7 for all pressures.

- From the plots it is very clear that for all 'n' values the initial nature of  $C_{r80}$  graph &  $C_{r50}$  graph decreases with initial applied pressure and at higher pressures it remains same that is nearly constant. It is because of the initial structural resistance existing in the clay water structure of the Kaolinite clay.
- From the plots of  $C_r$  for various 'n' values of various vertical drains it is very clear that for all 'n' values the initial nature of  $U_{r80}$  graph &  $U_{r50}$  graph decreases with initial applied pressure and at higher pressures it remains same that is nearly constant. Three reasons may be hypothesized for this: (i) for any given invrement of loading there will be dissipation of free pore water and depression of adsorbed water after pore water pressure becomes zero establishing hydrostatic equilibrium. This depression of adsorbed water may change orientation(slippage) of particle which we call 'plastic deformation' (secondary compression which was maximum in case of CJ drain of 'n'11.04 (ii) there is a change in pore size and shape at end of every load leading to dissipaiton of pore water pressure, this tubular pore channels are directly related to angle of orientation ( $\beta$ ) and tortousity. The path drawn by pore water particles vary with 'n' value and is dependant on velocity of frictional water present between two particles which helps to push solid particles nearer to each other. (iii) the change in compressibility of soil mass also depengs on discharge capacity of drains and pore size by which it attracts

and draws water by radial direction which is maximum in case of CJ of 'n'11.04 while 'n'16.93 is more efficient then 'n'21.71. This reason is true for any 'n' value of various vertical drains.

- Lesser variation in  $C_r$  value is observed for radial point's  $r_2$  and  $r_3$  for all drain materials and for all applied pressures. Though CJ of 'n'11.04 shows more inter-rate of dissipation of excess hydrostatic pore water pressure even at successive pressures in compare to other drains of 'n' values 16.93 and 21.71.

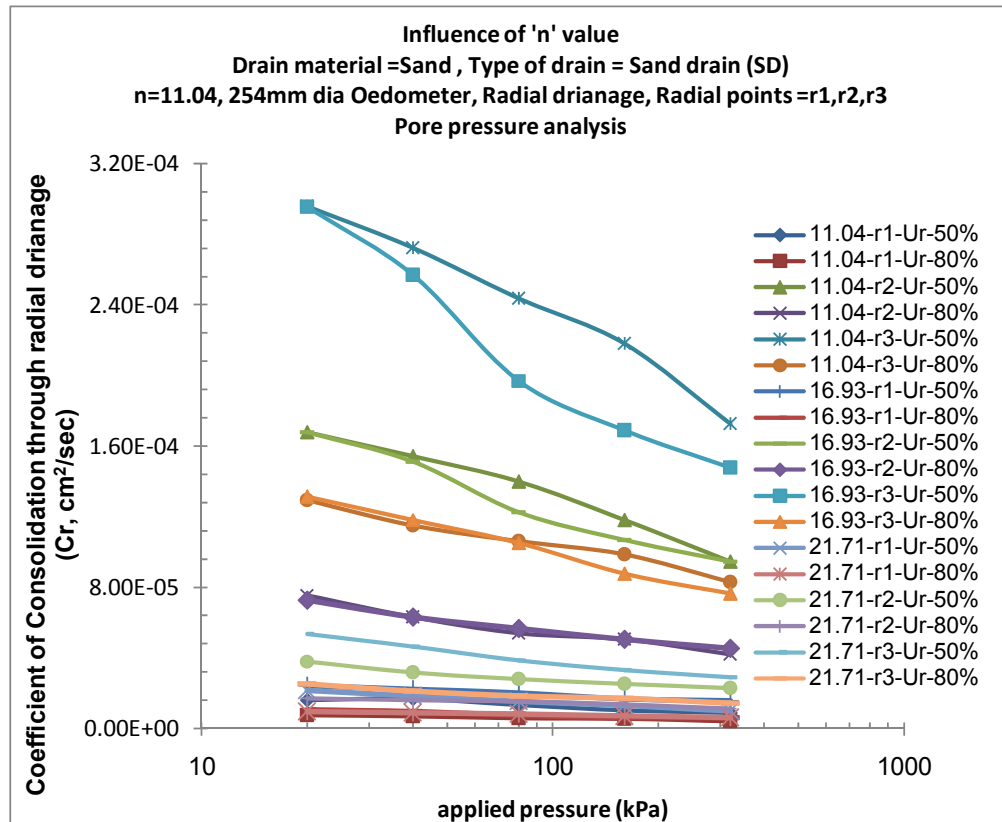


**Fig. 6.187:** Comparison of  $C_r$  against applied pressure for SD of various 'n' values at 50% and 80% degree of consolidation

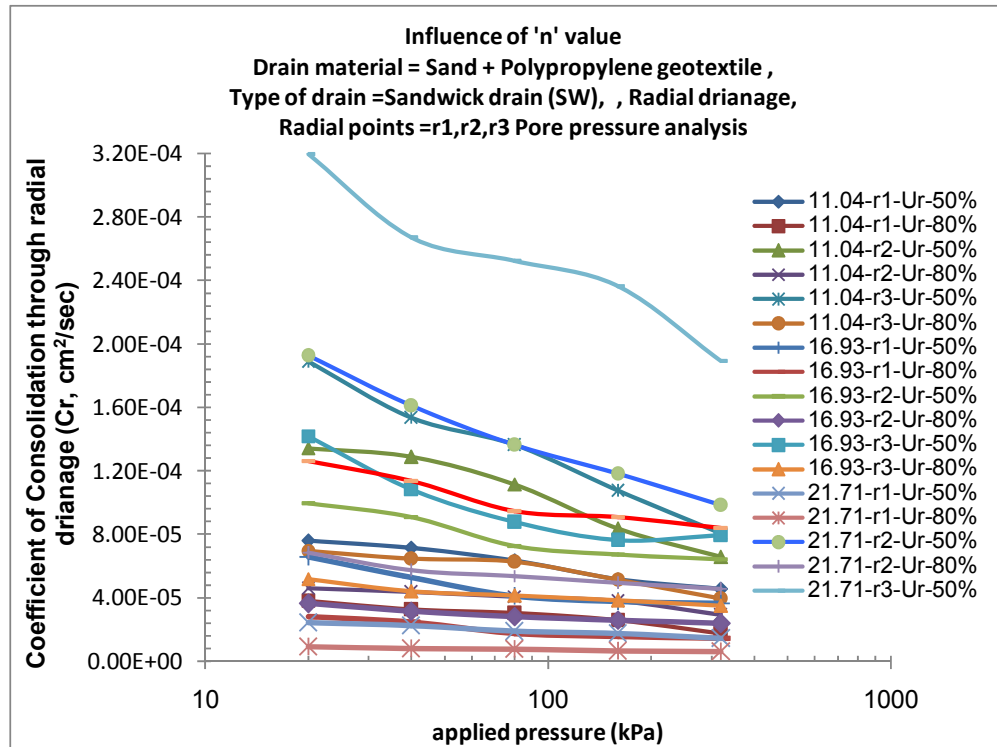


**Fig. 6.188:** Comparison of  $C_r$  against applied pressure for SW of various 'n' values at 50% and 80% degree of consolidation

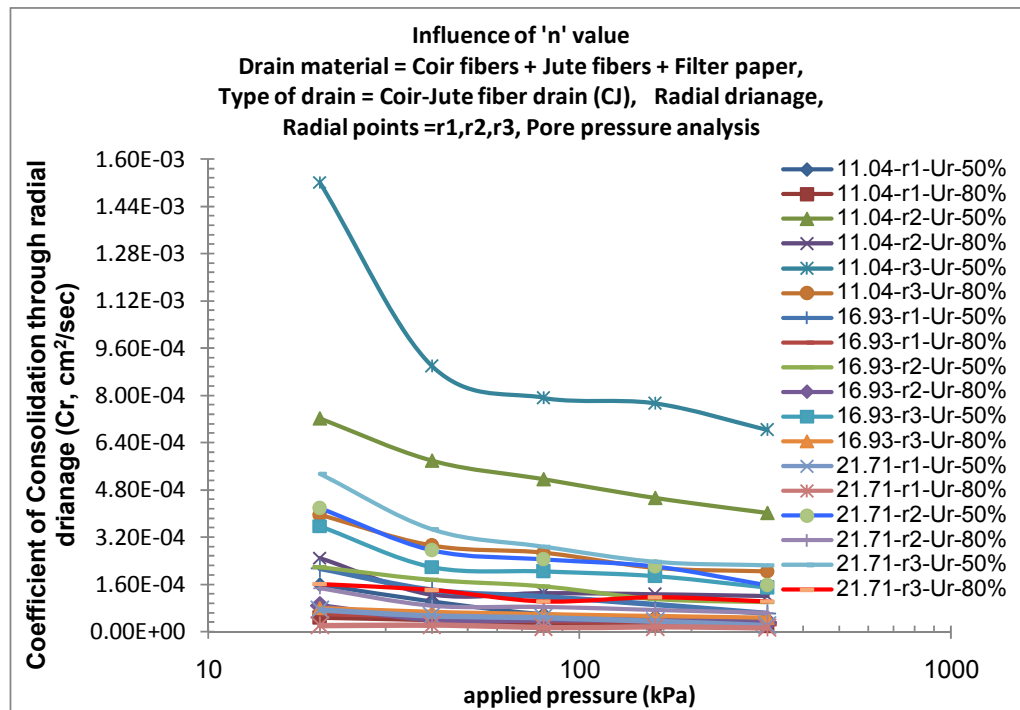


**Fig. 6.189:** Comparison of  $C_r$  against applied pressure for CJ of various 'n' values at 50% and 80% degree of consolidation



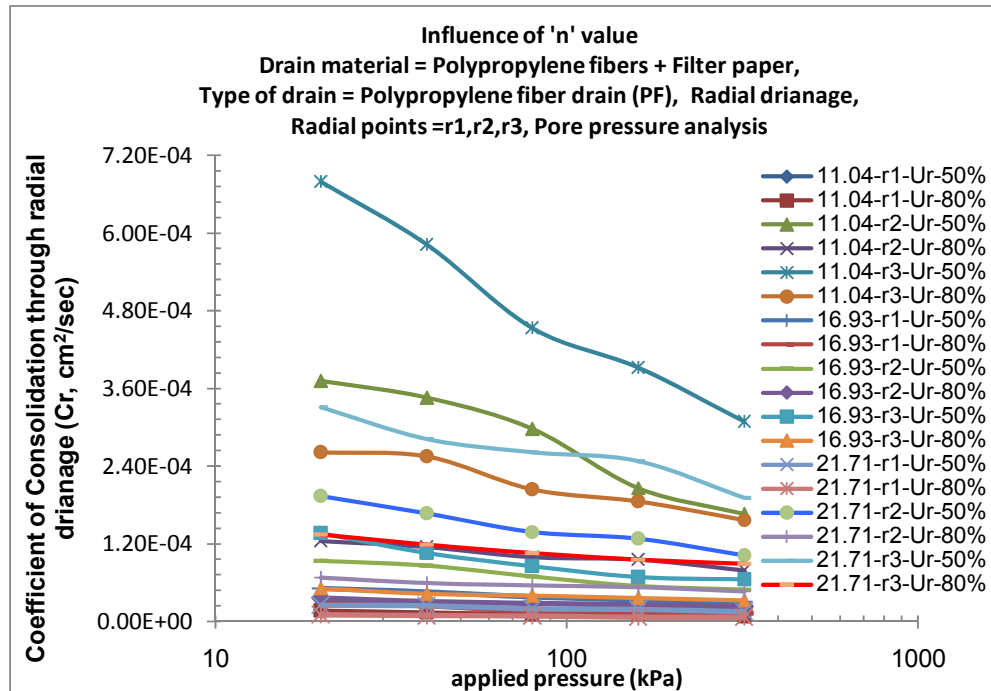


**Fig. 6.190:** Comparison of  $C_r$  against applied pressure for PF of various 'n' values at 50% and 80% degree of consolidation

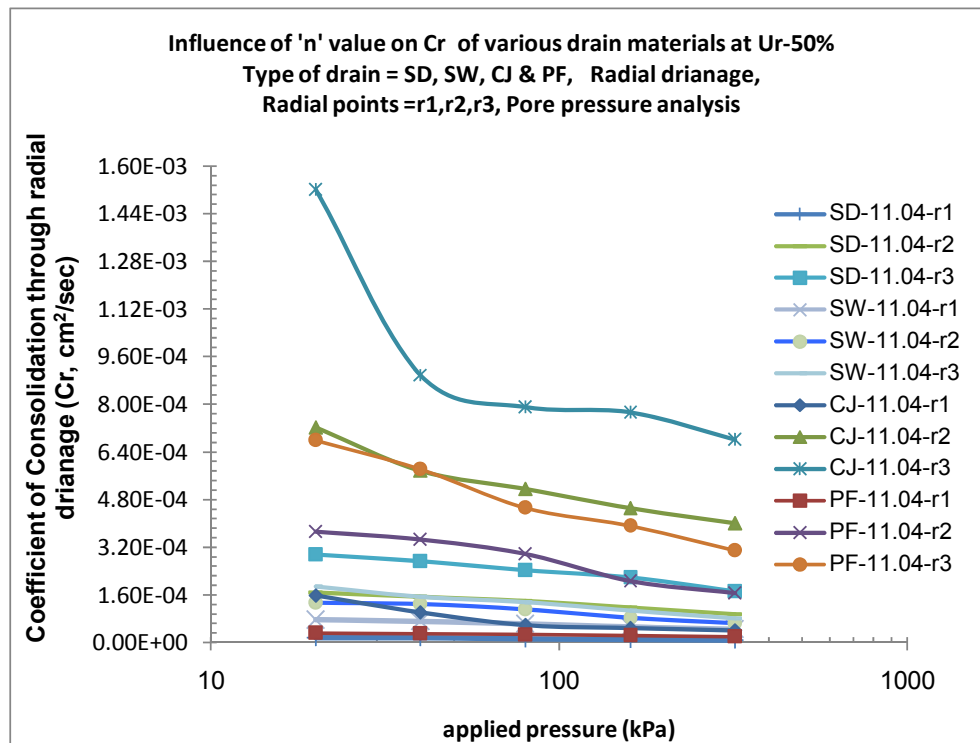


**Fig. 6.191:** Comparison of  $C_r$  value on drain material for same 'n' 11.04 at Ur =50%

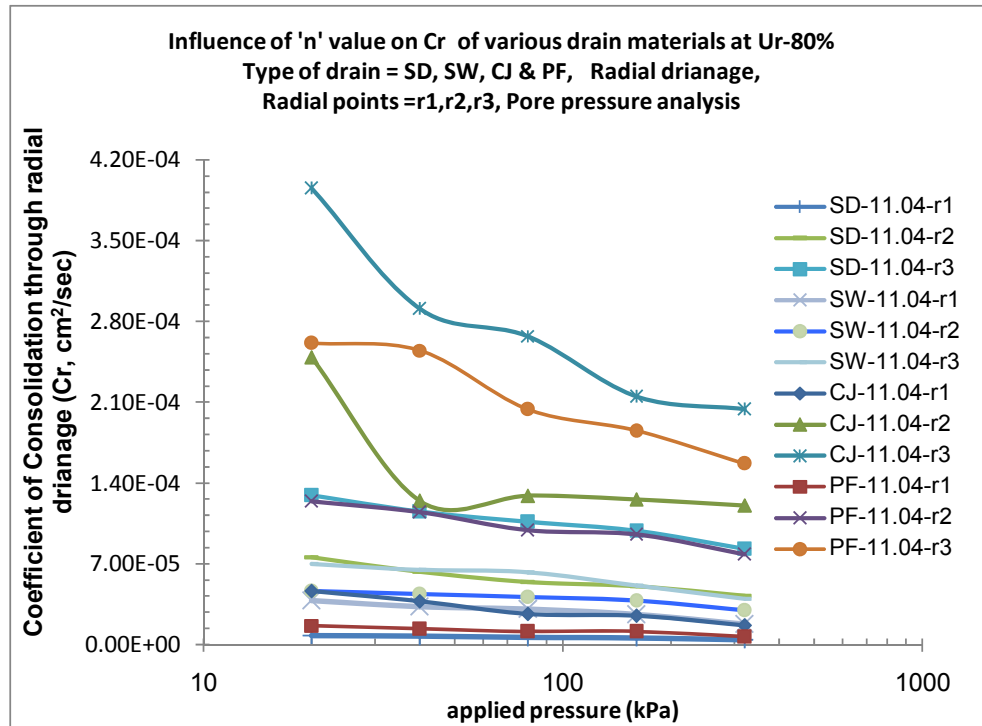


**Fig. 6.192:** Comparison of Cr value on drain material for same 'n' 11.04 at Ur = 80%

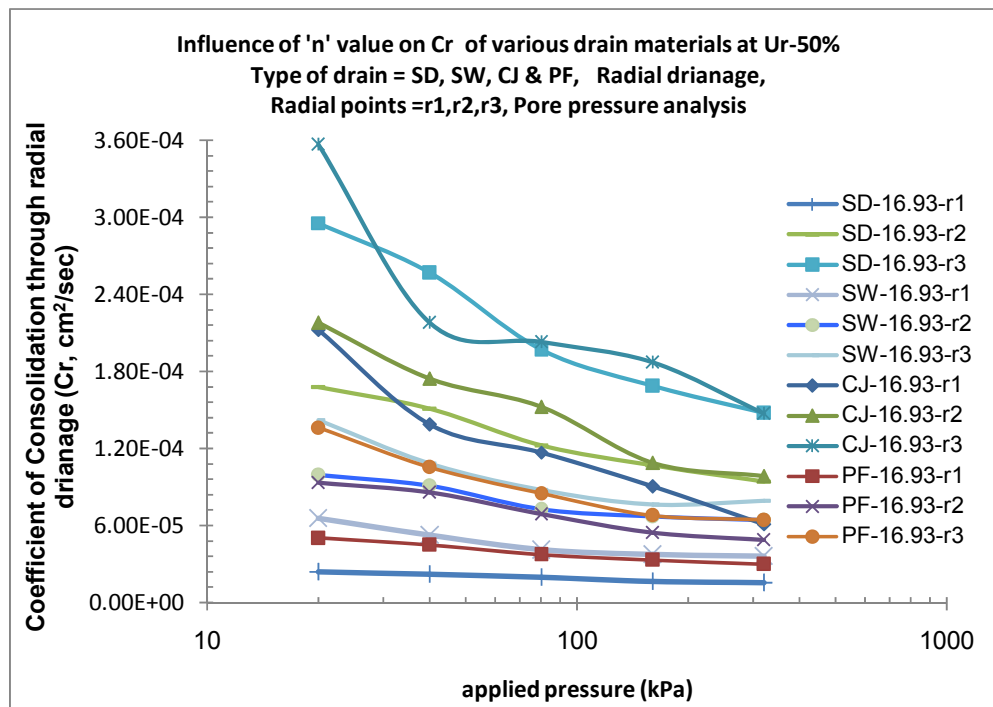


**Fig. 6.193:** Comparison of Cr value on drain material for same 'n' 16.93 at Ur =50%

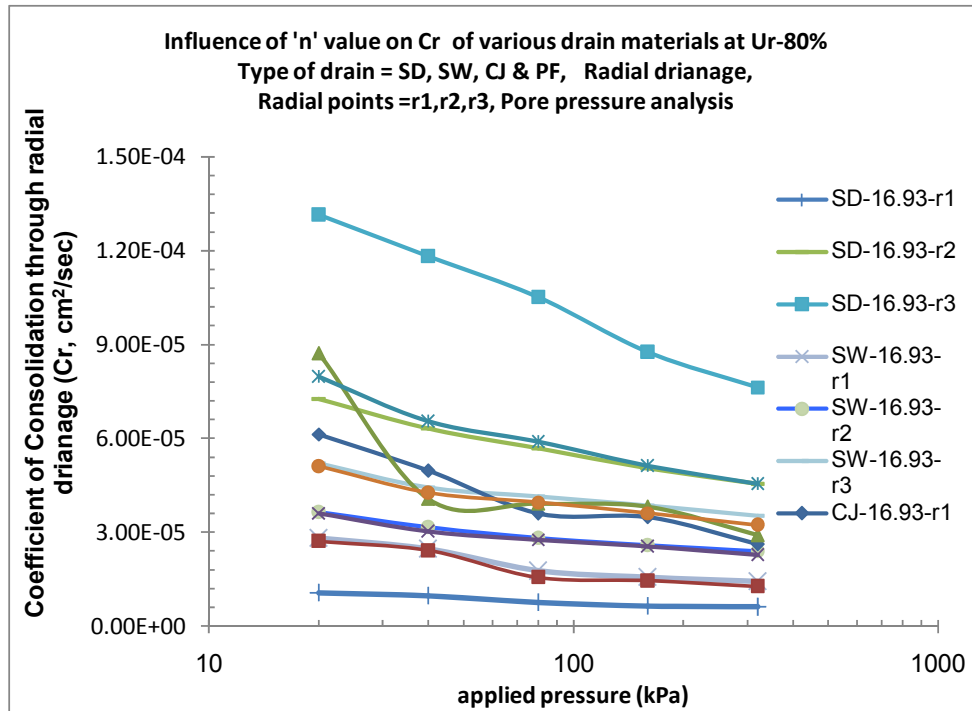


**Fig. 6.194:** Comparison of Cr value on drain material for same 'n' 16.93 at Ur =80%

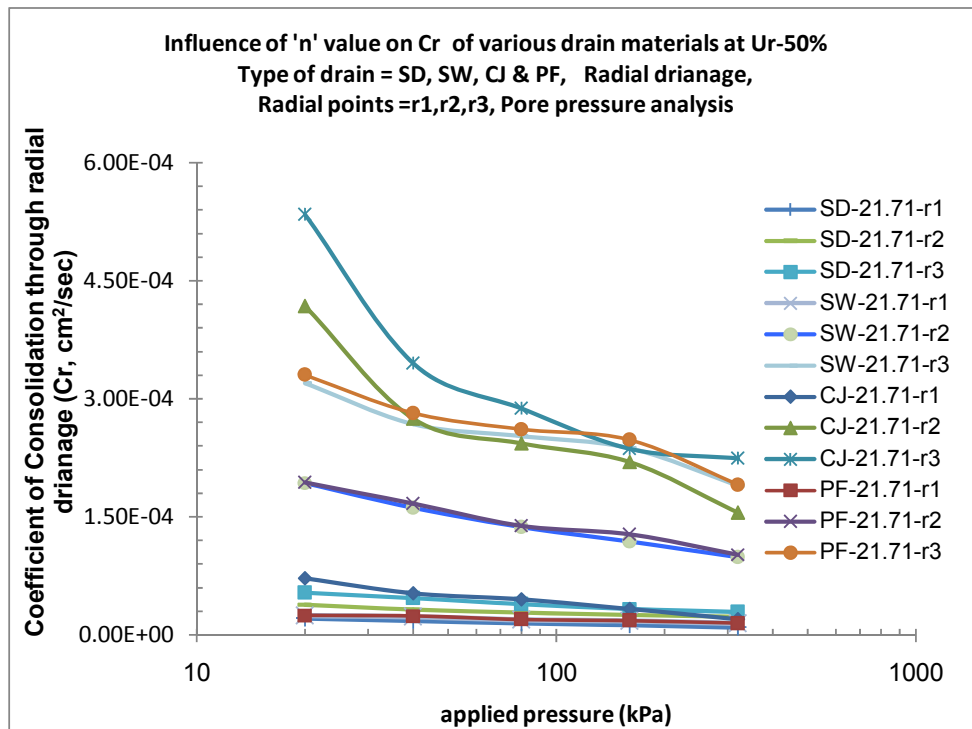


**Fig. 6.195:** Comparison of Cr value on drain material for same 'n' 21.71 at Ur =50%

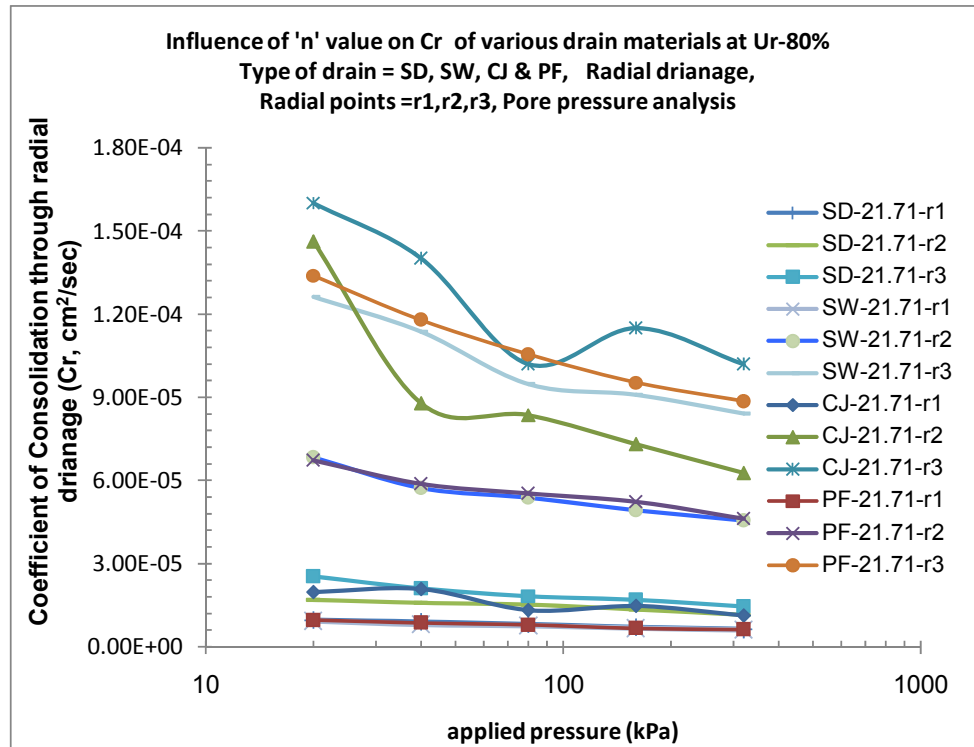


**Fig. 6.196:** Comparison of  $C_r$  value on drain material for same 'n' 21.71 at Ur =80%

#### 4) Void ratio (e) vs. applied pressure: Figures 6.197 to 6.201

**a) Settlement analysis:-** Fig.6.197 to Fig.6.201 shows a characteristic curve of normally consolidation soil for three 'n' value equal to 11.04, 16.93 and 21.71 for various drains viz. SD, SW, CJ & PF. The value of coefficient of compression ( $C_c$ ) for various vertical drains of 'n' values 11.04, 16.93 and 21.71 is 0.400, 0.409 and 0.466 for SD, while 0.315, 0.348 and 0.364 for SW, while 0.258, 0.310 and 0.384 for CJ, while 0.366, 0.353 and 0.373 for PF. From the above plots it is observed that lowest void ratio is achieved in case of  $n=11.04$  and subsequently at 'n' equal to 16.93 and 21.71. Comparing various drains lowest  $C_c$  value is observed in case of CJ of 'n'11.04 and highest value for SD of 'n'21.71. It can therefore be said that 'n' equal to 11.04 is most optimum (efficient) size of drain with greater rate of compressibility to compress soft soil thus accelerating rate of consolidation. From the void ratio obtained for various 'n' values the inter-compressibility rate was determined between two pressures and

it is observed that as pressure increases rate increases and highest gain of 49% was observed for 'n'11.04 while lowest gain of 46% was observed for 'n'21.71 for coir-jute fiber drain (CJ). This inter-compressibility rate clearly justifies efficiency of 'n' value 11.04 of CJ.

### **Discussion:**

- With the same drain  $C_c$  value shows increasing trend with higher 'n' value. It signifies that because of low rate of dissipation in higher 'n' values the magnitude of compressibility increases at particular period of interval. This behavior is similar for all drains.  $C_c$  value for coir-jute drain(CJ), Sandwich drain(SW), Polypropylene fiber drain(PF), Sand drain(SD) for  $n=11.04$  are 0.258, 0.315, 0.366, and 0.400 respectively.
- Amongst the various 'n' values the n equal to 11.04 provides optimum specific surface area to the saturated surrounding soil structure for a given diameter of influence zone of soil mass. Because of this gradient of radial flow during consolidation can help producing low level of structural resistance to compression in this case compare to other 'n' value of 16.93 and 21.71. The load component during higher level of loads can help structural breakdown or pushing the particles at a more rate leading to final consolidated mass at 320kPa. It is reflected in micro porosity, degree of orientation and tortousity measurement graphs drawn for the final load as shown in photographs 6.13 to 6.18 and figs. 6.138 to 6.140.

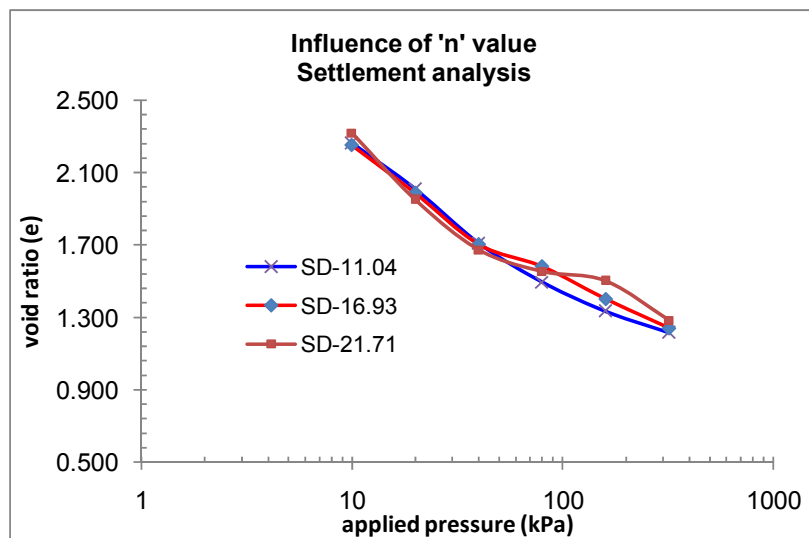


**Fig. 6.197:** Comparison of void ratio vs. applied pressure for SD

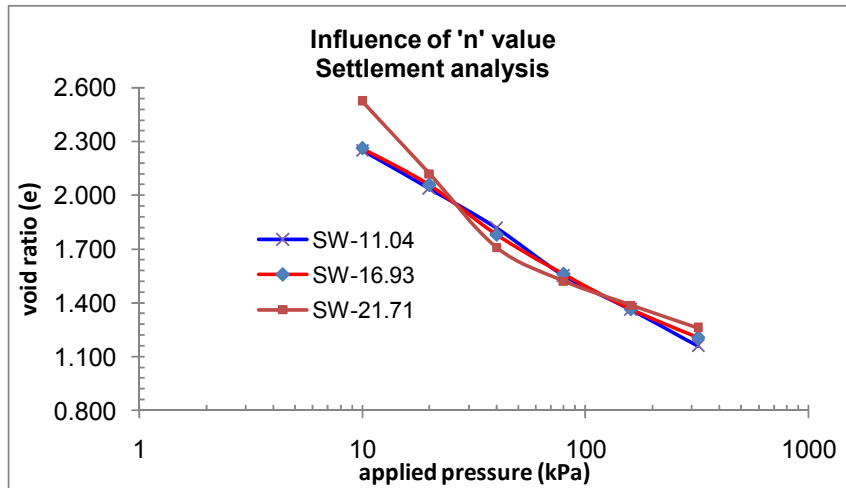


**Fig. 6.198:** Comparison of void ratio vs. applied pressure for SW

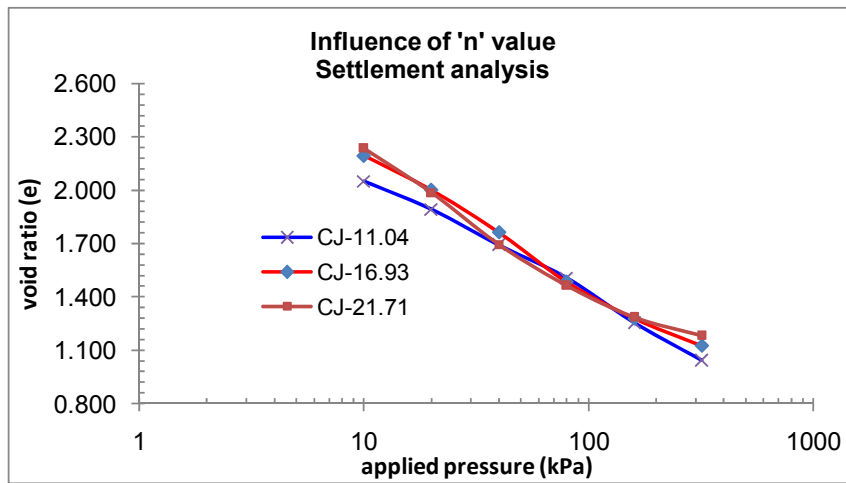


**Fig. 6.199:** Comparison of void ratio vs. applied pressure for CJ

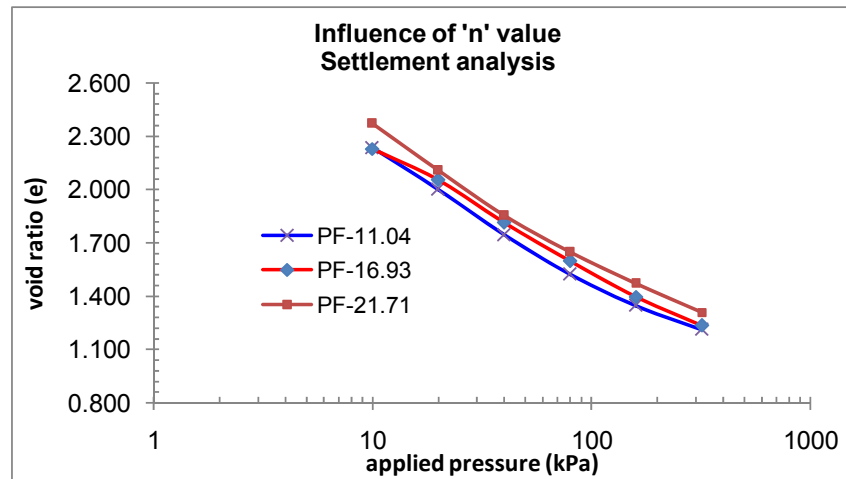


**Fig. 6.200:** Comparison of void ratio vs. applied pressure for PF

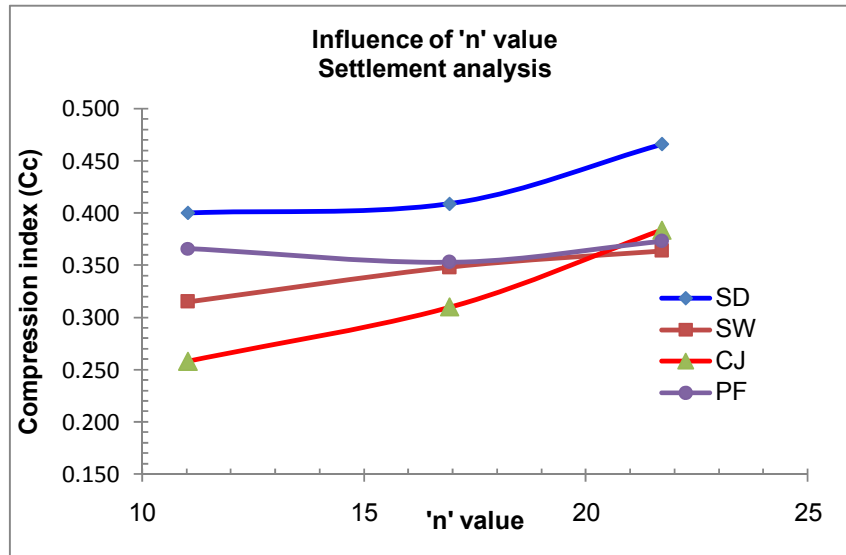


**Fig. 6.201:** Comparison of compression index ( $C_c$ ) against 'n' value for various vertical drains

### 5) Coefficient of horizontal permeability ( $k_h$ ) vs. applied pressure: Figures 6.202 to 6.215

**a) Settlement analysis-** : Fig.6.202 to Fig.6.207 shows the plots of coefficient of horizontal permeability ( $k_h$ ) versus applied pressure for various 'n' value i.e. 11.04, 16.93 and 21.71 for drains viz. SD, SW, CJ and PF at all applied pressures. Here for analysis time required for 50% ( $T_{50}$ ) consolidation and time required for 80% ( $T_{80}$ ) consolidation are taken for all pressures and for all 'n' values to get  $k_{h50}$  and  $k_{h80}$ .

- The horizontal permeability ( $k_{h50}$ ) obtained by settlement decreases with increase in the pressure for almost all drains and for all 'n' values. The value of horizontal permeability ( $k_{h50}$ ) at 160kPa for CJ for 'n' equal to 11.04, 16.93 and 21.71 is found as  $2.18 \times 10^{-7}$  cm/sec,  $3.67 \times 10^{-8}$  cm/sec,  $6.11 \times 10^{-8}$  cm/sec respectively. Similarly value of  $k_{h80}$  is found as  $7.33 \times 10^{-8}$  cm/sec,  $1.57 \times 10^{-8}$  cm/sec, and  $2.79 \times 10^{-8}$  cm/sec respectively.
- The value of horizontal permeability ( $k_{h50}$ ) at 160kPa for SW for 'n' equal to 11.04, 16.93 and 21.71 is found as  $3.36 \times 10^{-8}$  cm/sec,  $2.16 \times 10^{-8}$  cm/sec,  $1.97 \times 10^{-8}$  cm/sec respectively. Similarly value of  $k_{h80}$  is found as  $1.4 \times 10^{-8}$  cm/sec,  $9.76 \times 10^{-9}$  cm/sec, and  $1.18 \times 10^{-8}$  cm/sec respectively.

- The value of horizontal permeability ( $k_{h50}$ ) at 160kPa for PF for 'n' equal to 11.04, 16.93 and 21.71 is found as  $6.17 \times 10^{-8}$  cm/sec,  $1.94 \times 10^{-8}$  cm/sec,  $4.54 \times 10^{-8}$  cm/sec respectively. Similarly value of  $k_{h80}$  is found as  $2.79 \times 10^{-8}$  cm/sec,  $1.13 \times 10^{-8}$  cm/sec, and  $2.16 \times 10^{-8}$  cm/sec respectively.
- The value of horizontal permeability ( $k_{h50}$ ) at 160kPa for SD for 'n' equal to 11.04, 16.93 and 21.71 is found as  $7.97 \times 10^{-8}$  cm/sec,  $3.52 \times 10^{-8}$  cm/sec,  $2.06 \times 10^{-9}$  cm/sec respectively. Similarly value of  $k_{h80}$  is found as  $3.25 \times 10^{-8}$  cm/sec,  $2.41 \times 10^{-8}$  cm/sec, and  $1.1 \times 10^{-9}$  cm/sec respectively.
- With comparison of  $k_{h50}$  and  $k_{h80}$  with n' values it is found that for CJ, the  $k_{h50}$  of n=11.04 is 83% and 78% higher in compared to n=16.93 and 21.71 at 160kPa pressure, while  $k_{h80}$  of n=11.04 is 78% and 61% higher in compared to n=16.93 and 21.71 at 160kPa pressure.
- With comparison of  $k_{h50}$  and  $k_{h80}$  with n' values it is found that for SW, the  $k_{h50}$  of n=11.04 is 35% and 41% higher in compared to n=16.93 and 21.71 at 160kPa pressure, while  $k_{h80}$  of n=11.04 is 30% and 15% higher in compared to n=16.93 and 21.71 at 160kPa pressure.
- With comparison of  $k_{h50}$  and  $k_{h80}$  with n' values it is found that for PF, the  $k_{h50}$  of n=11.04 is 68% and 26% higher in compared to n=16.93 and 21.71 at 160kPa pressure, while  $k_{h80}$  of n=11.04 is 59% and 22% higher in compared to n=16.93 and 21.71 at 160kPa pressure.
- With comparison of  $k_{h50}$  and  $k_{h80}$  with n' values it is found that for SD, the  $k_{h50}$  of n=11.04 is 55% and 97% higher in compared to n=16.93 and 21.71 at 160kPa pressure, while  $k_{h80}$  of n=11.04 is 25% and 96% higher in compared to n=16.93 and 21.71 at 160kPa pressure.
- So from the above analysis it can be said that 'n' equal to 11.04 is better in compare to 16.93 and 21.71 for almost all pressures for all drains.



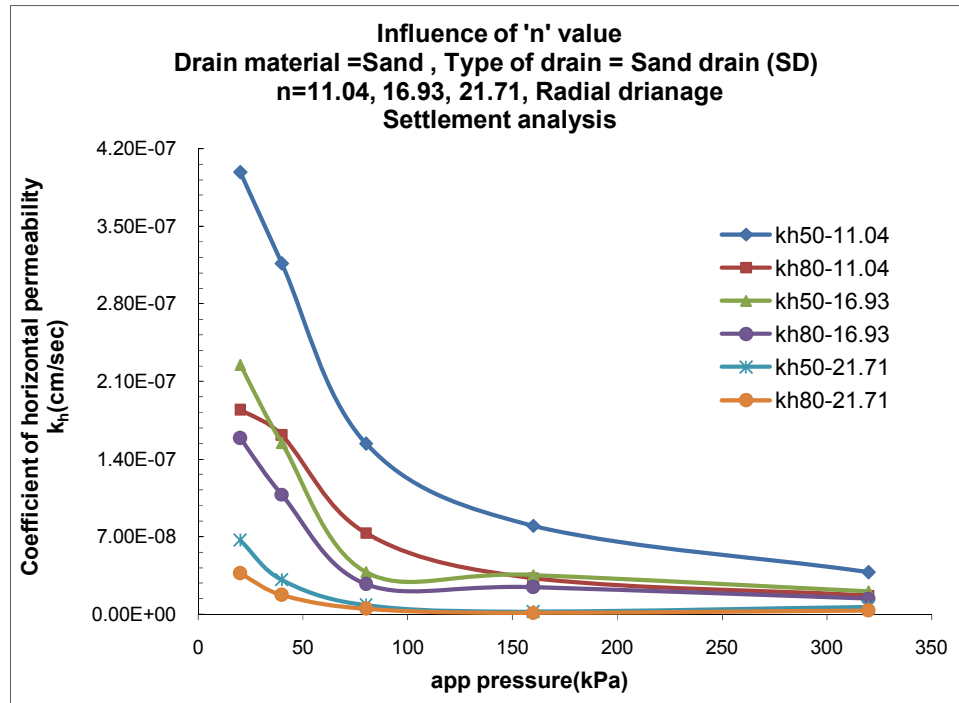


**Fig. 6.202:** Comparison of coefficient of horizontal permeability ( $k_h$ ) against applied pressure for SD of various 'n' values

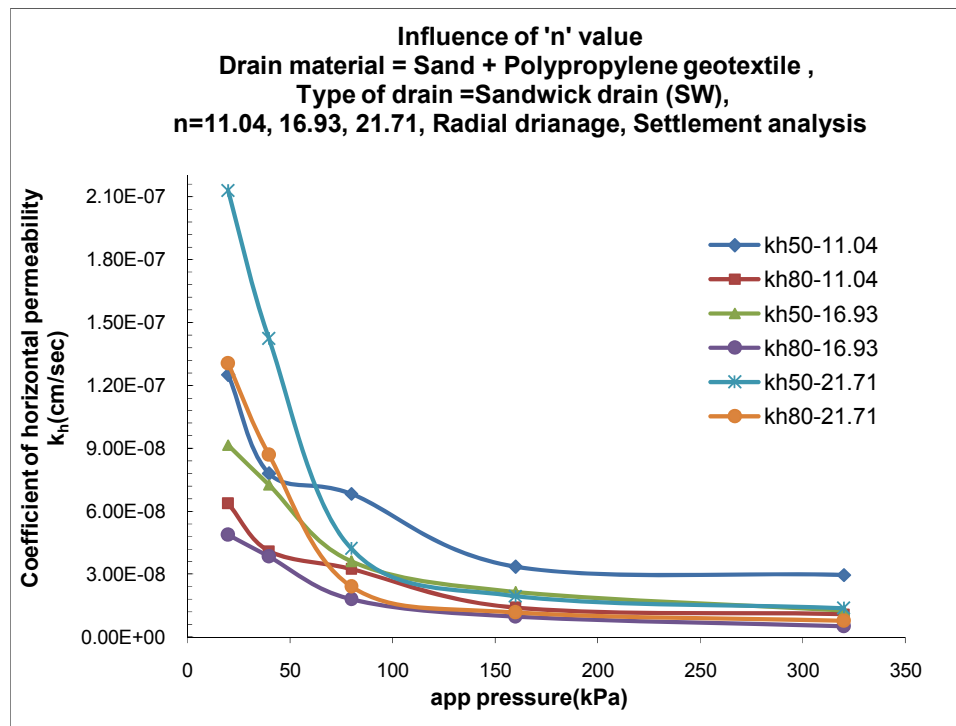


**Fig. 6.203:** Comparison of coefficient of horizontal permeability ( $k_h$ ) against applied pressure for SW of various 'n' values

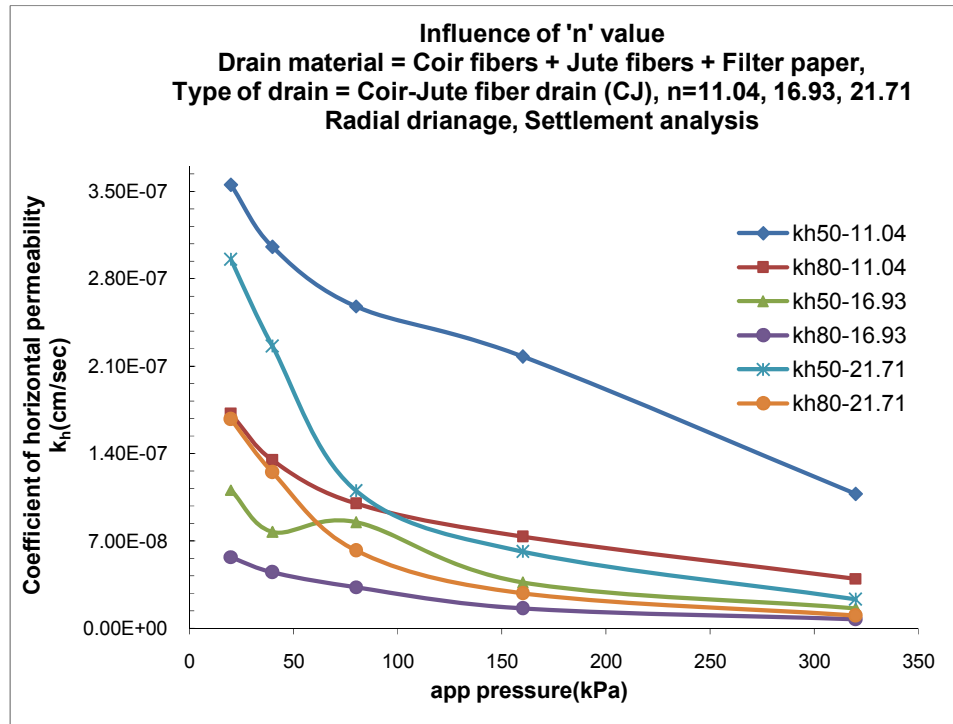


**Fig. 6.204:** Comparison of coefficient of horizontal permeability ( $k_h$ ) against applied pressure for CJ of various 'n' values

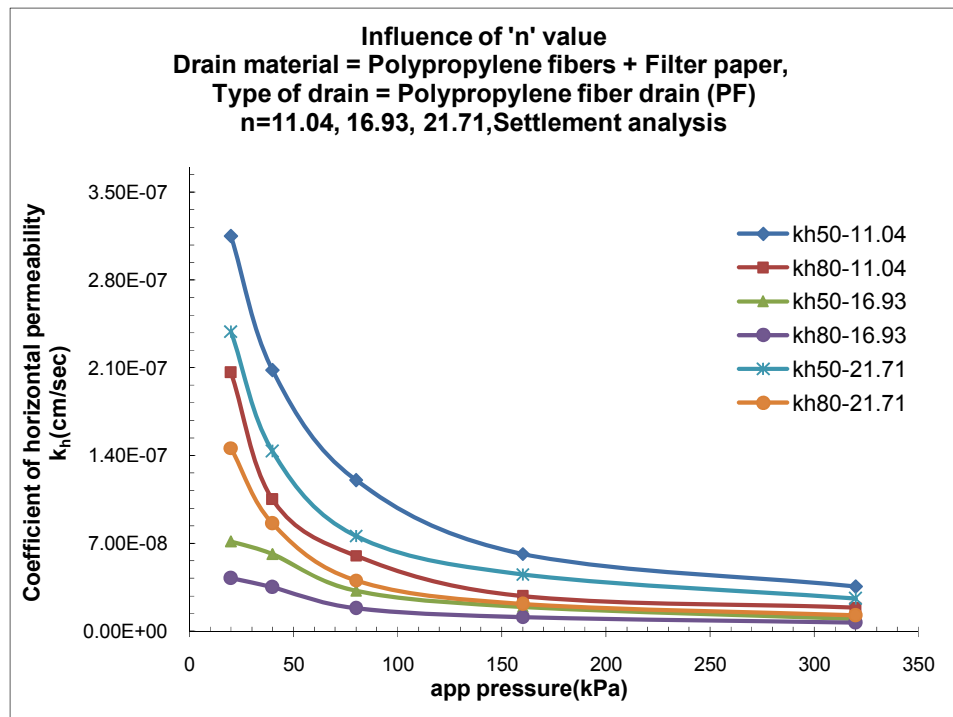


**Fig. 6.205:** Comparison of coefficient of horizontal permeability ( $k_h$ ) against applied pressure for PF of various 'n' values

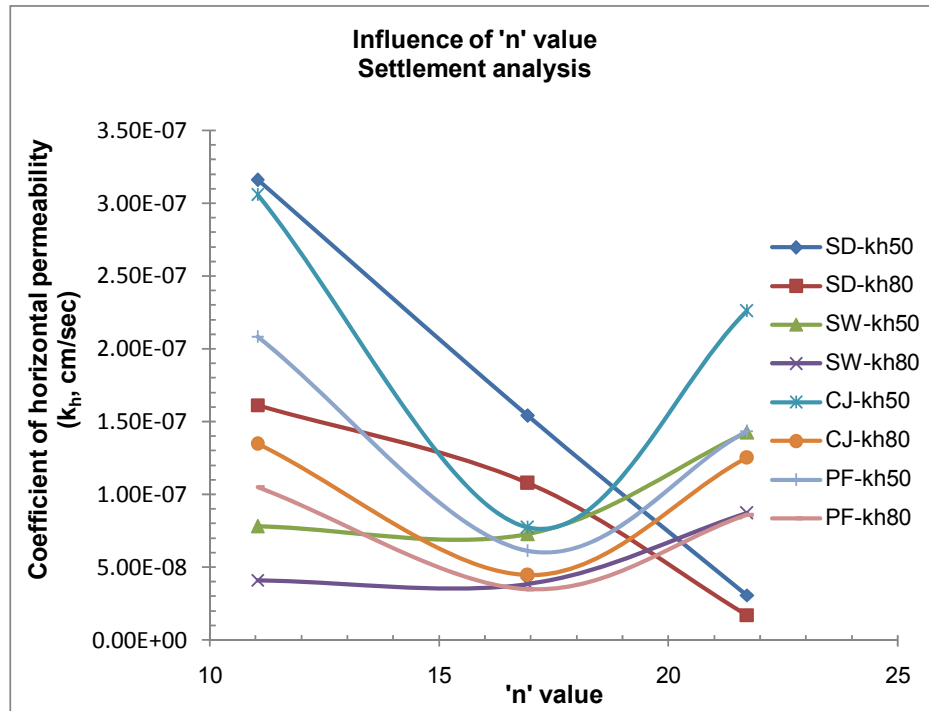


**Fig. 6.206:** Influence of 'n' value of various vertical drains on coefficient of horizontal permeability ( $k_h$ ) for Ur-50% & 80% at 40kPa pressure

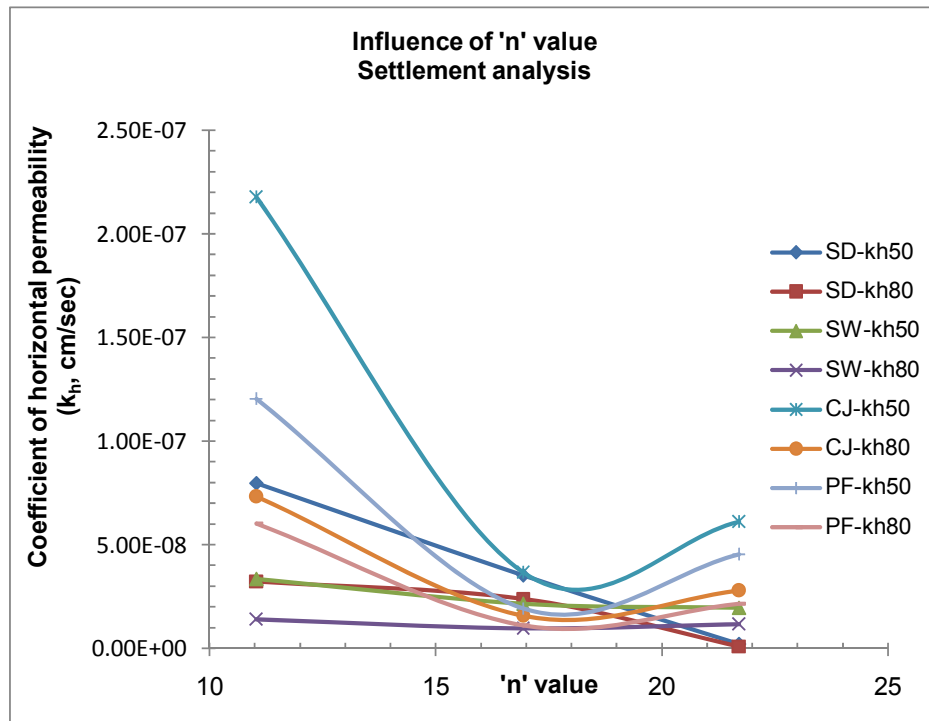


**Fig. 6.207:** Influence of 'n' value of various vertical drains on coefficient of horizontal permeability ( $k_h$ ) for Ur-50% & 80% at 160kPa pressure

**b) Pore pressure analysis:-** Fig.6.208 to Fig.6.215 shows the plots of coefficient of horizontal permeability ( $k_h$ ) versus applied pressure for various 'n' values of 11.04, 16.93 and 21.71 for various drains like SD, SW, CJ & PF for three radial points' r1, r2 & r3. Here for analysis time required for 50% ( $T_{50}$ ) consolidation and time required for 80% ( $T_{80}$ ) consolidation are taken for all pressures and all 'n' values to get  $k_{h,50}$  and  $k_{h,80}$ . The horizontal permeability at three different radial points' r1, r2 and r3 for 50% consolidation obtained by pore pressure readings decreases with increase in the pressure.

- For CJ as drain at 160kPa pressure for 'n'=11.04,16.93,21.71 at nearest radial point (r1),  $k_{h,50}$  is  $7.43 \times 10^{-9}$  cm/sec,  $1.04 \times 10^{-8}$  cm/sec,  $3.23 \times 10^{-9}$  cm/sec, while  $k_{h,80}$  for 160kPa it is  $9.27 \times 10^{-10}$  cm/sec,  $4.02 \times 10^{-9}$  cm/sec,  $1.44 \times 10^{-9}$  cm/sec respectively. Similarly at middle radial point (r2),  $k_{h,50}$  is  $6.81 \times 10^{-8}$  cm/sec,  $1.26 \times 10^{-8}$  cm/sec,  $2.15 \times 10^{-8}$  cm/sec, while  $k_{h,80}$  for 160kPa it is  $1.9 \times 10^{-8}$  cm/sec,  $4.41 \times 10^{-9}$  cm/sec,  $7.18 \times 10^{-9}$  cm/sec respectively. Similarly at outer radial point (r3),  $k_{h,50}$  is  $1.17 \times 10^{-7}$  cm/sec,  $2.16 \times 10^{-8}$  cm/sec,  $2.32 \times 10^{-8}$  cm/sec, while  $k_{h,80}$  for 160kPa it is  $3.25 \times 10^{-8}$  cm/sec,  $5.93 \times 10^{-9}$  cm/sec,  $1.13 \times 10^{-8}$  cm/sec respectively.
- For SW as drain at 160kPa pressure for 'n'=11.04,16.93,21.71 at nearest radial point (r1),  $k_{h,50}$  is  $5.31 \times 10^{-9}$  cm/sec,  $3.97 \times 10^{-9}$  cm/sec,  $1.35 \times 10^{-9}$  cm/sec, while  $k_{h,80}$  for 160kPa it is  $2.65 \times 10^{-9}$  cm/sec,  $1.63 \times 10^{-9}$  cm/sec,  $5.06 \times 10^{-10}$  cm/sec respectively. Similarly at middle radial point (r2),  $k_{h,50}$  is  $8.57 \times 10^{-9}$  cm/sec,  $7.08 \times 10^{-9}$  cm/sec,  $9.08 \times 10^{-9}$  cm/sec, while  $k_{h,80}$  for 160kPa it is  $3.88 \times 10^{-9}$  cm/sec,  $2.71 \times 10^{-9}$  cm/sec,  $3.98 \times 10^{-9}$  cm/sec respectively. Similarly at outer radial point (r3),  $k_{h,50}$  is  $1.10 \times 10^{-8}$  cm/sec,  $8.06 \times 10^{-9}$  cm/sec,  $1.82 \times 10^{-8}$  cm/sec, while  $k_{h,80}$  for 160kPa it is  $5.24 \times 10^{-9}$  cm/sec,  $4.05 \times 10^{-9}$  cm/sec,  $6.98 \times 10^{-9}$  cm/sec respectively.
- For SD as drain at 160kPa pressure for 'n'=11.04,16.93,21.71 at nearest radial point (r1),  $k_{h,50}$  is  $9.09 \times 10^{-10}$  cm/sec,  $1.6 \times 10^{-9}$  cm/sec,  $3.56 \times 10^{-10}$  cm/sec, while  $k_{h,80}$  for 160kPa it is  $4.85 \times 10^{-10}$  cm/sec,  $5.99 \times 10^{-10}$  cm/sec,  $1.92 \times 10^{-10}$  cm/sec respectively. Similarly at middle radial point (r2),  $k_{h,50}$  is  $1.04 \times 10^{-8}$  cm/sec,  $1.02 \times 10^{-8}$  cm/sec,  $6.98 \times 10^{-10}$  cm/sec, while  $k_{h,80}$  for 160kPa it is  $4.44 \times 10^{-9}$  cm/sec,  $4.82 \times 10^{-9}$  cm/sec,  $3.73 \times 10^{-10}$  cm/sec respectively. Similarly at outer radial point (r3),  $k_{h,50}$  is  $1.92 \times 10^{-8}$  cm/sec,

$1.61 \times 10^{-8}$  cm/sec,  $9.12 \times 10^{-10}$  cm/sec, while  $k_{h1,80}$  for 160kPa it is  $8.69 \times 10^{-9}$  cm/sec,  $8.37 \times 10^{-9}$  cm/sec,  $4.67 \times 10^{-10}$  cm/sec respectively.

- Comparing 'n' values for CJ it is observed that 'n' equal to 11.04 for 160kPa for  $k_{h1,50}$  is -41% and 56% higher in compare to n' equal to 16.93 & 21.71 while  $k_{h1,80}$  is -81% and 61% higher. Similarly  $k_{h2,50}$  is 81% and 68% higher in compare to n' equal to 16.93 & 21.71 while  $k_{h2,80}$  is 76% and 62% higher. While  $k_{h3,50}$  is 81% and 80% higher in compare to n' equal to 16.93 & 21.71 while  $k_{h3,80}$  is 81% and 65% higher respectively.
- Comparing 'n' values for SW it is observed that 'n' equal to 11.04 for 160kPa for  $k_{h1,50}$  is 25% and 74% higher in compare to n' equal to 16.93 & 21.71 while  $k_{h1,80}$  is -38% and 80% higher. Similarly  $k_{h2,50}$  is 17% and -5% higher in compare to n' equal to 16.93 & 21.71 while  $k_{h2,80}$  is 30% and 3% higher. While  $k_{h3,50}$  is 26% and -64% higher in compare to n' equal to 16.93 & 21.71 while  $k_{h3,80}$  is 22% and -33% higher respectively.
- Comparing 'n' values for PF it is observed that 'n' equal to 11.04 for 160kPa for  $k_{h1,50}$  is -55% and 27% higher in compare to n' equal to 16.93 & 21.71 while  $k_{h1,80}$  is -42% and 43% higher. Similarly  $k_{h2,50}$  is 70% and 40% higher in compare to n' equal to 16.93 & 21.71 while  $k_{h2,80}$  is 70% and 46% higher. While  $k_{h3,50}$  is 80% and 38% higher in compare to n' equal to 16.93 & 21.71 while  $k_{h3,80}$  is 78% and 50% higher respectively.
- Comparing 'n' values for SD it is observed that 'n' equal to 11.04 for 160kPa for  $k_{h1,50}$  is -76% and 60% higher in compare to n' equal to 16.93 & 21.71 while  $k_{h1,80}$  is -23% and 60% higher. Similarly  $k_{h2,50}$  is 2% and 93% higher in compare to n' equal to 16.93 & 21.71 while  $k_{h2,80}$  is -8% and 91% higher. While  $k_{h3,50}$  is 15% and 95% higher in compare to n' equal to 16.93 & 21.71 while  $k_{h3,80}$  is 4% and 94% higher respectively.
- So from the above analysis it can be said that 'n' equal to 11.04 is better in compare to 16.93 and 21.71 for almost all pressures for all drains. It is also concluded that coefficient of horizontal permeability ( $k_h$ ) for CJ is highest in compare to other drains for n=11.04. Also CJ of n=16.93 is more efficient in compare to n=21.71 for other drains.

### **Discussion:**

- The horizontal permeability ( $k_{h50}$ ) obtained by settlement decreases with increase in the pressure for almost all drains and for all 'n' values.
- From settlement analysis it concludes that  $n=11.04$  for 50% consolidation shows 278% and 289% higher  $k_h$  value compare to  $n=16.93$  and 21.71 for any drain material under light loading and 735% and 3025% under constructional loading. Similarly for 80% consolidation shows 190% and 200% higher  $k_h$  value compare to  $n=16.93$  and 21.71 for any drain material under light loading and 442% and 1862% under constructional loading.
- From pore analysis for middle radial point  $r_2$  it concludes that  $n=11.04$  for 50% consolidation shows 305% and 373% higher  $k_h$  value compare to  $n=16.93$  and 21.71 for any drain material under light loading and 732% and 2747% under constructional loading. Similarly for 80% consolidation shows 165% and 134% higher  $k_h$  value compare to  $n=16.93$  and 21.71 for any drain material under light loading and 454% and 1460% under constructional loading.
- $n=16.93$  shows more coefficient of transmissivity of pore water then  $n=21.71$  under both light and constructional loadings.
- From settlement analysis  $n=16.93$  shows averagely 47% and 512% higher  $k_h$  value under light loading and constructional loading compare to  $n=21.71$  but 37% and 77% lower compare to  $n=11.04$  under light loading and constructional loading for 50% consolidation under any drain material.
- From pore pressure analysis  $n=16.93$  shows averagely 63% and 411% higher  $k_h$  value under light loading and constructional loading compare to  $n=21.71$  but 45% and 73% lower compare to  $n=11.04$  under light loading and constructional loading for 50% consolidation under any drain material.
- From pore pressure analysis for 50% consolidation it concludes that  $k_h$  value of mid plane pore pressure for CJ works out to be 76% and 146% higher under light loading and constructional loading compare to PF for any 'n' value while for 80% consolidation CJ shows 33% and 77% higher value under light loading and constructional loading respectively.
- Two hypothesis can be presented here as why CJ is showing more horizontal permeability compare to other vertical drains viz. SW, PF & SD. One reason

is that fibers of coir and jute have high water absorbing capacity as well as good capillary action so pore water can travel at more faster rate and second reason lies in the microstructure of CJ drain. Not only more porosity is available on the surface of drain but arrangement of coir-jute fibers partially radial and partially vertical created tubular pore bewtten fibers and bunch of fibers which further helped pore water to dissipate faster. Even this tubular pores/channels which intersects each other at various levels of drain height and simultaneous rearrangement of this tubular pores under various stress levels indicate that there is little bit decrease in pore volume compare to microstructure behavior of other vertical drains. Even though PF drain also has fibers of polypropylene but they itself get attracted towards eachother due to water contact and interparticle attraction between two fibers decreases pore space and thus reduced discharge capacity under various stress levels.

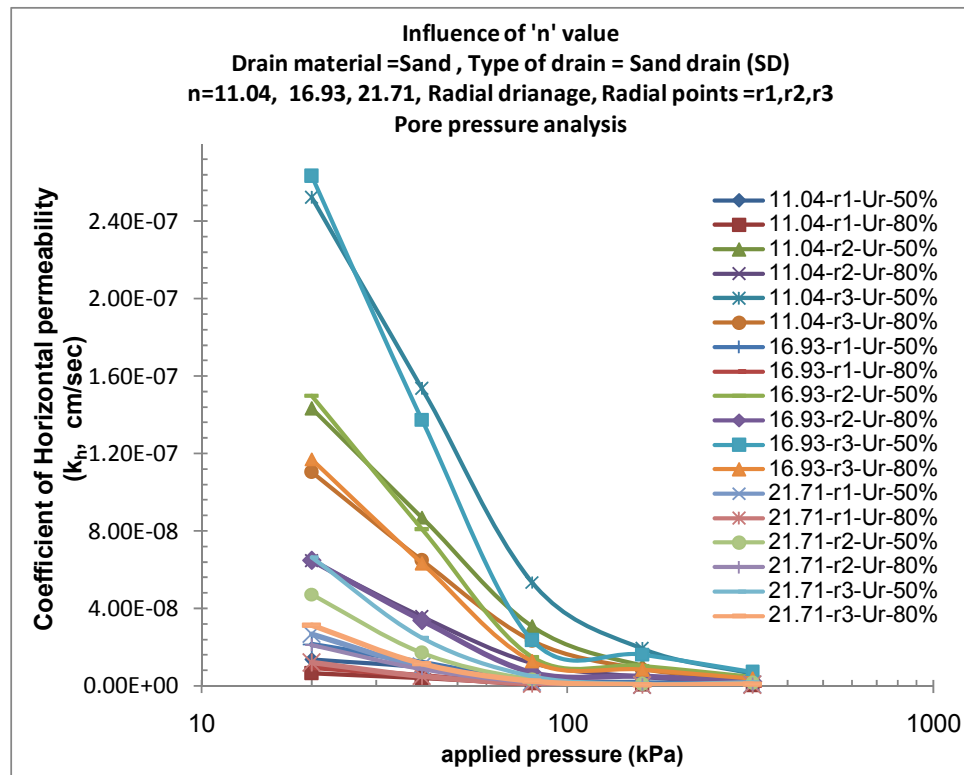


**Fig. 6.208:** Comparison of coefficient of horizontal permeability ( $k_h$ ) against applied pressure for SD of various 'n' values at radial point's r1, r2, r3

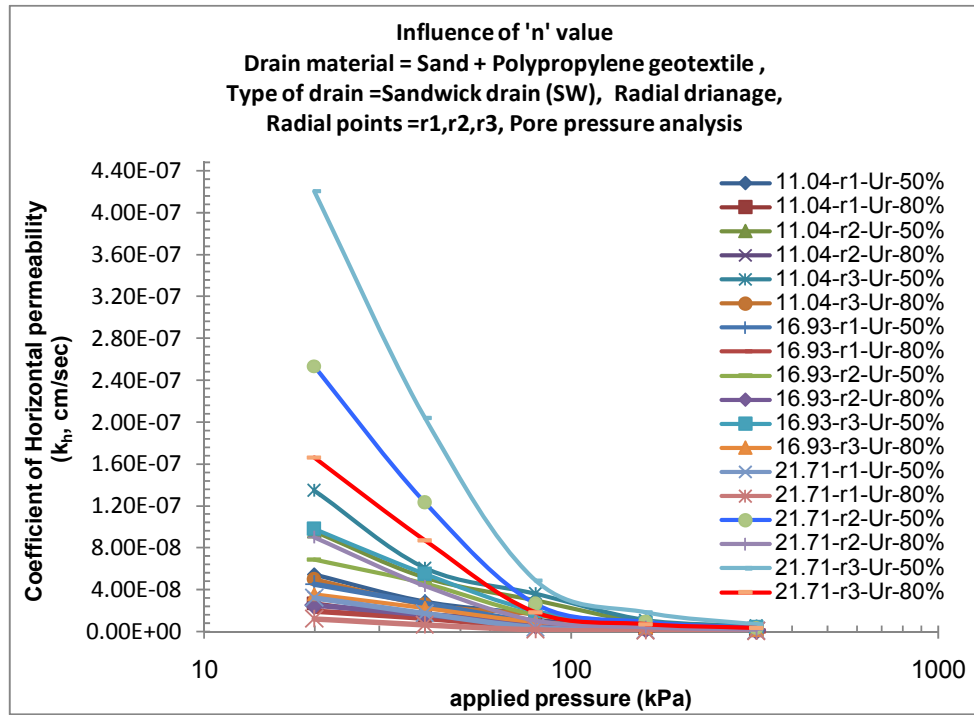


**Fig. 6.209:** Comparison of coefficient of horizontal permeability ( $k_h$ ) against applied pressure for SW of various 'n' values at radial point's r1, r2, r3

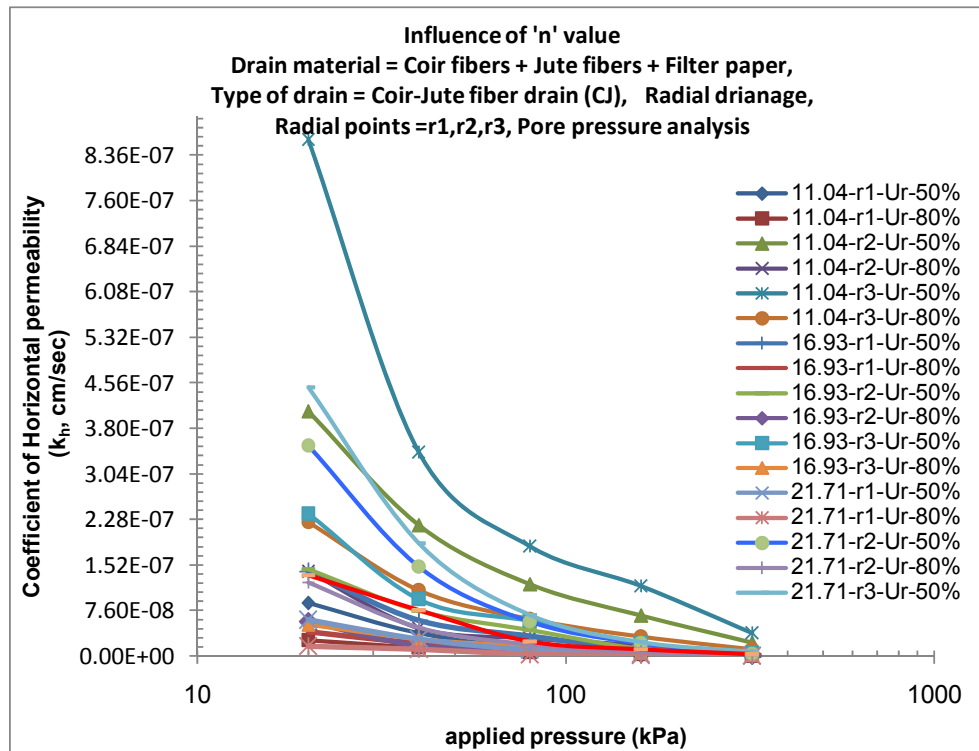


**Fig. 6.210:** Comparison of coefficient of horizontal permeability ( $k_h$ ) against applied pressure for CJ of various 'n' values at radial point's r1, r2, r3



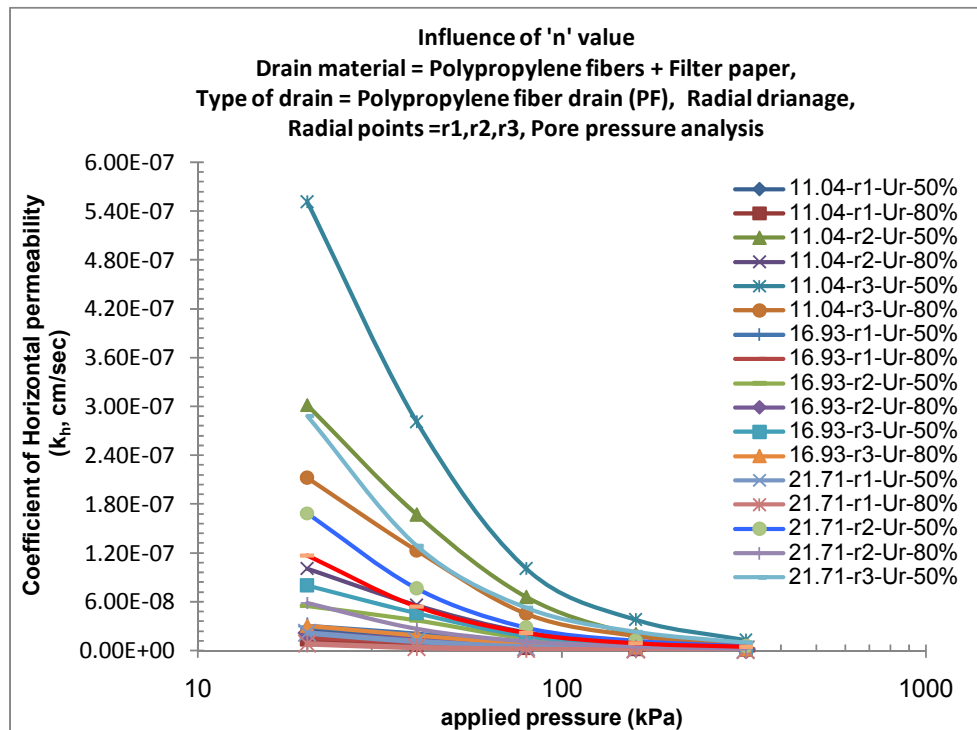


**Fig. 6.211:** Comparison of coefficient of horizontal permeability ( $k_h$ ) against applied pressure for PF of various 'n' values at radial point's r1, r2, r3

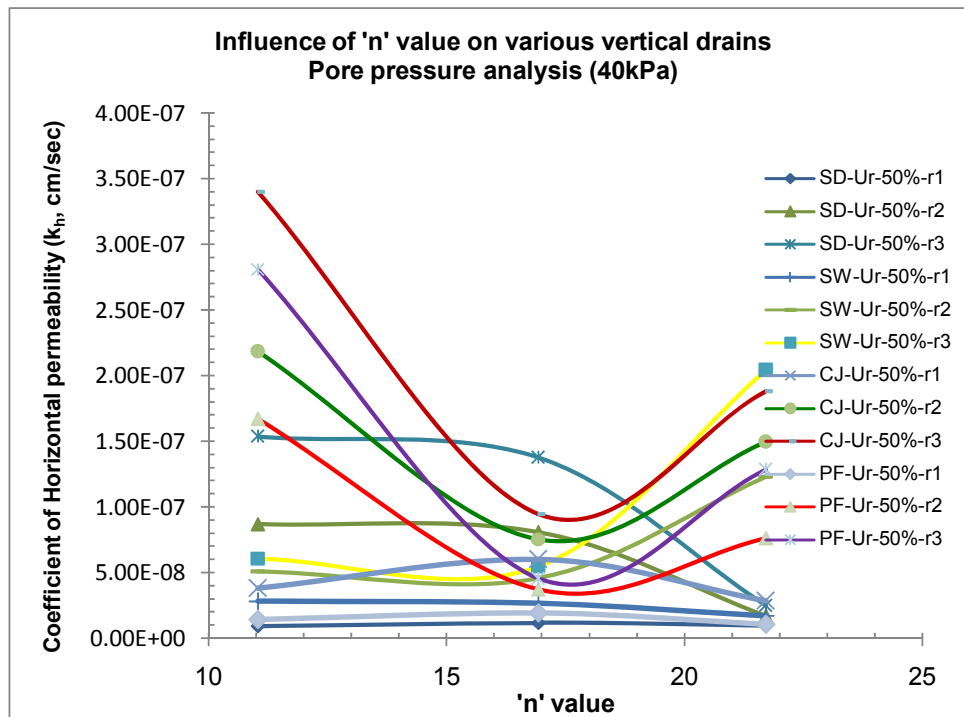


**Fig. 6.212:** Influence of 'n' value of various vertical drains on coefficient of horizontal permeability ( $k_h$ ) for Ur-50% at 40kPa pressure at three radial points

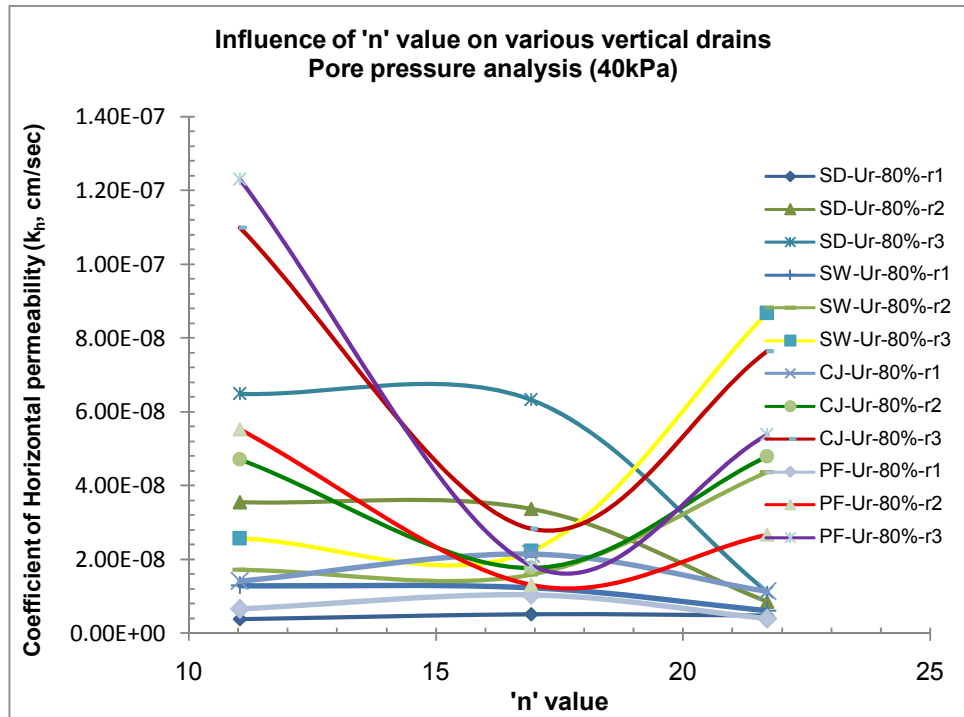


**Fig. 6.213:** Influence of 'n' value of various vertical drains on coefficient of horizontal permeability ( $k_h$ ) for Ur-80% at 40kPa pressure at three radial points

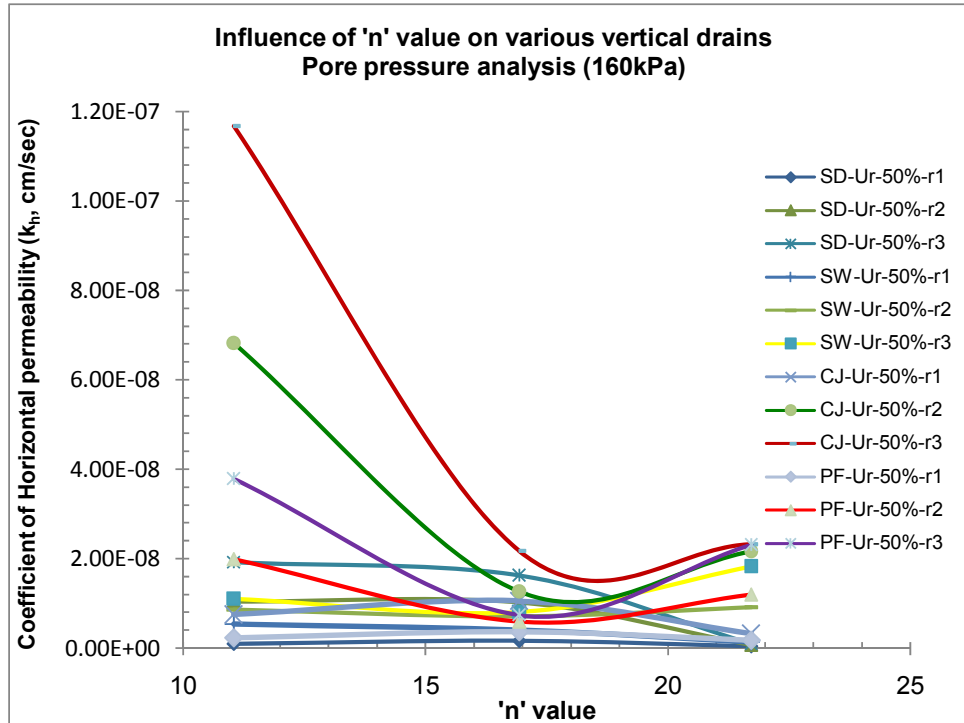


**Fig. 6.214:** Influence of 'n' value of various vertical drains on coefficient of horizontal permeability ( $k_h$ ) for Ur-50% at 160kPa pressure at three radial points

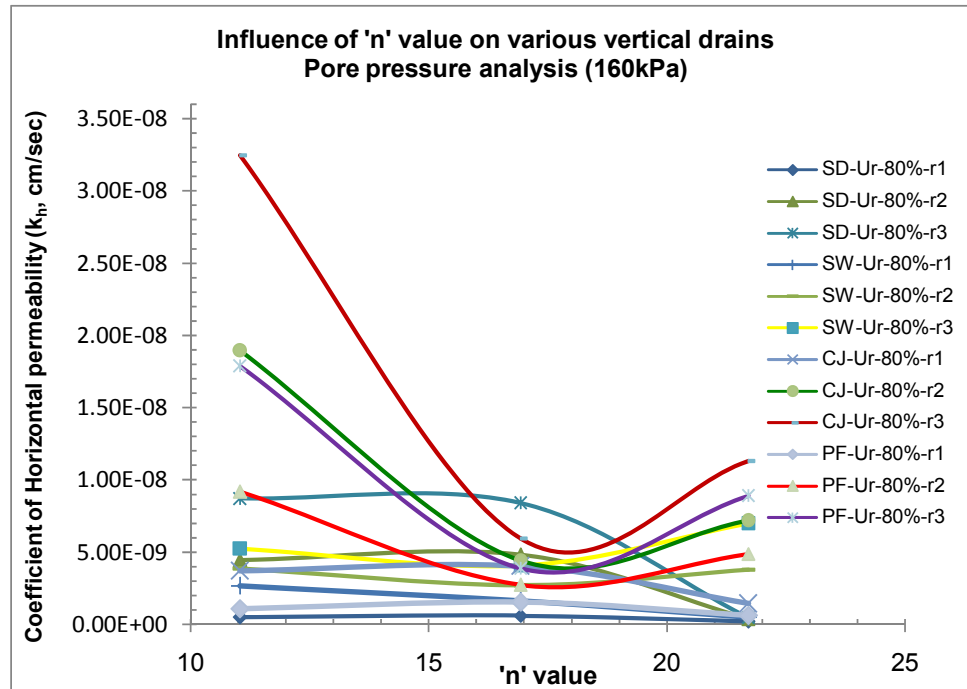


**Fig. 6.215:** Influence of 'n' value of various vertical drains on coefficient of horizontal permeability ( $k_h$ ) for Ur-80% at 160kPa pressure at three radial points

## 6) Isochrones: Figures 6.216 to 6.235

**a) Pore pressure analysis:-** Fig.6.216 to Fig.6.235 shows the plots of isochrones with respect to time and comparison of isochrones with respect to Time factor ( $T_r$ ) for various 'n' values 11.04, 16.93 and 21.71 for vertical drains viz. SD, SW, CJ and PF. Comparing initial slope of isochrones for various 'n' values against various vertical drain it interprets that CJ of 'n'11.04 shows more rate of dissipation at any time (initial linear portion of graph) compare to 'n'16.93 and 21.71 for any type of drain. While 'n'16.93 shows more inter-rate of dissipation of pore water pressure compare to 'n'21.71 for any type of vertical drain. This is true for any type of vertical drain viz. SD, SW, CJ and PF. Also it is observed that PF shows better rate of dissipation at all three radial points r1, r2 and r3 at all applied pressures. Almost for all drain materials nature of isochrones were similar except SW. Comparing theoretical and experimental isochrones using proposed theory it interprets that experimental isochrones

matches very well with theoretical isochrones for various time factors ( $T_r$ ). This is well observed for all drain materials viz. SD, SW, CJ and PF at all pressures.

For all 'n' values of any vertical drain, experimental time factor more than 0.24 exhibit concave shapes initially, while  $T_r$  less than 0.24 shows convex towards vertical axis. Comparing isochrones for various types of vertical drain it indicates that CJ of 'n'11.04 shows more magnitude of dissipation at same time factor for almost all pressures. Initial slope of SD and PF drain of 'n'16.93 and 21.71 indicates that their initial capacity of dissipation of pore water is faster up to 35% consolidation but thereafter its rate retard consistently, while SD of 'n'21.71 shows lowest rate of dissipation during entire process of consolidation thus indicating that 'n'21.71 is not effective in increasing rate of consolidation and this is almost true for all vertical drains. The reasons for this may be less surface area of drain, bulging and twisting of drain, fast clogging of drain, low strain compatability of drain with loads and as diameter is less, longer drainage path retards velocity of pore water. Reverse is the behavior of 'n'16.93 for any vertical drain but less effective compare to 'n'11.04 for any loads, also PF and SW shows nearly equal rate of diispation of pore water pressure either at low value of time factor at high value of time factor. Comparing groups of all the isochrones of various time factor of various vertical drains, SD curve are distinctly showing initial concave curve for 'n'21.71 and same pattern of curves are obtain for PF of 'n'16.93.

### **Discussion:**

As discussed already in above preeceding plots, the micro pore structures of the SW drain of 'n'11.04 are quite distinct that is initial micro porosity of SW is less compare to other drains while micro pore structures of PF of 'n'16.93 are quite distinct which also reflects in isochrones characteristics. Other 'n' values of various vertical drains shows more or less same micro porosity that wise initial slope of isochrones is same to some extent, but with increase of time factor micro-porosity decreases in other drains while in CJ drain of 'n'11.04 micro porosity remains almost same being the flexible nature of jute and coir fibers which helps in more dissipation of pore pressure indicating

more percentage of consolidation. Overall microporosity decreases with increase of 'n' value and same is the effect on angle of orientation.

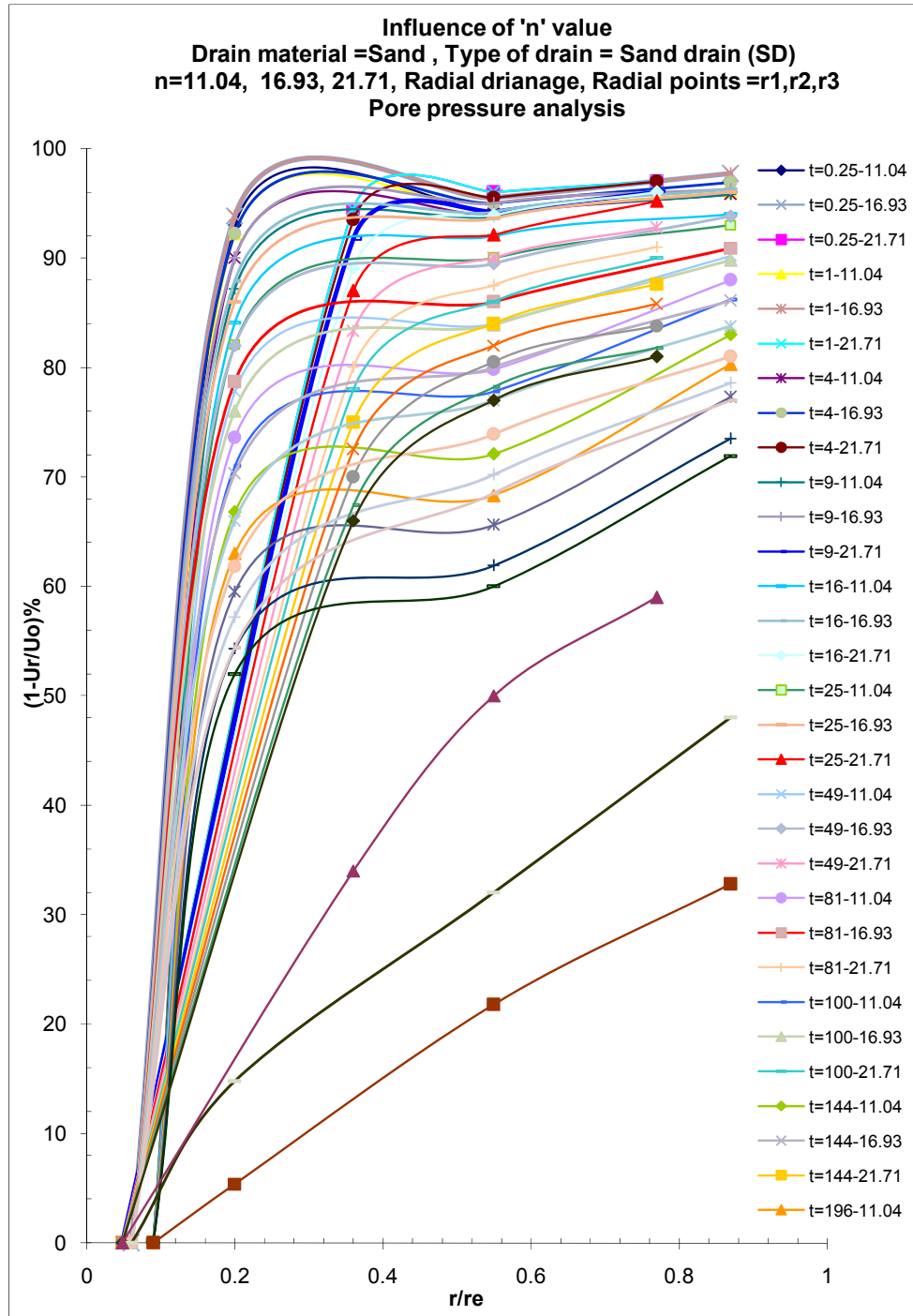


**Fig. 6.216:** Comparison of isochrones of 'n' values (dissipation of excess hydrostatic pore water pressure) w.r.t time against ratio of radial distance at 160kPa pressure

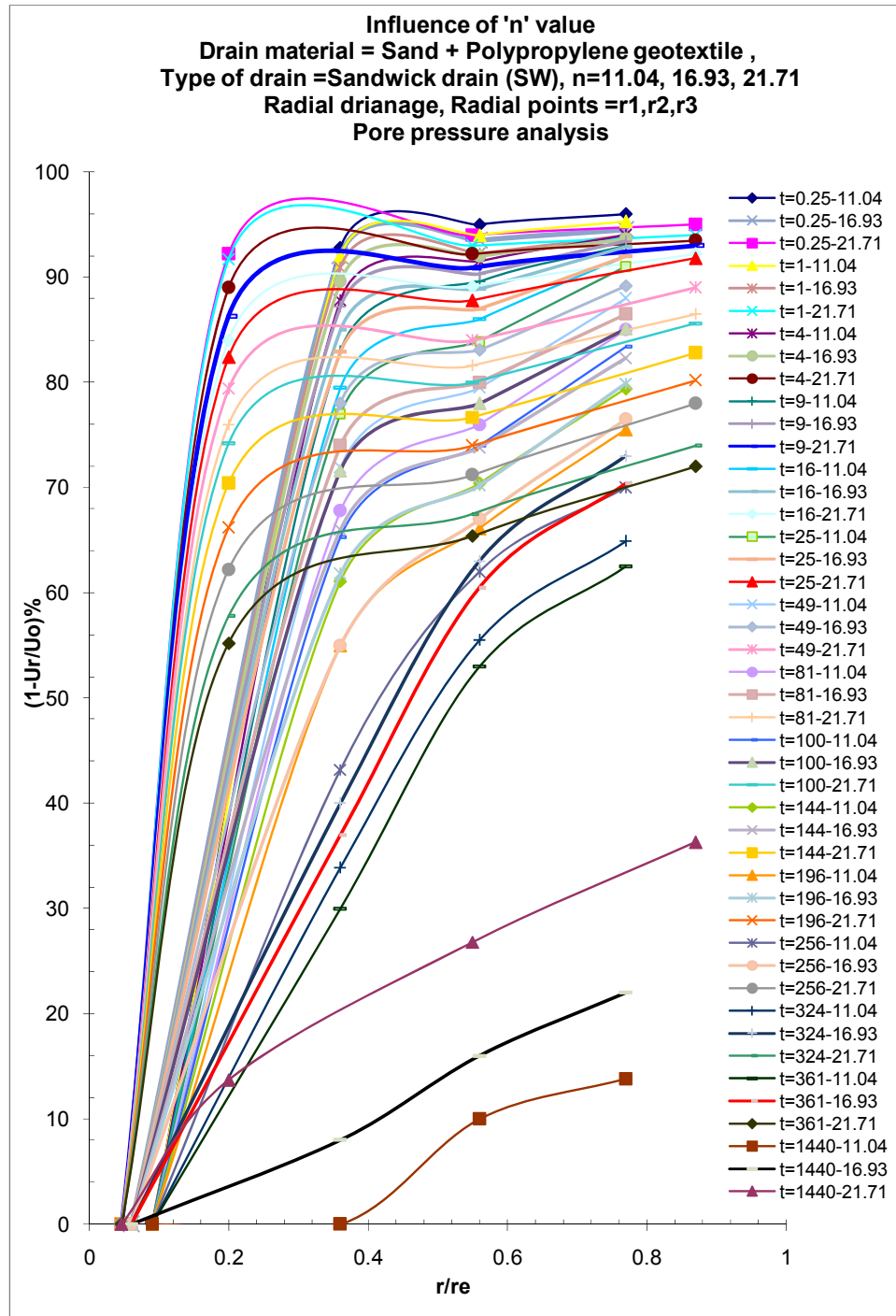


**Fig. 6.217:** Comparison of isochrones of 'n' values (dissipation of excess hydrostatic pore water pressure) w.r.t time against ratio of radial distance at 160kPa pressure

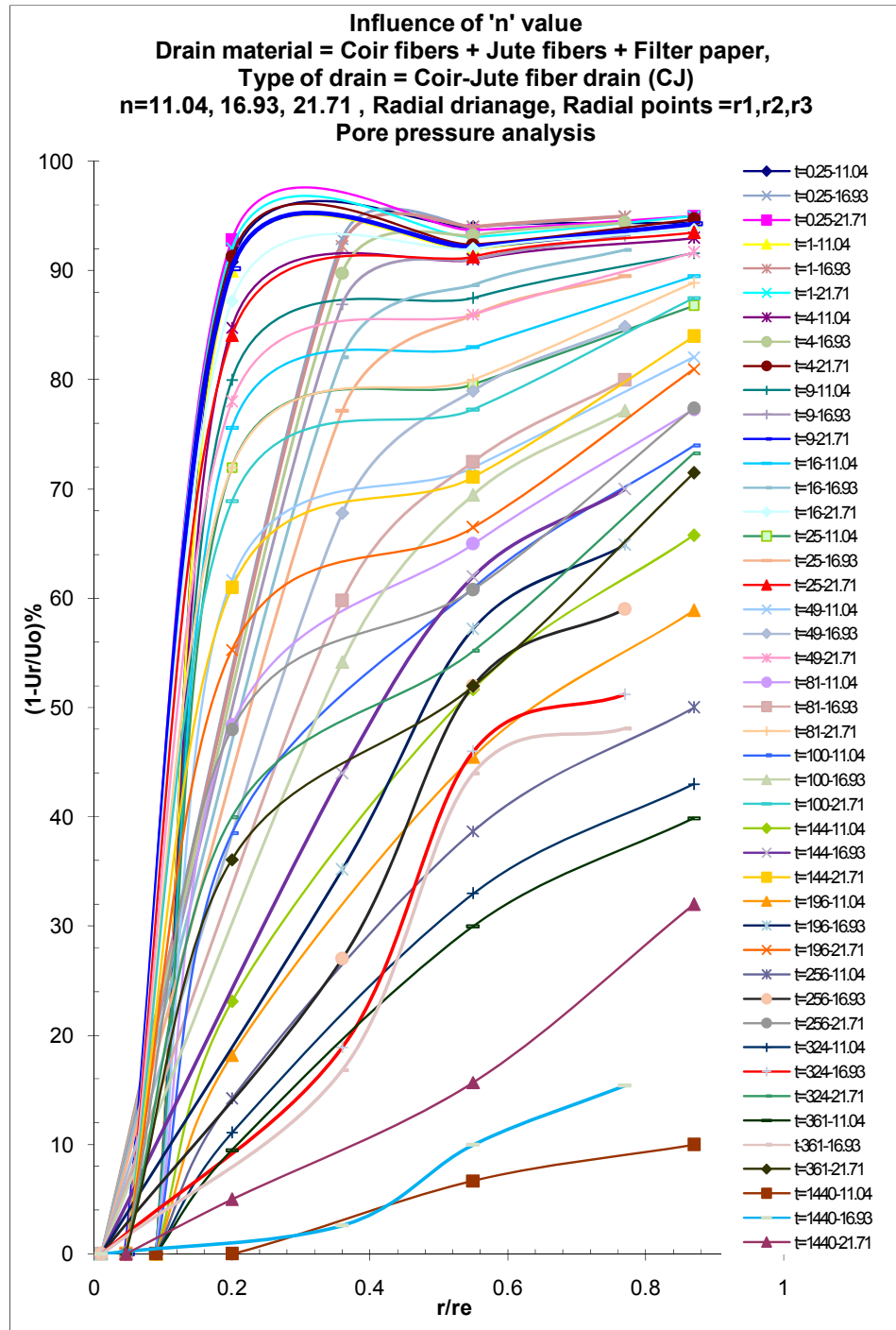


**Fig. 6.218:** Comparison of isochrones of 'n' values (dissipation of excess hydrostatic pore water pressure) w.r.t time against ratio of radial distance at 160kPa pressure

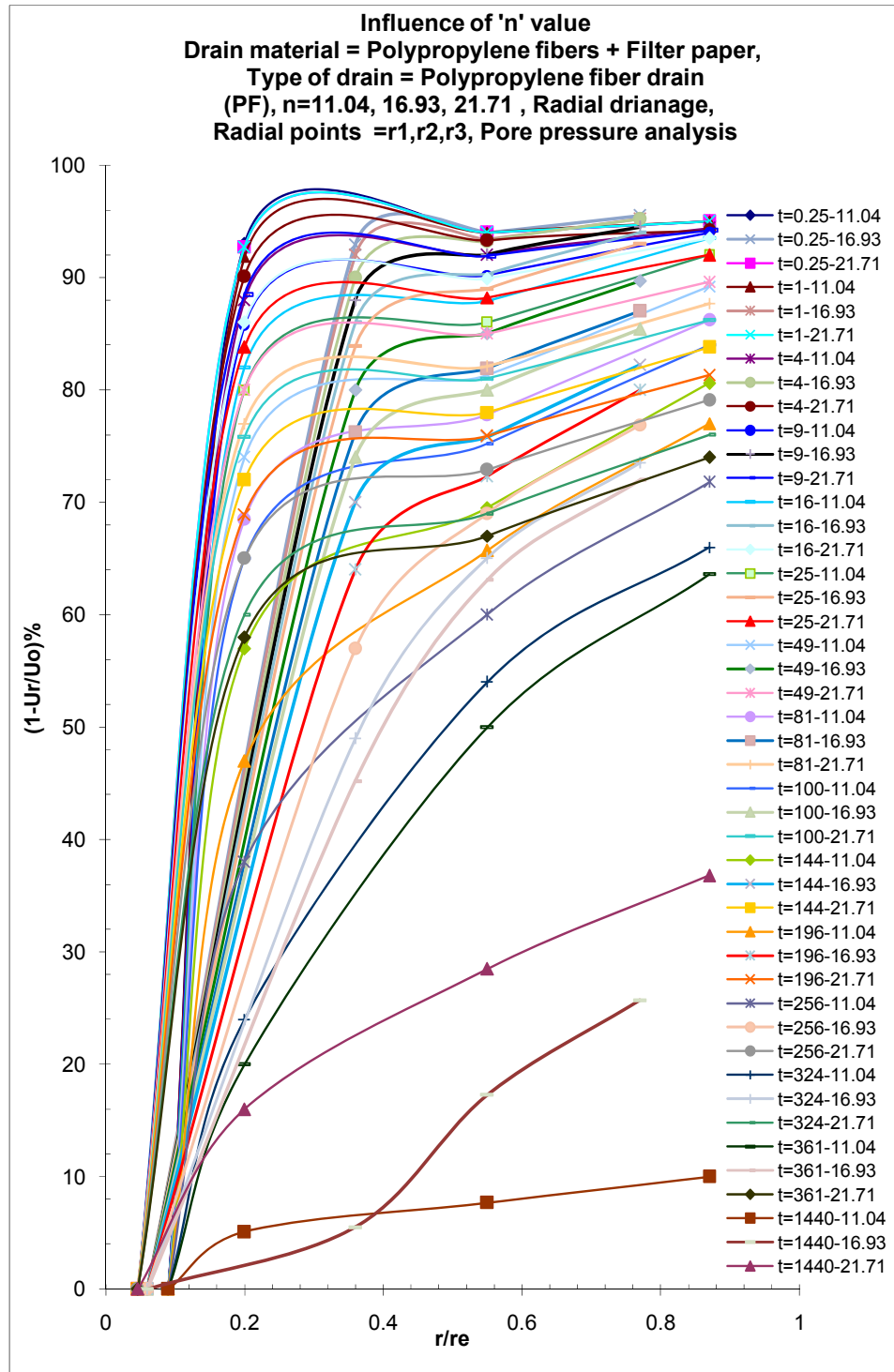


**Fig. 6.219:** Comparison of isochrones of 'n' values (dissipation of excess hydrostatic pore water pressure) w.r.t time against ratio of radial distance at 160kPa pressure



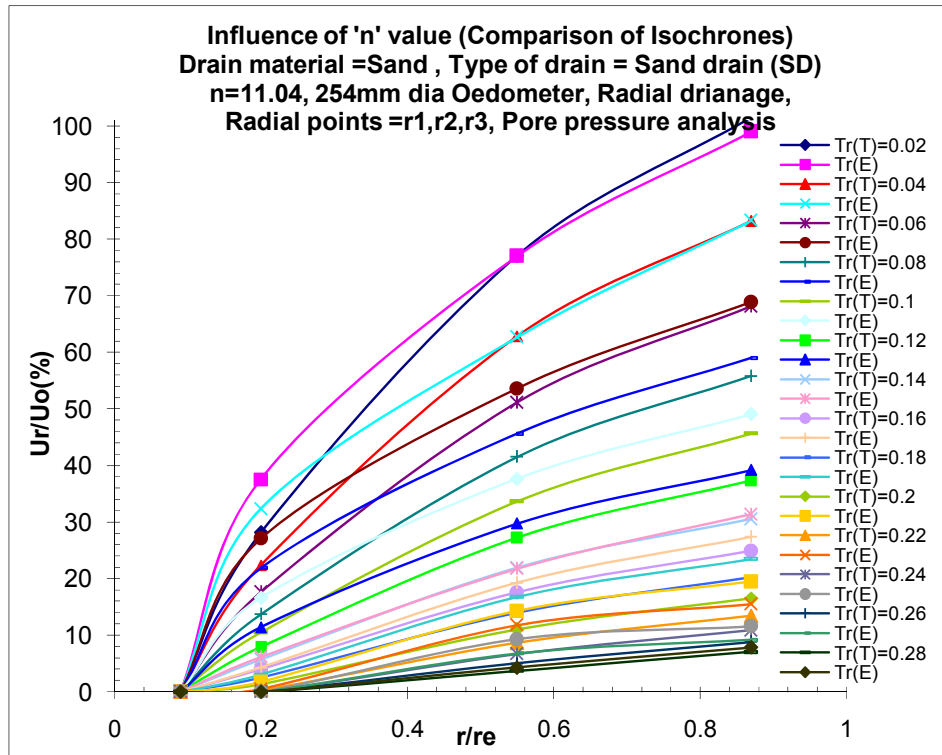


**Fig. 6.220:** Comparison of isochrones of 'n'11.04 of SD w.r.t experimental and theoretical Time factors ( $Tr$ ) at 160kPa pressure

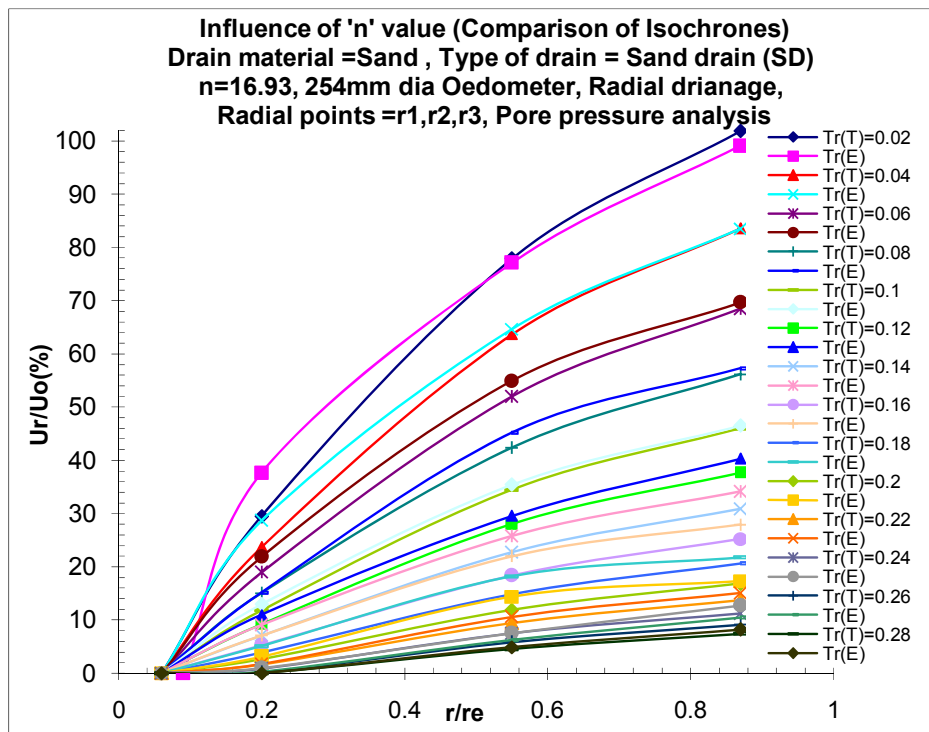


**Fig. 6.221:** Comparison of isochrones of 'n'16.93 of SD w.r.t experimental and theoretical Time factors ( $Tr$ ) at 160kPa pressure

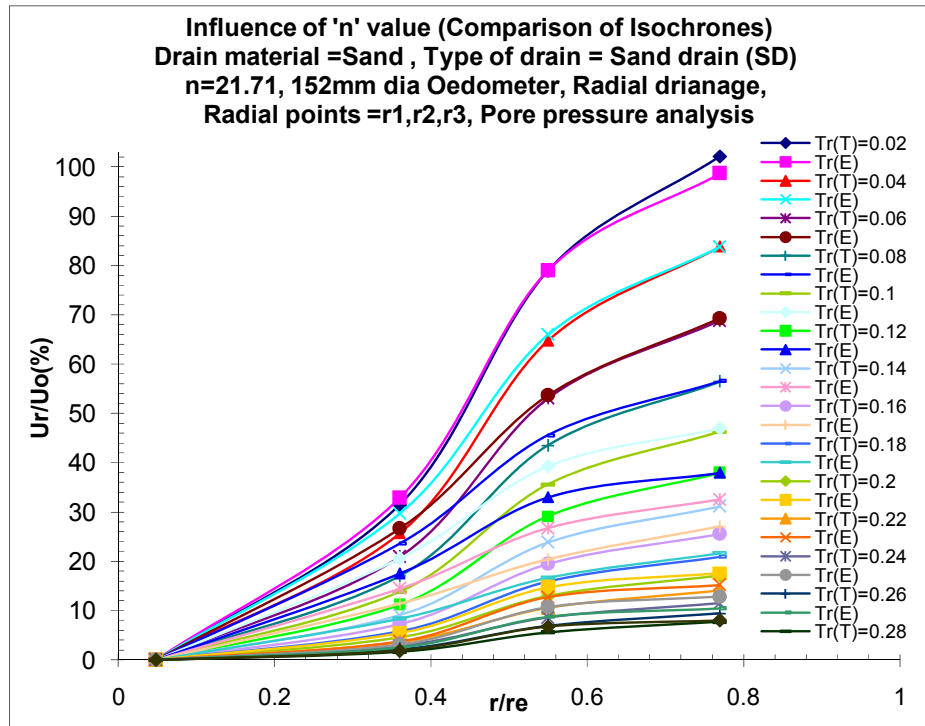


**Fig. 6.222:** Comparison of isochrones of 'n'21.71 of SD w.r.t experimental and theoretical Time factors ( $Tr$ ) at 160kPa pressure

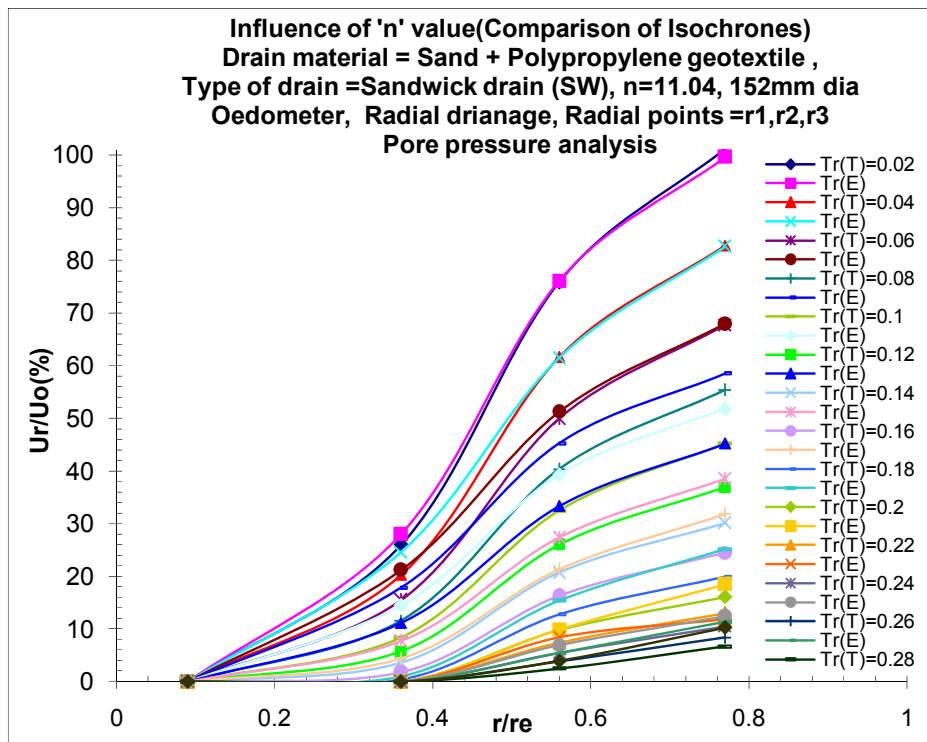


**Fig. 6.223:** Comparison of isochrones of 'n'11.04 of SW w.r.t experimental and theoretical Time factors ( $Tr$ ) at 160kPa pressure

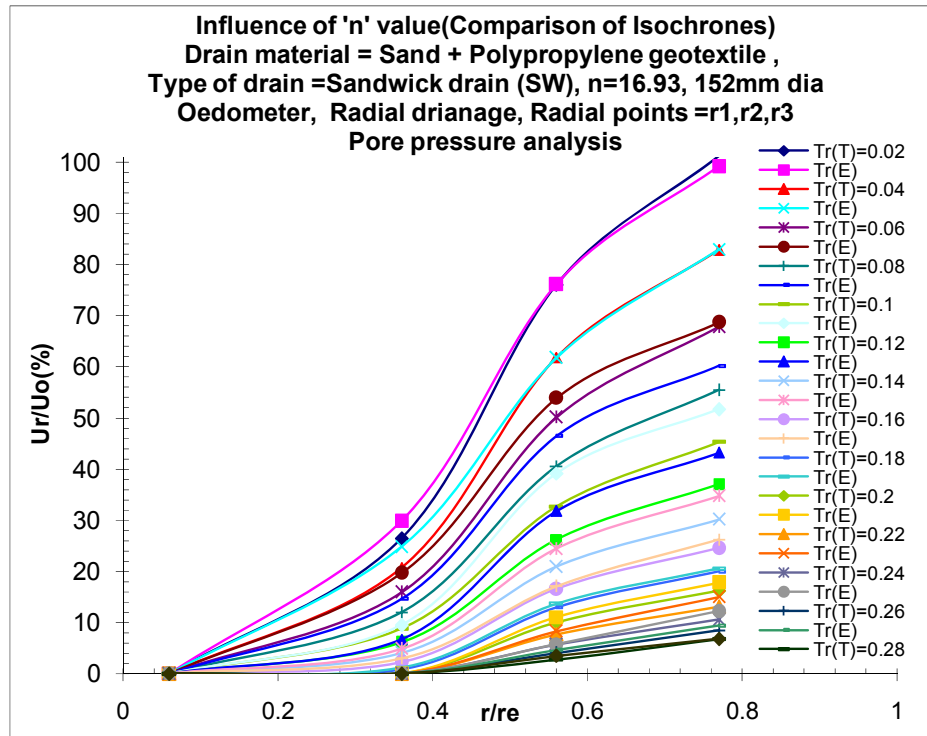


**Fig. 6.224:** Comparison of isochrones of 'n'16.93 of SW w.r.t experimental and theoretical Time factors ( $Tr$ ) at 160kPa pressure

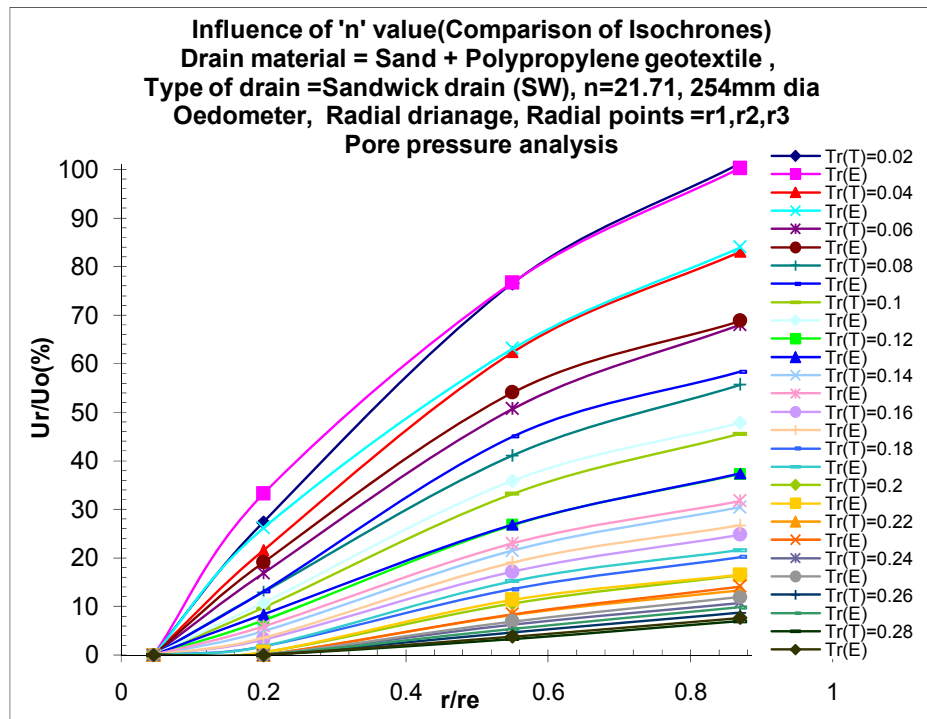


**Fig. 6.225:** Comparison of isochrones of 'n'21.71 of SW w.r.t experimental and theoretical Time factors ( $Tr$ ) at 160kPa pressure

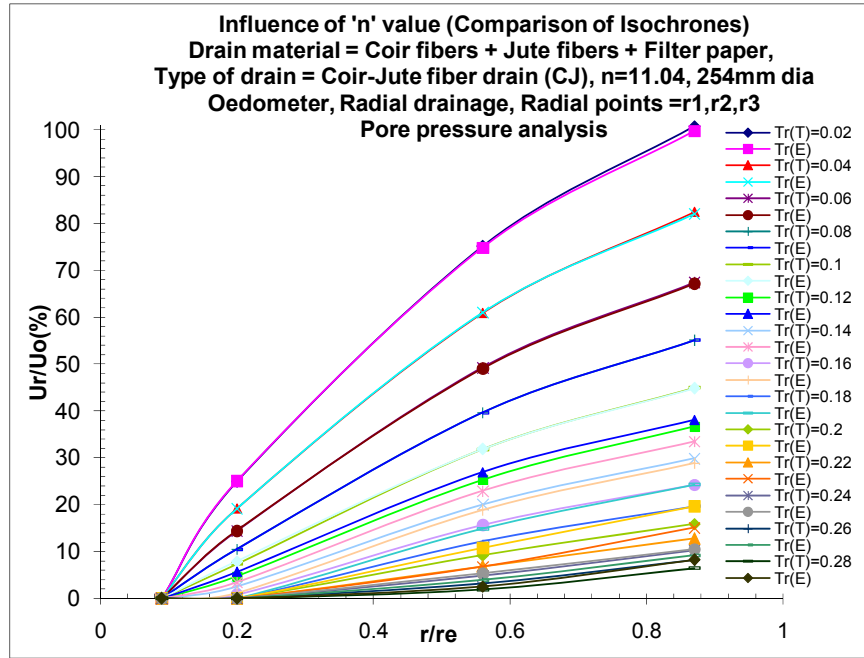


**Fig. 6.226:** Comparison of isochrones of 'n'11.04 of CJ w.r.t experimental and theoretical Time factors ( $Tr$ ) at 160kPa pressure

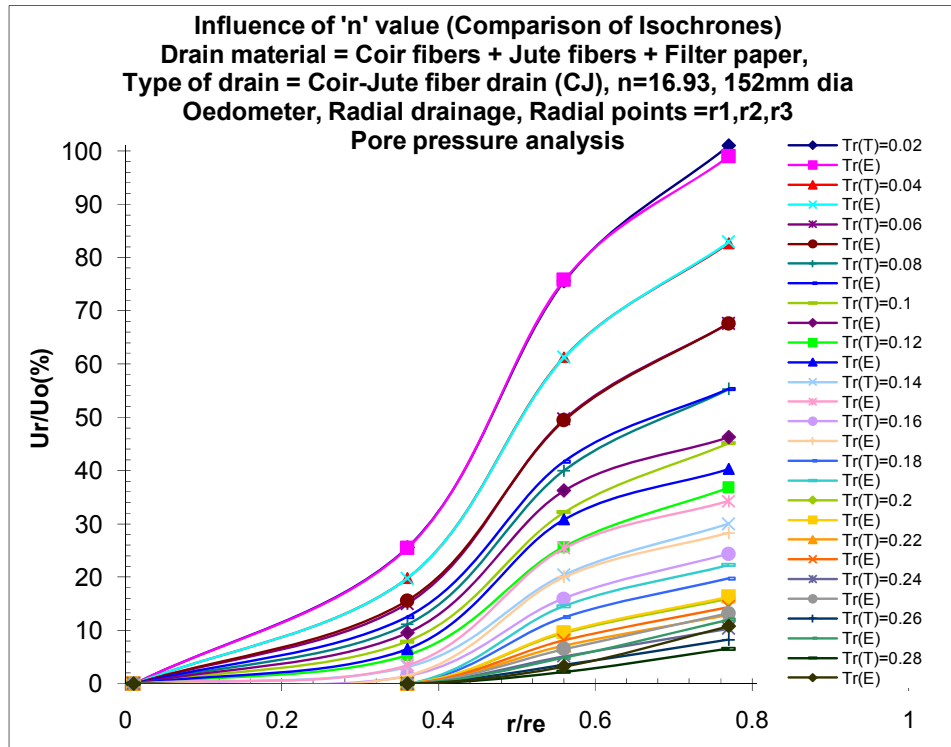


**Fig. 6.227:** Comparison of isochrones of 'n'16.93 of CJ w.r.t experimental and theoretical Time factors ( $Tr$ ) at 160kPa pressure

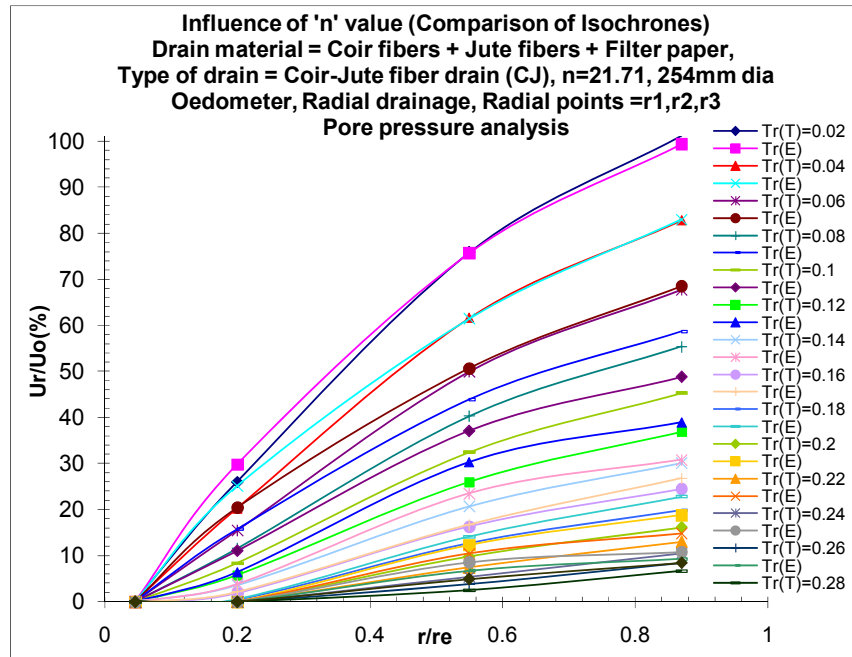


**Fig. 6.228:** Comparison of isochrones of ' $n$ '21.71 of CJ w.r.t experimental and theoretical Time factors ( $Tr$ ) at 160kPa pressure

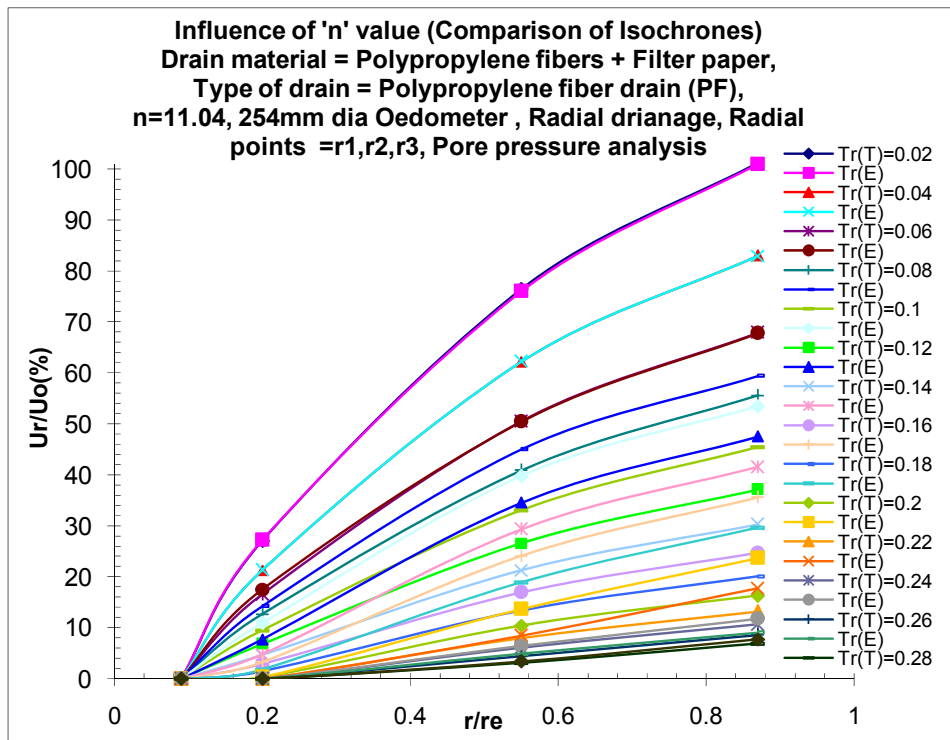


**Fig. 6.229:** Comparison of isochrones of ' $n$ '11.04 of PF w.r.t experimental and theoretical Time factors ( $Tr$ ) at 160kPa pressure

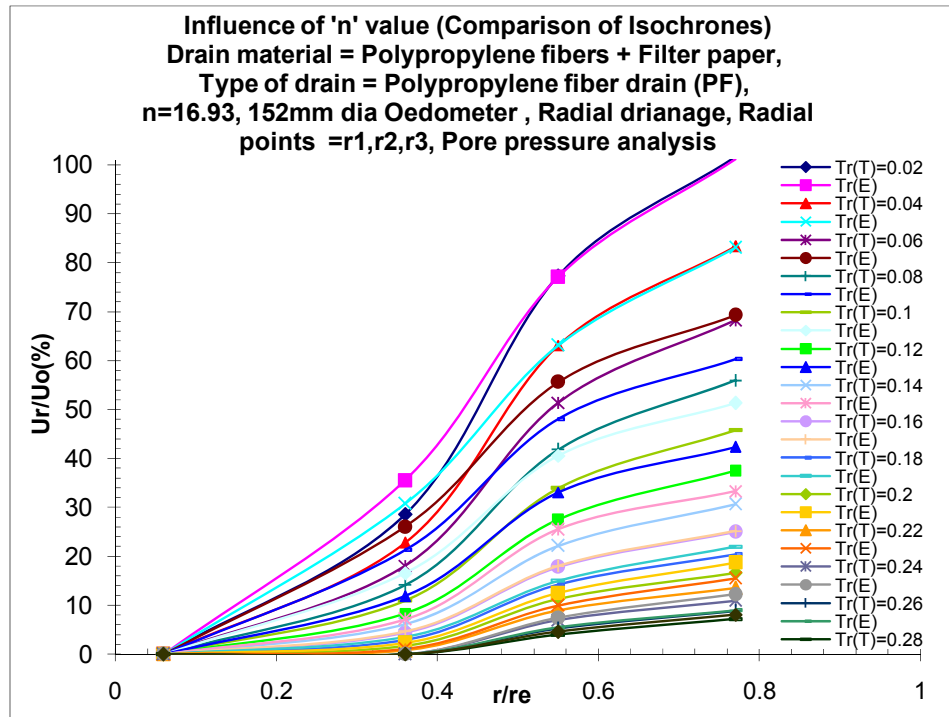


**Fig. 6.230:** Comparison of isochrones of 'n'16.93 of PF w.r.t experimental and theoretical Time factors ( $Tr$ ) at 160kPa pressure

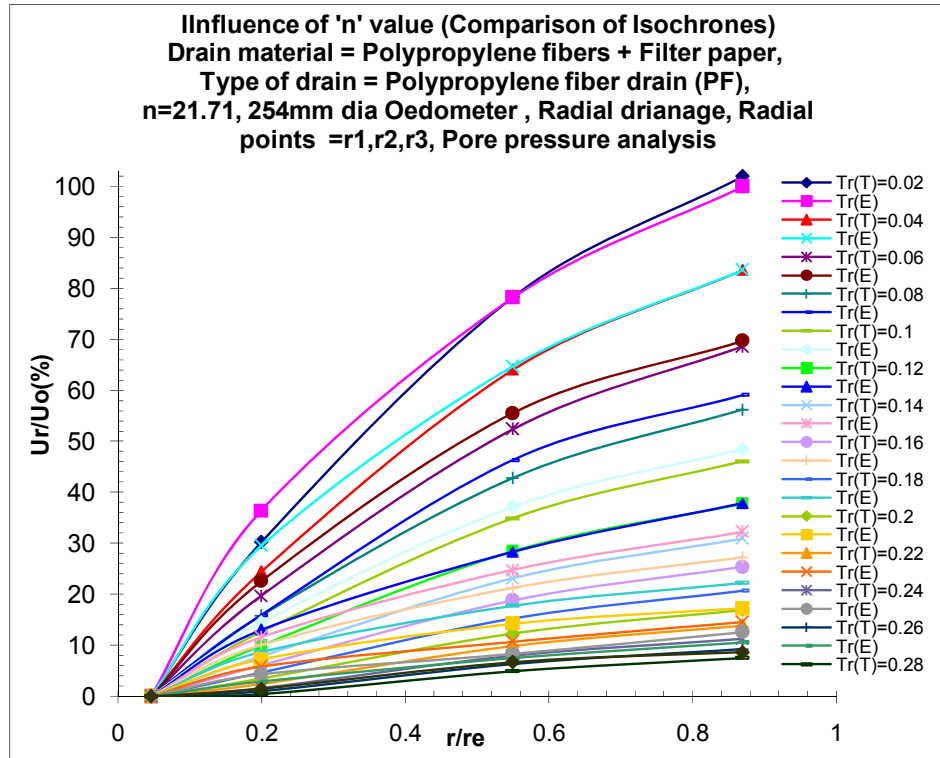


**Fig. 6.231:** Comparison of isochrones of 'n'21.71 of PF w.r.t experimental and theoretical Time factors ( $Tr$ ) at 160kPa pressure

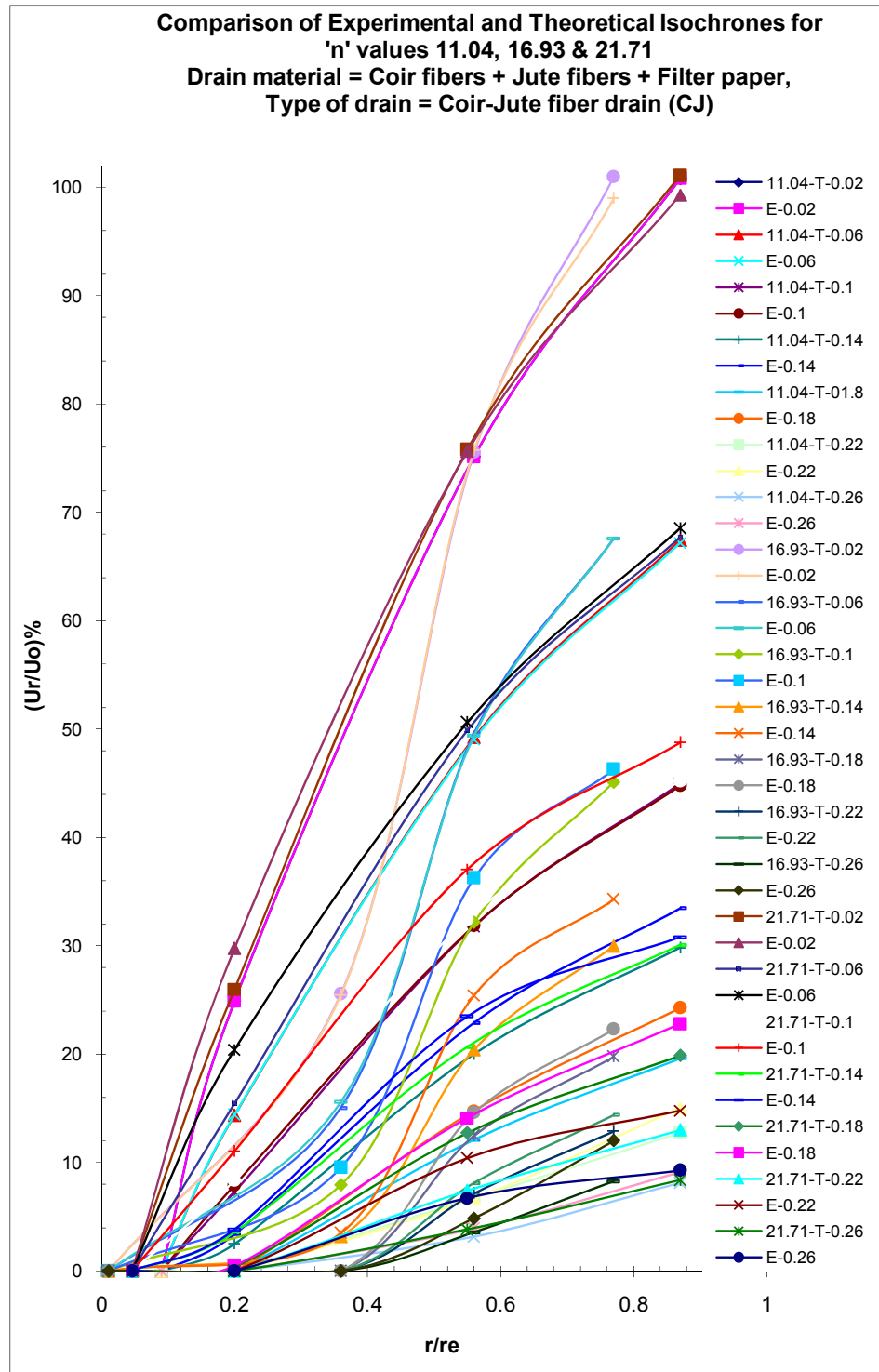


**Fig. 6.232:** Influence of isochrones on 'n' value w.r.t experimental and theoretical time factors ( $T_r$ ) for CJ at 160kPa pressure

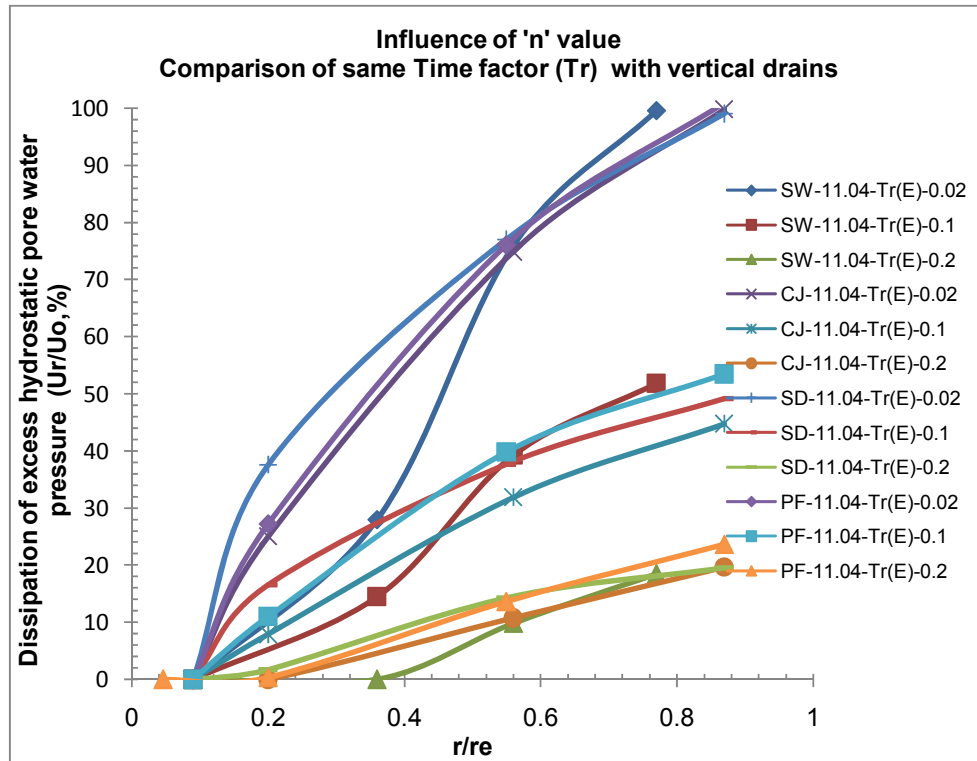


**Fig. 6.233:** Influence of 'n' value on experimental isochrones for various vertical drains of 'n' 11.04 at 160kPa pressure

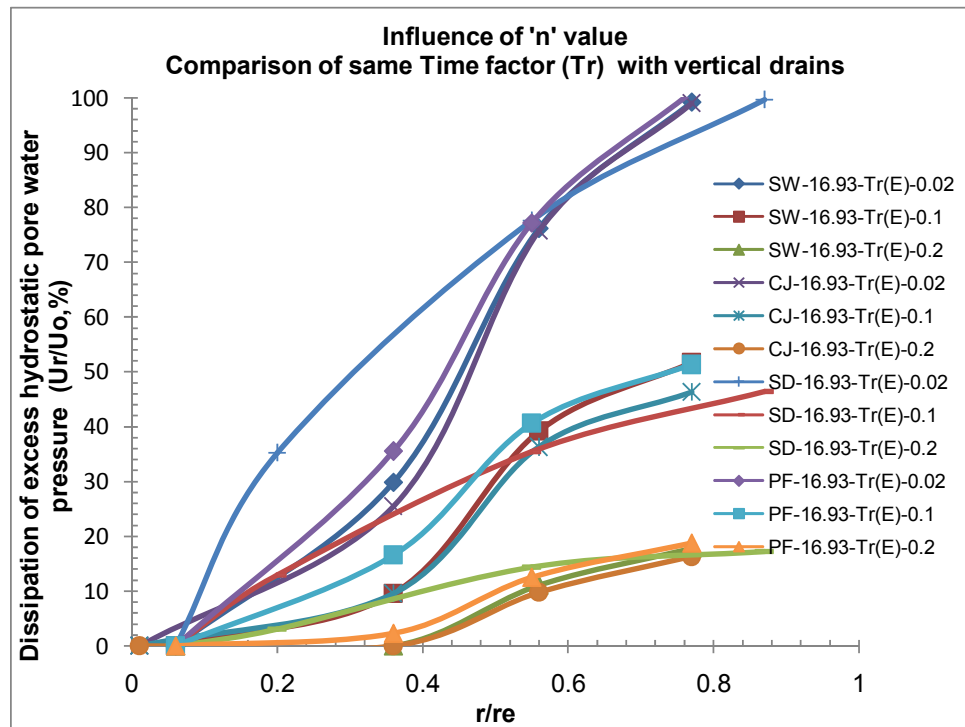


**Fig. 6.234:** Influence of 'n' value on experimental isochrones for various vertical drains of 'n' 16.93 at 160kPa pressure



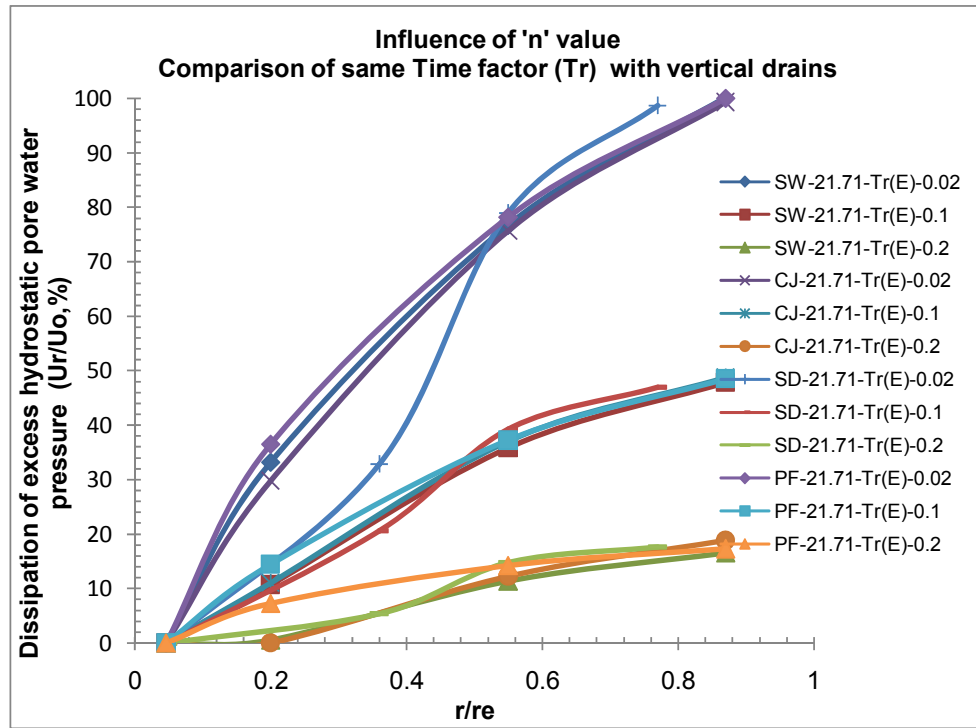


**Fig. 6.235:** Influence of 'n' value on experimental isochrones for various vertical drains of 'n' 21.71 at 160kPa pressure

## 7) Degree of consolidation ( $U_r$ ) vs. Time factor ( $Tr$ ): Figures 6.236 to 6.254

**a) Settlement analysis:-** Fig.6.236 to Fig.6.243 shows the comparative plots of various 'n' values of 11.04, 16.93 and 21.71 for degree of consolidation ( $U_r$ ) versus time factor ( $Tr$ ) for various drains like CJ, SW, PF & SD. For comparison between theoretical and experimental values two applied pressure of 40kPa and 160kPa are selected. The lumped parameter ' $\lambda$ ' is appropriately fitted for 'n' value of each drain with respect to time factors so as to study the influence of diameter (size) on vertical drain performance. Here it is determined that for three 'n' values of 11.04, 16.93, 21.71 for CJ the lumped parameter ' $\lambda$ ' is equal to -0.175, -0.16, -0.15 fits respectively. Similarly it is determined that for three 'n' values of 11.04, 16.93, 21.71 for SW the lumped parameter ' $\lambda$ ' is equal to -0.15, -0.14, -0.12 fits respectively. Similarly it is determined that for three 'n' values of 11.04, 16.93, 21.71 for PF the lumped parameter ' $\lambda$ ' is equal to -0.125, -0.09, -0.05 fits respectively, while for SD the lumped parameter ' $\lambda$ ' is equal to -0.1, -

0.07, -0.02 fits respectively. It is observed that ' $\lambda$ ' value of -0.175 is having maximum efficiency and as ' $\lambda$ ' value decreases diameter of drain decreases. It is observed from the above graphs that experimental results almost matches with theoretical results and this is true for ' $n$ ' values ,for all drains and for all applied pressures. Table shows the value of lumped parameter ' $\lambda$ ' fitted to each drain type.

| Sr.No. | Type of Drain                  | 'n' value | Lumped parameter ' $\lambda$ ' |
|--------|--------------------------------|-----------|--------------------------------|
| 1.     | Sand drain (SD)                | 11.04     | -0.125                         |
|        |                                | 16.93     | -0.11                          |
|        |                                | 21.71     | -0.1                           |
| 2.     | Sandwick drain (SW)            | 11.04     | -0.15                          |
|        |                                | 16.93     | -0.14                          |
|        |                                | 21.71     | -0.13                          |
| 3.     | Coir-Jute fiber drain (CJ)     | 11.04     | -0.2                           |
|        |                                | 16.93     | -0.19                          |
|        |                                | 21.71     | -0.18                          |
| 4.     | Polypropylene fiber drain (PF) | 11.04     | -0.175                         |
|        |                                | 16.93     | -0.17                          |
|        |                                | 21.71     | -0.16                          |

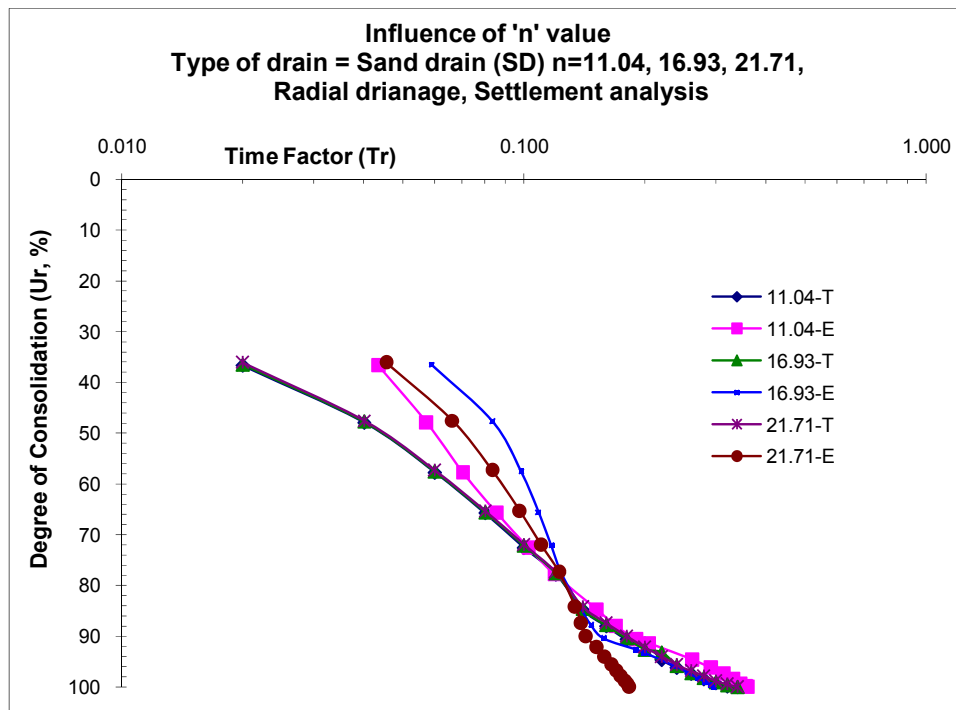


**Fig. 6.236:** Comparison of theoretical and experimental average degree of consolidation ( $U_r$ ) against Time factor ( $T_r$ ) for SD at 40kPa pressure

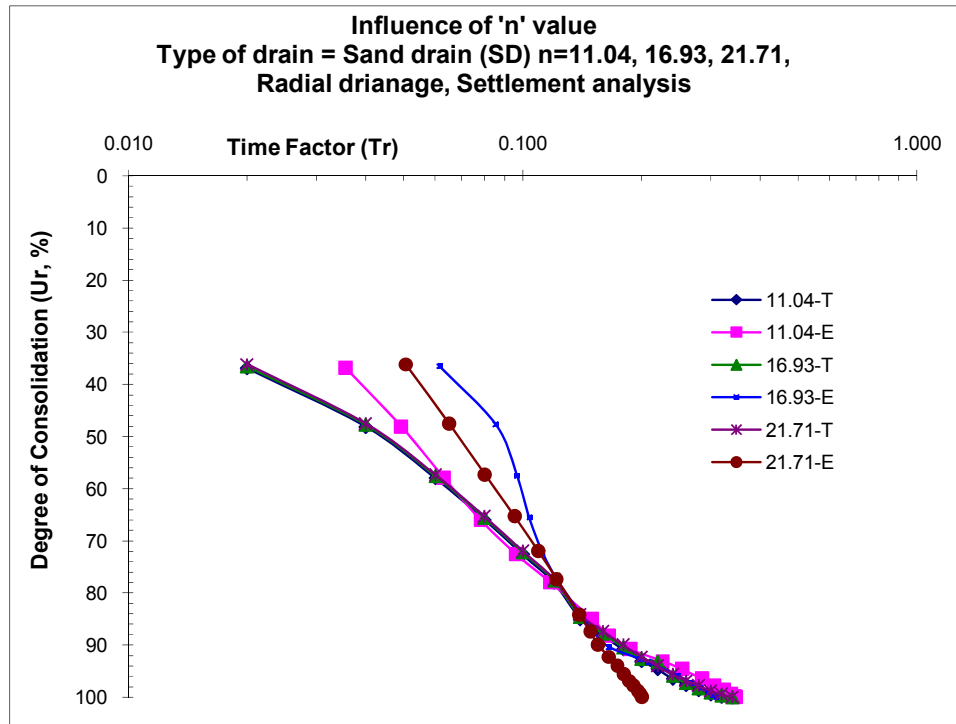


**Fig. 6.237:** Comparison of theoretical and experimental average degree of consolidation ( $U_r$ ) against Time factor ( $Tr$ ) for SD at 160kPa pressure

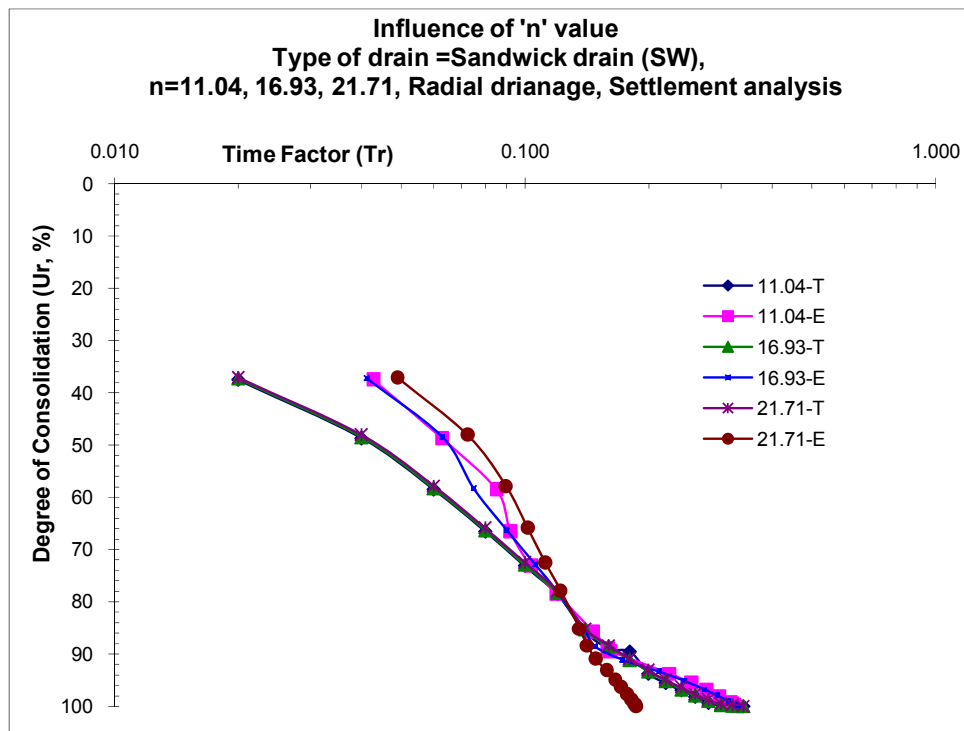


**Fig. 6.238:** Comparison of theoretical and experimental average degree of consolidation ( $U_r$ ) against Time factor ( $Tr$ ) for SW at 40kPa pressure

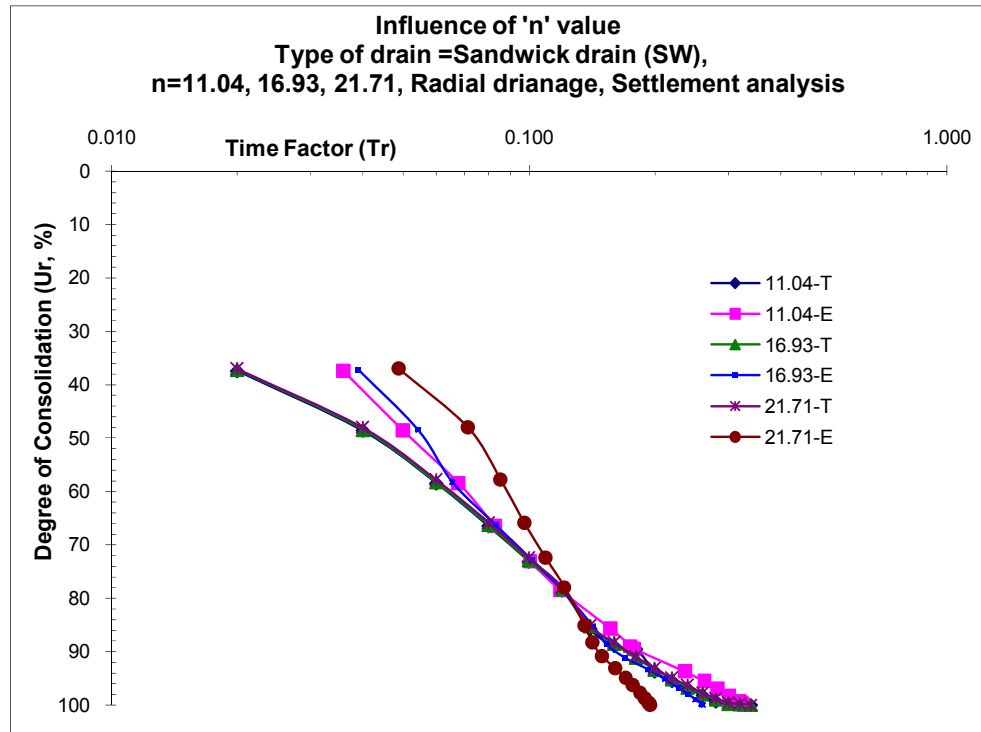


**Fig. 6.239:** Comparison of theoretical and experimental average degree of consolidation ( $U_r$ ) against Time factor ( $T_r$ ) for SW at 160kPa pressure

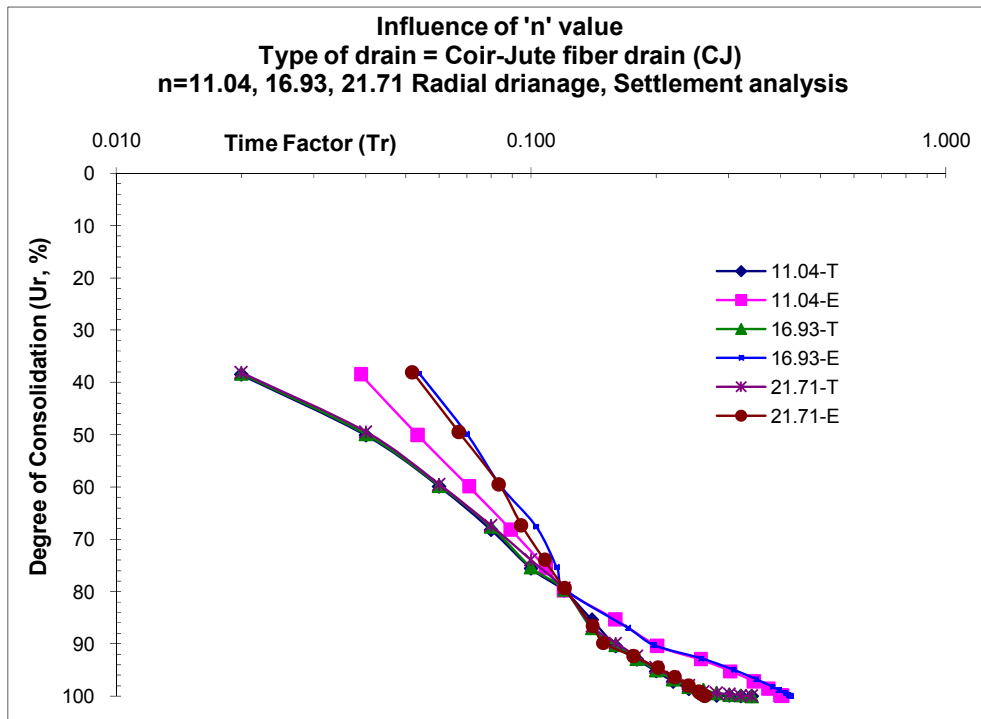


**Fig. 6.240:** Comparison of theoretical and experimental average degree of consolidation ( $U_r$ ) against Time factor ( $T_r$ ) for CJ at 40kPa pressure

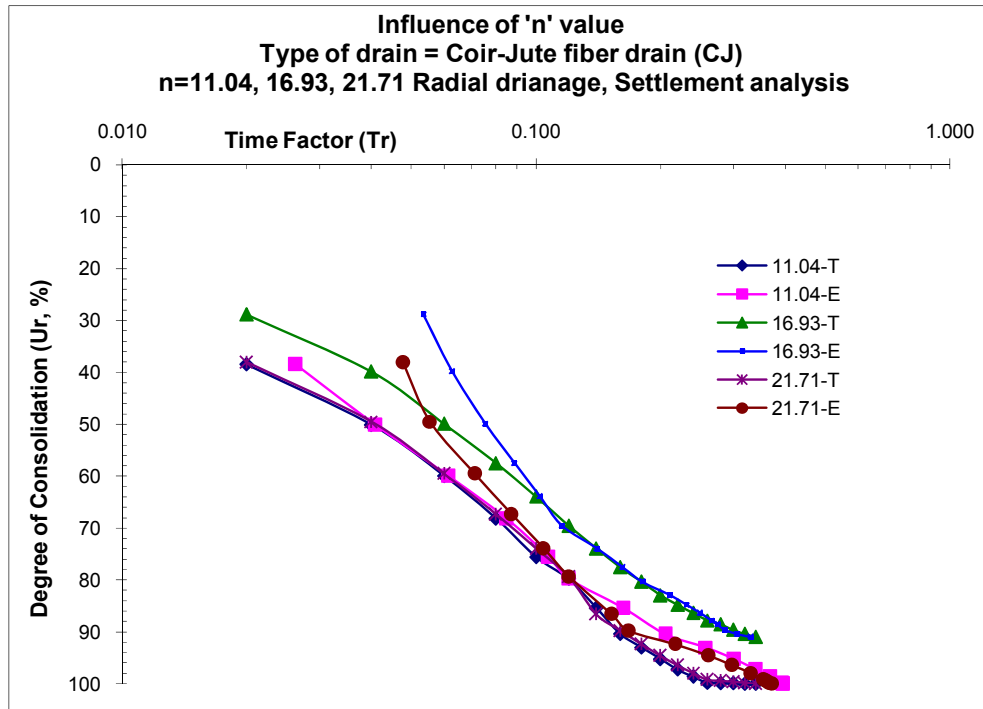


**Fig. 6.241:** Comparison of theoretical and experimental average degree of consolidation ( $U_r$ ) against Time factor ( $Tr$ ) for CJ at 160kPa pressure

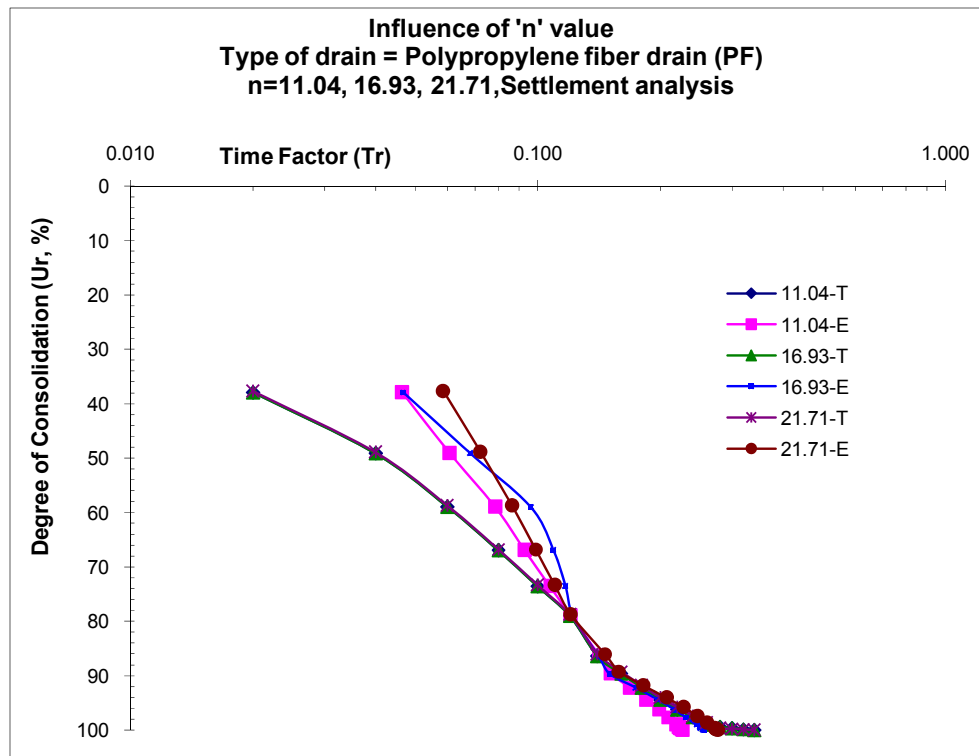


**Fig. 6.242:** Comparison of theoretical and experimental average degree of consolidation ( $U_r$ ) against Time factor ( $Tr$ ) for PF at 40kPa pressure

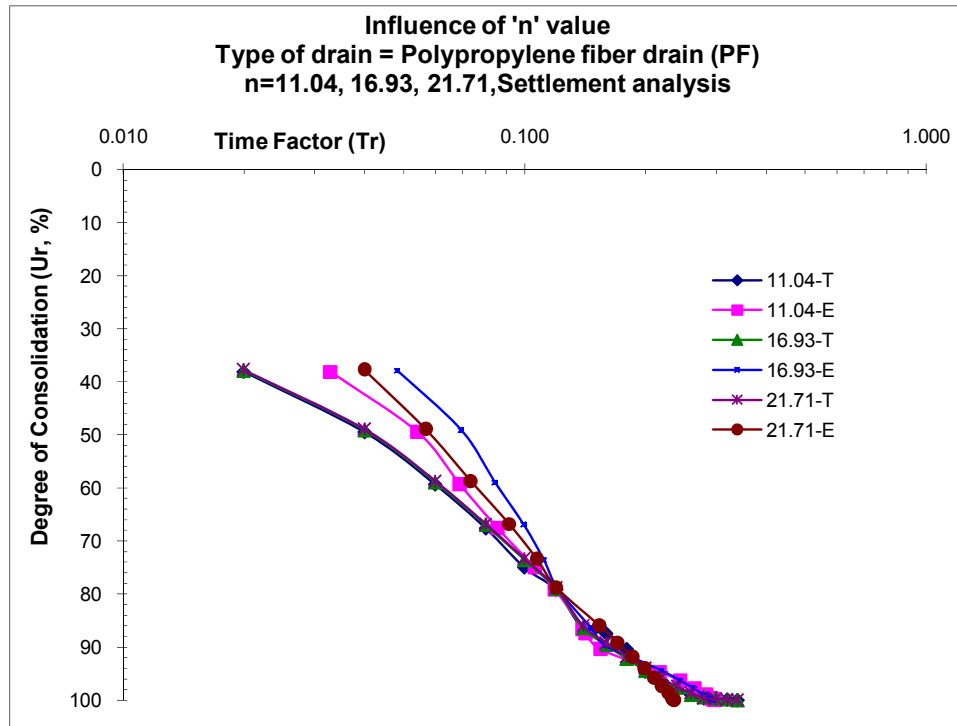


**Fig. 6.243:** Comparison of theoretical and experimental average degree of consolidation ( $U_r$ ) against Time factor ( $T_r$ ) for PF at 160kPa pressure

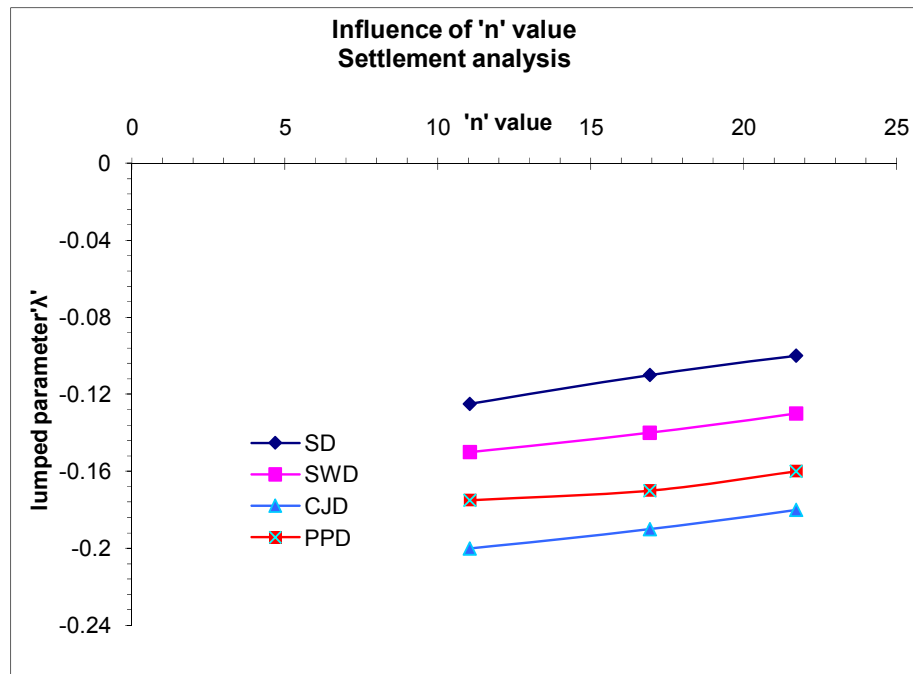


**Fig. 6.244:** Comparison of lump parameter ( $\lambda$ ) vs. 'n' value based on settlement analysis

**b) Pore pressure analysis:-** Fig.6.245 to Fig.6.251 shows the comparative plots of various 'n' values of 11.04, 16.93 and 21.71 for various drains like CJ, SW, PF, SD for degree of consolidation ( $U_r$ ) versus time factor ( $T_r$ ) at all pressures. For comparison between theoretical and experimental values two applied pressure of 40kPa and 160kPa are selected. The lumped parameter ' $\lambda$ ' is appropriately fitted for each 'n' value with respect to time factors so as to study the influence of diameter on vertical drain performance. Here it is determined that for three 'n' values of 11.04, 16.93, 21.71 for CJ the lumped parameter ' $\lambda$ ' is equal to -0.175, -0.16, -0.15 fits respectively. Similarly it is determined that for three 'n' values of 11.04, 16.93, 21.71 for SW the lumped parameter ' $\lambda$ ' is equal to -0.15, -0.14, -0.12 fits respectively. Similarly it is determined that for three 'n' values of 11.04, 16.93, 21.71 for PF the lumped parameter ' $\lambda$ ' is equal to -0.125, -0.09, -0.05 fits respectively, while for SD the lumped parameter ' $\lambda$ ' is equal to -0.1, -0.07, -0.02 fits respectively. It is observed that ' $\lambda$ ' value of -0.175 is having maximum efficiency and as ' $\lambda$ ' value decreases efficiency of drain diameter decreases. It is observed from the above graphs that experimental results almost matches with theoretical results and this is true for all vertical drains of all 'n' values and for all applied pressures. Table shows the value of lumped parameter ' $\lambda$ ' fitted to each drain type. It is observed that degree of consolidation determined from pore pressure readings suggest that SW is more efficient in compare to PF while settlement readings suggest that PF is more efficient in compare to SW.

| Sr.No. | Type of Drain                  | 'n' value | Lumped parameter ' $\lambda$ ' |
|--------|--------------------------------|-----------|--------------------------------|
| 1.     | Sand drain (SD)                | 11.04     | -0.1                           |
|        |                                | 16.93     | -0.07                          |
|        |                                | 21.71     | -0.02                          |
| 2.     | Sandwick drain (SW)            | 11.04     | -0.15                          |
|        |                                | 16.93     | -0.14                          |
|        |                                | 21.71     | -0.12                          |
| 3.     | Coir-Jute fiber drain (CJ)     | 11.04     | -0.175                         |
|        |                                | 16.93     | -0.16                          |
|        |                                | 21.71     | -0.15                          |
| 4.     | Polypropylene fiber drain (PF) | 11.04     | -0.125                         |
|        |                                | 16.93     | -0.09                          |
|        |                                | 21.71     | -0.05                          |

**Discussion:**

Appropriate fitting of lump parameter with experimental results:

- Type of the drain material in the prefabricated vertical geodrain has direct influence on the velocity with which it leaves the void space. In the theoretical derivation for the present investigation also it reflects that the rate of outflow of fluid, that is rate of change of fluid in the element is dependant on excess fluid pressure gradient which will be function of the type of drain material used in fabricating vertical geodrain being 'k' will be function of both porosity and void ratio 'e' which ultimately reflects in coefficient of consolidation ( $C_r$ ) in the derivation. Further lumped parameter ( $\lambda$ ) is the ratio of ( $C_e / C_r$ )  $r_e$ , (being) where  $C_r$  is coefficient of consolidation due to radial drainage and  $C_e$  is coefficient due to permeability and porosity which is to some extent due to small magnitude of radial strain which helps in redistributing loads to the surface at interface of drain giving same settlement supporting 'equal strain' condition. In turn  $C_r$  will vary with the drain material reflecting in the values of ( $\lambda$ ). Maximum and minimum drainage path related to various shapes of the central drain orientation is coordinated to related to rate of dissipation of the pore fluid, thereby degree of consolidation of clay with time. Longer the drainage path, lower the rate of consolidation and ( $\lambda$ ) will vary as per the above explanation. Change of tortousity because of particle orientation under load variation reflecting soil structural changes (from edge to face and edge to edge or face to face) orientation is also accounted in lumped parameter ( $\lambda$ ).
- As ' $\lambda$ ' value increases, drain diameter ('n' value) decreases. Experimental results almost match with theoretical results with  $\lambda = -0.2$  particularly for CJ for  $n=11.04$ ,  $\lambda = -0.19$  for  $n=16.93$  and  $\lambda = -0.18$  for  $n=21.71$  proves to be efficient amongst other drains. From theoretical considerations  $n=11.04$  proves to be efficient amongst other 'n' values.



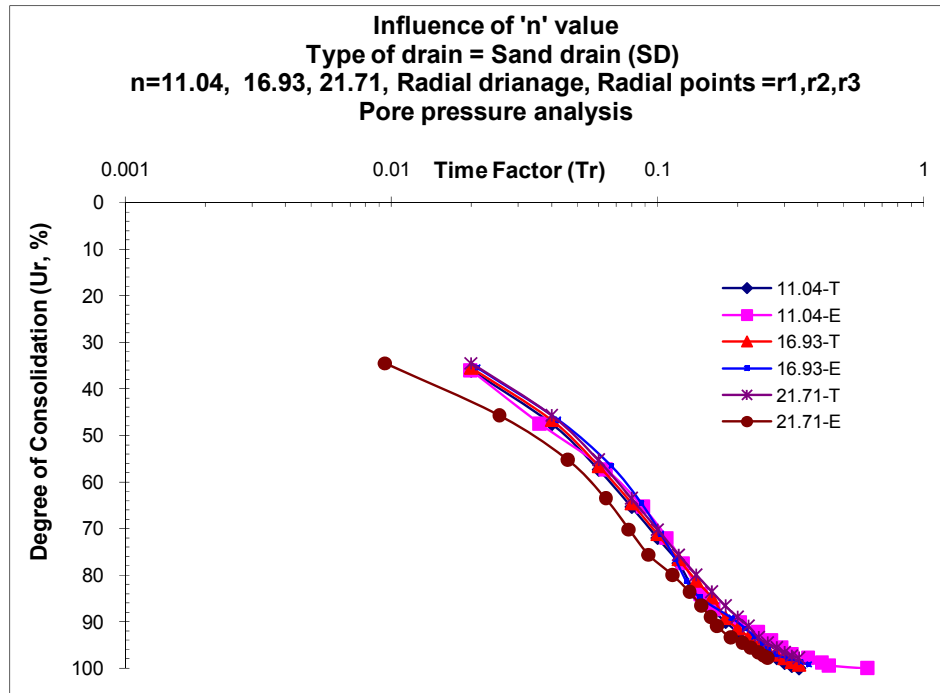


**Fig. 6.245(a):** Comparison of theoretical and experimental average degree of consolidation ( $U_r$ ) against Time factor ( $Tr$ ) for SD at 40kPa pressure

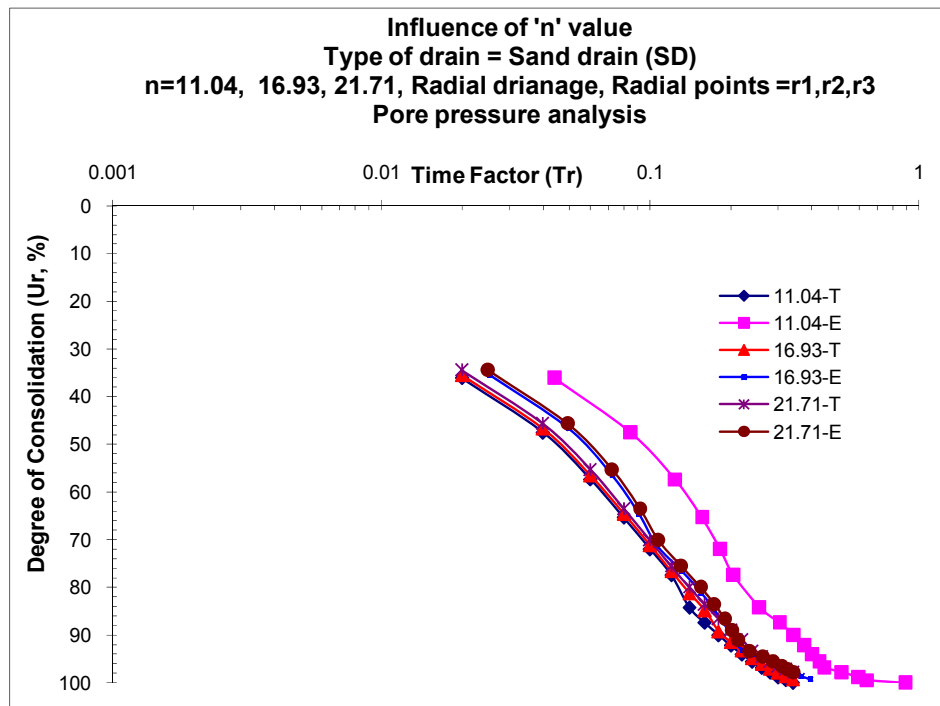


**Fig. 6.245(b):** Comparison of theoretical and experimental average degree of consolidation ( $U_r$ ) against Time factor ( $Tr$ ) for SD at 160kPa pressure

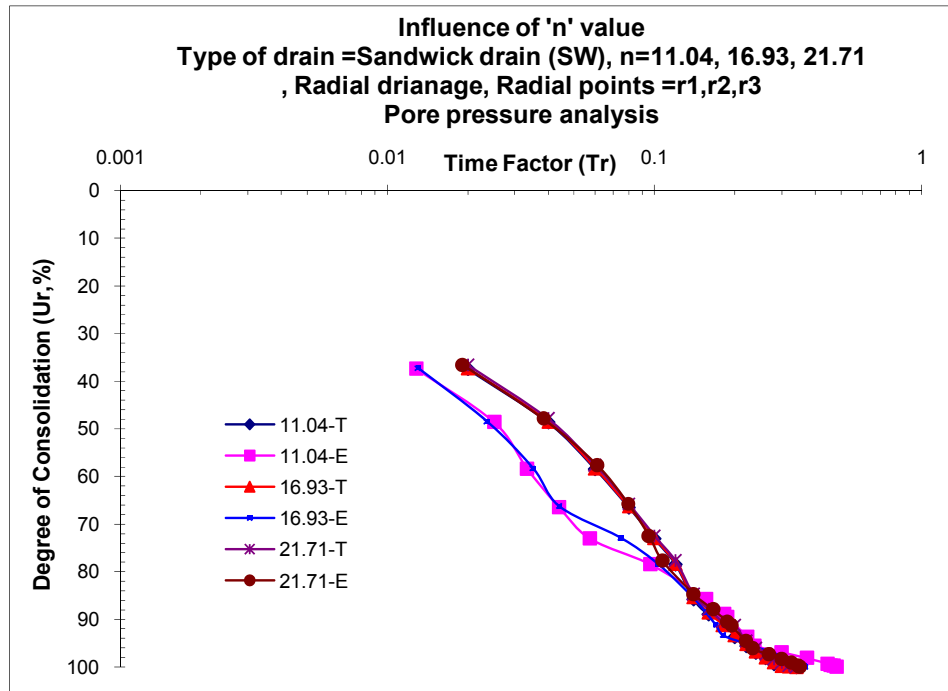


**Fig. 6.246:** Comparison of theoretical and experimental average degree of consolidation ( $U_r$ ) against Time factor ( $Tr$ ) for SW at 40kPa pressure

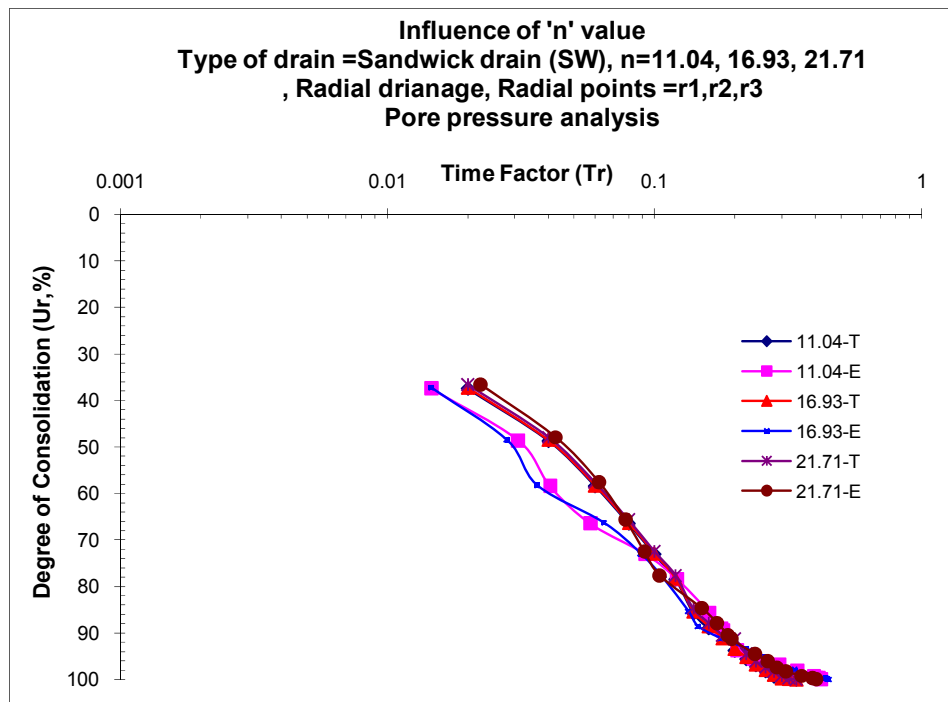


**Fig. 6.247:** Comparison of theoretical and experimental average degree of consolidation ( $U_r$ ) against Time factor ( $Tr$ ) for SW at 160kPa pressure

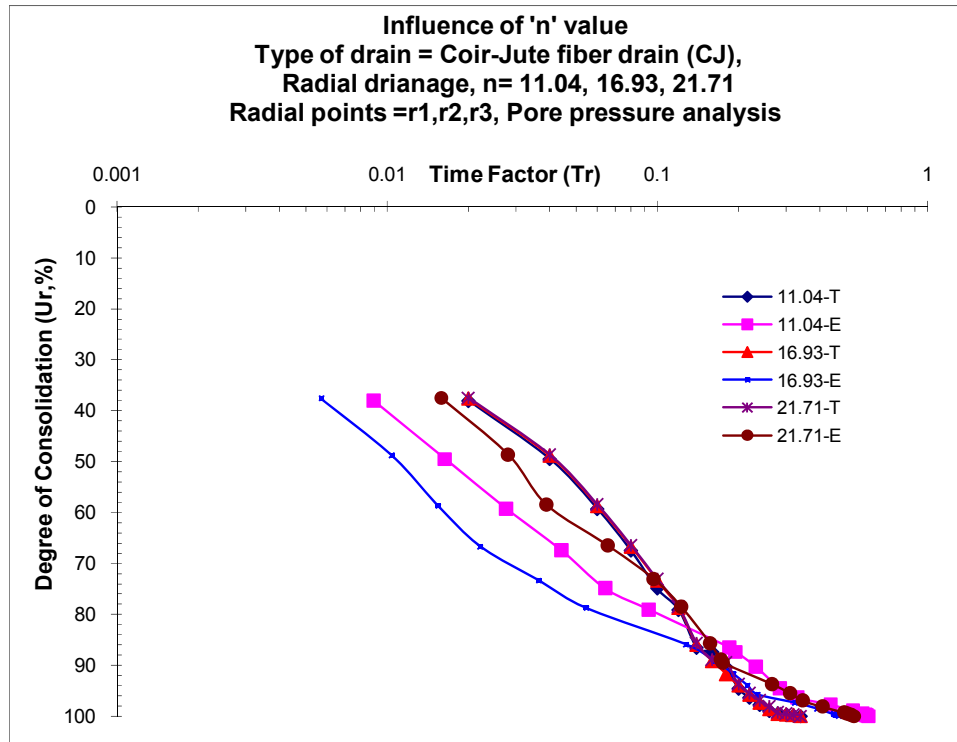


**Fig. 6.248:** Comparison of theoretical and experimental average degree of consolidation ( $U_r$ ) against Time factor ( $Tr$ ) for CJ at 40kPa pressure

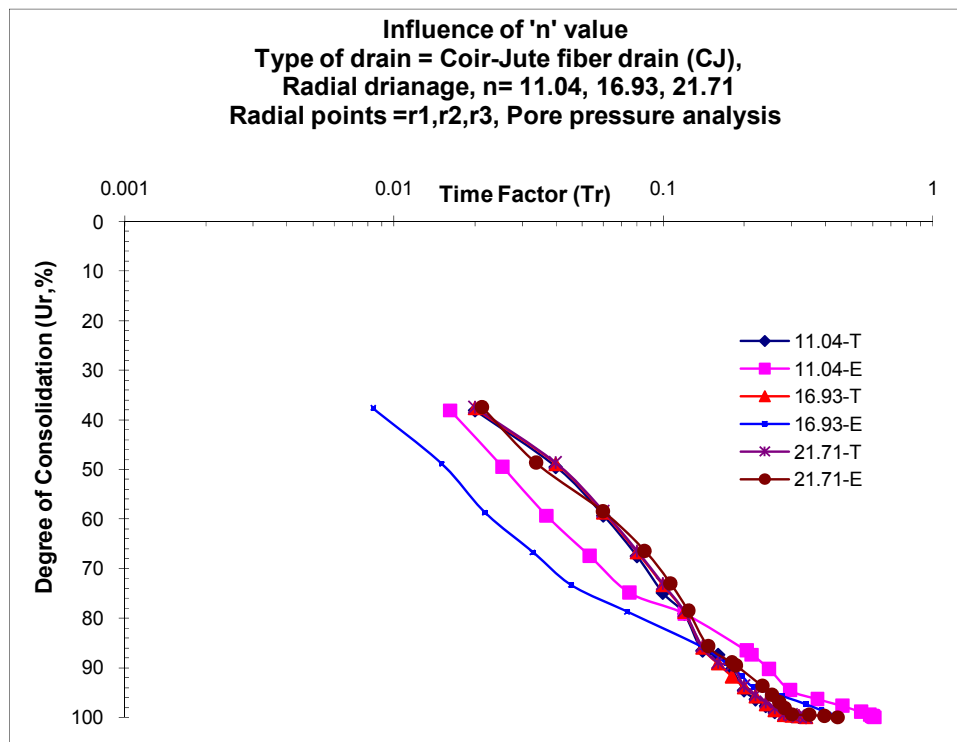


**Fig. 6.249:** Comparison of theoretical and experimental average degree of consolidation ( $U_r$ ) against Time factor ( $Tr$ ) for CJ at 160kPa pressure

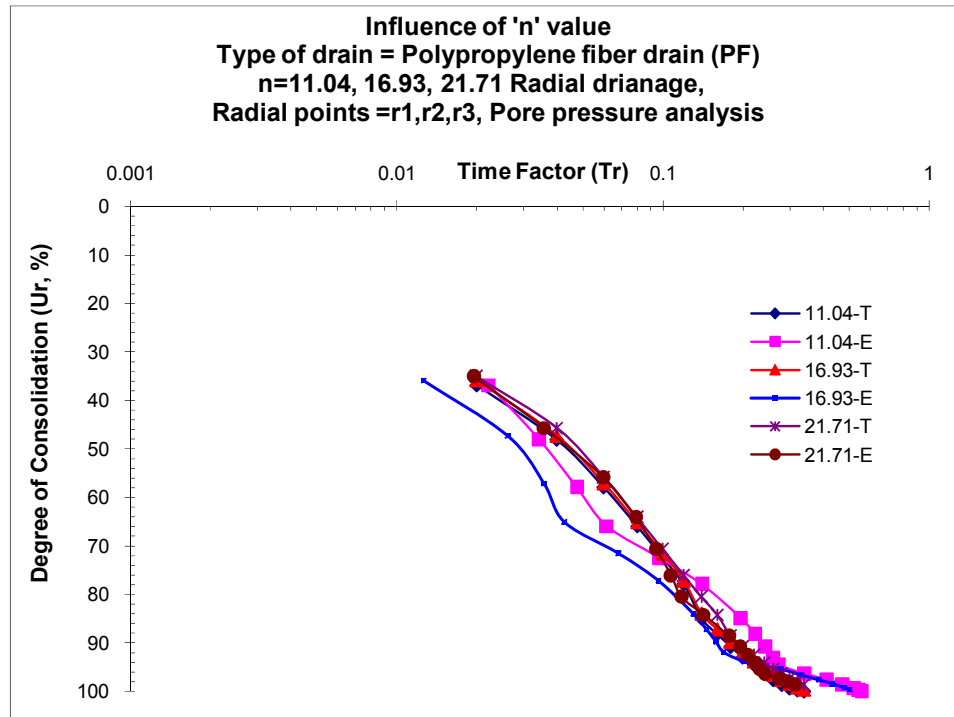


**Fig. 6.250:** Comparison of theoretical and experimental average degree of consolidation ( $U_r$ ) against Time factor ( $T_r$ ) for PF at 40kPa pressure

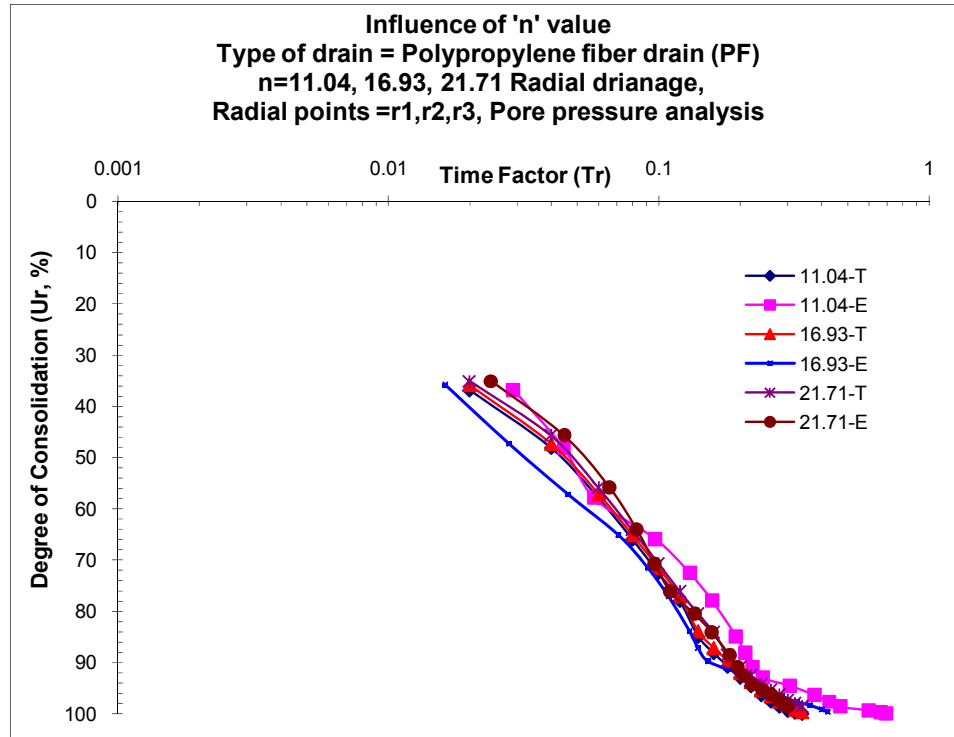


**Fig. 6.251:** Comparison of theoretical and experimental average degree of consolidation ( $U_r$ ) against Time factor ( $T_r$ ) for PF at 160kPa pressure

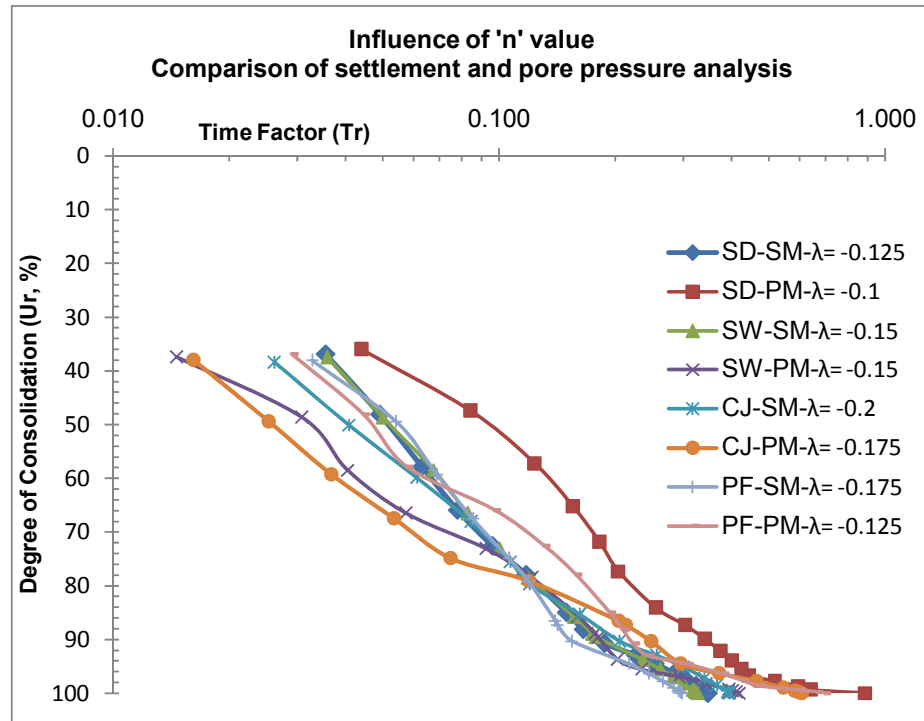


**Fig. 6.252:** Comparison of 'n' value w.r.t settlement and pore pressure analysis for vertical drains of 'n' 11.04

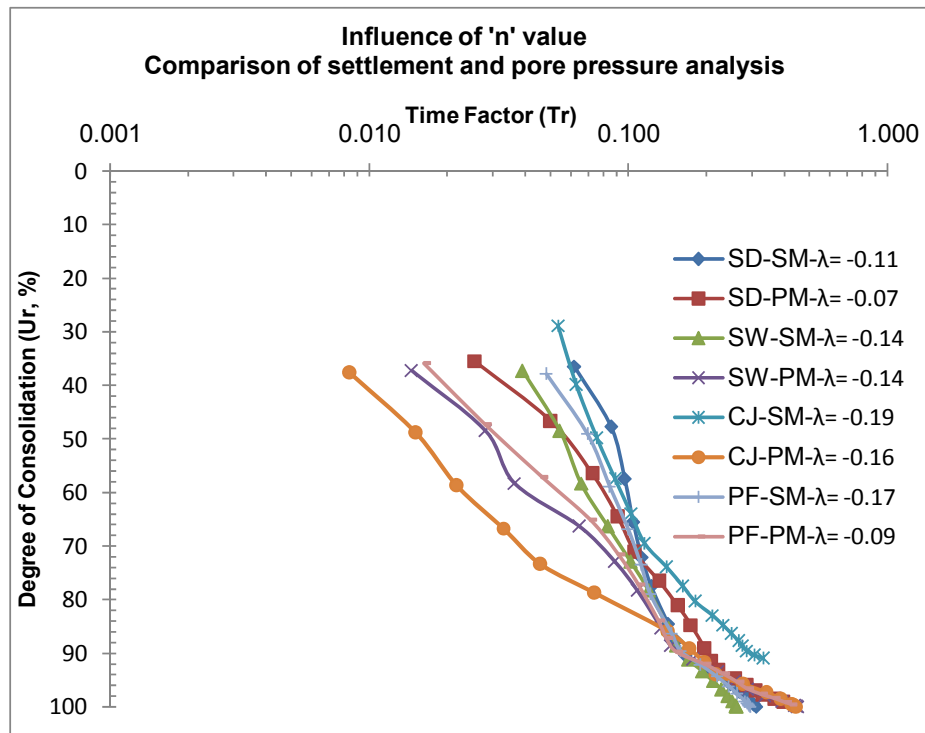


**Fig. 6.253:** Comparison of 'n' value w.r.t settlement and pore pressure analysis for vertical drains of 'n' 16.93

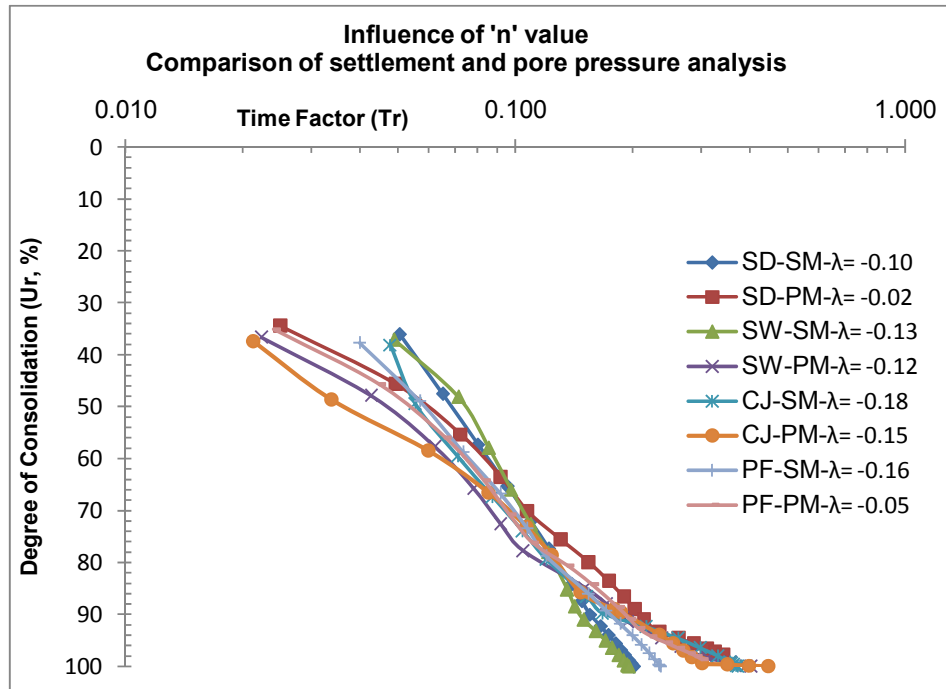


**Fig. 6.254:** Comparison of 'n' value w.r.t settlement and pore pressure analysis for vertical drains of 'n' 16.93

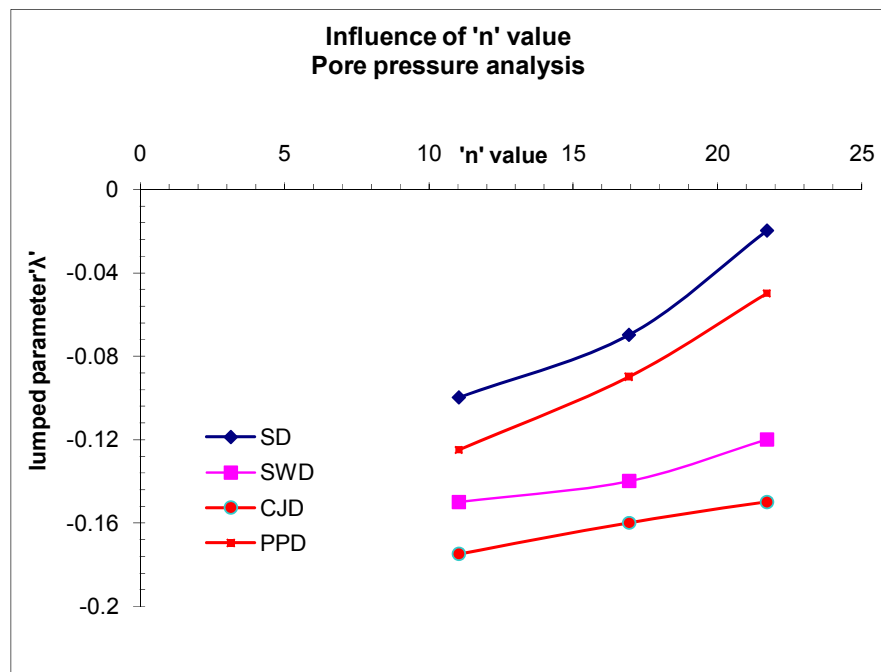


**Fig. 6.255:** Comparison of lump parameter ( $\lambda$ ) vs. 'n' value based on pore pressure analysis

**8) Vane Shear Strength and Images of Consolidated clay samples (end of 320kPa pressure) with central vertical drains:- Figures 6.256 to 6.259 and Photographs 6.19 to 6.24**

**Discussion:**

- Gain in shear strength was observed for all three 'n' values for any drain material after consolidation, but highest gain was observed in case of 'n' equal to 11.04 for any drain material. Average post shear strength increased to 150kPa from pre shear strength of 15kPa.
- Shear strength increases as 'n' value decreases (drain dia increases) for any drain material. Comparing effect of various 'n' values for CJ drain, the shear strength achieved at end of consolidation is highest for 'n' equal to 11.04 compare to 16.93 and 21.71. The shear strength achieved for n' equal to 11.04, 16.93 and 21.71 is 153kPa, 129kPa, and 109kPa respectively. Also more shear strength is observed for nearest radial point and this effect is true for any 'n' value. The curve of 11.04 lies above the curve of 'n'16.93 and 'n'21.71 for any drain material. Lowest gain in shear strength is observed in case of SD compare to CJ, SW, PF, while almost low strength is observed in case of 'n'21.71 for all drain materials. In general 'n' equal 11.04 provides more specific surface area being larger diameter of the particle which facilitate easy and more dissipation of pore water pressure under particular load thereby bringing the particle close together in a parallel orientation in more number.

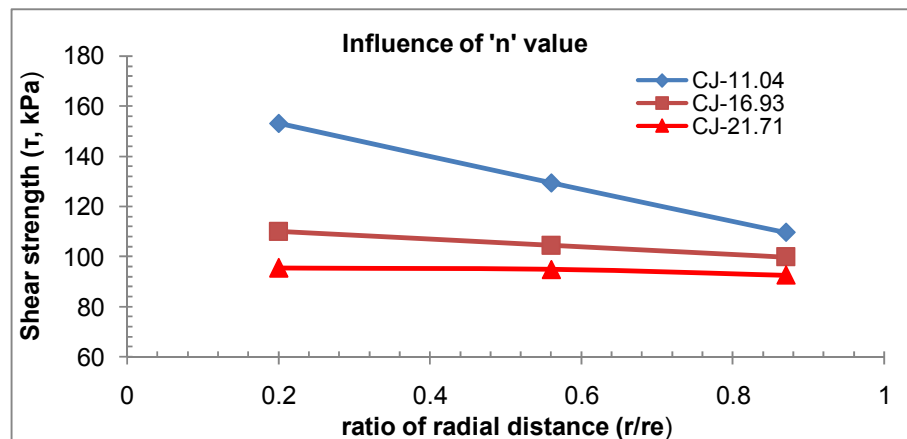


**Fig. 6.256:** Comparison of vane shear strength against ratio of radial distance for CJ of all 'n' values

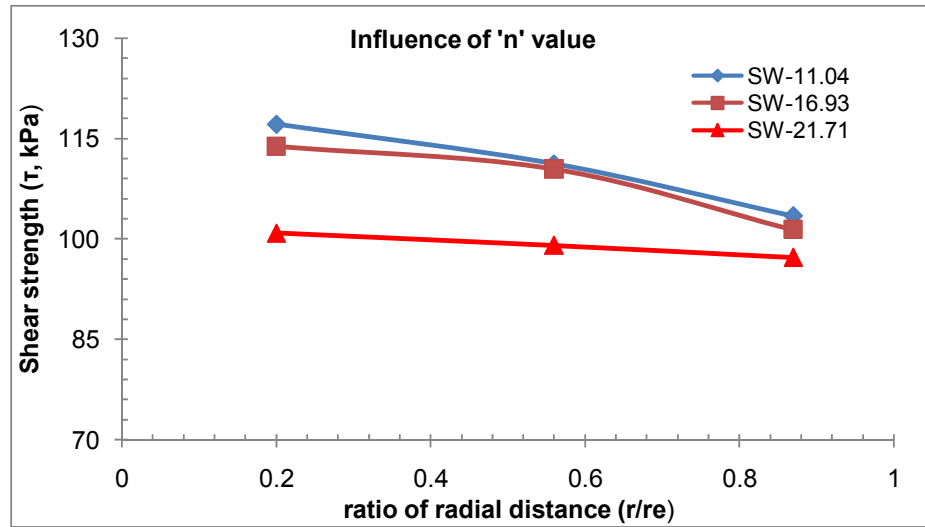


**Fig. 6.257:** Comparison of vane shear strength against ratio of radial distance for SW of all 'n' values

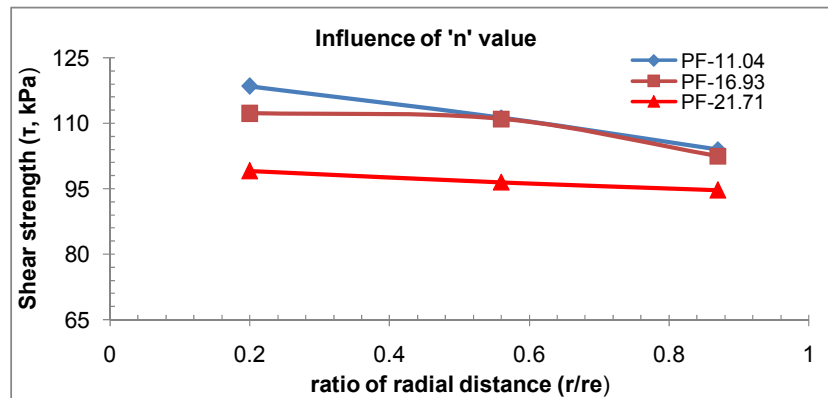


**Fig. 6.258:** Comparison of vane shear strength against ratio of radial distance for PF of all 'n' values

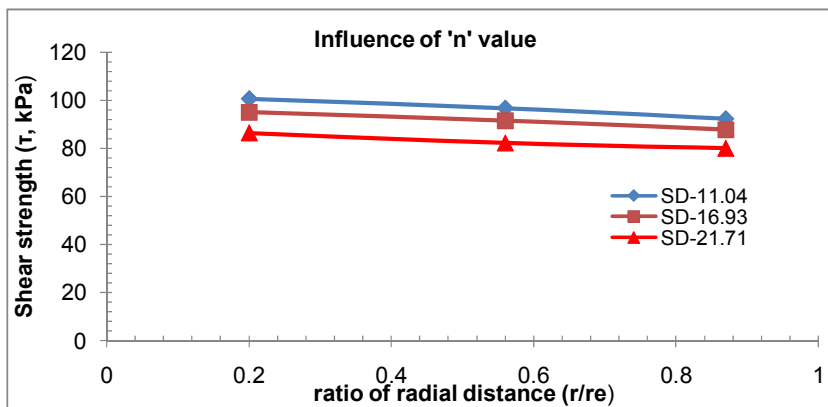
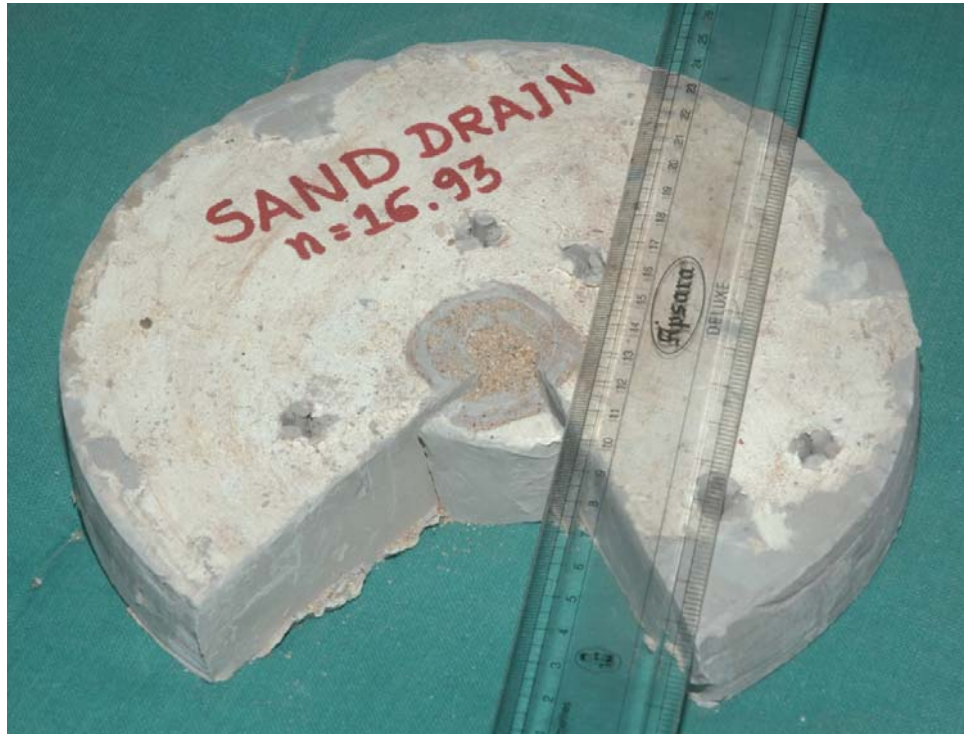
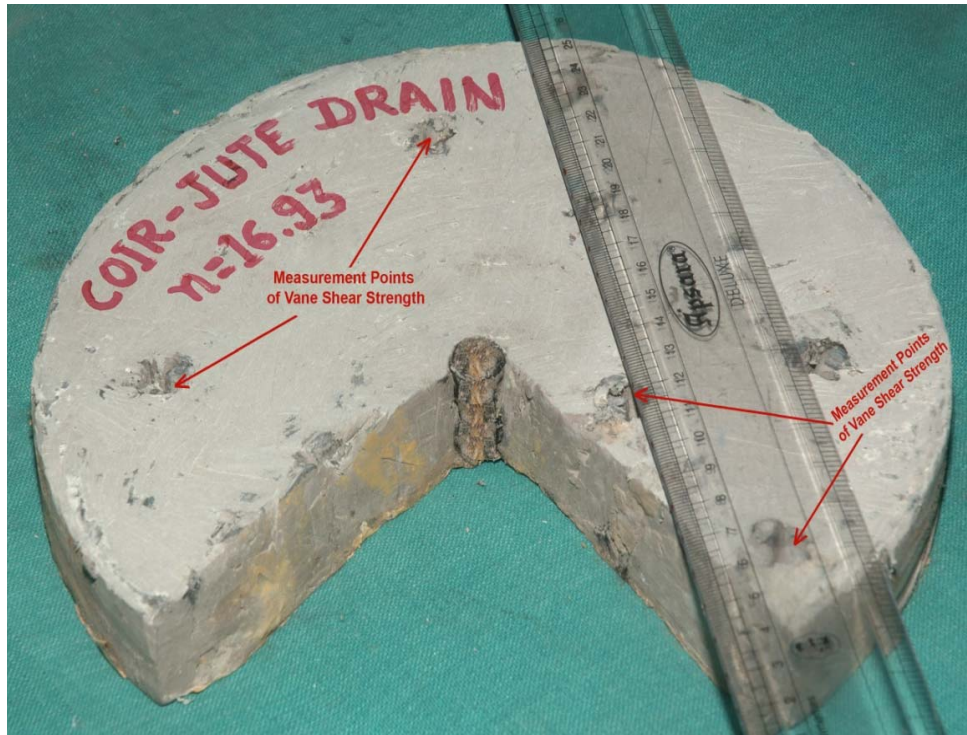


**Fig. 6.259:** Comparison of vane shear strength against ratio of radial distance for SD of all 'n' values

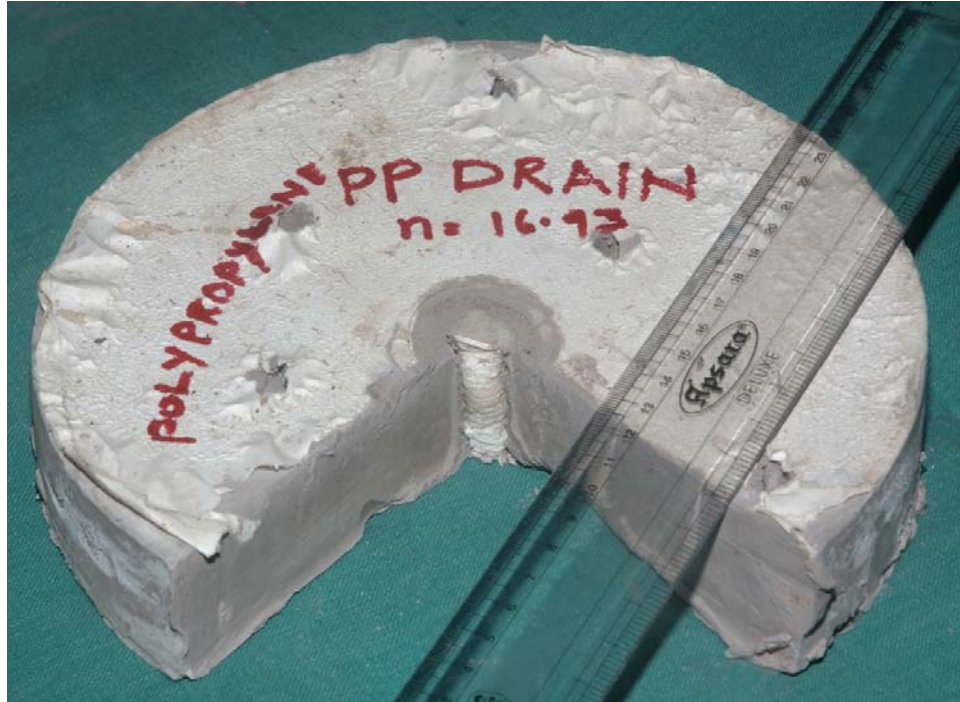




**Photograph 6.19:** Sectional view of consolidated clay sample (end of 320kPa pressure) with central vertical sand drain (SD) of  $n = 16.93$



**Photograph 6.20:** Sectional view of consolidated clay sample (end of 320kPa pressure) with central vertical sand drain (CJ) of  $n = 16.93$



**Photograph 6.21:** Sectional view of consolidated clay sample (end of 320kPa pressure) with central vertical sand drain (PF) of  $n = 16.93$



**Photograph 6.22:** Sectional view of consolidated clay sample (end of 320kPa pressure) with central vertical sand drain (SD) of  $n = 21.71$





**Photograph 6.23:** Sectional view of consolidated clay sample (end of 320kPa pressure) with central vertical sand drain (SW) of  $n = 21.71$



**Photograph 6.24:** Sectional view of consolidated clay sample (end of 320kPa pressure) with central vertical sand drain (CJ) of  $n = 21.71$

### 6.3.3) Geometry (shape) of vertical drain

Refer figures 6.260 to 6.318 which are derived from the settlement measurements and pore water pressure measurements. The following shapes of vertical sand drains are investigated and analysed.

- 1) **Circular** shape sand drain (CSSD)
- 2) **Plus** shape sand drain (PSSD)
- 3) **Tripod** shape sand drain (TSSD)
- 4) **Band** shape sand drain (BSSD)

#### 1) Degree of consolidation $U_r$ vs. Time: Figures 6.260 to 6.264

**a) Settlement analysis:-** Fig.6.260 to Fig.6.264 shows the plots of degree of consolidation versus time for various drain materials for all pressures and comparative plots are also shown for 40kPa and 160kPa as mentioned and it is observed as follows:

- The time required for 50% consolidation using Circular shape sand drain(CSSD) for  $n=11.04$  at 20kPa, 40kPa, 80kPa, 160kPa and 320kPa are 600min, 500min, 400min, 310min and 260min respectively while time required for 80% consolidation is 1300min, 980min, 840min, 760min and 580min respectively.
- The time required for 50% consolidation using Plus shape sand drain(PSSD) for  $n=11.04$  at 20kPa, 40kPa, 80kPa, 160kPa and 320kPa are 900min, 850min, 860min, 580min and 480min respectively while time required for 80% consolidation is 1800min, 1700min, 1500min, 1150min and 920min respectively.
- The time required for 50% consolidation using Band shape sand drain(BSSD) for  $n=11.04$  at 20kPa, 40kPa, 80kPa, 160kPa and 320kPa are 780min, 750min, 700min, 500min and 450min respectively while time required for 80% consolidation is 1750min, 1500min, 1400min, 1100min and 900min respectively.
- The time required for 50% consolidation using Tripod shape sand drain(TSSD) for  $n=11.04$  at 20kPa, 40kPa, 80kPa, 160kPa and 320kPa are 1050min, 980min, 820min, 760min and 580min respectively while time

required for 80% consolidation is 1900min, 1700min, 1650min, 1350min and 1050min respectively.

- Comparing all four drain geometry (shapes), CSSD takes lowest time both in terms of 50% and 80% consolidation. For 40kPa and for 50% consolidation CSSD takes 70%,96%,50% less time in compare to PSSD, BSSD, TSSD respectively, while for 80% consolidation CSSD takes 73.5%,73.5%,53% less time in compare to PSSD, TSSD, BSSD respectively. (for same 'n' value and for same pressure)
- Comparing all four drain geometry (shapes), CSSD takes lowest time both in terms of 50% and 80% consolidation. For 160kPa and for 50% consolidation CSSD takes 87%,145%,61% less time in compare to PSSD, BSSD, TSSD respectively, while for 80% consolidation CSSD takes 51%,77%,44% less time in compare to PSSD, BSSD, TSSD`respectively. (for same 'n' value and for same pressure)
- From the above observations it is clear that circular shape sand drain (CSSD) is most efficient shape of drain as it shows higher rate of compressibility (settlement) both for 50% and 80% consolidation, while BSSD is more economic then PSSD and TSSD.

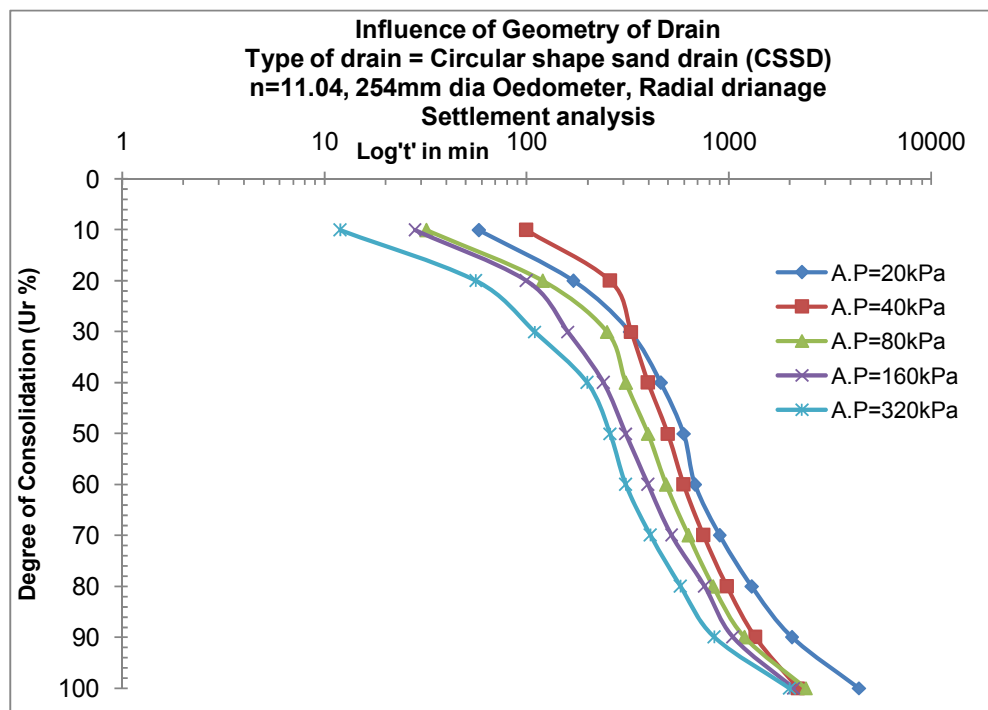


**Fig. 6.260:** Comparison of degree of consolidation vs. log't in min for CSSD

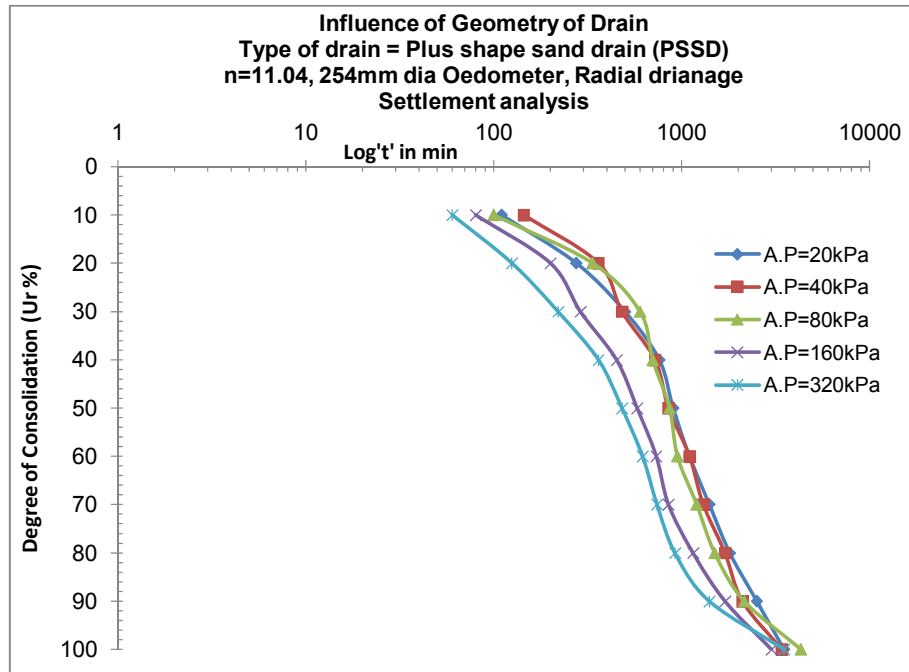


**Fig. 6.261:** Comparison of degree of consolidation vs.  $\log't$  in min for PSSD

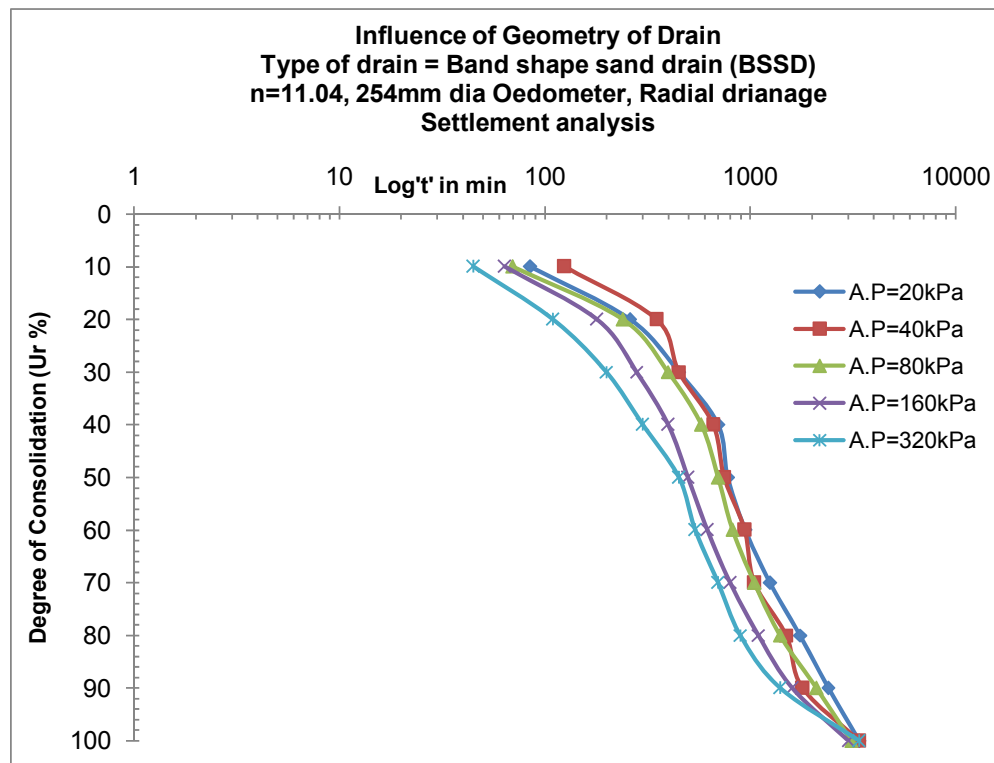


**Fig. 6.262:** Comparison of degree of consolidation vs.  $\log't$  in min for BSSD

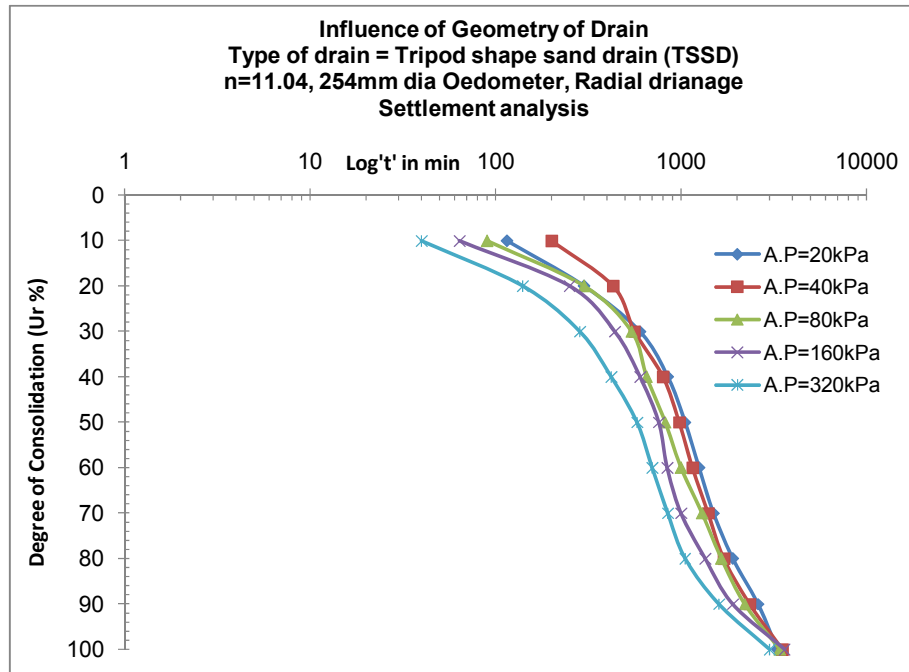


**Fig. 6.263:** Comparison of degree of consolidation vs.  $\log t'$  in min for TSSD

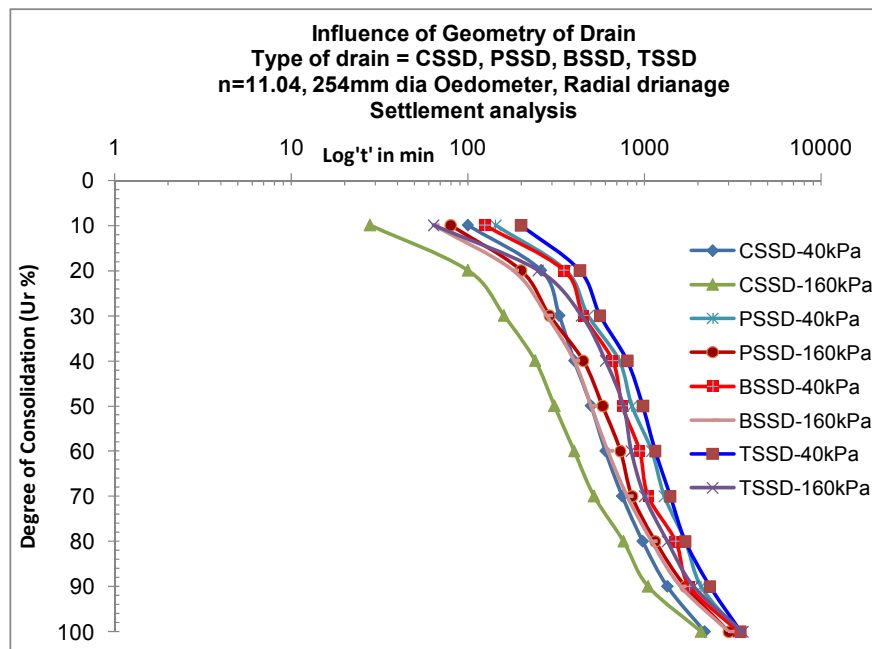


**Fig. 6.264:** Comparison of various geometry of sand drain at 40kPa and 160kPa pressure of 'n'11.04

**b) Pore pressure analysis:-** Fig.6.265 to Fig.6.271 shows the plots of degree of consolidation (dissipation of excess pore water pressure) versus time for various drain materials at all pressures and comparative plots are also shown for 40kPa and 160kPa at three radial point's r1, r2, r3 as mentioned and is observed as follows:

- The time required for 50 % consolidation using circular shape sand drain (CSSD) for  $n=11.04$  at 40kPa for radial point r1,r2 & r3 is 245min,490min,760min while for 160kPa for radial point r1,r2 & r3 is 400min,640min,950min respectively and time required for 80% consolidation at 40kPa for radial point r1,r2 & r3 is 600min,1200min,1800min while for 160kPa for radial point r1, r2 & r3 is 750min,1500min,2100min respectively.
- The time required for 50 % consolidation using Plus shape sand drain (PSSD) for  $n=11.04$  at 40kPa for radial point r1,r2 & r3 is 330min,560min,880min while for 160kPa for radial point r1,r2 & r3 is 500min,800min,1200min respectively and time required for 80% consolidation at 40kPa for radial point r1,r2 & r3 is 720min,1400min,2050min while for 160kPa for radial point r1, r2 & r3 is 950min,1800min,2500min respectively.
- The time required for 50% consolidation using Tripod shape sand drain (TSSD) for  $n=11.04$  at 40kPa for radial point r1,r2 & r3 is 361min,600min,950min while for 160kPa for radial point r1,r2 & r3 is 580min,900min,1250min respectively and time required for 80% consolidation at 40kPa for radial point r1,r2 & r3 is 800min,1550min,2250min while for 160kPa for radial point r1, r2 & r3 is 950min,2000min,2700min respectively.
- The time required for 50% consolidation using Band shape sand drain (BSSD) for  $n=11.04$  at 40kPa for radial point r1,r2 & r3 is 310min,540min,800min while for 160kPa for radial point r1,r2 & r3 is 450min,710min,1100min respectively and time required for 80% consolidation at 40kPa for radial point r1,r2 & r3 is 650min,1300min,1950min while for 160kPa for radial point r1, r2 & r3 is 880min,1700min,2300min respectively.



- Comparing all four drain geometry (shapes), CSSD takes lowest time both in terms of 50% and 80% consolidation. For 40KPa and for 50% consolidation cssd takes 34.7%,47.3%,26.5% less time in compare to pssd,tssd,bssd for radial point 'r1' respectively, while cssd takes 14.3%,22.4%,10.2% less time in compare to pssd,tssd,bssd for radial point 'r2' respectively,while cssd takes 15.8%,25%,5.3% less time in compare to pssd,tssd,bssd for radial point 'r3' respectively, Similarly for 80% consolidation cssd takes 20%,33.3%,8.3% less time in compare to pssd,tssd,bssd for radial point 'r1' respectively, while cssd takes 16.7%,29.2%,8.3% less time in compare to pssd,tssd,bssd for radial point 'r2' respectively,while cssd takes 13.9%,25%,8.3% less time in compare to pssd,tssd,bssd for radial point 'r3' respectively. (for same 'n' value and for same pressure)
- Comparing all four drain geometry (shapes), cssd takes lowest time both in terms of 50% and 80% consolidation. For 160KPa and for 50% consolidation cssd takes 25%,45%,12.5% less time in compare to pssd,tssd,bssd for radial point 'r1' respectively, while cssd takes 25%,40.6%,10.9% less time in compare to pssd,tssd,bssd for radial point 'r2' respectively,while cssd takes 26.3%,31.6%,15.8% less time in compare to pssd,tssd,bssd for radial point 'r3' respectively, Similarly for 80% consolidation cssd takes 26.7%,26.7%,17.3% less time in compare to pssd,tssd,bssd for radial point 'r1' respectively, while cssd takes 20%,33.3%,13.3% less time in compare to pssd,tssd,bssd for radial point 'r2' respectively,while cssd takes 19%,28.6%,9.5% less time in compare to pssd,tssd,bssd for radial point 'r3' respectively. (for same 'n' value and for same pressure)
- From the above observations it is clear that circular shape sand drain (cssd) is most efficient shape of drain as it shows higher rate of pore pressure dissipation both for 50% and 80% consolidation at three radial points r1, r2, r3, while bssd is more economic then pssd and tssd.

### **Discussion:**

- Considering settlement measurement it concludes that for 50% consolidation, CSSD of  $n=11.04$  takes 41% less time compared to any drain material under light loading and 48%, under constructional loading. Similarly for 80%

consolidation, CSSD takes 39% less time compared to any drain material under light loading and 36% under constructional loading.

- From pore pressure measurements, it infers that for 50% consolidation and mid plane radial point  $r_2$ , CSSD of  $n=11.04$  takes 13% less time compared to other drain shapes under light loading and 20% under constructional loading. Similarly for 80% consolidation, CSSD takes 15% less time compared to other drain shapes under light loading and 18% under constructional loading.
- CSSD of  $n=11.04$  takes lowest time in compare to BSSD, PSSD, TSSD both under light and constructional loading. However BSSD for 50% consolidation takes 12% & 23% lower time in compare to PSSD & TSSD but 50% higher in compare to CSSD under light loading. Also PSSD takes 13% lower time compare to TSSD but 70% higher in compare to CSSD. Similarly BSSD for 80% consolidation takes 12% & 12% lower time in compare to PSSD & TSSD but 53% higher in compare to CSSD under light loading. Also PSSD takes equal time compare to TSSD but 73% higher in compare to CSSD.
- For any load intensity and for any geometry of sand drain with 'n' value equal to 11.04, the time deformation curve with respect to pore pressure dissipation remain towards the vertical axis compare to curve of settlement, that is time require for 50% or 80% consolidation is less compare to settlement curve which also reflects in isochrones curves.
- Though from the point of rate of dissipation of pore pressure for a circular shape drain seems to be efficient, the band shape drain provide best construction facility during installation in terms of cost and speed of work.
- Based on the equivalent diameter concept the dimensions of various shapes of drain are worked out. Though surface area of plus shape and tripod shape drain work out to be higher then band shape and circular shape drain, the draining efficiency of circular and band shape is higher then other two shapes of drain. It may be due to right and acute angles of the drain which intercept the path of flow of water to some extent.
- Under compressional stresses the drain-clay interface are not remaining compatible with the deform shape of the drain, therefore the higher surface

area of plus and tripod shape drain are not remaining advantageous for the easy flow of water from the central drain.

- For any load intensity and for any geometry of sand drain with 'n' value equal to 11.04, the time deformation curve with respect to pore pressure dissipation remain towards the vertical axis compare to curve of settlement, that is time require for 50% or 80% consolidation is less compare to settlement curve which also reflects in isochrones curves. The curve of pore pressure for CSSD shift towards vertical axis compare to BSSD, PSSD and TSSD for any pressure for same specific surface area. The curve of CSSD remain towards vertical axis showing less time for 50% consolidation thereafter all curves merge to some extent. The curve of BSSD remains towards vertical axis more compare to curve of BSSD and TSSD for both pore pressure and settlement measurements. The above observation may be due to higher hindrance for the conductivity of the radial flow to the drain compare to other drains wise band, tripod and plus shape. This is in similitude with flow per unit time through various shaped notch under constant head. That is circular notch gives higher discharge compare to rectangular notch, plus shape notch and tripod shape notch. The hydraulic conductivity will always remain uniform through circular one, least quantum of vortex is observed in circular one compare to other shape notch. To some extent this is true for flow through different shape drain with a different hydraulic mean radius of capillary formed.

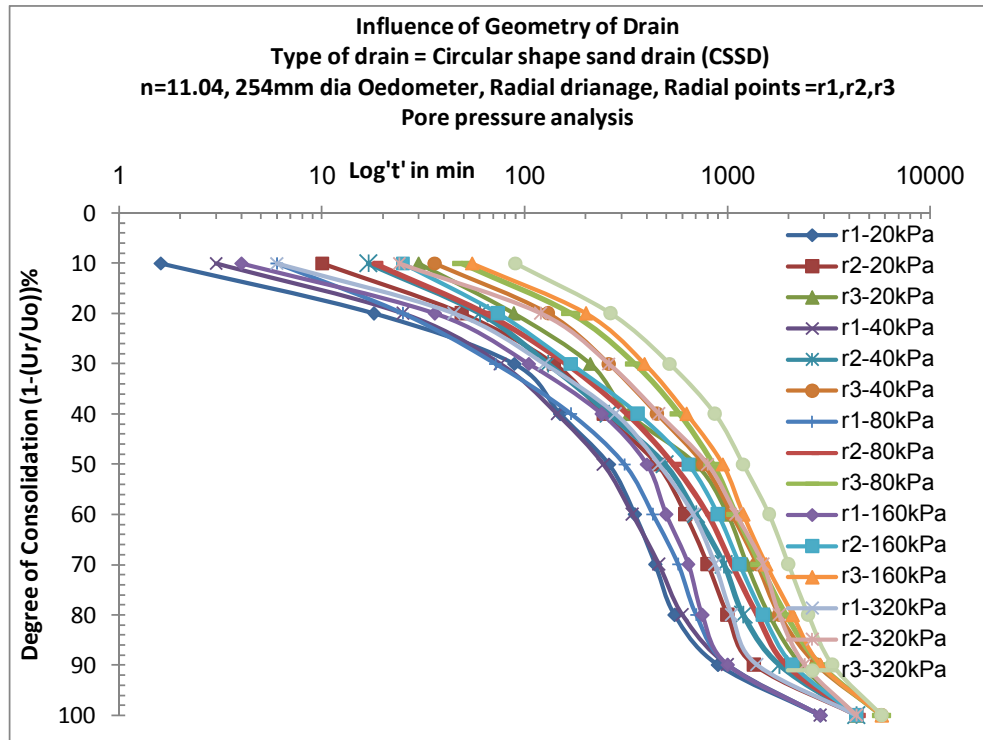


**Fig. 6.265:** Comparison of degree of consolidation vs.  $\log t'$  in min for CSSD at three radial points for all applied pressures

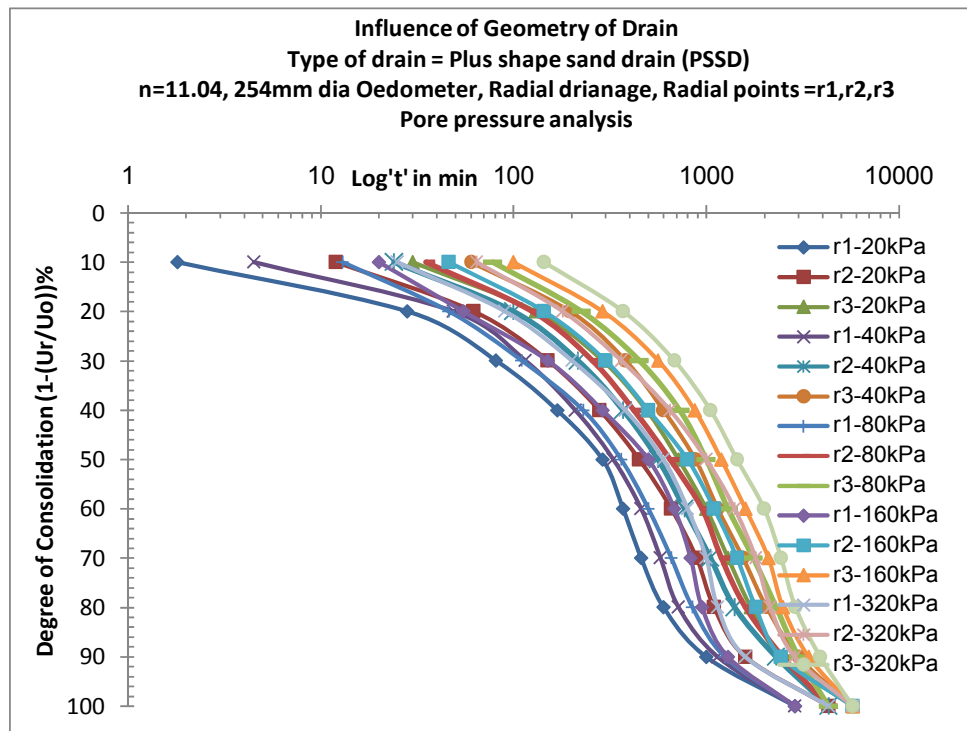


**Fig. 6.266:** Comparison of degree of consolidation vs.  $\log t'$  in min for PSSD at three radial points for all applied pressures

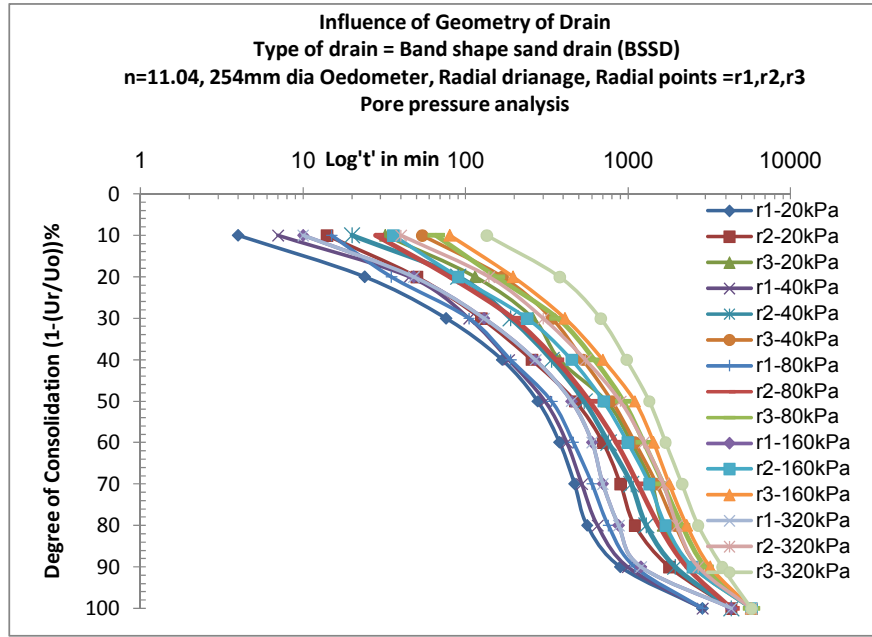


**Fig. 6.267:** Comparison of degree of consolidation vs.  $\log t'$  in min for BSSD at three radial points for all applied pressures

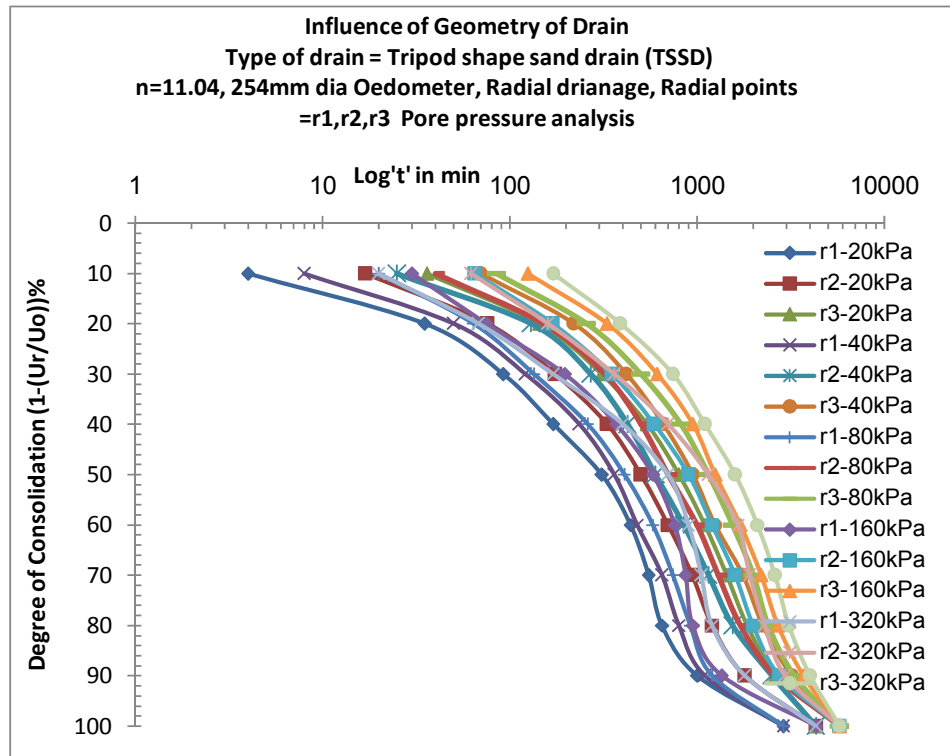


**Fig. 6.268:** Comparison of degree of consolidation vs.  $\log t'$  in min for BSSD at three radial points for all applied pressures

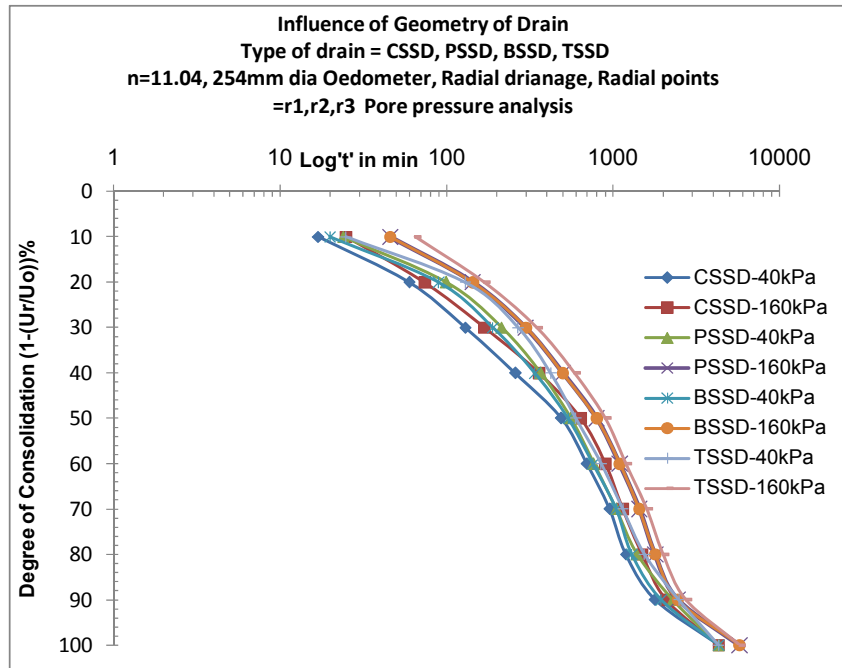


**Fig. 6.269:** Comparison of degree of consolidation for various geometrical sand drains of mid radial point  $r_2$  at 40kPa and 160kPa pressure

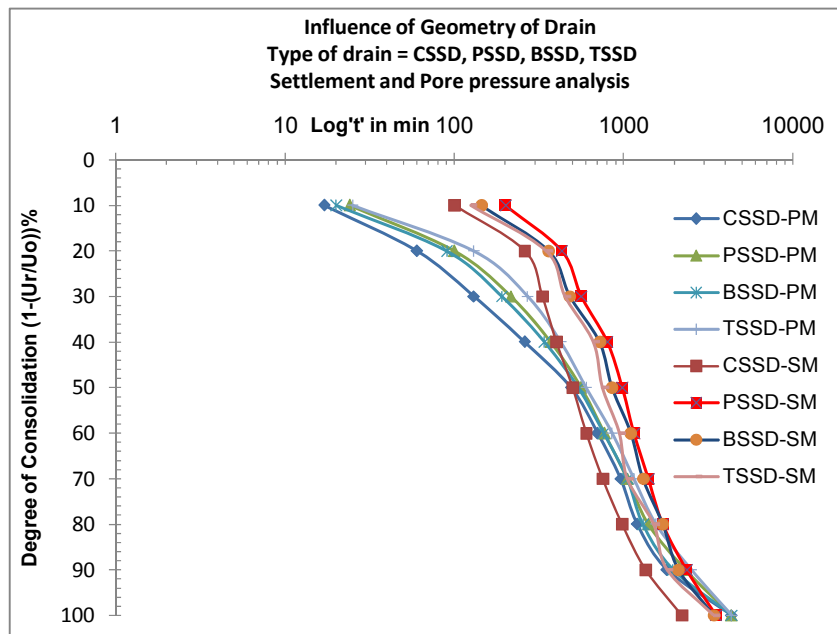


**Fig. 6.270:** Comparison of degree of consolidation for various geometrical sand drains based on settlement and pore pressure measurements at 40kPa pressure

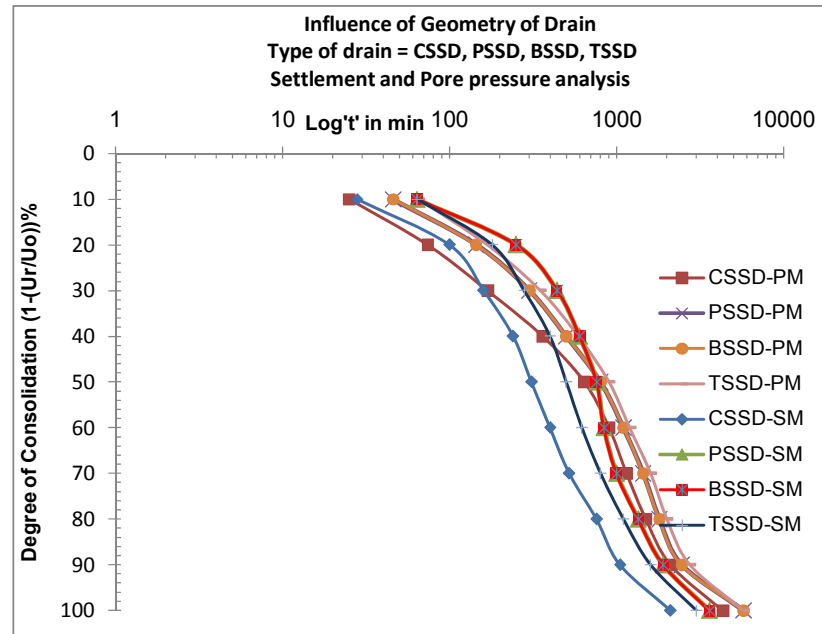


**Fig. 6.271:** Comparison of degree of consolidation for various geometrical sand drains based on settlement and pore pressure measurements at 160kPa pressure

**2) Coefficient of consolidation ( $C_r$ ) vs. Degree of consolidation ( $U_r$ ):**  
**Figures 6.272 to 6.282**

**a) Settlement analysis:-** Fig.6.272 to Fig.6.276 shows comparison plots of Coefficient of consolidation versus degree of consolidation for 'n' value of 11.04 for various geometrical shape sand drains i.e. CSSD, PSSD, TSSD & BSSD at 40kPa and 160kPa applied pressures.

- $n=11.04$ , for 50% consolidation CSSD shows 33.33%, 40.71%, 48.17% higher  $C_r$  value in compare to BSSD, PSSD, TSSD for 40kPa pressure, while for 80% consolidation CSSD shows 34.67%, 41.9%, 41.44% higher  $C_r$  value in compare to BSSD, PSSD, TSSD for 40kPa pressure, while BSSD shows 11% & 22% higher  $C_r$  value in compare to PSSD, TSSD and for 80% consolidation BSSD shows 11% & 10% higher  $C_r$  value in compare to PSSD & TSSD respectively.

- $n=11.04$ , for 50% consolidation CSSD shows 38%,46%,58% higher  $C_r$  value in compare to BSSD,PSSD,TSSD for 160kPa pressure, while for 80% consolidation CSSD shows 31%,33%,42% higher  $C_r$  value in compare to BSSD,PSSD,TSSD for 160kPa pressure, while BSSD shows 13% & 33% higher  $C_r$  value in compare to PSSD,TSSD and for 80% consolidation BSSD shows 3%& 17% higher  $C_r$  value in compare to PSSD & TSSD respectively.
- From the above discussions it is clear that out of four geometrical shapes of drains, the CSSD of 'n' equal to 11.04 is more efficient in compare to BSSD, PSSD & TSSD, while BSSD is more efficient in compare to PSSD & TSSD at all pressures.CSSD shows more rate of compressibility in compare to other shapes of sand drains.

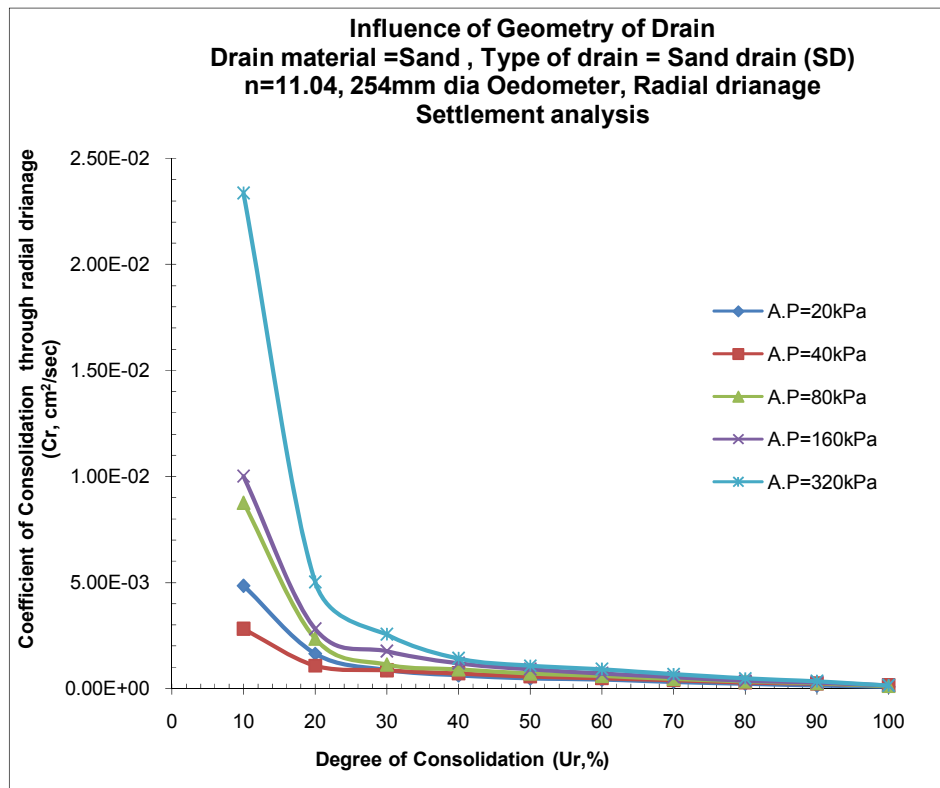


**Fig. 6.272:** Comparison of  $C_r$  vs.  $U_r$  for CSSD at all pressures



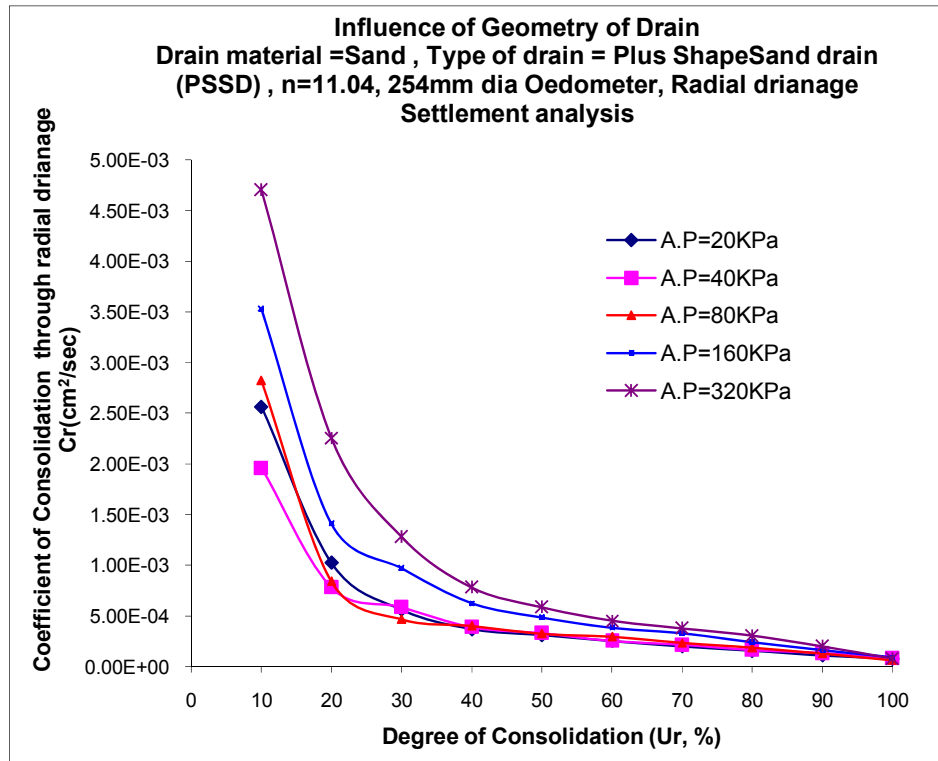


**Fig. 6.273:** Comparison of  $C_r$  vs.  $U_r$  for PSSD at all pressures

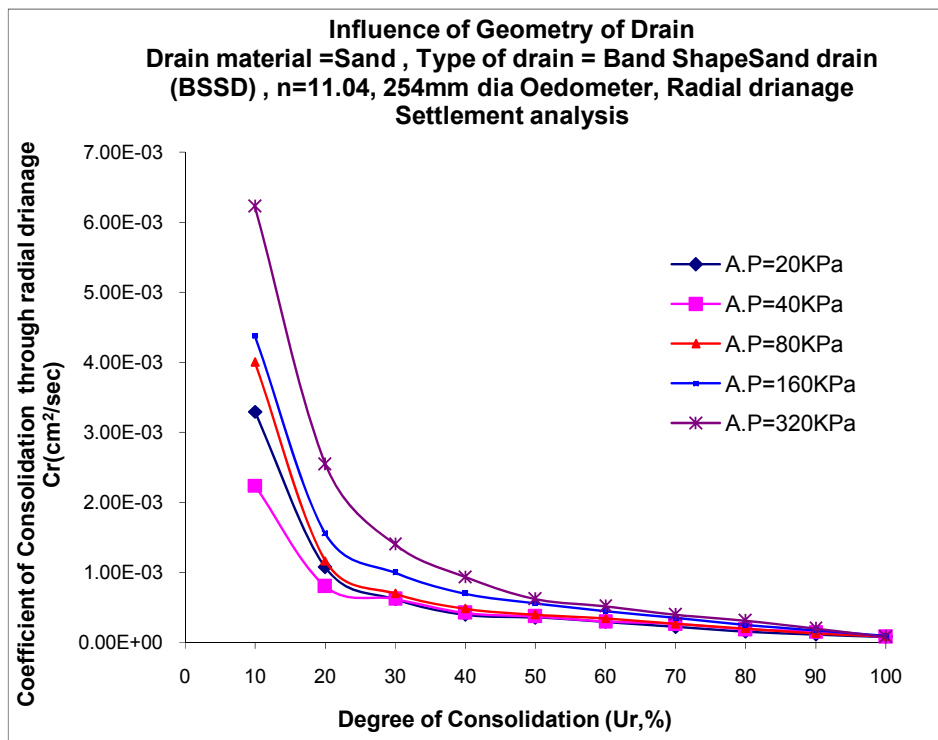


**Fig. 6.274:** Comparison of  $C_r$  vs.  $U_r$  for BSSD at all pressures

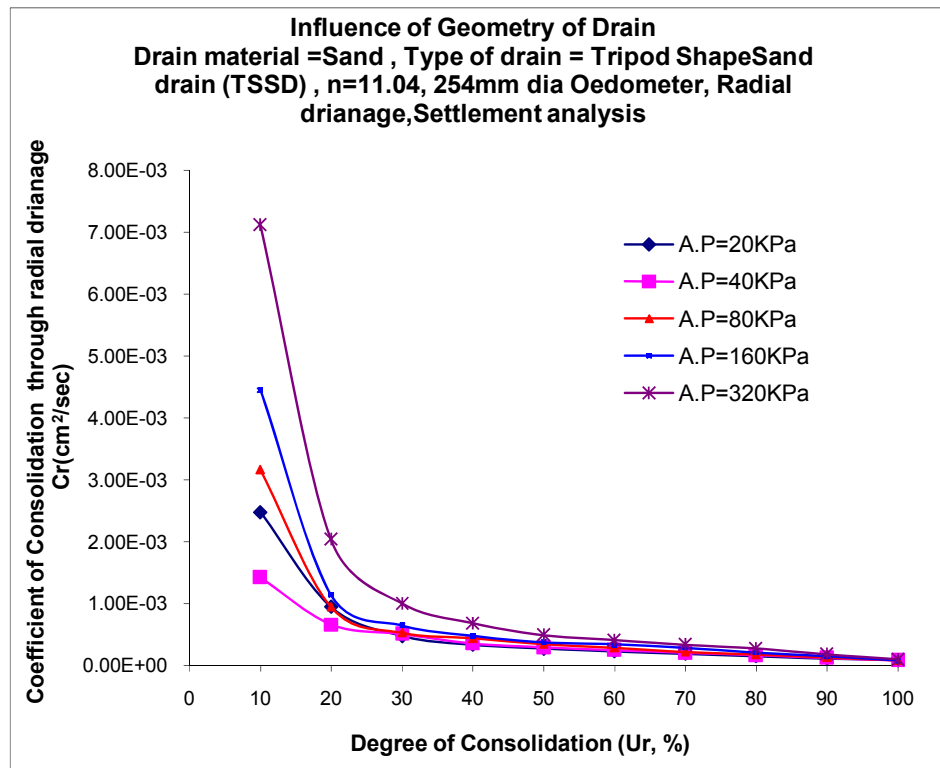


**Fig. 6.275:** Comparison of  $Cr$  vs.  $U_r$  for TSSD at all pressures

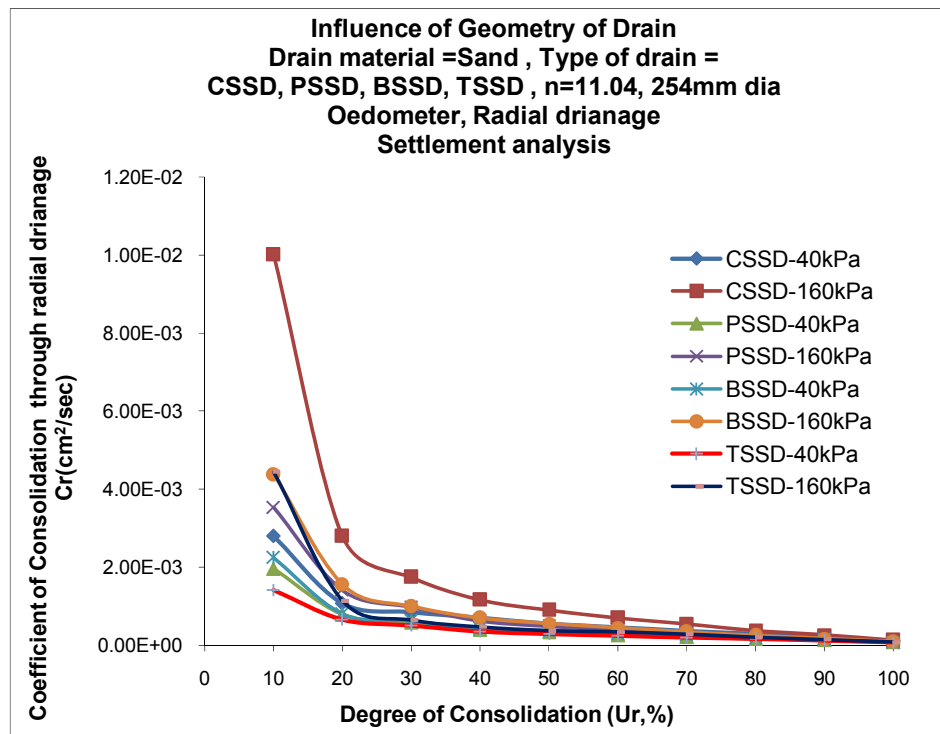


**Fig. 6.276:** Influence of various geometrical shape of drain on  $Cr$  vs.  $U_r$  for all pressures

**Pore pressure analysis:** Fig.6.277 to Fig.6.282 shows the comparison plots of Coefficient of consolidation( $C_r$ ) versus degree of consolidation( $U_r$ ) at three radial points'  $r_1$ ,  $r_2$ ,  $r_3$  for various geometrical sand drains i.e. CSSD, PSSD, TSSD & BSSD at all pressures. The analysis is carried out for 'n' value of 11.04 for all pressures. Comparative plots are also presented for 40kPa & 160kPa pressures. Atlast comparative plot is presented between settlement and pore pressure analysis.

- $n=11.04$ , for 50% consolidation, for radial point  $r_1$ , CSSD shows 22%, 20%, 28% higher  $C_r$  value in compare to PSSD, BSSD and TSSD for 40kPa pressure, while  $n=11.04$  for 80% consolidation CSSD shows 13%, 7%, 21% higher  $C_r$  value in compare to PSSD, BSSD and TSSD for 40kPa pressure. Similarly for radial point  $r_2$ , CSSD shows 8%, 9%, 14% higher  $C_r$  value in compare to PSSD, BSSD and TSSD for 40kPa pressure, while  $n=11.04$  for 80% consolidation CSSD shows 10%, 7.5%, 18% higher  $C_r$  value in compare to PSSD, BSSD and TSSD for 40kPa pressure. Similarly for radial point  $r_3$ , CSSD shows 9%, 5%, 15% higher  $C_r$  value in compare to PSSD, BSSD and TSSD for 40kPa pressure, while  $n=11.04$  for 80% consolidation CJD shows 8%, 7.5%, 15% higher  $C_r$  value in compare to PSSD, BSSD and TSSD for 40kPa pressure.
- Similarly  $n=11.04$ , for 50% consolidation, for radial point  $r_1$ , BSSD shows 9%, higher  $C_r$  value in compare to TSSD for 40kPa pressure, while  $n=11.04$  for 80% consolidation CSSD shows 14% higher  $C_r$  value in compare to TSSD for 40kPa pressure.
- $n=11.04$ , for 50% consolidation, for radial point  $r_1$ , CSSD shows 16%, 11%, 27% higher  $C_r$  value in compare to PSSD, BSSD and TSSD for 160kPa pressure, while  $n=11.04$  for 80% consolidation CSSD shows 17%, 14%, 16% higher  $C_r$  value in compare to PSSD, BSSD and TSSD for 160kPa pressure. Similarly for radial point  $r_2$ , CSSD shows 16%, 10%, 25% higher  $C_r$  value in compare to PSSD, BSSD and TSSD for 160kPa pressure, while  $n=11.04$  for 80% consolidation CSSD shows 13%, 11%, 21% higher  $C_r$  value in compare to PSSD, BSSD and TSSD for 160kPa pressure. Similarly for radial point  $r_3$ , CSSD shows 17%, 13%, 20% higher  $C_r$  value in compare to PSSD, BSSD and TSSD for 160kPa pressure, while  $n=11.04$  for 80% consolidation CJD

shows 12%,8.5%,18% higher Cr value in compare to PSSD, BSSD and TSSD for 160kPa pressure.

- n=11.04, for 50% consolidation, for radial point r1, BSSD shows 2%,10% higher Cr value in compare to PSSD and TSSD for 40kPa pressure, while n=11.04 for 80% consolidation BSSD shows 6%,14% higher Cr value in compare to PSSD and TSSD for 40kPa pressure. Similarly for radial point r2, BSSD shows -0.7%, 5% higher Cr value in compare to PSSD and TSSD for 40kPa pressure, while n=11.04 for 80% consolidation BSSD shows 3%, 12% higher Cr value in compare to PSSD and TSSD for 40kPa pressure. Similarly for radial point r3, BSSD shows 5%,11% higher Cr value in compare to PSSD and TSSD for 40kPa pressure, while n=11.04 for 80% consolidation BSSD shows 0.7%,9% higher Cr value in compare to PSSD and TSSD for 40kPa pressure.
- n=11.04, for 50% consolidation, for radial point r1, BSSD shows 6%,18% higher Cr value in compare to PSSD and TSSD for 160kPa pressure, while n=11.04 for 80% consolidation BSSD shows 3%,2.5% higher Cr value in compare to PSSD and TSSD for 160kPa pressure. Similarly for radial point r2, BSSD shows 7%, 17% higher Cr value in compare to PSSD and TSSD for 160kPa pressure, while n=11.04 for 80% consolidation BSSD shows 1.5%, 10% higher Cr value in compare to PSSD and TSSD for 160kPa pressure. Similarly for radial point r3, BSSD shows 4%,7% higher Cr value in compare to PSSD and TSSD for 160kPa pressure, while n=11.04 for 80% consolidation BSSD shows 4%,10% higher Cr value in compare to PSSD and TSSD for 160kPa pressure.
- n=11.04, for 50% consolidation, for radial point r1, PSSD shows 8% higher Cr value in compare to TSSD for 40kPa pressure, while n=11.04 for 80% consolidation PSSD shows 9% higher Cr value in compare to TSSD for 40kPa pressure. Similarly for radial point r2, PSSD shows 6% higher Cr value in compare to TSSD for 40kPa pressure, while n=11.04 for 80% consolidation PSSD shows 9% higher Cr value in compare to TSSD for 40kPa pressure. Similarly for radial point r3, PSSD shows 7% higher Cr value in compare to TSSD for 40kPa pressure, while n=11.04 for 80%

consolidation PSSD shows 8% higher  $C_r$  value in compare to TSSD for 40kPa pressure.

- $n=11.04$ , for 50% consolidation, for radial point  $r_1$ , PSSD shows 13% higher  $C_r$  value in compare to TSSD for 160kPa pressure, while  $n=11.04$  for 80% consolidation PSSD shows -0.7% higher  $C_r$  value in compare to TSSD for 160kPa pressure. Similarly for radial point  $r_2$ , PSSD shows 10% higher  $C_r$  value in compare to TSSD for 160kPa pressure, while  $n=11.04$  for 80% consolidation PSSD shows 9% higher  $C_r$  value in compare to TSSD for 160kPa pressure. Similarly for radial point  $r_3$ , PSSD shows 3% higher  $C_r$  value in compare to TSSD for 160kPa pressure, while  $n=11.04$  for 80% consolidation PSSD shows 7% higher  $C_r$  value in compare to TSSD for 160kPa pressure.
- From the above discussions it is clear that out of four geometrical shapes of drains, the CSSD of 'n' equal to 11.04 is more efficient in compare to BSSD, PSSD & TSSD, while BSSD is more efficient in compare to PSSD & TSSD at all pressures. CSSD shows more rate of dissipation of excess pore water pressure in compare to other shapes of sand drains.

#### **Discussion:**

- From settlement analysis it concludes that CSSD of  $n=11.04$  for 50% consolidation shows 71% higher  $C_r$  value compare to other geometry of drains under light loading and 96% under constructional loading. Similarly for 80% consolidation shows 65% higher  $C_r$  value compare to other geometry of drains under light loading and 57% under constructional loading.
- From pore pressure analysis for middle radial point  $r_2$  it concludes that CSSD of  $n=11.04$  for 50% consolidation shows 12% higher  $C_r$  value compare to other geometry of drains under light loading and 21% under constructional loading. Similarly for 80% consolidation shows 14% higher  $C_r$  value compare to other geometry of drains under light loading and 18% under constructional loading.

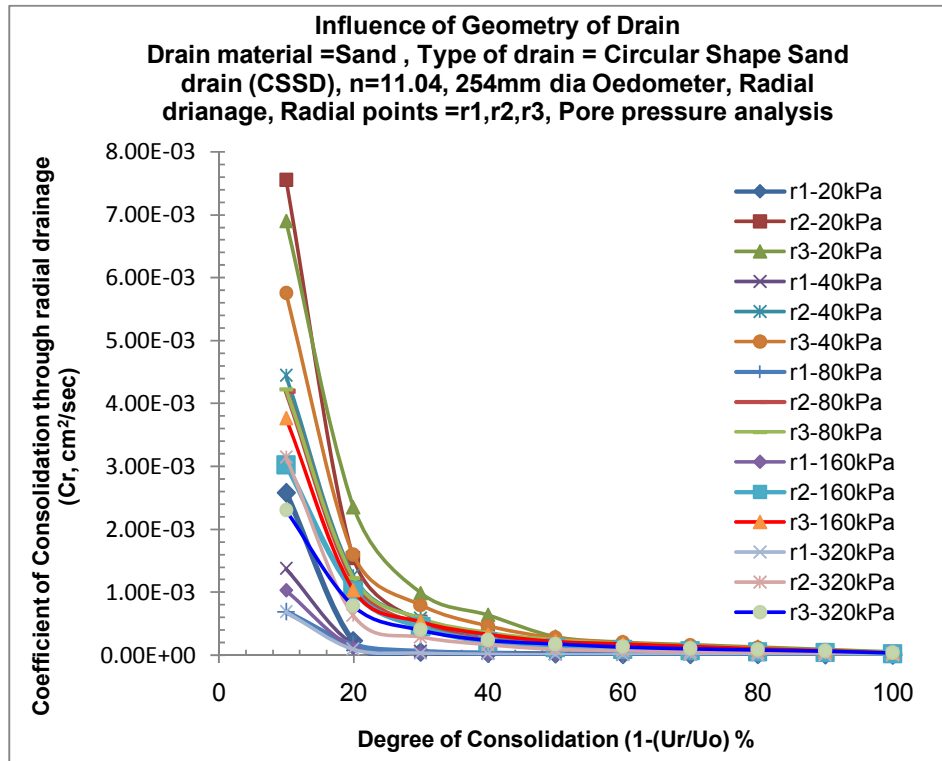


**Fig. 6.277:** Comparison of Cr vs. Ur for CSSD for all pressures at radial points r1, r2 and r3

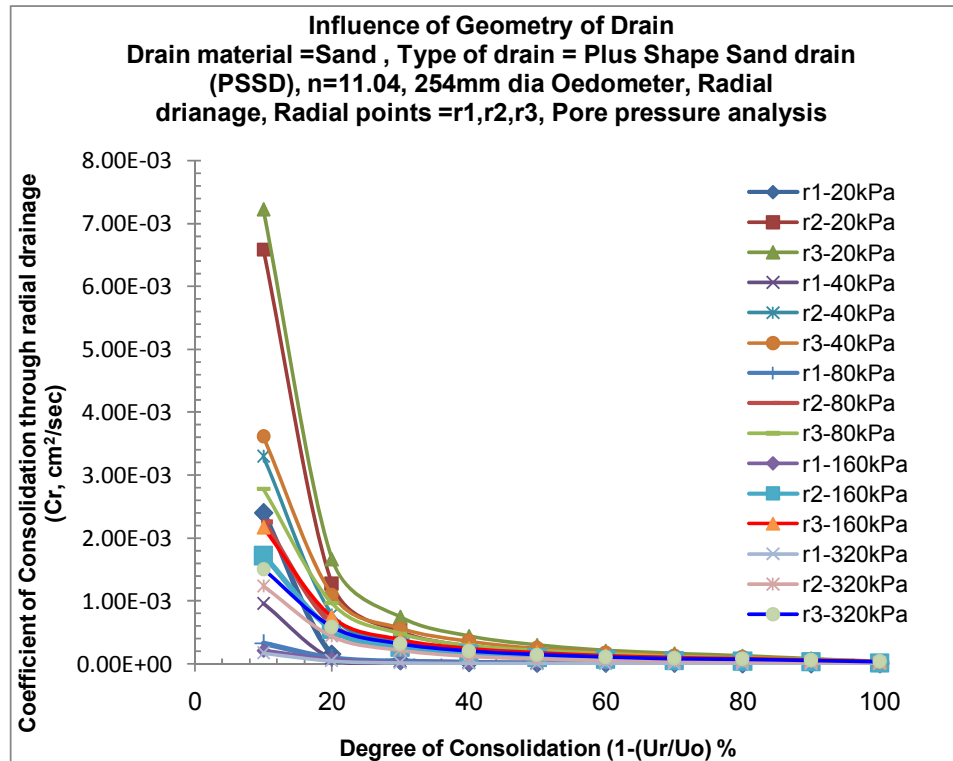


**Fig. 6.278:** Comparison of Cr vs. Ur for PSSD for all pressures at radial points r1, r2 and r3

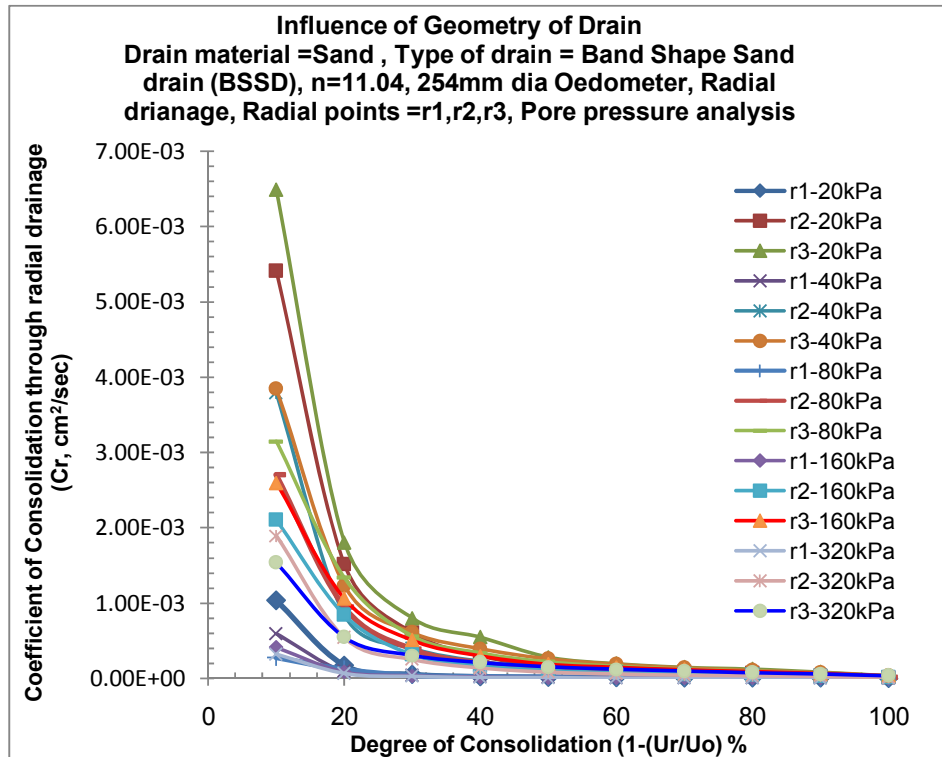


**Fig. 6.279:** Comparison of Cr vs. Ur for BSSD for all pressures at radial points r1, r2 and r3

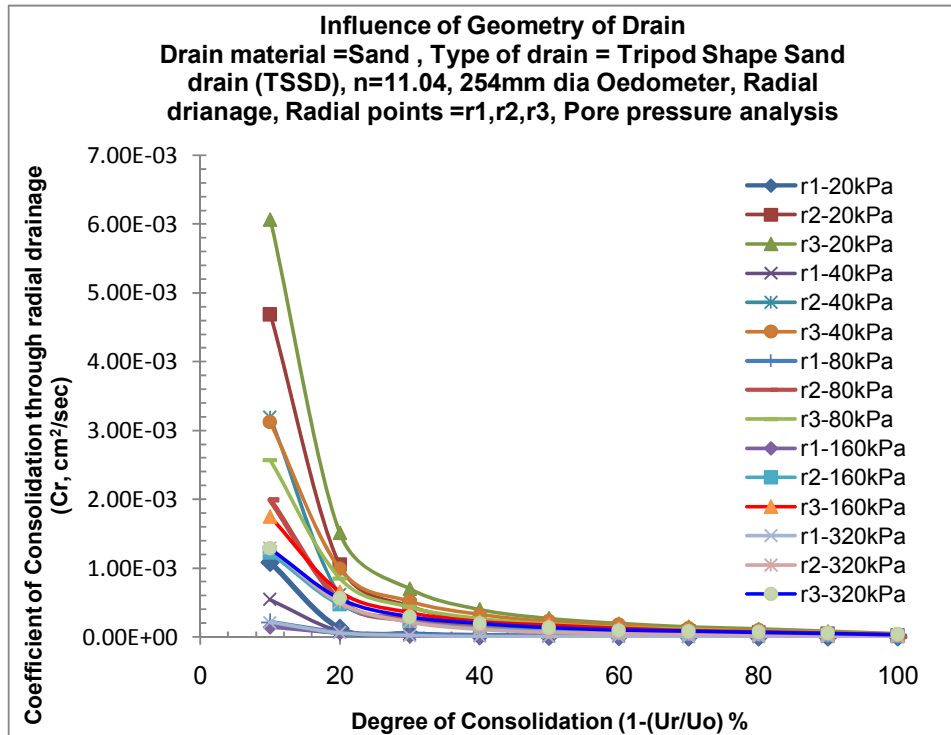


**Fig. 6.280:** Comparison of Cr vs. Ur for TSSD for all pressures at radial points r1, r2 and r3

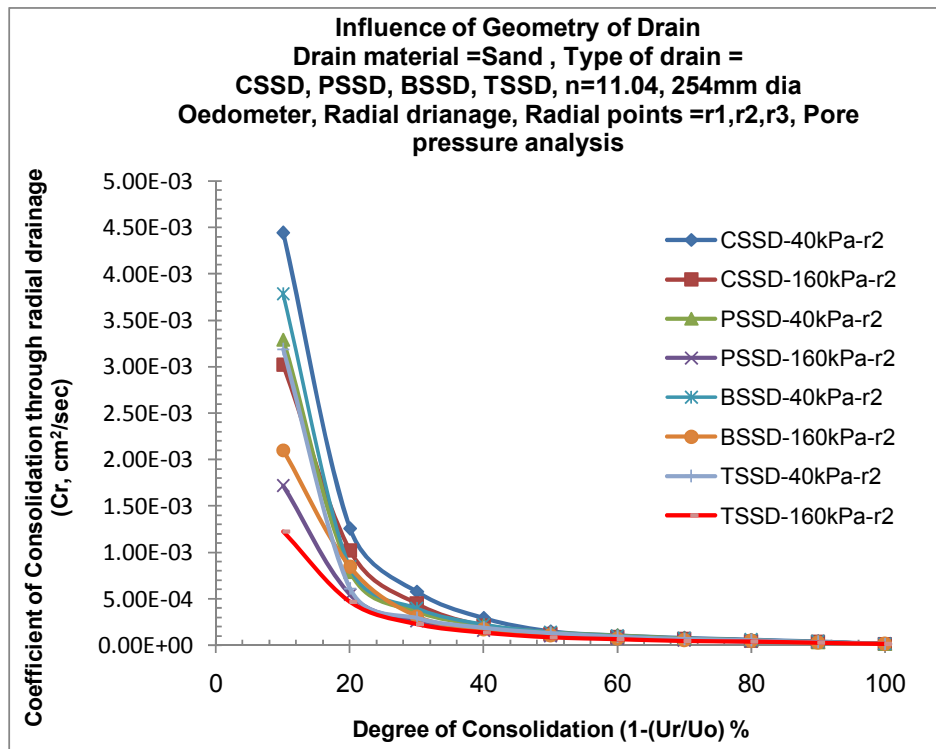


**Fig. 6.281:** Influence of Geometry of drain on  $C_r$  (of mid radial point  $r_2$ ) vs.  $U_r$  at 40kPa and 160kPa pressure

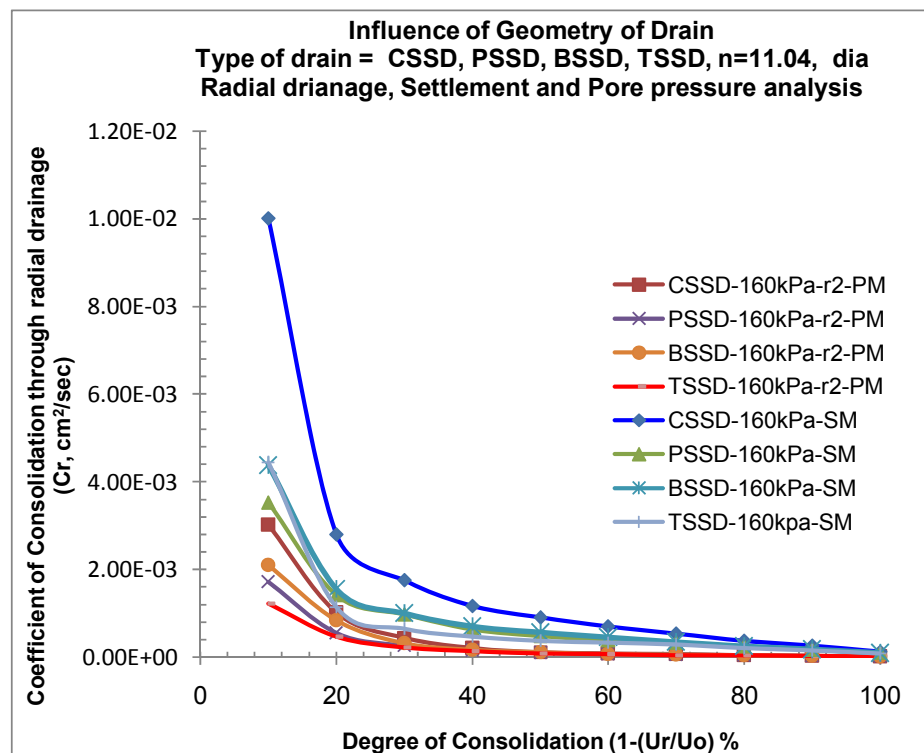


**Fig. 6.282:** Influence of Geometry of drain on  $C_r$  vs.  $U_r$  at 160kPa pressure based on settlement and pore pressure analysis



### 3) Coefficient of consolidation (Cr) vs. Applied pressure:- Figures 6.283 to 6.285

**a) Settlement analysis-** Fig.6.283 shows the plots of coefficient of consolidation due to radial drainage (Cr) versus applied pressure for various shapes of drains i.e. CSSD, BSSD, PSSD & TSSD for 'n' value of 11.04. Here for analysis time required for 50% ( $T_{50}$ ) consolidation and time required for 80% ( $T_{80}$ ) consolidation are taken for all applied pressures. From the plots it is very clear that the nature of  $U_r$ -80% graph remains same that is nearly constant or say linear increasing, while  $U_r$ -50% graph has much variation in initial pressures and thereafter Cr values increase rapidly for later higher pressures. This is true almost for all drains. There is no much variation in the value of Cr up to 50 kPa, change of Cr value indicates the initial structural resistance existing in the clay water structure in the Kaolinite clay.

- The value of  $Cr_{50}$  for CSSD, BSSD, PSSD and TSSD for 'n' equal to 11.04 and for 40 kPa was found to be  $5.60 \times 10^{-4} \text{ cm}^2/\text{sec}$ ,  $3.73 \times 10^{-4} \text{ cm}^2/\text{sec}$ ,  $3.32 \times 10^{-4} \text{ cm}^2/\text{sec}$ ,  $2.90 \times 10^{-4} \text{ cm}^2/\text{sec}$  and  $Cr_{80}$  was found as  $2.85 \times 10^{-4} \text{ cm}^2/\text{sec}$ ,  $1.86 \times 10^{-4} \text{ cm}^2/\text{sec}$ ,  $1.66 \times 10^{-4} \text{ cm}^2/\text{sec}$ ,  $1.67 \times 10^{-4} \text{ cm}^2/\text{sec}$  respectively. For higher engineering stress of 160 kPa the  $Cr_{50}$  for all four geometrical shapes was determined as  $9.03 \times 10^{-4} \text{ cm}^2/\text{sec}$ ,  $5.60 \times 10^{-4} \text{ cm}^2/\text{sec}$ ,  $4.86 \times 10^{-4} \text{ cm}^2/\text{sec}$ ,  $3.74 \times 10^{-4} \text{ cm}^2/\text{sec}$  and  $Cr_{80}$  was found as  $3.68 \times 10^{-4} \text{ cm}^2/\text{sec}$ ,  $2.54 \times 10^{-4} \text{ cm}^2/\text{sec}$ ,  $2.45 \times 10^{-4} \text{ cm}^2/\text{sec}$ ,  $2.10 \times 10^{-4} \text{ cm}^2/\text{sec}$  respectively.
- Looking to mentioned plots and values it is clear that of all four geometrical shapes the CSSD of  $n=11.04$  proves to be most economical shape of vertical drain and this is true for all pressures. Also BSSD is more superior in compare to PSSD, while PSSD is more economical than TSSD for all pressures. Out of all drains CSSD shows more rate of consolidation both at low and high pressures in compare to other shape of sand drains. So it can be said that CSSD shows more inter-rate of compressibility even at following pressures in compare to other geometrical shapes of drains for  $n=11.04$ .

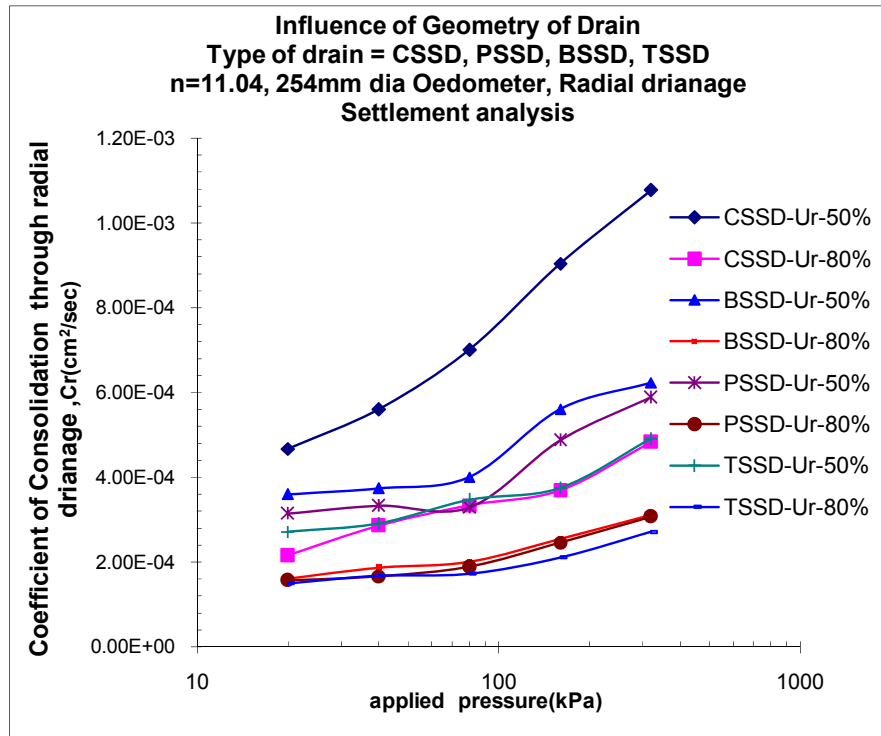


**Fig. 6.283:** Comparison of  $C_r$  vs. applied pressure for various geometrical drains at  $U_r$  50% and  $U_r$  80%

**b) Pore pressure analysis-** Fig.6.284 to Fig. 6.285 shows the plots of coefficient of consolidation due to radial drainage ( $C_r$ ) versus applied pressure for various geometrical shapes of sand drains like CSSD, PSSD, BSSD, TSSD for 'n' values of 11.04 at three radial points'  $r_1$ ,  $r_2$  and  $r_3$ . Here for analysis time required for 50% ( $T_{50}$ ) consolidation and time required for 80% ( $T_{80}$ ) consolidation are taken for all 40kPa and 160kPa pressures. From the plots it is very clear that for all shapes of drain the initial nature of  $T_{80}$  graph &  $T_{50}$  graph decreases with initial applied pressure and at higher pressures it remains same that is nearly constant. This is true for all shapes of drains. There is much variation in the value of  $C_r$  up to 50kPa, change of  $C_r$  value indicate the initial structural resistance existing in the clay water structure in the Kaolinite clay. Lesser variation in  $C_r$  value is observed for radial point's  $r_2$  and  $r_3$  for all 'n' values, for all shapes of drains and for all applied pressures.

- The value of  $C_{r1,50}$  at 40kPa for CSSD, PSSD, BSSD, TSSD for 'n' equal to 11.04 is  $1.7 \times 10^{-5} \text{ cm}^2/\text{sec}$ ,  $1.3 \times 10^{-5} \text{ cm}^2/\text{sec}$ ,  $1.3 \times 10^{-5} \text{ cm}^2/\text{sec}$ ,  $1.2 \times 10^{-5} \text{ cm}^2/\text{sec}$  while for 160kPa it was found to be  $1 \times 10^{-5} \text{ cm}^2/\text{sec}$ ,  $0.9 \times 10^{-5}$

cm<sup>2</sup>/sec,  $0.9 \times 10^{-5}$  cm<sup>2</sup>/sec,  $0.7 \times 10^{-5}$  cm<sup>2</sup>/sec respectively. Similarly value of  $C_{r2,50}$  is  $1.54 \times 10^{-4}$  cm<sup>2</sup>/sec,  $1.41 \times 10^{-4}$  cm<sup>2</sup>/sec,  $1.4 \times 10^{-4}$  cm<sup>2</sup>/sec,  $1.33 \times 10^{-4}$  cm<sup>2</sup>/sec while for 160kPa it was found to be  $1.18 \times 10^{-4}$  cm<sup>2</sup>/sec,  $9.88 \times 10^{-5}$  cm<sup>2</sup>/sec,  $1.07 \times 10^{-4}$  cm<sup>2</sup>/sec,  $8.85 \times 10^{-5}$  cm<sup>2</sup>/sec respectively. Similarly value of  $C_{r3,50}$  is  $2.72 \times 10^{-4}$  cm<sup>2</sup>/sec,  $2.46 \times 10^{-4}$  cm<sup>2</sup>/sec,  $2.59 \times 10^{-4}$  cm<sup>2</sup>/sec,  $2.3 \times 10^{-4}$  cm<sup>2</sup>/sec while for 160kPa it was found to be  $2.18 \times 10^{-4}$  cm<sup>2</sup>/sec,  $1.81 \times 10^{-4}$  cm<sup>2</sup>/sec,  $1.89 \times 10^{-4}$  cm<sup>2</sup>/sec,  $1.75 \times 10^{-4}$  cm<sup>2</sup>/sec respectively.

- The value of  $C_{r1,80}$  at 40kPa for CSSD, PSSD, BSSD, TSSD for 'n' equal to 11.04 is  $6.87 \times 10^{-6}$  cm<sup>2</sup>/sec,  $5.99 \times 10^{-6}$  cm<sup>2</sup>/sec,  $6.36 \times 10^{-6}$  cm<sup>2</sup>/sec,  $5.43 \times 10^{-6}$  cm<sup>2</sup>/sec while for 160kPa it was found to be  $5.5 \times 10^{-6}$  cm<sup>2</sup>/sec,  $4.54 \times 10^{-6}$  cm<sup>2</sup>/sec,  $4.69 \times 10^{-6}$  cm<sup>2</sup>/sec,  $4.58 \times 10^{-6}$  cm<sup>2</sup>/sec respectively. Similarly value of  $C_{r2,80}$  is  $6.3 \times 10^{-5}$  cm<sup>2</sup>/sec,  $5.6 \times 10^{-5}$  cm<sup>2</sup>/sec,  $5.8 \times 10^{-5}$  cm<sup>2</sup>/sec,  $5.1 \times 10^{-5}$  cm<sup>2</sup>/sec while for 160kPa it was found to be  $5 \times 10^{-5}$  cm<sup>2</sup>/sec,  $4.44 \times 10^{-5}$  cm<sup>2</sup>/sec,  $4.5 \times 10^{-5}$  cm<sup>2</sup>/sec,  $4 \times 10^{-5}$  cm<sup>2</sup>/sec respectively. Similarly value of  $C_{r3,80}$  is  $1.15 \times 10^{-4}$  cm<sup>2</sup>/sec,  $1.06 \times 10^{-4}$  cm<sup>2</sup>/sec,  $1.06 \times 10^{-4}$  cm<sup>2</sup>/sec,  $9.7 \times 10^{-5}$  cm<sup>2</sup>/sec while for 160kPa it was found to be  $9.86 \times 10^{-5}$  cm<sup>2</sup>/sec,  $8.67 \times 10^{-5}$  cm<sup>2</sup>/sec,  $9.02 \times 10^{-5}$  cm<sup>2</sup>/sec,  $8.09 \times 10^{-5}$  cm<sup>2</sup>/sec respectively.
- Looking to given plots and values it is clear that, out of all four geometrical shapes of 'n' 11.04, CSSD shows more rate of consolidation both at low and high pressures at all three radial points. The BSSD is better in compare to PSSD for all pressures. TSSD is not much efficient in dissipation pore water pressure because of smaller diameter and clogging problems. Out of all shapes of drains CSSD shows more rate of consolidation both at low and high pressures in compare to other shape of drains. So it can be said that CSSD shows more inter-rate of dissipation of excess hydrostatic pore water pressure even at following pressures in compare to other shape of drains for same 'n' value. At higher pressures though dissipation is fast at nearest radial point 'r1' during initial time but it ceases as consolidation proceeds and so middle radial point is taken for comparison as no much variation is observed in value of  $C_r$  at all pressures. This is true for all shapes of sand drains.

### **Discussion:**

- The general pattern of  $C_r$  vs. pressure for any shape of drain indicates that it increases with pressure, but at 50% consolidation variation in  $C_r$  value is

higher compare to 80% consolidation. In pore pressure measurement under lighter loading there is variation in  $C_r$  value, but constancy is maintained after 50kPa for any shape of drain.

- Average  $C_r$  value for BSSD remain in between CSSD and PSSD. The lowest average value of TSSD signifies inefficiency of the drain geometry compare to geometry of other drains. The nature of plot is almost nearly horizontal as load increases, variation in  $C_r$  value is observed in case of PSSD is because of hindrance offered by right angles of drain itself in dissipation of pore water pressure and also simultaneous effect of load and overburden disturbs the shape (deformation of layers) and thus it further reduces discharge thus reducing pore pressure dissipation and compressibility of soft mass. Though at one stage it seems that PSSD having more exposure for pore water to drain out, but there is colliding of water particle at right angles of drain whose action is further dismantling shape of drain and reducing discharge. In case of TSSD though individual limbs are at 120 degree to each other, but sharp corners (v-shape) creates hindrance in dissipation of pore water pressure and also some water particle have to travel longer path (longer side of limb) which also further reduces dissipation rate of TSSD. The shape of TSSD also gets disturbed one because of slenderness of limb and second is twisting action of drain by radial flow of pore water under load.
- CSSD shape acting as vertical cylinder and having both advantage of circular arc shape for every water particle to dissipate out in radial direction, there is no hindrance for pore water to drain out and as well as deformation of drain is compatible with deformation of soil mass, though some bulging action is observed at mid portion of drain under higher loads.

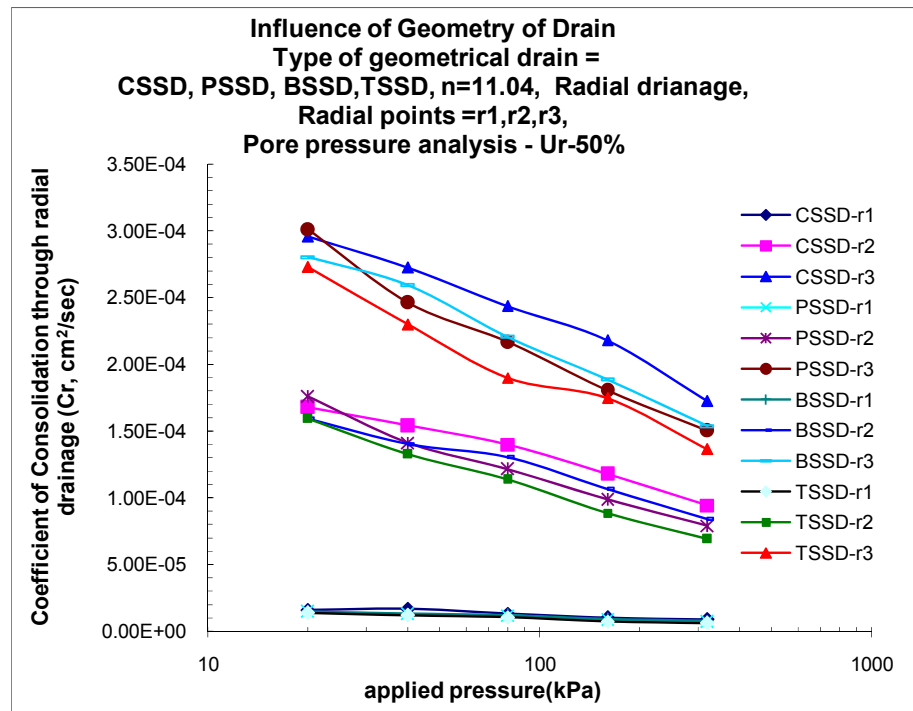


**Fig. 6.284:** Comparison of  $C_r$  vs. applied pressure for geometrical drains at  $U_r=50\%$  at radial points  $r_1$ ,  $r_2$  and  $r_3$

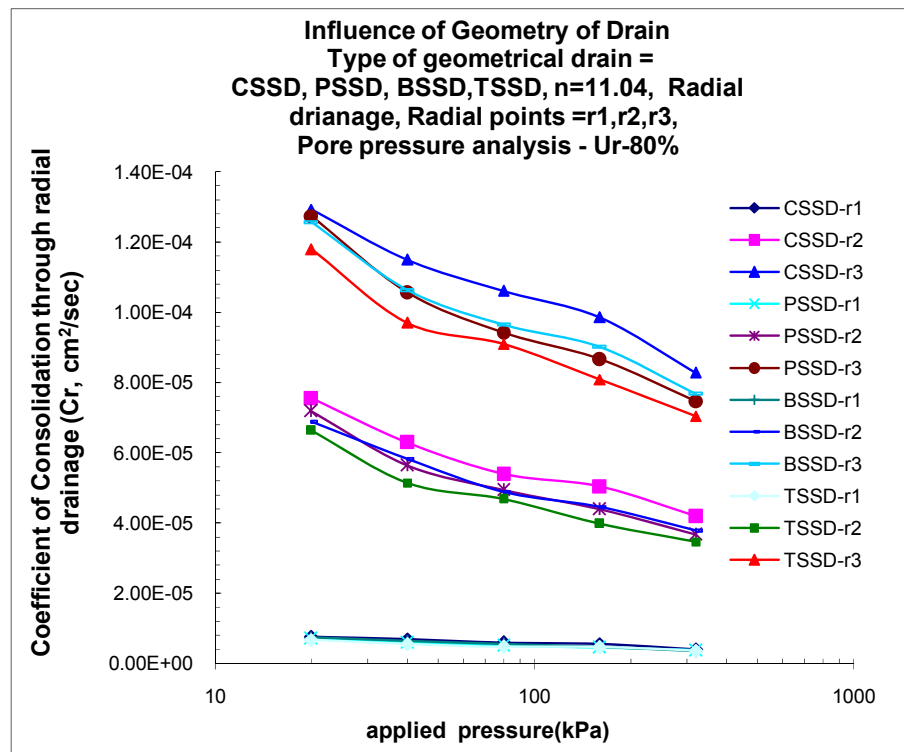


**Fig. 6.285:** Comparison of  $C_r$  vs. applied pressure for geometrical drains at  $U_r=80\%$  at radial points  $r_1$ ,  $r_2$  and  $r_3$

#### 4) Void ratio (e) vs. Applied pressure: Figures 6.286 to 6.287

**a) Settlement analysis:-** Fig.6.286 to Fig.6.287 shows a characteristic curve of normally consolidation soil for four geometrical sand drains viz. CSSD, BSSD, PSSD, TSSD of 'n' value equal to 11.04 and comparison of average compression index values for various shapes. The average value of coefficient of compression ( $C_c$ ) for various drain materials is 0.216 for CSSD, 0.266 for BSSD, 0.307 for PSSD, 0.324 for TSSD. From the above plots it is observed that lowest void ratio is achieved in case of CSSD and subsequently at BSSD and PSSD. From this it can be said that CSSD equal to 11.04 is most optimum shape of drain with maximum efficiency to compress soft soil.

#### Discussion:

- It is observed that for CSSD lower  $C_c$  value is obtained compared to other geometry of sand drains. It signifies that because of low rate of dissipation in other shapes of drains the magnitude of compressibility increases at particular period of interval. This behavior is similar for all drains.  $C_c$  value determined individually between two pressures to know efficacy of shape at various intermediate pressure levels for CSSD, BSSD, PSSD, and TSSD for  $n=11.04$ , out of which lowest values obtained are 0.161, 0.241, 0.271, and 0.282 respectively. Under no geodrain condition the value of  $C_c$  is 0.42.
- There is no much variation of Compression index with shape of drain, though the rate of drainage for a particular static loading seems to be faster in CSSD compared to others.
- Circular shape sand drain experience least interference of dissipation of radial flow compare to band drain, tripod shape and plus shape drain. This more and easy dissipation of pore pressure is because of the higher gradient of water flow through soil structure which has been cultivated under the load. Under lighter load because of the structural resistance it shows convex upward curve while after critical zone the particle orientation leading to parallel alignment exhibit higher slope of the curve (e vs.  $\log p$ ) tending to final consolidated soil mass having face to face bond.

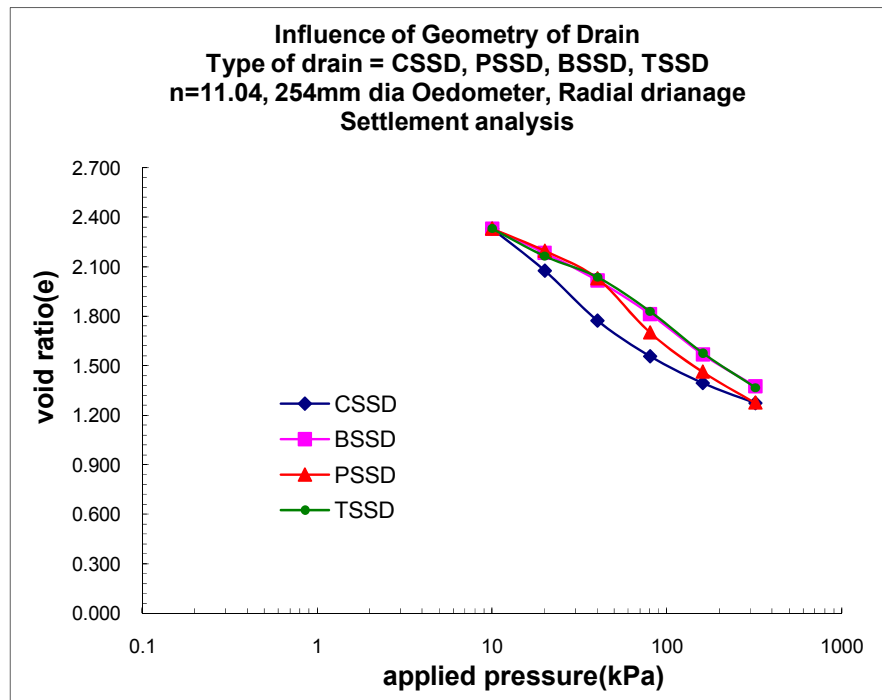


**Fig. 6.286:** Comparison of void ratio (e) vs. applied pressure for various geometrical shape sand drains

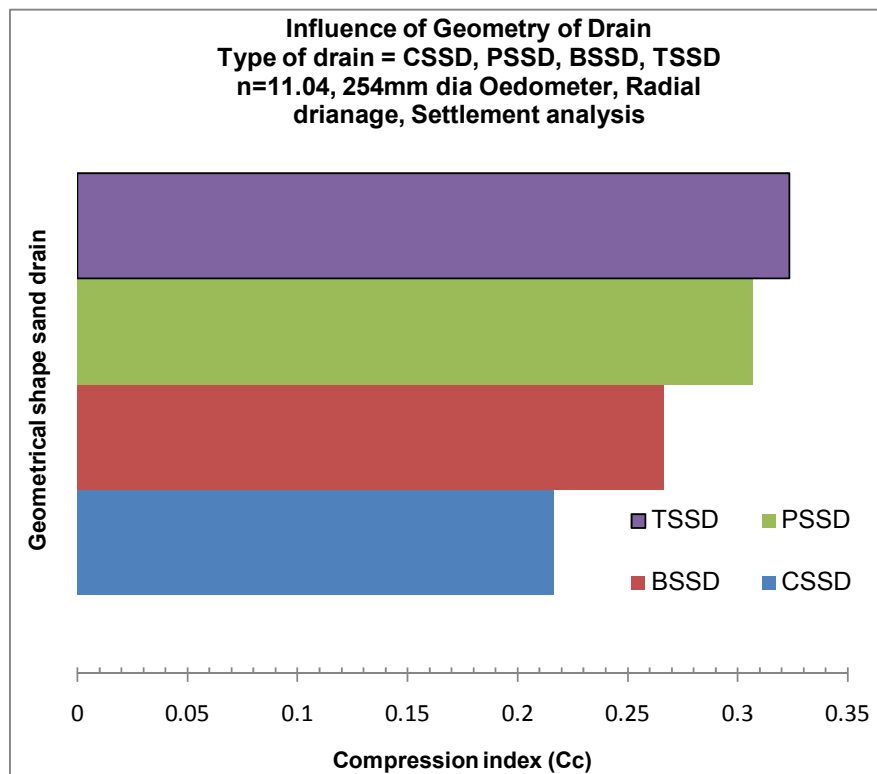


**Fig. 6.287:** Comparison of Compression index (Cc) vs. Geometrical shape sand drains of 'n'11.04

## 5) Coefficient of horizontal permeability ( $k_h$ ) vs. Applied pressure: Figures 6.288 to 6.292

**a) Settlement analysis-** Fig.6.288 shows the plot of coefficient of horizontal permeability ( $k_h$ ) versus applied pressure for various shapes of sand drains i.e. Circular shape sand drain (CSSD), Band shape sand drain (BSSD), Plus shape sand drain (PSSD), Tripod shape sand drain (TSSD) for all applied pressures. Here for analysis time required for 50% ( $t_{50}$ ) consolidation and time required for 80% ( $t_{80}$ ) consolidation are taken for all pressures and for shapes of drains to get  $k_{h,50}$  and  $k_{h,80}$ .

- The horizontal permeability ( $k_{h,50}$ ) obtained by settlement decreases with increase in the pressure for almost all shapes of drains for  $n=11.04$ . The value of horizontal permeability ( $k_{h,50}$ ) at 160KPa for CSSD, PSSD, BSSD, TSSD for 'n' equal to 11.04 is found as  $7.97 \times 10^{-8}$  cm/sec,  $6.03 \times 10^{-8}$  cm/sec,  $7.09 \times 10^{-8}$  cm/sec,  $4.85 \times 10^{-8}$  cm/sec respectively. Similarly value of  $k_{h,80}$  is found as  $3.25 \times 10^{-8}$  cm/sec,  $3.04 \times 10^{-8}$  cm/sec,  $3.22 \times 10^{-8}$  cm/sec,  $2.73 \times 10^{-8}$  cm/sec respectively.
- With comparison of  $k_{h,50}$  values with different shapes of drains it is found that for CSSD, the  $k_{h,50}$  of  $n=11.04$  is 11%, 24%, 39% higher in compared to BSSD, PSSD, TSSD at 160kPa pressure, while  $k_{h,50}$  of BSSD is 15% and 31% higher in compared to PSSD and TSSD at 160kPa pressure.
- With comparison of  $k_{h,80}$  values with different shapes of drains it is found that for CSSD, the  $k_{h,80}$  of  $n=11.04$  is 1%, 6%, 16% higher in compared to BSSD, PSSD, TSSD at 160kPa pressure, while  $k_{h,80}$  of BSSD is 5% and 15% higher in compared to PSSD and TSSD at 160kPa pressure.
- So from the above analysis it can be said that CSSD of 'n' equal to 11.04 is better in compare to BSSD, PSSD, TSSD for almost all pressures.



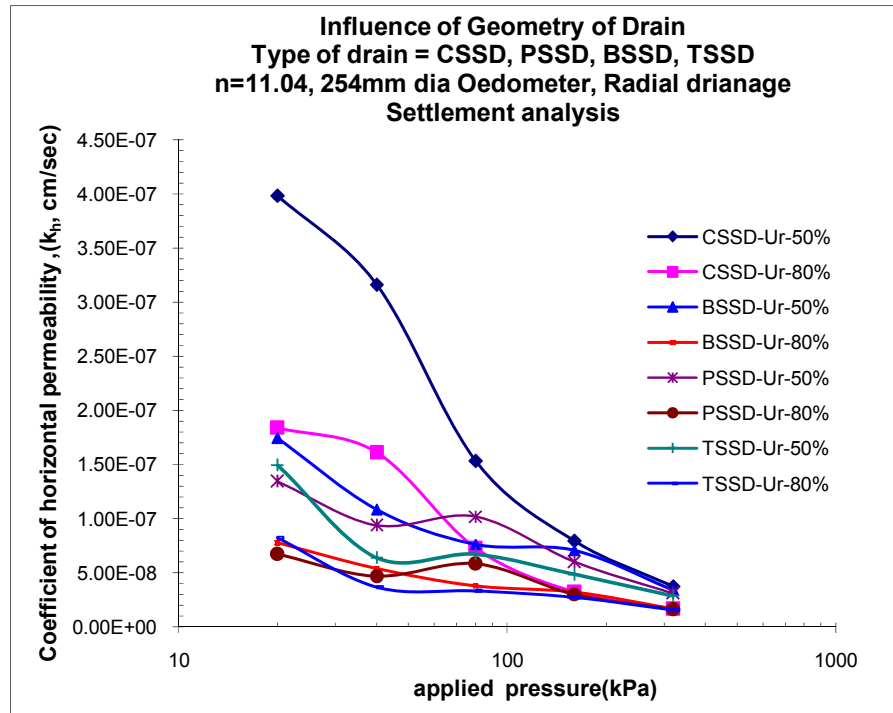


**Fig. 6.288:** Comparison of coefficient of horizontal permeability( $k_h$ ) against applied pressure for geometrical drains at Ur-50% and Ur-80%

**b) Pore pressure analysis-** Fig.6.289 to Fig.6.292 shows the plots of coefficient of horizontal permeability ( $k_h$ ) versus applied pressure for various 'n' values of 11.04 for various geometrical shapes of sand drains like CSSD, BSSD, PSSD & TSSD for three radial points' r1, r2 & r3. Here for analysis time required for 50% ( $t_{50}$ ) consolidation and time required for 80% ( $t_{80}$ ) consolidation are taken for all pressures and all 'n' values to get  $k_{h,50}$  and  $k_{h,80}$ . The horizontal permeability at three different radial points' r1, r2 and r3 for 50% consolidation obtained by pore pressure readings decreases with increase in the pressure.

- For CSSD, BSSD, PSSD, TSSD as geometrical drains at 160 kPa pressure for  $n=11.04$  at nearest radial point (r1),  $k_{h1,50}$  is  $9.09 \times 10^{-10}$  cm/sec,  $1.16 \times 10^{-9}$  cm/sec,  $1.07 \times 10^{-9}$  cm/sec,  $9.71 \times 10^{-10}$  cm/sec while  $k_{h1,80}$  for 160 kPa it is  $4.85 \times 10^{-10}$  cm/sec,  $5.94 \times 10^{-10}$  cm/sec,  $5.63 \times 10^{-10}$  cm/sec,  $5.93 \times 10^{-10}$  cm/sec respectively. Similarly at middle radial point (r2),  $k_{h2,50}$  is  $1.04 \times 10^{-8}$  cm/sec,  $1.35 \times 10^{-8}$  cm/sec,  $1.22 \times 10^{-8}$  cm/sec,  $1.15 \times 10^{-8}$  cm/sec while  $k_{h2,80}$  for 160 kPa it is  $4.44 \times 10^{-9}$  cm/sec,  $5.63 \times 10^{-9}$  cm/sec.

cm/sec,  $5.44 \times 10^{-9}$ cm/sec,  $5.16 \times 10^{-9}$ cm/sec respectively. Similarly at outer radial point (r3),  $k_{h3,50}$  is  $1.92 \times 10^{-8}$ cm/sec,  $2.39 \times 10^{-8}$  cm/sec,  $2.24 \times 10^{-8}$  cm/sec,  $2.26 \times 10^{-8}$ cm/sec while  $k_{h3,80}$  for 160KPa it is  $8.69 \times 10^{-9}$ cm/sec,  $1.14 \times 10^{-8}$  cm/sec,  $1.07 \times 10^{-8}$ cm/sec,  $1.05 \times 10^{-8}$ cm/sec respectively.

- Comparing CSSD values of various shapes of sand drains it is observed that 'n' equal to 11.04 for 160kPa for  $k_{h1,50}$  is -17.6%,-27.8%,-6.8% higher in compare to BSSD, PSSD, TSSD while  $k_{h1,80}$  is -16.1%,-22.5%,-22.3% higher. Similarly  $k_{h2,50}$  is -17.6%,-29.6%,-10.1% higher in compare to BSSD,PSSD,TSSD while  $k_{h2,80}$  is -22.5%, -26.9%, -16.2% higher. While  $k_{h3,50}$  is -16.4%, -24.2%, -17.7% higher in compare to BSSD, PSSD,TSSD while  $k_{h3,80}$  is -23.5%, -31.3%, -20.5% higher respectively.
- Comparing BSSD values of various shapes of sand drains it is observed that 'n' equal to 11.04 for 160kPa for  $k_{h1,50}$  is 8%, 16.4%, higher in compare to PSSD, TSSD while  $k_{h1,80}$  is 5.3%, 0.2%, higher. Similarly  $k_{h2,50}$  is 9.2%, 15% higher in compare to PSSD, TSSD while  $k_{h2,80}$  is 3.4%, 8.4% higher. While  $k_{h3,50}$  is 6.3%, 5.2% higher in compare to PSSD, TSSD while  $k_{h3,80}$  is 5.9%, 8.2% higher respectively.
- Comparing PSSD values of various shapes of sand drains it is observed that 'n' equal to 11.04 for 160kPa for  $k_{h1,50}$  is 9.2%, higher in compare to TSSD while  $k_{h1,80}$  is -5.3%, higher. Similarly  $k_{h2,50}$  is 6.4% higher in compare to TSSD while  $k_{h2,80}$  is 5.2% higher. While  $k_{h3,50}$  is -1.1% higher in compare to TSSD while  $k_{h3,80}$  is 5.2% higher respectively
- So from the above analysis it can be said that CSSD of 'n' equal to 11.04 is better in compare to BSSD, PSSD, TSSD for almost all pressures. It is also concluded that coefficient of permeability ( $k_h$ ) for CSSD is highest in compare to other geometrical sand drains for  $n=11.04$ . Also BSSD is more efficient in compare to PSSD & TSSD while PSSD is more efficient in compare to TSSD for all pressures.

### **Discussion:**

- From settlement analysis it concludes that  $n=11.04$  for 50% consolidation shows 274% higher  $k_h$  value compare to any shape of sand drain under light

loading and 36% under constructional loading. Similarly for 80% consolidation shows 259% higher  $k_h$  value compare to any shape of sand drain under light loading and 9% under constructional loading.

- From pore pressure analysis for mid plane radial point  $r_2$  it concludes that CSSD of  $n=11.04$  for 50% consolidation shows 143% higher  $k_h$  value compare to any shape of sand drain under light loading and 15% lower under constructional loading. Similarly for 80% consolidation it shows 149% higher  $k_h$  value under light loading and 18% lower under constructional loading.

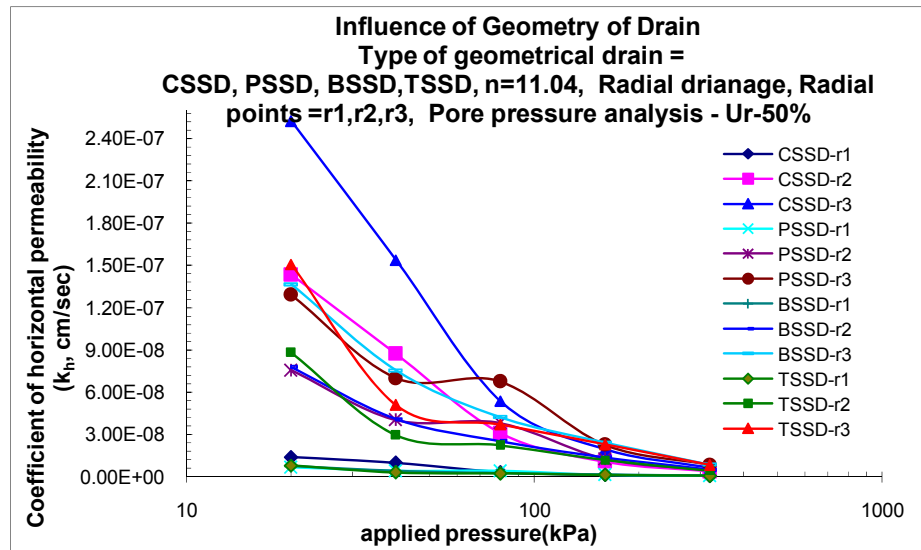


**Fig. 6.289:** Comparison of  $k_h$  vs. applied pressure for geometrical sand drains for Ur-50% at radial points  $r_1$ ,  $r_2$  and  $r_3$

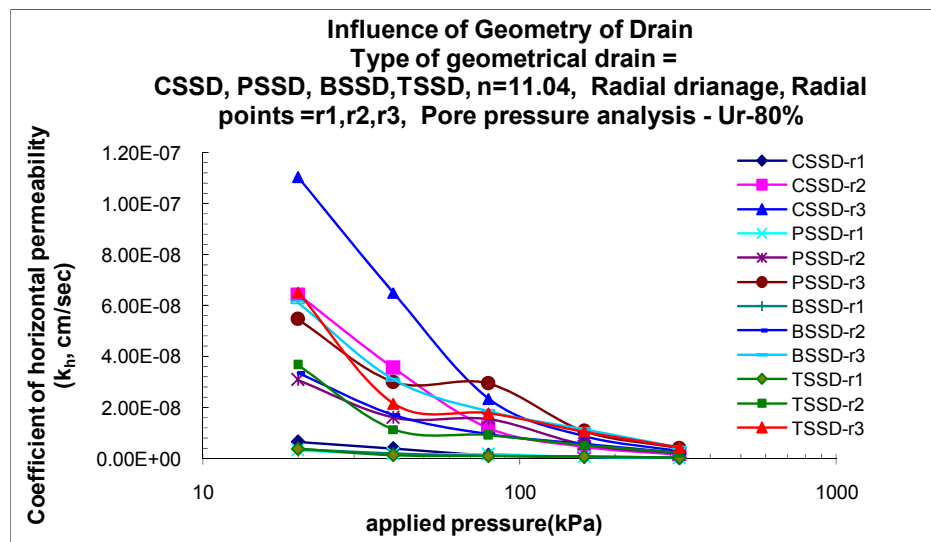


**Fig. 6.290:** Comparison of  $k_h$  vs. applied pressure for geometrical sand drains for Ur-80% at radial points  $r_1$ ,  $r_2$  and  $r_3$

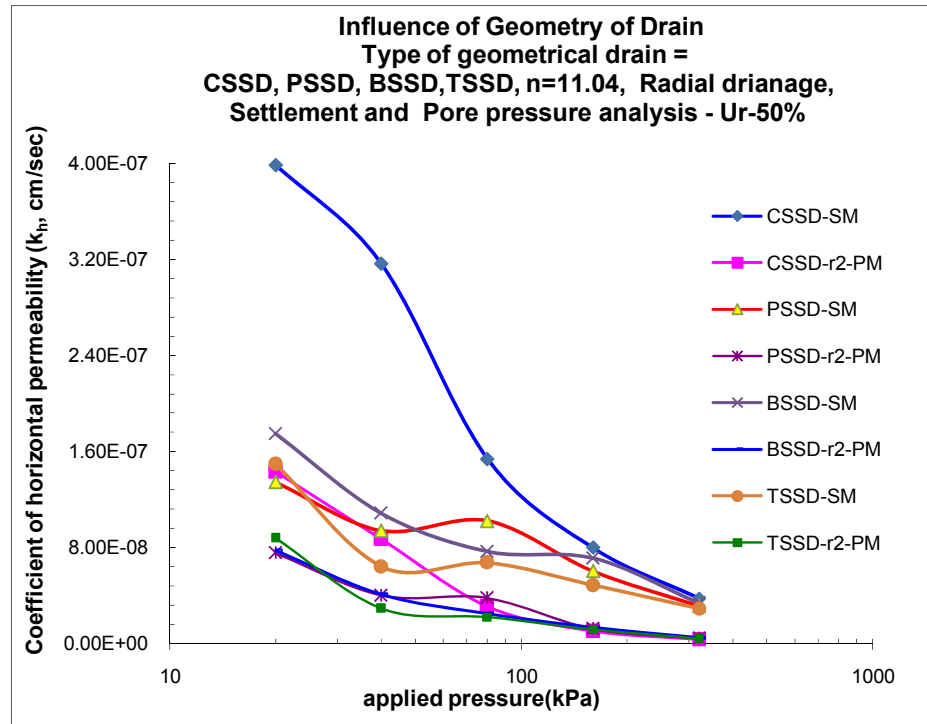


**Fig. 6.291:** Comparison of  $k_h$  vs. applied pressure for geometrical sand drains for Ur-50% based on settlement and pore pressure analysis

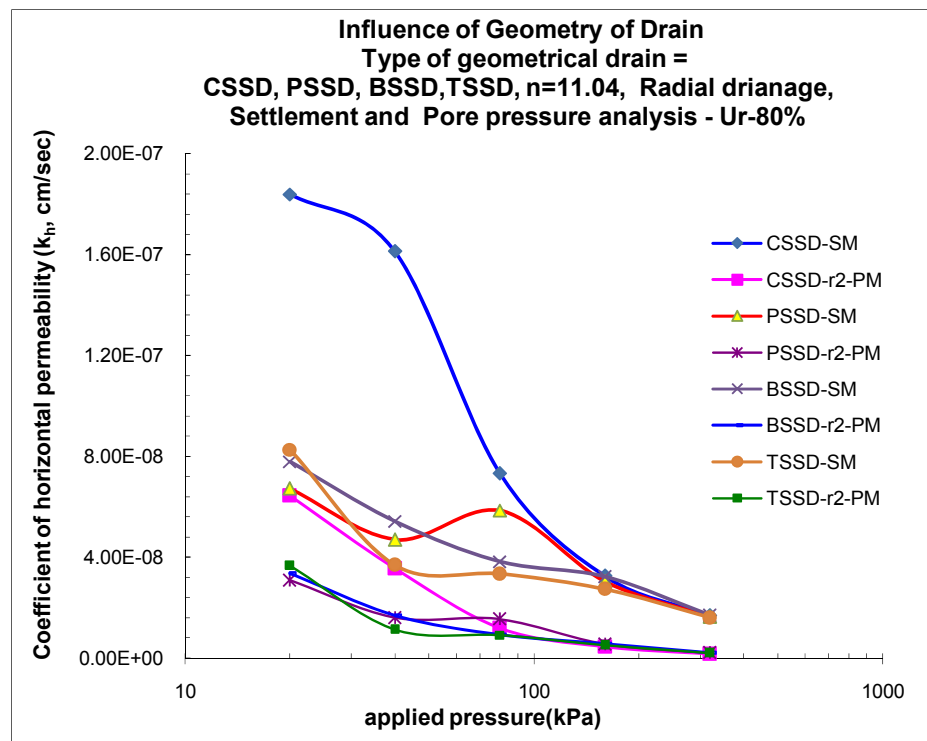


**Fig. 6.292:** Comparison of  $k_h$  vs. applied pressure for geometrical sand drains for Ur-80% based on settlement and pore pressure analysis

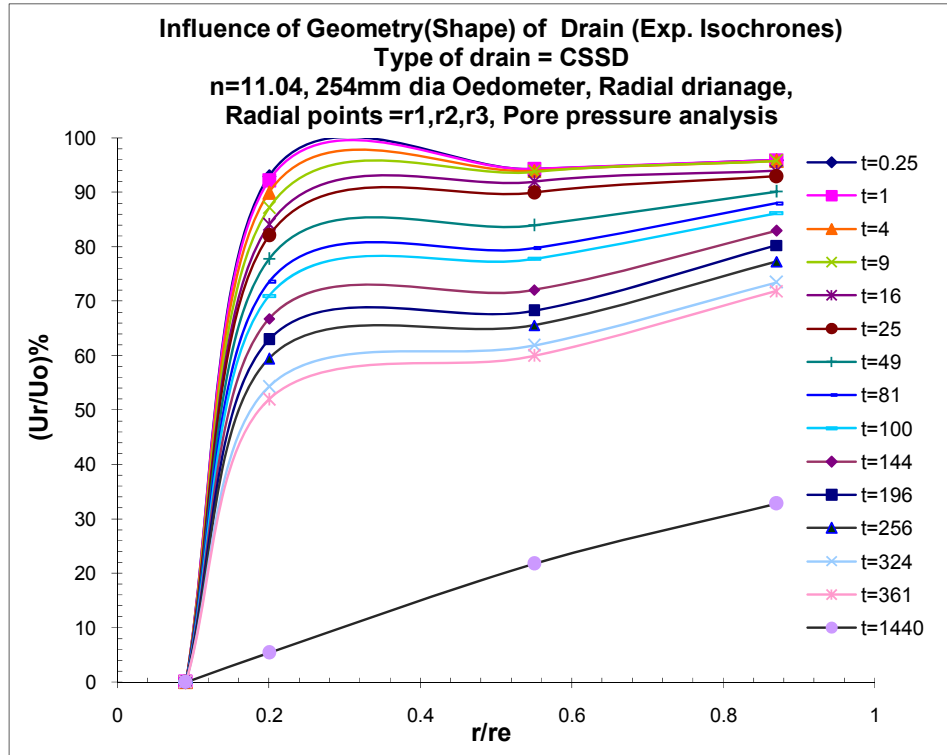
## 6) Isochrones: Figures 6.293 to 6.300

**a) Pore pressure analysis:** Fig.6.293 to Fig.6.300 shows the plots of isochrones with respect to time and comparison of isochrones with respect to Time factor ( $T_r$ ) for various geometrical shape sand drains viz. circular shape sand drain (CSSD), Plus shape sand drain (PSSD), Band shape sand drain (BSSD), Tripod shape sand drain (TSSD) of 'n' value 11.04. Comparing initial slope of isochrones for various geometrical sand drains against ratio of radial distance it interprets that CSSD of 'n' 11.04 shows more rate of dissipation at any time (initial linear portion of graph) compare to PSSD, BSSD, and TSSD for any value of time. While BSSD shows more inter-rate of dissipation of pore water pressure compare to PSSD and TSSD for any time both under light loading and heavy loading. Also it is observed that PSSD shows better rate of dissipation at all three radial points  $r_1$ ,  $r_2$  and  $r_3$  at all applied pressures compare to TSSD. Almost for all geometrical sand drain nature of isochrones were similar and presenting clear picture of dissipation of pore water pressure at various sequences of consolidation. Comparing theoretical and experimental isochrones using proposed theory it interprets that experimental isochrones matches very well with theoretical isochrones for various time factors ( $T_r$ ). This is well observed for all geometrical sand drain viz. CSSD, PSSD, BSSD and TSSD at all pressures.

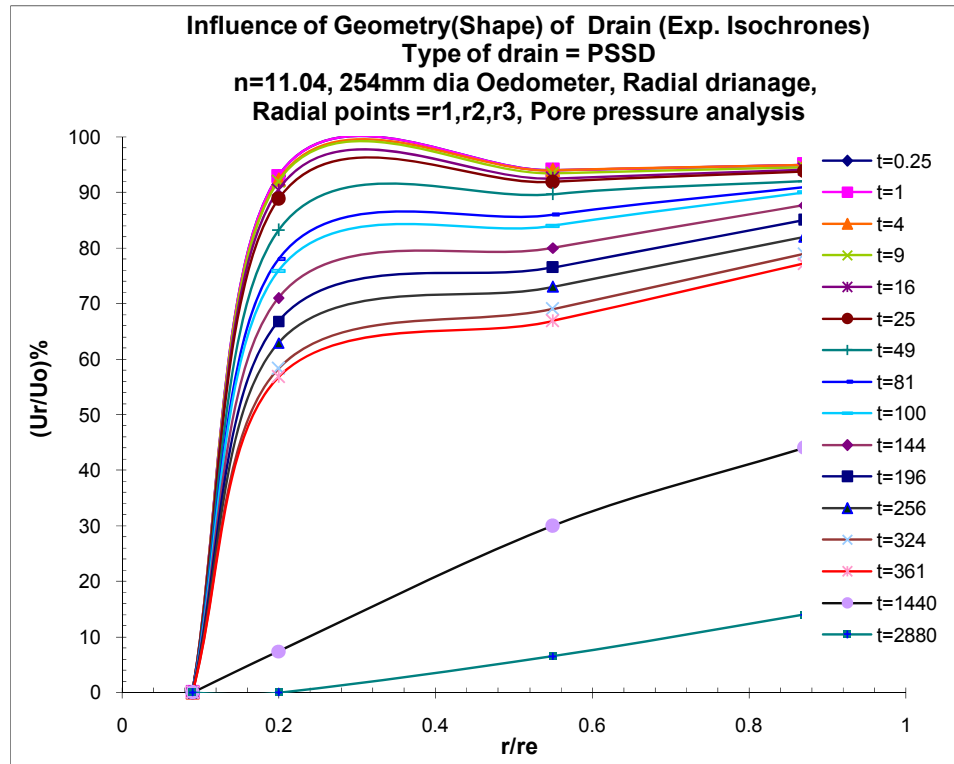
### Discussion:

- From the consolidation ratio vs. radius of influence for various  $T_r$  values reveals that sequence of consolidation for CSSD of  $n=11.04$  at any radius of influence seems to be effective compare to other geometry of drains. Comparing isochrones of all four shapes it is concluded that CSSD is more effective compare to others, while BSSD is superior compare to PSSD & TSSD for same drain material. Trajectory of isochrones for CSSD lies above the BSSD, PSSD, TSSD for both light and constructional loading. Overall TSSD is in-effective in increasing rate of compressibility and dissipation of pore water pressure.

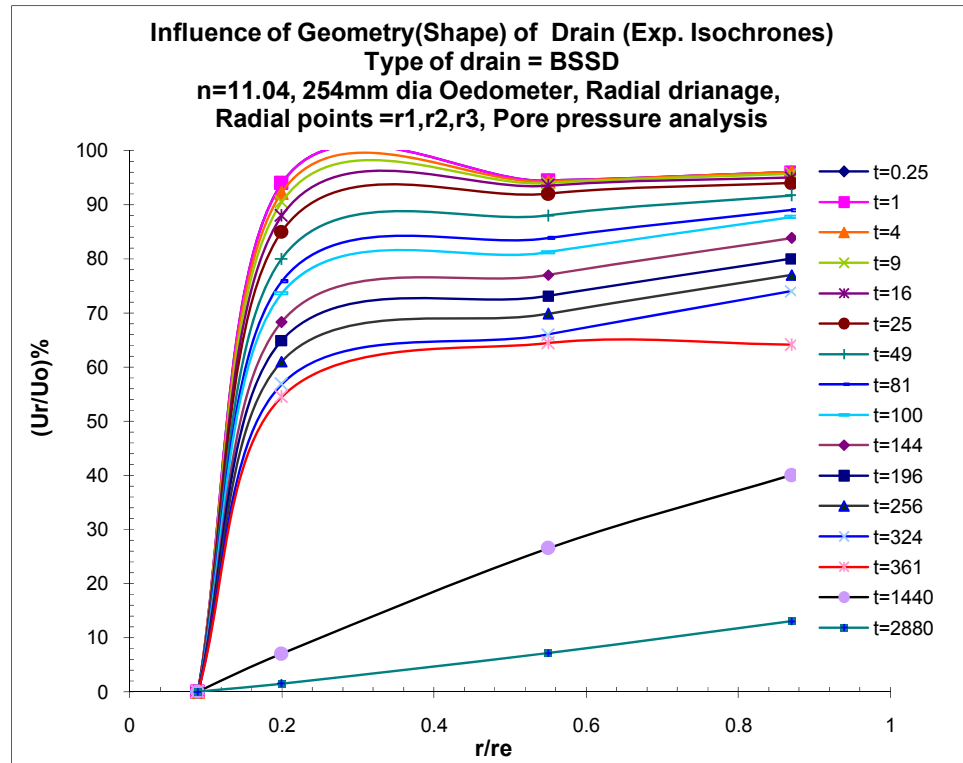
### **(i) Isochrones with respect to time (t):**



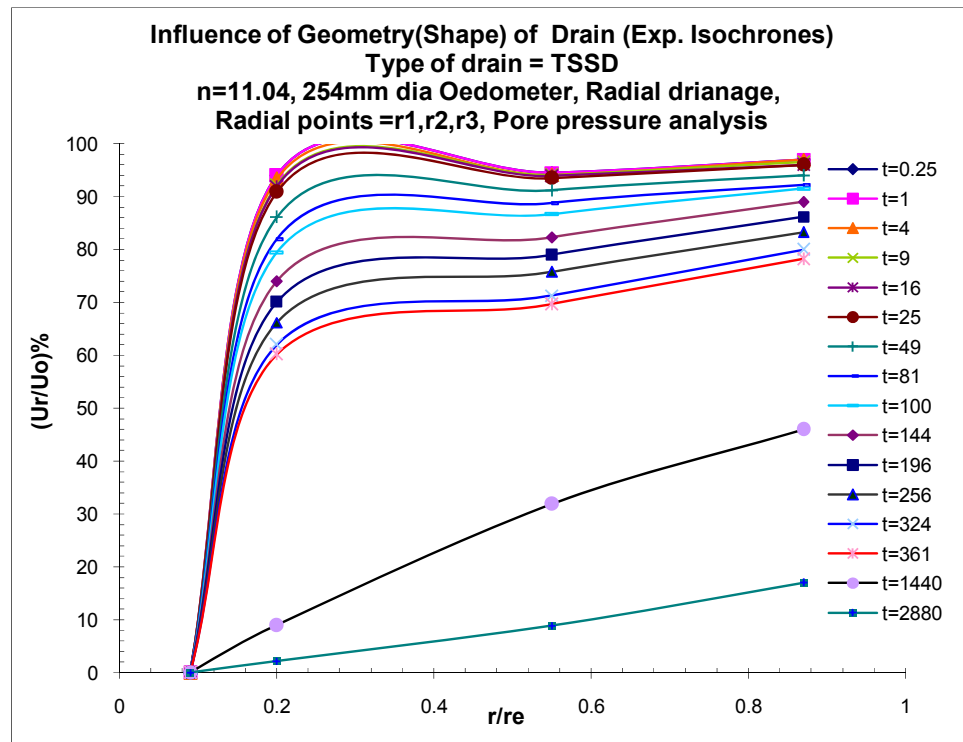
**Fig. 6.293:** Dissipation of hydrostatic excess pore water pressure ( $U_r/U_o$ ) vs. ratio of radial distance ( $r/r_e$ ) with respect to time for CSSD at 160kPa



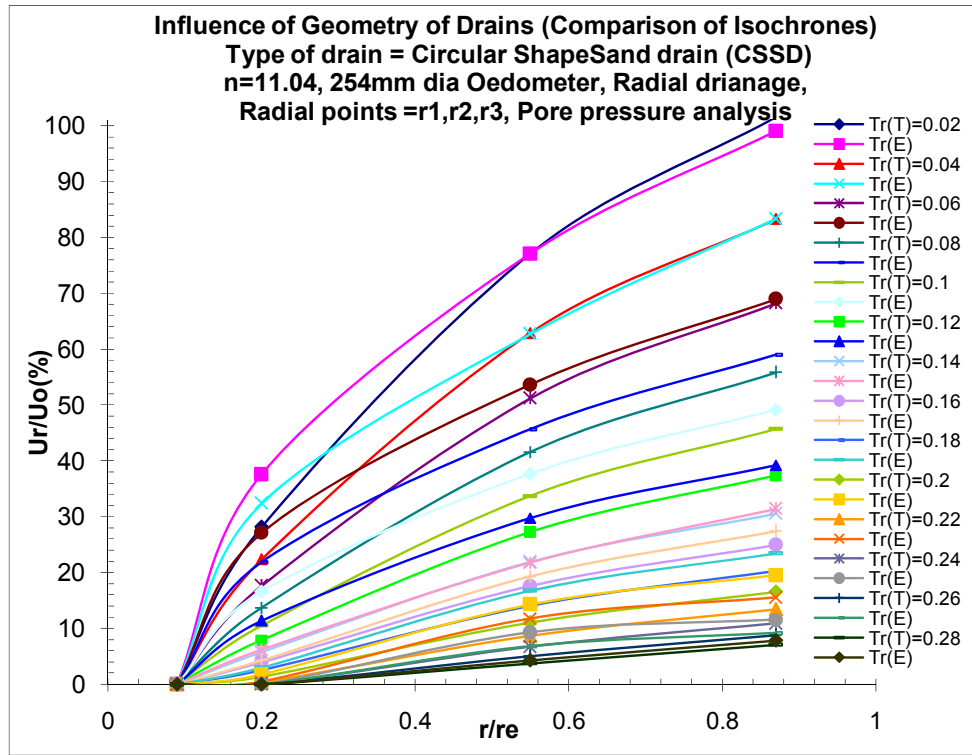
**Fig. 6.294:** Dissipation of hydrostatic excess pore water pressure ( $U_r/U_o$ ) vs. ratio of radial distance ( $r/r_e$ ) with respect to time for PSSD at 160kPa



**Fig. 6.295:** Dissipation of hydrostatic excess pore water pressure ( $U_r/U_o$ ) vs. ratio of radial distance ( $r/r_e$ ) with respect to time for BSSD at 160kPa



**Fig. 6.296:** Dissipation of hydrostatic excess pore water pressure ( $U_r/U_o$ ) vs. ratio of radial distance ( $r/r_e$ ) with respect to time for TSSD at 160kPa

(ii) Isochrones with respect to Time factor ( $Tr$ ):

**Fig. 6.297:** Comparison of theoretical isochrones and experimental isochrones with respect to time factor ( $Tr$ ) for CSSD at 160kPa pressure

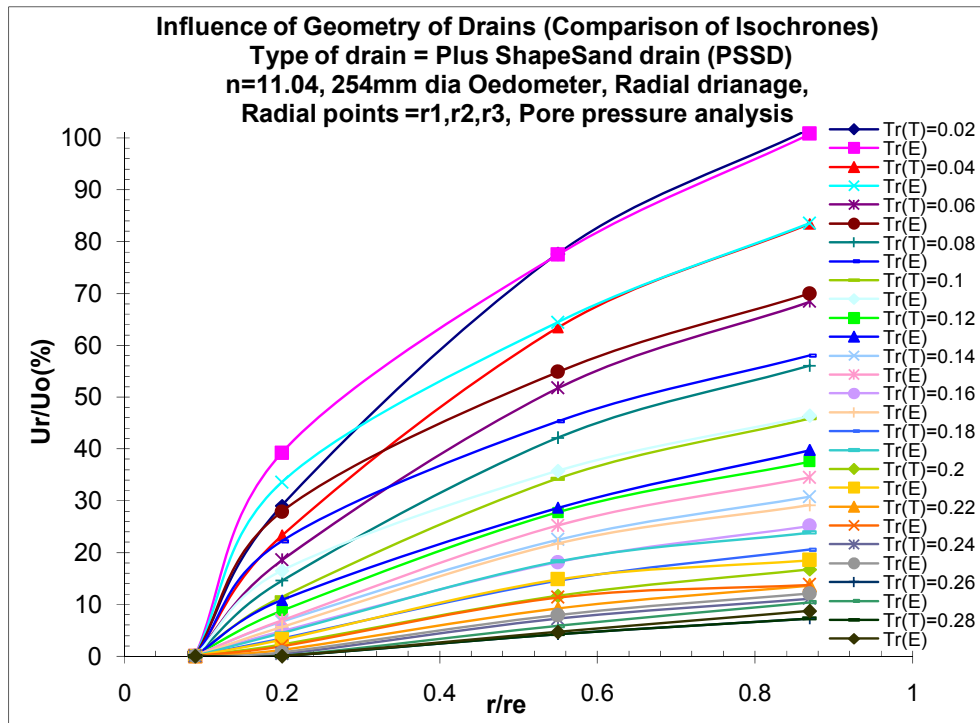


**Fig. 6.298:** Comparison of theoretical isochrones and experimental isochrones with respect to time factor ( $Tr$ ) for PSSD at 160kPa pressure



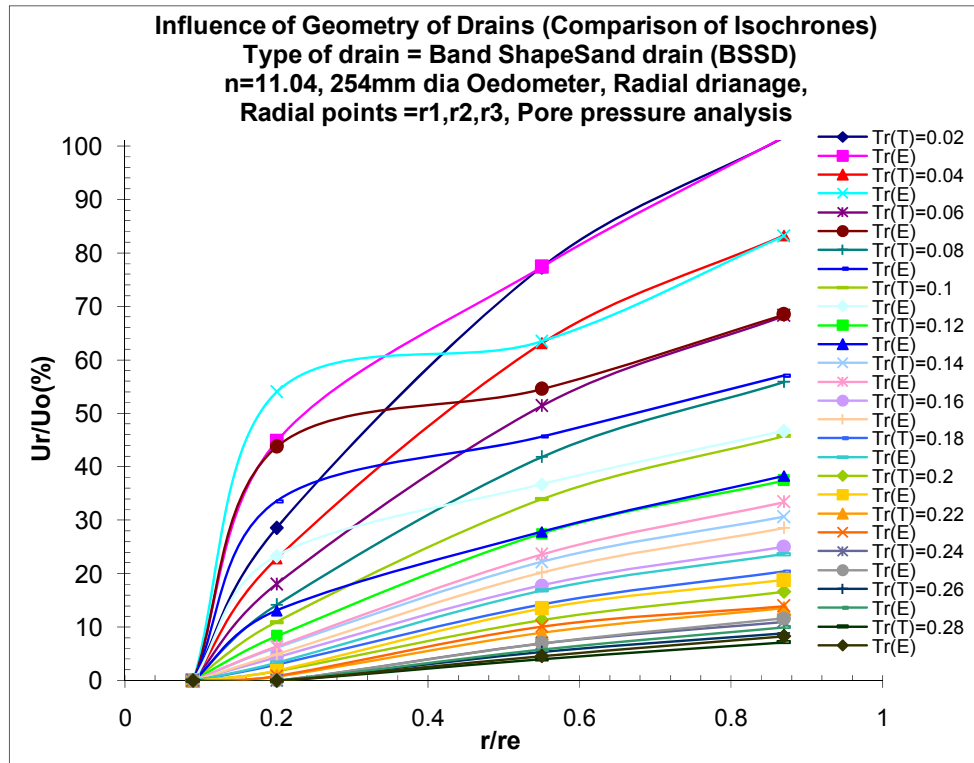


**Fig. 6.299:** Comparison of theoretical isochrones and experimental isochrones with respect to time factor ( $Tr$ ) for BSSD at 160kPa pressure

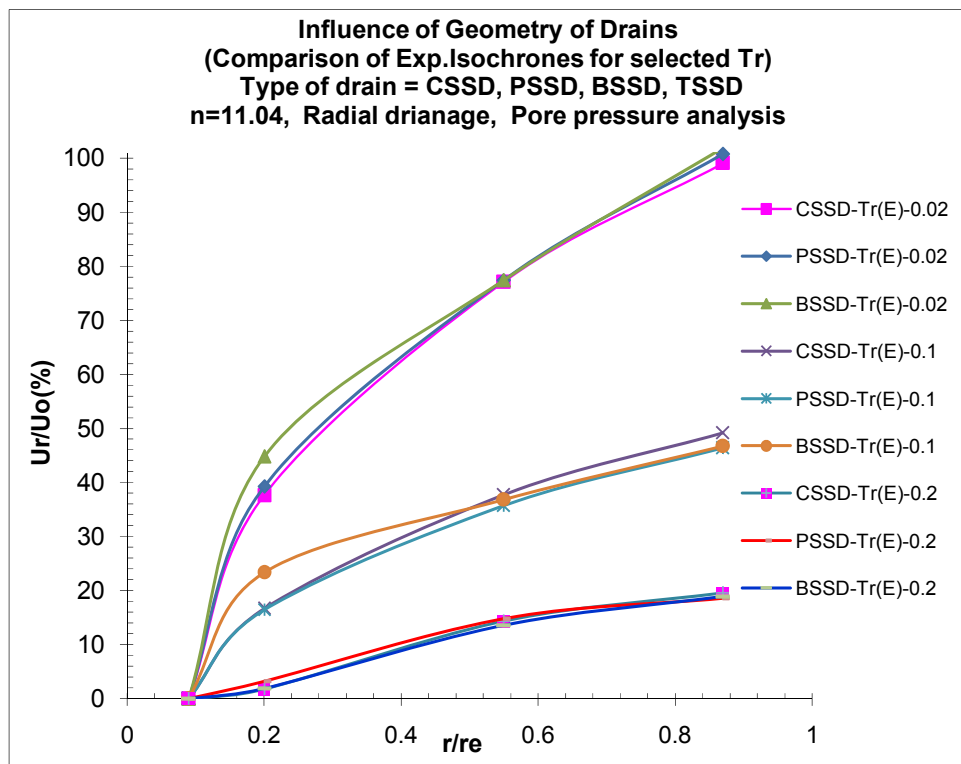


**Fig. 6.300:** Comparison of experimental isochrones with respect to selected time factor ( $Tr$ ) for geometrical sand drains at 160kPa pressure

## 7) Degree of consolidation ( $U_r$ ) vs. Time factor ( $T_r$ ): Figures 6.301 to 6.317

**a) Settlement analysis-** Fig.6.301 to Fig.6.308 shows the comparative plots of various geometrical sand drains of 'n' value of 11.04 for degree of consolidation ( $U_r$ ) versus time factor ( $T_r$ ) for various shape drains like CSSD, BSSD, PSSD & TSSD. For comparison between theoretical and experimental values two applied pressure of 40kPa and 160kPa are selected. The lumped parameter ' $\lambda$ ' is appropriately fitted for each geometrical sand drain with respect to time factors so as to study the influence of geometry (shape) on vertical drain performance. Here it is determined that for four shapes of sand drains of 'n' values of 11.04, for CSSD the lumped parameter ' $\lambda$ ' is equal to -0.125 fits appropriately. Similarly it is determined that for BSSD the lumped parameter ' $\lambda$ ' is equal to -0.12 fits respectively. Similarly it is determined that for PSSD the lumped parameter ' $\lambda$ ' is equal to -0.11 fits respectively, while for TSSD the lumped parameter ' $\lambda$ ' is equal to -0.1 fits respectively. It is observed that ' $\lambda$ ' value of -0.125 is having maximum efficiency and as ' $\lambda$ ' value decreases shape of drain decreases. It is observed from the above graphs that experimental results almost matches with theoretical results and this is true for all geometrical sand drains and for all applied pressures. Table shows the value of lumped parameter ' $\lambda$ ' fitted to each drain material.

| Sr.No. | Type of Geometrical Drain        | 'n' value | Lump parameter ' $\lambda$ ' |
|--------|----------------------------------|-----------|------------------------------|
| 1.     | Circular shape sand drain (CSSD) | 11.04     | -0.125                       |
| 2.     | Band shape sand drain (BSSD)     | 11.04     | -0.12                        |
| 3.     | Plus shape sand drain (PSSD)     | 11.04     | -0.11                        |
| 4.     | Tripod shape sand drain (TSSD)   | 11.04     | -0.1                         |

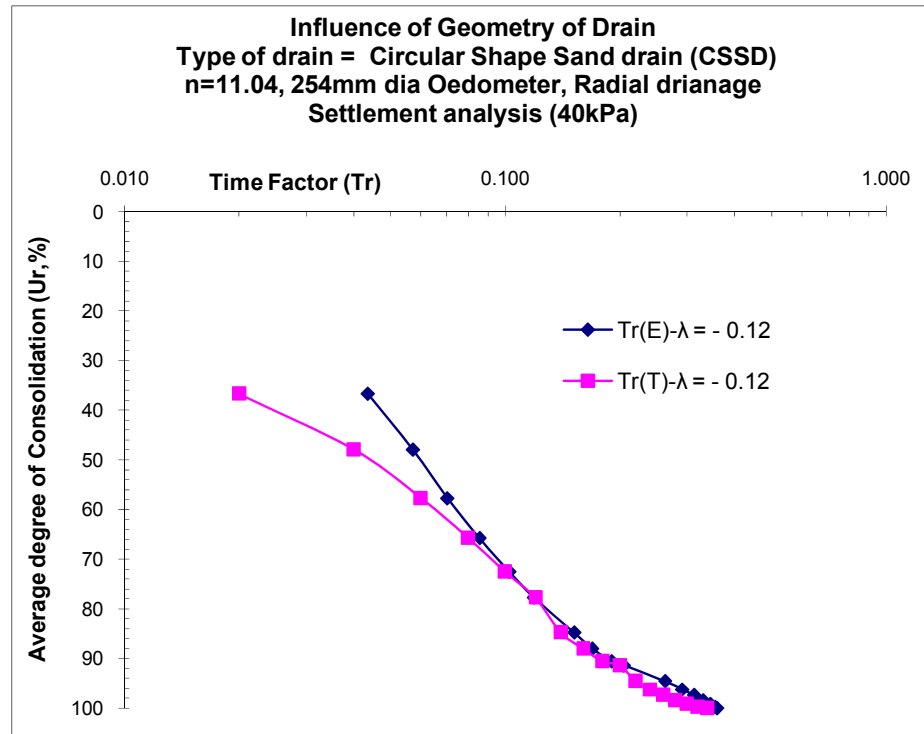


**Fig. 6.301:** Comparison of theoretical and experimental average degree of consolidation ( $U_r$ ) against Time factor ( $Tr$ ) for CSSD at 40kPa pressure

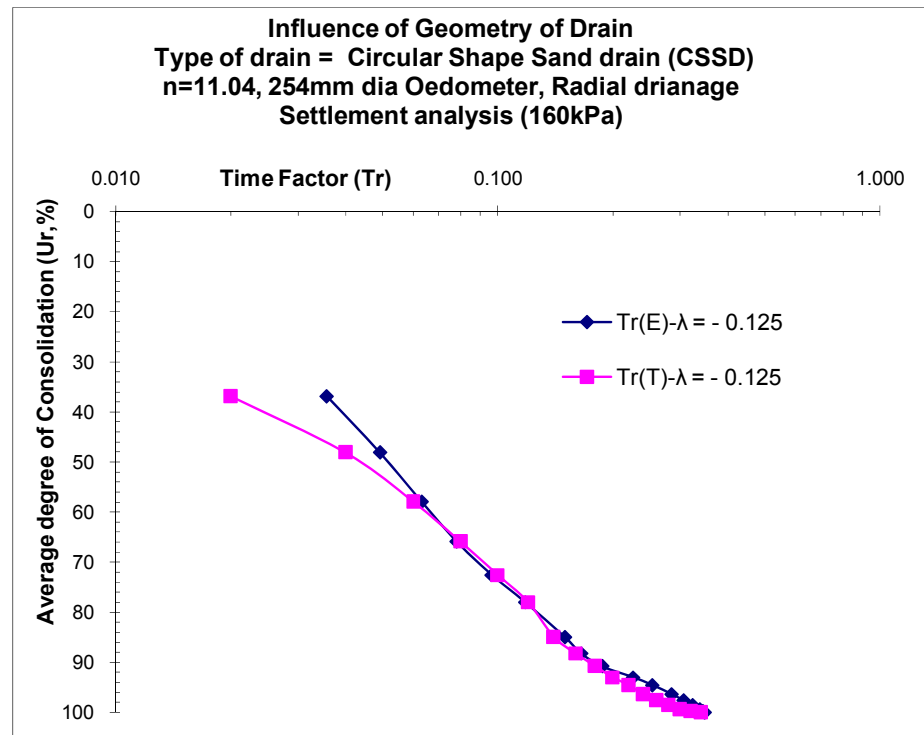


**Fig. 6.302:** Comparison of theoretical and experimental average degree of consolidation ( $U_r$ ) against Time factor ( $Tr$ ) for CSSD at 160kPa pressure

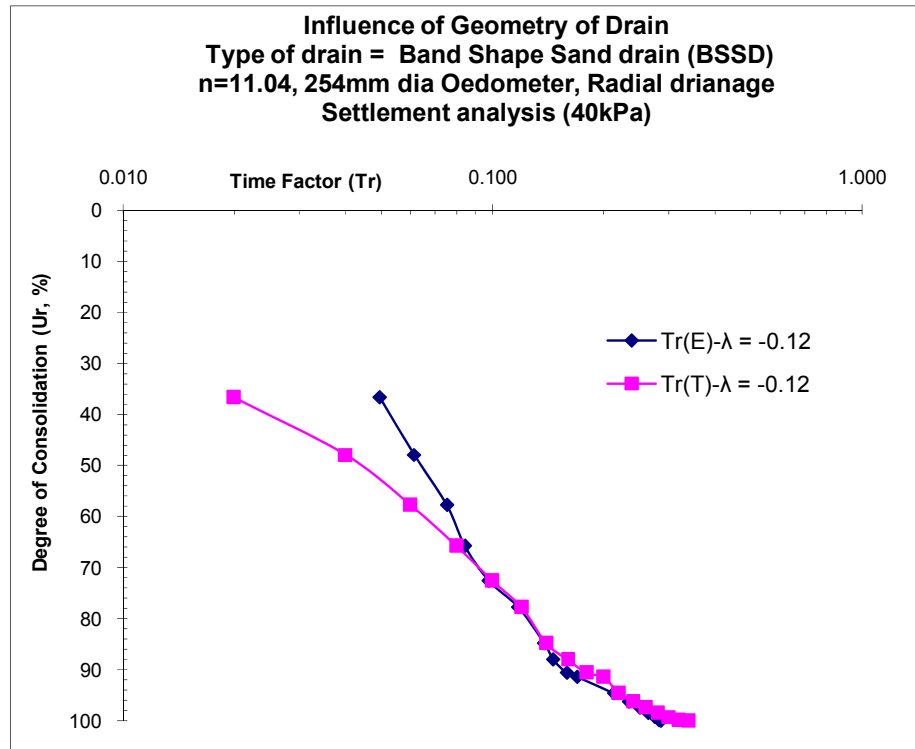


**Fig. 6.303:** Comparison of theoretical and experimental average degree of consolidation ( $U_r$ ) against Time factor ( $Tr$ ) for BSSD at 40kPa pressure

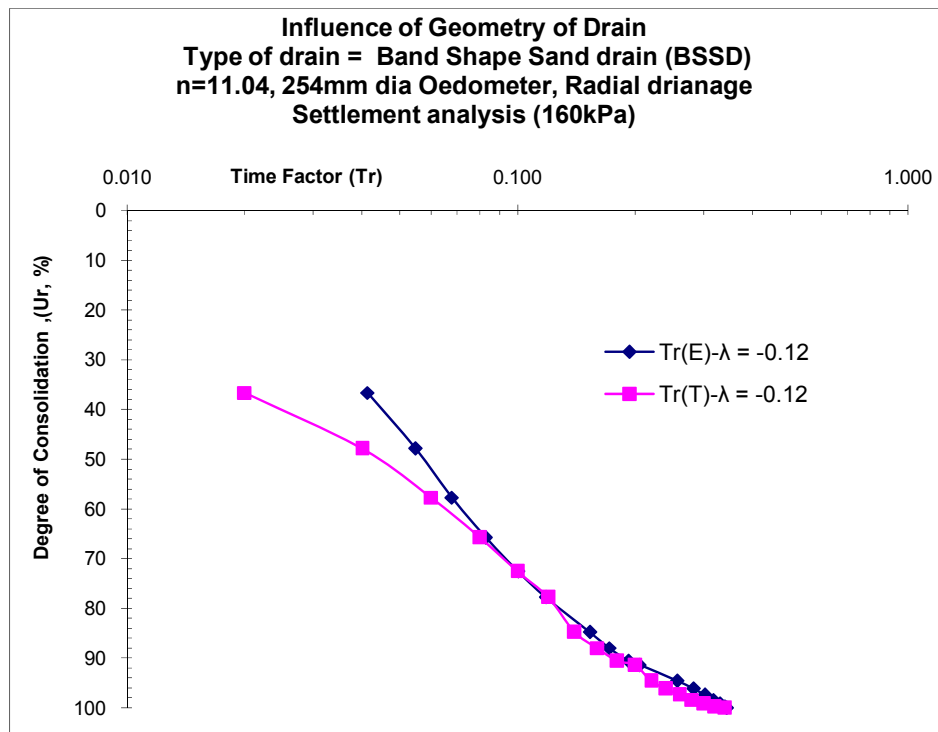


**Fig. 6.304:** Comparison of theoretical and experimental average degree of consolidation ( $U_r$ ) against Time factor ( $Tr$ ) for BSSD at 160kPa pressure

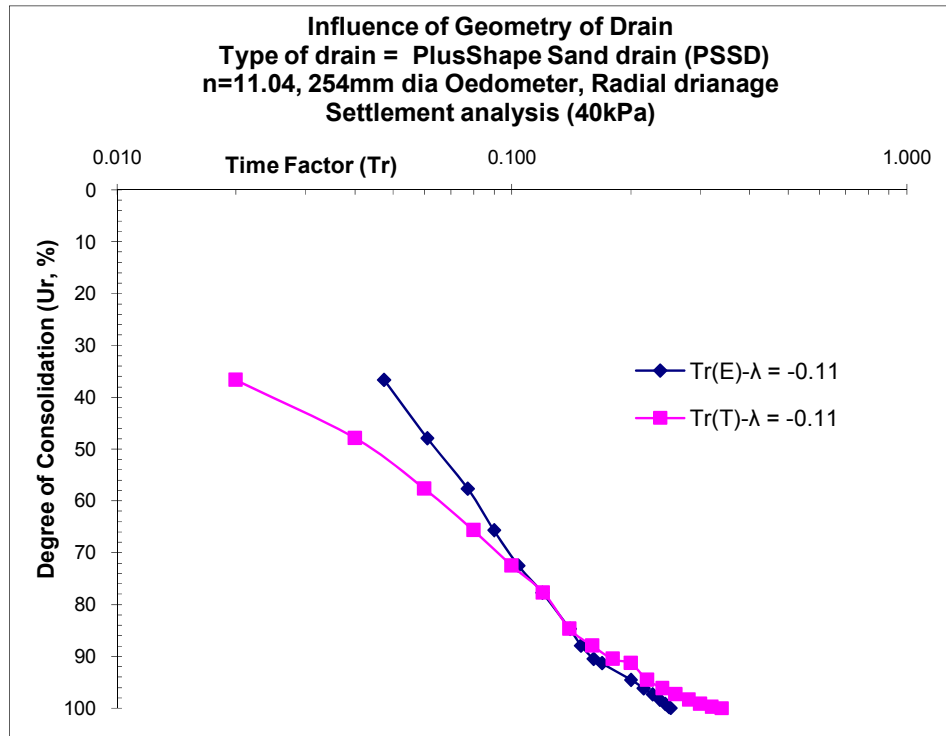


**Fig. 6.305:** Comparison of theoretical and experimental average degree of consolidation ( $U_r$ ) against Time factor ( $Tr$ ) for PSSD at 40kPa pressure

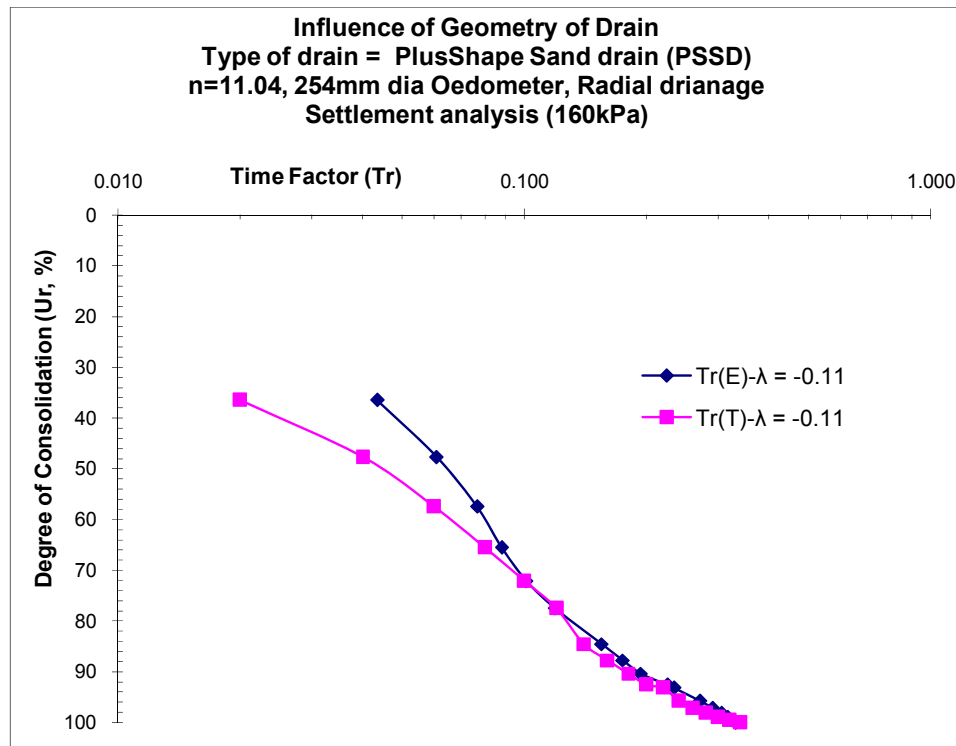


**Fig. 6.306:** Comparison of theoretical and experimental average degree of consolidation ( $U_r$ ) against Time factor ( $Tr$ ) for PSSD at 160kPa pressure

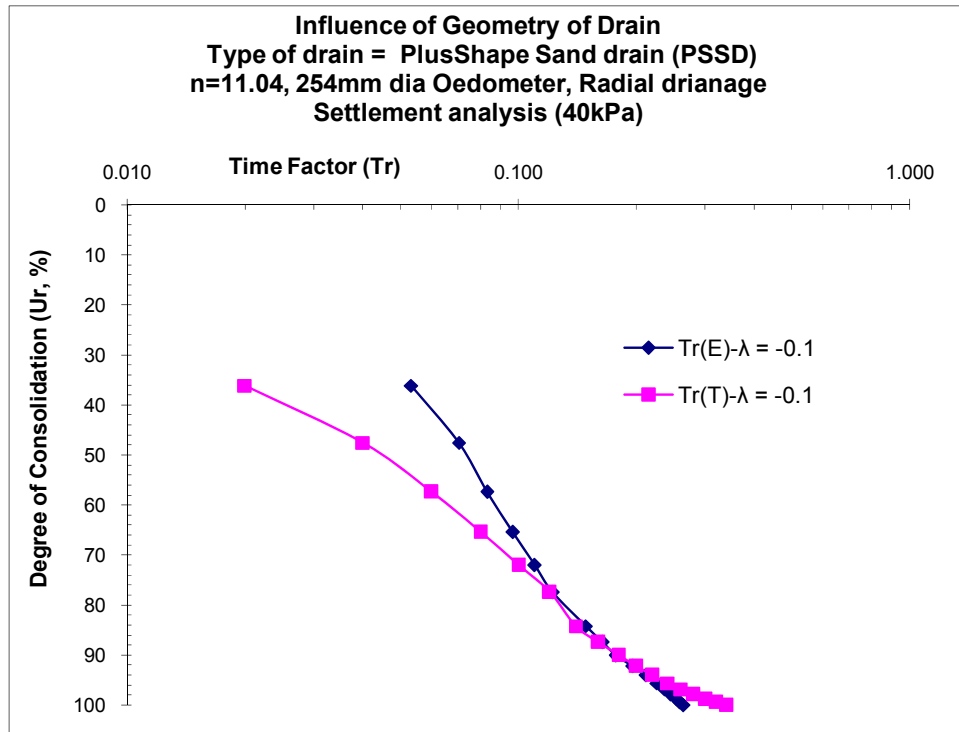


**Fig. 6.307:** Comparison of theoretical and experimental average degree of consolidation ( $U_r$ ) against Time factor ( $Tr$ ) for TSSD at 40kPa pressure

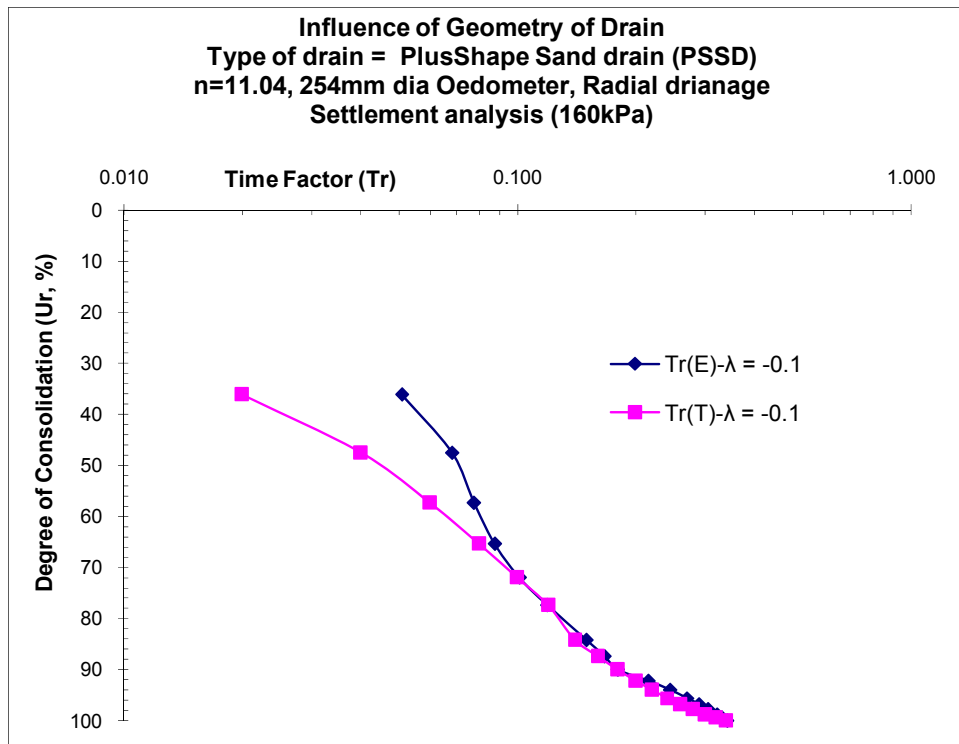


**Fig. 6.308:** Comparison of theoretical and experimental average degree of consolidation ( $U_r$ ) against Time factor ( $Tr$ ) for TSSD at 160kPa pressure

**Pore Pressure analysis: Fig.6.309 to Fig.6.317** shows the comparative plots of various geometrical sand drains of 'n' values of 11.04 for various shape drains like CSSD, BSSD, PSSD, TSSD for degree of consolidation ( $U_r$ ) versus time factor ( $T_r$ ) at all pressures. For comparison between theoretical and experimental values two applied pressure of 40KPa and 160KPa are selected. The lumped parameter ' $\lambda$ ' is appropriately fitted for each geometrical sand drain with respect to time factors so as to study the influence of geometry (shape) on vertical drain performance. Here it is determined that for four shapes of sand drains of 'n' values of 11.04 for CSSD the lumped parameter ' $\lambda$ ' is equal to -0.1 fits appropriately. Similarly it is determined that for BSSD the lumped parameter ' $\lambda$ ' is equal to -0.09 fits respectively. Similarly it is determined that for PSSD the lumped parameter ' $\lambda$ ' is equal to -0.08 fits respectively, while for TSSD the lumped parameter ' $\lambda$ ' is equal to -0.07 fits respectively. It is observed that ' $\lambda$ ' value of -0.1 is having maximum efficiency and as ' $\lambda$ ' value decreases efficiency of drain geometry decreases. It is observed from the above graphs that experimental results almost matches with theoretical results and this is true for all shape drains and for all applied pressures. It is observed that degree of consolidation determined from pore pressure readings and settlement readings suggest that CSSD is more efficient in compare to other geometrical sand drains. Table shows the value of lumped parameter ' $\lambda$ ' fitted to each drain shape.

| Sr.No. | Type of Geometrical Drain        | 'n' value | Lump parameter ' $\lambda$ ' |
|--------|----------------------------------|-----------|------------------------------|
| 1.     | Circular shape sand drain (CSSD) | 11.04     | -0.1                         |
| 2.     | Band shape sand drain (BSSD)     | 11.04     | -0.09                        |
| 3.     | Plus shape sand drain (PSSD)     | 11.04     | -0.08                        |
| 4.     | Tripod shape sand drain (TSSD)   | 11.04     | -0.07                        |

#### **Discussion:**

- Experimental results almost match with theoretical results with  $\lambda = -0.125$  particularly for CSSD,  $\lambda = -0.12$  for BSSD,  $\lambda = -0.11$  for PSSD and  $\lambda = -0.1$  for

TSSD proves to be efficient amongst other drains. From the above analysis it can be said that Circular shape is more efficient in compare to other shapes in accelerating rate of consolidation.

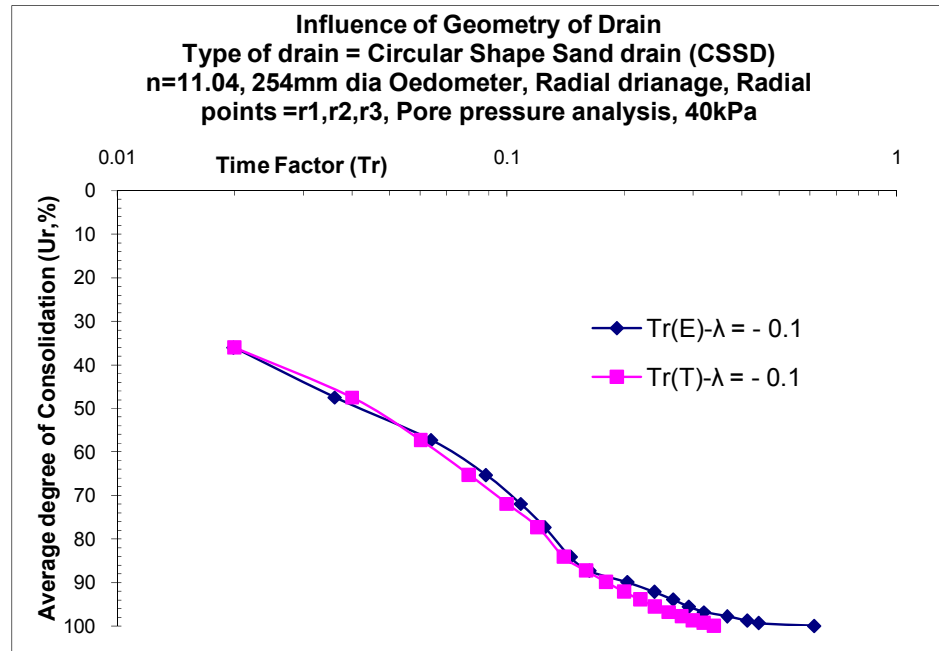


**Fig.6.309:** Comparison of theoretical and experimental average degree of consolidation ( $U_r$ ) against Time factor ( $Tr$ ) for CSSD at 40kPa pressure

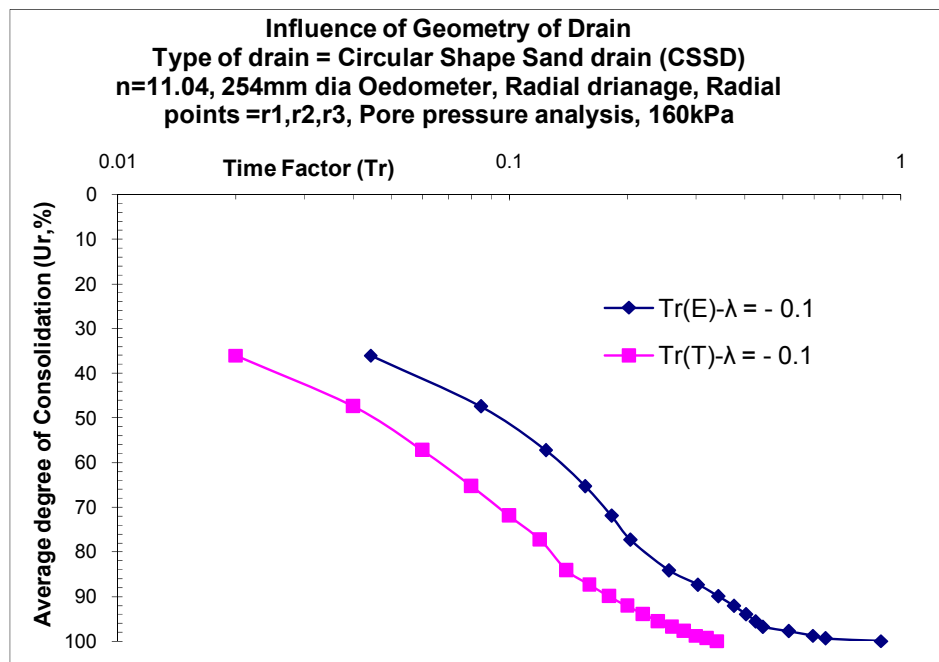


**Fig.6.310:** Comparison of theoretical and experimental average degree of consolidation ( $U_r$ ) against Time factor ( $Tr$ ) for CSSD at 160kPa pressure



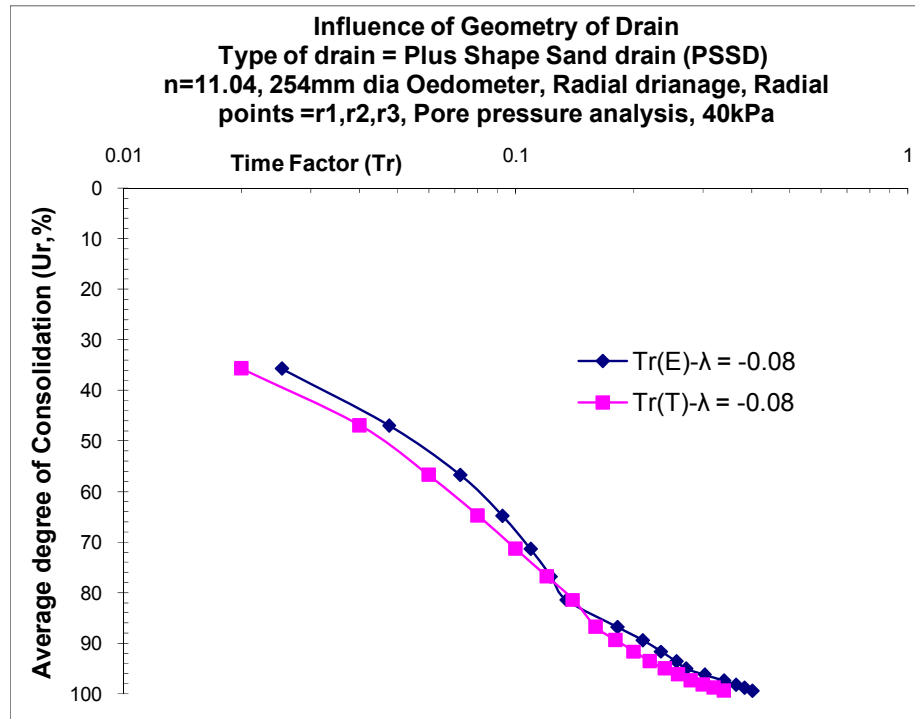


**Fig.6.311:** Comparison of theoretical and experimental average degree of consolidation ( $U_r$ ) against Time factor ( $T_r$ ) for PSSD at 40kPa pressure

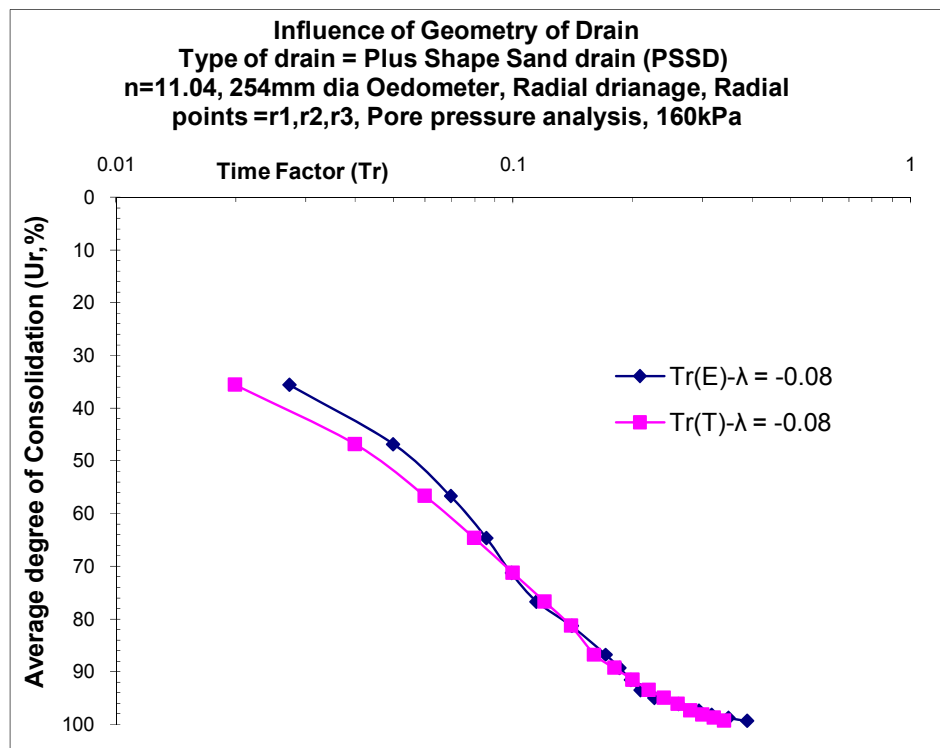


**Fig.6.312:** Comparison of theoretical and experimental average degree of consolidation ( $U_r$ ) against Time factor ( $T_r$ ) for PSSD at 160kPa pressure

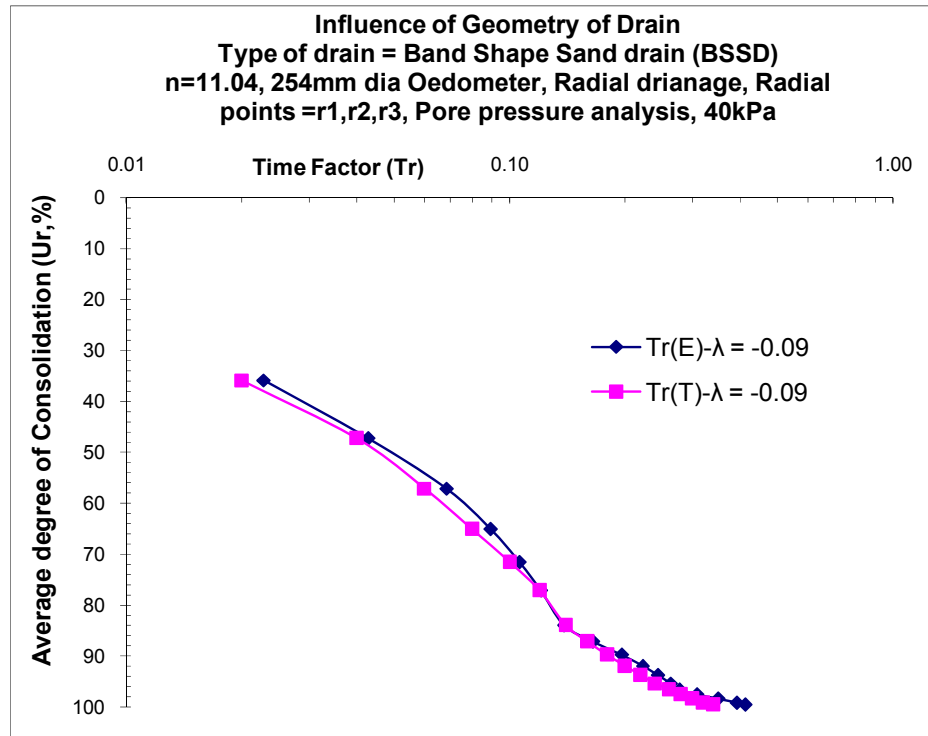


**Fig.6.313:** Comparison of theoretical and experimental average degree of consolidation ( $U_r$ ) against Time factor ( $Tr$ ) for BSSD at 40kPa pressure

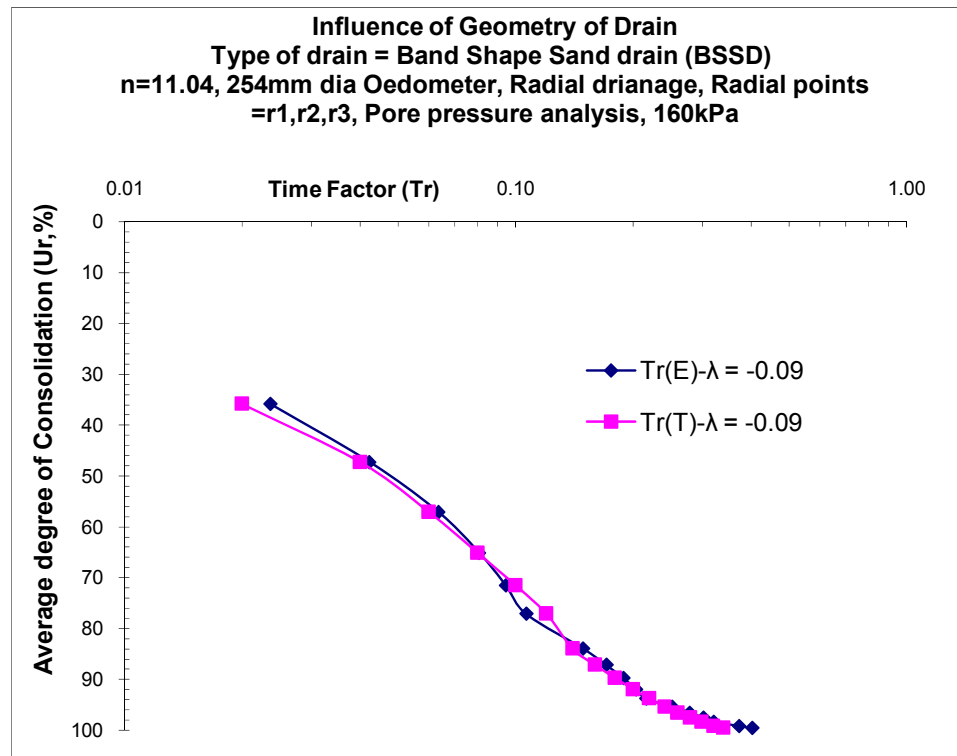


**Fig.6.314:** Comparison of theoretical and experimental average degree of consolidation ( $U_r$ ) against Time factor ( $Tr$ ) for BSSD at 160kPa pressure

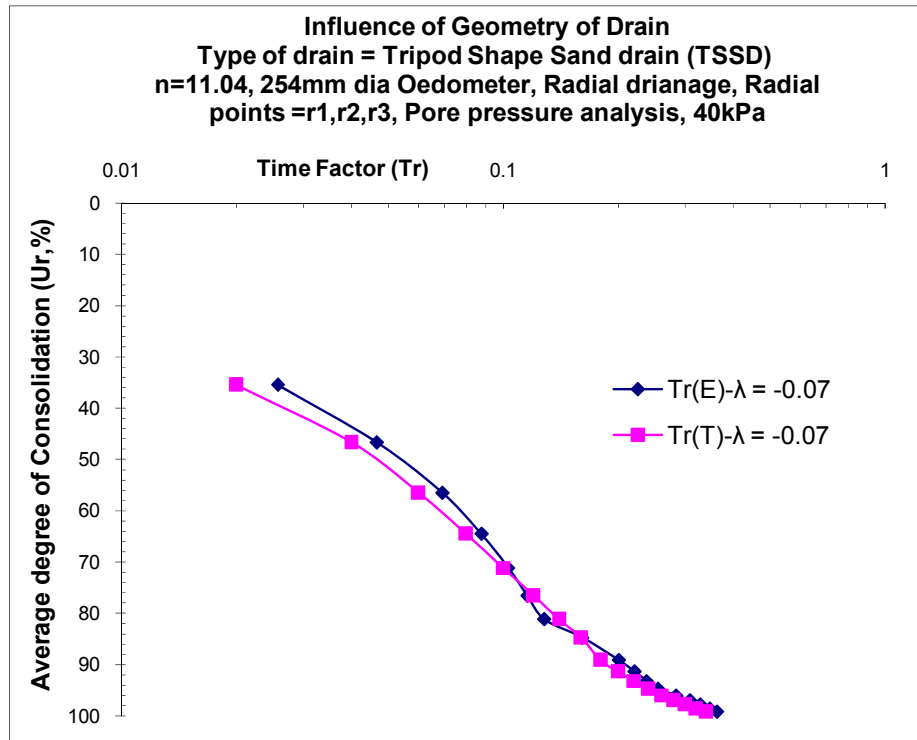


**Fig.6.315:** Comparison of theoretical and experimental average degree of consolidation ( $U_r$ ) against Time factor ( $Tr$ ) for TSSD at 40kPa pressure

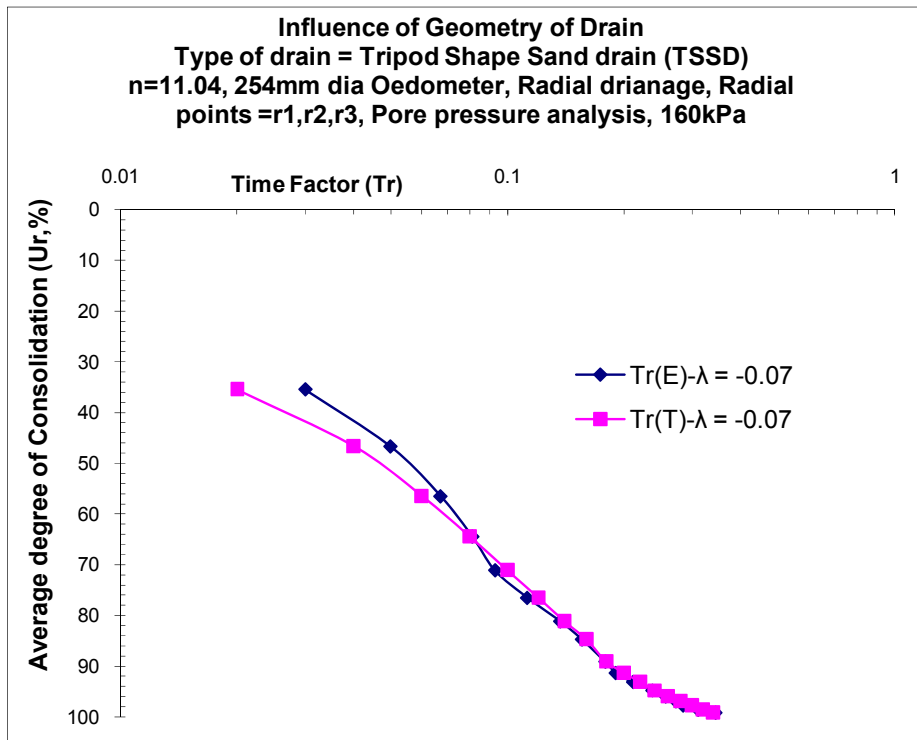


**Fig.6.316:** Comparison of theoretical and experimental average degree of consolidation ( $U_r$ ) against Time factor ( $Tr$ ) for TSSD at 160kPa pressure

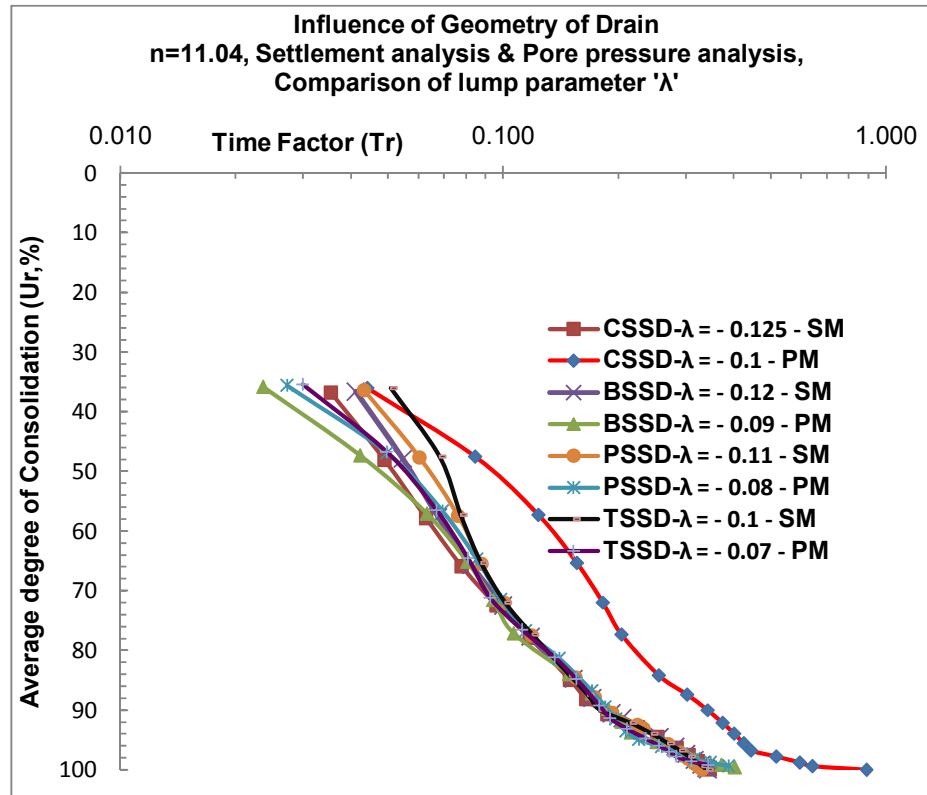


**Fig.6.317:** Influence of geometry of drain on experimental time factor (lump parameter) based on settlement and pore pressure analysis

**8) Vane Shear Strength and Images of Consolidated clay samples (end of 320kPa pressure) with central vertical drains:- Figures 6.318 and Photographs 6.25 to 6.27**

**Discussion:** (refer fig.6.318)

More gain in shear strength is observed in case of CSSD compare to PSSD, BSSD and TSSD for same 'n' value and same specific surface area. The shear strength observed in case of CSSD, PSSD, BSSD, and TSSD in terms of magnitude is 96kPa, 90kPa, 86kPa and 82kPa respectively. The initial shear strength(before consolidation) was in the range of 14-18kPa. The shear strength increases towards the drain for all shapes of drain. Sample having CSSD have marked strength compare to others. The strength is 1.07, 1.12, and 1.17 times higher compared to PSSD, BSSD and TSSD. The reasoning for the above is as follows. Though all the drains have same specific surface area, the radial flow

towards the drain experience hindrances in PSSD, TSSD and BSSD. BSSD has good versatility in the installation process but dissemination of pore pressure through BSSD takes more time and structure of soil produced may not be well oriented with face-to-face contact. Same is the story with other drains, then circular one. CSSD controls rate as well as magnitude of the pore pressure dissipation in achieving required strength.

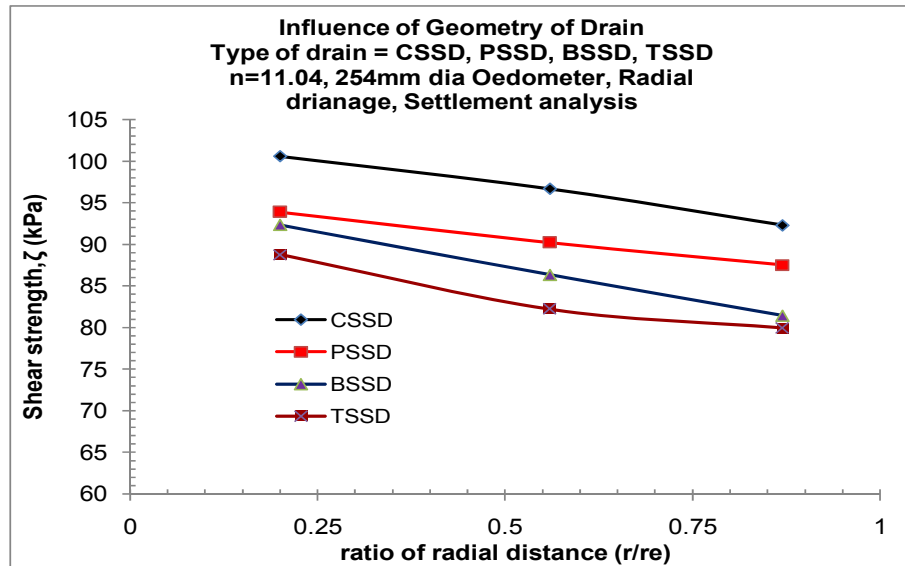
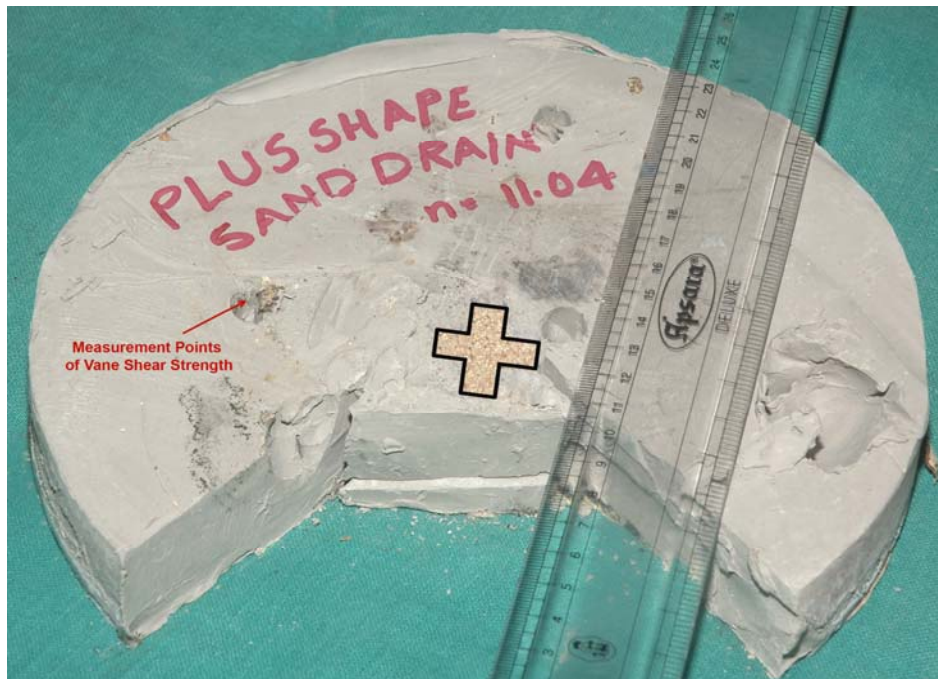
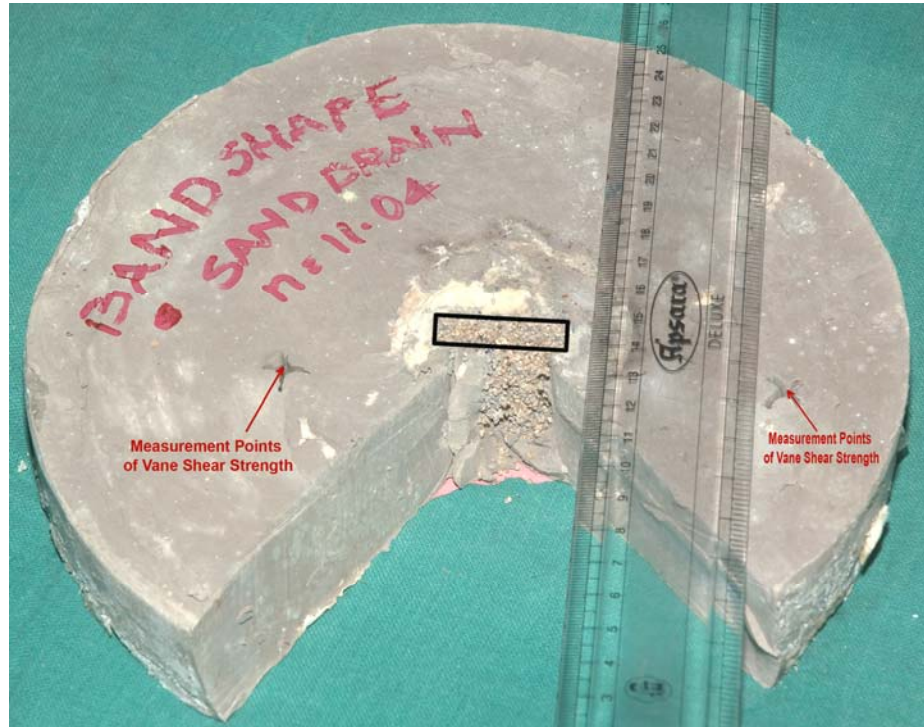


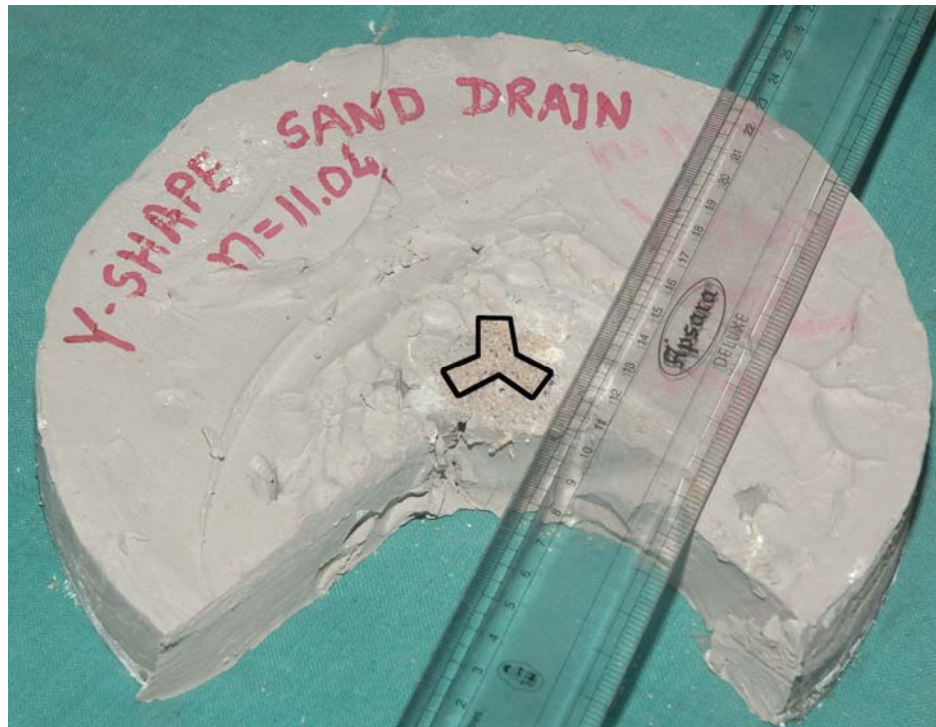
**Fig.6.318:** Comparison of vane shear strength of consolidated clay mass by CSSD, PSSD, BSSD, TSSD



**Photograph 6.25:** Sectional view of consolidated clay sample (end of 320kPa pressure) with central Plus shape sand drain (PSSD) of n'11.04



**Photograph 6.26:** Sectional view of consolidated clay sample (end of 320kPa pressure) with central Band shape sand drain (BSSD) of  $n'11.04$

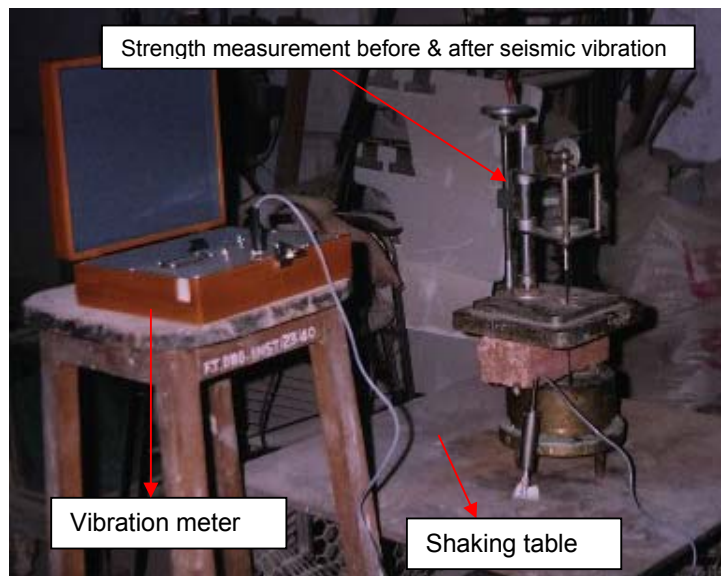


**Photograph 6.27:** Sectional view of consolidated clay sample (end of 320kPa pressure) with central Tripod shape sand drain (TSSD) of  $n'11.04$



### 6.3.3.1 Dynamic Analysis of Consolidated Clay Bed by Central Vertical Geodrain Sandwich of 'n'16.93 and 21.71

The set of experiment programme was made in the laboratory employing hydraulically pressurized Oedometer. The experimental model was conceived comprising of central prefabricated vertical Geodrain (sandwich) on a round sample of soft clay. The shear strength by vane shear was measured before installation of central vertical drain and after the consolidation of soft clay through radial drainage under different design embankment loadings post strength is attempted to measure by vane shear. Further this consolidated soil mass placed on a shaking table and simulating the insitu seismic stresses by vibrating table, the influence on strength is measured with respect to time as one of the variable. Seismic stresses of same intensity were applied with different interval of timings as 5s, 15s, 30s, 60s and 120s respectively. Sandwiches of two different 'n' values as 16.93 and 21.71 is analysed with reference to strength before and after the application of seismic stresses. The shaking table used for the investigation along with set-up of oedometer and vane shear test instrument is shown in the photograph 6.28. The vane shear strength was measured at the end of consolidation as well as at the end of each vibration period. This vibration was equivalent to seismic coefficient of 0.1g.



**Photograph.6.28:** Shaking table with Oedometer, vane shear and vibration meter

**Shear strength of consolidated soil mass using sandwich :** Table mention below gives detail of vane shear strength of clay bed consolidated using sandwich drain of 'n'16.93 and 21.71 before and after application of seismic stresses using shaking table.

**Table:** Vane shear strength before consolidation

| Vane shear strength ( $\zeta$ ) | $r_1$<br>(kPa) | $r_2$<br>(kPa) | $r_3$<br>(kPa) |
|---------------------------------|----------------|----------------|----------------|
| n=16.93                         | 14.6           | 13.0           | 13.0           |
| n=21.71                         | 12.1           | 12.1           | 12.9           |

**Table:** Vane shear strength after consolidation(end of 320kPa)

| Vane shear strength ( $\zeta$ ) | $r_1$<br>(kPa) | $r_2$<br>(kPa) | $r_3$<br>(kPa) |
|---------------------------------|----------------|----------------|----------------|
| n=16.93                         | 113.7          | 110.4          | 101.5          |
| n=21.71                         | 100.7          | 99.1           | 97.4           |

**Table:.** Vane shear strength at the end of seismic stresses equivalent to 0.1g under different durations by using shaking table

| Time in sec | Vane shear strength ( $\zeta$ ) in KPa |         |
|-------------|--|---------|
|             | n=16.93                                | n=21.71 |
| 0-5         | 51.10                                  | 46.30   |
| 0-15        | 58.40                                  | 42.20   |
| 0-30        | 63.30                                  | 31.60   |
| 0-60        | 58.40                                  | 32.40   |
| 0-120       | 57.60                                  | 31.60   |

**Table .6.5:** Percentage loss in strength at the end of each period due to seismic effect

| Time in sec | % loss in shear strength |         |
|-------------|--------------------------|---------|
|             | n=16.93                  | n=21.71 |
| 0-5         | 52.91                    | 53.23   |
| 0-10        | 46.18                    | 57.37   |
| 0-30        | 41.67                    | 68.08   |
| 0-60        | 46.18                    | 67.27   |
| 0-120       | 46.92                    | 68.08   |



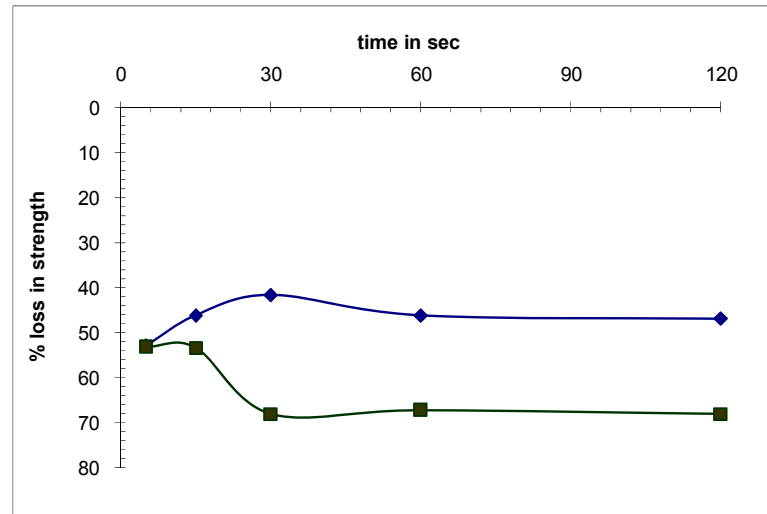


**Fig.6.319:** %loss of shear strength vs. time interval in seconds

**Discussion:** (Refer Fig. 6.319 and table 6.5)

Post vane shear strength of reinforced consolidated clay mass before application of seismic stresses

- For sandwich of  $n = 16.93$  the results of vane shear strength indicates that strength increases from 14.6kpa to maximum of 113.7kpa i.e. 88% increment. It was also observed that strength is more towards the first radial point  $r_1$  while it is less at  $r_3$  i.e. 101.5kpa. But generally for analysis the mid radial point ( $r_2$ ) is consider in design. For  $n=21.71$  the strength increased from 12.1kpa to 99.1kpa i.e. 87% increment without application of seismic stresses. In this case also the strength was maximum at  $r_1$  while it was minimum at  $r_3$  i.e. 97.4kpa. This results indicates that as the diameter of drain increases the soil shear strength also increases.
- In brief, before consolidation of the soil sample, the same strength (12.5kPa) for any radial distance is observed for all the 'n' value. The strength of consolidated soil mass at the end of 320kPa load intensity exhibit 9 times strength than 10kPa for  $n=16.93$ , while for  $n=21.71$  it is about 7.5 times. The strength at mid radial point is less than the strength nearer at drain and more than farthest radial point  $r_3$ .

Post vane shear strength of reinforced consolidated clay mass after application of seismic stresses

- Under dynamic analysis, SW of  $n=16.93$ , the vane shear strength indicates that the % loss in strength is more during first or initial vibration, afterwards the loss in strength is more or less constant. The average strength for  $n=16.93$  decreased from 108.53kpa to 51.10kpa i.e. 53% decrement for vibration period of 5 seconds. While for  $n=21.71$  the average strength decreased from 99.0kpa to 46.3kpa i.e. 53% decrement, Initial earthquake shock (period of vibration equal to 5 sec) is sufficient to cause metastable condition in card house structure of soft clay for any 'n' value but smaller the 'n' value more resistance is offered against strength loss. In any  $n=16.93$  the % strength loss(46%) is less than  $n=21.71$ . Percentage loss in strength for any period of vibration is less in smaller 'n' value compare to higher 'n' value 11.04.
- For  $n=16.93$  under seismic stresses the results of vane shear strength for seismic period of 15 secs, 30 secs, 60 secs and 120 secs indicates that %loss in strength is 46% averagely remains constant though seismic periods was increased while if we consider the net effect in strength then it is only 6 to 8% which may be an indication of particle rearrangement or the card house structure of soft clay to have become horizontal whose metastability was not affected by adsorbed water at later stages to some extent. While or  $n=21.71$  the % loss in strength was averagely 68% which is much higher compare to  $n=16.93$  values. Also it was observed that there was no change in in-situ placed condition of sandwich or even no settlement of only sandwich was observed nor any change in its diameter was observed indicating sandwich as a stable drain under seismic conditions which prevents the soft soil to get quick.
- Initial earthquake shock (period of vibration equal to 5 sec) is sufficient to cause metastable condition in card house structure of soft clay for any 'n' value but smaller the 'n' value more resistance is offered against strength loss. In any  $n=16.93$  the % strength loss(46%) is less than  $n=21.71$ . Percentage loss in strength for any period of vibration is less in smaller 'n' value compare to higher 'n' value 11.04.

**Derived Factors:****6.3.4 Variation of Water content ratio (WCR):**

| Water Content Ratio | Water content      |                    | Drain type                     | 'n' value | End of Load (kPa) | Water content (%) | Cc average from graph | *Cc as per load variation |
|---------------------|--------------------|--------------------|--------------------------------|-----------|-------------------|-------------------|-----------------------|---------------------------|
|                     | W <sub>i</sub> (%) | W <sub>f</sub> (%) |                                |           |                   |                   |                       |                           |
| 0.851               | 91                 | 47.67              | Sand drain (SD)                | 11.04     | 20                | 77.53             | 0.400                 | 0.896                     |
| 0.724               |                    |                    |                                |           | 40                | 65.95             |                       | 0.734                     |
| 0.634               |                    |                    |                                |           | 80                | 57.72             |                       | 0.619                     |
| 0.566               |                    |                    |                                |           | 160               | 51.54             |                       | 0.532                     |
| 0.523               |                    |                    |                                |           | 320               | 47.67             |                       | 0.468                     |
| 0.863               | 91                 | 45.48              | Sandwick drain (SW)            | 11.04     | 20                | 78.58             | 0.315                 | 0.911                     |
| 0.777               |                    |                    |                                |           | 40                | 70.10             |                       | 0.792                     |
| 0.657               |                    |                    |                                |           | 80                | 59.82             |                       | 0.648                     |
| 0.577               |                    |                    |                                |           | 160               | 52.52             |                       | 0.546                     |
| 0.499               |                    |                    |                                |           | 320               | 45.48             |                       | 0.437                     |
| 0.802               | 91                 | 41.52              | Coir-Jute drain (CJ)           | 11.04     | 20                | 73.00             | 0.258                 | 0.833                     |
| 0.717               |                    |                    |                                |           | 40                | 65.26             |                       | 0.724                     |
| 0.638               |                    |                    |                                |           | 80                | 58.10             |                       | 0.624                     |
| 0.531               |                    |                    |                                |           | 160               | 48.38             |                       | 0.488                     |
| 0.456               |                    |                    |                                |           | 320               | 41.52             |                       | 0.370                     |
| 0.847               | 91                 | 47.20              | Polypropylene fiber drain (PF) | 11.04     | 20                | 77.13             | 0.366                 | 0.891                     |
| 0.739               |                    |                    |                                |           | 40                | 67.28             |                       | 0.753                     |
| 0.645               |                    |                    |                                |           | 80                | 58.75             |                       | 0.633                     |
| 0.570               |                    |                    |                                |           | 160               | 51.92             |                       | 0.538                     |
| 0.518               |                    |                    |                                |           | 320               | 47.20             |                       | 0.465                     |

\* Where, Water content ratio is the ratio of existing water content at the end of particular load to water content at the end of initial load (10kPa).

W<sub>i</sub> and W<sub>f</sub>= Initial water content and Final water content of clay sample at the end of particular load. \* Cc calculated as per Nishida method

### Variation of Water content ratio (WCR):

#### Discussion: (Figs. 6.320 to 6.322)

- As water content ratio increases the value of  $C_c$  increases for any drain material and for same 'n' value as shown in table above. For same water content ratio the variation in compression index ( $C_c$ ) value for different drain material indicate 0.556 for coir-jute drain (CJ), 0.546 for sandwich drain (SW), 0.538 for polypropylene fiber drain (PF) and 0.532 for sand drain (SD). From the pattern of variation it infers that for same  $C_c$  value the WCR remains in the ascending order of CJ, SD, PF and SW. For same WCR, the  $C_c$  values are descending order of CJ, SW, PF and SD.
- Coir-jute drain show lowest water content at the end of any load amongs various drains proving its ability to consolidate soil more compare to others.

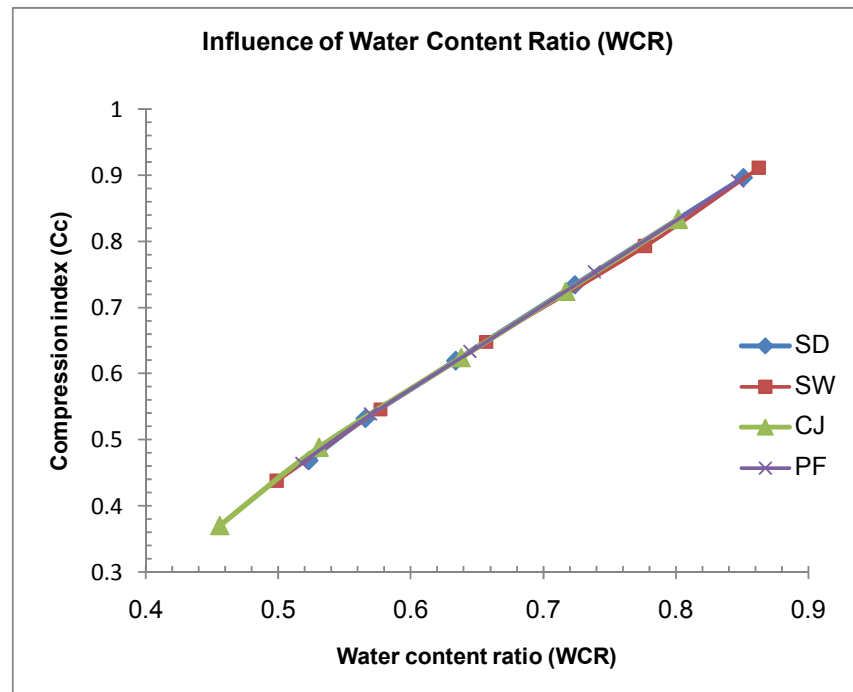


**Fig.6.320:** Comparison of  $C_c$  vs. WCR for various vertical drains

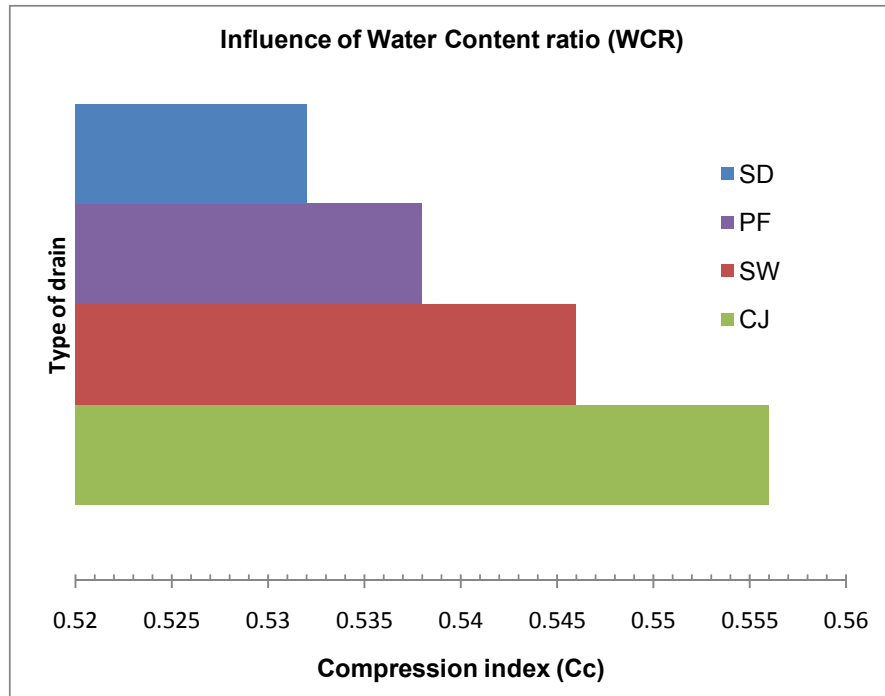


**Fig.6.321:** Comparison of Cc vs. Type of drain for same WCR (0.574 avg value)

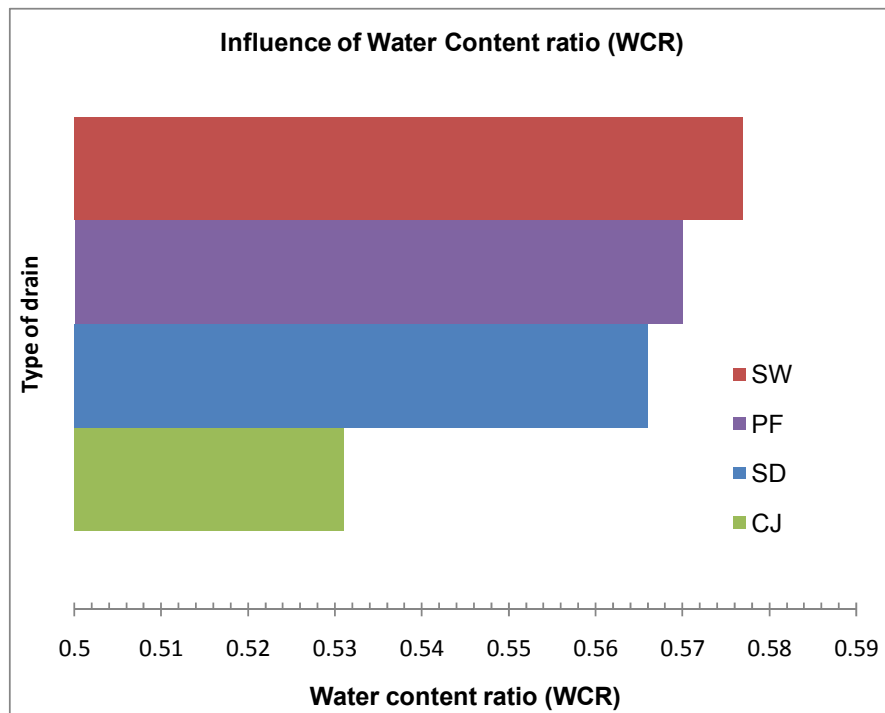


**Fig.6.322:** Comparison of WCR vs. Type of drain for same Cc (0.526 avg. value)

**6.3.5 Variation of Consolidation Pressure Ratio (CPR):**

| CPR | Drain Type           | 'n' value | Existing load (kPa) | $k_h$ (cm/sec)        | $k_v$ (cm/sec)        | $k_h/k_v$ | Cc value | Diameter of Oedometer |
|-----|----------------------|-----------|---------------------|-----------------------|-----------------------|-----------|----------|-----------------------|
| 2   | Coir-jute fiber (CJ) | 11.04     | 20                  | $3.55 \times 10^{-7}$ | $1.31 \times 10^{-7}$ | 2.71      | 0.227    | 254mm                 |
| 4   |                      | 11.04     | 40                  | $3.05 \times 10^{-7}$ | $4.67 \times 10^{-8}$ | 6.54      | 0.258    |                       |
| 16  |                      | 11.04     | 160                 | $2.17 \times 10^{-7}$ | $8.04 \times 10^{-9}$ | 27.1      | 0.286    |                       |
| 2   | Sandwick (SW)        | 11.04     | 20                  | $1.25 \times 10^{-7}$ | $1.31 \times 10^{-7}$ | 1.00      | 0.308    | 254mm                 |
| 4   |                      | 11.04     | 40                  | $7.81 \times 10^{-8}$ | $4.67 \times 10^{-8}$ | 1.67      | 0.312    |                       |
| 16  |                      | 11.04     | 160                 | $3.36 \times 10^{-8}$ | $8.04 \times 10^{-9}$ | 4.17      | 0.320    |                       |
| 2   | PP drain (PF)        | 11.04     | 20                  | $3.15 \times 10^{-7}$ | $1.31 \times 10^{-7}$ | 2.41      | 0.339    | 254mm                 |
| 4   |                      | 11.04     | 40                  | $2.08 \times 10^{-7}$ | $4.67 \times 10^{-8}$ | 4.46      | 0.353    |                       |
| 16  |                      | 11.04     | 160                 | $6.17 \times 10^{-8}$ | $8.04 \times 10^{-9}$ | 7.67      | 0.380    |                       |
| 2   | Sand drain (SD)      | 11.04     | 20                  | $3.98 \times 10^{-7}$ | $1.31 \times 10^{-7}$ | 3.03      | 0.255    | 254mm                 |
| 4   |                      | 11.04     | 40                  | $3.16 \times 10^{-7}$ | $4.67 \times 10^{-8}$ | 6.76      | 0.555    |                       |
| 16  |                      | 11.04     | 160                 | $7.97 \times 10^{-8}$ | $8.04 \times 10^{-9}$ | 9.91      | 0.928    |                       |

Where, CPR = ratio of existing pressure/initial pressure of 10kPa ,

Cc = Compression index (slope of e vs.log'p' graph)

Note: Data of Coefficient of vertical permeability of soil ( $k_v$ ) used in this table is obtained from laboratory test data of one-dimensional consolidation experiment.

### **Variation of Consolidation Pressure Ratio (CPR):**

#### **Discussion:**

- As CPR value increases the compression index ( $C_c$ ) value increases for any drain material. In the higher range of CPR value, the  $C_c$  value is in the order of CJ, SW, PF and SD while for lower range of same CPR value the sequence is in the order of CJ, SW, SD and PF.
- As CPR increases  $k_v$  and  $k_h$  increases for any drain material and therefore the ratio  $k_h/k_v$  increases as CPR increases for any drain material. Amongst various drains, CJ gives highest  $k_h/k_v$  of the order of 27 which indicates CJ drains facilitates more gradient of water towards drain forming displacement of particles in such a way that horizontal permeability of soil increases leading ratio more for end of any load.

## CHAPTER-7

### SUMMARY OF FINDINGS

---

The post Barron developments in consolidation due to radial flow theories could be classified into two distinct approaches namely 'free strain condition' and 'equal strain condition' supported either by analytical solutions or numerical solutions. The consolidation phenomenon in soft soils due to radial flow cannot be tackled by mathematical treatments based on gross idealization. The consolidation problem is different from the elasticity problem and is not adequately solved by simply satisfying a heat conduction type equation. One of the distinct feature of the consolidation phenomenon is the occurrence of large volume changes during the process. A physical process, however, attractive it may be, loses its value if it cannot be mathematically exploited to evaluate the parameters for the engineering analysis. A clearer picture of the phenomenon is possible if a proper linkage between the physico-chemical characteristics of clays and analytical procedure is established. The Lagrangian mathematical scheme followed by McNabb (1960) and Gibson et al. (1967) is versatile.

A differential equation: 
$$\frac{\partial e}{\partial T} = \left( \frac{r_e}{h} \right) \frac{\partial^2 e}{\partial R^2} \mp \lambda \frac{\partial e}{\partial R}$$
 of Shroff and Shah (2008, 2010, 2012) for the present work is derived from fundamental consideration based upon the above mathematical treatment. The equation has form identical to the differential equation for the nonsteady one dimensional flow of heat through moving media against Terzaghi classical concept of heat flow through isotropic bodies.

Taking ' $\lambda$ ' as a constant, solution of the differential equation is obtained by Laplace Transform technique. lumped parameter ( $\lambda$ ) is the ratio of ( $C_e / C_r$ )  $r_e$ , being  $C_r$  as coefficient of consolidation due to radial drainage and  $C_e$  as coefficient due to permeability and porosity. Change of tortousity because of particle orientation under load variation reflecting soil structural changes (from edge to face and edge to edge or face to face) orientation is also accounted in lumped parameter ( $\lambda$ ). lumped parameter ( $\lambda$ ) will vary with drain material,  $n'$  value and shape of drain because of vertical strain in



the soil structure due to radial gradient of flow. For solution of higher order partial differential equation derived from first principle an macro-EXCEL programme on computer is developed to compute theoretical relationships. The proposed theory is seen to agree adequately with experimental observations. The constant ' $\lambda$ ' of the equation emerges as a weighted factor to account for the deviation from Barron's 'equal strain' idealizations. It is suggested that it will be worthwhile to obtain the solution of the differential equation taking ' $\lambda$ ' as some function of ' $t$ '.

The degree of exposition of any physical process depends on the degree of exactitude of the experimental set-up. Major factors that influence the measurement of consolidation characteristics are sample disturbance, side friction and inadequacies in the measuring systems. The present investigations show that deposition of uniform slurry at double liquid limit consistency in a pot produce a uniform sample, the smearing of silicone grease to contacting surfaces help minimize side friction, and continuous maintenance and calibration of measuring devices ensure precise readings. The uses of electronic equipments demand stable electric power, constant temperature conditions and utmost vigilance for zero defects. The modified hydraulically pressurized Oedometer set-up is particularly better suited for pore pressure measurements and drainage control using central vertical drain. The measurement of local deformations and pore pressures within the clay bed using vertical drains employing displacement transducers, pore pressure transducers along with Bishop System interfaced with Data logger system connected to computer are worth a pursuit. Scanning electron microscopy of clay samples at various magnifications factors and use of Micro Structure Characterization (MIC) software helps to understand the role of various physico-chemical forces on consolidation characteristics of soft soil through radial flow under various vertical geodrains.

**General Inferences:**

- 1) There is a distinct behavior of soft soil during consolidation by vertical flow and only by radial flow.

- 2) Time – settlement curve (degree of consolidation) due to radial flow always lie below the vertical flow. This is because of shorter drainage path and horizontal permeability in radial flow compared to vertical flow.
- 3) Higher initial hydrodynamic lag is observed in dissipation of mid plane pore water pressure in vertical flow compared to radial flow. The tortousity of soil structure for a vertical flow causes delay in the dissipation in early stage of consolidation.
- 4) Under lighter load time taken for the consolidation due to radial flow is 16 times lesser than the vertical flow, while for 50% consolidation time taken for radial flow is 3 times; for 90% consolidation time taken is about 6 times lesser than the vertical one which also reflects in coefficient of consolidation due to radial drainage ( $C_r$ ) versus pressure relationship that is magnitude of  $C_r$  decreases at faster rate compare to vertical one.
- 5) The void ratio for a particular load decreases at faster rate in radial case compare to vertical one. Initial structural dynamic viscosity of the soil configuration resist the light consolidation load exhibiting initial hump more in vertical case.
- 6) The measurement of coefficient of radial permeability of vertical drain using special set-up developed in present research is very useful in knowing the exact discharge capacity of any vertical drain of any 'n' value under constant head and falling head condition. This set-up is even useful to measure radial permeability of soil.
- 7) The modification of hydraulically pressurized Oedometer for measurement of complete pore water pressures by drawing three radial points at  $120^\circ$  each covering complete radial influence of soil sample has proved its efficacy at various stages of consolidation and by maintaining 'equal strain' condition with help of 'rubber jack' under various loadings gives better and accurate picture of influence of various parameters intended to affect consolidation of soft soils.
- 8) The studies on consolidation of clayey soil due to vertical flow revealed that degree of saturation, drainage path; stress history, mineral type and soil structure play their important role on settlement characteristics of kaolinitic clays, Shroff et.al (1972). The conclusions of present work are drawn considering the above factors and the influence of diameter ('n'values), distinctive material and geometry of vertical drain with soil

structure effects on consolidation characteristics of kaolinitic clay due to only radial drainage using hydraulically pressurized oedometer.

### **Influence of Distinctive Drain Materials:**

#### **I) Rate of Consolidation**

##### *Degree of consolidation ( $U_r$ ) vs. Time*

- From settlement and pore pressure measurement considerations it infers that for 50% consolidation, CJ under light loading takes 46% less time in compare to SW, 49% in compare to PF, 56% in compare to SD, while for 80% consolidation, CJ takes 31% less time in compare to SW, 35% in compare to PF and 44% in compare to SD and under constructional loading CJ takes 45% less time in compare to SW, 58% less time in compare to PF, 58% in compare to SD, while for 80% consolidation CJ takes 29% less time in compare to SW, 41% in compare to PF and 47% in compare to SD for same 'n' value and permeability ratio.
- Rate of drainage of a radial points nearer to drainage being faster the time taken for particular % of consolidation is less in compare to radial points farther away, it also reflects this observation in settlement measurements to some extent showing more compressibility gradient towards central drain. It seems from the micrograph of several drains the pore space in terms of nanomeasurement is larger compare to other drains. This reflects the efficiency of CJ with respect to micro structure opening even under light and heavy constructional loading.
- Under light loading for 50% consolidation SW takes 26% less time in compare to PF while it takes 0% against SD while SD takes 26% less time compare to PF but 34% more time compare to CJ. Similarly under constructional loading SW takes 41% & 3% less time in compare to PF & SD. Also SD takes 37% lesser time in compare to PF while SD takes 3% & 40% more time compare to SW and CJ.
- Under light loading for 80% consolidation SW takes 31% less time in compare to PF while it takes 3% against SD while SD takes 27% less time compare to PF but 23% more time compare to CJ. Similarly under constructional loading SW takes 30% &

5% less time in compare to PF & SD. Also SD takes 23% lesser time in compare to PF while SD takes 5% & 27% more time compare to SW and CJ.

- For any load intensity and drain material, the time deformation curve with respect to pore pressure dissipation remain towards the vertical axis compare to curve of settlement, that is time require for 50% or 80% consolidation is less compare to settlement curve which also reflects in isochrones curves. This is because of direction of flow from the void space is radial which allows early dissipation compare to particle reorientation achieving same degree of consolidation. The role played here is by 'macrocompressibility' in settlement case while 'microcompressibility' in pore pressure case.
- The gradient of radial flow is also facilitated by type of drain material, CJ drain may facilitate easy dissipation compare to other drain material, because of more percentage of microporosity in CJ drain compare to others which is also mentioned earlier in chapter 3 in para drain characteristics which also explains describes 'permittivity' and 'transmissivity' of various drain material used in fabricating the circular drain. Further this data indicate the gradient of water formed because of the higher or lower transmissivity of geosynthetics material used in the present investigation. In plane permeability data also confirms the above reasoning.
- Because of the above reasoning the time-deformation curve and isochrones indicate early dissipation and early deformation as well as the magnitude of vertical consolidation in CJ drain compare to other drains.

Coefficient of consolidation due to radial drainage ( $C_r$ ) vs. Time

- Looking to above inferences it is clear that CJ shows more rate of consolidation both at low and high pressures in compare to other drain materials from settlement and pore pressure measurement considerations because of higher horizontal permeability of drain of CJ.
- Effectiveness of PF seems too remote from reality compare to functioning of other drains. While effectiveness of SW is less than CJ but higher than SD.
- Under any strain condition because of the flexibility CJ drain shows higher horizontal permeability compare to others.

- Cr for CJD for 50% consolidation from settlement readings work out to be averagely 73% & 78% more compare to other drain materials under light and heavy construction loading. Similarly for 80% consolidation it is averagely 63% & 66% more. This observation satisfies that higher horizontal permeability of CJD compare to other drain materials under light and heavy construction loading.
- Cr for CJD from mid plane pore pressure measurements for 50% consolidation work out to be averagely 154% & 155% more compare to other drain materials under light and heavy construction loading. Similarly for 80% consolidation it is averagely 48% & 81% more.
- For any load intensity and drain material, the time deformation curve with respect to pore pressure dissipation remain towards the vertical axis compare to curve of settlement, that is time require for 50% or 80% consolidation is less compare to settlement curve which also reflects in isochrones curves. This is because of direction of flow from the void space is radial which allows early dissipation compare to particle reorientation achieving same degree of consolidation. The role played here is by 'macrocompressibiliy' in settlement case while 'microcompressibility' in pore pressure case.
- The gradient of radial flow is also facilitated by type of drain material, CJ drain may facilitate easy dissipation compare to other drain material, because of more percentage of microporosity in CJ drain compare to others

Coefficient of consolidation due to radial drainage ( $C_r$ ) vs. applied pressure

- Under any strain condition because of the flexibility CJ drain shows higher horizontal permeability compare to others.

---

SD = Sand drain, SW = Sandwick drain, CJ = Coir-Jute fiber drain,  
PF = Polypropylene fiber drain, n= ratio of drain diameter to soil sample  
diameter

- From the plots it is very clear that for all drain materials the initial nature of  $T_{r80}$  graph &  $T_{r50}$  graph decreases with initial applied pressure and at higher pressures it remains same that is nearly constant. It is because of the initial structural resistance existing in the clay water structure of the Kaolinite clay.
- Lesser variation in  $C_r$  value is observed for radial point's  $r_2$  and  $r_3$  for all drain materials and for all applied pressures. Though CJ shows more inter-rate of dissipation of excess hydrostatic pore water pressure even at successive pressures in compare to other drain materials.

#### Isochrones

- From the consolidation ratio vs. radius of influence for various  $T_r$  values reveals that sequence of consolidation for CJ at any radius of influence seems to be efficient compare to all other drains.
- For all drain material experimental time factor more than 0.24 exhibit concave shapes initially, while  $T_r$  less than 0.24 shows convex towards vertical axis. Comparing isochrones for various drain materials it indicates that CJ shows more magnitude of dissipation at same time factor for almost all pressures. Initial slope of SD and PF drain indicates that their initial capacity of dissipation of pore water is faster up to 15% consolidation but thereafter its rate retard consistently, while CJ though not showing fast rate of dissipation during initial stage of consolidation but its performance is consistent and shows more degree of consolidation at less time factor. Reverse is the behavior of SW for pore pressure dissipation either at low value of time factor at high value of time factor. Comparing groups of all the isochrones of various time factor of drain materials, SW curve are distinctly showing initial concave curve.
- The micro pore structures of the SW drain and other drains are quite distinct that is initial micro porosity of SW is less compare to other drains which reflects in isochrones characteristics.

---

SD = Sand drain, SW = Sandwich drain, CJ = Coir-Jute fiber drain,  
PF = Polypropylene fiber drain,  $n$  = ratio of drain diameter to soil sample diameter

- Other drains shows more or less same micro porosity that wise initial slope of isochrones is same to some extent, but with increase of time factor micro-porosity decreases in other drains while in CJ drain micro porosity remains almost same being the flexible nature of jute and coir fibers which helps in more dissipation of pore pressure indicating more percentage of consolidation.

Lumped parameter ( $\lambda$ ) vs. Degree of consolidation ( $U_r$ )

- As ' $\lambda$ ' value decreases efficiency of drain material decreases. Experimental results almost match with theoretical results with  $\lambda=0.2$  particularly for CJ proves to be efficient amongst other drains.
- Time-deformation curve with respect to pore pressure dissipation and settlement follow a general trend of transmission of particle orientation from one stage to another against several physico-chemical forces initially and then thereafter achieving randomly oriented or parallel oriented soil structure. The quantum of initial resistance will depend on magnitude of load, characteristics of drain material and the ' $n$ ' value (particularly when consolidation by radial drainage is considered) and horizontal permeability that is tortuosity in horizontal direction. The initial flocculated structure of soil bed has edge to surface or edge to edge link bonds. When load is applied some resistance is offered by this link bond. Load has to overcome the edge to edge or edge to face attraction to alter the packing geometry. During this resistance the stage can be regarded as 'microcompressibility', Shroff (1972) and specific deformation can be expressed as slow decay as soon as local breakdown commences, the initial resistance to compression diminishes and the rate of consolidation increases to some extent. Progressive deformation can be visualized as 'macro compressibility', Shroff (1972) in which deformation is caused by sliding and lifting of plate shape particles, pressing out the pore water, at the same time it loosens the 'interfacial grip' of adsorbed water at links of plate shape particles. Under high loading microcompressibility and interfacial grip at links of plate shape clay particle have little relevance.

**II) Magnitude of consolidation**

Compression index ( $C_c$ ) vs. applied pressure

- Amongst various drain material fibers of CJ orient in such a way that the rate of dissipation remain faster in spite of pressure increase though pressure effects their orientation but compare to other drains it maintains its efficaciousness. These reflect in the value of  $C_c$  of SW and CJ which results into effective compressibility of soil.
- The  $e$  vs.  $\log p$  relationship and  $C_c$  vs. pressure indicate that because of effectiveness of CJ drain the compression index under lighter loading remains in the range of such a value that soil structure follow easy rate of dissipation showing low porosity compare to SD.
- Initial curvature portion of  $e$  vs.  $\log p$  relationship interpret soil structural resistance that is hydrodynamic lag against compressive load which giving resistance to deformation as mentioned earlier. This structural resistance or hydrodynamic lag against compression is more pronounced in SW and SD compare to PF and CJ drain. CJ or PF allows higher gradient of radial flow forming structural orientation of particle accordingly pushing the particles against face to edge bonds of random orientation bringing close to each other in a parallel orientation cultivating face to face bonds showing more shear strength of a consolidated mass. The same thing is reflected in values of compression index of the soil structure produced by various drains. In micrographs of sample collected after loading of 320kPa exhibit the same thing of above materials. (put three plots of micrograph)-
- For any depth the % porosity remains less at any consolidation pressure with coir-jute drain compare to sand drain exhibiting effective consolidation.
- In general the degree of orientation(decrease of angle between particles) of particles in the soil structure undergoing consolidation indicate comparatively more face-to-face contact towards drain. Also this pattern is exhibited depth wise for any radial distance and drain material.
- In case of SD the degree of orinetation during consolidation is more near the drain (radial point  $r_1$ ) compare to CJ, while more degree of orientation is observed in CJ at



middle radial point  $r_2$  compare to SD, and almost same degree of orientation is observed in CJ & SD at farthest radial point  $r_3$ .

- This is because of incase of SD consolidation proceeds faster near the drain thereby causing comparativley more surface settlment in that region, it could very well cause a redistribution of surface loading. While in case of CJ the condition of free strain develops which is implied that the settlment at the surface did not change the distribution of load to the soil at any location. At mid radial distance  $r_2$ , the plot indicates effectiveness of CJ drain in early achievement of face-to-face oreintation of particle.

Coefficient of horizontal permeability ( $k_h$ ) vs. applied pressure

- From the above discussion it indicates that  $K_h$  value of drain increases the efficacy of rate of drainage through soil thereby it reflects coefficient of transmissivity of water through soil. For any pressure the  $k_h$  value of CJ remains efficient compare to others.
- Void ratio-pressure relationship can be of initial flocculated structure or random type of structure. The magnitude of the bonding force defining the flocculated state will control the curvature middle region. This critical region is not well defined for the random structure clay, since the bonding forces are smaller than the flocculated structure. Our is the intermediate stage of flocculated and random soil structure. The critical region is defined to some extent exhibiting some bonding forces are prevalent edge to face bonds (which is already illustrated in chapter 6 of analysis) the resistance during 'microcompressibility' occurring under lighter load is clearly reflected in the critical zone. Viewed microscopically, particles in a randomly oriented particles sample are rotated into more parallel orientation and then pushed closed together. These two actions probably occur simultaneously. Pushing particles closer together involves action against interparticle forces of repulsion, but particle rotation must also be considered as an integral part of compression. After critical region of curve, the fall down of curve indicate structural breakdown that occurs under consolidation pressure sufficient large to disrupt the bonds formed in the soil structure as interpreted from various plots of micrograph. The abrupt

change in slope beyond preconsolidation pressure in the latter zone of curve might be viewed as the collapse of matrix. Tortuosity with respect to actual flow path and thickness of sample works out to tend towards unity from analysis of micrographs indicating soil particles more oriented having face to face configuration.

#### Shear strength

- Comparing effect of various drain materials, the shear strength achieved at end of consolidation it is observed that CJ gains highest shear strength compare to SW, SD, PF. Soft clay consolidated by CJ gained a shear strength of 153kPa compare to shear strength gained by SW, PF, SD as 120kPa, 118kPa and 100kPa respectively. The curve of CJ lies on the top for all three radial distances while curve of SW and PF are nearly at same level indicating similar strength and curve of SD lies below the curve of PF indicating achievement of lowest shear strength.

#### **Influence of Drain Diameter ('n' value)**

##### **I) Rate of Consolidation (Influence of 'n' value keeping same material of drain and same pressure)**

#### Degree of consolidation ( $U_r$ ) vs. Time

- It concludes that for 50% consolidation,  $n=11.04$  takes 48% and 71% less time compared to  $n=16.93$  and 21.71 for any drain material under light loading (upto 40kPa) and 53%, 63%, under constructional loading (160kPa and greater). Similarly for 80% consolidation,  $n=11.04$  takes 35% and 61% less time compared to  $n=16.93$  and 21.71 for any drain material under light loading and 37%,54% under constructional loading.
- From pore pressure measurements, it infers that for 50% consolidation and mid plane radial point  $r_2$ ,  $n=11.04$  takes 59% and 76% less time compared to  $n=16.93$  and 21.71 for any drain material under light loading and 65%,77%, under constructional loading. Similarly for 80% consolidation,  $n=11.04$  takes 42% and 61% less time compared to  $n=16.93$  and 21.71 for any drain material under light loading and 51%,67% under constructional loading.

- In case of coir-jute drain(CJ) at 50% consolidation,  $n=11.04$  takes lowest time of 330min & 185min amongst other drains under light and construction loadings respectively. Also for 80% consolidation CJ and  $n=11.04$  remain effective exhibiting lowest time of 750min & 550min time under light and constructional loading respectively as discussed earlier.
- It concludes that for 50% consolidation,  $n=11.04$  takes 135% and 300% less time compared to  $n=16.93$  and 21.71 for any drain material under light loading and 203%,413%, under constructional loading. Similarly for 80% consolidation,  $n=11.04$  takes 73% and 203% less time compared to  $n=16.93$  and 21.71 for any drain material under light loading and 86%,225% under constructional loading.
- From pore pressure measurements, it infers that for 50% consolidation and mid plane radial point  $r_2$ ,  $n=11.04$  takes 197% and 420% less time compared to  $n=16.93$  and 21.71 for any drain material under light loading and 239%,423%, under constructional loading. Similarly for 80% consolidation,  $n=11.04$  takes 81% and 180% less time compared to  $n=16.93$  and 21.71 for any drain material under light loading and 119%,228% under constructional loading.
- For any load intensity and 'n' value of any drain material, the time deformation curve with respect to pore pressure dissipation remain towards the vertical axis compare to curve of settlement, that is time require for 50% or 80% consolidation is less compare to settlement curve which also reflects in isochrones curves. The curve of pore pressure for 'n' equal to 11.04 shifts towards vertical axis compare to 'n' equal to 16.93 and 21.71 for any drain material and for any pressure. While curve of pore pressure of 'n' equal to 16.93 align left of 'n'21.71 for any drain material. The reasons for this is the specific surface area of drain which gives direct flow path to water particle for dissipation of pore water. More the specific surface area, more the discharge and higher the compressibility of soil mass. The above reason can be justified by the microporosity measured for all drains of different 'n' values which is presented in chapter 6.

Coefficient of consolidation due to radial drainage ( $C_r$ )-Degree of consolidation ( $U_r$ ) relationship

- During settlement measurements it concludes that  $n=11.04$  for 50% consolidation shows 76% and 69% higher  $C_r$  value compare to  $n=16.93$  and 21.71 for any drain material under light loading and 81% and 75% under constructional loading. Similarly for 80% consolidation shows 67% and 60% higher  $C_r$  value compare to  $n=16.93$  and 21.71 for any drain material under light loading and 69% and 63% under constructional loading.
- During pore pressure measurements for middle radial point  $r_2$  it concludes that  $n=11.04$  for 50% consolidation shows 405% and 583% higher  $C_r$  value compare to  $n=16.93$  and 21.71 for any drain material under light loading and 483% and 580% under constructional loading. Similarly for 80% consolidation shows 227% and 239% higher  $C_r$  value compare to  $n=16.93$  and 21.71 for any drain material under light loading and 290% and 298% under constructional loading.
- $n=16.93$  is found to be more efficient then  $n=21.71$  under both light and constructional loadings.  $n=16.93$  shows averagely 92% higher  $C_r$  value under light loading while 60% higher under constructional loading compare to  $n=21.71$  but 61% lower compare to  $n=11.04$  under light loading and 56% lower under constructional loading.
- The general pattern of  $C_r$  vs. pressure for any 'n' value indicates that it increases with pressure, but at 50% consolidation variation in  $C_r$  value is higher compare to 80% consolidation. In pore pressure measurement under lighter loading there is variation in  $C_r$  value, but constancy is maintained after 50kPa for any 'n' value.
- For  $n=11.04$  the maximum value of  $C_r$  is  $8.09 \times 10^{-4} \text{ cm}^2/\text{sec}$  &  $7.02 \times 10^{-4} \text{ cm}^2/\text{sec}$  at 50% and 80% consolidation for CJ from settlement consideration.
- For  $n=16.93$  average  $C_r$  value ranges from  $1.46 \times 10^{-4} \text{ cm}^2/\text{sec}$  &  $3.49 \times 10^{-5} \text{ cm}^2/\text{sec}$  for 80% consolidation for constructional loading from settlement and pore pressure measurements respectively.
- For  $n=21.71$  average  $C_r$  value ranges from  $1.78 \times 10^{-4} \text{ cm}^2/\text{sec}$  &  $4.7 \times 10^{-5} \text{ cm}^2/\text{sec}$  for 80% consolidation for constructional loading from settlement and pore pressure measurements respectively.

- Average  $C_r$  value for  $n=16.93$  remain in between  $n=11.04$  and  $n=21.71$ . The lowest average value of  $n=21.71$  signifies inefficiency of the drains of any material compare to drains of other 'n' value.

#### Isochrones

- From the consolidation ratio vs. radius of influence for various  $T_r$  values reveals that sequence of consolidation for CJ of  $n=11.04$  at any radius of influence seems to be efficient compare to all other drains. Comparing isochrones of all three 'n' values it is concluded that  $n=11.04$  is more effective compare to  $n=16.93$  and  $n=21.71$ , while  $n=16.93$  is more superior compare to  $n=21.71$  for all drain materials.
- Trajectory of isochrones for  $n=11.04$  lies above the  $n=16.93$  and  $n=21.71$  for both light and constructional loading. Also trajectory of isochrones for  $n=16.93$  lies above  $n=21.71$  for all drain materials and loadings.

#### Lumped parameter ( $\lambda$ ) vs. Degree of consolidation ( $U_r$ )

- As ' $\lambda$ ' value increases, drain diameter ('n' value) decreases. Experimental results almost match with theoretical results with  $\lambda=-0.2$  particularly for CJ for  $n=11.04$ ,  $\lambda = -0.19$  for  $n=16.93$  and  $\lambda = -0.18$  for  $n=21.71$  proves to be efficient amongst other drains. From theoretical considerations  $n=11.04$  proves to be efficient amongst other 'n' values.

## **II) Magnitude of Consolidation**

#### Compression index ( $C_c$ ) vs. applied pressure

- With the same drain  $C_c$  value shows increasing trend with higher 'n' value. It signifies that because of low rate of dissipation in higher 'n' values the magnitude of compressibility increases at particular period of interval. This behavior is similar for all drains.  $C_c$  value for coir-jute drain(CJ), Sandwich drain(SW), Polypropylene fiber drain(PF), Sand drain(SD) for  $n=11.04$  are 0.272, 0.279, 0.292, and 0.312 respectively.
- Amongst the various 'n' values the n equal to 11.04 provides optimum specific surface area to the saturated surrounding soil structure for a given diameter of

influence zone of soil mass. Because of this gradient of radial flow during consolidation can help producing low level of structural resistance to compression in this case compare to other 'n' value of 16.93 and 21.71. The load component during higher level of loads can help structural breakdown or pushing the particles at a more rate leading to final consolidated mass at 320kPa. It is reflected in micro porosity, degree of orientation and tortousity measurement graphs drawn for the final load.

Coefficient of horizontal permeability ( $k_h$ ) vs. applied pressure

- The horizontal permeability ( $k_{h50}$ ) obtained by settlement decreases with increase in the pressure for almost all drains and for all 'n' values.
- From settlement analysis it concludes that  $n=11.04$  for 50% consolidation shows 278% and 289% higher  $k_h$  value compare to  $n=16.93$  and 21.71 for any drain material under light loading and 735% and 3025% under constructional loading. Similarly for 80% consolidation shows 190% and 200% higher  $k_h$  value compare to  $n=16.93$  and 21.71 for any drain material under light loading and 442% and 1862% under constructional loading.
- From pore analysis for middle radial point  $r_2$  it concludes that  $n=11.04$  for 50% consolidation shows 305% and 373% higher  $k_h$  value compare to  $n=16.93$  and 21.71 for any drain material under light loading and 732% and 2747% under constructional loading. Similarly for 80% consolidation shows 165% and 134% higher  $k_h$  value compare to  $n=16.93$  and 21.71 for any drain material under light loading and 454% and 1460% under constructional loading.
- $n=16.93$  shows more coefficient of transmissivity of pore water then  $n=21.71$  under both light and constructional loadings.
- From settlement analysis  $n=16.93$  shows averagely 47% and 512% higher  $k_h$  value under light loading and constructional loading compare to  $n=21.71$  but 37% and 77% lower compare to  $n=11.04$  under light loading and constructional loading for 50% consolidation under any drain material.

- From pore pressure analysis  $n=16.93$  shows averagely 63% and 411% higher  $k_h$  value under light loading and constructional loading compare to  $n=21.71$  but 45% and 73% lower compare to  $n=11.04$  under light loading and constructional loading for 50% consolidation under any drain material.
- From pore pressure analysis for 50% consolidation it concludes that  $k_h$  value of mid plane pore pressure for CJ works out to be 76% and 146% higher under light loading and constructional loading compare to PF for any 'n' value while for 80% consolidation CJ shows 33% and 77% higher value under light loading and constructional loading respectively.

### Shear strength

- Gain in shear strength was observed for all three 'n' values for any drain material after consolidation, but highest gain was observed in case of 'n' equal to 11.04 for any drain material. Average post shear strength increased to 150kPa from pre shear strength of 15kPa.
- Shear strength increases as 'n' value decreases (drain diameter increases) for any drain material. Comparing effect of various 'n' values for CJ drain, the shear strength achieved at end of consolidation is highest for 'n' equal to 11.04 compare to 16.93 and 21.71. The shear strength achieved for n' equal to 11.04, 16.93 and 21.71 is 153kPa, 129kPa, and 109kPa respectively. Also more shear strength is observed for nearest radial point and this effect is true for any 'n' value. The curve of 11.04 lies above the curve of 'n'16.93 and 'n'21.71 for any drain material. Lowest gain in shear strength is observed in case of SD compare to CJ, SW, PF, while almost low strength is observed in case of 'n'21.71 for all drain materials. In general 'n' equal 11.04 provides more specific surface area being larger diameter of the particle which facilitate easy and more dissipation of pore water pressure under particular load thereby bringing the particle close together in a parallel orientation in more number.

### **Influence of Geometry (shape) of Drain**

## I) Rate of Consolidation

### Degree of consolidation ( $U_r$ ) vs. Time

- Considering settlement measurement it concludes that for 50% consolidation, CSSD of  $n=11.04$  takes 41% less time compared to any drain material under light loading and 48%, under constructional loading. Similarly for 80% consolidation, CSSD takes 39% less time compared to any drain material under light loading and 36% under constructional loading.
- From pore pressure measurements, it infers that for 50% consolidation and mid plane radial point  $r_2$ , CSSD of  $n=11.04$  takes 13% less time compared to other drain shapes under light loading and 20% under constructional loading. Similarly for 80% consolidation, CSSD takes 15% less time compared to other drain shapes under light loading and 18% under constructional loading.
- CSSD of  $n=11.04$  takes lowest time in compare to BSSD, PSSD, TSSD both under light and constructional loading. However BSSD for 50% consolidation takes 12% & 23% lower time in compare to PSSD & TSSD but 50% higher in compare to CSSD under light loading. Also PSSD takes 13% lower time compare to TSSD but 70% higher in compare to CSSD. Similarly BSSD for 80% consolidation takes 12% & 12% lower time in compare to PSSD & TSSD but 53% higher in compare to CSSD under light loading. Also PSSD takes equal time compare to TSSD but 73% higher in compare to CSSD.
- For any load intensity and for any geometry of sand drain with 'n' value equal to 11.04, the time deformation curve with respect to pore pressure dissipation remain towards the vertical axis compare to curve of settlement, that is time require for 50% or 80% consolidation is less compare to settlement curve which also reflects in isochrones curves.
- Though from the point of rate of dissipation of pore pressure for a circular shape drain seems to be efficient, the band shape drain provide best construction facility during installation in terms of cost and speed of work.

---

CSSD= Circular shape sand drain, PSSD = Plus shape sand drain

BSSD = Band shape sand drain, TSSD = Tripod shape sand drain



- Based on the equivalent diameter concept the dimensions of various shapes of drain are worked out. Though surface area of plus shape and tripod shape drain work out to be higher than band shape and circular shape drain, the draining efficiency of circular and band shape is higher than other two shapes of drain. It may be due to right and acute angles of the drain which intercept the path of flow of water to some extent.
- Under compressional stresses the drain-clay interface are not remaining compatible with the deform shape of the drain, therefore the higher surface area of plus and tripod shape drain are not remaining advantageous for the easy flow of water from the central drain.
- For any load intensity and for any geometry of sand drain with 'n' value equal to 11.04, the time deformation curve with respect to pore pressure dissipation remain towards the vertical axis compare to curve of settlement, that is time require for 50% or 80% consolidation is less compare to settlement curve which also reflects in isochrones curves. The curve of pore pressure for CSSD shift towards vertical axis compare to BSSD, PSSD and TSSD for any pressure for same specific surface area. The curve of CSSD remain towards vertical axis showing less time for 50% consolidation thereafter all curves merge to some extent. The curve of BSSD remains towards vertical axis more compare to curve of BSSD and TSSD for both pore pressure and settlement measurements. The above observation may be due to higher hindrance for the conductivity of the radial flow to the drain compare to other drains wise band, tripod and plus shape. This is in similitude with flow per unit time through various shaped notch under constant head. That is circular notch gives higher discharge compare to rectangular notch, plus shape notch and tripod shape notch. The hydraulic conductivity will always remain uniform through circular one, least quantum of vortex is observed in circular one compare to other shape notch. To some extent this is true for flow through different shape drain with a different hydraulic mean radius of capillary formed.

---

CSSD= Circular shape sand drain, PSSD = Plus shape sand drain

BSSD = Band shape sand drain, TSSD = Tripod shape sand drain

Coefficient of consolidation due to radial drainage ( $C_r$ )-Degree of consolidation ( $U_r$ ) relationship

- From settlement analysis it concludes that CSSD of  $n=11.04$  for 50% consolidation shows 71% higher  $C_r$  value compare to other geometry of drains under light loading and 96% under constructional loading. Similarly for 80% consolidation shows 65% higher  $C_r$  value compare to other geometry of drains under light loading and 57% under constructional loading.
- From pore pressure analysis for middle radial point  $r_2$  it concludes that  $n=11.04$  for 50% consolidation shows 12% higher  $C_r$  value compare to other geometry of drains under light loading and 21% under constructional loading. Similarly for 80% consolidation shows 14% higher  $C_r$  value compare to other geometry of drains under light loading and 18% under constructional loading.

Coefficient of consolidation due to radial drainage ( $C_r$ ) vs. applied pressure

- The general pattern of  $C_r$  vs. pressure for any shape of drain indicates that it increases with pressure, but at 50% consolidation variation in  $C_r$  value is higher compare to 80% consolidation. In pore pressure measurement under lighter loading there is variation in  $C_r$  value, but constancy is maintained after 50kPa for any shape of drain.
- Average  $C_r$  value for BSSD remain in between CSSD and PSSD. The lowest average value of TSSD signifies inefficiency of the drain geometry compare to geometry of other drains.

Isochrones

- From the consolidation ratio vs. radius of influence for various  $T_r$  values reveals that sequence of consolidation for CSSD of  $n=11.04$  at any radius of influence seems to be effective compare to other geometry of drains. Comparing isochrones of all four shapes it is concluded that CSSD is more effective compare to others, while BSSD is superior compare to PSSD & TSSD for same drain material. Trajectory of isochrones

for CSSD lies above the BSSD, PSSD, TSSD for both light and constructional loading. Overall TSSD is in-effective in increasing rate of compressibility and dissipation of pore water pressure.

Lumped parameter ( $\lambda$ ) vs. Degree of consolidation ( $U_v$ )

- Experimental results almost match with theoretical results with  $\lambda = -0.125$  particularly for CSSD,  $\lambda = -0.12$  for BSSD,  $\lambda = -0.11$  for PSSD and  $\lambda = -0.1$  for TSSD proves to be efficient amongst other drains. From the above analysis it can be said that Circular shape is more efficient in compare to other shapes in accelerating rate of consolidation.

**II) Magnitude of Consolidation (e vs. log P)**

Compression index ( $C_c$ ) vs. applied pressure

- It is observed that for CSSD lower  $C_c$  value is obtained compared to other geometry of sand drains. It signifies that because of low rate of dissipation in other shapes of drains the magnitude of compressibility increases at particular period of interval. This behavior is similar for all drains.  $C_c$  value for CSSD, BSSD, PSSD, and TSSD for  $n=11.04$  are 0.161, 0.241, 0.271, and 0.282 respectively. Under no geodrain condition the value of  $C_c$  is 0.42.
- There is no much variation of Compression index with shape of drain, though the rate of drainage for a particular static loading seems to be faster in CSSD compared to others.
- Circular shape sand drain experience least interference of dissipation of radial flow compare to band drain, tripod shape and plus shape drain. This more and easy dissipation of pore pressure is because of the higher gradient of water flow through soil structure which has been cultivated under the load. Under lighter load because of the structural resistance it shows convex upward curve while after critical zone the particle orientation leading to parallel alignment exhibit higher slope of the curve (e vs. log p) tending to final consolidated soil mass having face to face bond.

---

CSSD= Circular shape sand drain, PSSD = Plus shape sand drain

BSSD = Band shape sand drain, TSSD = Tripod shape sand drain

Coefficient of horizontal permeability ( $k_h$ ) vs. applied pressure

- From settlement analysis it concludes that  $n=11.04$  for 50% consolidation shows 274% higher  $k_h$  value compare to any shape of sand drain under light loading and 36% under constructional loading. Similarly for 80% consolidation shows 259% higher  $k_h$  value compare to any shape of sand drain under light loading and 9% under constructional loading.
- From pore pressure analysis for mid plane radial point  $r_2$  it concludes that CSD of  $n=11.04$  for 50% consolidation shows 143% higher  $k_h$  value compare to any shape of sand drain under light loading and 15% lower under constructional loading. Similarly for 80% consolidation it shows 149% higher  $k_h$  value under light loading and 18% lower under constructional loading.

Shear Strength

- More gain in shear strength is observed in case of CSSD compare to PSSD, BSSD and TSSD for same ' $n$ ' value and same specific surface area. The shear strength observed in case of CSSD, PSSD, BSSD, and TSSD in terms of magnitude is 96kPa, 90kPa, 86kPa and 82kPa respectively. The shear strength increases towards the drain for all shapes of drain. Sample having CSSD have marked strength compare to others. The strength is 1.07, 1.12, and 1.17 times higher compared to PSSD, BSSD and TSSD. The reasoning for the above is as follows. Though all the drains have same specific surface area, the radial flow towards the drain experience hindrances in PSSD, TSSD and BSSD. BSSD has good versatility in the installation process but dissemination of pore pressure through BSSD takes more time and structure of soil produced may not be well oriented with face-to-face contact. Same is the story with other drains, then circular one. CSSD controls rate as well as magnitude of the pore pressure dissipation in achieving required strength.

**Dynamic Analysis of Consolidated Clay Bed by Central Vertical Geodrain**

Post vane shear strength of reinforced consolidated clay mass before application of seismic stresses

- For sandwicks of  $n = 16.93$  the results of vane shear strength indicate that strength increases from 14.6 kPa to a maximum of 113.7 kPa i.e. 88% increment. It was also observed that strength is more towards the first radial point  $r_1$  while it is less at  $r_3$  i.e. 101.5 kPa. But generally for analysis the mid radial point ( $r_2$ ) is considered in design. For  $n = 21.71$  the strength increased from 12.1 kPa to 99.1 kPa i.e. 87% increment without application of seismic stresses. In this case also the strength was maximum at  $r_1$  while it was minimum at  $r_3$  i.e. 97.4 kPa. This result indicates that as the diameter of drain increases the soil shear strength also increases.
- In brief, before consolidation of the soil sample, the same strength (12.5 kPa) for any radial distance is observed for all the 'n' value. The strength of consolidated soil mass at the end of 320 kPa load intensity exhibits 9 times strength than 10 kPa for  $n = 16.93$ , while for  $n = 21.71$  it is about 7.5 times. The strength at mid radial point is less than the strength nearer to drain and more than farthest radial point  $r_3$ .

Post vane shear strength of reinforced consolidated clay mass after application of seismic stresses

- Under dynamic analysis, SW of  $n = 16.93$ , the vane shear strength indicates that the % loss in strength is more during first or initial vibration, afterwards the loss in strength is more or less constant. The average strength for  $n = 16.93$  decreased from 108.53 kPa to 51.10 kPa i.e. 53% decrement for vibration period of 5 seconds. While for  $n = 21.71$  the average strength decreased from 99.0 kPa to 46.3 kPa i.e. 53% decrement. Initial earthquake shock (period of vibration equal to 5 sec) is sufficient to cause metastable condition in card house structure of soft clay for any 'n' value but smaller the 'n' value more resistance is offered against strength loss. In any  $n = 16.93$  the % strength loss (46%) is less than  $n = 21.71$ . Percentage loss in strength for any period of vibration is less in smaller 'n' value compared to higher 'n' value 11.04.

- For  $n=16.93$  under seismic stresses the results of vane shear strength for seismic period of 15 secs, 30 secs, 60 secs and 120 secs indicates that %loss in strength is 46% averagely remains constant though seismic periods was increased while if we consider the net effect in strength then it is only 6 to 8% which may be an indication of particle rearrangement or the card house structure of soft clay to have become horizontal whose metastability was not affected by adsorbed water at later stages to some extent. While for  $n=21.71$  the % loss in strength was averagely 68% which is much higher compare to  $n=16.93$  values. Also it was observed that there was no change in in-situ placed condition of sandwich or even no settlement of only sandwich was observed nor any change in its diameter was observed indicating sandwich as a stable drain under seismic conditions which prevents the soft soil to get quick.
- Initial earthquake shock (period of vibration equal to 5 sec) is sufficient to cause metastable condition in card house structure of soft clay for any 'n' value but smaller the 'n' value more resistance is offered against strength loss. In any  $n=16.93$  the % strength loss (46%) is less than  $n=21.71$ . Percentage loss in strength for any period of vibration is less in smaller 'n' value compare to higher 'n' value 11.04.

#### **Influence of Water Content Ratio (WCR)**

- As water content ratio increases the value of  $C_c$  increases for any drain material and for same 'n' value. For same water content ratio the variation in compression index ( $C_c$ ) value for different drain material indicate 0.556 for coir-jute drain (CJ), 0.546 for sandwich drain (SW), 0.538 for polypropylene fiber drain (PF) and 0.532 for sand drain (SD). From the pattern of variation it infers that for same  $C_c$  value the WCR remains in the ascending order of CJ, SD, PF and SW. For same WCR, the  $C_c$  values are descending order of CJ, SW, PF and SD.
- Coir-jute drain show lowest water content at the end of any load amongs various drains proving its ability to consolidate soil more compare to others.

#### **Influence of Consolidation Pressure Ratio (CPR)**

- As CPR value increases the compression index ( $C_c$ ) value increases for any drain material. In the higher range of CPR value, the  $C_c$  value is in the order of CJ, SW, PF and SD while for lower range of same CPR value the sequence is in the order of CJ, SW, SD and PF.
- As CPR increases  $k_v$  and  $k_h$  increases for any drain material and therefore the ratio  $k_h/k_v$  increases as CPR increases for any drain material. Among various drains, CJ gives highest  $k_h/k_v$  of the order of 27 which indicates CJ drain facilitates more gradient of water towards drain forming displacement of particles in such a way that horizontal permeability of soil increases leading ratio more for end of any load.

### Scanning Electron Microscopy

Scanning electron microscopy (SEM) along with the quanti-image analyzer with system of MIC (micro-structure characterization) software has been employed to deduce the interpretation by this nano technology, which will give the relative compression of circular soil sample from extreme radial distance to interface of drain with soil.

#### *Influence of micro-porosity*

- From nano analysis of micrograph, it interprets that for same height level of sample the percentage micro pores are increasing from central drain radially to outer radial point. Between nearest radial point  $r_1$  and clay-drain interface the percentage decrease of micro pore is more compared to mid plane radial point  $r_2$  and outward radial point  $r_3$ . Because of faster rate of dissipation the achieved void ratio or porosity which is worked out is less in case of coir-jute drain compare to sand drain.
- Though, the micro pore distribution at interface(drain-soil) at any level (height) is less compare to  $r_1$ ,  $r_2$  and  $r_3$ , in general the distribution of the micro-porosity exhibit higher magnitude of consolidation with increase of depth at any radial point however, it has been confirmed this observation at mid plane radial point  $r_2$ . In general the degree of orientation(decrease of angle between particles) of particles in the soil structure undergoing consolidation indicate comparatively more face-to-face contact towards drain. Also this pattern is exhibited depth wise for any radial distance and drain material.

*Influence of angle of orientation*

- The software measurement for angle of angularity of one particle with other of various micrographs indicate that orientation of particle becomes more or less face to face to some extent as we approach towards drain from extreme radial point.
- In case of SD the degree of orientation during consolidation is more near the drain (radial point r1) compare to CJ, while more degree of orientation is observed in CJ at middle radial point r2 compare to SD, and almost same degree of orientation is observed in CJ & SD at farthest radial point r3.

*Influence of Tortousity*

- Tortousity is a real measure of actual flow path towards radial direction towards central drain during consolidation process. Tortousity tends to unity in case of CJ drain compare to SD as mentioned earlier. Soil structure because of the gradient of flow in horizontal direction and vertical load help causes more quantum of face-to-face contact in the former case. For the same drain the depth wise tortousity also indicate the effect of over burden to some extent. In case of coir-jute drain the tortouisty at interface and at mid radial point are almost same indicating uniform surface settlment unlike sand drain.

The theoretical relationship obtained between average degree of consolidation versus time factor for various values of ' $\lambda$ ' both for positive and negative range fits well with the experimental results obtained from the laboratory studies. The above findings will give definitely provide a ready solution to the design engineers and field persons in making the selection of effective drain material, optimum drain diameter(size) and easy workable drain geometry with respect to site conditions. The appropriate value of lumped parameter ' $\lambda$ ' will directly give the clue to design engineer regarding the selection of prefabricated vertical geodrain with respect to field conditions.



## LIST OF RESEARCH PUBLICATIONS

(BASED ON **PRESENT Ph. D WORK** - INTERNATIONAL CONFERENCES,  
NATIONAL CONFERENCES & JOURNALS)

### **INTERNATIONAL** CONFERENCES/SYMPOSIUMS/WORKSHOPS/SEMINAR

|   |
|---|
| 1) Settlement Performance Of Soft Clays Using Sandwich Drain With Varying Diameter “by M.V. Shah, Dr.A.V. Shroff, <b>Proc. of Int.Conf. on infrastructure development on expansive soils</b> , Erode Sengunthar Engg.College(A.P), Feb-2006   |
| 2) "Experimental Study On Performance Of Sand Drain On Kaolinite With Varying Drain Diameter“ by M.V. Shah, T.A. Khan,Dr. A.V. Shroff, <b>Proc. of XIII-Danube-European Conf. on Geotechnical Engineering</b> , Vol-I, pp-349-354,Danube,May-2006, ISBN(Vol-I) 961-90043-8-8 & ISBN(Vol-II) 961-90043-9-6   |
| 3) "Radial Consolidation By Using Sandwiches“by M.V. Shah, T.A. Khan, Dr. A.V. Shroff, <b>Proc. of Int.Conf. on Physical Modeling in Geotechnics</b> , HongKong University of Science and Technology, HongKong, Vol-I,Aug-2006,pp-565-570, ISBN:0-415-41586-1, 0-415-41587-X, 0-415-41588-8, Pub: Taylor & Francis/Balkema  |
| 4) "Effect Of Ratio Of Influence Zone And Type Of Vertical Drain On Consolidation Of Soft Clay Due To Radial Flow“ by M.V. Shah, Dr. A.V. Shroff,T.A. Khan,Dr. N.H. Joshi, <b>Proc. of IV Int.Conf.on Soft-soil Engineering</b> , Canadian Geotechnical Society, University of Alberta, Canada,Vol-I,pp-765-773,Oct-2006,Soft Soil Engg-Chan & Law(eds),Taylor& Francis Group, ISBN 13978-0-415-42280-2 |
| 5) "Effect On Coastal Soils Using Prefabricated Vertical Geodrains Under Seismic Stresses“byM.V.Shah,Dr.A.V.Shroff, <b>Proc.ofFirstSriLankanGeotechnicalSociety,(SLGS)International Conference on Soil and Rock Engg</b> , Colombo,Vol-I, Aug-2007  |
| 6) "Laboratory study on effect of shape of mandrel on consolidation of soft clays using oedometer“ by M.V.Shah,Dr.A.V.Shroff, <b>Proc.of 60<sup>th</sup> Canadian Geotechnical conference &amp; 8<sup>th</sup> Joint CGS/IAH – CNC Groundwater Conf.</b> , Ontario, Canada,Vol-I, Oct-2007  |
| 7) "Settlement performance of soft clays using coir-jute drain under  |

|  |
|--|
| radial drainage using Oedometer “by M.V.Shah,Dr.A.V.Shroff, <b>Proc.of 10<sup>th</sup> Australia New Zealand conference on Geomechanics</b> , Brisbane,Vol-I, Oct-2007   |
| 8) ”Consolidation of soft clays using polypropylene fibers through inward radial drainage “by M.V.Shah,Dr.A.V.Shroff, <b>Proc.of The First Pan American Geosynthetics conference &amp; Exhibition</b> , Mexico,Vol-I, March-2008   |
| 9) ”Laboratory experiment to study isochrones using plus shape sand drain“ by M.V.Shah,Dr.A.V.Shroff, <b>Proc.of Int.Conf.on The challenge of sustainability in the Geoenvironment, (GEOCONGRESS)</b> ,New Orleans, Louisiana, USA,March-2008  |
| 10) ”Effect Of Prefabricated Vertical Coir-Jute Geodrain On Pore Water Pressure Dissipation Using Oedometer“by M.V.Shah,Dr.A.V.Shroff, <b>Proc.of Int.Conf.on Geotechnical Earthquake Engg &amp; Soil Dynamics</b> , Sacramento, CA,May-2008   |
| 11) ”A Case Study On Stability Analysis Of Surajbari Bridge Approach Slope After Bhuj Earthquake” by M.V.Shah,Dr.A.V.Shroff,Jai Bhagwan, <b>Proc.of 6th Int.Conf. on Case Histories in Geotechnical Engg</b> , University of Missouri-Rolla,Vol-I, Aug-2008  |
| 12) ”Soft soil consolidation by radial flow using prefabricated vertical geodrains”, by M.V.Shah,Dr.A.V.Shroff, <b>Proc.of 17<sup>th</sup> ICSMGE</b> ,Egypt, Oct-2009   |
| 13) Laboratory Study On Effect Of Shape Of Mandrel On Consolidation Of Soft Clays Using Oedometer“ by M.V Shah, Dr. A.V Shroff, <b>Proc. of Int.Conf.on Sixth Asian Young Geotechnical Engineers Conference</b> -IISc-Banglore, Vol-I, Dec-2009  |
| 14) ”Consolidation Of Soft Clay Using Prefabricated Vertical Geodrains Through Radial drainage” by M.V Shah, Dr. A.V Shroff, <b>Proc. of Int. Symposium on Geotechnical Engineering, Ground Improvement &amp; Geosynthetics for sustainable mitigation and adaptation to climate change including global warming</b> , Thailand, Vol-I, Dec-2009 |
| 15) ”Theory of Consolidation through Radial Drainage for Soft Soils using Vertical GeoDrain“ by M.V Shah, Dr. A.V Shroff, <b>Proc. of Int. Symposium on GIT and Case Histories (ISG09)</b> ,Singapore, Vol-I, Dec-2009   |

|  |
|--|
| 16)"Influence Of Diameter And Geometry Of Vertical Sand Drain On Consolidation Characteristics Of Kaolinitic Clay Due To Radial Drainage" by M.V Shah, Dr. A.V Shroff, <b>Proc. of Int. Conf. on New Developments in Geotechnical Engineering Analysis, Modeling and Design</b> ,USA, Feb-2010   |
| 17)"Soil-Structure Interaction Of Soft Clay Using Prefabricated Vertical Geodrains Under Seismic Stresses" by M.V Shah, Dr. A.V Shroff, <b>Proc. of 5<sup>th</sup> Int. Conf. on Recent Advances on GTE &amp; Soil Dynamics</b> , California, May-2010, Paper no. 5.53a, ISBN(Abstract)1-8870009-16-7 & ISBN(Proceedings)1-887009-15-9 |
| 18)Consolidation Of Soft Clay Using Prefabricated Vertical Geodrains Through Radial Drainage" by M.V Shah, Dr. A.V Shroff, <b>Proc. of 9<sup>th</sup> International Conf. on Geosynthetics</b> , Brazil, May-2010  |
| 19)"Influence of Diameter and Geometry of Vertical Sand Drain on Consolidation Characteristics of Kaolinitic Clay through Radial Drainage" by M.V Shah, Dr. A.V Shroff, <b>Proc. of 17<sup>th</sup> Southeast Asian Geotechnical Conf.</b> , Taipei, Taiwan, May-2010  |
| 20)"General Equation of Consolidation through Radial Drainage for Soft Soils using Vertical Geodrains" by M.V Shah, Dr. A.V Shroff, <b>Proc. of 2<sup>nd</sup> International Conf. on Applied Physics &amp; Mathematics(ICAPM)</b> , Kuala Lumpur, Malaysia, May-2010  |
| 21)"Non-Linear Theory of Consolidation through Radial Drainage for Soft Soils using Vertical Drains" by M.V Shah, Dr. A.V Shroff, <b>Proc. of 14<sup>th</sup> Danube-European Conf. on Geotechnical Engg</b> , Bratislava, Slovakia, June-2010, pp113, Vol-I, Slovak University of Technology, Bratislava ISBN 978-80-227-3279-6       |
| 22)"Non-Linear Theory of Consolidation through Radial Drainage for Soft Soils using Vertical Drains" by M.V Shah, Dr. A.V Shroff, <b>Proc. of 63<sup>rd</sup> Canadian Geotechnical Conference (Geo2010)</b> , Calgary, Alberta, Canada, Sept-2010   |
| 23)"Modeling Of Vertical Drains Using Modified Hydraulically Pressurized Oedometer" by M.V Shah, Dr. A.V Shroff, <b>Proc. of 6<sup>th</sup> International Congress on Environmental Geotechnics</b> , New Delhi, India, Nov-2010, pp-1739-1746, Tata McGraw Hill Publications, ISBN (13):978-0-07-070710-8, ISBN (10):0-07-070710-3    |

|     |  |
|-----|--|
| 24) | "Influence of Vertical Geodrains on Pore Water Pressure Dissipation using Oedometer" by M.V Shah, Dr. A.V Shroff, <b>Proc. of Int. Conf. on Advances in Geotechnical Engg</b> , Dallas, Texas, USA, Geo-Frontiers-2011, March-2011   |
| 25) | "Consolidation of soft clays using vertical GeoDrains" by M.V Shah, Dr. A.V Shroff, <b>Proc. of 14<sup>th</sup> Asian Regional Conference</b> , Hong Kong, China, May-2011   |
| 26) | "Influence of Vertical Geodrains on Consolidation Characteristics of Soft Soils " by M.V Shah, Dr. A.V Shroff, <b>Proc. of 5<sup>th</sup> Int.Symposium on Deformation Characteristics of Geomaterials</b> , Korean Geotechnical Society, Seoul, Korea, Aug-2011                                   |
| 27) | "Consolidation Characteristics of Kaolinitic Clays using Vertical Geodrains" by M.V Shah, Dr. A.V Shroff, <b>Proc. of XV European Conf on Soil Mechanics &amp; Geotechnical Engg(ECSMGE)</b> , Athens, Greece, Sept-2011   |
| 28) | "Consolidation of Soft Clays through Radial Flow Using Hydraulically Pressurized oedometer ", by M.V Shah, Dr. A.V Shroff, <b>Proc. Of ISSMGE Workshop on Advances in Multiphysical Testing of Soils and Shales</b> , Lausanne, 2012   |
| 29) | "Study on Mechanics of Hydrostatic excess Pore Water Pressure through Consolidation by Vertical Drains using Isochrones", by M.V Shah, Dr. A.V Shroff, <b>Proc. of 5th European Geosynthetics Congress</b> , International Geosynthetics Society and European Organizations, Valencia, Spain. 2012 |
| 30) | "Study on Pore Water Pressure Dissipation Phenomena of Soft Clays through consolidation using Vertical Drains", by M.V Shah, Dr. A.V Shroff, <b>Proc of ISSMGE-TC211 International symposium on Ground Improvement (ISGI)</b> , Brussels, Belgium , May-31& June 1-2012                            |
| 31) | "Soft Soil Consolidation using Prefabricated Composite Vertical Geodrains ", by M.V Shah, Dr. A.V Shroff, <b>Proc. Of International conf. on Ground Improvement (ICGI)</b> , 30 Oct-2 Nov. 2012, University of Wollongong, Australia.  |

**NATIONAL** CONFERENCES/SYMPOSIUMS/WORKSHOPS/SEMINAR

|   |
|---|
| 1) "Use Of Prefabricated Vertical Geodrains In Coastal Soils Under Seismic Stresses" by M.V. Shah, Dr.A.V. Shroff,Dr.N.H Joshi, <b>Proc. of NDM</b> ,Andhra University, Visakhapatnam ,Vol-I,Feb-2005   |
| 2) "Experimental study on performance of Sand drains" by T.A. Khan, Manish Shah, Dr.A.V.Shroff,Dr.N.H.Joshi, <b>Proc. of GEOPRACTICE</b> ,II Sc Bangalore,Vol-I, pp-207-217,July-2005   |
| 3) "Influence of sandwick in soft clays on radial pore pressure dissipation during consolidation"by M.V. Shah, Dr.A.V. Shroff, <b>Proc. of Nat.Conf. on Corrective Engg. Practices in Troublesome Soils</b> , JNTU & IGS-Kakinada chapter,Vol-I,July-2006             |
| 4) "Effect of ratio of influence zone and type of vertical drain on consolidation of soft clay due to radial flow" by M.V. Shah,Dr. A.V. Shroff, <b>Proc. of GEOTECHNICA</b> , IGS Delhi chapter & CSMRS, New Delhi, Vol-I, April-2007                                |
| 5) " Settlement performance of soft clays using sand drains through radial drainage using Oedometer" by M.V. Shah, Dr.A.V. Shroff, <b>Proc.of NCFRS</b> ,IIT-Roorkee,Vol-I,May-2007   |
| 6) "Influence of sandwick in soft clays on radial pore pressure dissipation during consolidation" by M.V.Shah, Dr.A.V.Shroff, <b>Proc.of 13<sup>th</sup> ARC</b> , Kolkatta, India Vol-I,pp-817-820,10.1-8-IN,Dec-2007  |
| 7) "Laboratory Study On Effect Of Shape Of Mandrel On Consolidation Of Soft Clays Using Oedometer" by M.V.Shah, Dr.A.V.Shroff, <b>Proc. of 2<sup>nd</sup> Indian Young Geotechnical Engineer Conf.(IYGE)</b> ,JNTU, Kakinada,Vol-I, March-2009                        |
| 8) "Influence of sandwick in soft clays on radial pore pressure dissipation during consolidation" by M.V.Shah, Dr.A.V.Shroff, <b>Proc. of National Conf. on Emerging Vistas of Technology in 21<sup>st</sup> Century(NCEVT09)</b> , PIT,Vadodara,India,Vol-I,Sep-2009 |
| 9) "Influence Of Diameter And Geometry Of Vertical Sand Drain On Consolidation Characteristics Of Kaolinitic Clay Due To Radial Drainage", by M. V. Shah, Dr. A. V. Shroff, <b>Proc. of</b>   |

|  |
|--|
| <b><i>Int.Conf.on Advances in Concrete Structural and Geotechnical Engineering</i></b> , BITS Pilani, INDIA (ACSGE), Vol-I, Oct-2009.  |
| 10)"Laboratory Study On Effect Of Shape Of Mandrel On Consolidation Of Soft Clays Using Oedometer" by M.V. Shah, Dr. A.V. Shroff, <b><i>Proc. of Int.Conf.on Sixth Asian Young Geotechnical Engineers Conference-IISc-Bangalore</i></b> , Vol-I, Dec-2009  |
| 11)"Study Of Isochrones Using Vertical Plus & Band Shape Sand drain" by M.V. Shah, Dr. A.V. Shroff, <b><i>Proc. of Indian Geotechnical Conf(IGC)</i></b> , Guntur,India, Vol-I, Dec-2009   |
| 12)"Influence Of Vertical Geodrain With Soil Structure Effects On Consolidation Characteristics Of Kaolinitic Clay " by M.V Shah, Dr. A.V Shroff, <b><i>Proc. of IGC-2010</i></b> , IIT Bombay, Powai, India, Dec-2010   |
| 13)"Influence Of Vertical Geodrain With Soil Structure Effects On Consolidation Characteristics Of Kaolinitic Clay" by M.V Shah, Dr. A.V Shroff, <b><i>Proc. of 3<sup>rd</sup> Indian Young Geotechnical Conference</i></b> , IGS,New Delhi,India,March-2011   |
| 14)"Consolidation Characteristics of Kaolinitic Clay through radial drainage using geometrical vertical sand drains, <b><i>Proc. of Indian Geotechnical Conference-Geochallenges (IGC2011)</i></b> , Kochi, Kerala, India, Dec-2011  |
| 15)"Influence of Seismic Stresses on Consolidation of Soft Soil and Soil-Structure Interaction Using Prefabricated Vertical Geodrains", <b><i>Proc. of Technical Research Advances in Civil Engineering (TRACE-2011)</i></b> ,LDRP Institute of Technology and Research,Gandhinagar, India, Dec-2011 |
| 16)"Consolidation of Soft Clays using Sanddrains and Sandwicks through Inward Radial Flow", by M.V Shah, Dr. A.V Shroff , <b><i>Proc of Conf. on Recent Developments in Civil Engineering (RDCE)</i></b> , SRM university and Indian Concrete Institute , Kattankulathur, Tamil Nadu, India.         |
| 17)"Theory of Consolidation through Radial Drainage for Soft Soils using Vertical Drains", by M.V Shah, Dr. A.V Shroff, <b><i>Proc of National Conf. on Emerging Technologies (NCEVT)</i></b> , Parul Inst. & GTU Ahmedabad , India  |

## JOURNALS

- 1) "Theory of one-dimensional consolidation through radial flow using vertical drains", by M.V Shah, Dr. A.V Shroff, Int. ***Journal of Geomechanics and Engineering***, Techno-Press publications. (under print)
- 2) "Performance of Sand Drains with varying Drain Diameter" by Dr. A.V. Shroff, Manish Shah, T.A. Khan, Dr.D.L. Shah, Dr.N.H Joshi, ***Journal of Engg & Tech***, BVM Engineering College, Vallabh Vidhyanagar ,Vol-18,Dec-2005

## REFERENCES

---

- Abid, M. M., and Pyrah, I. C. (1991). "Consolidation Behavior of Finely Laminated Clays." *Comput. Geotech.*, pp.307-323.
- Aboshi H. (1963), "Determination Of Horizon Coefficient of Consolidation of An Alluvial Clay", *Proc. 4<sup>th</sup> Aug. New Zealand conf. S.M. and F.E*, pp 159-169
- Aboshi H. and Mohan H. (1961), "Three Dimensional Consolidation of Saturated Clays", *Proc. 5<sup>th</sup> ICSMFE, Paris*, vol.1 pp.559-562.
- Aboshi H. , Yoshikuni H. and Uchibayashni T. (1969), "Stability Soft Clay Foundations Underneath Embankments Consolidated By Means Of Cardboard Drains", *Soils And Foundations* , vol.9(2), pp. 1-14
- Aldrich, H.P. (1965). "Precompression For Support Of Shallow Foundations." *J. Soil Mech. Found. Div., ASCE*, 91(2), pp.5-20.
- Ali Ghandeharioon, Buddhima Indraratna,Cholachat Rujikiatkamjorn,(2010)," Analysis of Soil Disturbance Associated with Mandrel-Driven Prefabricated Vertical Drains Using an Elliptical Cavity Expansion Theory", *International Journal of Geomechanics*, Vol. 10, No. 2,pp. 53-64
- Anandkrishnan M. (1968), " Study Of Some of The Variables of Consolidation Theory As Applied To Vertical Sand Drain Design" Ph.D thesis, Univ.of Manchester, pp.602.
- Anandkrishnan M. and Kappuswami T.(1969), "Note on Effect of Smear In Sand Drain Construction Loading" *Jour.Ind. National Soc. of SM & FE.*, vol.8, no.33, pp.281-287.
- Anandarajah, A. (1994). "Discrete Element Method For Simulating Behavior of Cohesive Soils." *J. Geotech. Engrg. Div., ASCE*, 120(9), pp.1593-1613.
- Anandarajah, A., and Kuganenthira,N. (1995). "Some Aspects of Fabric Anisotropy of Soils." *Geotechnique*, London , England, 45(1),pp. 69-81.
- Anandkrishna M. (1968), " A Study Of Some Of The Variables Of Consolidation Theory As Applied To Vertical Sand Drain Design", Ph.d thesis, University of Manchester.
- Anjaneyulu V.S.R (1991), "Influence Of Strip Geodrain On Radial Consolidation of Clays", M.E.Dissertation Thesis, M.S.U., Baroda.



- Akagi T.(1979), "State Of The Art Report On Settlements And Time Rates of Consolidation", *Geotechnical Engineering* (10), pp. 179-198
- Akai K.and Oakabayashi L. (1983) , "Consolidation Mechanism And Performance Analysis Of Sand Drain", *Proc. of 8<sup>th</sup> European Conference on SM & FE*, vol 2, pp. 565-570.
- Aria H. (1955), "Pore Water Measurement During Consolidation Test", *Report of Transportation , Tech. res. Instt., Japan*
- Asundaria R.(1989), "Radial Consolidation Of Clay By Prefabrication Drain", *M.E. Thesis, M.S.U., Baroda*
- Asian Institute of Technology (AIT). (1995), "The Full-Scale Field Test Of Prefabricated Vertical Drains for the Second Bangkok International Airport." *Final Rep., Vol. 1, Bangkok, Thailand.*
- Atkinson, M.S., and Eldred, P.J. L. (1981). "Consolidation Of Soil Using Vertical Drains", *Geotechnique*, London, England, 31(1),pp.33-43
- Ayub Khan,P., Madhav,M.R. et.al (2010),"Effect of non-linear consolidation for radial flowon pore pressure dissipation, *Indian Geotechnical Journal*, 40(1), pp.47-54
- Babu Rao.D. And Bhaskara Rao D. (1973), "Effect Of Smear In Sand Drains", *Indian Geotechnique Journal*, vol 3 , no.4 , pp.285-293
- Barden L. (1965), "Consolidation of Clay with Non Linear Viscosity", *Geotechnique*, vol. 15, pp.345-362.
- Barron, R.A.(1948). "Consolidation Of Fine-Grained Soils By Drain Wells." *Trans. ASCE*, 113, pp.718-742.
- Barron R.A. (1940), "The Influence Of Drain Wells On The Consolidation Of Fine –Grained Soils", *Micrograpped , July, 1944.*
- Basu, D., Basu, P., and Prezzi, M. (2006) "Analytical Solutions For Consolidation Aided By Vertical Drains." *Geomech. Geoeng.*, 1(1), pp.63–71.
- Bear, J., and Bachmat, Y. (1990). "Introduction To Modeling Of Transport Phenomena In Porous Media". *Kluwer Academic Publishers, Dordrecht, The Netherlands.*
- Bell, F.G. (1993). "Sand Drains, Sandwicks And Band Drains Engineering Treatment Of Soils", *E & FN Spon, London, England*, pp.77-88.

- Bergado, D. T., Alfaro, M. C., and Balasubramaniam, A. S. (1993). "Improvement of soft Bangkok clay using Vertical Drains." *Geotextiles and Geomembranes*, 12, pp. 615-663.
- Bergado, D. T., Alfaro, M. C., and Balasubramaniam, A. S. (1991). "Improvement Of Soft Bangkok Clay Using Vertical Drains" *Geotechnical engg*, vol-1, no.2, pp.3-29
- Bergado, D. T., Anderson, L. R., Miura, N., and Balasubramaniam, A. S. (1996), "Soft Ground Improvement, In Lowland And Other Environments." ASCE, New York, pp. 427.
- Bergado, D. T., Asakami, H., .et.al (1991). "Smear Effects Of Vertical Drains On Soft Bangkok Clay" *J. Geotech. Engrg.*, ASCE, 117, pp.1509-1530.
- Bergado, D. T., Balasubramaniam, A. S., Fannin, R. J., Anderson, L. R., and Holtz, R. D. (1997). "Full Scale Field Test Of Prefabricated Vertical Drain (PVD) On Soft Bangkok Clay And Subsiding Environment." *Proc., Ground Improvement, Reinforcement and Treatment Devel. 1987 to 1997*, Geo-Logan 1997, Spec. Publ. No. 69, ASCE, New York, pp.372-393.
- Bergado D.T., Miuria N., Singh N. and Panichayatum B. (1988), "Improvement Of Soft Bangkok Clay Using Vertical Drains Based On Full Scale Test", *Proc. International Conference On Engg. Problems Of Regional Soils*, Beijing, pp.379-384.
- Berles, J. D. (1995). "A Numerical Model For The Consolidation Of Clay," MSCE Thesis, School Of Civ. Engrg., Purdue University, West Lafayette, Ind.
- Berry P.L. and Wilkinson W.B. (1969), "The Radial Consolidation Of Clay Soils", *Geotechnique*, vol. 19 , pp.253-284.
- Bhatt A.J. (1995), "Influence Of Prefabricated Polypropylene- Jute Fibre Geodrain On Radial Consolidation Of Kaolinitic Clay", M.E.Thesis , M.S.U. Baroda
- Biot M.A. (1941), "General Theory Of Three Dimensional Consolidation" , *J. Applied Physics* , vol. 12, pp.155-164.
- Bishop A.W. (1976), "The Influence Of System Compressibility On The Observed Pore Pressure Response To An Undrained Change In Stress In Saturated Rock", *Geotechnique*, vol.26, no 2, pp.370-375.
- Bishop A.W. (1973), "The Influence Of An Undrained Change In Stress On The Pore Pressure In Media Of Low Compressibility", *Geotechnique* , vol.23, no.3, pp.435-442.

- Bjerrum L. (1973), "Problems Of Soil Mechanics And Construction On Soft Clays", Proc. 8<sup>th</sup> Intl Conf. On SM& FE, Moscow,3, pp. 111-159.
- Bo, M. W., Chu, J., Low, B. K., and Choa, V. 2003." Soil Improvement; Prefabricated Vertical Drain Techniques", Thomson Learning, Singapore
- Borges, J. L. (2004). "Three-Dimensional Analysis Of Embankments On Soft Soils Incorporating Vertical Drains By Finite Element Method." Comput. Geotech., 31, pp.665–676.
- Brednev A.V, Svetinsky E.V and Stroganov A.S (1983), " Soil Consolidation By Means Of Band Shaped Drains", Proc. 8<sup>th</sup> Euro. Conf. On SM & FE, Helsinki, vol.1, pp.565.
- Brenner R.P. and Pbebaharan N. (1983), "Analysis Of Sand Wick Performance In Soft Bangkok Clay", Proc . 8<sup>th</sup> European Conf. On SM & FE, Helsinki, vol. 2, pp. 579-686.
- Brom B, "Soil Mechanics", pp 349-351.
- Bronwell L.G. and Lambe T.W. (1968), " A Comparison Of Laboratory And Field Valves Of MV For Baston Blue Clay" 47<sup>th</sup> Annual Meeting of HRB.
- Burn K.G.(1964), "A Transducer To Measure Pore Water Pressure In Soil Tests" ASTM, STP no.361, pp.390.
- Burke H.H. and Smneha S.S. (1981), " Geodrain Installation Of Lornex Tailings Dam", Proc 10<sup>th</sup> Intl. Conf. On SM & FE, Stockholm, pp.559-602.
- Cao, L. F., Teh, C. I., and Chang, M. F. (2001). "Undrained Cavity Expansion In Modified Cam Clay. I: Theoretical Analysis." Geotechnique, 51(4), pp. 323–334..
- Carillo, N.J. (1942). "Simple Two And Three-Dimensional Cases In The Theory Of Consolidation Of Soils, "J. Math. Phys., 21(1), pp.1-5.
- Casagrande L. and Populous S. (1969), " On The Effectiveness Of Sand Drains", Canadian Geotechnical Journal, vol.6, pp.287-326.
- Chai, J.C.(2001). "Linear  $\ln(E + E_c) \sim \ln(P')$  Relation Of Structured Natural Clay." Proc., 15<sup>th</sup> Int. Conf. On Soil Mech. And Geotech. Engrg., Vol. 1, Balkema, Rotterdam, The Netherlands.

- Chai, J. C., and Bergado, D. T. (1993). "Performance of Reinforced Embankment On Muar Clay Deposit." *Soils and Found.*, Tokyo, 33(4), pp.1-17.
- Chai, J. C., Bergado, D. T., Miura, N., and Sakajo, S. (1996). "Back Calculated Field Effect Of Vertical Drain." *Proc. 2<sup>nd</sup> Int. Conf. Soft Soil Engrg.*, Vol. 1, Hohai University Nanjing, China, pp.270-275.
- Chai, J. C., Carter, J. P., and Hayashi, S. (2005). "Ground Deformation Induced By Vacuum Consolidation." *J. Geotech. Geoenviron. Eng.*, 131(12), pp.1552-1561
- Chai, J. C., and Miura, N. (1999). "Investigation Of Factors Affecting Vertical Drain Behavior." *J. Geotech. And Geoenviron. Engrg.*, ASCE, 123(3), pp.216-226.
- Chai, J. C., Miura, N., Sakajo, S., and Bergado, D. T. (1995). "Behavior Of Vertical Drain Improved Subsoil Under Embankment Loading." *Soils and Found.*, Tokyo, 35(4), pp.49-61
- Chai, J. C., Miura, N., and Sakajo, S. (1997). "A Theoretical Study On Smear Effect Around Vertical Drain." *Proc. 14<sup>th</sup> Int. Conf. Soil Mech. And Found Engrg.*, Vol. 3, Balkema, Rotterdam, The Netherlands, pp. 1581-1584.
- Chai, J.C., Shen, S.L., Miura, N. and Bergado, D.T. 2001. "Simple Method Of Modelling PVD Improved Subsoil" *J. Of Geotechnical Engineering*, ASCE, 127(11) pp.965-972.
- Chapman, G. A., Wagstaff, J. P., and Seidel, J. P. (1991). "The Effect Of Bitumen Slip Coating In The Driveability Of Precast Concrete Piles." *Proc.*, 4<sup>th</sup> Int. Conf. On Piling And Deep Found., Deep Foundations Institute, Balkema, Rotterdam, The Netherlands, pp.193-199.
- Chaput D. and Thomatin G. (1975), "Consolidation Of A Soil With Vertical Drain Under Variable Loads- Analytical Solution Methods Of Finite Difference" *Lab. Points Chanss*, Paris rapp.no47, pp.1-67.
- Ceryer C.W.(1965), " A Comparison Of The Three Dimensional Consolidation Theories Of Boit And Terzaghi", *Applied Maths*, vol. 16, pp.401-412.
- Chew, S. H., Wong, W. K., Ng, C. C., Tan, S. A., and Karunaratne, G. P. (1999). "Strain gauging Geotextiles using External Gauge Attachments Method." *Grips, Clamps, Clamping Techniques and Strain Measurement for testing of Geosynthetics*, ASTM STP 1379, ASTM, Philadelphia, pp.97-110.
- Choa, V. (1989). "Drain And Vacuum Preloading Pilot Test." *Proc.*, 12<sup>th</sup> ICSMFE, A. A. Balkema, Rotterdam, The Netherlands, Vol. 2, pp.1347-1350.

- Choa V. (1985), "Preloading And Vertical Drains : Soil Improvement Methods", Proceedings Of The Third International Geotechnical Seminar Nanyang Technological Institute, Singapore, pp.87-99.
- Choa, V., and Bo, M. W. (2000). "Quality Assurance Of Prefabricated Vertical Drain In Changi Reclamation." Proc., Int. Seminar Of Geotechnics in Kochi, 24, 25 september, Kochi, Japan, pp.263-274.
- Choa, V., Bo, M. W., and Chu, J. (2001). "Soil Improvement Works For Change East Reclamation Project." Ground Improvement, 5(4), pp.141-153.
- Christian J.T. (1977), " Two and Three Dimensional Consolidation" , Numerical Methods in Geotechnical Engineering , eds. C.S. Desai and J.T. Christian , pp.399-426
- Christie I.F. (1966), " The Solution Of Consolidation Problems By General Analogue Computer", Geotechnique vol.16 ,no.2, pp.131-148.
- Chu, J., Yan, S. W., and Yang, H. (2000). "Soil Improvement By The Vacuum Proloading Method For An Oil Storage Station." Geotechnique, 50(6),pp. 625-632.
- Consolidation Of Soils: Testing And Evaluation, ASTM special publication ,1985
- Cognon, J. M., Juran, I., and Thevanayagam, S. (1994). "Vacuum Consolidation Technology-Principles And Field Experience." Proc., Conf. On Vertical And Horizontal Deformations Of Foundations And Embankments Deformations, College Station, Tex., pp.1237-1248.
- Cortlever, N., and Dijst, G. (2002), Proc., 4<sup>th</sup> Int. Conf. on Ground Improvement Techniques, 26-28 March, Kuala Lumpur, Malaysia, 1, pp.303-309.
- Crawford C.R. (1964), " Interpretation Of The Consolidation Test", Jour. Of SM &FE Dn. A.S.C.E., Vol. 96, SM 5.
- Cryer c.w. (1965), " A Comparison Of The Three Dimensional Consolidation Theories Of Biot And Terzaghi", Applied Maths vol-16,pp.401-412.
- Dastidar A.G., Gupta S., and Ghosh T.K. (1969), " Application Of Sandwicks In A Housing Project", Proceeding Of 7<sup>th</sup> International Conference On Soil Mechanics And Foundation Engineering , Mexico City, vol.2, pp.59-64
- Datye K.R. (1982), " Simpler Technique For Ground Improvements", 4<sup>th</sup> IGS Annual Lecture Ind. Geotech. Journal vol.3, jan .12(1), pp.1-82.
- Davis E.H. and Poulous H.G (1972), " rate of settlement under two and three dimensional conditions", geotechniques, vol.22, pp.95-111.

- Davis J. A., and Humpheson, C.(1981), "A Comparison Between The Performance Of Two Types Of Vertical Drain Beneath A Trial Embankment In Belfast" *Geotechnique*, London, England, 31(1), pp.19-31.
- De lean E.H. (1965), " A Theory Of Three Dimensional Consolidation Applied To Cylindrical Bodies ", *Proc. 6<sup>th</sup> Int. Conf. On SM & FE*, Montreal, vol.1,pp.287-292.
- Desai C.(1975), " Analysis Of Consolidation By Numerical Methods", *Soil Mechanics Recent Developments : Proceedings Of A Symposium held at Univ. of New South Wales, Australia*, pp. 143-179.
- Dewel J.A. (1953), " An Investigation Of Consolidation Of Plastic Soils" S.M. Thesis at MIT, USA.
- Dinesh Mohan, Jain U.S., Sengupta D.P. and Devendra Sharma (1977), "Consolidation of Ground by Vertical Rope Drain", *Indian Geotechnical Journal*, vol.7, pp.1407-115.
- Duncan, J.M. (1993). "Limitations Of Conventional Analysis Of Consolidation Settlement." *J. Geotech. Engrg.*, ASCE, 119(9), pp.1333-1359.
- Eriksson L., and Ekstrom A. (1983). "The Efficiency of Three Different Types of Vertical Drain Results from a Full Scale Test" , *Proceedings of the Eight European Conference on SMFE*, Helsinki, Vol.II, pp.605.
- Eriksson, U., Hansbo, S., and Torstensson, B. A. (2000). "Soil Improvement at Stockholm-Arlanda Airport." *Ground Improvement*, (4), pp.73-80.
- Escario V. and Uriel S. (1961), "Determining The Coefficient Of Consolidation And Horizontal Permeability By Radial Drainage" , *Proc. 5<sup>th</sup> Int. Conf. on SM & FE.*, Vol. 1, pp. 83.
- Faisal Haji and Yong Kong Why (1989), " Effect Of Consolidation Settlement On The Performance Of Vertical Drains ", *Symposium On The Application Of Geosynthesis And Geofibre In South East Asia* , Kuala Lampur , Malaysia , pp.31-35.
- Fellenius, B.H., and Castonguay, N. G. (1985). "The Efficiency Of Band-Shaped Drains. "Rep. To Nat. Res. Council Of Canada, Univ. Of Ottawa, Ottawa, Canada, pp.1-54.
- Fellenius, B. H., and Goudreault, P. A. (1997). *Unipile Version 3 For Windows, User Manual*, Unisoft Ltd., Ottawa.
- Fellenius, B. H., and Warer,O. (1977). "The Equivalent Sand Drain Diameter Of The Band-Shaped Drain. "Proc., 9<sup>th</sup> ICSMFE, A.A. Balkema, Rotterdam, The Netherlands, Vol. 3, pp.395-396.

- FinN F.N. (1951), "The Effect Of Temperature On The Consolidation Characteristics Of Remoulded Clay" ASTM stop no. 126.
- Fox, P. J., and Berles, J.D. (1997). "CS2: A Piecewise-Linear Model For Large Strain Consolidation." *Int. J. For Numer. And Analytical Methods In Geomech.*, 21(7), pp.453-475.
- Furstenberg A., Lechowica Z., Szymanska., and Wolski W. (1983), "Effectiveness of Vertical Drains in Organic Soils", *proc.eight European conf. soil mech. Found. Engg. Helsinki*, vol.2, pp.611-616.
- Gibson R.E. (1963), " An Analysis Of System Flexibility And Its Effects On Time Lag In Pore Water Pressure Measurements" *Geotech. Vol.13*.
- Gibson R.E. and Mcnamee J. (1963), " A Three Dimensional Problem Of Consolidation Of A Semi-Infinite Clay Stratum", *Quart, J.Mech. Applied Maths* ,vol.16,pp.115-127.
- Goughnour, R. R. (1994). "Finite Strain Consolidation For Vertical Drains. Vertical And Horizontal Deformations Of Foundations and Embankments", A. T. Yeung And G. Y. Felio, Eds., *Geotech. Spec. Publ. No.40*, ASCE, Newyork, N.Y., Vol.1,pp.688-700.
- Glyn T.E and Sepence P.(1961), " An Automatic Control For Pore Pressure Measurement", *Geotechnique*, vol.2.
- Griffiths D. V.and Huang j, et.al., "Probabilistic Analysis of Coupled Soil Consolidation", *Journal Of Geotechnical And Geoenvironmental Engineering*, ASCE, 2010, pp.417-431
- Hansbo, S. (1993). "Band drains." *Ground Improvement* , M.P.Moseley, ed., CRC Press Inc., Boca Raton, Fla., pp.40-62.
- Hansbo.S (1960), "Consolidation Of Clay , With Special Reference To Influence Of Vertical Sand Drains", *Proc.Swedish Geo-Tech Instt.no.18*.
- Hansbo, S. (1979). "Consolidation of Clay By Band-Shaped Prefabricated Drains. " *Ground Engrg.*, 12(5),pp.16-25.
- Hansbo, S. (1981). "Consolidation Of Fine-Grained Soils By Prefabricated Drains. " *Proc., 10<sup>th</sup> ICSMFE*, A. A. Balkema, Rotterdam, The Netherlands, Vol.3, pp.677-682.
- Hansbo, S. (2005) .Experience Of Consolidation Process From Test Areas With and Without Vertical Drains. In: B. Indraratna And J. Chu (Eds), *Ground Improvement—Case Histories*, Elsevier, Amsterdam, pp. 3–50.

- Hansbo, S. (1983). "How To Evaluate The Properties Of Prefabricated Drains."Proc., 8<sup>th</sup> ECSMFE, A. A. Balkema, Rotterdam, The Netherlands, Vol.2, pp.621-626.
- Hansbo S. (1981), "Soil Improvement Techniques In Design Of Coastal Structures", Symposium On Geotechnical Aspects Of Coastal Structures", Symposium On Geotechnical Aspects Of Coastal Structures, Bangkok, pp.189-206.
- Hansbo.S. (1983), "Techno Economic Trend For Subsoil Improvements Methods In Foundations Engineering", Spl. Lectures Proc. Eight European Conf. Soil Mechanics Found. Engg. , Helsinki, vol.2, pp.1333-1343.
- Hansbo. S. and Torstensson B.A. (1977), " Geodrain And Other Vertical Drain Behavior", Proc. 9<sup>th</sup> ICSMFE Tokyo, vol1, pp. 553-540.
- Hansbo, S., Jamiolkowski, M., and Kok, L.(1981). "Consolidation By Vertical Drains." Geotechnique, London, England, 31(1), pp.45-66.
- Hausmann, M. R. (1990). "Preloading and the use of vertical drains." Engineering Principles of ground modifications. McGraw-Hill Inc., New York, N. Y., pp.245-271.
- Hawlder, B. C., Imai, G., and Muhunthan, M. \_2002\_. "Numerical Study Of The Factors Affecting The Consolidation Of Clay With Vertical Drains." Geotext. Geomembr., 20(4), pp.213–239.
- Hegg U., Jamiolkowski M.B, Lancellotta R and Parvis E. (1983), "Behavior Of Oil Tanks On Soft Cohesive Ground Improved By Vertical Drains" Proc. 8<sup>th</sup> European Conf. on SM & FE, Helsinki, vol.2, pp.621
- Heni Ali P and Yong K.W (1988), "Performance Of Prefabricated Vertical Drains" First Indian Geotextiles Conf. On Reinforced Soil And Geotextile, pp e-9.
- Hibbitt, Karlsson, and Sorensen 2006. ABAQUS/Standard User's Manual, Published by HKS Inc.
- Hird, C. C., and Moseley, V. J. \_2000\_. "Model Study Of Seepage In Smear Zones Around Vertical Drains In Layered Soil." Geotechnique, 50(1), pp.89–97.
- Hird, C. C., Pyrah, I. C., and Russell, D. (1992). "Finite Element Modeling Of Vertical Drains Beneath Embankments Of Soft Ground." Geotechnique, London, 42(3), pp.499-511.



- Hird, C. C., Pyrau, I. C., Russell, D., and Cinicioglu, F. (1995). "Modelling The Effect Of Vertical Drains In Two-Dimensional Finite Element Analyses Of Embankmentson Soft Ground." *Can. Geotech. J.*, Ottawa,32, pp.795-807.
- Holtz R.D. (1987), "Preloading with Prefabricated Vertical Strip Drains", *Geotextile and Geomembrane* , vol.6, pp.109-121.
- Holtz, R. D., Jamiolkowski, M. B., Lancellotta, R., and Pedroni, R. (1991). "Prefabricated vertical drains: Design and Performance". Butterworth-Heinemann, Oxford, England.
- Holtz R.D., Jamiolkowski M., Lancellotta R. AND Pedroni S.(1987), "Performance Of Prefabrication Band Shaped Drains", Report CIRIA Research Project 364, Construction Industry Research And Information Association , London, UK.
- Holtz R.D., and Christopher B.R (1987), " Characteristics Of Prefabricated Drains For Accelerating Consolidation", *Proc. 9<sup>th</sup> European Conf. On SM & FE*, Dublin, vol.2, pp.903-906.
- Holtz R.D., and Christopher B.R (1985), "Geotextile Engineering Manual ",FHWA report THWA ts 86/203.
- Hong, H. P. (1992). "One-Dimensional Consolidation With Uncertain Properties." *Can. Geotech. J.*, Ottawa, 29, pp.161-165.
- Hong, H.P., and Shang, J. Q. (1998). "Uncertainty In Consolidation With Prefabricated Vertical Drains For Soil Improvement." *Can. Geotech. J.*, Ottawa, 35, pp.666-677.
- Huang, J. And Griffiths, D. V. (2010). "One-dimensional consolidation theories for layered soil and coupled and uncoupled solutions by the finite-element method", *Ge´otechnique* 60, No. 9, pp.709–713
- Hughes F.H. and Chalmers (1972) " Smell Diameter Sand Drains *Civ. Engg. Pub Wks. Rev.* 1972 March 3-6.
- Imai, G., and Tang, Y.- X. (1992). " A Constitutive Equation Of One-Dimensional Consolidation Derived From Inter-Connected Tests." *Soils and Found.*, Tokyo, 32(2) pp.83-96.
- Indraratana, B., Balasubramaniam, A. S., and Ratnayake, P. (1994). "Performance Of Embankment Stabilized With Vertical Drains On Soft Clay." *J. Geotech. Engrg.*, ASCE, 120(2),pp. 257-273.

- Indraratna, B., Bamunawita, C., and Khabbaz, H. (2004). "Numerical Modeling Of Vacuum Preloading And Field Applications." *Can. Geotech. J.*, 41(6), pp.1098-1110.
- Indraratna, B., and Chu, J. (2005). *Ground improvement—Case histories*, Vol. 3, Elsevier Science, U.K.
- Indraratna, B., and Redana, I.W. (1998). "Laboratory Determination Of Smear Zone Due To Vertical Drain Installation." *J. Geotech. Geoenviron. Eng.* 124(2), pp.180-184.
- Indraratna, B., and Redana, I. W. (2000). "Numerical Modeling Of Vertical Drains With Smear And Well Resistance Installed In Soft Clay." *Can. Geotech. J.*, 37, pp.132-145.
- Indraratna, B., and Redana, I. W. (1997). "Plane Strain Modeling Of Smear Effects Associated With Vertical Drains." *J. Geotech. Geoenviron. Eng.* 123(5), pp.474-478.
- Indraratna, B., Bamunawita, C., Redana, I. W., and McIntosh, G. (2003). "Modelling Of Prefabricated Vertical Drains In Soft Clay And Evaluation Of Their Effectiveness In Practice." *Ground Improv.*, 7(3), pp.127–137
- Indraratna, B., and Rujikiatkamjorn, C. (2004). "Laboratory Determination Of Efficiency Of Prefabricated Vertical Drains Incorporating Vacuum Preloading." *Proc., 15th Southeast Asian Geotechnical Conf.*, Vol. 1, Bangkok, Thailand, pp.453–456.
- Indraratna, B., and Sathananthan, I. (2003). "Comparison Of Field Measurements And Predicated Performance Beneath Full-Scale Embankments." *Proc., 6<sup>th</sup> Int. Symp. On Field Measurements In Geomechanics*, Oslo, Norway, pp.117-127.
- Indraratna, B., Rujikiatkamjorn C., and Sathananthan, I. (2005). "Analytical And Numerical Solutions For A Single Vertical Drain Including The Effects Of Vacuum Preloading". *Canadian Geotechnical Journal*, 42: pp.994-1014.
- Indraratna, B., Sathananthan, I., Bamunawita, C., and Balasubramaniam, A. S. (2005) "Theoretical and Numerical Perspectives and Field Observations for the Design and Performance Evaluation of Embankments constructed on soft marine clay." *Elsevier geo-engineering book series*, Vol. 3, Elsevier Science, U.K., pp.51–89.
- Indraratna, B., Sathananthan, I., Rujikiatkamjorn C. and Balasubramaniam, A. S. (2005). "Analytical And Numerical Modelling Of Soft Soil Stabilized By PVD

Incorporating Vacuum Preloading".International Journal Of Geomechanics, 5(2),pp. 114-124.

Indraratna. B, Rujikiatkamjorn, C., Shahin, M., and Christie, D. (2006). "Soft Soil Stabilisation With Special Reference To Railway Embankments". Proc. Of 4th International Conference On Soft Soil Engineering, Vancouver, Canada, (Edited by D. Chan and K. T. Law), pp.35-56.

Indraratna. B, Rujikiatkamjorn, C., "Soft Clay Stabilisation Using Prefabricated Vertical Drains and the Role of Viscous Creep at the Site of Sunshine Motorway, Queensland", University of Wollongong, NSW 2522, Australia

Indraratna. B , Rujikiatkamjorn, C and Ali g.,(2010), "Analysis of Soil Disturbance Associated with Mandrel-Driven Prefabricated Vertical Drains Using an Elliptical Cavity Expansion Theory", International Journal Of Geomechanics ,ASCE , pp.53-65

Indraratna. B ,Aljorany, A, and Sivakuga, N.(2008),"Analytical and numerical modeling of consolidation by vertical drain beneath a circular embankment", Int. Jl. Of Geomechanics, 8(3), 119-206

Indraratna. B and walker r.(2006) "Vertical Drain Consolidation with Parabolic Distribution of Permeability in Smear Zone", Journal Of Geotechnical And Geoenvironmental Engineering , ASCE,pp.937-942

Iyathurai Sathananthan, Buddhima Indraratna,Cholachat Rujikiatkamjorn(2008),"Evaluation of Smear Zone Extent Surrounding Mandrel Driven Vertical Drains Using the Cavity Expansion Theory", International Journal of Geomechanics, Vol. 8, No. 6,pp.355-365

Institution of Civil Engineers (ICE). (1982). "Vertical drains", Thomas Telford Ltd., London, England.

Ishi Yasumaru,T, Shinohora ,T. Tatish And S. Kurate (1953), "Estimation Of  $M_v$  And  $C_v$  Values For The Design Of Sand Drains", Proc. 3<sup>rd</sup> ICSMFE , pp.312-315.

Itoh, M., Shirasawa, M., Itoh, A., Kumagai, K., Fukuoka, M. (1994). "Well Documented Case Study Of A Reinforce Wall." Proc., 5<sup>th</sup> Int. Conf., On Geotextils Geomembrances, And Related Products, Singapore, 1.1, pp.49-52.

Johnson, S. J. (1970). "Precompression For Improving Foundation Soils." J. Soil. Mech. Found. Div., ASCE, 96(1) pp.111-144.

Johnson, S. J. (1970). "Foundation Precompression With Vertical Sand Drains." J. Soil. Mech. Found. Div., ASCE, 96(1), pp.145-175.

- Jamiolkowski, M., and Lancellotta, R. (1984). "Embankments On Vertical Drains-Pore Pressures During Construction." Proc., Int. Conf. On Case Histories In Geotech. Engrg., A. A. Balkema, Rotterdam, The Netherlands, Vol. 1, pp.275-278.
- Jamiolkowski, M., Lancellotta, R., and Wolski, W. (1983). "Precompression And Speeding Up Consolidation." Proc., 8<sup>th</sup> ECSMFE, A. A. Balkema, The Netherlands, Vol. 3, pp.1201-1226.
- Jansen, H. L., and Den Hoedt, G. (1983). "Vertical Drains: In-Situ And Laboratory Performance And Design Considerations In Fine Soils." Proc., 8<sup>th</sup> ECSMFE, A. A. Balkema, The Netherlands, Vol. 2, pp.647-651.
- Jumikis A.R., "Consolidation of Soil and Settlement of Structures", pp.451-460.
- Juran J and guerazi A (1987) "Settlement Response Of Soft Soils Reinforced By Compacted Sand Columns"
- Kamon, M., Pradhan, T. B. S., and Suwa, S. (1992). "Laboratory Evaluation Of The Discharge Capacity Of Prefabricated Band-Shaped Drains." Soil Improvement, T. Mise, K. Nishida, M. Kamon, And M. Mashima, Eds., Current Japanese Materials Research, Vol. 9, Elsevier Science Publishing Co. Inc., New York, N. Y., pp.23-38.
- Karunaratne, G. P., et al. (2003). "Installation Stress In Prefabricated Vertical Drains." J. Geotech. Geoenviron. Eng., 129(9), pp.858–860.
- Karunatate, G. P., Young, K. Y. Tan, T. S., Tan, S. A., Liang, K. M., Lee, S. L., And Vijiaratnam, A. (1990). "Layered Clay-Sand Scheme Reclamation At Changi South Bay." Proc., 10<sup>th</sup> Southeast Asian Geotechnical Conf., Southeast Asian Society Of Soil Mechanics And Foundation Engineering, 1.1, pp.71-76.
- Kirkgard, M. M., and Lade, P. V. (1993). "Anisotropy Of Normally Consolidated San Francisco Bay Mud." Geotech. Testing J., 14(3), pp.231-240.
- Kjeliman .W (1948), " Accelerating Consolidation Of Fine Grained Soils By Means Of Cardboard Wicks", Proc.2<sup>nd</sup> ICSMFE, Rotterdam, vol.II, pp.302-305.
- Klausner, Y. (1991). "Fundamentals Of Continuum Mechanics Of Soils". Springer-Verlag, London.
- Koerner, R. M. (1994). "Wick Drains." Design With Geosynthetics, 3<sup>rd</sup> Ed., Prentice-Hall, Inc., Englewood Cliffs, N.J., pp.734-745.
- Kremer R.H.J., Oostveen J.P., Van Weele A.F., Dejager W.F.J. and Meyvogel, I.Y..(1983), " The Quality Of Vertical Drainage", Proc.8<sup>th</sup> European Conf. SM & FE, Helsinki, Vol.2, pp. 721-726.

- Kuesel T.R. ,Schmidt B. and Rafaell D. (1973), “ Settlements And Strengthening Of Soft Clay Accelerated By Sand Drain”, Highway Research Board Record n.457, pp.18-26.
- Kuganenthira, N., Zhao, D., and Anandarajah, A. (1996). “Measurement Of Fabric Anisotropy During Triaxial Shearing.” Geotechnique, London, England.
- Laumans Q. (1983), “Soil Improvement By Vertical Drains Factors Determining The Settlements Behavior”, Proc. European Conf. On SM& FE, Helsinki, vol.1, pp.641.
- Lambe T.W.(1951), “Soil Testing For Engineers”
- Lambe T.W and Whitman R.V.(1969), “Soil Mechanics”
- Landau, R. E. (1966). “Method Of Installation As A Factor In Sand Drain Stabilization Design.” Hwy. Res. Rec., 133, Hwy. Res. Board, Washington, D.C., pp.75-97.
- Lee S.L., Karunathe G.P. Yong K.Y., and Ramaswami S.D (1989), “Performance Of Fiber Drain In Consolidation Of Soft Soils “, Proc. 12<sup>th</sup> ICSMFE, Rotterdam , vol.3, pp. 1667-1670.
- Leonard G.A and Girault P.(1961), “ Study Of The One Dimensional Consolidation Test” Proc. 5<sup>th</sup> Intl. Conf. on SM & FE., vol .1.
- Lekha, K. R., Krishnawamy, N. R., and Basak, P. (1998). “Consolidation Of Clay By Sand Drain Under Time-Dependent Loading.” J. Geotech. Geoenviron. Eng., 124(1) pp.91-94.
- Lemoine k. and Rathmayer H. (1983), “ Experience On Horizontal Oedometer Tests To Determine The Parameter Ch.”, Proceedings Of The 8<sup>th</sup> European conf. on SM& FE, Helsinki, vol.1, pp.647-652.
- Leroueil, S. (1997). “Closure To ‘Compressibility Of Clays: Fundamental And Practical Aspects.’ “ J. Geotech. And Geoenviron. Engrg., ASCE, 123(9), pp.895.
- Leroueil, S., Bouclin, G., Tavenas, F., Bergero, L., and La Rochelle, P. (1990). “Permeability Anisotropy Of Natural Clays As A Function Of Strain.” Can. Geotech. J., Ottawa, 27(5), pp.568-579.
- Leroueil, S., Lerat, P., Hight, D. W., and Powell, J. J. M. (1992). “Hydraulic Conductivity Of A Recent Estuarine Silty Clay At Bothkennar.” Geotechnique, London, 42 (2), pp.275-288.

- Li Xiaoyong , Zhang Hui (2010), "Monte Carlo Analysis of Probability of One-dimensional Consolidation in Saturated Clay Soil Ground", International Conference on Computer and Information Application (ICCIA 2010) , china
- Lo K.Y. (1960), "Correspondence On Measurement Of The Coefficient Of The Of Consolidation Of Lacustrine Clay", By P.W.Row , Geotechnique , vol.no.10,pp.36.
- Lo, D. O. K., and Mesri, G. (1994). "Settlement Of Test Fills For Chek Lap Kok Airport." Vertical And Horizontal Deformations Of Foundations And Embankments, A. T. Yeung And G. Y. Felio, Eds., Geotech. Spec. Publ. No. 40, ASCE, New York, N. Y., Vol. 2, pp.1082-1099.
- Loh, S. L. (1998). "Drainage Capacity of High Strength Geotextile in Residual soil for Reinforcement application." Thesis, National Univ. of Singapore.
- Long, R. P., and Fontaine, L.F. (1992). "Performance of Wick drains at Windsor, Connecticut." Advances In Geotechnical Engineering, Transp. Res. Rec. 1369, Transp. Res. Board, Washington, D.C.,pp. 1-7.
- Long, R, P., Fontaine, L. F., and Olmstead, B. (1994). "Performance Of Wick Drains Installed By Vibration." Vertical And Horizontal Deformations Of Foundations And Embankments, A.T. Yeung And G.Y. Felio, Eds., Geotech. Spec. Publ. No. 40,ASCE, New York, N.Y., Vol. 2, pp.1193-1201.
- Long, R. P., and Hover, W. H. (1984). "Performance Of Sand Drains In A Tidal Marsh." Proc., Int. Conf. On Case Histories In Geotech. Engrg., A. A. Balkema, The Netherlands, Vol. 3, pp.1235-1244.
- Madhav, M.R., Park, Y. M., and Miura, N. (1993). "Modelling And Study Of Smear Zones Around Band Shaped Drains." Soils And Found., Tokyo, 33(4), pp.135-147.
- Madhav, M.R, Ayub Khan (2011)", Consolidation of Soft Ground with Drains with no (PVDs) and Finite Stiffness (Granular Piles)", Proc. of Indian Geotechnical Conference, Kochi, India, Vol-I,pp.33-40
- MagnanJ.P. Pillot G. and Queyroi D. (1983), "Back Analysis Of Soil Consolidation Around Vertical Drains", proc. 8<sup>th</sup> Euro. Conf. on SM & FE, Helsinki, vol.2, pp.653-658.
- Mandal and Kanagi, "Centrifuge Modeling Of Vertical Drains", Indian Geotechnical Journal .,Vol.28, No.1 January 1998, pp.71-98.
- Masar M.A.(1974), "Consolidation With Sand Drain Votr. Bangrundtag, Frankfurt, Germany, Spozialbitzung" Dt.Ges. Erd-Und Grundban, Essen, pp.36-63.

- Massarch K.R. and Kamon M. (1983), "Performance Of Driven Sand Drains", Proc. 8<sup>th</sup> Euro. Conf. On SM&FE ,Helsinki, vol.2,pp.659-662.
- McGown, A., and Hughes, F. H.(1981). "Practical Aspects Of The Design And Installation Of Deep Vertical Drains." Geotechnique, London, England, 31 (1), pp.3-17.
- Mckinlay D.G (1961), " A Laboratory Study Of Rates Of Consolidation In Clays With Particular Reference To Conditions Of Radial Pore Water Drainage ", Proc. 5<sup>th</sup> ICSMFE, Paris, vol.1,pp.225-228.
- Meral Proctar, Mueser Rutledge. (1950) "Study Of Deep Soil Stabilization By Vertical Sand Drain" U.S Dept Of Navy Bureau Of Yards And Docks Tech. Services, pp15-16,92.
- Mesi G. and Choi Y.K. (1979), "Excess Pore Water Pressure During Consolidation ", Proc. 6<sup>th</sup> Asian Regional SM & FE , Singapore, vol .3,pp.151-154.
- Mesri, G., Lo, D. O. K., and Feng, T. – W. (1994). "Settlement Of Embankment On Soft Clays." Vertical And Horizontal Deformations Of Foundations And Embankments, Geotech. Spec. Publ. No. 40, A. T. Yeung, And G. Y. Felio, Eds., Vol. 1, ASCE, New York, pp.8-56.
- Mitchell, J. K. (1956), "The Fabric Of Natural Clay And Its Relation To Engineering Properties", Proc. Highway Research Board , vol.35
- Mitchell, J. K. (1981). "Soil Improvement-state-of –the-art." Proc., 10<sup>th</sup> ICSMFE, A. A. Balkema, The Netherlands, Vol. 4, pp.509-565.
- Miura, N., Chai, J. C., and Toyota, K. (1998)."Investigation On Some Factors Affecting Discharge Capacity Prefabricated Vertical Drain." Proc. 6<sup>th</sup> Int. Conf. On Geosynthetics, International Geosynthetics Society, Atlanta, pp. 845-850.
- Miura, N, Park, Y. M., and Madhav, M. R. (1993). "Fundamental Study On The Discharge Capacity Of Plastic Board Drain." J. Geotech. Engrg., Tokyo, 35(III), pp.31-40(in Japanese).
- Mogami T. and Shimju E. (1963), "Results On Three Dimensional Consolidation Of Clays", Proc. 2<sup>nd</sup> Asian Regional Conf. On SM & FE , vol.1, pp.163-166.
- Mohamedelhassan, E., and Shang, J. Q. (2002). "Vacuum And Surcharge Combined One-Dimensional Consolidation Of Clay Soils." Can. Geotech. J., 39, pp.1126-1138.
- Murray R.T. (1978), "Development in Two and Three Dimensional consolidation theory ", Sm-1, Applied Science London.

- Newland P.L. and alley B.H. (1960), "Study Of The Consolidation Characteritics Of A Clay" Geotech vol.10 ,pp.62.
- Nicholson, D. P., and Jardine, R. J. (1981). "Performance Of Vertical Drains At Queenborough Bypass." Geotechnique, London, England, 31(1), pp.67-90.
- Nogami, T., and Li, M. (2002). "Consolidation Of System Of Clay And Thin Sand Layers." Soils Foundations, Jpn. Geotech. Soc., in press.
- Northey r.d and Thomas r.f (1965), "Consolidation Test Pore Pressure" Proc. 6th Intl. Conf. On SM& FE. Vol .1.
- Onoue, A. (1991). "Permeability Of Disturbed Zone Around Vertical Drains." 26th Annu. Meeting Of The Japan Geotech. Soc., Pp.2015-2018(in Japanese).
- Olson, R. (1998). "Settlement Of Embankments On Soft Clays." J. Geotech And Geoenviron. Engrg., ASCE, 124(4), pp.278-288.
- Olson, R.E., Daniel, D.E., and Liu, T. K. (1974). "Finite Difference Analyses For Sand Drain Problems." Proc., ASCE Specialty Conf. on Anal. And Des. In Geotech. Engrg., ASCE, New York, N.Y., Vol. 1, 85-110.
- Park, Y. M. (1994). "A Research On The Mechanical Properties Of Low Land Marine Clay And Vertical Drain Improvement Method." Doctor Of Engineering Thesis, Saga University, Japan.
- Parikh P.V. and Verma A.P. (1975), "One Dimensional Theory Of Consolidation" Proc. 5<sup>th</sup> Asian Reg. Conf. vol.3.
- Perloff W.H., Nair K. and Smith J .G (1965), " Effect Of Measuring System On Pore Water Pressure In The Consolidation Test", Proc. 6<sup>th</sup> ICSMFE, pp.338-342.
- Prakash, K. (1997). "Settling, Compressibility And Permeability Behavior Of Fine Grained Soils." Ph.D Thesis, Indian Institute Of Science, Bangalore, India.
- Prawono S. (1981), " Sand Drain Model By Central Drain Oedometer", Proc. 10<sup>th</sup> ICSMFE,Stockolm,vol.1,pp.745-750.
- Qian, J.H., Zhao. W. B., Cheung, Y.K., and Lee, P.K.K.(1992). "The Theory and Practice of Vaccum Preloading." Comput. Geotech. 13, pp.103-118.
- Queroi D. and Soyebz (1987), "Laboratory characteristics of the hydraulic properties of prefabricated band shaped drains" proc. Inst. symp. on geotechnical Engg. of soft Mexico vol.1. pp.109-116.
- Ramanjaneya G.S.(1969)," Consolidation Characteristics Varved Clay", Ph.D Thesis, Univ. Of Connecticut.



- Rama Swamy S.V. Krishna kumar M., "Experimental Studies On The Vertical Drains", Indian Geotechnical Conf. Bangalore Dec.1995, vol.2.
- Rao and Raju (1990), " One Dimensional Consolidation With 3D Flow For Time-Dependent Loading", Journal Of Geotechnical Engineering ,vol.116, no.10, October 1990, ASCE., pp.1576-1580.
- Rao, D.K And Rao. D.J (1970), "Pore Pressure Set Up Using Sand Drains Under Construction Type Of Loading" Jour. SM & FE, India vol.9 no.3,pp.323-331.
- Raymond G.P. (1961), "Consolidation of Deep Deposit of Homogeneous Clay" Geotech, vol.19 no.3, pp.478-494.
- Raymond G.P. (1966), "Laboratory Consolidation Of Some Normally Consolidated Soils" Canadian Geot, Jour, vo.3 no.4, pp.217-235.
- Raymond G.P. and Davis E.H (1965), "Non Linear Theory Of Consolidation" Geotech, vol.15 no.2, pp.161.
- Reddy A.S. and Murthy M.V.K. (1969), " New Theory On Sand Drains", Indian Journal Soil Mech. Foundation Engg.,Vol.8.,pp.237-258.
- Richart, F.E. Jr(1959). "Review Of The Theories For Sand Drains." Trans. ASCE,pp.709-736.
- Rixner, J.J., Kraemer, S. R., and Smith, A.D. (1986). "Prefabricated Vertical Drains: Vol. 1, Engineering Guidelines." Rep. No. FHWA/RD-86/168, Federal Hwy. Admin., McLean, va.
- Robertson, P.K., Campanella, R.G., Brown, P.T., and Robinson, K.E.(1988). "Prediction Of Wick Drain Performance Using Piezometer Cone Data." Can. Geotech.J.,25(1) 56-61.
- Roscoe K.H and Burland J.B (1969), "Pore Pressure In Normally Consolidated Clays" geotech, Vol.19, pp.338-379.
- Rowe, P. W.(1964). "The Calculation Of The Consolidation Of Laminated Varved Or Layered Clays, With Particular Reference To Sand Drains." Geotechnique, London, England, 14(4), pp.321-340.
- Rowe, P. W.(1959), " Measurement Of Coefficient Of Consolidation Of Lacustrine Clay",Geotech.,vol.9, no.1,pp.107-118.
- Rowe, P. W.(1968), "The Influence Of Geological Features Of Clay Deposits On The Design And Performance Of Sand Drains", Proc. Inst. Civil Engns. Suppl.vol.1968,pp.1-72.

- Rowe, P. W. and Barden (1968), "A New Consolidation Cell", *Geotech.*, vol.16, pp.162-170.
- Rowe, P. W. and shields D.H. (1964), "Radial Drainage Oedometer For Laminated Clays", *Jour.SM & FE Divn. ASCE*, Vol.91, Smi, pp.15-23.
- Rowe, R. K. (1992). "Some Challenging Applications Of Geotextiles In Filtration And Drainage." *Proc., Conf. GEOFAD'92: Geotextiles in filtration and Drainage*, U.K.Chapter of the International Geotextile Society, Churchill College, Cambridge, U.K., September.
- Rujikiatkamjorn, C., Indraratna, B., and Chu, J. (2007), "Numerical Modelling Of Soft Soil Stabilized By Vertical Drains, Combining Surcharge And Vacuum Preloading For A Storage Yard." *Can. Geotech. J.*
- Rujikiatkamjorn, C., Indraratna, B., and Chu, J. (2008), "2D and 3D numerical modeling of combined surcharge and vacuum preloading with vertical drains. *Intl. Jl. Of Geomechanics*, 8(2), pp.114-156
- Ruohonen K (1983), "Founding An Athletics Field With Vertical Drain And Preloading", *Proc. Of The 8<sup>th</sup> Euro. Conf. On SM &FE*, Helsinki, vol.2, pp.669.
- Samsuke T.(1963), "Determination Of Process Of Consolidation By Sand Drain Under Variable Loading" *Proc. 3<sup>rd</sup> Intl. Conf. on SM & FE*, pp.242.
- Sathananthan, I. (2005). "Modelling Of Vertical Drains With Smear Installed In Soft Clay." *Ph.D. Thesis, School Of Civil, Mining And Environmental Engineering, Faculty Of Engineering, Univ. Of Wollongong*, New South Wales, Australia.
- Sathananthan, I., and Indraratna, B. (2006), "Laboratory Evaluation Of Smear Zone And Correlation Between Permeability And Moisture Content." *J. Geotech. Geoenviron. Eng.*, 132(7),pp. 942–945
- Sharma, J. S., and Xiao, D. (2000), "Characterization Of A Smear Zone Around Vertical Drains By Large-Scale Laboratory Tests." *Can. Geotech. J.*, 37(6), pp.1265–1271.
- Satyanarayana K G, Rohatgi P K And Kulkarni A G, "Structure and properties of coir fibres", *proc. Indian Acad. Sci. (Engg. Sci.)* Vol. 4, Pt. 4, December 1981, pp. 419-436
- Satyanarayana K G and Tomczak .f , "Studies on lignocellulosic fibers of Brazil. Part II: Morphology and properties of Brazilian coconut fibers", *Science direct*, pp.1710-1722

- Satyanarayana K G , Rohatgi P. K. ,et.al .,(1982), “ Structure Property Studies Of Fibres From Various Parts Of The Coconut Tree”, Journal Of Materials S C I E N C E ,pp.2453- 2462
- Schiffman R.L (1968), “Consolidation Of Soil Under Time Dependent Loading And Varying Permeability”, Proc. Highway Res. Board no.37, pp.584-617.
- Schiffman R.L (1950), “A Three Dimensional Theory Of Consolidation Including Temperature Effects” Univ Of Colarado rep. no.70.
- Shah P.V (1989), “ Influence Of Sandwich On Radial Consolidation Of Kaolinite Clay”, M.E. Dissertation Thesis, M.S.U., Baroda.
- Shah L.M. (1979), “Influence Of Radial Drainage On Consolidation Characteristics Of Kaolinite Clay”, M.E.. dissertation thesis, M.S.U., Baroda.
- Shields D.H. (1976),” Consolidation Test”, Geotechnique vol.26, pp.209-212.
- Shroff A.V. (1972), “Influence Of Mineral Of Mineral Type, Degree Of Saturation, Fabric Structure, Stress History And Drainage On The Consolidation Characteristics Of Clay “, Ph.D Thesis, M.S.U., Baroda
- Shroff and Shah, “ Soil Mechanics And Geotechnical Engineering”,pp.28-31
- Shen, S. L., Yang, C. W., Miura, N., and Chai, J. C. (2000). “Field Performance Of PVD Improved Soft Clay Under Embankment.” Coast. Geotech. Engrg. In Pract., A. Nakase And T. Tsuchida, eds., Vol. 1, Balkema, Rotterdam, pp.515-520.
- Singh. S. K. (2001). “Confined Aquifer Parameters From Temporal Derivative Of Drawdowns.” J. Hydraul. Eng., 127(6),pp.466-470.
- Singh G. and Hattab T.N. (1979), “ A Laboratory Study Of Effect Of Sand Drain In Relation To Method Of Installation And Spacing”, Geotechnique, vol.29,no.4,pp.395-442.
- Siva Reddy A. and Krishna Murthy (1969), “New Theory On Sand Drain” Jour. Indian nat. Soci. of SM & FE, Vol.b No.4, pp.337-358.
- Silveire I.P.(1953), “Consolidation Of A Cylindrical Clay Sample With External Radial Flow Of Water” Proc. 3<sup>rd</sup> Intl. Conf. on SM& FE, vol.1, pp.55.
- Soranzo M.(1983), “ Determination Of Horizontal Consolidation Coefficient Of A Silty Marine Clay”, Proc.8<sup>th</sup> European Conf. on SM &FE, Helsinki, vol.2, pp.685-690.

- Stamatopoulos, A.C., and Kotzias, P.C. (1985). Soil Improvement By Preloading. Wiley Interscience, Newyork, N.Y.
- Stanton F.E. (1948), "Vertical Sand Drains As A Means Of Foundation Consolidation On Accelerating Settlement Of Embankment Over Marsh Land ", Proc. 2<sup>nd</sup> ICSMFE, vol.5, pp.273-278.
- Suits, L. D., Gemme, R.L., and Masi, J.J.(1986). "Effectiveness Of Prefabricated Drains On Laboratory Consolidation Of Remoulded Soils." Consolidation Of Soils: Testing And Evaluation, ASTM STP 892, ASTM, Philadelphia, Pa., pp.663-683.
- Suzuki, S., and Yamada, M. (1990). "Construction of an artificial island for the Kansai Intl. Airport," Proc., 1989 Sem. On Coastal Dev., IEM and Kosai Club, Malaysia, pp.511-520.
- Tan T.K. (1957), "Three Dimensional Theory Of The Consolidation And Flow Of Clay Layers", Jour.Maths And Physics, vol.19, pp.167.
- Tan S.B and Simons N.E (1971), " Radial Consolidation Of Clays By Vertical Sand Drains ", Proc.4<sup>th</sup> Asian Regional Conf. On SM & FE Engg. Bangkok, vol .1, pp.75-80.
- Tan, S. A., Yong, K. Y., and Lee, S. L. (1992). "Drainage Efficiency Of Sand Layer In Layered Clay-Sand Reclamation." J. Geotech. Eng., 118(2), pp.209-228.
- Tanaka, H. (1994), "Consolidation Of Ground Reclaimed By Inhomogeneous Clay." Vertical And Horizontal Deformations Of Foundations And Embankments, A.T.Yeung And G.Y.Felio, Eds., Geotech. Spec. Publ. No. 40, Vol. 2, ASCE, New York, N.Y., Vol. 2, pp.1262-1273.
- Takagi (1957), "Determination Of The Process Of Consolidation By Sand Drain Under Variable Loading"
- Taylor D.W.(1948), " Fundamental Of Soil Mechanics", Asia Publishing House.
- Terzaghi K.(1943), "Theoretical Soil Mechanics", Published By John Wiley And Sons Inc., New York.
- Terzaghi K.(1945),"Drainage Of Clay Strata By Filler Well" Civil Engg. A.S.C.E.(oct)
- Terzaghi, K., Peck, R. B., and Mesri, G. (1996). "Soil Mechanics In Engineering Practice", 3<sup>rd</sup> Ed., Wiley Interscience, New York.

- Tiller, F. M., and Hsyung, N. B. (1995). "Role Of Porosity In Filtration: Xii. Filtration With Sedimentation." *Aiche J.*, 41, pp.1153.
- Tiller, F. M., and Hsyung, N. B. (1993). "Unifying The Theory Of Thickening, Filtration And Centrifugation." *Water Sci. Technol.*, 28, pp.1.
- Tiwari A.K. (1990), "Radial Consolidation Of Kaolinite Clay By Jute Drain ", M.E. Dissertation Thesis, M.S.U., BARODA.
- Toorman , E. A. (1996). "Sedimentation and self-weight consolidation: General unifying theory." *Geotechnique*, London, 46(1), pp.103-113.
- Townsend, F. D., and Mcvay, M. C. (1990). "SOA: Large strain consolidation predictions." *J. Geotech. Engrg.*, ASCE, 116(2), pp. 222-243.
- Tsytoich N.A., Ter-matirosoyan Z.Y and Kulkari K.R (1971), "Certain Problems In Consolidation Of Clayey Soils By Vertical And Horizontal Drainage Under Conditions Of Equal Deformation", *Proc. 4<sup>th</sup> Asian Reg. Conf. On SM & FE.*, Bangkok, vol .1, pp.81-86.
- Trautwein J.S.et al (1981), "Radial Flow Consolidation", *Xth ICSMFE*, vol .1, pp.481.
- Umesh dayal (1985), " Recent Trends Ion Wick Drain Design And Installation ", 146-1985, pp.165-170.
- Verma A.P. (1969),"Laplace Transform Solution of a One Dimensional Ground Water Recharge by Spreading", *Amnali di Geophisica*, Vol.22-1, pp.26-31.
- Voakamp, W., Troost, G., and Koerner, G. R. (1998). "The Mobilized Strength Of Prefabricated Vertical Drains." *Proc.*, 6<sup>th</sup> Int. Conf. On Geosynthetics, Atlanta, 2, pp.839-844.
- Vreeken C., Van den berg F. and Ioxham M. (1983), " The Effect Of Clay Drain Interface Erosion On The Performance Of Band Shaped Vertical Drains ", *Proc. Of The 8<sup>th</sup> European Conf. On Sm & Fe* , Helsinki, vol.II ,pp. 713-716.
- Vreeken C. and Duijn C.J (1983), "The Effect Of Soil Heterogeneityon The Consolidation By Vertical Drains ",*Proc. Of The 8<sup>th</sup> European Conf. On SM& FE*, Helsinki, vol.II ,pp. 707-712.
- Walker, R., Indraratna, B, and Sivakugan, N.(2009)", Vertical and radial consolidation analysis of multilayered soil using the spectral method, *J. of Geotech and Geoenv. Engg*, ASCE, 135(5), 657-663.
- Wang, Z. M., Xu, L. X., and Jian, Z. H. (1998), "Field Experimental Study On The Soft Ground Treatment Of Hongzhou-Niingbo (HN) Expressway

- Foundation." Soft Ground Treatment In Hangzhou-Ningbo Expressway, T. L. Cai, Ed., Hongzhou Press, Hongzhou, pp.183-222 (in Chinese.)
- Warren M.J.(1986), " Impact Of Design And Specifications Requirement Of Actual Wick Drain Construction", Transportation Research Circular (309), pp. 10-13.
- Weber, W.G.Jr.(1966)."Experimental Sand Drain Fill At Napa River." Hwy. Res. Rec. 133,Hwy. Res. Board, Washington, D.C., pp.23-44.
- Winterkorn H.P. (1943)," The Condition of Water in Porous System", Soil Science, Vol. 56, No.2, pp.109-116.
- Winterkorn H.P. (1941),"A Study of Changes in Physical Properties of Putam Soil by Ionic Substitution", HRB Proceedings, pp.416-433.
- Wolski W. et al (1983), "Effectiveness of Vertical Drain in Organic Soils", Proc. 8<sup>th</sup> European Conf. on SM & FE, Helsinki, vol.II, pp.611-616.
- Wood, D. M. (1990), "Soil Behavior And Critical State Soil Mechanics", Chapter 9, Cambridge Press, Cambridge, England, U.K.
- Woo, S.M., Van Weele, A.F., Chotivittayathanin, R., and Trangkarahart, T. (1989). "Preconsolidation Of Soft Bangkok Clay By Vacuum Loading Combined With Non-Displacement Sand Drains." Proc., 12<sup>th</sup> ICSMFE, A.A.Balkema, The Netherlands, Vol. 2, pp.1431-1434.
- Xie, K. H., Lee, P. K. K., and Cheung, Y. K. (1994). " Consolidation Of A Two-Layer System With Vertical Ideal Drains." Proc., 8<sup>th</sup> Int. Conf. On Computer Methods and Advances in Geomechanics, 1.1, Morgantown, W. V., pp.789-794.
- Yan, S. W., and Chu, J. (2003), "Soil Improvement For A Road Using A Vacuum Preloading Method" Ground Improvement, 7(4), pp.165–172.
- Ye, br.lu S.Y and tang Y.S (1983), "Packed Sand Drain Atmospheric Preloading For Strengthening Soft Foundation" Proc. Of The 8<sup>th</sup> Euro. Conf. on SM & FE, Helsinki, vol.1, pp717.
- Yoshikuni and Makando H. (1974), "Consolidation Of Soils By Vertical Drain Wells With Finite Permeability", Soils And Foundations, vol.14(2), pp. 35-46.
- Younger, J.S.(1968). "Design Procedure For Sand Drains." Civ. Engrg. & Public Works Rev., 63(740),pp.285-291.
- Young, R.N. and Warkentin, B.P. (1966)," Introduction to Soil Behaviour", The Macmillan Co., New York.

Zeng G.X., and Xie K.H. (1989)' "New Development Of The Vertical Drain Theories." Proc., 12<sup>th</sup> ICSMFE, A.A.Balkema, The Netherlands, Vol. 2, pp.1435-1438.

Zhu, G., and Yin, J.-H. (2004), "Consolidation Analysis Of Soil With Vertical And Horizontal Drainage Under Ramp Loading Considering Smear Effects." Geotext. Geomembr., 22(1), pp.63–74.

## LIST OF SPECIAL CODES REFEREED

|                     |  |
|---------------------|--|
| ASTM D4354-99(2004) | Standard Practice for Sampling of Geosynthetics for Testing  |
| ASTM D4354-99(2004) | Standard Practice for Sampling of Geosynthetics for Testing  |
| ASTM D5199-01(2006) | Standard Test Method for Measuring the Nominal Thickness of Geosynthetics  |
| ASTM D5261-92(2003) | Standard Test Method for Measuring Mass per Unit Area of Geotextiles   |
| ASTM D4751-99(2004) | Standard Test Method for Determining Apparent Opening Size of a Geotextile   |
| ASTM D4595-05       | Standard Test Method for Tensile Properties of Geotextiles by the Wide-Width Strip Method                                |
| ASTM D4632-91(2003) | Standard Test Method for Grab Breaking Load and Elongation of Geotextiles  |
| ASTM D4533-04       | Standard Test Method for Trapezoid Tearing Strength of Geotextiles   |
| ASTM D4833-00       | Standard Test Method for Index Puncture Resistance of Geotextiles, Geomembranes, and Related Products                    |
| ASTM D6241-04       | Standard Test Method for the Static Puncture Strength of Geotextiles and Geotextile-Related Products Using a 50-mm Probe |
| ASTM D6140-00(2005) | Standard Test Method to Determine Asphalt Retention of Paving Fabrics Used in Asphalt Paving for Full-Width Applications |
| ASTM D4759-02       | Standard Practice for Determining the Specification Conformance of Geosynthetics   |

|                          |  |
|--------------------------|--|
| IS 13321 : Part 1 : 1992 | Glossary of terms for Geo-Synthetics Part : Terms used in materials and properties |
|--------------------------|--|



|                          |   |
|--------------------------|---|
| IS 13325 : 1992          | Determination of Tensile Properties of Extruded Polymer Geogrids Using the Wide Strip-Test Method                             |
| IS 13326 : Part 1 : 1992 | Method of test for the evaluation of interface friction between Geosynthetics and soil Part 1 modified direct shear technique |
| IS 13162 : Part 3 : 1992 | Geotextiles – Methods of Test Part 3 : Determination of Thickness at Specified Pressures                                      |
| IS 13162 : Part 4 : 1992 | Geotextiles – Methods of Test Part 4 : Determination of puncture resistance by falling cone method                            |
| IS 13162 : Part 5 : 1992 | Geotextiles – Methods of Test – Part 5 : Determination of Tensile Properties Using a Wide Width Strip                         |
| IS 14293 : 1995          | Geotextiles – Method of test for trapezoid tearing strength   |
| IS 14294 : 1995          | Geotextiles – Method for determination of apparent opening size by dry sieving technique                                      |
| IS 14324 : 1995          | Geotextiles – Methods of test for determination of water Permeability-Permittivity  |
| IS 14706 : 1999          | Geotextiles – Sampling and Preparation of Test Specimens  |
| IS 14714 : 1999          | Geotextiles - Determination of Abrasion Resistance  |
| IS 14716 : 1999          | Geotextiles - Determination of Mass per Unit Area   |
| IS 14739 : 1999          | Geotextiles - Method for Determination of Creep   |
| IS 15060 : 2001          | Geotextiles - Tensile Test for Joint/Seams by Wide-Width Method   |

## DATA ACQUISITION SYSTEM

### STEP 1

Switch 'OFF' the power of the system if it is already switched 'ON'.

### STEP 2

Connect all the transducers to the channels on REAR PANEL.

### STEP 3

Connect RS-232C cable (from COM1 port of the computer) if it is required, to 25 pin 'D' connector on rear panel of the system. Similarly, connect printer cable.

### STEP 4

Now switch 'ON' the power of the system. Display shows DAS-16. If not, press CLR key to reset the system.

### STEP 5

Press SHIFT + C.S.Keys. Display shows –CS000

Enter the channel no. and press ENTER key to update the sequence. Press CLR/TERM to exit.

### STEP 6

Press SHIFT + MODE keys. Display shows – 0001 dc 00 CH code

Key in the proper Strain/LVDT code for all the channels using ENTER key and press CLR/TERM to exit.

### STEP 7

Press S.C. Key. Display shows - SC 0000.

Enter the required number of scan cycles and press ENTER key. Press CLR/TERM to exit.

### STEP 8

Press S.R. Key. Display shows - Sr 0000

Enter required number of samples/channel to be taken in each cycle and press ENTER key. Initialize with 0001 at least. Press CLR/TERM to exit.

### STEP 9

Press I.S.Key. Display shows - IS 0000

## APPENDIX - B

Enter inter scan delay if needed else press CLR/TERM to exit.

### STEP 10

Press A/M key. Display shows –A1 00

Give Auto mode (00)/Manual mode (01) code and press ENTER. Press CLR/TERM to exit.

### STEP 11

Press S.P. Key. Display shows SP00

Give prover code and press ENTER key. Press CLR/TERM to exit.

### STEP 12

Press SHIFT +C.F. keys. Display shows – 001 C 1.000

CH            C.F.

Enter the required calibration factor for all the channels using ENTER keys and press CLR/TERM to exit.

### STEP 13

Press SHIFT + D.P. keys. Display shows – 001 DP 00

CH            DP

Enter D.P. code for all the channels using ENTER key and press CLR/TERM to exit.

### STEP 14

Press SHIFT + UNIT keys. Display shows – 001 U1 00

CH    Unit code

Set proper unit codes for all the channels using ENTER key and press CLR/TERM to exit.

### STEP 15

Press SHIFT + P.I. Key. Display shows – PI 0000

HSMS

Set printing interval required in HSMS and press ENTER key. Press CLR/TERM to exit.

### STEP 16

## APPENDIX - B

Press CLR key. Display shows - t 00.01.02

Time. Check time and date. If required reinitialize or press CLR/TERM to exit.

### STEP 17

Press I/P CHK key. Display shows unbalance of the channel.

Balance it to zero or press IP save key to save the unbalance data. Do the above for all the selected channels and press CLR/TERM to exit.

### STEP 18

Press STORE key. Display shows – St 00

Set storing mode and press ENTER key. Press CLR/TERM to exit.

### STEP 19

Press RUN key. The system starts its execution and scans the selected channels as per the functional parameter set. Unbalance data is subtracted and display shows actual data. After completing the selected number of scans, the system will come to halt and display again indicates.

DAS-16

Press TERM key to stop the process any time.

NOTE: After three months, DAS 16 (MODEL 6101 P) was interfaced with LabVIEW 8.2 software of National Instruments, Netherlands (M/S-Micron, Roorkee, India)

## LABVIEW- 8.2 SOFTWARE

The *LabVIEW Data Acquisition Basics Manual* includes the information you need to get started with data acquisition and LabVIEW.

### STEP 1

After installing LabVIEW and the DAS-16 driver, install your hardware and complete the software configuration. LabVIEW uses the software configuration information to recognize your hardware and to set default DAQ parameters.

### STEP 2

Once you install and configure your hardware, you can configure your channels. LabVIEW DAQ software includes a channel configuration application, the DAQ Channel Wizard, you can use to configure the analog and digital channels on your DAQ device—DAQ plug-in boards, stand-alone DAQ products, or SCXI modules. In NI-DAQ 5.x only analog input channels can be configured. The DAQ Channel Wizard helps you define the physical quantities you are measuring or generating on each DAQ Hardware channel by querying for information about the physical quantity being measured, the sensor or actuator being used, and the associated DAQ hardware. As you configure channels in the DAQ Channel Wizard, you give each channel configuration a unique name which is used when addressing your channels in LabVIEW. The channel configurations you define are saved in a file that instructs the NI-DAQ Driver how to scale and process each DAQ channel by its name. You can simplify the programming required to measure your signal by using the DAQ Channel Wizard to configure your channels.

### STEP 3

Locating the Data Acquisition in LabVIEW:

You can find the Data Acquisition in the **Functions** palette from your block diagram in LabVIEW. When you put your cursor over each of the icons in the **Functions** palette, LabVIEW displays the palette name you are about to access at the top of the **Functions** palette. You can find the Data Acquisition icon near the bottom of the **Functions** palette, as shown in Figure 1.

The **Data Acquisition** palette contains six subpalette icons that take you to the different classes of DAQ VIs. Figure 2 shows what each of the icons in the **Data Acquisition** palette mean.

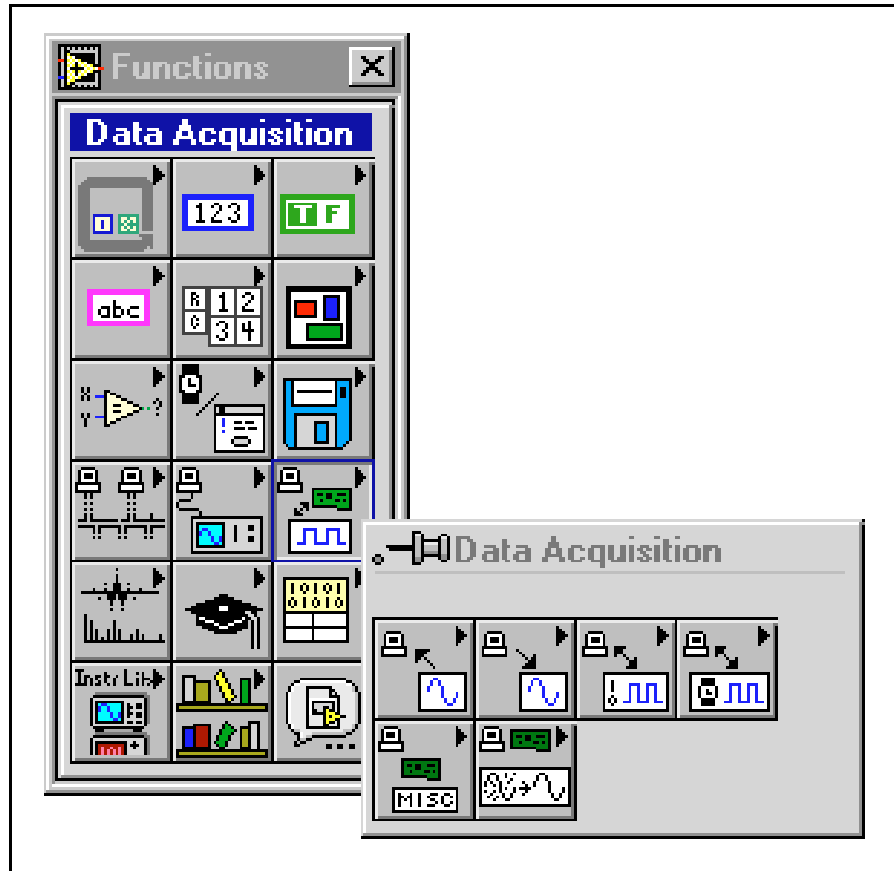


**Figure 1.** Accessing the Data Acquisition Palette

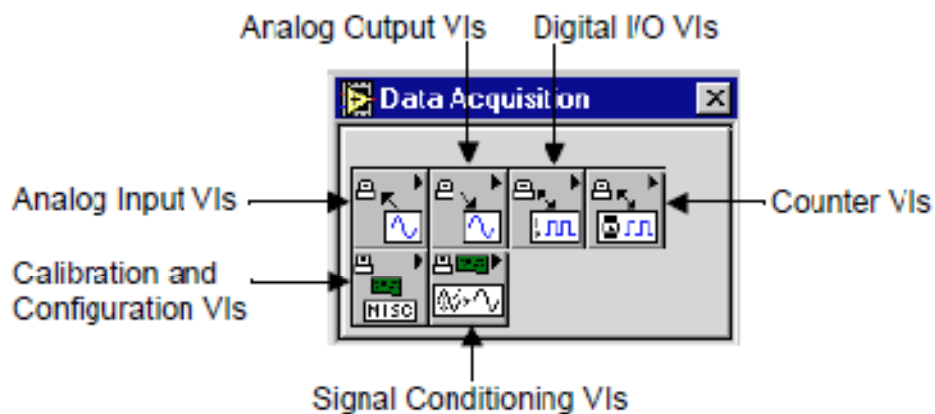


**Figure 2.** Data Acquisition VIs Palette Display of Palette Name

## Single-Channel, Single-Point Analog Input:

A single-channel, single-point analog input is an immediate, non-buffered operation. In other words, the software reads one value from an input channel and immediately returns the value to you. This operation does not require any buffering or timing. You should use single-channel, single-point analog input when you need one data point from one channel. You can connect the transducer that produces a voltage representing the fluid level to a single channel on your DAQ device and initiate a single-channel, single-point acquisition whenever you want to either to know the fluid level/displacement/deflection/pressure.

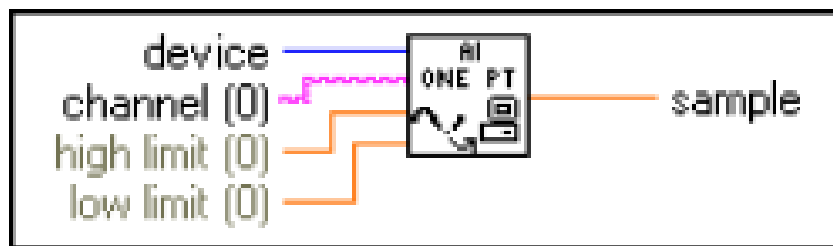


**Figure 3.** AI Sample Channel VI

STEP 5

Figure 4 shows how you program the Acquire 1 Point from 1 Channel VI, located in labview\examples\daq\analogin\analogin.llb, using the AI Sample Channel VI to acquire data.

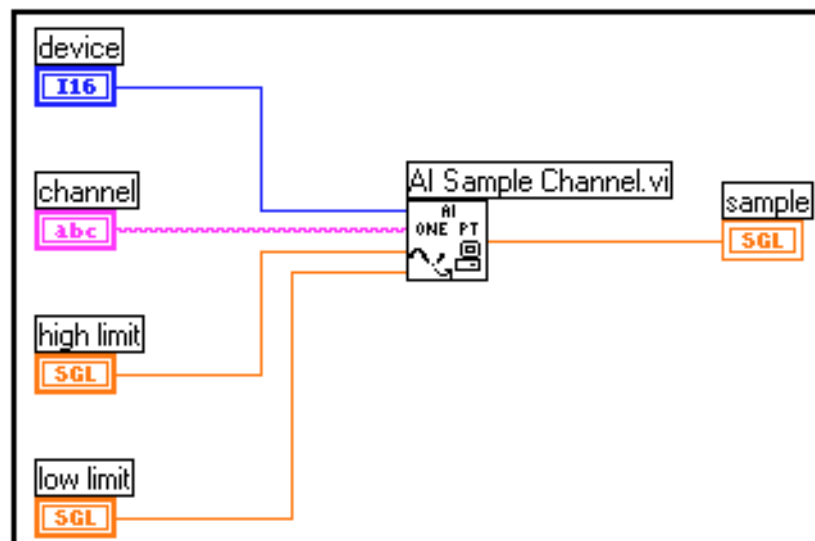


**Figure 4.** Acquiring Data Using the Acquire 1 Point from 1 Channel VI

With a multiple-channel, single-point read (or scan), LabVIEW returns the value on several channels at once. Use this type of operation when you have multiple

## APPENDIX - C

transducers to monitor and you want to retrieve data from each transducer at the same time. Your DAQ device executes a scan across each of the specified channels and returns the values when finished .

### STEP 6

With software-timed analog control loops the analog acquisition rate and subsequent control loop rate are controlled by a software timer such as the Wait Until Next Millisecond multiple timer. The acquisition is performed during each loop iteration when the AI Single Scan VI is called and the control loop is executed once for each time interval. Your loop timing can be interrupted by any user interaction, which means your acquisition rate is not as consistent as that which can be achieved through hardware-timed control loops. Generally, if you do not need a precise acquisition rate for your control loop, software timing is appropriate.



### **CURVE EXPERT 3 SOFTWARE**

1. Load data into CurveExpert. In this quickstart, we will simply read a sample text file supplied with CurveExpert. Choose File|Open (see Opening Data Files) , and double click the file BEANROOT.DAT. When the File Import (see Importing Data Files) dialog appears, simply click OK.

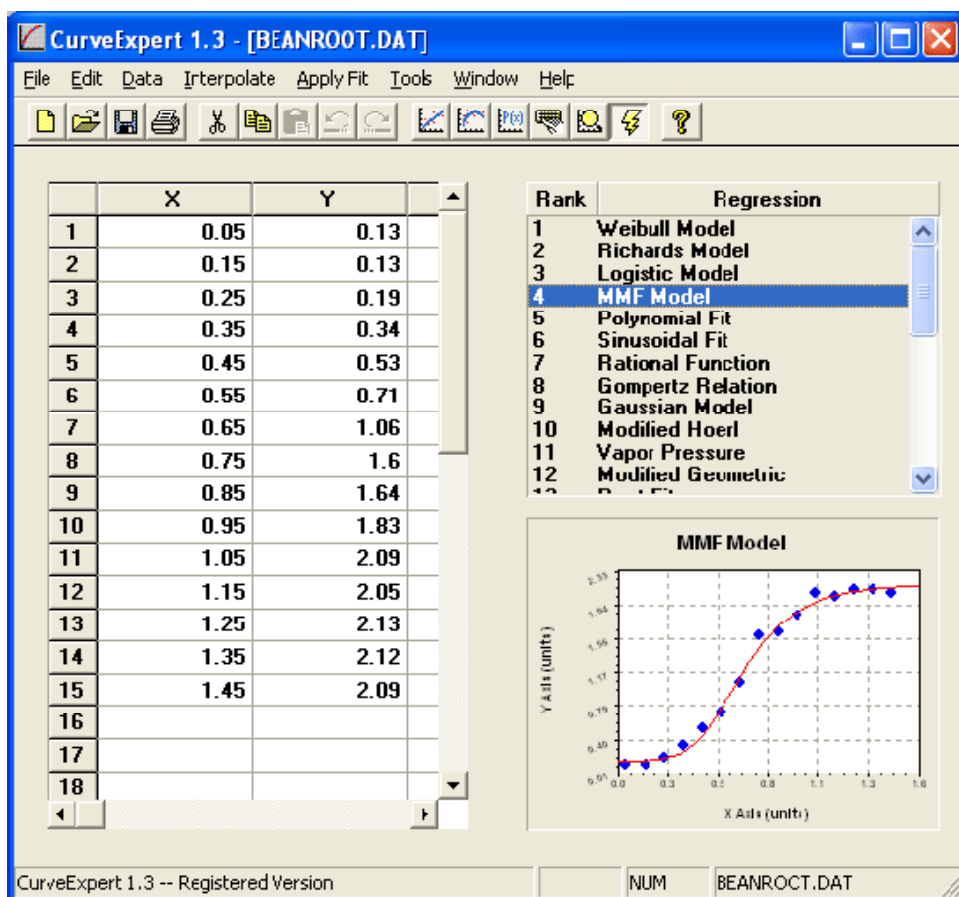
2. Perform all curve fits in CurveExpert's library. In most cases, you can select a particular model from the Apply Fit menu, but in this demo, we will just calculate them all. Choose Tools|CurveFinder (see Using CurveFinder), and then press OK in the following dialog.

3. Examine the curve fit information. A graph (see Graphing) for the Weibull model should now be displayed on your screen. Right click anywhere on the graph and select Information (see Model Information). Browse through the tabs as desired, and press Close when finished.

4. Export a table. Again right click anywhere on the graph and select Generate Table (see Creating a Table).

Navigate to a folder that you have permission to write a file to, and also type in the filename "weibull.tab", and set the minimum to 0, maximum to 2, and the increment to 0.01. Click OK. This will generate a text file with the Weibull model evaluated within the range just given.

## APPENDIX - D



**File Import Options**

Filename: C:\Program Files\CurveExpert\THREECOL.DAT

Number of Columns Detected: 3

Number of Points Detected: 15

1 First Column to Read

3 Number of Columns to Read

☐ AutoFill Independent Variable

0.00 Minimum

1.00 Increment

☐ Last Column is Std. Deviation Data

☒ Show this dialog next time

OK

Cancel

Help

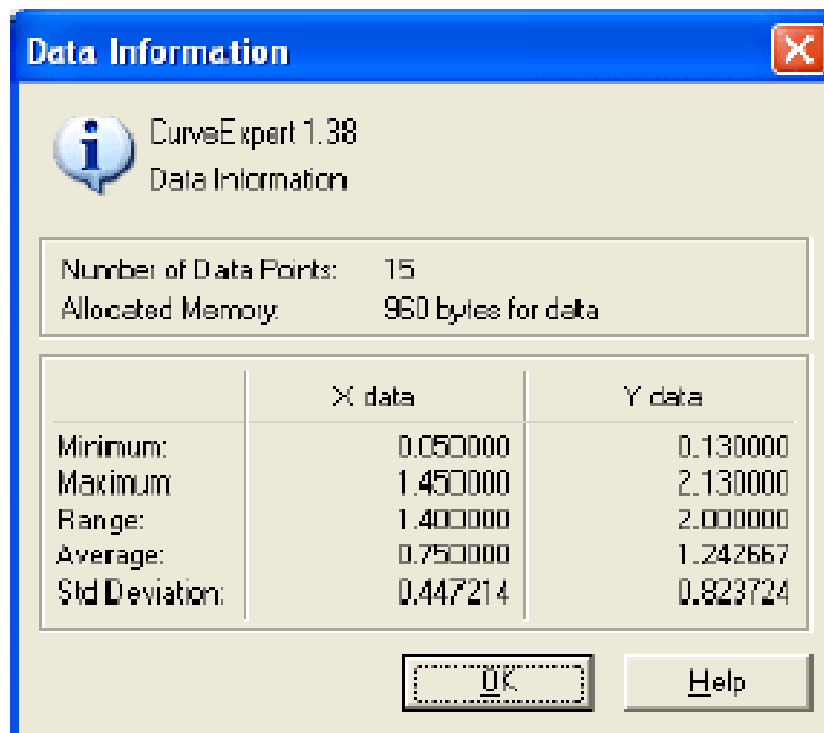
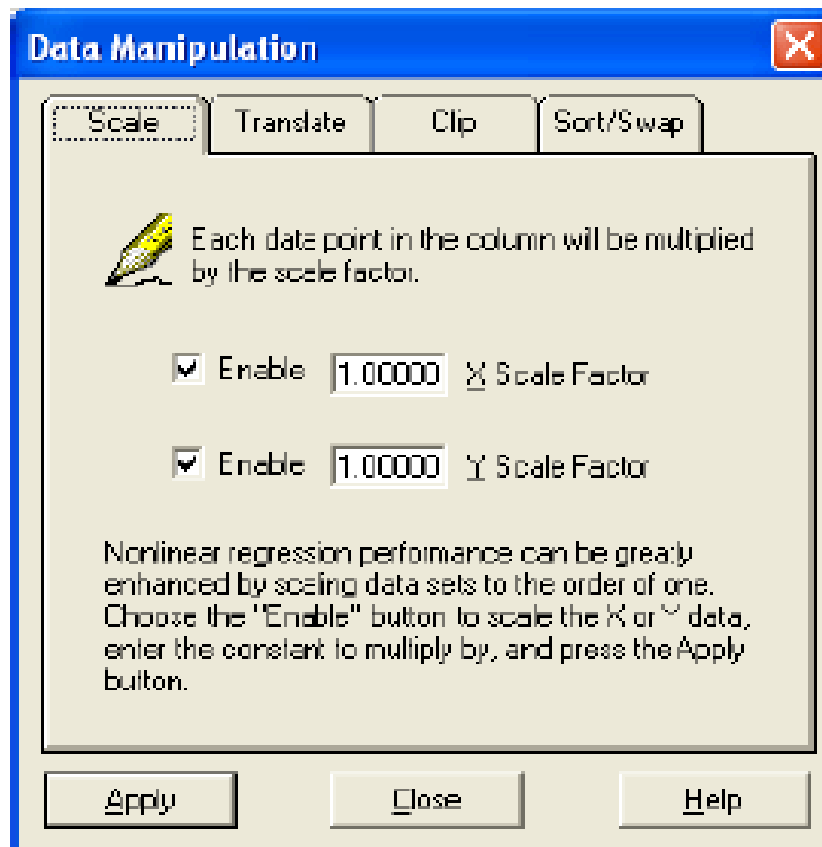
**Dataset Results**

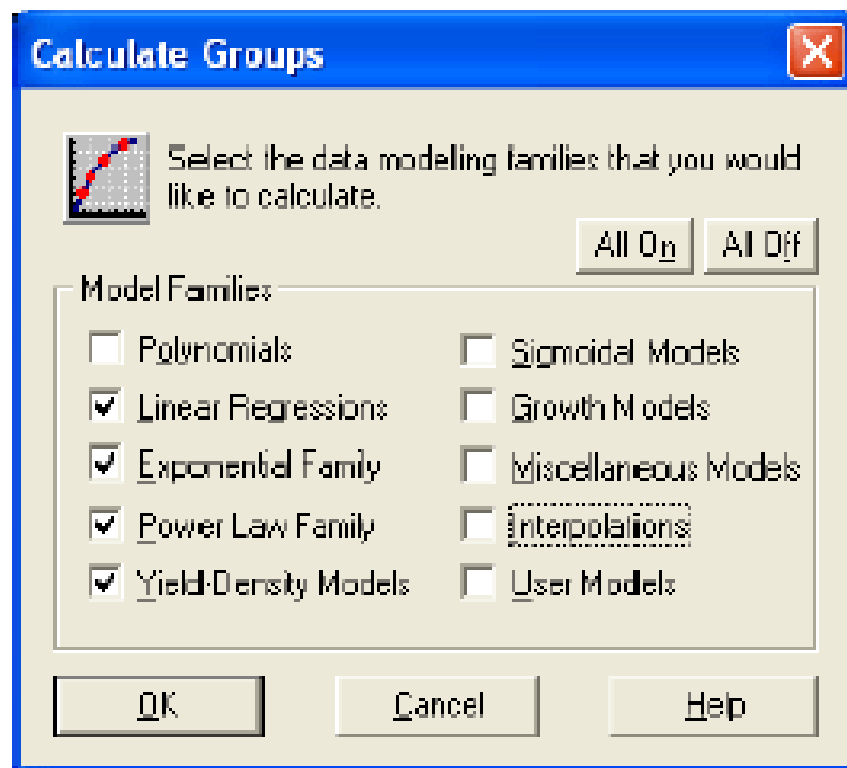
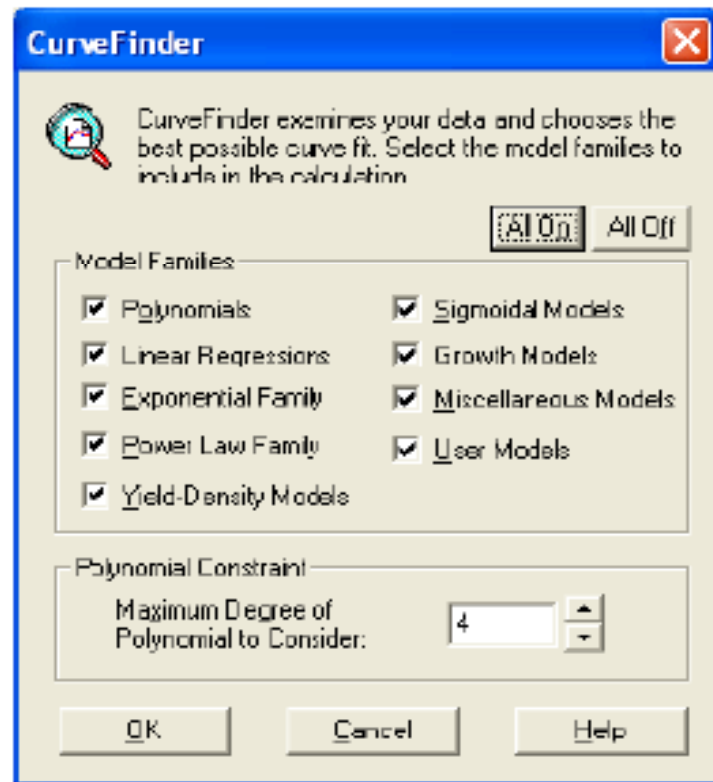
Independent Variables: 1

Dependent Variables: 2

Standard Deviation Data: no

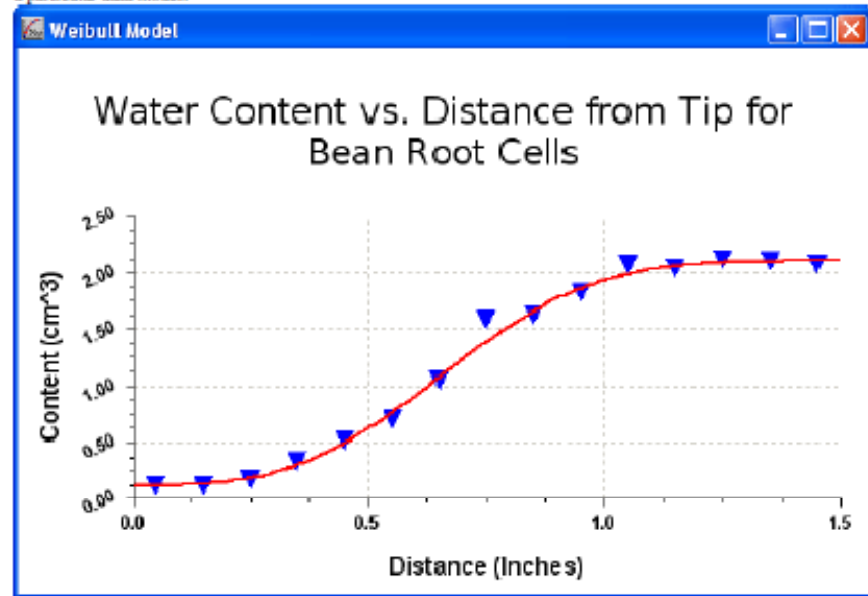
Total Number of Columns: 3





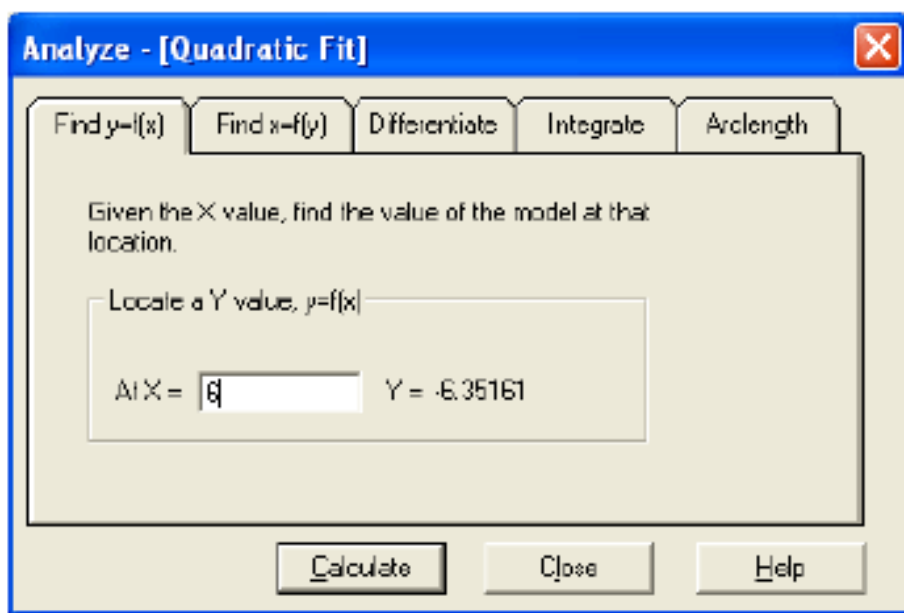
## APPENDIX - D

CurveExpert has extensive graphing capability. This capability gives you immediate feedback on the performance of a particular data model.



The 'Graph Properties - [Weibull Model]' dialog box is shown with the 'X Axis' tab selected. The 'X Axis' section includes a 'Label' field containing 'Distance (Inches)', a 'Show Label' checkbox (checked), a 'Show Grid Lines' checkbox (checked), a 'Grid Lines at Minors' checkbox (unchecked), a 'Ticks Inside' checkbox (unchecked), and a 'Line at X=0' checkbox (checked). The 'Y Axis' section includes a 'Label' field containing 'Content (cm<sup>3</sup>)', a 'Show Label' checkbox (checked), a 'Show Grid Lines' checkbox (checked), a 'Grid Lines at Minors' checkbox (unchecked), a 'Ticks Inside' checkbox (unchecked), and a 'Line at Y=0' checkbox (checked). The 'Point/Line' section includes a 'Show Points' checkbox (checked) and a 'Show Lines' checkbox (checked). The 'Overall' section includes a 'Scale Type' dropdown set to 'Normal', a 'Scale' dropdown set to 'High', a 'Low' dropdown set to '0', an 'Increment' dropdown set to '0.5', a 'No. of Minors' dropdown set to '3', a 'Fixed Point' radio button (selected), a 'Scientific' radio button (unselected), a 'Precision' dropdown set to '1', and a 'Rotation' dropdown set to '0'. The 'Font...' button is visible next to the 'Label' field in the 'X Axis' section. The 'OK', 'Apply', 'Apply To All', 'Cancel', 'AutoScale', 'Save Setup', and 'Help' buttons are at the bottom.

Using below window area under curve can be estimated using various models up to as many iterations as we require. Using particular model are under curve can be obtained using integration process.



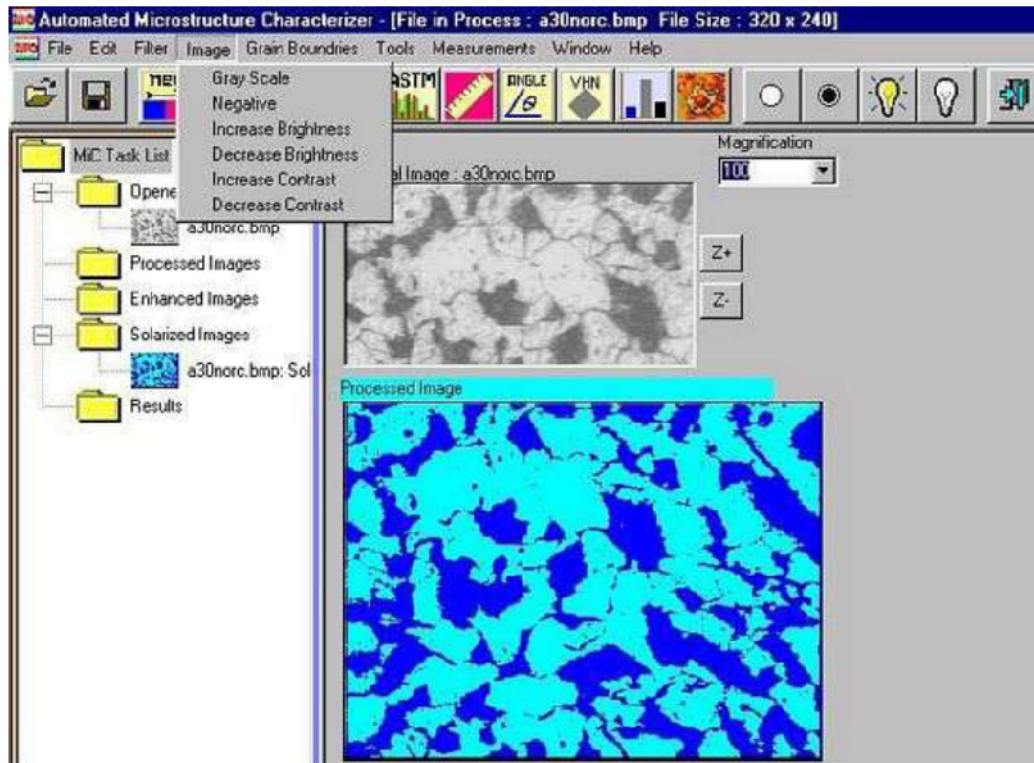
Nonlinear regression models come in all shapes and sizes – in CurveExpert, an attempt has been made to include as many models as possible, while at the same time providing relevant models to a wide range of applications. Also, keep in mind that if the model that you desire is not built-in to CurveExpert, you may define your own using the Define User Models facility. In CurveExpert, the nonlinear models has been divided into families based on their characteristic behavior.

### **Microstructure Characterizer Software (MIC)**

The Microstructure Characterizer (MiC) 2.0 is the powerful image analysis software for engineering use. Digital images taken from a Microscope are analyzed by Microstructure Characterizer, the software for microstructure interpretation. Using this software, a Material Science engineer can characterize different types of micro structural images for grain size, coating thickness and phases; get images from one or more files; and intensify the image using the filtering and enhancement features. Microstructure Characterizer Software version 2.0 offers following modules:

- Grain Size Measurement and Distribution Plots (Automatic and Manual modes)
- Volume Fraction (Automatic and Manual modes)
- Inclusion Rating (Automatic and Manual modes)
- Graphite Morphology (Automatic and Manual modes)
- Nodularity Assessment
- Bulk or micro Hardness Measurement and generating profile
- Particle Size Measurement and generating histogram of size distribution
- Linear and Angular Dimensioning.
- Percent of 'Delta Ferrite' phase present in the microstructure for color Metallography.
- Acquire images manually from one or more files.
- Increasing image detail using the filtering and enhancement tools.
- Create reports in 'Rich Text Format' or 'Custom Made' as per users' choice.
- Easy to operate - One Touch Calibration for different image resolutions.

Microstructure Characterizer Software (MiC) characterizes microstructural features using standard methods of material characterization such as ASTM grain size measurements, coating thickness, linear and angular measurements, comparison of super imposed grain size reticules, inclusion rating as per IS and ASTM standards, nodularity measurements, powder particle size distribution and so on.

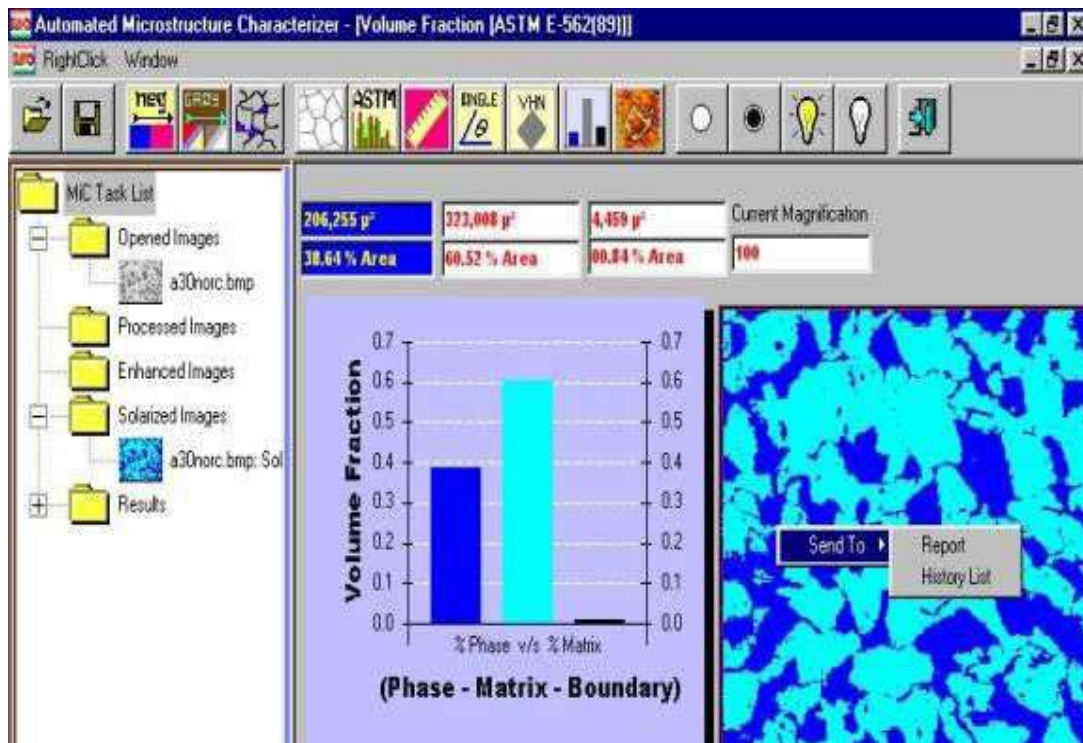


### Volume Fraction

Microstructure Characterizer Software (MiC) ships with a great feature of finding Volume fraction numbers (percentage and absolute area). These numbers are determined by automated point counting procedure for statistically estimation on a grid of one to one pixel resolution bases. Microstructure Characterizer Software is a user friendly tool that needs only dragging of color map counts volume fraction. The user can add up to five images for counting of volume fraction.

Following screen snap shot demonstrates how you get the result on screen using the Microstructure Characterizer Software.





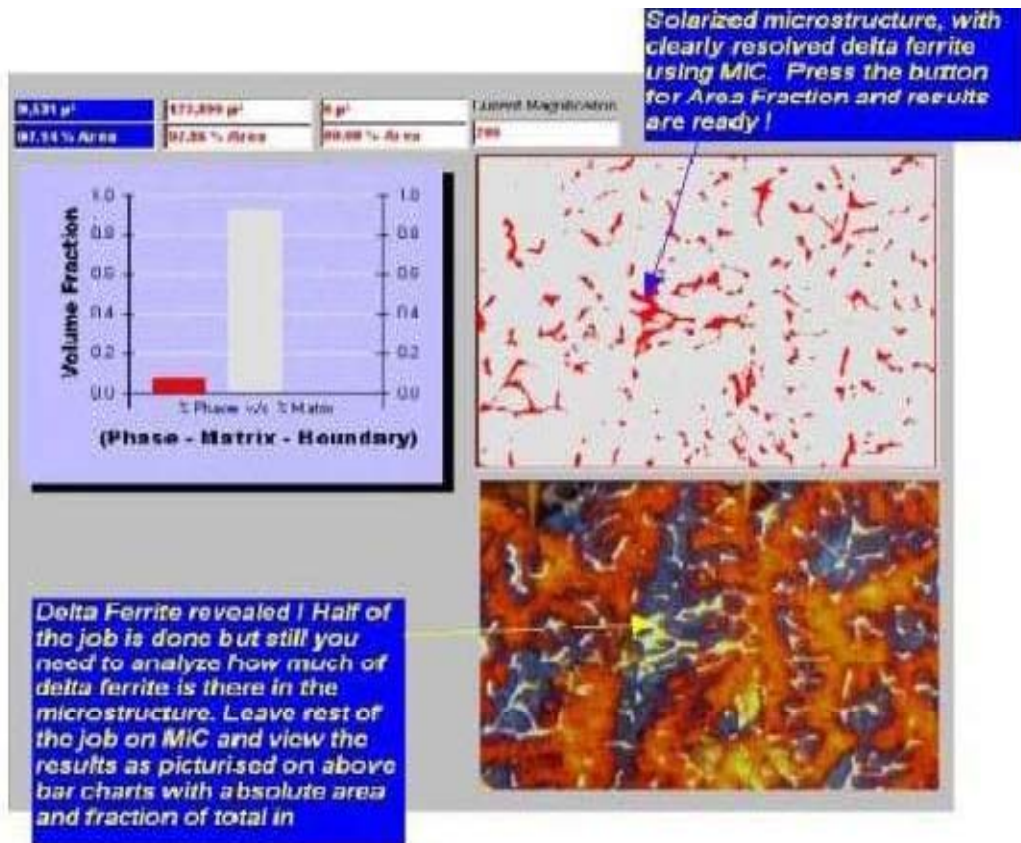
### Linear / Angular Measurement

Microstructure Characterizer Software provides facility to measure anything in any direction by means of click i.e one can measure Plating Thickness/PCB Layer Thickness/Nitrided Layer/Case hardened layer/Individual Nodule-Grin Diameter/PearliteLameale/Lathe Distance etc & that is with high accuracy & more precision.

### Reporting:

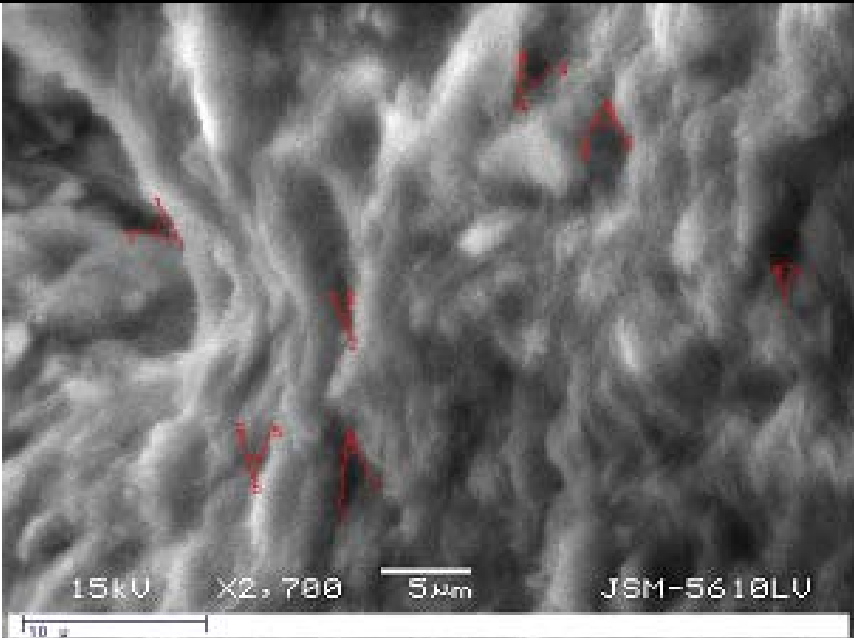
Any strength of customization is possible with MiC, right from new detection logic concept or image resolution or simultaneous image processing or with regard to reporting. What ever wished by the customer can be fulfilled with highest accuracy and repeatability algorithms. MiC has two built in modules for Reporting. Namely, report format in word 'Rich Text Format' that may be opened in standard text formatting editors like MS Word and second, 'Custom Report Format' that ships with MiC. Both of the report modules are easy to understand and does not require user input.

# APPENDIX - E



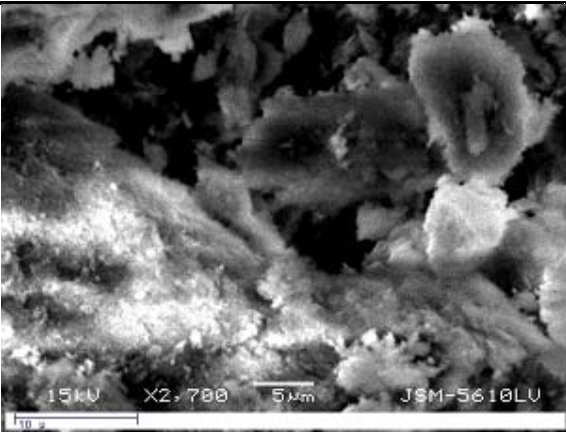
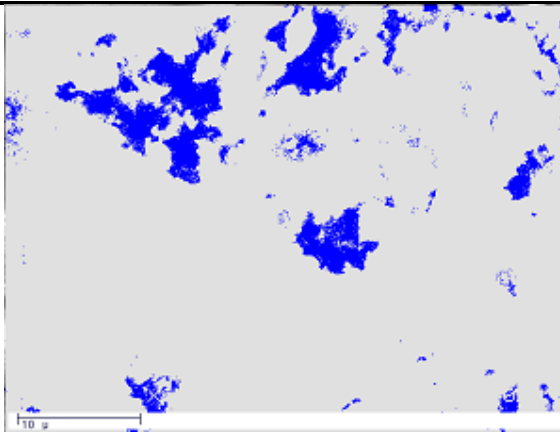
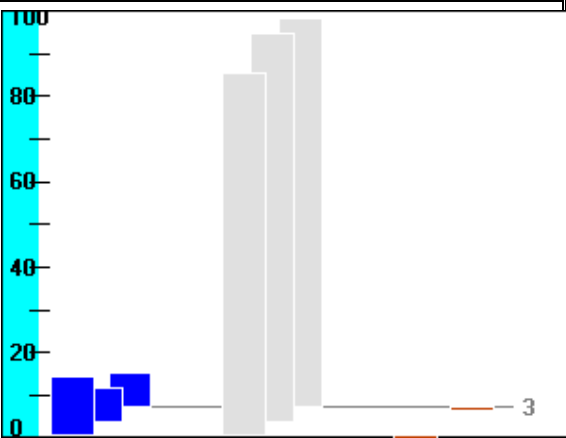
## APPENDIX - E

### Example of Data sheet/report for angular measurement:

| TEST REPORT   |   |
|---|---|
| Date: 21.04.2011  |   |
| <b>TEST: Angular Measurement.</b>   |   |
| Test Performed at   | : TCR Advanced Engineering Pvt. Ltd., Research Division |
| Instrument Utilized:  | : Optical Microscope                                    |
| Date of completion of test  | : 20.04.2011  |
| <b>SAMPLE ID: CJD-11.04- _AM</b>  |   |
|  |   |
| Plate: 1  | (2700X)   |
| Location  | Angle in Degree   |
| 1   | 0053.9  |
| 2   | 0019.9  |
| 3   | 0034.2  |
| 4   | 0045.8  |
| 5   | 0035.3  |
| 6   | 0056.1  |
| 7   | 0054.3  |

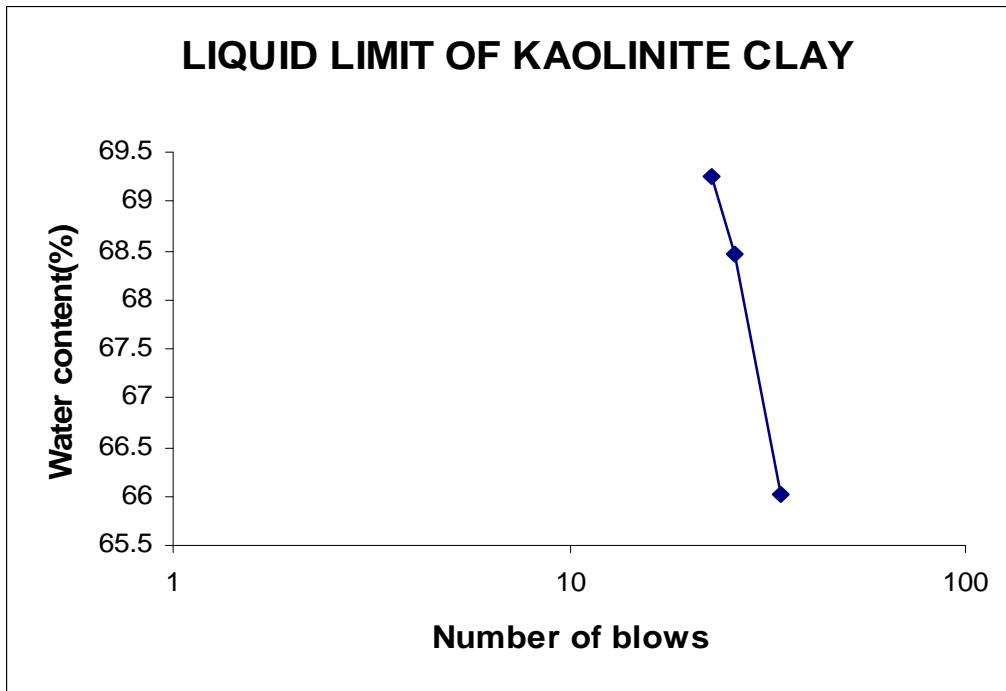
# APPENDIX - E

## Example of Data sheet/report for porosity/volume fraction measurement:

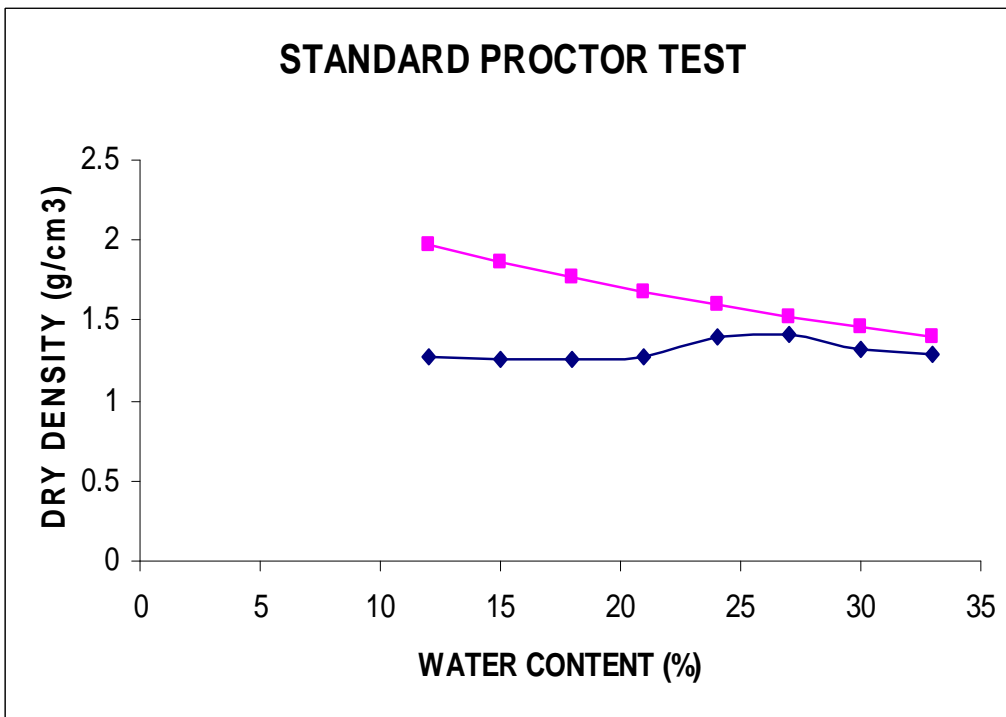
| TEST REPORT   |            |   |       |            |   |      |
|---|------------|---|-------|------------|---|------|
| Date: 21.04.2011  |            |   |       |            |   |      |
| <b>TEST: Porosity Measurement.</b>  |            |   |       |            |   |      |
| Test Performed at   | :          | TCR Advanced Engineering Pvt. Ltd., Research Division   |       |            |   |      |
| Instrument Utilized:  | :          | Optical Microscope  |       |            |   |      |
| Date of completion of test  | :          | 20.04.2011  |       |            |   |      |
| <b>SAMPLE ID: SD-11.04 - h<sub>tr2</sub>_VF</b>                                     |            |   |       |            |   |      |
|   |            |    |       |            |   |      |
| Plate: 1  | (2700X)    | Plate: 2 (2700X)  |       |            |   |      |
|  |            | <table border="1"> <thead> <tr> <th>Frame</th> <th>% Porosity</th> </tr> </thead> <tbody> <tr> <td>1</td> <td>8.48</td> </tr> </tbody> </table> | Frame | % Porosity | 1 | 8.48 |
| Frame   | % Porosity |   |       |            |   |      |
| 1   | 8.48       |   |       |            |   |      |

# VARIOUS TESTS ON CLAY

Determination of liquid limit:



Determination of MDD and OMC:



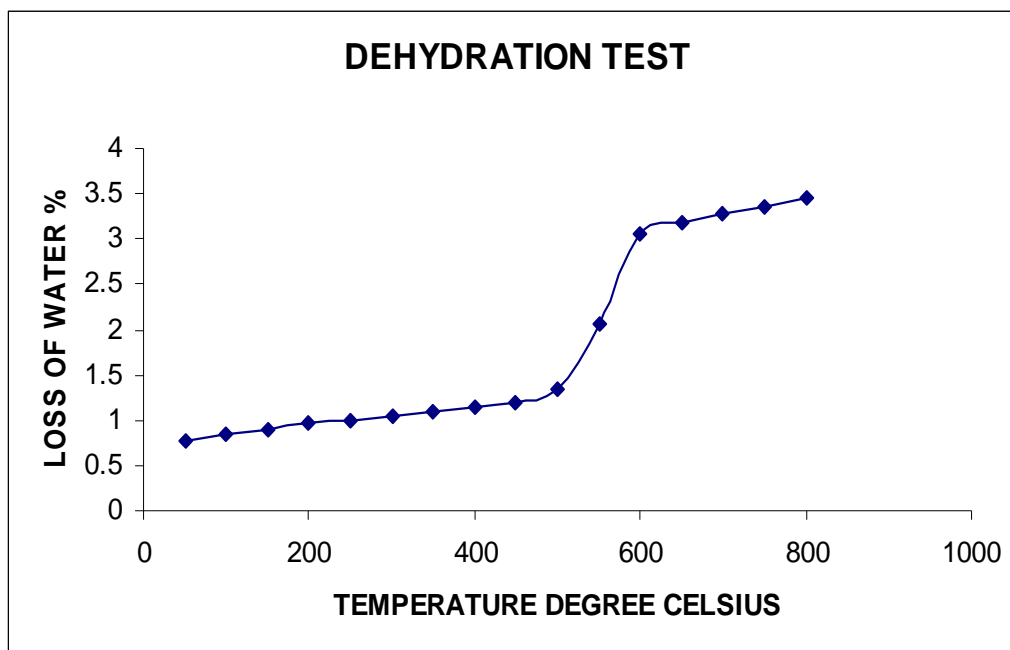
## APPENDIX - F

### Determination of Kaolin:

1. Weight of Platinum disc =19.476gms
2. Weight of sample taken = 5.0gms
3. Weight of sample and disc initially=24.476gms

| Sr.no. | Weight of sample in<br>gms | Temperature °C | % loss weight |
|--------|----------------------------|----------------|---------------|
| 1.     | 24.285                     | 50             | 0.78          |
| 2.     | 24.269                     | 100            | 0.845         |
| 3.     | 24.258                     | 150            | 0.89          |
| 4.     | 24.239                     | 200            | 0.968         |
| 5.     | 24.233                     | 250            | 0.993         |
| 6.     | 24.218                     | 300            | 1.054         |
| 7.     | 24.209                     | 350            | 1.090         |
| 8.     | 24.196                     | 400            | 1.143         |
| 9.     | 24.182                     | 450            | 1.20          |
| 10.    | 24.145                     | 500            | 1.35          |
| 11.    | 23.971                     | 550            | 2.06          |
| 12.    | 23.725                     | 600            | 3.068         |
| 13.    | 23.699                     | 650            | 3.174         |
| 14.    | 23.672                     | 700            | 3.28          |
| 15.    | 23.654                     | 750            | 3.358         |
| 16.    | 23.631                     | 800            | 3.452         |

Comparing the standard curve with test results **Kaolinite** mineral content of clay is reflected.



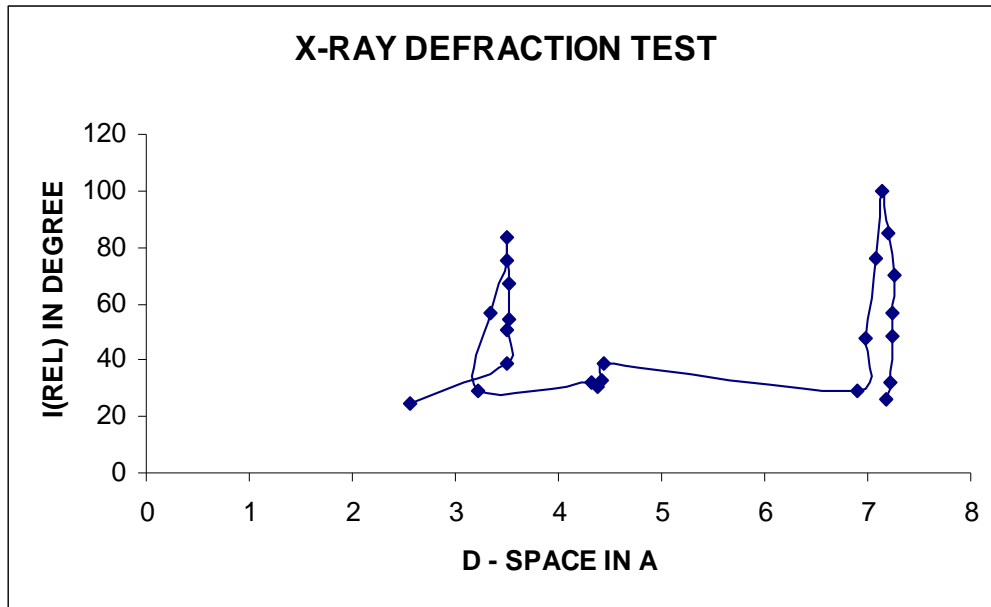
## APPENDIX - F

### X-RAY DEFRACTION TEST OF THE CLAY SAMPLE: Peak Finding Parameters

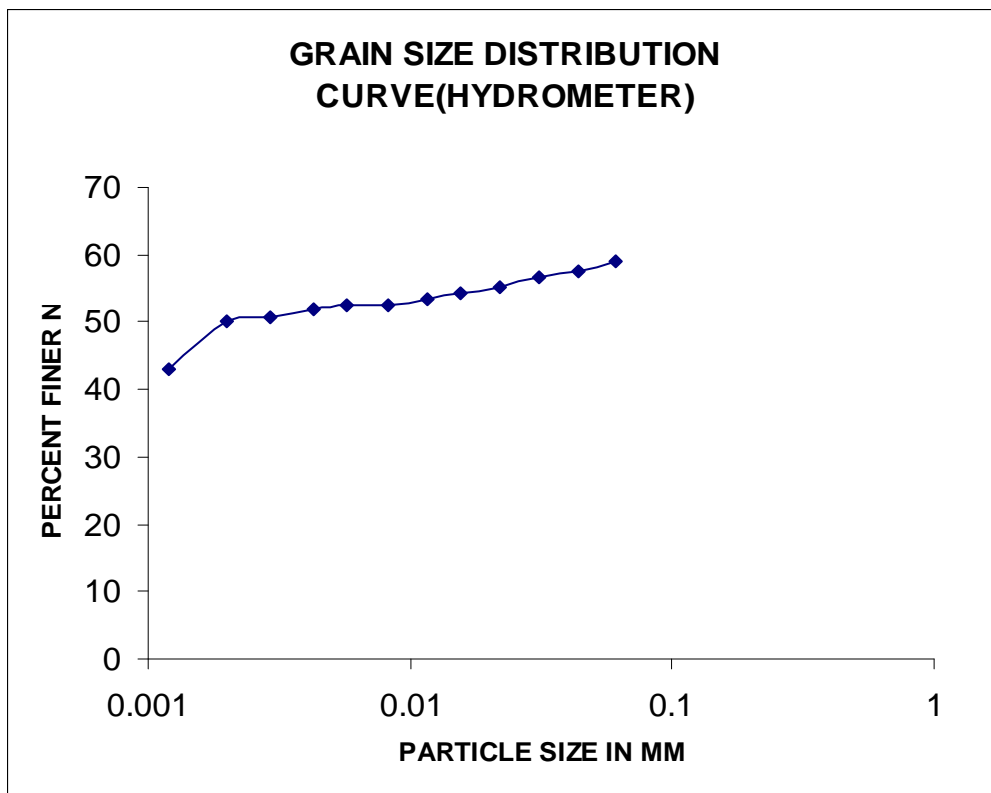
| PEAK | 2-THETA | D-SPACE | I(REL) | I(CPS) | FWHM  |
|------|---------|---------|--------|--------|-------|
| 1    | 11.74   | 7.1856  | 26.34  | 447.5  | 0.080 |
| 2    | 11.82   | 7.2281  | 32.19  | 547.0  | 0.169 |
| 6    | 11.98   | 7.2381  | 48.34  | 821.3  | 0.178 |
| 8    | 12.14   | 7.2464  | 56.56  | 961.0  | 0.209 |
| 9    | 12.19   | 7.2548  | 70.10  | 1191.0 | 0.200 |
| 10   | 12.29   | 7.1960  | 85.19  | 1447.4 | 0.190 |
| 12   | 12.37   | 7.1497  | 100.00 | 1699.0 | 0.390 |
| 14   | 12.5    | 7.0756  | 75.74  | 1286.7 | 0.180 |
| 16   | 12.66   | 6.9865  | 47.40  | 805.3  | 0.190 |
| 19   | 12.81   | 6.9051  | 28.77  | 462.4  | 0.090 |
| 22   | 19.95   | 4.4470  | 38.82  | 659.5  | 1.190 |
| 24   | 20.03   | 4.4294  | 32.68  | 555.3  | 0.130 |
| 28   | 20.24   | 4.3839  | 30.61  | 520.1  | 0.150 |
| 32   | 20.54   | 4.3206  | 32.12  | 545.8  | 0.780 |
| 36   | 24.54   | 3.2189  | 29.02  | 493.1  | 0.110 |
| 38   | 24.71   | 3.3481  | 56.57  | 961.1  | 0.179 |
| 40   | 24.83   | 3.4956  | 75.41  | 1281.2 | 0.210 |
| 42   | 24.95   | 3.5089  | 83.43  | 1417.5 | 0.760 |
| 44   | 25.06   | 3.5179  | 67.09  | 1139.9 | 0.429 |
| 46   | 25.23   | 3.5270  | 54.18  | 920.6  | 0.170 |
| 48   | 25.37   | 3.5079  | 51.04  | 867.1  | 0.179 |
| 50   | 25.46   | 3.4957  | 38.39  | 652.3  | 0.170 |
| 52   | 34.95   | 2.5652  | 24.58  | 417.5  | 0.060 |

Clay contains Kaolinite with a reflection at  $d_{001} = 0.715\text{nm}(7.15 \text{ \AA})$  Since any one mineral has a number of repeating planes running in many different directions through the crystal, each mineral gives a number of X- ray deflections. In present case **lower graph analysis** of whole soil sample shows strongest peak for **Kaolinite 0.35nm(3.5 \AA)**. In **upper graph 0.715nm(7.15 \AA)** represents **Kaolinite** for first order.

## APPENDIX - F



Determination of Grain size:





## APPENDIX - G

### VARIOUS TESTS OF SAND

#### Determination of coefficient of permeability:

| Sr. no | Description   | I                                   |
|--------|---|-------------------------------------|
| 1.     | Hydraulic head h(cm)  | 137.5                               |
| 2.     | Length of sample(L) (cm)  | 10.9                                |
| 3.     | Hydraulic gradient  | 12.614                              |
| 4.     | Cross sectional area of sample(cm <sup>2</sup> )                                  | 78.54                               |
| 5.     | Time of flow(sec)<br>(i) I test (min)<br>(ii) II test(min)<br>(iii) III test(min) | 2 : 00.61<br>1 : 58.83<br>1 : 59.42 |
| 6.     | Quantity of flow (Q)(ml)  | 1000                                |
| 7.     | Coefficient of permeability(cm/sec)   | $8.45 \times 10^{-3}$               |
| 8.     | Test temperature( °C)   | 27                                  |
| 9.     | Permeability at 27°C (cm/sec)   | $8.45 \times 10^{-3}$<br>cm/sec     |

#### Determination of Grain size:

$$C_u = \frac{D_{60}}{D_{10}} = 2.023$$

$$D_{10}$$

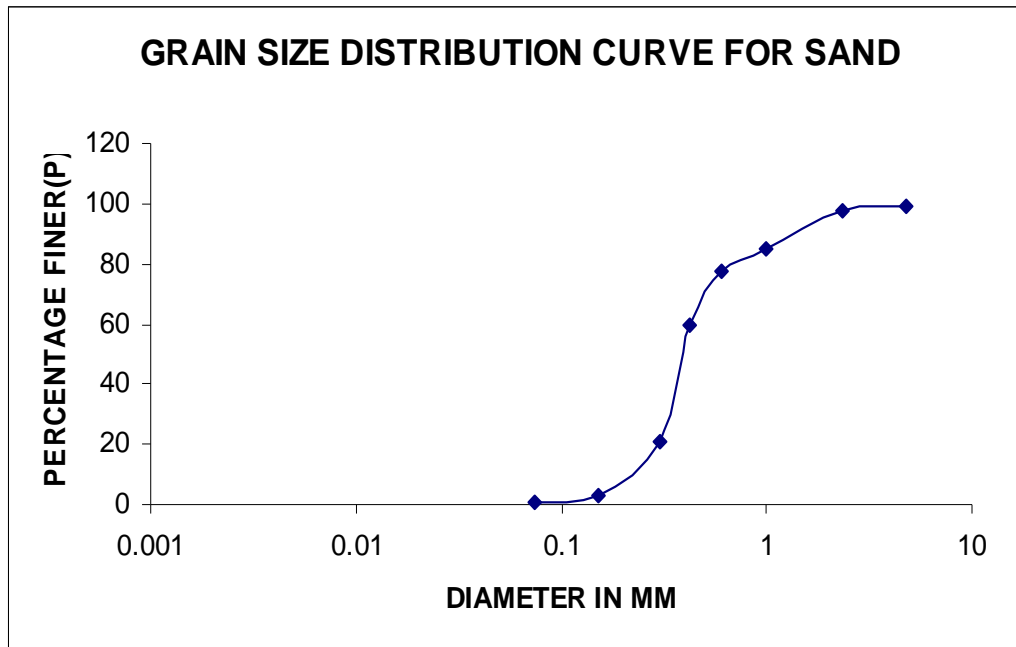
$$C_c = \frac{D_{30}^2}{D_{60} \times D_{10}} = 1.295$$

$$D_{60} \times D_{10}$$

$$C_u > 2, 3 > C_c > 1$$

Thus sand is not uniformly graded and it is well graded soil.

## APPENDIX - G



### Determination of Specific Gravity (G): Density Bottle Method

| Sr.No.                            | Description                         | Results |
|-----------------------------------|-------------------------------------|---------|
| 1.                                | Density bottle No.                  | 1       |
| 2.                                | Mass of density bottle(M1)gms       | 27.383  |
| 3.                                | Mass of bottle +dry soil(M2)gms     | 42.047  |
| 4.                                | Mass of bottle + soil +water(M3)gms | 88.383  |
| 5.                                | Mass of bottle + water(M4)gms       | 79.262  |
| Specific gravity(G) at 27°C=2.645 |                                     |         |

### Determination of Specific Gravity (G): Pycnometer Bottle Method

| Sr.No.                             | Description                      | Results |
|------------------------------------|----------------------------------|---------|
| 1.                                 | Pycnometer no.                   | 1       |
| 2.                                 | Mass of Pycnometer (M1)gms       | 442     |
| 3.                                 | Mass of pyc.+ soil(M2)gms        | 670     |
| 4.                                 | Mass of pyc.+ soil +water(M3)gms | 1592    |
| 5.                                 | Mass of pyc.+ watergms           | 1428    |
| Specific gravity(G) at 27°C=3.5625 |                                  |         |

## **VITAE**



### **BIOGRAPHICAL ITEMS ON THE AUTHOR OF THE THESIS**

MR. MANISH VRAJLAL SHAH

1. Born - December 22, 1976
2. Residential Address: 34, Maneklal Society, B/H-Buddhdev Colony, Karelibaug, Baroda-390018, Gujarat.
3. Attended M.S. University of Baroda from July 1995 to June 1998. Awarded the Degree of Diploma of Civil Engineering in June 1998.
4. Attended M.S. University of Baroda from July 1998 to June 2001. Awarded the Degree of Bachelor of Civil Engineering in June 2001.
5. Attended M.S. University of Baroda from July 2001 to Feb 2003. Awarded the Degree of Master of Civil Engineering with specialization Geotechnical Engineering in Feb 2003.
6. Worked as Lecturer in Applied Mechanics at Faculty of Polytechnic, M.S University of Baroda from July 2003 to May 2011.
7. Working as Assistant Professor in Applied Mechanics at L.D. College of Engineering, Ahmedabad appointed through Public Service Commission.
8. Membership in Professional societies ISSMGE, IGS, ISTE, IGS, ASCE(SM), ASTM(SM).
9. Published more than 60 research papers in various journals, International and National conferences.

**(M.V. SHAH)**